Conference Proceedings

Third ISEES International Conference On

Sustainable Energy and Environmental Challenges (III-SEEC)

18th Dec 2018 – 21st Dec, 2018

International Society for Energy, Environment and Sustainability

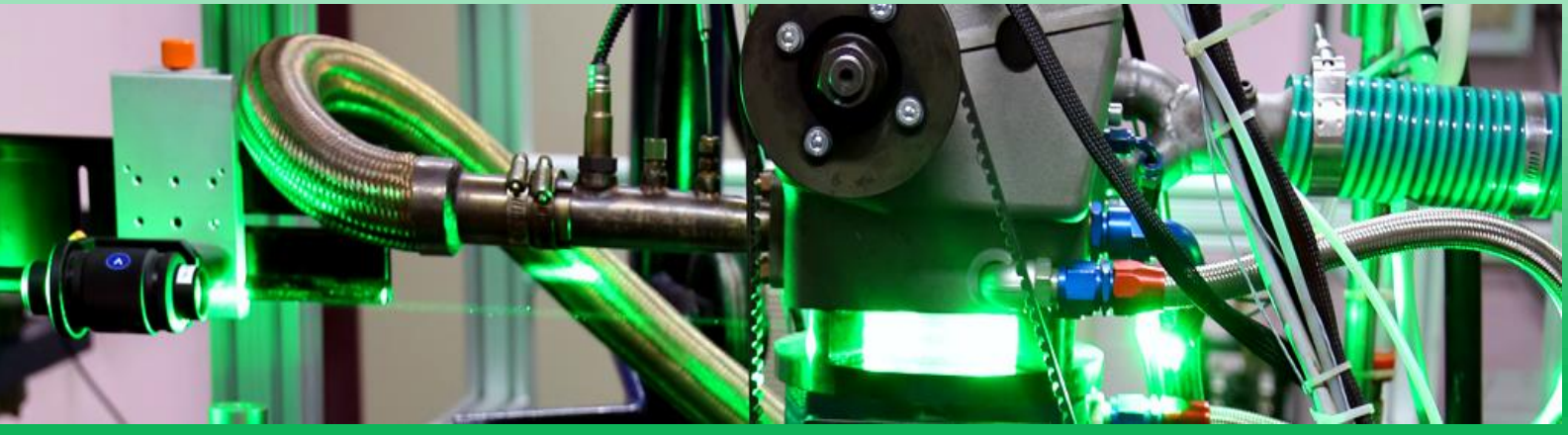

Indian Institute of Technology Roorkee

&

National Institute of Technology Uttarakhand

Conference Proceedings

III - ISEES International Conference
On

Sustainable Energy and Environmental Challenges (III SEEC)

18th Dec 2018- 21st Dec 2018

International Society for Energy, Environment and Sustainability

Indian Institute Technology Roorkee &
National Institute of Technology
Uttrakhand

Contents

About International Society for Energy, Environment and Sustainability (ISEES)

International Society for Energy, Environment and Sustainability

About the Society

The International Society for Energy, Environment and Sustainability was founded at IIT Kanpur in January, 2014 with an aim to spread knowledge in the fields of Energy, Environment, Sustainability and Combustion. In this changing environmental scenario, the time has come where more emphasis has to be laid on renewable energy resources. Moreover, in this dynamic scenario of swelling competition and reducing profits, staying environmentally responsible can be extremely challenging for any organization. More efficient systems have to be developed to meet the increasing energy demands keeping in mind its environmental impact. People have to become more aware and concerned about the environmental challenges which the world is facing today to make it a better place for us and our future generations. The Society aims to spread knowledge in the above mentioned areas among people and make them more aware about the environmental challenges which the world is facing today. The Society is involved in various activities like conducting workshops, seminars, conferences, etc. in the above mentioned domains. The society also recognizes young scientists and engineers for their contributions in this field. It comprises of experts from leading research institutions working in various domains related to energy

Aims and Objectives

1. To organize Workshops/ Symposia/ Conferences/ Lectures/ Courses for wide dissemination of knowledge to its members and society at large, in the areas related to energy, combustion, sustainability, and environment related subjects.
2. To publish technical papers, monographs, books and journals in the areas mentioned above.
3. Organizing events and activities for the benefits of the underprivileged in the society as per the capability of society members.

Journal of Energy and Environmental Sustainability (JEES)

Journal of Energy and Environmental Sustainability is official publication of the International Society for Energy, Environment and Sustainability dedicated to all the areas of conventional

and renewable energy that are relevant for environmental sustainability. The journal will publish two issues in a year and offer a platform for high-quality research in the interdisciplinary areas of energy and environmental science and engineering.

ISEES Membership

1. The Society shall have the grades of Student Member, Member, Fellow and Honorary Fellow. In addition, institutions and organizations will be given Institutional or Corporate membership on payment of dues and satisfying other eligibility criteria as specified by the executive body from time to time.
2. Fellow of the Society will be the highest grade of membership.
3. A graduate in engineering, technology, science, social sciences, humanities or having equivalent qualification as recognized by ISEES may apply for the membership of the Society. In case of unrecognized qualifications, ISEES executive committee (EC) will decide on the recognition of the qualifications. The same shall be updated in the membership documentation from time to time. Award of membership shall be at the sole discretion of the EC.
4. A member may withdraw permanently from the membership of the society at any time by giving a notice in writing to the secretary. In such cases, neither partial nor full refund of membership fee shall be done under any circumstances. There shall not be any exception to this provision.
5. The membership of any student member/ member/ fellow can be withdrawn by ISEES EC in case of unethical, immoral and criminal conduct of the individual concerned. Any action not in alignment with the objectives, interests and purpose of the society may also lead to suspension of the membership. The permanent withdrawal can only be done after an opportunity to present his/ her views to the EC has been given to the defaulting member. The decision of the ISEES EC in this regard shall be final and irrevocable in all such cases.

Privileges of Membership

1. A member whose subscription is paid up to date shall be entitled:
2. To be notified of all relevant activities of the Society.
3. To vote at all Annual General Body Meetings (AGBM) and special meetings of the Society and voting (online/ ballot) on various issues including elections and referendums.
4. Reduced registration fee in the events organized under the banner of the Society.
5. Receive a copy of the proceedings of the meetings (to the corporate members only).
6. To be included in a directory of experts along with the domain expertise to be published by the ISEES from time to time.

7. Corporate members will be able to send two delegates free/ subsidized rates to the events organized by the Society. They will also get partial fee waiver in the advertisement published in the society newsletters/ literature/ ISEES website.

Awards and Recognition

1. A member whose subscription is paid up to date shall be entitled:
2. To be notified of all relevant activities of the Society.
3. To vote at all Annual General Body Meetings (AGBM) and special meetings of the Society and voting (online/ ballot) on various issues including elections and referendums.
4. Reduced registration fee in the events organized under the banner of the Society.
5. Receive a copy of the proceedings of the meetings (to the corporate members only).
6. To be included in a directory of experts along with the domain expertise to be published by the ISEES from time to time.
7. Corporate members will be able to send two delegates free/ subsidized rates to the events organized by the Society. They will also get partial fee waiver in the advertisement published in the society newsletters/ literature/ ISEES website.

Membership Fees

	Type of membership	Annual Membership Fee	Five-Years Membership Fee NEW	Life Membership Fee (10 Years)
India/ SAARC Countries	Student Members	1000 INR	--	--
	Member/ Fellow	2000 INR	5000 INR	10000 INR
	Corporate	10000 INR	--	50000 INR
	Honorary Fellow	0	0	0
USA, Europe and Developed Countries	Student Members	50 US$	--	--
	Member/ Fellow	100 US$	250 US$	500 US$
	Corporate	500 US$	--	2500 US$
	Honorary Fellow	0	0	0

ISEES Executive Committee (2017-2018)

Chairman

Prof. Ashok Pandey

Secretary

Prof. A. K. Agarwal

Vice Chairman

Dr. Anirudh Gautam

Joint Secretary

Prof. B. R. Gurjar

Treasurer

Dr. Santanu De

Members

Dr. S. V. Mohan

Dr. Atul Dhar

Dr. T. Bhaskar

Dr. A. P. Singh

ISEES Executive Committee (2019-2020)

Chairman

Prof. Ashok Pandey

Secretary

Dr. A. P. Singh

Vice Chairman

Dr. Gautam Kalghatgi

Joint Secretary

Dr. Atul Dhar

Treasurer

Dr. Santanu De

Members

Prof. E Wintner

Dhananjay Kumar

Dr. P Binod

Prof. A. K. Agarwal

Committee for
III ISEES International Conference
on
Sustainable Energy and
Environmental Challenges
(III SEEC)

Chief Patron:	Dr. V.K. Saraswat, Member, NITI Aayog
Patron:	Prof. Ajit Kumar Chaturvedi, Director, IIT Roorkee
General Chair:	Dr. Ashok Pandey, Distinguished Scientist, IITR, Lucknow
Conference Chairs:	Prof. Shyam Lal Soni, Director, NIT Uttarakhand Prof. Avinash Kumar Agarwal, IIT Kanpur Prof. B.R. Gurjar, IIT Roorkee
Conveners:	Dr. Kaushik Pal, IIT Roorkee Prof. Vikas Pruthi, IIT Roorkee Dr. Pawan Kumar Rakesh, NIT Uttarakhand Dr. Aditya Kymar Anupum, NIT Uttarakhand Dr. Rakesh Kumar Mishra, NIT Uttarakhand

Intl. Advisory Board Members

Prof. Ramesh K. Agarwal, Washington University
Prof. S R Gollahalli, University of Oklahoma
Prof. Kalyan Annamalai, Texas A & M University, USA
Prof. Bui Xuan Thanh, Ho Chi Minh City University of Technology, Vietnam
Prof. Bassim H. Hameed, Universiti Sains Malaysia
Prof. Huu Hao Ngo, University of Technology, Sydney, Australia
Prof. Lee Keat Teong, Universiti Sains Malaysia, Malaysia
Dr. Michael Sauer, University of Natural Resources and Life Sciences, Austria
Dr. Zainul Akmar Zakaria, Universiti Teknologi Malaysia
Dr. Eldon Raj, UNESCO-IHE, Netherlands
Dr. Irem Deniz, Manisa Celal Bayar University, Turkey
Prof. D. Roekaerts, Delft University, Netherlands
Prof. Wan Azlina Ahmad, Universiti Teknologi Malaysia
Prof. Mohsen Assadi, University of Stavanger, Norway
Dr. Daniel Tsang, Hong Kong Polytechnic University, Hong Kong
Prof. Keshav S Varde, University of Michigan Dearborn, USA
Dr. Amit Bhatnagar, University Of Eastern Finland, Finland
Dr. Gabriel D Roy, CPNE Consultants, USA
Prof. E Gutheil, Heidelburg
Dr. Rod Gapp, Griffith University

National Advisory Board Members

Prof. A.B. Gupta, MNIT Jaipur
Prof. Dilip Sharma, MNIT Jaipur
Dr. Binod Parameswaran, CSIR-NIIST, Trivandrum
Prof. Rupam Kataki, Tezpur University, Tezpur
Prof. Vijayanand. S. Moholkar, IIT Guwahati
Dr. Sunita Varjani, GPCB, Gandhinagar
Dr. Deepak Pant, CUHP, Dharamshala
Dr. Ruhit Jyoti Konwar, Eternal University
Prof. P.S.Panesar, SLIET Longowal
Prof. Achintya Mukhopadhyay, Jadavpur University
Dr. R.S. Singh, Punjabi University
Dr. V.K. Garg, Central University of Punjab
Dr. Sathesh Mariappan, IIT Kanpur
Dr Praveen Kumar, Arunai Engineering College, Thiruvannamalai
Dr Baskar Gurunathan, St Joseph's College of Engineering, Chennai
Dr S Venkata Mohan, IICT, Hyderabad
D.Uma Maheshwar, GE Aviation, Bangalore
Prof. Gokare A.Ravishankar, CSIR- CFTRI, Mysore
Prof. Debabrata Das, IIT, Kharagpur
Prof. Sudipta De, Jadavpur University
Dr. S. Saravanamurugan, CIAB Mohali
Dr. Debasis Chakraborty, DRDL Hyderabad
Dr Himasnhu Tyagi, IIT Ropar
Dr.S.S.Thipse, ARAI Pune
Prof. M K G Babu, R M K Engineering College, Kavaraipettai
Prof. Tarun Gupta, IIT Kanpur
Prof. L. M. Das, IIT Delhi
Dr Atul Dhar, IIT Mandi
Prof. R. P. Sharma, IIT Delhi
Prof. R.P. Gakkhar, IIT Roorkee
Prof. Sudarshan Kumar, IIT Bombay
Dr. Rajeev K Sukumaramn, CSIR-NIIST, Trivandrum
Dr. Pravesh C. Shukla, IIT Bhilai
Dr. Sunil Kumar, CSIR-NEERI
Dr. Thallada Bhaskar, CSIR-IIP, Dehradun
Dr. Rajiv Kumar Garg, NIT Jalandhar

III SEEC ORGANISERS

Prof. Ashok Pandey
Distinguished Scientist
CSIR-Indian Institute of Toxicology Research,
Lucknow-226001, India
E-mail pandey@ciab.res.in; ashokpandey56@yahoo.co.in
Tel: +91-172-4990214
Fax: +91-172-4990204

Professor Ashok Pandey is currently Distinguished Scientist at CSIR-Indian Institute for Toxicology Research, Lucknow, India and Honorary Executive Director at the Centre for Energy and Environmental Sustainability- India. He has been Visiting Professor/Scientist and UNESCO Professor in many countries, including France, Brazil, UK, Switzerland, Malaysia, Thailand, etc. Formerly, he was Eminent Scientist at the Center of Innovative and Applied Bioprocessing, Mohali and Chief Scientist & Head of Biotechnology Division at CSIR's National Institute for Interdisciplinary Science and Technology at Trivandrum. Professor Pandey has ~ 1200 publications/communications, which include 16 patents, 54 books, 130 book chapters, 465 original and review papers, etc with h index of 84 and >29,000 citations (Goggle scholar).

Professor Pandey is the recipient of many national and international awards and fellowships, which include Life-Time Achievement Award from the International Society for Energy, Environment and Sustainability (2017); Fellow of Royal Society of Biology, UK (2016); Academician of European Academy of Sciences and Arts, Germany (2016); Fellow of International Society for Energy, Environment and Sustainability (2014); Fellow of National Academy of Science, India (2012); Fellow of Association of Microbiologists of India (2010); Fellow of International Organization of Biotechnology and Bioengineering (2008); Fellow of the Biotech Research Society, India (2005); Honorary Doctorate degree from Univesite Blaise Pascal, France (2007); Thomson Scientific India Citation Laureate Award, USA (2008); Lupin Visiting Fellowship, Best Scientific Work Achievement award, Govt of Cuba; UNESCO Professor; Raman Research Fellowship Award, CSIR; GBF, Germany and CNRS, France Fellowship; Young Scientist Award, etc.

Professor Pandey was Chairman of the International Society of Food, Agriculture and Environment, Finland (Food & Health) during 2003-2004. He is Founder President of the Biotech Research Society, India; International Coordinator of International Forum on Industrial Bioprocesses, France, Chairman of the International Society for Energy, Environment & Sustainability and Vice-President of All India Biotech Association.

Prof Pandey is Editor-in-chief of Bioresource Technology, Honorary Executive Advisors of Journal of Water Sustainability and Journal of Energy and Environmental Sustainability, Subject editor of Proceedings of National Academy of Sciences (India) and editorial board member of several international and Indian journals. He is editor-in-chief of a book series on Current Developments in Biotechnology and Bioengineering, comprising twelve volumes published by Elsevier and another series on Biomass, Biofuels and Biochemicals, comprising six volumes.

Prof. S L Soni
Director
National Institute of Technology Uttarakhand,
Srinagar, Pauri-Garhwal
Mobile No. +91-9829128150, 9557750888
Landline No.: +91-1346-257400 (O)
Fax: +91-1346-251095

Prof. S.L. Soni is currently Director of NIT Uttarakhand. His areas of interest include Thermal Engineering, Alternative Fuels, Emission Control, and Energy Conservation.

Prof. S.L. Soni received his B.E. degree from MREC, Jaipur, and M.Tech. and Ph.D. degrees from IIT Delhi.

He served Malviya National Institute of Technology (MNIT) Jaipur in various capacities including Professor and Head of the Department of Mechanical Engineering, Dean (Research and Consultancy), Faculty Coordinator (Training and Placement), Chairperson (Golden Jubilee Year Celebrations), Chief Vigilance Officer, and Registrar.

Prof. Soni has 32 publications in peer reviewed international journals and conferences, 370+ Scopus citation, 3 patents and 4 books to his credit.

He is a Fellow of Institute of Engineers, Member of SAE, Associate member of ASHRAE, Member of BIS sectional committee of Refrigeration and Air Conditioning, life member of ISEES, ISTE, Indian Association for Air Pollution Control, and Combustion Institute(I).

He is recipient of SAE India Foundation's "GURU award" as well as certificate of appreciation by MNIT Jaipur. He has supervised 12 doctoral student. As Chairperson of Golden Jubilee Year Celebrations of MNIT, Jaipur, he organized 30 International and National Conferences.

Prof. Avinash Kumar Agarwal
Professor
Department of Mechanical Engineering
Indian Institute of Technology Kanpur
Kanpur 208016
Phone: +91-512-259 7982 (office)
Fax: +91 -512-259 7408
Email: akag@iitk.ac.in

Prof. Avinash Kumar Agarwal obtained his B.E. (Mech Engg., 1994) from Malviya Regional Engineering College, Jaipur and M.Tech. (Energy, 1996) and Ph.D. (Energy, 1999) from Indian Institute of Technology Delhi. After his Post-Doctoral Fellowship (1999 – 2001) at the Engine Research Center, University of Wisconsin, Madison, USA, he returned to India in 2001 and joined Department of Mechanical Engineering, Indian Institute of Technology Kanpur as Assistant Professor, where he is serving as a Professor currently. He was a Visiting Professor to University of Loughborough, UK, Photonics Institute, University of Vienna, Austria, Hanyang University, South Korea and Korea Advanced Institute of Science and Technology, South Korea.

At IIT Kanpur, Prof. Agarwal worked in the areas of IC engines, combustion, conventional fuels, alternative fuels, hydrogen, fuel sprays, lubricating oil tribology, optical diagnostics, laser ignition, HCCI, particulate and emission control, and large bore engines. He has developed laser fired hydrogen and CNG engines in automotive sizes and developed the first electronic fuel injection system equipped locomotive engine for Indian Railways, which improved duty-cycle fuel economy and reduced particulate emissions substantially. Currently, Prof. Agarwal is involved in development of Methanol and DME fuelled vehicles for automotive sector. He is Editor-in-Chief of Journal of Energy and Environmental Sustainability and Associate Editor of Journal of Energy Resources Technology (Transactions of ASME), International Journal of Vehicle Systems Modelling and Testing and the Journal of the Institute of Engineers (Series C).

For his outstanding contributions, Prof. Agarwal is conferred upon Clarivate Analystics India Citation Award-2017 in Engineering and Technology, Prestigious Shanti Swarup Bhatnagar Prize (2016) in Engineering Sciences, Rajib Goyal Prize in Physical Sciences (2017); NASI-Reliance Industries Platinum Jubilee Award (2012); INAE Silver Jubilee Young Engineer Award (2012); Dr. C. V. Raman Young Teachers Award (2011); SAE International's Ralph R. Teetor Educational Award (2008); INSA Young Scientist Award (2007); UICT Young Scientist Award (2007); INAE Young Engineer Award (2005); Devendra Shukla Research Fellowship (2009-12) and Poonam and Prabhu Goyal Endowed Chair Professorship (2013-16) at IIT Kanpur; AICTE Career Award for Young Tecahers (2004); DST Young Scientist Award (2002); and DST BOYSCAST Fellowship (2002). He is a Fellow of Society of Automotive Engineers International, USA (SAE; 2012), American Society of Mechanical Engineers (ASME; 2013), Indian National Academy of Engineering (INAE; 2015) and International Society for Energy, Environment and Sustainability (ISEES; 2016). At IIT Kanpur, Prof. Agarwal has established a state-of-the art "Engine Research Laboratory" (www.iitk.ac.in/erl).

Dr. Bhola R. Gurjar
Professor
Department of Civil Engineering
Indian Institute of Technology
Roorkee 560012
Phone: +91 - 1332 - 285881
Email: bholafce@iitr.ac.in
Web: https://www.iitr.ac.in/~CE/bholafce

Prof. Gurjar received his bachelor's in Civil Engineering from J.N.V. University, Jodhpur, master's degree in Environmental Engineering from J.N.V. University and Ph.D. from IIT Delhi. He held Research Scientist positions at Max Planck Institute for Chemistry, Mainz, Germany before joining the Indian Institute of Technology, Roorkee as a faculty member in 2005.

Prof. Gurjar's research group focuses on Emissions and Air Quality, Health Risk Assessment, Urban Climate Change, Megacities & Global Change, Environmental Sustainability, Energy and Environmental Policy Evaluation Industrial Hazards and Disasters, Quantitative and Qualitative Risk Analysis

Prof. Gurjar has been elected Fellow of The Institution of Engineers (India), Kolkata, India and UKIERI; from the British Council Division of British High Commission, New Delhi. Among several other awards, Prof. Gurjar has received the award for Eminent Environmental Engineer conferred by Environ. Div. Board of the Institution of Engrs. (India), Highly Cited Author (Elsevier Journal Atmospheric Environment), National Design Award in Environmental Engineering from National Design and Research Forum – IEI, Highly Cited Author (Elsevier Journal Atmospheric Environment) and START Young Scientist Award.

Currently, Prof. Dutta is the Dean of Resources & Alumni Affairs and Head of Centre for Transportation Systems (CTRANS), I.I.T. Roorkee

Dr. Vikas Pruthi
Professor
Department of BiotechnologyIndian Institute
Technology
Roorkee 560012
Phone: 91-01332-285530
Email: vikasfbs[at]iitr.ac.in

Vikas Pruthi has done M.Sc. in Microbiology from University of Delhi, India, and Ph.D. in Biotechnology from Institute of Microbial Technology (CSIR), Chandigarh, India. Currently, he is a Professor at Department of Biotechnology, Indian Institute of Technology Roorkee (IITR), Roorkee, India, and Head, Centre for Transportation Systems, IITR. In his 30 years of academic and research experience, he has guided 21 Ph.D. thesis and more than 50 undergraduate and postgraduates students for their dissertation and project work. He has published more than 100 research papers and 05 book chapters and has filed Indian patents. He successfully completed 11 research projects funded by various national funding agencies. He was a recipient of Young Scientist Award and Better Opportunities for Young Scientists in Chosen Areas of Science and Technology (BOYSCAST) Fellowship for the year 2007 by the Department of Science & Technology, India. He is fellow member of American Society for Microbiology, Association of Microbiologist of India, The Biotech Research Society, India and Society of Biological Chemists. His main area of research is the development of novel strategies for the treatment and transforming pollutants to harmless substances, generating biodegradable materials from renewable sources and developing eco-friendly manufacturing and disposal processes.

Dr. Kaushik Pal
Adjunct faculty, Centre of Nanotechnology
Department of Mechanical Engineering,
IIT Roorkee
Ph: +91-1332-284761
E-mail: palkfme@iitr.ac.in

Dr. Kaushik Pal is Associate Prof. in Dept. of Mechanical and Industrial Engg. and adjunct faculty of Centre of Nanotechnology at IIT Roorkee. His main areas of research include, synthesis and modification of nanofillers (like SWCNT, GO, rGO, carbon dots, QDs, transition metal dichalcogenides) for energy harvesting and storage applications; gas and humidity sensing; barrier layers and packaging, bone implant and bio-medical applications; imaging and cellular drug delivery; aerospace applications. He is an author/co-author in more than 102 research articles and 09 book chapters. The major scientific contributions by Dr Pal in past few years include, modification of GO and rGO by raping and doping (Li and B) for gas and humidity sensor, transition metal dichalcogenides quatom dots for gas sensor, GNR and their modification for tribo-electric nanogenerator, synthesis of perovskite material for solar energy generation, PEG grafted TOCNC with rGO and GQD as a scaffold and antibacterial application, zirconia-reduced GO nanocomposite for hydrogen storage and PEM, modified SiC with nanocrystalline spinel LZO, ZnAl2O4 and GO for enhanced damping and mechanical properties etc. He has published some of his papers in very renowned journal like Nature Scientific Reports, ACS Omega, Langmuir, Electrochimica Acta, RSC Advances, Nanotechnology, Intl. J. of Biological Macromolecules, Materials & Design, Composites part B and so on. Recently, he has provided three course named Surface Engineering of Nanomaterials, Structural Analysis of Nanomaterials and for NPTEL online. Also he is the active member for so many prestigious professional bodies like NASI, MRSI, ISC, ACS, IE, ICS etc. So, Dr. Pal has a strong vision for materials development and, critically, application that will serve as a platform for new technological developments.

Dr. Pawan Kumar Rakesh
Department of Mechanical Engineering,
National Institute of Technology Uttarakhand, Srinagar,
Uttarakhand, India - 246174.
Email: pawanrakesh@nituk.ac.in

Dr. Rakesh is serving as an Assistant Professor, Department of Mechanical Engineering, National Institute of Technology Uttarakhand (NIT Uttarakhand). Currently, he is discharging the duties of the Associate Dean (Faculty Welfare) from 2016 to till date. He has also served as Head of Department, Mechanical Engineering (2013 - 2016). Working in a growing organization, he has got substantial exposure of several lab developments, academic Structure and student welfare. He has authored 36 articles published in reputed International/ National journals and conferences. He has contributed one book chapters in Mechatronics and Manufacturing Engineering.

ISEES FELLOWS

ISEES FELLOWS (2019)

Prof. Amitava Datta
Department of Power Engineering
Jadavpur University, Kolkata

Dr. Binod Parameswaran
Scientist
Microbial Process and Technology Division,
CSIR-NIIST Trivandrum, Kerala

Prof. Gnansounou Edgard
Professor
Modelling and Planning of Energy System
Swiss Federal Institute of Technology,
Lausanne (EPFL).

Prof. Vijaynad Mohalkar
Professor
Department of Chemical Engineering
Indian Institute of Technology, Guwahati

Dr. P.A. Lakshinarayanan
Professor
Department of Mechanical Engineering
Veltech Deemed University, Chennai

Prof. S.L. Soni
Director
National Institute of Technology,
Uttarakhand, India

Prof. Shantanu Bhattacharya
Department of Mechanical Engineering
Indian Institute of Technology Kanpur
Kanpur, 208016, UP, India

ISEES FELLOWS (2018)

Prof. Gautam Kalghatgi
Principal Professional, Saudi Aramco
PO Box 9290
Dhahran, Saudi Arabia 31311

Dr. Ajay Mathur
Director-General
TERI (The Energy and Resources Institute)
6C Darbari Seth Block IHC Complex, Lodhi Road
New Delhi 110003

Prof. V Ganeshan
Professor
Department of Mechanical Engineering
Indian Institute of Technology Madras

Prof. Franz Winter
Head of Chemical Process Engg and Energy Technology
Institute of Chemical, Environmental & Biological Engineering, TU-Wien,
Getreidemarkt 9/166
1060 Vienna, Austria

Dr. Nitin Labhasetwar
Sr. Principal Scientist & Head,
Energy & Resource Management Division,
CSIR-National Environmental Engineering Research Institute, Nehru Marg, Nagpur-440020, India

Prof. Achintya Mukhopadhyay
Professor
Mechanical Engineering Department
Jadavpur University, Kolkata, India

ISEES FELLOWS (2017)

Dr. V K Saraswat
Former Secretary Defence R&D
Member, NITI Aayog,
DRDO Guest House, Development Enclave,
Sankar Vihar Delhi Cantt., New Delhi-110010

Prof. Probir Kumar Bose
Campus Director, NSHM Knowledge Campus, GOI
Arrah, Shivtala, Via Muchipara, Durgapur - 713212

Prof. Ramesh Agarwal
William Palm Professor of Engineering
Washington University in St. Louis, USA

Prof. Bhola R. Gurjar
Professor in Civil (Environmental) Engineering, and
Head, Centre for Transportation Systems (CTRANS)
Indian Institute of Technology (I.I.T.) - Roorkee

Prof. Swarnendu Sen
Professor, Department of Mechanical EngineeringDepartment of Mechanical Engineering,
Jadavpur University, Kolkata - 700 032

Dr. Thallada Bhaskar
Principal Scientist,
Thermocatalytic Processes Area, Bio-Fuels Division,
CSIR-Indian Institute of Petroleum, Mohkampur,
Dehradun-248005, Uttarakhand, India

Dr. Anirudh Gautam
Executive Director
Special Railway Establishment for Strategic Technology and Holistic Advancement (SHRESHTA)
RDSO, Lucknow

ISEES FELLOWS (2016)

Prof. Avinash Kumar Agarwal
Department of Mechanical Engineering
Indian Institute of Technology Kanpur
Kanpur, 208016, UP, India

Dr. S. Venkata Mohan
Principal Scientist
Bioengineering and Environmental Sciences Lab, EEFF Department,
CSIR-Indian Institute of Chemical Technology, Hyderabad – 500 007, India

Prof. Ernst Wintner
Retired Professor of Applied Laser Technology
Vienna University of Technology (TU Vienna, Photonics Institute),
Vienna, Austria

Dr. Satish Kumar
Distinguished Scientist & Chief Controller R&D (TN) DRDO

Prof. Ryo Amano
Professor of Mechanical Engineering Department
University of Wisconsin-Milwaukee
Milwaukee, WI 53201

ISEES FELLOWS (2015)

Prof. L.M. Das
Emeritus Professor
Center for Energy Studies
IIT Delhi, Hauz Khas
New Delhi, 110016

Prof. Chang Sik Lee
Chair Professor
School of Mechanical Engineering
Hanyang University Seoul, Korea

Prof. O. N. Srivastava
Emeritus Professor
Faculty of Science, Department of Physics,
Banaras Hindu University
Varanasi

Dr. Gabriel D. Roy
CPnE Consultants,
Fairfax, VA 22030, USA

ISEES FELLOWS (2014)

Prof. Ashok Pandey
Distinguished Scientist
CSIR-Indian Institute of Toxicology Research,
Lucknow-226001, India

Prof. S. R. Gollahalli
School of Aerospace and Mechanical Engg.
University of Oklahoma
Norman. OK 73019

Dr. R. K. Malhotra
Director General
Federation of Indian Petroleum Industry (FIPI)
3rd Floor, PHD House, 4/2,
Siri Institutional Area,
August Kranti Marg,
New Delhi - 110 016

ISEES AWARDS - 2019

ISEES Young Scientist Awardees (2019)

Dr. Akhilendra Pratap Singh

Dr. Akhilendra Pratap Singh is currently a Post Doctoral fellow at Engine Research Centre, University of Wisconsin-Madicson, USA. His research interest includes Advanced Low Temperature Combustion, Optical Diagnostics with special reference to Engine Endoscopy and PIV, Combustion Diagnostics, Engine Emission Measurement, Particulates Characterization and their Control and Alternative Fuels. He has been awarded "Best Thesis Award" by ISEES and prestigious "Senior Research Associate Fellowship" by CSIR, New Delhi. He has 26 publications in peer reviewed journals, 10 conference papers and contribution to 17 book chapters.

Dr. Souvick Chatterjee

Dr. Souvick Chatterjee is an Educational Technical Evangelist at MathWorks, Bangalore. He is specialized in Liquid Transport in Physical System, Thermal Fluids and Integrated Research with focus on end–to-end product development. He has been awarded Pratt Fellowship (Virginia tech), Graduate Student Association Travel Award and Faydor Litvin Graduate Award (University of Illinois, Chicago). He has 2 patents, 14 peer-reviewed journal papers, 16 conference publications and 2 book chapters. His entrepreneurial drive also led him to be selected as one of the 2017 Think Chicago fellow.

Dr. Nikhil Sharma

Dr. Nikhil Sharma is currently a Post Doctoral Researcher at Division of Combustion and Propulsion System, Chalmers University of Technology, Sweden. His research areas include the Droplets Size and Velocity studies inside the Optical Engine using PDI, contributed in alternative fuels and reduction in emissions. He has been awarded Postdoctoral fellowship by Swedish Energy Agency, Senior Research Associate fellowship by CSIR and Best Ph.D. thesis award-2017 by ISEES. He has 7 refereed journal papers (SCI Indexed), 3 conference publications (Scopus indexed) and 10 book chapters.

Dr. Pooja Devi

Dr. Pooja Devi is a Scientist at CSIR, Chandigarh and Assistant Professor at ASIR, New Delhi. Her field of specialization is Material Science, Sensors and Energy Harvesting. She has been awarded BRICS Young Scientist fellow award, DST, New Delhi. She is also a recipient of Young Scientist Project under "Scheme for Young Scientist and Technologist". She is a member of Material Research Society of India, Electrochemical Society of India and Indian Science Congress Association. She has published 39 peer-reviewed journal paper, 51 conference paper and 2 books.

ISEES Best Ph.D. Thesis Awardees (2019)

Dr. Vikram Kumar

Thesis Title: Enhancement of Tribological properties of epoxy composite coatings for engine applications
Indian Institute of Technology Kanpur, India

Dr. Nithin K.S.

Thesis Title: Metallic Nanofillers Incorporated Polymer Nanocomposites for Energy Storage Applications

Visvesvaraya Technological University, Karnataka, India

LIST OF INVITED SPEAKERS of III SEEC

V. Ganesan	IIT Madras
Pravesh Chandra Shukla	Indian Institute of Technology Bhilai
Gabrial D. Roy	CPNE Consultants
Debasis Chakraborty	DRDL, Kanchanbagh
M. Razi Nalim	Purdue University Indianapolis
Santanu De	IIT Kanpur
P.A. Lakshminarayanan	Simpson and Co. Ltd, Chennai
S. Maji	Delhi Institute of Tool Engineering
Himanshu Tyagi	IIT Ropar
Rajiv Sharma	Amity University
Rajeev Kanth	Savonia University of Applied Sciences, Finland
V S Pruthi	IIT Roorkee
R.D. Garg	IIT Roorkee
Michael Sauer	BOKU Univ. of Natural Resources and Life Sciences, Austria
Thallada Bhaskar	CSIR-IIP, Dehradun
Binod Parmeshwaran	CSIR-NIIST, Triruvananthpuram
Vivek Kumar Morya	CEES, Lucknow
Amit Bhatnagar	University of Eastern Finland
R Praveen Kumar	Bharathidasan University
Daniel CW Tsang	The Hong Kong Polytechnic University, China
Sunil K. Khare	IIT Delhi
R P Gakkhar	IIT Roorkee
Anirudh Gautam	RDSO, Lucknow
Swarnendu Sen	Jadavpur University, Kolkata
Kirti Bhushan Mishra	IIT Roorkee
Shantanu Bhattacharya	IIT Kanpur
Dev Prakash Satsangi	B.T. Kumaon Inst. of Tech., Dwarahat
Nitin Labhasetwar	NEERI, Nagpur
Nirendra Nath Mustafi	Rajshahi University, Bangladesh
Amitava Datta	Jadavpur University, Kolkata
Rajat Agarwal	IIT Roorkee
V. S. Moholkar	IIT Guwahati
C. Balomajumder	IIT Roorkee
Arvind Kumar Bhatt	Himachal Pradesh University, Shimla
V.K. Garg	Central University of Punjab, Bathinda
Kashyap Kumar Dubey	Central University of Haryana, Mahendergarh
Inderdeep Singh,	IIT Roorkee
Bhola R. Gurjar	IIT Roorkee
S S Jain	IIT Roorkee
M Parida	IIT Roorkee
R. P. Singh,	IIT Roorkee
S N Naik	IIT Delhi
Deepak Pant	Central University of Harayana, Mahendergarh
Vinod Kumar	CIAB, Mohali
Akhilendra Pratap Singh	University of Wisconsin, Medison USA
Nikhil Sharma	Charlmers University, Sweaden

BIOGRAPHIES OF PLENARY SPEAKERS

Dr. V K Saraswat
Former Secretary Defence R&D
Member, NITI Aayog,
DRDO Guest House, Development Enclave,
Sankar Vihar Delhi Cantt., New Delhi-110010

Dr. Vijay Kumar Saraswat, India's most gifted scientist and an accomplished researcher with more than four decades of experience spaning over several fields and areas in both basic and applied sciences of defence research. Apart from being a scientist, he is a rare combination of an innovator, technologist and visionary. Born at Gwalior on 25 May 1949, Dr. Saraswat completed his engineering from Gwalior; Master of Engineering from IISc Bangalore followed by Ph.D from Osmania University. During his illustrious career, from Scientist to Scientific Adviser to Defence Minister, Director to Director General DRDO and Secretary to Dept of Defence R&D, Dr. Saraswat has been credited with development of Liquid Propulsion Rocket Engines and missiles namely PRITHVI, DHANUSH, PRAHAAR indigenously. He is the principal architect of the Ballistic Missile Defence programme which included major technology breakthroughs. The successive interceptions of incoming target ballistic missiles at Exo and Endo atmospheres are a testimony to his dedicated efforts and exploitation of limited technological resources. With this India joined the select nations that have the capability to develop BMD systems. Dr. Saraswat brought new dimensions to the strategic defence scenario through successful test firing of AGNI-5, SHOURYA, Initial Operational Clearance for Light Combat Aircraft TEJAS and induction of INS Arihant. Thus, today nation can boast of reaching any shores in the world with the nuclear capable missiles with different strike ranges. Under his leadership, DRDO provided the technologies developed by them for societal benefits namely Solar Powered Modular Green Shelters, Bio-Digesters, AAHAR programmes, explosive detection kit, Diagnostic Units for Dengu and Chickengunia etc. Dr. Saraswat's pioneering efforts have taken shape into establishment of Research & Innovation Centre at IIT Madras; MILIT-Centre for Training needs of armed forces on S&T ; CERT for reporting, auditing and handling emergency response of Information Security Incidents; CHESS - futuristic technology Centre for High Energy Laser and Microwave devices; Kyrgyz-Indian Mountain Bio-Medical Research Centre at Kyrgyzstan; The new international airport and Aerospace SEZ at Hyderabad and Advanced Combustion Research Centers at IISc and IIT(M). Till recently, Dr. Saraswat was DAE Homi Bhabha Chair and initiated development of technologies for Energy Security namely Bio-Mass, Solid Waste Management, Fuel Cells, Concentrated Solar Power, Multi Junction Photovoltaic Cells, Clean Coal Technologies etc., in the country at various Industrial and Academic Institutions in addition to bringing new dimensions to Aerospace Manufacturing. Honoris Causa was conferred upon him by more than 18 Universities including Andhra University (Visakhapatnam), NIT Surat. He has also authored and presented several papers for at National & International level journals / conferences and guided eight Ph.D Scholars. Dr. Saraswat presently is the Member NITI Aayog and shouldering many honorary positions in Government and Academic Institutions.

Dr. Gufran Beig
Joint Director at Indian Institute of Tropical Meterology Pune, India

Gufran-Ullah Beig is an Indian meteorologist and a scientist at the Indian Institute of Tropical Meteorology, Pune. He is the programme director of System of Air Quality Forecasting and Research (SAFAR), a network of air quality and weather monitoring stations, which assists in the forecast of air quality and in maintaining an emission inventory. An elected fellow of the Indian Academy of Sciences, he received the Norbert Gerbier-Mumm International Award of the World Meteorological Organization in 2005, the first Indian to receive the honor. The Council of Scientific and Industrial Research, the apex agency of the Government of India for scientific research, awarded him the Shanti Swarup Bhatnagar Prize for Science and Technology, one of the highest Indian science awards for his contributions to Earth, Atmosphere, Ocean and Planetary Sciences in 2006. His broad of research area is Air quality, weather and climate change. He did graduation from Rajasthan University in 1980 and obtained a master's degree in physics from Mohanlal Sukhadia University in 1983.Subsequently, he enrolled for doctoral studies at Physical Research Laboratory and after securing a PhD in atmospheric physics in 1990, he did his post-doctoral studies at National Center for Atmospheric Research. On his return to India, he joined Mohanlal Sukhadia University as an assistant professor in 1994 and after a service of two years, he moved to National Physical Laboratory of India in February 1994 as a scientist (B-Grade). His stay at NPL lasted only 5 months and in July 1996, he joined Indian Institute of Tropical Meteorology (IITM) as a scientist (Grade-C). Over the years, he rose through ranks to hold the position of a scientist (Grade-G) and also heads the System of Air Quality Forecasting and Research (SAFAR) programme as its director. He is known for his studies on anthropogenic emissions of green house gases and his studies have been documented in several peer-reviewed articles.

Prof. Ernst Wintner
Professor emeritus, Photonics Inst.
Vienna Univ. of Technology (TU Wien))
1040 Vienna, Austria
Phone: +43 6763094961
Email: ernst.wintner@tuwien.ac.at

Prof. Wintner received his Ph.D. in Physics in 1976 from University of Vienna with a thesis on "Electron Microscopy of Partial Dislocation Structures in CuAl Alloys". He changed to the field of Photonics when joining TU Vienna in 1976. In 1992 he was promoted titular full professor of Applied Laser Technology; since Oct. 2015 he is retired. His scientific work comprises nonlinear optics, fiber optic sensors, solid-state lasers, ultra-short pulse generation, and applications in materials processing and dental medicine. Together with GE Jenbacher, Austria, he founded the Laser Ignition Research Group in 1998. His external activities comprise visiting scientist at M.I.T. 1982–1984 and at Friedrich-Schiller-University, Jena in 1986, Visiting Professor to Institute of Laser Engineering, Osaka University, 2000-2001, and Indian Institute of Technology Kanpur in 2013. He is (co)author of more than 250 scientific publications including 7 book chapters and member of several professional organizations

Dr. Bharat Bhargava

Director General ONGC Energy Centre

Delhi, India

Dr. Bharat Bhargava is Director General, ONGC Energy Centre, since January 2013, working on various clean energy options, specially hydrogen energy, solar energy, geothermal energy, biotechnology for energy applications, uranium exploration and recovery by In Situ Leaching method, Helium recovery from oil/gas fields and energy efficiency & recovery in oil and gas sector etc. During this period several new processes and materials have been developed and patented by the Centre.

Dr. Bhargava has more than 46 years' experience in research, product development, quality assurance, production, policy, planning, management, in energy sector working on different aspects of clean energy technologies and more particularly on solar energy technologies in a research laboratory, industry and the Government. His areas of interest include material science, geophysics, semiconductor devices and micro-biology among others. Dr. Bhargava worked with the Ministry of New and Renewable Energy, Government of India, in different capacities, from 1989 to 2011. He was responsible for policy and all technical aspects of Solar technology development in India, Hydrogen & Fuel Cells Programme, Geothermal Energy Programme, Wind-Solar Hybrid Systems Programme etc. and among other activities, setting up of the PV Test Facility at Solar Energy Centre (now National Institute of Solar Energy) of the Ministry. Dr. B. Bhargava is one of the main architects of the Jawaharlal Nehru National Solar Mission, launched in 2010, which has given the Indian solar programme much needed thrust. He has also developed space grade solar cells. He was also involved in development of a number of solar applications in the country, most notable being solar lantern. He was also involved in indigenous development of several equipment, process steps, materials and test procedures associated with solar cells, modules and systems. He holds several national and international patents and involved in transfer of technology for manufacture of solar modules etc. He has written/presented papers in a large number of international and national technical journals and conferences, mainly in the area of solar PV and Hydrogen production. He has been recognized by several international and national institutions for his contributions in clean energy technologies. He is a member of several Expert Committees set up by various Ministries, State Governments and other organizations.

Prof. Ajit Kumar Chaturvedi
Director,
IIT Roorkee
Email: director@iitr.ac.in

Prof. Ajit Kumar Chaturvedi received the B.Tech., M.Tech., and Ph.D. degrees in Electrical Engineering from Indian Institute of Technology Kanpur in 1986, 1988, and 1995, respectively. He served the Department of Electronics Engineering at Indian Institute of Technology, Banaras Hindu University, Varanasi from 1994 to 1996. Subsequently, he joined the faculty of the Department of Electronics and Computer Engineering at Indian Institute of Technology Roorkee. In 1999, he moved to Indian Institute of Technology Kanpur where he also held the positions of Head of the Department of Electrical Engineering, Dean of Research & Development and Deputy Director. He is now the Director of IIT Roorkee. Prof. Chaturvedi was the Coordinator of the BSNL-IITK Telecom Centre of Excellence which has done a large number of projects for the Indian telecom sector. He is a recipient of the Distinguished Teacher award of IIT Kanpur and Tan Chin Tuan Fellowship of Nanyang Technical University, Singapore. Prof. Chaturvedi is a member of the Nomination and Election Committee of IEEE Communication Society. He has also served on the Teaching Awards Committee of IEEE. He is a founding member of the Telecom Standards Development Society of India (TSDSI) and the current Chair of the Joint Telematics Group which organizes the annual National Conference on Communications. Prof. Chaturvedi was a member of the DoT committee which recommended criteria for spectrum allocation to telecom operators, in 2008. His research interests are in Communication Theory and Wireless Communications. He has supervised a large number of graduate students and publishes regularly in IEEE journals in the area of Communications and flagship conferences of IEEE Communication Society. He is known for his contributions to waveform shaping and sequence design. Nowadays, he is working on the detection problem in massive MIMO system

Dr. Prashant Gargava
Member Secretary at Central Pollution Control Board,
New Delhi Area, India

Dr Prashant Gargava, Member Secretary at Central Pollution Control Board, is a Ph.D. in Environmental Engineering with more than 25 years of progressive and varied experience in the field of Environmental Management, particularly in environmental policies; sector specific statutory requirements and regulations; development of standards and compliance mechanism; air quality policy, strategy and action planning; and urban air quality management with substantive analytical, administrative and leadership skills.

A multifaceted environmental professional with extensive experience in academic and research as well as international exposure. His research interests include using mathematical models applied to an air quality control region for exhaustive mapping of air pollution scenario and planning control strategies; development of regulatory air quality model for India.

His did his Bachelor of Engineering, from SGITS, Indore, India, 1986, Master of Engineering from Government Engineering College, Jabalpur, 1988 and PhD from Nagpur University, 1994.

He is a Visiting faculty School of Planning & Architect, Delhi, since 1997, member internal jury, since 2000.

BIOGRAPHIES AND ABSTRACTS OF INVITED SPEAKERS

TRENDS IN AUTOMOTIVE ENGINES FOR EMISSION REDUCTION

V. GANESAN
FORMER PROFESSOR, I I T MADRAS

Abstract

In 19th century man was mainly depending on horses for mobility. Because of the unbearable semisolid and liquid pollution created by horses' man was forced find an alternative solution for mobility. In this, the ingenuity of two great scientists, viz., August Otto and Rudolf Diesel, the two engines, viz., gasoline and diesel engines were invented. The first horseless carriage rolled on American road in 1894. From then onwards engines were used for mobility. On seeing the first automobile on the road the American Congress commented, "This discovery begins a new era in the history of civilization. It may, someday, be more revolutionary in the development of human society than the invention of wheel, reported the Joint Committee of the US Congress in 1895." At the same time the congress cautioned *'Never in history has society been confronted with a power so full of potential danger and the same time so full of promise for the future of man and for the peace of the world.'* This is becoming true nowadays. The twentieth century was completely dominated by automobiles using these two engines. We are at the cross roads again because we are totally dependent on automobiles for our mobility. Environmentalists are concerned with pollution created by these two vehicles using conventional gasoline and diesel engines. A lot of research efforts are concentrated on emission reductions. The recent trends in this direction are concentrated on developing

1. **CRDI ENGINES**
2. DUEL FUEL & MULTI FUEL ENGINES
3. FREE PISTON ENGINES
4. **GDI ENGINES**
5. **HCCI ENGINES**
6. **LEAN BURN ENGINES**
7. STIRLING ENGINES
8. **STRATIFIED CHARGE ENGINES**
9. VCR ENGINES
10. **WANKEL ENGINES**

This lecture throws lights on the performance and emission characteristics of such engines. Not all the *ten* listed above are suited for automotive purpose. The *six* variants listed in block letters will be presented and discussed in this lecture.

Dr. V. Ganeshan
Professor (Superannuated)
Department of Mechanical Engineering
II T Madras
vganesan@iitm.ac.in

Prof. V. Ganeshan is a Professor Emeritus in Department of Mechanical Engineering, Indian Institute of Technology Madras. He is a Fellow of SAE, INAE, National Environmental Science Academy and IE(I). He is a life member of the Combustion Institute, ISTE and Aeronautical Society of India. He has authored 440 papers in peer reviewed journals and conferences and three books on IC Engines, Engine Simulation and Gas Turbines. He has supervised 40 doctoral students. Prof. Ganesan has received numerous prestigious award including Tamilnadu Scientist Award-2003, Automobile Engineer of the Year-2003, Khosla National Award-2004, Environmental Engineering Design Award-2006, SAE Cliff Garrett Turbomachinery Engineering Award-2007, and SAE Excellence in Engineering Education (Triple "E") Award.

Dr. Ganesan has so far published *more than 440* papers in national and international journals and conferences. He has attended many international conferences throughout the world and has chaired many technical sessions. He has organized many national and international conferences and workshops. Dr. Ganesan hasdedicated his life in writing technical books to service students' sector in the area of automotive engines and gas turbines. He has authored three popular books on IC Engines and Engine Simulation and a book on Gas Turbines and another on Heat Transfer, apart from editing several Proceedings by which thousands of undergraduate and post graduate students as well as hundreds of research scholars have been benefited. In July 2018 his book on 'THERMODYNAMICS: Basic and Applied" has been published by McGraw Hill education. His book on IC Engines is very popular and famous. McGraw Hill international has brought out the international edition of the first edition of this book and he is known to the international community throughout the world through his books. *Last but not the least he is one of the founder members of SAE India and serving the Society of Automotive Engineers India since its inception and has been honoured with three awards by SAE International*

Particle Number Emission from Compression Ignition Engines

Pravesh Chandra Shukla
Department of Mechanical Engineering
Indian Institute of Technology Bhilai.

Abstract

Diesel engine technologies have been improved a lot in the last two decades especially in terms of delivering higher efficiency and lower regulated emissions. Advancement of injection strategy in diesel injection reduced the particulate matter emission drastically. However, there is an increasing concern about particle number emission. These tiny particles are easier to inhaled deeper into the lungs and may be harmful. Future emission regulations are being designed to limit the particle number emission as well. This topic attempted to study the formation process, methods to control and recent advanced for particle number emission from compression ignition engines.

Dr. Pravesh Chandra Shukla
Assistant Professor
Department of Mechanical Engineering
Indian Institute of Technology Bhilai.

Dr. Pravesh Chandra Shukla is Assistant Professor in the Department of Mechanical Engineering at Indian Institute of Technology Bhilai. Dr. Shukla received his PhD from Indian Institute of Technology, Kanpur. He has also worked as Senior Research Associate (SRA, Pool Scientist) at IIT Kanpur. Prior to joining IIT Bhilai, he was a post-doctoral researcher in the Division of Combustion Engines, Department of Energy Sciences, Lund University, Sweden. He briefly worked in Ecole Centrale de Nantes, France in the field of dual fuel combustion. He is recipient of Young Scientist Award from the International Society for Energy, Environment and Sustainability.

Dr. Shukla mainly works in the field of Internal Combustion Engines and Alternative fuels for transportation. He worked on the development of additives for high compression ratio heavy duty engines fueled with alcohol. He is involved in investigating the emission characteristics for alternative fuels like biodiesel, HVO and alcohols for conventional and advanced heavy duty compression ignition engines. During his doctoral, he was mainly involved in physico-chemical characterization of diesel engine exhaust using non-noble metal based mixed oxides diesel oxidation catalysts. Till now, he has published more than 20 technical articles in international journals and conference proceedings.

Sustainable Propulsion Fuels: Challenges, Path Ahead

Gabriel D. Roy
CPNE Consultants

Abstract

Demand for propulsion fuels is on the increase due to increasing number of automobiles, airplanes and other transport vehicles. But the fuel price is also increasing, and the political uncertainties make the situation worse. Possible solutions are: (i) Alternate fuels - for bio fuels edible produce should not be the basic source nor could aural land be utilized for the source production. Genetic modification of plant resource to increase oil content, faster growth, capability to grow with less water will help. Coastal ground area can be saved by using multilevel ponds, and genetically modifying algae to grow faster. Bacteria enhanced conversion of waste material to propulsion fuel and similar innovations are in order. Strained hydrocarbon fuels need to be revisited, (ii) For the present and many more years to come, fossil fuel will still be the major market. So, it is necessary to improve the combustion process and make it more efficient by mixing enhancement, combustion control, plasma-assisted combustion and innovative emission and noise reduction technologies, (iii) New engines using thermodynamic cycles with better efficiency need to be developed. As an example, pulsed and continuous detonation engines offer higher efficiency, easier scalability and stand alone or topping engine capability. Though there are several programs address these, integrated multi-disciplinary research and development, major university, government, industry collaborations, substantial public and private funding, and collaboration of oil and alternate fuel producers and engine developers are still needed.

Dr. Gabriel D. Roy
CPNE Consultants
9944 Great Oaks Way
Fairfax, VA 22030, USA
Phone: +1 571418 9333
Email: roygd@aol.com

Dr. Gabriel Roy's last mission in Federal Government Service was as Associate Director at the Office of Naval Research Global, U.S. Embassy, Singapore. He was instrumental in building up joint research programs all over the world in the areas of propulsion, energy conversion, fuels and materials. Prior to this, he served as Program Manager for Propulsion and Energy Conversion at the U.S. Office of Naval Research in Arlington, VA, where he envisioned, sponsored and managed innovative research projects on Strained hydrocarbon fuels, Supersonic combustion, Combustion control, Plasma assisted emission control, pulsed and continuous detonation engines, jet noise control – to name a few. Dr. Roy has over 20 books to his credit and has authored over 100 journal articles and papers. He received the U.S. Secretary of the Navy Meritorious Civilian Service medal and award. His other recognitions include: AIAA Energy Systems medal and certificate, AIAA Air Breathing Propulsion Systems medal and certificate, ASME Jean F. Louis Energy Systems Award, JANNAF Combustion award, Dr. Roy is a Fellow of AIAA and served as an Associate Editor of AIAA Journal of Propulsion and Power. He is also a Fellow of ISEES. He is an artist and won the Lalitha Kala Academy Award in India and has recently published a book of poems, "Reality and Myth – When Two Worlds Collide."

Numerical Simulation of High Speed Combustion

Debasis Chakraborty
Design Group, Defence Research and Development Laboratory
Kanchanbagh

Abstract

Over the last few decades, CFD has developed into a rich and diverse subject and is emerged as a major component of applied and basic fluid dynamic research alongwith theoretical and experimental studies. Simultaneous development of new computers, numerical algorithms, physical and chemical models of flow physics are responsible for the great impact of CFD in both basic and applied scientific/engineering problems. Presently, CFD methods are employed routinely for the estimation of various complex propulsion flow parameters where experimental data cannot be obtained economically or feasibly.

Modeling combustion for high speed flows remains a formidable challenge in predicting high speed turbulent reacting flows. The development of combustion model for high speed turbulent reacting flows is in formative stage and some of the existing combustion models are too difficult to apply for engineering flows. Direct Numerical Simulations (DNS) are carried out for confined supersonic reacting mixing layers resolving all the spatial and temporal scales. The computed time series data are used to evaluate various empirical combustion models. Reasonable match of the models with the DNS data forms the basis of selecting the combustion model for practical applications.

3D RANS equations are solved alongwith turbulence and combustion models for the design and analysis of various missile propulsion systems using commercial softwares and important design modifications were made. These softwares were validated extensively against experimental results to find its error band and range of applications. Key performance parameters were predicted and propulsion systems were optimized through the analysis of various thermochemical parameters obtained from numerous numerical simulations. Simulation of scramjet combustor flow field of hypersonic airbreathing cruise vehicle is taken as a case study to demonstrate that how CFD methods can participate in the design exercise and help to arrive at optimized scramjet combustor.

Dr. Debasis Chakraborty, FNAE, FAeSI, FIE
Outstanding Scientist & Group Director
Design Group, Defence Research and Development Laboratory
Kanchanbagh P.O. Hyderabad -500058
Ph. 40-24583310, 40-24340037 (Fax), 9440909964 (Mob)
e-mail: debasis_cfd@drdl.drdo.in, debasisc.cfd@gmail.com

Dr. Debasis Chakraborty did his Ph. D in Aerospace Engineering from Indian Institute of Science (IISc), Bangalore. He has worked in VSSC and DRDL for the last 32 years and currently he is working as Group Director of Design Group in DRDL. He has worked extensively in numerical simulations of high speed reacting and non reacting flows and provided useful aerodynamics and propulsion design inputs for satellite launch vehicle, strategic and tactical missiles. He is the Fellow of Indian National Academy of Engineering, Institute of Engineers and Aeronautical Society of India and has received many awards including DRDO Scientist of the year, DRDO award for best innovation/futuristic development etc. He was the INAE-AICTE Distinguished Visiting Professor at IISc, Bangalore, and Visiting Professor at University of Hyderabad. He has published more than 235 research papers in various international journals and conferences in the area of CFD. As guest editor, He edited a special issue of Defence Science Journal on CFD. He was a member of aerodynamics and propulsion panels of AR&DB and expert panel member of National Supercomputing Mission and National Center for Combustion Research and Development (NCCRD).

Cost Reduction & Scale Expansion for Structural Carbon - A Path to Environment Decarbonization

M. Razi Nalim
Director, Combustion & Propulsion Research Laboratory
Indiana University - Purdue University Indianapolis

Abstract

Creation of high-value products such as structural carbon fiber from fossil and biomass hydrocarbons may disrupt the reliance on energy from burning of carbon and slow the emissions of carbon dioxide on a large scale, accelerating the transition to carbon-neutral energy. High-quality carbon fiber composites have already enabled substantial weight reduction of aircraft. Given the scale and economics of burning carbon for energy, and the absence todate of taxation on greenhouse gas externality, technological advances in diverting carbon to better uses may be more successful than focusing solely on slowing the burning. There may be significant opportunities to expand the range of feedstocks and precursors that can be used for expanding production of carbon fiber in quantities that may become comparable to other tensile structural materials such as steel and aluminum. In particular, the growing availability and low cost of natural gas and shale gas suggests new pathways from methane to carbon fiber that could include the use of commodity polymers such as polyethylene and polypropylene as precursors. Introduction of lower cost fiber, perhaps in non-aerospace grades, can drive more structural carbon use in automobiles and other mass-scale products. In addition, nanoscale carbon sturctures with unique properties can contribute to remarkable composite materials, but may not reach the scale of carbon diversion possible with macroscale carbon fiber.

Prof. M. Razi Nalim, P.E., Ph.D.
Director, Combustion & Propulsion
Research Laboratory
Indiana University - Purdue University
Indianapolis
799 West Michigan St, ET215,
Indianapolis, IN 46202
Phone: +91 900 3835011
Email: mnalim@iupui.edu

Dr. Razi Nalim is Executive Associate Dean for Research and Graduate Programs at the Purdue University School of Engineering & Technology in Indianapolis (currently on leave, and serving as Visiting Professor at Vellore Institute of Technology, Vellore, India). He has three decades of experience in higher education and professional practice – in industry, academia, and government. Working at NASA Glenn Research Center and Purdue University, he pioneered novel concepts for pressure-gain combustion engines and non-steady flow pressure-wave machines, aimed at efficiency, power and emissions improvement of aircraft and power generation engines. He helped to establish multiple industry-university research consortia, especially with Rolls-Royce Corporation. His research has led to 7 patents, and over 100 publications, supported by over $10 million in grants from NASA, US National Science Foundation (NSF), Rolls-Royce, and other sponsors. He previously led R&D at two small start-up companies, and has launched a startup company to commercialize his research. He has received the IUPUI Bynum Faculty Mentor award for guiding undergraduate research, University Trustees teaching award for innovative learning contributions, and the highest honors of his school for research and service. He has conducted workshops on project-enhanced active learning in engineering education, supported by the NSF. Internationally, Dr. Nalim has served as NATO AGARD Scholar and twice as a Fulbright Scholar. He is an Associate Fellow of the American Institute of Aeronautics & Astronautics.

Modeling of Turbulent Reacting Sprays

Santanu De
Department of Mechanical Engineering
IIT Kanpur

Abstract

Reacting sprays are important in a number of practical applications, such as liquid-fuelled furnaces, gas turbines, direct injection, and rocket engines. Due to the two-phase nature, the predictive models for turbulent spray combustion are complex, which further gets complicated due to finite-rate chemistry effects and turbulence-chemistry-spray interactions. In the talk, the presumed FDF based approaches, such as flamelet model and the conditional moment closure (CMC) methods will be reviewed, followed by a discussion on the transported FDF method. Numerical results from some of these combustion models will be presented and discussed.

Dr. Santanu De
Department of Mechanical Engineering
IIT Kanpur
Kanpur, India 208016
Phone: +91 512 2596478
Email: sde@iitk.ac.in

Dr. Santanu De is an Assistant Professor in the Mechanical Engineering, IIT Kanpur, since December 2014. He received a Bachelor of Engineering from the North Bengal University in 2002 and an M.Tech. from the IIT Kanpur in 2004, both in Mechanical Engineering. He received his Ph.D. in Aerospace Engineering from the Indian Institute of Science, Bangalore, in 2012. Prior to his joining at IIT Kanpur, he served 2 years at the Michigan Technological University as a postdoctoral research associate and 1 year at the Institute of Combustion Technology (ITV), University of Stuttgart. He also worked as a Scientist at the Liquid Propulsion Systems Center, Indian Space Research Organization, between 2004 and 2005. His primary areas of research are numerical modelling of turbulent combustion, spray atomization and combustion, coal gasification and combustion. He is a member of the editorial board of 'Journal of Energy, Environment and Sustainability.'

Understanding some Aspects of in-Cylinder Behaviour of a Direct Injection Diesel Engine by Experiments

P.A. Lakshminarayanan
Technical Adviser
Simpson and Co. Ltd

Abstract

The combustion and flow in a direct injection diesel are studied with increasing complexity using zero dimensional models to full 3-d models. The involved models are very useful to understand the minute details and then fine-tune the engine either upfront or after the engine is developed. However, they consume computer time as well as resources. Also, experimental verification of the models is necessary to have confidence. On the other hand, a designer would like to follow a medium path, which is neither zero- nor multi-dimensional, with support from experimental data on individual systems at the bench, so that iterations can be performed economically and fast. The presentation looks at: (1) gas flow, (2) ignition delay, (3) mixing controlled combustion model to consider the phenomenon at the wall and different types of injection systems, namely mechanical and electronic injection with single shot or multiple injection. The model is validated over many engines of bore size ranging from 75 mm to 280 mm. 4) Also, presented are the phenomenological models of formation of smoke and hydrocarbons, validated in engines and combustion bomb.

Dr. P.A. Lakshminarayanan
Technical Adviser
Simpson and Co. Ltd.
861/862 Mount Road
Chennai, 600 001
Phone: +9840850068
Email: Gautam.kalghatgi@aramco.com
kalghatgig@gmail.com

Dr. P.A. Lakshminarayanan graduated from the Indian Institute of Technology, Madras in 1971 and obtained M.S. and Ph.D. degrees from the IC Engines Laboratory of the same institute. Then, he was a Research Associate at Loughborough University of Technology, England for about five years and conducted research on petrol and diesel combustion. In 1983, he joined Tech Centre, Kirloskar Oil Engines Ltd., Pune. He worked there on many designs of engines and engine subsystems for nearly 20 years. In 2002, he was called to head the Engine R&D at Ashok Leyland, Hosur. During this tenure of ten years till 2011, he was responsible for development of new diesel and CNG engines up to Euro-5 emission norms and 230 hp. Till 2016, he was the Chief Technical Officer at Simpson and Co. Ltd. where his teams developed compact engines and upgraded and uprated existing diesel engines. Now he is the Technical Advisor. He has published 53 research papers in ASME, SAE and IMechE. Four of them received prizes for integrity and quality of the contents from the SAE (intl.), Combustion Society (India), AVL (Graz) and AVL (Pune) in 1983, 1993, 2005 and 2010 respectively. He has five patents to his credit. He has co-authored a book on "Modelling Diesel Combustion" published by Springer Verlag (2010). His next book "Critical Component Wear of Parts in heavy Duty Engines" was published in 2011 by John Wiley International. He is co-editing his third book on Design of Heavy-Duty Diesel engines, which is a collaborative effort of about 35 authors and it is intended for publication in 2019. He is a recipient of Arch Colwell Award of the SAE. He is a life member of ISEES and Combustion Institute (India). He is a Fellow of the SAE and Indian National Academy of Engineering (INAE).

Vehicular Emissions and its impact on AQI in Urban Areas

S. Maji
Director, Delhi Institute of Tool Engineering.

Abstract

AQI or Air quality index is a tool which tells about the relative quality of the air in terms of clean air. It gives a relative amount of pollutants present in air. AQI computation requires an air pollutant concentration over a specified averaging period, obtained from an air monitoring devices which are installed at selected places in a city. The quantity of the particulate material and other toxic gases with respect to a time duration represents the concentration of the air pollutant present in the air at a particular location. AQI has been found to be affected by the volume of traffic, fuel quality, vehicle maintenance etc. As the number of vehicles increase the AQI level also increases proportionally. AQI level is thus attributed to be impacted by the vehicular emissions to a larger extent in addition to other pollution sources like industrial pollution, burning of crops etc.

Prof. S. Maji
Director, Delhi Institute of Tool Engineering
Govt. Of NCT of Delhi
New Delhi

Prof. S. Maji is presently serving as Director, Delhi Institute of Tool Engineering. He has done his graduation in Mechanical Engineering from Delhi College of Engineering in 1981, M.Tech. from IIT-Delhi and Doctorate from Faculty of Engineering, University of Delhi. In the past he has worked as Scientist at CSIR – IIP, Dehradun. His area of research is "use of fuels and lubricants including alternate fuels in IC engines" and combustion generated pollution. He has served as Associate Professor / Professor for 24 years at DCE/DTU. In DTU, he was Head (Mechanical Engineering), Head (Production Engineering) and Head (Automobile Engineering). He was also Dean (Research & Development) and Professor Incharge (Alumni Affairs) and Principal, GB Pant Govt. Engineering College, Delhi.

Prof. Maji was conferred Guru Award by SAEINDIA Foundation for extraordinary contribution to Automotive Engineering Education; Ralph R. Teetor Educational Award in 2001 by SAE International, USA; National Award for "Development of New Cost Effective Product for Manufacture". Prof. Maji was invited by Michelin Tyre to deliver lecture in Bibendum-2011 at Berlin, Germany. Prof. Maji was UNDP fellow in 1986-87 at University of Zwickau, Germany and SERC fellow during 1998 at IIT-Delhi. Prof. Maji has more than 120 publications; 2 patents. He has guided 10 Ph.Ds. His academic and professional activities include Member of Expert Committee of NATRIP, BIS, GGSIPU, ISM, NIT-Kurukshetra, YMCA, MNES, IUAC. Expert / Advisor for recruitment for UPSC, CSIR & DRDO. Prof. Maji is also Member, Society of Automotive Engineers(SAE); Fire & Security Association of India (FSAI); SAE-India Publication Board; SAE-India, SAE-India Foundation; Faculty Advisor-SAE International Students Chapter; Vice-Chairman(Publication)-SAE India, NIS; Faculty Advisor-SAE Student Chapter-DCE.

Sustainable Energy Application: Water Purification

Himanshu Tyagi

School of Mechanical, Materials & Energy Engineering,

IIT Ropar

Abstract

Worldwide water scarcity and the contamination of existing fresh water resources (by various pollutants) is one of the serious global challenges. In order to augment the fresh water supply, desalination has been practised by many countries such as Middle East and North African countries, India, United States etc. Majority of the desalination plants in these countries are based on Multi Stage Flash (MSF) and Reverse Osmosis (RO) technologies. Both these technologies are capital and energy intensive and suitable for large scale water production applications and are having high cost for small scale applications. Hence, there is a need to develop such technologies which may be economical for small scale applications, can be combined with renewable energy sources such as solar and geothermal and are suitable for such regions in the world which does not have resources to install MSF or RO plants. Humidification-dehumidification (HDH) desalination technology is one such technology (based on thermal desalination technology) which has been found to be ideal for small scale water productions (1-100 m3/day), requires less maintenance and can be combined with the renewable energy sources such as solar or geothermal due to lower temperature operation.

Dr. Himanshu Tyagi
Associate Professor,
School of Mechanical, Materials & Energy Engineering,
IIT Ropar, Rupnagar – 140001, Punjab, India
Phone: +91-97796-12972
Email: himanshu.tyagi@iitrpr.ac.in

Dr. Himanshu Tyagi is currently working as Associate Professor in the School of Mechanical, Materials and Energy Engineering, IIT Ropar. He has previously worked at the Steam Turbine Design Division of Siemens (Germany and India) and at the Thermal and Fluids Core Competency Group of Intel Corp (USA). He received his Ph.D. from Arizona State University, in the field of Heat Transfer and specifically looked into the radiative and ignition properties of nanofluids. He won the Best Paper Award at the ASME Energy Sustainability Conference at Long Beach, CA in 2007. He obtained his master's degree from University of Windsor, Canada, and his bachelor's from IIT Delhi, in Mechanical Engineering. Among other awards, he has received Summer Undergraduate Research Award (SURA) from IIT Delhi, International Graduate Student Scholarship from University of Windsor Canada, Indo-US Science and Technology Forum (IUSSTF) grant awarded for organizing an Indo-US Workshop on 'Recent Advances in Micro/Nanoscale Heat Transfer and Applications in Clean Energy Technologies' at IIT Ropar.

Funding Opportunities in India for Clean Energy Research

Rajiv Sharma

Amity University

Abstract

Government of India has placed a great importance on clean energy to meet its growing energy demand with little or nil impact on the environment. India is a leading member of the Mission Innovation promoting research in clean energy with an ambitious target of doubling the expenditure in this area. To meet this target, a number of schemes have been launched promoting research in solar energy, biofuels, alternate fuels, clean energy materials, off grid energy storage, smart grid, energy demand reduction in built environment etc. India has also entered into bilateral and multilateral arrangements with various countries for joint research in these areas. The talk will cover some of these research funding opportunities.

Name: Dr. **Rajiv Sharma**
Designation: Director General
Amity Foundation for Science, Technology
& Innovation Alliances

Dr Rajiv Sharma is a Ph.D. in mathematical modeling of physiological fluid system from IIT Kanpur in 1987. He has a very extensive experience of over 33 years in promotion of science and technology through various positions in the Department of Science and Technology, Government of India. This includes about 20 years in development and implementation of international bilateral/ multilateral programmes with other countries and has widely travelled across the world for this purpose.

Dr Rajiv Sharma holds the distinction of being the first Indian Co-Chair of the Indo-German Science and Technology Centre as well as of the US-India S&T Endowment Board. He became the second Executive Director of the bi-governmental Indo-US Science and Technology Forum promoting science, technology and innovation collaboration, covering a large number of stakeholders ranging from students to senior scientists to entrepreneurs.

In 2016, Dr Sharma became the Mission Director of 4 important technology missions related to Nano Science & Technology; Clean Energy; Water; and Supercomputing. He later held the position of the Secretary of Science and Engineering Research Board for about 16 months before superannuation from Government of India.

He is presently a Senior Vice President of the Ritnand Balved Education Foundation (RBEF), the sponsoring foundation for Amity Universities in India and abroad and alsi the Director General of Amity Foundation for Science, Technology and Innovation Alliances (AFSTIA).

Role of Big-Data and Learning Analytics in Innovative Education System

Rajeev Kanth
Savonia University of Applied Sciences

Abstract

In the recent years, big data and learning analytics have been emerging as fast-growing research fields. The application of these emerging research areas is gradually addressing the contemporary challenges of school and university education. Tracing out the information regarding students' misconceptions and dropping-out probabilities from the courses at the right instant of time, development of detectors of a range of educational importance and achieving the highest level of quality in the higher education are becoming more challenging. Moreover, providing well timed and the best suitable solutions to the students at-risk are even more strenuous. In this concept paper, we aim to address these contemporary challenges of school, the university education, and their probable solutions by utilizing our research experiences of automated assessment, immediate feedback, learning analytics and the IT technologies. Solving such problems by knowing the history of students' activities, submissions, and the performances data is possible. The identification of students' misconceptions during the learning process, examining behavioral patterns and significant trends by efficiently aggregating and correlating the massive data, improving the state-of-the-art skills in creative thinking and innovation, and detecting the drop-outs on-time are highlighted in this article. We are aiming at extracting such knowledge so that adaptive and personalized learning will become a part of the current education system. Not only the available algorithm of supervised learning methods such as support vector machine, neural network, decision trees, discriminant analysis, and nearest neighborhood method but also new engineering and distillation of relevant data features can be carried out to solve these educational challenges.

Prof. Rajeev Kanth, D.Sc. (Tech.)
Savonia University of Applied Sciences
Senior Research Scientist
University of Turku, Finland
Opistotie 2, 70101 Kuopio Finland
Phone: +358 440210074
Email: rajeev.kanth@savonia.fi

Dr. Rajeev Kanth is currently working as an Associate Professor at the Savonia University of Applied Sciences, Kuopio, Finland and he has been supporting AI research lab at the University of Turku as a senior research scientist. He received Doctor of Science (D.Sc.) in Information and Communication Technology from University of Turku, Finland, in 2013. At the Savonia University of Applied Sciences, Finland, he has also been also working as a program chair for the Bachelor Degree Program in Internet of Things focusing both teaching and research. Previously, he has worked at the Indian Space Research Organization (ISRO), Ahmedabad India, Royal Institute of the Technology (KTH), Stockholm, Sweden and the University of Turku (UTU), Finland, where he has been a Researcher, Post-doctoral Researcher, and the Senior Researcher respectively. His current research interests include educational Technology, Internet of Things, Big Data Analytics, and the Artificial Intelligence. He has published more than 50 scientific articles in peer-reviewed conference proceedings and refereed journals in the field of computer science and communication technology and the data analytics. He is also a recipient of a certification from Stanford Centre for Professional Development, Stanford University and has presented keynote talks, invited lectures and research work in more than 30 countries across the world. He has been a member of IEEE communication society, IEEE cloud computing community, IEEE Earth Observation Community, and green ICT community.

Bio-Removal of Cadmium by Microalgae Synchronized with Enhanced Lipid Production

Vikas Pruthi
Indian Institute of Technology Roorkee, Roorkee,
Uttarakhand- 247667, India.

Abstract

Heavy metal contamination of soil and aquatic bodies caused due to enhanced industrialization is one of the major threats worldwide. Among all, cadmium is the most toxic and carcinogenic metal having extensive utilization in various industries making its accumulation easier in food chain. Nowadays, microalgae have emerged as potential candidates having capability to remove significant amount of cadmium from aqueous media. In present investigation, different microalgae species were screened for their tolerance capacity in varying cadmium concentrations on the basis of their IC_{50} value. Among the tested species, two oleaginous microalgae, *Scenedesmus* sp. IITRIND2 and *Chlorella minutissima* were found to show highest IC_{50} value of 84 and 76 mg/L with removal efficiency of 94 and 89% respectively at these concentrations of cadmium. Further examinations showed significant increase in lipid content of 27-36% in both the species with simultaneous decrease in protein, carbohydrate and photosynthetic pigments, which suggests their survival mechanism at high cadmium concentration. The amount of cadmium biosorbed and bioaccumulated within the cells were also measured. This coherent approach of coupling heavy metal remediation with enhanced lipid production by microalgae provides solution to two major problems, in terms of efficient bio-removal of heavy metals from contaminated sites as well as induced lipid that can be utilized for biodiesel production.

Dr. V. S. Pruthi
Professor
Department of
BiotechnologyIndian Institute
Technology
Roorkee 560012
Phone: 91-01332-285530
Email: vikasfbs[at]iitr.ac.in

Prof. Vikas Pruthi has done M.Sc. in Microbiology from University of Delhi, India, and Ph.D. in Biotechnology from Institute of Microbial Technology (CSIR), Chandigarh, India. Currently, he is a Professor at Department of Biotechnology, Indian Institute of Technology Roorkee (IITR), Roorkee, India, and Head, Centre for Transportation Systems, IITR. In his 30 years of academic and research experience, he has guided 21 Ph.D. thesis and more than 50 undergraduate and postgraduate students for their dissertation and project work. He has published more than 100 research papers and 05 book chapters and has filed Indian patents. He successfully completed 11 research projects funded by various national funding agencies. He was a recipient of Young Scientist Award and Better Opportunities for Young Scientists in Chosen Areas of Science and Technology (BOYSCAST) Fellowship for the year 2007 by the Department of Science & Technology, India. He is fellow member of American Society for Microbiology, Association of Microbiologist of India, The Biotech Research Society, India and Society of Biological Chemists. His main area of research is the development of novel strategies for the treatment and transforming pollutants to harmless substances, generating biodegradable materials from renewable sources and developing ecofriendly manufacturing and disposal processes.

Solar Energy with Geomatics for Sustainable Development

Rahul Dev Garg
Geomatics Engineering Group, CED, Indian Institute of Technology Roorkee, Roorkee, Uttarakhand, India

Abstract

Solar energy is the cleanest form of energy available on Earth. It can be harnessed to meet the daily needs of electricity consumption. Unavailability of electricity for agricultural requirements is a major problem in the rural areas. To cater this problem, this study has been performed for evaluating the feasibility of the solar energy for the farmers. Under the aegis of Unnat Bharat Abhiyan (UBA), Indian Institute of Technology Roorkee, India has recognized 5 villages and Beladi Salhapur is one of them. In this research work, the solar potential of the Beladi Salhapur village has been assessed for the sustainable development of this village.

Our study finds an optimum tilt angle to get the maximum quantum of the solar energy falling on the Solar Photovoltaic (SPV). Geomatics techniques have been used in assessing and digitizing the required area of interest. Solar irradiance data have been downloaded from the website of the National Renewable Energy Laboratory (NREL). The geodatabase has been created in QGIS software by digitizing the rooftops of the residential areas to obtain the usable area for SPV installation. Programming script programming for implementing an algorithm to convert irradiance at optimum tilt angle has been performed to get the maximum solar potential available at the location with the best tilt angle. Energy requirements have been calculated using a number of households and population to check whether SPV panels can be installed on the available rooftop area or not.

It has been analyzed from this study that enough solar potential is available to feed the requirements of all the households in the Beladi Salhapur village. Annually 0.167 GWh/year of the energy can be generated using SPV panels on the rooftops of this village (average data 2002-2008). The average of the 15 years i.e. from 2000 to 2014 is 0.163 GWh/year. This is the pilot study conducted in this village. The approach used in this study can be replicated at other locations such as hilly terrain, remote areas, etc.

Keywords: solar potential; renewable energy; remote sensing; QGIS; script

Dr. R.D. Garg
Department of Civil Engineering
IIT Roorkee
Email: 2garg_fce@iitr.ac.in,

Dr. R.D. Garg is Associate Professor in the Department of Civil Engineering, IIT Roorkee. He has about 24 years of experience in the field of Geomatics at ISRO and IIT. His research interests are land surveying, satellite image processing, optical thermal microwave and hyperspectral remote sensing, sub-surface investigations using GPR (ground penetrating radar), GIS and GPS. He has supervised 15 PhDs and 47 M.Tech. theses. He has published 100 research papers in international/ national refereed journals with high impact factors, 8 Book Chapters and presented 102 papers in the Conferences in India and abroad. He is involved in a number of international/ national research projects and consultancy work. He is Associate Editor of 'Journal
of Indian Society of Remote Sensing', 45 years old prestigious publication by Springer. He has won prestigious ISRS-SPECK Award in year 2003. He has been conferred five more 'Best Paper Awards'. He was awarded 15 months' fellowship by The Netherlands government to pursue research work at ITC, The Netherlands. He has organized 28 international and national training courses and delivered expert lectures in different parts of country and abroad. He is Fellow of IEI and IWRS, senior member of IACSIT, Singapore and member of several professional bodies. Received 'Uttarakhand Eminent Engineers Award 2018' by Institution of Engineers (India), Uttarakhand State Chapter. He has been conferred 'Outstanding Teacher Award 2012' by IIT Roorkee for Excellence in Teaching and Research. Also, received "Excellence Award 2017" by Institution of Engineers (India), RLC.

Industrial Microbiology for the Valorization of Carbon Containing Side Streams

Michael Sauer
Department of Biotechnology
BOKU University of Natural Resources and Life Sciences
Muthgasse 18 1190 Vienna, Austria

Abstract

In our societies quest to mitigate greenhouse gas emissions and petroleum use, processes for fuel and chemical production from renewable resources are a key for the future. However, care must be taken for the choice of the renewable resources, if the concept shall be sustainable. Sustainability includes not only the environment but also societal impact and economic considerations. Currently unused side streams of actual production processes are promising sources of carbon as they are in no competition with food or feed production. In fact, they are prone to cause environmental problems as long as they remain unused. So, valorizing them instead of wasting them makes sense. The fact that they are not used now, implies that their valorization might be difficult or expensive, so the development of the right techniques is required. Industrial microbiology plays a key-role for the provision of the desired technical solutions. Such solutions require the right choice of the production organism and diligent development of the bioprocess to ensure optimal performance of the microorganism. Industrial production conditions are generally very harsh. Nevertheless, the host cells should be very efficient, which opens a vast area of conflict for the industrial microbiologist. Synthetic biology and metabolic engineering provide optimal tools for the rational design of biocatalysts. However, biodiversity is a major resource which should be tapped first. Nature solved many problems, which we face in industrial context – be it natural stress resistance or efficiency of metabolic pathways. However, all too often the rich source of natural diversity is neglected in favor of "pet" or model organisms. I propose that the fastest and most reliable path to efficient and economically viable microbial production processes uses both – natural diversity and synthetic biology. This concept shall be exemplified with entirely oil palm based 1,3-propanediol (PDO) production with the bacterial host Lactobacillus diolivorans. The use of plant oil derived long chain fatty acids for oleochemical production processes leads to vast amounts of remaining crude glycerol (mio t scale world wide) as side stream. The price of this crude glycerol is rather low (0.05 – 0.25$ per pound). Furthermore, plant oil production leaves huge amounts of biomass behind, which is often unused and in worst case burnt, which leads to severe environmental problems. One example for such plant material are empty fruit bunches (EFB) from palm oil production.
Due to their high content of cellulose (45% w/w) and hemicellulose (18% w/w) they are a potential source of sugars. To make these sugars available, a pre-treatment of the EFBs such as steam explosion followed by enzymatic hydrolysis is necessary.
We present a concept for an entirely palm oil based biorefinery producing a variety of products.

Dr. Michael Sauer
Department of Biotechnology
BOKU University of Natural Resources
and Life Sciences
Muthgasse 18
1190 Vienna, Austria
Phone: +43 1 47654 79105
Email: michael.sauer@boku.ac.at

Pro. Michael Sauer is Senior Researcher at the Department of Biotechnology. His research is dedicated to microbial chemical production from renewable resources. The philosophy of his team is to combine synthetic biology with natures' diversity and to develop processes as close as possible to industrial realities. One focus is on the characterization and optimization of natural producers, thus exploiting natural diversity. A second line of research is dedicated to the development of synthetic tools aiding metabolic engineering approaches with a focus on the spatial organization of metabolic pathways within a given cell.

Conversion of Biomass to Low-Sulfur Boiler Fuel and High Value Chemicals

Thallada Bhaskar, Yenumula Sudhakara Reddy, Jitendra Kumar
Bio-Fuels Division (BFD), CSIR-Indian Institute of Petroleum (IIP)

Abstract

The growing interest in biofuels from lignocellulosic feedstock can provide a path towards replacing petroleum-based fuels. The sustainable biofuels are the potential alternative and lower the greenhouse gas (GHG) emissions. Various feedstock and combinations of processes are used in a bio-refinery for the production of several products. India has agro-based economy with huge source of biomass availability 120 – 150 million metric tons per annum covering agricultural and forestry residues and being burnt in open lands causing environmental problem. These residues can be a renewable carbon resource and can be converted to energy products, chemicals and bio fertilizer. Thermochemical conversion processes are the promising route to convert the residual biomass/carbon such as pyrolysis, hydrothermal liquefaction, gasification and combustion.

Pyrolysis process yields liquid, solid and gaseous products includes bio oil, syngas, and bio char. The possible applications for these products are as follows. The bio-oil from the process (25-27 MJ/kg) as a blending agent in furnace oil/boiler fuel/stationery power/energy applications and co-processed with petroleum fractions in refinery, non-condensable gases for the energy applications and bio char for the soil enrichment (bio fertilizer), water purification, and energy/heat applications. The syngas produced from the gasification is the build block molecule for various chemical processes/ fertilizer industry. The bio oil produced can be source/ raw material for the different process to produce chemicals and fuels. CSIR-IIP has mobile pyrolysis developed in collaboration with Aston University, UK; European Bioenergy Research Institute (EBRI) can help to provide technology/large-scale units to biomass rich countries. In addition, the process developed for wet biomass/lignin converted into high value functional chemicals may contribute for economically viable integrated bio refinery systems.

The utilization of renewable carbon resources will reduce the dependency on fossil fuel derived products. The Biomass-energy systems help in economic development without contributing to the greenhouse. It will also generate new income for farmers and rural population, revitalizes the retarded rural & agricultural economies.

Dr. Thallada Bhaskar
Principal Scientist & Associate Professor
Bio-Fuels Division (BFD)
CSIR-Indian Institute of Petroleum (CSIR-IIP)
Dehradun 248005
Phone: +911352525820
Email: tbhaskar@iip.res.in

Dr. Bhaskar, Principal Scientist, is currently heading the Thermo-catalytic Processes Area, Bio-Fuels Division (BFD) at CSIR-Indian Institute of Petroleum, Dehradun, India. He received PhD for his work at CSIR-Indian Institute of Chemical Technology (IICT), Hyderabad. He carried out Postdoctoral Research at Okayama University, Okayama, Japan after which he joined as Faculty at the level of Research Assistant Professor for ~7 years. He has 130 publications in SCI journals of international repute with *h-index* of 38 and around 4400 citations, contributed 28 book chapters to renowned and 14 patents to his in his field of expertise. Research experience cover various fields in heterogeneous catalysis, thermo-chemical conversion of biomass (lignocellulosic and aquatic biomass including macro and micro algae) waste plastics and e-waste (WEEE) plastics into value added hydrocarbons. He is on the editorial board of international peer reviewed journals and editor for 4 books. He received awards from AIST (2013), Japan, FSRJ, Japan; JSPS Visiting Scientist to TIT, Japan; SINTEF, Norway. He is also the Fellow of RSC, BRSI, IBA, ISEES, TAS. He received the Raman Research Fellowship, CAS, China Presidential award. Dr Bhaskar is a subject expert in various committees under DST/TIFAC/NITI Aayog/CII/MDWS/MoPNG.

Utilization of Oil Palm Front Biomass for the Production of 2,3-Butanediol

Binod Parameswaran
CSIR-National Institute for Interdisciplinary Science and Technology

Abstract

2,3-Butanediol (BDO) is a valuable chemical that is commonly synthesized from petrochemical derivatives. It is an important platform chemical for the manufacture of aviation fuels, printing inks, perfumes, fumigants, explosives, plasticizers, food additives, moistening and softening agents. It is important and challenging to find an economical, safe and green route for the large scale fermentative production of such petroleum based bulk chemicals. The present study reporting the fermentative production of BDO from Oil Palm Front (OPF) biomass using an *Enterobacter sp.*SG1. The study also aims to develop a process for the production of 2,3 BDO using Simultaneous Saccharification and Fermentation (SSF). The study showed that SSF is one of the most attractive techniques for the microbial production of 2,3 BDO using OPF. The enzymatic digestibility and fermentative capacity of dilute acid pre-treated OPF biomass was checked and the role of various experimental parameters during SSF like enzyme loading and inoculum loading in the BDO yield were estimated. A comparison of effectiveness of SSF over separate hydrolysis and fermentation (SHF) on 2,3 BDO production using OPF was evaluated.

Dr Binod Parameswaran
Scientist
Microbial Processes and Technology Division
CSIR-National Institute for Interdisciplinary Science and Technology
Pappanamcode, Thiruvananthapuram-695019
Phone: +91 9447014980
Email: binodkannur@niist.res.in
binodkannur@gmail.com

Dr. Binod Parameswaran is currently working as Scientist at CSIR-National Institute for Interdisciplinary Science and Technology, Trivandrum. He obtained his PhD in Biotechnology in 2008 and did post-doctoral research at Korea Institute of Energy Research, South Korea. His focus of research has been on bioprocess technology. Dr Parameswaran has published over 140 papers, reviews and book chapters. He is recipient of several national and international awards and fellowships, including Young Scientist Award-2011 by International Forum on Industrial Bioprocesses, France; Kerala State Young Scientist Award – 2014; Elsevier Renewable Energy Best Paper Award – 2014, Elsevier Impactful Research Award – 2018; Fellowship from EPFL, Switzerland; Marie Curie Fellowship, etc. He is National Honorary Advisory Board Member of Centre for Energy and Environmental Sustainability and Central Office Executive of the Biotech Research Society, India.

Developments in Enzyme-Mediated Single-Pot Fermentable Sugar Production from Lignocellulosic Biomass

Vivek Kumar Morya
SSMASER Technology Pvt Ltd, India
Centre for Energy and Environmental sustainability
(A Govt. of India Approved Center)

Abstract

Lignocellulosic biomasses (LCB) are the most abundant and nonfood-based reduced carbon source on earth. However, the structural complexity of these biomasses is major challenge for microbial fermentation based process development for their conversion into simple sugar for biotechnological applications. Therefore, an efficient cost-effective pre-treatment process is being needed. In recent years, Ionic liquids (ILs) and the Deep Eutectic solution solvents have gained immense attention for pre-treatment of LCB. The major constrains is toxicity and recovery of these expensive solvents. Thus, the present study was designed to minimize the process in with enzymes and extracellular culture filtrate for enhanced production of the fermentable Sugar from LC. Enzymes from the IL tolerant microbes as well as extremophile were used for saccharification of the Partially ILs exposed LCB. In order to optimize the efficacy of bio-conversion several ionic liquids were screened duly for biomass treatment as well as enzyme compatibility. The experimental result showed that the yield of reducing sugars from [Mmim][DMP] treated biomass was found to be significantly higher than the untreated one. In order to ensure the efficient process, the production optimization of enzyme from the fungi was evaluated and 96 hours of incubation time was found to be optimum. Approximately 40-60 % bio-conversion was achieved from the biomass in 48 hours by 2.0 mg/ml protein (culture supernatant) in reaction mixture. The optimization for up-scaling, product and ILs recovery is in progress. Based on the results, it is anticipated that this single-pot cost effective process may be helpful in the development of a commercially compatible sugar production from LCB.

Keywords: Lignocellulosic biomass, bioethanol, single-pot saccharification, Ionic Liquid

Dr. Vivek Kumar Morya
Chief Scientist
SSMASER Technology Pvt Ltd, India
Centre for Energy and Environmental sustainability
(A Govt. of India Approved Center)
4/63, Jakipuram Extension
Lucknow 226021, India
Phone: +91-94151514268
Email: moryavivek@gmail.com

Dr. Vivek is currently a Chief Scientist at SSMASER Technology Pvt Ltd. working in association with CSIR-IITR, Lucknow. He is also Scientific officer at Centre for Energy and Environmental sustainability, India. Earlier He was scientist as DST-Centre for Policy Research during 2017-2018. Dr. Vivek Served as Assistant professor in the Department of Biological Engineering, Inha University, (2010-2017). He is pioneer for development of the courses on 'Biosimilar'; 'Bionanotechnology'; 'Applied statistics'. Dr. Vivek has organized three days' workshop for future farmers, supported by Biotech research society of India. Dr. Vivek has delivers several invited-talk in India and overseas. Dr. Vivek was awarded Gold medal and young scientist award for his PhD work. He also recipient of Best poster award in AFOB conference Manila, Philippine. Dr. Vivek has 08 Patents (05 Granted 03 Under process), Deposited 28 industrially Important Aspergillus at MTCC (07) and NIICC (21), and 06 Book chapters, and 01 book. He published 45 research/review papers in the Journals of international repute. He is editorial board member in 17 journals, serving as consultant to sevral companies, founding member for three successful startups.

Microalgae: A Sustainable Solution for Diverse Environmental Challenges

Amit Bhatnagar
Associate Professor
University of Eastern Finland
Department of Environmental and Biological Sciences, P.O. Box 1627

Abstract

Microalgae have received notable attention for their various environmental applications, due to their unique features. In this work, the potential of a freshwater (Scenedesmus quadricauda) and a marine water (Tetraselmis suecica) microalga was explored for dairy wastewater treatment, lipid extraction (for biodiesel production) and pharmaceutical removal. Results of this study revealed that microalgae grew well in dairy wastewater without adding nutrients. It was found that both species of microalgae successfully removed total nitrogen, phosphate, and total organic carbon from dairy wastewater (in the range of 40-90%). Fatty acid methyl esters (FAMEs) analysis demonstrated that both species of microalgae had eight fatty acids in total, in different percentages. C16 and C18 were the dominant fatty acids in the cultivated microalgae. The percentage of saturated fatty acids was significantly higher in Scenedesmus quadricauda. On the contrary, higher percentage of polyunsaturated fatty acids was observed in Tetraselmis suecica. Lipid extracted microalgae was finally used for the removal of pharmaceutical from water, which showed promising results. This study exhibits that microalgae, as a renewable resource, has the potential to solve different environmental issues in a sustainable way, after careful selection of correct microalgae species and conducting proper optimization studies.

Dr. Amit Bhatnagar
Associate Professor
University of Eastern Finland
Department of Environmental and Biological Sciences, P.O. Box 1627
FI-70211, Kuopio, Finland
Phone: +358 50 3696419
Email: amit.bhatnagar@uef.fi; dr.amit10@gmail.com

Dr. Amit Bhatnagar is currently Associate Professor in University of Eastern Finland, Kuopio Campus, Finland. He obtained his PhD from Indian Institute of Technology (IIT) Roorkee, in 2003. He has conducted postdoc research in various international universities/institutes such as Linnaeus University, Sweden; University of Porto, Portugal; Hamburg University of Technology (TUHH), Germany; University of Kuopio, Finland; Yonsei University, South Korea; Swiss Federal Institute of Environmental Science and Technology (EAWAG), Switzerland; Central Building Research Institute (CBRI)/CSIR, India. He has published 146 research/review articles in peer-reviewed journals. His current H-index is 46 (Google Scholar) with over 9800 citations. He is serving as an Associate Editor for Critical Reviews in Environmental Science and Technology, and in the Editorial Board of Nature Scientific Reports and PLOS ONE journals. He has been identified as one of the 2018 Highly Cited Researchers from Clarivate Analytics

Agro Industry Based Biorefineries: Opportunities for Integrated Biorefinery Systems in Cassava Sago Industries

R Praveen Kumar
Arunai Engineering College, Tiruvannamalai

Roots of Cassava (Manihot esculenta Crantz) a tuber crop is being primarily used in starch and sago processing industries. Tamilnadu a southern state in India is having many such industries (around 200 – approx). The process of producing starch and sago discharges enormous amount of waste both as liquid and solid form. Solid wastes were produced as three forms in different stages: as peels in initial processing, fibrous byproducts during crushing and sieving and bagasse or thippi during cassava starch and flour processing. Whereas the liquid waste as starch residues after starch settling, and wastewater effluents. It was estimated that per ton of processed root generates at least 600L of wastewater which are high in starch content and COD thereby. Generally, the disposed waste consists starch, cellulose, hemicellulose, lignin and other organic and inorganic constituents, out of which the amount of starch alone would be 55-60% of, 25% of cellulose and 6% of hemicellulose. Disposal of these wastes having high COD is the biggest challenge for sago industries which may cause several harmful effects to the environment. Biorefinery concept may suit to utilize these wastes as there are research evidences for the production of biofuels, organic acids and several other products through biological route. This review articulates the potential utilization of those wastes to produce value added products.

Prof. R. Praveen Kumar
Head – Biotechnology
Arunai Engineering college
Tiruvannamalai – 606 603
Tamil Nadu, India
Phone: +91 9842073165
Email: praveenramanujam@gmail.com

Prof. R. Praveen Kumar is working as Head of the Department in Department of Biotechnology, Arunai Engineering Colleg. His area of research includes biorefineries, renewable energy from biomass and municipal waste. He is having more than 50 research publications, 6 book chapters, co-author of 3 books and provisional registration for 4 patents. He had organized various National and International Conferences and served as Scientific Advisory Committee member in several National and International events. He has chaired sessions and delivered invited talks in various National and International conferences. He is a life member in various professional societies which includes BRSI, IICHE, IFIBiop, BigFin, ISTE, EWBIndia. He has served as Management council member in Biotech Research Society of India (BRSI) and currently serving as Vice-President in "Engineers Without Borders – India (EWB-India)" Chennai chapter. He is a recipient of "ISTE-Syed Sajid Ali National Award for Outstanding Research work in the field of Renewable Energy" for the year 2017.

Urban Food Waste Valorization into Bio-Based Chemicals and Energy

Daniel C.W. Tsang

Department of Civil and Environmental Engineering, The Hong Kong Polytechnic University, Hung Hom, Kowloon, Hong Kong, China

Abstract

Food waste that amounts to over one billion tonnes per year globally is a potential renewable feedstock for biorefineries. Our research focuses on the development of high-throughput catalytic systems to produce value-added platform chemicals, such as hydroxymethylfurfural (HMF) and levulinic acid, from various selected food waste that is rich in starch, cellulose, or sugars. Homogeneous (e.g., $SnCl_4$ and $AlCl_3$) and heterogeneous catalysts (e.g., zeolites) were evaluated, which carry different Brønsted acidity and Lewis acidity for controlling HMF yield and selectivity. These acidities maneuver the kinetics of desirable tandem reactions (hydrolysis of glycosidic bonds, isomerization of glucose, and dehydration of fructose) and side reactions (polymerization and rehydration). In particular, our recent studies highlight biochars functionalized via N-doping, metal impregnation, sulfonation, and acid activation as novel solid catalysts in different important reactions, for achieving sustainable and circular biorefineries. Solvents are also evidenced to play an important role beyond serving as a reaction medium, e.g., the production of HMF in the presence of acetone is substantially faster than that in dimethyl sulfoxide/H_2O and tetrahydrofuran/H_2O. Replacing the industrial co-solvent by greener alternatives, i.e., propylene carbonate and γ-valerolactone, can further accelerate the conversion of food waste. The solvent medium interacts with the substrates and catalysts, altering their reactivity during catalysis. In addition to platform chemicals, hydrochar as a potential solid fuel can be co-generated via a demonstrated microwave-assisted hydrothermal treatment of red seaweed. These research efforts elucidate the roles of different parameters in conversion systems and demonstrate a good potential of food waste valorization for the synthesis of bio-based products in real-life applications.

Acknowledgement: The author appreciates the financial support from the Hong Kong Research Grants Council and Environment and Conservation Fund.

Dr. Daniel CW Tsang
Department of Civil and Environmental Engineering
Faculty of Construction and Environment
Hong Kong Polytechnic University
Hung Hom, Kowloon, Hong Kong
Phone: 852-2766-6072
Email: dan.tsang@polyu.edu.hk

Dr. Daniel Tsang is currently an Associate Professor in the Department of Civil and Environmental Engineering at the Hong Kong Polytechnic University (HK PolyU). He was an IMETE Visiting Scholar at Ghent University in Belgium (2015), Visiting Scholar at Stanford University in the US (2011-2013), Senior Lecturer (2011-2012) and Lecturer (2008-2010) at the University of Canterbury in New Zealand, and Post-doctoral Fellow at Imperial College London in the UK (2007-2008) and the Hong Kong University of Science and Technology (2006-2007). Dan holds BEng (2002) and PhD (2006) from the Hong Kong University of Science and Technology. With a strong link to real-world environmental challenges, Dan's research group strives to develop cost-effective and low-impact solutions to ensure sustainable urban development, enhance the engineering infrastructure, and create new ways in which we manage contaminated soils/sediments, municipal solid waste, and urban waters. Dan has published over 130 SCI journal papers, and he is chair/co-chair and organizer of 2nd Biological Waste as Resource Conference (BWR2017, Hong Kong), 2nd International Conference on Bioresources, Energy, Environment, and Materials Technology (BEEM2018, Korea), and 4th Contaminated Land, Ecological Assessment and Remediation Conference (CLEAR2018, Hong Kong).

. Halophiles as sources of novel biocatalysts

Sunil K. Khare
Enzyme and Microbial Biochemistry Laboratory, Department of Chemistry,
Indian Institute of Technology, Delhi

Abstract

Enzyme stability is a prerequisite for their applications in industrial processes. Our primary focus has been to develop novel enzyme preparations and understand molecular basis of their stability. The extremophiles and their extremozymes have been studied in this context.
Extremophiles are microorganisms that inhabit some of earth's most hostie environments and perceived to be an excellent source of hyperstable macromolecule s, particularly enzymes (extremozymes). The halophilic enzymes have proved to be robust catalysts in peptide synthesis, enhanced oil recovery, bioremediation and hypersaline waste treatment over non-halophilic counterparts which denature under harsh reaction conditions. Some novel halophiles inhabiting saline/hypersaline environment and solvent tolerant extremophiles have been isolated and characterized. Thirty-five such extremophiles gene sequences have been deposited into GenBank, NCBI USA.
Some of their novel enzymes have been purified and characterized by our group.
The applications of these halophiles have been quite noteworthy with far reaching implications. The solvent-tolerant protease from the haloalkaliphilic bacterium Geomicrobium sp. EMB2 (MTCC 10310) was purified to homogeneity by hydrophobic interaction chromatography on Phenyl Sepharose 6 Fast Flow matrix and cloned. Similarly, enzymes from other halophiles i.e. protease from Virgibacillus sp. EMB13, (GU059913), lipase from Marinobacter sp. EMB5 (FJ525429) and amylase from Marinobacter sp. EMB8 (GU059908) have been purified and studied in detail. Application of Marinobacter sp. amylase has been demonstrated in synthesizing maltotriose and maltotetrose rich maltooligosaccharide, which are highly desirable in baking applications. The differential interaction of nanoparticles and extracellularly secreted halophilic and non-halophilic enzymes has also been studied extensively. The proteomic insights achieved on responses of gram-positive and gram-negative halophilic bacteria grown in different salt concentrations have contributed to understanding of the protein diversity and osmoadaptive strategies in moderately halophilic bacteria.

Keywords: Extremophiles; Biocatalyst; Enzyme tolerance; Nanomaterials; Microbial diversity

Prof. Sunil Kumar Khare
Assoc. Dean R&D & Professor of Biochemistry
Enzyme and Microbial Biochemistry Lab
Department of Chemistry
Indian Institute of Technology Delhi
New Delhi-110016
Tel: +91 11 2659 6533
E-mail: skkhare@chemistry.iitd.ac.in;
skhare@rocketmail.com

Prof. Sunil K. Khare is presently working as Professor of Biochemistry at the Department of Chemistry, Indian Institute of Technology Delhi. He received his PhD from IIT Delhi and carried out Postdoctoral Research at National Food Research Institute, Tsukuba, Japan and has been DBT visiting scientist at Northern Regional Research Laboratory, Illinois, USA. He has more than 29 years of academic and industrial research experience which led to >150 publications with h-index of 36 (citation-4507 with i-10 value 77), 2 patents, 1 book, 18 book chapters, 50 NCBI gene bank submissions, 15 PhD thesis, 42 master's thesis supervision to his credit. His current noteworthy contributions have been in differential proteomics of solvent-tolerant and halophilic class of extremophiles and deciphering nanotoxicity mechanisms in plant and microbial systems. Prof. Khare has been honoured with awards like United Nations -Amway award in 1998, Malaviya Memorial Award Senior Faculty-BRSI in 2018. He is also an elected fellow of prestigious societies like Royal Society of Chemistry (FRSC), International Forum on Industrial sBioprocesses (IFIBiop), France, Biotech Research Society of India Fellow of BRSI (FBRS), UNU-Kirin Fellow, Japan (1997) and Fellow of National Academy of Sciences (FNAAS), India. Currently, he serves as the Associate Dean, Research & Development, IIT-Delhi.

Exergy Analysis as an Input for Better Engine

R. P. GAKKHAR
Dept. of Mech. & Ind. Eng.
IIT Roorkee

Abstract

The concept of exergy stems from second law of thermodynamics. Whenever a system which is at different state than its exergy reference environment, interacts and comes to equilibrium with it then there is an opportunity for developing work. Exergy is the maximum which can be obtained from such an interaction. Exergy is an extensive property of the system and its magnitude indicates the extent to which the state of the system departs from that of the environment. Unlike energy, it is not conserved but gets destroyed because of irreversibilities. Exergy analysis is quite useful for achieving better and more efficient energy resource use as it helps in identifying the locations at which significant irreversibilities occur and determining their nature and magnitude. This certainly is helpful in the better design of equipment and in selecting appropriate processes involving minimum irreversibilities. With an exergy analysis of the operating engine exergetic parameters such as exergy input, exergy distribution to various heads, exergetic efficiency etc are determined and scope for improvement ascertained.

a

Dr R P GAKKHAR
Former Professor
Dept. of Mech. & Ind. Eng.
IIT Roorkee, Roorkee
Uttarakhand, 247667
Phone: +91 9837422780
Email: gakhrfme@gmail.com

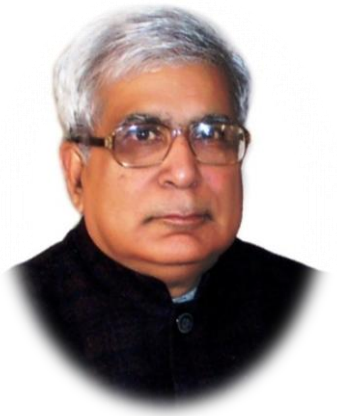

Dr. Gakkhar is a former Professor from IIT Roorkee. His interests include Combustion, IC Engines, and Thermodynamics. He has supervised 8 PhD and 40 M.Tech theses. He is co-author of QIP monograph on Combustion Charts, two book chapters and more than sixty papers in international and national journals. He was recipient of Khosla Annual Research Award (1992). He is life member of Combustion Institute (Indian Section)-Member National Executive Committee (2012-14), Society of Automotive Engineers (SAE), American Society of Mechanical Engineers (ASME), Institute of Liquid Atomization & Spray Systems (ILASS), South East Asia Section, International Society for Energy, Environment and Sustainability. He was actively involved in various academic activities including PG and doctoral level research, conducting short-term continuing education and specialist courses, member of organizing committees of various conferences etc. Produced TV film on Basic Principle of IC Engines for UGC education program.

Development of Methanol fuelled Trainset for Bangalore Suburban Railways

Anirudh Gautam

Executive Director SRESTHA (RDSO)

Lucknow - 226011

Abstract

Bangalore Suburban Railway system is being developed to decongest the city. Availability of a suburban system will assist in reduction of fuel consumption and improvement of environment. Quality of commuting will be improved for the passengers and coupling to metro trains will provide a breath of life to the city. Indian Railways has planned a large electrification program in order to run MEMU EMU trains in the suburban trains. Author has argued for an alternative to the proposed system. It is brought out the hybrid methanol based systems will lead to carbon neutral transportation at substantially lesser cost to the government. Comparative technology merits and economic benefits have been computed and presented. It is proved that methanol based transportation is better than electrification across economy efficiency and environmental parameters.

Dr. Anirudh Gautam

Executive Director SRESTHA (RDSO) Lucknow - 226011

Dr. Anirudh Gautam is a mechanical and electrical engineer from prestigious SCRA scheme of Indian Railways. He has served initial years on the Indian Railways in the maintenance of the carriage and wagon, maintenance and operation of steam locomotives, operation and maintenance of diesel locomotives and train and crew management in the challenging Eastern Sector of Indian Railways. He then worked in the area of manufacture of diesel locomotives at Diesel Locomotive Works, Varanasi and moved to the niche area of design and development of diesel engines for the locomotives. He is credited with design of the first hotel load feature on an export locomotive and was instrumental in building the first indigenous EMD design locomotive in India at DLW. He has developed the worlds first ALCO locomotive electronic fuel injection system which has been commercially successful. He developed the mobile Emission Test Car which has been used for measuring pollutants levels from diesel locomotives of Indian Railways. He has been working on the research and development of alternate and advanced propulsion systems. His main areas of interest are energy production devices, fuel cells, hybrid power trains and sustainable motive power systems, control systems development and structures optimization. His other area of specialization is Reliability Engineering and he has been instrumental in setting up a Center for Reliability and Integrated Systems Engineering at RDSO. Dr. Gautam is recipient of various awards by the Ministry of Railways, including the coveted National Award for Outstanding service by the Minister of Railways. He is currently working on development of highly fuel efficient engine technologies for locomotive engines, design and development of natural gas engine technologies, use of methanol on locomotive engines and reduction of emissions from locomotive engines. He is the chairperson of the National Task Force for conversion of IC engines to operate on methanol. He is working on developing fuelcell based hybrid trainsets which is the future of railway traction. He holds a Masters in Quality management from BITS Pilani, a Masters of Engineering in Engine Systems from University of Wisconsin, Madison, USA and a PhD in renewable energy and transportation from IIT Kanpur.

Instability Control in Natural Circulation Loop

Swarnendu Sen
Professor, Department of Mechanical Engineering, Jadavpur University

Abstract

The reliable and sustainable cooling of a heat generating system is one of the biggest concerns in the field of thermal engineering. For this purpose, today's world is focusing on such cooling systems which do not involve any active components (passive systems) for its high reliability and compact size. For this reason, in heat transfer, natural circulation loop (NCL) is highly used. NCL works as a cooling system by removing heat from the lower elevated heat source and deposit the heat to a higher elevated heat sink by the moving fluid present in it. As spontaneous dynamics of the working fluid plays a very important role in the performance of the system, it is necessary to study proper fluid flow dynamics. With increase in heater power, a change in loop fluid flow dynamics has been observed. For the comparatively low heater power we observed steady flow and with the increase in heater power first we got the oscillatory flow and then with the addition of more heater power we observed flow reversal. In this paper, first we investigated the instability associated with the loop fluid flow with the help of recurrence plot. Along with recurrence plot we also compute the recurrence quantification analysis. From the recurrence quantification analysis, we can predict early about the change in flow pattern from oscillatory region to flow reversal region. For the numerical simulation in single phase, a small scale square natural circulation loop set-up has been used. 1-D control volume technique has been employed for the solution of governing equations of mass, momentum and energy. Numerical simulations are carried out by Simulink model. On-Off controller is used to control the instability. We trigger the control signal depending on the mass flux. When the value of the mass flux becomes higher than the mean value of mass flux distribution control signal is fired. From the numerical results, it can be observed that with the increase in power we need higher perturbation in controller to control the instability.

Prof. Swarnendu Sen
Professor, Department of Mechanical Engineering, Jadavpur University,
Kolkata – 700032, India
Phone: +91 9830561574
Email:
swarnendu.sen@jadavpuruniversity.in
sen.swarnendu@gmail.com

Prof. Sen is working in Department of Mechanical Engineering at Jadavpur University in Kolkata, India. He is in teaching and research for about 30 years. He did his bachelor and masters in mechanical engineering and PhD (Engineering) from Jadavpur University. He did his post-doctoral work at University of Illinois at Chicago, USA; Virginia Tech, USA and at Technical University of Munich Germany. He was awarded with DAAD fellowship. He is a fellow of International Society for Energy, Environment and Sustainability and West Bengal Academy of Science and Technology. He has authored more than 200 technical papers in various reputed journals and conferences. He has guided 25 PhD scholars so far. His research area covers reacting & multiphase flow, magnetic fluid &nanofluid transport, heat transfer augmentation and nano-structure synthesis.

What Do We Reliably Know About the Technological Risks of Biofuels?

Kirti Bhushan Mishra
IIT Roorkee

Abstract

This talk will introduce the audience to possible types of risks that the biofuels may pose to the people, infrastructure and the environment when being processed, stored and transported in technological scales. Common scenarios and deduced consequences of fire, explosion and dispersion for conventional fuels (crude products) may not be applicable to biofuels without certain modifications. Highlighting such modifications based on convincing scientific evidences are the key issues that will be discussed. Once such know-hows are developed the safety of people, process, plant and environment can be much better assured. Computational modelling assisted risk assessment of critical scenarios of fire, explosion and dispersion likely to occur with biofuels will also be briefly touched upon.

Dr. Kirti Bhushan Mishra
Assistant Professor,
Department of Mechanical Engineering
Indian Institute of Technology Roorkee
Roorkee-247667, India
Phone: 7248186701; Fax:
Email: kirti.fme@iitr.ac.in
Web: https://www.iitr.ac.in/trag/

Principal Field of Activities: Combustion, Fuels, Fire Safety, CFD modeling, Disaster prevention.

Dr. Kirti Bhushan Mishra is an Assistant Professor in Department of Mechanical and Industrial Engineering at Indian Institute of Technology (IIT) Roorkee. He is also the founder of Technological Risk Research and Analysis Group TRAG and in-charge of fuels, combustion and IC engines lab at IIT-R. Dr. Mishra obtained his B.E. from RGPV, Bhopal in 2001 and M.Tech from MANIT, Bhopal in 2003, both with distinctions. Subsequently, he completed his PhD on fire safety and combustion from University of Duisburg-Essen (UDE), Germany in the year 2010. After his PhD, he worked as Senior Scientific Officer at BAM Federal Institute for Materials Research and Testing in Berlin, Germany for more than five years. Since July 2015 he has been working as faculty in mechanical engineering department at IIT Roorkee. He has 22 journal papers, 20 patents and 42 conference papers to his credit. He is also the recipient Early Career Research Award -2016 by Science and Engineering Research Board, Govt. of India. He is currently supervising 4 PhD students working on different fields of combustion, fuel, fire, explosion and emission control.

From Cellulose Paper to High- performance Supercapacitors for Efficient Energy Storage for Flexible Electronic Applications

Poonam Sundriyal[a,b], and Shantanu Bhattacharya[a,b,*]

a. Department of Mechanical Engineering, Indian Institute of Technology, Kanpur, India, 208016

b. Microsystems Fabrication Laboratory, Indian Institute of Technology, Kanpur, India, 208016

Abstract

With the recent advancements in the energy generation technologies, there is an urgent requirement for the high-performance energy storage devices. The rapidly growing demand of the flexible and miniaturized devices also needs the development of the flexible, environment- friendly, low- cost and portable energy storage devices that can be integrated on various flexible electronic gadgets. Recently our group has successfully developed the cellulose paper-based super-capacitors through inkjet printing solutions. The devices developed have excellent output performance.

More specifically in one of the work, we have fabricated the sandwich configuration of the supercapacitor with a separator in between the positive and negative electrodes. The printed paper supercapacitor device with a combination of the reduced graphene oxide- MnO2 as positive electrode, activated carbon as a negative electrode, and poly(vinyl) alcohol – LiCl as the electrolyte have shown a stable potential window of 0 to 2 V. This device has displayed excellent electrochemical performance with a specific capacitance of 1023 F/g at 4 mA/cm2, high energy density of 22 mWh/cm3, and ~ 90 % capacitance retention upto 9000 charge-discharge cycles. Further, in the second work, we have tried to develop the fully inkjet- printed, planar micro-supercapacitors for flexible and miniaturized electronics application. The interdigitated electrodes are printed on cellulose papers and their dimensions are optimized to get the high-performance micro-supercapacitors. The developed paper-based supercapacitor devices are able to light up a 3 V LED and shows excellent output performance under different mechanical deformation conditions which indicat their suitability to wearable flexible devices. The goal here is to develop scalable paper capacitors and batteries which can serve as low cost high storage solutions to some of the chanllenges posed by flexible devices and wearable electronics.

Prof. Shantanu Bhattacharya

Head, Design Program
Dr. Gurumukh T. and Veena M.
Mehta Chair
Professor, Mechanical Engineering
Indian Institute of Technology
Kanpur
Phone: +91 05122596056
Email: bhattacs@iitk.ac.in

Prof. Shantanu Bhattacharya is currently holds the Dr. Gurumukh T. and Veena M. Mehta Chair at the Department of Mechanical Engineering at the Indian Institute of Technology Kanpur. He also heads the Interdisciplinary program of Design in the same place. Prof. Bhattacharya has been intricately associated with many R&D activities in the broad domain of Advanced Engineered Materials with domain expertise in Nano-engineering and Technology, Biomedical Micro-devices, Water treatment, Sensors and actuators, fabrication solutions for electronic devices, design and development of products etc. He has been involved with the design and development of a Dengue detection paper microfluidic platform which can recognize the infection of dengue patients early on, a 10KLD water treatment filtration unit which cleans textile effluents and processes them to Inland water discharge grade. He is also well known for design and development of acoustic meta-structure through 3-D printing solutions which today find their way into the Boeing technology roadmap. He has several credits to his honor which includes the IEI young engineers award, the ISSS young scientist Award, NDRF design award of IEI, Boeing outstanding technical leadership award, Fellow grade memberships in IEI and ISEES etc. He has many international peer reviewed journal publications, conference proceedings, books and monographs to his credit.

Impact of Miscibility Additives for Methanol-Diesel Blends and Their Impact on Noise, Vibrations and Combustion Characteristics

Dev Prakash Satsangi
Assistant Professor
Department of Mechanical Engineering
B.T.Kumaon Institute of Technology, Dwarahat

Abstract

Stationary diesel engines are very noisy, pollute air, vibrate excessively, and contribute to global warming. Thus there is a need to find alternatives to diesel for such applications. Blends of alcohols and diesel (diesohols) may work as such alternatives. However, many such blends exhibit phase stability only in the presence of miscibility additives. Butanol and 1-dodecanol are two popular miscibility additives used to stabilize methanol-diesel blends. In this study, investigations have been conducted to assess their influence on noise, vibrations, and combustion characteristics. Investigations show that diesohols with butanol as the miscibility additive perform better in terms of total and exhaust noises. In contrast, the performance of diesohols with 1-dodecanol has marginally better performance in terms of vibrations, and combustion noise.

Dr. Dev Prakash Satsangi
Assistant Professor
Department of Mechanical Engineering
B.T.Kumaon Institute of Technology, Dwarahat
(Almora)-263653, India
Email: devprakashsatsangi2017@gmail.com

Dr. Dev Prakash Satsangi is currently working as Assistant Professor in Department of Mechanical Engineering, B.T.Kumaon Institute of Technology, Dwarahat (Almora)-263653, India. He did his B.Tech. in 2006 and M. Tech in 2008 from G.B. Pant University of Agriculture and Technology, Pantnagar. Thereafter, he completed his Ph.D. degree (Mechanical Engineering) from IIT Kanpur in the year 2018. His area of interests are Acoustics, Vibrations, and IC Engines.

Nano- and other Low-cost Materials for Cleaner Energy and Environmental Applications

Nitin Labhasetwar

CSIR-National Environmental Engineering Research Institute, Nehru Marg, Nagpur-440020, India

Abstract

Cleaner and sustainable energy and other environmental issues are among the most important challenges world is facing today and therefore attracting a lot of R&D attention in recent years. These have also become a matter of great public concern and therefore Government agencies are all serious as never before to find adequate solutions. Although electric and hydrogen mobility has been pitched as a future of automobiles, the energy mix outlook, clearly suggests that oil/hydrocarbon will dominate the energy and transport sector for another two decades or so. Looking at the air pollution scenario, especially in urban settlements, there is no assimilative capacity left for any additional pollution loads. This has now prompted the Government to leapfrog to Euro-6 emission norms effective 2020. As next few decades are likely to witness continued vehicular growth in India and with such stringent emission norms in place, advanced after-exhaust catalyst technologies will be inevitable. Vehicular emission control has been traditionally one of the major areas for catalyst applications in environmental point of view, and responsible for consumption of sizable fraction of noble metal production in the world.

Low cost, non-noble metal based catalysts can also show good potential for their applications, mainly due to lowering of sulphur content in fuel, as well as due to the higher cost of noble metals. Although, their activity and stability cannot be often compared with those noble metal based catalysts, efforts are ever increasing to explore the possibility of their applications for both automobiles and stationary applications. We are exploring perovskites and other transition metal/mixed oxide based catalysts for diesel soot oxidation and we have recently tested one such substituted perovskite on engine dynamometer with encouraging results on PM mass and number reduction. Emission control from old/in-use vehicles as and several other issues also need serious attention to expect substantial reduction in air pollution on a sustainable basis.

Dr. Nitin Labhasetwar
Chief Scientist & Head,
Energy & Resource Management Division,
CSIR-National Environmental Engineering Research Institute, Nehru Marg, Nagpur-440020, India
Phone: 9850316799; Fax: 0712-2249900
Email: nk_labhsetwar@neeri.res.in
Web: http://www.neeri.res.in

Principal Field of Activities: Cleaner Energy, Automobile Emission Control, GHG Emission Control, Chemical Looping Combustion, Environmental Catalysis.

Dr. Nitin Labhasetwar is a Ph.D. in Chemistry with 32 years of research experience in environmental and energy related research. He has worked as *STA/JSPS Fellow* and *Visiting Overseas Researcher* at NIMS, Tsukuba, Japan and as a *Visiting Professor* at Kyushu University, Japan under the GCOE programme. He has also worked at other International Laboratories on development of materials and processes including low cost and nano-materials for their applications in energy & environmental applications, vehicular emission control, photocatalysis, GHG emission control, cleaner energy generation, heterogeneous catalysis etc. He has over 158 research publications with over 4300 citations and 22 international patents in addition to a few contributions in books. He has received 9 awards for excellence in research and also received various fellowships in India and abroad. He is a reviewer for more than ten SCI journals and member of Editorial Advisory Boards of two international journals. He has supervised 15 students for PhD and several others for Master courses. He is currently involved in more than 15 R&D projects.

Energy Sector and Sustainability – Bangladesh's Perspective

Nirendra Nath Mustafi
Rajshahi University of Enginering & Technology, Rajshahi, Bangladesh

Abstract

Bangladesh being a populated country in the Southeast Asia has been facing an energy crisis due to its rapid infrastructural and economic growth. It is now a low meddle-income country with an estimated GDP growth rate of about 7.8% in the fiscal year of 2017-18 and the growth rate is expected to be higher in the coming fiscal years. Bangladesh aims to cross the low middle-income threshold by 2021 and to acquire the status of a developed nation by 2041. However, in order to attain such progress Bangladesh needs to ensure reliable energy (electricity in particular) supplies in different sectors and to maintain its sustainability. The availability of electrical power is a prerequisite for sustainable economic growth and hence Bangladesh needs a manifold increase in the power availability from the current level of about 11 GW to 24 GW by 2021, 40 GW by 2041 and so on. Bangladesh, not being blessed by natural energy sources availability, faces numerous challenges in its efforts to ramp up the electricity supplies. Indigenous natural gas, which is still the main primary energy source (~64% in the fuel mix of electricity generation) in the country, is depleting fast. Unless new reserves are discovered and developed, the present reserves are expected to get exhausted by the year 2023. Domestic coal supply, on the other hand, is facing issues like high cost of extraction (unavailability of local technology), and the location of the mines in densely populated regions. Therefore, Bangladesh has to depend on the imported petroleum oils for its rest of power generation (currently ~36%). Currently, the country is heavily dependent on private power generations (~46% share) which may not be sustainable in the long run. The public sector generation is usually affected by the plant overall efficiency (less than 40%), and high transmission and system losses. The GoB has taken mega projects of power generation (based on coal, LNG or gas) in the coming years which will affect badly to the country's landscape, and its ecosystem. Bangladesh being an agricultural country will face land shortage problems significantly and can affect the food security and sustainability in supplies along with the energy supplies. So, along with building the new plants, improvement of the existing plants (converting them to gas-steam combined cycle plants) is crucial so that they run at an overall efficiency not less than 50%. The building of nuclear plants is always controversial due to its technology and the waste disposals issues. The other option of importing power from neighboring countries (currently from India) which is being in practice and the GoB has to take necessary steps to increase its share in future. In these circumstances, the incorporation of renewable energy sources in the fuel/energy mix has become essential. Although there is a set-target to raise the power generation from renewable energy to 5 percent by 2021, it needs significant attentions from the government as well as from private stakeholders. Its share should be increased from 5 to 10 percent in the coming years. Unfortunately, hydropower and wind power potentials are limited due to the country's landscape pattern which is almost flat. So, the enormous source of biomass energy has to play a great role to fulfil the goals and of course, the waste-to-energy resources should be given priority.

Dr. Nirendra Nath Mustafi

Prof., Dept. of Mechanical Engineering
Rajshahi University of Eng. & Tech.
Rajshahi, Bangladesh
& Currently, Visiting Fellow
Dept. of Mech. Engineering
IIT Kanpur, India
Phone: +91 8334046240
Email: nnmus@iitk.ac.in,
nnmustafi@gmail.com

Dr. Nirendra Nath Mustafi is a Professor in Mechanical Engineering at Rajshahi University of Engineering & Technology (RUET), Rajshahi, Bangladesh. Currently he is working as a Visiting Fellow in Mechanical Engineering at IIT Kanpur with Prof. Avinash Agarwal. He has a B.Tech. from RUET, Bangladesh (1995) and Masters in Sustainable Energy Engineering from KTH, Sweden (2003) and Ph.D. from The University of Auckland, New Zealand (2008) in Mechanical Engineering. He went to the University of Ghent, Belgium in 2013 and worked there as a fellow for three months with Prof. Roger Seirens and Dr. Sebastian Verhelst with the PhD Plus Scholarship. He served as the Head of Mechanical Engineering Department (in 2010-12) and Dean, Faculty of Mechanical Engineering (in 2015-17) at RUET. Prior to joining at IIT Kanpur, he was serving as the Director of the Institute of Energy & Environmental Studies at RUET. He has published about 44 papers in peer-reviewed journals and conferences in the field of IC Engines, Alternative fuel, PM Emissions, Renewable and Sustainable Energy and Environment.

Sustainability Transition in Indian Power Sector: Role of Distributed Generation

Amitava Datta
Department of Power Engineering Jadavpur University
Salt Lake Campus Kolkata, India 700098

Abstract

Energy is a fundamental requirement in the modern society which influences the economic growth and human development index. The utility generation of energy takes place in the power plants and gets distributed in the form of electrical energy. Indian power sector has seen a tremendous growth in the last seventy years since independence. The installed capacity of power generation has risen from a paltry 1350 MW in 1947 to a mammoth 340 GW at present. The growth is particularly rapid in the last ten years when more than 200 GW of capacity addition has taken place. Considering the availability of fossil fuel reserves in the country, most of the capacity addition has occurred in the thermal sector. However, the lack of good quality fuel, adverse effects of the thermal plants on the environment and the worldwide endeavour towards sustainable growth have driven the government to go towards green energy production in the country. India has pledged to reduce emission intensity by 35% from 2005 level and to have 40% share of non-fossil fuel power generation in the total mix by 2030. As a step towards these goals, the Government of India has set a target to install 175 GW renewable energy generation by 2022.

At the same time, there is a thrust for the supply of reliable and quality power for all. The challenge in this direction is to maintain the voltage and frequency, particularly with the variability of the renewable sources. Storage of energy will play a big role in the stability of the grid. Long distance transmission is to be avoided, particularly at remote locations, through distributed generation. India being an agricultural country can rely on biomass as a back up to solar and wind based power generation. Regarding the generation of power from biomass, it is important to identify the correct route of energy transition and the proper prime mover to generate electricity from the resource. Finding the right mix of resources is a challenge along with the other challenges related to power system and its protection. All these open up much potential for research and study towards the sustainability transition in the energy sector.

Prof. Amitava Datta
Department of Power Engineering
Jadavpur University
Salt Lake Campus
Kolkata, India 700098
Phone: +91 33 23355813
Email:
amitava.datta@jadavpuruniversity.in
amdatta_ju@yahoo.com

Dr. Amitava Datta is a professor in the Department of Power Engineering of Jadavpur University. He completed his graduate education in Mechanical Engineering from Jadavpur University and his PhD from IIT Kharagpur. Dr. Datta is a recipient of Alexander von Humboldt Fellowship in Germany in the year 2000 and worked at Lehrstuehl fuer Technische Thermodynamik in the University of Erlangen Nuernberg. His research interests include combustion, atomization, energy, thermodynamic modeling and application of CFD in reacting flows. Dr. Datta has completed guidance of 14 PhD theses and several Masters theses. He has published 90 peer reviewed research papers in various International Journals and also presented and published several papers in National and International conferences. He also has authored one text book on Combustion. Dr. Datta has undertaken several sponsored research projects and has received awards and recognitions from different national and international bodies. He is also involved in various administrative responsibilities in his University. Presently Dr. Datta is serving his second term as Head of Power Engineering Department.

Competitive Advantage through Sustainable Transportation System

Rajat Agrawal
Centre for Transportation Systems, IIT Roorkee

Abstract

India is passing through a transition stage where it is expected that share of manufacturing in national GDP will increase to more than 20% by 2020. For strengthening manufacturing sector, a sustainable transportation system is the most important enabler. A sustainable transport system must provide mobility and accessibility to raw material and finished products from different corners of the country in a safe and environment friendly mode of transport. This is a complex and difficult task when the requirements of different products and markets are not only different but also often conflicting. For example, if a large part of any state is not having access to Railways- then limited industrial development will take place in this part. But development of railway infrastructure is also not a guarantee of industrial development and may result in large scale migration of people to other parts due to easy mobility.

Prof. Rajat Agrawal
Department of Management Studies
Indian Institute of Technology Roorkee
rajatfdm@iitr.ac.in
01332-285737

Prof. Rajat Agrawal is a member of faculty at Department of Management Studies, Indian Institute of Technology Roorkee, Roorkee. He is also associate faculty member at Center of Excellence for Disaster Mitigation and Management and Center of Excellence for Transportation Management, IIT Roorkee. He administers various initiatives of IIT Roorkee in the field of IPR, incubation and entrepreneurship in different capacities. He initiated incubation centre at IIT Roorkee. He is co-coordinator of Design innovation centre at IIT Roorkee. He is also IPR Chair Coordinator at IIT Roorkee.

Dr. Rajat is a visiting fellow to Copenhagen Business School, Copenhagen, Denmark. His area of interest is Production and Operations Management including Supply Chain Management, Manufacturing Strategy and World Class Manufacturing. He has guided fourteen Ph D thesis in these areas and published papers in journals of Emerald, Sage, Springer, Taylor and Francis, Elsevier, and Inderscience. Currently, ten students are working under him for Ph D thesis. He has more than 90 research papers in refereed journals and more than 25 research papers in refereed conference proceedings.

He has developed more than 20 case studies on various aspects of supply chain management, organisational development, natural resource management, social entrepreneurship, and value co-creation. He has developed more than 15 programmes for All India Radio on various subjects of rural development and technical, management education. He has completed 10 research and consultancy projects. He was also involved in some of the international projects funded by Danish Innovation Council and European Union. He has more than 200 hours of corporate training experience with organisations like BHEL, THDC India Ltd., Power Finance Corporation Ltd., Syndicate Bank, Everest Industries, and Rockman Industries etc.

He received Best Teacher Dainik Bhaskar National Education Leadership Awards-2013. He received Noel Deere Gold Medal for paper in management stream in 71st and 72nd annual convention of STAI, consecutively. One of his paper was considered one of the best articles of the Year 2014 by Business Standard. He was also awarded ISOL Research Award 2015 at 5th International conference at Chicago USA. He was also awarded ICCR chair professorship at Indonesia.

Xylitol Production from Sugarcane Bagasse

V. S. Moholkar
Indian Institute of Technology, Guwahati

Absract

This study has investigated ultrasound-assisted xylitol production through fermentation of dilute acid (pentose-rich) hydrolysate of sugarcane bagasse using free cells of Candida tropicalis. Sonication of fermentation mixture at optimum conditions was carried out in ultrasound bath (37 kHz and 10% duty cycle). Time profiles of substrate and product in control (mechanical shaking) and test (mechanical shaking + sonication) fermentations were fitted to kinetic model using Genetic Algorithm (GA) optimization. Max. xylitol yield of 0.56 g/g and 0.61 g/g of xylose was achieved in control and test fermentations, respectively. The biomass yields also increased marginally (~17%) with sonication. However, kinetics of fermentation increased drastically (2.5×) with sonication with 2× rise in xylose uptake and utilization by the cells. With comparative analysis of kinetic parameters in control and test experiments, this result was attributed to enhanced permeability of cell membrane that allowed faster diffusion of nutrients, substrates and products across cell membrane, higher enzyme-substrate affinity, dilution of toxic components and reduced inhibition of intracellular enzymes by substrate. Similar enhancement effects were also seen in case of xylitol production from sugarcane bagasse using C. tropicalis MTCC 184 immobilized on PU foam. Application of 37 kHz sonication @10% duty cycle during fermentation at optimum conditions resulted in marked intensification of fermentation kinetics. Xylitol yield of 0.66 g/g of xylose has been obtained in ultrasound-assisted fermentation in just 15 h.

Dr. V. S. Moholkar, PhD, CEng, FIChemE, FRSC, MAICHE (Sr)
Professor, Department of Chemical Engineering and
Head, Center for Energy
Indian Institute of Technology Guwahati
Guwahati – 781 039, Assam, INDIA
Phone: +91 361 258 2258/3126/3150 (landline)
+ 91 9954709058 (mobile)
Fax: +91 361 258 2291
E-mail: vmoholkar@iitg.ernet.in,
vmoholkar1972@gmail.com

Dr. V. S. Moholkar (b. 1972) is a Full Professor of Chemical Engineering and Head of Center for Energy at Indian Institute of Technology (IIT) Guwahati. He received Bachelors (1993) and Masters (1996) degree in Chemical Engineering from Institute of Chemical Technology (ICT) Mumbai, followed by Ph.D. from University of Twente in 2002. He has been Head of the Chemical Engineering Department at IIT Guwahati between 2012-2015. His main research interests are sonochemistry, cavitation assisted physical, chemical and biological processing, and thermo- and biochemical routes to biofuels. As of November 2018, he has published more than 140 papers in renowned international journals that have received more than 5000 citations (with *h*-index of 43). He has also filed 3 US patents (in collaboration with CTI Nanotech, CA, USA) on application of hydrodynamic cavitation reactors for biomass pretreatment and bioalcohol synthesis. He has graduated 15 Ph.D. and 26 M.Tech. students. He has been elected as Fellow of Royal Society of Chemistry (FRSC) in July 2016. He has also been elected as Fellow of Institution of Chemical Engineers, UK. He is a Chartered Engineer (CEng) registered with Engineering Council of UK. He was admitted as Senior Member of American Institute of Chemical Engineers (MAIChE (Sr.)) in August 2016.

Delignification and Microbial Hydrolysis for Bioethanol Production

Bahiru Tsegaye[1], Chandrajit Balomajumder[1], Partha Roy[2]
[1]Department of Chemical Engineering, Indian Institute of Technology Roorkee, Roorkee 247667, Uttarakhand, India
[2]Department of Biotechnology, Indian Institute of Technology Roorkee, Roorkee 247667, Uttarakhand, India

Abstract

The change in environment mainly caused by the use of fossil fuels is a major concern in today's world politics and academicians. This problem opens the opportunity for the scientific community to search for alternative renewable energy sources. Among the renewable energy sources biofuel (bioethanol) production from lignocellulose biomass are gaining much attention due to the vast availability and potential to replace fossil fuel. In this study, straw was used for enhancing the production of bioethanol via chemical pretreatment and microbial hydrolysis followed by fermentation. Alteration of the structure of straw was observed after chemical pretreatments due to depolymerization of lignin, which leads to the release of cellulose and hemicellulose. Removal of lignin and carbohydrate releases were confirmed by XRD and FTIR analysis. A significant amount of lignin was removed in 5% and 7% chemicalpretreatment, which implies higher cellulose and hemicellulose removal at this point. The maximum amount of lignin was removed at 7% chemical solution pretreatment (79.82%) and release of 86.28% polysaccharides. The efficiency polysaccharide conversion to reducing sugars are analyzed by 3, 5 dinitrosalycilic acid method. About 87.25% conversion was achieved after the 11th day of hydrolysis. Chemical modification followed by bacterial hydrolysis was seen as an efficient and cost-effective way to obtain ethanol from lignocellulose.

Keywords: Hydrolysis; delignification; straw; pretreatment; bioethanol

\

Dr. Chandrajit Balomajumder
Professor
Chemical Engineering Department,
IIT Roorkee

Dr. Chandrajit Balomajumder is a Professor in Department of Chemical Engineering, Indian Institute of Technology, Roorkee. He is a Fellow of *Jr. of Chemistry & Environment, IIChE (Indian Institute of Chemical Engineers – Life Member)* and *Life Member, IIT Roorkee Alumni Assoc*. His area of interest includes Bio Energy, Removal of Toxic and Hazzardous Pollutants from Industrial Waste Waters and from Waste gases. He has authored 225 papers in peer reviewed journals and has 125 conferences papers to his name. He has supervised 22 doctoral students 131 M. Tech students and 96 B. Tech project. He has received Siksha Ratan Purashkar and U.P. Government Research Fellowship.

Biobutanol: A Combustion Engine Friendly Biofuel through Biotechnological Intervention

Arvind Kumar Bhatt, Ranju Kumari Rathour, Ravi Kant Bhatia
Department of Biotechnology, Himachal Pradesh University, Summer Hill, Shimla-171005, India

Abstract

Global energy demands are primarily met through non-renewable sources such as coal, natural gas and oil. However, the scarcity and rising prices of fossil fuels, coupled with the unprecedented environmental problems lead the researchers to find out a microbial alternative to address these issues. Biofuel has emerged as an attractive and economically viable solution which can be effectively used in the current scenario. Among the probable list of alternates, biobuatnol is an important renewable source of biofuel which can be easily accommodated in existing fuels due to its better performance and other advantages over other biofuels. Bio-butanol can be efficiently produced from industrial, agricultural and domestic waste material through microbial fermentation. Industries produce a huge amount of waste and if not managed properly, it can be a major cause of different pollution related to soil, water and air. Many microorganisms can utilize carbohydrate rich waste material to produce bio-butanol through aerobic and anaerobic fermentation. Production of biobutanol from industrial wastes not only provides an ideal, eco-friendly clean/ green energy source but has potential to address the global issues of pollution, global warming and greenhouse effect etc. to a greater extant.

Dr. Arvind Kumar Bhatt
Department of Biotechnology
Himachal Pradesh University, Shimla
Email: bhtarvind@yahoo.com,

Dr. Bhatt is currently serving as Professor (Industrial Biotechnology) in Department of Biotechnology, Himachal Pradesh University, Shimla teaching and guiding Master's, M. Phil. and Ph. D. students with major focus on Industrial Biotechnology.

Earlier, Dr. Bhatt has successfully headed the Industrial Biotechnology Division and advised Himachal Pradesh Government on various policy matters related to Biotechnology and Science & Technology, has worked with Himachal Pradesh University, Dr. YS Parmar University UHF-Solan, Beck & Co., Bremen-Germany and scientific consultant to various Industries.

Dr. Bhatt has also obtained advanced professional trainings in Industrial Biotechnology at GBF, Braunschweig-Germany, *DBT GOI/ AICTE* sponsored trainings on DNA Finger Printing, Mol. Biology Techniques, Bioresource Management at Bose Institute Calcutta, IARI-New-Delhi, BITS-Pilani, Ranbaxy and CFTRI-Mysore besides several other professional trainings.

Dr. Bhatt is also working as Convener-Working Group on Environment, Inter Quality Assurance Cell (IQAC), Member Central Placement Committee, Committee for Generation of Grants through various Funding Agencies, Secretary Association of Biotechnologists of Himachal Pradesh (ABHI), Treasurer-Vigyan Bharti Himachal Pradesh and is also involved in University - Industry linkages besides other different departmental activities.

Dr. Arvind Kumar Bhatt has more than 50 *research papers* to his credit published in Scientific Journals of repute and has presented more than 60 research papers in several National/International Conferences /workshops/ seminars within India and abroad and has guided/is guiding students for Masters, M.Phil. and Ph. D. Degrees.

Solid Waste Management Using Vermitechnology

V.K. Garg
Central University of Punjab

Abstract

There has been a significant increase in solid waste generation during the last few decades and its management has become a major issue because the poor waste management practices affect the health and amenity of the cities. In recent years, there is a marked trend towards the use of novel technologies, mainly based on biological processes, for recycling and efficient utilization of organic residues. Among these, "vermicomposting" has been arising as an innovative and low cost biotechnology for the conversion of organic wastes into value added products, which can be utilized for improving the soil structure and fertility in organic farming. Vermicomposting involves the conversion of organic solid waste of domestic, industrial and agricultural origin into organic fertilizers, which serve as a rich source of plant nutrients. These waste materials contain energy, protein and nutrients, which would otherwise be lost if they are disposed as such in the open dumps. With the use of vermicompost as organic amendments in the agriculture, recycling of the nutrients to soil takes place, in turn, maintain the sustainability of the ecosystem.

Vermicompost is a peat like material containing most nutrients in plant available forms such as nitrates, phosphates, calcium, potassium, magnesium etc. It has high porosity, water holding capacity and high surface area that provides abundant sites for microbial activity and for the retention of nutrients. The plant growth regulators and other plant growth influencing materials i.e. auxins, cytokinins and humic substances etc. produced by the microbes have been found in vermicomposts

This paper reports the vermicomposting of different solid wastes. The results showed that there is a significant decrease in pH, organic carbon, C:P ratio and C: N ratio, but increase in ash content, electrical conductivity, nitrogen content, potassium content, and phosphorus content after vermicomposting of the solid wastes. The heavy metals content in vermicomposts was higher than initial substrates. The results indicated that solid wastes can be converted into good quality manure. Investigations were also to assay the influence of vermicomposts, on the growth and productivity of plants in pot culture experiments. The fertility status of soil and vermicomposts was quantified. There were significant differences in the fertilizer quality of soil and vermicomposts. Results showed that the addition of vermicompost, in appropriate quantities, to potting media has synergistic effects on growth and flowering of plants. These experiments demonstrate that vermicomposting can be an alternate technology for recycling and environmentally sustainable management of solid wastes using an epigeic earthworm Eisenia fetida.

Prof. V.K. Garg
Professor and Dean
Central University of Punjab, Bathinda
151001, Punjab
Phone: +91 9812058109
Email:
vinodkgarg@yahoo.com

Prof. Garg is currently working as Professor at Department of Environmental Science and Engineering, Central University of Punjab, Bathinda, Punjab, India. He has held professorial appointments in the past at Guru Jambheshwar University of Science and Technology, Hisar, Haryana, India and CCS Haryana Agricultural University, Hisar, India. He is a fellow of the Biotechnology Research Society of India and is on the editorial boards of several journals. He has published around 200 papers and three books.

Strategies for Treatment of Hospital Wastewater Using Integrated Technology

Kashyap Kumar Dubey[1,*], Ankush[1], Mrinal Kanti Mandal[2], Shailesh Pandey[2], Joao G. Crespo[3], Patricia Luis[4]

[1]Department of Biotechnology, Central University of Haryana, Mahendargarh, Haryana-India

[2]Department of Chemical Engineering, National Institute of Technology Durgapur, West Bengal

[3]Department of Chemical Engineering, University of Nova de Lisbon (UNL), Portugal

[4]Department of Chemical Engineering, University of Leuven, Leuven-Belgium

Abstract

India is lacking of hospital wastewater treatment process to remove antineoplastic agents from wastewater in hospitals (mainly in metro city). European Union countries like Portugal and Belgium are sharing the same situation in which antineoplastic agents are not removed specifically, reaching conventional wastewater treatment plants that are not able to destroy these persistent components, reaching the aquatic environment. In addition, the increasing rate of cancer patients all over the world has become a global fact during the last two decades. Keeping in the view, the necessity of specific treatment methods for removal of antineoplastic agents (Cyclophosphamide, 5-flurouracil, Etoposide) developed with the integration of biological and membrane technology.

Kashyap Kumar Dubey (Ph.D, M.Tech.) M.N.A.Sc.
Associate Professor and Head,
Department of Biotechnology
Central University of Haryana, Mahendergarh
Mobile No. +91-9996122280
E-mail: kashyapdubey@gmail.com

Prof. Dubey is currently working as Associate Professor at Central University of Haryana and is also a Visiting Researcher at IIT, Kanpur. Dr. Dubey has research interest in biochemical engineering and wastewater treatment which includes process development of value-added pharmaceutical products (3-demethylated colchicine, betulin, CoQ10, pullulan and lipstatin), through optimization of enzyme reactions and toxicological studies of micro-pollutants.
He is having grants from European Commission (IPP1) on Clean Water for Health, BIRAC-DBT and DBT on microbial process development. He has completed two major research projects and published 50 research articles in International reputed Journals. He is a Member of Various Scientific societies like BRSI, NASc, ISCA, SBC, DST-INSPIRE, MSI, ISCB, IFbioP, and AMI. He has organised Four National Conferences, Conducted 02 GIAN courses, and 01 STTP. He has delivered several expert lectures in various scientific events.

Effect of Pavement Conditions on Road Safety

Dr. S.S.Jain
Professor
Transportation Engineering Group
Department of Civil Engineering
Indian Institute of Technology Roorkee

Dr. S.S. Jain is a Professor, Transportation Engineering Group in Department of Civil Engineering at Indian Institute of Technology, Roorkee. Prof Jain had been Founder Head of Centre of Excellence in Transportation Systems at IIT Roorkee. He has contributed over 550 research papers in Indian and foreign Journals and Conference Proceedings. He has guided 18 Ph.D's and over 200 M.Tech Thesis. He has completed 32 sponsored research projects including three nationally coordinated projects on "Urban Transport Environment Interaction", "Road Traffic Safety" and "Integrated Development of Public Transport System".
Dr. Jain is the Fellow of Institution of Engineers (India) and Fellow of Indian Institution of Bridge Engineers. Prepared more than 22 IRC Codes/Specifications/Guidelines/Manuals for the Design & Maintenance Management of Roads & Highways. He is the recipient of 45 Medals/Prizes/Awards which includes University Gold Medal, Khosla Research Prizes and Medals, First Recipient of Jawahar Lal Nehru Award from Indian Roads Congress, President of India Prize from Institution of Engineers (India), U.P. Government National Award from Indian Society for Technical Education, Prof. S.R. Mehra National Award. Certificate of Excellence Award from AICTE.

Prof. Jain had been the Member Editorial Board of Institution of Civil Engineers (UK) Journal. He is the Member of various Technical Committees of Indian Roads Congress and Member, World Roads Congress, Technical Committee, PIARC, France.

- Chairman, Roorkee Local Centre, Institution of Engineers (India).
- Chairman Regional Chapter of Institute of Urban Transport (India).
- Member, Board of Governors, IIT Roorkee.

Member, Executive Council, DSR University of Science & Technology, Sonepat.

Sustainable Urban Mobility Strategies for Indian Cities

Dr. M. Parida
Professor
Indian Institute of Technology Roorkee
Email: mprdafce@iitr.ac.in
Phone : +91 - 9837423963

DR. MANORANJAN PARIDA is a B.Sc. Engg. (Civil) from Sambalpur University, Sambalpur, M.Planning (Urban Planning) from School of Planning & Arch., New Delhi and Ph.D. from IIT Roorkee. He was Junior Town Planner at Cuttak Dev. Authority, Research Associate at School of Planning & Architecture, New Delhi, Assistant Town & Country Planner at TCPO, Min. of Urban Affairs & Employment, Govt. of India before joining IIT Roorkee. His research is focused on Urban Transport Planning. He has guided 8 PhD and & 71 M.tech students successfully and published 284 papers including 95 journals. He has accomplished 14 Sponsored Research Projects and 304 Consultancy Project. He is life member of Indian Roads Congress, Indian Society for Technical Education, Institution of Engineers, India, Institute of Urban Transport (IUT), Indian Society for Continuing Engineering Education, University of Roorkee, Roorkee and Indian Society of Construction Material & Structures. (ISCMS).

Microalgal Biofuel: Molecular Strategies and Implications

R. P. Singh* and Jyoti Singh
Department of Biotechnology, Indian Institute of Technology Roorkee, Roorkee

Abstract

The rising price for fossil fuels and depleting resources has necessitated to look for alternative resources for energy generation. Distinct biological resources that are available appear promising for developing a robust and sustainable technology for biofuel production. Microalgae are photosynthetic microorganisms which can grow rapidly and live in diverse environments due to their simple cellular structure. Their size range varies from a few micrometers to a few hundreds of micrometers. Examples of some typical microalgae currently being looked at as feedstocks for biofuels include *Nanochloropsis salina, Chlorella sp., Tetraselmis sueica and Botryococcus braumii* based on high productivities and high neutral lipid content. Microalgae have very high surface productivity, and can be cultivated on non-arable land. Because microalgae are photosynthetic organisms, their use provides green house gas mitigation benefits. However, the real technological challenge is to mass produce microalgae with higher lipid content for the production of a low-value-high-volume product to make it economically viable. In this regard, strategies to maximize biomass and lipid production are crucial for improving the economics of microalgal-based biofuels. Lipid metabolic cascades are pivotal for achieving algal stains with high lipid content. Identification and targeting the regulatory steps for improving lipid accumulation may enable in developing the engineered algal strains for biofuel production. The revolutions in whole-genome-based technologies, together with systems biology, metabolic engineering and synthetic biology approaches, would enable the rational design and engineering of algal feedstock and help to fill the gaps between the technical and economical reality and the huge potential of algal biofuels.

Prof. R. P. Singh,
Indian Institute of Technology
Roorkee, India

Prof. R. P. Singh has contributed over three decades of his dedicated service for research and science education. He is currently a Senior Professor at Department of Biotechnology, Indian Institute of Technology Roorkee, India. Prof. Singh received his Master's in Biochemistry from G.B. Pant University of Agriculture & Technology, India and Doctoral degree in Microbial biochemistry from Central Drug Research Institute, Lucknow, India. He had continued as a Research Associate at Institute of Microbial Technology, Chandigarh. Further he worked at National Institutes of Health, USA and Harvard Medical School, USA as a Visiting Fellow and as a Research Officer for more than five years. He was also a visiting faculty for a year at University of Arkansas for Medical Sciences, USA. His research interests primarily include enzyme engineering, biofuels, biopolymers and targeted drug delivery. He is associated with several International and National organizations mainly Process Innovation and Process Intensification Network, UK; European Federation of Biotechnology, Committees on Genetically Modified Organisms and Food, Food Safety and Standards Authority of India; Expert Committees of Department of Science & Technology and Department of Biotechnology, Govt. of India and Life Science Research Board, DRDO, Govt. of India. He is a member of editorial board of journals and had served as a reviewer for several reputed international journals. He has authored several original research articles, review papers and book chapters and has one US patent to his credit. He has supervised more than 20 doctoral theses and several Master's and Undergraduate dissertations. Prof. Singh had delivered several invited lectures and had visited countries mainly USA, UK and Germany. He has handled various research projects till date. He is life member of several scientific bodies and is on the board and committees of several institutions.

Sustainable Composite Materials: Expectations and Reality

Inderdeep Singh
Department of Mechanical and Industrial Engineering
Indian Institute of Technology Roorkee

Abstract

Sustainable development is a key word and efforts are being put worldwide for ensuring judicious as well as optimal utilization of resources. Composite materials represent a class of materials with a plethora of opportunities and have the potential to be exploited in diverse application spectrum ranging from aerospace to biomedical components and devices. The use of composite materials has multiplied manifold owing to their superior combination of properties, usually difficult to achieve using traditional/conventional engineering materials. However, the non-biodegradability of most of the currently used composite materials is a major limitations and is motivating the researchers and scientists to explore the feasibility of conceptualizing, designing and developing composite materials based on sustainable resources. The talk will address the key expectations from the materials in the future and will aim at attempting a realistic check on the status of the composite materials based on natural fibers and the bio-plastic matrix. The focus will be to showcase the successful application of composite materials in the area of sustainable energy.

Dr. Inderdeep Singh
Associate Professor
Department of Mechanical and
Industrial Engineering
Indian Institute of Technology Roorkee
-247 667
Email: inderfme@iitr.ac.in

Dr. Inderdeep Singh is currently working as Associate Professor with the Department of Mechanical and Industrial Engineering, IIT Roorkee. He completed B. Tech from National Institute of Technology Hamirpur (H.P) in 1998 and Master of Technology and PhD from Indian Institute of Technology Delhi in 2004. His PhD research work was awarded by the *Foundation for Innovation and Technology Transfer (FITT),* IIT Delhi as the "Best Industry Relevant PhD Thesis of the Academic Year 2004-2005". His area of interest includes processing of composite materials with focus of bio-degradable composites often termed as green composites. He has supervised 12 PhD candidates towards successful completion of their research work and is currently supervising 05 PhD candidates. He has published more than 200 research articles in the area of development, characterization, machining and joining of composite materials. He has edited a book with the title "Primary and Secondary Manufacturing of Polymer Matrix Composites", published by CRC press. He has also contributed 20 book chapters in books published by internationally renowned publishers. He was awarded the "Outstanding Teacher Award" on the Teacher's Day in 2013 by IIT Roorkee.

Current Status of PM 2.5 Pollution and Its Mitigation in India

Bhola Ram Gurjar, Rajmal Jat and Veerendra Sahu
Department of Civil Engineering
Indian Institute of Technology Roorkee, India

Abstract

Ever increase industrialization, transportation, urbanization and population growth impacted the air quality significantly in many cities of India (CPCB, 2011; Gurjar et al., 2008). Given this increase, fluctuating trend is observed for the particulate matter in Indian megacities (Gurjar et al., 2016). PM 2.5 referred to as the fine particulate matter with the aerodynamic diameter of less than 2.5 μm and found to have adverse health impact by cardiovascular and respiratory disease in terms of mortality and morbidity (Dockery et al., 1993; Pope et al., 2009). Studies in India and South Asia reported the premature mortalities due to exposure to the particulate matter and pollutant gases (Gurjar et al., 2010; Ghude et al., 2017). Exposure to fine particulate matter (PM 2.5) in India has increased exponentially due to increase in urbanization, industrialization and
biomass burning. In this study, we have analyzed the PM 2.5 mean concentration for year 2017 and its trend analysis from 2014 to 2017 using the ground based measurement data provided by the Central Pollution Control Board (CPCB), India through online and manual monitoring stations. Results indicate that north Indian states in Indo Gangetic plain show the higher annual mean PM 2.5 concentration ranging from 73.7 ± 39.5 μg/m 3 to 135.2 ± 71.1 with maximum values in Bihar (135.2 ± 71.1 μg/m 3) followed by Delhi (126.3 ± 63.6 μg/m 3). Whereas, south Indian states are found having lower concentration ranging from 51.0 ± 9.5 μg/m 3 to 24.9 ± 13 μg/m 3. Lowest concentration of PM 2.5 for the year 2017 was found in Kerala i.e. 24.9 ± 13 μg/m 3. Seasonal variation in 2017 is also investigated that shows higher concentration in winter season attributed to lesser depth of planetary boundary layer. Trend analysis illustrates the decreasing trend in Bihar, Rajasthan and Madhya Pradesh and increasing trend in Delhi, Gujarat, Haryana, Maharashtra and Goa. In Delhi 57.8 % increase is found until 2017 with respect to the base year 2014. To curb the pollution several mitigation measures are taken and proposed by the Government of India attributed to various source sectors. There are large uncertainties in observed data and more studies are required to get the better insight of fine particulate matter in India.

Keywords: Exposure; Fine particulate matter; Mitigation measures: Source apportionment;

Dr. Bhola R. Gurjar
Professor
Department of Civil Engineering
Indian Institute of Technology
Roorkee 560012
Phone: +91 - 1332 - 285881
Email: bholafce@iitr.ac.in
Web: https://www.iitr.ac.in/~CE/bholafce

Prof. Gurjar received his bachelor's in Civil Engineering from J.N.V. University, Jodhpur, master's degree in Environmental Engineering from J.N.V. University and Ph.D. from IIT Delhi. He held Research Scientist positions at Max Planck Institute for Chemistry, Mainz, Germany before joining the Indian Institute of Technology, Roorkee as a faculty member in 2005.

Prof. Gurjar's research group focuses on Emissions and Air Quality, Health Risk Assessment, Urban Climate Change, Megacities & Global Change, Environmental Sustainability, Energy and Environmental Policy Evaluation Industrial Hazards and Disasters, Quantitative and Qualitative Risk Analysis

Prof. Gurjar has been elected Fellow of The Institution of Engineers (India), Kolkata, India and UKIERI; from the British Council Division of British High Commission, New Delhi. Among several other awards, Prof. Gurjar has received the award for Eminent Environmental Engineer conferred by Environ. Div. Board of the Institution of Engrs. (India), Highly Cited Author (Elsevier Journal Atmospheric Environment), National Design Award in Environmental Engineering from National Design and Research Forum – IEI, Highly Cited Author (Elsevier Journal Atmospheric Environment) and START Young Scientist Award.

Currently, Prof. Dutta is the Dean of Resources & Alumni Affairs and Head of Centre for Transportation Systems (CTRANS), I.I.T. Roorkee.

A Biorefinery Approach for the Utilization of Waste Generated from Natural Indigo Dye Production Process

Satya Narayan Naik
Centre for Rural Development & Technology, Indian institute of Technology Delhi, Delhi 110016, India

Abstract

Due to recalcitrant, toxic and carcinogenic nature of synthetic dyes, the demand of natural dye are accelerating in textile, cosmetics, pharmaceutical and food sectors. In the current scenario, the most effective source for natural dyes are plants and different parts of plant. Among various plant sources *Indigofera tinctoria* (commonly known as Neel) is the primary source of natural indigo in India and other Asian countries.The plant was not only used in dye production, but also used for different therapeutic and medicinal purposes. This plant is categorized under leguminous plant and can be grown in a broad range of soil conditions. It is a good nitrogen catch crop, reducing the amount of fertilizer leaching to the groundwater. The plant was also used as cover crop because of its soil erosion control potential.

Despite of several benefits of this plant, it has only been utilized for dye production in rural village of southern India in traditional way. From initial field survey it was found that, approximately 750-1000 hectares of land have been utilized for cultivation and production of approximately 30-40 Gg of *Indigofera tinctoria* plant biomass. The natural indigo dye production process consists of three steps: steeping, beating and dye recovery. A large amount of plant biomass and water were utilized during the steeping process. For a single batch of dye production process (10 kg of indigo cake) approximately 1Mg of biomass and 12000 L of water were utilized. For a product recovery of 1%, approximately 99% of plant biomass and water after the dye extraction process remains unused and usually discarded. To make natural indigo dye production process more economical and eco-friendly, reuse of waste plant biomass generated from indigo dye production processes is essential.

Dr. **Satya Narayan Naik**
Centre for Rural Development & Technology,
Indian institute of Technology Delhi,
Delhi 110016, India

Fax 091-11-26591121

Cell No:9818294067
E-mail: snn@rdat.iitd.ac.in, naiksn@gmail.com

Dr. S N Naik is Master in Chemical Technology specialization in Oils, Fats and Waxes from Nagpur University and Ph.D in "Supercritical Fluid Extraction of Natural Product" from IIT Delhi . During Ph.D he has **worked at University of Siegen, Germany under Volkswagen Research Fellowship in 1986.** He has handled many research projects sponsored by DST, DBT, Ministry of food processing, Ministry of Agriculture, Ministry of Tribal Affairs, GIZ Germany, General Motors R & D Centre USA. He has produced 34Ph.Dthesis and published more than 180 research publications in international and national journals and also 7 patents. He has transferred patented Technology to various Industries. He has been offered visiting faculty position in of Siegen (Germany),UniversityUniversity of Saskatchewan (Canada) and University of Aston (U.K.) Kyoto Institute of Technology (Japan). He has also awarded with Dr. H S Zaheer Memorial Award(2010) by Oil Technologist Association of India and Dr. D. R. Dhingra Memorial Award (1989) by Essential Oil Association of India. His research interest is Extraction of Natural Plant Products (Essential oils, Oleoresins, Food Colors, Biopesticides, Nutraceutical and Cosmoceuticals) by using Subcritical and Supercritical fluids as well as processing of non-edible oil seeds for production of Bio-fuels, Bio-lubricants and Oleo-chemicals, Value addition to Non timber Forest Produce.

Economy in Waste Plastic Recycling

Deepak Pant
Central University of Harayana (CUH), Mahendergarh

Abstract

Value addition is a new technique involves an effective utilization of any plastic waste intermediate/ final product formed during any of existing recycling processes. The involving pathways are mixed polymer recycling, composite of same polymer intermediates through different routes (formed during its management/recycling), mixing of different waste process intermediates and chemical, mechanical modification of various intermediate or final products etc. The existing technologies for recycling plastic waste require high temperature or involving utilization of carcinogenic solvents, but both the technologies are not safer in terms of environmental and economic aspects. This research consists of the development of technique for the conversion of plastics waste like PC, PFT and PVC to value added product for making the recycling as an economic affair.

Prof. Deepak Pant
Professor in Chemistry
Dean, Chemical Sciences
Central University of Harayana (CUH),
Mahendergarh
Phone: +919816639032
Email: dpant2003@gmail.com

Dr. Deepak Pant is currently working as a Professor in Chemistry in Central University of Harayana (CUH), Mahendergarh, India is the recipient of Silver Jubilee Research Fellowship Award for the year 2003 by Kumaun University, Nainital (India); UCOST Young Scientist Award 2009, INSA Fallow 2010, DST-SERC Visiting Fallow 2010, DST- SERC Young Scientist Award 2011 and Visitor award 2017 by president of India for his research activities. This year also he is nominated for 8th National Award for Technology Innovation (2018) by Ministry of Chemicals and Fertilizers, Government of India. Dr Pant has 05 patents in the area of waste management by green techniques and published 10 books, 40 research papers in various national and international journals. He has guided 02 M. Phil, 04 Ph. D. thesis and 48 M. Sc. dissertations. He is current Dean of the school of Chemical Sciences, CUH. Before joining CUH, he was working as Dean and Head, Environmental Science, Central University of Himchal Pradesh, Dharamshala, Himachal Pradesh. He is in the editorial board of The Journal of Environmental Science and Sustainability (JESS).

Production and purification of a robust L-asparaginase having low-glutaminase activity from Bacillus Sp.: In vitro evaluation of anti- cancerous properties

Vinod Kumar
Technical officer
Microbial Technology
Center of Innovative and Applied Bioprocessing (CIAB)

L-asparaginase with low glutaminase is a crucial therapeutic for the treatment of acute lymphpoblastic leukemia (A.L.L). The current study highlights the characterization of a purified extracellular L-asparaginase having low glutaminase activity, produced by isolated *Bacillus* spp. Protein was found to be specific for its natural substrate i.e. L-asparagine. The enzyme showed an increased activity in presence of monovalent cations such as Na^+ and K^+, however activity presence of divalent cations and thiol group blocking reagents. The purified enzyme was maximally active over the range of pH 6.0 to 10.0 and temperature of 40^{o}C and enzyme was stable maximum at pH 9.0. The purified L-asparaginase had cytotoxic activity against various cancerous cell lines viz. Jurkat clone wil-1, Raji and L-929-562. However the enzyme should be considered potential candidate for further pharmaceutical use as an anticancer drug.

Dr. Vinod Kumar
Technical officer
Microbial Technology
Center of Innovative and Applied Bioprocessing (CIAB)
Sector – 81, Manauli, Mohali, Punjab- 140306
Phone: +8427595494
Email: vinodudsc@gmail.com

Dr. Vinod Kumar is Technical Officer (Microbial and Enzyme Bioprocessing) at the Center of innovative and Applied Bioprocessing (National Institute under Department of Biotechnology, Govt of India), Mohali, Punjab, India. He obtained PhD degree in Microbiology from the University of Delhi (2014) for which he had obtained a fellowship from MNRE, New Delhi. Before that he worked at CIAB, Mohali as Research Associate and Young Scientist under the DST-SERB (Govt of India) program. He was awarded EPFL Visiting Fellowship in 2016 and worked there during Sep-Oct 2016. His current research interests include production of bacterial cellulose and xylitol from un-utilized bioresources. His main research interests are in the areas of Industrial Microbiology and Biotechnology. He has published 28 papers and three patents filled. He has visited to Korea, China and Switzerland.

Energy recovery from petroleum refinery waste using thermal plasma pyrolysis

Prof. (Dr.) V. K. Srivastava
Sankalchand Patel University, Sankalchand Patel Vidyadham, Visnagar

Thermal plasma pyrolysis converts carbon-containing materials, under high temperature and pressure, into synthesis gas. Synthesis gas or **syngas** is generally composed of hydrogen and carbon monoxide but can be manufactured to contain methane and other higher molecular weight compounds. Syngas can be used as a fuel to generate electricity or as a basic chemical building block for use in the petrochemical and refining industries. Syngas generally has a heating value that is approximately two-thirds that of natural gas and, when burned as fuel, produces emissions that are similar to natural gas. In the petroleum refining industry alone, about seven to ten million tons of hazardous byproducts containing carbon, currently managed under the Resource Conservation and Recovery Act (RCRA), could be converted into energy as useable fuel or chemicals using thermal plasma pyrolysis methods.

Prof. (Dr.) V. K. Srivastava
Provost (Vice Chancellor)
Sankalchand Patel University,
Sankalchand Patel Vidyadham, Visnagar (Gujarat)
Email: vc@spu.ac.in; drvks9@gmail.com
Mobile: 09426163888, 07490025201

Prof.(Dr.)V.K.Srivastava completed his Bachelors and Masters in Science from the BU, Jhansi, and he was awarded with two Gold Medals for securing First Rank in Bachelors and Masters Degree respectively. He also completed his Post Graduate Diploma Business Management from RPICM-Mumbai and PhD Degree from BU Jhansi. His wide array of experience includes one year serving in the Industry and with over 22 years of experience in teaching, research and administration at different Institutes and world class Universities. In past, he has worked at senior academic administrative positions like Dean/Director, Head of Department, Chairman-Board of Studies2014 at reputed world class Universities. He had been instrumental in formulating MoUs with other reputed Universities, Research centers and Industries for achieving the bench marks of academic excellence.

He has published more than 45 research papers in National and International Journals and Conference, published 3 books and 10 Chapters, completed several funded research projects and Consultancy projects. He has organised number of Seminars, Conferences, Short Term Training Programmes (STTP) and other Faculty Development Programmes.

Advanced Combustion Techniques for Internal Combustion Engines: Strategies, Achievements and Future Directions

Akhilendra Pratap Singh
Engine Research Center
University of Wisconsin, Madison
Wisconsin, USA

Abstract

Universal concerns about degradation of ambient environmental conditions, stringent emission legislations and depletion of petroleum reserves have motivated research and development of engines towards alternative combustion concepts. Low temperature combustion (LTC) is an advanced combustion concept for internal combustion (IC) engines, which offers prominent benefits in terms of simultaneous reduction of both oxides of nitrogen (NOx) and particulate matter (PM) emissions in addition to utilization capability of renewable fuels. In last two decades, massive research efforts have been done on different derivatives of LTC such as partially homogeneous charge compression ignition (PHCCI) combustion and premixed charge compression ignition (PCCI) combustion for low-load applications in light-duty and heavy-duty engines. However full-load applications, even in light-duty engines have not been experimentally demonstrated until now due to lack of control over ignition timing and heat release rate. This limits the commercial application of LTC technologies in production-grade engines. To tackle this problem, an intermediate solution namely 'mode switching technique' has been demonstrated. In mode switching technique, engine can operate in both PCCI as well as compression ignition (CI) combustion mode depending on engine operating condition, which is an effective solution for commercializing LTC technology. In last few years, a new derivative namely "reactivity controlled compression ignition (RCCI)" combustion has been demonstrated. This is a dual fuel technique, in which auto-ignition can be controlled by the global reactivity of fuel-air mixture by varying the relative quantities of two fuels (low reactivity and high reactivity fuels). In RCCI combustion, a long range of alternative fuels namely alcohols, hydrogen, etc. can be used as low reactivity fuels. RCCI combustion in mode switching strategy can further improve the overall engine efficiency and reduce harmful emissions. Use of RCCI combustion engine as a fossil fuel energy source in hybrid vehicles may be the future research area for the development of the next generation road transport vehicles.

Dr. Akhilendra Pratap Singh
Engine Research Center
University of Wisconsin, Madison
Wisconsin, USA
Email: akhilendrapdf@gmail.com
asingh98@wisc.edu
Mobile No. +1 6086987815
+91 7458902505

Dr. Akhilendra Pratap Singh is currently working as an Indo-US postdoctoral fellow at Engine Research Center, University of Wisconsin, Madison. Dr. Singh received his Masters and Ph.D. in Mechanical Engineering from Indian Institute of Technology Kanpur, India. He has worked as a CSIR Pool Scientist at Indian Institute of Technology Kanpur from 2014 to 2017. His areas of research include advanced low temperature combustion; optical diagnostics with special reference to engine endoscopy and PIV; combustion diagnostics; engine emissions measurement; particulate characterization and their control; and alternative fuels. Dr. Singh has published more than 25 international journal articles and presented 10 papers in international and national conferences. Dr. Singh has edited 7 books and written more than 20 book chapters. He is a member of the editorial board of the 'Journal of Energy, Environment, and Sustainability'. He has been awarded with 'ISEES Best Ph.D. Thesis Award' (2017), 'SERB Indo-US Postdoctoral Fellowship' (2017) and 'IEI Young Engineer Award' (2017).

Particulate Bound Trace Metals and Soot Morphology of Gasohol Fueled Gasoline Direct Injection Engine

Nikhil Sharma
Chalmers University of Technology

Abstract

Direct injection spark ignition or gasoline direct injection (GDI) engines are superior in terms of relatively higher thermal efficiency and power output compared to multipoint port fuel injection engines and direct injection diesel engines. In this study, a 500 cc single cylinder GDI engine was used for experiments. Three gasohol blends (15% (v/v) ethanol/methanol/butanol with 85% (v/v) gasoline) were chosen for this experimental study and were characterized to determine their important fuel properties. For particulate investigations, exhaust particles were collected on a quartz filter paper using a partial flow dilution tunnel. Comparative investigations for particulate mass emissions, trace metal concentrations, Raman spectroscopy, Fourier transform infrared spectroscopy (FTIR) analyses, and high-resolution transmission electron microscopy (HR-TEM) imaging of the particulate samples collected from different test fuels at different engine loads were performed. For majority of the experimental conditions, gasohols showed relatively lower trace metal concentration in particulates compared to gasoline. HR- TEM images showed that higher engine loads and presence of oxygen in the test fuels increased the soot reactivity. Multicore shells like structures were visible in the HR-TEM images due to growth of nuclei, and rapid soot formation due to relatively higher temperature and pressure environment of the engine combustion chamber. Researches world-over are trying to reduce particulate emissions from GDI engines; however, there is a vast research gap for such investigations related to gasohol fueled GDI engines. This paper critically assesses and highlights comparative morphological characteristics of gasohol fueled GDI engine.

Dr. Nikhil Sharma

Post Doctoral Researcher
Combustion and Propulsion System
Chalmers University of Technology
Email: sujeet20186@gmail.com

Dr. Nikhil Sharma is currently a Post Doctoral Researcher at Division of Combustion and Propulsion System, Chalmers University of Technology, Sweden. His research areas include the Droplets Size and Velocity studies inside the Optical Engine using PDI, contributed in alternative fuels and reduction in emissions. He has been awarded Postdoctoral fellowship by Swedish Energy Agency, Senior Research Associate fellowship by CSIR and Best Ph.D. thesis award-2017 by ISEES. He has 7 refereed journal papers (SCI Indexed), 3 conference publications (Scopus indexed) and 10 book chapters.

III SEEC Contributed Papers/ Posters

Proceedings of theThird International Conference on Sustainable Energy and Environmental Challenges (3rd SEEC)

18 –21 December, 2018, IIT Roorkee, India

SEEC No.003

FEASIBILITY OF UTILIZING SOLAR DRYING TECHNIQUE AS ENERGY EFFICIENT PROCESS FOR THE QUALITATIVE BIODIESEL PRODUCTION FROM A LOCALLY ISOLATED MICROALGA *SCENEDESMUS OBLIQUUS*

Sourav Kumar Bagchi[1,2]
[1]Agricultural and Food Engineering Department, Indian Institute of Technology Kharagpur, West Bengal-721302, India

[2]Present address: Molecular Microbiology Laboratory, Department of Biotechnology, Indian Institute of Technology Roorkee, Uttarakhand-247667, India
Email: skbmka@gmail.com

P. Srinivasa Rao[1]
[1]Agricultural and Food Engineering Department, Indian Institute of Technology Kharagpur, West Bengal-721302, India
Email: psraoiit@gmail.com

Nirupama Mallick[1*]
[1]Agricultural and Food Engineering Department, Indian Institute of Technology Kharagpur, West Bengal-721302, India
*Email: nm@agfe.iitkgp.ernet.in

ABSTRACT

In this present investigation, the wet biomass of the indigenous isolated microalga Scenedesmus obliquus (Turp.) Kütz. was solar dried varying the sample thickness with the different seasonal variations. The test alga was cultivated with a low cost medium in the semi-large tanks at 15 cm culture depth (560 L culture volume) under the outdoor conditions for lipid followed by biodiesel production. After harvesting, the thick microalgal slurry was spread in petridishes at three sample thicknesses, viz. 5, 7.5, 10 mm and were dried in solar drier. Solar drying was found to be quite effective during the summer, autumn, as well as during the winter seasons with the maximum lipid yield was recorded as ~420 mg g^{-1} in the month May-June with a drying time of only 24-30 h, respectively for 5 mm initial thick samples Rainy season was really found as troublesome for the solar drying in this tropical regions.

***Keywords*:** Biodiesel, Microalgae, Solar drying.

1. INTRODUCTION

Since the last couple of decades, scientists are paying a strong drive towards the development of alternative and renewable fuel technologies based on the sustainable use of various plant biomass sources to produce the non-polluting biofuels. Currently, the foremost attention is being focused on the third generation biodiesel source, 'microalgae' that are often coined as the 'Green gold' for biodiesel production. Generally wet microalgae contain >80% moisture. It has already been estimated that microalgal drying can alone account for 30% of the total production costs of algae biomass to biodiesel [1]. The intensive energy utilized in various drying techniques is a big hurdle for the production of microalgal biodiesel in a commercial scale. For tropical and sub-tropical countries, solar drying is the foremost method that has been mostly recommended by scientists to be used commercially as solar drying is basically very cheaper than other kinds of microalgal biomass drying methods like oven, tray, freeze, drum, vacuum, and/ or spray drying [2]. However, the algal biomass drying by using the solar drying method is infrequently practiced and rarely reported till date for the biodiesel production from microalgae. In this present investigation, the wet biomass of the indigenous isolated microalga *Scenedesmus obliquus* (Turp.) Kütz. was solar dried varying the sample thickness with the different seasonal variations. The lipid extraction followed by the transesterification and biodiesel production was also investigated thoroughly for the solar dried biomass of *S. obliquus*.

2. MATERIALS AND METHODS

2.1 Identification and maintenance of cultures

The test microalga was isolated following the standard microbial techniques from a local pond near Subarnarekha river side, Bhasraghat, Jhargram, West Medinipur (latitude 22° 04' N, longitude 87° 17' E), West Bengal, India, and was identified by the Cryptogamie section, Botanical Survey of India (BSI), Howrah, India, as *Scenedesmus obliquus* (Turpin) Kützing. The laboratory grown batch cultures of the test microalga was tried to be cultured initially at outdoor in plastic trays. These tray cultures were used as inoculum for small size fiber-reinforced plastic (FRP) tanks (1.25 × 0.60 × 0.45 m). Subsequently, these cultures were re-inoculated in the semi-large size FRP tanks (3.6 × 1.1 × 0.3 m) at 15 cm culture depth (560 L

culture volume of each tank) under the outdoor conditions. The growth medium was used as the normal farm fertilizer low-cost grade medium.

2.2. Biphasic strategy

The harvested biomass of *S. obliquus* from the first phase was transferred again into the nitrogen starved medium and incubated for 7 days [3] to boost up and stimulate maximum lipid accumulation.

2.2 Drying of wet algal biomass

After harvesting, the thick microalgal slurry was spread uniformly in glass petridishes (9 cm inner diameter and 1.5 cm depth) at three different sample thicknesses, viz. 5, 7.5, and 10 mm for all the drying experiments and were recorded at different time intervals like 1, 2, 3, 5, 7, 9, 12, 15, 18, 24, 30 h, and beyond that so on.The solar dryer (RM Enterprises, Andul, West Bengal, India) was comprised with large glass-plated surface area called as collector plates, which collected the sun-light and converted it to heat energy (Figure. 1a, b).

2.3 Determination of moisture content

The moisture content in term of % wb, denoted as '*m*' of the samples was calculated based on their weight loss at various time intervals following the protocol of Chakraverty [4].

$$m = \left\{ \frac{Wm}{(Wm + Wd)} \times 100 \right\} \quad \text{(Eq. 1)}$$

Where, W_m is the weight of the moisture present, and W_d is the weight of the bone dry materials. Bone drying means drying the samples in an oven dryer at 103 ± 2 °C for 24 h [4]. The solar drying experiments were performed throughout the year for a period of three consecutive years to confirm the variation and data reproducibility.

2.4 Determination of biomass and lipid yield

Biomass concentration was recorded in every third day following the gravimetric analysis with a little modification of Rai *et al.* [5], and expressed as g L^{-1}. Lipid extraction was carried out at room temperature using the technique of Bligh and Dyer [6] with binary solvents as chloroform and methanol.

2.5 Transesterification

Transesterification was performed with a molar ratio of oil: methanol: HCl :: 1: 82: 4 at 65 °C temperature and reaction time of 6.4 h, as optimized in our laboratory [7].

2.6. Estimation of biodiesel in Gas Chromatography Mass Spectrometry (GC-MS)

For confirmation of FAMEs present in the biodiesel samples, 0.2 µL of the biodiesel filtrate was taken for Gas Chromatography Mass Spectrometry (GC-MS) analysis using the GC (Model: Clarus 680; Make: Perkin-Elmer, Shelton, CT, USA) equipped with an Elite-1 methyl polysiloxane capillary column (30 m × 0.25 mm × 0.25 µm) and Turbomass Gold Mass Spectrometer (Model: Clarus 600 T MS).

3. Results

3.1 Drying time and lipid yield with varying sample thickness under solar drying of S. obliquus biomass during different seasons/ months

3.1.1 Lipid yield, drying time, and moisture content during summer season

Solar drying of the harvested *S. obliquus* biomass was found to be highly effective during summer season (March - June). The maximum lipid yield was recorded as 418.0 ± 8.6 mg g^{-1} dry biomass in the month of May followed by 414.1 ± 8.3 mg g^{-1} in the month of June with a drying time of 24 and 30 h, respectively for 5 mm thick samples. It was also depicted that 10 mm initial sample thickness was not found to be suitable for solar drying due to prolonged drying period. For 7.5 mm thick samples, maximum lipid yield was recorded as 410.2 ± 10.2 mg g^{-1} dry biomass in the month of May. The drying time taken was 30 h.

3.1.2 Lipid yield, drying time, and moisture content during rainy and autumn seasons

Rainy season was found troublesome due to cloudy and rainy days. In July, the maximum lipid yield was recorded as 367 ± 9.1 mg g^{-1} dry biomass with a drying time of 54 h, whereas the value was reduced to 331.6 ± 9.2 mg g^{-1} dry biomass with a drying time of 66 h in August for 5 mm initial sample thickness. It was also seen that the drying times were so lengthened as 72 to 84 h in August and September for 7.5 and 10 mm thick samples. However, during autumn days (October), the solar drying was proved to be quite effective as the maximum lipid yield was recorded as 385 ± 6.2 mg g^{-1} dry biomass with a residual moisture content of 3.15% (wb) at a drying time of 48 h for 5 mm initial sample thickness.

3.1.3 Lipid yield, drying time, and moisture content during winter season

During winter season, the maximum lipid yield was recorded as 401.0 ± 7.3 and 387.2 ± 7.1 mg g^{-1} dry biomass for 5 and 7.5 mm thick samples with a drying time of 42 and 48 h, respectively in the month of February, whereas

378.2 mg g^{-1} dry biomass in the month of November with a drying time of 48 h for 5 mm thick samples.

The month-wise hierarchy for lipid yield with 5 mm initial sample thickness was as follows:

May ≥ June ≥ April ≥ March ≥ February > October ≥ November ≥ December ≥ January ≥ July > September > August

3.2 GC-MS Analysis of the produced biodiesel

The fatty acid methyl ester (FAME) profile for the biodiesel produced from the lipids of the solar dried biomass in different seasons demonstrated the presence of five major FAMEs, i.e. palmitic, stearic, oleic, linoleic, and linolenic acid methyl esters. The very high amount of saturated and mono-unsaturated fatty acid mixtures (~88%) were recorded for the test microalgal biodiesel dried under solar drying conditions during the winter season.

4. CONCLUSION

The locally isolated microlaga *S. obliquus*, cultivated in the FRP tanks in outdoor condition with low-cost farm fertilizer medium, was dried in a solar drier and was found to be quite effective drying during the summer, autumn and winter seasons with a maximum lipid yield of 418.0 ± 8.55 mg g^{-1} dry biomass in the month of May. Considering the energy requirement, the solar drying protocol so developed carries the immense potential for drying the microalgal biomass in tropics and sub-tropics particularly in India throughout the year except for some days during the rainy season. It was also highly striking that the total saturated and monounsaturated fatty acid contents of the biodiesel were found to be ~90% under the solar drying techniques studied, thus demonstrating that the high quality of biodiesel was produced through this solar dried algal biomass.

FIGURES

FIGURE 1a. OUTDOOR CULTIVATION OF S. *OBLIQUUS* IN FRP TANKS

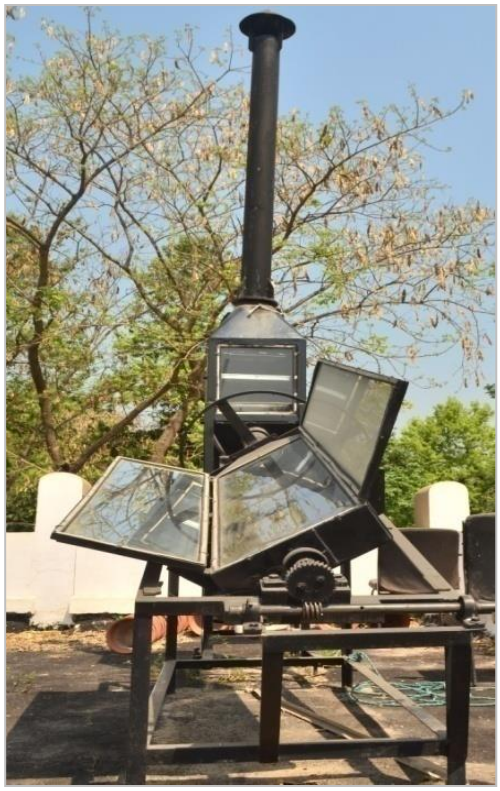

FIGURE 1b. PICTORIAL VIEW OF A SOLAR DRIER INSTALLED AT THE AGFE DEPARTMENT, IIT KHARAGPUR, INDIA

FIGURE 1c. OUTDOOR CULTIVATED *S. OBLIQUUS* BIOMASS DRIED UNDER SOLAR DRYING METHOD

ACKNOWLEDGMENTS

The authors are grateful to Indian Institute of Technology Kharagpur, India, for providing the basic instrumentations and research facilities. The first author SKB would like to acknowledge Prof. Vikas Pruthi, Professor of Biotechnology and Head of CTRANS, Indian Institute of Technology Roorkee, for providing the chance to do the Post Doctoral work under his mentorship and carry on the research work further for the lab scale and outdoor chlorophycean microalgae cultivation and biofuel production.

REFERENCES

[1] Becker, E. W., 1994. Large-scale cultivation. In: Microalgae: Biotechnology and Microbiology. Cambridge University Press. p. 165.

[2] Show, K. Y., Lee, D. J., and Chang, J. S., 2013, Algal biomass dehydration. Bioresource Technology, 135, 720-729.

[3] Bagchi, S. K., Rao, P. S., and Mallick, N., 2015, Establishment of an oven drying protocol for extraction of lipids for production of biodiesel from a locally isolated chlorophycean microalga *Scenedesmus* sp. Bioresource Technology, 180, 207-213.

[4] Chakraverty, A., 1988, Theory of Grain Drying: Post Harvest Technology of Cereals, Pulses and Oilseeds. Oxford and IBH Publishing Co. Pvt. Ltd. p. 26.

[5] Rai, L. C., Mallick, N., Singh, J. B., and Kumar, H. D., 1991, Physiological and biochemical characteristics of a copper tolerant and a wild type strain of *Anabaena doliolum* under copper stress. Journal of Plant Physiology, 138, 68-74.

[6] Bligh, E. G., and Dyer, W. J., 1959, A rapid method of total lipid extraction and purification. Canadian Journal of Biochemistry and Physiology, 37, 911-917.

[7] Mandal, S., Patnaik, R., Singh, A. K., and Mallick N. (2013) Comparative assessment of various lipid extraction protocols and optimization of transesterification process for microalgal biodiesel production. Environmental Technology, 34, 2009-2018.

SEEC No. 004

THERMODYNAMIC MODELLING AND EXERGY ANALYSIS OF A TRI-GENERATION PROCESS

Abhimanyu Bandyopadhyay
Department of Mechanical Engineering
Jadavpur University, Kolkata-700037
abhimanyu.bandyopadhyay@gmail.com

Sudipta De
Department of Mechanical Engineering
Jadavpur University, Kolkata-700037
de_sudipta@rediffmail.com

ABSTRACT
Tri-generation process is a multi-utility process which integrates different components like turbines, combustor, pumps, gasifier, heat exchangers etc to get multiple outputs like power, utility heat and refrigeration . Agricultural wastes like rice husk is used as raw material to generate the multiple outputs of the plant.This study deals with the thermodynamic modelling and exergetic analysis of different parts of a tri-generation process and looks forward for optimizing the exergy efficiency by varying different parameters like steam to biomass ratio, operating temperature, degree of superheat etc.

***Keywords*:**
Tri-generation, thermodynamic modelling, exergy analysis, operating parameters

NOMENCLATURE

h_f	Enthalpy in kJ/kg
h_T	Enthalpy rise due to temperature change in kJ/kg
$g_{f,T}$	Gibbs energy of formation in kJ/kmol
p	Partial pressure of a component in bar
P	Total pressure in bar
K	Equilibrium constant
E_{phy}	Physical Exergy in kJ
E_{chem}	Chemical Exergy in kJ
T_o	Ambient temperature ($25o_C$)
C_p	Specific heat of flue gas in kJ/KgK
x	Mole fraction

INTRODUCTION
With fast depleting fossil fuels and impact of climate change, high efficiency energy systems using renewable resources is an imperative need at present[2]. Agricultural wastes are abundantly available in India and may be used as useful biomass to supply different energy utilities including power[1]. Also integrating different energy utilities in a single unit increases overall efficiency of the energy systems. Tri-generation integrates power, utility heat and cooling in a single unit with overall improved efficiency. Analysis using thermodynamic modeling helps to assess expected performance of a new energy system. Study of variation of performances of such systems with design and operational parameters helps to determine the possible optimum design and operational conditions of such possible new systems. Exergy analysis identifies loss of work potential and associated inefficiency of an energy system. Thus exergy analysis helps to determine possible improvement of energy systems evaluated through exergy loss or exergetic efficiency of different components of the system[4].

A tri-generation using rice husk available as agricultural waste in India is modeled thermodynamically. Analysis using this developed model assesses and recommends possible optimum design and operational parameters for acceptable performance of this energy system. Exergy analysis[10] is also included to assess the performance of components of this plant with variations of different parameters of design and operation.

1. SYSTEM DESCRIPTION

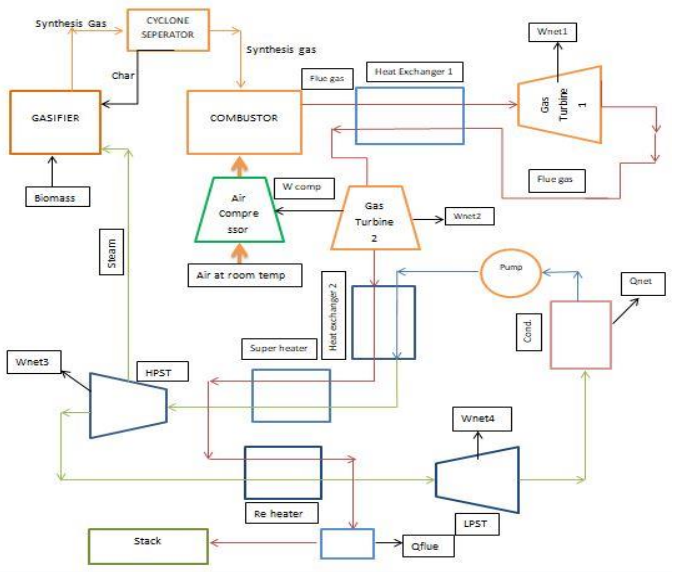

Fig 1.1

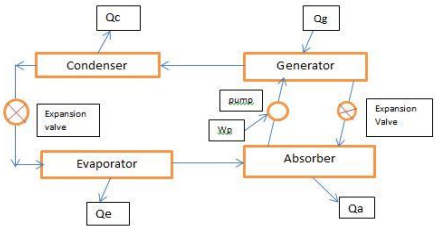

Fig 1.2

The system consists of a topping Gas cycle followed by a bottoming Vapour cycle. The different parts of the Gas cycle are Gasifier, Combustor, Gas Turbines, Air Compressors, Heat Exchangers, Cyclone separators etc. The components of the bottoming Vapour cycle are pump, Super heater, High Pressure Steam Turbine (HPST), Re-heater, Low Pressure Steam Turbine (LPST), Condenser etc. The different parts of the refrigeration system are Generator, Absorber, Evaporator, Condenser, Pump etc. Here the outputs from the chosen tri-generation process are work, sensible heat and refrigeration effect. The work is extracted from the turbines and heat is extracted from the flue gas or from condenser. A part of the heat extracted is supplied to the generator of a Vapour Absorption Refrigeration System (VARS) at generator temperature (Tg) $156o_C$. The inputs to the system are biomass (Rice Husk is used here), air and water at room temperature.

2. THERMODYNAMIC MODELLING

2.1 Gasifier

The governing equation of gasification of biomass with steam is:

$$CH_xO_y + mH_2O = n_{H2}.H_2 + n_{CO}.CO + n_{CO2}.CO_2 + n_{CH4}.CH_4 + n_{H2O}H_2O + n_c.C$$

To the left of CBP, we have 6 unknowns (n_{H2} n_{CO},n_{CO2},n_{H20},n_{CH4},n_C) and to the right of CBP there are 5 unknowns without the last one, so we need 6 and 5 equations respectively to solve these unknowns.

First 3 equations are carbon hydrogen and oxygen balance equations and the remaining 3 equations are equilibrium constant relations of the following equations.

Heterogeneous water-gas reaction:
C + H_2O = CO + H_2
$K_1=(P_{CO} * P_{H2})/P_{H2O} = (x_{CO} * x_{H2})/x_{H2O}$ (1)

Bouduourd reaction:
C + CO_2 =2CO
$K_2=(P_{CO})^2/P_{H2O} = (x_{CO})^2/x_{H2O}$ (2)

Methanation reaction:
C + 2H_2 = CH_4
$K_3 =(P_{CH4})/(P_{H2})^2 = (x_{CH4})/(x_{H2})^2$ (3)

Water-gas shift reaction:
CO + H_2O= CO_2 + H_2 (4)

The equilibrium constants in the above equations are not unknowns they are calculated by the following equations.

LnK= -(ΔG^o)/RT (5)
$\Delta G^o = \sum_{p=product}(\gamma_p \Delta g^o_{f,T,p}) - \sum_{r=reactant}(\gamma_p \nabla g^o_{f,T,r})$ (6)

2.2 Exergy analysis

Exergy= $E_{phy} + E_{chem}$
$E_{phy} = \int_{To}^{T} C_p.dT - T_o.\int_{To}^{T}(C_p/T).dT = h - h_o - T_o(s - s_o)$ (7)
E_{chem} =x.(e_{chem} +R$T_o$log(x)) (8)

C_p here is a function of temperature(T) and the function and chemical exergy of each compound are known. [1]
$E_{biomass} = \beta * LHV_{biomass}$ (9)

2.3 Combustion process:

At 700 o_C and steam-biomass ratio, the composition of synthesis gas can be written as
Syngas=1.0611.H_2 +0.4779.CO +0.4684.CO_2 + 0.0538.CH_4 + 0.644H_2O = CH_xO_y
After calculation, the values of x and y came as 3.6217 and 2.0566 respectively. Hence the syngas can be written as $CH_{3.6217}O_{2.0566}$

Governing Equation for Combustion:
$CH_{3.6217}O_{2.0566} + a\,[O_2 + 3.76N_2] = CO_2 + (\frac{3.6217}{2})\,H_2O + 3.76aN_2$ (10)
Where $a=[1+\frac{3.6217}{4} - \frac{2.0566}{2}] = 0.8771$

Adiabatic Flame Temperature Calculation:

It was assumed that the entire heat generated from combustion process is used to rise the temperature of the flue gas and no heat is rejected from the surrounding. This is used to calculate the temperature of flue gas.
$H_{syngas} + H_{air} = H_{flue\ gas}$ (11)
$\sum_{i=reactant} H_i = \sum_{j=syngas} n_j(h^0_{f,j} + \Delta h_{T,j}) + a(h^0_{f,O2} + \Delta h_{T,O2}) 3.76\,(h^0_{f,N2} + \Delta h_{T,N2})$
$\sum_{j=fluegas} H_j = \sum_{j=fluegas} n_j(h^0_{f,j} + \Delta h_{T,j})$

Steam turbine inlet temperature is 1300o_C and the adiabatic flame temperature calculated was 2182K and so excess air(2 moles) and excess air (1.2 moles) with a flue gas reheater were used to lower the fluegas temperature in 2 cases.

2.4 Turbines, compressors and heat exchangers

This part comprises of the Gas Turbines and Steam turbines or the work producing devices and the Heat Exchangers like the Flue Gas Heat Exchanger, Steam Generator, Super Heater.
The temperature and pressure values of each state point are calculated. The pressure of the flue Gas eliminated from the stack is assumed to be atmospheric pressure or 1 Bar. It is assumed that there is no pressure drop in the Heat exchangers and the combustor and Gasifier. The isentropic efficiency of the Gas Turbines are assumed to be 90% and the pressure ratio (P_{out}/P_{in}) in the Gas Turbines are 8. All the calculations of the Gas Cycle or Brayton cycle are done by assuming flue gas to be an ideal gas with specific heat as a function of temperature. The Steam Turbines have pressure ratio (P_{out}/P_{in}) of 5. All the calculations of the Rankine Cycle are done using Steam Tables.
From isentropic process relationship, pv^{γ}= **constant** and ideal gas equation and isentropic efficiency, the outlet temperature of each state point was found out.

3. RESULTS AND DISCUSSIONS

3.1 Variation of composition of synthesis gas

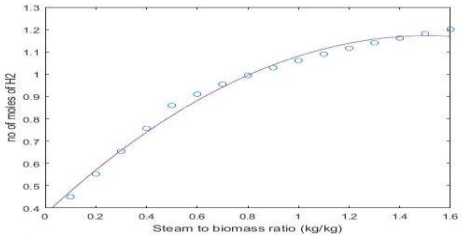

Fig 3.1.1

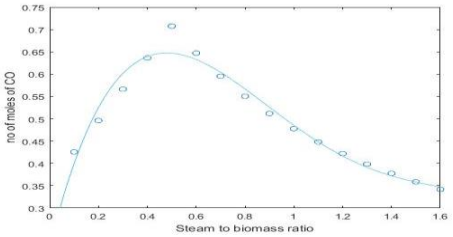

Fig 3.1.2

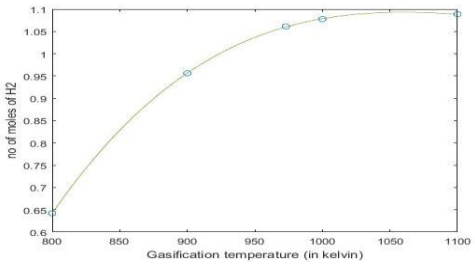

Fig 3.1.3

The above 3 figures shows the variation of the composition of different constituents of synthesis gas like H_2 and CO with steam to biomass ratio or gasification temperature respectively. More the amount of H_2 and CO released, more is the heating value of the synthesis gas and more power is produced in the gas turbine after combustion. But temperature of the turbine inlet and combustor and ducts are a limitation so optimum composition must be used and so here gasification temperature is 700o_C and steam to biomass ratio is 1.

3.2 Excess air in combustion

Combustion process	Stoichiometic	Excess air (Case 1)	Excess air (Case 2)
Number of moles of air	0.8771	1.2	2
Flue gas temperature (in kelvin)	2181.84	1893.55	1475.96
Exergy efficiency (in %)	-	71.19	32.26

Table 3.2.1

3.3 Calculated Temperature and pressure values at different state points

3.3.1 For Gas Cycle

State points	Temperature(in kelvin)	Pressure(in bar)
1. Flue gas from combustor	1893.55	64
2. Gas Turbine 1 inlet	1573	64
3. Gas Turbine 1 outlet	938.83	8
4. Reheater outlet/GasTurbine2 inlet	1303.32	8
5. Gas Turbine 2 outlet	777.85	1
6. Steam Generator outlet	705.9	1
7. Superheater outlet (for 3 cases- 100^o,200^o, 300^o superheat)	700.2 694.5 688.81	1
8. Re-Heater outlet		1
9. Stack outlet	373 (assumed)	1

The Re-heater outlet temperature of the flue gas can have 9 temperatures based on the degree of super heat of steam in both the steam turbines. The degree of super heat of steam in super heater and re heater is varied from 100^o,200^o, 300^o superheat.

3.3.2 For Vapour Cycle

State Points	Temperature (in celcius)	Pressure (in bar)
a. Water from pump outlet	25	25
b. Steam temperature from steam generator outlet	100	25
c. Super heater (degree of super heat is 100^o,200^o, 300^o)	200 300 400	25
d. High Pressure Steam Turbine outlet	43.08 109.9 176.728	5
e. Re heater outlet (degree of re heat is 100^o,200^o, 300^o)	200 300 400	5
f. Low Pressure Steam Turbine outlet	43.08 109.9 176.728	1
g. Water inlet to the pump	25	1

COMPONENTS	Work done (in kJ)
Gas Turbine 1	227.264
Gas Turbine 2	183.84
Flue Gas Heat Exchanger	-
Gas Turbine if flue gas re heater was not there	299.68

3.4 Vapour Absorption Refrigeration System

COMPONENTS	Work done (in kJ)	
Super Heat degree	**For 200 degree super heat**	**For 300 degree super heat**
High Pressure Steam Turbine	235.26	432.58
Low Pressure Steam Turbine	368.16	442.63
Pump (work consumed)	-544.1	-544.1
Net Work output from the Vapour Cycle	59.32	331.11

3.4 Vapour Absorption Refrigeration System

Condenser pressure (Pc)	20.3 bar
Evaporator pressure (Pe)	2.1 bar
Generator Temperature (Tg)	156 o_C
Absorber Temperature (Ta)	40o_C
Heat added to the Generator (Qg)	2468 KJ
Pump Work (Wp)	11.6 KJ
Refrigeration effect (Qo)	837 KJ
Heat rejected in absorber (Qa)	1865 KJ
Heat rejected in Condenser (Qc)	1440 KJ
Coefficient of Performance (COP)	0.34

3.5 Net Outputs from the Tri-generation process

	Heat Extracted (Q) (in KJ)	Work extracted (W) (in KJ)	Refrigeration Effect (Qo) (in KJ)
Topping Gas Cycle	80.616	402.58	-
Bottoming Vapour Cycle	2723.9	331.11	-
Refrigeration Cycle	-2468		837
Net Outputs	336.52	733.69	837

These are the net outputs extracted from the Tri-generation process at 300 degree superheat condition. A part of the net heat extracted from both the gas and vapour cycle is absorbed in the Vapour Absorption Refrigeration System to give the net cooling effect

3.6 Exergy and irreversibilities of different components

Exergy efficiency and hence the irreversibilities in the different components of the Tri-generation process was calculated and depicted in the form of a chart.

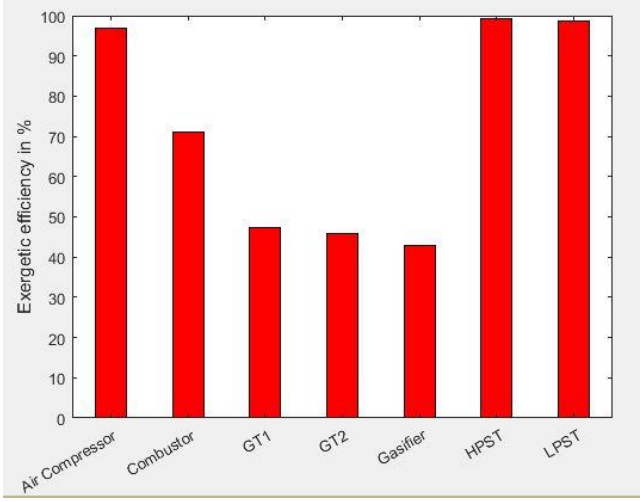

Fig 3.6.1

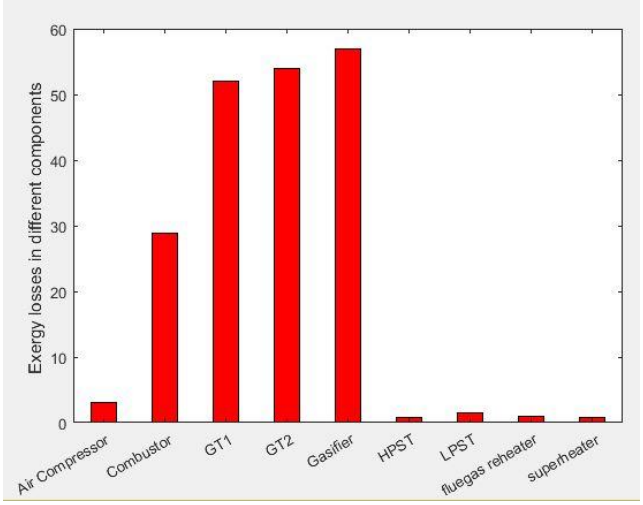

Fig 3.6.2

4. CONCLUSION

The thermodynamic modelling of the entire tri-generation system is done to estimate the outputs of the system in different form from a given set of inputs like biomass and air. Different parameters like gasification steam to biomass ratio, gasification temperature, pressure ratio in the turbines, superheat temperature etc can be varied to optimise the output requirements for the process. In place of biomass,even coal or agricultural wastes can be used as the raw material. Exergy losses of different components in the powerplant are estimated and design optimisation is required to minimize the losses as far as possible without increasing the cost much. The inlet temperature of Gas turbine is fixed so the flue gas temperature can be reduced by adding excess air or by adding excess air and then passing through a flue gas reheater. The exergy efficiency of the second case is much higher but the cost required to make the flue gas reheated operating at such high temperature is quite costly, so we need to optimise both efficiency and cost.

5. REFERENCES

[1] Loha C, Chatterjee PK, Chattopadhyay H. Thermodynamic analysis of hydrogen rich
Synthesis gas generation from fluidized bed gasification of rice husk. Energy 36(2011)4063-4071

[2] 2017_JEES_3_37-42

[3] 2015_Energy (Elsevier) 91, 540-555

[4] 2000_IMechE_214 (A1), 53-60

[5] Thermodynamics and Heat Transfer-P.K. NAG

[6] Gasification- Christopher Nigman and Maarten van der Burgt

[7] Steam Tables and charts

[8]Air conditioning and Refrigeration- C.P Arora

[9] water-ammonia refrigerant table

[10] Energy and Exergy Analysis of High Temperature Agent Gasification of Biomass
Yueshi Wu, Weihong Yang and Wlodzimierz Blasiak

Proceedings of the International ConferenceonSustainable Energy and Environmental Challenges (SEEC-2018)
18 – 21 December, 2018, Roorkee, India

SEEC No.005

Performance assessment of an Organic flash cycle (OFC) using R1234ze(Z) as the alternative working fluid of R245fa

Subha Mondal
Department of Mechanical Engineering
Aiah University, Kolkata-700156
Subhamondal53@gmail.com

Sudipta De
Department of Mechanical Engineering
Jadavpur University, Kolkata-700037
de_sudipta@rediffmail.com

ABSTRACT

Organic flash cycle (OFC) is appearing as one of the preferable options for the partial conversion of lowgrade heat into useful power due to the absence of pinch limitation. It should be noted that either dry or isentropic working fluids are considered for running OFCs as there is no superheater in the system layout. Though OFC with R245fa yields satisfactory thermal efficiency use R245fa will be restricted as GWP of R245 fa is close to 1050.
In this situation, highly flammable hydrocarbons are to be used in place of R245fa. On the other hand, R1234ze(Z) is having almost similar thermodynamic property as that of R245fa and corresponding GWP is close to 10. R1234ze(Z) is less flammable compared to Hydrocarbons. Thus R1234ze(Z) may appear as the most suitable alternative of R245fa.

***Keywords*:**
Organic flash cycle, R245fa, R1234ze(Z), low grade heat

NOMENCLATURE

c_{Pg}	Specific heat of fluegas (kJ kg^{-1}K)
h	Specific enthalpy (kJ kg^{-1})
$I_{Component}$	Component irreversibility
I_{Cycle}	Cycle irreversibility (kJ kg^{-1} of FG)
P_{TI}	Turbine inlet pressure (MPa)
P_{CR}	Critical pressure (MPa)
s	Specific entropy (kJ kg^{-1}K)
t_{CR}	Critical temperatur (^{o}C)
T_0	Ambient temperature (K)
T_{gi}	Flue gas inlet temperature (K)
T_{go}	Flue gas exit temperature (K)
η_I	First law efficiency
x	quality

ABBRIVIATION

FG	Flue gas
GWP	Global warming potential
HRU	Heat recovery unit
HPTV	High pressure throttle valve
LPTV	Low pressure throttle valve
ODP	Ozone depletion potential

1. INTRODUCTION

Conversion of low-grade heat into power is appearing as one of the possible technology that would reduce fossil fuel consumption to some extent. Organic flash cycle is appearing as one of the promising options for conversion of lowgrade heat into power. OFC is preferred due to the absence of pinch limitation in the heat recovery unit (HRU). An OFC was capable of producing utilization efficiency which was comparable to that of an organic Rankine cycle.[1]. Mondal and De [2] revealed that an OFC would appear as an economical option compared to a transcritical CO_2 power cycle if a slightly smaller power output per unit mass of flue gas was acceptable. On the other hand, the OFC configuration could be modified for achieving better cycle performance [3-4].

R245fa is a preferable working fluid for an OFC as it is having vapour line with positive slope and zero ODP. It yields thermodynamic performance which is comparable to hydrocarbons like Butane, Isopentane etc.. However, due to the moderately higher value of GWP (i.e ~1050) use of R245fa is to be phased out by 2047 [5]. Though hydrocarbons are having reasonably small GWP, replacing R245fa by hydrocarbons will be a risky option as hydrocarbons are highly flammable On the other hand, R1234ze (z) may replace R245fa as GWP of R1234ze(Z) is close to 10. R1234ze(Z) is much less flammable compared to hydrocarbons. Safety and environmental safety data for R245fa and R1234ze (Z) are summarized in table-1 for the better comparison.

1: Safety and environmental data of R245fa and R1234ze(Z)

Working Fluid	R245fa	R1234ze(Z)
Category	HFC	HFO
Nature of working fluid	Dry	Dry
P_{CR} (MPa)	3.64	3.533
t_{CR} (°C)	154.05	150.12
ODP	0	0
GWP	1050	<10
ASHRAE Safety group	B1	A2L

2. SYSTEM DESCRIPTION

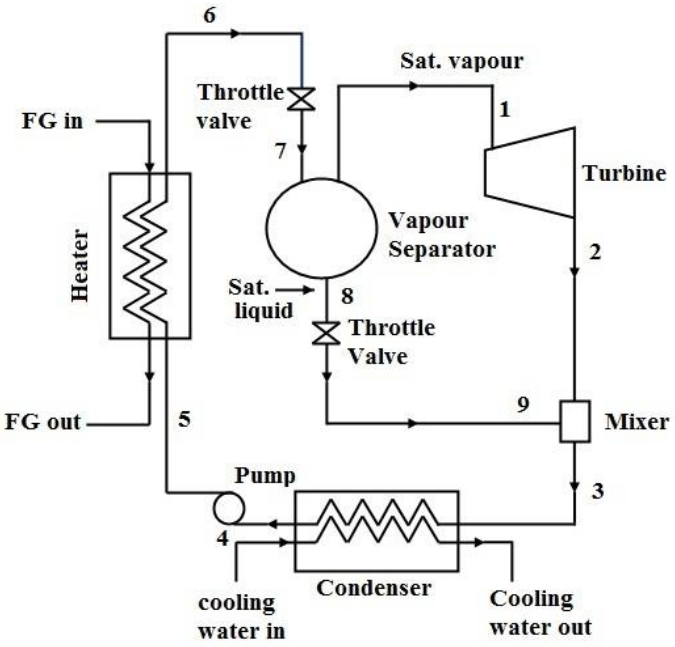

Fig.1: Layout of an OFC

The layout of an OFC is presented in Fig.1. The OFC consists of a heat recovery unit (HRU), a vapour separator, a turbine, a condenser, a mixer and two throttle valves. Working fluid after being heated (process 5-6) to saturated liquid state in the heat recovery unit is throttled to turbine inlet pressure (state-7). After throttling dry saturated vapour gets separated from the saturated liquid and expands (process 1-2) through the turbine to produce a power output. The saturated liquid stream leaving the vapour separator (state-8) undergo another throttling process (process 8-9) and finally mixes with working fluid exiting the vapour separator. After the mixing process total working fluid mass is condensed (process 3-4) in the condenser and pressurized to the HRU pressure (state-5)by using a pump.

3. MATHEMATICAL MODELLING

During the analysis a mathematical modelling is done based on the following assumptions:

a) The temperature of the working fluids exiting the HRU is assumed to be 140°C. Corresponding condenser temperature is 40°C.
b) Turbine and pump isentropic efficiencies are assumed to be 90% and 85% respectively.
c) Terminal temperature difference at the low temperature end of the HRU is 25°C.
d) The flue gas inlet temperature is 150°C
e) The pressure drop across different components are negligible.
f) There is no extraneous heat flow except flue gas outflow.
g) Ambient temperature is 25°C

Now, first law efficiency of the proposed cycle can be expressed as follows:

$$\eta_I = \frac{x(h_1 - h_2) - (h_5 - h_4)}{(h_6 - h_5)} \quad (1)$$

Ireeversibility of each of the component can be expressed as follows:

$$I_{Turbine} = m_f x T_0 (s_2 - s_1) \quad (2)$$

$$I_{MIXER} = m_f T_0 [s_3 - x s_2 - (1 - x) s_9] \quad (3)$$

$$I_{Condenser} = m_f T_0 (s_4 - s_3) - m_w T_0 (s_{wo} - s_{wi}) \quad (4)$$

$$I_{Pump} = m_f T_0 (s_5 - s_4) \quad (5)$$

$$I_{HRU} = m_f T_0 (s_6 - s_5) + c_{Pg} \ln \frac{T_{go}}{T_{gi}} \quad (6)$$

$$I_{HPTV} = m_f T_0 (s_7 - s_6) \quad (7)$$

$$I_{LPTV} = m_f T_0 (1 - x)(s_9 - s_8) \quad (8)$$

3. RESULTS AND DISCUSSION

In the present study performance of OFCs are compared condsidering R245fa and R1234ze(Z) as the working fluid. First law efficiency, irreversibility of each of the components and cycle irreversibility are considered as the performance parameter.

Effects of varying turbine inlet pressure on varying first law efficiencies of OFCs using R245fa as well as R1234ze(Z) is presented in Fig.1. For both of the working fluids, there exists an optimum turbine inlet pressure corresponding to the peak value of

thermal efficiency. This is occuring due to counteracting effects of the varying turbine in let pressure on variations of working fluid mass flow to the turbine and specific enthalpy change of working fluid during expansion in the turbine. It is observed for both of the working fluids peak values of first law efficiency ar almost same. However, optimum turbine inlet pressure for as R1234ze(Z) is slightly higher.

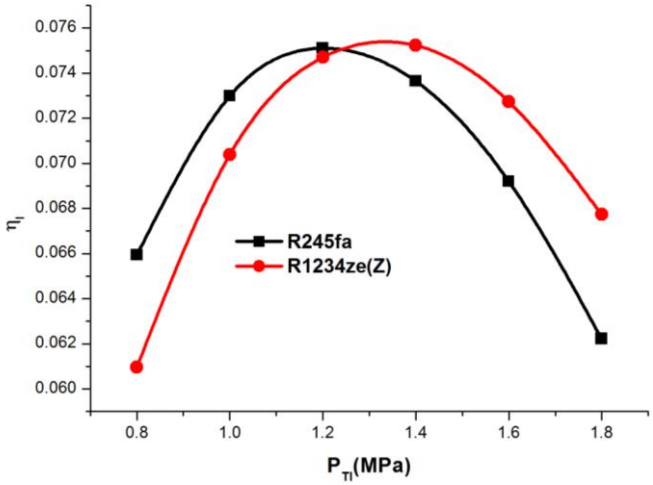

Fig.2: First law efficiency vs turbine inlet pressure

It is observed in Fig.3 that at the optimum turbine inlet pressure irreversibility of the HRU reduces appreciably as R245fa is replaced by R1234ze(Z). This also helps to reduce irreversibility of the high pressure throttle valve. However irreversibility in low pressure throttle valve increases appreciably as R245fa is replaced by R1234ze(Z). The ultimate result of replacing R245fa with R1234ze(z) is a very slight reduction in overall cycle irreversibility at optimum turbine inlet pressure as shown in Fig.4.

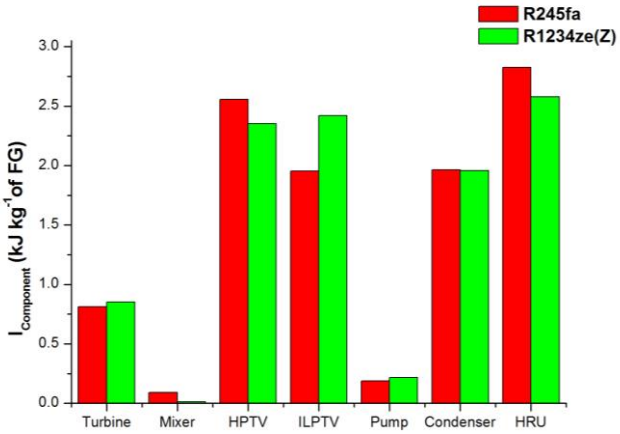

Fig.3: Comparison of component irreversibility for two working fluids

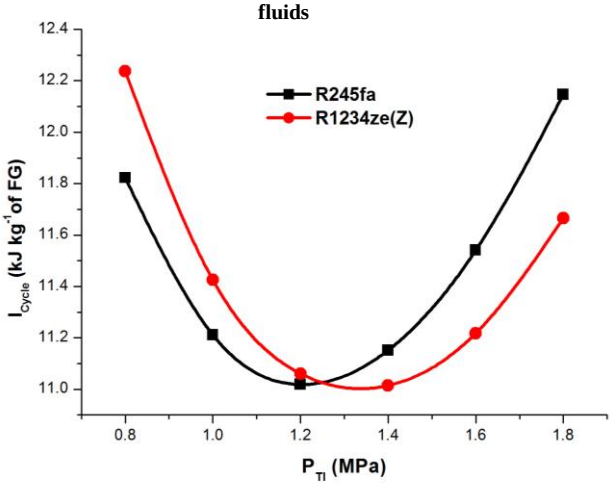

Fig.4: Comparison of cylet irreversibility for two working fluids

5. CONCLUIONS

Organic flash cycle is one of the preferable options for producing power from low-grade heat especially if minimum exit temperature of heat source from the HRU is not restricted by factors like acid condensation. R245fa is a preferable working fluid for running an OFC if heat source temperature lies betwwen 150 to 180^{o}C. R245fa is more preferable compared to hydrocarbons as it is nonflammable. R1234ze(Z) is mildly flammable, having zero ODP and its critical temperature is also close to 150^{0}C. The added advantage R1234ze(Z) is its very low value of GWP. The present analysis reveals that OFC with R1234ze(Z) can yield first law efficiency which is comparable to first law efficiency of OFC that is utilizing R245fa. Minimum cycle irreversibility with both of the working fluid are also comparable. Thus, R1234ze(Z) is the possible future working fluid for the OFC that may replace R245fa as well as hydrocarbons .

REFERENCES

[1] Ho T, Mao Samuel S, Greif R. Comparison of the Organic Flash Cycle (OFC) to other advanced vapor cycles for intermediate and high temperature waste heat reclamation and solar thermal energy. Energy 42(2012)213-223.

[2] Mondal S and De, S. Power by waste heat recovery from low temperature industrial flue gas by Organic Flash Cycle (OFC) and Transcritical-CO2 power cycle:

a comparative study through combined thermodynamic and economic analysis. Energy 121(2017) 832-840

[3] Ho T, Mao Samuel S, Greif R. Increased power production through enhancements to the Organic Flash Cycle (OFC). Energy 45(2012)686-695.

[4] Mondal S, De S. Ejector based organic flash combined power and refrigeration cycle (EBOFCP&RC) – A scheme for low grade waste heat recovery, Energy 134(20170 638-648.

[5] Powell, R.L. CFC phase out; have we met the challenge. Journal of Fluorine Chemistry 114(2002) 237-250.

Proceedings of Third International Conference on Sustainable Energy and Environmental Challenges (SEEC), December 18-21, 2018, IIT Roorkee, India

SEEC No. 008

PERFORMANCE ANALYSIS OF C.I. ENGINE BY USING DME FUEL

A.B.KOLEKAR
Asistant Professor, Department of Technology,
Shivaji University, Kolhapur
Email: abk_tech@unishivaji.ac.in

A.S.JOSHI
Department of Technology,
Shivaji University, Kolhapur
Email: aditya3909@gmail.com

ABSTRACT

Imperativeness is a key commitment for social and money related change of any country and upgrading individual fulfillment. The enthusiasm for oil things in India has been extending at a rate higher than the development in private availability. Meanwhile there is extended weight on the surge control through irregularly settled bearings particularly for urban networks. In the wake of this condition there is a sincere need to propel use of alternative fields as substitute for diesel engines. Diesel engines are the standard prime movers for open transportation vehicles, stationary power time unit and for agrarian applications. Regardless, diesel engines are critical supplier of various sorts of toxins, for instance, particulate issue (PM), carbon monoxide (CO), oxides of nitrogen (NOx) and other frightful blends. The twin issues of both utilization of uncommon resources and climatic pollution expedited by vehicles continue running on petro things are appealing to find a sensible and provoke differentiating alternative to fossil fills. Dimethyl ether (DME) is a substitution fuel that is created from fossil feedstock including normal gas and coal and what's more from sustainable feedstock and waste. From the present research consider results in liberal decreasing of unburnt carbons (HC), CO and particulate issue (PM) diverged from outpourings from diesel. Also erformances levels of Brake power, Efficiencies, Fuel Consumptions etc. gives better results as compared to Diesel fuel. The genuine vapor defilements both unburnt hydrocarbons and nitrogen oxides are ozone debilitating or darker cloudiness molding precursors. The usage of DME fuel realizes diminishment of unburnt hydrocarbon in the midst of start. In light of engine testing, using the most stringent radiations testing procedure, the general ozone molding capacity of the speculated hydrocarbon releases from DME fuel was half not as much as that think for diesel. Test work is finished to picture the likelihood of using DME fuel under moved exploratory conditions especially with complement on directing air tainting.

Keywords: dimethyl ether (DME), C.I. engine, performance, analysis

I] INTRODUCTION

The world imperativeness supply has depended strongly on non-unlimited crude oil gathered (fossil) liquid stimulates, out of which 90% are assessed to be exhausted for essentialness period and transportation region. It is moreover understood that release from the consuming of oil fills are the huge purposes behind an unnatural climate change and various countries has passed establishment to catch their negative effect on condition coming about to the snappy addition in masses. Many making countries are becoming their mechanical base and yield in general essentialness demand will without a doubt increase of course, known crude oil stores could be depleted in next 50 years at the present rate of use. This condition began and dealt with the excitement for perceiving boundless rough materials into the deliver of liquid or gasses elective forces. Vegetable oil isn't another fuel for CI engine as more than hundred years earlier; Rudolf Diesel attempted his engine with vegetable oil as bio fuel. In 1911 he has coordinated preliminary on engine and uncovered that vegetable oil would help altogether in the change of Agriculture of the countries. It has in like manner been represented that vegetable oils both acceptable oils would be a promising differentiating alternative to diesel oil since they are economical and made easily in nation territories.DME is the least complex ether communicated by its compound recipe CH3OCH3 comprising of two methyl bunches attached to a focal oxygen particle. The substance structure of DME is fairly like methanol; it contains oxygen and no carbon-carbon bonds in this manner restricting the likelihood of framing carbonaceous particulate discharges amid ignition.

DME is a manufactured fuel can be produced using an assortment of fossil feedstock including gaseous petrol and coal and in addition from inexhaustible feedstock and waste. The most practical feedstock for both DME and methanol is gaseous petrol at remote areas.

In diesel engine Particulate Matter (PM) and Oxides of Nitrogen (NOx releases) are the two indispensable surges. To decrease such releases diverse fuel associations and the particular researchers all around the world are meticulously working with different ways. Assorted blending of fuel and plan change of consuming chamber is the crucial mean to diminish such surges. In show audit try will be made by the examiners for finding suitable alternative fuel for CI engine. Among different available choice empowers, Di-Methyl Ether (DME) fuel has potential as an alternative fuel for CI engine. Also Di-Ethylene Glycol Di-Methyl Ether (DGME), Di-Methoxy Methane(DMM), Methyl Tertiary Butyl Ether (MTBE), Di-Butyl Ether (DBE), Di-Methyl Carbonate (DMC), methanol, ethanol and Di-Ethyl Ether (DEE-a Cetane Improver)has accepted their part to reduce diesel surges. The closeness of oxygen in the fuel sub-nuclear structure adds to essential properties of fuel to diminish PM and other dangerous transmissions from CI engine. These empowers are blend with standard diesel fuel or used clearly in CI engine. The present work tries to find and evaluate the effect of DME fuel on diesel execution and exhaust outpourings without blending with diesel fuel. The survey is in like manner gone for finding the vapor transmissions including PM, carbon monoxide (CO), smoke and engine noise with DME invigorates. Beside this the audit also endeavors to measure and evaluate NOx outpourings for various engine stack conditions using DME fuel. Reducing of vapor gas releases are depended on upon the rate of oxygen substance in the fuel.

DME fuel has oxygen substance of 34.7% and is one of the promising elective powers for CI motor. It can be gotten from flammable gas, coal and biomass sources. Nonattendance of C-C bond, shorter start delay, high Cetane number and quick vaporization properties of DME add to finish burning in CI motor. Due to similarity in the properties DME gives better operational performances.

II] EXPERIMENTAL

Experimental set up consist of single Cylinder Vertical Water Cooled Diesel Engine Test Rig. It was divided mainly into 4 parts.

1. Single Cylinder 4 Stroke Diesel Assembly.
2. Electrical Dynamometer Assembly.
3. Fuel Consumption Measuring Unit.
4. Exhaust Gas Calorimeter.

To ensure the best results from the equipment, the installation and subsequent maintenance was planned carefully.

III] PERFORMANCE GRAPHS

The exploratory outcomes are displayed in three sections as those are given underneath concentrating on investigation of execution and outflows of CI motor,

1. DME fuel activity in air bay port and complex infusion with improved air bay valve opening planning (12º BTDC).
2. DME fuel activity in air bay port and complex infusion with improved DME stream rate with the assistance of manual control valve.
3. DME fuel enters in gulf complex by utilizing LPG gas pack as a supply source in the burning chamber.

1] Comparison of Brake Power

The recorded parameters for Diesel and DME was revealed that, for constant set of loads the BP for DME tends to be more than Diesel by 9 % (One load) to 37 % (Full load). Figure 1 shows the effect of engine load versus brake power. A difference in the break power for a load was observed. At higher engine loads, the break power reaches its maximum. For all loads DME fuelled engine develop more power than diesel fuelled engine. The mixture of DME and air was injected in the manifold 12° BTDC, which increases the temperature of the mixture leading towards complete combustion.

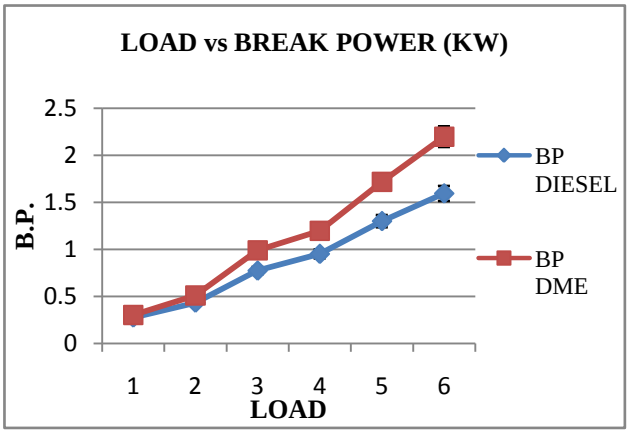

Figure 1. Effect of Load on Break Power

2] Comparison of Volumetric Efficiency

Figure 2 shows the variation of volumetric efficiency with respect to load. For all loads, volumetric efficiency of DME fuelled engine was less than diesel fuelled engine. This variation was in line with the variation of A/F ratio. Volumetric efficiency was measure of success with which the air supply, and thus the charge, was inducted in to the engine. It was indicated by the breathing capacity of the engine.

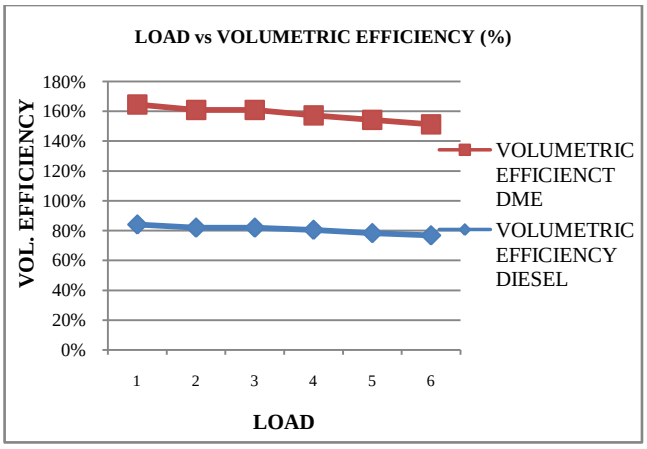

Figure 2. Effect of Load on Volumetric Efficiency

3] Comparison of Thermal Efficiency

The effect of engine load on brake thermal efficiency is shown in Figure 3. The presence of DME can enhance the thermal efficiency when compared to diesel fuel at increase of engine load. After 60 % of total engine load, it was found that the brake thermal efficiency increased significantly and recorded parameters for Diesel and DME was revealed that, for constant set of loads the Thermal Efficiency for DME fuel tends to be increased than Diesel fuel by 4% (One load) to 31 % (Full load).

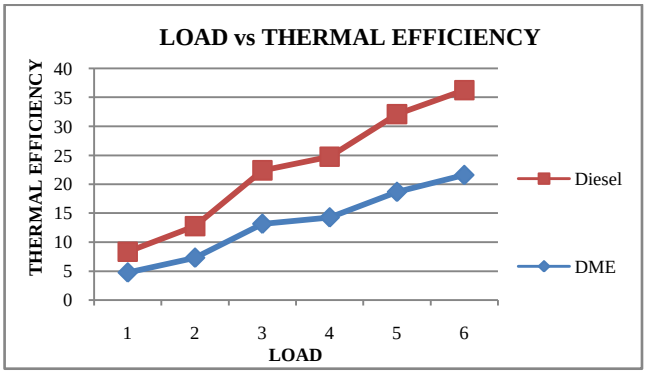

Figure 3. Effect of Load on Thermal Efficiency

4] Comparison of Break Specific Energy consumption (BSFC)

For all load, DME fuelled engine BSFC was higher than diesel fuelled engine. From the recorded parameters for Diesel and DME it was revealed that, for constant set of loads the BSFC for DME tends to be more than Diesel by 15.72% (One load) to 3.56% (Full load). Figure 4 depicted that the effects of engine load on brake specific fuel consumption (BSFC). A difference in the BSFC for a load can be observed.

Due to better combustion of fuel in the low temperature range, specific energy consumption and power improved. Fuel consumption was found to have increased at increased in load, due to reduction of the heating value of DME fuel. Therefore, BSFC for DME fuel shows a significant improvement

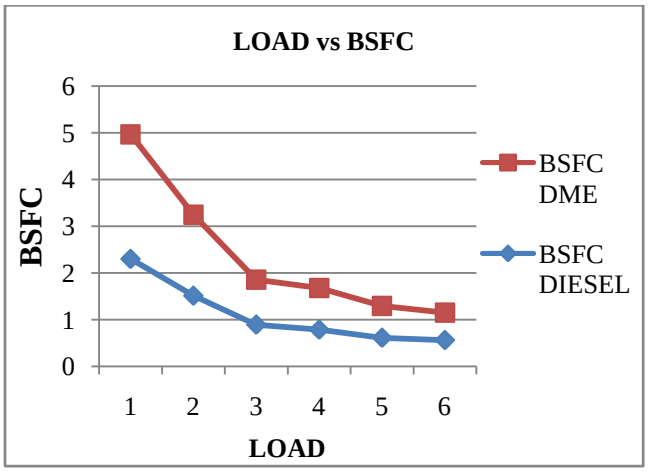

Figure 4. Effect of Load on BSFC

Chemical characteristics of DME are different from diesel petroleum. The current work was carried out to understand the impact of DME and Diesel on performance of C.I. Engine at different loads were investigated and compared with the diesel fuel. All the experiments were conducted at a constant speed of 1500 rpm. The properties of DME as well as diesel as a substitute for C.I. engine fuel.

III] CONCLUSION

The accompanying are the imperative conclusions drawn from the present examinations on an immediate infusion diesel motor.

- Thermal proficiency ascend by 4% to 31%, BSFC 4% to 16% and Volumetric productivity is 2% to 4.75% are better in the DME fuel and since CI motors give better effectiveness can be suggested.
- Engine vibration was smoother. In any case, there was sure measure of high recurrence ignition and limit of activating explosion.
- DME was turned out to be more good when contrasted with diesel fuel.
- The brake control got with diesel fuel is less by 9% to 37% than as contrast with DME fuel. This was principally a result of a higher Cetane number of DME in contrast with diesel fuel.
- High execution were seen DME in view of the consequence of warm proficiency than diesel. The brake particular vitality utilization demonstrated a diminishing pattern with diesel as higher BSFC.

In terms of engine performance parameters the DME fuel is suitable than that of diesel fuel.

IV] ACKNOWLEDGMENTS

I would like to thank to all whose names, which do not figure here, but have helped me during the tenure of my research work.

V] REFERENCES

1. Troy A. Semelsberger a, b, Rodney L. Borup a, Howard L. Greene, "Dimethyl ether (DME) as an alternative fuel", Journal of Power Sources, PP 497–511, 2006.
2. Prabhakaran, Thennarasu, Karthick, "Performance and Characteristics of a CI Engine Using DME (Dimethyl Ether)", International Journal of Innovative Research in Science, Engineering and Technology, Vol. 4, Special Issue 2, February 2015.
3. Z H Huang, H W Wang, H Y Chen, L B Zhou and D M Jiang, "Study of combustion characteristics of a compression ignition engine fuelled with dimethyl ether", Technical Note, Institute of Internal Combustion Engines, School of Energy and Power Engineering, Xi'an Jiaotong University, Xi'an, People's Republic of China.
4. Sho Fukuda, Kazutoshi Chaki and Toshiya Wakatsuki, Japex, "Feasibility Study of Production of Methanol and Dimethyl Ether from Flare Gas", Technical Research Center Division, Japan Petroleum Exploration CO., LTD., Chiba, Japan.
5. Y. Adachia, M. Komotob, I. Watanabec, Y. Ohnoc, K. Fujimotoa, "Effective utilization of remote coal through dimethyl ether synthesis", Fuel 89, PP 229–234, 2000.
6. H.Erdener, A.Arinan, S.Orman, Hulya Erdener, Ayca Arinan, Sultan Orman, "Future Fossil Fuel Alternative Di-methyl Ether (DME) A Review", International Journal Of Renewable Energy Research, IJRER, Vol.1, No.4, PP.252-258, 2011.
7. D. D .Nagdeote, M. M. Deshmukh, "Experimental Study of Diethyl Ether and Ethanol Additives with Biodiesel-Diesel Blended Fuel Engine", International Journal of Emerging Technology and Advanced Engineering, Vol. 2, Issue 3, March 2012.
8. K.Rajkumar And P. Govindarajan, "Experimental Investigation of Oxygen Enriched air intake on Combustion Parameters of a Single Cylinder Diesel Engine", International Journal of Engineering Science and Technology Vol. 2(8), PP 3621-3627, 2010.
9. H. M. Patel, V. H. Chaudhari, S.A.Shah, "Design and Optimization of Fuel Injection System in Diesel Engine Using Biodiesel – A Review", International Journal of Innovations in Engineering and Technology (IJIET), PP 70-78, 2013.
10. Kitae Yeom, Jinyoung Jang, Jungseo Park and Choongsik Bae, "Liquefied Petroleum Gas and Dimethyl Ether Compression Ignition Engine", Korea Advanced Institute of Science and Technology.
11. Mark Sellnau, James Sinnamon, Kevin Hoyer, Harry Husted, "Gasoline Direct Injection Compression Ignition (GDCI) - Diesel-like Efficiency with Low CO2 Emissions", SAE International, 2011.
12. Kitae Yeom and Choongsik Bae, "Di-methyl Ether Homogeneous Charge Compression Ignition Engine with Gasoline Port Injection", Korea Advanced Institute of Science and Technology (KAIST).
13. Denis Gill, Josef Erhart, Ludwig Bürgler, "Characterizing Injection System Behaviour under Real Operating Conditions", AVL List GmbHeribert Kammerstetter, Manfred Werner,AVL Pierburg Instruments Flow Technology GmbH.
14. Yi Ren, Zuohua Huang, Haiyan Miao, Yage Di, Deming Jiang, Ke Zeng,Bing Liu, Xibin Wang, "Combustion and emissions of a DI diesel engine fuelled with diesel-oxygenate blends", Fuel 87,PP 2691–2697, 2008.
15. Shivaji Bhandarkar, "Vehicular Pollution, Their Effect on Human Heatlh and Mitigation Measures", Vehicle Engineering (VE), Volume 1, Issue 2, June 2013.
16. M. Loganathan, A. Anbarasu and A. Velmurugan, "Emission Characteristics of Jatropha - Dimethyl Ether Fuel Blends on A DI Diesel Engine", International Journal of Scientific And Technology Research Vol. 1, Issue 8, 2012.
17. Y. Ashok Kumar Reddy B. V. Appa Rao, "Experimental Investigations on the Engine Performance and Emission Characteristics of Indirect Injection (IDI) Diesel Engine using Preheated Jatropha Methyl Ester as Alternate Fuel", International Journal of Engineering Research and Technology (IJERT), Vol. 3 Issue 3, 2014.
18. T.G.Arul M Gokul S.Sasidhran S.Parthasarathi, "Emission Test on S.I Engine Using Alternative Fuels and Ethanol", IJSRD - International Journal for Scientific Research and Development, Vol. 2, Issue 09, 2014.

Proceedings of the Third International Conference on Sustainable Energy and Environmental Challenges (3rdSEEC)
18 –21 December, 2018, IIT Roorkee, India
SEEC No. 010

THERMAL PERFORMANCE ANALYSIS OF EARTH-AIR-PIPE-HEAT EXCHANGER SYSTEM WITH DIFFERENT BACKFILLING MATERIALS

Kamal Kumar Agrawal*
Mechanical Engineering Department,
Malaviya National Institute of Technology, Jaipur, India, kamal.rightway@gamil.com

Rohit Misra
Mechanical Engineering Department,
Government Engineering College, Ajmer, India,
rohiteca@gmail.com

Sandeep Parmar
Mechanical Engineering Department,
Malaviya National Institute of Technology, Jaipur, India, sandeepparmar1995@gmail.com

Ghanshyam Das Agrawal
Mechanical Engineering Department,
Malaviya National Institute of Technology, Jaipur, India, gdagrawal2@gmail.com

ABSTRACT

Earth-air-pipe-heat exchanger (EAPHE) is a promising passive technique for building heating and cooling, but it required long pipes for heat transfer to/from soil and large land area for installation of pipes. The required length of pipe can be reduced by improving thermal properties of soil at the vicinity of EAPHE pipe using different backfilling materials. The purpose of the present study is to compare the effect of different backfilling materials (different types of soils and industrial waste materials) on the performance of EAPHE systems. For this purpose, a laboratory scale experimental setup of EAPHE system (EAPHE simulator) has been developed and installed in a controlled environment. Four backfilling materials viz., native soil of Ajmer city, black soil, granite powder, and coarse particles of quartz have been considered for experimentation. It was observed that after 6 hours of continuous operation, the air temperature drop was of 9.1 °C for the native soil of Ajmer and 9.4 °C, 9.7 °C, 10.8 °C, for black soil, granite powder and coarse particles of quartz respectively.

Keywords: *EAPHE simulator, Backfilling materials, Air temperature drop, effectiveness, Pipe length*

1. INTRODUCTION

The earth-air pipe heat exchanger (EAPHE) system is geothermal energy based passive system which is used to produce heating effects in winter and cooling effects in summer. The sub-soil temperature at a depth of 3-4 from the earth's surface is almost constant all over the year and equivalent to the annual mean temperature of that location. This sub-soil at constant temperature can be used as heat source or sink.

In a typical EAPHE system, outdoor air is passed through the buried pipes and heat is exchanged between flowing air and subsoil. As a result, the temperature of the air at the outlet of EAPHE is considerably cool down in summer and get heated in winter. This outlet air from EAPHE system can be directly used for cooling in summer and for heating in winter season [1–4]. The working principle of EAPHE system is depicted in Figure 1.

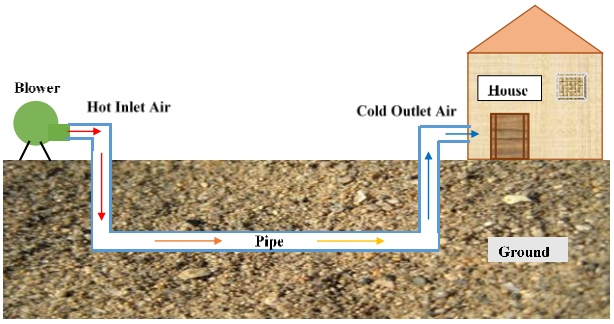

FIGURE 1: WORKING PRINCIPLE OF EAPHE SYSTEM [5]

EAPHE system is a promising passive technique for building heating and cooling, but it required long pipes for heat transfer to/from soil and large land area for installation of pipes. The required pipe length can be reduced by increasing heat transfer rate between air and soil, by enhancing soil thermal properties at the vicinity of the pipe. Thermal conductivity is the primary property of the soil, which influences the heat transfer and it mainly be governed by moisture content, mineralogical composition and density of the soil [6]. Soil thermal conductivity at the vicinity of buried pipe can be upgraded by increasing moisture in soil or by using thermally enhanced backfilling materials [7]. Therefore Efforts should be made to enrich the thermal properties of underground sub-soil.

Allan and Kavanaugh [8] utilized thermally enhanced backfilling material for ground-source heat pump (GSHP) system and found that by using thermally enhanced backfilling material, the required bore length can be reduced up to 37%. Cuny et al. [9] applied three kinds of coating soils (viz. in-situ earth soil, sand and, sand-bentonite mixture) at different parts of the buried EAPHE pipe and found that mixture of sand-bentonite coating provides better thermal performance compared to other two types of coating. Sipio et al. [10–12] used five types of thermally enhanced backfilling material (viz., sand 0-5 mm, sand 0-5 mm with 15% bentonite, fine sand 0-1 mm, fine sand 0-1 mm with 15% bentonite and sandy clay) in horizontal ground heat exchanger system to augment the heat transfer rate. The study revealed that the fine sand 0-1 mm with 15% bentonite provides best results. Elminshawy et al. [13] developed a laboratory scale EAPHE system for experimental study and evaluated the impact of soil compaction levels on performance of EAPHE system. From the experimental results, it was observed that the performance of EAPHE system improves by increasing compaction level of soil.

Literature shows that the thermal performance of a ground coupled heat exchanger may be improved by using thermally enhanced material at the vicinity of the buried pipe. However, very few experimental studies are available for analysing the effect of locally available backfilling materials on the performance of the ground heat exchanger system. Therefore, there is a necessity to experimentally investigate the impact of locally available backfilling materials on the overall performance of EAPHE system.

The primary objective of the current experimental investigation is to explore the effect of four different locally available backfilling materials *(*viz., native soil of Ajmer city, black soil, granite powder, and coarse particles of quartz) on the performance of EAPHE system by carrying out the experiments on laboratory scale experimental setup.

2. EXPERIMENTAL SET-UP

A laboratory scale experimental setup of EAPHE system was used to investigate the effect of different backfilling materials on the thermal performance of EAPHE system. The experimental set-up of EAPHE system was installed inside a room (dimension of 3m×3 m×3m) of the Mechanical Workshop at Government Engineering College, Ajmer, India.

The laboratory scale experimental set up has a soil container of dimension 2.4 m × 0.46 m × 0.46 m as shown in Figure 2(a). The soil container has two compartments in which two steel pipes of the inner diameter of 0.014 m and length 2.5 m each, installed parallel as shown in figure 2(b).

(A) EMPTY SOIL CONTAINER

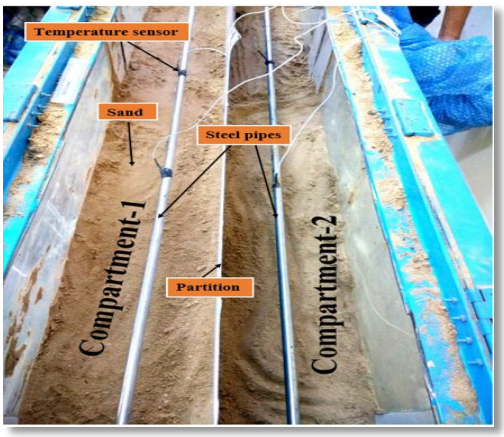

(B) SOIL CONTAINER WITH TWO COMPARTMENTS

FIGURE 2: SOIL CONTAINER FOR LABORATORY SCALE EAPHE SYSTEM

In both the compartments initially ordinary sand was filled up to the height of 13 cm from the bottom and after that a 10 cm layer of a backfilling material laid down in compartment-1, while another backfilling material filled in compartment-2.

After that RTDs (PT-100) sensors were installed in both the pipes at different locations (0 m, 0.6 m, 1.2 m, 1.8 m and 2.4 m from the inlet section of soil box) to measure the temperature of air along the length of pipes. Temperature sensors were also installed in the soil to measure the soil temperature variation with time. After the installation of the sensor, a layer of 10 cm thickness of a backfilling material was laid down in compartment 1, and similarly, a 10 cm thick layer of another backfilling material was laid down in compartment-2. After that, both the compartments were filled further with sand up to the top of the soil container. Finally, the air-pipes were connected with an air heater, and air blower and RTD sensors were linked with a data logger. The schematic of the laboratory scale experimental setup is depicted in Figure 3.

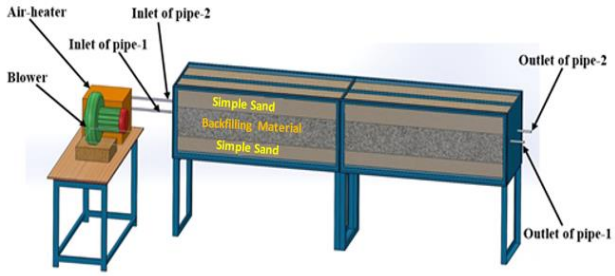

FIGURE 3: SCHEMATIC OF THE LABORATORY SCALE EXPERIMENTAL SETUP

3. EXPERIMENTAL PROCEDURE AND MEASUREMENT

Experimentations were carried out with different soil temperature (maintained by an air-conditioner unit in the room), different air inlet temperature (maintained by an air-heater with a variac) and with different velocity of air (maintained by a blower with a variac) but for the present study, only one set of the parameter has been considered. The present research is mainly based on a soil temperature of 26 °C, the inlet air temperature of 43 °C and inlet air velocity of 20 m/s.

The data has been recorded hourly basis, and the measurement and recording of hourly data included the temperature of the air at inlet and outlet of EAPHE pipes, the temperature of air in the buried pipes at three different locations and temperature of the soil at various locations. EAPHE system was operated for six hours and after that soil was allowed to get regenerated during the next 18 hours. Regeneration of soil was augmented by using an air conditioner, and this air-conditioning unit also helped to get the desired soil temperature. For experimentation, first of all, environmental air passed through the centrifugal blower and then it passed through an air heater box (for achieving desired air temperature) and then finally the air is supplied simultaneously through both the pipes of EAPHE system. Thermal performance of EAPHE system was evaluated in terms of temperature drop of air and effectiveness of EAPHE system.

Air temperature variation along the length of pipe of EAPHE system (with soil at 26 °C, constant inlet air temperature of 43 °C and velocity of 20 m/s) after 1 hour and 6 hours is presented in Table 1(A) and (B).

TABLE 1 (A) : VARIATION IN AIR TEMPERATURE ALONG THE LENGTH OF PIPE FOR FOUR DIFFERENT BACKFILLING MATERIALS AFTER 1 HOUR OF OPERTION

Section at length of pipe (m)	Air temperature (°C) after 1 hour of operation			
	Native soil of Ajmer	Black soil	Granite powder	Coarse particles of quartz
0	43.0	43.0	43.0	43.0
0.6	39.0	38.8	38.4	37.6
1.2	35.7	35.4	35.1	33.7
1.8	33.5	33.3	32.9	31.7
2.4	32.1	31.7	31.2	30.2

TABLE 1 (B) : VARIATION IN AIR TEMPERATURE ALONG THE LENGTH OF PIPE FOR FOUR DIFFERENT BACKFILLING MATERIALS AFTER 6 HOURs OF OPERTION

Section at length of pipe (m)	Air temperature (°C) after 6 hours of operation			
	Native soil of Ajmer	Black soil	Granite powder	Coarse particles of quartz
0	43.0	43.0	43.0	43.0
0.6	39.9	39.7	39.5	38.6
1.2	37.1	36.9	36.6	35.4
1.8	35.2	35.0	34.7	33.4
2.4	33.9	33.6	33.3	32.2

4. RESULTS AND DISCUSSION

From Table 1 it is observed that the drop in air temperature along the length of pipe is highest for coarse particles of quartz, and minimum for the native soil of Ajmer even after 6-hours of continuous operation.

From Table 1 and Figure 4, it is noticed that after 1-hour of continuous operation, the total air temperature drop of 10.9 °C is obtained at the exit of pipe (2.4 m length) for the native soil of Ajmer. However, for the coarse particles of quartz almost the same air temperature drops of 11.3 °C is obtained, at a pipe length of 1.8 m only. In the same way, it can also be seen that After 6 hours of continuous operation, the total air temperature drop of 9.1 °C is obtained at the exit of pipe (2.4 m length) for the native soil of Ajmer. However, for the coarse particles of quartz approximately same air temperature drops of 9.6 °C is obtained at a pipe length of 1.8 m only. Therefore it can be concluded that the required length of pipe of EAPHE system can be reduced by more than 25% by using coarse particles of quartz as backfilling material compared to native soil of Ajmer.

From table 1, it is also noticed that the other backfilling materials (black soil and granite powder) also giving better results compared to native soil of Ajmer. It is maybe because of the higher thermal conductivity of black soil,

granite powder and coarse particle of quartz than the native soil of Ajmer.

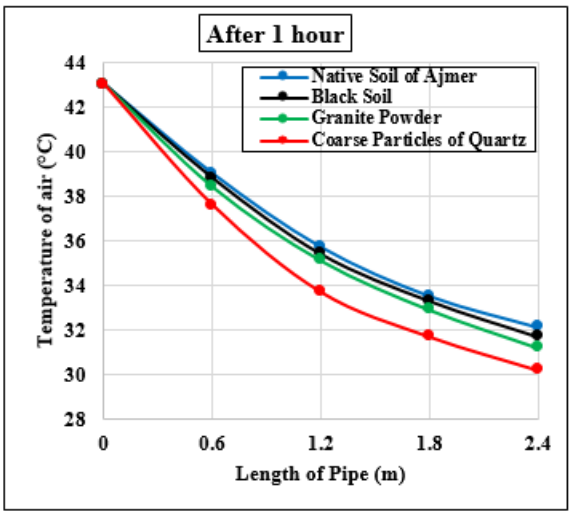

(A)

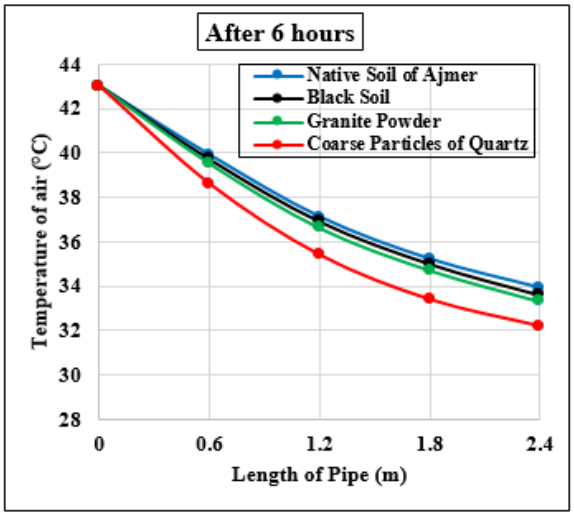

(B)

FIGURE 4: AIR TEMPERATURE VARIATION ALONG THE LENGTH OF PIPE FOR DIFFERENT BACKFILLING MATERIALS AFTER (A) 1 HOUR AND (B) 6 HOURS

Apart from the air temperature drop along the pipe length, thermal performance of EAPHE system can also be evaluated using temperature effectiveness of the EAPHE system. The effectiveness of an EAPHE system is defined as the ratio of actual temperature drop along the length of the pipe to the maximum possible temperature drop that can be obtained through pipes [14]. Following equations are used for calculation of effectiveness:

$$\varepsilon = \frac{T_{air,in} - T_{air,out}}{T_{air,in} - T_{wall,in}}$$

For the present study, the temperature effectiveness is calculated hourly basis and for that outlet air temperature is taken hourly, however, inlet air temperature, and pipe wall temperature (initial soil temperature) was considered constant 43 °C and 26 °C respectively. The obtained results of effectiveness are presented in graphical form in Figure 5.

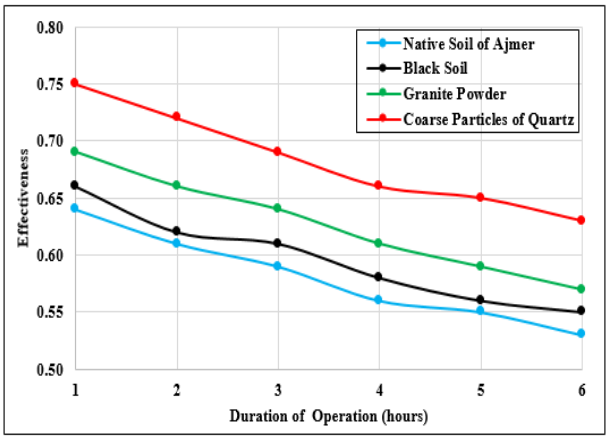

FIGURE 5: PLOT BETWEEN EFFECTIVENESS AND DURATION OF OPERATION

The average effectiveness of EAPHE system also calculated by considering average outlet temperature of air for 6 hours of operation and it was observed that the effectiveness of EAPHE system is highest with coarse particles of quartz (0.68), then followed by granite powder (0.63), black soil (0.60), and native soil of Ajmer (0.59).

5. CONCLUSION

In the present study, thermal performance of EAPHE system with four different backfilling materials has been investigated experimentally for cooling operation. Thermal performance of EAPHE system was assessed in terms of air temperature drop along the length of pipe and temperature effectiveness of EAPHE system. The primary outcomes and observations of the study are:

1. After 6-hours of continuous operation, the air temperature drop was 9.1 °C for the native soil of Ajmer and 9.4 °C, 9.7 °C, 10.8 °C, for black soil, granite powder and coarse particles of quartz respectively.
2. After 1-hour of continuous operation, the effectiveness of EAPHE system was 0.64, 0.66, 0.69, and 0.75 for the native soil of Ajmer, black soil, granite powder and coarse particles of quartz respectively. However, after 6-hours of continuous operation, the effectiveness of EAPHE system reduced, and it became 0.53, 0.55, 0.57, and 0.63 respectively.

3. Thermal performance of EAPHE system was better, when coarse particles of quartz used as a backfilling material, and it may be because of its higher thermal conductivity.
4. The required length of pipe of EAPHE system can be reduced by more than 25 % when coarse particles of quartz used as backfilling material, compared to native soil of Ajmer.
5. It is concluded that EAPHE system with thermally enhanced backfilling materials, can improve heat transfer rate between air & soil, and reduce the required length of pipe of EAPHE system, which able to reduces overall installation cost (pipe cost, excavation and refilling cost) of EAPHE system.

References:

[1] M.S. Sodha, A.K. Sharma, S.P. Singh, N.K. Bansal, A. Kumar, Evaluation of an earth-air tunnel system for cooling/heating of a hospital complex, Build. Environ. 20 (1985) 115–122.

[2] D.Y. Goswami, A.S. Dhaliwal, Heat Transfer Analysis in Environmental Control Using an Underground Air Tunnel, J. Sol. Energy Eng. 107 (1985) 141.

[3] M. Santamouris, G. Mihalalalou, C.A. Balaras, J.O. Lewis, M. Vallindras, A. Argiriou, Energy conservation in greenhouses with buried pipes, Energy. 21 (1996) 353–360.

[4] G. Mihalakakou, J.O. Lewis, M. Santamouris, On the heating potential of buried pipes techniques - Application in Ireland, Energy Build. 24 (1996) 19–25.

[5] K.K. Agrawal, M. Bhardwaj, R. Misra, G.D. Agrawal, V. Bansal, Optimization of Operating Parameters of Earth Air Tunnel Heat Exchanger for Space Cooling : Taguchi Method Approach, Geotherm. Energy. 6 (2018) 1–17. doi:10.1186/s40517-018-0097-0.

[6] K.K. Agrawal, R. Misra, T. Yadav, G.D. Agrawal, D.K. Jamuwa, Experimental study to investigate the effect of water impregnation on thermal performance of earth air tunnel heat exchanger for summer cooling in hot and arid climate, Renew. Energy. 120 (2018) 255–265. doi:10.1016/j.renene.2017.12.070.

[7] K.K. Agrawal, G. Das Agrawal, R. Misra, M. Bhardwaj, D.K. Jamuwa, A Review on Effect of Geometrical, Flow and Soil Properties on the Performance of Earth Air Tunnel Heat Exchanger, Energy Build. 176 (2018) 120–138. doi:10.1016/j.enbuild.2018.07.035.

[8] M.L. Allan, S.P. Kavanaugh, Thermal conductivity of cementitious grouts and impact on heat exchanger length design for ground source heat pumps, HVAC&R Res. 5 (1999) 85–96.

[9] M. Cuny, J. Lin, M. Siroux, V. Magnenet, C. Fond, Influence of coating soil types on the energy of earth-air heat exchanger, Energy Build. 158 (2018) 1000–1012. doi:10.1016/j.enbuild.2017.10.048.

[10] E. Di Sipio, D. Bertermann, M. Psyk, T. Popp, Improving thermal efficiency of horizontal ground heat exchangers, in: Eur. Geotherm. Congr. 2016 Strasbourg, Fr. 19-24 Sept 2016, 2016.

[11] E. Di Sipio, D. Bertermann, Influence of different moisture and load conditions on heat transfer within soils in very shallow geothermal application: An overview of ITER project, in: Proceedings, 42nd Work. Geotherm. Reserv. Eng. Stanford Univ. Stanford, California, Febr. 13-15, 2017 SGP-TR-212, 2017.

[12] E. Di Sipio, D. Bertermann, Factors Influencing the Thermal Efficiency of Horizontal Ground Heat Exchangers, Energies. 10 (2017) 1897. doi:10.3390/en10111897.

[13] N.A.S. Elminshawy, F.R. Siddiqui, Q.U. Farooq, M.F. Addas, Experimental investigation on the performance of earth-air pipe heat exchanger for different soil compaction levels, Appl. Therm. Eng. 124 (2017) 1319–1327. doi:10.1016/j.applthermaleng.2017.06.119.

[14] T.M. Yusof, H. Ibrahim, W.H. Azmi, M.R.M. Rejab, Thermal analysis of earth-to-air heat exchanger using laboratory simulator, Appl. Therm. Eng. 134 (2018) 130–140. doi:10.1016/j.applthermaleng.2018.01.124.

Proceedings of the Third International Conference on Sustainable Energy and Environmental Challenges (3rd SEEC)
18 –21 December, 2018, IIT Roorkee, India

SEEC **No.** 011

EFFECT OF SOIL MOISTURE CONTENTS ON THERMAL PROPERTIES OF SOIL FOR EARTH-AIR-PIPE HEAT EXCHANGER SYSTEM

Kamal Kumar Agrawal*
Mechanical Engineering Department,
Malaviya National Institute of Technology, Jaipur, India,
kamal.rightway@gamil.com

Rohit Misra
Mechanical Engineering Department,
Government Engineering College, Ajmer, India,
rohiteca@gmail.com

Ghanshyam Das Agrawal
Mechanical Engineering Department,
Malaviya National Institute of Technology, Jaipur, India,
gdagrawal2@gmail.com

Abstract:

Earth air pipe heat exchanger (EAPHE) system works well for a short period of operation, but for long continuous operation, its performance gets deteriorated due to thermal saturation of sub-soil in the vicinity of buried pipe. This thermal saturation problem is more prominent with the soil of poor thermal conductivity. The thermal conductivity of soil can be improved by adding the moisture into it, and soil thermal saturation problem in EAPHE can be resolved to a great extent. In the present study, the effect of moisture contents on the thermal properties of soil is measured, and its impact on the thermal performance of EAPHE system is studied. For this purpose, soil samples with different moisture contents (0-30% volumetric water content) were tested in the laboratory, and the thermal properties of soil have been determined with the help of Thermal Constants Analyser (Hot Disk TPS-500). It is observed that by increasing the soil moisture content, the thermal conductivity of soil initially improves at a high rate and after that the rate of improvement diminishes. By increasing moisture contents of soil from 0 to 30%, the thermal conductivity of soil increased up to 236 %. Moreover, the heat transfer rate of EAPHE system increased up to 28.6 %.

Keywords: *EAPHE, Soil moisture content, Specific heat, Thermal conductivity, Thermal Diffusivity.*

1. INTRODUCTION

Soil temperature at the ground surface fluctuates diurnal as well as seasonal. However this soil temperature fluctuation reduces rapidly with increasing depth from the surface of the ground and becomes negligible at a depth of 3-5 m, and at this depth, the soil temperature becomes almost stable [1–3]. This undisturbed temperature of underground soil is equal to the average ambient temperature at that latitude [4], and this undisturbed soil temperature is always lower than that of the outside temperature in summer, whereas higher during the winter. When pipes are buried at this depth and ambient air flows through these underground buried pipes, the air gets cooled in summer and heated in winter. Thus this system is called earth-air-pipe heat exchanger (EAPHE) system. The schematic of an EAPHE system for summer cooling operation is shown in Figure 1.

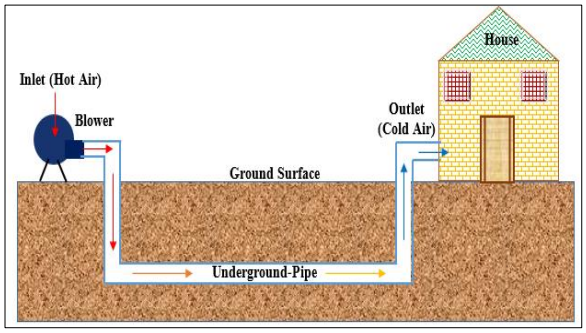

FIGURE 1: SCHEMATIC DIAGRAM OF AN EAPHE SYSTEM FOR SUMMER COOLING OPERATION

Various researchers noticed that the thermal performance of ground heat exchanger systems highly depends on thermal conductivity of sub-soil, and it predominantly depends on moisture contents in soil [5]. Leong et al. [6] assessed the influence of soil moisture content on the performance of ground source heat pump and found that the COP of system increased up to 35% by increaeing soil moisture from 0 to 12.5 % degrees of saturation.

In the literature, few studies are available in which the impact of soil moisture content on EAPHE system performance has been considered. The primary objective of the present work is to measure experimentally thermal properties of local soil (soil of Ajmer city) with different soil moisture contents and then evaluate its impact on the thermal performance of EAPHE system. For this purpose, a Hot Disk TPS-500 apparatus has been used to measure the soil thermal properties, and a simulation study is carried out to evaluate the impact of different soil properties on the thermal performance of an EAPHE system.

2. MATERIALS AND METHODS

For the measurement of soil thermal properties with different soil moisture contents, a Thermal Constants Analyser (Hot Disk TPS-500 apparatus) has been used in

Tribology lab, MNIT-Jaipur, India. The Hot Disk equipment depend on on the transient plane source (TPS) method, and this can measure thermal conductivity, volumetric heat capacity, and thermal diffusivity simultaneously in the range of 0.03 to 100 W/m-K (accuracy 2%) , 0.10 to 4.5 MJ/m^{3}K (accuracy 12 %) , 0.02 to 40 mm^2/sec (accuracy 10 %) respectively [7].

2.1 Sample Preparation

For the present study, the soil is collected from the test site of Ajmer (loamy-sand), and then it passes through a 600-micron sieve, and this filtered soil has been used to prepare test samples. Seven sets of test samples were made with different moisture contents.

For each set of the test sample, 80 gram of soil was taken, and water was added in the soil according to the requirement of sample set (for each set of sample different volumetric percentage of water was added), and then water was mixed with soil properly. After that with the help of a cylindrical cup of plastic, two cylindrical soil samples, (as shown in Figure 2) were made for each set of test. Each soil sample has a diameter of 2.5 cm and height of 2 cm. For the moisture measurement in soil samples, the Gravimetric method has been used. For the test set-1(i.e. dry soil, 0% moisture), the soil samples were made oven dry before the test.

FIGURE 2: SNAPSHOT OF CYLINDRICAL SOIL SAMPLES

2.2 Test Procedure

For the measurement of thermal properties, electrically conducting metallic (nickel) sensor with insulating layers (Kapton insulated sensor) is positioned between two pieces of the sample (as shown in Figure 3) and a light pressure applied on top sample piece to ensure good contact between sample and sensor.

Then input experiment parameters are given to the software. Sample identity, sensor type and radius, available probing depth, measurement time, measurement temperature and heating power are the main input parameters. For the present study, probe depth was 4-6 mm, the sensor was Kapton insulated sensor with 3.189 mm radius, measurement temperature was 33 ^{o}C, measurement time was 10 sec and heating power was 200 mW. After that, a baseline temperature drift is checked before the experiment, and required correction is applied, then run the test and after that, a graph between temperature increases v/s time is plotted, from which thermal conductivity is derived [8]. For each set of samples, three repetitive measurements have been taken at the room temperature.

In Hot Disk Transient Plane Source (TPS) Technique, when the electric current passes through the sensor, its temperature increases and concurrently, the temperature resistance (function of time) is measured. Therefore, the sensor functions as a heat source and a dynamic temperature sensor [9].

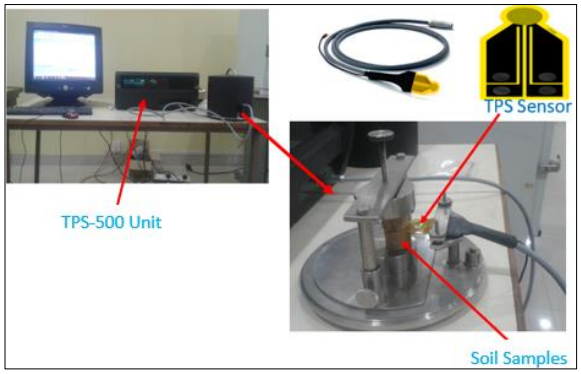

FIGURE 3: TPS-500 UNIT WITH SENSOR AND SOIL SAMPLES

2.3 Experimental Results

Thermal properties of seven test samples of soil with different moisture contents have been measured using TPS-500 apparatus. The obtained thermal properties of tested soil samples are presented in Table 1 and Figure 4.

TABLE 1: MEASURED THERMAL PROPERTIES OF SOIL WITH DIFFERENT MOISTURE CONTENTS

Soil Type	Conductivity (W/m-K)	Sp. Heat (MJ/m^{3}K)	Diffusivity (mm^2/sec)
$Soil_1$ (Dry soil)	0.5	0.97	0.52
$Soil_2$ (Soil with 5% moisture)	0.9	1.18	0.76
$Soil_3$ (Soil with 10% moisture)	1.18	1.38	0.85
$Soil_4$ (Soil with 15% moisture)	1.36	1.57	0.86
$Soil_5$ (Soil with 20 % moisture)	1.52	1.74	0.87
$Soil_6$ (Soil with 25% moisture)	1.62	1.93	0.84
$Soil_7$ (Soil with 30% moisture)	1.68	2.13	0.79

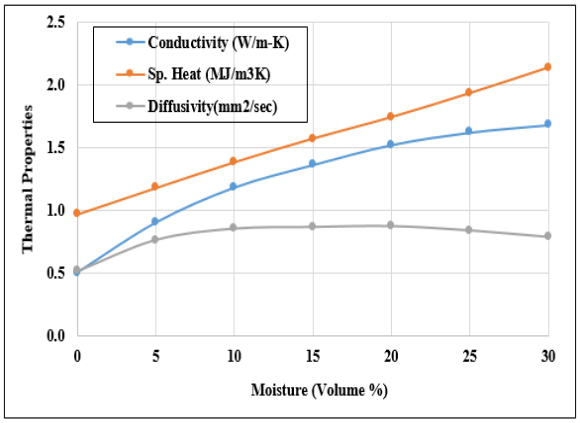

FIGURE 4: VARIATION OF SOIL THERMAL PROPERTIES WITH MOISTURE CONTENTS

2.4 Validation of Measured Results

For the reliability of the measurements results, the measured thermal conductivity is compared with literature values [10–14], and the experimental results of soil with different moisture contents found good agreement with literature results.

3. EFFECT OF SOIL THERMAL CONDUCTIVITY ON THE PERFORMANCE OF EAPHE SYSTEM

For the evaluating the effect of soil thermal properties on EAPHE system, a published [15] three-dimensional CFD simulation model (with ANSYS FLUENT environment) of the EAPHE system has been considered. For the simulation study, a straight EAPHE pipe of length 30 m and diameter of 0.1 m was taken, and the control volume of EAPHE system was defined by generating a cylindrical volume of soil around the pipe with 1 m diameter.

For the EAPHE system performance evaluation, total seven cases were run, and the thermo-physical properties of air, PVC pipe and soil for these cases is presented in Table 2.

TABLE 2: THERMO-PHYSICAL PROPERTIES OF MATERIALS USED FOR SIMULATION

Material	Density (kg/m^3)	Specific heat (J/kg-K)	Thermal conductivity (W/m-K)
Air	1.22	1006	0.02
PVC pipe	1380	900	0.16
$Soil_1$ (Dry soil)	1550	625	0.50
$Soil_2$ (Soil with 5% moisture)	1600	736	0.9
$Soil_3$ (Soil with 10% moisture)	1650	838	1.18
$Soil_4$ (Soil with 15% moisture)	1700	924	1.36
$Soil_5$ (Soil with 20 % moisture)	1750	994	1.52
$Soil_6$ (Soil with 25% moisture)	1800	1072	1.62
$Soil_7$ (Soil with 30% moisture)	1850	1153	1.68

For 6 hours of continuous operation, the inlet air temperature (Ti) and velocity was taken 319.35 K and 5 m/s respectively however initial soil temperature were considered 300 K. The result obtained after 6 hours of continuous operation in terms of outlet air temperature (To) and heat transfer rate (Q), are presented in Table 3.

TABLE 3: OUTLET AIR TEMPERATURE AND HEAT TRANSFER RATE IN EAPHE SYSTEM AFTER 6 HOURS OF OPERATION

	Outcomes of Simulation study		
Soil Samples	**Ti (K)**	**To (K)**	**Q (Watt)**
$Soil_1$ (Dry soil)	319.35	306.05	627.04
$Soil_2$ (Soil with 5% moisture)	319.35	304.37	707.45
$Soil_3$ (Soil with 10% moisture)	319.35	303.42	752.92
$Soil_4$ (Soil with 15% moisture)	319.35	302.96	774.94
$Soil_5$ (Soil with 20 % moisture)	319.35	302.64	790.26
$Soil_6$ (Soil with 25% moisture)	319.35	302.44	799.83
$Soil_7$ (Soil with 30% moisture)	319.35	302.3	806.53

4. RESULTS AND DISCUSSION

Table 1 and 3 shows that by increasing the soil moisture contents from 0 % to 10 %, the thermal conductivity of soil is increased by 136 %, and heat transfer rate in EAPHE system is increased by 20 %, however, by increasing the soil moisture contents from 10 % to 20 %, the thermal conductivity of soil is increased only by 28.8 %, and heat transfer rate in EAPHE system is increased only by 5 %. Furthermore, by increasing the soil moisture contents from 20 % to 30 %, the thermal conductivity of soil is increased only by 10.5 % and heat transfer rate in EAPHE system is increased only by 2 %.

When the moisture contents increases in the soil, the thin water films bridged the voids present in the soil, which subsequently increases the contact area between the soil particles hence, the heat flow and thermal conductivity of soil improve. However, after a certain limit of soil moisture content, the thermal conductivity of soil not increases because the voids in the soil get completely filled with water.

5. CONCLUSION

In the present study, the thermal properties of the soil with different moisture contents have been measured experimentally and the measured value of the soil is used for the evaluating the effect of soil moisture contents on

thermal performance of EAPHE system. The key outcomes and observations of the study are:

1. It is observed that the soil thermal properties are very sensitive to the soil moisture contents.
2. By increasing the soil moisture contents, the thermal conductivity of soil at first increases rapidly but beyond 10 % of moisture content, the rate of the increase becomes slow, and after 20 % of moisture contents it becomes very low (almost negligible).
3. By increasing soil moisture contents from 0% to 10 %, the heat transfer rate in EAPHE system increased by 20 %, however it increases 5 % only when soil moisture contents increases from 10 % to 20 %, Furthermore, it increases 2 % only, by increasing soil moisture contents from 20 % to 30 %.
4. It is concluded that EAPHE system with moist soil, can improve the heat transfer between air & soil. However, it is reasonable to increase soil moisture contents up to 20 % only.

REFERENCES

[1] S.S. Bharadwaj, N.K. Bansal, Temperature distribution inside ground for various surface conditions, Build. Environ. 16 (1981) 183–192.

[2] N.K. Bansal, M.S. Sodha, S.S. Bharadwaj, Performance of earth air tunnels, Energy Res. 7 (1983) 333–345.

[3] T. Kusuda, P.R. Achenbach, Earth temperature and thermal diffusivity at selected stations in the United States, (No. NBS-8972). National Bureau of Standards Gaithersburg MD, 1965.

[4] C.O. Popiel, J. Wojtkowiak, B. Biernacka, Measurements of temperature distribution in ground, Exp. Therm. Fluid Sci. 25 (2001) 301–309. doi:10.1016/S0894-1777(01)00078-4.

[5] M. Habibi, A. Hakkaki-Fard, Evaluation and improvement of the thermal performance of different types of horizontal ground heat exchangers based on techno-economic analysis, Energy Convers. Manag. 171 (2018) 1177–1192. doi:10.1016/j.enconman.2018.06.070.

[6] W.. Leong, V.. Tarnawski, A. Aittomäki, Effect of soil type and moisture content on ground heat pump performance, Int. J. Refrig. 21 (1998) 595–606. doi:10.1016/S0140-7007(98)00041-3.

[7] Thermtest, Instruction manual, Hot Disk TPS-500, 2009. http://www.thermtest.com/tps-500.

[8] Thermtest Thermophysical Instruments, Hot Disk Transient Plane Source (TPS) Technique-Intruction Manual, 2014.

[9] M.A. Pagola, R.L. Jensen, S. Madsen, S.E. Poulsen, Measurement of thermal properties of soil and concrete samples. Aalborg: Aalborg University. Department of Civil Engineering. DCE Technical Reports, No. 235, 2017.

[10] O. Johansen, Thermal Conductivity of Soils, 1977. doi:10.1063/1.1699752.

[11] S. Lu, T. Ren, Y. Gong, R. Horton, An Improved Model for Predicting Soil Thermal Conductivity from Water Content at Room Temperature, Soil Sci. Soc. Am. J. 71 (2007) 8–14. doi:10.2136/sssaj2006.0041.

[12] S. Nikoosokhan, H. Nowamooz, C. Chazallon, Effect of dry density, soil texture and time-spatial variable water content on the soil thermal conductivity, Geomech. Geoengin. 11 (2016) 149–158. doi:10.1080/17486025.2015.1048313.

[13] B. Tong, Z. Gao, R. Horton, Y. Li, L. Wang, An Empirical Model for Estimating Soil Thermal Conductivity from soil water content and porosity, J. Hydrometeorol. 17 (2016) 601–613. doi:10.2136/sssaj2014.05.0218.

[14] J. Côté, J. Konrad, A generalized thermal conductivity model for soils and construction materials, Can. Geotech. J. 42 (2005) 443–458. doi:10.1139/T04-106.

[15] K.K. Agrawal, M. Bhardwaj, R. Misra, G.D. Agrawal, V. Bansal, Optimization of Operating Parameters of Earth Air Tunnel Heat Exchanger for Space Cooling : Taguchi Method Approach, Geotherm. Energy. 6 (2018) 1–17. doi:10.1186/s40517-018-0097-0.

SEEC No. 013

COMPUTATIONAL SIMULATION OF DOMESTIC BURNER WITH DIFFERENT FUELS AND VARYING BORES GEOMETRY

Harishchandra Dhumal*, Amardeep Dongare*

***Students, B.Tech, Mechanical Engineering**

Department of Technology,

Shivaji University, Kolhapur.

harishdhumal6@gmail.com

amardongare3996@gmail.com

Nikhil Raut[1], Ajit Kolekar[2]

[1 2]Assi.Prof.Mechanical Engineering.

Department of Technology,

Shivaji University, Kolhapur.

nikhilraut44@gmail.com

abk_tech@unishivaji.ac.in

Corresponding Author: - harishdhumal6@gmail.com

ABSTRACT

In today's developing world, energy resources have got a great value, but the biggest problem is their depletion with time. Hence the proper and wise use of these energy resources is very essential. In this paper we have worked to enhance the efficiency of the domestic burners using computational simulation. It has been stated by Bureau of Indian Standards (BIS) 4246:2002 that the efficiency of these conventional burners (CB) is 64%, but its efficiency under critical condition found is 52%. Hence the efficiency of the domestic burner could be increased by a considerable percentage. Thus efficiency can be enhanced by a) changing fuel (LPG and biogas) and their composition b) complete combustion of the fuel used by proper air-fuel mixture ratio (A/F ratio) with appropriate speed of the fuel ejecting from cylinder and c) the transfer of the heat from combustion region to its useful region which can be achieved by modifying the design of the bores of the burner and using the proper height of the pan support. This can be achieved by changing the geometry of the bore from cylindrical to conical with varying diameters. Results are obtained by simulation with these geometries using software ANSYS 15.0. The highest efficiency obtained by varying these geometries is 54%, which is higher than the critical condition efficiency. We have obtained this efficiency by simulating the various parameters on ANSYS Fluent 15.0. Thus increased efficiency will save fuel as well as help in improving economy of rural India, since it is the primary energy source for domestic uses in the rural parts of India.

Keywords: Simulation, Domestic burner, bore geometry, efficiency, ANSYS 15.0

SEEC No. 014

REMOVAL OF ARSENIC BY ADSORPTION USING NEEM LEAVES (AZADIRACHTA INDICA)

Sonam Tantuvoy
Department of Civil Engineering/
Water and Environment Division
National Institute of Technology,
Warangal - 506004, India
Research Scholar
Email: sonam.edu24@gmail.com

Dr. P Hari Prasad Reddy
Department of Civil Engineering/
Water and Environment Division
National Institute of Technology,
Warangal 506004, India
Associate Professor
Email: ponnapuhari@gmail.com

ABSTRACT

The measurement of inorganic arsenic in the environment has received ample and serious attention over the past several years due to its persistence and presence in the ground water. Among the various removal technologies, adsorption is a relatively simple and efficient. The proposed work is concerned for the cost effective arsenic removal using waste matured neem leaves. In this study neem leaves adsorbent was prepared for removing arsenic from the synthetically prepared solution. FTIR and XRD techniques were used to characterize the structure of the neem leaves powder (NLP) and to track the functional group present on its surface. The removal of arsenic was investigated at 5mg/l concentration using batch studies. The particle size of 300µm was considered for all the experiments. Batch experiments indicated that the time to attain equilibrium was 1h, optimum pH was 7, and optimum dosage was 0.5 g. The percentage removal efficiency of NLP was recorded as 82%. Adsorption isotherms were applied to the experimental results. The adsorption data fitted well to the D-R isotherm. Kinetic studies were carried out using Lagergren Pseudo-First Order model and Pseudo Second-Order model. And the adsorption mechanism was better explained by pseudo II-order kinetics.

Keywords: Adsorption; Neem leaves powder (NLP); Batch study; Adsorbent; Kinetics; Isotherms.

INTRODUCTION

Heavy metals present in the wastewater causes ill effects on all forms of life when discharged directly to the environment by anthropogenic activities/sources. It can be recovered from municipal wastewater and industrial effluents. The untreated effluents discharged from industries are highly toxic and percolates into the surface and ground waters. Arsenic is also known as king of the poisons and is one of the WHO's top 10 chemicals concern for deadly diseases. Arsenic contamination in groundwater is a major problem because ground water is the chief source of drinking water supply in many regions. It is reckoned that umpteen lives of people in Bangladesh are at menace of being exposed to arsenic concentrations higher than the stated WHO guidelines (10µg/L) as well as the National standard level (50µg/L) [12]. Arsenic levels can be lethal for human well-being for long term exposures and can cause extreme adverse health effects which includes cardiovascular, respiratory, gastrointestinal, mutagenic, genotoxic and carcinogenic effects.

Widely available techniques for the heavy metals eviction from groundwater are ineffective and uneconomic. Therefore there is an urgent need that, all possible optimum conditions for arsenic removal should be explored and their feasibility should be studied in detail. This has triggered the search for simple and economically viable alternatives such as adsorption. In a nutshell adsorption techniques are promising for pollutant removal from the industrial effluents and wastewater. Thus, this work is propounded to study the adsorption behavior of bioadsorbent alike neem leaves for the arsenic removal from the synthetically prepared solution [6,7,10].

MATERIALS AND METHODS

The motive of the present work is conversion of bio-material like Neem leaves into adsorbent, it's characterization and study of utility of neem leaves for adsorbing arsenic from the synthetic solution.

For the adsorbent preparation matured neem leaves were obtained from the NIT Warangal campus. These leaves were douched with water for cleaning dust and water soluble impurities and were dried subsequently under the sun. Futher neem leaves were oven dried at 60 ºC, for 24 hours till leaves turned to pale yellow. The leaves were grounded in the grinding mixer and sieved to different (300, 450, 600µm) size fractions. In addition to this neem leaves powder (NLP) adsorbent was preserved in glass bottles for further study as shown in Figure 1.

Characterization has been done using FTIR (Fourier transform infra-red Analysis) and XRD (X-Ray diffraction Analysis).
The investigations were carried out using batch studies, adsorption isotherm analysis and kinetic studies.

Characterization of the adsorbent

For the characterization purpose FTIR (Fourier transform infra-red Analysis) and XRD (X-Ray diffraction Analysis) were utilized. FTIR measurements for the NLP exhibited the presence of variety of functional groups as shown in Figure 2 and 3 which is in congruence with the presence of several elements on the surface of Neem leaves. Moreover, it was carry forwarded that when NLP are oven dried at different temperatures of 60ºC and 100ºC, there was no considerable change noticed in its intensity and peak distribution of FTIR spectra which showed that surface structure of the NLP particles stayed stable even at higher temperature.
The XRD patterns of NLP are shown in Figure 4 and 5 before and after the treatment respectively. A number of Bragg reflections with 2θ values of 26.5º, and 39º for neem were observed. Different peaks were observed which hints the distance between hydrogen-bonded sheets in cellulose. Two broad peaks at 15 º and 31º were observed which are associated with monoclinic unit cell and cellobiose units of the cellulose respectively in. Arsenoroesslerite compound is formed after adsorption process at peaks 26.5º and 49º.

Batch Study

Batch study was panned out to know the potential influencing factors like contact time, pH and amount of adsorbent dosage. Solutions were prepared synthetically in each 250 mL volumetric flasks, of known concentrations varied in the range of 5 to 25 mg/L with a known amount of adsorbent. The solutions were kept in orbital shaker for different time periods succeeded by filtration process through whatmann Filter Paper No. 42 and then the quantitative analysis of adsorbed arsenic was done by ICP-OES (Inductively Coupled Plasma Optical Emission Spectrometry).

RESULTS AND DISCUSSIONS

Effect of contact time

Arsenic removal was done from the aqueous solution for contact time ranging from 30-240 min with 5mg/L of initial metal ion concentration, pH 7, adsorbent dosage of 0.5 g/100mL at 150 rpm speed to determine the equilibrium time. Time required for adsorbate concentration to attain a stable curve which is also known as equilibrim time was obtained by plotting graph between % removal of arsenic versus different contact times as shown in Figure 6. It indicated that percentage removal of the metal ion increased with an increase in the contact time until equilibrium was reached and these values increased progressively from 69% to 82% as a function of contact time from 30 to 60 minutes. In the beginning, degree of adsorption was high because vacant sites were present on the adsorbent's surface [1-3]. Increase in contact time subsequently shows the percentage removal of arsenic remains constant (81%), indicating equilibrium was reached at 60 minutes only.

Effect of pH

To bring forward the pH effect in the present investigation, adsorption of arsenic by NLP was studied with metal ion concentration of 5mg/L having adsorbent dosage of 0.5g/100mL at agitation speed of 150 rpm by pH variation of metal solution from 1 to 9. The percentage removal versus pH effect on the adsorption of arsenic by NLP is displayed in the Figure 7. Arsenic removal was amplified as pH approaches to 7 and subsequently decreased from 7 to 9 showing the maximum value at pH 7. The increased % removal of arsenic was observed when pH ranges 5 to 7, the reason may be attributed to the fact that adsorption increase with the decrease in acidity. When pH is low, arsenic ions gets tough competition for the adequate sites on the adsorbent surface. Thereupon pH reached to 7, the hydrogen ions were almost got finished ,hence high amount of arsenic ions got adsorbed on the NLP adsorbent. Therefore the value reduced from 82% to 78.3% again when pH reached beyond 7. The major reason for this is the electrostatic interaction. High interaction results in intense adsorption process [5,7-9].

Effect of Adsorbent Dose

Arsenic adsorption process is further figured out with varying dosages of NLP adsorbent from 0.3 to 1.5 g/100mL by fixing other parameters (pH, contact time and agitation speed) constant. The variations in percentage removal and adsorption capacity of arsenic on NLP with different adsorbent dose are presented in Figure 8. The removal efficiency of arsenic improved from 73.5% to 89.93% on increasing adsorbent dosage from 0.3 to 1.0 g/100mL, whereas adsorption capacity was decreased by 1.23 to 0.45 mg/g. The maximum removal efficiency at the dosage of 1gm/100mL can be attributed to the fact that more dosage of the adsorbent provides more availability of exchangeable sites [2,6,8]. Furthermore, from the Figure 8, it can be observed that there is no significant increase in adsorption with increase in adsorbent dosage from 1.0g/100mL to 1.5g/100mL. With increasing adsorbent dose beyond 1 g/100mL ,adsorption process decreases which may be attributed to overlapping of adsorption sites because of too many adsorbent particles. As the removal efficiency is 82% so based on this 0.5g/100mL can be taken as the optimum adsorbent dose.

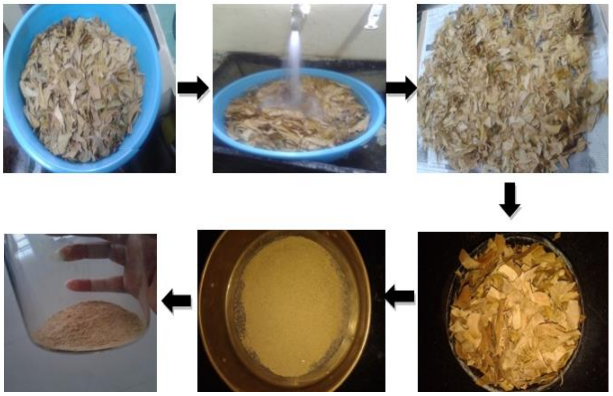

FIGURE 1. Preparation of adsorbent

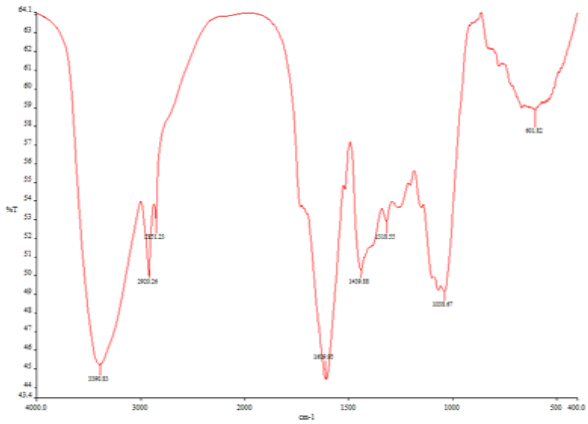

FIGURE 2. NLP (at 60ºC) sample analysed in FTIR

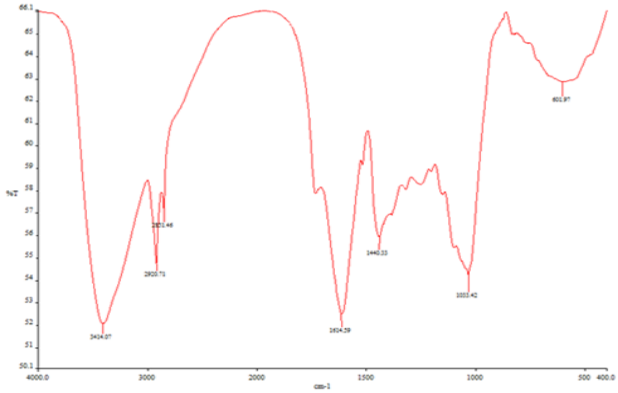

FIGURE 3. NLP (at 100ºC) sample analysed in FTIR

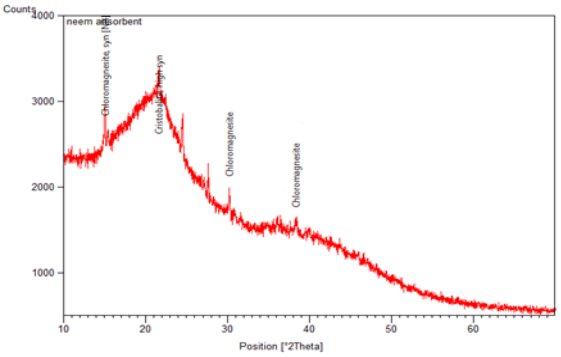

FIGURE 4. NLP analysed in XRD instrument before treatment

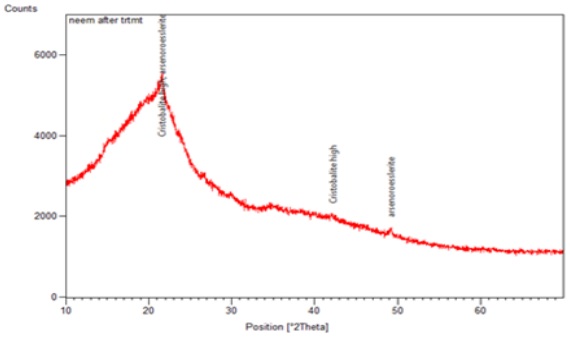

FIGURE 5. NLP analysed in XRD instrument after adsorption process

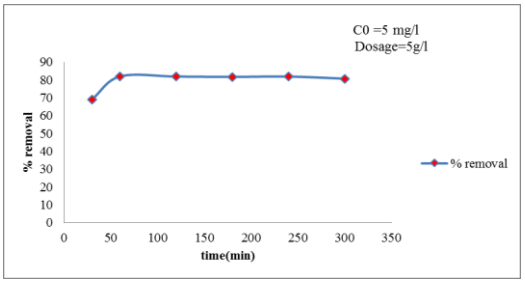

FIGURE 6. Variation of contact time on adsorption of arsenic by NLP.

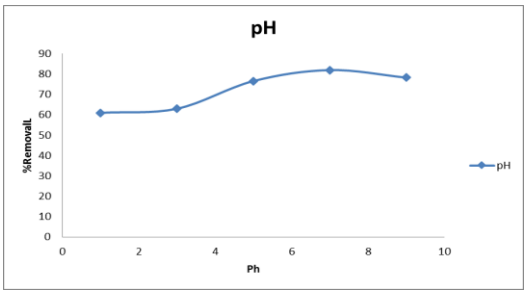

FIGURE 7. pH effect on the arsenic adsorption by NLP.

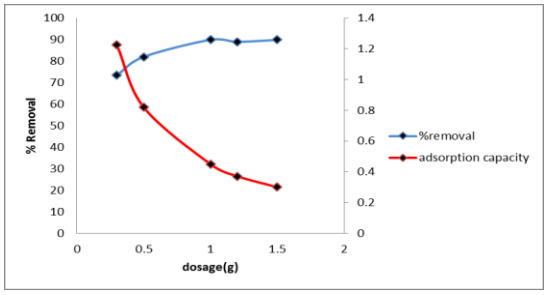

FIGURE 8. NLP adsorbent dosage effect on the arsenic adsorption

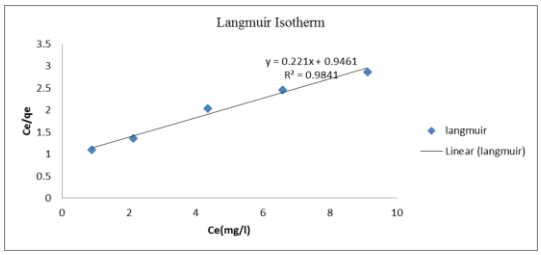

FIGURE 9. Langmuir isotherm for arsenic adsorption

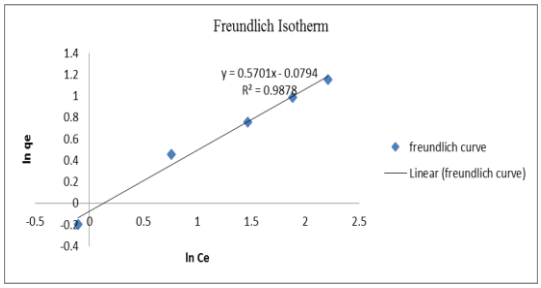

FIGURE 10. Freundlich isotherm for arsenic adsorption

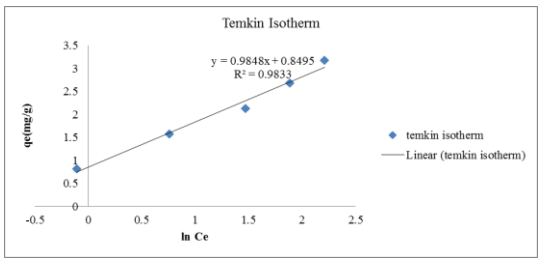

FIGURE 11. Temkin isotherm for arsenic adsorption

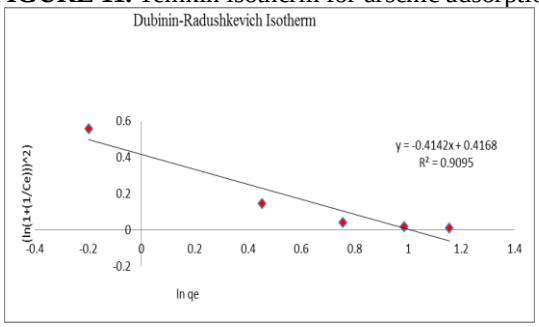

FIGURE 12. Dubinin-Radushkevich Isotherm for arsenic adsorption by NLP.

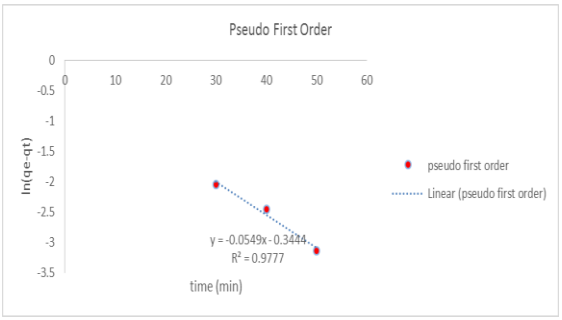

FIGURE 13. Pseudo first order kinetics for arsenic adsorption

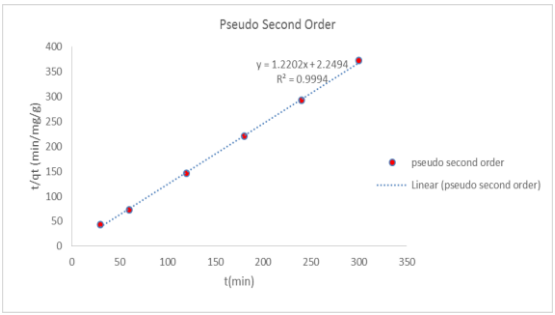

FIGURE 14. Pseudo second order kinetics for arsenic adsorption

ADSORPTION ISOTHERMS

The present equilibrium sorption studies of the arsenic metal ion on the NLP was performed to quantify the rate of reaction under different experimental conditions.

Langmuir Isotherm

A graph between C_e/q_e and C_e has been plotted as shown in Figure 9. This curve gives the constants Q_0 and K_L which indicates slope and intercept respectively. Langmuir adsorption capacity 'Q_0' has been calculated from the graph which has a value of 4.525 mg/g and the Langmuir adsorption intensity 'K_L' has a value of 0.2335 L/mg. Futhermore coefficient of determination 'R^2 = 0.9841' value proves that it is in congruence with the experimental values. In addition , we have one more chief parameter R_L which is a dimensionless constant also known as separation factor, it indicates the affinity between the sorbate and sorbent.The R_L values between 0 and 1 supports favourable adsorption process. Here the R_L value was computed as 0.461, indicating that adsorption of the arsenic metal ion onto NLP is conducive.

Freundlich isotherm

A graph between ln q_e and ln C_e has been plotted as shown in Figure 10. This curve gives the constants n and K_f which indicates the slope and intercept respectively. The Freundlich isotherm constant 'n' changes with the degree of heterogeneity and K_f is the relative adsorption capacity which is manifestion of bonding energy. Moreover the slope of 1/n ranging from 0 to 1 reveals surface

heterogeneity or adsorption intensity. It hitns heterogeneous nature of the adsorbent as its value approaces to zero. The values of 'n' amidst 1 to 10 showcase conducive adsorption process. The arsenic values observed from the Freundlich curve gave maximum adsorption capacity (K_f) of 0.9236 mg/g. The affinity value (n) was found equal to 1.754 and the value of 1/n = 0.5701 indicating that the sorption of arsenic onto NLP is favourable . The correlation factors R^2 value is 0.9878 for Freundlich model, which shows relevancy between theoretical models and experimental outcomes presented in the study.

Temkin Isotherm

A graph between q_e and ln C_e has been plotted as shown in Figure 11. This curve gives the constants B and K_T which indicates the slope and intercept respectively. Further temkin isotherm constant 'B' has been calculated from the graph which has a value of 0.9848 and the Temkin adsorption potential 'K_T' has a value of 2.3693 L/mg.

Dubinin-Radushkevich Isotherm

A graph between $(\ln(1+1/C_e))^2$ and ln q_e has been plotted and shown in Figure 12. This curve gives the constants B_D and q_D which indicates the slope and intercept respectively. The constant 'B_D' is associated to the mean free energy of sorption per mole of the sorbate and has been calculated from the graph has a value of 6.658E-08 and the theoretical isotherm saturation capacity 'q_D' has a value of 1.5170 (mg/g).

ADSORPTION KINETICS

The adsorption kinetic parameters are useful for giving the adsorption rate which is of paramount importance for the modelling and designing purpose. In the present investigation pseudo first-order and pseudo second-order kinetic model were used.

Pseudo First Order Kinetic Model

The kinetics of arsenic adsorption onto NLP was analysed using pseudo first order kinetics model. The present experiment has been done at a concentration of 5 mg/L at different time intervals for 0.5g/100mL dosage of NLP at 150 rpm. Graphs are drawn between $\ln(q_e-q_t)$ and time 't' as shown in Figure 13. The coefficient of correlation was found to be 0.9777 which proves that pseudo first order kinetic was relevant for arsenic removal by NLP as an adsorbent.

Pseudo Second Order Kinetics

The pseudo second order kinetics was computed by plotting t/q_t versus t graph as shown in Figure 14. The obtained value of coefficient of correlation was 0.9994 which indicates that the pseudo II-order kinetic is well fitted.

CONCLUSION

Thus coupled with the literary evidence following conclusions can be made for the suitability of Neem leaf powder (NLP) as an adsorbent:

i. NLP is proved to be an efficacious adsorbent for arsenic removal.
ii. The Contact time, pH of the medium and adsorbent dosages influence the adsorption process.
iii. There are huge number of polar and non-polar functional groups on the adsorbent surface of NLP and few of these have strong binding property of forming strong chemisorptive bonds.
iv. From batch studies optimum conditions for arsenic uptake capacity were found as, pH of the solution 7, adsorbent dosage of 0.5 g adsorbent/100 mL and contact time of 1h.
v. NLP has been found potential adsorbent for capturing the arsenic from the synthetic solution with efficiency of 82 %.
vi. The data fitted well with Dubinin-Radushkevich isotherm indicating favourable conditions of adsorption.
vii. The study of adsorption kinetics unfolded that the pseudo second order kinetic model fitted well to the adsorption process.

ACKNOWLEDGMENTS

The authors extend sincere thanks to the Department of Chemistry and CAI building for providing FTIR and XRD facilities at NIT Warangal.

REFERENCES

[1] Ajmal M., Mohammad A., Yousuf R. & Ahmad A. (1998) "Adsorption behaviour of cadmium, zinc, nickel & lead from aqueous solution Mangifera indica seed shell", Indian Journal of Environmental Health, 40: 15–26.

[2] Arunima Sharma, Krishna G. Bhattacharyya(2005), "Azadirachta indica (Neem) leaf powder as a biosorbent for removal of Cd(II) from aqueous medium" Journal of Hazardous Materials B125 (2005) 102–112.

[3] Baral S. S., Das S. N., Rath P., Chaudhary G.R. (2007), "Chromium (VI) removal by calcined bauxite", Biochem. Eng. J. 34(1): 69-75.

[4] Krishna G Bhattacharyya, Arunima Sharma (2004), "Adsorption of Pb(II) from aqueous solution by *Azadirachta indica* (Neem) leaf powder", Journal of Hazardous Materials B113 (2004) 97–109.

[5] Mohanty, K., Jha, M., Biswas, M.N., Meikap, B.C., 2005. Removal of chromium (VI) from dilute aqueous solutions by activated carbon developed from Terminalia arjuna nuts activated with zinc chloride.Chem. Eng. Sci. 60, 3049–3059.

[6] Mumtazuddin S. and Azad AK. (2012), “Removal of Arsenic Using Mango, Java Plum and Neem Tree Barks” IJAPBC – Vol. 1(3).
[7] Onundi Y. B.; Mamun A. A.; Khatib M. F. Al; Ahmed Y. M. (2010),”Adsorption of copper, nickel and lead ions from synthetic semiconductor industrial wastewater by palm shell activated carbon”, Int. J. Environ. Sci. Tech,7 (4): 751-758.
[8] Reena Malik ,Suman lata and Sushila Singhal(2012), “Neem Leaf Utilization for Copper and Zinc Ions Removal from Aqueous Solution”, International Journal of Science and Research ISSN : 2319-7064:3.358
[9] Sharma A., Bhattacharya K.G. (2005). “Adsorption of chromium (VI) on Azadirachta indica (neem) leaf powder”, Adsorption, 10(4): 327-338.
[10] Sud D., Mahajan G. and Kaur M. P.(2008) “Agricultural waste material as potential adsorbent for sequestering heavy metal ions from aqueous solution - A review”.,Bioresource Technology,99: 6017-6027.
[11] Volesky B. and Holan Z. R. (1995) “Biosorption of Heavy Metals”, Biotechnol. Prog. 1995, 11, 235-250.
[12] ISI, Drinking water specifications (DWS), IS 10500 (1991).

Proceedings of the Third International Conference on Sustainable Energy and Environmental Challenges (3rd SEEC)
18 –21 December 2018, IIT Roorkee, India

SEEC No. 015

NUMERICAL STUDY OF A LAMINAR FLAT PLATE BOUNDARY-LAYER DIFFUSION FLAME WITH FUEL INJECTION

Debjit Kundu
Department of Mechanical Engineering
Jadavpur University
Kolkata-700032, India

Sourav Sarkar
Department of Mechanical Engineering
Jadavpur University
Kolkata-700032, India

Achintya Mukhopadhyay
Department of Mechanical Engineering
Jadavpur University
Kolkata-700032, India

Swarnendu Sen
Department of Mechanical Engineering
Jadavpur University
Kolkata-700032, India

ABSTRACT

This paper presents the numerical simulation of a laminar, two-dimensional, non-premixed methane-air reacting flow over a flat plate. Methane is injected perpendicularly in the air stream from a porous plate. A numerical model is developed which includes multi-step chemical kinetic mechanism, thermal diffusion, multi-component species diffusion and radiation heat transfer. In exothermic reacting flows, thermal radiation absorption by the product gases (which include species like H_2O and CO_2) plays a significant role. Therefore, the consideration of the effects of participating media in radiation heat transfer is necessary. In the present study, Discrete Ordinates (DO) radiation heat transfer model is used for radiation modeling where the absorption coefficient is calculated using weighted sum of gray-gas model (WSGGM). The results obtained from numerical simulation are validated against experimental results reported in literature. The effect of thermal radiation absorption in flame characteristics is investigated and reported.

***Keywords*:** Boundary layer , Non-premixed flame , Absorption coefficient , WSGGM , Discrete Ordinates (DO) radiation .

INTRODUCTION

The study of boundary layer formed over a flat plate with fuel injection is important due to its simplistic representation of fundamental phenomena like heat and mass transfer in a chemically reacting gas stream. The study of aerodynamics, heat and mass transfer processes is significant to the development of theory and practical applications. Many investigations has been carried out on diffusion flames formed on a boundary layer by the researchers. Hirano and Kanno [1] conducted an experimental study of diffusion flame in a laminar boundary layer with upward injection of gaseous fuel (methane and propane) in an air stream flowing along the horizontal porous plate. They observed that within the flame zone, velocity far exceeded the free stream velocity (velocity overshoot). Gravitational effects, effects of thermal expansion and the local pressure distribution around the boundary layer have been proposed as the primary causes of this velocity overshoot. Ramachandra and Raghunandan [2] as well as Ueda et al. [3] carried out similar experiments but with both upward and downward injection of fuel and reported the absence of velocity overshoot in the case of downward injection. Numerical modeling of laminar diffusion flames is crucial from analysis and design perspective, therefore, chemically reacting flows in boundary layer have been simulated by several investigators. Chen et al. [4] carried out a two-dimensional numerical simulation of a diffusion flame over a flat plate with one-step overall chemical reaction to study the flame stabilization and blow-off phenomena over a wide range of Damköhler numbers. Wang et al. [5] performed a two dimensional computational study of a chemically reacting boundary layer over a porous horizontal wall with a diffusion flame considering a single-step reaction mechanism and studied the velocity anomaly and hydrodynamic instability induced by formation of counter-rotating vortices. E.D.Gopalakrishnan et al. [6] studied the effects of upward and downward injection of fuel as well as the introduction of a backward facing step on the flame characteristics. P.K.Shijin et al. [7] conducted a numerical study of laminar non-premixed methane-air flames in the presence of a square cylinder bluff-body. In their work, the effect of varying the air velocity on the location of flame anchoring was analyzed in detail. The implementation of radiation sub-models in numerical simulation is of great importance. Previously used radiation models followed emission approximation, i.e. only emission was considered and absorption of radiation was neglected because the amount of energy emitted was much more than that absorbed. Daguse et.al [8] presented a comparison between calculations considering radiation absorption and without considering it. Further studies showed significant improvement of predictions by considering radiation absorption by participating media in numerous cases. Barlow et al. [9]

conducted experiments on non-premixed flames and compared their characteristics with predicted numerical results while considering thermal absorption by the major species. Kim et al. [10] and Zhu et al. [11] studied the effects of self-absorption in partially premixed flames by calculating the absorption coefficients of the gases present by weighted sum of gray gas model (WSGGM) which was first proposed by Hottel & Sarofim [12]. It assumes the gas mixture present in a combusting flow to consist of several gray gases. The local emission coefficient is calculated as the sum of the products of absorption coefficient of each of the constituent gray gases and their mole fraction. This model is a reasonable compromise between oversimplified gray gas model and computationally expensive comprehensive approach considering temperature and wavelength dependency of emissivity values.

The objective of the present study is to carry out a comparative study between predicted results obtained by employing different radiation sub-models in numerical simulation of a combusting flow and indicate the effect of each model on calculated flame characteristics. The simple case of diffusion flame in the boundary layer formed over a flat plate is chosen for this study. Three separate cases were simulated in the present study - by not considering radiation, by considering radiation without absorption, by considering of radiation with absorption. Absorption coefficients were calculated by implementing WSGGM.

PROBLEM DESCRIPTION

Computational Domain: The geometry under consideration is same as that of experimental investigation of Hirano & Kanno [1]. A combustion chamber (30 mm×100 mm cross-section and 160 mm long) with a porous plate (30 mm×120 mm surface area) mounted on the bottom of the chamber had been used and air & fuel were supplied at a steady volume flow rate. For computation, the two-dimensional domain, illustrated in Figure 1 has been used.

Boundary Conditions: Both air and fuel was assumed to have uniform velocities at the inlet.

1. Methane Inlet: At the fuel inlet boundary, a constant velocity of 20mm/s is specified as the injection velocity of methane with inlet temperature of 300K.
2. Air inlet: At the air inlet boundary, a constant velocity of 650mm/s is specified as the velocity of air with inlet temperature of 300K.
3. Outflow: At the exit, outflow boundary condition is specified, wherein all the variables are calculated by extrapolation from interior.
4. Wall: All the walls were considered no-slip surfaces. The walls were set to a convective condition (h=30 W/m^{2}K) with an ambient temperature of 300K.

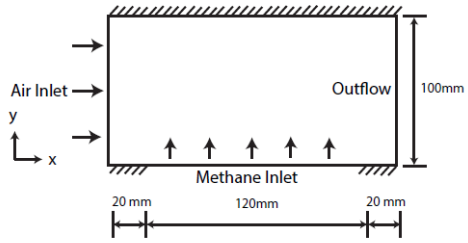

FIGURE 1: COMPUTATIONAL DOMAIN AND BOUNDARY CONDITIONS

NUMERICAL METHODOLOGY

Two-dimensional, unsteady, laminar, incompressible reacting flow calculations have been carried out by the commercial software ANSYS FLUENT 14.5. Full multi-component diffusion, thermal diffusion and inlet diffusion was considered. The equations for conservation of mass, momentum, energy and species were solved for 2D planar geometry. A multi-step chemical reaction mechanism with 16 species and 46 reactions is used to model chemistry of the combustion phenomena [13]. A pressure-based solver is used and SIMPLE scheme is applied for pressure-velocity coupling. A second-order upwind scheme is used for solving momentum, species and energy equations. A time step of 10^{-4}s has been considered. Convergence criteria of mass and momentum balance were set to 10^{-3} and that of energy and species balance were set to 10^{-6}. Discrete Ordinates (DO) method was implemented to model radiation in the cases where radiation is considered. A structured two-dimensional mesh with 240x200 cells (48000) for the entire domain has been used. The grid size is gradually refined near the bottom of the domain where the flame is formed.

RESULTS AND DISCUSSION

The x-velocity and temperature profiles at two locations (10 and 30 mm downstream from the leading edge of the fuel inlet) are obtained from three cases, namely,

1. No Radiation.
2. Radiation but no absorption.
3. Radiation and absorption with WSGGM.

These profiles are compared against the experimental results of Hirano&Kanno [1].

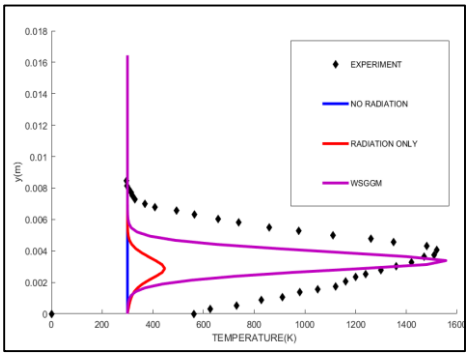

FIGURE 2: Temperature profiles at x=10 mm

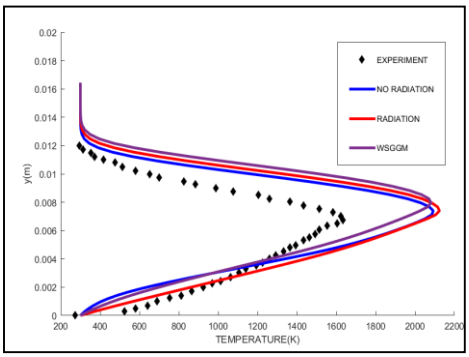

FIGURE 3: Temperature profiles at x=30 mm

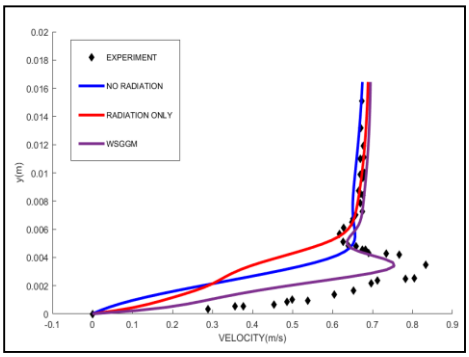

FIGURE 4: Velocity profiles at x=10 mm.

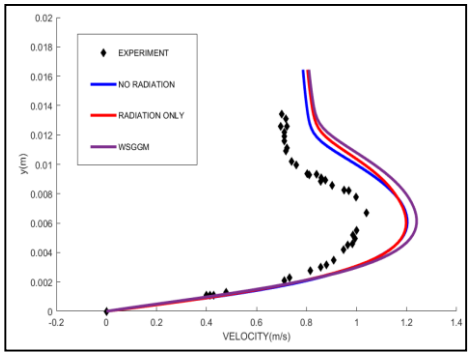

FIGURE 5: Velocity profiles at x=30 mm.

It is observed that the results obtained by modelling radiation with WSGGM agree well with the experimental calculations as compared to the other two cases. It is observed that at a distance of 10 mm from the fuel inlet, calculated temperature using WSGGM deviate only 4.54%from the experimental data. At 30 mm away from the fuel inlet, reported peak temperature is 1630 K. Calculations without considering radiation show a peak temperature of 2092 K (28.3% error), by considering radiation but no absorption gives a peak temperature of 2123 K(30.25% error). Whereas, using WSGGM a peak temperature of 2081 K (27% error) is reported.

Here, a three-dimensional setup is simulated in two dimensions, which might be a source of error. Also, a reduced chemical mechanism is considered which might cause differences between the calculations from the actual scenario. In spite of accurately predicting the locations of velocity overshoot and peak temperature, their values are over-predicted. This might be due to the fact that Hirano&Kanno [1] did not correct their temperature measurements for thermometric errors.

The contours of temperature, x-velocity are presented in the Figure 6 and Figure 7.

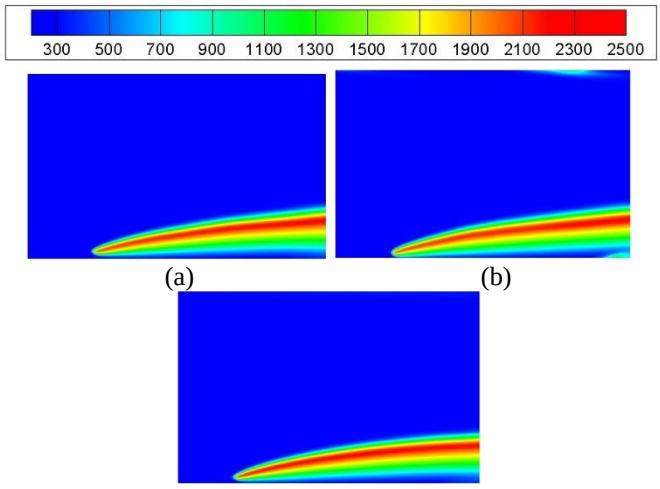

FIGURE 6: Temperature contours for (a) No Radiation (b) Radiation and (c) Radiation with WSGGM, respectively.

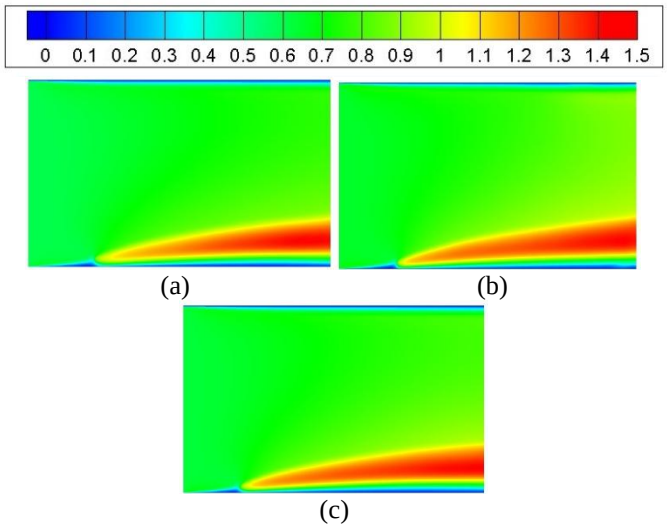

FIGURE 7: X-Velocity contours for (a) No Radiation (b) Radiation and (c) Radiation with WSGGM, respectively.

It is clearly visible from the Figures 6 and 7 that thermal expansion of the gases due to high temperature in the flame region is responsible for velocity overshoot in the boundary layer. The absorption coefficients of H_2O and CO_2 much higher than that of other species present in the reaction. The mass fraction contours of the product gases like H_2O and CO_2 reported in Figure 8. It is observed that the value of absorption

coefficient is higher in those regions where H_2O and CO_2 mass fractions are significantly large.

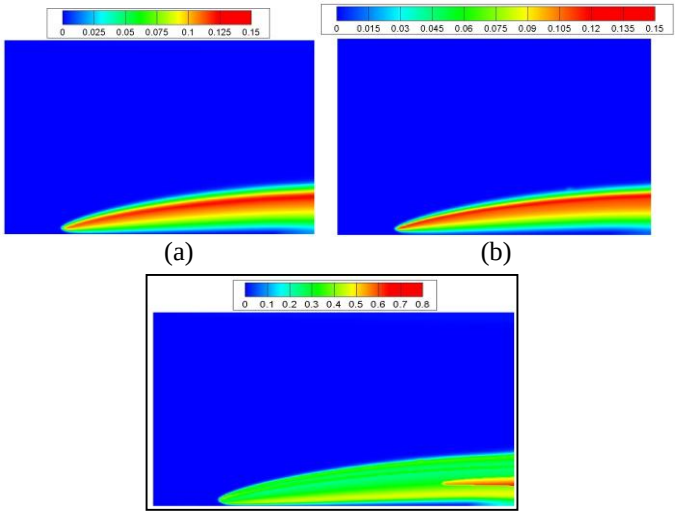

FIGURE 8: (a) H_2O mass fraction contour (b) CO_2 mass fraction contour (c) Absorption Coefficient contour for WSGGM.

CONCLUSION

A two dimensional numerical model has been developed for the simulation of a laminar flat plate boundary-layer diffusion flame with fuel injection. The numerical model has been validated with experimental results reported in the literature. The effect of radiation in numerical calculations has been investigated. It is found that the consideration of radiation heat transfer in combusting flow calculations is necessary and the inclusion of absorption of radiation by the participating media further improves the predictions of flame characteristics.

REFERENCES

[1] Hirano,T., and Kanno,Y., Aerodynamic and thermal structures of the laminar boundary layer over a flat plate with a diffusion flame, Proc. Combust. Inst. 14 (1973), pp. 391–398.

[2] Ramachandra,A., and Raghunandan,B.N, Buoyancy effects on the characteristics of a laminar boundary layer diffusion flame in a confined flow, Combust. Flame 58 (1984), pp. 191-196.

[3] Ueda,T., Ooshima,A., Saito,N., and Mizomoto,M., Aerodynamic structure of a laminar boundary layer diffusion flame over a horizontal flat plate–experimental analysis, JSME Int. J. Ser. 234-II(4) (1991), pp. 527–532.

[4] Chen,C.H, and T'ien,J.S, Diffusion flame stabilization at the leading edge of a fuel plate, Combust. Sci. Technol. 50 (1986), pp. 283–306.

[5] Wang, X., Suzuki, T., Ochiai, Y., and Ohyagi, S., Numerical studies of reacting flows over flat walls with fuel injection: Part 1 – Velocity anomaly and hydrodynamic instability, JSME Int. J. Ser. B 41(1) (1998), pp. 19–27.

[6] Gopalakrishnan ,E.D. and Raghavan,V., Numerical investigation of laminar diffusion flames established on a horizontal flat plate in a parallel air stream, Int. J. Spray Combust. Dynam. 3(2) (2011), pp. 161–190.

[7] Shijin, P.K, Sundaram,S.S, Raghavan,V. & Babu,V. (2014) Numerical investigation of laminar cross-flow non-premixed flames in the presence of a bluff-body, Combustion Theory and Modelling, 18:6, 692-710

[8] Daguse, T., Croonenbroek,T., Rolon,J.C., Darabiha,N., and Soufiani,A., Study of Radiative Effects on Laminar Counterflow H2/O2/N2 Diffusion Flames, Combustion and Flame, vol. 106, pp. 271–287, 1996

[9] Barlow, R.S., Karpetis,A.N., Frank,J.H, and Chen,J.Y., Scalar profiles and NO formation in laminar opposed-flow partially premixed methane/air flames, Combust. Flame 127 (2001), pp.2102–2118.

[10] Kim,O.J., Gore,J.P. , Viskanta,R., & Zhu,X.L, (2003) Prediction of self-absorption in opposed flow diffusion and partially premixed flames using a weighted sum of gray gases model (wsggm)-based spectral model, Numerical Heat Transfer: Part A: Applications.

[11] Zhu,X.L., Gore,J.P., Karpetis,A.N, Barlow,R.S., The Effects of Self-Absorption of Radiation on an Opposed Flow Partially Premixed Flame, Combustion and Flame 129:342-345, 2002.

[12] Hottel,H.C., and Sarofim,A.F., Radiative Transfer, McGraw-Hill, New York, 1967

[13] Kee, R. J., Rupley, F. M., Miller, J. A., Chemkin-II: A Fortran Chemical Kinetics Package for the Analysis of Gas Phase Chemical Kinetics; Sandia National Laboratories Report No. SAND89-8009B, 1991.

Proceedings of the Third International Conference on Sustainable Energy and Environmental Challenges(3rd SEEC)
18 –21 December, 2018, IIT Roorkee, India

SEEC No. 017

VOLTAGE PROFILE ANALYSIS OF A GRID-TIED PV SYSTEM DURING KNOWN INTERMITTENT PHENOMENON

Shahinur Rahman
Electrical and Computer Engineering
Florida International University
Email: srahm026@fiu.edu

Arif I. Sarwat
Electrical and Computer Engineering
Florida International University
Email: asarwat@fiu.edu

ABSTRACT

Grid-tied Photovoltaic (PV) systems supply a part of the total power to consumers and reduce energy demand upon the utility grid. Despite these advantages, there exist several technical limitations when PV penetration exceeds a minimum threshold. The proliferation of PV integration to the grid degrades the existing system performance and causes severe power quality issues. The rapid cloud transients reduce PV generation and consequently, cause significant voltage fluctuations, overvoltage, and frequent operation of voltage regulating devices. This paper investigates voltage profile and operations of voltage regulating devices of a grid-tied PV system during a known intermittent phenomenon. A simulation study has been done using OpenDSS software, where IEEE 123 Standard bus is remodeled and connected to a PV system with a real irradiation profile. This paper also presents a case study on feeder voltage analysis of a real 1.4 MW grid-tied PV plant, located at Florida. This study will help the distribution network operator (DNO) to take decisions and designers to keep consideration while making a distribution plan in the future.

Keywords

Smart Grid, Solar eclipse, PV penetration, voltage profile, high penetration PV, point of interconnection

INTRODUCTION

The worldwide electric energy consumption is increasing at a fast and consistent rate with the economic growth and estimated a rise of 28% within the next 20 years [1]. Greenhouse gas emission from fossil fuel power plants and the advancement of power electronic semiconductor devices have made a shift from the centralized grid network to the highly distributed energy sources, commonly known as a smart grid (fig. 1). A smart grid is an electrical grid, which includes a variety of renewable energy sources and energy storage systems.

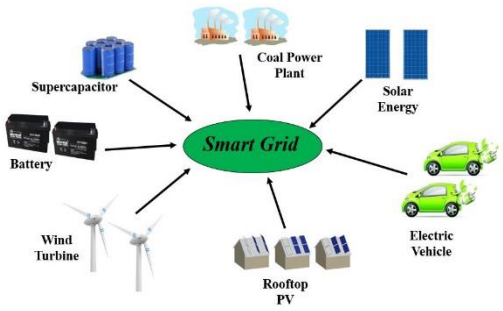

Figure 1: Smart Grid with Different Renewable Energy Sources and Energy Storage Systems

Solar energy is emission-free, inexhaustible, and clean that provides benefits to service providers and at the same time causes some technical issues [2]. PV generation depends on several environmental factors, such as solar irradiance, ambient temperature, wind velocity, and cloud transients. One of the environmental events is a solar eclipse, which reduces PV generation and consequently, affects voltage profile and operation of the voltage regulating devices (VRs and OLTCs) in the network. Frequent change of tap settings degrades the lifespan of VRs and OLTCs. The severity of these effects depends on the location and ratings of the PV system and the control settings of voltage regulating devices.

This paper explores the impacts of the solar eclipse of August 21, 2017 on voltage profile at the point of interconnection (POI) and operation of the voltage regulating devices close to a grid-tied PV system. IEEE 123 Standard bus is reconfigured in OpenDSS software [3] and integrated to a PV system with real irradiation and temperature profile of that day to observe the intermittency impact. A comprehensive feeder voltage profile analysis has been conducted on a real 1.4 MW grid-tied PV system to quantify the severity of solar eclipse effect on the grid.

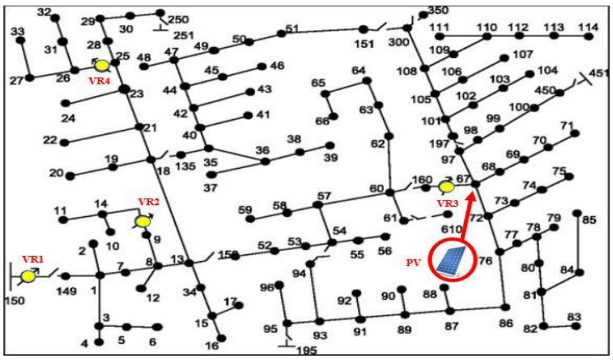

Figure 2: IEEE 123 bus Integrated to a PV System and Four Voltage Regulators (VR1, VR2, VR3, and VR4)

SIMULATION CIRCUITS:

The IEEE 123 standard bus in fig. 2 operates at nominal voltages of 4.16kV and 2.4kV. The feeder contains both balanced and unbalanced loads and three voltage regulators (VR2, VR3, and VR4) with tap-changeable substation transformer (VR1). To observe the impact on feeder voltage and voltage regulators' operation of a grid-tied PV system during solar eclipse time, the IEEE Standard 123 bus is reconfigured in OpenDSS software and connected a 1.4MW PV system at bus 67 with 2500kVA, 2.4/0.48kV transformer. The voltage change at bus 67 affects VR3 operations severely as they are located very close. The irradiance and temperature profiles during the eclipse were used for the PV system modeling. For this simulation, the line characteristics and load profiles are kept as like as the standard model. The simulation has been divided into two parts (with a PV system and without a PV system) to clarify the impact of connected PV to the standard bus.

Simulation Results:

Figure 3(a) shows the dynamic changes of three-phase RMS voltage profile at bus 67 and figs 3(b-d) present the operations of VR3 when PV was not connected to the model. The bus voltage varied between 282-291V and VR3 changed its tap position 5, 3 and 1 for phase A, B and C respectively but did not change tap during eclipse time (13:30-16:00). Load variations inside the distribution network are mainly responsible for the voltage variation and tap settings change of VR3. Figure 4 shows the solar irradiation profile of 21 August 2017 and corresponding PV power obtained from simulation when PV was connected to the model. Both irradiation and PV power gradually first decreases and then, increases from 13:30 to 16:00 due to solar eclipse effect, which consequently causes voltage fluctuations at bus 67 (fig. 5(a)). The dynamic changes in the voltage profile cause the VR3 to tap change in other to control the voltage within the ANSI C84.1-2011 voltage standard. Figures 5 (b-d) shows the various tap changing done by the VR3. VR3 tapped 7 times on phase A, 5 times on phase B and 1 times on phase C during the eclipse time.

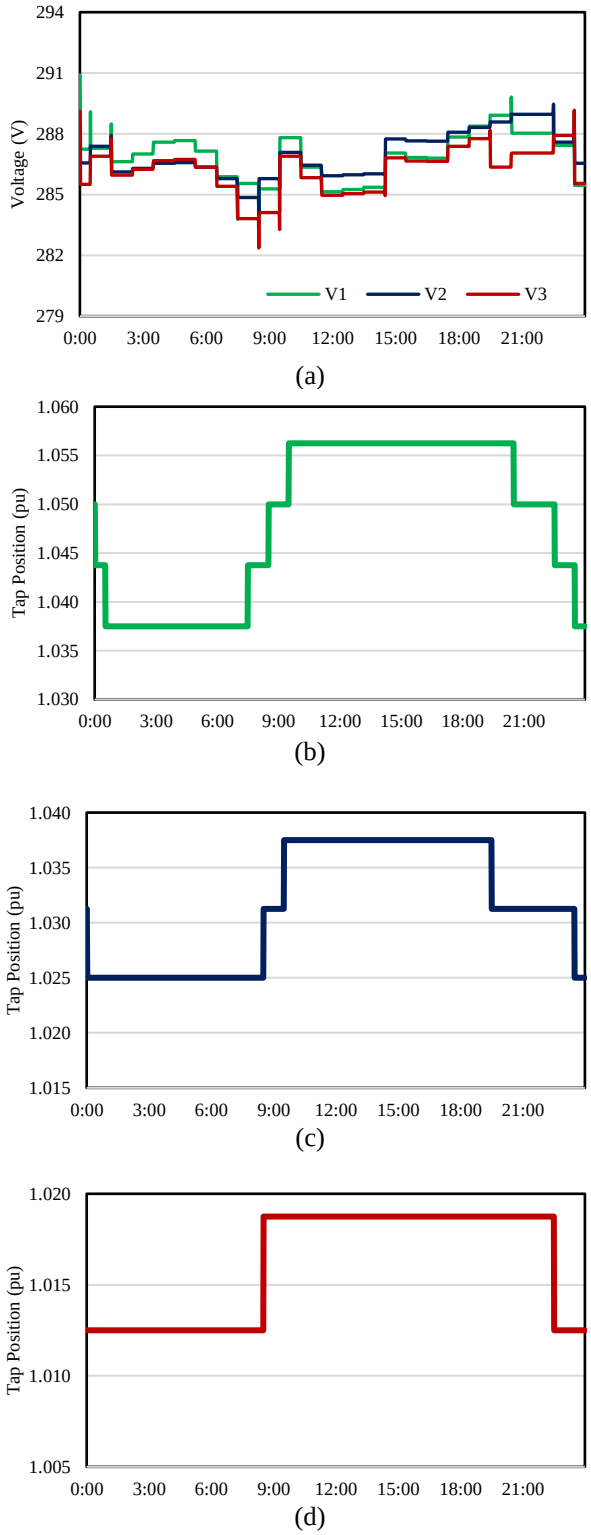

Figure 3: Voltage Profile and VR3 Regulator Operations without PV system (a) Three Phase RMS Voltages (V) at Bus 67 (b) VR3 Tap Position of Phase A (c) VR3 Tap Position of Phase B (d) VR3 Tap Position of Phase C.

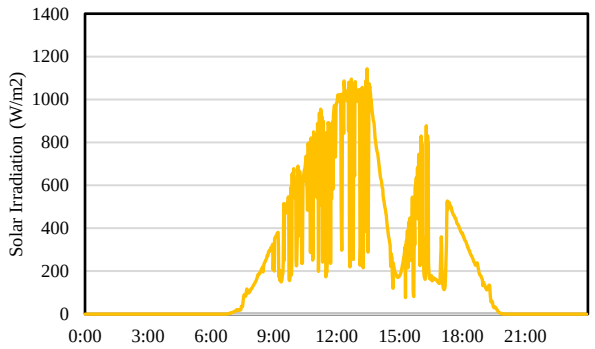

(a)

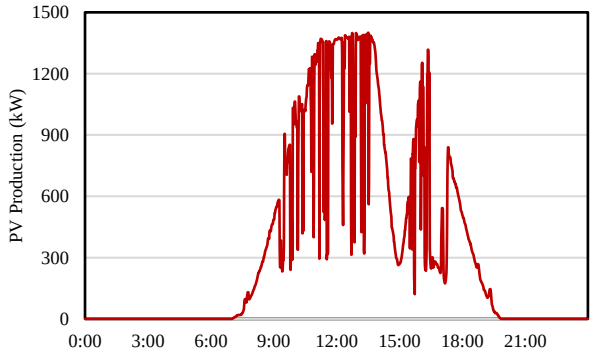

(b)

Figure 4: (a) Solar Irradiation Profile at Miami, Florida during Solar Eclipse of 21 August, 2017 (b) PV power generation obtained from the simulation study

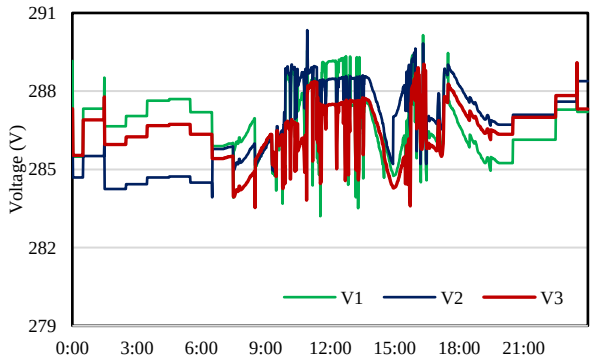

(a)

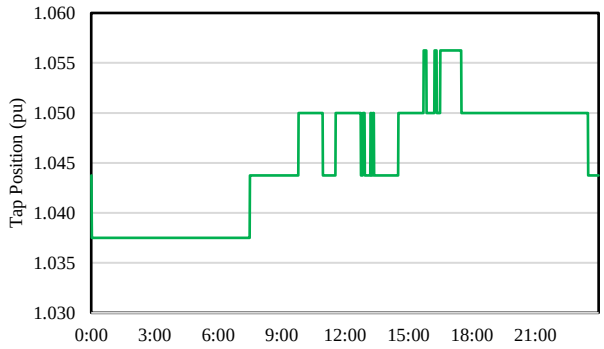

(b)

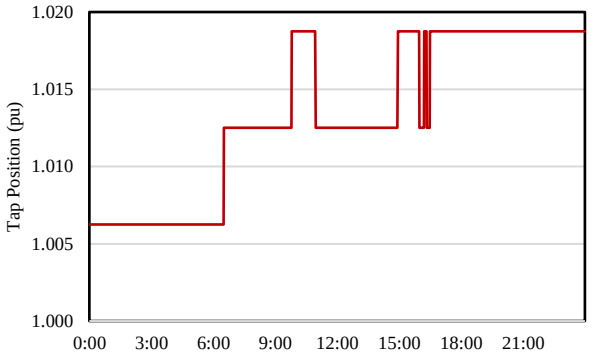

(c)

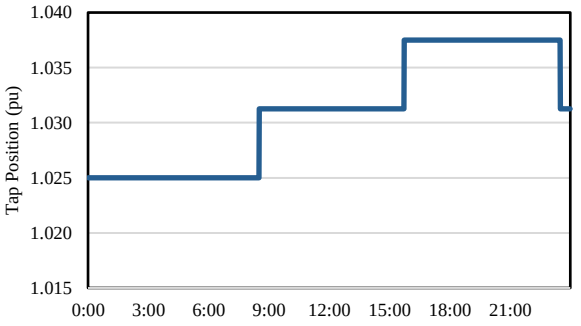

(d)

Figure 5: Voltage Profile and VR3 Regulator Operations with PV system (a) Three Phase RMS Voltages (V) at Bus 67 (b) VR3 Tap Position of Phase A (c) VR3 Tap Position of Phase B (d) VR3 Tap Position of Phase C.

CASE STUDY ON FIU GRID-TIED PV SYSTEM:

A case study was performed on a real 1.4MW grid-connected PV system to analyze the impact of the solar eclipse on PV power production and feeder voltage profile. The PV plant is located at Florida International University (FIU), Florida (fig. 6(a)), which has 4,460 modules **(**each 315W rated power) and 46 smart string inverters (each 24kW). The inverters convert DC Power to AC and inject power to the grid through a 480V /277V, 2000 KVA oil-cooled step-down transformer. A weather station records solar irradiance, ambient temperature, and module temperature locally. An Elkor production meter records the PV plant's net energy production. A Data Acquisition System (DAS) collects time-series data from the weather station, inverters, and meters and stores those data in a cloud server (fig. 6(c)). A RevolutionR Wireless Power Quality Meter connected to the low voltage side of the transformer, records three phase RMS voltage data with the 1-minute time interval at POI (fig. 6(b)). The plant generates maximum 1MW on a sunny, bright, and clear day. The peak demand on the feeder under study is about 6.7MW and the plant runs at about 16% penetration. The concerned feeder has one voltage regulator, two transformers and three capacitor banks that serve approximately 200 industrial customers and 700 households.

(a) (b) (c)

Figure 6: (a) Grid-integrated PV System situated at Florida International University (FIU) (b) RevolutionR Wireless Power Quality Meter (c) Data Acquisition System (DAS) that collects data from the weather station, meter, and inverters.

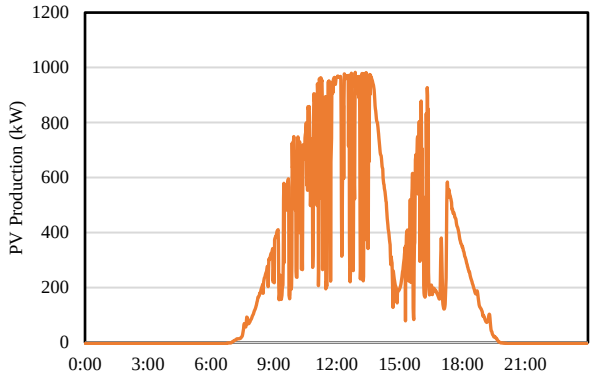

(a)

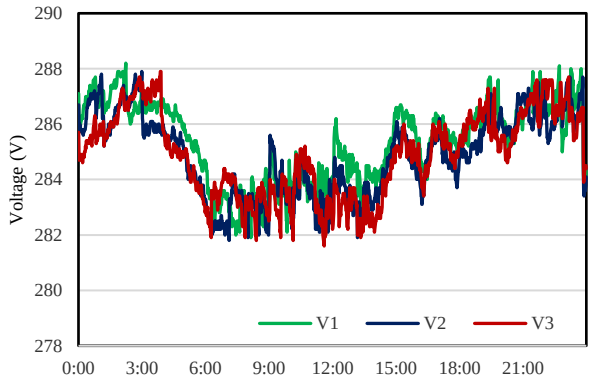

(b)

Figure 7: (a) PV power Production from FIU PV system on 21 August, 2017 (b) voltage variation at POI

Case Study Result:

The solar eclipse started about 13:30 and ended 16:00 in Miami, Florida and maximum 80% coverage happened at 15:00. It is clearly observed in figure 7 (a) that the PV power production of FIU PV plant decreased from 1000kW to 200kW which was almost 80% decrease of peak generation. The decrease of production caused the corresponding feeder voltage variations. The average RMS voltage at the POI during the eclipse is illustrated in Fig. 7(b). According to IEEE Standard 1547-2018, the feeder voltage at a low voltage distribution network can vary within ±5% of the base voltage. Therefore, the minimum and maximum allowable ranges of average RMS voltage at the POI are 265 V and 292 V, respectively. It is clearly observed in fig 7(b) that at the peak of the eclipse on PV System the voltage was within the safe boundary. The penetration level of this PV system did not produce any significant impact on the voltage profile during the eclipse event. These impacts could become severe at higher PV penetration level.

CONCLUSION:

Although solar energy has enough potential to meet the increasing energy demand, service providers face several technical challenges when PV is integrated into the utility grid. This paper explores voltage related issues and investigates the operation of voltage regulating devices of a grid-tied PV system during the known intermittent event through a simulation and comprehensive case study. Although the results obtained from simulation and observed in a real grid-tied PV system seem to have an insignificant impact on the grid, the dynamics will change when the penetration level increases drastically. This study will help system planners to design the distribution network and take necessary steps to avoid the drastic impact of intermittency of a solar eclipse.

ACKNOWLEDGEMENTS:

The material published is a result of the research supported by the National Science Foundation under the Award number CNS-1553494 and 174582.

REFERENCE:

[1] International Energy Outlook 2017. https://www.eia.gov/outlooks/ieo/

[2] Shibani Ghosh, Saifur Rahman: 'Global deployment of solar photovoltaics: Its opportunities and challenges', ISGT-Europe, 2016, pp. 1 - 6

[3] EPRI Simulation Tool – OpenDSS. http://smartgrid.epri.com/SimulationTool.aspx

SEEC No.018

TO MAKE A FRAME WORK OF INPUT-OUT FOR SUSTAINABLE DEVELOPMENT OF CLEAN ENERGY- A REVIEW OF NEW HOLLAND FRAM INDUSTRY

Ms. Saloni Chaudhary[1], Dr. Raghavendra G. Rao[2]

[1,2] SRM University, Sonepat (Haryana) (India)

[1]salonichaudhary140@gmail.com, [2]raghavgrao@gmail.com

ABSTRACT

Globally clean energy demandable for the sustainable development of achieving the higher height of the economic and social level of the world. Nowadays it became centre of all energies. For the achieving higher heights for economic growth of any country worldwide, with satisfying the basic need of humanities without an intensive use of energy it's challenging. On another hand, the main cause of energy use is greenhouse gases released by energy source; it shows the negative impact on global climate. Agricultural implements industries are highly energy intensive. Some of these industries are use fossil fuel as an energy source and release greenhouse gases. There is a need to use clean energy resources in agriculture implements for the preservation of our environment and natural resources.

This paper presents a New Holland has worked with clean energy strategies by using renewable resources in the agricultural equipment for protecting our environment by greenhouses gases.

Keywords: ***Clean Energy, New Holland, Sustainable Development***

Proceedings of the Third International Conference on Sustainable Energy and Environmental Challenges (3rd SEEC)
18 –21 December, 2018, IIT Roorkee, India

SEEC No.019

NOVEL EXPERIMENTAL STUDY OF INTERNALLY COOLED DEHUMIDIFIER FOR LIQUID DESICCANT SYSTEM

Geleta Fekadu
Department of Mechanical and Industrial Engineering, IIT Roorkee, 247667 Roorkee, India
Email: gelefeke@gmail.com

Sudhakar Subudhi
Department of Mechanical and Industrial Engineering, IIT Roorkee, 247667 Roorkee, India
Email: subudhi3@gmail.com

ABSTRACT

The energy crisis has become an issue in recent time. Replacing conventional technologies with a new that remove moist by desiccant promotes renewable energy usage. To alleviate the use of fossil fuel, the investigation of the ways to utilize renewable energy which are eco-friendliness and sustains development. Absorption of moisture by desiccant is one among the system to condition indoor air quality (IAQ). Some of the desiccants are regenerated by low-temperature heat source obtained from low-grade energy. The experiments have been initiated using 40% of calcium chloride solution by mass. An internally-cooled dehumidifier is used to cool and dehumidify the process air simultaneously in a single design. Dehumidification of 15% -26% by calcium chloride solution is obtained but further investigation will be conducted to obtain more reduction in temperature. This increment of temperature may be as a result of the exothermic reaction generated in the dehumidifier. So using desiccant as air conditioning is promising due to its low regeneration temperature, which is achieved from solar and other waste energy sources from industries.

Keywords: Liquid desiccant, internally cooled, dehumidifier, Air conditioning, Thermal comfort.

INTRODUCTION

Controlling indoor thermal comfort and energy consumption are paramount. Demand for fossil fuel for air conditioning makes depletion of fuels. Renewable energy for a liquid desiccant air-conditioning system is very essential. Some absorbents, like $CaCl_2$, are reactivated at a low temperature of the heat sources like solar energy. In the present system, a single storage tank for calcium chloride is used in place of double tanks for concentrated, diluted solution and water. Both cooling and dehumidification are done in an internally cooled dehumidifier [1-3].

Controlling of indoor humidity for thermal comfort, building material sustainability, and energy consumption are important. Demand for energy consumption and its coupling to fossil fuel (Coal, Petroleum, and Natural Gas), makes depletion of fuels. Sustainable energy is important for one country's development. Renewable energies viz. solar, wind, biomass, geothermal and hydropower etc. are used for heating, lighting, cooking and air conditioning [4-7]. Recent demand for Air conditioning causes a significant rise in energy resources. Apart from depletion of primary energy, burning of these fuels causes CO_2 emission. Heating ventilation and air conditioning load of the world is estimated to rise 6.2% per year. The objective of this study is to experimentally investigate internally cooled and dehumidified process air by using single storage desiccant solution tank [8-10].

THERMAL COMFORT: ASHRAE defines comfort as "the condition of mind that expresses satisfaction with the thermal environment, it requires subjective evaluation." There are three main factors for thermal comfort viz. environmental; air temperature, air movement, humidity, radiation, personal factor; metabolic rate, and clothing, contributing factors; food and drink acclimatization, subcutaneous fat, body shape, age and gender, and state of health [11-12].

MOTIVATIONS: Energy crisis, global warming, pollution, population increasing, urbanization,

industrialization, modernization and demand for standard living, advancement of science–technology in solving the thermal comfort are the main initiators for this desiccant of air conditioning.

DESICCANTS: A substance that is natural or synthetic has capable of showing a strong affinity for water vapor (moist air), viz. some of the liquid desiccant used as air conditioning in a hybrid to with conventional air conditioning and stand alone. Some of the liquid desiccants are saline salts, like are lithium chloride, lithium bromide, calcium chloride, calcium-lithium chloride mixture, and organic compounds ionic liquids (ILs) and New organic compounds, Like 1-butyl-3-methylimidazolium tetrafluoroborate and mono-ethylene glycol etc. For this experimental study, we used the calcium chloride solution due to its cost and availability. Fig. 1. indicates the powder of $CaCl_2$ used for the experiment [12].

FIGURE 1. CALCIUM CHLORIDE POWDER (90+%AGE. ($CaCl_2$)

EXPERIMENTAL METHODS

EXPERIMENTAL SETUP: The schematic line diagram for the complete set up is indicated in Fig. 2. Fabrication of internally cooled dehumidifier is from the following materials; namely aluminum sheet of 0.4cm thickness, polycarbonate sheet of 0.8cm thickness, wick surface of the cotton cloth for wetting purpose and PVC piping system for dispersing solution and coolant. (0.8cm diameter of with 0.2cm x 11holes) as Fig.3 and Fig.4

Fabrication of stratified single storage tank of 30x30x60cm was made from thick Perspex Sheet two side and bottom 6mm thickness, thick transparent glass on two side sheet 6mm thickness, 14 copper tube size 3/8" O.D, and inlet-outlet manifold at the top and bottom diameter of 24mm O.D as Fig.5 and Fig.6. Fabrication of shell and tube heat exchanger for regeneration is made of mild steel diameter of 12.7cm and length of 30cm, copper tube dia. 2.4cm and length of 38cm. For taking data the Devices Used are Hygrometers (Measuring range RH% 1-100%, Accuracy RH$\pm$1.8% RH; Temperature($-20-60^0$C) accuracy $\pm\ 0.5^0C$), Flow meter and control valve, thermocouples (accuracy $\pm 0.3^O$c), Fan, pump, data logger, computer and constant bath temperature.

EXPERIMENTAL PROCEDURE: The experimental procedure has been done as follows. The calculation for maximum possible concentration is found to be 74.4%, but concentrations of 35% - 45% is used for experiments, making a solution and storing in a storage tank. Then the selection of constant bath temperature approximately same as that of solar energy heat flux is used in the storage tank. The measurement of temperatures of regenerators (inlet-outlet), dehumidifiers, and inlet-outlet humidity are done. The setting of constant bath temperature for coolers using data acquisition systems.

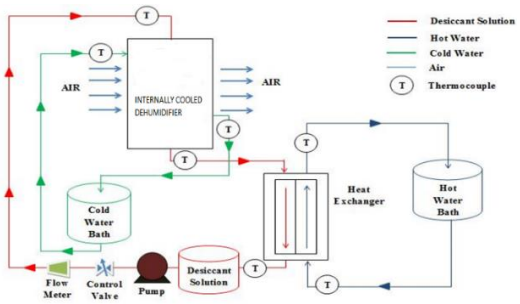

FIGURE 2. SCHEMATIC LINE DIAGRAM OF THE EXPERIMENTAL SETUP

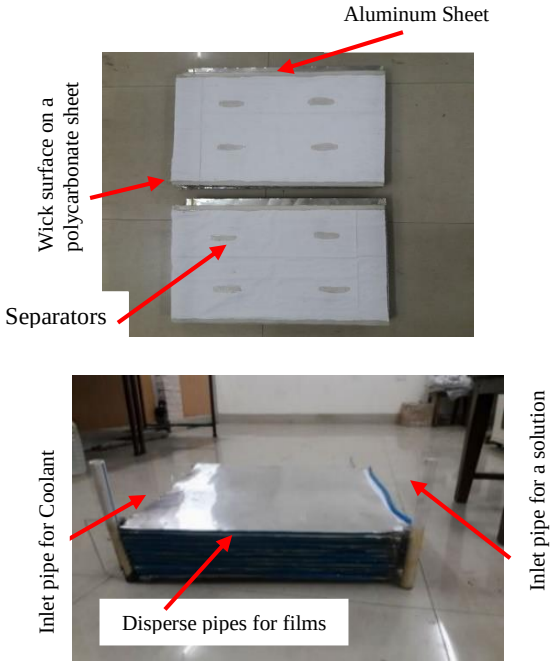

FIGURE 3. FABRICATION OF INTERNALLY COOLED DEHUMIDIFIER

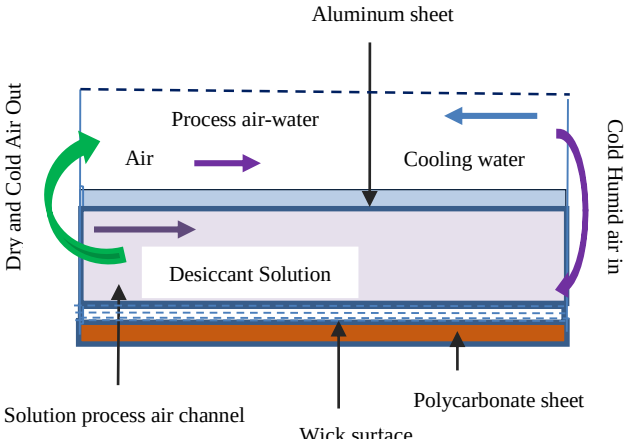

FIGURE 4. CROSS-SECTIONAL VIEW OF INTERNALLY COOLED DEHUMIDIFIER

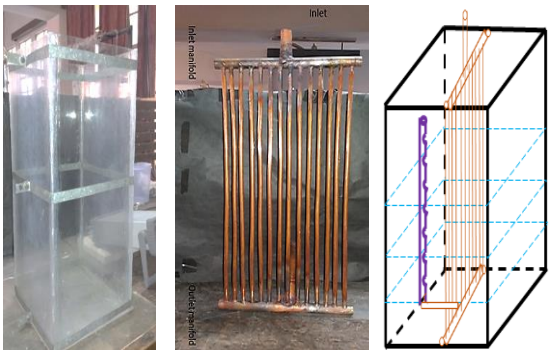

FIGURE 5. STRATIFIED SINGLE STORAGE TANK AND VERTICAL HEAT EXCHANGER

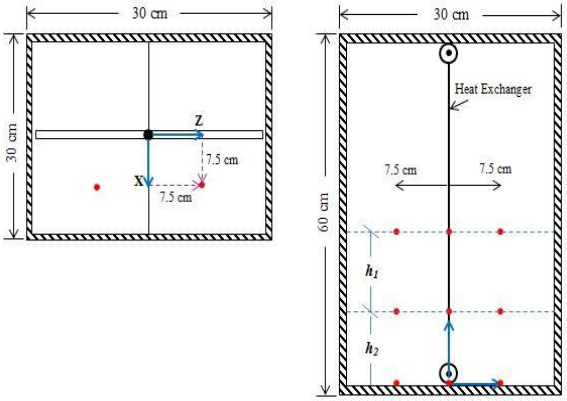

FIGURE 6. PROTOTYPE STORAGE TANK AND THERMOCOUPLE POSITIONS

RESULTS AND DISCUSSION

Based on experimental data collected for two hours for a week the data was analyzed using graphs.

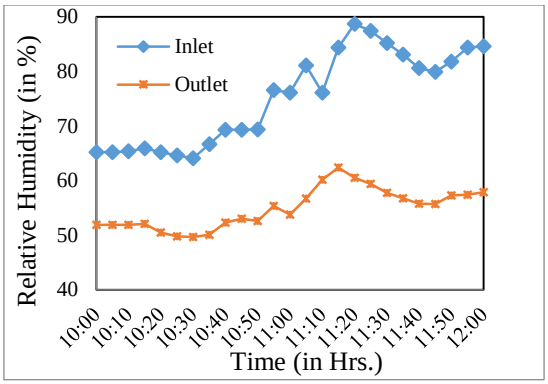

FIGURE 7. RELATIVE HUMIDITY (%) VS TIME

From Fig.7 above the relative humidity (%) reduction increases with time up to some point and then becomes stable. Maximum humidity reduction is seen at about 26%.

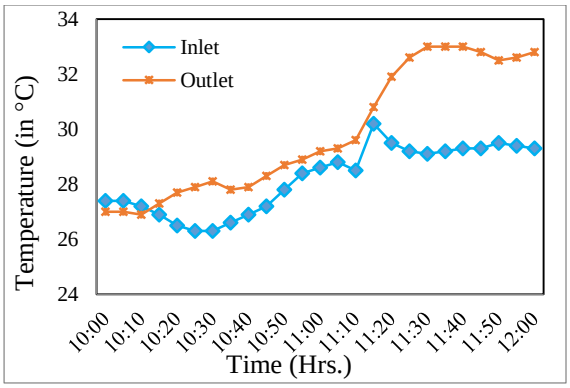

FIGURE 8. TEMPERATURE VS TIME

Fig.8 above shows as outlet temperature increases up to some point and then becomes stable.

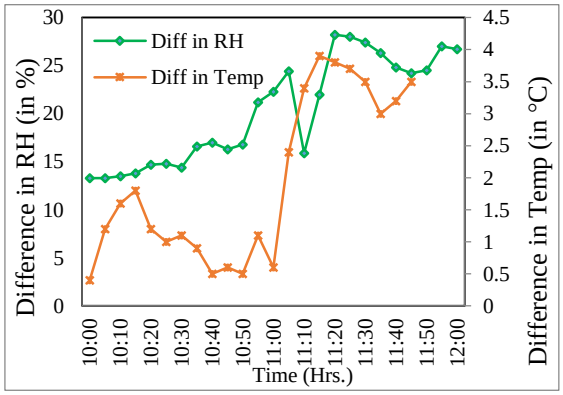

FIGURE 9. DIFFERENCE IN TEMPERATURE, RELATIVE HUMIDITY (%) VS TIME

Generally, the experiments have been conducted for the difference in relative humidity (%) reduction in the range 15% -26% and temperature increase in the range of 0.5^0C-4^0C as shown in Fig.9 above.

CONCLUSIONS

The dehumidification reduction is observed in the system for 40% mass concentration of $CaCl_2$-H_2O solution. But further experiments are required for observation of temperature reduction.

REFERENCES

[1] K. Gommed, G. Grossman, (2006). "Experimental investigation of a liquid desiccant system for solar cooling and dehumidification". Solar Energy 81, 131-138.

[2] P. Bourdoukan, E. Wurtz P. Joubert, (2009). "Experimental investigation of a solar desiccant cooling installation". Solar Energy 83, 2059–2073.

[3] Jan Wrobel, Pablo Sanabria Walter, Gerhard Schmitz, (2013). "Performance of a solar assisted air conditioning system at different locations". Solar Energy 92, 69–83.

[4] A. Ali, K. Vafai, (2004). "An investigation of heat and mass transfer between air and desiccant film in an inclined parallel and counter flow channels". International Journal of Heat and Mass Transfer 47, 1745– 1760.

[5] Sanjeev Jain, P.K. Bansal, (2007). "Performance analysis of liquid desiccant dehumidification systems". International Journal of Refrigeration 30, 861- 872

[6] Ertac Hurdogan, Orhan Buyukalaca, M. Tolga Balta, Arif Hepbasli, Tuncay Yılmaz, (2013). "Experimental exergoeconomic assessment of a desiccant cooling system". Energy Conversion and Management 69, 9–16.

[7] S. Bouzenada, C. Mc Nevinb, S. Harrison, A. N. Kaabid, (2015). "An experimental study on the dehumidification performance of a low- flow falling-film liquid desiccant air-conditioner", Procedia Computer Science 52, 796 – 803.

[8] W. Kessling, E. Laevemann and C. Kapfhammer, (1998). "Energy storage for desiccant cooling systems component development" Solar Energy Vol. 64, Nos 4–6, 209–221.

[9] A.S.A.Mohamed, M.S.Ahmed, A.A.M. Hassan, M.Salah Hassan, (2016). "Performance evaluation of gauze packing for liquid desiccant dehumidification system" Case Studies in Thermal Engineering 8, 260–276.

[10] M. Mujahid Rafique, P. Gandhidasan, Shafiqur Rehman, Luai M. Al-Hadhrami, (2015). "A review on desiccant based evaporative cooling systems". Renewable and Sustainable Energy Reviews 45, 145–159.

[11] ASHRAE Handbook-Fundamentals. Sorbents and desiccants. Atlanta, GA: American Society of Heating, Refrigeration and Air-Conditioning Engineers, Inc.; 2005.

[12] Afshin M. Selection of the liquid desiccant in a run-around membrane energy exchanger [M.Sc. thesis]. Saskatoon: University of Saskatchewan;2010.(ttp://ecommons.usask.ca/handle/10388/etd 05262010-175310).

Proceedings of the Third International Conference on Sustainable Energy and Environmental Challenges (3rd SEEC)
18 – 21 December, 2018, IIT Roorkee, India

SEEC No.020

REDUCTIVE LEACHING OF SPENT LI-ION BATTERIES TO RECOVER COBALT OXALATE USING SULPHURIC ACID AS A LEACHANT

Sandeep S. Anwani
Department of Chemical Engineering
Visvesvaraya National Institute of Technology
Email: sandeepanwani@gmail.com

Ravi N. Methekar*
Department of Chemical Engineering
Visvesvaraya National Institute of Technology
Email: methekar.vnit@gmail.com

ABSTRACT

Excessive consumption of Lithium-ion batteries in mobile phones and electric vehicles create tones of e-waste after their useful life which needs to be disposed safely and economically. This urges recycling process which not only minimizes the e-waste but also recover the value added products from the spent Li-ion batteries. Recycling process consists of peeling, dissolution and extraction steps. The peeling of active cathode material from cathode surface has enhanced to 82% with ultra-sonic cleaning. In this paper, sulphuric acid leaching of spent lithium ion batteries followed by precipitation of value added metals using suitable reagent have been investigated. The dissolution of active cathodic material was found to be 95.15% using 2 M H_2SO_4, 2 vol.% H_2O_2, 10 g/l Solid to liquid ratio at 95°C temperature with 2 h stirring time and a particle size of 25µm. The extraction efficiency and purity of cobalt oxalate are found to be 91 % and 90 % respectively.

Keywords: ***Lithium ion batteries, Recycling, Spent batteries, Dissolution, e-waste***

INTRODUCTION

Lithium ion batteries (LIBs) are widely used in mobile phones, laptops, cameras and other portable electronic gadgets because of high energy density, light in weight, low self-discharge, longer durability and safer operations. LIBs consists of cathode, anode, separator, steel casing. The $LiCoO_2$ material is adhered to an aluminum sheet to form cathode while graphite is adhered to a copper sheet to form anode electrode. The separator is a thin plastic porous film which separates the two electrodes from short circuiting. The separator is generally soaked in an electrolyte which may vary depending upon the brand or battery model which is generally $LiPF_6$, $LiBF_4$, $LiClO_4$ (Xu et al., 2008). In the period between 2000 and 2010, the annual production of LIBs increased by 800% worldwide (Zeng et al., 2014). Recently LIBs have been used in battery operated vehicles such as cars and auto-rickshaws in many countries. The lithium ion batteries contain 5-20% cobalt, 5-10% nickel, 5-15% manganese, copper, aluminum, 5-7% lithium and many valuable metals in trace amount of varying manufactures and different chemistries which can be recycled and reuse in their respective stable forms may lead in economic benefits. (Shin et al., 2005).

Several routes such as pyrometallurgy, hydrometallurgy, and bioleaching have been adopted in recent times to recover these valuable metals. Current study mainly deals with the hydrometallurgical route which is highly energy efficient and more environmental-friendly. Many researchers have worked on reductive leaching of spent LIBs using H_2SO_4 (Nan et al.,2005, Atkas et al.,2006, Meshram et al.,2015, Jha et al.,2015, Chen et al.,2011, Wang et al.,2012, Li et al.,2009, Kang et al.,2010).

In the recovery process, a combined method of acidic leaching and selective precipitation were employed to recover metals from the leach solution. Among all methods acidic leaching is an environment-friendly, cost effective technique to recover cobalt and lithium. In our study cobalt, manganese and lithium were precipitated successively at a particular pH to recover cobalt oxalate, manganese carbonate and lithium carbonate respectively. Furthermore the products obtained from this process would be of industrial interest. The purpose of this paper is to develop an efficient, cost effective and environmentally benign recycling process to minimize the e-waste, ground water pollution and mineral exploitation.

EXPERIMENTAL STUDY

Materials

All the reagents used in the experiment were all of analytical grade. The spent mobile phone batteries mainly

of Nokia BL-5C were procured from the local market of Nagpur.

Sample preparation and pretreatment

The fully discharged batteries were dismantled manually through an angle grinder with proper safety precautions. The plastic casing and inner steel casing was successively scrapped off from the main internal core. The cathodic film was separated and cut into square pieces with scissor. The resultant pieces were dissolved in a particular volume of N-Methyl-2-Pyrrolidone (NMP) solvent to peel off the active cathodic material from the aluminum films via ultra-sonication cleaning which basically dissolves the fluoro-polyvinylidene glued to these films. The black slurry thus obtained was centrifuged at 4000 RPM for about 20 minutes to separate the active cathode material from the NMP solution, and dried at 150°C for 1 hour. The dried materials was fed to ball mill for size reduction followed by manual sieving with a mesh size of 25µm.The smaller diameter particles are needed for efficient dissolution of the material in the acid. Finally the material was calcined in a muffle furnace at 750°C for 5 h to burn off the carbon, and residual NMP if left any in the material.

2.3 Dissolution study for active cathodic material

Leaching of metals from the cathode active material was carried out in a 250-ml three necked round bottom flask with a four flat bladed impeller fitted with an overhead motor agitator, thermometer. The conical flask is heated in a heating mantle and a reflux condenser assembly is provided to the flask to avoid the loss due to evaporation. The leaching experiments were performed by taking pre-calculated charge of 2 g in a 2M H_2SO_4 solution with 1.7 H_2O_2 (v/v%), pulp density 20 g/l as the initial operating conditions. The charge was leached at 95°C for 2 hours with an impeller speed of 300 RPM.

The dissolution efficiency was calculated by using the expression:

$$D\% = \frac{\times^{\circ} - \times}{\times^{\circ}} \times 100$$

Where: D% is the percent dissolution efficiency; $\times^{\circ}$ is the initial mass of the solid reactant and $\times$ is the mass that remains unreacted after the reaction. The residue thus obtained was filtered and dried overnight in a hot oven at 90°C. The clear leached pink solution (filtrate) was analyzed by an inductively coupled plasma (ICP) emission spectrometer for their metallic concentrations. The optimum dissolution efficiency was found out by varying solid to liquid ratio, acid molarity, leaching time, particle size and concentration of reducing agent. Fig. 1 shows the schematic representation of the complete process including acidic leaching.

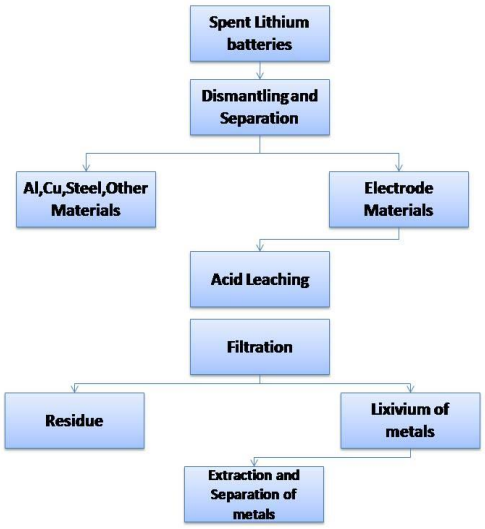

Figure 1. FLOW-SHEET OF THE HYDROMETALLURGICAL RECYCLING PROCESS OF LITHIUM-ION SECONDARY RECHARGEABLE BATTERIES

RESULTS AND DISCUSSIONS

Characterization active cathodic material

The active cathodic material was characterized by X-Ray diffractometry (Fig.2) and the inductively coupled plasma emission spectroscopy. The XRD test confirms that the major peaks are of $LiCoO_2$ along with the peaks of Cobalt oxide (Co_3O_4) a performance degrading product formed during battery operation with minor phases of magnesium aluminum silicate, phosphorus pentoxide, ferroferric oxide. The ICP analysis of the untreated cathode material presented in Table 1 shows that the cobalt (45.1 weight %), manganese (11.8 weight %) and lithium (6.3 weight %) metals are present in the significant amount as transition metals. Calcium, sodium, magnesium and iron, etc. are present in small quantities (Table 1) and the rest was surely be the oxygen as all the metals are present in their oxides form as indicated by the XRD analysis.

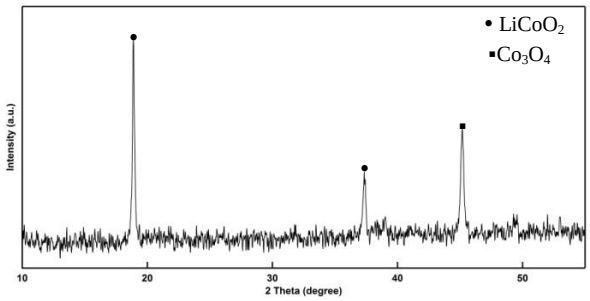

Figure 2. PHASE ANALYSIS OF ACTIVE CATHODE MATERIAL USING XRD ANALYSIS

Table 1. COMPOSITION OF ACTIVE CATHODE MATERIAL USING XRF ANALYSIS

Metal	Weight %	Metal	Weight %	Metal	Weight %	Metal	Weight %	Metal	Weight %
Li	6.3	Cu	0.6	K	0.02	Si	0.09	Fe	0.11
Co	45.1	Al	0.67	Ca	0.03	Cl	0.02	Zr	0.01
Mn	11.8	P	0.32	Na	0.23	Ti	0.02	Nb	0.01
Ni	0.30	S	0.16	Mg	0.41	Cr	0.09	O_2	Rest

Synthesis of cobalt oxalate from spent batteries using oxalic acid

In order to separate cobalt from the leach solution 100% excess amount of oxalic acid in solid form has been directly added to the solution at an optimum pH of 1.75 which is maintained by 5 M NaOH solution. The mixture was agitated for 2 hours at a temperature of 50°C. The proper agitation time and temperature were necessary for the efficient recovery of the cobalt. The pink precipitate obtained after filtration was washed efficiently to reduce the contamination by the Na^+ ions. The product is then dried at 95°C and weighted. The obtained product was analyzed through the X-Ray diffractometer (Fig. 4). The shape and position of the peaks confirmed that the product obtained was cobalt oxalate with two moles of water of hydration attached to it (Nayaka et al., 2015). Minor spikes of MnC_2O_4 were also identified indicates the co-precipitation of manganese in smaller proportion. Additionally the material has been characterized by ICP-OES to detect the percentage of various metals and the extraction efficiency of cobalt oxalate. The test showed that leaching efficiency of cobalt oxalate (Fig. 3) has been 91%.

Figure 3. COBALT OXALATE RECOVERED FROM LEACHING SOLUTION AT 1.5 pH

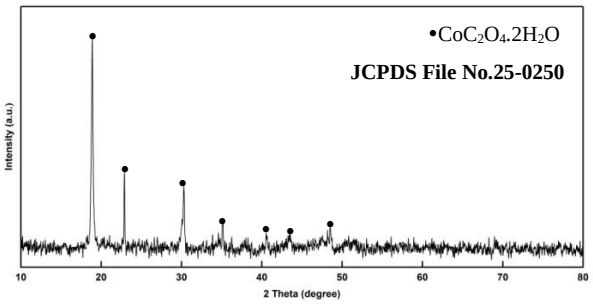

Figure 4. PHASE ANALYSIS OF COBALT OXALATE USING XRD ANALYSIS

Then this sample is analyzed for purity of the cobalt oxalate using ICP-AES technique which is shown in Table 3. It is found that cobalt and carbon are present in significant amounts. It is also found that Mn and Ni are also present in the sample along with Fe and Na in very small quantities. From ICP-AES analysis, the purity of cobalt oxalate is found to be 90 %.

Table 2.COMPOSITION OF COBALT OXALATE USING ICP-AES ANALYSIS

Metal ions	Weight Percentage
Co	28.96
C	10.03
Li	0.02
Mn	1.07
Ni	1.01
Na	0.128
$CoC_2O_4.2H_2O$ Purity	89.8%

Precipitation of $MnCO_3$

The pH of leached liquor was adjusted to pH 7.5 by using 5 M NaOH solution, then a saturated solution of Na_2CO_3 was added drop by drop with continuous stirring at room temperature till a light brownish precipitate of $MnCO_3$ was obtained, filtered and dried overnight in an oven for recovery of $MnCO_3$.The precipitate obtained was not analyzed further since it was not used in the latter stages of cathode material preparation.

CONCLUSIONS

The optimum conditions for the dissolution active cathodic material have been identified as an acid concentration of 2M H_2SO_4 at a temperature of 95°C with a

leaching time of 2 h. We found that the dissolution efficiency of active cathodic material were high at a solid to liquid ratio of 10 gl^{-1}. A higher dissolution efficiency of 95.15% has been reported in this paper. Cobalt oxalate extraction efficiency found to be 91% with purity of 90%. This material can be used as a precursor for lithium cobalt oxide preparation, while fabricating coin cells.

ACNOWLEDGEMENT

The authors acknowledge the department of science and technology, Government of India for financial help for carrying out this work under the DST-SERB-ECR scheme (ECR/2016/000422).

REFERENCES

[1] Zeng, X.; Li, J.; Shen, B., Novel approach to recover cobalt and lithium from spent lithium-ion battery using oxalic acid. Journal of hazardous materials 2015, 295, 112-118.

[2] Pagnanelli, F.; Moscardini, E.; Granada, G.; Cerbelli, S.; Agosta, L.; Fieramosca, A.; Toro, L., Acid reducing leaching of cathodic powder from spent lithium ion batteries: Glucose oxidative pathways and particle area evolution. Journal of Industrial and Engineering Chemistry 2014, 20, (5), 3201-3207.

[3] Granada, G.; Moscardini, E.; Pagnanelli, F.; Trabucco, F.; Toro, L., Product recovery from Li-ion battery wastes coming from an industrial pre-treatment plant: Lab scale tests and process simulations. Journal of Power Sources 2012, 206, 393-401.

[4] Chen, X.; Fan, B.; Xu, L.; Zhou, T.; Kong, J., An atom-economic process for the recovery of high value-added metals from spent lithium-ion batteries. Journal of Cleaner Production 2016, 112, 3562-3570.

[5] Sun, L.; Qiu, K., Organic oxalate as leachant and precipitant for the recovery of valuable metals from spent lithium-ion batteries. Waste management 2012, 32, (8), 1575-82.

[6] Li L., Fan, E., Guan Y., Zhang X., Xue Q., Wei L., Wu, F., Chen, R., Sustainable Recovery of Cathodic Materials from spent li-ion batteries using lactic acid leaching system**,** ACS Sustainable Chem. Eng, (2017), 5 (6), 5224–5233.

[7] Zhang X., Cao H., Xie Y., Ning P., An H., You H., Nawaz F., A closed process for recycling LiNi1/3Co1/3Mn1/3O2 from the cathode scraps of lithium-ion batteries: Process optimization and kinetics analysis, Sep. Puri. Technol, (2015), 150, 186-195.

[8] Jha, M. K., Kumari A., Jha A. K., Kumar V., Hait J., Pandey, B. D., Recovery of lithium and cobalt from waste lithium ion batteries of mobile phone, Waste Management, (2013), 33 (9), 1890-1897.

[9] Zhang P., Yokoyama T., Itabashi O., Suzuki M.T., Inoue K., Hydrometallurgical process for the recovery of metal values from spent lithium ion spent batteries, Hydrometallurgy, (1998), 47, 259–271.

[10] Castillo S., Ansart F., Laberty-Robert C., Portal J., Advances in the recovering of spent lithium battery compounds, J. Power Sources, (2002), 112, 247–254.

[11] Lee C., Rhee K., Reductive leaching of cathodic active materials from lithium ion battery wastes, Hydrometallurgy, (2003), 68, 5-10.

[12] Shin M.S., Kim N., Sohn J., Yang H.D., Kim H.Y., Development of a metal recovery process from Li-ion battery wastes, (2005), Hydrometallurgy, 79, 172-181.

[13] Meng Q., Zhang Y., Dong P., Use of glucose as reductant to recover Co from spent lithium ions batteries, Waste Management, (2017),64, 214–218.

[14] Li-Po He., Shu-Ying Sun., Yan-Yu Mu., Xing-Fu Song., Jian-Guo Yu., Recovery of Lithium, Nickel, Cobalt, and Manganese from Spent Lithium-Ion Batteries Using L-Tartaric Acid as a Leachant, ACS Sustainable Chem. Eng., (2017), 5 (1), 714–721.

Proceedings of the International Conference on Sustainable Energy and Environmental Challenges (3rdSEEC)
18th– 21st, December, 2018, IIT Roorkee, India

SEEC No.021

DEVELOPMENT OF BATCH MODEL FOR MICROBIAL FUEL CELL

Ashish Yewale, Ravi N. Methekar, Shailesh Agrawal

Visvesvaraya National Institute of Technology, Nagpur

ABSTRACT

Demand for energy and clean water is increasing at a faster rate. To meet the required quantity of energy, non-renewable energy sources depleting at a faster rate. This urges scientific society to find better alternative. Microbial fuel cell is a process which generate electricity and produces clean water from waste water or organic matter simultaneously. A batch model is developed to get detailed understanding of the physics of the system. As substrate concentration depleted, it affects the current generation and produces low power. Also the accumulation of protons at the biofilm and anode chamber reduces current generation. This can be improved by pH neutralization. Higher amount of current can be achieved by maintaining pH close to microbial activity.

Keywords: ***Microbial fuel cell, batch model, pulse input, pH***

NOMENCLATURE

a	*Anode*
b	*Tafel coefficient*
c	Cathode
ρ	Density of biomass [$kg.m^{-3}$]
R	Gas constant [$Jmol^{-1}\ K^{-1}$]
F	Faradays constant $coloumb.mol^{-1}$]
$C_{H,b}$	Proton bulk concentration [$kg.m^{-3}$]
$C_{H,bf}$	Proton biofilm concentration [$kg.m^{-3}$]
$C_{OH,b}$	Hydroxide bulk concentration [$kg.m^{-3}$]
$C_{OH,bf}$	Hydroxide biofilm concentration [$kg.m^{-3}$]
V_L	Bulk liquid volume [m^3]
A_m	Membrane area [m^2]
A_b	Biofilm surface area [m^2]
D_H	Diffusivity of protons [$m^2.day^{-1}$]
D_{OH}	Diffusivity of hydroxide ion [$m^2.day^{-1}$]
L_l	Diffusional sublayer thickness [m]
T	MFC chamber temperature [K]
d_m	Membrane thickness [m]
d_{cell}	Distance between electrode [m]
k_{aq}	Solution conductivity [$mS.m^{-1}$]
k_m	Membrane conductivity [$mS.m^{-1}$]
i, I	Current [mA]
$i_{0,\ ref}$	Exchange current density [mA]
η	Activation over potential [mV]

INTRODUCTION

Energy and water necessity have been increasing exponentially. Renewable and non-renewable energy sources are used to meet the current energy requirement, which are economically and environmentally incompatible [1]. Also, Millions of people die due lack of drinking water and water related disease. These problems drive to find the alternative which should be economical, efficient, environment friendly. The consensus is that a multi-faceted approach is needed to solve this energy crisis [2]. In this context, microbial fuel cell (MFC) can be a savior, which treats wastewater and yields electricity at the same time. MFC is a device, which convert the chemical energy present in organic matter into electrical energy under anaerobic condition using microorganisms. Despite its ease of feed stock and extensive range of applications, commercialisation of MFC did not happened till date. The major limitation for the commercialisation process is low power density and scale of process. To improve the power performance, it is important to understand the dynamic of MFC. The dynamic of MFC can be evaluated by performing experiment or modeling. The former is costly and time consuming affair compared to later.

A very few researchers worked on the modeling of MFC. Very scanty literature available for the dynamic modeling of MFC batch process. In 1995, Zhang *et al* [3] developed first 1-D dynamic model for batch MFC, and mediator is used for electron transfer. The influence of

mediator and substrate concentration on current production is captured. Later on, Marcus *et al*. [4] developed a 1-D conduction based dynamic model for batch MFC, where electron is directly transferred to electrode. The 1-D model for multispecies electron donor and acceptor for biofilm anode based on the material balance, Ohm's law and Nernst-Monod kinetics to describe the rate of electron donor oxidation. Conductivity of biofilm is limiting factor in electron transfer mechanisms and current production. Picioreanu *et al* [5] developed a 3-D biofilm based model for batch MFC, using mediator to transfer electrons. They enhance the model by capturing competition between anodophilic and methanogenic bacteria for substrate utilization [6] and pH and anode geometry to increase current generation [7]. Few researchers [8, 9] utilized the model developed by Marcus *et al* [4] and evaluated the impact of anode geometry [8] and parameter estimation [9]. In 2017, Esfandyari *et al* [10], developed batch process model considering direct electron transfer through biofilm to the electron acceptor. Protons gets accumulated in the anode chamber, due to low transport rate. This results into drop in pH and it can hamper the inhibition rate of microbial activity. To improve the power performance of MFC, pH inside anode chamber should be maintain close to the microbial environment.

The substrate utilization in biofilm produces electrons and protons. Proton gets diffused into bulk of anode chamber from biofilm, then into the cathode chamber through the PEM. The main hindrance for the transport of proton are transport through the biofilm and membrane. This result into accumulation of protons in the anode as well as biofilm. In the batch process, substrate is completely consumed and this hamper the rate of substrate utilization and thus current production.

In this paper, we will present the development of dynamic model for batch microbial fuel cell. The model includes the mass balance for substrate, CO_2 and protons between biofilm and bulk liquid. This paper includes pH neutralization for maintaining the pH in anode chamber also the impact of pulse input of substrate on power performance is studied.

MATHEMATICAL MODEL OF BATCH MFC

The MFC operates on the principle of transport and migration of ions along with bio-electrochemical reactions. As the MFC is a complex process, which includes biological, chemical, electrochemical and electrical reactions in the bulk as well as in the biofilm. In this fuel cell, *Shewanella oneidensis* taken as a microorganism and lactate as a substrate. The substrate at the anode chamber gets diffuse into the biofilm from the anode chamber. The substrate available in bulk gets diffuse into the biofilm attached to the anode electrode. Substrate is oxidized by the action of available microorganism in biofilm and generates electrons and protons. Electrons then collected at electrode and transferred to cathode chamber through external circuit producing power. The protons diffused back into bulk liquid and migrates into cathode chamber via proton exchange membrane (PEM). In cathode chamber, reduction reaction occurs between the electrons from the external circuit, migrated protons and supplied oxygen producing water. These phenomena are captured through the mathematical model. In this paper, we used the model presented by Esfandyari *et al* [10]. This is a one dimensional batch model. We converted this batch model into pH controlling and pulse injecting model. We have added the equation for adding substrate once it gets completely oxidized. The pH balance is carried out by adding the equation for buffer balance. NaOH is used for maintaining the pH of anode chamber. For sake of brevity, we are presenting here only modified equations, however other equations used in model can be found in Esfandyari *et al* [10].

Assumptions:

1) MFC is considered as lumped parameter system
2) Temperature of anode and cathode chamber maintained constant at 303 K
3) pH of the cathode chamber is maintained

Half reaction at anode

$$C_3H_6O_3 + 3H_2O \rightarrow 3CO_2 + 12H^+ + 12e^- \quad (1)$$

Half reaction at cathode

$$O_2 + 4H^+ + 4e^- \rightarrow 2H_2O \quad (2)$$

Change in the concentration protons in the biofilm is captured by following equation

$$\frac{d\left(C_{H,bf}(t)\right)}{dt} = \left(C_{H,b}(t) - C_{H,bf}(t)\right)\left(\frac{D_H}{L_f L(t)}\right) + 12\rho r_s - \frac{C_{H,bf}(t)}{L(t)}\frac{d}{dt}\left(L(t)\right) - K_{bf}C_{H,bf}(t)C_{OH}(t) \quad (3)$$

The first term in above equation represents diffusion of protons from biofilm into bulk, second term represents production of protons, third term represents balance term comes after applying chain rule due to change in volume with time and fourth term represents the consumption of produced proton.

Change in the concentration protons in the bulk liquid of anode is given by following equation

$$\frac{d\left(C_{H,b}(t)\right)}{dt} = -\left(C_{H,b}(t) - C_{H,bf}(t)\right)\left(\frac{D_H A_{bf}}{L_f V_L(t)}\right) - \left(C_{H,b}(t) - C_{HC}(t)\right)\left(\frac{D_{mem}}{L_f d_m(t)}\right) - K_{bk}C_{H,b}(t)C_{OH,b}(t) \quad (4)$$

The first term in above equation represents diffusion of protons from biofilm into bulk, second term represents diffusion of proton from bulk liquid into cathode chamber via PEM and third term represents the consumption of accumulated proton in the bulk.

Change in the concentration of bufferin bulk liquid is given by

$$\frac{\mathrm{d}\left(C_{OH,b}(\mathrm{t})\right)}{\mathrm{dt}} = -K_{bk}C_{H,b}(t)C_{OH,b}(t) - \left(C_{OH,b}(\mathrm{t}) - C_{OH,bf}(\mathrm{t})\right)\left(\frac{D_{OH}A_{bf}}{L_l V_L(t)}\right) \tag{5}$$

The first term in above equation represents the consumption of excess proton in the bulk chamber and second term represents the diffusion of buffer into the biofilm.

Change in the concentration of buffer in biofilm is given by

$$\frac{\mathrm{d}\left(C_{H,b}(\mathrm{t})\right)}{\mathrm{dt}} = \left(C_{OH,b}(\mathrm{t}) - C_{OH,bf}(\mathrm{t})\right)\left(\frac{D_{OH}A_{bf}}{L_l L(t)}\right) - K_{bf}C_{H,bf}(t)C_{OH,bf}(t) - \frac{C_{OH,bf}(t)}{L(t)}\frac{d}{dt}\left(L(t)\right) \tag{6}$$

The first term represents diffusion of buffer into biofilm, second term represents consumption of protons inside biofilm and third term represent the balance term came after applying chain rule.

The cell voltage obtained from continuous MFC is given as

$$\mathrm{E_{out}} = E_{thero} - \frac{b}{2.303}\sinh^{-1}\left[\frac{i}{2i_{0,ref}}\right] - \left(\frac{d_m}{k_m} + \frac{d_{cell}}{k_{aq}}\right)i - \frac{RT}{nF}\ln\left(\frac{\frac{nFD_sC_{sb}}{L_l}}{\frac{nFD_sC_{sb}}{L_l} - i}\right) \tag{7}$$

Solution procedure

The data for the base case considered in this paper is given in table 1. This model consists of thirteen ordinary differential equations with one algebraic equation. Equation (7) is solved for current after setting voltage at a fixed value. After obtaining current all differential equation is solved using ode solver (ode23) in MATLAB for required time period. As the voltage is fixed at particular value, current is calculated at operating condition. Due to this solution approach, trial error method of solution has been avoided.

Model validation

We have validated our batch model with literature. As mentioned earlier, the model equations are taken from Esfandyari *et al* (10). Hence, some key dynamic is validated with Esfandyari *et al* as well as Picioreanu *et al*[5] such as substrate consumption, current production and biofilm thickness. Fig. 1 shows the dynamics of the above mentioned variables with the Picioreanu *et al*[5] work. It is found that the key dynamics are qualitatively in good agreement with Picioreanu et al[5] work.

RESULTS AND DISCUSSION

Pulse injection of substrate

In the batch process, substrate is fed into the anode chamber at the start of reaction. Over the evolution of time substrate gets consumed in the biofilm and produces electrons and protons and thus current. Fig. 1 show, the development of current with time. It shows that, current decreased after reaching optimum value due to depletion in substrate concentration. Fresh substrate is injected into the bulk of anode chamber to extract more current shown in Fig. 2. The current very quickly reach maximum and remains constant until adequate amount of substrate is available. This second batch will produce more current compared to previous because the excess quantity of active fraction of biomass is available when compared to old batch. This excess amount of biomass increases the utilization rate and produces more electrons and protons resulted into higher current generation.

pH neutralization in batch process

The accumulation of protons in the biofilm as well as bulk liquid results into acidification of MFC. This will drop the pH of biofilm and anode chamber and thus effect the inhibition of microorganisms. Fig. 3 show the effect of buffer concentration on the current generation and maintaining pH at constant value close to 7. As we increase the concentration of buffer solution, the pH reaching towards 7 and thus current increases. Further increase in buffer concentration results into decreases in current generation due to excess consumption of proton in the biofilm as well as bulk liquid. Current generation is highly dependent on buffer concentration. It is decreased in absence or excess buffer concentration.

CONCLUSION

The batch model for microbial fuel cell has been developed and simulated. The batch model is validated with the work of Picioreanu *et al*[5]. A novel method for solution of MFC model is presented. The model is updated for pulse injection of substrate and maintaining pH in the anode as well as biofilm. The pulse input shows that the current rapidly increased to a maximum value and then drops down with the decrease in substrate concentration. pH neutralization shows the impact of buffer solution on the current generation. Excess or deficient amount of buffer decrease the current generation in MFC.

FIGURES AND TABLES

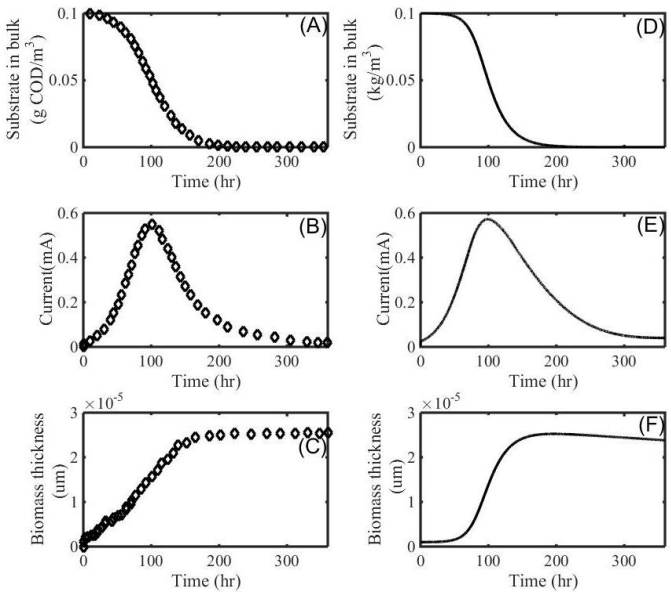

FIGURE 1. QUALITATIVE VALIDATION OF MODEL WITH LITERATURE, (A-C) TRENDS FROM MODEL SIMULATION, AND (D-F) TRENDS FROM LITERATURE

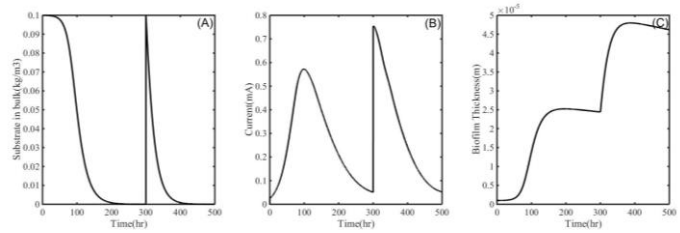

FIGURE 2. PULSE INJECTION IN THE ANODE CHAMBER (A) BULK SUBSTRATE CONCENTRATION (B) CURRENT PRODUCED (C) BIOFILM THICKNESS

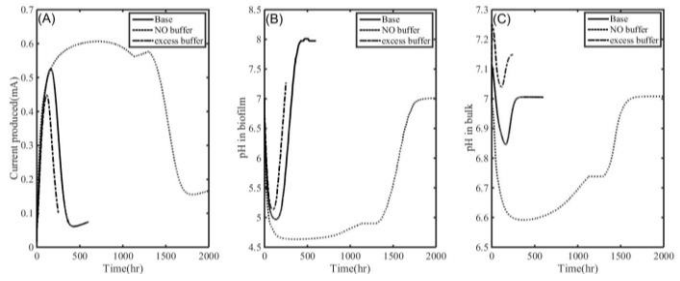

FIGURE 3. PH NEUTRALIZATION IN THE ANODE CHAMBER (A) CURRENT PRODUCED (B) PH IN BIOFILM (C) PH IN BULK LIQUID

TABLE 1. DATA FOR THE BASE CASE

Input variable	values
$C_{sb,0}$ (kg/m^3)	0.1
$C_{OH,0}$ (kg/m^3)	1.48×10^{-2}
A_b(m^2)	22.4×10^{-4}
Eset (mV)	35×10^{-3}
T (K)	303

REFERENCES

[1] Rahimnejad M., Adhami A., Darvari S., Zirepour A., Oh S., 2015. "Microbial fuel cell as new technology for bioelectricity generation: A review", Alexandria Engineering Journal, 54, pp. 745–756.

[2] Capodaglio A., Molognoni D., and Pons A.,2016. "A multi-perspective review of microbial fuel-cells for wastewater treatment: Bio-electrochemical, microbiologic and modeling aspects" AIP Conference Proceedings, 1758, 030032.

[3] Zhang X. and HalmeA.,1995. "Modelling of a microbial fuel cell process", Biotechnol. Lett. 17, pp. 809–814.

[4] Marcus A., Torres C., and Rittmann B., 2007. "Conduction-Based Modeling of the Biofilm Anode of a Microbial Fuel Cell" Biotechnology and Bioengineering, 98 (6), June, pp. 1171-1182.

[5] Picioreanu C., Head I., Katuri K., Loosdrecht M. van, Scott K., 2007. "A Computational Model for Biofilm-Based Microbial Fuel Cells" Water Research,41, May, pp. 2921-2940.

[6] Picioreanu C., Katuri K., Head I., Loosdrecht M. van, Scott K.,2008. "Mathematical model for microbial fuel cells with anodic biofilms and anaerobic digestion" Water Sci. Technol. 57, pp. 965–971.

[7] Picioreanu C., Mark C.M. van Loosdrecht M.C.M. Van, Curtis T., Scott K.,2010. "Model based evaluation of the effect of pH and electrode geometry on microbial fuelcell performance", Bioelectrochemistry, 78, pp. 8-24.

[8] Merkey B., and Chopp D., 2012. "The Performance of a Microbial Fuel Cell Depends Strongly on Anode Geometry: A Multidimensional Modeling Study", Bull Math Biol 74 pp. 834–857.

[9] Sedaqatvand R., Esfahany M., Behzad T., Mohseni M., Mardanpour M.,2013. "Parameter estimation and characterization of a single-chamber microbial fuel cell for dairy wastewater treatment", Bioresource Technology, 146, pp. 247–253.

[10] Esfandyari M., Fanaei M., Gheshlaghi R., and Mahdavi M., 2017. "Mathematical modeling of two-chamber batch microbial fuel cell with pure culture of *Shewanella*" Chemical Engineering Research and Design, 7, pp. 34-42.

Proceedings of International Conference on Sustainable Energy and Environmental Challenges (3rd SEEC), December 18-21, 2018, IIT Roorkee, India

SEEC No. 022

PREDICTION OF POTENTIAL OF ENERGY GENERATION FROM MUNICIPAL SOLID WASTE THROUGH INCINERATION TECHNOLOGY

Abhishek Kumar[1]

[1]PG Student, Thermal Engineering, Bundelkhand Institute of Engineering and Technology, Jhansi, U.P., India
Email: akj.mechanical@gmail.com

Dr. N. P. Yadav[2]

[2]Professor, Department of Mechanical Engineering, Bundelkhand Institute of Engineering and Technology, Jhansi, U.P., India
Email: npyadava@gmail.com

ABSTRACT

This paper focuses on the energy generation from the municipal solid waste of Jhansi city through incineration process. However, the potential energy capacity has been calculated by four most commonly used empirical relations after finding out the chemical composition of MSW considering it as fuel. The samples have been collected from five wards and then manual segregation were done to categorise the waste. These segregated portions were also quantified by weighing them. The chemical composition is found out by performing ultimate analysis. On behalf of ultimate analysis reports of the waste samples, approximate quantity of categorised waste is calculated for all the sixty wards of Jhansi city by keeping population of the city as a factor. These values are used in empirical relations for quantifying heating value of fuel in MJ/kg and Net Electric Power Generation capacity in MWh/day and MW. In the worst case it can be said that 4 MW power can be extracted from the MSW daily. So, ultimately, this paper deals with estimating the daily MSW of Jhansi city and potential of energy generation from it. The paper focuses on technical feasibility only.

Keywords: Municipal Solid Waste, Waste to Energy, Ultimate Analysis, Jhansi City

NOMENCLATURE

MSW	Municipal Solid Waste
WTE	Waste-To-Energy
TPD	Tonnes Per Day
MNRE	Ministry of New and Renewable Energy
JNN	Jhansi Nagar Nigam
HHV	Higher Heating Value
LHV	Lower Heating Value
NEPG	Net Electric Power Generated

INTRODUCTION

All societies produce some kind of waste as per their need, e.g., organic or inorganic; toxic or non-toxic, etc. So, it was observed that management of waste is very essential. Few theories were also proposed about the reusing and recycling of waste. Then an idea which opened a new door of research and analysis was to produce energy from this waste by incineration (a waste-to-energy technology). The idea seems to be attractive since it not only reduced the volume of waste to a numerable extent but also saved the land which earlier was required to dump it, solved up to some extent the environmental concern of GHG, land water pollution and odour. On the other hand, it produced thermal energy which could be used in house heating or in thermal power plants to generate electricity. And since, the waste is something which will get produced regularly, this source of energy generation may also be referred to as an everlasting source. It will also reduce our dependency on conventional fossil fuels.

Various components of MSW have an economic value because of their calorific value. Over 81% of MSW is disposed at open dump sites annually without any treatment. With planned efforts to Reduce, Reuse, Recover, Recycle and Remanufacture (5Rs) and appropriate technology adoption, the country can profitably utilize about 65% of the waste in producing energy and/or compost and another 10 to 15% to promote recycling industry and bring down the quantity of wastes going to landfills/dumps under 20%. [1]

In Indian context, there is an urgent need to manage the MSW generated. According to the MNRE, in comparison to the levels of the developed world of 1 to 2.5 kg/capita/day, average MSW generation in India is 450 gm/capita/day. This amount is further less in the country is 200-300 gm/capita/day for small towns, 300-400 gm/capita/day for medium cities and 400-600 gm/capita/day for large cities. This seems to be impressive but due to large population, cumulative amount of waste produced daily becomes very huge. Plastic wastes and its composites are high calorific value materials and decisive ingredients for MSW based WTE plants. Under the Indian context, following Waste-To-Energy (WTE) technologies are suitable of [2]:

I. **Bio-methanation for wet bio-degradable wastes**
II. **Combustion of Refuse-Derived Fuel (RDF)**
III. **Mass burning of MSW/Incineration**

IV. In addition to the above, two other technologies which are currently under Research and Development and piloting phase are of:
   i) Gasification
   ii) Pyrolysis

There is an approximate potential of 500 MW in present as per the waste collected from cities/towns in India, which can be enhanced to 1075 MW by the year 2031 and further to 2780 MW by 2050 [2]. The above data gives a glance on how India can create an alternate source of energy through the waste generated in its urban localities and also contribute in Swachh Bharat Mission by getting rid of from this waste.

Most of the modern WTE plants use incineration facilities. The reason behind that it can be applied even when the MSW is received without pre-treatment, such as mechanical fine sorting or chemical treatment, and fed directly to the incinerator. [3]

The total amount of waste generation in the country is estimated at around 1.43 lakh metric tonnes/day. Out of which, 82% is being collected and remaining 18% is littered. Out of this total collected waste, only 28% is being treated and disposed cleanly. [4]

STUDY AREA

Jhansi city is extended between 24°11' N to 25°57' N and 78°10' E to 79°25' E and has an average elevation of 284 meters. As per the census report of 2011 the population of the city is 505,693. The city's municipal body is Nagar Nigam which administers 152 square kilometres of area which is divided in 5 circles containing 60 sanitary wards.

Jhansi Nagar Nigam (JNN) is responsible for the collection, transportation and disposal of all solid waste generated in the city, except the untreated bio-medical waste and hazardous industrial waste, which is taken care by the respective generators.

The statistics of existing and future land use categories within Jhansi city, obtained from the Jhansi Master Plan are summarized in Table 1. [5]

TABLE 1: Land Use Categories in Jhansi city [5]

Land Use Category	2001	2021
Residential	44.3%	50.75%
Commercial	3.17%	1.32%
Institutional	8.51%	9.85%
Industrial	11.55%	7.08%
Govt. & Other Offices	3.03%	2.49%
Roads	10.64%	12.27%
Community Services	10.84%	9.93%

The total waste generated in Jhansi city is 197 Tonnes Per Day (TPD) (approx.), out of which about 150 TPD (approx.) is collected and transported daily. [5]

CHARACTERISTICS OF SOLID WASTE IN JHANSI CITY

There are 60 wards in Jhansi city and each ward produces around 3 to 4 TPD of waste as per the information gathered from Jhansi Nagar Nigam (JNN). It is quite hard to represent exact day-to-day quantity of waste from each ward daily because of the absence of proper waste monitoring mechanism. Thus, a solution is applied in this regard by making out small samples from five wards of 5 kg each. These five wards are chosen on random basis and are located at enough distance from each other, so that approximation becomes better. The chosen wards are – Ward No. 3 (Bahar Saiyar Gate), Ward No. 18 (Gudri), Ward No. 20 (Bangla Ghat), Ward No. 29 (Pichhor), Ward No. 41 (Dadiyapura First).

Efforts are made to maintain the uniformity of each sample by collecting it in parts and not just picking up the whole sample from the top of the heap of MSW unloaded. These sample are then segregated manually in six categories – Food Waste, Plastic, Paper, Cardboard, Garden Trimming and Residual Material. The weights of each category from each sample is measured separately and has been shown in Table 2.

TABLE 2: Composition of Solid Waste generated in Ward No. 3, 18, 20, 29, 41 of Jhansi city

Waste Component	**Quantity (kg/day) (Out of 5 kg sample)**				
	Ward No. 3	**Ward No. 18**	**Ward No. 20**	**Ward No. 29**	**Ward No. 41**
Food Waste	1.167	1.135	1.247	1.262	1.277
Plastic	0.505	0.521	0.563	0.559	0.563
Paper	0.662	0.551	0.539	0.538	0.498
Cardboard	0.296	0.279	0.281	0.293	0.312
Garden Trimming	1.446	1.516	1.328	1.456	1.496
Residue	0.924	0.998	1.042	0.892	0.854
Total	**5.000**	**5.000**	**5.000**	**5.000**	**5.000**

Ultimate Analysis is done on dry basis (% by wt.). Average Moisture Content (MC) is assumed on the basis of Tchobanoglaus G. et al. (1997) mentioned in Ankit Singh et al. (2014) [6]. This is 75% for food waste, 2% for plastic, 7% for paper, 7% for cardboard, 60% for garden trimming.

$$Dry\ wt.of\ Component\ (kg) = \frac{Wet\ wt.of\ Component\ (kg)\ X\ (100\ -\ \%\ MC)}{100}$$

From the above-mentioned formula dry weight composition of solid waste can be formulated which has been mentioned in Table 3.

TABLE 3: Dry wt. Composition of Solid Waste generated in Ward No. 3, 18, 20, 29, 41 of Jhansi city

Waste Component	**Dry Quantity (kg/day) (Out of 5 kg sample)**				
	Ward No. 3	**Ward No. 18**	**Ward No. 20**	**Ward No. 29**	**Ward No. 41**
Food Waste	0.29175	0.28375	0.31175	0.31550	0.31925
Plastic	0.49490	0.51058	0.55174	0.54782	0.55174
Paper	0.61566	0.51243	0.50127	0.50034	0.46314
Cardboard	0.27528	0.25947	0.26133	0.27249	0.29016
Garden Trimming	0.57840	0.60640	0.53120	0.58240	0.59840
Residue	0.924*	0.998*	1.042*	0.892*	0.854*
Total	**3.17999**	**3.17063**	**3.19929**	**3.11055**	**3.07669**

**Since Average Moisture content for Residue cannot be calculated due to its unpredictably changing composition, therefore, it is presented as it is.*

As the total waste generated in Jhansi city is about 197 TPD and the population of Jhansi city is 5,05,693 as per census 2011 and there are 60 wards in the city, thus, it can be averaged that per capita waste generation in the city is 0.388 kg/person/day and per ward waste generation is 3.283 TPD. Based on this averaging, total quantity of waste components on ward basis can be calculated. Table 4 gives the description of total averaged weight of waste components in ward no. 3, 18, 20, 29, 41.

TABLE 4: Total dry wt. composition of Solid Waste generated in Ward No. 3, 18, 20, 29, 41 of Jhansi city

Waste Component	**Total Quantity (kg/day)**				
	Ward No. 3	**Ward No. 18**	**Ward No. 20**	**Ward No. 29**	**Ward No. 41**
Food Waste	191.5825	186.3292	204.7158	207.1783	209.6408
Plastic	324.9843	335.2809	362.3093	359.7351	362.3093
Paper	404.2834	336.4957	329.1673	328.5566	304.1286
Cardboard	180.7672	170.3853	171.6067	178.9351	190.5384
Garden Trimming	379.8160	398.2027	348.8213	382.4427	392.9493
Residue	606.7600	655.3533	684.2467	585.7467	560.7983
Total	**2088.1934**	**2082.0471**	**2100.8671**	**2042.5945**	**2020.3597**

The percentage compositions of dry wt. of these five wards have been represented through Table 5.

TABLE 5: Ward-wise waste percent compositions of Ward No. 3, 18, 20, 29, 41 of Jhansi city

Waste Component	**Ward-wise Dry wt. Percent Compositions**				
	Ward No. 3	**Ward No. 18**	**Ward No. 20**	**Ward No. 29**	**Ward No. 41**
Food Waste	9.17	8.95	9.74	10.13	10.38
Plastic	15.56	16.10	17.25	17.61	17.93
Paper	19.36	16.16	15.67	16.09	15.05
Cardboard	8.66	8.18	8.17	8.76	9.43
Garden Trimming	18.19	19.13	16.60	18.73	19.45
Residue	29.06	31.48	32.57	28.68	27.76

ULTIMATE ANALYSIS OF SOLID WASTE AND FEASIBILITY OF SAMPLE EXPERIMENTATION

The ultimate analysis of a waste component typically involves the determination of the percent of C (carbon), H (hydrogen), O (oxygen), N (nitrogen), S (sulphur), and ash or inert material.

Since, assumption is of same types of waste, only the relative quantity is varying, thus ultimate analysis would be done for the waste types of a single ward to find the percentage of chemical elements. The quantity in kilograms would be found out on sample basis. Thus, Table 6 describes about ultimate analysis in percent of categorised waste, while Table 7 describes about the ultimate waste composition in kg/day of ward no. 3, 18, 20, 29, 41 respectively.

TABLE 6: Ultimate Analysis per unit weight (dry basis) of Solid Waste Components in percent

Waste	**C (%)***	**H (%)***	**O (%)***	**N (%)***	**S (%)***	**ASH (%)***
Food Waste	47.83	6.1	36.8	2.4	0.36	6.51
Plastic	58.64	6.9	22.5	0.05	0.03	11.68
Paper	43.2	5.8	42.9	0.3	0.2	7.6
Cardboard	42.6	5.6	43.9	0.28	0.19	7.43
Garden Trimming	47.25	5.7	37.75	3.1	0.25	5.95

Residue	48.7	6.0	38.5	0.09	0.03	6.68

**% by weight (dry basis)*

TABLE 7: Ultimate Composition of Solid Waste from Ward No 3, 18, 20, 29, 41 of Jhansi city

SOURCE WARD	COMPOSITION (kg/day of waste)					
	C	H	O	N	S	ASH
Ward No. 3	1008.81	125.74	773.40	18.80	3.07	157.72
Ward No. 18	1010.99	125.58	765.80	19.06	2.95	117.99
Ward No, 20	1023.76	127.12	768.50	17.99	2.92	160.01
Ward No. 29	994.17	123.48	746.56	19.03	3.00	155.78
Ward No. 41	984.06	122.15	707.04	19.33	2.98	154.20
Total	**5021.79**	**624.07**	**3761.30**	**94.21**	**14.92**	**745.70**

**Appendix shows the individual ward-wise composition*

To check the feasibility of samples, it is required to consider the population of the places of sample collection. Thus, Table 8 gives a glance of the population of the wards from where samples has been collected.

TABLE 8: Population of Ward No. 3, 18, 20, 29, 41 of Jhansi city as per Census 2011. [7]

WARD NO.	WARD NAME	POPULATION
3	Bahar Saiyar Gate	8009
18	Gudri	8102
20	Bangla Ghat	8490
29	Pichhor	12647
41	Dadiyapura First	13704
Total		**50952**

Since as per the survey of census India 2011, the total population of Jhansi city is 505,693 and the samples has been collected for the population of 50,952, which is almost 10.08 % of the total population, thus a fair approximation of chemical constituents of total municipal solid waste can be made on behalf of these five wards. So, Table 9 indicates the composition of total waste in kg/ day, in kg/tonne and in % from the Jhansi city. This data has also shown in terms of percent in Fig 1.

TABLE 9: Approximate Composition of Chemical Constituents of Solid Waste generated from Jhansi city

Source	Composition (kg/day)					
	C	H	O	N	S	Ash
All 60 Wards of Jhansi city	49840.71	6193.83	37330.49	935.02	148.08	7400.99
	Composition (kg/tonne)					
	C	**H**	**O**	**N**	**S**	**Ash**
	253.00	31.44	189.49	4.75	0.75	37.57
	Composition (%)					
	C	**H**	**O**	**N**	**S**	**Ash**
	48.94	6.08	36.65	0.92	0.15	7.27

Thus, out of one tonne of solid waste, only 517 kg of waste can be considered as dry waste, which is to be 51.70 %. Thus, out of 197 tonnes of MSW generated daily by the residents of Jhansi city 101.85 tonnes is dry only.

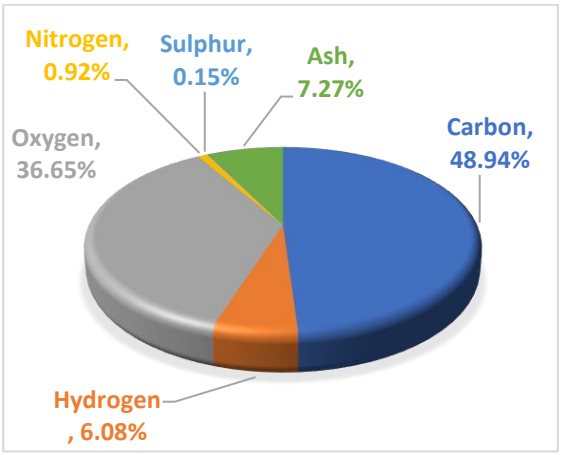

FIGURE 1: Percentage Waste Composition of Jhansi city

COMPUTATION OF ENERGY POTENTIAL

To calculate the electrical energy potential, it is first necessary to calculate the heat energy generated from the MSW of Jhansi city. This can be achieved by putting the above percent values of chemical constituents in any empirical correlation such as Dulong Formula and other formulas mentioned in equation (1), (2), (3) and (4) respectively. In this paper four empirical correlations are used to find the end results. However, these end results also depend on some efficiency assumptions. Further calculations have been done by considering steam conversion efficiency as 70%, electrical energy conversion efficiency as 31.6%, station service allowance as 6% and unaccounted heat loss as 5 %. [8], [9]

(A). Using Dulong's Formula [10]

$$\mathbf{HHV = 4.185 * (78.4 * C + 241.3 * H + 22.1 * S)} \quad (1)$$

= 22211.11 kJ/kg

Heat Energy Generated = 22211.11 kJ/kg

This Heat Energy Generated is used to produce steam.

Steam Energy Available = 70 % of Heat Energy generated = (0.70 x 22211.11) = 15547.78 kJ/kg

This calculated Steam Energy is utilized to run the Steam Turbines which are further coupled to Power Generators which produce electricity. Heat Rate is the heat input required to produce one unit of electricity (i.e. kWh), and 1 kWh = 3600 kJ/h

Since, no energy conversion is perfect or 100% efficient. Thus, to get fair results, losses must be taken into consideration.

Considering the conversion efficiency of 31.6%. Thus, in a power plant the heat input which is required is 3600/31.6% = 11392.405 kJ/kWh

So, to produce 1 kWh Electrical Energy 11393 kJ of steam energy is required.

Electrical Energy Generation = Steam Energy / 11393 = (15547.78 / 11393) kWh/kg = 1.3647 kWh/kg

Total weight of Dry Solid Waste generated in Jhansi city = 101.849 tonnes/day = 101849 kg/day

Total Electric Power generation = (1.3647 x 101849) kWh/day = 138993.3 kWh/day

Considering Station Service Allowance = 6% of the total electric power generation = (0.06 x 138993.3) kWh/day = 8339.6 kWh/day

Unaccounted Heat Loss = 5% of the total electric power generation = (0.05 x 138993.3) kWh/day = 6949.665 kWh/day

Net Electric Power Generation = Total Electric Power Generation – (Station Service Allowance + Unaccounted Heat Loss)

= [117187.5 – (8339.6 + 6949.665)] kWh/day

= 123704.03 kWh/day = 123.7 MWh/day

The above generated electricity is for one day or for 24 hours.

Thus, for per hour basis,

Net Electric Power generated = 123.7/24 = 5.15 MW

(B). Using Modified Dulong's Formula [10]

$$\mathbf{HHV = 4.18 * \{78.4*C + 241.3*(H - O/8) + 22.1*S\}} \quad (2)$$

= 17563.77 kJ/kg

Heat Energy Generated = 17563.77 kJ/kg

Thus, again implementing the same procedure;

Steam Energy available = 70% of Heat Energy Generated = 0.70 x 17563.77 = 12294.64 kJ/kg

Heat input required in a power plant is 3600/31.6% = 11392.405 kJ/kWh

So, to produce 1 kWh Electrical Energy 11393 kJ of steam energy is required.

Electrical Energy Generation = Steam Energy / 11393 = (12294.64 / 11393) kWh/kg = 1.0791 kWh/kg

Total weight of Dry Solid Waste generated in Jhansi city = 101.849 tonnes/day = 101849 kg/day

Total Electric Power generation = (1.0791 x 101849) kWh/day = 109905.26 kWh/day

Station Service Allowance = 6% of the total electric power generation = (0.06 x 109905.26) kWh/day = 6594.31 kWh/day

Unaccounted Heat Loss = 5% of the total electric power generation = (0.05 x 109905.26) kWh/day = 5495.26 kWh/day

Net Electric Power Generation = Total Electric Power Generation – (Station Service Allowance + Unaccounted Heat Loss)

= [109905.26 – (6594.31 + 5495.26)] kWh/day

= 97815.69 kWh/day = 97.8 MWh/day

The above generated electricity is for one day or for 24 hours.

Thus, for per hour basis,

Net Electric Power generated = 97.8/24 = 4.07 MW

(C). Using Vandralek Formula [10]

$$\mathbf{HHV = 4.18 * \{85 * C + 270 * H + 26 * (S - O)\}} \quad (3)$$

= 20283.45 kJ/kg

Heat Energy Generated = 20283.45 kJ/kg

Using the same procedure again;

Steam Energy available = 70% of Heat Energy Generated = 0.70 x 20283.45 = 14198.415 kJ/kg

Heat input required in power plant is 3600/31.6% = 11392.405 kJ/kWh

So, to produce 1 kWh Electrical Energy 11393 kJ of steam energy is required.

Electrical Energy Generation = Steam Energy / 11393 = (14198.415 / 11393) kWh/kg = 1.2462 kWh/kg

Total weight of Dry Solid Waste generated in Jhansi city = 101.849 tonnes/day = 101849 kg/day

Total Electric Power generation = (1.2462 x 101849) kWh/day = 126924.22 kWh/day

Station Service Allowance = 6% of the total electric power generation = (0.06 x 126924.22) kWh/day = 7615.45 kWh/day

Unaccounted Heat Loss = 5% of the total electric power generation = (0.05 x 126924.22) kWh/day = 6346.21 kWh/day

Net Electric Power Generation = Total Electric Power Generation – (Station Service Allowance + Unaccounted Heat Loss)

= [126924.22 – (7615.45 + 6346.21)] kWh/day

= 112962.56 kWh/day = 112.9 MWh/day

The above generated electricity is for one day or for 24 hours.

Thus, for per hour basis,

Net Electric Power generated = 112.9/24 = 4.70 MW

(D). Using Direct Formula for LHV [10]

$$\mathbf{LHV = 4.18 * (94.19 * C – 0.5501 – 52.14 * H)} \quad (4)$$

= 17940.97 kJ/kg

Heat Energy Generated = 17940.97 kJ/kg

Steam Energy available = 70% of Heat Energy Generated = 0.70 x 17940.97 = 12558.68 kJ/kg

Heat input required in a power plant is 3600/31.6% = 11392.405 kJ/kWh

So, to produce 1 kWh Electrical Energy 11393 kJ of steam energy is required.

Electrical Energy Generation = Steam Energy / 11393 = (12558.68 / 11393) kWh/kg = 1.1023 kWh/kg

Total weight of Dry Solid Waste generated in Jhansi city = 101.849 tonnes/day = 101849 kg/day

Total Electric Power generation = (1.1023 x 101849) kWh/day = 112268.15 kWh/day

Station Service Allowance = 6% of the total electric power generation = (0.06 x 112268.15) kWh/day = 6736.09 kWh/day

Unaccounted Heat Loss = 5% of the total electric power generation = (0.05 x 112268.15) kWh/day = 5613.41 kWh/day

Net Electric Power Generation = Total Electric Power Generation – (Station Service Allowance + Unaccounted Heat Loss)

= [112268.15 – (6736.09 + 5613.41)] kWh/day

= 99918.65 kWh/day = 99.9 MWh/day

The above generated electricity is for one day or for 24 hours.

Thus, for per hour basis,

Net Electric Power generated = 99.9/24 = 4.16 MW

RESULTS AND DISCUSSION

The potential for net electric energy has been calculated by using different formulas and thus the results obtained by them are also different. These results have been tabulated in Table 10

TABLE 10: Results of Energy in different units obtained by different formulas

METHOD USED	**HEATING VALUE (MJ/kg)**	**NET ELECTRIC POWER GENERATED (NEPG)**	
		(MWh/day)	**(MW)**
Dulong Formula	HHV = 22.211 MJ/kg	123.7 MWh/day	5.15 MW
Modified Dulong Formula	HHV = 17.564 MJ/kg	97.8 MWh/day	4.07 MW
Vandralek Formula	HHV = 20.283 MJ/kg	112.9 MWh/day	4.70 MW
Direct Formula for LHV	LHV = 17.941 MJ/kg	99.9 MWh/day	4.16 MW

From the above table, it can be interpreted that even in the worst case there is a potential of 4 MW of electricity generation by the heat recovered from the Jhansi city.

CONCLUSION

A thorough analysis has been done on the amount of MSW generation in Jhansi city and an effort has been made in order to quantify the energy potential of this MSW to produce heat energy for power generation. The generation of municipal solid waste in Jhansi city is around 197 TPD, out of which as per the sample survey and experimentation it was found that it comprises of around 48.3% of wet waste. Thus, the quantity of dry waste is 51.7% or 101.849 TPD. Four empirical relations have been used to find out the heating value and net electric power generation capacity of dry portion of MSW of Jhansi city. These relations provide different results but still by considering the worst case, there is a potential of 4 MW of electricity generation by the heat recovered from the MSW of Jhansi city. On the other hand, it will reduce the quantity of waste going to landfill to a significant amount.

REFERENCES

1. Report of the Task Force on Waste to Energy (WTE), May, 2014. NITI Aayog (erstwhile Planning Commission), Govt. of India.

2. "Power Generation from Municipal Solid Waste", 20th report, August, 2016. Standing Committee on Energy (2015-16), Sixteenth Lok Sabha, Ministry of New and Renewable Energy.
3. Paul Cheremisinoff, 1992. "Incinerator Types", Waste Incineration Handbook, pp. 49-67.
4. Report of Central Pollution Control Board; February, 2015.
5. Detailed Project Report, 2015-2016. "Solid Waste Management in Jhansi (Uttar Pradesh)", Regional Centre for Urban and Environmental Studies.
6. Ankit Singh and Remya Neelancherry, 2014. "Solid Waste Management: A Case Study of Ultimate Analysis and Landfill Design for NIT Calicut", International Journal of Scientific and Engineering Research, 5(7), July, pp. 174-182.
7. Census Report of India, 2011.
8. Shubham Gupta and R. S. Mishra, 2015. "Estimation of Electrical Energy Generation from Waste to Energy using Incineration Technology", International Journal of Advance Research and Innovation, 3(4), pp. 631-634.
9. Shubham Rathi and Dr. Pradeep Kumar, 2014. "Electrical Energy Recovery from Municipal Solid Waste of Kanpur city", International Journal of Scientific Research Engineering and Technology (IJSRET), 3(5), August.
10. Jean Fidele NZIHOU, Salou Hamidou, Medard Bouda, Jean Koulidiati and B. Gerard Segda, 2014. "Using Dulong and Vandralek Formulas to Estimate the Calorific Heating Value of a Household Waste Model", International Journal of Scientific & Engineering Research (IJSER); 5(1), January, pp. 1878- 1883.
11. Jhansi Nagar Nigam.

Proceedings of the third International Conference on Sustainable Energy and Environmental Challenges (3rdSEEC)
18 –21 December, 2018, IIT Roorkee, India

SEEC No.023

Comparative Evaluation of Energy and GHG Emissions of Diesel and Biodiesels from Jatropha Oil and Waste Cooking Oil

Suvam Bhadra
Automotive Research Centre
Vellore Institute of Technology
Email : suvam.bhadra2015@vit.ac.in

Arnab Das
Automotive Research Centre
Vellore Institute of Technology
Email : arnab.das2015@vit.ac.in

J. Thangaraja
Automotive Research Centre
Vellore Institute of Technology
Email : thangaraja.j@vit.ac.in

ABSTRACT

Recent studies have evaluated the life cycle analysis of biofuels and highlighted the reduction in overall Greenhouse Gases (GHG) relative to fossil diesel. The current work contributes to the sustainability characteristics of biodiesel fuels by estimating the energy and GHG Emissions of jatropha and waste cooking methyl esters. The energy and GHG emission analysis are evaluated using the Greenhouse gases, Regulated Emissions, and Energy use in Transportation (GREET) Model. In comparison to fossil diesel, jatropha biodiesel consumed 32.28% lower energy, while in the case of WCO biodiesel it was found to be lowered by 14.61%. Further, biodiesel fuels exhibits lower GHG than fossil diesel, and WCO shows a significant reduction in the carbon dioxide emissions

Keywords

Life Cycle Analysis, Jatropha, Waste Cooking Oil, Fossil Energy Ratio

.

NOMENCLATURE

WCO : Waste Cooking Oil
LCA : Life Cycle Analysis
JBD : Jatropha Biodiesel
GHG : Green House Gas
FER : Fossil energy ratio
NER : Net energy ratio
NEG : Net energy gain
CO2 : Carbon dioxide
NOx : Oxides of nitrogen

INTRODUCTION

Biodiesel is a promising alternative fuel for usage in compression ignition engines. Several feedstocks has been identified globally for potential use as biodiesel. However, the sustainability of these resources depends on the social, environmental and economic indicators. Life cycle analysis (LCA) is a comprehensive study that evaluates the feasibility of a source by taking into account the technical, economic, environmental and social factors. Metrics like the net energy ratio, fossil energy ratio and Greenhouse Gases (GHG) Emissions are indicative of the suitability of a feedstock. Jatropha is being recognized as a suitable feedstock for the Indian scenario. However, Waste Cooking Oil (WCO) has certain advantages over the conventional feedstock. According to the Food Safety and Standards Authority of India (FSSAI), 3 million tons of WCO could be recovered annually in India [1]. The Government is also keen in the process of establishing WCO collection mechanisms. The typical processes involved in the production of WCO and jatropha biodiesel are shown in Fig. 1. Each of the processes consumes energy and generates GHG emissions, further in the case of Indian scenario; food security is given more priority over the energy security. The diversion of land from agricultural and production to the cultivation of energy crops like jatropha is quite debatable. However WCO is an unused product and does not require cultivation and extraction stages. This ensures significant reductions in water consumption, fossil energy consumption with WCO. Since there are no systematic disposal systems in India, these oils are dumped into fresh water resources and contribute to water pollution. Besides oil spread into thin and broad membranes which hinders the oxygenation of water, and thus are potential candidate to the environmental contaminant [2]. Hence, thermochemical conversion of WCO to biodiesel has a substantial positive environmental impact.

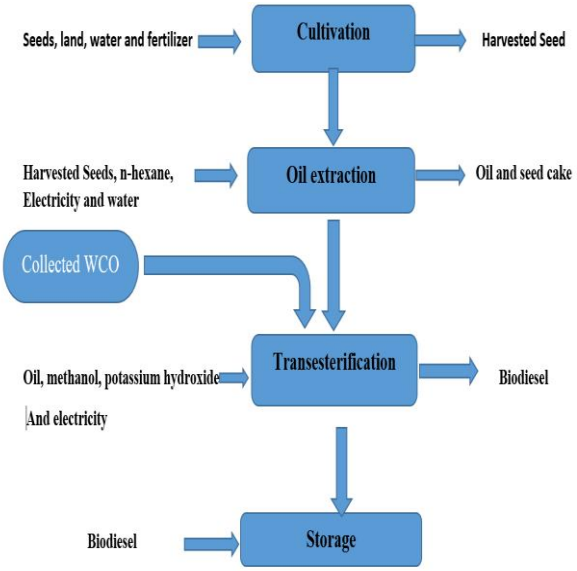

FIGURE 1: Typical processes involved in the production of WCO and Jatropha biodiesel

METHODOLOGY

In an approach to analyze the energy inflows and outflows of a system, one typically executes the following steps: establishing an inventory list and processes inherent in the production, use and final disposal of the system. The above pathways are evaluated using the GREET model developed by the Argonne National Laboratory to estimate the energy and GHG emission. The GREET model is an analytical tool that evaluates the energy consumption and emissions of different energy resources. The emissions GHG that are evaluated are carbon dioxide (CO_2), methane (CH_4) and nitrous oxide (NO_2). The processes involved in the life cycle of the fuel are simulated by setting up process pathway in GREET. The process pathway for jatropha biodiesel has been shown in Figure 2. As WCO is directly collected from vendors, the cultivation and extraction processes are eliminated in the evaluations. The required data for estimating the energy and emission requirements for the biodiesel fuels of interest are carried out following the literature [3-4].

The transesterification process to be used depends on the free fatty acid (FFA) value of the oil. Higher FFA values require a two-stage transesterification process. Due to low FFA values of JBD, a single stage transesterification is considered for the evaluations. However, due to the higher FFA value of WCO, a two-stage alkali based transesterification process is being considered. Various co-products are also formed during the biodiesel production process. A significant amount of biomass is generated during the oil extraction process which can be used further as a fuel and the glycerin produced during the transesterification process has applications in the chemical industry. As theses co products also consume resources, an appropriate distribution of primary process energy and GHG emissions should be done [3]. In this study distribution based on the mass of the products and co products has been adopted.

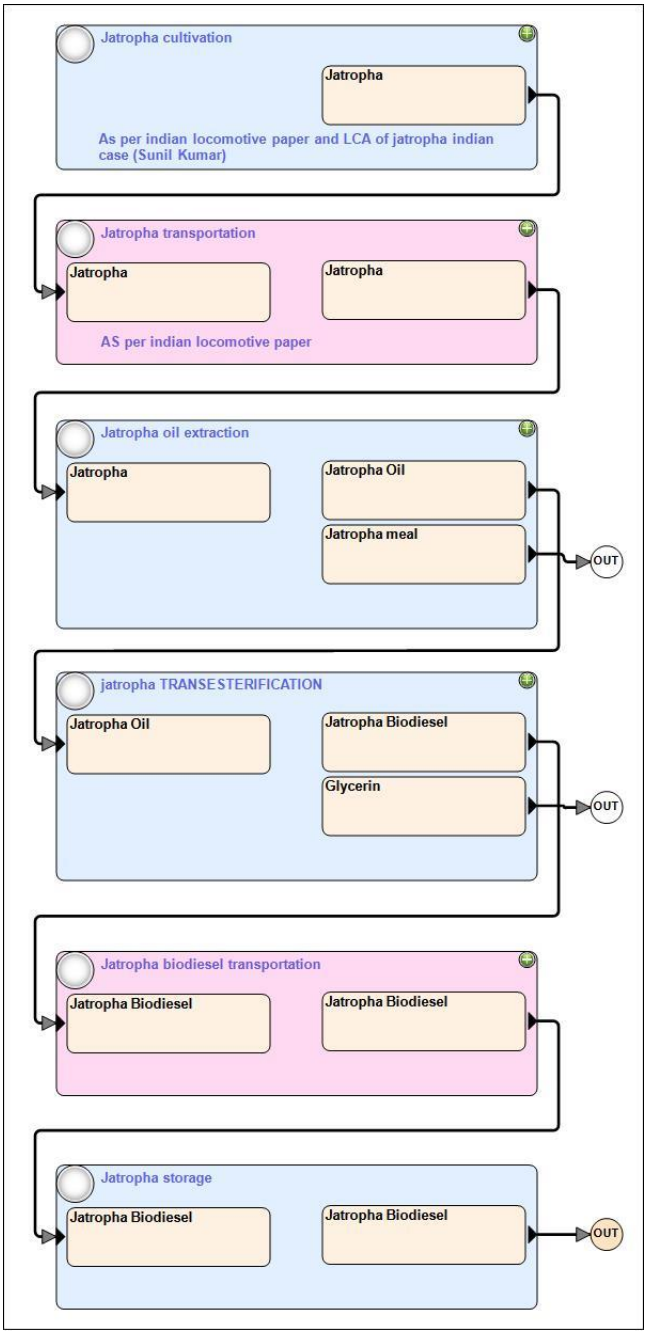

FIGURE 2 : JBD production pathway in GREET

In this study, the functional unit considered is one mega joule (1MJ) and hence the comparisons between the energy and emissions are carried out for producing 1 MJ of fuel. The energy indices considered inclides [5]:

$$Net\ Energy\ Ratio\ (NER) = \frac{Output\ Energy\ Obtained}{Input\ Energy\ Supplied} \quad \ldots(1)$$

$$Fossil\ Energy\ Ratio(FER) = \frac{Output\ Energy\ Obatained}{Fossil\ Energy\ Supplied} \quad \ldots(2)$$

$$Net\ Energy\ Gain(NEG) = Output\ Energy\ Obtained - Input\ Energy\ Supplied \quad \ldots(3)$$

RESULTS & DISCUSSION

The total energy consumed in the production process for the two fuels has been shown in figure 3. The overall energy consumption for producing 1MJ of WCO biodiesel and JBD was found to be 1034 kJ and 820.64 kJ respectively. In comparison to fossil diesel, JBD consumed 32.28% lower energy, while in the case of WCO biodiesel it was found to be lowered by 14.61%.

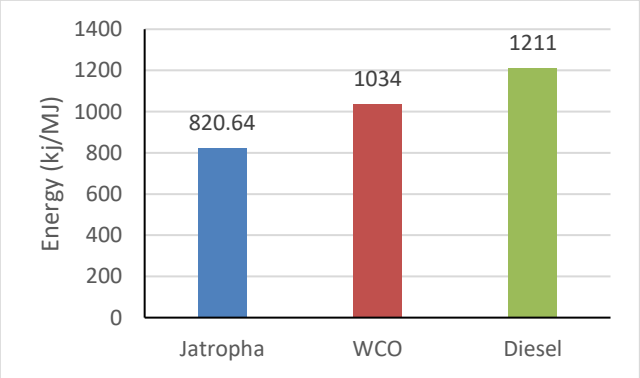

FIGURE 3: Comparison of total energy consumption

The net energy ratio and fossil energy ratio are depicted in figures 4 and figure 5 respectively. The NER of JBD and WCO biodiesel were 1.21 and 0.966 which were lower than the NER of diesel. JBD has a higher NER due to lower overall energy consumption. However, WCO biodiesel has a higher FER than JBD as evident from the figures. JBD shows higher FER as the cultivation process is highly dependent on diesel fuel as an energy source. On the other hand, major energy consumption in WCO production is in the form of electricity during the transesterification process which significantly reduces its FER.

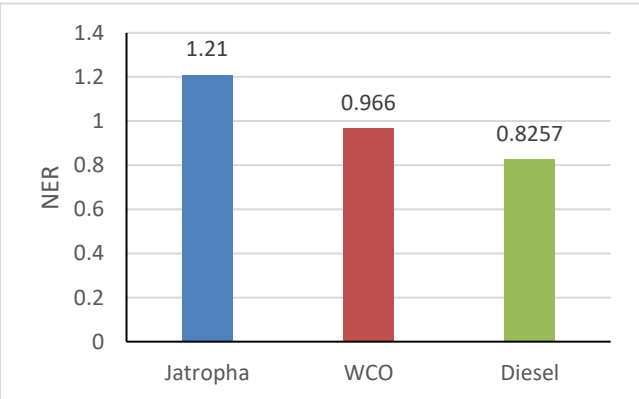

FIGURE 4 : Comparison of net energy ratio

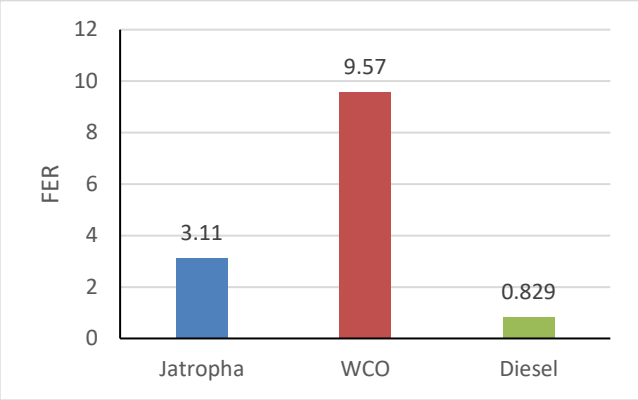

FIGURE 5: Comparison of fossil energy ratio

Nitrous oxide emissions have been shown in figure 6. The nitrous oxide emissions of JBD are significantly higher due to use of nitrogen-rich fertilizers during the cultivation process.

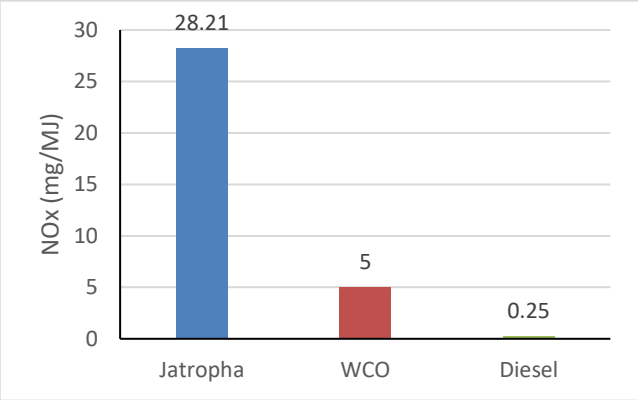

FIGURE 6 : Comparison of NOx emissions

The CO_2 emission is shown in figure 7. Biodiesel fuels show lower carbon dioxide emissions than fossil diesel. This is coherence with the trend in FER, as higher carbon dioxide emissions indicate a higher consumption of fossil energy.

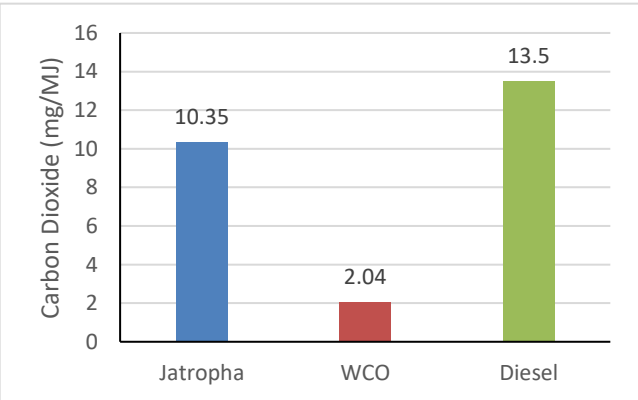

FIGURE 7 : Comparison of CO_2 emissions

SUMMARY

WCO biodiesel exhibits higher sustainability indices than JBD. There is a significant reduction in the GHG emissions as compared to JBD. The environmental advantage of thermochemical conversion of WCO to biodiesel and continual availability of WCO makes it a reliable and sustainable source for producing biodiesel.

ACKNOWLEDGEMENTS

The authors acknowledge the Department of Science and Technology (No. ECR/2016/001059), India for supporting this work.

REFERENCES

[1] New regulations for 'used cooking oil' come into effect, retrieved on August 10, 2018,URL:https://www.fssai.gov.in/dam/jcr:7a401427-8af2-4c0c-9fb2-f64e39d1fc7b/FSSAI_News_Cooking_Oil_BusinessLine_03_07_2018.pdf

[2] Mangesh G. Kulkarni and Ajay K. Dalai," Waste Cooking Oils An Economical Source for Biodiesel: A Review", *Ind. Eng. Chem. Res.*, 2006, *45* (9), pp 2901–2913

[3] Sunil Kumar, Jasvinder Singh , S.M. Nanoti and O. Garg, " A comprehensive life cycle assessment (LCA) of Jatropha biodiesel production in India", *Bioresource Technology*,110(2012),pp 723-729

[4] Sergio Morais, Teresa M Mata, Antonio A Martinsa, Gilberto A Pintoc and Carlos A.V. Costa," Simulation and life cycle assessment of process design alternatives for biodiesel production from waste vegetable oils*" Journal of Cleaner Production* ,18 (2010), pp 1251-1259

[5] Himanshu Sharma and Thangaraja J, "Comparative Evaluation of Energy and GHG Analysis of Diesel and Biodiesel Fuels*",* International Conference on Trends and Advanced Research in Green Energy Technologies, *ICTARGET-2017,* VIT Vellore, 30 - 31 March, 2017

Proceedings of the Third International Conference on Sustainable Energy and Environment Challenges (3rd SEEC)
18 –21 December, 2018, IIT Roorkee, India

SEEC No.025

Studies of Methanol Production Processes from Various Sources and It's Applications

Sukanta R.
Mechanical Engineering Department, Visvesvaraya National Institute of Technology Nagpur-440010
Assistant Professor
rogasukanta@vnit.ac.in

K.V.S.K. Abhinash
Mechanical Engineering Department, Visvesvaraya National Institute of Technology Nagpur-440010
UG Student
abhinashkanigelpula@gmail.com

G.P. Yathindra
Mechanical Engineering Department, Visvesvaraya National Institute of Technology Nagpur-440010
UG Student
pavanyathindra@gmail.com

ABSTRACT

This paper provides different possible ways of methanol production. It is believe that the methanol is the most versatile synthetic fuel available and its use could stretch or eventually substitute for, the disappearing reserves of low cost petroleum resources. Methanol could be used now as a means for marketing economically the natural gas that is otherwise going to waste in remote locations if methanol were used as an additive to gasoline at a rate of 5 to15%, for use in internal combustion engines, there would be an immediate in atmosphere pollution, there would be less need for lead in fuel and automobile performance would be improved. With increase in production of fuel grade methanol from coal and other sources it is foresee the increasing use of methanol for electrical power plants for heating and for other fuel applications. It is expected that a practical methanol fuel cell will be commercially available by the time that methanol becomes plentiful for fuel purposes.

Energy is considered as of the key inputs for economic development of the Country. India is poised to play a significant role in the Global energy space, as it is likely to account for 25% of the rise in global energy demand by 2040. India energy demand is expected to rise at a compounded annual growth rate (CAGR) of 3.5% till 2040 as it advances on the path of development. However, there has been a dismal growth in domestic oil (CAGR -1.4%) and natural gas (0.01%) production over the last decade. Methanol and Dimethyl ether (DME) can play an important role in order to contain the rising imports and improve the energy security of India. Methanol (CH_3OH) is a single carbon compound which can be produced from coal, natural gas, biomass (i.e. products which are capable of producing syngas), whereas DME (CH_3OCH_3) which is the simplest ether compound can be produced from methanol or directly from syngas. Methanol is an efficient fuel (octane number 100) and emits lesser NOx and Particulate matter (PM) than gasoline and produces no SOx as there is no sulphur in methanol. It can be blended (or be completely substituted) with gasoline to use as a transport fuel along with other applications.

However, methanol is more corrosive than gasoline and may require new equipment for storage and distribution of the same and is also toxic to humans if ingested. It burns with invisible flame but make it visible by adding additives (e.g., gasoline).

China is leading the world with the largest production of Methanol and DME. It is to be noted that China produces 70% of its methanol from Coal as it has the third largest coal reserves in the World, although, other countries (US, South America, Iran) are largely producing methanol from natural gas due to its abundant availability in those countries at low prices. India can also follow the footsteps of China as our Country has the 5th largest coal reserves in the World and if used efficiently, can contribute significantly in methanol production.

India is at a nascent stage in methanol production and usage, but it has a large potential given its wide applications. There are 5 main producers of methanol in India – Gujarat Narmada Valley Fertilizer and Chemicals limited, Deepak Fertilizers, Rashtriya Chemicals and Fertilizers, Assam Petrochemicals and National Fertilizers Limited. From this coal the produced methanol has many advantages.

Methanol has attractive features for use in transportation:

- It is a liquid fuel which can be blended with gasoline and ethanol and can be used with today's vehicle technology at minimal incremental costs.
- It is a high octane fuel with combustion characteristics that allow engines specifically designed for methanol fuel to match the best efficiencies of diesels while meeting current pollutant emission regulations.
- It is a safe fuel. The toxicity (mortality) is comparable to or better than gasoline. It also biodegrades quickly (compared to petroleum fuels) in case of a spill.
- Produced from renewable biomass, methanol is an attractive greenhouse gas reduction transportation fuel option in the longer term.

The production of methanol usually consists of three basic steps independent of feedstock material: synthesis gas preparation, methanol synthesis and methanol purification.In order to properly understand the challenges of different processes to produce the synthesis gas, it is need to be understand the process from synthesis gas to methanol, the methanol synthesis. In essence the process consists of the three following equations:

$$CO + 2H_2 \rightleftharpoons CH_3OH \quad \Delta H298K = -21.7 \text{ kcal/mol} \quad (1)$$

$$CO_2 + 3H_2 \rightleftharpoons CH3OH + H_2O \quad \Delta H298K = -11.9 \text{ kcal/mol} \quad (2)$$

Reverse Water gas shift reaction:

$$CO_2 + H_2 \rightleftharpoons CO + H_2O \quad \Delta H298K = 9.8 \text{ kcal/mol} \quad (3)$$

All three equations are reversible and thus the process conditions regarding temperature, pressure and synthesis gas mixture are important to control. It can also be noted that equation (1) and (2) are exothermic, i.e. the processes produce heat and require cooling. Some heat is normally recovered and used for other parts of the synthesis.

While it was originally believed that the main process that produce methanol was the reaction between carbon monoxide and hydrogen (equation 1) it is now understood that carbon dioxide is just as important in the synthesis process. CO_2 even used to be scrubbed from the reactant mixture but a scrubber failure at Imperial Chemical Industries (ICI) with a resulting increase of methanol production showed that CO_2 was active and important in the reaction. Subsequent studies have shown that it is mainly the CO_2 that is converted to methanol while CO acts as a reducing agent for oxygen at the surface of the catalyst. The equation (3) describes the reverse water gas shift reaction that produces carbon monoxide from carbon dioxide and hydrogen. The carbon monoxide then reacts with hydrogen to produce methanol (equation 2). Equation 2 is actually merely the

sum of (1) and (3). To synthesise methanol, not only is a specific H_2/CO ratio of 2 in the synthesised gas needed but also a $(H_2-CO_2)/(CO+CO_2)$ ratio, called stoichiometric number, equal to or slightly above.

Production of Methanol from Indian Coal and Solid Waste:

The main ingredient used for methanol production is synthesis gas .Methanol can be produced from Indian coal and solid wastes through synthesis gas production. The process to convert Indian coal to synthesis gas is a combination of partial oxidation and steam treatment called Gasification.

$$C + 0.5*O_2 \rightleftharpoons CO \quad \Delta H298K = -29.4 \text{ kcal/mol} \quad (4)$$

$$C + H_2O \rightleftharpoons CO + H_2 \quad \Delta H298K = 31.3 \text{ kcal/mol} \quad (5)$$

$$CO + H_2O \rightleftharpoons CO2 + H_2 \quad \Delta H298K = -9.8 \text{ kcal/mol} \quad (6)$$

$$CO_2 + C \rightleftharpoons 2CO \quad \Delta H298K = 40.8 \text{ kcal/mol} \quad (7)$$

The design and processing conditions vary greatly depending on the composition of the coal used as feedstock. The synthesis gas produced have a deficit of hydrogen and must be subjected to the water gas shift reaction (equation 6) in improve the H_2/CO ratio. The synthesis gas produced from coal is usually in higher need of purification than that produced from natural gas, especially sulphur compounds must be removed before the methanol synthesis to protect the sensitive catalysts from poisoning.The conventional method to produce methanol from solid wastes is through gasification of the feedstock material .The gasification process of biomass is similar to the synthesis gas process from coal. For gasification of solid wastes the feedstock is first dried and pulverized. The moist content should generally be no higher than 15-20 wt%. The first step in a two-step gasification process is called pyrolysis, or destructive distillation. The dried solid waste is heated to 400-600 °C in an oxygen deficient environment to prevent complete combustion. Carbon monoxide, carbon dioxide, hydrogen, methane as well as water and volatile tars are released. The remaining biomass (≈10–25 wt%), called charcoal. is further reacted with oxygen at high temperature (1300-1500 °C) to produce mainly carbon monoxide.

Other Methods:

An attractive alternative for synthesis of natural gas to methanol would be if the energy consuming step of synthesis gas could be avoidable by directly inserting an oxygen atom in the methane molecule by direct oxidation. The difficulty is that the high reactivity of the products themselves easily results in complete combustion of the methane to carbon dioxide and water. Despite the desire of success no method has been found to achieve a high enough selectivity, productivity and catalyst stability for industrial applications. With the advances of renewable energy as well as greater utilization of existing energy sources such as the sun and geothermal heat methanol evolves not as an energy source but as an energy carrier with great potential. While biomass and other waste materials is a possible and probable route to gradually decrease our dependence on fossil energy sources there are technologies available that allows us to produce methanol and at the same time reduce the carbon dioxide emissions in our atmosphere. The process consists of combining hydrogen and carbon dioxide to produce methanol with the only by-product being oxygen from the electrolysis of water.

The idea is to produce methanol from carbon captured from the atmosphere, mainly from local emitters such as power plants and industrial facilities but with improving technologies also from the atmosphere itself. To accommodate the need for hydrogen in the synthesis process electrolysis of water is performed with electricity. Electrolysis of water is an old technology that has been used for more than a century but as the energy consumption is very high only a small part with high purity demands of the world production of hydrogen is through electrolysis. The best energy efficiency is today around

73% with the expectancy to reach toward 85 % with current research and development programmes. The success of this technology relies of an abundance of energy that can come from mainly solar, wind and thermal sources that lack any efficient mean of storage in other ways. Carbon Recycling International (CRI) is currently operating one plant on Iceland that use available geothermal energy to produce 5000m^3 Methanol per year and Mitsui Chemicals has announced construction of a demonstration plant capable of producing 100 tonne methanol per year from CO_2.

Recently M.I.T proposed ultrahigh efficiency methanol engines with advanced exhaust heat recovery. This invention pertains to an engine system using alcohol Rankine heat recovery where the engine heat converts alcohol into hydrogen-rich gas which is then introduced into the engine cylinders. The engine system includes a source of liquid alcohol along with an internal combustion engine generating a high-temperature exhaust. A structure is provided for introducing a first portion of the liquid alcohol into the engine and a series of heat exchangers forming a Rankine heat recovery cycle is provided to extract heat from the exhaust and transferring the heat to a second portion of the liquid alcohol, causing it to change phase to a gaseous alcohol. A heat exchanger/catalyst is heated by the exhaust to reform the gaseous alcohol into a hydrogen-rich reformate. Valve structure rapidly introduces the reformate into the engine for combustion and a control system is provided for controlling the ratio of the first and second portions of the liquid alcohol to maximize the amount of the second portion of the liquid alcohol while using a minimum amount of the first portion needed to prevent knock. The heat recovery system uses metallic foams on fin heat exchangers. By this invention efficiency is found to be 55-60%.

Keywords: Indian coal, Methanol, Solid waste

Proceedings of the Third International Conference on Sustainable Energy and Environmental Challenges (3rd SEEC) 18 –21 December, 2018, IIT Roorkee, India

SEEC No. 026

PARAMETRIC ANALYSIS OF POROUS BURNER WITH PRESSURE KEROSENE COOKING STOVE

First Author
Gyan Sagar Sinha
School of Mechanical Engineering
Kalinga Institute of Industrial Technology
Bhubaneswar, Orissa
Email: gyan_it002@yahoo.co.in

Second Author
Niraj K Mishra
Department of Mechanical Engineering
NIT Uttarakhand, Srinagar,
Uttarakhand
Email: nkm.iitg@gmail.com

Third Author
P Muthukumar
Department of Mechanical
Engineering, IIT Guwahati,
Guwahati
Email: pmkumar@iitg.ac.in

ABSTRACT

This paper discuss about the performance analysis of porous burner with pressure kerosene stove in terms of emissions and thermal efficiency. This paper also discuss about the effect of nozzle diameter on thermal efficiency and thermal emissions (NOx and CO). Weather change in India is the important factor for human life. Therefore, thermal performance at different weather of kerosene pressure stove with porous radiant burner has been examined in this paper.

Keywords: Porous burner, Nozzle diameter, Ambient temperature.

.

NOMENCLATURE

η_{th}	Thermal efficiency
C_w	Specific heat of water (kJ/kg-K)
m_w	Mass of water (kg)
T_2	Final temperature of water (°C)
T_1	Initial temperature of water (°C)
m_f	Mass of fuel consumed (kg)
m_p	Mass of vessel (kg)
C_p	Specific heat of vessel (kJ/kg-K)

1. INTRODUCTION

In rural areas, the main source of energy for cooking are firewood and cow dung cake, which are used in generally in mud stove. But this type of cooking device produces more emissions resulting in a poor efficiency. Moreover, large consumption of firewood leads to deforestation and highly necessitates the urge in the modification of the existing less efficient combustion systems. Due to the poor supply of electricity in rural areas, the usage of electric stove is restricted. Because of the technical and management issues, usage of solar and biogas stoves is also limited. It is of course no doubt that LPG is a cleaner fuel when compared to other fuels for cooking purpose. But in rural areas, because of inadequate distribution and high cost, people could not afford LPG [1]. It is known that kerosene is of lower cost and easy to handle and transport (as compared to LPG). In addition, the government also gives subsidies for kerosene purchase. Hence, kerosene is affordable for low-income group people in rural, suburban and urban areas. Also by the usage of kerosene for cooking purpose, it may reduce the dependency on biomass especially in rural areas.

Two types of kerosene stoves are generally used for cooking purpose, viz., wick type and pressure type. Wick type stove works on the capillary action of the kerosene, in which the wick draws kerosene from the fuel tank. At the end of wick, ablaze is done for flame production and that flame is used for cooking purpose. In pressure type stoves, the preheated kerosene in the form of vapor is pressurized and passed through the nozzle. It is then mixes with air and ignites for producing the flame. This flame is used for cooking purpose, and so it is called as free flame combustion. The thermal efficiency of pressure kerosene cooking stoves is higher than the wick type kerosene stoves. Average thermal efficiency of pressure kerosene cooking stoves are 45 % [2-3], while in the case of BIS stoves, it varies from 55 – 58 % [4]. A brief discussion about the general conventional burner is presented

here. As shown in Figure 1, the general conventional burner consists of two ascending and two descending tubes. These tubes touch the vaporizer (which is a flat circular chamber) and the ascending tubes remain connected with the riser. Middle section of the descending tubes contains the spray nozzle, through which kerosene vapor is sprayed in air. For ignition of the kerosene stove, little amount of kerosene is put in spirit cup initially and is burned with ablaze wick.

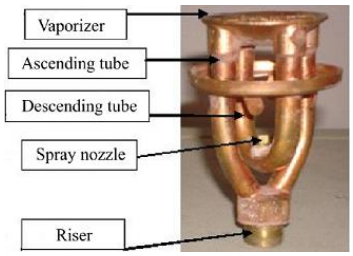

Figure 1: Construction of general conventional burner.

During the burning of kerosene, pressure pushes the liquid kerosene to vaporizer through the riser and ascending tube. Vaporizer gains heat from the burning kerosene through convection and becomes hot. Liquid kerosene becomes vapor when they pass through the hot vaporizer. Under the force of pressure, vapor kerosene passes through the descending tubes and finally emits from the spray nozzle and then mixes with air and burns with yellowish orange (as shown in Figure 2) flame in the place between the vaporizer and flame holder. The initial flame in the spirit cup is quenched and vaporizer takes heat continuously from the kerosene-air flame.

Combustion in conventional pressure stove is free flame, which is treated as gas whose emissivity and thermal conductivity are very low. Because of this reason, convection mode of heat transfer is predominant in the conventional pressure kerosene cooking stove. Due to insignificant conduction and radiation modes of heat transfer, performance of the pressure kerosene cooking stoves is very low like low thermal efficiency and high emissions (CO: 610 – 915 ppm, NO_x: 19 – 35 ppm) [4]. The emissions are higher than the prescribed limit of the World health organization (WHO) for indoor air pollution [5-6]. Reason for the low efficiency and high emission is the incomplete combustion.

A promising concept called porous media combustion can be used for reduction of emissions and improvement in thermal efficiency. The combustion in PM (porous media) makes use of a porous solid matrix wherein fuel and air are entered and they are ignited using a pilot flame. Once the heat of combustion is released, a premixed or diffusion (non-premixed) flame is enveloped within the matrix and it got stabilized at a particular location depending on the operating conditions [7-9]. The chemical enthalpy of gas is then absorbed by the solid and the media becomes radiatively participating. The PM being highly conductive starts transferring heat through conduction too to the upstream and the large surface area of it makes convective heat transfer sufficiently large. The incoming air fuel mixture is thus preheated with the recirculated heat coming though the combined modes of radiation, conduction and convection. Figure 3(a)-(b) shows the heat transfer mechanisms of CB and PRB (porous radiant burner) respectively.

Figure 2: Pictorial view of the free flame in conventional cooking kerosene stove

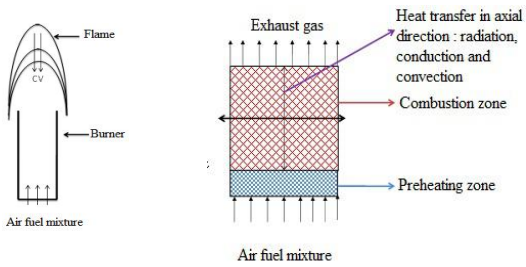

Figure 3: (a) Convection dominated free-flame in CB (b) radiation dominated PRB [4].

Porous media concept has been used by many researchers in different application, in which they used the highly conductive and emissive solid porous. However, few researchers used this solid porous in LPG stove and kerosene pressure stove called porous radiant burner. The very first investigation was carried out by Kakati et al. [10], where they examined the thermal efficiency, kerosene consumption rate and emission of domestic burner with porous inserts of pottery clay, sodium silicate and saw dust and compared the results with the conventional one. Later, Sharma et al. [11] investigated the performance of the same stove by replacing the inserts with four different porous materials, viz. silicon carbide (SiC), zirconia (ZrO_2), wire mesh roll filled with metal balls and alumina (Al_2O_3). They found an optimum value for mass flow rate (130-140 g/hr) and vessel size (260 mm diameter) which resulted in increased thermal efficiency for all the inserts with maximum 7% increase exhibited in SiC inert. Sharma et al. [12] further modified the stove by incorporating ceramic heat shield of low conducting and radiating alumina (Al_2O_3) which resulted in 15% increase in thermal efficiency. Recently, Sharma et al. [13] extended their research by changing the burner geometry and also incorporated exergy analysis. Experimental stove consisting of two-layer porous matrix of alumina (Al_2O_3) balls and honeycomb structured silicon carbide (SiC) was experimented with three different shapes of burner casing, viz. straight cylindrical, taper and conical. Performance with conical burner casing was found to be the best of all with 10% increase in thermal efficiency at air and fuel flow rate of 120-130 lpm and 220 g/hr respectively. The burner with 70 mm diameter proved to be the best among the three studied burner diameters of 60 mm, 70 mm and 80 mm. In another study on kerosene stove, Sharma et al. [11] found the optimal thickness

of the combustion zone of the PM and it was 20 mm. At this thickness better emissions and higher efficiencies were reported.

Aforesaid PRBs require the supply of external air for its operation, which constrained its potential for commercialization in domestic cooking application. Henceforth, the researchers put in their efforts to make a PRB which would work on naturally induced draft as in the conventional one. This was achieved by bringing changes in the supply pressure of kerosene, design of orifice, the burner port, the mixing chamber, the preheating zone and the casing (as shown in Fig. 4). After the experiment, stable combustion was found and thermal efficiency was higher than CB present in market and also reductions of emissions were found in the same burner.

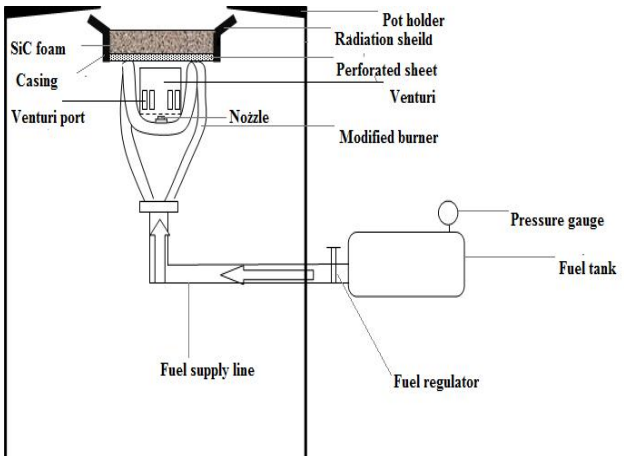

Figure 4: Schematic of the PRB setup without external air supply.

2. EXPERIMENTAL PROCEDURE

The thermal efficiency was measured by conducting water boiling test (WBT) following the guidelines of bureau of Indian standard (IS 10109:2002)[14]. The emission analysis has been done by the hood method. Operating principle of PRB with BIS kerosene pressure stove are following. Ignition of the stove is done by burning wick. Optimal size of aluminum vessel along with lid and stirrer for the experiment are selected and filled with a known amount of water at room temperature (~30 C). In the WBT, initially the stove is allowed to operate for 5 min (according to BIS for the attainment of steady state) and then it is kept over the platform (dimension: 400 mm x 300 mm) of the weighing machine, for measuring the initial weight of the stove. Weight of the vessel (with lid and stirrer) along water is measured separately with the help of a weighing balance machine. Initial temperature (T_1) of water is measured using glass-in-mercury thermometer (accuracy ± 0.5 °C). After measuring the initial weight of stove, it is unloaded from platform and then vessel is kept above the burner. Water is heated up to 90 °C and for maintaining the uniform temperature in the vessel, stirring is done parallel and continued until the end of the test, when the temperature of water is reached (T_2) 90 ± 0.5°C. At this phase, the burner is quenched. The time required to heat the water from room temperature to 90 °C is noted and the mass of the fuel consumed during this period is recorded by the difference in weights of the stove before and after heating. In every case, the experiments were repeated at least three times and the average of the three was taken for the analysis. The percentage of thermal efficiency η_{th} of the stove is calculated based on IS 10109:2002 guidelines. Prescribed formula given by Equation (1) .Where m_w is the mass of water, C_w is the specific heat of water, m_p is mass of vessel along with the lid and stirrer, C_p is the specific heat of the vessel material (aluminium), m_f is the mass of the kerosene consumed and CV is the lower calorific value of kerosene (43890 kJ/kg). The calorific value is taken from the BIS standard (IS 10109:2002).The uncertainty in the thermal efficiency was found to be ± 1.40 %.

$$\eta_{th} = \frac{Heat\ Output}{Heat\ Input} = \frac{\left(m_w \cdot C_w + m_p \cdot C_p\right)\left(T_2 - T_1\right)}{m_f \cdot \mathrm{CV}} \quad \ldots\ldots(1)$$

3. RESULTS AND DISCUSSION

Figure 5(a) and Figure 5(b) show the thermal efficiency and emission, respectively for CB (conventional burner) at different power. Lean combustion on CB (conventional burner) is not suitable because of the lift-off phenomena occur in lean combustion. To avoid the phenomena of lift-off, conventional pressure kerosene cooking stove is configured for a fuel rich combustion and hence the CO becomes very high and due to the very high global temperature, CB produces high NO_x. With increased thermal power, flame size increases results in more heat loss to surrounding subsequently decreasing of thermal efficiency.

In case of porous burner, after the repeated experiments it was found that the nozzle diameter of modified burner (called vaporizer tube) also affects the thermal efficiency, because, Due to reduction in the nozzle diameter, velocity of the upcoming vaporized kerosene increases resulting in the creation of a higher pressure difference between the nozzle section and the surrounding air. Because of this, more air is sucked in the mixing chamber (venture region), which increases the air entrainment. This increased air entrainment not only improves the combustion but also increases the thermal efficiency. Figure 6 and Fig. 7 show the measured thermal efficiency and thermal emission (NO_x and CO), respectively for different input power for PRB with the two different nozzle diameters, 0.454 mm and 0.376 mm. The thermal efficiency of the PRB varies from 52.5 – 61.3 % for 0.454 mm nozzle and 55.5 – 64.3 % for 0.376 mm nozzle in the input power range of 1.5-3 kW. With the usage of PRB, conduction, radiation and convection heat transfer modes become active which leads to better combustion of the fuel. This results in the higher thermal efficiency. It is further observed from Figure 6 that with the increase in the input power, thermal efficiency was found to decreases in both CB

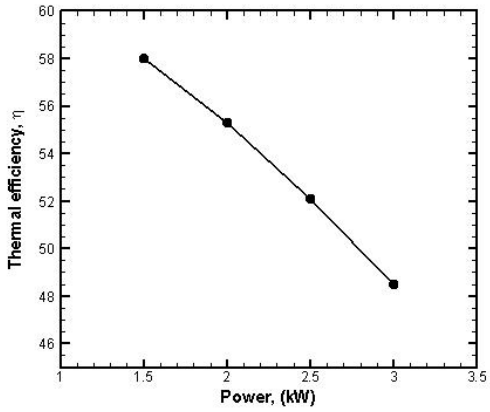

Figure 5(a): Effect of power intensity on the thermal efficiency of the conventional pressure kerosene cooking stove [4].

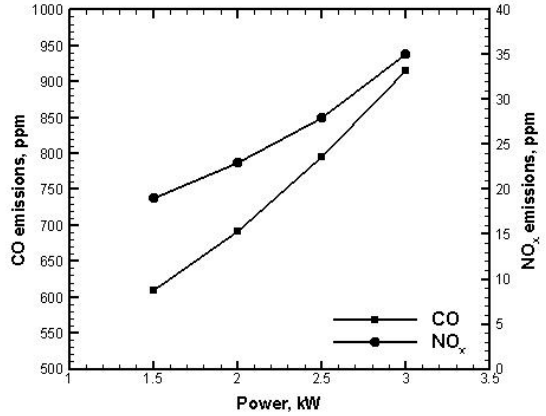

Figure 5(b): Typical emission characteristics of a pressure kerosene cooking stove with CB [4].

and PRB. The reason behind this is the higher heat loss to the surrounding at higher power input, due to which the net power output decreases as compared to the input power. Further, in PRB with smaller nozzle diameter (0.376 mm), the downward movement of the reaction zone takes place, and this increase the volumetric heat release. From the Figure 6, it can be observed that for nozzle diameter 0.376 mm, the maximum thermal efficiency of the Porous burner is 64.3 % at thermal input power 1.5 kW. Figure 7 shows the NO_x and CO for CB burner. Greenline 8000 portable flue gas analyzer was used to measure CO and NO_x. Measured emissions of PRB are lower than that of CB because of better combustion and more residence time, which leads to lower CO emissions. In the PRB, NO_x emission was found much lower than the CB. The reason behind of this was the low surface temperature of the porous burner. In the case of PRB with venture effect, the increased air entrainment plays an important role on both efficiency and emissions

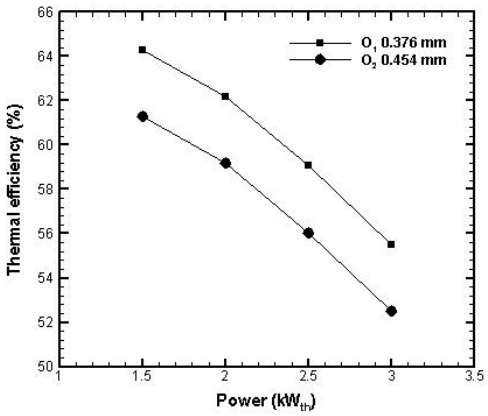

Figure 6: Thermal efficiency at different nozzle diameter at different power input for PRB.

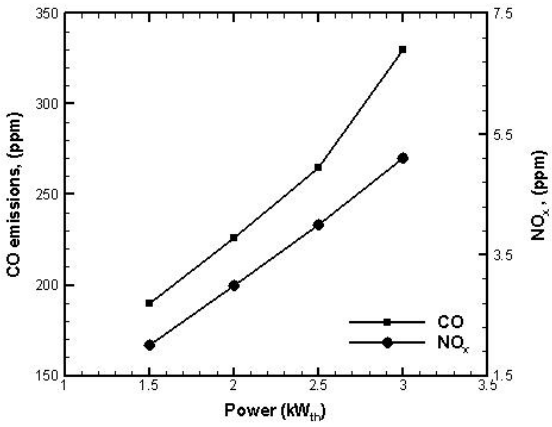

Figure 7 (a): Emissions of PRB at 0.454 mm diameter nozzle.

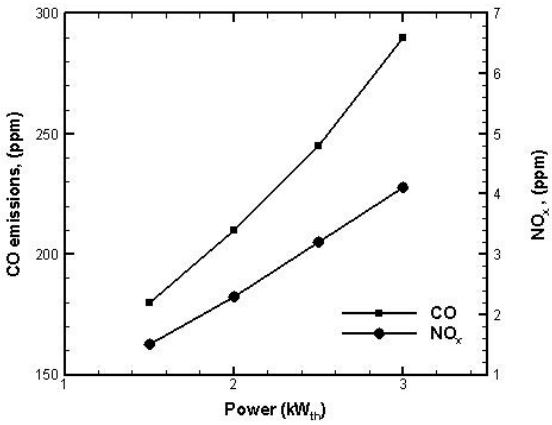

Figure 7(b): Emission of PRB at 0.376 mm diameter nozzle.

In PRB, two types of heat losses occur: convective and radiative heat loss. But in the case of CB, only convective heat loss takes place. Hence the rate of heat loss is lower in CB as compared to PRB. Also in cold weather conditions, more heat loss occurred as compared to the hot weather conditions. So in order to investigate the thermal efficiency with ambient temperature, the thermal efficiencies of both CB and PRB were measured at different ambient temperatures (10 ˚C, 15 ˚C, 20 ˚C, 25 ˚C, and 30 ˚C). The maximum thermal

efficiency for both CB and PRB was obtained at 30 ˚C (as shown in Figure 8).

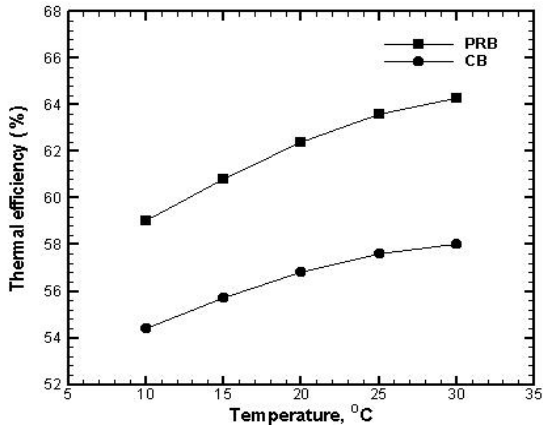

Figure 8: Variation of thermal efficiency with ambient temperature.

4. CONCLUSIONS

Performance analyses of the pressurized kerosene cooking stove with PRB (1.5 – 3 kW) have been carried out in terms of thermal efficiency, CO and NO_x emission characteristics. Porous burner without external air supply is a promising concept which is not only decrease the emission while it will help to reduce energy crisis. It may useful in rural area because of two reason first is people are below to poverty level area and second one is incomplete distribution of LPG connection.

3. REFERENCES

[1] Dixit,C. S. B., Paul, P. J., and Mukunda, H. S., 2006. "Experimental studies on a pulverized fuel stove". Biomass Bioenergy, 30, pp. 673-683.

[2] Thukral, K., Bhandari, P. M., 1994. "The rationale for reducing the subsidy on LPG in India". Energy Policy, 22 pp. 81-87.

[3] Smith, K., Uma, R. K. V. V. N., 2000. "Greenhouse gases from small-scale combustion devices in developing countries". Phase IIa, Household Stoves in India, USEPA, EPA (2000) 600-00-052.

[4] Sinha, G. S., 2018. "Development and performance analysis of self-aspirated porous radiant burners for kerosene pressure stove", PhD thesis, IIT Guwahati, see also URL. http://gyan.iitg.ernet.in/handle/123456789/902.

[5] Kandpal, J. B., Maheshwari, R. C., and Kandpal, T. C., 1995. "Indoor air pollution from domestic cookstoves using coal, kerosene and LPG, Energy Conversion and Management". 36, pp. 1067-1072.

[6] Zhang, J., Smith, K. R., and Uma, R., 1999. "Carbon monoxide from cookstoves in developing countries: 1. Emission factors". Chemosphere-Global Change Science, 1, pp. 367-375.

[7] Marbach, T L., Agrawal. A K., 2003. "Experimental study of surface and interior combustion using composite porous inert media". Journal of Engineering for Gas Turbines and Power, 127, pp. 307-13.

[8] Marbach, T L., Sadasivuni, V., and Agrawal, A K., 2007. "Investigation of a miniature combustor using porous media surface stabilized flame". Combustion science and technology, 179, pp. 1901-1922.

[9] Nakamura, Y., Itaya, Y., Miyoshi, K., and Hasatani, M., 1993. "Mechanism of methane-air combustion on the surface of a porous ceramic plate". Journal of Chemical Engineering of Japan, 26, pp. 205-211.

[10] Kakati, S., Mahanta, P., and Kakoty, S., 2007. "Performance analysis of pressurized kerosene stove with porous medium inserts". Journal of Scientific & Industrial Research, 66 pp. 565-569.

[11] Sharma, M., Mishra, S. C., and Acharjee, P., 2009. "Thermal efficiency study of conventional kerosene pressure stoves equipped with porous radiant inserts". International Energy Journal, 10 pp. 247-254.

[12] Sharma, M., Mishra, S. C., and Mahanta, P., 2011. "An experimental investigation on efficiency improvement of a conventional kerosene pressure stove". International Journal of Energy for a Clean Environment, 12, pp. 79-93.

[13] Sharma, M., Mahanta, P., and Mishra, S. C., 2016. "Usability of porous burner in kerosene pressure stove: An experimental investigation aided by energy and exergy analyses". Energy, 103, pp. 251-260.

[14] Indian Standard, Burners for oil pressure stoves and oil pressure heaters, specification, (Second Revision): IS 10109, 2002, Bureau of Indian Standard.

Proceedings of the Third International Conference on Sustainable Energy and Environmental Challenges (3rd SEEC)
18 –21 December, 2018, IIT Roorkee, India

SEEC No.027

ELEMENTAL AND HEAT LOSS ANALYSIS OF DIFFERENT FEEDSTOCK IN THE DOWNDRAFT GASIFIER

Anil Kumar Sakhiya
Institute of Technology,
Nirma University, Ahmedabad
16mmet22@nirmauni.ac.in

Apoorv Chaturvedi
Institute of Technology,
Nirma University, Ahmedabad
15bme006@nirmauni.ac.in

Vivek Barasara
Institute of Technology,
Nirma University, Ahmedabad
16bme014@nirmauni.ac.in

Krunal Panchal
Ph.D. Research Scholar,
Indian Institute of Technology, Madras
me18d005@smail.iitm.ac.in

Darshit Upadhyay
Institute of Technology,
Nirma University, Ahmedabad
darshit.upadhyay@nirmauni.ac.in

Rajesh Patel
Institute of Technology,
Nirma University, Ahmedabad
rnp@nirmauni.ac.in

ABSTRACT
Gasification is a thermochemical biomass conversion technique in which biomass is converted into low / medium calorific value producer gas with partial amount of oxidizer. It is one of the most suitable technologies for rural electrification for the country like India where plenty of biomass is available. Thermodynamic and heat transfer analysis is very important aspect to understand the utilization of feedstock in the gasifier reactor. For the analysis purpose, five different feedstock such as lignite, cumin briquette + sawdust briquette (40:60, w/w), sawdust briquette, wood and lignite + wood (50:50, w/w) were used. Mass balance, element balance and heat transfer analysis were carried out in the present study. Mass Balance Closure (MBC) and Element Balance Closure (EBC) were found in the range of 0.95-1.03 and 0.84-1.09 respectively. Convective and radiative heat loss were calculated for 10 kWe atmospheric pressure downdraft gasifier. It was found that total heat loss remained in the range of 0.76 kW to 1.23 kW.

***Keywords*:** Downdraft gasifier, Element balance, Heat transfer analysis, Mass balance

INTRODUCTION
Requirement of electricity is increasing globally day by day. The cause is the rapid growth of infrastructure and economy of the developing nations such as India, China, Indonesia etc. India's economy is one of the fastest growing economy in the World. Installed capacity and per capita electricity consumption of India is around 327 GW and 1122 kWh year^{-1} [1]. Compound annual growth of India is around 8.52% of the installed capacity in electricity generation [2]. India is blessed with large biomass reserves and nearly 500 million tonnes of biomass is produced in India every year [3]. Despite of this huge potential for bio-energy, a large number of people in rural India don't have access to electricity. It can be due to unfeasible or uneconomic grid connection at some interior parts of India. People in those areas generally depend on firewood, agricultural waste, animal dung for cooking, lighting, heating applications [4]. But this direct combustion technique has its own drawbacks and has very less thermal efficiency. One of the major drawback is the harmful gases formed at the end of the process resulting in sever human health and environment degradation. Apart from that, continuously increasing fossil fuel prices and GHGs emissions are the motivations for the researchers to look into new and commercially viable options in renewable energy. Gasification is one of the suitable technologies which convert biomass effectively into producer gas with sub-stoichiometric oxidizer (such as air, steam, oxygen etc.). Fuel flexibility is the major advantage of the gasifier and any carbonaceous fuel can be used as a feedstock in the gasification system. This century old technology has gained prominence during World War II and after that reduce the growth rate due to viability of cheaper crude oil [5].

Different types of gasifiers such as fixed/moving bed, fluidized/bubbling bed, and entrained flow gasifiers with different capacities and designs are commercially available in the market. In the downdraft gasifier, gasification process could be divided into four zones i.e drying zone, pyrolysis zone, combustion zone and reduction zone. Combustion zone provides the thermal energy required for the pyrolysis and reduction zones. Some amount of heat is utilized to dry up the feedstock too. Pyrolysis of feedstock produces the non-condensable gases, char and tar that is again utilized in combustion and reduction zone. Thermodynamic analysis is very important aspect to understand any gasification system. The mass balance is one of the way to examines the reliability of information composed [6]. Element balance can be drawn from the feedstock proximate/ultimate analysis and producer gas and tar concentration [7].

In the present study, an atmospheric pressure 10 kWe downdraft gasifier was used for the experiments. Five different feedstock were opted for the thermodynamic analysis. Mass - element balances and heat transfer analysis were carried out for the selected feedstock.

EXPERIMENTAL SETUP

An atmospheric pressure 10 kWe downdraft gasifier was used for the experiments which are illustrated in Figure 1. Feedstock was fed from the top cover of the gasifier reactor. The Vibrating mechanism was installed to prevent system from chocking/bridging the feedstock. Air nozzles are provided to supply sufficient oxidizer to the reactor to maintain equivalent ratio 0.38. The water pump, scrubber and tank arrangement enabled smooth flow of air-gas and washing of producer gas (to remove tar, dust and other particulate matter). The surge tank maintained the pressure of the gas and remove ash-dust-water particles from the gas. Bag type fabric filter collect remaining suspended particulate matter in such a way that clean gas flow was available at the burner section. Calibrated orifice meter and K type thermocouples were used to measure gas flow rate and temperature respectively. Hotwire anemometer with data logger (Fluke make Amprobe TMA-21HW) and gas chromatograph (Shimandzu 2010) were used to measure air flow rate and producer gas concentration. Details of gasification system, its instrumentations, performance parameters and results such as temperature profile, producer gas concentration, cold gas efficiency, tar and particulate matters are available elsewhere [8]–[10].

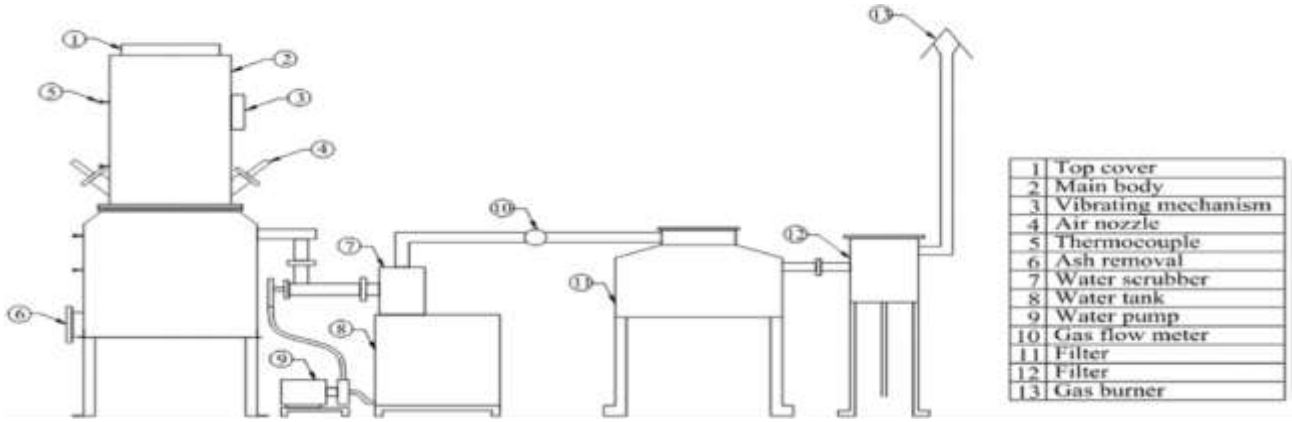

FIGURE 1. SCHEMATIC DIAGRAM OF THE 10 KWE DOWNDRAFT GASIFIER SYSTEM [8]–[10]

TABLE 1: CHARACTERIZATION OF FEEDSTOCK

Analysis	Lignite	Cumin + Sawdust (40:60, w/w)	Sawdust	Wood	Lignite + Wood (50:50, w/w)
Proximate[a]					
Volatile Matter	45.72	74.2	74.63	77.75	61.74
Ash	15	3.95	4.87	7.3	11.15
Moisture	8.28	4.81	8.7	8.88	8.58
Fixed Carbon[b]	31	17.04	11.8	6.07	18.53
Ultimate Analysis					
Carbon	37.80	43.25	42.8	45.8	41.8
Hydrogen	4.93	5.6	5.17	6.3	5.42
Nitrogen	1.625	1	1.48	0.4	1.2125
Sulphur	0.141	0.15	0.05	0.02	0.0775
Oxygen[b]	55.50	50	50.5	47.48	51.49
Heating Value[c] (MJ kg^{-1})	16.37	15.95	15.15	13.25	14.81
Bulk Density (kg m^{-3})	776	532	526	413	594
Particle size (mm)	22-25	150*90 (L*D)	150*90 (L*D)	50*50*5	N/A

[a] Test method IS 1350 (Part I)-1984
[b] By difference
[c] Test method IS 1350 (Part II)-1970

TABLE 2: MASS BALANCE OF DIFFERENT FEEDSTOCK

Fuel	Inputs (kg h^{-1})			Outputs (kg h^{-1})					MBC
	Fuel	Air	Total	Dry gas	Char	Water	Ash	Total	
Lignite	10.67	18.31	28.98	24.86	0.30	1.80	1.65	28.61	0.98
Cumin + Sawdust (40:60, w/w)	10.55	18.23	28.78	23.77	0.28	1.82	1.63	27.50	0.95
Sawdust	10.25	18.01	28.26	24.03	0.27	1.89	1.57	27.76	0.98
Wood	10.01	17.66	27.67	22.99	0.23	1.79	1.54	26.55	0.95
Lignite + Wood (50:50, w/w)	10.7	17.81	28.51	26.37	0.35	1.64	1.19	29.55	1.03

MASS BALANCE

In present study, five feedstock were used for the mass balance. Data required for mass balance were collected from the experiments carried out on 10 kWe gasifier. It is essential that, total mass input to the gasifier (fuel and oxidizer) must be equal to total mass output (gas, water, ash, tar etc.). Total mass input comprises of feedstock and air, while total mass output holds dry producer gas, char, tar, ash and water output. The tar was found very less in quantity compared to other products so it was neglected for the analysis. The usual way to quantify the inconsistencies in the mass balance is the mass balance closure (MBC) which is defined as the ratio of total mass output to that of total mass input. It is very difficult to obtained 100% closure due to error in measuring instruments, round-off error and unaccounted losses. Despite of this, the closures are found within 95%-100%. Characterization of feedstock and mass balance were shown in Table 1 and Table 2 respectively.

ELEMENT BALANCE

The feedstock contains various elements but the major contribution is due to these elements: Nitrogen (N_2), Oxygen (O_2), Carbon (C), Hydrogen (H_2) and Sulphur (S). But as Sulphur content, as shown in Table 1, is very less, hence is neglected for the element balance analysis. The producer gas is mainly comprised of N_2, H_2, CO, CH_4 and CO_2 gases. Hence the elements present in producer gas are N, H, O and C. The char is the unburnt fixed carbon content, hence it is assumed to contain only Carbon. Ash is obtained in solid form and is composed of oxides of potassium, manganese, aluminium, iron, calcium, etc. As these elements are not adequate at input side as well as at product side, their contents are very negligent and not considered in calculation. Hence ash is considered to be composed of mostly of oxygen. The molar flow rate of O_2 from ash were calculated from X- ray Fluorescence (XRF) of ash.

The corresponding elements in the feedstock can be obtained from Table 1. The molar flow rate of each element species that comprise feedstock and air can be calculated using Eq. (1).

$$\ddot{M}_i = \frac{\dot{M}_J * v_i}{M_i} \quad (1)$$

Where, $\ddot{M}_i$ and $\dot{M}_J$ are the molar flow rates of ith species and mass flow rate of jth input component respectively. v_i is the molar fraction of the ith species and M_i is the molecular weight of the ith species.

The output elements comprised mainly of producer gas, ash, char and water. The mass flow rate for each output component were obtained from Table 2. The Amagat's law was used to convert the volumetric flow rate of gas mixture to molar flow rate [11]. The moisture from air and gas was obtained by measuring relative humidity and dry bulb temperature of both gas and air throughout the experiment and taking average of it. Eq. (1) was used to find the molar flow rates for each of the output elements. Table-3 represents the element balance of different feedstock.

TABLE 3: ELEMENT BALANCE

Feedstock	Element	Input mol h^{-1}	Output mol h^{-1}	EBC
Lignite	N	481.42	515.10	1.06
	H	103.51	105.21	1.01
	O	381.49	321.5	0.84
	C	275.38	297.42	1.08
Cumin + Sawdust (40:60, w/w)	N	492.46	489.22	0.98
	H	216.89	204.17	0.94
	O	404.04	380.82	0.94
	C	382.17	405.85	1.06
Sawdust	N	495.53	497.31	1.00
	H	213.21	192.18	0.90
	O	408.62	374.02	0.91
	C	364.06	396.53	1.08
Wood	N	486.63	490.88	1.00
	H	197.87	179.13	0.90
	O	383.56	368.32	0.96
	C	391.83	382.91	0.97
Lignite + Wood (50: 50, w/w)	N	484.34	490.42	1.01
	H	190.59	172.3	0.90
	O	387.23	357.03	0.92
	C	352.76	361.76	1.09

HEAT TRANSFER ANALYSIS

Only convective and radiative heat transfer was considered for the analysis, while conductive heat transfer was neglected due to the poor conductivity of warm air surrounding the gasifier surface. The surface temperatures of various zones were measured using thermal imager (Fluke TIA759HZ) and infra-red temperature gun (TESTO 835-T2). The height of various zones war measured from the surface temperature profile on the gasifier for each feedstock. Eq. (2) was used to calculate the convective heat transfer [12].

$$Nu = \left\{ 0.825 + \frac{0.387 * {Ra_L}^{1/6}}{\left[1+\left(\frac{0.492}{Pr}\right)^{\frac{9}{16}}\right]^{8/27}} \right\}^2 \quad (2)$$

Where, Nu is the nusselt number which is used to calculate convection heat transfer coefficient ($h = {Nu.K}/{Lc}$, where K and Lc are thermal conductivity of air and characteristic length respectively. Ra, Pr and Gr are the Rayleigh, Prandtal and Grashof number respectively. $Nu = f(Gr, \mathrm{Pr})$ and $Gr = f(Ra, \mathrm{Pr})$. Rayleigh number can be calculated using $Ra_L = \frac{g*\beta*(T_S - T_\infty)*{L_C}^3}{\vartheta^2} * Pr$, where g is gravitational acceleration (m^2/s). $\beta = \frac{1}{T_f}$ is coefficient of volume expansion, where T_f is the average temperature and β is coefficient of thermal expansion, ϑ is the kinematic viscosity of air, T_s and T_∞ are the surface and

ambient temperature (K). Prandtal number can be calculated as $Pr = \frac{\mu_i * Cp_i}{k_i}$, where μ_i is the dynamic viscocity of air (Ns/m), Cp_i is the specific heat capacity of air (kJ/kgK) and k_i is the heat conductivity of air (W/mK). Heat loss due to convection can be calculated as $Q_{convective} = h * A * \Delta T$, where ΔT is the temperature difference between surface and surroundings (303 K). For the calculation of heat transfer by radiation was calculated using Stefan's law of radiation [13], where emissivity of gasifier reactor material was considered. The total heat transferred was taken as sum of convection and radiation heat transfer.

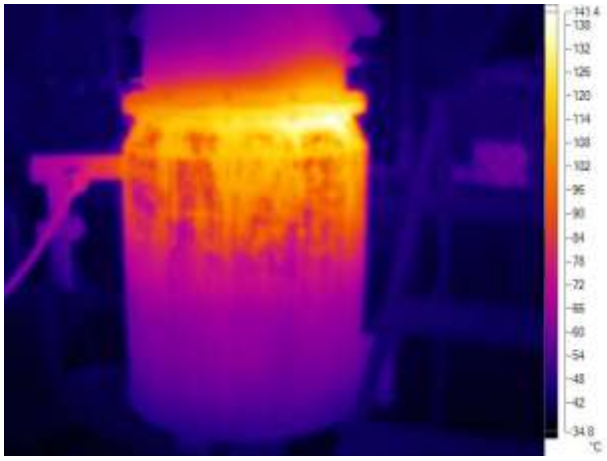

FIGURE 2. THERMOGRAPHY OF GASIFIER AT STEADYSTATE CONDITION

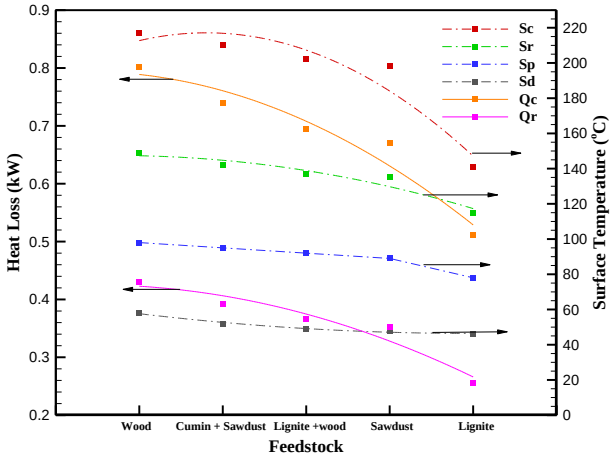

FIGURE 3: HEAT LOSS ANALYSIS OF DIFFERENT FEEDSTOCK

Figure 2 shows the variation of temperature along the surface after the steady state was reached. The convection (Q_c) and radiation (Q_r) heat loss along with surface temperature for combustion (S_c), reduction (S_r), pyrolysis (S_p) and drying (S_d) zones were mentioned in Figure 3. Surface temperatures distribution is directly influenced by the combustion zone temperature inside. Convective and radiative heat losses were found in the range of 0.511 kW to 0.802 kW and 0.255 kW to 0.431 kW for the selected feedstock. It was observed that total heat loss was found maximum with wood as a feedstock (1.23 kW) and minimum with lignite feedstock (0.76 kW). This was because the temperature for wood gasification was highest and for lignite, it was lowest among all selected feedstock.

CONCLUSIONS:

Following are the major conclusions from the present study.

1. Mass and element balance closure were found in the range of 0.95-1.03 and 0.84-1.09 respectively.
2. Convective and radiative heat loss were calculated and found in the range of 0.511 kW - 0.802 kW and 0.255 kW - 0.431 kW.
3. The minimum and maximum heat loss was observed with lignite and wood feedstock.

ACKNOWLEDGEMENT:

Authors are sincerely appreciated Department of Science and Technology, New Delhi (Project No: SR/S3/MERC-0114/2010) and Nirma University, Ahmedabad (Project No: NU/PhD/MRP/IT-ME/16-17/851) for the financial assistance.

REFERENCES:

[1] Ministry of Power, "Growth of Electricity Sector in India From 1947-2017," Government of India, 2017.

[2] Govt. of India, "Energy Statistics 2017," 2017.

[3] "India Biomass Energy." [Online]. Available: http://www.eai.in/ref/ae/bio/bio.html. [Accessed: 31-Aug-2018].

[4] V. C. J. Singh and S. J. Sekhar, "Performance studies on a downdraft biomass gasifier with blends of coconut shell and rubber seed shell as feedstock," *Appl. Therm. Eng.*, vol. 97, pp. 22–27, 2016.

[5] H. V Makwana, D. S. Upadhyay, J. J. Barve and, "Strategies for Producer Gas Cleaning in Biomass Gasification : A Review," in *International Conference on Recent Advances in Bioenergy Research*, 2018, pp. 115–127.

[6] Dogru, M., C.R. Howarth and A. A. M. Akay G. B. Keskinler, "Gasification of hazelnut shells in a downdraft gasifier," *Energy*, vol. 27, pp. 415–427, 2002.

[7] M. Simone, F. Barontini, C. Nicolella, and L. Tognotti, "Bioresource Technology Gasification of pelletized biomass in a pilot scale downdraft gasifier," *Bioresour. Technol.*, vol. 116, pp. 403–412, 2012.

[8] V. R. Patel, D. S. Upadhyay, and R. N. Patel, "Gasification of lignite in a fixed bed reactor: Influence of particle size on performance of downdraft gasifier," *Energy*, vol. 78, pp. 323–332, 2014.

[9] V. R. Patel, D. Patel, N. S. Varia, and R. N. Patel, "Co-gasification of lignite and waste wood in a pilot-scale (10 kWe) downdraft gasifier," *Energy*, vol. 119, pp. 834–844, 2017.

[10] D. S. Upadhyay, H. V. Makwana, and R. N. Patel, "Performance evaluation of 10 kWe pilot scale downdraft gasifier with different feedstock," *J. Energy Inst.*, Inpress, pp. 1–10, 2018.

[11] W. Woo and S. I. Yeo, "Dalton's Law vs, Amagat's Law for the Mixture of Real Gases," *SNU J. Educ. Res.*, vol. 5, pp. 127–134, 1995.

[12] Yunus Cengel and Afshin Ghajar, *Heat and Mass Transfer: Fundamentals and Applications*, 5th ed. McGraw-Hill Education, 2014.

[13] C. A. Forero-Núñez and F. E. Sierra-Vargas, "Heat Losses Analysis Using Infrared Thermography on a Fixed Bed Downdraft Gasifier," *Int. Rev. Mech. Eng.*, vol. 10, no. 4, p. 239, 2016.

Proceedings of International Conference on Sustainable Energy and Environmental Challenges (3rd SEEC), December 18-21, 2018, IIT Roorkee, India

SEEC No.028

Application of Condensed Distillers syrup Ethanol Industry waste for Heavy metal removal from wastewater

First Author- Bedotroyee Chowdhury
Food Technology & Biochemical Engineering
JadavpurUniversity
Email: bedotroyeechowdhury@yahoo.in

Second author- L.Roy[1*], DebabrtaBera[2*]
1.Techno India, Saltlake
2. Jadavpur University

ABSTRACT

Water is one of the most important resources on our planet. Currently availability of clean water available is becoming scarcer each year with the improper strategies of waste disposal. Heavy metals in waste are primarily a consequence of the intended use of heavy metals in industrial products. Heavy metals removal from industrial wastewater is a another challenging task for scientists, due to multi-facet contamination of water bodies. On the other hand the ethanol industry waste by product .i.e. condensed distillers syrup (CDS) is on an increasing trend as the bioethanol industry is expanding significantly. In this present study a novel composite has been employed by utilizing waste i.e.CDS for the preparation of a composite biofilm. CDS composite material after cross-linking with humic acid was used to examine the metal removal activity from water. Lead, cadmium, and mercury ions in water were almost completely removed when 1% humic acid was used. Under the same conditions, copper concentration was reduced .This outcome of research is an interesting and enticing contribution to the waste treatment strategies.

Keywords: Distillery waste, heavy metals, humic acid.

INTRODUCTION

Throughout the past several years, increased demand for ethanol and use of its co-products has expanded because the population is increasing. This rising population is creating an impact on both the demand for food as well as energy [14]. To cater to the fuel energy there is more focus on bio-energy production. As the ethanol is a good source of bio-energy so demand is creating. To meet up this demand the ethanol industry is flourishing. From the statistic, it is predicted that the production of ethanol will increase 20-30% by the year of 2030. It is very well known that along with the main products there would be generating huge quantity of by products which will be generating during the processing. Hence during the processing of ethanol there is also generating enormous byproduct. We are using corn grains, rice grains, wheat grains etc as a substrate for production of ethanol. In the eastern region of our country, we are producing approximately 35000 thousand tons rice every year. The post-harvest process of the rice industry, the waste generated from that industry like broken rice or the substandard rice grain is the rice grain has been exploited by the ethanol industry in the eastern part of our country for the production of ethanol. For production of the ethanol the grains are undergoes fermentation process in the presence of yeast during which the carbohydrate ultimately concerted to alcohol. The reaming remains in the same unit. This is referring as a stillage. This stillage mainly consist of residual matter after starch has been utilized. This stillage have both soluble and insoluble component in it. When it is subjected to the centrifugation during which the supernatant which contain soluble portion of it is refer to as a thin stillage and that is your distilleries soluble syrup. This all condensation yields condensed distilleries syrup (CDS). After the centrifugation remaining portion is called wet distilleries grains (WDG). When this WDG mixed with solubles and subjected to drying then it is called as distilleries drying grain soluble (DDGS) [15]. So we need to know the basic composition of the DDGS and CDS so that we can use DDGS and CDS in different aspect. As a first step, the numerical data generated during this study will help fill a current void in design information for the utilization of DDGS in other way.

The production of ethanol and byproducts are directly proportional so generation of the ethanol byproducts will increase day by day. So we need one direction where we can use this huge quantity of ethanol by-products to be utilized. In this study we are using condensed distilleries syrup (CDS) for preparation of bio-films.

Bio-based films are derived from renewable polymers obtained from biomass. These films have received increasing interest as potential substitutes for certain polymers since they are biodegradable. Basically there are three types of bio-based films

polysaccharide, protein and lipid film [6]. The polysaccharide films are starch, alginate films etc. They are exhibit excellent gas permeability properties but poor barriers for water vapour due to hydrophilic nature. The lipid films are excellent moisture barriers due to the tightly packed crystalline structure but poor for mechanical strength. Protein films provide good barriers for carbon dioxide and oxygen but do not resist Water diffusion [7]. To overcome individual's drawbacks of those films we came down a new concept which is composite film. We are making composite film with a good homogeneous blend of carbohydrate, protein and fat [2]. Now we are getting all the advantages of individual film's together. In the ethanol production after the starch has been utilized the stillage mainly have protein, lipid and carbohydrate. The yeast also gives the contribution on the total percentage to protein, fat and lipid in the stillage. So it is a good blend of protein, lipid and carbohydrate. Hence our hypothesis is that this CDS could be a good candidate for the composite films.

Heavy metals removal from industrial wastewater is a challenging task for scientists, due to multi-facet contamination of water bodies [1,8,9]. Heavy metals are elements having atomic weights between 63.5 and 200.6, and a specific gravity greater than 5.0 [10]. With the rapid development of industries such as metal plating facilities, mining operations, fertilizer industries, tanneries, batteries, paper industries and pesticides, etc., heavy metals wastewaters are directly or indirectly discharged into the environment increasingly, especially in developing countries. Heavy metals are not biodegradable and tend to accumulate in living organisms and many heavy metal ions are known to be toxic or carcinogenic. Toxic heavy metals of particular concern in treatment of industrial wastewaters are including Zn, Cu, Ni, Hg, Cd, Pb and Cr [3,11,13]. Different techniques such as ion exchange, chemical precipitation, ultra filtration, electrochemical have been used for removal of metals from industrial wastewater employing different adsorbent materials [4]. To detect the metals at trace level is economically infeasible due to their relatively high costs. Therefore, developing countries can't afford these composites. To overcome these challenging points, there is a need to investigate a cost effective and economical alternate materials as well as method for water purification. The focus of this study is to add the absorbent material in film making formula and use it as a metal removal film. The CDS itself is a waste material so it is a cost effective process.

Humic acid (HA) is a absorbent material so it is used for removal of metal from industrial waste water [5,16]. Generally, there are three possible structures for the adsorption of heavy metals in the presence of HA. When HA coexists with metal ion, the metal ion is absorbed by forming ligand-bridging ternary surface complexes (M-HA) or surface complexes in which the metal ion remains directly bonded to functional groups of the mineral, that is, binary M-S or metal-bridging ternary surface complexes (HA-M-S), where S represents the adsorption site on the solid surface and M is the metal ion [12]. The effects of HA on the removal of heavy metals by adsorbents depend on the relative contribution of the above individual sorption complexes, types of adsorbents and metal ions, and geochemical conditions. Blending both the concept means add humic acid during the preparation of film so that CDS film shows the metal absorbing properties. CDS composite material after cross-linking with humic acid was used to examine the metal removal activity from water. The cross-linked composite material film was suspended in aqueous solutions of divalent metal ions (Cu, Pb, Cr, Cd and Hg, t 200 ppm), and the film–metal complex was filtered. Removal efficiency of the metal ions from their aqueous solutions increased proportionally with the humic acid in the film solution. Lead, cadmium, and mercury ions in water were almost completely removed when 1% humic acid was used. Under the same conditions, copper concentration was reduced.

MARERIALS AND METHODS

Preparation of Films

CDS syrup was mixed with distilled water in the ratio of 2:25. The plasticizer (glycerol), texture improver (sodium alginate), humic acid and 2-3 drops of oil added to the solution. All components were homogenized at 10000 rpm for 30 min. The solution was heated at 75°C for 30 min. Cooled the solution at room temperature. The film-solution was poured onto the I.R meter. After one hour Film sample was peeled off and stored in plastic bags and held in desiccators at 55+5 % RH for further testing.

Removal of Metal Ions From Water

An aqueous solution of copper ions (Cu 203 ppm) was prepared by dissolving cupric sulfate ($CuSO_4 \cdot 5H_2O$, 0.8 g) in distilled water (1 l). Cross-linked carboxymethyl starch (0.5–3.0 g, db) was added in the copper solution (100 ml), and the dispersion was stirred for 10–30 min for the humic to form a complex with the metal ions. The humic–metal complex was removed by filtration (Whatman

No. 41), and the filtrate was used for the residual metal analysis.

To compare the removal effect of other metal ions, Pb (203 ppm), Hg (208 ppm), and Cd (194 ppm) solutions were prepared by dissolving lead acetate (Pb(CH3CO2)2•3H2O,0.19 g), mercuric acetate (Hg(CH3CO2)2, 0.33 g) and cadmium sulfate (CdSO4, 0.25 g) in distilled water (1 l), respectively. Film is suspended into the solution for 2hrs and after 2hrs cheek the metal concentration in the solution.

Analysis of Metal Ions

After the metal solution was treated with the cross-linked carboxymethyl starch, residual metal ion content in the filtrate was measured either by a colorimetric method (Helrich, 1990) for Cu, chromium and by AAS for others.

RESULT AND DISCUSSION

For lead removal from a lead acetate solution (437 ppm Pb), the film showed a positive correlation with the removal efficiency, as was the case of Cu. The result showed that the degree of Pb removal was more than twice of that of copper ions. This difference could be explained by the significantly higher molecular weight of lead ion compared to the copper ion (207.2 vs 63.5). The molar concentrations of lead (437 ppm) and copper (203 ppm) in the solutions were 2.11 *1023 and 3.20 * 1023, respectively. Therefore, the reduced concentration of both the metal ions were similar in molar concentration (t 2 mmol/l). This result may indicate that the functional groups in film display relatively equal binding affinity to both divalent metal ions. By using 1% (w/v) of the humic acid, cadmium and mercury ions (194 and 208 ppm, respectively) could be almost completely removed (over 99%), in the tested range.

Table 1: Results of metal concentration in the solution after absorption

Metal	Initial	Final
Cupper	201ppm	150ppm
Lead	203ppm	78ppm
Cadmium	194ppm	24ppm
Mercury	208ppm	49ppm
Chromium	100ppm	31ppm

CONCLUSION

The primary aim of this study was to removal of heavy metal from the industrial waste water as it is harmful for living organism as well as human. Presently the technique are available those are very costly so another aim of this study was to develop a simple, reliable, reproducible and inexpensive method for the removal of heavy metals. To achieve this purpose, 1st we developed a film from CDS. Formation of CDS films are itself economic and environment friendly process because CDS is a waste material. In the film we added humic acid as a substance. Humicsubstances, with high reactivity and strong binding ability, play a significant role in altering surface properties, aggregation, transportation and toxicity of nanoparticles and in controlling removal, mobility and bioavailability of metal ions in the environment. After adding humic acid the film is also showing the same feature. Hence this film can useful for metal removal from aquatic environmental.

REFERENCES

1. Ali, I., 2012. "New generation adsorbents for water treatment". Chemical reviews, *112*(10), pp.5073-5091.

2. Bourtoom, T., 2008. "Edible films and coatings: characteristics and properties". International Food Research Journal, *15*(3), pp.237-248.

3. Fu, F. and Wang, Q., 2011. "Removal of heavy metal ions from wastewaters: a review". Journal of environmental management, *92*(3), pp.407-418.

4. Gupta, V.K. and Rastogi, A., 2009. "Biosorption of hexavalent chromium by raw and acid-treated green alga Oedogonium hatei from aqueous solutions". Journal of Hazardous Materials, *163*(1), pp.396-402.

5. Hyung, H. and Kim, J.H., 2008. "Natural organic matter (NOM) adsorption to multi-walled carbon nanotubes: effect of NOM characteristics and water quality parameters". Environmental science & technology, *42*(12), pp.4416-4421.

6. Janjarasskul, T. and Krochta, J.M., 2010. "Edible packaging materials". Annual Review of Food Science and Technology, *1*, pp.415-448.

7. López, O., García, M.A. and Zaritzky, N.E., 2010. "Novel sources of edible films and coatings". Stewart Postharvest Review, *3*(3), pp.1-8.

8. Pandey, N., Shukla, S.K. and Singh, N.B., 2015. "Zinc oxide-urea formaldehyde nanocomposite film as low-cost adsorbent for removal of Cu (II) from aqueous solution". Adv. Mater. Lett., *6*(2), pp.172-178.

9. Patil, B.N. and Acharya, S.A., 2014. "Preparation of ZnS-graphene nanocomposite and its photocatalytic behavior for dye degradation". Adv. Mat. Lett, *5*(3), pp.113-116.

10. Srivastava, N.K. and Majumder, C.B., 2008. "Novel biofiltration methods for the treatment of heavy metals from industrial wastewater". Journal of hazardous materials, *151*(1), pp.1-8.

11. Shukla, S.K., Nidhi, S., Pooja, N., Charu, A., Silvi, M., Rizwana, A.B. and Dubey, G.C., 2014. "Metal decontamination from chemically modified rice husk film". Advanced Materials Letters. 5(6), 352-355.

12. Tang, W.W., Zeng, G.M., Gong, J.L., Liang, J., Xu, P., Zhang, C. and Huang, B.B., 2014. "Impact of humic/fulvic acid on the removal of heavy metals from aqueous solutions using nanomaterials: a review". Science of the total environment, *468*, pp.1014-1027.

13. Zhang, Q., Zhong, S.W., Su, J.L., Li, X.J. and Zou, H., 2013. "Determination of trace chromium by square-wave adsorptive cathodic stripping voltammetry at an improved bismuth film electrode". Journal of the Electrochemical Society, *160*(4), pp.H237-H242.

14. Going global 2015 ethanol industry outlook, renewable fuels association

15. Hertrampf, J. W. and F. Piedad-Pascual. 2000. Handbook on Ingredients for Aquaculture Feeds. Kluwer Academic Publishers, Boston, MA, USA. 573 p.

16. *WM'01 Conference* 2001. February. Application of humic substances in environmentalremediation. https://s3.amazonaws.com/academia.edu.documents/45775883/Application_of_humic_substances_in_envir20160519-245051wkrv60.pdf?AWSAccessKeyId=AKIAIWOWYYGZ2Y53UL3A&Expires=1536138217&Signature=sOIbGLdeA0seNnO9uHN0e79U8GI%3D&response-contentdisposition=inline%3B%20filename%3DApplication_of_humic_substances_in_envir.pdf

Proceedings of theThird International Conference on Sustainable Energy and Environmental Challenges (3rd SEEC)
18 –21 December, 2018, IIT Roorkee, India

SEEC No. 029

PREPARATION OF ELECTROCHEMICALLY GENERATED ADSORBENT USING ULTRASONICATION FOR FLUORIDE REMOVAL

Kunjan C Junghare
Chemical Engineering Dept, VNIT
Research Scholar
Email: kunjanjunghare@gmail.com

Dr. Shyam M Kodape
Chemical Engineering Dept, VNIT
Assistant Professor
Email address: samkodape@gmail.com

ABSTRACT

Humankind required water for their daily usage, according to United States Geological Survey (USGS) only 2.5% fresh water is available for drinking purpose on earth. Out of which many sites are contaminated with fluoride which has a hazardous impact on mankind. This brings the concern of fluoride removal from the available groundwater. In the present work, a novel ultrasound-assisted method for preparation of electrochemically generated adsorbent. This method reduces the particle size of adsorbents which increase the active sites. The prepared adsorbent is used for fluoride removal using an electrolytic method and ultrasonication. The effect of different electrolyte and electrodes was studied and a quantitative analysis of produced gases is carried out. The SEM-EDX analysis shows a passive layer on the electrodes. The increase in surface area of adsorbent is confirmed by BET analysis. The fluoride removal using ultrasonicated and non-ultrasonicated adsorbent were carried out and it is found to be 85% and 75% respectively within 2 hours. Using ultrasonic approach efficiency of fluoride removal is increased along with the reduction in the time required.

***Keywords*:** Electrolytic, Ultrasonification, Fluoride removal, SEM.

INTRODUCTION

According to United States Geological Survey (USGS) only 2.5% fresh water is available on earth. Out of these availability, there is fluoride contamination seen in the available ground water. There are many other contamination but fluoride is brought into concern because of worst impact it has on mankind. This is because a low dose of <1.5 mg/l of fluoride prevents decay of teeth, whereas concentrations above 1.5 mg/l in drinking water cause skeletal fluorosis, cardiovascular disease and many other. WHO in 1984 has prescribed a maximum tolerance limit of fluoride as 1.5 mg/l[1]. The Central Pollution Control Board standard allows 1.5mg/l and 15 mg/l for drinking and industrial waste water respectively[2]. Specifically in India the major sources are found in the area characterized by high-grade metamorphic rocks such as khondalite, charnockite, and leptynite. Other minerals in rocks and anthropogenic sources such as industries that manufacture pesticides, fertilizers and aluminium[3][4]. Many areas are also characterized by the presence of a hot spring, one such occurrences is seen in the eastern part of Orissa[5]. In Maharashtra places like solapur, karanja, washim also found high fluoride level[6]. Occurrence of the high fluoride levels in groundwater is found in Punjab, Orissa and many other states in India was reported by Das et al (2000) Kundu (2001).

The history of fluoride removal was started by NEERI in 1987. The main contents of the fluoride is removed along with the flocs, probably due to a combination of sorption and ion exchange also called as a co-precipitation[7][8]. But sludge generated has a disposal issue. Then next technique used was electrolytic defluoridation also called as electrocoagulation was used as an alternative[9].

Electrocoagulation means apply an electrical charge to water in the process of changing the particle surface charge, allowing suspended matter to form an agglomerate or flocs which is further used for the treatment. It effectively removes suspended solids in a wide range, breaks emulsions such as oil and grease or latex, and oxidizes and eradicates heavy metals from water without the use of filters or the addition of separation chemicals. The sludge generated here also has the same disposal problem. Especially during electrocoagulation the sludge obtained is a waste and is considered for no further use.

Our aim is to prepare adsorbent using electrolytic method which is named as electro-chemically generated adsorbent. Further this adsorbent is exposed to ultrasonification to inhance the fluoride removal efficiency. Literature proved that ultrasonification can enhance defluoridation via increasing the surface areas. Ultrasound is a wave of frequency 2×10^4 to $\times$ 10^{10} Hz. When ultrasonic wave passes through a liquid medium, a large no of micro bubbles form, grow and collapse in a very short time about a few microseconds, which is called ultrasonic cavitaion, which all results in reduction of surface area[10].Also Sonication is the act of applying sound energy to agitate particles for various purposes such as the extraction of multiple compounds from plants, microalgae and seaweeds. .

INTERNATIONAL AND NATIONAL STATUS

Till 2017 a lot research work is being done at international level. A. Oulebsir et al. have generated adsorbents along with regeneration using electrochemical technique at constant parameters, direct use of those adsorbents have been done for fluoride removal[11]. H. Lounici a et al used a combination of activated alumina column and electrochemical system for fluoride removal[12]. Electrocoagulation on pharmaceutical industry wastewater to remove high and varied refractory organic compounds content was tested[13]. Simple treatments like activated carbon adsorbent are also used effectively but also bring along the waste dumping problems[14]..While here in India Nalgonda technique developed by NEERI 1987 still plays a dominant role during application for defluoridation. But this method has disposal problem. Bhise R.M. et al used activated charcoal adsorption and electrocoagulation for colour removal of spent wash[22]. Naba Kumar et al used aluminium impregnated coconut fiber along characterization to confirm the removal of fluoride but again will be pure adsorbent with no regeneration option also having environmental impacts by increasing the carbon credits[6]. M. Barathi, et al is directly preparing adsorbent zirconium impregnated cellulose using ultrasonication method for effective fluoride adsorption[7]. Study on real soya oil refinery wastewater was done by K. Rajkumar for comparison of the amount of sludge generated using conventional treatment process and electrochemical process[17]. Review paper by NEERI Sanghratna et al for defluoridation using adsorbent prepared by industrial, agricultural and biomass waste[23]. Papers on novel adsorbents like marble wastewater powder for removal of fluoride ions form aqueous solution[24].

MECHANISM

A electrolytic process basically consists of an electrochemical cell which can be a batch or continuous reactor with metal electrodes connected to a DC power supply. In mechanism of electrolytic method, the coagulant is generated by electrochemical dissolution of sacrificial anode[26]. When the sacrificial anode is made up of aluminum metal, the supply of electric current produces trivalent aluminum hydroxide flocs[27]. Reactions occurring in this process when aluminum is used as a sacrificial anode can be represented as follows[28]

Anode: $Al_{(s)} \rightarrow Al^{3+} + 3e^-$

Cathode: $2H_2O + 2e^- \rightarrow H_{2(g)} + 2OH^-$

Formation of coagulant species:

$$Al^{3+} + 3H_2O \rightarrow Al(OH)_{3(s)} + 3H^+$$

After electrolytic process this electro generated adsorbents will be ultrasonified. Literature shows that ultrasonification can be used to increase the surface area of the adsorbents. Ultrasonic frequencies (>20 kHz) are usually used, leading to the process also being known as ultrasonication. This sludge will be used as an adsorbent. Adsorption is a surface phenomena, in this adhesion of atoms, ions or molecules from a gas, liquid or dissolved solid to a surface happens. Here optimization and statistical modeling of electrocoagulation process will be done using Taguchi. Taguchi is a statistical modeling technique used to create empirical models, study interactions among factors and to find out optimized parametric conditions for a target response. The main advantage of using Taguchi for designing experiments is that it allows us to study interactions among different variables and optimize the specified response with a limited number of planned experiments. Also it allows us to find the error percentage in the experiment carried which clearly tells us weather the results are correct or not.

METHODOLOGY

This combination of the three different principles is applied in one approach. So basically we will use electrolytic method, ultrasonification and adsorption. Adsorbent preparation will be done using electrolytic method and ultrasonification. Further defuoridation will be done by adsorption. The major steps involved to

prepare this Electro-chemically generated adsorbents are given below:

Preparation of electrolytic solution: Electrolyte solution can be prepared using different salts e.g. NaCl, KCl, Na_2SO_4 and various concentration of solution will be prepared ranging from 1 N-10 N etc.

- Preparation of stock solution
- Electro chemically generated adsorbent preparation:
- Preparation of nanosized adsorbents using ultrasonification
- Optimization of operating parameters using Taguchi

CHARACTERIZATION AND ANALYSIS

1. SEM -EDX (Scanning Electron Microscope) : This is to be used to show the passive layers on electrodes before and after experiment. Also composition of adsorbent will be studied. To study the formation of passive layers on electrodes[31]

2. Fourier transform infrared spectroscopy (FTIR) analysis : The adsorbent will be analysed. S. Zaidi et al used FTIR to study formation of new bonds between carbonyl oxygen and aluminum ions (of flocs)[11].

3. Gas Chromatograph : The gases which will be generated during sludge preparation by electrolytic method will be used to study analytical chemistry for analyzing gases present qualitatively and quantitatively without decomposition. Literature shows that gases are released during this process, so there will be chance to use it further. Abdalhadi D et al showed the release of hydrogen gas during electrolytic process[32].

4. Brunauer–Emmett–Teller : Here it will be used to find the surface area of the adsorbents i.e the sludge generated during electrolytic process.

PERFORMANCE STUDY

Objective 1. Study on defluoridation using sonicated and non-sonicated adsorbents.

Objective 2. Optimizating the process parameters for the removal of fluoride using Taguchi method

Objective 3. Application of different electrolyte and electrodes in electrolytic process.

Objective 4. To study the effect of other ions on defluoridation using electrochemically generated adsorbents.

Objective 5. To study the thermodynamic aspects, kinetics of reactions and adsorption isotherm.

Objective 6. To study output gases composition released during the sludge generation.

Objective 7. To Validate the results using Analytical Techniques.

Objective 8. Regeneration of the adsorbents will be done to reuse them.

OVERALL OUTCOME:

A novel approach for defluoridation of wastewater in electrolytic method, adsorption and ultrasonification will be studied successfully. Kinetic of the above experiments will be studied. Effect to ultrasonication on adsorbents will be seen. Optimizating the process parameters using Taguchi method. Effect of different electrolyte and electrodes in electrolytic process. The effect of other ions on defluoridation using electrochemically generated adsorbents. The thermodynamic aspects, kinetics of reactions and adsorption isotherm will be known. Different Analytical Techniques to identify output gases composition released during the sludge generation and lastly regeneration of the adsorbents.

FUTURE SCOPE

The preparation of adsorbent form any industrial wastewater is not studied. Also naturally available electrolytes like sea water which already has NaCl is not taken into consideration. Only flouride removal is focused, we can also study simultaneous removal of other adsorbents. We can also implement this as a continuous process for forming a bed of adsorbent prepared.

REFERENCES

[1] T. Edition, “International standards for drinking-water,” 1971.

[2] S. Vi, “GENERAL STANDARDS FOR DISCHARGE OF ENVIRONMENTAL POLLUTANTS PART-A : EFFLUENTS,” vol. 2, no. 174, pp. 545–560, 1993.

[3] S. Shekhar, A. C. Pandey, and M. S. Nathawat, “Evaluation of fluoride contamination in groundwater sources in hard rock terrain in Garhwa district , Jharkhand , India,” vol. 3, no. 3, pp. 1022–1030, 2012.

[5] N. K. Æ. M. K. Panigrahi and Æ. S. P. S. Æ. S. Tripathy, “Delineation of fluoride contaminat- ed groundwater around a hot spring in Nayagarh , Orissa , India using geochemical and resistivity studies,” pp. 228–235, 2002.

[6] N. K. Mondal, R. Bhaumik, and J. K. Datta, “Removal of fluoride by aluminum impregnated coconut fiber from synthetic fluoride solution and natural water,” *Alexandria Eng. J.*, vol. 54, no. 4, pp. 1273–1284, 2015.

[7] E. Dahi, F. Mtalo, B. Njau, and H. Bregnhj, “Defluoridation using the Nalgonda Technique in Tanzania The Nalgonda technique,” pp. 266–268, 1996.

[8] B. Maniraj, “A novel ultrasonication method in the preparation of zirconium impregnated cellulose for effective fluoride adsorption,” no. December, 2014.

[9] “Assessment of electrolytic process for water defluoridation,” vol. 1, no. November, pp. 175–182, 2014.

[10] T. J. Mason, “Theory , Applications and Uses of

Ultrasound in Chemistry Sonochemistry , Theory , Applications and Uses of Ultrasound in Chemistry Timothy James Mason , J . P . Lorimer," no. January 1989, 2014.

[11] A. Oulebsir *et al.*, "Preparation of mesoporous alumina electro-generated by electrocoagulation in NaCl electrolyte and application in fluoride removal with consistent regenerations," *Arab. J. Chem.*, 2017.

[12] H. Lounici *et al.*, "Study of a new technique for fluoride removal from water Qm â€™ b â€™ Ce," vol. 114, pp. 241–251, 1997.

[13] A. R. Miron, A. A. Chivu, A. Abdul, K. Klaif, and P. C. Albu, "Pharmaceutical Industry Wastewater Treatment through Electrocoagulation," pp. 1399–1406.

[14] E. Science and J. Kaur, "Removal of fluoride from drinking water using activated carbon," no. June, 2013.

[15] M. Malakootian and N. Yousefi, "THE EFFICIENCY OF ELECTROCOAGULATION PROCESS USING ALUMINUM ELECTRODES IN REMOVAL OF HARDNESS FROM WATER," vol. 6, no. 2, pp. 131–136, 2009.

[16] N. Drouiche, S. Aoudj, M. Hecini, N. Ghaffour, H. Lounici, and N. Mameri, "Study on the treatment of photovoltaic wastewater using electrocoagulation : Fluoride removal with aluminium electrodes — Characteristics of products," vol. 169, pp. 65–69, 2009.

[17] K. Rajkumar, "STUDIES ON COMPARISON OF SLUDGE PRODUCED FROM CONVENTIONAL TREATMENT PROCESS AND ELECTROCHEMICAL PROCESSES OF SOYA OIL REFINERY PROCESSING WASTEWATER," vol. 32, no. 2, pp. 562–571, 2016.

[18] F. E. Bulletin, M. Sciences, and M. Sciences, "Performance evaluation of electrocoagulation process for phenol removal from aqueous solutions," no. April 2014, 2012.

[19] S. Bibi, A. Farooqi, K. Hussain, and N. Haider, "Evaluation of industrial based adsorbents for simultaneous removal of arsenic and fl uoride from drinking water," *J. Clean. Prod.*, vol. 87, pp. 882–896, 2015.

[20] U. Tezcan and E. Ozel, "Electrocoagulation of yogurt industry wastewater and the production of ceramic pigments from the sludge," *Sep. Purif. Technol.*, vol. 120, pp. 386–391, 2013.

[21] M. A. Nasution, Z. Yaakob, E. Ali, N. B. Lan, S. Rozaimah, and S. Abdullah, "A Comparative Study Using Aluminum and Iron Electrodes for the Electrocoagulation of Palm Oil Mill Effluent to Reduce its Polluting Nature and Hydrogen Production Simultaneously," vol. 45, no. 2, pp. 331–337, 2013.

[22] R. M. Bhise, A. A. Patil, A. R. Raskar, P. J. Patil, and D. P. Deshpande, "Removal of Colour of Spent Wash by Activated Charcoal Adsorption and Electrocoagulation," vol. 1, no. 6, pp. 66–69, 2012.

[23] S. S. Waghmare and T. Arfin, "FLUORIDE REMOVAL BY INDUSTRIAL , AGRICULTURAL AND BIOMASS WASTES AS ADSORBENTS : REVIEW," no. 4, pp. 628–653, 2015.

[24] D. Mehta, P. Mondal, and S. George, "Journal of Environmental Chemical Engineering Utilization of marble waste powder as a novel adsorbent for removal of fl uoride ions from aqueous solution," *Biochem. Pharmacol.*, vol. 4, no. 1, pp. 932–942, 2016.

[25] A. Kumar, P. Kumar, D. Pal, A. Chandrakar, and R. Choudhary, "Journal of Water Process Engineering Electrocoagulation treatment of rice grain based distillery effluent using copper electrode," *J. Water Process Eng.*, vol. 11, pp. 1–7, 2016.

[26] P. Loganathan, S. Vigneswaran, J. Kandasamy, and R. Naidu, "Ac ce pt ed cr t," *J. Hazard. Mater.*, no. 2010, 2012.

[27] D. T. Moussa, M. H. El-naas, M. Nasser, and M. J. Al-marri, "A comprehensive review of electrocoagulation for water treatment : Potentials and challenges," *J. Environ. Manage.*, 2016.

[28] K. S. Hashim, A. Shaw, and D. Phipps, "De fl uoridation of drinking water using a new fl ow column- electrocoagulation reactor (FCER) - Experimental , statistical , and economic approach," vol. 197, pp. 80–88, 2017.

[29] Y. H. Tan, M. O. Abdullah, C. Nolasco-hipolito, and N. A. Zauzi, "Application of RSM and Taguchi methods for optimizing the transesterification of waste cooking oil catalyzed by solid ostrich and chicken-eggshell derived CaO," *Renew. Energy*, 2017.

[30] S. M. Baligidad, U. Chandrasekhar, K. Elangovan, and S. Shankar, "ScienceDirect RSM Optimization of Parameters influencing Mechanical properties in Selective Inhibition Sintering," *Mater. Today Proc.*, vol. 5, no. 2, pp. 4903–4910, 2018.

[31] S. Zaidi, T. Chaabane, and T. A. M. Msagati, "Electro-coagulation coupled electro-flotation process : Feasible choice in doxycycline removal from pharmaceutical effluents," *Arab. J. Chem.*, pp. 0–11, 2015.

SEEC NO.030

STUDY OF SPECIFIC OUTPUTS AND EMISSION CHARACTERISTICS OF ENGINES BY USING SUITABLE HCNG FUEL BLENDING

Sukanta R.
Mechanical Engineering Department, Visvesvaraya National Institute of Technology Nagpur-440010
Assistant Professor
rogasukanta@vnit.ac.in

S. Shiva Teja
Mechanical Engineering Department, Visvesvaraya National Institute of Technology Nagpur-440010
UG Student
sherishivateja@gmail.com

G.M.S.R Pavan Kumar
Mechanical Engineering Department, Visvesvaraya National Institute of Technology Nagpur-440010
UG Student
pavangundumogula@gmail.com

ABSTRACT:

With increasing concern about energy shortage and environmental protection, research on reducing exhaust emissions, reducing fuel consumption, reducing engine noise and increasing specific outputs has become the major researching aspect in combustion and engine development. Depleting petroleum reserves and stringent emission legislations demand introduction of alternative automotive fuels in order to reduce global emissions and lower the consumption of conventional fuels such as gasoline and diesel.

Several alternative fuels have emerged such as alcohol, biodiesel and LPG but none of them are available commercially are widely successful except natural gas. Natural gas is used in the form of compressed natural gas (CNG) or liquefied natural gas (LNG). Although LNG storage has been used in few vehicles at present, refueling cost of LNG tanks is not competitive with CNG. Until such time most vehicles using natural gas will store it in compressed form. CNG produces low HC and CO_2 emissions and negligible SOx and particulate matter (PM) emissions, making it a "clean" fuel. Over last couple of decades, number of on-road CNG vehicles has drastically increased and several surveys project further increase.

Most important quality of CNG is its lower emissions. An additional advantageous characteristic of compressed natural gas is its high research octane number of 130. This means that a natural gas engine may be run at higher compression ratios than petrol engine without knocking, thus increasing its thermal efficiency. However CNG suffers from severe shortcomings because of its properties such as lower diffusivity, poor lean limit, high ignition energy, high COV, low flame speed and high flame quenching distance. These adverse properties of CNG can be improved by addition of hydrogen.

Pure hydrogen has serious safety concerns for its implementation in internal combustion engines due to its low ignition energy and wide flammability range, which causes backfire and engine knocking. However many of the excellent properties of hydrogen can be effectively utilized in Hydrogen-CNG mixtures which contain mixture of hydrogen and CNG. Therefore hydrogen and CNG blends (HCNG) may be considered as an automotive fuel without

any major modification in the existing CNG engine and infrastructure.

In general, under precise circumstances the indicated thermal efficiency of the HCNG engine is much better than CNG engines without tolerating the high level of harmful emissions. Therefore the above discussion reveals us the importance of HCNG fuel. But the efficiency and combustion of HCNG fuel depends upon the proportions of hydrogen and CNG and mixing of each other. Mixing of hydrogen and CNG must be done in a specially designed HCNG fuel chamber.

There are various designs for the combustion chambers which are used in modern day engines. In this study it is considered a combustion chamber which consists of an inlet valve through which hydrogen blended with CNG (HCNG) is introduced into the chamber and ignited it with the help of spark plug to initiate the combustion required for driving the engine. However this discussion is mainly on the influence of the HCNG on emission norms. The properties of HCNG due to which it holds upper hand over the usage of CNG as a fuel are:

- Carbon free emission leading to decrease in the emission of greenhouse gases.
- Requirement of low ignition energy.
- High reactivity of hydrogen present in HCNG.
- High diffusivity and high burning velocity.
- Improves the engine efficiency and lowers the fuel consumption.
- It extends the lean misfire limit of CNG.
- It requires only small hydrogen storage and a column for the mixing of hydrogen with natural gas.
- Minor modifications are required in the engine due to the moderate concentration of hydrogen in the fuel mixture; the excellent anti-knock characteristics of CNG are not undermined.
- Safety properties are similar to CNG. HCNG is safer to handle than hydrogen, because of lower risk due to very low energy content from hydrogen (only up to 30 vol.%).

Although many properties of hydrogen are favorable for proper combustion, engines cannot be fueled with pure hydrogen because of the lower volumetric energy density and higher combustion temperature of hydrogen which makes pure hydrogen fueled engine produces lower power output and much higher NOx emissions than gasoline-fueled engine at stoichiometric air-fuel ratio. Therefore blending of hydrogen with CNG is done to produce a blended gas known as HCNG. HCNG allows customers early hydrogen deployment with nearly commercial technology. It is being treated as the first step towards future hydrogen economy. Any natural gas engine is compatible to run on HCNG and can do so with minimum modifications. It also allows governments and agencies to promote the use of hydrogen to greater number of people at less cost. HCNG can help the hydrogen industry to develop volume and transportation solutions while reducing costs. HCNG can take advantage of existing investment in natural gas infrastructure and also has much higher volumetric energy storage density than pure hydrogen.

The variation of various kinds of efficiencies in engines due to the usage of HCNG fuels can be depicted in the form of following charts in which the gradual increase in thermal efficiency of HCNG engines with increase in air ratio is due to increase in the temperature of engine cylinder because of complete combustion which is observed from the figure 1. It is observed from the figure 2 that at low hydrogen contents in fuel volumetric efficiency is decreasing with increase in rpm because the process of pushing the exhaust gases out and sucking the fresh charge inside the cylinder gets lesser and lesser in time. Hence the marginal increase in the mass of air induced decreases with increase in rpm. But with increase in the hydrogen content the volumetric efficiency approaches a steady mean value which is independent on engine speed.

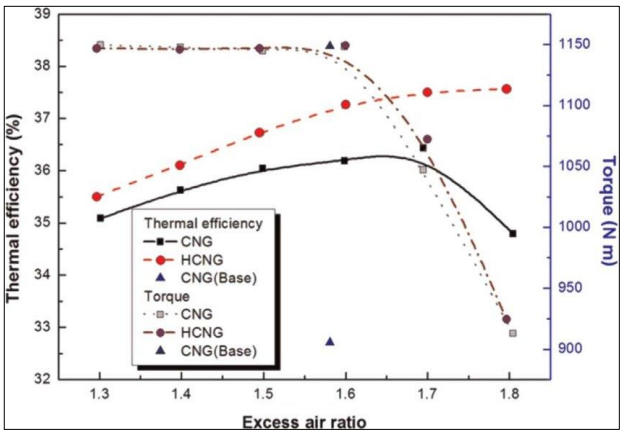

Fig.1: Thermal efficiency vs. excess air ratio in various engines

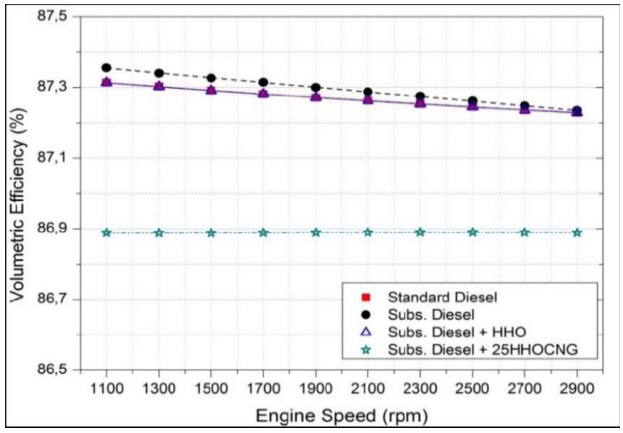

Fig.2: Volumetric efficiency vs. excess engine speed in various engines

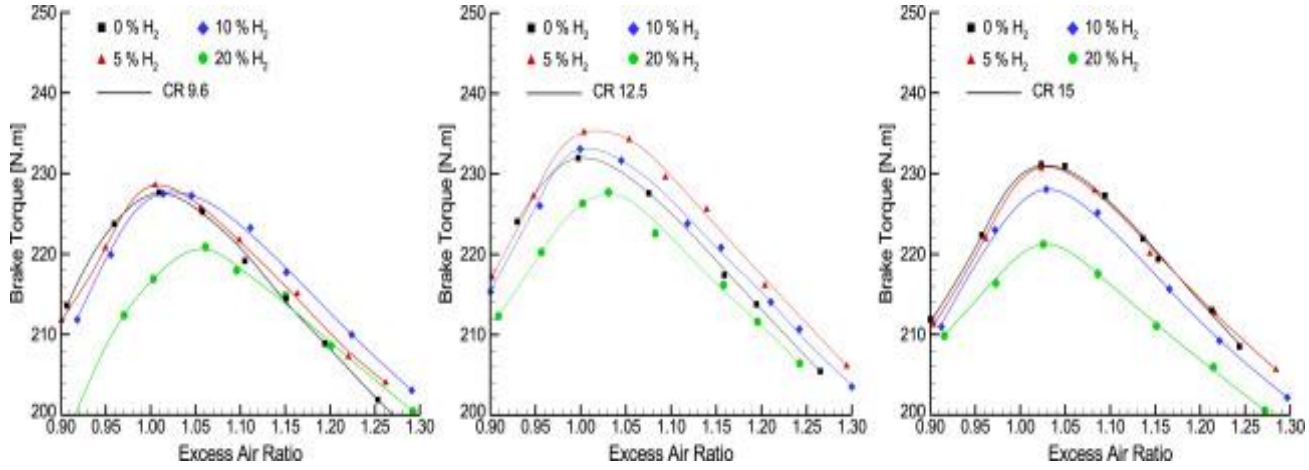

Fig.3: Brake torque vs. excess air ratio

The figure 3 shows the variation of brake torque vs. excess air ratio at various percentage compositions of hydrogen and various compression ratios of different engines using an HCNG fuel. A similar tabular chart is also prepared to describe the variation of other properties.

Properties	H_2	HCNG	CH_4	Gasoline
Limits of flammability in air, vol%	4-75	5-35	5-15	1.0 -7.6
Stoichiometric composition in air, vol%	29.53	22.8	9.48	1.76
Maximum energy for ignition in air, mJ	0.02	0.21	0.29	0.24
Auto ignition temperature, K	858	825	813	501-744
Flame temperature in air, K	2318	2210	2148	2470
Burning velocity in NTP of air, cms^{-1}	325	110	45	37-43
Quenching gap in NTP of air, cm	0.064	0.152	0.203	0.2
Normalized flame emissivity	1.0	1.5	1.7	1.7
Equivalence ratio flammability limit in NTP of air	0.1-7.1	0.5-5.4	0.7-4	0.7-3.8
Methane number	0	76	80	-

Challenges of using HCNG:

- HCNG storage and supply infrastructure.
- Efforts to be focused on responding to fuel system performance, material compatibility.
- Emission testing with more ranges hydrogen in HCNG blends
- Continuous availability of HCNG needs to be assured before embarking on its major use in I.C engines.
- Continued engine performance, emissions and durability testing in variety of engine types and sizes need to be developed to increase consumer and manufacturer confidence.
- Development of less expensive quality tests.

Therefore, as the demand of fuel is rapidly increasing according to the industrial development all over the world the amount of fossil fuel reduces very fast. CNG one of the alternative fuels is really important to support the transportation sector. Currently, most of the CNG engine vehicle is a converted version whether from the diesel vehicle or gasoline vehicle. To widespread the use of CNG, the refueling network must establish all over the country within the CNG engine vehicle driving range and at the same time the refueling technology and the dedicated CNG engine vehicle technology must be improved. This is very important as preparation of the gas-age (when the fossil fuel totally out of resource). Although at present bi-fuel gasoline conversions seem to be a convenient way to spread the use of CNG in the passenger car market, it is expected that as the gas distribution network expands and the number of refueling stations increase, increasingly more dedicated single-fuel engines will be developed for mass production which will be designed from scratch and will be fully optimized to accommodate the characteristics physical and chemical properties of natural gas. However, every effort will be made to use as many as possible common parts with gasoline engines. The end result could be more efficient engines with simultaneous reduction of all major pollutants relative to gasoline engines of equivalent capacity.

Keywords: CNG, Emission characteristics, HCNG fuel blending, SOx

SEEC No. 031

NOVEL APPROACH OF THE EFFECT OF MICROENCAPSULATION ON ANTIOXIDANT ACTIVITY FROM RICE WASTE DISTILLER'S DRIED GRAINS WITH SOLUBLE

Puja Mukherjee[1], Samayeeta Ghosh[1], Dr. Debabrata Bera[1], Dr. Lakshmishri Roy[2]

[1] Department of food technology and biochemical engineering, Jadavpur university, Kolkata
pmpujamukherjee068@gmail.com, samayeeta03@gmail.com, beradebabrata@yahoo.co.in
[2] Department of food technology, Techno India, Kolkata, lakshmi1371@gmail.com

ABSTRACT

Increasing dependence on non-renewable energy resources has resulted in the escalation of bioethanol industry growth. Consequently the phenomenal quantity of ethanol industry processing residues is predicted to create a significant impact on its future. DDGS i.e. distillers dried grain with solubles is the nutrient rich non fermentable residue of this industry which is produced significantly. Microencapsulation technology is an alternative to protect food ingredients or additives, which include environmentally sensitive bioactive principles in protective matrices to increase their functionality and life span. So this is the novel approach that production of antioxidants powder from ethanol industry waste that is rice distiller's dried grains with solubles (DDGS). In this research, microencapsulation of antioxidants using different proportion sodium alginate coating (0.5%, 1%, 2%, 3%) with freeze drying method will be done. The results of sonicated method is much higher than vortex method. The antioxidant activities, TPC and TFC in the initial sample were higher than those of encapsulated samples. Results are indicative of the alternative novel mode of utilization and revenue generation of the alcohol industry waste. So further processing need to standardise the process.

Keywords: DDGS, antioxidants, freeze drying, encapsulated powder

INTRODUCTION

Distiller dried grains with soluble (DDGS) is waste material of ethanol industry. In India, bio ethanol production increased from about 52.8 million of gallons in 2007 to over 225 million of gallons in 2016 [7]. Grains are the primary resources for ethanol production using either a wet milling or dry-grind process DDGS is produced from cereal grains like whole wheat, corn, soybean, barley, sorghum and their blends. Conventional ethanol production consists of 6 sequential steps, which include dry milling, liquefaction, saccharification, fermentation, distillation, and co-product recovery. During the last step of co-product recovery, condensed soluble (CDS) are mixed with distillers wet grains to become wet distillers grains with solubles (WDGS) and then dried into DDGS [2]. Distillers Dried Grains with Solubles (DDGS) is produced from the non-fermentable grains which remain after the starch has been converted to ethanol. 100 kg grains produce 32 kg DDGS and CDS, and 32 kg carbon di oxide along with 40 litre ethanol. In India the low quality rice and broken rice is increasingly being used in the ethanol industry. So in future, a large amount of rice based distillery by-products is likely to be available in the country. Distillers Grain with Soluble (DDGS) is a very good source of protein, fibre and minerals. But till date DDGS is considered as waste material and utilized only as animal and poultry feed [6]. Rice DDGS is a good source of nutrients. The taste of is bitter because of presence of high amounts of antioxidants. Its modification and suitable treatment may open up avenues of its application in development of valuable products for human consumption, at low cost.

As reported by Schrooyen et al (2001), bioactive compounds could slowly degrade and lose their activity, become hazardous (by oxidation reactions), react with other components present in the food system and/or change colour or taste of food products. Recently, microencapsulation has become suitable for food industry applications, in particular for the production of high value aliments and nutraceuticals. One of the most important reasons for microencapsulation of active ingredients is to improve stability in final products and during processing.

Microencapsulation is used to remove bitter taste during eating and astringency of polyphenols and others antioxidant compounds that limit their food application. Shahidi and Han (1993) listed six reasons for employing microencapsulation in food industry [5]:

• To reduce the core reactivity with environmental factors;
• To decrease the transfer rate of the core material to the outside environment;
• To promote easier handling;
• To control the release of the core material;
• To mask the core taste;
• To dilute the core material when it should be used in only very small amounts.

The objective of this study is to analyse the polyphenols and antioxidants extraction of rice distiller's dried grains with solubles and examine microencapsulation of these comounds.

METHODOLOGY

Experimental Design:

Ethanol industry solid wastes i.e. rice Distillers dried grains with solubles were obtained from IFB Agro industry pvt ltd. The sample was dried at 50°C in a hot air oven. The dried sample was taken for grinding. The grinding was carried out with the help of laboratory grinder. Then it was taken for particle size analysis and it was performed with the help of sieve shaker. The final size obtained was 150 and 250 microns. The powder of this two particle size mixture was then subjected to analysis.

Extraction Procedure:

The extraction of liquid was prepared by adding ethanol. Sample / solid ratio was 10:55 (g/ml). Extraction was carried out under shaking incubator at a speed of 120 rpm at 30 ± 2°C temperatures. After 24 hours extraction process the sample was separated from residual solids and stored at -20°C. Extraction solvent, solid:sample ratio, rpm, temperature and time were determined and fixed after optimisation.

Microencapsulation of Antioxidants:

Sample preparation for coating material is sodium alginate containing 0.5%, 1%, 2% and 3% solids. The prepared coating material solutions were then combined with antioxidant extract (core), at certain core: coating ratios (1:2v/v). Then the mixture was spread on calcium chloride solution. After 2 hours then filter the solution. Then freeze dried the solid portion. It is most suitable technique for dehydration for all heat sensitive materials and also for microencapsulation.

Sample Preparation for Analysis:

Sample was prepared by two modified methods –

Sample Preparation by Vortex Method [3]:

Approximately 1gm encapsulated sample was weighed and mixed with 10ml methanol stirred for 5 minutes in a regular vortex mixer. They were then frozen at -18°C for 90 minutes and thawed at room temperature. Sample was stirred in a vortex mixer for 2 minutes and centrifuged at 6000 rpm for 15 minutes.

Sample Preparation by Sonication Method [1]:

1gm of encapsulated powder was dissolved in 10ml of Methanol, mixed for 1 minute and sonicated twice for 20 minute. Sample was then centrifuged at 6000 rpm for 15 minutes.

Antioxidants analysis [4]:

Determination of Total Polyphenols Content (TPC):

The total phenolic content was determined by using the Folin- Ciocalteu assay. 1ml aliquot of extracts and standard solution of Gallic acid was added to 25ml volumetric flask, containing 9ml distilled water. Reagent blank was prepared by distilled water. 1ml of Folin-Ciocalteu phenol reagent was added to the mixture. After 5 minutes 10ml of 7% Na_2CO_3 was added to the mixture. The volume was then made up to the mark. After incubation for 45 minutes at room temperature, the absorbance against the reagent blank was determined spectrophotometer at 750nm. Total phenolic content was expressed as mg Gallic acid Equivalents.

Determination of Total Flavonoids Content (TFC):

Flavonoids were analysed by aluminium trichloride method. Briefly, 1ml of sample was mixed with 4ml of distilled water and 0.5ml of 5% sodium nitrite ($NaNO_3$) solution. After 5 minutes 0.3ml of 10% aluminium chloride ($AlCl_3$) solution was added. After 6 minutes of reaction, 2ml of 2M NaOH and 2.2 ml of water were added to the mixture. The solution was measured at 510nm at spectrophotometer. Quercetin solutions were used as standard.

Determination of Free Radical Scavenging Activity:

The free radical scavenging activity of extract was measured using DPPH free radical scavenging method with some modifications. 1 ml of sample extract was added to 3 ml DPPH solution (4 mg in methanol). The mixture was shaken vigorously and allowed to stand for 30 minutes at room temperature in the dark. Then the absorbance was measured at 539 nm. Methanol was used instead of sample for control measurements. The inhibition of DPPH was determined according to the following equation.

% inhibition = [(A Control – A Sample) / A control] × 100

A control: absorbance of control at 539 nm
A sample: absorbance of sample at 539 nm

RESULTS

The total phenolics content (TPC) of rice distiller's dried grain with solubles is 230.4 mg of GAE per 100gm. The total flavonoids content of sample is 1037mg of quercetin equivalent per 100gm. And percentage of free radical inhibition is 57%. These all results were found after optimisation. Fig. 1 and 2 are showing the standard curve of gallic acid and quercetin respectively.

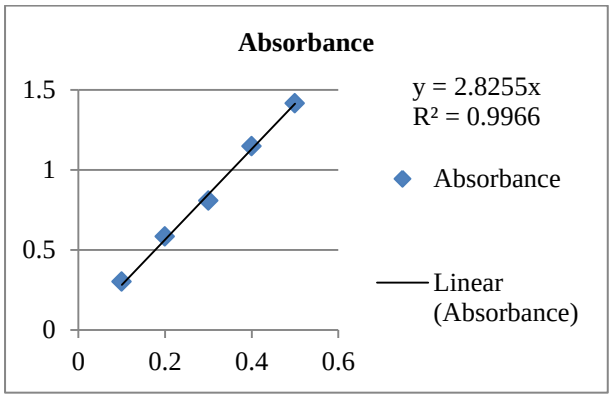

FIGURE 1: STANDARD CURVE OF GALLIC ACID

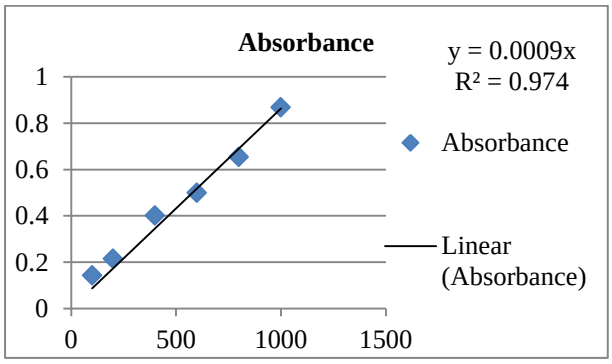

FIGURE 2: STANDARD CURVE OF QUERCETIN

The total phenolic content of concentrated sample (which is used for encapsulated product) is 844mg of GAE per 100 ml, flavonoids content is 6465 mg quercetin equivalent per 100 ml and percentage of free radical scavenging is 83.58%.

Fig. 3 is showing the pictures of encapsulated powders.

Results of antioxidants by Vortex method:

The total phenolics content (TPC) of 0.5%, 1%, 2%, 3% sodium alginate content of 5ml encapsulated sample is 34 mg, 56.17 mg, 51.23 mg, 48.618 mg of GAE per 100gm. The total flavonoids content of 0.5%, 1%, 2%, 3% sodium alginate content of 5ml encapsulated sample is 510 mg, 530.22 mg, 482.8 mg, 500.14mg of quercetin equivalent per 100gm respectively. And percentage of free radical inhibition is 83%, 97%, 91%, 83.58%.

Results of antioxidants by Sonicate method:

The total phenolics content (TPC) of 0.5%, 1%, 2%, 3% sodium alginate content of 5ml encapsulated sample is 55.53 mg, 71.13 mg, 78.578mg, 88.15 mg of GAE per 100gm. The total flavonoids content of 0.5%, 1%, 2%, 3% sodium alginate content of 5ml encapsulated sample is 718.76 mg, 787 mg, 862.44 mg, 845mg of quercetin equivalent per 100gm respectively. And percentage of free radical inhibition is 85%, 97%, 94%, 88%.

Tab. 1 is showing the percentage of antioxidants presents in initial concentrated sample and encapsulated samples.

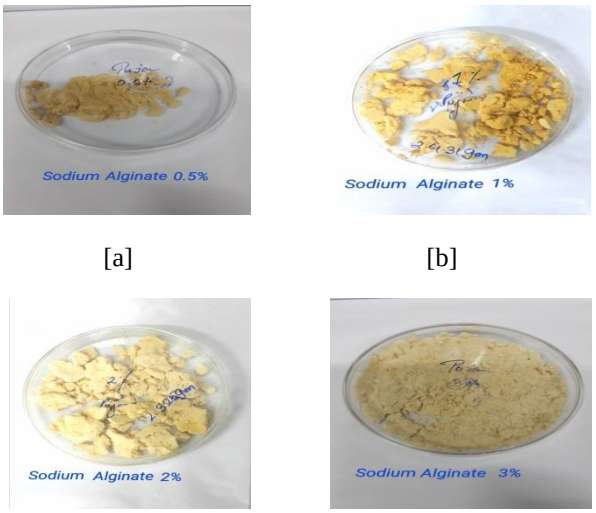

[a] [b]

[c] [d]

FIGURE 3: ENCAPSULATED POWDER – [a] 0.5% SODIUM ALGINATE [B] 1% SODIUM ALGINATE [C] 2% SODIUM ALGINATE [D] 3% SODIUM ALGINATE

TABLE 1: PERCENTAGE OF ANTIOXIDANTS

	TPC (mg of GAE / 100 gm)	TFC (mg of Quercetin / 100 gm)	DPPH %
Concentrated sample	844	6465	83.58
0.5% sodium alginate - vortex	34	510	83
0.5% sodium alginate - sonicate	55.53	718.76	85
1% sodium	56.17	530.22	97

alginate - vortex			
1% sodium alginate - sonicate	71.13	787	97
2% sodium alginate - vortex	51.23	482.8	91
2% sodium alginate - sonicate	78.57	862.44	94
3% sodium alginate - vortex	48.618	500.14	83.58
3% sodium alginate - sonicate	88.15	845	88

CONCLUSION

Different solid content effect on the antioxidant activities of encapsulated product. The changes in the concentration of sodium alginate affect the final product of encapsulated sample. The antioxidant activities, total polyphenol contents and total flavonoids contents in the initial sample were higher than those of encapsulated samples. So further processing need to standardise the process and the composite film.

ACKNOWLEDGMENTS

The authors are thankful to the university grant commission (UGC), New Delhi for providing the NET-JRF fellowship to Puja Mukherjee for this research. And also thankful to the IFB Agro Industry for providing us rice DDGS sample.

REFERENCES

1. Bahar Aliakbarian, Marco Paini et.al, 2015, "Effect of Encapsulating Agent on Physical-Chemical Characteristics of Olive Pomace Polyphenols-Rich Extracts", The Italian association of chemical engineering, 43, 97 - 102.
2. Jianchun Han and Keshun Liu, 2010, "Changes in composition and amino acid profile during dry grind ethanol processing from corn and estimation of yeast contribution toward DDGS proteins", Journal of agricultural and food chemistry, 58, 3430–3437.
3. Leslie Vidal J, Marcia Avello L, and Cristina Loyola C et.al, 2013, "Microencapsulation of maqui (*Aristotelia chilensis* [Molina] Stuntz) leaf extracts to preserve and control antioxidant properties", Chilean journal of agricultural research, 73 (1), 17 – 23.
4. Meral, R and SaitDogan, I, 2013, "Quality and antioxidant activity of bread fortified with flaxseed", Italian journal of food science, 25 (1), 51 – 57.
5. Shahidi, F. and Han, X., 1993, "Encapsulation of food ingredients", Critical Review in Food Science and Nutrition, 33, 501–547.
6. Weijie Xu, Narendra Reddy, and Yiqi Yang, 2007, "An acidic method of zein extraction from DDGS", Journal of agricultural and food chemistry, 55, 6279 – 6284.
7. Ethanol Industry Outlook, 2016, RFA analysis of public and private data sources, Fuelling a High OctaneFuture. http://www.ethanolrfa.org/resources/industry/statistics/#1454099103927-61e598f7-7643

Proceedings of the Third International Conference on Sustainable Energy and Environmental Challenges (3rd SEEC), 18 –21 December, 2018, IIT Roorkee, India

SEEC No.032

ROOFTOP PV ASPIRATIONS OF THE NATIONAL SOLAR MISSION AND THE RENEWABLE ENERGY NORMS OF GRIHA: THE MISSING LINK?

Rhythm Singh

Department of Electrical Engineering and Computer Science

Indian Institute of Technology Bhilai, Sejbahar, Raipur-492015, Chhattisgarh, India

Email: rhythms@iitbhilai.ac.in

ABSTRACT

The National Solar Mission of India aims for a total installed capacity of 100 GWp of solar photovoltaic installations in the country by 2022. Of this, 60 GWp is envisaged to come from utility-scale grid-connected solar PV parks, and another 40 GWp from rooftop PV installations. However, the recent data released by MNRE shows that while around 12.8 GWp of utility-scale solar photovoltaic installations have already been commissioned, the cumulative capacity of rooftop solar photovoltaic technology is barely touching 1 GWp. Clearly, the rooftop PV segment has not picked up in the country as the policy planners would have hoped for. Though the GRIHA framework adopted by MNRE stipulates some guidelines for incorporating renewable energy in the built environment, these guidelines are too diffused and too cursory to be effective. This paper investigates possible policy prescriptions, in the context of the GRIHA framework, which can help bolster the rooftop PV aspirations of India, as envisaged under the National Solar Mission.

Keywords: Solar rooftop PV policy, National Solar Mission, GRIHA

NOMENCLATURE

C	Annual electricity consumption per unit area
FA	Floor area of a building
G	Annual rooftop PV generation per unit area
I_{year}	Annual solar insolation per unit area
IA	Total inhabited area of a building
N_{sh}	Number of sunshine hours in a year
PTC	Power-temperature coefficient
PVAr	PV-available area ratio
PVSR	PV sufficiency ratio
$T_{panel,h}$	Hourly panel temperature during sunshine
η_{PCU}	Power conditioning unit efficiency
η_{PV}	PV panel rated conversion efficiency

INTRODUCTION

Various policy mechanisms have been used by different governments across the world for promoting renewable energy technologies. In fact, without any prejudice towards renewable energy technologies, it has been a standard practice across different countries and different ages, to promote a technology/ practice deemed beneficial for the "greater social good" with supportive policy formulations. In the context of renewable energy technologies, these supportive policy mechanisms broadly fall under two major categories – i) Price mechanisms, and ii) Quota mechanisms. In the price mechanism, the price for renewable energy generation is fixed, and the market forces decide upon the volume of renewable energy produced, as in feed-in tariff mechanism. On the other hand, quota mechanisms stipulate a mandatory share of energy to be generated from renewable sources, and accordingly the market forces act to decide upon the price at which this energy would be generated or traded. Usually, any government applies a mix of price and quota mechanisms for promoting renewable energy.

As a part of the National Solar Mission (NSM) of India, an ambitious target of having 100 GWp of total installed solar photovoltaic capacity by 2022 has been taken up. In pursuance of this ambitious target, the Government of India has been adapting a host of supportive policy mechanisms over the last few years – both of the price mechanism type, like feed-in tariff

mechanism and net metering etc., as well as quota mechanism type, like the renewable purchase obligations (RPOs). However, the quota mechanisms like RPOs have been put in place only for utilities, and not for retail consumers. Interestingly, at the same time, one finds that whereas the growth of utility-scale grid-connected solar PV has been quite good in pursuance of the targets envisaged for 2022 (almost 12.8 GWp of the 60 GWp target for utility-scale grid-connected PV has already been installed), the progress on the rooftop solar PV segment has been much sluggish (only around 1 GWp of the 40 GWp target for rooftop PV has been installed so far). This raises the question that will a quota mechanism for the rooftop segment, an equivalent of the RPO mechanism for utilities, help boost the sluggish growth of the installed capacity in this segment?

GRIHA AND RENEWABLE ENERGY NORMS

In recognition of the deep linkage between buildings' energy demand and the ensuing environmental impacts and sustainability issues, the Ministry of New and Renewable Energy (MNRE), Government of India, has adopted a set of norms for promoting "green building" practices in the country, known as "**G**reen **R**ating for **I**ntegrated **H**abitat **A**ssessment", or GRIHA, in short. The National Rating System for Green Buildings, developed under the GRIHA framework, envisages a holistic "green building" standard encompassing several aspects of "green" building design and implementation, like site planning, building envelope design, renewable energy incorporation in building design and functionality, usage of recyclable and/or eco-friendly building materials, energy efficiency measures in buildings, etc.

Interestingly, though the GRIHA rating system is supposed to be focussed on "greening" the buildings, it talks about renewable energy utilization in buildings as only one of the 34 criteria in the evaluation procedure. Moreover, renewable energy utilization has been placed as a "partly mandatory" criteria, with a weight of only 5 points out a total of 104. Furthermore, the description of this criterion is not so focussed and free of ambiguity so as to be able to provide a clear roadmap to the building developers/ owners regarding renewable energy incorporation in their respective projects.

Criterion 18 of the rating system, which deals with renewable energy utilization in buildings, says the buildings must have "renewable energy system with capacity equivalent to 1% of connected load for lighting and space conditioning", and further, the building must "meet energy requirements for a minimum of 5% of the internal lighting load (for general lighting) or its equivalent from renewable energy sources". While these descriptions provide an indication regarding how much renewable capacity and renewable generation is expected in a building, a more focussed guideline in form a prescription with regard to a particular renewable energy technology is expected to reap a larger dividend on this front. Furthermore, if this prescription can be made in regard to rooftop solar PV technology, which is not only one of the most mature renewable energy technologies at distributed generation level, but is also the subject of the ambitious National Solar Mission, it has the potential to become a doubly rewarding endeavour – promising to help push the sluggish rooftop PV component of the NSM targets.

A FRAMEWORK FOR DEVELOPING ROOFTOP PV NORMS

Rooftop PV, by definition, is deployed on the rooftops of buildings. Hence there is an intrinsic relationship between building design and rooftop PV deployment and proliferation. This inherent relationship can be evolved further to develop focussed prescriptions for renewable energy deployment under GRIHA rating system, based entirely on rooftop PV technology.

The electricity consumption of a building is usually related to the total inhabited area in a building. Let's say there is a sample building having a total inhabited area of IA m^2, including all the floors. Also, say that the electricity consumption is C kWh/m^2/year for the total inhabited area. Therefore, a total inhabited area of IA m^2 will have total annual electricity consumption of (IA).(C) kWh/year.

On the other hand, the generation from rooftop PV for a building depends on the floor area, which almost entirely translates into the rooftop area; and a reduction factor for taking care of the reduction in the available floor area for PV, due to utilities on the rooftop and the near-shading effects. Singh and Banerjee (2015) have indicated this reduction factor as the PVA ratio, the ratio of the PV-available area on the rooftop to the building footprint area. Singh and Banerjee (2015) have also documented the values of PVA ratio used by other researchers for similar analysis. Table 1, which is referenced from Singh and Banerjee (2015), shows the PVA ratio values from literature; also appended to this table is the result from Singh and Banerjee (2015). In this paper we abbreviate PVA ratio as PVAr, for the sake of simplicity for putting in mathematical formulae.

Further, let our sample building has a floor area (same as the gross roof area) of FA m^2. And, let's say that the generation from rooftop PV system is G kWh/m^2/year for the roof area (same as the Floor Area). Thus the total annual generation from the rooftop PV system for the sample building will be (FA).(G).(PVAr) kWh/year.

Based on the above, one can define PV Sufficiency Ratio (PVSR) for the sample building as given in Eqn. (1) – Eqn. (4). This PVSR can be used as a measure of efficacy of rooftop PV potential usage in a building.

TABLE 1. Values of PVA Ratio from literature (Ref: Singh and Banerjee (2015))

Reference	Area Covered	PVA ratio
IEA (2002)	World	0.4
Scartezzini et al. (2002)	Switzerland	0.49-0.95
Montavon et al. (2004)	Switzerland	
Pillai and Banerjee (2007)	India	0.3
Izquierdo et al. (2008)	Spain	0.22–0.43
Ordo´n˜ez et al. (2010)	Andalusia, Spain	0.535
Wiginton et al. (2010)	Ontario, Canada	0.3
Bergamasco and Asinari (2011)	Italy	0.145, 0.405
Yue and Huang (2011)	Taiwan	0.4 – 0.5
Theodoridou et al. (2012)	Thessaloniki, Greece	0.146
Karteris et al. (2013)	Greece	0.25
Greenpeace India (2013)	Delhi, India	0.26
Singh and Banerjee (2015)	Mumbai, India	0.28

$$PVSR = \frac{Annual\ PV\ Generation}{Annual\ Electricity\ Consumption} \quad (1)$$

$$PVSR = \frac{FA \times G \times PVAr}{IA \times C} \quad (2)$$

$$PVSR = PVAr \times \left(\frac{FA}{IA}\right) \times \left(\frac{G}{C}\right) \quad (3)$$

$$PVSR = PVAr \times \left(\frac{1}{No.of\ Floors}\right) \times \left(\frac{G}{C}\right) \quad (4)$$

Equation (4) follows from Eqn. (3) because the total inhabited area in the building is, generally, the summation of the floor areas of all the floors in the building. Further, there is an implicit assumption in this conversion that the floor area of all the floors is almost the same. As is evident from Tab. 1, the values of PVA ratio for Indian conditions, used by different researchers, varies in the narrow band of 0.26 – 0.30. Taking this set of values for Indian context as the reference, Eqn. (4) can be further simplified to Eqn. (5), for the general case. For estimating the PV Sufficiency Ratio (PVSR) of a specific building, however, simple building-specific analysis can be done for estimating the PVA ratio of the particular building. This analysis would entail estimation of the rooftop area used for utilities, and near-shading analysis of the rooftop, based on a 3D model of the building and the adjoining structures in some PV sizing and estimation software, like PVSyst.

$$PVSR = 0.28 \times \left(\frac{1}{No.of\ Floors}\right) \times \left(\frac{G}{C}\right) \quad (5)$$

The G value used in Eqn. (2) – Eqn. (5), which is the electrical energy output from a rooftop PV system per unit area per year, depends on i) the annual solar irradiation profile at the location of interest, ii) the solar PV panel technology used, its conversion efficiency and power-temperature coefficient, specifically, and iii) the efficiency of the power conditioning unit. Together, these factors combine to determine the G value. Let's say the rated PV panel conversion efficiency is η_{PV}, and the power-temperature coefficient of the PV panels deployed is PTC. Further, let's say that the efficiency of the power conditioning unit is η_{PCU}, and the total annual solar insolation received at the location of the interest is I_{year} kWh/m^2/year. As we know, the annual electrical energy output per unit area (G) of such a system is given by Eqn. (6), where $T_{panel,h}$ is the hourly panel temperature for all the solar insolation hours around the year and N_{sh} is the number of sunshine hours in the entire year.

$$G = I_{year} \times \eta_{PCU} \times \eta_{PV} \left(1 + \frac{1}{N_{sh}} \sum_{N_{sh}} \frac{PTC \times \left(T_{panel,h} - 25\right)}{100}\right) \quad (6)$$

Relevant analysis has been done for Mumbai city in India, with a sample polycrystalline Si module of BP Solar (BP 4175N) of rating 30V, 175 Wp, having a fixed tilt of 19° (same as the latitude angle of Mumbai) (Singh and Banerjee, 2016) and power conditioning unit consisting of 60 kW, 405-750V, 50/60 Hz Ingecon Sun 60 Inverter. This analysis gives a G value for this sample system for Mumbai city as 201.22 kWh/m^2/year.

The C value is the annual electricity consumption per unit area. A lot of variation can occur in this parameter depending on a host of factors, like the building location, building usage type, local weather and its fluctuations around the year, energy efficiency measures and behavioral patterns of the residents and/or users of the building. Table 2 lists the C values for some sample buildings in Indian conditions.

TABLE 2. C values for sample buildings in India

Reference	Type of building	C (kWh/m^2/ year)
BEE National Benchmark	Commercial	180
ECBC Compliant Building	Commercial	110
Bhatt et al. (2005)	Residential	12 – 36
Bhatt et al. (2005)	Commercial	60 – 300
Microsoft building, Hyderabad	Commercial	150

Putting together the results for the sample PV system in Mumbai city and the sample consumption values presented in Tab. 2, and substituting them in the generic PVSR equation, given in Eqn. (5), the generic PVSR results given in Tab. 3 can be obtained for buildings of different heights.

TABLE 3. PVSR results for sample buildings in India

No. of Floors	PVSR value	
	BEE National Benchmark	ECBC Compliant Building
3	0.104	0.171
5	0.063	0.102
7	0.045	0.073
10	0.031	0.051
14	0.022	0.037

INTEGRATING THE PVSR RESULTS WITH GRIHA NORMS

The analysis presented in the previous section provides a simple, yet effective, analytical framework for developing norms for the efficacy of rooftop PV potential utilization in a building. The PV Sufficiency Ratio (PVSR) developed in the last section takes into account not only the realizable rooftop PV potential, in terms of the available solar insolation, the building geometry and location specific constraints, but also the electricity consumption parameters; and integrates the two aspects to give a practical measure of the extent of rooftop PV potential utilization.

The PVSR value can be easily modified to take into account i) the variation in the PVA ratio due to the site-specific and/or structural variations of the building ii) the variations in the annual incident solar energy from location to location, iii) the variations produced in the electrical energy output of the rooftop PV systems due to modifications in the PV panel and/or power conditioning unit technology, and, last but not the least, iv) the variations in consumption patterns of different buildings.

Thus, it can be a really a promising move for the MNRE and the NSM to tweak with the GRIHA framework to formulate region specific and/or city-specific mandatory requirements for buildings to comply with the necessary PVSR requirements. For instance, with reference to Tab. 3, one can see that for a typical 3-storeyed BEE National Benchmark-compliant commercial building in Mumbai, it is expected to have a PVSR value of 0.104, considering typical average values for all the parameters involved. Thus, for instance, the GRIHA framework can be tweaked to say that for a 3-storeyed commercial building in Mumbai, the following specifications would hold in regard to rooftop PV utilization:

i) The building must have a minimum PVSR value of 0.08, for the necessary construction approval.

ii) If the building is designed to have a PVSR value in the range of 0.12 – 0.14 then it would attract, let's say, a 30% reduction in the municipal taxes for the first three years after commissioning.

iii) If the building is designed to have a PVSR value of more than 0.14, then it would attract, let's say, a 50% reduction in the municipal taxes for the first three years after commissioning.

iv) The evaluation of municipal taxes for the building would be linked to the rooftop PV generation from the building, via a smart meter which records the in-house rooftop PV generation. This linkage can then help decide penalties and waivers in the taxes, in accordance with the suitable cut-off values for rooftop PV generation, decided for each city/ region, for each financial year, by the MNRE or a competent representative thereof.

Similar guidelines can be formulated for different building sizes for each city, and the results can be integrated together in form of a lookup table for rooftop PV performance norms for a given location. The impetus for implementation of these norms can then be provided by making some minimum norms as mandatory and incentivizing the application of the higher norms.

CONCLUSION

The paper provides a framework for developing rooftop PV norms for Indian buildings, in the backdrop of the ambitious National Solar Mission. Sample values have been used to illustrate the framework for some simple cases. Linking this rooftop PV implementation and performance framework with financial incentives and penalties, via some standard mechanism, like municipal taxes for one, might help provide a significant boost to the sluggish growth of the rooftop PV segment in India.

REFERENCES

[1] Singh, R., Banerjee, R. 2015. Estimation of rooftop solar photovoltaic potential of a city. Solar Energy, 115, pp. 589-602.

[2] Scartezzini, J.L., Montavon, M., Compagnon, R., 2002. "Computer evaluation of the solar energy potential in an urban environment". Eurosun 2002 Conf.

[3] Montavon, M., Scartezzini, J.L., Compagnon, R., 2004. Solar energy utilisation potential of three different Swiss urban sites. Energie und Umweltforschung im Bauwesen, Zurich, pp. 503–510.

[4] Pillai, I.R., Banerjee, R., 2007. Methodology for estimation of potential for solar water heating in a target area. Sol. Energy 81 (2), pp.162–172.

[5] Izquierdo, S., Rodrigues, M., Fueyo, N., 2008. A method for estimating the geographical distribution of the available roof surface area for large-scale photovoltaic energy-potential evaluations. Sol. Energy 82 (10), pp.929–939.

[6] Ordo´n˜ ez, J., Jadraque, E., Alegre, J., Martı´nez, G., 2010. Analysis of the photovoltaic solar energy capacity

of residential rooftops in Andalusia (Spain). Renew. Sustain. Energy Rev. 14 (7), pp.2122–2130.

[7] Wiginton, L.K., Nguyen, H.T., Pearce, J.M., 2010. Quantifying rooftop solar photovoltaic potential for regional renewable energy policy. Comput. Environ. Urban Syst. 34 (4), pp.345–357.

[8] Bergamasco, L., Asinari, P., 2011. Scalable methodology for the photovoltaic solar energy potential assessment based on available roof surface area: application to Piedmont Region (Italy). Sol. Energy 85 (5), pp.1041–1055.

[9] Yue, C.D., Huang, G.R., 2011. An evaluation of domestic solar energy potential in Taiwan incorporating land use analysis. Energy Policy 39 (12), pp.7988–8002.

[10] Theodoridou, I., Karteris, M., Mallinis, G., Papadopoulos, A.M., Hegger, M., 2012. Assessment of retrofitting measures and solar systems' potential in urban areas using geographical information systems: application to a mediterranean city. Renew. Sustain. Energy Rev. 16 (8), pp.6239–6261.

[11] Karteris, M., Slini, T., Papadopoulos, A.M., 2013. Urban solar energy potential in Greece: a statistical calculation model of suitable built roof areas for photovoltaics. Energy Build. 62, pp.459–468.

[12] Greenpeace India, 2013. Rooftop Revolution: Unleashing Delhi's Solar Potential.

[13] Singh, R., Banerjee, R., 2016. Impact of Solar Panel Orientation on Large Scale Rooftop Solar Photovoltaic Scenario for Mumbai. Energy Procedia, 90, pp.401-411.

[14] Bhatt, M.S., Rajkumar, N., Jothibasu, S., Sudirkumar, R., Pandian, G. Nair, K.R.C., 2005. Commercial and residential building energy labeling. Journal of Scientific and Ind. Research, 64, pp. 30-34.

VALUE ADDITION OF KINNOW PROCESSING INDUSTRY BY-PRODUCTS USING GREEN SOLVENTS

Gisha Singla[1], Meena Krishania[1]*, Pankaj P. Sandhu[1], Rajender S. Sangwan[2], Parmjit S. Panesar[3]

1 Center of Innovative and Applied Bioprocessing (CIAB), Sector-81, S.A.S Nagar, Mohali, Punjab 140306, India
2 Academy of Scientific and Innovative Research (AcSIR), CSIR-Human Resource Development Centre, Sector 19, Ghaziabad, Uttar Pradesh 201 002, India
3 Food Biotechnology Research Laboratory, Department of Food Engineering & Technology, Sant Longowal Institute of Engineering & Technology Longowal 148106, Punjab

ABSTRACT

Processing of citrus fruits yields a significant amount of by-products as waste but bitterness of these by-products needs considerable attention. This study has been focused on debittering of kinnow juice industry by-products such as kinnow pulp residue and kinnow pomace by using green solvent method and the optimization of process parameters. In solventogenesis method, compounds responsible for bitterness such as naringin and limonin got solubilized in acetone with sample: solvent ratio 1:5 at ambient temperature for 3hr. However, naringin and limonin content in acetone treated kinnow pulp residue and pomace has been reduced considerably which indicates debittering of kinnow industry by-products. Therefore, these acetone treated kinnow pulp residue and pomace can be used as a raw material for development of different food products at commercial scale. This process is not only an effective utilization of agro-industrial by-product but also a solution to the environmental pollution caused by kinnow juice industry.

Keywords Kinnow pulp Residue, Kinnow Pomace, green solvents, solventogenesis, debittering compounds

INTRODUCTION

Kinnow is one of the major citrus fruit crops in northern region of India, especially in Punjab, Haryana, Rajasthan and Himachal Pradesh (Sharma et al. 2007). "Kinnow" is hybrid between king and willow mandarins (*Citrus nobilis Lour* × *C. deliciosa Tenore*). India ranks fourth in citrus fruit production. Its annual production in India is more than 1.0 MMT. Kinnow peel and pulp are the major by-products of the kinnow juice processing industry, which accounts for 55-60% of the fresh fruit weight (Kour et al. 2014), whereas around 30% of the produce of citrus fruits is processed to make juice. More than 40 million tons of industrial waste has been generated worldwide, residue content of citrus waste comprises almost 50% of whole fruit mass (Marin et al. 2007). Industrial processing of citrus fruits generated large amount of peel waste (19 Mt annually) which can be used as bio-refinery raw material (Bustamante et al. 2016). Dumping of byproducts of orange juice processing industry has created various disposal and environmental problems and also resulted in loss of nutrients as these peels were rich source of cellulose, pectin, hemicelluloses, lignin, essential oils and phenolic compounds (Hou et al. 2013).

Little research has been done on utilization of kinnow processing waste. Previous studies have been focused on extraction of pectin, flavonoids, carotenoids or ethanol from the waste and rest of the material left is again wasted (Baskar et al. 2018). The main drawback in utilization of the kinnow industy by-products is low shelf life as it deteriorates due to high moisture and sugar content, caused by the huge load of molds and yeast. The other formidable problems are its bitterness and delayed bitterness, thereby affecting its consumer acceptability. So in the present study, two-step method has been developed, which can be easily upgraded to industrial level economically. The investigation involves treating the kinnow juice processing industry residues with green solvents that will also help in enhancing the shelf life of pulp reisdue and pomace. Debittered edible pomace and pulp residue powder can be incorporated in various food products or can be used as such.

MATERIALS AND METHODS

Procurement of Raw Material

Kinnow pulp residue which has been obtained as waste during clarification of juice and kinnow pomace which contains peel, sac and seeds of kinnow, were procured from Punjab Agro Juices Limited Village Alamgarh, near Abohar, District Ferozepur (Punjab), India.

Physico-Chemical Characterization of Kinnow Juice Processing Waste (Pulp Residue and Pomace)

Physico-chemical study of kinnow juice industrial waste (pulp residue and pomace) was carried out for its different constituents/ nutritional and functional properties such as moisture (using moisture analyser, MA35, Saritorius), Protein (lowry et al. 1951), crude fat (Rosenthal et al. 1996). Pectin, crude fiber, total carbohydrates, total phenols and ash has been done according to standards of association of analytical communities (AOAC 2000).

Debittering of Kinnow Pulp Residue and Kinnow Pomace

Various green solvents such as acetone, hexane, ethanol and ethyl acetate have been employed for debittering of kinnow pulp residue and pomace.

Debittering by Solventogenesis of Kinnow Pulp Residue and Pomace

Kinnow juice industrial waste (pulp residue and pomace) was subjected to maceration technique as prescribed by Elfalleh et al. (2012) with minor modifications. Experiments were performed using different green solvents with the different ratios of sample: solvent (1:5, 1:10 and 1:15) at 25ºC. These solvent mixtures were homogenised for 1, 2, 3, 4 and 5 hr at 2000 rpm. Extracts were centrifuged (Eppendorf Centrifuge 5810 R) at 8000 rpm for 3 minutes at ambient temperature. Supernatant has been collected and the solvent was recovered using rotary evaporator (IKA, HB 10 Control) system under vacuum at temperature of 45ºC which was then stored for further reuse. Debittered residue obtained was air dried for overnight (12 hrs) and ground for further use.

Sensory Evaluation

Sensory analysis was performed according to Hou et al. (2013). The bitterness of each sample was determined by a panel of ten people. Before the sample was tasted, the mouth was fully rinsed with distilled water. The sample was tested in the mouth for 10 s, and the taste of each sample was averaged. Lyophilized pomace, which was bitter, has been used as the reference.

Quantification of bitterness causing Soluble Components

Compounds responsible for debittering were filtered through 0.45-µm membrane filter and then injected into Waters Acquit UPLC H-Class (WAT-176015007) (Milford, MA, USA) equipped with quaternary pump (Waters Quaternary Solvent Manager), injector (Waters Sample Manager-FTN (Flow Through Needle)), column compartment with Eclipse RP C18 column (150 × 4.6 mm; 5 µm), Waters 2998 PDA (Photodiode Array) detector and interfaced to mass detector (Waters TQ (Tandem Quadrupole, WAT-176001263). 0.1% orthophosphoric acid in water (v/v) (solvent A) and acetonitrile (solvent B) were used as mobile phase (Ignat et al. 2011). The temperature of column was kept at 30°C using a thermostat. The wavelength of detector scan range was set between 200 and 400 nm. Flow rate of 1ml/min has been induced for analysis having sample volume 20µl with UV detector set at 254 nm for phenolic acids.

RESULTS AND DISCUSSION

Physico-Chemical Characterization of Kinnow Pulp Residue and Pomace

Physico-chemical characterization of kinnow juice industry by-products (pulp residue and pomace) has been shown in Table 1. The major content is crude fiber in kinnow pulp residue and kinnow pomace was 16.94 and 17.85 mg/g after moisture 89.11% and 71.79 % respectively. This shows that it can use as fiber source as well.Total carbohydrates in kinnow pomace was 74.35 mg/g which was slightly higher than only kinnow pulp residue 73.84 mg/g and ash content in kinnow pulp residue was 0.50% and 0.61 % in kinnow pomace. Kinnow pomace is rich in minerals as compare to only pulp residue so its shows higher ash content Fallahi et al. (1985). Kinnow pomace includes peel and pulp residue, moreover peels are enriched with essential oils which have compounds with antimicrobial activity (food-info, 1999). The chemical composition of kinnow residues are in similar pattern as mentioned in previous literature (Kour et al. 2014).

Table 1 Chemical characterization of kinnow juice industrial waste on dry weight basis

Experiment	Kinnow pulp residue (%)	Kinnow pomace (%)
Moisture	89.11 ± 1.76	71.79 ± 1.57
Ash	0.50± 0.02	0.61 ± 0.05
Crude fat	4.2± 0.08	1.61 ± 0.71
Hemicellulose	1.01 ± 0.49	4.28 ± 1.65
Crude Fiber	16.94± 1.98	17.85 ± 2.94
Pectin	3.02± 1.43	5.42 ± 1.26
Protein	10.9± 1.03	12.02 ± 1.04

Debittering of kinnow pulp residue and pomace

Solventogenesis

Among various green solvents it was observed that the acetone was more effective to solubilize the bitterness causing phenols as mentioned in Fig.1. The kinnow pulp residue and pomace were solubilized 27% (w/w) and 30% (w/w) of initial dry biomass after acetone treatment. Insoluble fibers settled down at bottom which was recovered by filtration and the acetone mixture of kinnow pulp residue contains 331.25 mg/g sugars, 58.3 mg/g phenolic compounds, where as in kinnow pomace contains 427.75 mg/g sugars, 127.7 mg/g phenolic compounds. The pomace shows more phenolic compounds as it also contains peel. Peels have higher amount of bitterness causing compounds as compared with pulp residue because peels are outer coating of fruit, so they got more disposed to synthesis of phenolic compounds and narginin has been responsible for bitterness (Ignat et al. 2011).

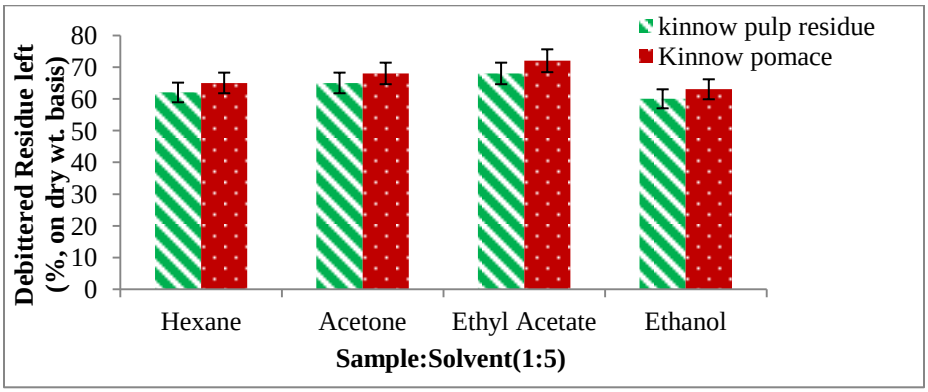

Fig. 1 Percentage of debittered antioxidant rich residue left after treatment with different food grade solvents

Marketability and consumer response depends upon sensory evaluation. Panelists analyzed it for appearance, taste color, aroma, body/texture, flavor, astringency and overall acceptability (Amerine et al. 1965). The original flavor of kinnow without bitterness was observed in acetone treated pulp (debittered, 5) and acetone treated pomace was also obtained (4) hedonic reading which was maximum among all the four solvents.. The acetone treated fibers are rich in antioxidants as majorly bitterness causing naringin, limonin and hesperidin were solubilized and remaining present in left residues (Fallahi and Moon, 1988).

It has been found that naringin and limonene compounds responsible for bitterness were in accordance to previous work (Kanaze et al. 2003) but due to influence of environment, climatic change, geographical area, method used for analysis, so variation in results have been found. It has been found that naringin, limonene and hesperidin, were present in 7.8, 5.497 and 31.22 mg/g of kinnow pulp residue extract after acetone treatment and 9.70, 17.14 and 41.21 mg/g of kinnow pomace extract respectively as shown in Table 2. So, the acetone treatment process was optimized. Higher quantity of hesperidin has been obtained by solvent extraction method of orange peel as compared with water extraction. According to Sharma et al. (2017) amount of hesperidin extracted from pre-treated and dried peels ranges between 3.7% and 4.5% respectively and it was 1.8% and 2.3% from fresh orange peels. Higher yield after solvent extraction was due to solubilisation of pectin.

Table 2 Analysis of extract obtained after solvent treatment of kinnow pulp residue and kinnow pomace.

Kinnow	**Debittering Process**	**Naringin (mg/g)**	**Limonin (mg/g)**	**Hesperidin (mg/g)**
Pulp residue	**Ethanol**	2.33	3.62	31.9
	Ethyl Acetate	1.88	4.44	4.28
	Acetone	7.88	5.97	31.22
	Hexane	0.43	3.01	2.41
Pomace	**Ethanol**	2.83	14.5	40.9
	Ethyl Acetate	2.38	15.39	13.46
	Acetone	9.7	17.14	40.21
	Hexane	3.33	12.34	11.82

Effect of Solvent Concentration on Extract Yield

The effect of solid-solvent ratio on maximum solubilisation of bitterness causing compounds has been shown in Fig. 2. Results showed that with increase in concentration of solvent their rate of extraction got increased and then equilibrium stage has been reached at 1:5 solid solvent ratio, when maximum extraction of bitterness causing compounds- naringin and hesperidin was observed with solvent treatment in pulp and pomace after time period of 3hr which were 20% and 23% respectively at sample to solvent ratio of 1:5. The extract yield was containing phenols and majorly naringin, limonin which are bitterness causing compounds in kinnow pulp residue and pomace.

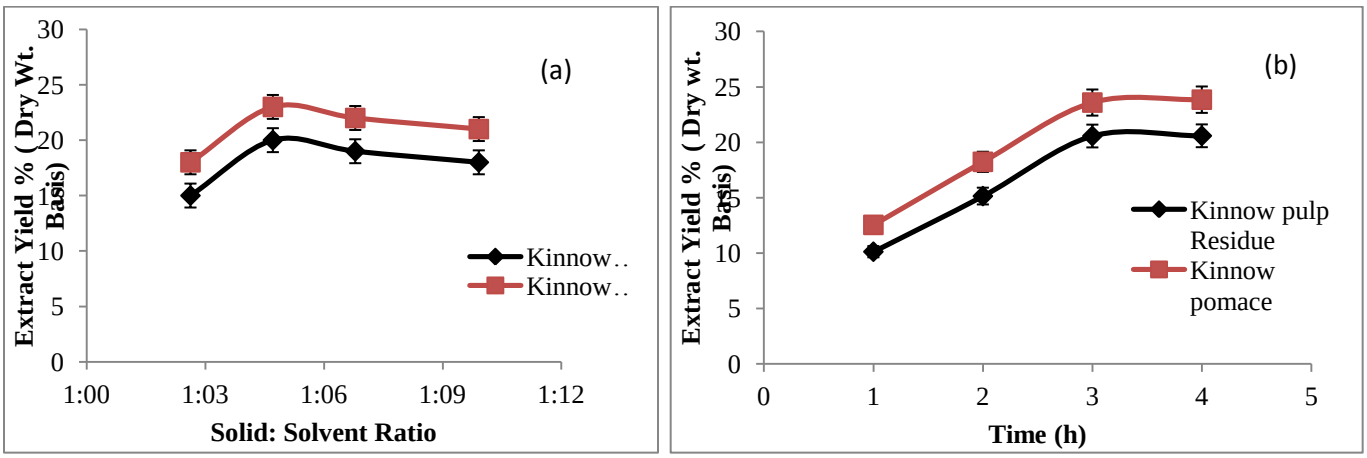

Fig. 2(a) Effect of solvent ratio on extract yield after acetone treatment at room temperature on kinnow industry by-products

2(b) Effect of time on extract yield after acetone treatment at different time intervals on kinnow industry by-products

Effect of Extraction Time

The effect of extraction time indicated that Fig. 2(b) that maximum extraction of soluble solids containing bittering compounds got extracted upto 3 hr after that there has been no significant increase in the naringin and hesperidin. This shows that the extraction process is sensitive to extraction time and solid-sample ratio (Pekic et al. 1998). It was observed from the data that after 3 hrs, soluble solids in case of kinnow pulp residue and pomace has been found to be 18% and 20% respectively. After 3 hrs no significant change in increase of soluble solids has been found both in case of pulp, pomace

Conclusion

The present study reveals that in the solventogenisis method, acetone treated pulp residue with hedonic scale 5 and acetone treated pomace with hedonic reading 4 has been maximum debittered. Fibers with no bitter taste and flavor have been obtained. It can be used as a raw material for food product development. The pulp residue and pomace can be useful in preparation of dietary fiber rich food product without any off flavor and bitterness. This process is not only an effective utilization of agro-industrial by-products/wastes but also a solution to the environmental pollution caused by kinnow juice industry.

Acknowledgement

Authors gratefully acknowledge the financial support given by SERB, DST under ECR project (ECR/2016/001237) for conducting this research and also grateful to Centre of Innovation and Applied Bioprocessing, Mohali for provisional support and facilities.

References

[1] Amerine, M.A., Pangborn R.M., Roessler E.B., 1965. “Principles of sensory evaluation of food”. Academic Press, Elsevier, London, UK. 602

[2] Association of Analytical Chemistry. 2000. “Official Methods of Analysis. Association of official Analytical Chemists”, 16thedn. Washington, USA

[3] Bustamante, J., Van Stempvoort, S., García-Gallarreta, M., Houghton, J.A., Briers, H. K., Budarin, V.L., Matharu,A.V., Clark, J.H., 2016. “Microwave assisted hydro-distillation of essential oils from wet citrus peel waste”, Journal of Cleaner Production, 137, pp. 598-605

[4] Elfalleh, W., Hannachi, H., Tlili, N., Yahia, Y., Nasri, N., Ferchichi, A., 2012. "Total phenolic contents and antioxidant activities of pomegranate peel, seed, leaf and flower", Journal of. Medicinal Plants Research, 6, 4724-30.

[5] Fallahi, E., Moon Jr. J.W., 1988. "Effects of Canopy Position on Quality, Photosynthesis and Mineral Nutrition of Four Citrus Varieties", Citrus Research *Report*. http://hdl.handle.net/10150/215697.

[6] Fallahi, E., Richardson, D.G., Westwood, M.N., Chaplin, M.H., 1985. "Relationships among mineral nutrition, ethylene, and postharvest physiology in apples on six root stocks". Scientia horticulturae., 25, 163-175.

[7] Food–info.net, 1999. Questions-Answers, Food products, fruits and Vegetables. Waheningen University. http://www.food-info.net/uk/qa/additives.htm.

[8] Hou, X., Chen, X., Cheng, Y., Xu, H., Chen, L., Yang, Y., 2013. "Dyeing and UV-protection properties of water extracts from orange peel". Journal of Cleaner Production, 52, pp. 410- 419

[9] Ignat, I., Volf, I., Popa, V. I., 2011. "A critical review of methods for characterization of polyphenolic in fruits and vegetables", Food Chemistry. 126, pp. 1821-1835.

[10] Kanaze, F.I., Gabrieli, C., Kokkalou, E., Georgarakis, M., Niopas, I., 2003. "Simultaneous reversed-phase high-performance liquid chromatographic method for the determination of diosmin, hesperidin and naringin in different citrus fruit juices and pharmaceutical formulations", Journal of Pharmaceutical and Biomedical Analysis, 33,pp. 243–9

[11] Kour, K., 2014. "Phenolic compounds and flavonoids from kinnow peel and their microbial activity", Thesis, Department of Chemistry, College of basic sciences and humanities Punjab Agricultural University, Ludhiana.

[12] Lowry, O.H., Rosenbrough, N.J., Farr, A., Randall, R. J., 1951. "Protein measurement with the Folin phenol reagent". Journal of Biological Chemistry, 193:265-75

[13] Marın, F.R., Soler-Rivas, C., Benavente-Garcıa, O., Castillo, J., Perez-Alvarez, J.A. 2007. "By-products from different citrus processes as a source of customized functional fibers". Food Chemistry, 100, pp 736–41

[14] Pekic, B., Kovac, V., Alonso, E., Revilla. E., 1998. "Study of the extraction of proanthocyanidins from grape seeds". Food Chemistry, 1/2(61), pp. 201-6

[15] Rosenthal, A., Pyle, D.L., Niranjan, K., 1996. "Aqueous and enzymatic processes for edible oil extraction". Enzyme *and* Microbial Technology. 19, pp. 402-420

[16] Sharma, K., Mahato, N., Cho, M.H., Lee, Y. R., 2017. "Converting citrus wastes into value-added products: Economic and environmently friendly approaches", Nutrition. 34, pp. 29–46

[17] Sharma, N., Kalra, K.L., Oberoi, H., Bansal, S., 2007. "Optimization of fermentation parameters for production of ethanol from kinnow waste and banana peels by simultaneous saccharification and fermentation", Indian Journal of Microbiology. 47(4), 310-6

Proceedings of theThird International Conference on Sustainable Energy and Environmental Challenges (3rd SEEC)
18 –21 December, 2018, IIT Roorkee, India

SEEC No. 035

EXPERIMENTAL ANALYSIS ON THE EFFECT OF HYDROGEN INDUCTION AND MANIFOLD INJECTION IN A DIESEL DUAL FUEL ENGINE

Saket Verma
Centre for Energy Studies, Indian Institute of Technology (IIT) Delhi, India
Email: saketverma@hotmail.com

K. Kumar
Centre for Energy Studies, Indian Institute of Technology (IIT) Delhi, India

L.M. Das
Centre for Energy Studies, Indian Institute of Technology (IIT) Delhi, India

S.C. Kaushik
Centre for Energy Studies, Indian Institute of Technology (IIT) Delhi, India

S.K. Tyagi
Centre for Energy Studies, Indian Institute of Technology (IIT) Delhi, India

ABSTRACT

An experimental investigation on dual fuel (DF) operation of a diesel engine with hydrogen as the main fuel and diesel as the pilot fuel has been performed. The focus has been made on gaseous fuel delivery system for performance enhancement during DF operations. Two techniques of hydrogen delivery namely, manifold port induction and manifold port injection are compared in the DF engine. In the case of manifold induction, the gas is introduced with the help of a gas mixture in the intake manifold, whereas in the case of manifold injection, the gas is introduced with the help of an injector. The injector is located close to the intake valve and its timing is controlled through an electronic control unit. It was found that hydrogen manifold injection improves the diesel substitution and thermal efficiency of the DF engine as compared to manifold induction technique. The diesel substitution was improved by 2.3% and 1.5% at low and high loads respectively. Similarly, the brake thermal efficiency was improved by 0.4% and 0.5% at low and high loads respectively.

***Keywords*:** Dual fuel, Diesel, Hydrogen, Injection, Induction

INTRODUCTION

The continuously increasing energy demand of the world has brought unprecedented situations of energy insecurity and environmental instability in the past couple of decades. It has been well understood that sole reliance on fossil sources is unsustainable and a prudent mix of renewable energy sources is indispensable. In this context, hydrogen is considered as the future fuel due to its unique properties and potential to zero emissions. However, utilization of hydrogen in internal combustion engines (ICEs) poses some technical challenges such as knocking, backfire and safety concerns. In addition to that the major issues with the use of renewable energy sources are their lack of availability and uncompetitive economics against the fossil based energy sources. These challenges can be effectively tackled for the near terms if the renewable fuels can be utilized in combination with the fossil fuels in the existing engines. In this context, dual fuel (DF) engine technology is an excellent option, which can utilize hydrogen as the gaseous fuel in the existing diesel engines. In the DF engines, small amount of pilot fuel (e.g. diesel) is required to initiate the combustion and bulk combustion

is achieved with the gaseous fuel. Utilization of hydrogen in the DF mode is constrained by excessive engine knock, backfire and high levels of NOx emissions. Mathur et al. [1] tried charge dilution as a possible technique to improve the performance. It was found that Helium was better able to control the engine knock, whereas, water showed highest level of improvement in diesel substitution. Saravanan and Nagarajan [2] studied hydrogen-air enrichment in DF engine and found that 90% hydrogen substitution showed highest efficiency, however resulted in knocking. It was reported that smooth operations were found with 30% hydrogen substitution and performance was also improved. The DF operation is also affected by the methodology of introducing the gaseous fuel in the engine. Chintala and Subramanian [3] found that there is a critical distance at which the gaseous fuel must be introduced to avoid fuel accumulation and backfire. Jemni et al. [4] studied the effect of intake manifold design using numerical simulation in a diesel engine converted to LPG gas fuelled. They found that the geometry of intake manifold plays vital role in fuel-air mixing and their distribution and ultimately affects the engine performance. Verma et al. [5] reported that in the DF mode, introduction of gaseous fuel in the intake manifold replaces air and hence lowers the volumetric efficiency. This effect is vital at higher engine loads, where rich fuel-air ratio exists and affects the combustion. Bedoya et al. [6] studied the effect of mixing system using simple 'T' shaped mixture and a specially designed supercharged and longer length of intake manifold in a biogas DF engine. It was found that specially designed mixture offered improved thermal efficiency and diesel substitution. In the spark ignition (SI) engine configuration, Das [7] examined various fuel induction techniques for hydrogen supply. It was found that the time manifold injection was the most suitable to counter undesirable combustion phenomena. Similar results with timed manifold injection were found with acetylene fumigated diesel DF engine reported by Lakshmanan and Nagarajan [8]. As the operation of a DF engine is significantly affected by the methodology of gaseous fuel induction, an experimental investigation is presented in this article to compare hydrogen port induction and hydrogen port injection techniques.

MATERIAL AND METHODS
LENGTH OF THE PAPER

The experiments were performed in a single cylinder, four-stroke diesel engine for which the specifications are given in Table 1. The conventional diesel engine was slightly modified to operate in DF mode with diesel and hydrogen as the pilot fuel and main fuel respectively. The pilot diesel fuel is supplied in conventional direct injection method with the help of a diesel injector. The gaseous fuel supply system consists of a high pressure hydrogen cylinder, pressure regulator, gas piping arrangement, safety devices and manifold gas mixture. In the case of hydrogen port induction, gas mixture is placed in the intake line near intake manifold. The gas is supplied from the high pressure cylinder, mixes with the incoming air and supplied to the engine. In the case of hydrogen port injection technique, a hydrogen injector is placed very near to intake valve and controlled by an electronic circuit and in-house computer code. The schematic diagram of the experimental setup is shown in Fig. 1.

TABLE 1: SPECIFICATION OF EXPERIMENTAL DIESEL ENGINE

Parameters	Technical specifications
Make & model	Kirloskar TAF1
Type	Single cylinder
Bore & stroke	87.5 × 110 mm
Swept volume	661 cm^3
Compression ratio	17.5:1
Rated brake power	6 bhp / 4.4 kW
Rated speed	1500 rpm

The engine was started with the conventional diesel injection and required engine load was applied to the engine. The engine was allowed to properly warm up before the gas supply was started and as a result, pilot fuel supply was automatically reduced to control the engine speed. The gas supply was increased to maximum limit which is defined as the maximum diesel substitution (DS) as following:

$$DS(\%) = \left[\frac{\dot{m}_{D,D} - \dot{m}_{D,DF}}{\dot{m}_{D,D}} \right] \times 100 \qquad (1)$$

where $\dot{m}_{D,D}$ and $\dot{m}_{D,DF}$ are the diesel fuel flow rates at diesel only (single fuel) and DF modes respectively. The experimental results are presented at two engine loads of low load that is BMEP of 1.16 bar and high load that is BMEP of 5.32 bar in this paper.

RESULTS AND DISCUSSION

The variation in diesel substitution with two different modes of hydrogen fuel supplies viz. port induction and port injection is shown in Fig. 2. It was found that the diesel substitution increased with hydrogen port injection as compared to port induction both at low and high loads. The diesel substitution was improved by 2.3% and 1.5% at low (BMEP of 1.16 bar) and high loads (BMEP of 5.32 bar) respectively. It is more important to achieve improvements in the diesel substitution at high loads with hydrogen as the main gaseous fuel. This is because very low diesel substitution was found at high loads as compared to low loads owing to server knocking. With

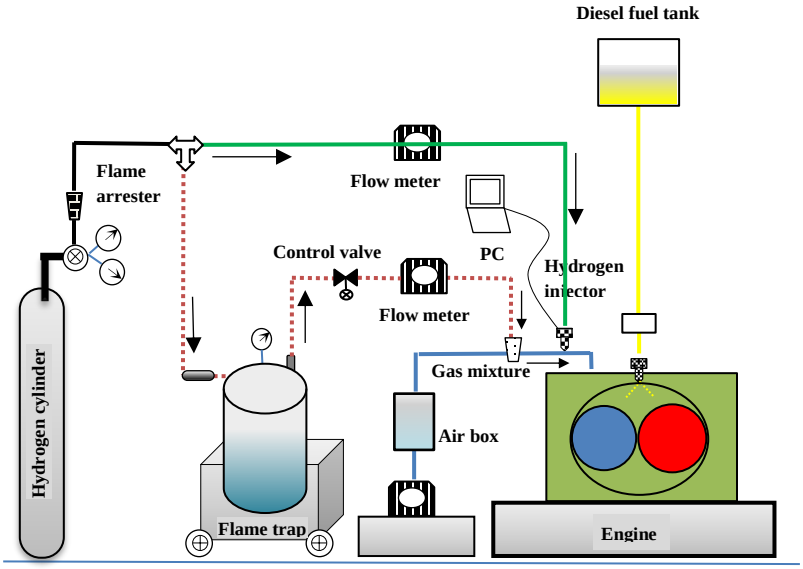

FIGURE 1: SCHEMATIC DIAGRAM OF THE EXPERIMENTAL SETUP

higher hydrogen addition at high load in DF mode, the combustion rate is significantly enhanced leading to engine knock. Another important reason for lower diesel substitution is decreased volumetric efficiency with hydrogen DF combustion and backfire. The addition of hydrogen in the intake manifold was found to cause frequent backfire, especially at high loads. Furthermore, hydrogen being significantly less dense than the air, replaces some amount of air and lowers the volumetric efficiency. The variation in volumetric efficiency with two different modes of hydrogen fuel supplies viz. port induction and port injection is shown in Fig. 3 for low and high loading conditions.

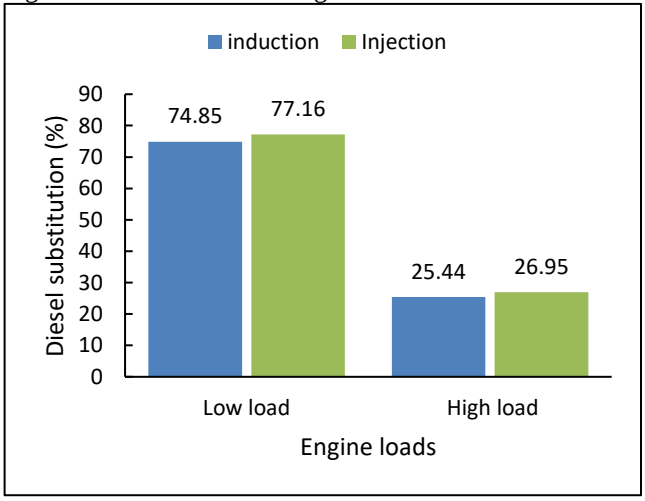

FIGURE 2. VARIATION IN THE DIESEL SUBSTITUTION WITH HYDROGEN PORT INDUCTION AND PORT INJECTION TECHNIQUES AT LOW AND HIGH LOADS

It is clearly evident that port injection technique improves the volumetric efficiency and helps in the better diesel substitution. The volumetric efficiency is increased as the hydrogen is discontinuously supplied and replaces lesser amount of air.

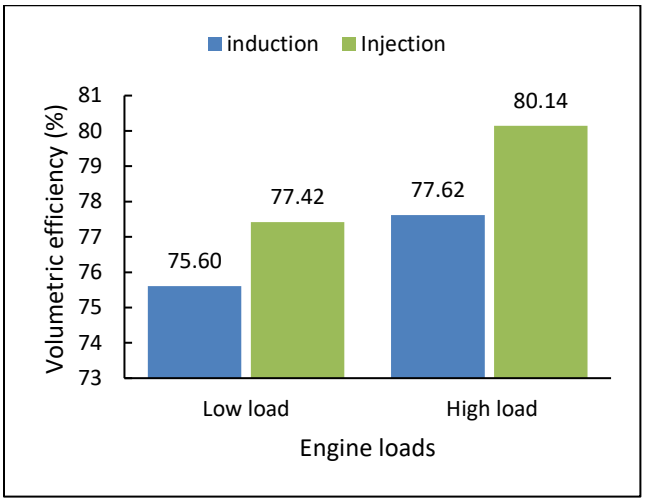

FIGURE 3. VARIATION IN THE VOLUMETRIC EFFICIENCY WITH HYDROGEN PORT INDUCTION AND PORT INJECTION TECHNIQUES AT LOW AND HIGH LOADS.

The effect of hydrogen fuel induction techniques (port induction and port injection) on engine brake thermal efficiency is shown in Fig. 4 for low and high loads. It was found that the brake thermal efficiency was improved by 0.4% and 0.5% at low and high loads respectively with hydrogen port injection technique. This could mainly be due to improvement in the diesel substitution with hydrogen port injection. The higher amount of gaseous fuel causes better homogeneity of the mixture formation. Furthermore, hydrogen has significantly higher flame speed than the diesel fuel which leads to much faster rate of energy release and improves combustion. As a result of these effects, the thermal efficiency of hydrogen port injection DF engine is improved as compared to port induction.

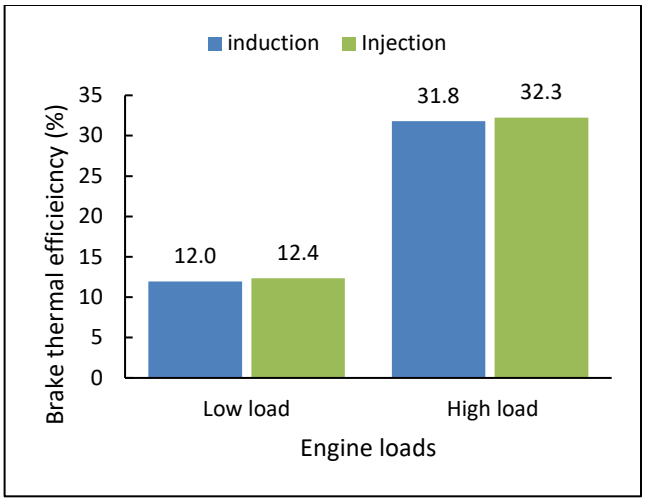

FIGURE 4. VARIATION IN THE BRAKE THERMAL EFFICIENCY WITH HYDROGEN PORT INDUCTION AND PORT INJECTION TECHNIQUES AT LOW AND HIGH LOADS.

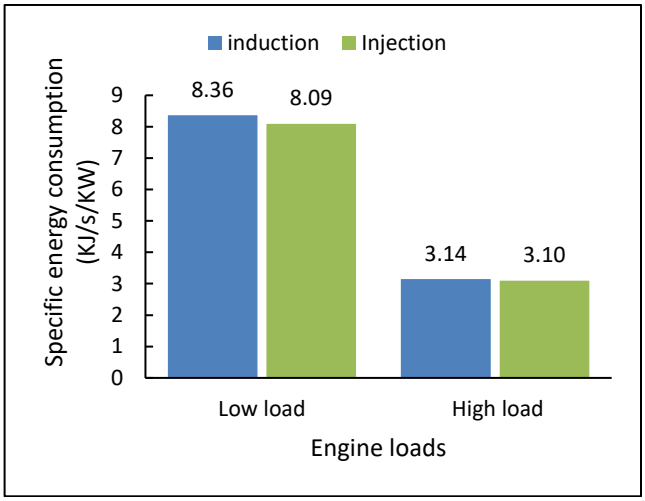

FIGURE 5. VARIATION IN THE SPECIFIC ENERGY CONSUMPTION WITH HYDROGEN PORT INDUCTION AND PORT INJECTION TECHNIQUES AT LOW AND HIGH LOADS.

The variation in specific energy consumption with hydrogen port induction and port injection strategies are shown in Fig. 5. It confirms that the combined (pilot fuel+main fuel) energy consumption from DF engine with hydrogen port injection is lower than the port induction strategy. The specific energy consumption was found higher with the lower load as compared to higher load. This is because of relatively leaner air-fuel mixture at low load, which lead to slower combustion and produces lower conversion efficiency. Whereas, at high load, rich air-fuel mixture produces high temperature combustion and lead to lower specific energy consumption.

CONCLUSIONS

An experimental investigation of diesel-hydrogen DF operation of diesel engine is presented with focus on strategies to supply the gaseous fuel. The comparison is made between hydrogen with hydrogen port induction and port injection techniques and results are presented at low and high loads. It was found that the hydrogen port injection technique provides improved diesel substitution and volumetric efficiency as compared to port induction technique. In addition to that it was also possible to better tackle the combustion anomaly of backfire with the port injection technique. As a result, improved brake thermal efficiency and better combustion can be achieved along with increased utilization of hydrogen at high load in DF engines.

ACKNOWLEDGMENTS

We would like to acknowledge the support of Council of Scientific & Industrial Research (CSIR), New Delhi, India. Research facility provided by Indian Institute of Technology Delhi (IITD) is also gratefully acknowledged.

REFERENCES

[1] Mathur HB, Das LM, Patro TN. Hydrogen-fuelled diesel engine: performance improvement through charge dilution techniques. International journal of hydrogen energy. 1993 May 1;18(5):421-31.

[2] Saravanan N, Nagarajan G. An experimental investigation of hydrogen-enriched air induction in a diesel engine system. International Journal of Hydrogen Energy. 2008 Mar 1;33(6):1769-75.

[3] Chintala V, Subramanian KA. A CFD (computational fluid dynamics) study for optimization of gas injector orientation for performance improvement of a dual-fuel diesel engine. Energy. 2013 Aug 1;57:709-21.

[4] Jemni MA, Kantchev G, Abid MS. Influence of intake manifold design on in-cylinder flow and engine performances in a bus diesel engine converted to LPG gas fuelled, using CFD analyses and experimental investigations. Energy. 2011 May 1;36(5):2701-15.

[5] Verma S, Das LM, Bhatti SS, Kaushik SC. A comparative exergetic performance and emission analysis of pilot diesel dual-fuel engine with biogas, CNG and hydrogen as main fuels. Energy Conversion and Management. 2017 Nov 1;151:764-77.

[6] Bedoya ID, Arrieta AA, Cadavid FJ. Effects of mixing system and pilot fuel quality on diesel–biogas dual fuel engine performance. Bioresource technology. 2009 Dec 1;100(24):6624-9.

[7] Das LM. Hydrogen engine: research and development (R&D) programmes in Indian Institute of Technology (IIT), Delhi. International Journal of Hydrogen Energy. 2002 Sep 1;27(9):953-65.

[8] Lakshmanan T, Nagarajan G. Experimental investigation of timed manifold injection of acetylene in direct injection diesel engine in dual fuel mode. Energy. 2010 Aug 1;35(8):3172-8.

Biotreatment of Acid Magenta Dye by Rice Husk : A Sustainable Tool for Agro-Waste Management

Dr. Riti Thapar Kapoor

Assistant Professor

Amity Institute of Biotechnology

Amity University, Noida - 201 313, India

E.mail: rkapoor@amity.edu

Abstract

The present paper deals with the effect of activated rice husk on removal of acid magenta dye from aqueous solution under different experimental conditions such as pH, exposure time and different amount of adsorbent. The activated rice husk showed better response in comparison to untreated rice husk. Maximum colour removal of acid magenta dye (94 %) was observed after 120 minutes at pH 6.2 with 2 g of activated rice husk. The results revealed that activated rice husk can be used as low cost and effective adsorbent for the removal of acid magenta dye from aqueous solution.

Keywords: Acid Magenta, Biosorption, Rice husk, Waste management.

Introduction

Water pollution from textile effluent is a serious concern that adversely affect environment and economic growth of nation. Wastewater discharged from textile industries is often not treated properly before discharge into the water bodies [4, 5, 15]. The disposal of untreated textile effluent into the environment is harmful not only to the aquatic system but also to the biodiversity [1]. Textile effluent is often intense in colour with high COD and BOD, heavy metals, dye and suspended solids [10]. Approximately 7×10^5 tonnes of dyes are produced annually worldwide [14].

Dyes are toxic to aquatic flora and fauna due to the presence of aromatic compounds, chlorides and metals etc [8]. Earlier workers have utilized various techniques for dye removal from industrial effluent such as chemical coagulation, ozonation, ion exchange, oxidation process, reverse osmosis and ultra-filtration etc [2]. The drawbacks related with all the above mentioned techniques is the high cost of application, energy requirement, complex process and generation of sludge which causes secondary pollution [13]. The commercially available activated carbon is also used as adsorbent for dye removal but it is very expensive [9]. Some workers have utilized agricultural wastes such as wheat straw, corn and maize cob, pinewood and sawdust for dye removal [12]. The adsorption process has an edge over the other methods as it is feasible, efficient, affordable, economically viable and sludge free clean operation for complete removal of dye from textile effluent [9].

Rice (*Oryza sativa* L.; family - Poaceae) is the most widely consumed staple food for large part of the world's population. Rice husk is an undesirable agricultural waste which is byproduct of rice milling industry and abundantly available in most of the parts of the world. In India, 20 million tonnes of rice husk are produced annually [3]. Rice husk is insoluble material with high mechanical strength and it contains cellulose, hemicellulose, lignin and silica etc. The burning of rice husk generates toxic gases which may cause health related problems such as asthma and bronchitis in human-beings. Studies have reported that rice husk acts as an adsorbent for removal of reactive blue 2, reactive orange 16, methylene blue and reactive yellow 15 dye [7]. Rice husk was also used for the treatment of dairy wastewater [11]. No study has been done till date to study the effect of rice husk on removal of acid magenta dye. In the present study, rice husk was selected as an adsorbent material for removal of acid magenta dye due to its availability, low cost and removal efficiency. Hence, present investigation was conducted to study the adsorption capacity of rice husk for removal of acid magenta dye from aqueous solution and its suitability as an adsorbent material.

Materials and methods

The experiments were conducted in Plant Physiology Laboratory, Amity Institute of Biotechnology, Amity University, Noida.

Preparation of activated rice husk

Rice husk was collected from rice mill located at Gautam Budh Nagar district of Uttar Pradesh. Rice husk was washed with tap water then three times with distilled water to remove dust and dried in shade for 48 hours. The dried rice husk was powdered in grinder and sieved to 30 - 40 mesh size and it was kept in hot air oven at 105^0C for 12 hours. Rice husk powder was separated into two parts to prepare modified rice husk adsorbent: (a). rice husk powder was pre-treated with distilled water several times until the pH of washed water become 6 - 7 (b). rice husk powder was pre-treated with 10% NaOH solution for 12 hours, after that washed with distilled water several times until the pH of washed water become 6 - 7. The modified rice husk adsorbent was dried again in hot air oven at 110^0C for 24 hours. The modified adsorbents were stored in sealed desiccator and designated as untreated rice husk (URH) and activated rice husk (ARH) which were used for further experiments.

Procurement of dye

Triarylmethane dye [Acid magenta (Acid Voilet 19)], [Molecular formula: $C_{20}H_{17}N_3Na_2O_9S_3$; molecular weight: 585.54 g/mol] is an anionic dye was obtained from a dye supplier company of New Delhi.

Dye adsorption experiment

Batch experiments were conducted to study the effect of different parameters i.e. pH, exposure time and amount of adsorbent (untreated and activated rice husk) for the removal of acid magenta dye from aqueous solution. A solution of acid magenta dye (100 PPM) was prepared by using distilled water and pH was measured. An aliquot of 100 ml of acid magenta dye solution was treated with different amount of untreated and activated rice husk such as 0.5 g, 1 g, 1.5 g and 2 g at different pH (5.7, 6.2 and 7.1) and exposure period such as 60, 90, 120 and 150 minutes respectively. The absorbance was measured at 527 nm by using spectrophotometer.

The removal percentage of acid magenta dye was estimated by using the following formula:

Removal efficiency (%) = (Co - Ce/Co) x 100
Where Co = initial concentration of dye (mg/l)
Ce = final concentration of dye (mg/l)

Results and Discussion

The effect of rice husk (untreated and activated) on the removal of acid magenta dye was analyzed at different pH, exposure time and with different amount of adsorbent. Rice husk untreated and activated was used as adsorbent in the present study. The different amount of untreated and activated rice husk (0.5g, 1g, 1.5g and 2g) was taken in the experiment to evaluate their adsorption capacity for the adsorption of acid magenta dye. The increase in rate of adsorption of acid magenta dye was observed with increase in the adsorbent amount and exposure time (Figure - 1, 2 and 3).

The results of the present study indicated that activated rice husk was more effective in removal of acid magenta dye from aqueous solution in comparison to untreated rice husk. It may be due to increased surface area and availability of more adsorption sites on the activated rice husk. The increase in adsorption capacity of activated rice husk showed the following trend: 2g > 1.5g > 1g > 0.5 g.

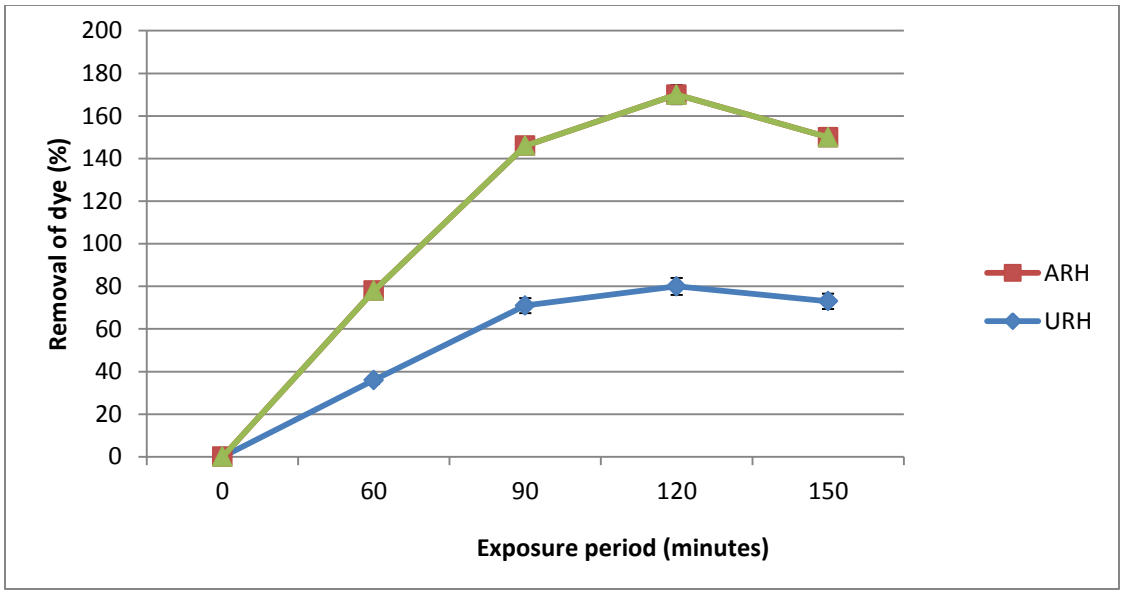

Figure 1. Removal of acid magenta dye by rice husk (2g) at pH 5.7 with different exposure period (URH = Untreated rice husk; ARH = Activated rice husk).

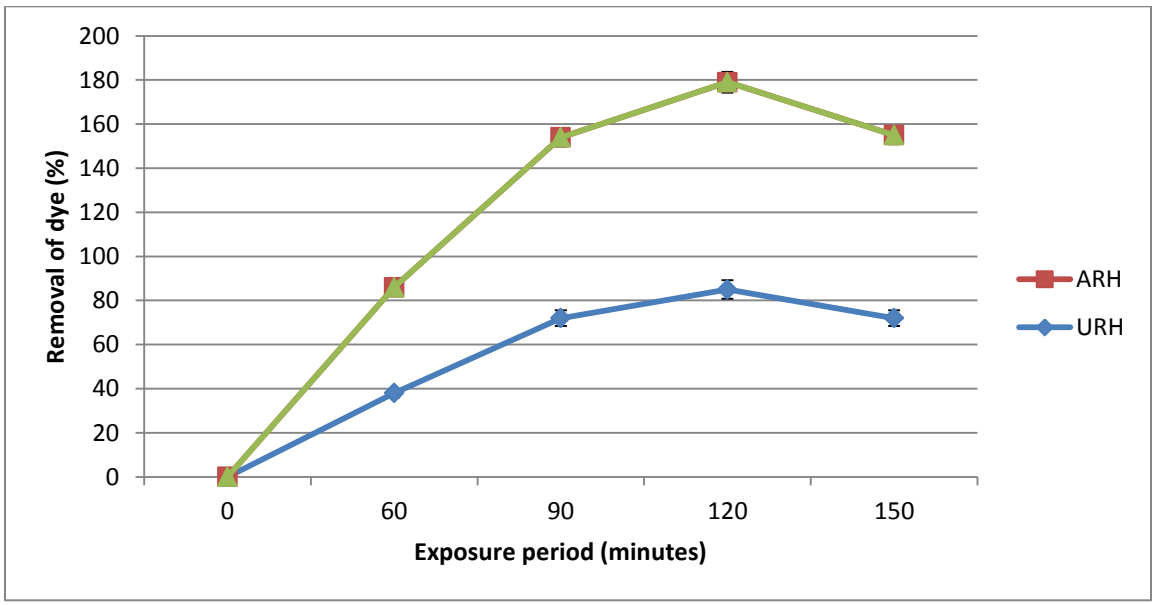

Figure 2. Removal of acid magenta dye by rice husk (2g) at pH 6.2 with different exposure period (URH = Untreated rice husk; ARH = Activated rice husk).

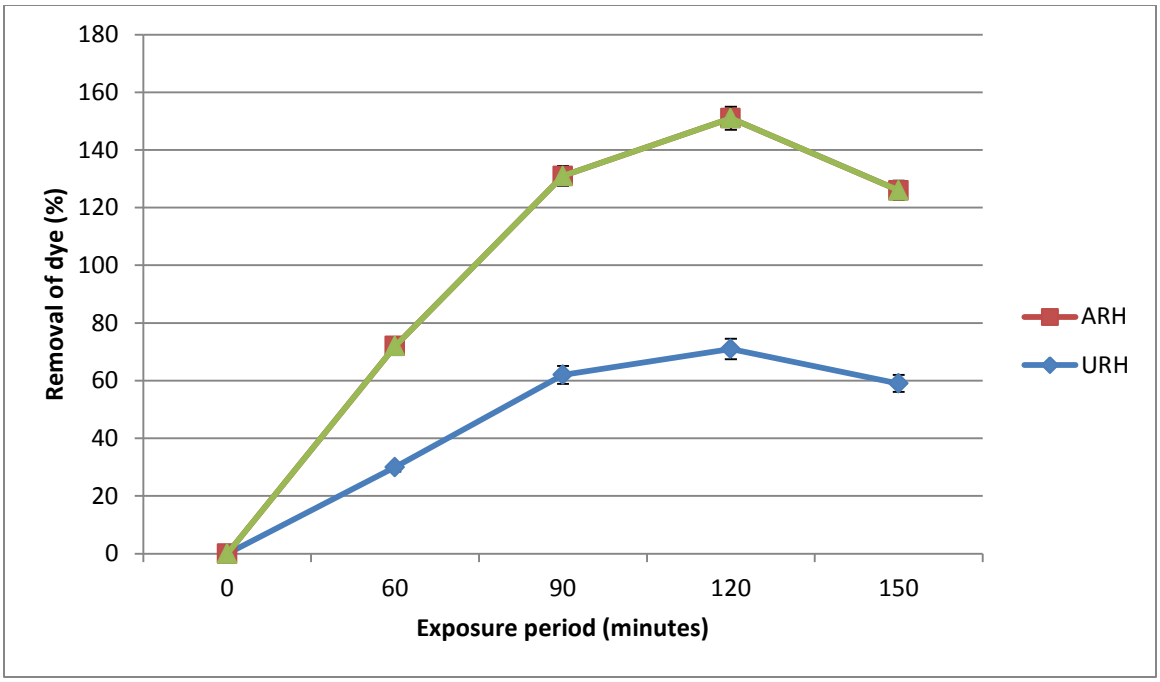

Figure 3. Removal of acid magenta dye by rice husk (2g) at pH 7.1 with different exposure period (URH = Untreated rice husk; ARH = Activated rice husk).

It was observed that after 120 minutes of exposure period, 80 and 90% acid magenta dye was removed at pH 5.7 whereas 71 and 80% dye removal was observed at pH 7.1 with untreated and activated rice husk respectively (Figure - 1 and 3). Maximum 85 and 94% removal of acid magenta dye was observed with untreated and activated rice husk respectively at pH 6.2 after 120 minutes of exposure period (Figure - 2). Treatment of rice husk with sodium hydroxide significantly increased the surface area and negative charges on the surface of rice husk. Activated rice husk showed significant increase in acid magenta dye adsorption efficiency in comparison to untreated rice husk [6]. The findings of the present investigation may lead to the development of economically feasible and eco-friendly alternative for dye removal from textile effluent.

Conclusion

The present study revealed that the treatment of acid magenta dye by using activated rice husk is a simple, low cost and eco-friendly technology as it has significant potential of reducing colour. The present study may be useful in fabrication of economically viable treatment system by utilization of activated rice husk for the removal of acid magenta dye from textile effluent.

Acknowledgement

The author is thankful to Dr. Chanderdeep Tandon, Director, Amity Institute of Biotechnology, Amity University, Noida for providing laboratory facilities to carry out this study.

References

1. Aksu Z, Eyda S, Gatay A and Onen F (2007). Continuous fixed bed biosorption of reactive dyes by dried *Rhizopus arrhizus*: determination of column capacity. Journal of Hazardous Materials. 143: 362-371.
2. Deniz F and Karaman S (2011). Removal of Basic Red 46 dye from aqueous solution by pine tree leaves. Chemical Engineering Journal. 170: 67-74.
3. GiddeMilind R, Dutta J and Jadhav S (2009). Comparative adsorption studies on activated rice husk and rice husk ash by using methylene blue as dye. International Congress on Environmental Research at BITS Pilani, Goa. 8: 1- 11.
4. Gumel SM, Usman MT and Ado A (2015). Colouration industry wastewater treatments in Nigeria–hazard and treatment: a review. International Journal of Chemical and Biomolecular Science. 1(2): 27-33.
5. Gupta VK, Khamparia S, Tyagi I, Jaspal D and Malviya A (2015). Decolourization of mixture of dyes: A critical review. Global Journal of Environment Science and Management. 1 (1): 71-94.
6. Janthai K, Warodomrungsimun C and Singhakant C (2017). Decolourization of basic and direct dyes by adsorption on chemically modified rice husk. Journal of Thai Interdisciplinary Research. 12(1): 35-42.

7. Khan T, Chaudhuri M, Isa MH and Hamid AZBA (2013). Use of incinerated rice husk for adsorption of reactive dye from aqueous solution. International Journal of Energy Technology and Policy. 3 (11): 234-239.

8. Li WH, Yue QY, Gao BY, Ma ZH, Li YJ and Zhao HX (2011). Preparation and utilization of sludge-based activated carbon for the adsorption of dyes from aqueous solutions. Chemical Engineering Journal. 171: 320-327.

9. Marzouk I, Chaabane L, Dammak L and Hamrouni B (2013). Application of donnan dialysis coupled to adsorption onto activated alumina for chromium (VI) removal. American Journal of Analytical Chemistry. (4): 420-425.

10. Olaoye RA, Oladeji OS, Olaniyan OS and Salami M O (2018). Remediation of textile wastewater using activated rice husk. IOSR Journal of Engineering. 8(6): 8 - 15.
11. Pathak U, Das P, Banerjee P and Datta S (2016). Treatment of wastewater from a dairy industry using rice husk as adsorbent: treatment efficiency, isotherm, thermodynamics and kinetics modelling. Journal of Thermodynamics. pp. 1 - 7.
12. Pekkuz H, Uzun I and Güzel F (2008). Kinetics and thermodynamics of the adsorption of some dyestuffs from aqueous solution by poplar sawdust. Bioresource Technology. 99: 2009-2017.
13. Ramya M, Anusha B, Kalavathy S and Devilaksmi S (2007). Biodecolourization and biodegradation of reactive blue by *Aspergillus* sp. African Journal of Biotechnology. 6:1441-1445.
14. Saravanan R, Sacari E, Gracia F, Khan MM, Mosquera E and Gupta VK (2016). Conducting PANI stimulated ZnO system for visible light photocatalytic degradation of coloured dyes. Journal of Molecular Liquids. 221: 1029-1033.
15. Senthilkumar S, Perumalsamy M and Prabhuet HJ (2011). Decolourization potential of white-rot fungus *Phanerochaete chrysosporium* on synthetic dye bath effluent containing Amido black 10B. Journal of Saudi Chemical Society.30:1-9.

Proceedings of International Conference on Sustainable Energy and Environmental Challenges (3rd SEEC), December 18-21, 2018, IIT Roorkee, India

SEEC No.041

BULK UTILISATION OF FLY ASH IN MINING

R.S KRISHNA

GOVERNMENT COLLEGE OF ENGINEERING KEONJHAR, MECHANICAL STUDENT
krishnaskull@gmail.com

Abstract

Indian coal is high in ash content and low in calorific value which signifies that for generation of energy, thermal power plants consume more coal and generate more fly ash as compared to the other countries. Problems related with Fly ash are land required for disposal and air pollution. Coal based Power Generation has been the backbone of any developing country. Thus, a large amount of ash is being generated by the coal based TPPs. Fly ash can prove to be an environmental hazard if not disposed properly. Fly ash is one , which has been treated as a waste material, in India, some years ago and has now emerged not only as a resource material but also as an environment saviour. This paper present details about Fly ash & its bulk utilization in mining sectors of India.

Keywords:- ESP, PCC, TPP, Pozzolanic, Cementitious

NOMENCLATURE:

%	Percentage
µm	Micrometre
ASTM	American Society for Testing and Materials
ha	Hectare
m	Metre
MW	Megawatt

Proceedings of the Third International Conference on Sustainable Energy and Environmental Challenges (3rd SEEC), 18 –21 December, 2018, IIT Roorkee, India

SEEC No.042

INDOOR POTTED PLANT BASED BIOFILTER: PERFORMANCE EVALUATION AND KINETICS STUDY

Anugunj Pal[a], Asmita Sarowgi[a], Sangeeta Kumari[a], Yeshaswi Kaushik[b], Abhishek Jaiswal[c], V Thivaharan[d], B. S. Giri[c*], R. S. Singh[c*]

[a]Department of Botany, Institute of Science, Banaras Hindu University, Varanasi 221005, Uttar Pradesh , India
[b]Department of Biotechnology, Thapar Institute of Engineering and Technology, Patiala, Punjab 147004, India.
[c]Department of Chemical Engineering and Technology, IIT(BHU), Varanasi 221005, UP (East), India.
[d]Department of Biotechnology, Manipal Institute of Technology, Manipal Academy of Higher Education, Manipal-576 104, Karnataka, India

*Corresponding author: Dr. Balendu Shekher Giri; Professor R.S. Singh
Department of Chemical Engineering, IIT (BHU), Varanasi 221005, India; (balendushekhergiri23@gmail.com; rssingh.che@iitbhu.ac.in)

Abstract

Recently, plant-based Bio filters associated with microorganisms have gained popularity in controlling odorous compounds like VOCs as they are cost-effective and an environment-friendly alternative to conventional air pollution control techniques. Attempting the same, the main objective of this work was to evaluate the performance of potted plants based Clairy biofilter for the biodegradation of benzene. A sealed Perspex chamber with lid and fan was designed to ensure minimum leakage, proper aeration and distribution of benzene inside the chamber. Five different ornamental indoor plants were placed inside the chamber sequentially and exposed to a concentration of 5 PPM benzene for 30 hours each. The leakage of benzene was checked beforehand. It was found out that Epipremnum aureum (Money plant) showed the maximum benzene degradation in the aforementioned time period with a removal efficiency of 98%. The µmax and Ks values for 100 PPM concentration of benzene were calculated to be 0.284 h^{-1} and 0.427 g/m^3 respectively.

Keywords: Plant-based Clairy biofilter; VOCs; Removal efficiency; Minimal salt media (MSM)

Introduction

In contrast to the lifestyle of our predecessors, the current generation is facing a major crisis in the form of environmental pollution. Owing to population explosion, rapid industrialization, urbanization, commercialization and other human activities for a luxurious lifestyle, the quality of water we drink the air we breathe and the land we live on has deteriorated significantly. As compared to outdoor air pollutants, the risk of exposure to indoor pollutants is much higher. This level of pollutants has proved to be hazardous to our health due to the amount of time spent indoors like offices, residential buildings etc. Thus, it is of utmost importance to understand the role of clean air and adopt different techniques to purify the air around us.

One such indoor air pollutant is Volatile Organic Compounds (VOCs). The high vapor pressure at ordinary room temperature is due to a low boiling point as a result of which the phenomenon of volatility takes place. For example, the boiling point of formaldehyde is only –19 °C (–2 °F). The association of poor indoor air quality and these anthropogenic pollutants is relatively high. The sources of VOCs range from pesticides, gasoline, perfumes, paints etc. The presence of acetone, acetaldehyde, methanol and other aldehydes has been reported as a result of metabolism in humans. A sub-group of VOCs include mono-aromatic hydrocarbons called BTEX (Benzene, toluene, Ethylbenzene and xylene) containing one substituted or methyl-substituted benzene ring. They can be found in the environment due to emissions from motor vehicles and aircraft exhaust, fuel operations, refineries, gasoline stations, and gasification sites. Introduction into water can be due to industrial effluents and atmospheric pollution, spills of petrol and petroleum products or proximity to natural deposits of petroleum and natural gas. In the air surrounding areas with a high traffic density, the concentrations for BTEX are up-to 349, 1310, 360 and 775 µg/m^3 respectively. As compared to air, the concentration of BTEX in water is comparatively lower. The health risks involved are drowsiness, dizziness, rapid heart rate, headaches, tremors, confusion, and unconsciousness. Cancer of blood-forming organs (leukemia) can be a result of long-term exposure to benzene. Other health hazards associated with benzene are vomiting, irritation of the stomach, dizziness, sleepiness, convulsions, rapid heart rate, coma, and sometimes death (ATSDR 2007a). Toluene

mainly affects the brain and nervous system which can be evident from symptoms such as fatigue and drowsiness (ATSDR 2000). Similarly, exposure to ethylbenzene causes enlargement of liver and kidney (IPCS 1996) and xylene can cause damages to the nervous system like lack of muscle coordination, dizziness and confusion (ATSDR 2007c, IPCS 1997). The harmful effects of BTEX have been reported in aquatic organisms too. Thus, due to this toxic nature of BTEX and VOCs to human health, it is of utmost importance to purify the air around us. Different types of bioreactors can be employed for the treatment of VOCs. The criteria for selection depend on loading capacity, physical and chemical properties of the target molecules along with the design, configuration, operational parameters of the bioreactor etc. [1]. Examples of various bioreactors along with their advantages and disadvantages are mentioned in table 2. Owing to its low cost and lack of secondary pollutant production, bio filtration is an attractive air treatment technology for the degradation of VOCs. Our experiments demonstrate that bio filtration using a potted-plant based Clairy's filter is a viable treatment technology for removing and degrading VOCs. Indoor plants play an important role in the removal of VOC. The root zone of plant is very effective for removal of VOC and under controlled conditions.

In this study, potted plants are the simplest and most economical choice for indoor air purification, although they remove pollutants at a slower rate. If passive potted plant systems are designed to exhibit greater VOC removal rates, then their benefits will be experienced from people inhabiting locations with poor electricity access.

METHODOLOGY

Experimental setup:

Firstly, to check the leakage of benzene, 0.9 µl of 5 PPM benzene was added in the perplex chamber and was sealed for a period of 30 hours to check the decrease in the benzene concentration. After the leakage was checked, a potted plant was placed on aluminium support in the centre and same concentration of benzene was added in the chamber. The fan was switched on and other conditions like temperature and moisture content was regulated as per the needs of the plant. The set-up was kept for 30 hrs and the decrease in benzene concentration was noted after every 2 hours using a sensor. The experiment was repeated for all the 5 plants for the same aforementioned time period to do a comparative study. The removal efficiency for each plant was calculated as follows:

$$\textit{Removal Efficiency (\%)} = (Cin - Cout)/Cin \times 100$$

Where: Cin and Cout are the concentrations of Benzene at inlet and outlet respectively.

Isolation, enrichment, and biochemical test for bacterial isolates:

From the soil of each of the plant before and after exposure to VOC, bacteria was isolated for obtaining the total no of bacteria present vs. the no of bacteria capable to degrading benzene. For this, the soil samples were collected and diluted up to 10-6 dilution. 100 µl of 10-4 and 10-5 dilutions were spread on NA plates using a L-shaped spreader. The plates were kept for overnight incubation (35°C). The total number of colonies was counted in CFU/ml using the following formula:

$$CFU/ml = (\text{Number of bacteria} \times \text{Dilution factor})/(\text{Volume of culture spread on the plate})$$

Few colonies were picked up and streaked on MSM plates following which 1 ml of 100 PPM benzene was spread on top of the streaked plates and kept at 35°C for incubation. The colonies which appeared on the MSM plates after a few days were specific for benzene and could utilise benzene as a carbon source. Streaking of the obtained colonies was done on NA plates for storage purpose and further use.

PCR Amplification:

The extracted bacterial genomic DNA was subjected to PCR amplification of 16SrRNA gene with universal primers. The amplifications were carried out in a thermocycler (Bio-Rad Laboratories, Inc, Australia). The reaction mixture was prepared in a final volume of 50 µL containing tris-HCl, MgCl2, dNTPs, Taq DNA polymerase, and universal primer and DNA template.

AGAROSE GEL ELECROPHORESIS:

Agarose gel electrophoresis is used to separate mixtures of DNA fragments on the basis of molecular weight and sizes. 1% agarose gel (made in TAE buffer) was used to resolve DNA fragments. Ethidium Bromide (EtBr), the DNA intercalating dye, was added to the gel before casting to visualize the DNA fragments. The solidified gel was then loaded with DNA samples containing gel loading dye and ran in 0.5% TAE buffer at 90 volt. The gel was finally visualised under UV-transilluminator. The microorganism was grown as pure culture and further sent for molecular characterisation.

GROWTH CURVE OF BACTERIA:

A growth curve of the benzene degrading bacteria was prepared by inoculating 200 ml of MSM broth with a loopful of culture and adding 100 PPM benzene. The OD value was taken after every 2.5 hours. A similar

growth curve was prepared by adding 150 PPM of benzene. A control was also made in which benzene was not added. The amount of substrate (Benzene) degradation with respect to the growth of bacteria was also noted. The growth curve obtained is used for calculating the values of μmax and Ks using the Monod kinetics.

RESULTS

PERFORMANCE EVALUATION:

A comparative study of all the 5 plants was done to check the removal efficiency of each plant. Our experiments showed that Epipremnum aureum showed the highest removal efficiency of 98% in 30 hours. The graph showing the rate of benzene degradation is and the performance evaluation of each plant is shown in Figure 1 and 2.

BACTERIAL ISOLATION AND NUMBER:

In case of Spider plant, the bacterial number present in the soil decreased from 2.08x106 CFU/mL to 3.88x104 CFU/mL before and after the plant was exposed to benzene respectively. The molecular characterisation results showed Bacillus sp. For PCR and PAGE, the amplified DNA was analysed in a UV-trans illuminator after gel running. The image of the amplified DNA is shown in the figure below.

GROWTH CURVE:

The growth curve obtained for the bacteria for concentrations of 100 PPM and 150 PPM respectively has been studied and results shows the curve for control in which substrate is not added. The μmax and Ks values for 100 PPM concentration of benzene were calculated using the Monod equation s and O.D. values obtained for the growth curve and was found to be 0.284 h-1 and 0.427 g/m^3 respectively.

OPTIMISATION OF GROWTH CONDITIONS:

From the graph below, it was evident that the optimum temperature for the growth of bacteria is 35° C. pH- The optimum pH for growth of the organism is 7. INHIBITION- At a benzene concentration of 400 PPM, the growth of the bacteria is inhibited.

CONCLUSION AND DISCUSSION

It is the need of the hour to formulate effective techniques to reduce air pollution owing to its association with both morbidity and mortality. VOC is one of the pollutants which have to be degraded to breathe healthy pollutant-free air. VOCs can found to be degraded using a lot of techniques both chemical and biological. The biological method of VOC degradation using microorganisms can be used to obtain a cost-effective and environment-friendly technique over traditional chemical technologies. A potted-plant (ornamental plant) based Claire's biofilter has been developed which can be used to degrade VOC. The efficiency of VOC degradation depends on a lot of factors like the leaf's surface area, physico-chemical properties of the VOC present, moisture conditions and many more. The microorganisms present in soil can utilise them as a substrate for metabolism. It is essential to develop techniques to increase the rate of VOC biodegradation so that it can be both economical and efficient. From our experiment using benzene, results showed that out of the 5 plants used, Money plant showed the maximum removal efficiency of 98%. 5 PPM of benzene was degraded at a higher rate by this plant as compared to others. Optimum temperature, pH and moisture conditions need to be maintained to ensure maximum growth of VOC-degrading organisms. Studies with potted plants in closed chambers continue to be useful for isolating factors that may enhance removal efficiency and therefore contribute towards the improvement of plant-based systems. Plants and their associated microorganisms have been proved to highly important for the bettering of indoor air quality and therefore further research on such strategies becomes a necessity.

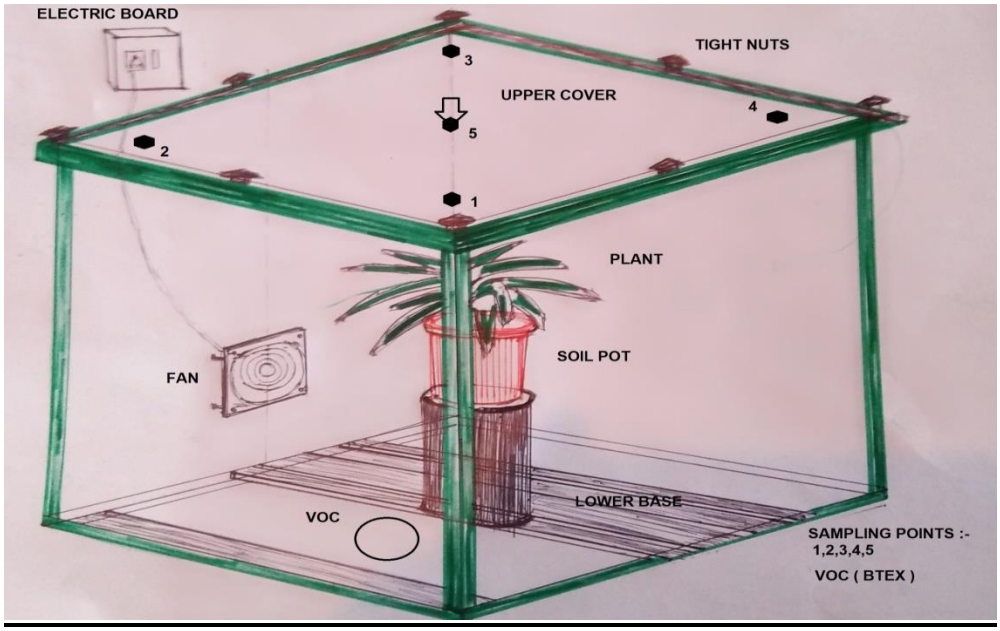

Figure 1: Sealed perspex chamber covered with a lid using nuts and bolts with a fan attached to one side of the chamber to ensure equal distribution of all components present in the air inside and sampling points for noting down the concentration of VOC at a given point of time.

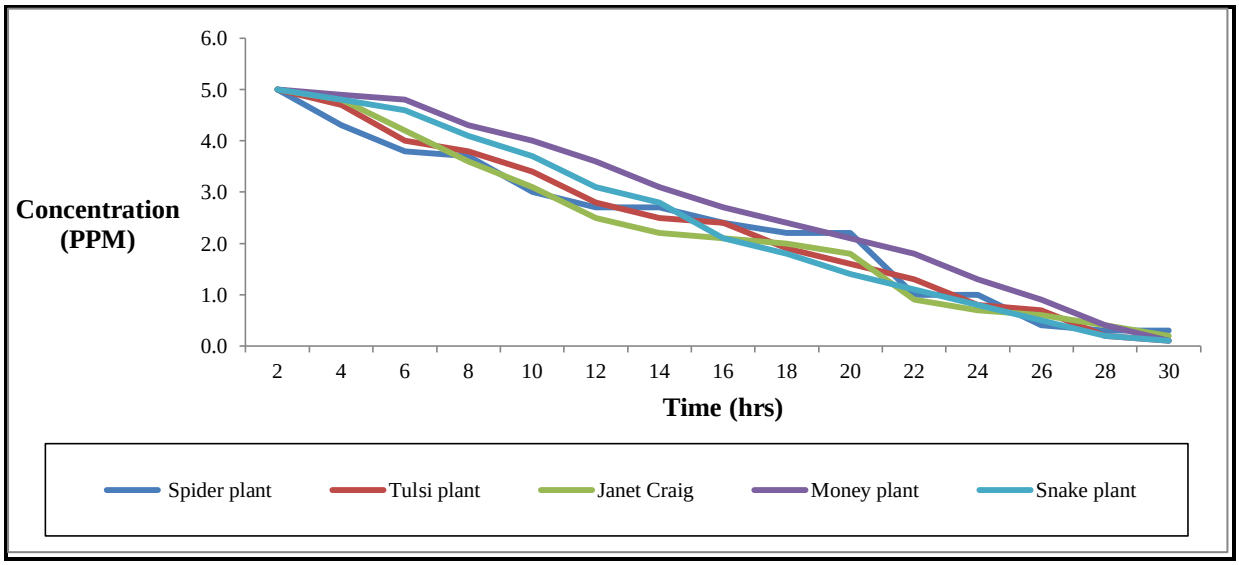

Figure 2: Performance evaluation of the 5 plants (Spider plant, tulsi plant, janet craig, money plant and snake plant) for benzene degradation with an initial concentration of 5 PPM. As per our results, money plant shows the maximum removal efficiency of 98%.

Acknowledgements

The authors are thankful to Mr. Sudheer Kumar for the preparation of biochar.The authors also acknowledge the DIH and Project Varanasi for their financial support and the staff of the SAIF department for their great cooperation in carrying out all the described analyses.

References

- Balendu Shekher Giri, Ki Hyun Kim, R.A. Pandey, Jinwoo Cho, Hocheol Song, Yoon Shin Kim (2014). Review of biotreatment techniques for volatile sulfur compounds with an emphasis on dimethyl sulphide. *Process biochemistry* 49 (9), 1543-1554.
- Sandeep Mudliar, Balendu Giri, Kiran Padoley, Dewanand Satpute, Rashmi Dixit, Praveena Bhatt, Ram Pandey, Asha Juwarkar, Atul Vaidya, 2010. Bioreactors for treatment of VOCs and odours–a review. *Journal of Environmental Management* 91 (5), 1039-1054.

Proceedings of the Third International Conference on Sustainable Energy and Environmental Challenges (3rdSEEC)
18 –21 December, 2018, IIT Roorkee, India

SEEC No. 045

Wind-Solar PV Hybrid Electricity Generation and Application to Electric Vehicles, a Sustainable Solution to Carbon Emission Reduction in India

***Gado Abubakar**
Department of Environmental Science
Central University of Kerala
gadoabubakar@cukerala.ac.in

Anbazhagi Muthukumar
Department of Environmental Science
Central University of Kerala
sanbazhagi@gmail.com

Muthukumar Muthuchamy
Department of Environmental Science
Central University of Kerala
mmuthukumar@cukerala.ac.in

ABSTRACT

Global warming and climate change which we are already seeing today, requires serious shift from business as usual in electricity and transportation sectors, to sustainable energy solutions in keeping the global warming below the dangerous two-degree scenario. Electricity generation and transportation sectors, are responsible for about 60% of the global energy related GHG's emission, and their emissions are increasing in faster rate in comparison to all other energy sources. In this study, a novel approach is adopted in the analysis of wind/solar PV hybrid system for micro electricity generation, and application to electric vehicles. Spline interpolation method is adopted in wind power output estimations from 1kW small scale wind turbine, while the global accepted formulation is utilised for 520Wp solar PV system output estimations from hourly meteorological datasets (2006-2016) obtained from PVGIS5. The simulations shows that, the typical household electricity demand, as well as the 1.8kW electric vehicle demand can be achieve with 0.28kW excess energy that can be exported to the national grid across summer equivalent season. It appear from our analysis that, the hybrid renewable technology can significantly help in the reduction of electricity and transportation related emissions, and can help greatly in achieving Indian government 2022 renewable energy mission under National Action Plan on Climate Change.

***Keywords*:** Electric Vehicles; Wind; Solar PV; Hybrid; *India*

INTRODUCTION

The utilization of fossil fuels for transportation and energy related issues, is among the biggest culprit of anthropogenic carbon emission accounting for about 60% of the global CO_2 emission. Electricity as the backbone of development of any society, has already contributed 37.5% of the total CO_2 emission in the globe, releasing of 7700 million tonnes of CO_2 annually, this is an indication that, serious transition is necessary in decarbonising electricity across the globe [1-3]. However, literature highlighted the potential solutions to sustainable electricity generation for large, medium and small scale electricity generation, but renewable energy sources turns to be the sustainable solution among all the suggested solution highlighted by different studies [4,5], although renewable energy sources are prone to several limitations in electricity generation, the most important and challenging issue being intermittency effect, since they depend on climatic conditions and seasons of the year unlike the conventional energy sources.

Renewable energy sources such as wind energy, solar energy, small hydro, geothermal energy etc. are clean energy sources that offer the promise of meeting energy demand for both on-grid and off-grid applications as well as application to electric vehicles, and other electric motors utilised in the transportation sector. Several studies are conducted to address the effect of renewable energy intermittency in electricity generation in the real time and simulation environments. However, conclusion can be made that, the best way of addressing the effect of renewable energy intermittency in electricity generation is to look at the generation at diurnal level i.e. hourly level of generation and Complimenting different renewable energy technologies in form of hybrid as the technology have been developed and practically proven to generate autonomous, stable and sustainable power for both on grid and off grid applications [6, 7].

the aim of this paper is to analyse the viability of wind-solar PV hybrid system performance for electricity generation and application to electric vehicles, in a location in southern part of India. The system is proposed to deliver smoother power to the end-user according to the electricity demand of a typical household, and electricity demand of the selected electric vehicle for the study using (2006-2016) meteorological datasets for the location under study.

Micro electricity generation

Decentralized renewable energy production, is commonly the main vision and solution to carbon emission in electricity generation. Decentralized or micro- electricity generation, has tendency of yielding significant benefits in terms of energy efficiency, reduction in carbon emission, mitigation to electricity transmission and distribution losses and enhancing energy security [8].

India is blessed with abundant renewable energy resources that can be harness for sustainable electricity generation at both small scale, medium and grid size electricity generation, and application to electric vehicles [9]. Micro electricity generation refers to, generation of electricity in a reliable and environmentally sustainable way by individuals, small business, communities etc. as alternative to the grid connected power with relative low carbon emission to the environment [10]. Transition from the current mode of fossil fuels transportation and electricity generation to sustainable and green electricity in India, requires deployment of renewable energy technologies at all level of mass transportation, personal transportation and electricity generation in form of micro electricity generation. This involves the configuration of highly diverse set of renewable energy technologies such as wind, solar, solar thermal, geothermal, renewable hybrid technologies etc. coupled for the generation of electricity without carbon emission to the environment.

Materials and methods

Meteorological Datasets

Renewable energy sources are intermittent in electricity generation, due to the dependence on atmospheric nature. This dependence on atmospheric conditions makes it quite difficult and complex, and challenging in terms of understanding their variability in electricity generation [11]. Several studies have been carried out in the literature on the modelling and forecasting of renewable energy sources in electricity generation, but the widely accepted approach is believed to be, diurnal approach in modelling of the resources, which is believed to have tendency of providing clear information on the stochastic and dynamic nature of renewable energies in short-term, middle-term and long-term scales, in renewable electricity forecasting and generation [12].

However, based on standards, accumulative measurement of data set from 5-10 years at any site of interest is adequate to predict long-term behaviour of meteorological parameters with 90% confidence [3]. In this study, hourly meteorological datasets (2006-2016) of Kasaragod, obtained from PVGIS5, is scaled to Typical Meteorological Year (TMY) which is later sorted and converted to typical day across the season of the year (summer, winter, monsoon and post monsoon), is utilised to identify the performance of hybrid wind/solar PV system electricity generation in the summer equivalent season using Matlab Simulink.

Meteorological Datasets Modelling

Hourly wind speed data recorded at 10m height, is extracted from PVGIS5 metadata using Matlab Simulink intervention script. However, wind power depends directly on the cubic wind speed, and wind speed changes with height in the boundary layer (wind shear), therefore, it is necessary to scale the wind speed data to the desired hub height of the chosen wind turbine.

Several models have been adopted by different literatures, in scaling the reference wind speed to desired hub height, and power law is the most common model adopted by several studies despite its limitations that can promote errors in the estimation of wind speed at hub height. In this study, Millward-Hopkins model Eqn. (1) is adopted in scaling the reference wind speed to the desired hub height. This model is more realistic because, it has taken account of any correction made to the atmospheric stability.

$$V_{hub} = V_{ref} \frac{\ln(Z_{hub}/Z_{0-ref})}{\ln(10/Z_{0-ref})} \quad (1)$$

Where, V_{hub} =Wind Speed at hub height V_{ref} = Wind Speed at reference height = 10m Z_{hub} = Reference height Z_{0-ref} = Reference height roughness length

However, several models are available in the literature for calculating energy output from Wind Energy Conversion Systems (WECs). Techniques such as, Gamma, Lognormal, Three parameter Beta, Rayleigh and Weibull distributions has successfully been used by different studies in the literature in calculating power output from wind [11]. In this study, spline interpolation model is utilised in estimating the performance of the chosen WECs based on the wind resource of the study site.

$$E = A * r * H * PR \quad (2)$$

E = Energy Output (W, kW, kWh), A = Total solar panel Area (m²) r = solar panel yield (%),
H = Insolation on tilted panels PR=Performance ratio

The insolation data utilised in this study is extracted from the data sets obtained from PVGIS 5 using MATLAB Simulink intervention script. Using Eqn. (2), the actual D.C power delivered by the solar system, can be estimated with the use of the solar panel parameters, and the insolation data of the location in question.

The extracted datasets (wind and solar), are all converted to months of the year, for subsequent conversion to seasons of the year (summer, winter, monsoon and post-monsoon). The conversion of the datasets to typical day across the seasons of the year will be useful for comparison with typical electricity demand, and electric vehicle electricity demand for identifying the viability of the system in addressing the intermittency effect of renewable energies in electricity generation which is among the major objectives of the study.

Electricity Demand and Hybrid System Components

Electricity demand data is one of the stochastic parameters required in the designing of this research. Hourly electricity consumption of a typical household in countries like India is very difficult because of the erratic nature of electricity supply across the states. However, Several methods based on estimates have been adopted by several studies in generating a typical household electricity demand profile. Methods such as, interpolation method, ANN (Artificial Neural Networks), non-linear and multiple regression method, have been utilised by several studies in this regard. In this study, PVGIS electricity demand profile is adopted for a typical household, and the electric vehicle electricity demand and specifications is shown in Tab. 1.

An indigenous solar module is adopted in this research to ensure maximum accuracy from simulation results. However, Futurenergy 1kW wind turbine is chosen in this study in estimating the wind power output from the wind datasets. The chosen wind turbine has an efficient rotor design and can operate at low wind speeds which makes it suitable for micro hybrid renewable electricity generation applications. The specifications and parameters of the chosen solar PV system at Standard Test Condition (STC) and the Futurenergy 1kW small wind turbine specifications are shown in Tab. 2.

Table1. Electric Vehicle Electricity demand and Specifications

Power	1800W
Power supply	Lead Battery
Battery	72V/120ah
Voltage	DC/60V
Top speed	38~40km/h
Mileage	120km
Full charge time	8~10 hours
Motor	Brushless motor
Charger	60V copper wire charger
Ground clearance	150mm
Net weight	380Kg (with battery)

Table 2: Hybrid system Specifications

Wind System Properties		Solar System Properties	
Properties	**Specification**	**Properties**	**Specification**
Turbine type	**HAWT**	**Nominal Power (Pmax)**	**260Wp**
Rotor diameter	**1.8m**	**Panel Area (m^2)**	**1.67m^2**
Nominal Power Output	**1kW**	**Maximum Power Current (Impp)**	**8.5A**
Power Coefficient (C_p)	**0.42**	**Open Circuit Voltage (V_{OC})**	**37.9V**
Cut-in Wind Speed	**3.5 m/s**	**PV efficiency (%)**	**15.6%**
Survival wind speed:	**52m/s**	**Power Tolerance (W)**	**0 ~ +5**
Rated Wind Speed	**12.5m/s**	**Short Circuit Current (I_{SC})**	**8.80A**
Generator type	**3-Phase AC**	**Voltage at Maximum Power (I_{MMP})**	**30.6V**

Results and Discussions

This section shows the results of wind and solar resource analysis, and simulation. The output of the hybrid optimisation model is also highlighted and discussed.

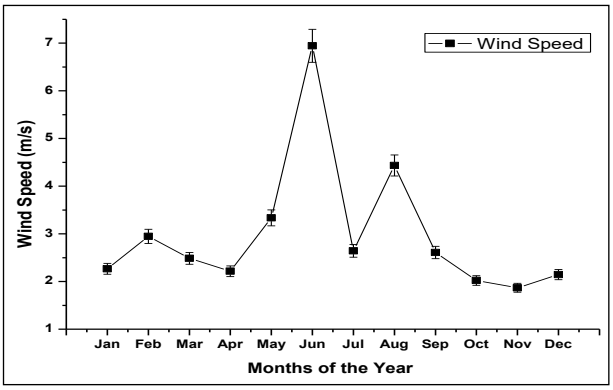

(a)

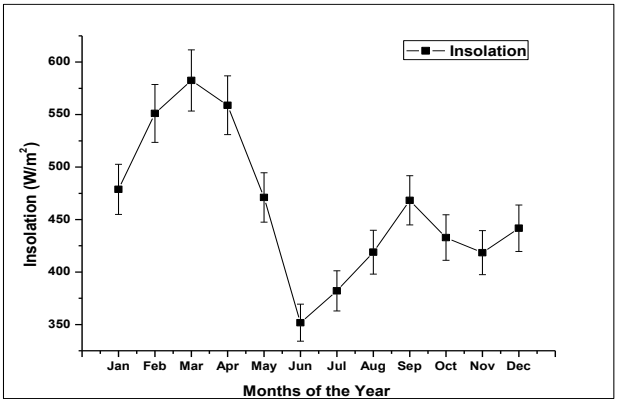

(b)

Fig 1. Average Monthly resources: a), Insolation b), wind speed at 25m height; the whiskers represents the max. and min. values.

The monthly average solar irradiation and wind speed at 25m height, across the study site is illustrated in Fig. 1 (a and b). Evidence from the figure shows that, the highest wind speed is observed in the month of June and the lowest solar irradiation also in the month of June. However, highest insolation is observed in

the month of March with corresponding lower wind speed across the month. The distinctive profile the wind and solar resources across the study site shows that, combination of the two renewable energy systems to formed hybrid, can offer unique opportunity for the elimination of intermittency effect of renewable energy resources in electricity generation.

The diurnal wind speed data measured at 10m, has average wind speed of 2.82ms^{-1} and it varies from 0.15ms^{-1} to 7.75ms^{-1}. The observations on the annual average values shows that, when the data is extrapolated to required hub height, the study site has a reasonable wind resources that can be employed for small scale, medium and large scale wind electricity generation. The spline interpolation method employed on the extrapolated wind speed data at 25m height, based on the power curve values of the chosen wind turbine, shows a very good results in the estimation of the wind power output from the chosen WECs as shown in Fig. 2a. From the results, a clear trend of higher wind speed is observed during the peak sunshine hours which is also accompanied in direct proportion with wind power output. Fig. 2b shows the hourly insolation and simulated power output from 520Wp solar PV system utilised in the study during the summer equivalent season. The results shows higher power output during mid-noon hours, signifying the direct correlation between power output and insolation falling on the surface of the PV system (Equ. 2). The results indicates that, solar PV electricity generation can play a very vital role in eradicating electricity shortage which is endemic to the study site, especially with the lower temperature of the site, which can enhance the efficiency of the solar PV module.

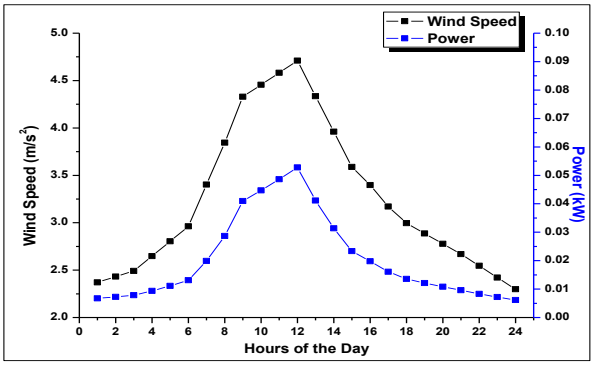

(a)

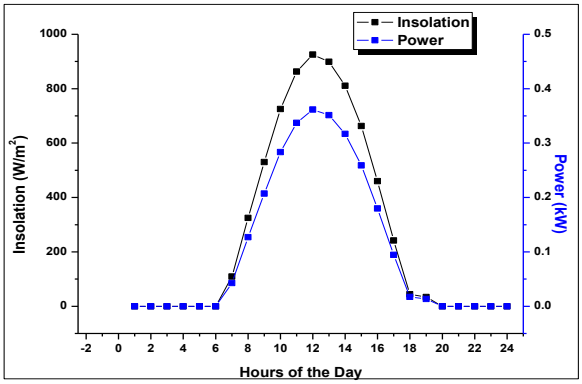

(b)

Fig. 2. Diurnal renewable energy resources across summer equivalent season: a) wind resources at 25m and corresponding power output b) Insolation and corresponding power output

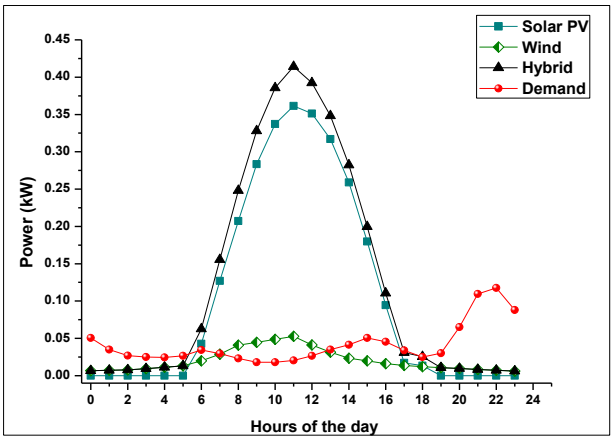

Fig. 3. The hybrid systems performance across summer equivalent season

Fig. 3 , shows the hourly power output of wind system, solar PV, hybrid system and typical household hourly electricity demand during summer equivalent season. It is evident from the plot that, there is higher power output from the solar PV system and wind turbine during peak sunshine hours. However due to higher power output from the solar PV system, the hybrid output contour followed the characteristics of the solar PV output during the sunshine hours. It also clear from the plot that, during the sunshine hours, solar and wind power generations exceeded the electricity demand and hence, hybrid output exceeded the demand greatly, this shows that, storage is required during the sunlight hours for the hybrid design to substantially power the demand at all time. The analysis of the results also shows that, 1800W electricity demand of Zhufeng ZF1260 electric vehicle can be supplied by the hybrid system during sunshine hours, and by storing the excess energy in the sunshine hours, 0.28kW excess power can be exported to the national grid after delivering full electricity demand of a typical household based on the electricity demand profile utilised for the study.

Conclusion

A novel approach is adopted in the analysis of renewable energy hybrid system consisting of wind and solar PV system, in a coastal area in Kerala state, southern India, for typical household electricity generation, and application to 1.8kW Zhufeng electric vehicle in summer equivalent season. The assessment of the proposed hybrid system using the novel methodology adopted shows that, the two clean energy sources can be utilised in delivering full electricity demand of a typical household, and application to electric vehicles at the study site. The results however, demonstrate that, Kasaragod has sufficient wind and solar energy potential for small scale, medium and large scale electricity generation applications. it is clear from the findings that, solar PV system produced more energy than wind energy system, and for the system to deliver uninterrupted power to the end-user, storage option is required. On the other hand, the analysis of the results shows that, 1800W electricity demand of Zhufeng ZF1260 electric vehicle can be deliver by the hybrid system with 0.28kW excess power that can be exported to the national grid. since The future suggestion of this research may

include the utilisation of sustainable storage option that will substitute the conventional lead acid batteries, which are carcinogenic and harmful to the environment since storage option appears to be inevitable if the effect of renewable resources intermittency in electricity generation is to be eliminated. It is expected that, the results from this novel hybrid system design would be a guiding information to the district policy makers and Kerala state government at large, in achieving the Indian government 2022 renewable energy mission under National Action Plan on Climate Change, and India's 2030 Vision on Electric Vehicle which aimed at converting all vehicles in India to electric vehicles by the year 2030.

REFERENCES

[1] Victor Moutinho, Margarita Robaina, 2016. Is the share of renewable energy sources determining the CO_2 kWh and income relation in electricity generation? Renewable and Sustainable Energy Reviews, 65, pp. 902–914

[2] Bonfils Safari, 2011. Modeling wind speed and wind power distributions in Rwanda. Renewable and Sustainable Energy Reviews, 15, pp. 925–935

[3] Ahmed Shata Ahmed, 2012. Potential wind power generation in South Egypt. Renewable and Sustainable Energy Reviews, 16, pp. 1528–15

[4] Mason, I.G., Page S.C., and Williamson A.G., 2010. A 100% renewable electricity generation system for New Zealand utilising hydro, wind, geothermal and biomass resources. Energy Policy. **38**(8), pp. 3973-3984

[5] Taher Maatallah, Souheil El Alimi, Anour Wajdi Dahmouni, Sassi Ben Nasrallah, 2013. Wind power assessment and evaluation of electricity generation in the Gulf of Tunis, Tunisia. Sustainable Cities and Society, 6, pp. 1–10

[6] Guorui Ren, Jinfu Liu, Jie Wan, Yufeng Guo and Daren Yu., 2017. Overview of wind power intermittency: Impacts, measurements, and mitigation solutions. Applied Energy. 204 (15): pp. 47-65

[7] Edmond Baranesa, Julien Jacqminb, Jean-Christophe Poudouc, 2017. Non-renewable and intermittent renewable energy sources: Friends and foes? Energy Policy. 111, pp. 58-67

[8] Jouni K. J., and Sampsa Hyysalo, 2015. Renewable and micro- generation of heat and electricity-Review on common and missing socio-technical configurations. Renewable and Sustainable Energy Reviews, 49: pp. 857-870

[9] Yoshiyuki Shimoda, Ayako Taniguchi-Matsuoka, Takuya Inoue. Masaya Otsuki, Yohei Yamaguchi, 2017. Residential energy end-use model as evaluation tool for residential micro-generation. Applied Thermal Engineering. 114 (5): pp. 1433-1442.

[10] Jouni K. J., and Sampsa Hyysalo, 2015. Renewable and micro- generation of heat and electricity-Review on common and missing socio-technical configurations. Renewable and Sustainable Energy Reviews, 49: pp. 857-870

[11] Fatma GülAkgül, Birdal Şenoğlu, Talha Arslan, 2016. An alternative distribution to Weibull for modelling the wind speed data: Inverse Weibull distribution. Energy Conversion and Management, 114, pp. 234-240

[12] Yeliz Mert Kantar, Ilhan Usta, 2015. Analysis of the upper-truncated Weibull distribution for wind speed. Energy Conversion and Management, 96, pp. 81-88

Proceedings of the Third International Conference on Sustainable Energy and Environmental Challenges (3rd SEEC)
18 – 21 December, 2018, IIT Roorkee, India

SEEC No. 046

ECONOMIC AND ENVIRONMENTAL ANALYSIS OF RECYCLING PROCESS FOR SPENT LI-ION BATTERIES USING STRONG ACIDS

Sandeep S. Anwani
Department of Chemical Engineering
Visvesvaraya National Institute of Technology
Email: sandeepanwani@gmail.com

Ravi N. Methekar*
Department of Chemical Engineering
Visvesvaraya National Institute of Technology
Email:methekar.vnit@gmail.com

ABSTRACT

The aim of the present study is twofold. Firstly, laboratory based economic analysis of recycling of spent LIBs has been carried out purely based on the laboratory cost of the chemicals and electricity consumption involved in the leaching and extraction process. Secondly it attempts to calculate the economics of the overall recycling process. Since economical processes have the higher potential to be adopted in an industry. This necessitates the scope of the economic analysis to be done for a recycling process. In the latter part environmental analysis of the recycling process has been carried out for four acids mainly sulphuric acid, hydrochloric acid, nitric acid and phosphoric acid thorough a Gabi software. It was found that all four acids have relatively same impact on the environment in terms of kilograms of CO_2 emission. On the other hand, recycling of spent LIBs using Nitric acid costs 30% lesser than other strong acids studied here, hence it is found to be an economical leaching agent for the recovery of cobalt oxalate, manganese carbonate and lithium carbonate.

Keywords: ***Leaching, Spent LIBs, Recycling, Gabi software***

INTRODUCTION

Lithium ion batteries (LIBs) are widely used in mobile phones, laptops, cameras and other portable electronic gadgets because of high energy density, light in weight, low self-discharge, longer durability and safer operations (Zeng X., 2015). Recently lithium ion batteries have also found their application in electric vehicles creating greener route for transportation. LIBs consist of mainly cathode, anode, separator and electrolyte. The cathode is made up of Lithium cobalt oxide which is adhered to an aluminum sheet while anode is made up of graphite adhered to a copper sheet. The separator is a thin plastic porous film which separates the two electrodes from short-circuiting. The separator is generally soaked in an electrolyte which may vary depending upon the brand or battery model which is generally $LiPF_6$, $LiBF_4$, $LiClO_4$ (Xu et al., 2008).

Due to the immense use of LIBs for various applications in all parts of the world creates massive amount of dead batteries which needs to be disposed off in a most efficient and economical way to minimize e-waste generation and hence ensuring safety of the environment. This leads to the urgency of recycling spent lithium ion batteries to boost e-waste management, reducing adverse environmental impacts and also to ensure sustainable material supply.

Recycling of spent lithium ion batteries from strong acids such as sulphuric acid, hydrochloric acid, nitric acid and phosphoric acid have been in practice since last decade (Meshram et al., 2017, Jha et al., 2015, Barik et al., 2015, Castillo et al., 2002, Pinna et al., 2016). Many researchers have worked on reductive leaching of spent LIBs using H_2SO_4(Nan et al., 2005, Atkas et al., 2006, Meshram et al., 2015, Jha et al., 2015, Chen et al., 2011, Wang et al., 2012, Li et al., 2009, Kang et al., 2010), HCl(Zhang et al., 1998, Barik et al., 2015, Fernandes et al., 2012, Barik et al., 2017), HNO_3(Castillo et al., 2002, Lee and Rhee., 2003), and H_3PO_4(Pinna et al., 2016).

Recycling of spent LIBs have an immense potential to solve major issues like e-waste generation, lithium scarcity, etc. Furthermore spent LIBs are the rich source of precious metals such as Co, Mn, Ni and Li which needs to recycled for their further use in battery material preparation, this gives birth to the idea of environmental-friendly and cost effective recycling process. Chemical processes are often cost intensive, so the biggest task is to make the process economically feasible and viable. Hence it is extremely important to estimate the cost involved in the recycling process.

In the recovery of valuable metal, a combined method of acidic leaching and selective precipitation were

employed in this paper, to recover valuable metals from the leach solution. Among all methods acidic leaching is an environment-friendly, cost effective technique to recover cobalt and lithium (Barik et al., 2017). In our study cobalt, manganese and lithium were precipitated successively at a particular pH to recover cobalt oxalate, manganese carbonate and lithium carbonate respectively. Furthermore, the products obtained from this process would be of industrial interest. The purpose of this paper is to develop an efficient, cost effective and environmentally benign recycling process for LIBs.

EXPERIMENTAL STUDY

Materials

All the reagents used in the experiment were all of analytical grade. The spent mobile phone batteries mainly of Nokia BL-5C were procured from the local market of Nagpur.

Methodology

Sample preparation and pretreatment

The fully discharged batteries were dismantled manually through angle grinder with proper safety precautions. The plastic casing and inner steel casing was successively scrapped off from the main internal core. The cathodic film was separated and cut in minute square pieces with scissor. The resultant pieces were dissolved in a proper volume of N-Methyl-2-Pyrrolidone (NMP) solvent to peel off the active cathodic material (ACM) from the aluminum films via ultra-sonication cleaning which basically dissolves the fluoro-polyvinylidene glued to these films. The black slurry thus obtained was centrifuged at 4000 RPM for about 20 minutes to separate the active cathode material from the NMP solution, dried at 150°C for 1 hour. The dried ACM was fed to ball milling for size reduction followed by manual sieving with a mesh size below 25µm.The smaller diameter particles are needed for efficient dissolution of the material in the acid lixivium. Finally, the material was calcined in a muffle furnace at 750°C for 5 h to burn off the carbon, and residual NMP if any left in the material.

Dissolution of active cathodic material

2 grams of active cathodic material was used in each leaching experiment, keeping solid to liquid ratio constant which is fixed at 10g/L for all strong acids. The molarity of the acids, temperature, time, concentration of reducing agent for leaching valuable metals was directly obtained from the literature. The leaching solution obtained was centrifuged to separate the residue which was hen dried at 373K and weighed to calculate the dissolution efficiency. The dissolution efficiency is the ratio of difference between mass of original sample fed for leaching and reside left after leaching to the mass of original sample fed forleaching. Mathematically, γ (dissolution efficiency) is given by

$$\gamma = \frac{m_o - m_r}{m_o} * 100\%$$

Where m_o =mass of original sample fed for leaching,
m_r =residue left after leaching
The dissolution efficiencies thus obtained were compared to select the best leaching acid used to extract valuable metals such as Co, Mn, and Li in their stable form.

RESULTS AND DISCUSSIONS

Economic analysis of the recycling of spent LIBs

Laboratory based economic analysis have been carried out purely based on the laboratory cost of the chemicals used in leaching and extraction processes. An electricity cost per unit has been taken from the electric board of the state. Consumption of the electricity is calculated from the rating and time of utilization of the particular equipment. The complete economic analysis with example is given in Table. 1. This gives us the idea about the expenditure of the recycling process which helps in finalizing the acid on economic grounds. Basically economical processes have the higher potential to be adopted in an industry. This necessitates the scope of the economic analysis to be done of the process.

Table: 2 shows the chemicals and electricity requirement in detail for recycling process using hydrochloric acid. For simplicity recycling process has been further divided into four steps viz., Leaching of valuable metals into the liquid, recovery of $CoC_2O_4.2H_2O$, recovery of $MnCO_3$ and recovery of Li_2CO_3. Individual cost in each of the process has been determined by the price and quantity of a particular chemical consumed, whereas overall cost is the summation of total process cost and electricity cost. The average electricity per unit cost has been taken as 5.2 Rs/u.

Environmental analysis in term of Kg-CO_2 equivalent

Cleanliness index in term of kg equivalent CO_2 is found out using GaBi software. Environmental analysis showed that almost all strong acids have relatively equal impact on the environment, however both extraction efficiency and dissolution efficiency of active cathodic material were observed highest for sulphuric acid so it will be an obvious choice to select sulphuric acid as the best leaching acid for recycling of spent lithium ion batteries.

Table: 3 shows the kilograms of CO_2 emitted into the atmosphere involved in the recycling process with different strong acids studied.As the GaBi software does not have data for the Phosphoric acid and hence assumed to be equivalent to nitric acid.

Table: 1 LABORATORY BASED COST ANALYSIS

Acid	Leaching Cost (Rs.)	Cobalt Oxalate Extraction Cost (Rs.)	$MnCO_3$ Extraction Cost (Rs.)	Li_2CO_3 Extraction Cost (Rs.)	Total Extraction Cost (Rs.)	Total Electricity Cost (Rs.)	Overall Process Cost(Rs.)
H_2SO_4	28.96	29.54	15.724	8.788	83.04	18.096	101
HNO_3	32.16	9.839	1.98	8.788	52.771	18.096	71
HCl	37.9	11.2776	2.922	8.788	60.967	18.096	79
H_3PO_4	53.6	8.976	11.438	8.788	82.854	18.096	101

Table: 2 SAMPLE CALCULATION FOR HYDROCHLORIC RECYCLING PROCESS OF SPENT LIBS

Process	HCl (ml)	H_2O_2 (ml)	D.I. Water (ml)	NaOH (g)	Oxalic acid (g)	Na_2CO_3 (g)	Individual Process Cost (INR.)	Total Electricity Cost (INR.)	Overall Process Cost (INR.)
Leaching	24.635	16	159.36				37.9794		
$CoC_2O_4.2H_2O$ Recovery			40	8g	3.76 g		11.2776	18	79
$MnCO_3$ Recovery			9.8	1.96 g		1.20 g	2.922		
Li_2CO_3 Recovery			100			7 g	8.788		

Table: 3 ENVIRONMENTAL ANALYSIS IN TERMS OF KG-CO_2 EQUIVALENT

Acids	H_2SO_4	HCl	HNO_3	H_3PO_4
Kg-Equivalent CO_2	3.87	3.59	3.67	3.67(Assume equivalent to nitric acid)

CONCLUSIONS

The recycling of spent lithium-ion battery is necessary from the environment point of view as well as from the sustainable metal supply. In this study, recycling of mobile phone's lithium-ion spent batteries is carried out using strong acids. Environmental impacts of acidic leaching process by the strong acids have been carried out using the software called GaBi. Laboratory based economic analysis of

the leaching process have been carried out.It was found that all four acids have relatively same impact on the environment in terms of kilograms of CO_2 emission. Recycling of spent LIBs using. Nitric acid as a leaching agent has found economical and costs 30% lesser than other acids used for the recovery of cobalt oxalate, manganese carbonate and lithium carbonate.

ACNOWLEDGEMENT

The author (RMN) acknowledge the department of science and technology, Government of India for financial help for carrying out this work under the DST-SERB-ECR scheme (ECR/2016/000422)

REFERENCES

[1] Zeng, X.; Li, J.; Shen, B., Novel approach torecover cobalt and lithium from spent lithium-ion battery using oxalic acid. Journal of hazardous materials, 2015,295, 112-118.

[2] Pagnanelli, F.; Moscardini, E.; Granada, G.; Cerbelli, S.; Agosta, L.; Fieramosca, A.; Toro, L., Acid reducing leaching of cathodic powder from spent lithium ion batteries: Glucose oxidative pathways and particle area evolution. Journal of Industrial and Engineering Chemistry, 2014, 20 (5), 3201-3207.

[3] Li L., Fan, E., Guan Y., Zhang X., Xue Q., Wei L., Wu, F., Chen, R., Sustainable Recovery of Cathodic Materials from spent li-ion batteries using lactic acid leaching system**,** ACS Sustainable Chem. Eng, 2017, 5 (6), 5224–5233.

[4] Jha, M. K., Kumari A., Jha A. K., Kumar V., Hait J., Pandey, B. D., Recovery of lithium and cobalt from waste lithium ion batteries of mobile phone, Waste Management, 2013, 33 (9), 1890-1897.

[5] Zhang P., Yokoyama T., Itabashi O., Suzuki M.T., Inoue K., Hydrometallurgical process for the recovery of metal values from spent lithium ion spent batteries, Hydrometallurgy, 1998, 47, 259–271.

[6] Castillo S., Ansart F., Laberty-Robert C., Portal J., Advances in the recovering of spent lithium battery compounds, J. Power Sources, 2002, 112, 247–254.

[7] Lee C., Rhee K., Reductive leaching of cathodic active materials from lithium ion battery wastes, Hydrometallurgy, 2003, 68, 5-10.

[8] Jha M. K., Kumari A., Jha A. K., Kumar V., Hait J., Pandey B. D., Recovery of lithium and cobalt from waste lithium ion batteries of mobile phone, Waste Management, 2013, 33 (9), 1890-1897.

[9] Castillo S., Ansart F., Laberty-Robert C., Portal J., Advances in the recovering of spent lithium battery compounds, J. Power Sources, 2002, 112, 247–254.

[10] Aktas S., Fray D. J., Burheim O., Fenstad J., Acma E., Recovery of metallic values from spent lithium ion secondary batteries, Miner. Process. Ext. Metal, 2006, 115 (2), 95-100.

[11] Nayaka P.G., Pai V.K., Santhosh G., Manjanna J., Recovery of cobalt as cobalt oxalate from spent lithium ion batteries by using glycerin as leaching agent, J. Envn. Chem. Eng., 2016, 4, 2378–2383.

[12] Junmin Nan, Dongmei Han, Xiaoxi Zuo, Recovery of metal values from spent lithium-ion batteries with chemical deposition and solvent extraction, Journal of Power Sources, 2005, 152, 278–284.

[13] Jingu Kang, Gamini Senanayake, Jeongsoo Sohn, Shun Myung Shin, Recovery of cobalt sulfate from spent lithium ion batteries by reductive leaching and solvent extraction with Cyanex-272, Hydrometallurgy, 2010, 100, 168-171.

[14] Eliana G.Pinna, M.C.Ruiz Manuel W.Ojeda Mario H.Rodriguez, Cathodes of spent Li-ion batteries: Dissolution with phosphoric acid and recovery of lithium and cobalt from leach liquors, Hydrometallurgy, 2017, 167,66-71.

[15] Aline Fernandes, Julio Carlos Afonso, Achilles Junqueira Bourdot Dutra, Hydrometallurgical route to recover nickel, cobalt and cadmium from spent Ni–Cd batteries, Journal of Power Sources, 2012, 220, 286-291.

[16] Jianbo Wang, Mengjun Chen, Haiyan Chen, Ting Luo, Zhonghui Xu, Leaching study of spent Li-ion batteries, Procedia Environmental Sciences, 2012, 16, 443 – 450.

[17] Pratima Meshram, B.D.Pandey, T.R.Mankhand, Recovery of valuable metals from cathodic active material of spent lithium ion batteries: Leaching and kinetic aspects, 2015, 45, 306-313.

[18] S.P.Barik, G.Prabaharan L.Kumar, Leaching and separation of Co and Mn from electrode materials of spent lithium-ion batteries using hydrochloric acid: Laboratory and pilot scale study, Management, Journal of Cleaner Production, 2017, 147, 37-43.

[19] S.P.Barik, G.Prabaharan, B.Kumar, An innovative approach to recover the metal values from spent lithium-ion batteries, Waste Management, 2016, 51, 222-226.

SEEC No.047

WASTEWATER TREATMENT CONTAINING OIL USING POLYVINYLIDENE FLUORIDE (PVDF) ULTRAFILTRATION MEMBRANE MODIFIED WITH FUNCTIONALIZED SiO_2 NANOPARTICLES

Bharti Saini

Department of Chemical Engineering, School of Technology, Pandit Deendayal Petroleum University, Gandhinagar, Gujarat, India
Email:bhartisaini100@gmail.com

Manish Kumar Sinha

Department of Chemical Engineering, School of Technology, Pandit Deendayal Petroleum University, Gandhinagar, Gujarat, India
Email:manish.sinha@sot.pdpu.ac.in

ABSTRACT

For treatment of wastewater containing oil using polyvinylidene fluoride (PVDF) ultrafiltration membrane were fabricated by phase inversion method. In order to achieve less fouling and high rejection, modification of PVDF membrane has been done by blending hydrophilic Poly(ethylene glycol) methyl ether methacrylate functionalized - SiO_2 nanoparticles (NPs). Successful functionalization of SiO_2 NPs and size were confirmed by energy dispersive X-ray spectroscopy (EDX) analysis and particle size analyzer, respectively. The morphology and hydrophilicity of the plain and modified membranes were evaluated by scanning electron microscope (SEM) and contact angle (CA) investigation respectively. The hydrophilicity resultrs reveals that the antifouling property of modified membrane enhanced. Plain PVDF membrane showed less oil rejection of about 69% which on functionalized NPs helped to improve oil rejection to the maximum value of 89%. Hence the PVDF/functionalised NPs membrane is desirable in the treatment of wastewater containing oil.

Keywords: Wastewater treatment, o/w emulsion, polymer membrane, polyvinylidine fluoride, removal percentage

NOMENCLATURE

SEM: scanning electron microscope; NPs: nanoparticles; o/w: oil-in-water; PVDF: poly(vinylidine fluoride); R(%): removal (%)

INTRODUCTION

Every year huge amount of oil containing wastewater is generated by petrochemical, food, pharmaceutical and metallurgical industries which results poor environmental pollution and trouble in resource utilization. Conventional oily wastewater treatment methods namely gravity separation and skimming, air flotation, coagulation, de-emulsification and flocculation have the inherent drawbacks such as low efficiency, high operating cost, corrosion and recontamination problems [1] that then lead to ineffective removal of emulsified oil droplets (size: micron and sub-micron) [2]. Moreover, emulsified oily wastewater by the addition of surfactants is extremely hard to remediate because of the efforts required to crack down the interfacial films created between oil and water [3,4]. In consideration of these limitations in conventional treatment methods, numerous kinds of polymeric membrane separation processes such as ultrafiltration (UF), nanofiltration (NF) and reverse osmosis (RO) have been recently utilized for oil-water treatment [5,6]. On account of its appropriate pore sizes (2–50 nm) and the ability of separating emulsified oil droplets without any de-emulsification processes, UF has been established as an capable method in the treatment of oil-water emulsions [7,8]. However, fouling is a severe problem intrinsic in UF membranes due to hydrophobic nature of polymer. Fouling caused by either deposition of oil on the membrane surface or inside of membrane pores that that ends up in a substantial flux loss [9]. The membrane properties such as pore structure, surface characteristics, as well as process and operating conditions are the factors which affects the membrane fouling. Hydrophilic rich moieties like inorganic nanoparticles, organic solvents, macromolecules and amphiphilic copolymers have been set up to impart antifouling property by means of membrane modification.

In this work PVDF membrane modification using Poly(ethylene glycol) methyl ether methacrylate functionalized - SiO_2 have been reported. The functionalized NPs were characterized by EDX and particle size analyzer. The plain and modified membranes were characterized by SEM, EDX pure water flux (PWF) and water contact angle. Afterwards the ultrafiltration study was conducted using oil-in-water (o/w) emulsion to represent as an industrial model pollutant. Finally, the separation performance of plain and modified membrane for o/w emulsion was

evaluated in terms of percentage removal of o/w emulsion and fouling parameters.

EXPERIMENTAL

PVDF pellets, PEGMA and DMAc were purchased from M/s. M/s. Sigma Aldrich, India. PEG was purchased from M/s, Loba chemicals, India. Silicon oxide (SiO_2) nanoparticles were supplied by Otto Chemie Private Limited, India. All chemicals were used as received without further purification. Initially, the Poly(ethylene glycol) methyl ether methacrylate functionalized - SiO_2 NPs were synthesized via radical polymerization of SiO_2 NPs and PEGMA in methanol using AIBN as initiator. Modified NPs were characterized for particle size distribution by particle size analyzer (Malvern Mastersize 2000, Model, MAL1083109) and successful functionalization of NPs by energy dispersive X-ray spectroscopy (EDX) analysis. After that the optimize concentration of functionalized NPs (0.5 wt%) was used to modify the PVDF membrane. Plain PVDF membranes was synthesized with 15 wt% of PVDF pellets with 5 wt% of pore forming agent without NPs on dissolving into DMAc solvent and subsequent fabrication by phase inversion method. The optimized modified membrane was synthesized by 15 wt% of PVDF pellets with 5 wt% of pore forming agent and 0.5 wt% of functionalized NPs on dissolving into DMAc solvent. The synthesis steps for membrane fabrication by phase inversion method are shown in figure 1.

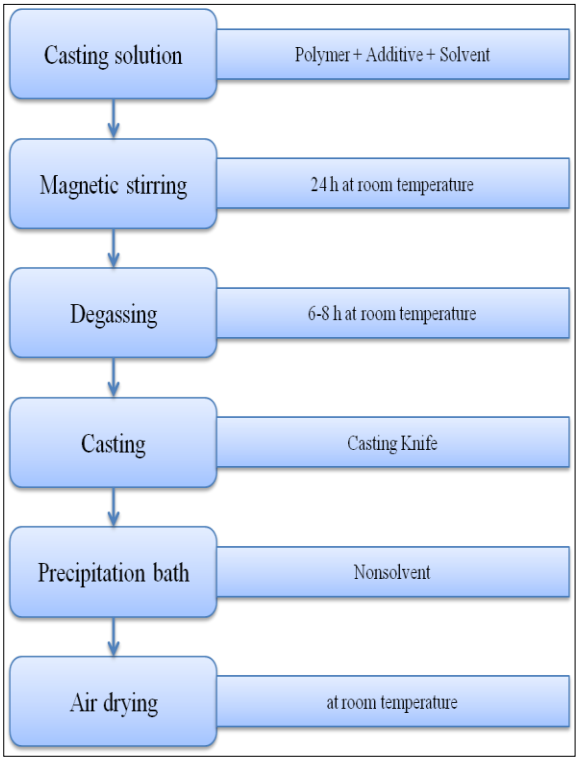

FIGURE 1. STEPS FOR MEMBRANE FABRICATION BY PHASE INVERSION METHOD

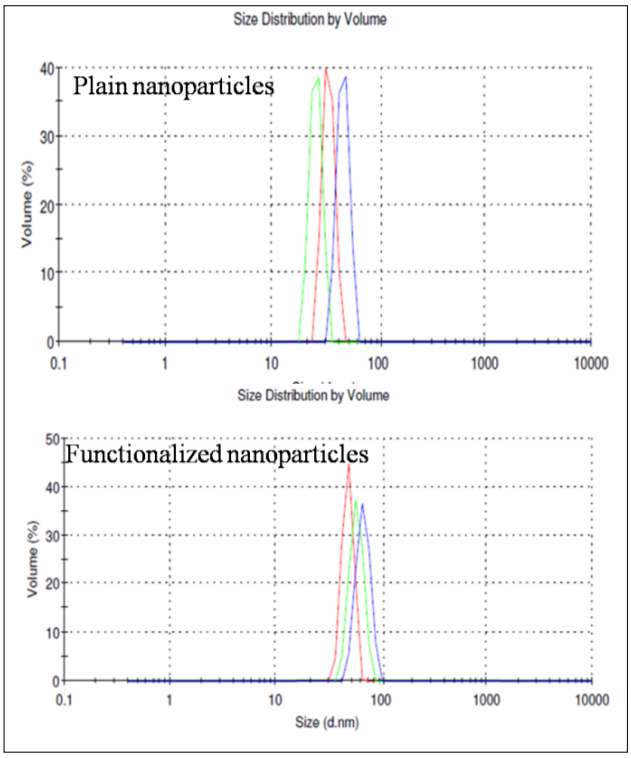

FIGURE 2. PARTICLE SIZE ANALYSIS FOR PLAIN AND FUNCTIONALIZED NPs

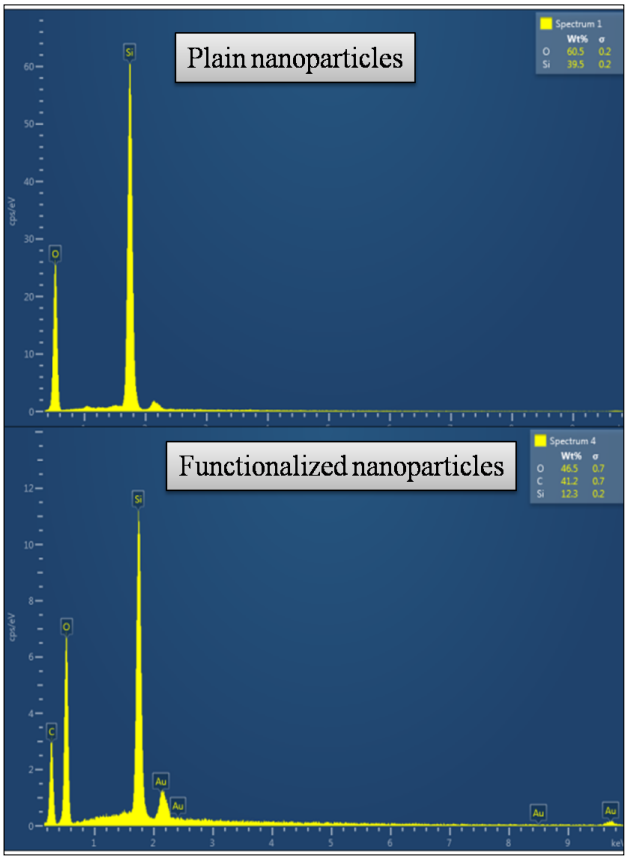

FIGURE 3. EDX IMAGES FOR PLAIN AND FUNCTIONALIZED NANOPARTICLES

Membrane hydrophilicity was analysed by measuring contact angle made by water drop on the membrane surface. Plain and modified membrane were analysed for top surface morphology by SEM (LEO 1430VP, UK) and existence of modified NPs in the membrane by EDX. In order to evaluate membrane performance o/w emulsion (100ppm) as feed was used in dead end batch filtration setup. The turbidity of the o/w emulsion feed and permeate were determined using a portable nephlometer turbidity meter (Model: 2100Q, Hach) and the feed turbidity was 259 NTU. The removal percentage of o/ w emulsion was calculated using feed and permeates concentration with the help of UV–vis spectroscopy at wavelength of 202 nm.

RESULT AND DISCUSSION

To ensure the nano size range of plain and functionalized NPs, the particle size analysis on volume (%) basis had been done. Figure 2. shows the particle size distribution of plain and functionalized NPs. The size of functionalized NPs was slightly larger compare to plain NPs. However, it was in the nanometre range. The EDX analysis of plain and functionalized NPs is shown in figure 3. In plain NPs spectra only Si and O elements peaks on wt% basis were observed. Whereas, functionalized NPs have one extra peak of C element on wt% basis, to confirm the successful functionalization of SiO_2 NPs by hydrophilic polymer chains.

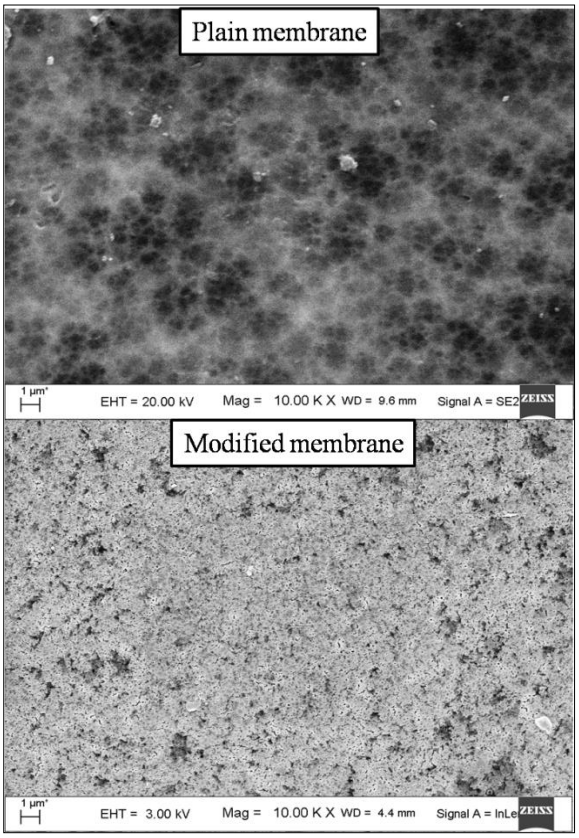

FIGURE 4. SEM IMAGES OF PLAIN AND MODIFIED MEMBRANE

The plain PVDF membrane has the highest water contact angle of 68.7°, showing poor hydrophilicity and it decreased around 55° with addition of functionalized NPs. Lower water contact angle higher the hydrophilicity which shows the improved antifouling property. These results showing that functionalized NPs were capable of significantly improving the membrane surface hydrophilicity. In order to analyse the effect of functionalized NPs on the microstructure of the fabricated membranes, SEM micrographs of top surface was analysed. The top surface SEM images showed that the blending of NPs have power on membrane formation mechanism and final structure of the membranes. Figure 4 shows the top surface images of plain and modified membranes. From figure 4 it was observed that with addition of functionalized NPs, the pore density of membranes was increased. The EDX images of plain and modified membrane are shown in figure 5. Plain membrane EDX spectra depicts that the wt% of Si element is zero, which confirms the non-existence of functionalized NPs the respective membrane. Whereas, modified membrane spectra shows that the wt% of Si element for the existence of functionalized NPs in PVDF membrane. After the characterization of membranes, all membranes were analysed for their performance in terms of percentage removal of o/w emulsion in a batch filtration setup of effective membrane surface area of 5.0 cm. O/w emulsion (100 ppm) was prepared using Indian crude oil (density: 911.2 kg/m3) collected from ONGC India without any treatment. Crude oil was used as oil phase in deionised water and concentration in water was kept at the desired value. Mixture of crude oil and water was so- nicated by probe sonicator (Model: VCX 500, Ultrasonic Processor 500 W, 20 Khz) for 6–8 h at 30 °C to prepare the o/w emulsion. The size of oil droplets was 311.5nm with a volume average which was determined using particle size analyzer (Malvern Mastersize 2000, Model, MAL1083109). The photograph of o/w emulsion is shown inset of figure 6. The turbidity of the feed was 259 NTU, after permeation this value decreased upto 1.4 NTU and 0.4 NTU for plain and modified membranes, respectively. As shown in figure 7, The flux through modified membrane is 4.5 times of plain membrane flux with in o/w emulsion feeds. This may be due to higher pore percent or pore density of modified membrane compare to plain membrane which were determined in our previous work [10]. It was observed that the $Flux_{RR}$ was increased from 0.53 (for plain membrane) to 0.84 (for modified membrane) in o/w emulsion ultrafiltration process. The significant increment of rejection percentage of o/w emulsion was observed from plain to modified membrane. For plain to modified membrane, the rejection percentages of BSA and o/w emulsion were increased from 71 69% to 89%. Therefore, retention property of modified membrane against o/w emulsion ultrafiltration was higher than plain membrane due to high surface hydrophilicity and smaller pore size.

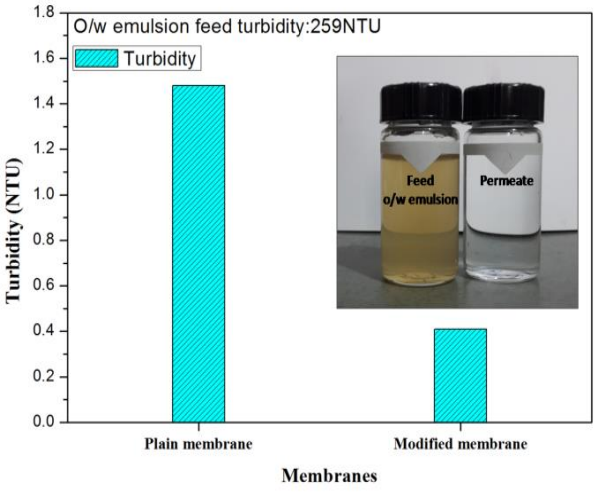

FIGURE 6. TURBIDITY VALUES OF PERMEATE THROUGH PLAIN AND MODIFIED MEMBRANE; (INSET: IMAGE OF FEED AND PERMEATE)

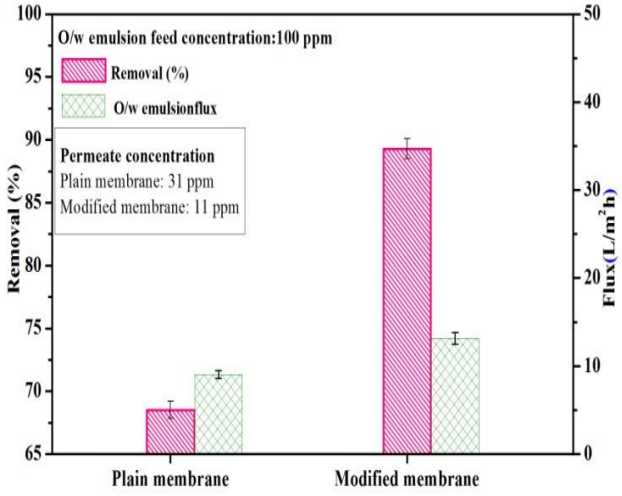

FIGURE 7. O/W EMULSION FLUX AND REMOVAL PERCENTAGE THROUGH PLAIN AND MODIFIED MEMBRANE

CONCLUSION

Functionalized NPs were successfully synthesized and blended in PVDF membrane and were able to modify the hydrophilicity and performance of the membrane for o/w emulsion removal from wastewater. Hydrophilicity and performance of PVDF membrane were found to enhance with functionalized NPs. For plain to modified membrane, the rejection percentages of BSA and o/w emulsion were increased from 71 69% to 89%. In summary, functionalized NPs were found to be an effective hydrophilic additive to improve the performance of ultrafiltration PVDF membrane. PVDF/ PEG6000/functionalized NPs membrane shows enhanced hydrophilicity, antifouling property, and o/ w emulsion flux compared to plain membrane.

ACKNOWLEDGEMENT

This work is financially supported by grant from Pandit Deendayal Petroleum Univesity, Gandhinagar under student research program with Project No.- ORSP/R&D/SRP/2016/TPBS.

REFERENCES

[1] A. Honga, A.G. Fane, R. Burford, Factors affecting membrane coalescence of stable oil-in-water mixtures, J.Membr. Sci. 222 (2003) 19–39.

[2] A. El-Kayar,M. Hussein, A.A. Zatout, A.Y. Hosny, A.A. Amer, Removal of oil from stable-oil-water mixture by induced air floatation technique, Technology 3 (1993) 25–31.

[3] Y.B. Zhou, L. Chen, X.M. Hu, J. Lu, Modified resin coalescer for oil-in-water mixture treatment: effect of operating conditions on oil removal performance, Ind. Eng. Chem. Res. 48 (2009) 1660–1664.

[4] P. Canizares, F. Martinez, J. Lobato, M.A. Rodrigo, Break-up of oil-in-water mixtures by electrochemical techniques, J. Hazard.Mater. 145 (2007) 233–240.

[5] R.J. Peterson, Composite reverse osmosis and nonofiltration membranes, J. Membr. Sci. 83 (1993) 81–150.

[6] B.D. Freeman, I. Pinnau, Gas and liquid separations using membranes: an overview, ACS Symp. Ser. 876 (2004) 1–23.

[7] C.V. Vedavyasan, Pretreatment trends-an overview, Desalination 203 (2007) 296–299.

[8] Y. Yang, H.Wang, J. Li, B. He, T.Wang, S. Liao, Novel functionalized nano-TiO2 loading electrocatalytic membrane for oily wastewater treatment, Environ. Sci. Technol. 46 (2012) 6815–6821.

[9] N. Hilal, O.O. Ogunbiyi, N.J. Miles, R. Nigmatullin, Methods employed for control of fouling in MF and UF membranes: a comprehensive review, Sep. Sci. Technol. 1957 (2005) 1957–2005

[10] B. Saini, M.K. Sinha, S.K. Dash, Mitigation of HA, BSA and oil/water emulsion fouling of PVDF Ultrafiltration Membranes by SiO_2-g-PEGMA nanoparticles, J Water Process Eng. (2018).

Proceedings of theThird International Conference on Sustainable Energy and Environmental Challenges (3rd SEEC)
18 –21 December, 2018, IIT Roorkee, India

SEEC No.048

AN ASSESSMENT ON THE CHARACTERISTICS OF ACID MINE DRAINAGE (AMD) IN NORTH EASTERN PARTS OF INDIA

Shweta Singh
Department of Civil Engineering, Indian Institute of Technology Guwahati, Guwahati, Assam, India.
Email: shwetasingh@iitg.ernet.in

Saswati Chakraborty
Department of Civil Engineering, Indian Institute of Technology Guwahati, Guwahati, Assam, India.
Email: saswati@iitg.ernet.in

ABSTRACT

The characteristic water quality assessment of the mine discharge from different coalmines of Meghalaya and Assam were carried out for its safe discharge onto the land and surface waters. The pH of mine water was found to be mostly acidic, ranging from 2.27 to 2.62. High electrical conductivity (EC) varying from 1.53 to 3.45 mS/cm, accompanied with very high total dissolved solids (TDS) which ranged from 1012 to 1868 mg/L. Mine waters were majorly contaminated with elevated concentrations of anions, especially sulfate (1028 to 1890 mg/L) and to some extent chloride ion (1.23 to 16.92 mg/L). Major contributing cations of AMD were Ca^{2+} and Mg^{2+}, which imparted total hardness to the water and other heavy metals, predominantly iron, aluminium, zinc, cobalt, nickel and manganese were found to be overhead the permissible discharge limit of EPA. In addition, EDAX analysis of nearby soil samples revealed heavy metal contamination due to the untreated discharge of AMD.

***Keywords*:** Acid mine drainage (AMD), Coalmines, Water quality.

INTRODUCTION

Acid mine drainage (AMD) pose a grave threat to ecology and environment owning to its inherent nature of continuous discharge of acidic mine wastewater from active as well as abandoned mines even after decades of closure of mining activity [1]. Due to which the surrounding vegetation, soil and waterbodies get severely affected. AMD is mostly characterized by its low pH in the range of 2–4, high sulfate content, low organic matter and presence of various soluble metals.

The mechanism involved in the formation of acidic mine water from coalmines can be well understood from the subsequent Eqns. (1–3) showing the oxidation of a mineral sulfide (mostly, pyrite as an example) in oxygenated conditions [2]. The ferric iron (Fe^{3+}) produced as per Eqn. (2) is capable of oxidizing pyrite at much faster rate of about 17–180 times even under anoxic conditions as shown in Eqn. (3) [3]. Although bacteria also plays a significant role in carrying out the biological oxidation of mineral sulfides.

$$FeS_2 \text{ (pyrite)} + 3.5O_2 + H_2O \rightarrow Fe^{2+} + 2SO_4^{2-} + 2H^+ \quad (1)$$

$$Fe^{2+} + H^+ + 0.25\ O_2 \rightarrow Fe^{3+} + 0.5\ H_2O \quad (2)$$

$$FeS_2 + 14Fe^{3+} + 8H_2O \rightarrow 15Fe^{2+} + 2SO_4^{2-} + 16H^+ \quad (3)$$

In the present study, some of the mines of northeastern states (i.e. Meghalaya and Assam) were selected to assess the mine water quality as well as the metal contamination in surrounding soil was quantified. Coals occurring in this part of country has distinctive low ash and high sulfur content. The coalmines chosen for the study were Northeastern coalfields Ltd (NEC, a subsidiary of Coal India Ltd) in Assam and mines situated in Jaintia hills of Meghalaya. The NEC coalfield is bounded by latitude 27°15'N to 27°25'N and longitude 95°40'E to 96°5'E, where mine water was collected from opencast mines Tirap colliery (an active mine) and Ledo colliery (declared abandoned recently). The Jaintia hills district of Meghalaya is bounded between latitude 25°5'N to 25°4'N and longitude 91°51'E to 92°45'E. Mine discharge from rat hole mines in Sutnga and Lamyrsiang (near river Wah Myrsiang) were collected and analyzed. Fig. 1 shows the map of the sampling stations.

FIGURE 1. MAP OF SAMPLING STATIONS

MATERIALS AND METHODS

The mine water were collected directly from the mine source and soil samples were also collected from the nearby mining sites (Fig. 2). Periodical sampling were carried out during the months of March–May 2018. All the samples were collected in triplicates. Prior to each sampling, the polyethylene bottles were cleaned and then rinsed twice with milli-Q water. For the measurement of the cations, 250 mL samples were acidified with HNO_3 to bring the pH < 2 and preserved separately. The non-acidified samples were stored for the analysis of anions. pH and EC of the samples were measured in laboratory using Microprocessor pH meter (Labtronics, India) and Digital Conductivity meter– 4 (VSI 04 Deluxe, VSI electronics Pvt. Ltd), respectively. Turbidity was measured using Digital Nephelo–Turbidity meter 132 (Systronics, India). Concentrations of metals (Co, Zn, Fe, Al, Mn, Ni, Mg) were determined using flame Atomic Absorption Spectrophotometer (SpectrAA 55B, Varian) after filtering the samples with 0.45 µm membrane filter. Concentration of cations such as Na^+, K^+ and Ca^{2+} were measured using Flame Photometer 128 (Systronics, India). Chloride and sulfate concentrations were determined using Ion Chromatograph (792 Basic IC, Metrohm); while ammonia concentration was determined using Phenate method as described in APHA [4]. Hardness of the samples were measured using EDTA titrimetric procedure whereas dissolved oxygen (DO) level was measured using permanganate modification [4]. The soil samples were collected in clear plastic bags and later analyzed for the metal concentrations in Atomic Absorption Spectrophotometer (AAS) following HNO_3 and H_2O_2 soil digestion procedure as described in EPA method 3050B [5]. The elemental composition of soil samples subjected to X-ray energy dispersion analysis in SEM/EDAX coupled system (Sigma, Ziess) were performed.

RESULTS AND DISCUSSIONS

The results obtained from the geochemical analysis of water and soil samples collected from different coalmine sites are discussed in the subsequent sections.

FIGURE 2. AMD COLLECTION AT A) SUTNGA, B) LAMYRSIANG, C) TIRAP AND D) LEDO COLLIERY

Coal Mine Water Discharge

The general characteristics of the AMD from the selected coalmines are presented in Tab. 1. The pH of the source AMD varied from 2.27 to 2.62, with an average of 2.41; whereas EC values in these coalmines discharge varied from 1.53 to 3.45 mS/cm (averaged 2.68). Total hardness (TH) varied from 36.67 to 90 mg/L $CaCO_3$ in mine water samples of Meghalaya. However, higher TH values were obtained in water samples of Tirap and Ledo colliery, ranging from 800 to 977 mg/L $CaCO_3$ due to higher concentration of contributing cations Ca^{2+} and Mg^{2+}. The DO level were found to be substantially low in all mine discharges (varied from 1.2 to 3.6 mg/L) majorly due to oxygen consumption during the oxidation process of various sulfide minerals. Total dissolved solids (TDS), which represents the sum total concentration of all dissolved ions ranged from 1012 to 1868 mg/L (averaged 1506 mg/L). Thus, EC and TDS values of water samples from different coalmines seemed to satisfy the correlation [6].

Sulfate was found to be the major dominating anion in both opencast and rat hole mine discharge. The average SO_4^{2-} concentration ranged from 1028 mg/L at Sutnga to 1890 mg/L at Ledo colliery. Higher amount of sulfate content is a very common characteristic of any coalmine water because of the oxidative leaching of sulfide bearing minerals usually present in coals, mostly pyrite (FeS_2) including others such as chalcopyrite ($CuFeS_2$), sphalerite (ZnS), galena (PbS), molybdenite (MoS_2) and tungstenite (WS_2). Chloride concentration ranged from 1.23 to 16.92 mg/L, with an average of 7.60 mg/L. The ammonia concentration ranged from 0.36 to 3.33 mg/L, with an average of 1.43 mg/L.

TABLE 1: WATER QUALITY PARAMETERS OF AMD (AVERAGED VALUES)

Site	pH	EC (mS/cm)	TH (mg/L $CaCO_3$)	DO (mg/L)	TDS (mg/L)	SO_4^{2-} (mg/L)	NH_4^+ (mg/L)	Metals (mg/L)							
								Fe	Al	Zn	Co	Ni	Mn	Mg	Ca
Sutnga	2.420	2.650	90.00	2.150	1640	1028	0.5700	157.8	24.00	0.6093	0.5611	0.6676	1.897	2.265	3.867
Lamyr-siang	2.270	3.440	36.67	1.430	1785	1212	1.428	171.8	28.27	0.2113	1.2900	0.4769	0.3771	1.275	4.067
Tirap	2.620	1.640	800.0	2.400	1066	1602	2.930	11.50	14.07	0.6544	0.2440	0.2120	0.8360	78.83	50.02
Ledo	2.540	1.530	977.0	3.540	1326	1890	3.328	9.407	11.15	0.6261	0.1790	0.1810	1.060	70.41	62.65

Major dominating cations in mine water were divalent Ca^{2+} (ranged from 3.80 to 62.65 mg/L) and Mg^{2+} (ranged from 1.26 to 78.8 mg/L). Relatively lower concentrations of other cations such as Na^+ and K^+, ranged from 2.30 to 10.71 mg/L and 1.2 to 5.19 mg/L, respectively.

Heavy metals contamination in water is another serious concern of AMD, many metal ions (present in dissolved state at lower pH) are often found to be present in mine water under varying range of concentrations depending upon the type of mine and geochemical nature of the underlying rocks. Tab. 1 shows the extent of heavy metals present in coalmine water. Iron was found to be most abundantly present in all the water samples, ranging from 9.41 to 171.58 mg/L, thus surfeiting the desirable limit of 2 mg/L. Aluminium (ranged from 11.15 to 28.91 mg/L) was found to be second most available metal ion exceeding the permissible discharge limit of 5 mg/L set by EPA [7]. Manganese exceeded the permissible limit of 0.2 mg/L in all coal mine water samples. However, zinc was detected to be present in the range of 0.20 to 0.65 mg/L and well below the discharge limit of 2 mg/L in all water samples. The maximum permissible limit of cobalt and nickel metal in any industrial discharge is 0.05 and 0.1 mg/L. In contrast, the amount of Co and Ni detected in all mine water samples were found to be more than the mentioned limit, ranged from 0.18 to 1.4 mg/L and 0.18 to 0.76 mg/L, respectively. Concentrations of other very toxic metals such as cadmium, total chromium and lead were found to fall below the permissible discharge limit of 0.01, 0.05 and 0.05 mg/L, respectively in water samples collected from Sutnga and Lamyrsiang. However, water samples of Ledo and Tirap colliery were found to exceed marginally cadmium and about ten times total chromium permissible concentration.

Soil Contamination

The untreated discharge of coalmine water onto land surface as well as to water bodies leads to ingress of different pollutants into the ecosystem. Thus, the nearby surrounding soil of the mine area were analyzed for the estimation of heavy metal contamination. EDAX analysis showed the chemical and elemental characteristics of the soil samples from different coal mining sites as illustrated in Fig. 3. The EDAX spectrum of the soil samples clearly revealed the presence of the dominating metals i.e., iron and aluminium found in coalmine water discharge as well. However, only to some extent the presence of other heavy metals such as Zn, Co, Ni and Mn were detected in soil samples of Tirap and Ledo colliery. Tab. 2 shows the amount of metals (in mg) present in per gram of the soil samples.

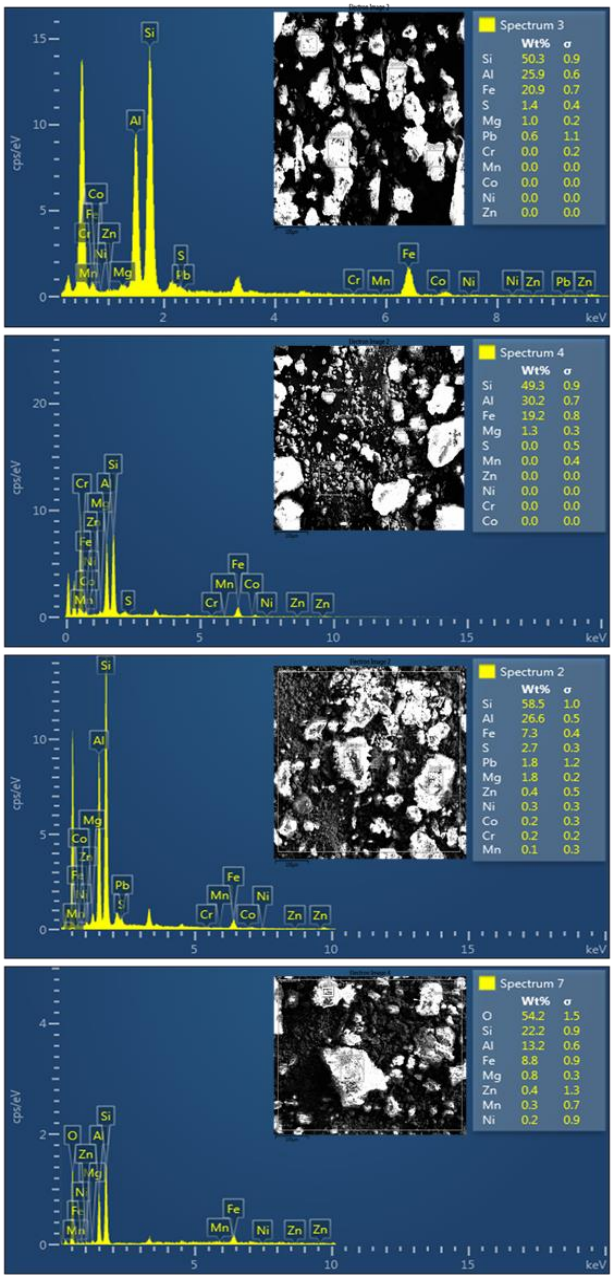

FIGURE 3. EDAX SPECTRUM OF SOIL SAMPLES FROM A) SUTNGA, B) LAMYRSIANG, C) TIRAP AND, D) LEDO COLLIERY

Table 2: METAL CONTENT (mg/g) IN NEARBY SOILS OF COALMINES

Soil	Average metals (mg/g)					
	Fe	Mn	Co	Ni	Zn	Mg
Sutnga	25.21	0.0710	0.5016	0.0060	0.0559	0.8169
Lamyrsiang	19.47	0.0610	0.4536	0.0068	0.0308	0.1851
Tirap	21.24	0.1897	0.0878	0.1003	0.1080	1.229
Ledo	26.78	0.4489	0.0779	0.1007	0.1409	0.5308

Average iron concentration were found to be 25.21, 19.47, 21.24 and 26.78 mg/g for Sutnga, Lamyrsiang, Tirap and Ledo soils, respectively. Manganese concentration in soil samples ranged from 0.06 to 0.45 mg/L. Concentration of other metals such as Co, Ni and Zn in Meghalaya soil samples ranged from 0.43 to 0.51 mg/L, 0.006 to 0.007 mg/L and 0.03 to 0.06 mg/L, respectively. Soil samples from Tirap and Ledo colliery showed comparatively higher concentration of Co, Ni and Zn than Meghalaya soils, ranging from 0.42 to 0.50 mg/L, 0.09 to 0.1 mg/L and 0.11 to 0.14 mg/L, respectively.

CONCLUSIONS

The mine water discharge from the open cast mines of northeastern coalfields and rat hole mines of Meghalaya were found to be extremely acidic (pH 2–3) in nature. Mining activities cause fissures in rock formation and thereby further weathering process escalates the formation of AMD. The geochemical assessment of collected mine water samples shows very high values of EC, TH, TDS, SO_4^{2-}, Fe and other heavy metals exceeding the recommended discharge limit set by EPA, thereby deteriorating the quality of nearby soils. Thus, adapting proper control strategies can improve the water quality. Limestone is the most common chemical treatment practiced for raising the pH but it further adds the cost of chemical and sludge management. Therefore, biologically active (such as sulfidogenic bioreactors) and passive (aerobic/ anaerobic wetlands, compost reactors) treatment systems needs more exploration for AMD remediation.

ACKNOWLEDGMENTS

The authors would like to express their gratitude to the Indian Institute of Technology Guwahati for the infrastructure, instrument facilities and financial assistance as research fellowship. We are also grateful to north-eastern coalfields, Margherita for their assistance during field.

REFERENCES

[1] Colmer, A.R., Temple, K.L. and Hinkle, M.E., 1950. "An iron-oxidizing bacterium from the acid drainage of some bituminous coal mines". Journal of bacteriology, 59(3), Mar, pp. 317–328.

[2] Singer, P.C. and Stumm, W., 1970. "Acidic mine drainage: the rate-determining step". Science, 167(3921), Feb, pp. 1121–1123.

[3] Zheng, C.Q., Allen, C.C. and Bautista, R.G., 1986. "Kinetic study of the oxidation of pyrite in aqueous ferric sulfate". Industrial & Engineering Chemistry Process Design and Development, 25(1), Jan, pp. 308–317.

[4] Standard Method for the Examination of Water and Wastewater, 21st ed., American Public Health Association (APHA), Washington (2005).

[5] U.S. Environmental Protection Agency. 2007. Method 3050B: Acid digestion of sediments, sludges, and soil. 3rd ed. Office of Solid Waste, Washington, pp. 1–12.

[6] Metcalf, Eddy, I., Tchobanoglous, G., Burton, F. and Stensel, H.D., 2002. Wastewater Engineering: Treatment and Reuse, 4th ed. McGraw-Hill Education. New York, Chap. 2, pp. 56–57.

[7] Environmental Protection Act, 2002. Standards for Effluent Discharge Regulations. General Notice No. 44. of 2003. Available from: http://faolex.fao.org/docs/texts/mat52519.doc (accessed 27.09.18).

Biodiesel production from microalgal oil using mixed oxide base catalyst

Authors:
Reena Singh and Prof.Yogesh Chandra Sharma

Abstract

Spirulina platensis was cultivated in a vertical aligned photobioreacter for biodiesel synthesis. The culture was harvested by centrifugation and subsequently obtained biomass was dried in oven. Oil extraction was carried out solvothermally in microwave at 60°C for 30 min and 750 w. The mixed metal oxide (Barium-calcium-Zinc) heterogeneous catalyst was synthesized and used in biodiesel synthesis from *spirulina* oil. The catalyst was characterized by using a number of techniques viz TGA-DSC, powder XRD, ATR-FTIR, SEM-EDX, and surface area analyser. The optimization study was performed on several reaction parameters such as temperature, time, molar ratio, catalyst weight and stirring speed. The maximum FAME conversion was found to be 98.94% at optimized parameter of 2.5 wt% catalyst, 1:18 molar ratio (methanol:oil), 600 rpm stirring speed and 65°C temperature for 120 min. Reusibilty test of catalyst was approved up to six cycle with 69.56 %. Basic site of catalyst was a function of catalyst activity which relay on barium content. Kinetic parameters have been evaluated by applying pseudo first order kinetic equation for transesterification of spirulina oil. The activation energy (Ea) for the catalyzed transesterication reaction found to be 48.02 kJ mol^{-1}.

Introduction

The rapid increment in population with industrialization and living standards of the society in the world are the major cause of the energy scarcity and global warming. The continuous decreasing in fossil fuel reservoir and increasing environmental pollution have compelled scientist to examine the suitable alternative source of energy.[1, 2] Biodiesel has emerged as the alternative source of the diesel fuel. Biodiesel is not only renewable but also

biodegradable, eco-friendly and non-toxic.[3] Biodiesel is carbon neutral i.e. no net accumulation of CO_2 in the atmosphere. Biodiesel exhibits relevant properties like petroleum diesel and it also certifies with high flash point, high cetane number, low viscosity and high lubricity. Biodiesel has the potency to achieve economic with environmental sustainability and accomplish the world energy demand.[4] Biodiesel is the mixture of mono alkyl ester of long chain fatty acid which is derived from feedstock (containing major component of triglyceride) such as the vegetable oil, animal fat and microalgal oil by the esterification or transesterification or both process. These process depend upon the free fatty acid of feedstock and type of catalyst (acid and basic) which is used in the biodiesel synthesis.[5] Feedstock selection also performs main role to decide the total biodiesel production cost.[6] Recently microalgae have been reported as potential feedstock over the conventional oil crops for biodiesel production. Microalgae have high photosynthesis rate and high lipid productivity as compare to the conventional oil crops.[7] The lipid content of microalgae is about 15-300 times higher than the conventional oil crops.[8] Besides this, microalgae have many aptitudes such as high growth rate, non-food sources, not require arable land for their growth and acquire 1.8 gm of CO_2 per 1gm of dry biomass during cultivation period.[9] So it is helpful to reduce the CO_2, the main global warming increasing factor in the environment. Therefore, microalgae has drawn much attention in order to reduce the total cost of biodiesel production and make to easily applicable at commercial level with environmental sustainability. Besides biodiesel production, microalgae also produce other biofuel such as biomethane and bioethanol.[10] In addition the biofuel, microalgae can be used as animal feed, cosmetic product and valuable pharmaceutical product. This makes the microalgal based biodiesel more economically feasible as compared to the conventional oil crop. Shin et al reported biodiesel production from *scendesmus sp*., Guldhe et al have studied on *scenedesmus obliquus* microalgae and found 90.81% of conversion in biodiesel production. Sharma et al.

have studied on chlorella vulgaris and obtained 84.03% yield by acid based catalyse transesterification in microwave assisted reactor. H. I. EI-Shimi et al have repoteted biodiesel production from *spirulina platensis* microalgae and 84.7% conversion was observed by using acid homogenous catalyst. Mostafa and Gendy also published article on biodiesel synthesis from *spirulina platensis* and examined its fuel properties and its blend with petro diesel.

The most predominant method for Biodiesel synthesis is the transesterification of triglycerides with alcohol in the presence catalyst (homogenous/heterogeneous). Numerous heterogeneous catalysts have been reported such as alkali-doped oxide, alkali earth metal oxides, acid solids, mixed metal oxides and hydrotalcites in biodiesel synthesis.

Nowadays, heterogeneous base catalyst was frequently used at large scale due to fast reaction, easy separation and no demands of large amount of water for biodiesel washing. It can be revitalized and recycled many times. In addition, heterogeneous base catalyst is cheaper, less corrosive and environment friendly as compared to homogenous catalyst. CaO catalyst has been widely used as heterogeneous base catalyst in large scale production of biodiesel due to cheap, easily available, high catalytic activity and long catalyst life. However leaching properties of CaO catalyst was also examined in transesterfication reaction. Therefore some supports have been used to improve the stability of CaO catalyst. Cao mainly perform as active component in mixed metal oxide catalyst for methanolysis reaction. ZnO is inactive catalyst for transesterification, some researchers ZnO used as supporting material for active catalyst preparation. ZnO is pours material having large surface area and prevents the lixivation of the active phase. Alkali metals can be added to increase the base strength and catalytic activity of CaO. MacLeod et al. have studied the doping effect the of alkali metals salt ($LiNO_3$, $NaNO_3$, and KNO_3) and showed the better catalytic activity of CaO in the transesterifincation reaction. Watkins et al. also reported the

effective tranesterificaction by $LiNO_3$ impregnated CaO catalyst. Kesic et al. prepared CaO.ZnO catalyst and studied the catalytic activity of CaO.ZnO by adding different amount of K_2CO_3. To our best knowledge no study was investigated on the performance of barium impregnated CaO-ZnO catalyst in transesterification of microalgal oil.

The main intention of present work is microalgal cultivation, lipid extraction and synthesis of barium impregnated CaO-ZnO mixed oxide catalyst. The synthesized catalyst was characterised and used for transesterification of *spirulina* oil. The optimum condition of reaction parameter (catalyst weight, temperature, molar ratio, and time) and reusability of the catalyst was investigated. Kinetic study of transesterification process was also executed to determine the activation energy and the value of pre-exponential factor from Arrhenius plot.

1. Pan, H., et al., *Mesoporous polymeric solid acid as efficient catalyst for (trans)esterification of crude Jatropha curcas oil.* Fuel Processing Technology, 2016. **150**: p. 50-57.
2. Rawat, I., et al., *Biodiesel from microalgae: A critical evaluation from laboratory to large scale production.* Applied Energy, 2013. **103**: p. 444-467.
3. Baskar, G., I. Aberna Ebenezer Selvakumari, and R. Aiswarya, *Biodiesel production from castor oil using heterogeneous Ni doped ZnO nanocatalyst.* Bioresource Technology, 2018. **250**: p. 793-798.
4. Gardy, J., et al., *Synthesis of Ti(SO4)O solid acid nano-catalyst and its application for biodiesel production from used cooking oil.* Applied Catalysis A: General, 2016. **527**: p. 81-95.
5. Malins, K., et al., *Synthesis of activated carbon based heterogenous acid catalyst for biodiesel preparation.* Applied Catalysis B: Environmental, 2015. **176-177**: p. 553-558.
6. Farooq, W., et al., *Water use and its recycling in microalgae cultivation for biofuel application.* Bioresource Technology, 2015. **184**: p. 73-81.
7. Chueluecha, N., A. Kaewchada, and A. Jaree, *Enhancement of biodiesel synthesis using co-solvent in a packed-microchannel.* Journal of Industrial and Engineering Chemistry, 2017. **51**: p. 162-171.
8. Zhuang, L.-L., et al., *Soluble Algal Products (SAPs) in large scale cultivation of microalgae for biomass/bioenergy production: A review.* Renewable and Sustainable Energy Reviews, 2016. **59**: p. 141-148.
9. Suganya, T., et al., *Macroalgae and microalgae as a potential source for commercial applications along with biofuels production: A biorefinery approach.* Renewable and Sustainable Energy Reviews, 2016. **55**: p. 909-941.
10. Hernandez, D., et al., *Biofuels from microalgae: Lipid extraction and methane production from the residual biomass in a biorefinery approach.* Bioresource Technology, 2014. **170**: p. 370-378.

Proceedings of theThird International Conference on Sustainable Energy and Environmental Challenges (3 SEEC) 18 –21 December, 2018, IIT Roorkee, India

SEEC No. 050

EFFECT OF INTERCOOLER ON THE PERFORMANCE PARAMETERS OF AXIAL FLOW COMPRESSOR

Vimal Patel
Assistant Professor
Mechanical Engineering Department
Sardar Vallabhbhai National Institute of Technology, Surat
vimal.iitbombay@gmail.com

Mohsinali Batti
Research scholar
Mechanical Engineering Department
Sardar Vallabhbhai National Institute of Technology, Surat
vimal.iitbombay@gmail.com

ABTRACT

Performance of gas turbine and jet engine highly depends upon the performance of its compressor. In present investigation, attempt is made to investigate the effect of intercooling on compressor performance. The compressor efficiency generally depends on temperature rise or entropy generation of gas during flow from compressor blades. Higher blade temperature or irreversibility leads to high power requirement and subsequently loss of efficiency. In addition, high blade temperature leads to increase thermal stress on compressor blades. In present investigation, the effect of intercooling is investigated on the performance parameters of highly loaded compressor blades using numerical simulation using AxStream software. The effect of intercooling is investigated for efficiency, power output and temperature condition of the blades. The current simulation indicates 239.51kW of power shaving using appropriate intercooler.

Keywords: *Gas turbine, Inter cooling, Compact turbine, AxStream, Axial flow compressor, compressor*

NOMENCLATURE

p_{si}	Averaged work coefficient $p_{si}=\frac{H}{U_2^2}$
P_{hi}	Averaged work coefficient $p_{hi}=\frac{C_{2s}}{U_2}$
eff_tt	Total to total efficiency
N	Power required
H	Heat loss
Om	Total pressure loss coefficient
D_{eqx}	Equivalent diffusion factor
R	Degree of reaction
AC	Axial compressor
G_{out}	Outlet mass flow rate
Ps	Static pressure
Pt	Total pressure
eff_pt	Polytrophic efficiency
c	Absolute velocity
W	Relative velocity
U	Blade velocity
A	Flow angle
B	Blade angle
K_1	Blade inlet metal angle
K_2	Blade outlet metal angle

I. INTRODUCTION

Due to high power to weight ratio, the applications of gas turbine extensively blowouts, specifically in the field of aircraft propulsion. In the industrial gas turbine, there is not such strict requirement of size and weight of the plant, even exit velocity of the gas from the gas turbine plant can be kept as low as possible. It has an ability to produce full power from cold condition within very short time; hence it is generally used for peak load plant and emergency applications i.e. standby plants for the hydroelectric power plants. Today, the gas turbine is used in several different modes in industries such as power generation, oil and gas, marine propulsion, process plants, Transport, and smaller related industries, as well. Due to vast applications, large growth for gas turbine technology observed in the last 20 years. This development is spear headed by the increase in compressor pressure ratio, advanced combustion techniques, improved technology for materials, the appearance of new coatings and new cooling schemes. The main limitation of the gas turbine is, large amount of the power, developed by the turbine, is utilised to operate the compressor. Hence, net power output is quite less compared to the other types of the power plants. In the present investigation, the attempt is made to investigate the reduction in the power requirement to the compressor with appropriate location of the intercooler and to analyse its effect on other parameters. The effect of intercooling on degree of reaction, flow and work, losses, static and total pressure, power requirement are investigated in the present investigation.

II. PRELIMINARY DESIGN

For preliminary analysis, design of high pressure compressor is considered without use inter cooler. The preliminary considered data for the investigation are shown in Tab. 1. The working fluid is considered as ideal gas and total 20 stages are considered for the investigation.

The preliminary calculations are carried out using AxStream software. From the available physible solutions from the preliminary design sets, a solution which is best match with the requirements is selected for the further analysis. The values of the initial output

values, which are calculated form the AxStream software are indicated in the Tab. 2

Table 1 Preliminary considered data for investigation

Sr. No.	Parameter	Value
1	Inlet total pressure	101.3kPa
2	Inlet total temperature	15 ºC
3	Total Outlet pressure	2000kPa
4	Mass flow rate	24.9kg/s
5	IGV exit angle	70deg
6	Rotational speed	10747rpm

Using the preliminary considered parameters, flow path and blade shapes are derived from AxStream software. The temperature rise along the axial direction of the compressor is shown in Fig. 1, along with the calculated power required (N), politropic efficiency (eff_pt), total to total efficiency (eff_tt) and mass flow rate (Gout).

Table 2 Output derived from AxStream

Sr. No.	Parameter	Value
1	Volume flow rate at outlet	2.2031m^3/s
2	Specific flow rate	0.0039
3	Average work coefficient	0.2323
4	Average flow coefficient	0.5268
5	Heat drop	-356731J/kg
6	Specific speed	0.10702

Figure 2 indicates the losses associated with different stages, along the axial flow direction. It is observed that, at the starting stage losses are high due to large fluctuation of inlet gas and higher abstract ratio. Later, the losses decrease at second and third stage but there after again it increases due to the temperature rise.

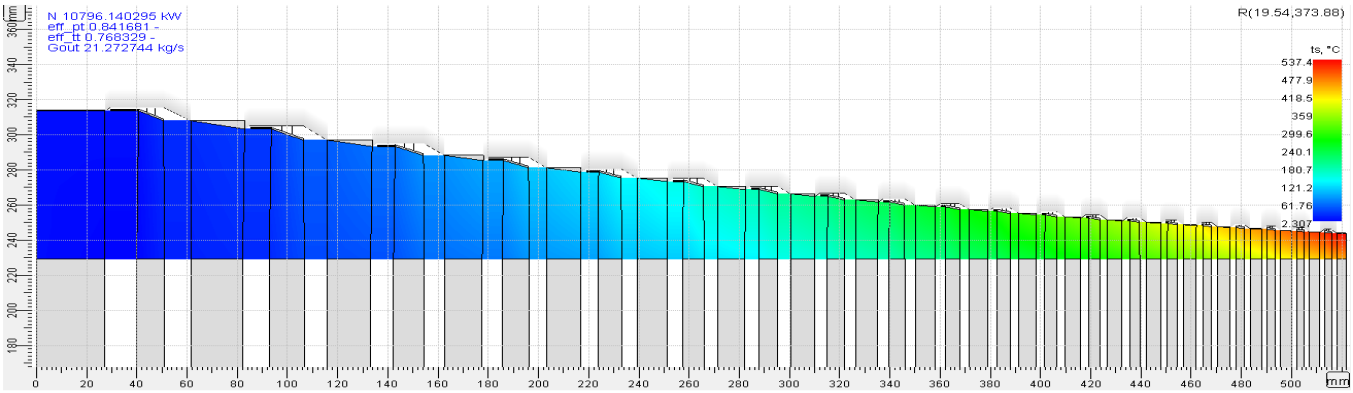

Figure 1. Temperature variation along the flow path without intercooler

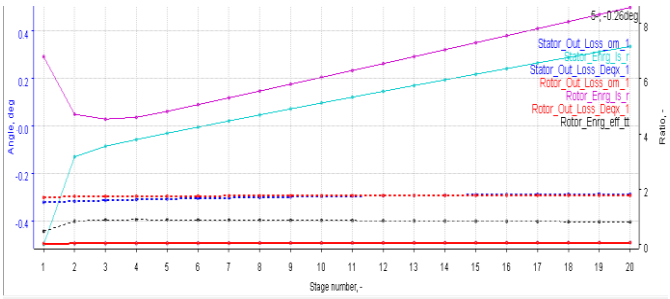

Figure 2. Rotor and stator losses associated at different stages

Figure 3 shows the variation of degree of reaction, flow coefficient and work coefficient at different stages of the compressor. The degree of reaction in first stage is maximum because in first stage load is higher compare to the other stages.

Figure 4 indicates the pressure variation in each stage. The static pressure inlet, total pressure exit and static pressure exit is gradually increases along the axial direction.

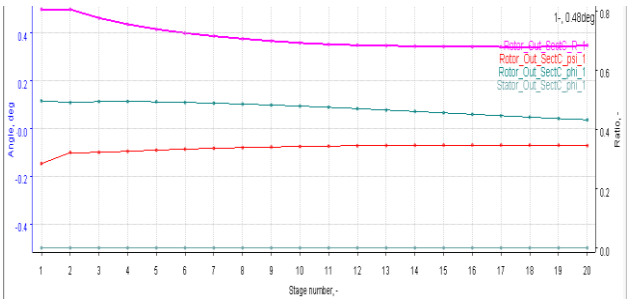

Figure 3. Degree of reaction, flow and work coefficient

Figure 5 indicates the power requirement at different stages, along the axial direction of the rotor. In the present investigation, intercooler is arranged after sixth stage. Figure 6 and 7 represents velocity triangle and pressure variation at the seventh stage.

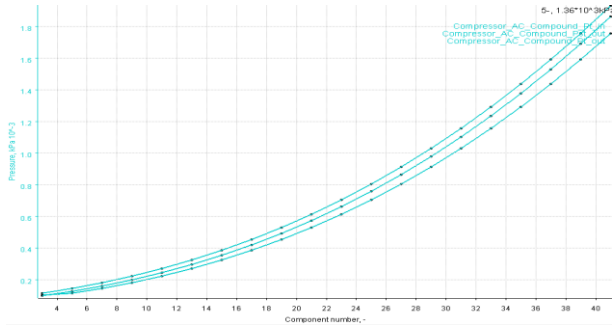

Figure 4. Static & total pressure outlet and total pressure inlet

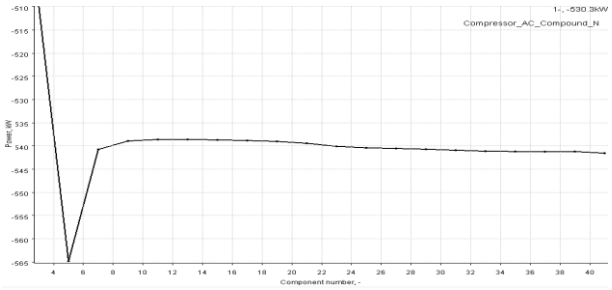

Figure 5. Power requirement at different stages

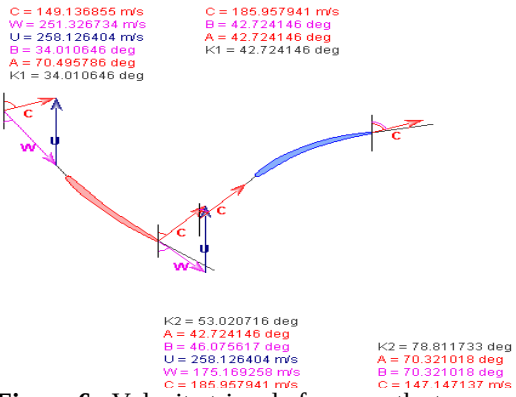

Figure 6. Velocity triangle for seventh stage

III. MODIFIED DESIGN

The design is modified using intercooler after the sixth stage. Same preliminary data for the investigation is consider the case of without intercooler.

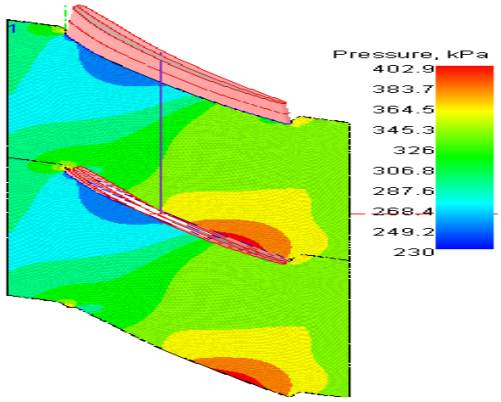

Figure 7. CFD calculation for seventh stage rotor

The temperature of gas enhances due to energy transferred from the compressor. The effectiveness of intercooler is considered as 0.8. The revised flow path and variation of the gas temperature along the axial direction is shown in Fig. 8. Tab. 3 indicates the comparison between different compressor parameters with using intercooler and without use of inter cooler.
Figure 9 indicates the stator and rotor losses associated with the different stages. Due to use of intercooler energy removes from the gas. Also presence of the intercooler creates the pressure loss, after the sixth stage.

Table 3. Comparison between performances of both the compressors.

Parameter	Without intercooler	With intercooler	Difference
Power[kW]	10796.14	10556.63	239.51
Total to total Efficiency	76.86%	86.25%	9.36%
Polytropic efficiency	84.16%	90.65%	6.49%
Mass flow rate [kg/s]	21.27	23.35	2.08

Figure 10 indicates the degree of reaction associated with different stages. To overcome the pressure between the stages 6 and 7, the degree of reaction also suddenly enhances. However, in later stages, it normalized.

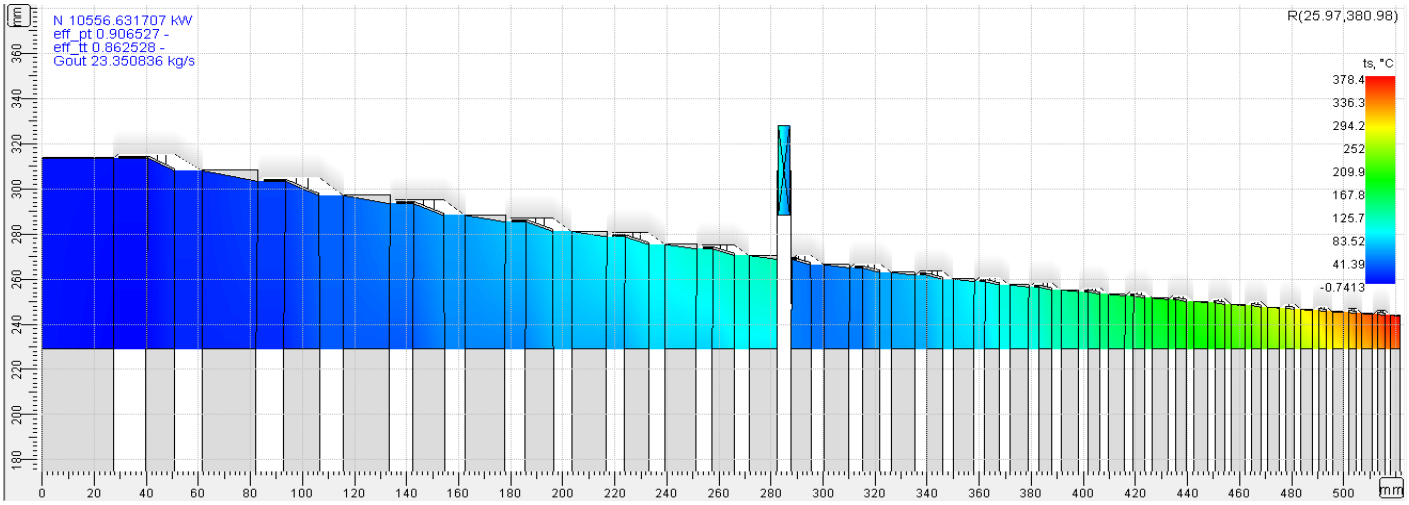

Figure 8. Flow path with intercooler

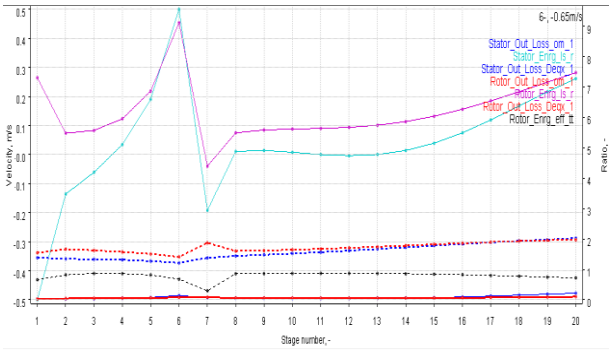

Figure 9. Losses with intercooler

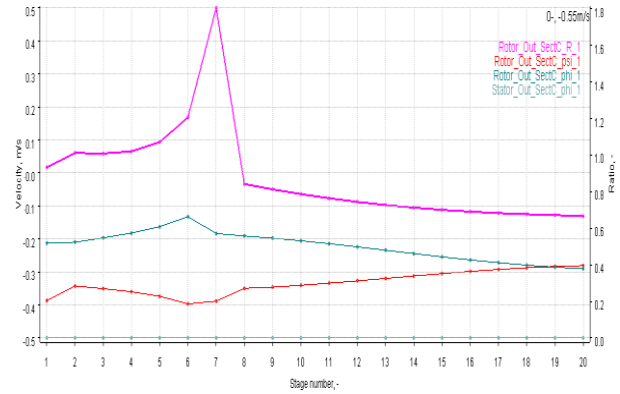

Figure 10. Degree of reaction with intercooler

Figure 11 and 12 indicates the variation of the pressure and power required at different components along the axial direction. Due to the presence of the intercooler, the total static pressure at inlet changes abruptly. After the seventh stage the pressure increase gradually.

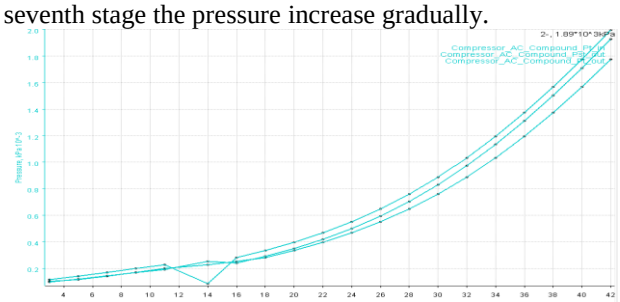

Figure 11. Static and total pressure with intercooler

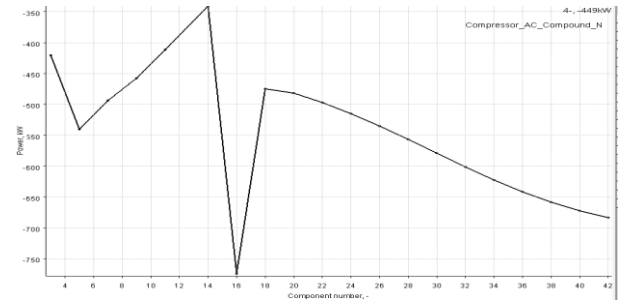

Figure 12. Power graph with intercooler

Also, due to no mechanical energy gain by the gas from the compressor and energy transferee from the gas to inter cooler, the power required along the path of intercooler is drastically falls.

Figure 13 indicates the absolute velocity, flow angle, blade angle and metal angle for both stator vane and rotor vane specifically for the seventh stage. It can be observed that, with use of the intercooler, the absolute velocity of gas at the rotor vane inlet and outlet is higher than the case of without use of inter cooler. The reason is the enhancement of the compressor capacity in form of mass flow rate. Figure 14 represents pressure variation at the seventh stage.

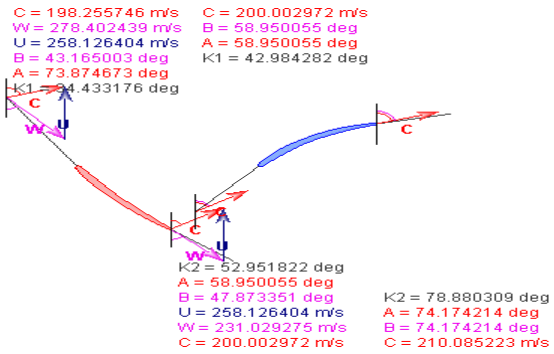

Figure 13. Velocity triangle for seventh stage

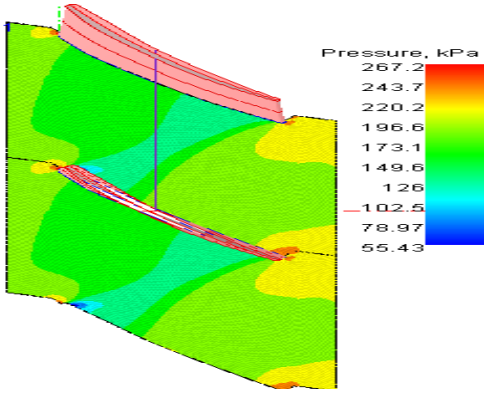

Figure 14. CFD analysis for seventh stage rotor.

IV. CONCLUSION

Present investigation indicates the effect of intercooler on power requirement, efficiency and heat loss of compressor. The investigation is carried out without using the intercooler and with use of the inter cooer using AxStream software. The investigation indicates the reduction of the compressor work requirement up to 239.51kW. The total efficiency and polytropic efficiency increases by 9.36 % and 6.49 % respectively. The modified design reduce the blade stresses compare to old design due to lower temperature in the later stages of the compressor blades, so it increases the blade life and decrease internal irreversibility. The additional benefit is the outlet pressure and mass flow rate also increase by use of the intercooler.

REFERENCE

[1] Boiko, A.V., Govorushchenko, Y.N., Yershov, S.V., Rusanov, A.V. and Severin, S.D., 2002. Aerodynamic Computation and Optimal Projection of Turbomachine Flow Paths. *Kharkov, NTU "KhPI.*

[2] Miller, M.J., Durschmidt, D.F., Medlock, A. and Sandel, W.A., 2004, January. An Integrated Design System for Fans, Compressors, and Turbines: Part 1—Overview. In *ASME Turbo Expo 2004: Power for Land, Sea, and Air* (pp. 1573-1582). American Society of Mechanical Engineers.

Proceedings of the third International Conference on Sustainable Energy and Environmental Challenges (3rd SEEC)

18 –21 December, 2018, IIT Roorkee, India

SEEC No.051

PERFORMANCE ANALYSIS OF PbS COLLOIDAL QUANTUM DOT SOLAR CELL AT DIFFERENT ABSORPTION COEFFICIENT

ANKITA SHARMA
Dept. of Electronics and Communication Engineering
Madan Mohan Malaviya University of Technology
Gorakhpur, India
ankitasharma6397@gmail.com

RAVI SHANKAR YADAV
Dept. of Electronics and Communication Engineering
Madan Mohan Malaviya University of Technology
Gorakhpur, India
ravisy1992@gmail.com

Dr. BRAMHA P. PANDEY
Dept. of Electronics and Communication Engineering
Madan Mohan Malaviya University of Technology
Gorakhpur, India
pandey.bramha@gmail.com

ABSTRACT

This paper is based on the modelling of absorption model for PbS colloidal quantum dot solar cell using SCAPS. The main objective is to predict the best absorption coefficient (cm^{-1}) for the PbS colloidal quantum dot (CQD) at which the solar cell performance can be improved. In the present work, the modelling and simulation have been performed for the five different absorption model included in CQD layer and obtained different performance parameter such as open-circuit voltage (V_{oc}), short-circuit current (J_{sc}), fill factor (FF) and power conversion efficiency (PCE). The best absorption coefficient (cm^{-1}) is 10^5 having V_{oc}, J_{sc}, FF and QE (quantum efficiency) values are 1.64V, 7.6 mA/cm^2, 0.91 and 47.2%, respectively. The quantum efficiency significantly changes with the absorption coefficient (cm^{-1}) for the 250nm to 1050nm wavelength range.

Keywords- Colloidal quantum dot, Absorption coefficient, Open circuit voltage (V_{oc}), Short-circuit current (J_{sc}), Fill factor (FF) and Power conversion efficiency (PCE).

INTRODUCTION

The incredible supply of solar energy is received by earth through the sun[1]. Solar power is a renewable resource that is freely available. A solar cell is a type of electrical device that uses the sun energy i.e. light and converts directly into the electricity. The conversion of sun energy (light) into electricity is caused by the phenomenon of photovoltaic effect, which is a chemical and physical phenomenon[2].The solar cell material have some property in order to absorb sunlight. There are basically two configuration of solar cell. The conventional solar cells can use light absorbing material as one single layer or can use multiple physical configuration for various charge separation and absorption mechanism[3]. The solar can be categorized into first, second and third generation solar cells[4]. Polysilicon and monocrystalline silicon materials are included in the first generation solar cell . First generation solar cell are also known as traditional, conventional or wafer based solar cells[5,6]. Second generation cells are thin film solar cell, that includes CdTe, CIGS and amorphous silicon. It avoid the use of silicon wafer and have lower consumption of material[7,8]. Third generation solar cells made up of organic materials such as polymer or small molecules. Dye sensitized and perovskite cells are also used in the third generation [9,10,11].

Quantum dots which is working as the absorbing photovoltaic material used in quantum dot solar cell (QDSCs) [12]. In this paper, lead chalcogenide (PbS) CQD as the absorbing photovoltaic material is used[13]. Colloidal quantum dots (CQDs) used in photovoltaic and optoelectronic devices for wide application such as solar cells, photo detectors and light emitting diodes due to their low temperature fabrication, low cost, high stability and their peculiar photovoltaic and optoelectronic properties[14]. CQDs are also attracted much attention for their solution based processing which is advantageous for their integration into the variety of the solar cells [15,16].

In this work, the solar cell CQD are constructed with the three different layer i.e. p-type CQDs as the absorbing layer, MZO (MgZnO) as the buffer layer and n-type metal oxide layer (such as ZnO). The absorption coefficient (cm^{-1}) is defined in the PbS CQD-TBAI layer and improved performance of the CQDs solar cell with respect to absorption coefficient is simulated. To enhance the quantum efficiency through selecting the best absorption coefficient, there is construction and comparison of different absorption model for PbS-TBAI CQD layer and calculated the V_{oc}, J_{sc}, FF and QE.

A SINGLE SOLAR CELL MODEL

A CQD solar cell device architecture with a buffer layer (BL) of MZO is shown in Figure 1. The ZnO layer is firstly deposited on the surface of a cleaned FTO glass with a thickness of ~40 nm and subsequently there is a deposition of MZO layer with a thickness of ~20nm. The deposition of CQD is on the surface of MZO layer and this layer working as a light absorber layer in solar cell device. With the bilayer

of tetrabutylammonium iodide (TBAI) and 1,2-ethanedithiol (EDT) performance of PbS QDs improved and result in higher signal to noise ratio (SNR), broader linear dynamic range (LDR), several times faster light response and many times higher detectivity[13]. Finally, the device designing completed with the thermally deposition of an electrode that is Au on the top of the surface of the CQD-EDT layer as shown in figure 1 [16]. The device become different and more efficient by the adding the absorption model in the PbS-TBAI material.

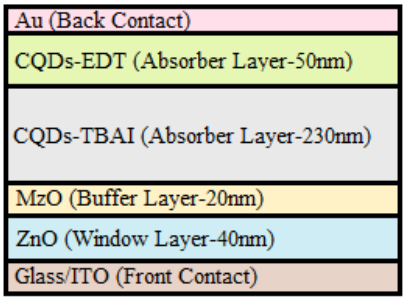

Figure 1: Architecture of single CQD solar cell device [16].

MATERIALS PARAMETER

The materials parameter used for the simulation is tabulated in following table.

Table 1: Details of Material parameter in SCAPS simulation. Part of these material parameter are taken from literature [16,18,19].

	PbS EDT	PbS TBAI	ZnO (or MZO)
Thickness (nm)	50	230	60 (40+20)
Bandgap edge (eV)	1.2	1.2	3.2(or up shift)
Electron affinity (eV)	3.9	4.15	4.3
Permittivity (er)	20	20	66
CB/VB DOS (cm^{-3})	10^{19}	10^{19}	10^{19}
Electron mobility (cm^2/Vs)	$2x10^{-4}$	$2x10^{-2}$	$5x10^{-2}$
Ndonor (cm^{-3})	10^{14}	10^{15}	10^{17}
Nacceptor (cm^{-3})	10^{16}	10^{15}	0
Radiative recombination coefficient (cm^3/s)		10^{-3}	
EDT/TBAI defect (neutral)	Total density (integrated over all energies) (cm^{-2}): 10^{16}		
Capture cross section (cm^2)	$1.2x10^{-13}$	$1.2x10^{-13}$	
Position below Ec (eV)	0.5	0.5	
Density (cm^{-3})	10^{16}	10^{17}	
TBAI-ZnO interface defects (neutral)	Total density (integrated over all energies) (cm^{-2}): 10^{16}		
Capture cross section (cm^2)			10^{-19}
Position above Ev (eV)			0.6
Density (cm^{-3})			10^{16}

In these parameter there are two most important parameter which are added in this work. The first parameter is radiative recombination coefficient and second parameter is absorption coefficient. The current is converted from the p-contact hole current to the n-contact electron current in diode. It shows that somewhere in the diode recombination must take place. So the recombination should define at least one place (in a layer, at a contact or at an interface) in the diode.

The absorption coefficient (α) can be set from an experimental data file or from a model. The absorption coefficient for PbS CQD material is 10^5 (cm^{-1}). The α(λ) can be measured using the following equation [17];

$$\alpha(\lambda) = \left(A + \frac{B}{hv}\right)\sqrt{hv - Eg} \quad (1)$$

where α, hv and Eg are absorption coefficient (cm^{-1}), photon energy (eV) and energy band gap (eV) respectively. A and B are wavelength dependent absorption constant.

RESULT AND DISCUSSION

In order to improve the system there are different calculation for different absorption coefficient to explore its performance under various operative conditions. In this work the model is simulated at five absorption coefficient (cm^{-1}) i.e. at 10^3, 10^4, 10^5, 10^6 and 10^7 respectively which is added in PbS-CQD layer. The calculation is made under dark and light illumination. In the dark illumination calculation the working point voltage is zero. In the light illumination the simulation is done at the open circuit voltage (V_{oc}). At the five absorption coefficient (cm^{-1}) i.e. 10^3, 10^4, 10^5, 10^6 and 10^7 there are different measurement which is as following table:

Table 2: Different calculated value (V_{oc}, J_{sc}, FF and QE) for the different absorption file.

	V_{oc} (V)	J_{sc} (mA/cm^2)	FF	QE (%)
10^3 (cm^{-1})	1.89	0.177	0.92	2.78
10^4 (cm^{-1})	1.8	1.58	0.92	18.34
10^5 (cm^{-1})	1.64	7.6	0.91	47.2
10^6 (cm^{-1})	3.53	17.51	0.95	89.39
10^7 (cm^{-1})	7.14	25.85	0.97	98.98

The first simulation of the system is with the 10^3 absorption coefficient (cm^{-1}) in PbS-CQD layer and get the value of V_{oc} and J_{sc} 1.89V and 0.177 mA/cm^2 respectively. The voltage at which no current flows through the external circuit is known as open circuit voltage (V_{oc}) [20]. The calculation of FF from V_{oc} is done by the following equation [9]:

$$FF = \frac{voc - \ln(voc + 0.72)}{voc + 1} \quad (2)$$

In which, $voc = \frac{Voc}{(mkB\frac{T}{q})}$

Therefore, from the Eq.(2), the value of FF is 0.9284. The quantum efficiency graph for 10^3 absorption coefficient (cm^{-1}) is plotted with open circuit voltage i.e. 1.89V.

The second simulation of the system is with the 10^4 absorption coefficient (cm^{-1}) in PbS-CQD layer and get the value of V_{oc}, J_{sc} and FF 1.8V, 1.58 mA/cm^2 and 0.9256 respectively. Again the quantum efficiency graph for 10^4 absorption coefficient (cm^{-1}) is plotted at the open circuit voltage of 1.8V (V_{oc}).

The third simulation with 10^5 absorption coefficient (cm^{-1}) is consider. After the simulation, value of V_{oc} and J_{sc} are 1.64V and 7.6 mA/cm^2 respectively are obtained. The quantum efficiency is simulated with open circuit voltage of 1.64V. The FF at 10^5 absorption coefficient (cm^{-1}) is 0.9198.

Fourth simulation is with 10^6 absorption coefficient (cm^{-1}) and again after simulating, the value of V_{oc} and J_{sc} are 3.53V and 17.51 mA/cm^2 respectively are obtained. The FF at 10^6 absorption coefficient (cm^{-1}) is 0.9569. The quantum efficiency graph for 10^4 absorption coefficient (cm^{-1}) is plotted with open circuit voltage i.e. 3.53 V.

Fifth simulation is with 10^7 absorption coefficient (cm^{-1}). After simulating, the value of V_{oc} and J_{sc} are 7.14V and 25.85 mA/cm^2 respectively are obtained. The FF at 10^7 absorption coefficient (cm^{-1}) is 0.9761. The quantum efficiency graph for 10^4 absorption coefficient (cm^{-1}) is plotted with open circuit voltage i.e. 3.53 V.

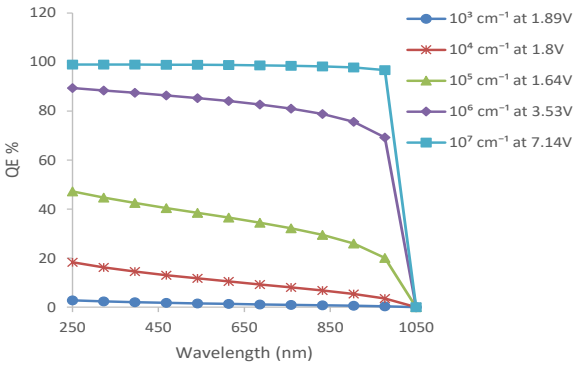

Figure 2: Comparison of different quantum efficiency with different absorption coefficient (cm^{-1}) i.e. 10^3, 10^4, 10^5, 10^6 & 10^7 respectively with their corresponding Voc.

When there is no connection of solar cell to the any load then there is no current flowing and voltage across the solar cell becomes maximum. This is known as open circuit voltage (V_{oc}). Changing the absorption coefficient the V_{oc} are also changed. To show the effect of V_{oc} at different absorption coefficient, there are five absorption coefficients (cm^{-1}) taken, which are 10^3, 10^4, 10^5, 10^6 & 10^7 respectively.

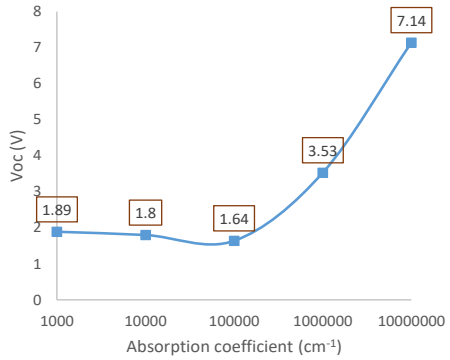

Figure 3: Measurement of V_{oc} with different absorption coefficient.

The changes in J_{sc} over different absorption coefficient is summarizing as following figure;

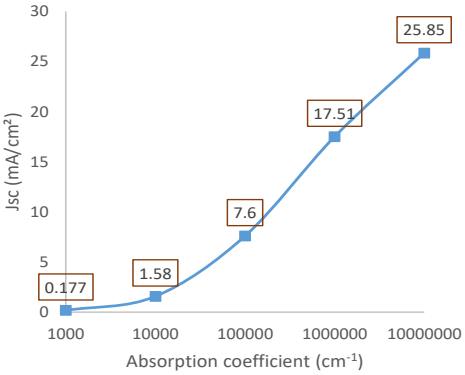

Figure 4: Measurement of J_{sc} with different absorption coefficient.

The fill factor is a measure of quality of solar cell essentially. The FF is also defined as the ratio of maximum power from actual solar cell to the maximum power to the ideal solar cell [10]. The value of FF with different absorption coefficient 10^4, 10^5, 10^6 are different which are shows as following:

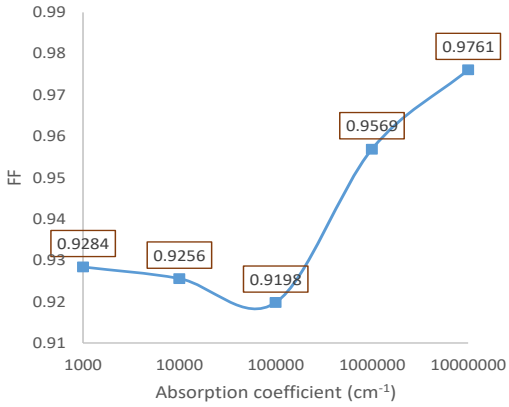

Figure 5: Measurement of FF with different absorption coefficient.

CONCLUSIONS

In this study, the improved performance parameter of solar cell have been calculated using the different absorption coefficient. The value of V_{oc}, J_{sc}, FF and QE vary with the different absorption model including in particular material or layer of solar cell. The different absorption model have been added in quantum dot layer of PbS-TBAI and shows their corresponding results. The best absorption coefficient (cm^{-1}) is 10^5 having V_{oc}, J_{sc}, FF and QE (quantum efficiency) values are 1.64 V, 7.6 mA/cm2, 0.91 and 47.2%, respectively. By introducing the absorption model the efficiency of solar cell is improved significantly. In this work there are five absorption model with five absorption coefficient (cm^{-1}) i.e. $10^{3,}$ 10^4, 10^5, 10^6 and 10^7 and simulating these value at different voltage. The quantum efficiency for $10^{3,}$ 10^4, 10^5, 10^6 and 10^7 are 2.78%, 18.34%, 47.2%, 89.39% and 98.98% respectively.

REFERENCES

[1] Askari Mohammad Bagher, "Solar Cell Quantum Dots"American Journal of Renewable and Sustainable Energy Vol. 2, No. 1, 2016, pp. 1-5

[2] Shruti Sharma, Kamlesh Kumar Jain, Ashutosh Sharma, "Solar Cells: In Research and Applications-A Review", Materials Sciences and Applications, 2015, 6, 1145-1155

[3] Askari Mohammad Bagher, Mirzaei Mahmoud Abadi Vahid, Mirhabibi Mohsen, "Types of Solar Cells and Application", American Journal of Optics and Photonics 2015; 3(5): 94-113

[4] Manjot Kaur, Harjit Singh, "A Review: Comparison Of Silicon Solar Cells And Thin Film Solar Cells", International Journal Of Core Engineering & Management (IJCEM), May 2016

[5] Kiran Ranabhat, Leev Patrikeev, Aleksandra Antal, Kirill Andrianov, Valerii Lapshinsky Frumkin ,Elena Sofronova, "An Introduction To Solar Cell Technology" Journal of Applied Engineering Science 14(2016)4, 405

[6] Andrew Blakersa, Ngwe Zina , Keith R. McIntoshb , Kean Fong," High Efficiency Silicon Solar Cells", Energy Procedia 33 (2013) 1 – 10

[7] Yongye Liang, Zheng Xu, Jiangbin Xia, Szu-Ting Tsai, Yue Wu, Gang Li, Claire Ray, and Luping Yu, "For the Bright Future-Bulk Heterojunction Polymer Solar Cells with Power Conversion Efficiency of 7.4%", Adv. Mater. 2010, 22, E135–E138

[8] Rasika Ganvir, "Modelling of the Nanowire Cds CdTe Device Design for Enhanced Quantum Efficiency in Window Absorber Type Solar Cells" 2016.

[9] NandiWu, YiliangWu, Daniel Walter, Heping Shen, TheDuong, Dale Grant, Chog Barugkin, Xiao Fu, JunPeng, Thomas White,Kylie Catchpole,and Klaus Weber, "Identifying the Cause of Voltage and Fill Factor Losses in Perovskite Solar Cells by Using Luminescence Measurements", Energy Technol. 2017, 5, 1827–1835

[10] A.B. Djurisic, F.Z. Liu, H.W. Tam, M.K. Wong, A. Ng, C. Surya, W. Chen, Z.B. He, "Perovskite solar cells - An overview of critical issues", Progress in Quantum Electronics 53 (2017) 1–37

[11] Di Zhou, Tiantian Zhou, Yu Tian, Xiaolong Zhu, and Yafang Tu, "Perovskite-Based Solar Cells: Materials, Methods, and Future Perspectives", Journal of Nanomaterials 2018.

[12] Lan X, Vozny O, Kiami A, Garcia De Arquer FP, Abbas As, Kim Gh, Liu M, Yang Z, Walters G,xu J, Yuan M, Ning Z, Fan F, Kanjanaboos P, Kramer I, Zhitomirsky D, Lee P Perelgut A, Hoogland S, Sargent Eh, "Passivation Using Molecular Halides Increases Quantum Dot Solar Cell Performance",Adv Mater 2016 Jan 13;28(2):299-304.

[13] Zhenwei Ren, Jiankun Sun, Hui Li, Peng Mao, Yuanzhi Wei, Xinhua Zhong, Jinsong Hu, Shiyong Yang, and Jizheng Wang, "Bilayer PbS Quantum Dots for High-Performance Photodetectors" Adv. Mater. 2017, 1702055

[14] Tianshuo Zhao, Earl D. Goodwin,Jiacen Guo, Han Wang, Benjamin T. Diroll, Christopher B. Murray, and Cherie R. Kagan, "Advanced Architecture for Colloidal PbS Quantum Dot Solar Cells Exploiting a CdSe Quantum Dot Buffer Layer", ACS Nano 2016, 10, 9267−9273.

[15] Chuang, C.-H. M.; Brown, P. R.; Bulović, V.; Bawendi, M. G. Improved Performance and Stability in Quantum Dot Solar Cells through Band Alignment Engineering. Nat. Mater. 2014, 13, 796−801

[16] Xiaoliang Zhang, and Erik M. J. Johansson, "Reduction of Charge Recombination in PbS Colloidal Quantum Dot Solar Cells at the Quantum Dot/ZnO Interface by Inserting a MgZnO Buffer Layer", J. Mater Chem. A, 2017, **5**, 303-310.

[17] Jaymin Ray, Tapas K. Chaudhuri, Chetan Panchal, Kinjal Patel, Keyur Patel, Gopal Bhatt, Priya Suryavanshi, " PbS-ZnO Solar Cell: A Numerical Simulation" in journal of nano electronics and physics-January 2017.

[18] G. H. Kim, F. P. Garcia de Arquer, Y. J. Yoon, X. Lan, M. Liu, O. Voznyy, Z. Yang, F. Fan, A. H. Ip, P. Kanjanaboos, S. Hoogland, J. Y. Kim, and E. H. Sargent, "Nano Lett." 2015, 15, 7691-7696. 3.

[19] M. Liu, F. P. de Arquer, Y. Li, X. Lan, G. H. Kim, O. Voznyy, L. K. Jagadamma, A. S. Abbas, S. Hoogland, Z. Lu, J. Y. Kim, A. Amassian, and E. H. Sargent, "Adv. Mater." 2016, 28, 4142-4148.

[20] Jizhong Yao, Thomas Kirchartz, Michelle S. Vezie, Mark A. Faist, Wei Gong, Zhicai He, Hongbin Wu, Joel Troughton, Trystan Watson, Daniel Bryant, and Jenny Nelson, "Quantifying Losses in Open-Circuit Voltage in Solution-Processable Solar Cells", Phys. Rev. Applied 4, 014020 (2015)

SEEC No. 052

TO INVESTIGATE MACROSCOPIC SPAY CHARACTERISTICS FOR METHANOL BLENDED FUELS

Utkarsha Sonawane
Engine Research Laboratory
Design Program
Indian Institute of Technology Kanpur
Email: utkarsha@iitk.ac.in

Avinash Kumar Agarwal
Engine Research Laboratory
Department of Mechanical Engineering
Indian Institute of Technology Kanpur
Email: akag@iitk.ac.in

ABSTRACT
To meet emissions norms, it is necessary to study the spray characteristics of any new fuel. Methanol has potential for wide use as compared to other alcohols in the automotive sectors. Addition of methanol to gasoline can significantly reduce emissions. Gasohol can be used to reduce the dependence of the transport sector on imported petroleum. The objective of this study is to investigate the macroscopic spray characteristics of different methanol blends (M15, M85, and M100) and gasoline (G100). In this experiment, an injector of a MPFI engine powered motorcycle (500 CC) was used. Macroscopic characteristics such as Spray penetration spray cone angle and spray area were measured. A high-speed camera, image processing software and light source were used to capture the images of the spray at different points in time after the start of injection in order to compare its comparative evolution with respect of baseline gasoline.

Keywords*: *Methanol-gasoline blends, macroscopic spray characteristics.

INTRODUCTION
Traditional fossil fuels are non-renewable sources of energy and expected to get exhausted in a few decades. A large amount of harmful emissions are generated by combustion of such fossil fuels. Therefore it is necessary to find alternative solutions to these fossil fuels in order to meet the prevailing emission standards applicable for various applications in different sectors of the economy. Methanol has been relatively widely used as a fuel supplements/ alternative to petroleum. Methanol is a clean burning, high octane fuel made from natural gas, coal, coal and biomass. Spay characteristics of fuel also affect the emission and performance characteristics of the engine. In this experimental study, we are investigating the macroscopic spray characteristics of various gasoline-methanol blends w.r.t. baseline gasoline such as spay penetration, spray cone angle and spray area.

Sharma et al. [1] performed experiments on a GDI engine to understand the GDI spray characteristics using gasoline, gasoline-ethanol blend (E15) and gasoline methanol blend (M15). They investigated both microscopic and macroscopic characteristics at different fuel injection pressures (FIP) of 40, 80, 120, 160, 200 bars. Microscopic spray characteristics such as arithmetic mean diameter (AMD), and Sauter mean diameter (SMD) were investigated using phase Doppler interferrometry (PDI). Macroscopic characteristics of the spray were evaluated using a high-speed CCD camera. It was found that with increasing FIP, spray penetration length increases. Also, spray droplet size distribution reduced and droplet velocity increased.

Xie et al. [2] investigated macroscopic spray characteristics of biodiesel blends (BD0, BD20, BD50, BD80, and BD100) for different injection pressures (60, 70, 80, 90, 100 MPa) and varying ambient pressures (0.1, 0.3, 0.5, 0.7, 0.9 MPa). Results showed that as the ambient pressure increased, spray cone angle increased and spray penetration decreased. As the fuel injection pressure increased, spray penetration and spay cone angle increased. As blends ratio of biodiesel increased, spray penetration and spray angle decreased due to higher viscosity and surface tension compared to baseline diesel.

Gupta et al. [3] investigated the effect of varying FIP on microscopic and macroscopic spray characteristics of Karanja biodiesel blends and baseline mineral diesel in a constant volume spray chamber (CVSC). The objective of this study was to investigate the effect of different methanol blends and methanol on macroscopic spray characteristics such as spray penetration length, spray cone angle and spray area, as well as microscopic spray characteristics. It was observed that biodiesel blend produced larger sized droplets in large numbers compared to baseline diesel. The spray cone angle of baseline diesel was wider than biodiesel blends. As the fuel injection pressure increased, Sauter means diameter (SMD; D_{32}) and arithmetic mean diameter (AMD; D_{10}) decreased.

Shayan et al. [4] studied the effect of Methanol blends with gasoline (M5, M7.5, M10, M12.5, and M15) on the performance and combustion characteristics of a four stroke, four-cylinder engine with multi-point injection system (Ford, Zetec-E). Performance parameters such as brake torque, brake power, brake thermal efficiency, volumetric efficiency, equivalence air-fuel ratio, and brake specific fuel consumption were evaluated along with regulated exhaust emission characteristics for CO, CO_2, HC, NO_x in the engine speed range of 1500- 5000 rpm. Performance of engine improved with use of methanol and CO and HC emissions reduced with increasing methanol content, while CO_2 and NO_x emissions increased.

From the literature review, It can be summarized that spray characteristics have major effects on the engine performance and emission characteristics. In order to comply with stringed emission norms being adopted in future and fuel efficiency norms, it is important to study spray characteristics of new fuels. In this study, experiments are conducted to analyze three important macroscopic spray characteristics namely spray penetration, spray cone angle and spray area for methanol blends vis-à-vis baseline gasoline for a two wheeler engine using MPFI engine technology.

EXPERIMENTAL SETUP

A cubic spray chamber of 15"x15" was fabricated using flat glass. Experiments were conducted using a MPFI injector of a 500 cc motorcycle (Royal Enfield; Thunderstorm) at ambient temperature and pressure and spray characteristics were evaluated. The experimental setup compromised of a high-speed CCD camera, a fuel injection and control system and an imaging software. Two flicker-free white light sources were used to illuminate the chamber interiors for spray imaging (Figure 1). An Arduino micro-controller based system was customized and used to control the solenoid injector using a custom-fabricated circuit and Arduino software.

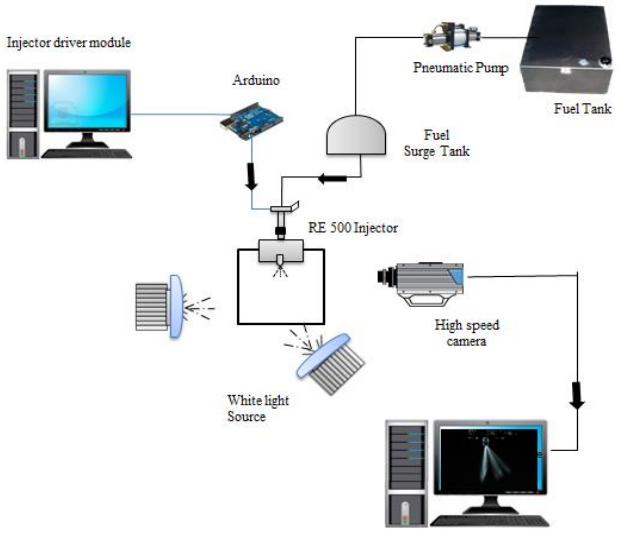

Figure1: Schematic of macroscopic spray characteristisation setup

RESULTS AND DISCUSSION

In the present experimental study, four test fuels namely M15 (15% v/v methanol blended with 85% v/v gasoline), M85 (85% v/v methanol blended with 15% v/v gasoline, M100 (100% v/v methanol) and baseline gasoline (100% v/v gasoline) were investigated to extract information about the Spray penetration, spray cone angle and spray area at different times after the start of spray and the evolution of the sprays was also studied comparatively.

Macroscopic Spray Images

To get a fair estimate of spray characteristics and spray evolution, it is necessary to perform imaging on a single spray plume by avoiding interaction between multiple plumes emerging out of the solenoid MPFI injector. For this, an injector cap was used such that it has only one orifice exposed to the atmosphere and only single spray plume comes out of the injector.

Table 1: Test matrix for macroscopic spray characterization of Methanol blends

	t1	t2	t3	t3	t4	t5
M15	Yes	Yes	Yes	Yes	Yes	Yes
M85	Yes	Yes	Yes	Yes	Yes	Yes
M100	Yes	Yes	Yes	Yes	Yes	Yes
G100	Yes	Yes	Yes	Yes	Yes	Yes

REFERENCES

[1] Nikhil Sharma, Avinash Kumar Agarwal, "Microscopic and Macroscopic Spray Characteristics of GDI Injector Using Gasohol Fuels at Various Injection Pressures" SAE Technical Paper No. 2016-01-0868 (DOI: 10.4271/2016-01-0868).

[2] Hongzhan Xie, Lanbo Song, Yizhi Xie, Dong Pi, "An Experiment to Study on the Macroscopic Spray Characteristics of Biodiesel and Diesel in a Constant Volume Chamber". Energies, 8(6), pp 5952-5972, 2015. (DOI:10.3390/en8065952).

[3] Jai Gopal Gupta, Avinash Kumar Agarwal, "Macroscopic and Microscopic Spay Characteristics of Diesel and Karanja Biodiesel Blends", SAE Technical Paper 2016-01-0869. (DOI: 10.4217/2016-01-0869).

[4] S. Babazadeh Shayan, S. M. Seyedpour, F. Ommi, S. H. Moosavy and M. Alizadeh, "Impact of Methanol–Gasoline Fuel Blends on the Performance and Exhaust Emissions of a SI Engine", International Journal of Automotive Engineering, Vol. 1, Number 3, July 2011.

BIOSORBING POTENTIALS OF *PSEUDOMONAS AERUGINOSA* SFP1 TO COMBAT Cr(VI) STRESS IN *CICER ARIETINUM* SEEDLINGS

Saima Saif*, Mohammad Saghir Khan*

*Department of Agricultural Microbiology, Faculty of Agricultural Sciences, Aligarh Muslim University, Aligarh, Uttar Pradesh-202002

Correspondence to; saima.saif3@gmail.com, Mob no. 9557632645

ABSTRACT:

Hexavalent chromium among metal pollutants is a major threat due to its mutagenic and carcinogenic impacts. Considering these, bacterial strain SFP1 was isolated from metal polluted soil (identified as Pseudomonas aeruginosa using 16SrRNA gene sequencing) showed significant tolerance to Cr (VI) and displayed chromium reducing ability under variable environmental conditions. The dead biomass of the adsorbed chromium maximally at pH 6 and 30±2^{0}C which decreased consistently with increase in Cr concentration. The values obtained for chromium sorption by strain SFP1 using both Langmuir (R^2=0.992) and Freundlich isotherms (R^2=0.999) were strongly and positively correlated. The surface functional groups of dried biomass detected by Fourier transform infrared (FTIR) spectroscopy were amino, carboxyl, hydroxyl, and carbonyl groups. Also SEM-EDX revealed significat deposition of Cr and modification of bacterial cells after Cr(VI) exposure. Also, chickpea seeds primed with SFP1 strain displayed enhanced germination compared with metal treated but uninoculated plants. The present study suggests that the bacteria removes chromium efficiently and hence, could be used for the management of industrial wastes and other environmental contaminants.

Keywords: *Chromium (VI) toxicity, Biosorption, Pseudomonas aeruginosa, Chickpea-Germination*

1. Introduction:

Among heavy metals, Chromium has been described as a priority pollutant by US EPA and is considered carcinogen. Among different oxidation states , the trivalent chromium (Cr (III) and hexavalent chromium (Cr(VI) has been reported to be approximately 100 times more toxic [1] and 1000 times more mutagenic than Cr (III) [2]. Due to limitations of widely employed physico-chemical methods such as high cost and environmentally unfriendly nature, the bioremediation approach using microorganisms have been exploited as an inexpensive and environmentally safe strategy that offers the possibility to destroy toxic chromium to harmless forms [3,4]. Biosorption involving bacteria is efficient method employed for the removal of Cr (VI) from industrial effluents [5] which decrease the concentration of chromium ions in solution. Realizing the chromium threat and importance of microbes in toxicity abatement on the other hand, the present study was aimed at identifying bacteria capable of biosorbing chromium under different conditions and used to assses the bioremeditaion potential using chickpea (*Cicer arietinum* L.)

2. Materials and methods

2.1 Isolation of bacteria, chromium tolerance, identification and phylogenetic tree

The bacterial strain SFP1 was isolated from rhizosphere grown in metal polluted fields of Unnao (26°32'25.0"N 80°29'14.3"E), UP India. The ability of bacterial strains to grow under increasing concentrations of chromium was tested both on solid agar plate and in liquid culture medium. For this, bacterial strains were aseptically streaked on nutrient agar plates supplemented with 100–2000µg/ml potassium dichromate, and checked for growth after incubation at 30±2^{0}C for 48 h. The bacterial strain SFP1 exhibiting the highest tolerance to Cr (VI) was selected for further studies. Chromium containing NB (0-100µg/ml) was inoculated with overnight grown cultures and incubated at 30±2^{0}C for 4 days under continuous shaking (120 rpm) in a rotary shaker. Further SEM micrographs of both untreated and Cr(VI) treated cells was observed for morphological alterations while EDX analysis was carried to determine the metal deposition. The chromium tolerant strain SFP1 was selected and characterised by standard morphological and biochemical methods [6]. The nucleotide sequence of strain SFP1 was analysed commercially by Macrogen Inc,, Seoul, South Korea using the 16S rRNA genes) involving universal primers, 785F (GGATTAGATACCCTGGTA) and 907R (CCGTCAATTCMTTTRAGTTT). The sequence (859 bp) so obtained were analyzed by adopting BLASTn tool (http://www.ncbi.nlm.nih.gov/BLAST) to accurately identify and match the sequence of isolates with the nearest neighbour sequence obtainable at the NCBI database. All the sequence were aligned using Clustal W and the aligned data was used for phylogenetic analysis using MEGA7 by neighbour-joining method with 1000 boot strap replicates.

2.2 Biosorption efficiency

To assess the biosorbing potential of the selected bacterial strain, biomass of SFP1 was produced by growing bacterial culture in nutrient broth (pH 7) at 30± 2^{0}C for 24 h. Cells were harvested by centrifugation (at 8000rpm) for 20 min. Cell pellets were washed three times with distilled water and dry biomass was prepared by overnight vacuum drying (at 90^{0}C). The sorption of chromium by dried dead biomss of SFP1 was determined by batch equilibrium method [7]. For this, metal stock solution was prepared by adding appropriate amount of $K_2Cr_2O_7$ in 100 ml of double distilled water. All set of experiments were conducted employing fixed volume (100 ml) of single metal ion solution in a 250 ml Erlenmeyer flask. Bacterial biomass was exposed to metal solutions for 96h on an orbital shaking incubator (Remi, India) at 160 r/min. Biomass was separated by centrifugation at 8000 rpm for 15 min. and the supernatant was analysed for residual metal concentration by flame atomic absorption spectrophotometer (Model: GBC 932B Plus). Furthermore, the

conditions that influenced the metal removal efficiency by the bacterial strain such as pH (2, 4, 6, 8 and 10), contact time (12h, 24h, 48h, 72h, 96h, 120h) and initial concentration (25, 50, 100, 200, 400 µg/ml) were also studied. .

2.3 Biosorption isotherms and FTIR anlaysis

Biosorption process using batch technique necessitates an understanding of the relationships between metal ions and biosorbent. The biosorption experiments were performed taking into account using the following equation: Metal adsorbed % = $\frac{(C_o-C_f)}{C_o}\times 100$; where C_0 and C_f represent initial and final Cr(VI) concentration. The biosorption capacity was estimated as- $Q=\frac{(C_o-C_f)}{M}\times V$ where Q indicates the extent of adsorbed metal ion onto the biomass surface at equilibrium (mg/l), M signifies the amount of biomass in the suspension (L), and V is the volume of the suspension (L). The Langmuir model considers monolayer accumulation of adsorbents on homogenous biosorbent surface and can be expressed as $Q=\frac{Q_{max}bC_f}{1+bC_f}$. The binding constant ($Q_{max}$,) and the sorbent capacity (b) are estimated by plotting $1/Q$ against C_f [8]. The model simulations for Cr(VI) with the calculated values of K_L and b are given in Fig 5 respectively. The Freundlich isotherm is an experimental model that highlights the adsorption intensity of the sorbent to the biosorbent. The isotherm is applied to depict the reversible adsorption among the adsorbing species and does not consider the monolayer formation. The Freundlich isotherm model can be represented as- $\log Q = \log K_F + (1/n)\log C_f$; A plot of logQ versus $\log C_f$ gives a straight line with slope $b_F = 1/n$ and intercept K_F. The shape of the isotherm can be used to predict whether adsorption system is favourable or unfavourable in a batch adsorption system. Accordingly, the important aspect of Langmuir isotherm was stated in terms of separation factor as $S_F=\frac{1}{(1+bC_0)}$. The bacterial biomass unexposed (control) and exposed to Cr (VI) at concentration of 100 mg/l was obtained by centrifugation (at 8000 rpm) for 15 min. at 4°C was dried at 80^0C. The harvested biomass was washed, dried in oven at 40°C and crushed to powder form after biosorption of chromium ions under the same conditions. For FTIR analysis, a 2.5 mg dried bacterial biomass was mixed and ground with 75 mg of KBr in an agate mortar and was immediately analysed with a spectrophotometer in the range of 400–4000 cm^{-1} with a resolution of 5 cm^{-1} using a FTIR Spectrometer (Thermo Nicolet, Nexus 670).

2.4 Germination assay

Seeds of chickpea (var. avrodhi) were surface sterilized both uninoculated and inoculated were placed on soft agar (0.8%) were amended with different concentrations (25-400 ug/ml) of chromium and growth parameters were measured at 7 days after sowing (DAS). Uninoculated and untreated seeds soaked in water served as control.

2.5 Statistical analysis of data

One way ANOVA, Duncan multiple range test on experimental data were evaluated by the computer software package, SPSS 17 (SPSS Inc., Chicago, USA).

3. Results and Discussion

3.1 Bacterial characterisation, 16SrRNA gene sequencing and phylogenetic tree construction

The bacterial strain SFP1 recovered from metal polluted rhizosphere tested positive for citrate utilization, nitrate reduction, and oxidase test, and hydrolyzed starch and gelatin. The strain however showed variable potential to utilise different carbohydrates (data not shown). Based on morphological and biochemical parameters, the bacterial strain SFP1 was presumptively identified to genus level as *Pseudomonas*. The nucleotide sequence of 16S rRNA of SFP1 obtained was approximately 859 bp in size which was identified as *P. aerugionosa* later on submitted to GenBank (accession number KU522247. A phylogenetic tree constructed by MEGA7 software, based on 16S rRNA partial gene sequence is presented in Fig. 1(a).

3.2 **Chromium tolerance and bacterial growth under chromium stress**

The bacteria strains recovered from the metal polluted soil were screened for their ability to tolerate toxic levels of hexavalent chromium. The strain SFP1 grew well on agar plates amended with 800 mg/l of potassium dichromate. Furthermore, chromium tolerance was proved by growing strain SFP1 in NB medium treated with different concentration of Cr (VI). Strain SFP1 continued to grow well until 200 mg/l of Cr (VI), but the bacterial population decreased thereafter, with prolonged lag period of 8 h. Also SEM images revealed significant alteratins in cell surface compared to untreated cells while the EDX showed desition of Cr at cell surface (Fig 1(b)). The reduction in growth, however, at higher concentrations of Cr (VI) could possibly be due to altered genetic composition and metabolic and physiological responses of bacteria under stress [9].

3.3 Biosorption studies and optimisation studies

In the present study, the biosorption efficiency of *P. aeruginosa* SFP1 was investigated. Strain SFP1 showed the sorption of chromium under different conditions of pH, temperature and initial Cr (VI) concentration. It was observed that an increase in the initial metal concentration resulted in a gradual decrease in the percentage removal of chromium. For example, it was 89.48% at 25 mg /l while it was 89.02% at 50 mg/l initial Cr (VI) concentration. The rate of biosorption was influenced by (i) competition among increasing chromium molecules for the available binding sites on the bacterial surface and (ii) the restriction of movement of chromium ions due to changes in charge distribution at high Cr(VI) concentrations [10]. Among different pH tested, the maximum removal of chromium occurred at acidic pH for the biosorbent and the sorption capacity increased constantly from pH 2 to 6.0 which decreased drastically thereafter. The maximum biosorption however, occurred at pH 6 (90.5%). As the pH of the solution affects different species of chromium in the solution [11] and the ionization states of the functional groups present on the biosorbent. Also, the

decrease in chromium removal rate with the increase in pH beyond pH 6 might be due to the osmotic changes and hydrolyzing effect [12]. The maximum biosorption was observed at 120 hr (89%) and it was observed that metal uptake increased in contact time from 12h to 96h however, till 120h there was no significant increase in the biosorption attaining an equilibrium position. The rapid adsorption in the initial hours of exposure followed by equilibrium supports the metal adsorption models that involves adsorption and desorption that depends on residence time between the adsorbing species [13].

3.4 Biosorption isotherms and functional group characterisation on cell surface

The metal ions deposited at the bacterial surface including cell wall is generally represented by conventional isotherms. In biosorption studies, the term Freundlich and Langmuir isotherm models represents heterogeneous and homogeneous processes of biosorption, respectively (Fig 2). From the calculated maximum metal uptake (Q) Langmuir isotherm, the achievable Cr uptake was 78.7 mg/gdw. It was observed that the Freundlich isotherm performed better than Langmuir isotherm because of their higher r^2 . The Freundlich constants where K_F (1.15 mg/.gdw) corresponded to the binding capacity (maximum adsorption capacity), and b_F (1.0341) characterises the affinity (adsorption intensity) between the isolates (sorbent) and Cr (sorbate) (Fig. 6). The separation factor (S_f) indicates the shape and nature of biosorption process and principally the separation factor value between 0 and 1 represents favourable isotherm. It has been discovered that the adsorption is irreversible when $S_f = 0$ while linear adsorption occurs when $S_f = 1$ [14]. Our results in this respect were favourable according to adsorption equation because all values of S_f were >0 and less than 1 at all the tested concentrations of chromium (0.453-0.049). Since, both adsorption of Cr to the biological surface of *P. aeruginosa* and conjugation of Cr to the functional groups present in the cell wall occur simultaneously, it indicated a heterogeneous binding process While comparing the FTIR spectra of untreated cells (control) with Cr (VI) treated cells, Cr (VI) treated cells showed several distinct, medium and weak bands at different wavelength. From Fig. 3, it was evident that the peak appearing before metal loading 3294 cm^{-1} was stretched to 3303 cm^{-1} which indicates the presence of amine and hydroxyl group (Park et al. 2005). The peak at 2967 cm^{-1} could be due to the–CH stretch in the biomass [15]. After contacting with the metal solution, -COO shifted from 1403 to 1405 cm^{-1} suggesting the affinity of carboxyl group to metal ions. The shift in 1400 cm^{-1} band is due to the vibration of O–H carboxylate ions. The peak around 1243 cm^{-1} shows the presence of carboxyl group. The peak at 1541 and 1458 cm^{-1} reveals the presence of C=O which plays a vital role in the chromium biosorption [16].

3.5 Enhancement of seed germination by metal tolerant strain SFP1

A considerable decline in chickpea growth was observed which further increased with increasing concentration of toxic chromium (Table 1). However, chickpea seeds inoculated with strain SFP1 showed better growth even in the presence of chromium. At 400 µg Cr/ml, the radicle length and shoot length was remarkably reduced each by 85%. In contrast, inoculated plants exhibited improved growth and reduction in radicle length (81.5%) and shoot length (80.7%) was significant at 400 µgCr/ml. This reduction in growth may be due to the toxic effect of chromium leading to inhibition of protein synthesis [17]. Also, it was observed that the seedling growth was enhanced maximally in presence of strain SFP1 at lower concentrations of chromium than at higher concentrations. The growth enhancement by inoculated seeds may be attributed to the both the chromium reducing and biosorbing ability of strain SFP1 which limits the toxic effect of chromium.

4. Conclusion

The Cr (VI) tolerant Gram negative strain SFP1 possessed significant biosorbing potential and reduced the toxic levels of Cr (VI) under different environmental variables. Also, the chromium tolerant strain enhanced the growth of chickpea even under metal stress. Considering these, *P. aeruginosa* SFP1 may be developed to optimize their viability and biological activity under field applications to be efficiently used for bioremediation of chromium contaminated soils.

5. Acknowledgements

One of the author, Saima Saif would like to acknowledge the UGC, Delhi for the financial assistance provided under the Maulana Azad National fellowship scheme and the USIF, AMU for providing the SEM analysis for completing the work.

9. REFERENCES

[1] Novotnik, B., Zuliani, T., Scancar, J. and Milacic, R. 2014 Inhibition of the nitrification process in activated sludge by trivalent and hexavalent chromium, and partitioning of hexavalent chromium between sludge compartments. *Chemosphere.* **105:**87–94.

[2] Barrera, L.M., Jimenez, F.M.G., Moreno, A.O., Urbina, E.C., 2008. Isolation, identification and characterization of a *Hypocrea tawa* strain with high Cr(VI) reduction potential. Biochem Eng J 40:284–292.

[3] Cicatelli, A., Guarino, F., Castiglione, S., 2017. Reclamation of Cr-contaminated or Cu-contaminated agricultural soils using sunflower and chelants. Environ Sci Pol Res.1-8.

[4] Kang, C., Wu, P., Li, L., Langfeng, Yu., Bo Ruan, Beini Gong, Nengwu, Zhu., 2017 Cr (VI) reduction and Cr(III) immobilization by resting cells of *Pseudomonas aeruginosa* CCTCC AB93066: spectroscopic, microscopic, and mass balance analysis. Environ Sci Pollut Res 24: 5949.

[5] Fatnassi, I.C., Chiboub, M., Saadani, O., Jebara, M., Jebara, S.H., 2015. Impact of dual inoculation with *Rhizobium* and PGPR on growth and antioxidant status of *Vicia faba* L. under copper stress. Comptes rendus biologies, 338:241-254.

[6] Holt, J.G., Krieg, N.R., Sneath, P.H.A., Staley, J.T., Williams, S.T, 1994. Gram negative aerobic/microaerophilic rods and cocci, in: Bergey's Manual of Determinative Bacteriology, ninth ed., Williams and Wilkins, Lippincott, Philadelphia 93 168.
[7] Khodaverdiloo, H., Samadi, A., 2011. Batch equilibrium study on sorption, desorption, and immobilisation of cadmium in some semi-arid zone soils as affected by soil properties. Soil Res 49:444–454.
[8] Bilgili, M.S., 2006. Adsorption of 4-chlorophenol from aqueous solutions by xad-4 resin: Isotherm, kinetic, and thermodynamic analysis. J Hazard Mat 137:157-164.
[9] Losi, M.E., Amrhein, C., Frankenberger, W.T., 1994. Environmental Biochemistry of Chromium. Rev Envi Contamin Toxicol 36:91–121.
[10] Horsfall Jr, M., Ogban, F., Akporhonor, E.E., 2006. Sorption of chromium (VI) from aqueous solution by cassava (*Manihot sculenta* CRANZ) waste biomass. Chem. Biodivers. 3: 161-173.
[11] Kumar, M., Pal, A., Singh, J., Garg, S., Bala, M., Vyas, A., Khasa, Y.P., Pachour, U.C., 2013 Removal of chromium from water effluent by adsorption onto *Vetiveria zizanioides* and Anabaena species. Nat. Sci. 5:341–348.
[12] Fomina, M., Gadd, G.M., 2014. Review Biosorption: Current perspectives on concept, definition and application. Bioresour Technol. 160:3-14.
[13] Zhang, H., Hu, X., Lu, H., 2017. Ni (II) and Cu (II) removal from aqueous solution by a heavy metal-resistance bacterium: kinetic, isotherm and mechanism studies. Water Sci Tech: wst 2017275.
[14] Gupta, S., Babu, B., 2009. Removal of toxic metal Cr(VI) from aqueous solutions using sawdust as adsorbent: equilibrium, kinetics and regeneration studies. Chem Eng J 150:352–365.
[15] Clothup, N.B., Daly, L.H., Wiberley, S.E., 1990. Introduction to Infrared and Raman Spectroscopy. 3rd edition, Academic Press, Inc., London. 310-319.
[16] Hassen, R., 2013. Biosorption of chromium by using *Spirulina* sp. Arabian J. Chem. 1-8.
[17] Medda, S., and Mondal, N.K., 2017. Chromium toxicity and ultrastructural deformation of *Cicer arietinum* with special reference of root elongation and coleoptile growth. An Agr Sci.

Tables and Figures

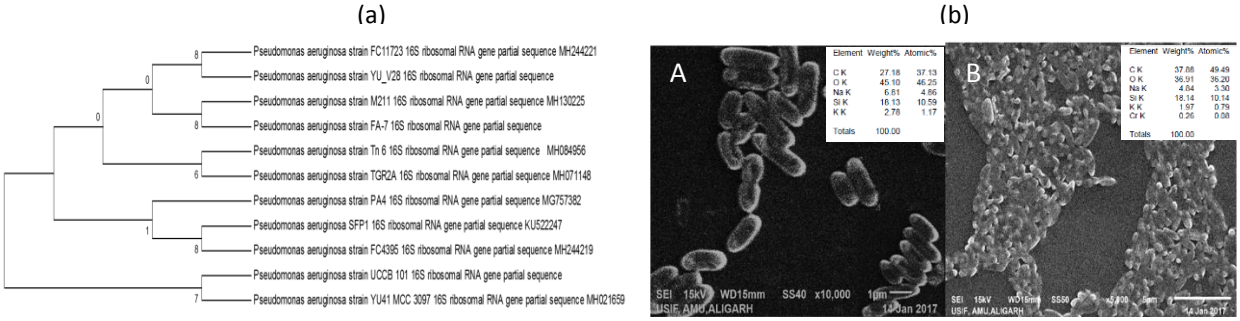

Fig 1. (a) Phylogenetic analysis based on 16S rRNA comparison of 859bp showing relationship between *Pseudomonas aeruginosa* **SFP1** (GenBank accession no. KU522247) and other closely related *P. aeruginosa* strain and values at node represents percentage of 1000 bootstrap replicates. (b) Effect of Chromium concentrations (µg/ml): 0 and 200 on growth of *P. aeruginosa* as observed under SEM.

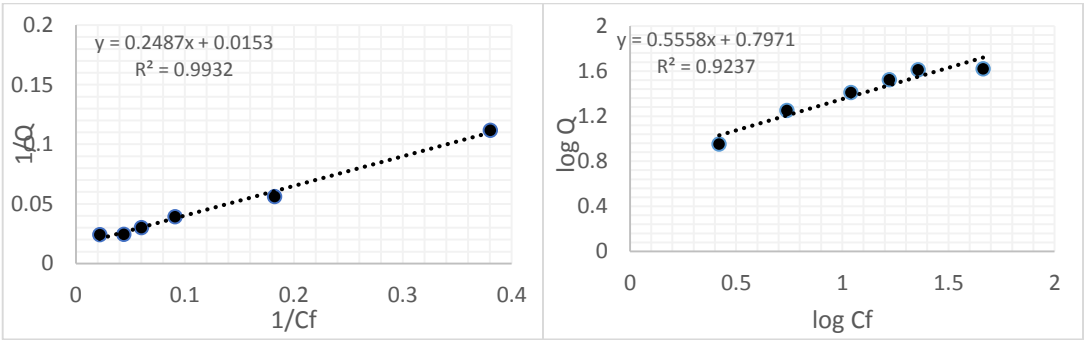

Fig 2. Linearised Langmuir (a) and Freundlich (b) adsorption isotherm for heavy metal ions on biosorbent biomass of *Pseudomonas aeruginosa* SFP1.

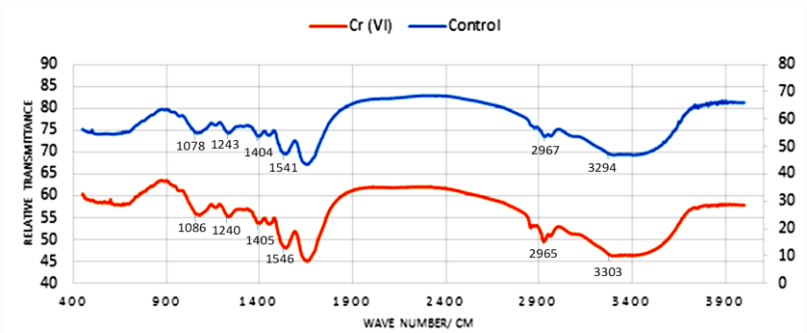

Fig 3. FTIR spectra of *P. aeruginosa* prepared in KBr disks: control and Cr(VI)-treated.

Table 1. Effect of heavy metals and PGP activity of strain SFP1 on germination attributes of chickpea after 7 days of incubation.

Treatment	Dose rate (µg/ml)	Germination percentage		Mean Shoot length (cm)		Mean Radicle length (cm)	
		Uninoculated	Inoculated	Uninoculated	Inoculated	Uninoculated	Inoculated
Control	0	100	100	5.4±0.8a	6.7±1.2a	7.8±0.8a	9.2±0.5a
Chromium	25	98	100	4.7±0.3b	6.5±0.8b	6.5±1.2b	7.2±0.7b
	50	85	90	3.8±1.2c	5.9±1.3b	4.5±1.5c	6.4±0.3b
	100	80	84	2.5±0.4d	4.8±0.7c	3.6±0.5d	5.3±0.5c
	200	60	79	1.7±0.4d	3.7±0.4d	3.0±0.4d	4.6±1.0d
	400	50	63	0.8±0.7f	1.0± 0.1e	1.2±0.2e	1.5±0.9e
F vlaue	-	-	-	19.2	18.9	47.3	42.4

Values indicate mean of three independent replicates. Uninocualted: No bacteria; Inoculated: *P. aeruginosa* SFP1. Means followed by similar alphabets are not significantly different from each other according to post hoc Turkey's HSD.

Proceedings of International Conference on Sustainable Energy and Environmental Challenges (3rd SEEC), December 18-21, 2018, IIT Roorkee, India

SEEC No.058

BIODEGRADATION OF HEXAVALENT CHROMIUM BY ACCLIMATIZED *PSEUDOMONAS PUTIDA*: OPTIMIZATION AND KINETIC STUDY

Ravi Kumar Sonwani, Prarabdh Jain, Balendu Shekhar Giri, Ram Sharan Singh, Birendra Nath Rai*

Department of Chemical Engineering & Technology Indian Institute of Technology (BHU), Varanasi-221005, Uttar Pradesh, India

E-mail: raviks.rs.che16@itbhu.ac.in; prarabdh.jain.che16@itbhu.ac.in

Paper No. 58

ABSTRACT

Hexavalent Chromium (Cr (VI)) is considered as precedence pollutants since they are inimical to organisms and classified as precarious pollutants because of their adverse effects on human health and environment. USEPA has set the maximum permissible limit of Cr (VI) for domestic uses of water is 0.05 mg/L. In the present work, the acclimatized culture of Pseudomonas putida (MTCC 1072) was used during the biodegradation study. The process variables such as pH, temperature, and process time were optimized and found to be 7.0±0.2, 35±2 °C, and 8.0 days, respectively in the batch reactor. The optimized process condition was used to scale up the batch reactor. The maximum removal of 86.4% was observed at optimum condition. The growth and inhibition kinetics were studied using Monod and Andrew-Haldane model and found to be μ_{max}*: 0.154 day*$^{-1}$*; Ks:22.35mg/L by Monod while* μ_{max}*: 0.247 day*$^{-1}$*; Ks: 23.51 mg/L; 42.34 mg/L by Andrew – Haldane.*

Keywords*: Pseudomonas putida, Hexavalent chromium, Kinetic study, Bioreactor*

Highlights

- *Process parameters such as pH, temperature, and process time were optimized.*
- *Acclimatized Pseudomonas putida was used during biodegradation process.*
- *Maximum removal of 86.4% was found at optimized condition.*
- *Kinetic parameters were studied using Monod and Andrew-Haldane model.*

Introduction

The industrial effluents contain Cr (VI) which is one of the most toxic heavy metal and is carcinogenic, mutagenic, and is a concern for the environmentalist (Pandey et al., 2016). It has adverse effect on human and aquatic life. Industrial processes like leather tanning, electroplating, steel production, textile industries and chromate preparation discharge effluent that contains chromium ions (Sultan and Hasnain 2017). Chromium is the major industrial pollutant found in the wastewater and it exists in nature in their valence states from -2 to +6 in solution (Shukla et al., 2012). According to World Health Organization and Environmental Protection Agency of the USA, the maximum permissible limit of Cr (VI) for domestic use of water is 0.05 mg/L. Based on the literature survey, various chemical and physical methods have been used to the removal of hexavalent chromium from wastewater. The method such as chemical reduction (Qim et al., 2005), precipitation (Gheju and Balcu 2011; Kongsricharoern et al., 1996), ion exchange, reverse osmosis, adsorption and electro dialysis are efficient methods for the removal of Cr (VI). But these methods generate secondary pollutant and require high operating cost (Zahoor and Rehman 2005). To overcome these demerits, bioremediation can be used for removal of Cr (VI), as it is cost-effective and an environment friendly technique. Bioremediation of Cr (VI) was studied by Nandi *et al.*(2015) in wastewater and found that blue-green algae has the ability for bioremediation of Cr (VI). Similarly, Shimei *et al*. (2015) isolated two strains of bacteria from chromium contaminated soil and observed that species were able to remove Cr (VI) in wastewater.

To the best of our knowledge, very few works are available on the kinetic study of Cr (VI) biodegradation. Keeping this fact in the mind, the aim of study is to optimize the process parameter alongwith kinetic study using Monod and Andrew-Haldane model. In the present study, the acclimatized culture of *Pseudomonas putida* was used in biodegradation of Cr (VI).

Materials and Methods

Chemical and culture medium

An analytical grade (>99% purity) potassium dichromate was acquired from Sigma-Aldrich to the preparation of Cr (VI) stock solution. The acclimatization of bacterial culture was performed in mineral salt medium (MSM) which was supplemented with 25 mg/L of Cr (VI). This process was repeated thrice by gradually increasing the Cr (VI) concentration to acclimatize the *Pseudomonas putida*. The composition of MSM (g/L) was; KH_2PO_4:1.5

(g/L), Na_2HPO_4:1.5 (g/L), NaCl: 2 (g/L), $CaCl_2.2H_2O$: 0.2 (g/L), $MgSO_4.7H_2O$: 0.3 (g/L), and yeast extract: 2.0 (g/L) (Mahmood et al., 2013). Initially, the stock solution was filtered through 0.22 µm filtration unit to sterilize the solution.

Batch Study

The batch experiment was performed in Erlenmeyer flasks containing sterilized MSM, $K_2Cr_2O_7$ (40 mg/L), and inoculated with 2.0 mL *Pseudomonas putida* culture. The flasks were incubated at 37 °C and 120 rpm in rotary shaker (NSW 256) for 10 days. The scale up process was performed in a cylindrical borosilicate reactor of 1424 mL (Fig. 1). The treated samples were taken at regular interval for the analysis of residual Cr (VI). The samples were centrifuged at 8000 rpm for 15 min and supernatant was used to measure the Cr (VI) concentration using 1, 5-diphenylcarbazide (DPC) method at 540 nm (APHA, 2005).

The pellets of centrifuged samples were re-suspended in same amount of distilled water (DW) and optical density of bacterial suspension was measured by UV-Vis spectrophotometer (ELICO SL 210) at 600 nm (Kumari et al., 2016). The percentage removal of Cr (VI) was measured by following equation:

$$\% \text{ Removal} = \left(\frac{C_i - C_f}{C_i}\right) \times 100 \quad (1)$$

where, C_i is the initial Cr (VI) conc. (mg/L) and C_f is the final Cr (VI) conc. (mg/L).

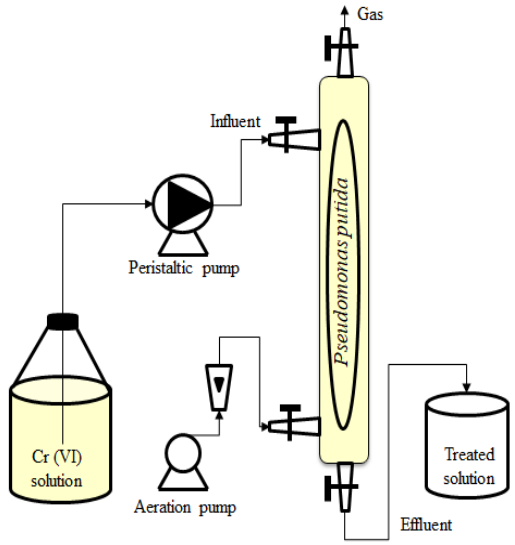

Fig. 1 Schematic diagram of experimental set up.

Kinetic study

The kinetics of Cr (VI) degradation is related to the specific growth rate of microorganisms. Monod model was used for calculation of specific growth rate. The experimental data of log phase was used to estimate the specific growth rate eq.(2)

$$\mu = \frac{1}{X}\frac{dX}{dt} = \frac{\mu_{max} S}{K_s + S} \quad (2)$$

where, X_o is the intial biomass concentration (mg/L); X is the biomass concentration (mg/L) at time t (day); µ is the specific growth rate (day^{-1}); μ_{max} is the maximum specific growth rate (day^{-1}); S is the substrate concentration (mg/L).

When the concentration of substrate was increased, the Monod model was irrelevant due to substrate inhibition. The substrate inhibition was well studied by Andrew-Haldane Model using eq.(3)

$$\mu = \frac{\mu_{max} S}{K_s + S + \frac{S^2}{K_i}} \quad (3)$$

where K_i is the substrate inhibition constant (mg/L).

Results and Discussion

Process optimization

The effective degradation of substrate during biological process depends on the process variables such as pH, temperature, substrate concentration, and process time. The effect of process time on Cr (VI) removal has been shown in Fig. 2. As shown in the Fig. 2, by increasing the time from 0 to 2 days, the removal increased by 16.2%. The maximum Cr (VI) removal efficiency was observed to be 76.8% on 8th day of process and above this no increment was found.

The pH of the solution was varied from 5 to 10. As can be seen in Fig. 3, by increasing the pH at constant time and temperature, the removal increased up to 7.0 pH and on further increasing pH to 10, the removal decreased. The maximum Cr (VI) removal was obtained to be 76.7% at 7.0 pH. Poornima *et al.* (2010) reported the maximum removal of Cr (VI) was obtained at the optimum pH 7.

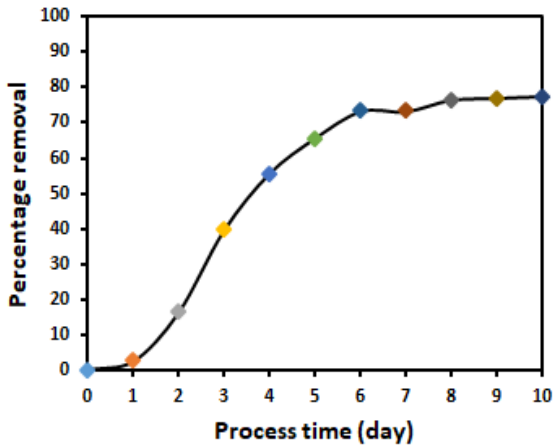

Fig. 2 Effect of process time on biodegradation of Cr (VI)

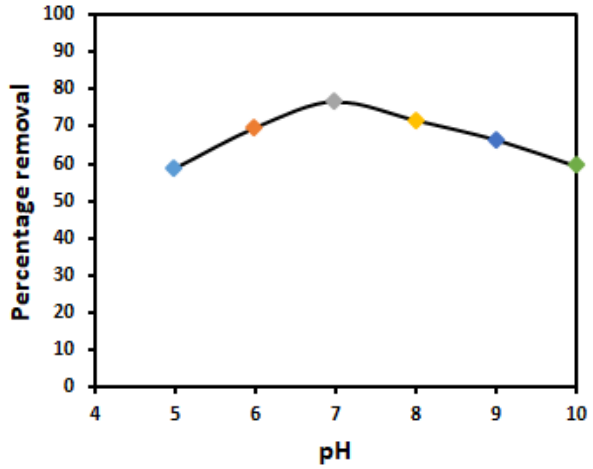

Fig. 3 Effect of pH on biodegradation of Cr (VI)

Temperature of the process is one of the important factor that affects the biological process. In the present work, temperature of the process was varied between 25-45 °C. As can be seen in Fig. 4, by increasing the temperature, the response was increased up to 35 °C and further increase in the temperature, the removal of Cr (VI) decreased. The maximum removal was observed to be 81.3% at 35°C (Fig. 4). The obtained result was similar to Polti *et al*. (2014), which reported that the maximum removal was obtained at 35 °C.

.

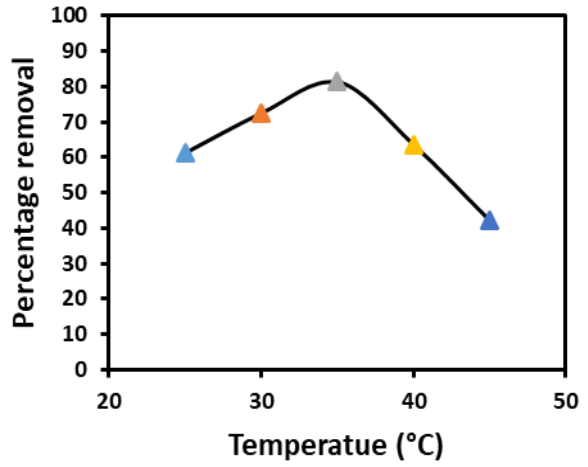

Fig. 4 Effect of temperature on biodegradation of Cr (VI)

The optimized process conditions (pH 7.0, temperature 35.0°C, and process time 8.0 days) was used to scale up the batch process. For this, a cylindrical borosilicate reactor of volume 1424 mL was fabricated and operated at optimized condition. Fig. 5, represents the biodegradation of Cr (VI) in scale up bioreactor at optimized condition. Initially, the rate of Cr (VI) removal (%) was slow which futher increased with process time. As shown in the figure, the amount of Cr (VI) decreased with increasing process time. The equilibrium of Cr (VI) removal was observed in 8.0 days. The maximum removal efficiency was observed to be 86.4% (Fig. 5).

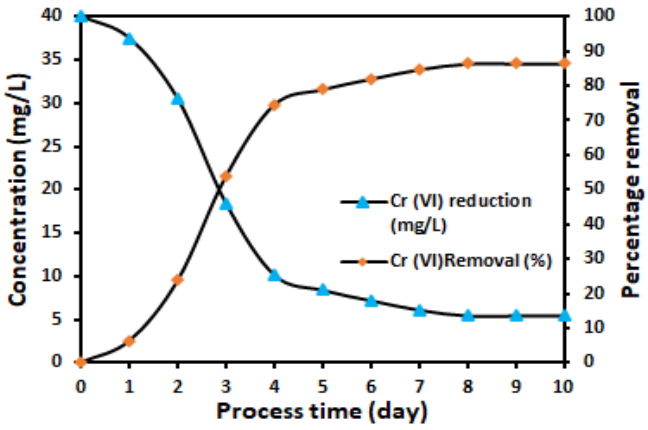

Fig. 5 Biodegradation study of Cr (VI) in scale up bioreactor at optimized condition (pH 7.0, temperature 35.0 °C, and process time 8.0 days)

Kinetic Study

The growth kinetics of *Pseudomonas putida* during Cr (VI) removal was described by Monod model. The model has used to find out the kinetic parameters for free cell between 10- 50 mg/L concentration. The details of kinetic parameters has been given in Table 1. The value of specific growth rate (μ_{max}) and half saturation rate constant (K_s) were found to be 0.154 (day^{-1}) and 22.53 (mg/L), respectively (Fig. 6A). Under substrate inhibition condtion, Andrew-Haldane model was used to predict the kinetic parameters. The value of specific growth rate (μ_{max}), half saturation rate constant (K_s), and inhibition constant (K_i) were found to be 0.047 (day^{-1}), 23.51 (mg/L), and 42.31 (mg/L), respectively (Fig. 6B). The small value of Ks and large value of μ_{max} are preferable during biodegradation process. it is dsirable to use ratio (μ_{max}/ Ks) as useful index to show the biodegradation potential of microbes for particular substrate (Sonwani et al., 2018; Geed et al., 2017; Kureel et al., 2017). The value of μ_{max}/ Ks for Monod and Andrew-Haldane model has been summarized in Table 1.

Table 1: Monod growth kinetics and Andrews-Haldane inhibition kinetics

Substrate concentration (mg/L)	μ_{max} (day^{-1})	K_s (mg/L)	K_i (mg/L)	μ_{max}/ K_s	R^2
10-50 (Monod)	0.154	22.53	-	0.0068	0.98
10-100 (Andrews-Haldane)	0.247	23.51	42.34	0.0105	0.96

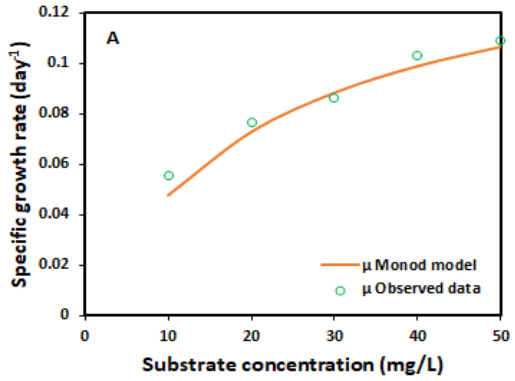

Fig. 6 (A) Experimental data fitted with monod model

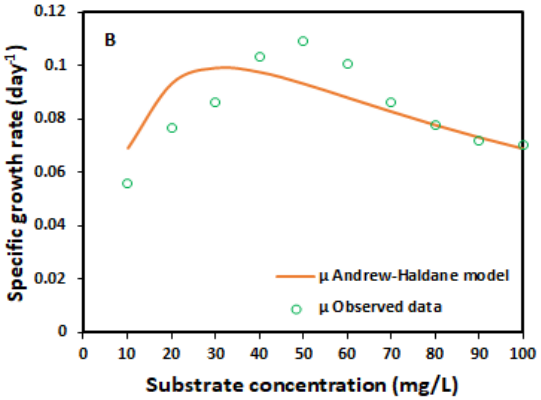

Fig. 6 (B) Experimental data fitted with Andrew-Haldane model

Conclusion

In the present study, biodegradation of Cr (VI) has been studied by Pseudomonas putida. The process parameter such as pH, Temperature, and process time were optimized and found to be 7.0±0.2, 35±2°C, and 8.0 days, respectively in the batch reactor. The maximum removal of Cr (VI) was found to be 86.4% at optimized condition in scale up bioreactor. The growth and inhibition kinetics were studied by Monod and Andrew-Haldane model and observed to be μ_{max}: 0.154 day^{-1}; Ks:22.35mg/L by Monod while μ_{max}: 0.247 day^{-1}; Ks: 23.51 mg/L; 42.34 mg/L by Andrew – Haldane. This study would be helpful in the designing of bioreactor and practical application of *Pseudomonas putida* culture for removal of Cr (VI) in the wastewater.

Acknowledgements

The authors gratefully acknowledged the Indian Institute of Technology (BHU) Varanasi, UP, India, for providing laboratory facility to complete the work. The authors also acknowledged the Ministry of Human Resource Development (MHRD) for the financial support to conduct the work.

References

[1] Apte, A.D., Verma, S., Tare, V. and Bose, P., 2005. "Oxidation of Cr (III) in tannery sludge to Cr (VI): field observations and theoretical assessment". *Journal of Hazardous Materials*, *121*(1-3), pp.215-222.

[2] Geed, S.R., Kureel, M.K., Giri, B.S., Singh, R.S. and Rai, B.N., 2017. "Performance evaluation of Malathion biodegradation in batch and continuous packed bed bioreactor (PBBR)". *Bioresource technology*, *227*, pp.56-65.

[3] Gheju, M. and Balcu, I., 2011. "Removal of chromium from Cr (VI) polluted wastewaters by reduction with scrap iron and subsequent precipitation of resulted cations". *Journal of hazardous materials*, *196*, pp.131-138.

[4] Kongsricharoern, N. and Polprasert, C., 1996. "Chromium removal by a bipolar electro-chemical precipitation process". *Water Science and Technology*, *34*(9), pp.109-116.

[5] Kureel, M.K., Geed, S.R., Giri, B.S., Rai, B.N. and Singh, R.S., 2017. "Biodegradation and kinetic study of benzene in bioreactor packed with PUF and alginate beads and immobilized with Bacillus sp. M3". *Bioresource technology*, *242*, pp.92-100.

[6] Nandi, R., Mukherjee, K. and Saha, B., 2015. "Surfactant assistant enhancement of bioremediation rate for hexavalent chromium by water algae". *Biochem. Physiol*, *4*, p.173.

[7] Mukherjee, K., Ghosh, D. and Saha, B., 2016. "Reliable bioremediation of hexavalent chromium from wastewater using mango leaves as reductant in association with the neutral and anionic micellar aggregation as redox accelarators". *Desalination and Water Treatment*, *57*(36), pp.16919-16926.

[8] Pandey, S., Singh, N.K., Bansal, A.K., Arutchelvan, V. and Sarkar, S., 2016. "Alleviation of toxic hexavalent chromium using indigenous aerobic bacteria isolated from contaminated tannery industry sites. *Preparative Biochemistry and Biotechnology*, *46*(5), pp.517-523.

[9] Polti, M.A., Aparicio, J.D., Benimeli, C.S. and Amoroso, M.J., 2014. "Simultaneous bioremediation of Cr (VI) and lindane in soil by actinobacteria". *International Biodeterioration & Biodegradation*, *88*, pp.48-55.

[10] Poornima, K., Karthik, L., Swadhini, S.P., Mythili, S. and Sathiavelu, A., 2010. "Degradation of chromium by using a novel strains of Pseudomonas species". *Journal of Microbial and Biochemical Technology*, *2*(4).

[11] Qin, G., McGuire, M.J., Blute, N.K., Seidel, C. and Fong, L., 2005. "Hexavalent chromium

removal by reduction with ferrous sulfate, coagulation, and filtration: A pilot-scale study". *Environmental science & technology*, *39*(16), pp.6321-6327.

[12] Ge, S., Ge, S., Zhou, M. and Dong, X., 2015. "Bioremediation of hexavalent chromate using permeabilized Brevibacterium sp. and Stenotrophomonas sp. cells". *Journal of environmental management*, *157*, pp.54-59.

[13] Shukla, D., Vankar, P.S. and Srivastava, S.K., 2012. "Bioremediation of hexavalent chromium by a cyanobacterial mat". *Applied Water Science*, *2*(4), pp.245-251.

[14] Sonwani, R.K., Giri, B.S., Geed, S.R., Sharma, A., Singh, R.S. and Rai, B.N., 2018. "Combination of UV-Fenton oxidation process with biological technique for treatment of polycyclic aromatic hydrocarbons using Pseudomonas pseudoalcaligenes NRSS3 isolated from petroleum contaminated site". *Indian Journal of Exp. Bio.* 56 (July) 460-469).

[15] Sultan, S. and Hasnain, S., 2007. "Reduction of toxic hexavalent chromium by Ochrobactrum intermedium strain SDCr-5 stimulated by heavy metals. *Bioresource technology*, *98*(2), pp.340-344.

[16] Thacker, U., Parikh, R., Shouche, Y. and Madamwar, D., 2006. "Hexavalent chromium reduction by Providencia sp". *Process Biochemistry*, *41*(6), pp.1332-1337.

[17] Zahoor, A. and Rehman, A., 2009. "Isolation of Cr (VI) reducing bacteria from industrial effluents and their potential use in bioremediation of chromium containing wastewater". *Journal of Environmental Sciences*, *21*(6), pp.814-820.

Proceedings of the Third International Conference on Sustainable Energy and Environmental Challenges (3rd SEEC)
18-21 December, 2018, IIT Roorkee, India

SEEC No.059

THERMODYNAMIC REVIEW OF TRIGENERATION SYSTEMS FOR POWER, HEATING AND COOLING REQUIREMENTS

Dr.Onkar Singh
Professor, Mechanical Engg. Dept.
Harcourt Butler Technical University,
(UP) India.
onkpar@rediffmail.com

Krishna Mani Mishra
PhD Scholar, Mechanical Engg. Dept.
Harcourt Butler Technical University,
(UP) India.
halkmmishra@gmail.com

Abstract

Changing climate conditions have been burdening the present civilization with excessive cooling and heating requirements, apart from the industrial requirements for these. Trigeneration refers to simultaneous power, heating and cooling from any system. The requirement of heating and cooling if met from the low grade energy available in conventional gas/steam combined cycle power plant offers potential solution to the endangering environment for meeting heating and cooling needs. Present paper deals with the thermodynamic review of trigeneration technology and aims at introspection into its state of study across the world.

Keywords: Energy, Exergy, Economical and environmental study, combined cooling, heating and power

1.INTRODUCTION

Global energy consumption has grown steeply since last many decades and is expected to increase by around 40% between 2006 & 2030 **[1] [2009].**In general the availability of energy in useable form depends upon the numerous renewable & non-renewable sources of energy with varying lifecycle of their replenishment. The major portion of energy requirement is being met from the non-renewable sources of energy, i.e. fossil fuels which have very long life cycle of replenishment and the fast depletion of fossil fuel is becoming a cause of concern for sustainability in the future. Amongst various options for ensuring sustainability, the energy conservation, energy efficiency & environmental concerns happen to be some of the key initiatives for meeting future energy challenges.

Combined cycle power plants are a consequence of initiatives for optional utilization of the energy sources in which gas turbine (GT) exhaust from topping cycle is used to run steam turbine (ST) based bottoming cycle through a heat recovery steam generator (HRSG). In view of increasing demand for cooling and heating along with power, it is worthwhile to explore efficient system, which can be combined cooling, heating & power (CCHP) option, i.e. three different objectives being taken care of in a power plant for meeting the power & heating/ cooling requirements of utilities with the help of single energy source. Such arrangements are also known as Trigeneration (TG) systems. In CCHP or trigeneration systems, the lost heat is utilized to generate a cold e□ect, in addition to power and heat.

The present paper aims at reviewing the present state of trigeneration technology starting from its evolution. The emergence and development of trigeneration systems for cooling, heating and power as reported in literature from time to time has been studied and compiled for creating a ready reckoner for those working in this field. Chronological developments in the trigeneration and related field have been suitably detailed in this paper.

NOMENCLATURE

APG	Absorption Power Generation	HRSG	Heat Recovery Steam Generator

AWKRC	Ammonia Water Kalina Rankine cycle	ORC	Organic Rankine Cycle
CCHP	Combined Cooling, Heating, and Power	SOFC	Solid Oxide Fuel Cell
CHP	Combined Heating, and Power	ST	Steam Turbine
GHG	Greenhouse Gas	TG	Trigeneration
GT	Gas Turbine	TLC	Trilateral Cycle

2. Evolution of CCHP around the world

All over the world, the evolution of CCHP was categorized broadly into four main zones along with their: the US in 1978, Europe in 1970, Asia and the Pacific in 1980 and rest of the world in early 2000.Trigeneration made its impact in India in early 2000 **[2] [2006].**

The world is facing dramatic increase in greenhouse gas emissions. Russia, India and China were all ranked among the five largest emitters, with China taking the top spot. All things equal, the U.S. Energy Information Administration has indicated that the worldwide energy related CO_2 emissions will increase to 46% by 2040 **[3]**. Therefore, finding more efficient energy systems is more crucial now than at any time since the beginning of the industrial revolution. The efficiency of conventional power plants that are based on single prime movers is usually less than 39%. Thus, most of the energy is lost as waste heat. Integrating cooling and heating subsystems in a conventional plant could increase the plant efficiency significantly where the CHP efficiency could reach 80%.In terms of electricity produced, the CHP accounted for more than 11% of the electricity produced in the G8 countries, as well as Brazil, China, India, Mexico, and South Africa in 2008.This percentage was expected to increase to 15% in 2015 and to 24% in 2030. In other words, the electricity produced by CHP is expected to reach around 430 GWe in 2015 and more than 830 GWe in 2030 **[4] [2008].**

The review of trigeneration plants can be carried out based on the thermodynamic cycle used, energy sources used, application, or analysis type. Significant contribution by some of the researchers in this area is detailed ahead in brief:

2.1. Thermodynamics Cycle

Calin Zamfirescu et al. [5] [2008] thermodynamically assessed the performance of an ammonia–water Rankine excluding boiler. **Johann Fischer [6] [2011]** compared and optimized trilateral cycle (TLC) systems with water as working fluid and optimized organic Rankine cycle (ORC) systems with pure organic working fluids. The study includes the heat transfer to and from the cycles. **Pouria Ahmadi et al. [7] [2012]** studied the performance of an integrated organic Rankine cycle for trigeneration. **Xingyang Yang et al. [8] [2016]** analysed a novel combined power and ejector-refrigeration cycle using zeotropic mixture. **G. Praveen Kumar et al. [9] [2017]** studied combination of NH3-H2O absorption refrigeration cycle and Kalina extraction turbine cycle that uses low-grade energy. **Zhiwei Ma et al. [10] [2017]** studied one double-effect, one half-effect and one ejector-combined absorption power generation (APG) cycles based on one of the most widely studied APG cycles – Kalina KCS-11.**JieJia et al. [11] [2017]** simulated and analysed an ORC system driven by the waste heat recovered from a trigeneration system. **Simin Anvari et al. [12] [2017]** analysed thermo- economical consideration of regenerative organic Rankine cycle coupled with the absorption chiller systems.**K.F. Fong et al**. **[13] [2017]** thermodynamically investigated climatic effect on the energy performance of trigeneration.

2.2. Energy, Exergy, Economical and Environmental Study Based Systems

Bassols et al. [14] [2002] studied energy, exergy analysis of trigeneration plants in the food industry. **Minciuc et al. [15-16] [2003]** analysed trigeneration systems from the point of view of fuel saving and environmental impact. **Temir and Bilge [17] [2004]** studied and analysed trigeneration plants from the thermos-economic point of view which produces electrical power with a natural gas fed reciprocating engine. **Ribarov and Liscinsky [18] [2007]** discussed the CCHP system for achieving economic viability through significant improvements in fuel utilisation. **Khaliq and Kumar [19] [2008]** analysed energy and exergy of gas turbine based trigeneration system and reported the effect of pressure ratio and process heat pressure on the performance parameters. **Khaliq [20] [2009]** further reported the impact of operating parameters on energetic and energetic efficiency of trigeneration system for optimisation purposes. **Mohammad Ameri et al. [21] [2010]** studied energy and exergy analysis of a tri-generation system based on micro-gas turbine with a steam ejector refrigeration system.**Yaping Chen et al. [22] [2015]** analyzed an integrated system of AWKRC (Ammonia Water Kalina Rankine cycle) for power and heating. **Giovanni Angrisani et al. [23] [2016]** studied performance indices such as energy based indices, environmental indices and economic indices and methodologies to assess the performances of cogeneration and trigeneration systems.**Keyvan Bahlouli et al. [24] [2016]** reported that the energy content of exhaust gases of the HCCI engine are used to drive the bottoming cycles including a steam turbine cycle and an absorption heat transfer cycle in a cogeneration system. **Mahesh. N. Shelar et al. [25] [2016]** compared energy and exergy analysis of diesel engine powered two trigeneration systems integrated with absorption chillers.**K.F. Fong [26] [2017]** investigated

trigeneration system using two sets of diesel-engine prime movers for a high-rise reference office building in a subtropical city. Many researchers analysed thermodynamically, exergo-economically and environmentally of trigeneration systems **[27-32] [2014, 2017, 2018].**

2.3. Energy Sources Based Systems

W.R. Wagar et al. [33] [2010] studied an ammonia–water Rankine cycle where renewable energy (solar, geothermal, biomass, oceanic-thermal, and nuclear as well as industrial waste heat) was used as energy source. **Hanna Mergner et al. [34] [2015]** studied ammonia water based cycles for power generation from low enthalpy heat sources.

2.3.1. Fuel Cell Based Systems

Faramarz Ranjbar et al. [35] [2014] analyzed a novel trigeneration system based on a solid oxide fuel cell (SOFC). **Paul E. Dodds et al. [36] [2015]** studied hydrogen and fuel cell technologies for heating. **M. Mortazaei et al. [37] [2016]** performed thermodynamic and environmental analysis of CCHP system via biomass based SOFC. **Leyla Khani et al**. **[38] [2016]** evaluated a CHP system from exergoeconomic point of view based on a SOFC.

2.3.2. Solar Based Systems

Ioan Sarbu et al. [39] [2015] reviewed solar closed sorption (absorption and adsorption) refrigeration systems and analysed environmental aspect of the systems. **Deb et al. [40] [2016]** proposed solar thermal system which facilitates the process heat for industrial purposes. Many researchers reported thermodynamic, exergoeconomic and environmental studies of different trigeneration systems with solar as primary energy source **[41-44] [2016, 2017].**

2.3.3. Biomass Based Systems

Antonio M Pantaleo et al. [45] [2017] analyzed energy performance and thermo-economic assessment of a micro turbine-based dual-fuel gas-biomass trigeneration system. **Joaquin Navarro-Esbrí et al. [46] [2017]** analyzed CCHP system, based on an ORC, using biomass as a renewable heat source for energy saving and emissions reduction in a supermarket. Thermodynamic analysis, exergy analysis and multiobjective optimization of biomass gasification based multigeneration system has been studied by different researchers **[47-48] [2014, 2016].**

CONCLUSION

Most conventional power generation systems are based on fossil fuels, which result in a huge amount of greenhouse gases (GHG) emissions. Hence, it is need of the day to explore the renewable sources or to use the low-grade waste heat from the power generation process for heating and/or cooling. It will be one of the solutions to save the energy squandering, and thus trigeneration technologies are quite relevant in present perspective. Present study shows that the degree of improvement of a trigeneration system is sensitive to the performance and operating parameters of each unit and the approach used to integrate these units into the single system. Therefore, energy, exergy, and environmental study of any proposed system are important to assess the system performance and to examine the possible degree of improvement in the system. The exergy analysis helps in identifying and quantifying the sources of the irreversibilities in the system that are associated with each component. The environmental analysis shows how much reduction in CO_2 emissions when the trigeneration system is used, as compared to a simple electrical power system. Economical study reports how generation of power locally and its consumption from the distribution companies and using it for the cooling and heating most of the times proves to be costlier.

REFERENCES

[1] Energy Information Administration. International Energy Outlook 2009. U.S.A., 2009.

[2] D.W. Wu, R.Z. Wang: 'Combined cooling, heating and power: A review', Progress in Energy and Combustion Science, 2006, 32,459–495.

[3] https://www.statista.com/statistics/271748/the largest-emitters-of-co2-in-the-world/.

[4] International Energy Agency. Combined heat and power: evaluating the benefits of greater global investment. France, 2008.

[5] Calin Zamfirescu, Ibrahim Dincer: 'Thermodynamic analysis of a novel ammonia–water trilateral Rankine cycle', Thermochimica Acta, 2008, 477, 7–15.

[6] Johann Fischer: 'Comparison of trilateral cycles and organic Rankine cycles', Energy, 2011, 36, 6208-6219.

[7] Pouria Ahmadi, Ibrahim Dincer, Marc A. Rosen: 'Exergo-environmental analysis of an integrated organic Rankine cycle for trigeneration', Energy Conversion and Management, 2012, 64, 447-453.

[8] Xingyang Yang , Nan Zheng , Li Zhao, Shuai Deng, Hailong Li , Zhixin Yu : 'Analysis of a novel combined power and ejector-refrigeration cycle', Energy Conversion and Management, 2016, 108,266–274.

[9] G. Praveen Kumar, R. Saravanan, Alberto Coronas: 'Experimental studies on combined cooling and power system driven by low-grade heat sources', Energy, 2017, 128, 801-812.

[10] Zhiwei Ma, Huashan Bao, and Anthony Paul Roskilly: 'Principle investigation on advanced absorption power generation cycles', Energy Conversion and Management, 2017, 150, 800–813.

[11] Jie Jia ,Cui He ,Zheng Xiao ,Chunqiong Miao ,Liqi Luo ,Haisheng Chen, Xinjing Zhang, Huan Guo, Yaod Wang,Tony Roskilly:'Simulation study of an ORC system driven by the waste heat recovered from a trigeneration system', Energy Procedia, 2017, 105, 5040 – 5047.

[12] Simin Anvari, Hadi Taghavifar, Alireza Parvishi: 'Thermo- economical consideration of Regenerative organic Rankine cycle coupling with the absorption chiller systems incorporated in the trigeneration system', Energy Conversion and Management, 2017, 148, 317-329.

[13] K.F. Fong, C.K. Lee: 'Investigation of climatic effect on energy performance of trigeneration in building application', Applied Thermal Engineering, 2017, 127, 409-420.

[14] J. Bassols, B. Kuckelkorn, J. Longneck and R. Schneider: 'Trigeneration in the food industry', Appl. Therm. Eng., 2002, 22, 595–603.

[15] E. Minciuc, O. L. Corre, V. Athanasovici, M. Tazerout and I. Bitir: 'Thermodynamic analysis of trigeneration with absorption chilling machine', Appl. Therm. Eng., 2003, 23, 1391–1405.

[16] E. Minciuc, O. L. Corre, V. Athanasovici and M. Tazerout: 'Fuel saving and CO2 emissions for trigeneration system', Appl. Therm. Eng., 2003, 23, 1333–1346.

[17] G. Temir and D. Bilge: 'Thermoeconomic analysis of trigeneration system', Appl. Therm. Eng., 2004, 24, 2689-2699.

[18] L. A. Ribarov and D. S. Liscinsky: 'Microgrid viability for small scale cooling heating, and power', J. Energ. Resour. ASME, 2007, 129, 1071–78.

[19] A. Khaliq and R. Kumar: 'Thermodynamic performance assessment of gas turbine tri generation system for combined heat cold and power production', J. Eng. Gas Turb. Power, 2008, 130, 1–4.

[20] A. Khaliq: 'Energy analysis of gas turbine trigeneration system for combined production of power heat and refrigeration', Int. J. Refrig., 2009, 32, 534–545.

[21] Mohammad Ameri, Ali Behbahaninia, Amir Abbas Tanha: 'Thermodynamic analysis of a tri-generation system based on micro-gas turbine with a steam ejector refrigeration system', Energy, 2010, 35, 2203-2209.

[22] Yaping Chen, Zhanwei Guo, Jiafeng Wu, Zhi Zhang, Junye Hua: 'Energy and exergy analysis of integrated system of ammonia water Kalina Rankine cycle', Energy, 2015, 90(2), 2028-2037.

[23] Giovanni Angrisani, Atsushi Akisawa, Elisa Marrasso , Carlo Roselli , Maurizio Sasso: 'Performance assessment of cogeneration and trigeneration systems for small scale applications', Energy Conversion and Management, 2016, 125, 194-208.

[24] Keyvan Bahlouli, Rahim Khoshbakhti Saray: 'Energetic and exergetic analyses of a new energy system for heating and power production purposes', Energy, 2016, 106, 390-399.

[25] Mahesh. N. Shelar, S.D.Bagade, G.N. Kulkarni: 'Energy and Exergy analysis of diesel engine powered trigeneration systems', Energy Procedia, 2016, 90, 27-37.

[26] K.F. Fong: 'Investigation on year-round dispatch of multiple chillers in trigeneration system for high-rise building application', Energy Procedia, 2017, 142, 1502-1508.

[27] Ioan Sarbu, Calin Sebarchievici: 'Energy and exergy assessments of a novel trigeneration system based on a solid oxide fuel cell', Energy Conversion and Management, 2014, 87, 318-327.

[28] Roberto Leiva-Illanes, Rodrigo Escobar, José M. Cardemil, Diego-César Alarcón-Padilla: 'Thermoeconomic assessment of a solar polygeneration plant for electricity, water, cooling and heating in high direct normal irradiation conditions', Energy Conversion and Management, 2017, 151, 538-552.

[29] Xiaofeng Zhang, Hongqiang Li, Lifang Liu, Chengying Bai, Shuang Wang, Quanbin Song, Jing Zeng, Xiaobo Liu, Guoqiang Zhang: 'Exergetic and exergoeconomic assessment of a novel CHP system integrating biomass partial gasification with ground source heat pump', Energy Conversion and Management. 2018, 156, 666-679.

[30] Pooria Behnam, Alireza Arefi, Mohammad Behshad Shafii:'Exergetic and thermoeconomic analysis of a trigeneration system producing electricity, hot water, and fresh water driven by low-temperature geothermal sources', Energy Conversion and Management,2018,157, 266-276,

[31] Hialeah Rashidi, Jamshid Khorshidi: 'Exergoeconomic analysis and optimization of a solar based multigeneration system using multiobjective differential evolution algorithm', Journal of Cleaner Production., 2018, 170, 978-990.

[32] Suthida Authayanun, Viktor Hacker:'Energy and exergy analyses of a stand-alone HT-PEMFC based trigeneration system for residential applications', Energy Conversion and Management, 2018, 160, 230–242.

[33] W.R. Wagar, C. Zamfirescu, I. Dincer: 'Thermodynamic performance assessment of an ammonia–water Rankine cycle for power and heat production', Energy Conversion and Management, 2010, 51, 2501–2509.

[34] Hanna Mergner, Thomas Weimer: 'Performance of ammonia water based cycles for power generation from low enthalpy heat sources', Energy, 2015, 88, 93-100.

[35] Faramarz Ranjbar, Ata Chitsaz, S.M.S. Mahmoudi, ShahramKhalilarya, Marc A. Rosen: 'Energy and exergy assessments of a novel trigeneration system based on a solid oxide fuel cell', Energy Conversion and Management, 2014, 87,318–327.

[36] Paul E. Dodds , Iain Staffell , Adam D. Hawkes , Francis Li , Philipp Grunewald , Will McDowall, Paul Ekins : 'Hydrogen and fuel cell technologies for heating: A review', International journal of hydrogen energy,2015, 40, 2065 -2083.

[37] M. Mortazaei, M. Rahimi: 'A comparison between two methods of generating power, heat and refrigeration via biomass based Solid Oxide Fuel Cell: A thermodynamic and environmental analysis', Energy Conversion and Management, 2016, 126, 132–141.

[38] Leyla Khani, S. Mohammad S. Mahmoudi, Ata Chitsaz, Marc A. Rosen: 'Energy and exergoeconomic evaluation of a new power/cooling cogeneration system based on a solid oxide fuel cell', Energy, 2016, 94, 64-77.

[39] Ioan Sarbu, Calin Sebarchievici: 'General review of solar-powered closed sorption refrigeration systems', Energy Conversion and Management, 2015, 105, 403–422.

[40] S.K Deb, B.C.Sharma:'Trigeneration Solar Thermal System', Procedia Computer Science, 2017, 111,427–434.

[41] A. Baghernejad, M. Yaghoubi, K. Jafarpur: 'Exergoeconomic optimization and environmental analysis of a novel solar-trigeneration system for heating, cooling and power production purpose', Solar Energy, 2016, 134,165-179.

[42] Luca Cioccolanti, Mauro Villarini, Roberto Tascioni, Enrico Bocci: 'Performance assessment of a solar trigeneration system for residential applications by means of a modelling study', Energy Procedia, 2017, 126, 445-452.

[43] R. Borgogno, S. Mauran, D. Stitou, G. Marck: 'Thermal-hydraulic process for cooling, heating and power production with low-grade heat sources in residential sector', Energy Conversion and Management, 2017, 135,148-159.

[44] Dheeraj Kishor Johar,Dilip Sharma,Shyam Lal Soni,Rahul Goyal,Pradeep K. Gupta:'Experimental investigation of thermal storage integrated micro trigeneration system',Energy Conversion and Management , 2017,146,87-95.

[45] Antonio M Pantaleo, Sergio M Camporeale, Christos N Markides, Giacomo Scarascia, Mugnozza, Nilay Shah: 'Energy performance and thermo-economic assessment of a microturbine-based dual-fuel gas-biomass trigeneration system', Energy Procedia, 2017,105, 764-772.

[46] Joaquín Navarro-Esbrí, Fracisco moles, Bernardo Peris, Adrian Mota- Babiloni, Jose Pascual Marti, Robertos Collado, Manuel Gonzalez: 'Combined cold, heat and power system, based on an organic Rankine cycle, using biomass as renewable heat source for energy saving and emissions reduction in a supermarket', Energy Procedia, 2017, 129, 652-659.

[47] Bahra Saadatfara, Reza Fakhrai, Torsten Franssona: 'Exergo-environmental analysis of nano fluid ORC low-grade', Energy Procedia, 2014, 61, 1879-1882.

[48] M. Mortazaei, M.Rahimi:'A comparison between two methods of generating power, heat and refrigeration via biomass based SOFC: A thermodynamic and environmental analysis', Energy Conversion and Management, 2016, 126, 132-141.

Proceedings of theThird International Conference on Sustainable Energy and Environmental Challenges (3rd SEEC)
18 –21 December, 2018, IIT Roorkee, India

SEEC No.060

IMPACT OF THIOCYANATE (SCN^-) ON GRANULAR CHARACTERISTICS AFTER DISINTEGRATION OF GRANULES

Sachin Kumar Tomar*
Department of Civil Engineering
Indian Institute of Technology Guwahati, Guwahati
Email: sachintomar306@gmail.com

Saswati Chakraborty
Department of Civil Engineering
Indian Institute of Technology Guwahati, Guwahati
Email: saswati@iitg.ac.in

ABSTRACT

The effect of thiocyanate (SCN^-) addition on characteristics of disintegrated aerobic granules was evaluated in a sequencing batch reactor (SBR). Granules were cultivated with phenol (400 mg L^{-1}) and ammonia-nitrogen (NH_4^+-N) (100 mg L^{-1}) in a SBR. After 75 day of stable recator opration with volatile suspended soilds of 3.67 g L^{-1} and granule size of 1202.03± 487.78 µm, the granules started to deteriorate and disintegration continued up to 84 day. Reformation of disintegrated granules were observed after gradual addition of SCN^- with granules having larger size (1819.87±43.44 µm), higher granule settling velocity (57.32±0.96 m h^{-1}) and higher extracellular polymeric substances (EPS) (101.45±1.06 mg $gVSS^{-1}$). It was found that SCN^- played an important role in the granule reformulation by provoking the secretion of EPS, a very high binding capacity substance.

***Keywords*:** aerobic granules, granule settling velocity, extracellular polymeric substances

INTRODUCTION

Aerobic granules have excellent settling behavior, denser, compact microbial structure and better pollutant removal ability as compared to conventional activated sludge [1]. But poor granule stability is a major issue for prolonged reactor operation which results into limited application for treating toxic wastewater [2]. Therefore, a sound and prolonged aerobic granular sludge reactor operation is needed.

The bacterial extracellular polymeric substances (EPS) is a key factor in maintaining granular integrity because of it's excellent binding capacity which results into microbial aggregation [1]. The EPS secretion is the bacterial action for the survival against harsh conditions imposed on the bacteria like exposure to toxic substances. This bacterial survival action helps in providing strength to the granules [3]. Thiocyanate (SCN^-) is a toxic compound, present in the coal gasification and liquefaction wastewater along with phenol and ammonia nitrogen [4]. SCN^- enhances the EPS secretion because of toxic nature, thus promotes the granule integrity[3].

The present research work aims to evaluate the impact of toxic SCN^- on granular reformulation from the disintegrated granules and also describes the change in granular characteristics after addition of SCN^-.

MATERIALS AND METHODS

REACTOR SET UP. This study was performed in a sequencing batch reactor (SBR) of 6 L working voume with working height and inner diameter of 212 and 6 cm, respectively. Air compressor was used to provide air with a air flow rate of 2.0 L min^{-1} through the rotameter.

FEED COMPOSITION. The influent feed composition is given in Tab.1. The influent feed contained phenol, ammonia nitrogen (NH_4^+–N as NH_4Cl), thiocyanate (SCN^- as KSCN), trace metals and phosphate buffer. Sodium

hydrogen carbonate and phosphate buffer were used to maintain 7.5-8.0 pH inside the reactor. Phosphate buffer and trace metal composition were adopted from the Sahariah and Chakraborty [5].

TABLE 1: FEED COMPOSITION

Day	75-84	85-115	116-126	133-146
	Feed composition[a]			
Phenol	400	400	400	400
NH_4^+–N	100	100	100	100
SCN^-	0	10-200	240	350

[a]All units in mg L^{-1}

REACTOR OPERATION. The SBR was regulated with a cycle and hydraulic retention time of 6 and 12 h, respectively. Feeding (30 min), reaction (320 min), settling of granular sludge (5 min) and effluent withdrawal from the SBR (5 min) were the four stages of the each 6 h cycle. 50% volume exchange ratio was maintained in the SBR. The seed sludge was taken from the Indian Oil Corporation Limited (IOCL), Guwahati. The SBR was operated with phenol and NH_4^+–N concentartions of 400 and 100 mg L^{-1}, respectively, up to 84 days. Form the day 85, the SCN^- concentration was gradually increased and was kept 240 mg L^{-1} for 10 days (day 116-126). Afterwards, it was raised up to 350 mg L^{-1} and the SBR was operated for next fifteen days at 350 mg L^{-1} for steady state data (Tab.1).

ANALYTICAL PROCEDURES. The granule size and granule settling velocity (GSV) were determined according to Tomar and Chakraborty [4]. Total and Volatile suspended solids (TSS and VSS) and sludge volume index (SVI_{30}) were measured according to standard methods [6]. Heat extraction procedure was used for determining EPS [7]. The protein (PN) content of EPS was determined by Lowry assay [8] and the polysaccharide (PS) content was evaluated by phenol-sulphuric acid method [9].

RESULTS AND DISCUSSION

The change in granule size with operational time is given in Fig.1a. The granule size was around 1202.03± 487.78 µm on day 75, since then a reduction was observed in granule size up to 87 day (911.19 µm), indicating the granule instability. After the addition of 25 mg L^{-1} SCN^-, an improvement in granule size was observed and it was continued up to 146 day of SBR operation. Granule reformulation was confirmed form the average granule size of 1819.87±43.44 µm formed after operating the reactor for 15 days (day 133-146) with SCN^- concentration of 350 mg L^{-1}.

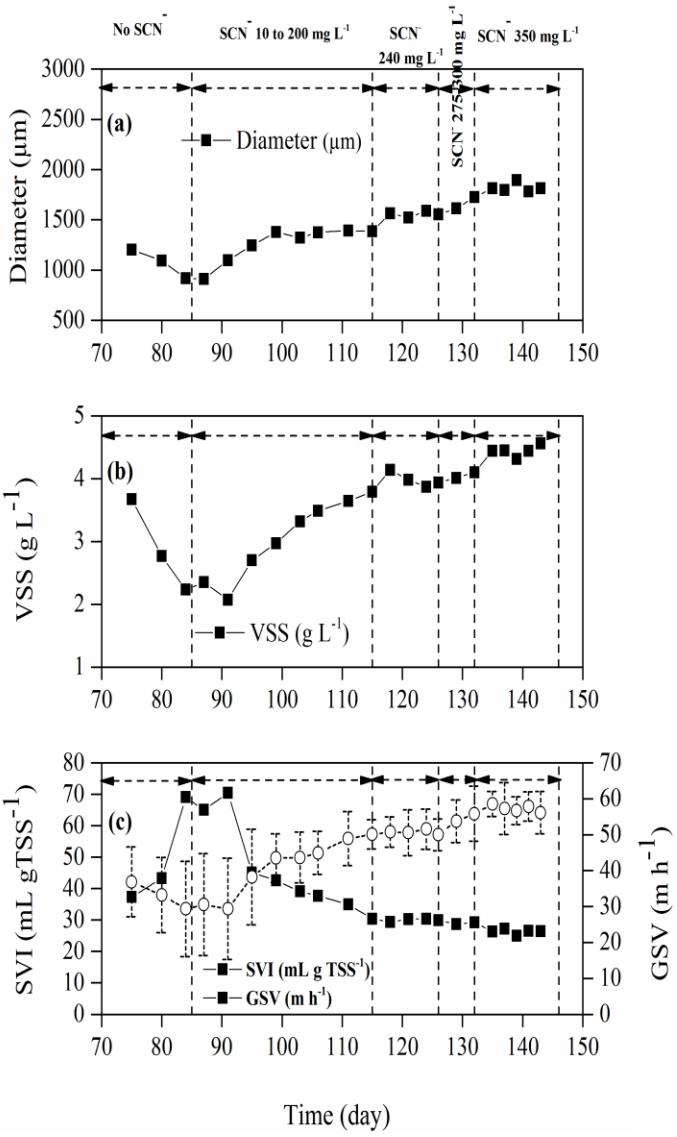

FIGURE 1. CHARACTERISTICS OF GRANULES (A) SIZE, (B) VSS, AND (C) SVI, GSV

A reduction in VSS was observed form VSS value of 3.67 g L^{-1} (day 75) to 2.07 g L^{-1} (day 91). After addition of SCN^-, a rise in VSS was noticed and it was reached up to 3.98±0.12 g L^{-1} during 118-126 day of SBR operation (240 mg L^{-1} of SCN^- concentration). The SCN^- concentration was again raised up to 350 mg L^{-1} to observe the impact of higher concentration of SCN^- on granuler biomass and a

higher average VSS of 4.44±0.086 g L^{-1} was observed during the day 135-143 (Fig. 1b).

From the Fig.1c, it was observed that as the SCN^- was increased, a reduction in SVI and an increment in GSV values were observed. SVI value decresed from 70.42 mL $gTSS^{-1}$ (day 91) to 26.31±0.80 mL $gTSS^{-1}$ (day 135-143). Whereas, GSV was increased from 29.35±14.11 m h^{-1} (day 91) to 57.32±0.96 m h^{-1} (day 135-143). A week after addition of SCN-, granules showed adaptability towards SCN- and afterwards, a significant positive impact was abserevd on granul characteristics. From Fig.1, it was concluded that after the addition of SCN^-, a progress was observed in granule characteristics, confirming the granule reformation and no negative impact of SCN^- on aerobic granules was observed up to a concentration of 350 mg L^{-1}.

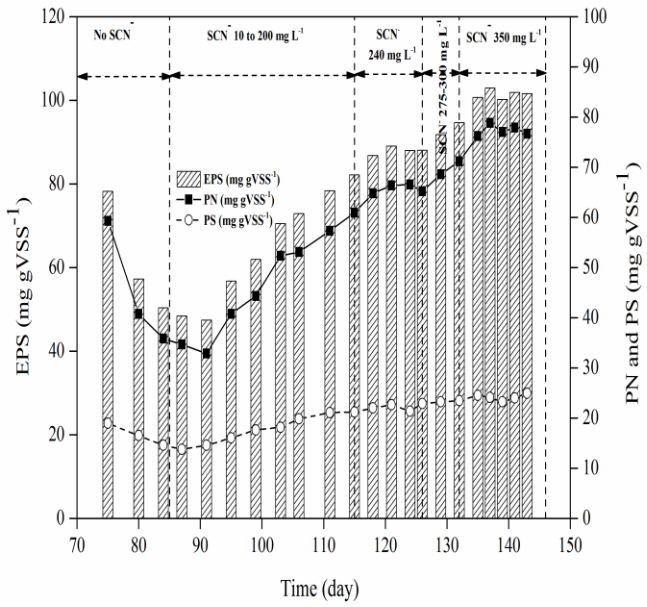

FIGURE 2. CONCENTRATION OF TOTAL EPS, PN AND PS

EPS content plays a key role in maintaining the stability of granules [4]. EPS content profile is illustrated in Fig.2. Initially on day 75, EPS was around 78.23 mg $gVSS^{-1}$ and moved down to the lower value of 47.44 mg $gVSS^{-1}$ on day 91. The reduction in EPS might be due to both lower VSS and size which were resulted from the granule instability. Thereafter, a rise in EPS content was observed and it was continued throughout the study. During steady state (day 133-146), the average value of EPS was found to be 101.45± 1.06 mg $gVSS^{-1}$. PN content was more profound than PS content. Form the EPS value, it was concluded that SCN^- was having a convincing impact on granul stability and also provoked the secretion of EPS for maintaining granular structure, which is having a very high binding affinity [1]. The secretion of EPS is the self adaptive action of granular biomass against the exposure to the toxic substance for their existence. Chen et al. [3] also observed the higher EPS value after the addition of SCN^- in granule based annamox process.

CONCLUSION

SCN^- was having a significant impact on granule reformulation by inducing the secretion of a very high binding affinity substance, EPS. Larger granules (average diameter of 1819.87±43.44 µm) with higher VSS (4.44±0.086 g L^{-1}), lower SVI value (26.31±0.80 mL $gTSS^{-1}$) and GSV (57.32±0.96 m h^{-1}) were reformed after the addition of SCN^-. SCN^- addition also encouraged the higher EPS secretion (101.45± 1.06 mg $gVSS^{-1}$).

ACKNOWLEDGMENT

Authors acknowledge the Indian Oil Corporation Limited (IOCL), Guwahati for providing sludge.

REFERENCES

[1] Liu, Y., Liu, Z., Wang, F., Chen, Y., Kuschk, P., and Wang, X., 2014. "Regulation of aerobic granular sludge reformulation after granular sludge broken: Effect of poly aluminum chloride (PAC)". Bioresour. Technol. 158, 201-208.

[2] Wang, X.H., Zhang, H.M., Yang, F.L., Xia, L.P., and Gao, M.M., 2007. "Improved stability and performance of aerobic granules under stepwise increased selection pressure." Enzyme Microb. Technol. 41, 205-211.

[3] Chen, Q.Q., Chen, H., Zhang, Z.Z., Guo, L.X., and Jin, R.C., 2017. "Effects of thiocyanate on granule-based anammox process and implications for regulation". J. Hazard. Mater. 321, 81-91.

[4] Tomar, S.K., Chakraborty, S., 2018. "Effect of air flow rate on development of aerobic granules, biomass activity and nitrification efficiency for treating phenol, thiocyanate and ammonium". J. Environ. Manag. 219, 178-188.

[5] Sahariah, B.P., and Chakraborty, S., 2011. "Kinetic analysis of phenol, thiocyanate and ammonia-nitrogen removals in an anaerobic–anoxic–aerobic moving bed bioreactor system". J. Hazard. Mater. 190, 260-267.

[6] APHA, 2005. Standard methods for the examination of water and wastewater, 21st ed. American Public Health Association, Washigton, DC.

[7] Li, X., and Yang, S., 2007. Influence of loosely bound extracellular polymeric substances (EPS) on the

flocculation, sedimentation and dewaterability of activated sludge. Water Res. 41, 1022-1030.
[8] Lowry, O.H., Rosebrough, N.J., Farr, A.L., and Randall, R.J., 1951. Protein measurement with the Folin phenol reagent. J. Biol. Chem. 193, 265-275.
[9] Dubois, M., Gilles, K.A., Hamilton, J.K., Rebers, P., and Smith, F., 1956. Colorimetric method for determination of sugars and related substances. Anal. Chem. 28, 350-356.

Proceedings of International Conference on Sustainable Energy and Environmental Challenges (3rd SEEC), December 18-21, 2018, IIT Roorkee, India

SEEC No.061

Monitoring Of Wastewater Quality: A Review

Varun Singh
Department of civil engineering,
BIET Jhansi
singhvarun900@gmail.com

Mohd Wasi
Department of civil engineering,
NIT kurukshetra
mohdwasi5191@gmail.com

ABSTRACT

Real-time monitoring of wastewater quality remains as unresolved problem to the waste water treatment industry .In order to comply with increasingly stringent environmental regulation, plant operators as well as industrial manufactures have expressed the the need of new standard and improved comparability of existing techniques. A review of currently available methods for monitoring global organic parameters (BOD,COD,PH,DO etc) is given .The study review both existing standard techniques and new innovative technologies with the focus on the sensors' potential for on-line and real-time monitoring and control. Current developments of virtual sensors for the monitoring of wastewater organic load are presented and the interests and limitations of these techniques with respect to their application to the wastewater monitoring are discussed.

Key words: BOD, COD, DO, PH, waste water, virtual sensor.

1. INTRODUCTION

Water is the valuable gift of nature to the human being. The European Community decided in 1991 to oblige all EU Member States to equip with wastewater treatment plants all cities whose wastewater organic load is greater than 15 000 equivalent in habitants (to be implemented before 3 1 December 2000) and 2000 equivalent-inhabitants (to be implemented before 31 December 2005). The characterization of wastewater at the inlet and outlet of the treatment plants is an effective way to control the process efficiency and to verify the final quality of treated waters. Usually, wastewater quality is characterized both by global parameters like biological oxygen demand (BOD), chemical oxygen demand (COD), total organic carbon (TOC) or total suspended solids (TSS), and by nitrogen and phosphorus compounds. All values must be lower than the maximal permissible values, depending on specific regulations. These dispositions are of great importance but unfortunately the great importance but unfortunately the monitoring procedures presently performed are not very satisfactory because they involve sampling, storage and laboratory analysis - a succession of sample handlings which considerably enhances the risk of errors. There is now an expanding need to limit sample handlings and to develop fast and accurate devices enabling a range of parameters to be monitored by direct field measurements. The aim of this study was to review both existing standard techniques and new innovative technologies with the focus on the sensors' potential for on-line and real-time monitoring and control.

2. REVIEW OF LITERATURE

The world is faced with difficulty related to the management of wastewater. This is due to large industrialization, increasing population density and high urbanized societies (EPA, 1993; McCasland et al., 2008). The effluents generated from domestic and industrial activities constitute the major sources of the natural water pollution load. This is a great burden in terms of wastewater management and can consequently lead to a point-source pollution problem, which not only increases treatment cost considerably, but also introduces a wide range of chemical pollutants and microbial contaminants to water sources (EPA, 1993, 1996; Eikelboom and Draaijer, 1999; Amir et al., 2004). The prevention of pollution of water sources and protection of public health by safeguarding water supplies against the spread of diseases, are the two fundamental reasons for treating wastewater. This is accomplished by removing substances that have a high demand for oxygen from the system through the metabolic reactions of micro organisms, the separation and settling of solids to create an acceptable quality of wastewater effluents, and the collection and recycling of microorganisms back into the system, or removal of excess microorganisms from the system (Abraham et al., 1997). In municipal wastewater treatment systems, the common water quality variables of concern are biological oxygen demand (BOD), chemical oxygen demand (COD), dissolved oxygen (DO), suspended solids, nitrate, nitrite and ammonia nitrogen, phosphate, salinity and a range of other nutrients and trace metals (DeCico, 1979; Brooks, 1996). The presence of high concentrations of these pollutants above the critical values stipulated by national and international regulatory bodies is considered unacceptable in receiving water bodies. This is because, apart from causing a major drawback in wastewater treatment systems, they also lead to eutrophication and various health impacts in humans and animals (EPA, 2000; CDC, 2002; Runion, 2008). In recent years, the reuse of treated effluent that is normally discharged to the environment from municipal wastewater treatment plants is receiving an increasing attention as a reliable water resource. In many countries, wastewater treatment for reuse is an important dimension of water resources planning and implementation. This is aimed at releasing high quality water supplies for potable use. Some countries, such as Jordan and Saudi Arabia have

national policies to reuse all treated wastewater effluents, thus have made considerable progress towards this end. In China, sewage use in agriculture has developed rapidly several decades ago and millions of hectares are irrigated with sewage effluent. The general acceptance is that wastewater use in agriculture is justified on agronomic and economic grounds, although care must be taken to minimize adverse health and environmental impacts (FAO, 1992; Metcalf and Eddy, 2003; Rietveld et al., 2009; Sowers, 2009). [2004] have studied the industrial wastewater and ground water, and pollution problem in ground water. V. Singh and C.P. S. Chandel [2006] have analyzed the wastewater of Jaipur City, which is used for agricultural purpose Furthermore, wastewater reuse is increasingly becoming important for supplementing drinking water needs in some countries around the world. The option of reuse of wastewater is becoming necessary and possible as a result of increased climate change, thus leading to droughts and water scarcity, and the fact that wastewater effluent discharge regulations have become stricter leading to a better water quality (Rietveld et al., 2009).

2. PRINCIPLES AND CLASSIFICATION OF EXISTING TECHNIQUES

In addition to traditional laboratory-based analytical techniques used in the water industry, recent years have seen the development of a range of innovative monitoring equipment. Although only a small number of such product has yet reached the market or has been accepted, there is already a great diversity of techniques and technologies available, both commercially and in research laboratories, which are reported in the literature. As a consequence, different schemes have been used in an attempt to classify existing sensors and analysers according to their respective properties.(Lynggaard-Jensen1999) listed eight different sensor/analyser properties (Table1).

Property	Example
1.Placement of sensor	In-situ, at-line, in-line; on-line, off-line
2.Principle of sampling	External sampling, no external sampling
3.Principle of filtration	Filtration, no filtration
4.Principle of sample treatment	Continuous, batch
5.Principle of measurement	Photometric, colorimetric, enzymatic, titrimetric, etc
6.No. measurants	Single parameter, multi parameter
7. Need for supplies	Consumables, no consumables
8.Service intervals	Long, medium or short intervals

Table 1: Relevant sensor properties (after Lynggaard-Jensen A 1999)

which should be taken into consideration before their introduction into wastewater systems (ie for monitoring or process control). Indeed key features such as the cost of ownership, ease of use, placement of the sensors, as well the response time, will influence the consumer's choice. Other technical aspects such as the principle of measurement , reliability, accuracy and detection limits will also dictate whether or not the technology will be accepted and promoted as a standard (or alternative) method by the end user and relevant authorities. It is, therefore, evident that both the performance characteristics (range, linearity, accuracy response time , limit of detection, etc.) and the intrinsic properties of the sensors (single or multi parameter, need for external sampling and filtration , intrusive/non-intrusive) are of major importance when looking at existing and new methodologies for wastewater systems.

3. ASSESSMENT OF WASTEWATER QUALITY

For the assessment of waste water pollution status of the water bodies, the following (as shown in Table 2) water quality parameters were analyzed. :

Characteristic	Sources
1.Turbidity	Erosion from upland, riparian, stream bank, and stream channel areas;
2.Color	Domestic and industrial wastes, natural decay of organic materials
3.Odour	Decomposing wastewater, industrial wastes.
4.Temperature	Domestic and industrial wastes
5.PH	Domestic, commercial, and industrial wastes
6.Chlorides	Domestic wastes, domestic water supply, groundwater infiltration
7.Nitrogen	Domestic and agricultural wastes

Table 2: Characterstics and source of wastewater

3.1 Turbidity

Sewage is normally turbid, resembling dirty dish water or wastewater from baths having other floating matter like fecel matter, pieces of paper, cigarette-ends, match-sticks, greases, vegetable debris, fruit skins, soaps, etc., The turbidity increases as sewage becomes stronger.
The degree of turbidity can be measured and tested by turbidity rods or by turbidimeters, as is done for testing raw water supplies.

3.2 Colour

The colour of sewage can normally be detected by the naked eye, and it indicates freshness of sewage. If its colour is yellowish, grey, or light brown, it indicates fresh sewage. However, if the colour is black or dark

brown, it indicates stale and septic sewage. Other colour, may also be formed due to the presence of some specific industrial wastes.

3.3 Odour

Fresh sewage is practically odourless. But however, in 3 to 4 hours, it becomes stale with all oxygen present in sewage being practically exhausted. It then starts omitting offensive odours, especially that of hydrogen sulphide gas, which is formed due to decomposition of sewage.The odour of water or wastewater can be measured by a term called the Threshold odour number (TON), which represents the extent of dilution required to just make the sample free of odour. The minimum odour of the sample that can be detected after successive dilutions with odourless medium, is, thus, known as the threshold odour.The Threshold odour number (TON) can be calculated by the equation :

$$TON=(V_s+V_d)/V_s$$

Where

TON=Threshold Odour Number

V_s=Volume of the sewage

V_d=Volume of distilled or odourless water added to just make the sewage sample loss its colour.

3.4 Temperature

The temperature has an effect on the biological activity of bacteria present in sewage, and it also affects the solubility of gases in sewage. In addition, temperature also affects the viscosity of sewage, which, in turn, affects the sedimentation process in its treatment.

The normal temperature of sewage is generally slightly higher than the temperature of water, because of additional heat added during the utilisation of water. The average temperature of sewage in India is 20ºC, which is near about the ideal temperature for the biological activities. However, when the temperature is more, the dissolved oxygen content (D.O.) of sewage gets reduced.

3.5 The pH

The hydrogen ion concentration expressed as pH, is a valuable parameter in the operation of biological units. The pH of the fresh sewage is slightly more than the water supplied to the community. However, decomposition of organic matter may lower the pH, while the presence of industrial wastewater may produce extreme fluctuations. Water and wastewater can be classified as neutral, acidic or alkaline according to the following range:

PH=7 neutral.

PH>7 alkaline.

PH<7 Acidic.

3.6 Chlorides

Concentration of chlorides in sewage is greater than the normal chloride content of water supply. The chloride concentration in excess than the water supplied can be used as an index of the strength of the sewage. The daily contribution of chloride averages to about 8 gm per person. Based on an average sewage flow of 150 LPCD, this would result in the chloride content of sewage being 50 mg/L higher than that of the water supplied. Any abnormal increase should indicate discharge of chloride bearing wastes or saline groundwater infiltration, the latter adding to the sulphates as well, which may lead to excessive generation of hydrogen sulphide.

3.7 Nitrogen

The principal nitrogen compounds in domestic sewage are proteins, amines, amino acids, and urea. Ammonia nitrogen in sewage results from the bacterial decomposition of these organic constituents. Nitrogen being an essential component of biological protoplasm, its concentration is important for proper functioning of biological treatment systems and disposal on land. Generally, the domestic sewage contains sufficient nitrogen, to take care of the needs of the biological treatment. For industrial wastewater if sufficient nitrogen is not present it is required to be added externally. Generally nitrogen content in the untreated sewage is observed to be in the range of 20 to 50 mg/L measured as TKN.

3.8 Biochemical Oxygen Demand (BOD)

The BOD of the sewage is the amount of oxygen required for the biochemical decomposition of biodegradable organic matter under aerobic conditions. The oxygen consumed in the process is related to the amount of decomposable organic matter. The general range of BOD observed for raw sewage is 100 to 400 mg/L. Values in the lower range are being common under average Indian cities. Hence the BOD of water during 5 days at 20 C is generally taken as the standard demand, and is about 68/ of the total demand. A 10 day BOD is about 90/ of the total. The following are the theoretical equations used to calculate the BOD. The Figure shown is used to describe the change of BOD with time. From the figure 1 the following correlations are derived:

L_0 = (BOD ultimate) or UBOD.

$Y_t = BOD_t$ (BOD exerted).

$L_t = L_0\, e^{-kt}$ (BOD remain).

$BOD_t = L_0 - Lt = L_0 - L_0e^{-kt} = L_0(1-e^{-kt})$

$BOD_5 = L_0\,(1-e^{-k5})$

$K = 0.23d^{-1}$ usually, $k_T = k_{20}\,\Phi^{T-20}$

, $\Phi = 1.047$ or as given

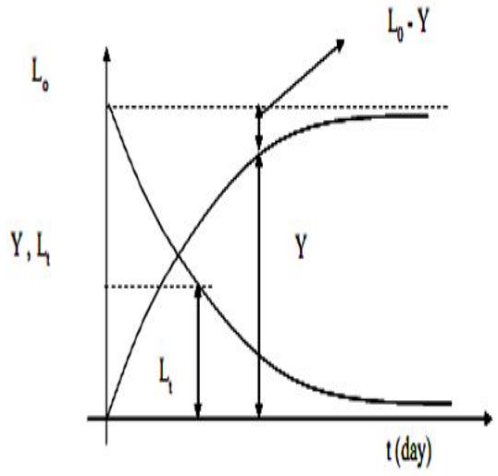

Figure 1: shown is used to describe the change of BOD with time

3.9 Chemical Oxygen Demand (COD)

The COD gives the measure of the oxygen required for chemical oxidation. It does not differentiate between biological oxidisable and nonoxidisable material. However, the ratio of the COD to BOD does not change significantly for particular waste and hence this test could be used conveniently for interpreting performance efficiencies of the treatment units. In general, the COD of raw sewage at various places is reported to be in the range 200 to 700 mg/L.

3.10 Dissolved Oxygen

The determination of dissolved oxygen present in sewage is very very important, because : while discharging the treated sewage into some river stream, it is necessary to ensure at least 4 ppm of D.O. in it ; as otherwise, fish are likely to be killed, creating nuisance near the vicinity of disposal. treatment processes. The D.O. content of sewage is generally determined by the Winkler's method which is an oxidation-reduction process carried out chemically to liberate iodine in amount equivalent to the quantity of dissolved oxygen originally present.

4. ALTERNATIVE NEW TECHNIQUES

A review of the techniques currently available is now presented with emphasis on automatic on-line methods for real-time monitoring. There is a plethora of new techniques and technologies available for monitoring changes in organic load in wastewater. The purpose of these is to obtain specific information about change in wastewater quality (particularly at the inlet) and to ensure treatment efficiency for compliance assessment and process control. Accordingly, several instrument manufactures are now offering device to perform rapid monitoring of wastewater BOD, but little experience with the technology has yet accumulated (Iranpour R et al 1997) Here is a selection of more or less developed systems described in the literature.

In order to meet the requirements for real-time and on-line monitoring in the real world, all methods must be simple, fast and reliable, as well as cost effective (reagents, maintenance, energy, operator's time, etc). With this in mind, several studies have been carried out to test and compare various types of analysers (Gernaey K et al 1999, Londong J et al 1996, Osbild D et al (1998). (Brookman and SKE 1997) noted the wide range of existing methods for the determination of BOD. These include the use of a microbial sensor;(Riedel K et al 1990) potentiometric stripping analysis;(Fayyad M et al 1987) incubation in acidified N/80 permanganate for 4h to give the permanganate value;(Lowden G et al 1981) and the use of a scanning optical sensor based on the oxygen quenching of luminescence(Li XM et al 1994). Accordingly, it is possible to distinguish between a few major types of techniques: biosensor and chemical, optical, or even 'virtual'(software, modeling) sensors.

Virtual sensors

Software sensors, or 'virtual sensors', have been defined by (Jacobsen S and Lynggaard-Jensen A 1998) as a term used for 'signals' obtained from calculations using measured signals from reliable, available sensors in combination with other signals such as on/off indications and time counters. Such 'sensor' emerged from the need for rapid evaluation /prediction of essential parameters for which data are not readily available. In most cases, the lack of real-time/continuous data is associated with technical limitations or cost restrictions. Some virtual sensors have been used as filters or as real-time quality controls of datasets and sensor validation procedures. The technique has also proved useful in the field of modeling and the determination of environmental parameters, such as in the case of wastewater treatment plant designs. This allows the rapid prediction of the effect of changes of a number of factors on the variable of interest. One such mathematical tool is the neural network model, which was used for on-line prediction of mill effluent BOD.

The method uses artificial intelligence to build nonlinear multivariate models based on large amounts of data. These techniques are not based on fundamental physical or chemical, or even biochemical principles and must be combined with practical insight to be effective. Similarly, in an early evaluation of the modeling of activated sludge processes,(Henze M. 1992) reported that there are still many problems to be solved with regard to wastewater characterization for modeling purposes. Indeed there are many difficulties associated with the lack of experience and/ or basic understanding.

5. CONCLUSION

Rapid monitoring of wastewater organic load is of major concern to the water industry. At present there does not seem to be a commercially available instrument that satisfies all the requirements for wastewater treatment monitoring, which will allow real-time control of effluent quality in compliance with the latest environmental regulations. Traditional methods are inadequate for providing continuous and real-time monitoring of water quality. For many years the approach to the measurement of global parameters

such as BOD, COD and DO has been off-line, requiring sample collection and retrospective laboratory analysis. In this review, the limits of the current standard procedures together with the importance of on-line and real-time control for automated systems have been demonstrated. Potentially suitable techniques such as biosensor and optical (absorption) sensors were presented and discussed. Many of these are still typically limited by environmental factors, short lifetime or fouling problems. New innovative and noninvasive techniques using virtual sensors have also been described. However, these promising new methods are still in their infancy and require further development.

Despite the increasing range and diversity of techniques and technologies available for wastewater monitoring, there are still a number of barriers to be overcome before they are accepted and implemented by the wastewater treatment operators. For instance, improvement in comparability and reliability of measurement is clearly needed. Similarly, clear definition and standardized validation of water quality determinants is also essential. Finally, a system's success and commercial viability will be determined by its robustness, simplicity, rapidity and cost considerations.

REFERENCES

[1] Amir HM, Ali RM, Farham K (2004). Nitrogen removal from wastewater in a continuous flow sequencing batch reactor. Pak. J. Biol. Sci. 7(11): 1880-1883.

[2] Abraham PJV, Butter RD, Sigene DC (1997). Seasonal changes in whole-cell metal levels in protozoa of activated sludge. Ecotoxicol. Environ. Saf. 38: 272-280.

[3] Brooks PC (1996). Investigation of temperature effects on denitrifying bacterial populations in biological nutrient removal (BNR) system. MS. Thesis: Virginia Polytechnic Institute and State University, Blacksburg, Virginia, USA.

[4] Brookman SKE, Estimation of biochemical oxygen demand in slurry and effluent using ultra-violet spectrophotomentry. Water Res 31:372-374 (1997).

[5] CDC (2002). U.S. Toxicity of Heavy Metals and Radionucleotides. Department of Health and Human Services, Centers for Disease Control and Prevention. Savannah river-site health effects subcommittee (SRSHES) meeting: Available from http://www.cdc.gov/nceh/radiation/savannah/SRSHES_Toxicity_jan02.htm. Accessed 07/12/2007.

[6] Decicco BT (1979). Removal of eutrophic nutrients from wastewater and their bioconversion to bacterial single cell protein for animal feed supplements phase II. Water Resources Research Centre Report 15.

[7] EPA (1993). Constructed wetlands for wastewater treatment and wildlife habitat. Available from http://www.epa.gov/owow/wetlands/construct. Accessed 14/01/2008

[8] EPA (1996). U.S. Environmental Protection Agency, American Society of Civil Engineers, and American Water Works Association. Technology Transfer Handbook: Management of Water Treatment Plan Residuals. EPA/625/R-95/008. Washington DC.

[9] EPA (2000). Nutrient criteria technical guidance manual-rivers and streams. EPA-822-B-00-002. Washington DC.

[10] Eikelboom DH, Draaijer A (1999). Activated sludge information system (ASIS). Available from http://www.asissludge.com. Accessed 09/11/2007.

[11] Fayyad M, Tutunji M, Ramakrishna RS and Taha Z, Dissolved oxygen: method comparison with potentiometric stripping analysis. Anal Lett 20:529-535 (1987).

[12] FAO (1992). Wastewater treatment and use in agriculture. Food and Agriculture Organization (FAO) of the United Nations Irrigation and Drainage Paper 47. Available from http://www.fao.org/../docrep/T0551E/T0551E00.htm. Accessed 10/11/2010.

[13] Gernaey K, Petersen P, Ottoy JP and Vanrollenghem P, Biosensing activated sludge. WQI May/June pp 16-21 (1999).

[14] Henze M, Characterization of wastewater for modeling of activated sludge processes. Wat Sci Technol 25:1-15 (1992).

[15] Iranpour R, Straub B and Jugo T, Real time BOD monitoring for wastewater process control. Environ Eng February: 154-159 (1997).

[16] Jacobsen S and Lynggaard-Jensen A, On-line measurement in wastewater treatment plants: sensor development and assessment of comparability of on-line sensors, In Monitoring of Water Quality, Elsevier. pp 89-102 (1998).

[17] Lowden G, Tests for assessing the oxygen demand of effluents. Wat Res Tkop 1:142-147 (1981).

[18] Li XM, Ruan FC, Ng WG and Wong KY, Scanning optical sensor for the measurement of dissolved oxygen and BOD. Sensors and Actuators B 21:143-149 (1994).

[19] Londong J and Wachtl P, Six years of practical experience with the operation of on-line analysers. Wat Sci Technol 33:159-164 (1996).

[20] Lynggaard-Jensen A, Trends in monitoring of waste water systems. Talanta 50:707-716 (1998).

[21] McCasland M, Trautmann N, Porter K, Wagenet R (2008). Nitrate: Health effects in drinking water. Available from http://pmep.cee.comell.edu/facts.slides–self/facts/nit-heefgrw85.html. Accessed 05/04/2008.

[22] Metcalf X, Eddy X (2003). Wastewater Engineering: Treatment and Reuse. In: Wastewater Engineering, Treatment, Disposal and Reuse. Techobanoglous G, Burton FL, Stensel HD (eds), Tata McGraw-Hill Publishing Company Limited, 4th edition. New Delhi, India.

[23] Osbild D and Vasseur P, Microbiological sensors for the monitoring of water quality, In Monitoring of Water Quality, Elsevier. pp 37-49 (1998).

[24] Riedel K, Lange KP, Stein HJ, Khum M, Ott P and Scheller F, A microbial sensor for BOD. Water Res 24:883-887 (1990).

[25] Runion R (2008). Factors to consider in wastewater-2. Ezine Articles (April 14). Available from http://ezinearticles.com/?factors-To-Consider-Wastewater--2& id= 11 08477. Accessed 09/05/2008.

[26] Rietveld LC, Meijer L, Smeets PWMH, van der Hoek JP (2009). Assessment of *Cryptosporidium* in wastewater reuse for drinking water purposes: a case

study for the city of Amsterdam, The Netherlands. Water SA, 35(2): 211-215
[27] Singh V. and Chandel C.P. S., Res. J. of Chem. And Environ. 2006: 10 (1): 30.
[28] Sowers AD (2009). The effect of wastewater effluent on fish and amphibians species. A Doctoral Dissertation presented to the Graduate School of Clemson University.
[29] Sharma S.K., Singh V.and Chandel C.P. S., Environ. And Eco. 2004: 22 (2): 319. 17.
[30] Singh V. and Chandel C.P. S., Res. J. of Chem. And Environ. 2006: 10 (1): 30.

A PRACTICAL FRAMEWORK FOR PURSUING "WEALTH FROM WASTE" IN INDIAN INDUSTRIES

RENGARAJAN MANIVANNAN

Keywords: Waste-to-Wealth, Sustainability, 3R's, Closed-loop-manufacturing, Life-cycle-assessment, Design-thinking.

1. RESEARCH OBJECTIVE

A resource-constrained world is facing a double whammy of a growing population and massive economic growth. If it has to aspire for a development pathway that is sustainable, resource efficiency through Material and Energy Recovery is a key. For an emerging economy like India, it is an imperative to balance the intertwined objectives of People, Planet and Profit.

India faces monumental environmental challenges associated with waste generation and their inadequate collection, transport, treatment and disposal. *"Environmentally sound waste management is one of the key elements for sustainable development"* (UNEP, 2018). The current abysmal state of and challenges in industrial waste management in India and the opportunities presented by a sustainability approach is the motivation for the present study

2. THE RESEARCH PROBLEM: THE CHALLENGE OF WASTE IN INDIAN INDUSTRIES

Studies have shown that the world is on a growth trajectory where waste generation is expected to more than double population growth, and touch 3.40 billion tonnes by 2050 (WBG, 2012 and 2018). Most studies on urban planning highlight the problems associated with solid waste (industrial, municipal, biomedical, electrical and electronic) management only. Untreated solid wastes alone have ramifications of leading to poor and serious public health issues, unsafe waste handling conditions, and environmental impacts – air pollution, water contamination, soil contamination due to leaching of hazardous chemicals, odour pollution, and emissions of greenhouse gases, estimated at 1.6 billion tonnes of carbon dioxide–equivalent in 2016 (WBG, 2018). If the problems posed by liquid and gaseous wastes are also taken into account, the challenge of waste management becomes even more formidable.

Waste management is a complex challenge to developing countries like India. About 50% of the world's population does not have access to proper waste collection (World Bank, 2016), while over 3 billion people lack access to controlled waste disposal facilities (UNEP, 2018). To cite just one more issue: The world had generated 44.7 million M.T. of e-waste by 2016, of which only 20% was recycled through appropriate channels (Balde et al, 2017).

European Union (2008, 2012) defines waste as the by-products and/or the end products of the production and consumption processes respectively. Our current model of resource consumption is linear - resources are extracted, processed, transformed, used and discarded at the end of their life to nature in the form of solid, liquid and gaseous wastes.

It has been seen that, globally, current resource and waste management is ad-hoc and lacks a coherent perspective that covers the entire value chain of product design, raw material

extraction, production, consumption, life extension, recovery and recycling, and waste disposal (Singh, 2014).

The true cost of waste is indeed manifold. It not only includes the costs of all the materials that go into making a product – raw materials, auxiliary materials (packing, consumables, stores and spares), manpower, and energy – but also includes the costs associated with managing wastes and their disposal (Kane, 2010). The costs become huge when one looks at the costs from a value chain perspective – the costs incurred across the 'extended enterprise'. The costs are much higher if the costs of externalities and opportunities are factored in.

Waste hierarchy is as follows (adapted from Kane, 2010):

The subject of waste management is vast, in terms of their state, points of origin, characteristics, and so on. Business organizations are at once the cause of many problems but are also the ones that can provide the solutions. They consume large resources, generate huge wastes, but also have the wherewithal to provide resources and expertise to solve the problems. The scope of this paper is limited to that of wastes emanating from and processed in Indian manufacturing operations, and their conversion to wealth.

3. RESEARCH METHODOLOGY

This paper examines the underlying issues of Resource Efficiency through Waste minimization initiatives in global and Indian industries and opportunities for converting wastes into wealth.

The Literature survey spans: (a) Academic publications; (b) Sustainability and other reports of major global and Indian resource-intensive companies; and industry institutions - CII, BEE, and CDP; (c) Performance of global industry leaders to identify best practices. Deductive Content Analysis (DCA) is used as the research methodology to analyze the potential for material and energy recovery. It is a systematic and objective means of describing and quantifying phenomena (Krippendorff, 1980), and is used when the structure of analysis is operationalized on the basis of previous knowledge and the purpose of the study is theory testing (Kyngaॅs & Vanhanen 1999).

4. KEY CONCEPTS AND TOOLS FOR CONVERTING WASTE TO WEALTH

A number of concepts and tools have been developed in guiding organizations in their efforts to convert wastes to wealth. Some of the important ones are discussed briefly below:

4.1 Sustainability Thinking: The concept of Sustainability perforce warrants a long-term approach involving intra- as well as inter-generational considerations. The whole concept of

Sustainable Development got a fillip and direction with the publication of the report "Our Common Future" by the World Commission on Environment & Development in 1987: *"Development that meets the needs of the present without compromising the ability of future generations to meet their own needs".*

4.2 Resource Conservation: The problem of finite resources and limited carrying capacity has been highlighted long before sustainability became a commonplace topic (Ehrlich, 1968 and 2008). The wise utilisation of resources and knowledge that are open to all will provide a competitive advantage to companies and communities, and a basis for environmental innovation and a sustainable economy. From the initial 3 R's (Reduce-Reuse-Recycle), the growing awareness on resource conservation has spawned a number of conservation approaches (CII, 2018) as listed in Table 4.1.

Table 4.1 Conservation Approaches – The Various R's

Refuse	Reduce	Reuse	Recycle
Restore	Regenerate	Repair	Recover
Refurbish	Redesign	Remodel	Remanufacture
Rethink	Retain	Retrieve	Reclaim
Redeem	Restore	Reinvent	Redevelop
Restrict	Reschedule	Refrain	

4.3 Life Cycle Thinking (LCA): It is a comprehensive method to assess the environmental impacts of a product, process or activity throughout its life cycle; from the extraction of raw materials through their processing, transport, use and disposal. LCA helps in determining the risks and environmental optimization potential for a product/process at each stage of its life cycle. It generates an understanding of life cycle thinking and helps integrate it into everyday activities of business at all levels (Rainey (2006).

4.4 The Circular Economy: The Ellen MacArthur Foundation has the goal of *"accelerating the transition to a regenerative, circular economy"* (2013). The concept is focused on a regenerative economic model which creates more value by reducing the dependence on scarce resources (McKinsey 2014a). The emphasis is on better design and optimization of products for multiple cycles of disassembly and reuse, thus bringing in a cradle-to-cradle approach, in short, Closed Loop Manufacturing. It works contrary to the liner model of extraction, production, use and disposal. In short, the shift is towards 'designing for the circular economy' (Wharton, 2017). Industries use circular-economy concepts to capture more value from resources (McKinsey 2016). In a very recent special report on waste management, The Economist (2018) has highlighted the growing problem in emerging economies, of which India is one, and has brought into focus how applying the principles of circular economy can help in mitigating the problem.

4.5 Design Thinking: Design thinking encompasses concept development, applied creativity, prototyping, and experimentation. When design thinking approaches are applied to business, the success rate for innovation has been seen to improve substantially (MIT, 2018). It includes Design for Environment, and Design for Sustainability, and focuses at the design stage, besides customer expectations, on aspects such as environmentally-friendly, recyclability, etc.

4.6 Lean Thinking: Lean-management thinking can be applied in resource-intensive industries to reduce the amount of energy and other resources used to increase resource productivity and reduce costs (McKinsey, 2014b).

4.7 Sustainable Supply Chain: In order to achieve the objective of creating a sustainable supply chain, organizations adopt a purchasing policy of sourcing their materials and services from suppliers, who fulfil the requirements of being environmentally-friendly and socially responsible (Kane, 2010). This also ensures low resource intensity of the final product and helps in achieving life cycle objectives.

5. FINDINGS OF THE STUDY - THE WAY FORWARD

The study indicates that India can achieve high levels of efficiency in waste management and reap the benefits by adopting a holistic wealth-from-waste management framework:

1. Recovery of resources - materials and energy - from the waste streams is the precursor to Recycling and Reuse.
2. Practised across several resource-intensive sectors by industry leaders: Automobiles, Cement, Chemicals, Construction, Electronics, FMCG, Oil & Gas, Pharmaceuticals, Power generation, Metallurgical industries, Paper, Steel, Sugar, etc. The principles of Resource conservation, resource optimization, reduction of resource intensity, enhancement of resource efficiency, closed-loop manufacturing, etc., are illustrated. However, wide-spread practice across all levels, especially the medium and small scale industries is not evident. Even in large companies, the practices are not uniform and yet to mature into a long-term strategy.
3. The benefits to the companies and society at large, include: (a) reduction in - consumption of virgin materials, energy; (b) lower cost of manufacturing; (c) reduced volatility in availability and prices of input resources; and (d) reduced environmental impact, waste management expenses, and landfill.
4. Several barriers exist: Segregation, Poor infrastructure for collection, transport, and treatment, Legal, Finance, Systems and Processes, Governance.
5. An integrated approach would consist of: (a) adopting circular economy or closed loop manufacturing as a core philosophy/value of the organization. (b) building an awareness and consciousness on the importance of waste management and its associated true costs. (c) mapping of the complete value chain, (d) accounting of all inputs and outputs, (e) mapping the life cycle of waste from generation to collection, treatment, and reuse, and/or disposal. (f) identifying potential opportunities for waste minimization, conversion into valuable products, and waste elimination, (g) creating a market structure for sourcing and collection, pre-processing, (h) identifying the risks and developing risk mitigation approaches, (e) conducting a full-fledged cost-benefit analysis; (i) developing complete infrastructure; (j) providing investments for wealth-from-waste initiatives; (k) installing supportive legislation, (l) benchmarking and pursuing relentlessly the waste minimization efforts through innovation, (m) developing new business models for integrated waste management and including a larger set of stakeholders, and (n) driving the concept across the value chain, to derive larger benefits to society, and achieve scale.

6. APPLICATION OF THE STUDY

The generic and practical framework can be adopted, with a sense of urgency, by all Indian companies across various manufacturing sectors to drive resource recovery; achieve reduction in resource consumption, cost, and environmental footprint; improve operational efficiency; and achieve wealth from waste.

Proceedings of International Conference on Sustainable Energy and Environmental Challenges (3rd SEEC), December 18-21, 2018, IIT Roorkee, India

SEEC No.063

GREEN SYNTHETIC APPROACH OF 1,7-BIS(SUBSTITUTED PHENYL)1,6-HEPTADENE-3,5-DIONES

Suhasini K.P

Dept. of Chemistry, Vignan Institute of Engineering for Women, Visakhapatnam, Andhra Pradesh
E-mail : suhasini.kl@gmail.com

Mangaveni P

Dept. of Organic Chemistry, St. Joseph College for Women (A), Visakhapatnam, Andhra Pradesh
E-mail : mangaveni@gmail.com

ABSTRACT

Green chemistry, also called sustainable chemistry. The objective of green chemistry is to achieve sustainable environment and good health. Solid support based green chemistry is obtaining popularity in present day context basing on number of fruitful green reactions. *Curcuma longa* (turmeric) is a ginger-like plant that grows in tropical regions. It possess broad spectrum of biological properties viz., anti-microbial, anti-biotic, anti-oxidant, anti-inflammatory agent, anti-fungal, anti-HIV. Due to its significant pharmacological importance a group of curcumin analogs has been synthesized with solid support i.e., in the absence of any organic solvents like chloroform, methylene chloride, carbon tetra chloride etc which are not only costly but are environment destructive and also harmful for those who are handling them. In green chemistry, an attempt has been made to minimize or eliminate these effects by using solvent free/solid support synthesis. Thus, a new synthetic route was developed to obtain a series of 1,7-bis(substituted phenyl)1,6-heptadene-3,5-diones by employing Silica-sulphuric acid as a solvent free/solid support method.

Keywords: Green Synthesis, Solid Support, Silica-sulphuric acid, Solvent free reactions.

INTRODUCTION

Green chemistry, also called sustainable chemistry, is a philosophy of chemical research and engineering that encourages the design of products and processes which minimize the usage and generation of hazardous substances [1]. Green chemistry applies to organic chemistry, inorganic chemistry, biochemistry, analytical chemistry and physical chemistry. The objective of green chemistry is to achieve sustainable environment and good health. These objectives are achieved by focusing on main areas as alternative synthetic pathways using a solvent that has less effect on environment, increased selectivity or solvent free synthesis [2]. The new scaffolds are designed by the process which reduce or to eliminate the usage of hazardous substances. The generation of unwanted and harmful byproducts is completely avoided. The Green chemistry mainly emphasizes on atom economy at every stage of design, manufacturing and utility.

Solid support based green chemistry is obtaining popularity in present day context basing on number of fruitful green reactions. R. Bruce Merrifield's Peptide Synthesis [3] in 1963 using cross linked polystyrene support opened an exciting area of research and since then many new reagent bound, substrate bound and catalyst bound methods have been developed. The polymer bound complex was found to be more effective than homogeneous counterpart. It was also found recyclable and reusable. Solid acids and especially those based on micelle-template silica and other mesoporous high surface area support materials are began to play a significant role in the greening of fine and significant chemical manufacturing processes. A wide range of important organic reactions can be efficiently catalyzed by these materials, which can be designed to provide different types of acidity as well as high degrees of reaction selectivity. The solid acids [4] generally have high turnover numbers and can be easily separated from the organic components. The combination of this chemistry with innovative reaction engineering offers exciting opportunities for innovative green chemical manufacturing in the future. Now a day's solvent free approach for organic synthesis involving microwave [5] exposure of neat reactants is proving to be a green tool. Selective absorption of microwave energy by polar molecules, enhanced reaction rates, improved yields are the major achievements which has been extended to modern drug discovery in complex multi step synthesis. This technology has been proved to be successful in formation of various carbon heteroatom bonds in organic synthesis.

Curcuma longa (turmeric) is a ginger-like plant that grows in tropical regions. The roots contain a bright yellow substance that contains curcumin and other curcuminoids. Turmeric has been used in Ayurvedic and Chinese medicine for centuries. Studies have shown that curcumin is not toxic to humans [6]. It possess broad spectrum of biological properties viz., anti-microbial, anti-biotic, anti-oxidant, anti-inflammatory agent, anti-

fungal, anti-HIV [7]. Among its many benefits, curcumin has vital role in inhibiting the colon cancer, breast cancer, liver cancer, prostate cancer. In the past few years, the extraordinary actions of curcumin against cancer have been scientifically documented. Chemo protective anti cancer effects were well documented by Gupta *et al* [8]. Due to its significant pharmacological importance we have synthesized the following curcumin analogs **(3a-3d)** with solid support i.e., in the absence of a solvent.

RESULTS & DISCUSSION

Generally chloroform, methylene chloride, carbon tetra chloride etc are used as solvents in organic synthesis which are not only costly but are very harmful for those who are handling them also. Among them, carbon tetrachloride is worst solvent as it is highly environment destructive. In green chemistry, an attempt has been made to minimize or eliminate these effects by using solvent free/solid support synthesis. Thus, a new synthetic route was developed to obtain 1,7-bis(substituted phenyl)1,6-heptadene-3,5-diones **(3a-3d)** by employing Silica-sulphuric acid as a solvent free/solid support method.

Synthesis of 1,7-bis(substituted phenyl)1,6-heptadene-3,5-diones (3a-3d):

Acetyl acetone **(1) (**1 mmole) is treated with substituted benzaldehydes (**2a-2d)** (2 mmole) in presence of Silica-sulphuric acid and ground thoroughly. The reaction mixture was further heated to 80^0C. At the interval of 15-20 min, the completion of the reaction was checked with TLC. After the completion of the reaction, the reaction mixture was recovered with 10ml of ethyl acetate. The solvent is recovered and catalyst was separated by filtration, residual compound was recrystallized to attain the target compounds i.e. 1,7-bis(substituted phenyl)1,6-heptadiene-3,5-diones **(3a-3d)**. Yield and melting points were recorded. The synthetic steps in the synthesis are illustrated in the **Scheme-1.**

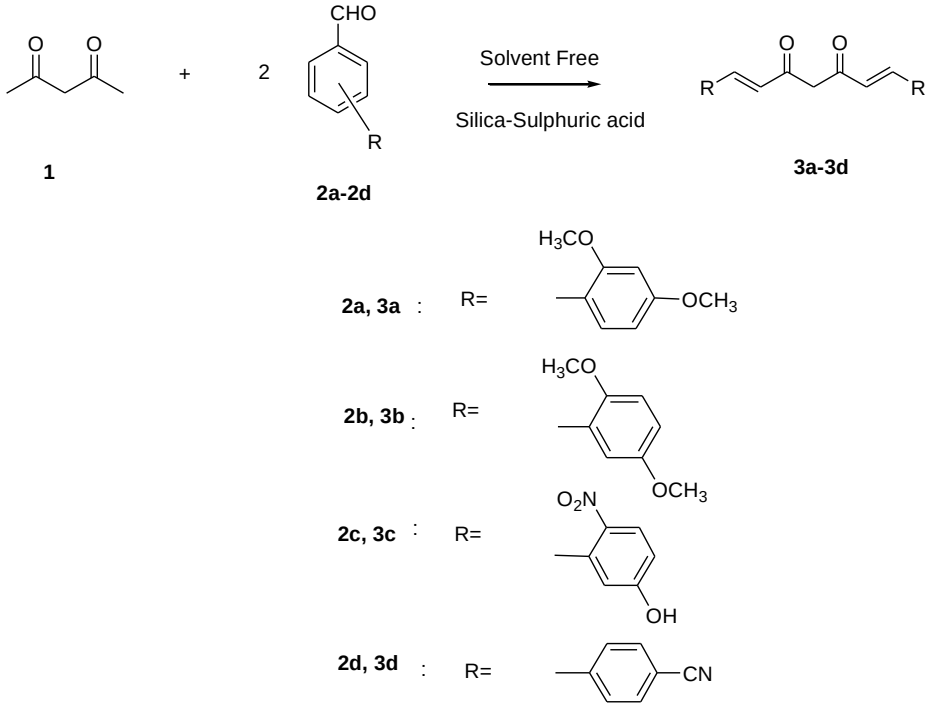

Scheme-1: Synthesis of 1,7-bis(substituted phenyl)1,6-heptadene-3,5-diones **(3a-3d)**

Characterization of 1,7-bis(substituted phenyl)1,6-heptadiene-3,5-diones (3a-3d) :

1,7-bis(2,4-dimethoxy phenyl)1,6-heptadiene-3,5-dione (3a)

Yellow crystalline compound, yield 90%, m.p.: 138°C.

IR (ν_{max}, KBr, cm^{-1}) : 2900, 2850, 1660, 1500, 1250, 1180, 1150, 1001.

^{1}H NMR (90 MHz, $CDCl_3$, TMS) δ : 3.74 (s, 6H, 2xOCH_3), 3.82 (s, 6H, 2xOCH_3), 5.58 (s, 2H, CH_2), 6.09 (s, Ar-H), 6.45-6.53 (d, Ar-H), 6.74-6.93 (d, olefinic

protons), 7.10-7.23 (d, Ar-H), 7.44- 7.53 (d, Ar-H), 7.91-8.09 (d, olefinic protons).

^{13}C NMR (22.5 MHz, $CDCl_3$, TMS) δ : 190.0, 162.8, 160.0, 137.0, 130.2, 124.2, 117.3, 105.1, 98.1, 55.8, 55.0, 29.6.

Mass m/e : 396.

Elemental analysis : calc. C, 69.68, H, 6.16; found C, 69.60, H, 6.13.

1,7-bis(2,5-dimethoxy phenyl)1,6-heptadiene-3,5-dione (3b)

Yellow amorphous solid, yield 80%, m.p. : 140°C.

IR (ν_{max}, KBr, cm^{-1}) : 1650, 1509, 1288, 1211, 1157, 1118, 1033, 979, 835.

^{1}H NMR (90 MHz, $CDCl_3$, TMS) δ : 3.84 (s, 6H, 2xOCH_3), 3.88 (s, 6H, 2xOCH_3), 5.27 (s, 2H, CH_2), 6.47-6.55 (d, Ar-H), 6.97-7.15 (d, oliefinic protons), 7.50-7.60 (d, 1H, Ar-H), 7.69-8.07 (s, olefinic proton).

^{13}C NMR (22.5 MHz, $CDCl_3$, TMS) δ : 199.0, 198.9, 159, 142.9, 112.9, 127.8, 127.4, 114.2, 56.9, 55.9.

Mass m/e : 396.

Elemental analysis : calc. C, 69.68, H, 6.16; found C, 69.65, H, 6.10.

1,7 bis(2-nitro, 4-hydroxy phenyl)1,6-heptadiene-3,5-dione (3c)

Yellow crystalline solid, yield 75%, m.p. : 186°C.

IR (ν_{max}, KBr, cm^{-1}) : 1680, 1570, 1500, 1212, 1160, 1034, 933, 830.

^{1}HNMR (90 MHz, $CDCl_3$, TMS) δ : 5.0 (s, OH), 5.83 (s, 2H, CH_2), 6.70 (d, 1H, olefinic proton), 7.07 (d, 2H, Ar-H), 7.4 (d, 2H, Ar-H), 7.61 (s, 2H, Ar-H).

^{13}C NMR (22.5 MHz, $CDCl_3$, TMS) δ : 198.9, 198.8, 158.6, 128.7, 122.6, 121.9, 110.0, 107.0, 51.9.

Mass m/e : 498.

Elemental analysis : calc. C, 57.29, H, 3.54, N, 7.03; found C, 57.30, H, 3.50, N, 7.00.

1,7 bis(4-cyano phenyl)1,6-heptadiene-3,5-dione (3d)

Yellow crystalline solid, yield 85%, m.p. : 210°C.

IR (ν_{max}, KBr, cm^{-1}) : 2254, 1684, 1568, 1512, 1219, 1174, 1025, 974, 845.

^{1}HNMR (90 MHz, $CDCl_3$, TMS) δ : 5.88 (s, 2H, CH_2), 6.77 (d, 1H, olefinic proton), 7.14 (d, 2H, Ar-H), 7.51 (d, 2H, Ar-H), 7.72 (s, 2H, Ar-H).

^{13}C NMR (22.5 MHz, $CDCl_3$, TMS) δ : 198.4, 198.1, 158.7, 128.4, 122.3, 121.3, 110.8, 108.3, 52.1.

Mass m/e : 326.

Elemental analysis : calc. C, 77.29, H, 4.32, N, 8.58; found C, 77.30, H, 4.33, N, 8.55.

CONCLUSION

It is clear that Green chemistry not only helps us in designing of new ways to synthesize the desired product economically, user friendly and it also helps to save the environment. A good flow of knowledge between the Industries and research institutions/universities undergoing such types of research topics will not only enable us to expand our knowledge but it would also help to protect the environment.

ACKNOWLEDGMENTS

Our Immense and heartfelt thanks to our Professor Dr. YLN Murthy, dept. of Organic Chemistry, Andhra University, Visakhapatnam for his constant support and guidance in the successful completion of this novel chore.

REFERENCES

[1] Bianca Aparecida deMarco, Barbara Sau Rechelo, Ana Carolina Kogawa, Herida Regina Nunes Saogado., 2018. "Evolution of green chemistry and its multidimensional impacts: A review". Saudi Pharmaceutical Journal, July, https://doi.org/10.1016/j.jsps.2018.07.011.

[2] Sangita Sanjay Makone, Sandeep Nivruttirao Niwadange. 2015. "Green Chemistry Alternatives for Sustainable Development in Organic Synthesis". Inter. Adv. Res. J. Sci. Eng. Tech., (IARJSET), 3(6), June, pp.113-115.

[3] R.B. Merrifield., 1963. "Solid Phase Peptide Synthesis". J. Am. Chem. Soc., 85 (14), July, pp 2149–2154.

[4] Mahesh K Dalal, 2012. "Green Chemistry on Solid Support". APCBEE Procedia, 3, May, pp.276-280.

[5] Sangeeta Verma, Sachin Goyal, Shivali Shingla, 2018. "Green Chemistry: A New Approach to The Synthesis, Processing and Application of Chemical Substances". Int. J Biotech & Bioeng. 4(4), April, pp. 89-95.

[6] Susan J. Hewlings, Douglas S. Kalman, 2017. "Curcumin: A Review of Its' Effects on Human Health". Foods, 6(10), October, pp.92-98.

[7] Augustine Anmalraj, Anitha Pius, Sreerag Gopi, Sreeraj Gopi, 2017. "Biological activities of curcuminoids, other biomolecules from turmeric and their derivatives - A review". J. Tradit. Complement. Med., 7(2), April. pp.205-233.

[8] Gupta A.P, Khan S, Manzoor MM, Yadav AK, Sharma G, Anand R, Gupta S. 2017. "Chapter 10 - Anticancer Curcumin: Natural Analogues and Structure-Activity Relationship". Stud. Nat. Prod. Chem. 54, 355-401.

SEEC No.64

Nitrate supplemented medium for enhanced biomass of *Chlorella sp.* DBRF-1

Sweta Singh
Defence Institute of Bioenergy Research (DRDO)
Email: swetasinghbt22@gmail.com

Atul Grover
Defence Institute of Bioenergy Research (DRDO)
iatulgrover@gmail.com

Madhu Bala
Defence Institute of Bioenergy Research (DRDO)
director@diber.drdo.in

ABSTRACT

Microalgae can potentially prove to be a viable alternative and a viable source of biofuels. Carbohydrate, protein and lipids are all extractable in sufficiently high quantities from microalgae. Here, we report Chlorella sp. DBRF-1 isolated locally, which has potential to be grown for the biomass. The strain was identified by 18S rRNA sequencing. The Phylogenetic analysis of nuclear-encoded small-subunit rDNA sequences of isolate; DBRF-1 showed 99% similarity with Chlorella sorokiniana (green algae which grows in freshwater ecosystem) isolate PCPBEC (Accession Number: KY471550.1) and the DNA sequence data was published in Genbank, assigned with a unique accession no. MH725912. The influence of different nitrogen sources (sodium nitrate, potassium nitrate, calcium nitrate, ammonium nitrate and urea) of varying concentrations (5mM, 10mM and 15mM) on biomass production of green algae DBRF-1 was investigated. Nitrate was found to be a preferred form of nitrogen source. The DBRF-1 strain produced 0.62 g/l dry mass when the BG-11 medium was supplemented with 10 mM sodium nitrate as compared with control and 15mM sodium nitrate. Urea (0.4 g/L) also resulted in almost significant biomass growth as nitrates, making it an economical substitute for nitrogen source in large scale culturing of algae being commercially available. We sincerely believe that efforts to enhance biomass will lead to an economical method towards development of algal biomass to biofuel approach.

ACKNOWLEDGMENTS

Defence Research and Development Organisation (DRDO), New Delhi is duly acknowledged for funding the project.

Proceedings of theThird International Conference on Sustainable Energy and Environmental Challenges (3rd SEEC)
18 –21 December, 2018, IIT Roorkee, India

SEEC No.066

NUMERICAL ANALYSIS OF EFFECT OF ASPECT RATIO AND FLOW RATE ON THE PERFORMANCE OF PCM BASED THERMAL ENERGY STORAGE SYSTEM

Kedumese u Mekrisuh
Research Scholar
Department of Mechanical Engineering
National Institute of TechnologyManipur
Email: kedumeseumekrisuh@gmail.com

Dr. Dushyant Singh
Assistant Professor
Department of Mechanical Engineering
National Institute of Technology Manipur
Email: dushyant@nitmanipur.ac.in

Dr. Udayraj
Assistant Professor
Department of Mechanical Engineering
Indian Institute of Technology Bhilai
Email: udayraj@iitbhilai.ac.in

ABSTRACT

A thermal energy storage system filled with PCM in an annular space was numerically studied considering three aspect ratios (4.13, 11.20, 19.84) while maintaining constant PCM volume. Studies were also carried out with three different mass flow rate (0.008316 kg/s, 0.01663 kg/s, 0.02495 kg/s) of heat transfer fluid. Effects of geometrical parameters of the energy storage system and flow rate of heat transfer fluid were studied on performance of the storage system. Thermal response rate of the system improved with the increase of the aspect ratio of the energy storage system and also with the increase in mass flow rate of heat transfer fluid. The maximum improvement in the melting rate of 61 % was observed at an aspect ratio of 19.84 and mass flow rate of 0.02495 kg/s.

***Keywords*:**latent heat storage system, phase change material, numerical modeling, liquid fraction, heat transfer fluid.

NOMENCLATURE

H	Total enthalpy,(kJ/kg)
L	Latent heat, (kJ/kg)
P	Pressure, (Pa)
$\vec{S}$	Source term, (kg/m^{3}s)
T	Temperature, (K)
$\vec{V}$	Velocity vector, (m/s)
β	Liquid fraction

INTRODUCTION

Utility of phase change material (PCM) in the field of solar power plant, air-conditioning, heating/cooling of space, textile industry, cooling of electronic chips and other areas has been identified in the last six decades. An important area where PCMs are being used widely is the thermal energy storage systems. They are used to store excess energy which can be utilized later as per the demand. This system lead to the effective utilization of renewable energy technologies that are intermittent in nature. Attention is also focused on the latent heat storage systems because of its higher heat storage capacity at nearly isothermal conditions. However, one major disadvantage associated with such systems is the lower thermal conductivity of PCMs (0.2-0.5 W/mK) leading to slower thermal response during their charging and discharging. Enhancement of the thermal response rate of PCMs has been the area of great interest to the researchers. Agyenim et al. [1] presented a review on the enhancement techniques that includes incorporation of metallic wool, foam, powder inserts with a honeycomb structure, porous media, fins and nanoparticles additives. With the advancement of nanotechnology, highly conductive particles were added in PCMs to compensate for the lower thermal conductivity of PCMs.

Researchers have worked on various geometries of energy storage systems incorporating various enhancement techniques for renewable energy technology. A rectangular enclosure heated from a vertical side was experimentally investigated by Wang et al. [2] to study the thermal characteristics of the melting process of PCM. A flat plate heat pipe was utilized to provide a near uniform wall temperature at all time. They have provided appropriate correlations for volume fraction and Nusselt number of PCM in rectangular enclosure. Hosseinizadeh et al. [3] performed both numerical and experimental investigations of PCM inside a spherical container during unconstrained melting of n-octadecane. Agyenim et al. [4] analyzed a horizontal concentric tube latent heat based energy storage system incorporating erythritol which has a melting temperature of 117.7 °C. Circular and longitudinal fins in the annular region was used to improve the thermal response rate of PCM. They have reported that the longitudinal fins provided better results. Al-Abidi et al. [5] experimentally investigated a triplex-tube heat exchanger with internal and external fins provided in the annular region filled with PCM where heat transfer fluid (HTF) flows in the innermost and outermost tubes. They studied

the influence of inlet temperature and mass flow rate of HTF on the heat exchanger performance. It was found that increasing inlet temperature was more effective than increasing mass flow rate. Hosseini et al. [6] conducted experimental and numerical study to analyze thermal behavior and heat transfer characteristics of paraffin RT50 in a shell and tube heat exchanger during a constrained melting and solidification process. The experimental findings revealed that increase in inlet temperature of HTF from 70 °C to 80 °C increased the theoretical efficiency during charging by 7.3 % thereby decreasing the melting time by 37 %) and discharging by 1.7 %. Kurnia et al. [7] evaluated numerically the heat transfer performance of a PCM based thermal storage system with different designs of tube such as U-tube, U-tube with inline and staggered fins, and U-tube of festoon design. Tube with festoon design provided the best heat transfer performance. Effect of volume expansion during melting was also analyzed in a vertical cylinder filled with paraffin wax and significant effect of considering volumetric expansionwas reported at low Biot number [8]. Tao et al. [9] studied the effect of natural convection in a shell and tube type latent heat storage unit and reported that the effect of natural convection was significant especially when PCM was filled in the tube region so it should not be neglected.

In the present study, thermal response rate of PCM in vertically oriented double-pipe thermal energy storage system is analyzed numerically. Paraffin wax is used as PCM and it is filled in the annular space and HTF which is water flows in the inner vertical tube. Effect of different aspect ratio of the energy storage systems of same volumetric capacity was analyzed for different flow rate of HTF.

PHYSICAL MODEL

TABLE:1 Cases Under Studied

Height H (m)	ID d (m)	Aspect ratio (H/D)	Mass flow rate (l/min)
1.5	0.035	19.84	1.5
1.5	0.035	19.84	1.0
1.5	0.035	19.84	0.5
1.0	0.035	11.20	1.5
1.0	0.035	11.20	1.0
1.0	0.035	11.20	0.5
0.5	0.035	4.13	1.5
0.5	0.035	4.13	1.0
0.5	0.035	4.13	0.5

Figure 1 shows the physical model of the problem considered in the present study. The problem consists of a double-pipe, vertically orientated heat storage system. PCM (paraffin wax) is filled in between inner and outer

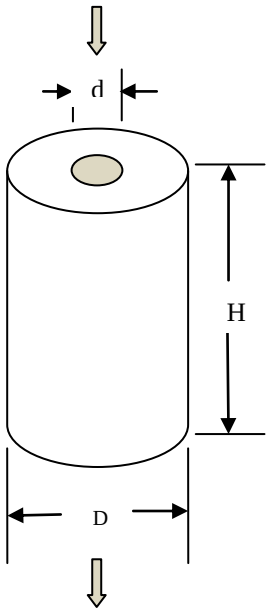

FIGURE 1. Schematic representation of the energy storage system.

cylinders. HTF flows in the inner tude in vertically downward direction. Dimensions of the physical model under consideration are given in the Table 1. Parametric study has been performed by considering storage system of different aspect ratio while keeping the PCM volume same. In order to maintain same PCM volume in all the cases, both height of the tube (H) and outer diameter (D) were changed.

NUMERICAL MODELING AND VALIDATION

Numerical modeling of phase change problem involving melting which takes place over a range of temperature is studied considering enthalpy-porosity formulation. In this, the phase change front is not tracked explicitly but treated as a porous zone with porosity equal to the liquid fraction. Governing equations solved considering unsteady, incompressible and laminar flow of HTF and phase change phenomenon are as follows [10]:

Continuity equation:

$$\nabla.\vec{V} = 0 \qquad (1)$$

Momentum equation:

$$\frac{\partial \vec{V}}{\partial t} + \vec{V}.\nabla\vec{V} = \frac{1}{\rho}\left(-\nabla p + \mu\nabla^2\vec{V} + \rho\beta\vec{g}\left(T - T_{ref}\right)\right) + \vec{S} \qquad (2)$$

$$\text{where } \vec{S} = \frac{(1-\beta)^2}{\beta^3} A_{mush}\vec{V} \qquad (3)$$

where, A_{mush} is a mushy constant and β is liquid fraction.

$\beta = 0$ if $T < T_{solidus}$

$\beta = 1$ if $T > T_{liquidus}$

If, $T_{solidus} < T < T_{liquidus}$, $\beta = \dfrac{T - T_{solidus}}{T_{liquidus} - T_{solidus}}$ (4)

Energy equation:

$$\frac{\partial h}{\partial t} + \frac{\partial H}{\partial t} + \nabla.\left(\vec{V}h\right) = \nabla.\left(\frac{k}{c_p}\nabla h\right) \quad (5)$$

The total enthalpy of the material is computed as the sum of the sensible enthalpy, h, and the latent heat, ΔH.

$$H = h + \Delta H \quad (6)$$

The latent heat content can now be written in terms of the latent heat of the material, L:

$$\Delta H = \beta L \quad (7)$$

The latent heat content can vary between zero for a solid and L for a liquid.

To deal with natural convection, Boussinesq approximation was taken into consideration. The SIMPLE scheme is utilized for pressure-velocity coupling. The energy and momentum equations were solved using the QUICK differencing scheme. The PRESTO scheme is utilized for the pressure correction equation.The lateral surface (boundary) of the outer tube is considered insulated. PCM is considered initially at 293 K and the HTF enters into the tube at 343 K.

In order to validate the numerical model, results were validated with Seddegh et al. [11]. It can be observed from Figure 2 that the present results agrees very well with the previously published results.

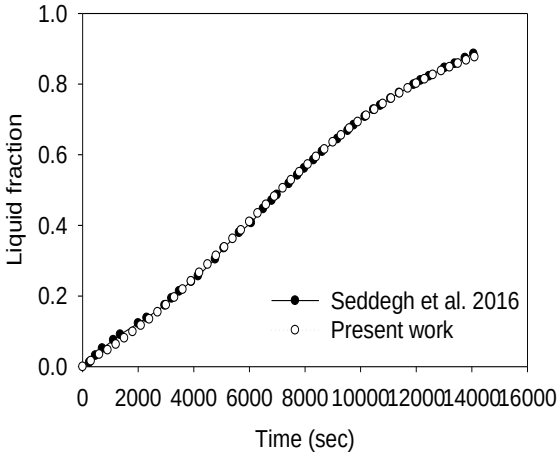

FIGURE 2. Comparison of liquid fraction obtained from thepresent study and Seddegh et al. [11].

RESULT AND DISCUSSION

Grid independence test was conducted and it is found that 3998 nodes is sufficient for the present study. For time step size independence study, time step size of 1.0, 0.5, 0.1, 0.05 s were studied. No difference were noted in results obtained by considering time step sizes of 0.5 and 0.1 s.

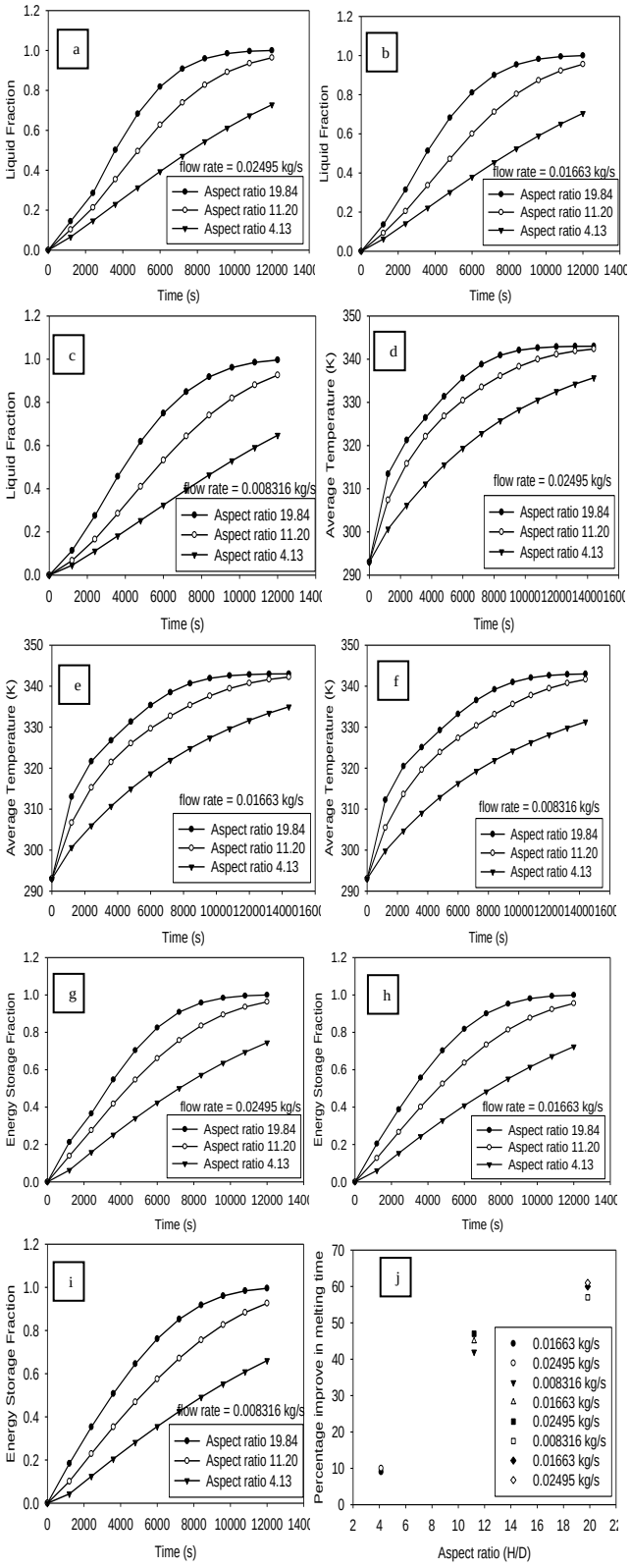

FIGURE 3.(3a-3i)Effect of aspect ratio on systemperformance for different mass flow rate of HTF. (3j) Improvement of melting rate of PCM.

Hence, a time step size of 0.5 s is chosen for the study keeping in mind the associated computational cost.It is to be noted that the entire performance comparison on PCM is done for a complete melting of PCM and the tube diameter and storage volume of PCM is kept constant for the entire cases of studies.

Figures 3a, 3b and 3c shows variation of liquid fraction of PCM with time at different mass flow rate of HTF and different aspect ratio. By increasing the aspect ratio to 19.84, the melting time can be improved by 56.67% as compared to the 4.13 aspect ratio case for a mass flow rate of 0.02495 kg/s. Whereas when the aspect ratio is fixed at 19.84, an enhancement of 9.30 % in melting rate can be achieved by increasing mass flow rate from 0.008316 kg/s to 0.02495 kg/s. Figure 3b, shows the effect of aspect ratio on PCM liquid fraction at a mass flow rate of 0.01663 kg/s. when the aspect ratio is increased from 4.13 to 11.2, there is an improvement of melting time by 39.56 % and further from 4.13 to 19.84 improves the melting time by 56.04 %. As the mass flow rate is increased from 0.008316 kg/s to 0.02495 kg/s while maintaining the aspect ratio at 11.2, there is an improvement of melting time by 8.6 %. Figure 3c, shows the effect of aspect ratio while maintaining a constant mass flow rate of 0.008316 kg/s and increasing the aspect ratio from 4.13 to 19.84 improves the melting time by 57%. When constant aspect ratio of 4.13 is maintained and the mass flow rate is increased from 0.008316 kg/s to 0.02495 kg/s, it improves the melting time by 10 %. From the above discussion, it can be noted that the effect of aspect ratio on melting rate is significant while flow rate have relatively lower effect on the melting rate of PCM.

Figures 3d-3f show the variation of PCM average temperature with time at different flow rates of HTF. Higher aspect ratio lead to larger heat transfer surface area and hence, higher heat transfer to the PCM from the HTF and higher PCM temperature. This is also the reason to have higher melting rate at higher aspect ratios of the system. Figures 3g-3i show the change in energy storage fraction with time, which is defined as the ratio of instantaneous energy stored tothe maximum possible energy storage by PCM. The energy storage fraction is higher at higher aspect ratio for all the three mass flow rates of HTF because of the higher melting rate of PCM at higher aspect ratios. The plot on the performance of PCM on melting time when aspect ratio of 4.13 and mass flow rate of 0.008316 kg/s is compared with each parametric cases of study is shown in figure 3j.

CONCLUSIONS

Following conclusions can be drawn from the present studies.

1. Melting rate of PCMs in latent heat storage system increases with increase in aspect ratio of the system and massflow rate of HTF.
2. Effect of the aspect ratio is more pronounced in the performance of the energy storage system as compared to the HTF mass flow rate.
3. Melting rate enhancement as high as 56.67 % can be achieved by increasing aspect ratio from 4.13 to 19.84 at 0.02495 kg/s HTF flow rate..

REFERENCES

[1] F. Agyenim, N. Hewitt, P. Eames, M. Smyth, A review of materials, heat transfer and phase change problem formulation for latent heat thermal energy storage systems (LHTESS), Renewable and Sustainable Energy Reviews 14 (2010) 615-628.

[2] Y. Wang, A. Amiri, K. Vafai, An experimental investigation of the melting process in a rectangular enclosure. International Journal of Heat and Mass Transfer 42 (1999) 3659-3672.

[3] S.F. Hosseinizadeh, A.A.R. Darzi, F.L. Tan, J.M. Khodadadi, Unconstrained melting inside a sphere, International Journal of Thermal Sciences 63 (2013) 55-64.

[4] F. Agyenim, P. Eames, M. Smyth, A comparison of heat transfer enhancement in a medium temperature thermal energy storage heat exchanger using fins, Solar Energy 83 (2009) 1509-1520.

[5] A.A. Al-Abidi, S. Mat, K. Sopian, M.Y. Sulaiman, A.T. Mohammad, Experimental study of melting and solidification of PCM in a triplex tube heat exchanger with fins, Energy and Buildings 68 (2014) 33–41.

[6] M.J. Hosseini, M. Rahimi, R. Bahrampoury, Experimental and computational evolution of a shell and tube heat exchanger as a PCM thermal storage system, International Communications in Heat and Mass Transfer 50 (2014) 128–136.

[7] J.C. Kurnia, A.P. Sasmito, S.V. Jangam, A.S. Mujumdar, Improved design for heat transfer performance of a novel phase change material (PCM) thermal energy storage (TES), Applied Thermal Engineering 50 (2013) 896-907.

[8] M.A. Hassab, M.M. Sorour, M.K. Mansour, M.M. Zaytoun, Effect of volume expansion on the melting process's thermal behavior, Applied Thermal Engineering 115 (2017) 350–362.

[9] Y.B. Tao, Y.K. Liu, Y. He, Effects of PCM arrangement and natural convection on charging and discharging performance of shell-and-tube LHS unit, International Journal of Heat and Mass Transfer 115 (2017) 99–107.

[10] ANSYS FLUENT Theory Guide, ANSYS Inc, USA, 2011 (Chapter 18).

[11] S. Seddegh, X. Wang, A. D. Henderson, Numerical investigation of heat transfer mechanism in a vertical shell and tube latentheat energy storage system, Applied Thermal Engineering 93 (2016) 348–358.

Proceedings of the Third International Conference on Sustainable Energy and Environmental Challenges (3rd SEEC)
18-21 December, 2018, IIT Roorkee, India

SEEC No.067

Design, Construction and Thermal Performance of a Solar House

Rahul Dev*
Mechanical Engineering Department, Motilal Nehru National Institute of Technology Allahabad, Allahabad, U.P., India.
*Email:*rahuldsurya@mnnit.ac.in*

Ajaya Bharti
Applied Mechanics Department, Motilal Nehru National Institute of Technology Allahabad, Allahabad, U.P., India.
Email: abharti@mnnit.ac.in

Aman Kumar
Mechanical Engineering Department, Motilal Nehru National Institute of Technology Allahabad, Allahabad, U.P., India.
Email:amankumar2343@gmail.com

Ankit Meena
Mechanical Engineering Department, Motilal Nehru National Institute of Technology Allahabad, Allahabad, U.P., India.

Amaresh Kumar Singh
Mechanical Engineering Department, Motilal Nehru National Institute of Technology Allahabad, Allahabad, U.P., India.

Amarendra Kumar
Mechanical Engineering Department, Motilal Nehru National Institute of Technology Allahabad, Allahabad, U.P., India.

Mohit dev
Department of Architecture and Planning,
Indian Institute of Technology Roorkee, Roorkee, U.K., India
Email: mohidev@gmail.com

Abstract:
Buildings consumes electricity to provide thermal comfort but to protect our environment from effects of pollution and global warming, thermal comfort can be provided using concepts of solar architecture. Whereas, energy efficiency of any existing or planning stage building, can be improved using solar energy technologies. In the present work, a solar house is designed with a major focus on concepts of solar architecture as well as use of photovoltaic system (for electricity generation to be used during day/night) for maintaining the inside temperature of a chamber of dimensions 5×6×6 ft^3. An experimental thermal analysis has been done for the solar house for the climatic condition of Allahabad, Uttar Pradesh, India.

Keywords: *Solar Architecture, Thermal Comfort, Fibre Reinforced Plastic.*

Introduction:

Buildings consume electrical energy in very high proportion in various applications such as cooling, heating, ventilation and lighting for proper providing thermal comfort. The total energy required for thermal comfort is increasing as number of buildings is also increasing because of continuous increase in population and living standards of human being which adds in global warming, disruption of climate, and crisis in energy security [1]. In today's scenario, to reduce anthropogenic CO_2 emission especially from buildings, a building giving an year round thermal comfort without using conventional sources of energy based electrical devices such as air conditioning unit, and room heater etc, is a good solution to problems arising from conventional buildings made in cities mainly [2].

In this communication, a solar house is designed and constructed to study its behaviour from the thermal comfort point of view, for the climatic condition of Allahabad (25.4358°N, 81.8463°E), Uttar Pradesh, India.

Materials and Methods:

The dimensions of the chamber (5×6×6 ft^3) is taken for small scale applications such as designing the security guard's chamber, outdoor laboratory room, farmer's field room. Whereas depending upon the capacity and activity, the dimensions can be varied. The walls thickness including thicknesses of material used for fabricating walls and roof are calculated and considered with a criteria of equivalent thickness compared to brick-cement wall [3]. Some provisions for daylighting and ventilation are also given in the walls and roof to provide proper illumination and air circulation in the chamber. The walls of the chamber is made of fibre reinforced plastic and thermocol. The support structure for walls and roof is made of iron angles to prevent bucking of walls and to protect walls from bearing the load of the roof. The un-conventional materials (Fibre reinforced plastic (FRP), Thermocol, and Ashbricks) have been selected because of their low thermal conductivity, and good strength of composite made of FRP and thermocol for making walls and roof and supported by L-shape G.I. angles. Simple glass is selected for window and PV module is used for generating electricity to be used for illumination during day or night time as per requirement. Use of FRP, Thermocol, Ashbricks and PV module are a technological advancement in the building [3].

Figure 1 shows the schematic diagram and Figure 2 shows the photograph of the solar house. The following considerations based on principles of passive architecture [4,5] have been used in the solar house.

.

(i) Orientation for heating and cooling of the proposed room, (ii) Ventilation, (iii) Daylight, (iv)

Composite walls for self cooling, (v) Electricity generation, (vi) Dimensions of the room.

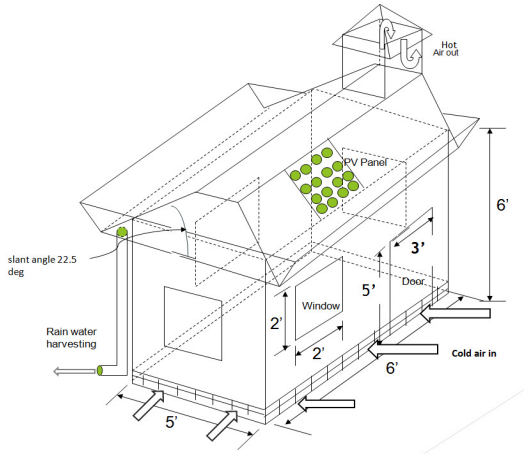

Figure 1: Schematic diagram of Solar house.

Figure 2: Photograph of Solar house.

Results and Discussion:

The calculation, results and analysis involves:
(i) Determination of optimum thickness of wall, (ii) Design of roof overhang, (iii) Types of window, (iv) Foundation of the room, (v) Designing of roof for low weight, (vi) Buckling test for L-shaped GI angles, (vii) Bending test of wall due to high wind velocity.

After all the calculations and test results, observations have been taken in April, 2018 during day and night (from 7:00 AM to 6:00 AM next day), which are shown in Figure (3-9), which are as follows:

- Out of four walls, the temperature of north wall is found lowest and the difference between outer and inner wall is also minimum for the north wall. Whereas, temperature on upper side of south wall is greater than middle and lower value because of trough. The variation in the temperature of the north wall is less than that of east, south and west walls. It has the minimum temperature throughout the day.

- By using two air gap of 3 mm between FRP sheets and thermocol. Maximum temperature difference of 10˚C between the outer and inner wall surfaces are achieved. The surface temperature of the wall is greater than ambient temperature.
- The major source of heat gain is the mild steel rod used in the wall. Because of this the temperature difference of 6-7℃ is obtained between the ambient and room.
- In the morning, east wall is directly facing the sun. Hence in morning the temperature of east wall is maximum. In afternoon the location of sun reaches in the west direction. West wall faces direct solar radiation. Its temperature starts rising from afternoon till evening. The maximum temperature of the west wall is at 3:00 pm.
- In the night the temperature is falling at greater rate. The temperature of the walls is less than ambient temperature. The temperature of all the walls is approximately same in the night. The thermal comfort in terms of temperature up to 35℃ is achieved.

Figure 3: Observations during night for Solar house.

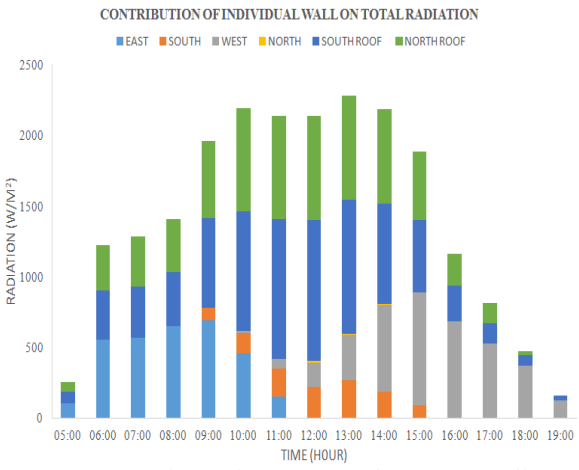

Figure 4: Solar radiation contribution on walls.

- Figure 4 shows the solar radiation contribution on walls.
- Figures (5-8) are plotted as temperature of walls of house inside and outside, and Figure 9 shows house temperature, air temperature at exit of chimney, and ambient for twenty four hour duration. The variation in the temperature of solar house is very less. The maximum temperature of the solar house

is 35 ℃ in the afternoon. Solar chimney is installed with the objective to set a convection current because of density difference in the air. The maximum temperature of the solar chimney is around 48℃. Ambient temperature is somewhat greater than the room temperature. The temperature difference obtained between ambient and room is about 6-7 ℃.

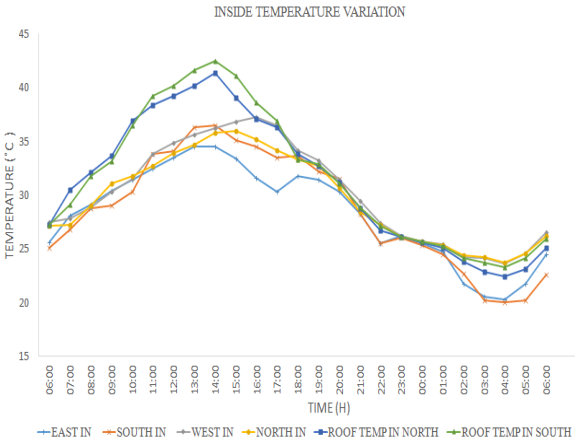

Figure 5: Temperature variation of walls (inside).

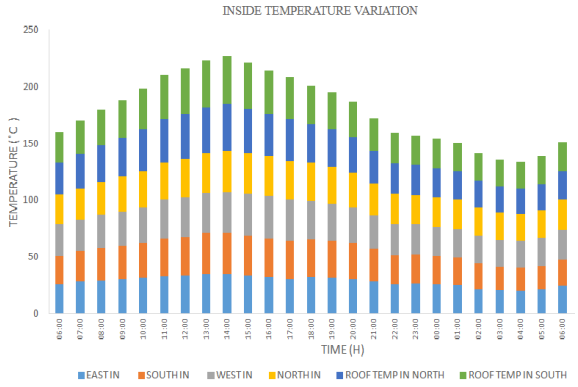

Figure 6: Temperature variation of walls (inside).

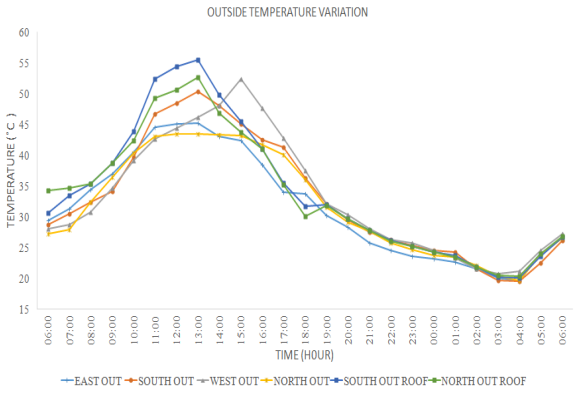

Figure 7: Temperature variation of walls (outside).

The temperature difference obtained between chimney and room is about 14℃. The maximum outside temperature on the day of reading was around 41℃. A PV panel with battery is also used to store the electricity produced to run electric bulb etc, during the night.

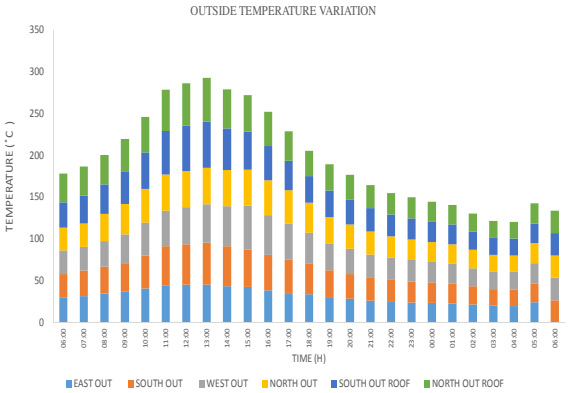

Figure 8: Temperature variation of walls (outside).

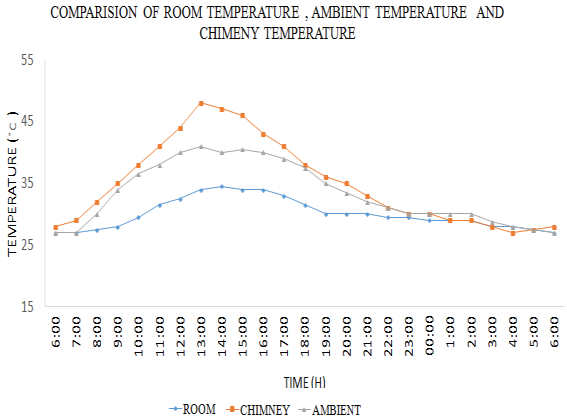

Figure 9: Variations of various temperatures.

Conclusion:

The following are the conclusions:

(i) A Solar house has been designed, constructed using concepts of passive solar architecture and experimentally studied for the thermal behaviour point of view.

(ii) Un-conventional materials have been used for small scale (size) buildings. These materials suited to construct and lowering down the inside solar house temperature in respect to high ambient temperature.

Acknowledgement:

Authors are thankful to Coordinator, TEQIP-III, MNNIT Allahabad, Allahabad for providing necessary fund for the present work.

References:

[1] Tiwari, G.N. (2012), "Solar Energy : Fundamentals, Design, Modelling and Application" (Revised Edition), Narosa Publishing House Pvt. Ltd. - New Delhi, **ISBN-13:** 978-8184872774.

[2] Kachadorian J., (2006) "Passive Solar House: The Complete Guide to Heating and Cooling Your Home", Chelsea Green Publishing; Revised and

expanded second edition edition , ISBN-13: 978-1933392035.

[3] Dev R., Bharti A., "Estimation of Performance of Proposed Room Designed on Solar Architectural Concepts", 2nd International Conference on Renewable Energy and Environmental Engineering (ICREEE 2017), Godavari academy of science and Technology, Khajuraho (UNESCO World Heritage Site), December 09-11, 2017, Conference Proceedings Page 26. ISBN 13: 978-81-930222-4-5, Published by: Basha Research Corporation, Hyderabad, India.

[4] Chiras D.D., (2002) "The Solar House, Passive Heating and Cooling", Chelsea Green Publishing; 1st Edition Later Printing edition, ISBN-13: 978-1931498128.

[5] Dutta B.N., "Estimating and Costing in Civil Engineering Theory and Practice Including Specifications and Valuations, UBS Publishers & Distributors Ltd., ISBN-13: 978-8174767295.

SEEC No.069

EMBODIED ENERGY, PAY-BACK PERIOD AND COST ANALYSIS OF TRIPLE SLOPE SOLAR STILL INTEGRATED WITH GLASS-GLASS PV MODULE

Gaurav Kumar
Mechanical Engineering Department
Kamla Nehru Institute of Technology Sultanpur, Sultanpur–228118, Uttar Pradesh, India
Email: gaurav_kumar500@yahoo.com

Piyush Pal*
Department of Mechanical Engineering
Motilal Nehru National Institute of Technology Allahabad, Allahabad–211004, Uttar Pradesh, India
Email: piyushpal19@gmail.com, rme1454@mnnit.ac.in
*Corresponding Author

Pulkit Agarwal
Department of Mechanical Engineering
Motilal Nehru National Institute of Technology Allahabad, Allahabad–211004, Uttar Pradesh, India
Email: pulkithtc830@gmail.com

Rahul Dev
Departmea nt of Mechanical Engineering
Motilal Nehru National Institute of Technology Allahabad, Allahabad–211004, Uttar Pradesh, India
Email: rahuldsurya@mnnit.ac.the in

Akhilesh Kumar Chauhan
Mechanical Engineering Department
Kamla Nehru Institute of Technology Sultanpur, Sultanpur–228118, Uttar Pradesh, India
Email: akc.knit@gmail.com

ABSTRACT

In this paper, the embodied energy, pay-back period and cost analysis of triple slope solar still (TSSS) are studied which is compared with the double slope solar still (DSSS). The embodied energy is an important factor in determining optimum material for solar still whose value depends on local availability of materials and their manufacturing processes. The total embodied energy of TSSS comes out to be 2595.22 MJ. Energy pay-back time is 0.202 and the total cost for constructing TSSS is Rs. 14049. The TSSS embodied energy comes out to be 40% less than double slope solar still. EPBT of TSSS comes out to be 242% smaller than of DSSS.

Keywords: Triple Slope Solar Still (TSSS), Fibre Reinforced Plastic (FRP), Energy Payback Time (EPBT), Double Slope Solar Still (DSSS).

INTRODUCTION

As long as hundreds of millions of years ago the water we drink today is been around in one form or other. Over time, the amount of freshwater on earth is remained fairly constant by recycling continuously. But at the same time, the human population is growing at an alarming rate i.e. in 2018 at the growth rate of around 1.09% (i.e. 83 million people per year) resulting in a shortage of freshwater.

Today, the world fresh water need is mostly fulfilled by using devices that run on non-renewable resources of energy like coal, oil, gas etc. This way of purification of water is not only high on cost but also requires experienced personnel to deal with the complexity of it. Also, it causes a significant amount of environmental pollution.

To ease the burden on conventional sources of energy a solar distillation technology is been worked upon. Solar still is a device which is used for purifying saline water with the help of solar radiation. There is an immense diversity of solar stills available, both active and passive. Several forms of solar still are made such as hemispherical solar still, pyramid solar still, spherical solar still, double basin glass solar still, tubular solar still, concentrator coupled single slope solar still, and tubular solar still coupled with pyramid solar still [1]. Many types of research have been done to enhance the output yield of solar stills. Badran et al. [2] research work suggests that with a rise in ambient temperature and solar intensity results in increased productivity. Also, by lowering the water depth from 3.5 cm to 2 cm there is a rise in productivity. The rate of evaporation is also found out to be proportional to the basin temperature.

Malaiyappan et al. [3] raised the temperature of the basin by coupling it with several elements like aluminum fins, a long hollow stainless-steel tube, helical copper coil and an iron plate. The solar still integrated with aluminium fins give the highest yield. El-Sebaii et al. [4] find out the thermal performance of a finned single basin solar still using different materials for finned basin liner such as, glass, stainless steel, mica, aluminium, iron, copper and brass. He concluded that the fin material does not have a significant effect on productivity and efficiency. Rather by adding fins to basin improve productivity by 16.39%. Rufuss et al. [5] shows the effects of nanoparticle-enhanced phase change material (NPCM) on solar still productivity. Two properties are important for melting and solidification of NPCM namely thermal conductivity and latent heat respectively. High thermal conductivity helps in decreasing the melting time of PCM (paraffin); while increased latent heat helps in releasing more heat during solidification. Improvements of 23.0, 39.3, 43.2 and 18% were obtained for SSPCM, SSNPCM-1, SSNPCM-2, and SSNPCM-3, against the productivity of a conventional still. (NPCM-1, NPCM-2, and NPCM-3 contains TiO2, CuO and GO nanoparticles, respectively impregnated in paraffin). Kabeel et al. [6] studied the productivity of solar still using jute cloth knitted with sand heat energy storage. He found out that the yield of fresh water is dependent on the mass of sensible energy material and depth of water present inside the basin. The average rise in temperature of the water was found to be 25% higher in the case of jute cloth knitted to sensible heat storing material as compared to conventional solar still. Pal et al. [7] studied the energy matrices, exergo-economic and enviro-economic analysis of modified multi-wick basin type double slope solar still. The total cost of setup comes out to be Rs. 14000 and EPBT are 0.69. Also, total embodied energy comes out to be 3635.98 MJ.

The objective of the present paper is to find out the embodied energy, energy pay-back period and cost analysis of Triple slope solar still integrated with the glass-glass PV module.

SOLAR DISTILLATION SYSTEM

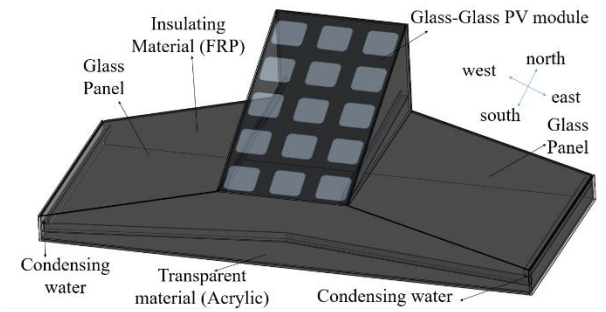

FIGURE 1: MODEL OF TRIPLE SLOPE SOLAR STILL

Fig. 1 shows the isometric view of the proposed design of triple slope solar still, which is modeled using SolidWorks 2018 software. Solar still is a box-type structure. It consists of a rectangular base, known as a basin, of dimension 0.825 m × 2 m in which saline water is filled from the holes provided on the north wall. FRP (5 mm thickness) is used as the material of construction of north and base wall of the solar still. The setup is East-West oriented so as to have glass covers on both east and west side which are inclined at an angle of 15º. Transparent acrylic sheet (3 mm thickness) is used as a material of construction for East, West and South walls. Condensed water from the glass cover and walls is collected through three troughs, one trough on each wall i.e. east, west and south. A glass-to-glass photovoltaic panel facing south is kept at an angle of 25 degrees (latitude of Allahabad). At the end of each trough, the outlet pipe is provided for collecting condensed water. One inlet pipe is used for feeding brackish water into the basin through a hole in the north wall. Walls height at East-West ends is 11 cm and a peak height of the south wall from the base is 31 cm. To generate electric power, glass-to-glass PV module is mounted on the solar still. Table 1 shows the various specification of triple slope solar still.

WORKING PRINCIPLE

Solar still is filled with brackish water from the hole provided in the north wall. Solar radiation is incident on the still and passes through the glass panel and transparent acrylic sheet in order to be absorbed by the basin and saline water present in it. This results in the rise of water temperature which causes evaporation of the top water layer. Water vapor gets mixed with air inside the solar still and raises its temperature. It increases the kinetic energy of water and air molecules such that when they collide with walls and glass cover, they release latent heat of vaporization to undergo a process of phase change from vapor to liquid state. During the course of the day more solar radiation is absorbed by water, thus further raising water temperature and enhancing the rate of evaporation. The condensate is collected in the collecting vessel placed outside the solar still at east, west and south walls. The output from the above process gives safe and potable water. The electricity produced by glass-glass PV module can be used for running DC operated devices like water pump (to lift the water and heat it by a north wall which is having a high temperature) or rotating the stirrer (to agitate water in the basin) in order to increase the rate of evaporation.

METHODOLOGY

EMBODIED ENERGY is defined as “the quantity of energy required by all of the activities associated with a production process, including the relative proportions consumed in all activities upstream to the acquisition of natural resources and the share of energy used in making energy equipment and in other supporting functions i.e. direct energy plus indirect energy” [8].

TABLE 1: DESIGN SPECIFICATIONS OF TRIPLE SLOPE SOLAR STILL

Parameters	Specification
Orientation	East – West
Location	MNNIT, Allahabad,
Location Coordinates	25.4358° N, 81.8463°
Climate	Warm and humid
Body material (Base & north wall)	FRP (Fibre-Reinforced Plastic)
Body material (East, west & South wall)	Acrylic
Basin area	0.825 m × 2 m
Thickness of FRP	5 mm
Thickness of Acrylic	3 mm
Height at ends	0.11 m
Height at center	0.31 m
Glass cover dimension	815.7 mm × 755.57 mm × 4 mm
Number of the glass cover	3
The inclination angle of the glass	15°
The color of the inside of north	Black
Number of inlets to saline water	1
Number of troughs	5
The inclination of the PV module	25°

The embodied energy of various components used in solar still is shown in Table 2.

TABLE 2: EMBODIED ENERGY OF TRIPLE SLOPE SOLAR STILL

Name of Component	Mass of Component (kg)	Mass Density (kg/m^3)	Energy Density (MJ/m^3)	Embodied Energy (MJ)
FRP (5 mm thickness)	21.5	1850	92.2	1982.44
Glass (4mm thickness)	14.95	2600	15.9	237.78
Acrylic (3mm thickness)	3.75	1200	100	375
Total	**40.2**			**2595.22**

The total embodied energy of solar still comes out to be 2595.22 MJ.

ENERGY PAYBACK TIME(EPBT) of the solar still defines the approximate time period required to recover the total energy consumed in the material preparation for constructing the solar still. EPBT depends on the embodied energy of various components used in the solar still and the annual energy output i.e. distillate yield obtained from the triple-slope solar still [7]. EPBT can be evaluated as

$$EPBT = \frac{Embodied\ energy\ in}{Annual\ energy\ out} \quad (1)$$

ANNUAL ENERGY OUT ($E_{out, ann}$) is given by:

$E_{out, ann}$ = Average daily yield x number of clear days in a year x latent heat of vaporization of water (2)

From the theoretical analysis of the above setup average daily yield was estimated to be 11.75 kg/m^2. Also, assuming 300 clear days in a year and latent heat of vaporization to be 0.627 kWh/kg.

By using the above data, the EPBT of triple slope solar still is estimated to be around 0.202.

COST ANALYSIS of triple slope solar still is shown in Table 3. FRP material is available at Rs. 400/kg and similarly Acrylic sheet at Rs. 182.50/kg. Total cost for constructing the triple-slope solar still comes out to be Rs. 14,049.

TABLE 3: COST OF VARIOUS COMPONENTS USED IN TRIPLE SLOPE SOLAR STILL

Component	Cost (Rs.)
FRP body @ 400/kg	8600
Acrylic body @182.50/kg	684
Glass cover	1245
Iron stand	600
Inlet/Outlet nozzle	120
Silicon gaskets	550
Black paint and glass putty	250
Labour and other charges	2000
Total Cost of Still	**14049**

CONCLUSION

1. As per the literature survey and the above analysis, the embodied energy of triple slope solar still is found to be less than double slope solar still by 40%.
2. The total money spent on the construction of triple slope solar still is found to be almost equal to the double slope solar still.
3. Also, the EPBT value of TSSS is significantly smaller than that of double slope solar still by 242%.

REFERENCES

[1] Arunkumar, T., Vinothkumar, K., Ahsan, A., Jayaprakash, R., & Kumar, S. (2012). “Experimental Study on Various

Solar Still Designs". ISRN Renewable Energy, 2012, 1–10.

[2] Badran, O. O., Abu-Khader, M. M. (2007). "Evaluating thermal performance of a single slope solar still. Heat and Mass Transfer", 43, 985–995.

[3] Malaiyappan, P., Elumalai, N. (2016). "Productivity enhancement of a single basin and single slope solar still coupled with various basin materials". Desalination and Water Treatment, 57, 5700–5714.

[4] El-Sebaii A. A., El-Naggar M. (2017). "Year-round performance and cost analysis of a finned single basin solar still. Applied Thermal Engineering", 110, 787–794.

[5] Rufuss D. D. W., Suganthi L., Iniyan S., Davies P. A. (2018). "Effects of nanoparticle-enhanced phase change material (NPCM) on solar still productivity". Journal of Cleaner Production, 192, 9–29.

[6] Kabeel, A. E., El-Agouz S. A., Sathyamurthy R., Arunkumar T. (2018). "Augmenting the productivity of solar still using jute cloth knitted with sand heat energy storage". Desalination, 443, 122–129.

[7] Pal, P., Dev, R., Singh, D., Ahsan, A. (2018) "Energy matrices, exergoeconomic and enviro-economic analysis of modified multi-wick basin type double slope solar still". Desalination, 447, 55-73.

[8] Tiwari, G.N., Tiwari, A., Shyam, 2016. Handbook of Solar Energy- Theory, Analysis, and Applications. Springer. Chapter 14, 556.

Proceedings of International Conference on Sustainable Energy and Environmental Challenges (3rd SEEC), December 18-21, 2018, IIT Roorkee, India

SEEC No.070

Tannery wastewater treatment with constructed wetland using Biochar mixed substrate as an adsorbent.

J. S. Sudarsan[1*], Payal Maharathi[2], B. Pranjal Singh[3], V.Srihari[4]

[1,3] National Institute of Construction Management and Research (NICMAR), Balewadi, Pune,411045, India.

[2]Department of Civil and Environmental Engineering, SRMIST, Kanchipuram Dt., Kattankulathur – 603 203, Tamil Nadu, India.

[4]National Institute of Construction Management and Research (NICMAR), Hyderabad, 500101, India.

***ssudarsan@nicmar.ac.in,sudarsanjss@yahoo.com**

Abstract – **In the developing countries increase in population, improper urbanization and industrialization causing many issues to the ecosystem and the environment. Industrial Pollution has been a great concern for decades. Mainly Tanning industries located in many places of India as small scale industry. These small scale industries mostly running in the houses discharge partially treated and untreated effluents with high concentration of Chromium V1 into the water bodies. Research Study was initiated with proto type lab scale model to identify a suitable alternative technique to reduce the concentration toxic compound present in Chrome tannery wastewater. Coupling of two techniques like constructed wetland and Biochar as adsorbent. Main objective is to identify the efficiency of constructed wetland with coconut shell biochar as an adsorbent. Constructed wetlands (CWs) are artificial engineered systems which are designed and constructed to utilize the natural processes like wetland vegetation, natural soils, with associated microbial assemblages helps in treating wastewaters by the action of filtration, adsorption, sedimentation and phytoremediation. Biochar was produced from the coconut shell which was heated to temperatures between 250 and 750°C, under less oxygen concentrations. Constructed wetland coupled with Biochar. The biochar was mixed into the substrate of constructed wetlands. By using the biochar substrate the constructed wetland coupled with biochar was developed as lab scale model. Different trails were carried with the model using tannery wastewater collected from local tannery unit. The adsorbent biochar acts as a treating media which reduces the color of the wastewater and also reduction in chromium concentration of wastewater.**

The constructed wetland assemblage helps in reduction of other organic concentration and total solids of the wastewater. Based on the different trials in the lab scale model a good reduction in color, chromium , BOD,COD can be observed. More than 60 to 70 % reduction efficiency was achieved with the help lab scale model. It is possible to achieve 4'R (Reduce, Reuse, Recycle and Recovery) if the same was carried out in a large scale.

Keywords: Constructed wetland, Coconut shell Biochar, Wastewater, lab scale model.

INTRODUCTION

Environmental Pollution has been the major concern for a very long time now. The pollution of water bodies by disposal of waste untreated water directly in them has caused many rivers and other water bodies to be unfit for use. Other pollutions include air pollution, land pollution etc. The problem of water pollution is increasing at a brisk pace. The unrestrained dumping of municipal, industrial and agricultural waste, solid and gaseous wastes to the environment establishes one of the greatest grave fears to the sustainability of human civilization by polluting the water, land, and air and by adding to global warming.[1,2]

Constructed Wetland is similar to that of the normal wetland but is artificially constructed in a controlled environment.They are cost effective, reliable systems with no energy sources or chemical requirements and a minimum of operational requirement. [3] There are two types of constructed wetlands, surface flow wetlands, with shallow flow of wastewater over saturated soil substrate and subsurface flow wetlands which have gravel as the main media to support the growth of plants. The classification of subsurface flow wetlands include vertical flow (VF) and horizontal flow (HF) systems and a combination of VF and HF systems are recently developed combining both principles of vertical flow (VF) and horizontal flow (HF) systems which are known as hybrid wetlands. [4.5]

The most important removal mechanism occurring in constructer wetland is filtration, several microbial-mediated processes, chemical networks, volatilization, sedimentation, sorption, photo degradation, plant uptake, ammonification,

nitrification, denitrification and many more. [6.7]
Different unconventional wetland media are used for treating different types of wastewaters. The treatment efficiency offered by each type of media is different due to variations in pH, conductivity, porosity and the bacterial composition offered by them.[8] One of the recent developments in the modification of wetland media is the use of biochar. Biochar is a steadied, organic carbon based compound, produced when biomass is heated to temperatures more often than not in the vicinity of 300 and 1000°C, under low oxygen fixations. It is produced from a variety of raw materials which includes horticultural buildups, wood chips, compost, coconut shells and municipal solid waste.[9,10]

Indian Leather Industry – sixth biggest in the World is plentifully supplied with a fortune of crude materials, gifted labor, inventive innovation and expanding industry consistence. Tannery wastewater contains an intricate blend of both natural and inorganic contaminations. The significant worry over tanneries has been about scents and water contamination from untreated releases. Critical contaminations related with the tanning business incorporate chlorides, chromium, colors and also synthetic solvents.[11] Biochar consists of certain bacteria along with activated carbon or zeolite which acts as an adsorbing media which adsorbs chromium ions and other associated contaminants from tannery waste water. In this paper we focus on the treatment of tannery wastewater and the reduction of chromium content in it using a cheaper and rather sophisticated technique of Construction Wetland coupled with Biochar. Chromium occurs in the earth basically in two valence states: trivalent chromium and hexavalent chromium. Introduction may occur from typical or mechanical wellsprings of chromium. Trivalent chromium is significantly less hurtful than hexavalent chromium. Hexavalent chromium has had extensive, whole deal use in industry for its ability to thwart the course of action of rust. It is in like manner a known human disease bringing on operator. [12,13]The tannery waste water is allowed to pass through the constructed wetland where biochar present along with the soil in the constructed wetland media adsorbs the chromium ions either hexavalent or trivalent in state and allows considerably good and harmless water to be disposed of in the natural water bodies.

2.0 METHODOLOGY

The overall experimental method is represented in a schematic diagram (Fig.1). The experiment starts with the collection of raw materials and wastewater. The experimental trial was carried out of a retention time of 5 days.

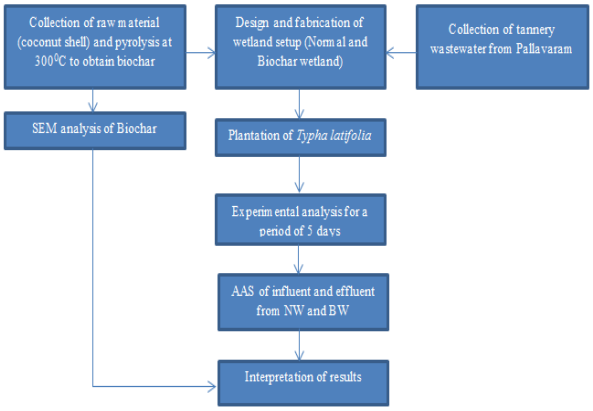

Fig. 1: Methodology adapted for the study

1) *Study area*: The exploratory work was done in SRM University, situated in SRM Nagar of Potheri Village (12° 9′ N to 12° 49′ N and 80° 2′ E to 80° 3′ E), in Kancheepuram locale, Tamil Nadu, India. The temperature ranges from 20-40°C and a yearly precipitation of 1213mm.

2) *Design of constructed wetland*: The study included two experimental setups. Each constructed wetland setup consisted of a PVC tub which is 0.6m in length, 0.4m wide and 0.3m deep. The two wetland systems were named as Normal Wetland (NW) and Biochar Wetland (BW) and were constructed with a slight inclination of 1-2% between inlet and outlet region. The setup was divided into three parts. The first part consisted of gravel alone for the elimination of bigger grit particles existing in the domestic wastewater. The second region of setup NW consisted of gravel, sand and soil while setup BW contained layers of gravel, sand and soil mixed with the coconut shell (CS) biochar.[14]The different stages of the wetland unit design are shown in Fig. 2. Figure 2(a) shows lining of constructed wetland unit with Gravel (b) lining of constructed wetland unit with sand (c)

plantation of *Typha latifolia* and (d) experimental trial using Tannery wastewater.

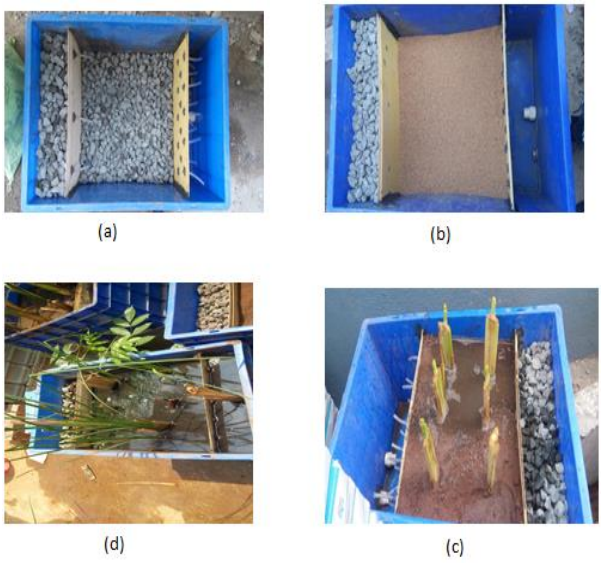

Fig.2. Stages of development of Constructed wetland setup and experimental trial.

3) *Wetland vegetation*: Plants in wetlands utilize the phytoremediation system in built wetlands. *Typha latifolia*, a local wetland species is to be used for the study.

4) *Biochar preparation*: The utilization of coconut shell biochar for treatment of wastewater is picking up significance in the present world. The coconut shells produced from oil industry and different employments of coconut should be used legitimately. The coconut shell was bought from the nearby markets and pounded into little pieces. The crushed pieces were cleaned and dried under sun and afterward sieved through a standard test sifter of 1.18mm strainer. Coconut shell when pyrolysed under 250 - 600°C by slow pyrolysis method showed effective biochar properties. For the production of biochar, the sieved coconut shell was undergone pyrolysis in a muffle furnace at the temperature range of 300°C for a time period of 5 hours. Fig. 3 shows the different stages of biochar preparation which include (a) Coconut shell before sieving through 1.18mm sieve (b) Coconut shell after sieving through 1.18mm sieve and (c) Coconut shell biochar after pyrolysis.

5) *Collection of tannery wastewater*: The tannery wastewater was collected from the CETP (Common Effluent Treatment Plants), Pallavaram, Chennai, which has a cluster of 150 tanneries. The tannery wastewater was collected according to the Standard Methods for Examination of Water and Wastewater, APHA.[15]

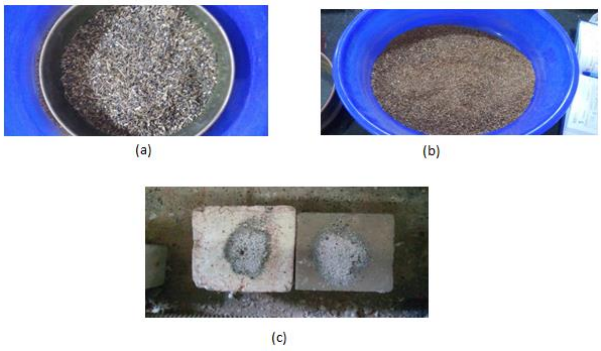

Fig. 3. Preparation of Biochar

6) *SEM analysis*: Scanning Electron Microscopy (SEM) investigation is used for the morphological examination of the biochar. It is a kind of electron amplifying instrument that produces photos of a case by separating it with a drew in light discharge. SEM images clearly demonstrate the physical nature of the compound, the surface topography and association. Illustrations can be found in high vacuum, in low vacuum, and in wet conditions.

7) *Experimental trial for analysis of chromium*: The tannery wastewater was passed through the wetland systems A and B and the water samples were collected after a retention time of 24, 48, 72, 96, and 120 hours from the outlet zones. Chromium in tannery wastewater was analyzed using Atomic Absorption Spectroscopy (AAS).

3.0 RESULTS AND DISCUSSION

A.SEM analysis results of Coconut shell biochar:

The SEM analysis of the coconut shell biochar was conducted. Figure 4.1 shows the SEM analysis images of coconut shell biochar under 2500X magnification. Fig. 4 shows the particle lengths of different particles. The figure shows that coconut

fiber pyrolysed at 300°C has an irregular structure. The mean length of the particles was calculated as 6913.184 nm and the mean area as 2784519 nm^2. It can be observed from the image that the biochar does not exhibit a porous structure but rather an irregular structure. Table 1shows the particle size analysis of coconut shell biochar using ImageJ.

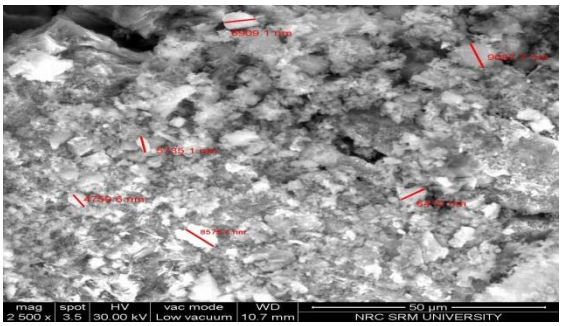

Fig. 4 SEM image of coconut shell biochar under 2500X magnification

TABLE 1
PARTICLE SIZE ANALYSIS OF COCONUT SHELL BIOCHAR USING IMAGEJ

	Label	Area	Angle	Length
1		1027703	-45.556	8575.355
2		3249763	9.782	6909.181
3		4388569	-71.801	9087.76
4		2013742	-60.255	4759.651
5		3249763	-143.13	6412.046
6		2777575	-79.38	5735.108
7	Mean	2784519	-65.057	6913.184
8	SD	1156411	49.7	1659.417
9	Min	1027703	-143.13	4759.651
10	Max	4388569	9.782	9087.76

B. Reduction of Cr in constructed wetlands:

The analysis of Cr by Atomic Absorption Spectroscopy (AAS) revealed that the initial levels of Cr in tannery effluent reached approximately 60 mg/l against the permissible limits of 2.0mg/l. Again when the tannery effluent is passed through normal constructed wetland and biochar wetland the concentration reduced to less than 20mg/l in biochar wetland and less than 25mg/l in normal constructed wetland.

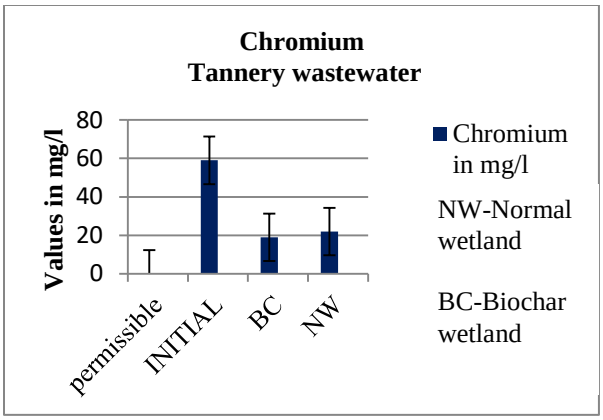

4.0 CONCLUSION

Concentration of Cr has been diminished marginally more in biochar wetlands, but there is no much significant difference in reduction of chromium from biochar wetland and normal wetland. The adsorption of chromium by using coconut shell biochar should be studied for future works.

REFERENCES

[1] K. Prasanna, J. S. Sudarsan, Nithiyanantham. "Wastewater Treatment Using Combined Biological and Constructed Wetland Techniques in Paper mills", *Sustainable Water Resources Management*, Springer, Vol. 3 Issue 2 pp 1-9, 2017.

[2] Atif Mustaf, "Constructed Wetland for Wastewater Treatment and Reuse: A Case Study of Developing Country", *International Journal of Environmental Science and Development*, Vol. 4, No. 1, 2013.

[3] J. Vymazal. "Horizontal sub-surface flow and hybrid constructed wetlands systems for wastewater treatment". *Ecological engineering*, *25*(5), 478-490, 2005.

[4] J. Vymazal "Removal of nutrients in various types of constructed wetlands". *Science of the total environment*, *380*(1), 48-65, 2007.

[5] L. Cui, Y. Ouyan, Q. Lou, F. Yang, Y. Chen, W. Zhu, & S. Luo. "Removal of nutrients from wastewater with Canna indica L. under different vertical-flow constructed wetland conditions". *Ecological Engineering*, 36(8), 1083-1088, 2010.

[6] U. Stottmeister, A. Wießner, P. Kuschk, U. Kappelmeyer, M. Kästner, O. Bederski, &H.

Moormann. “Effects of plants and microorganisms in constructed wetlands for wastewater treatment”. *Biotechnology advances*, *22*(1), 93-117, 2003.

[7] M. G. Prathap, J. S. Sudarsan, M. Mukhopadhyay, D. J. Reymond, & S. Nithiyanantham . “Constructed wetland-an easy and cost-effective alternative for the treatment of leachate”. *International Journal of Energy Technology and Policy*, *11*(4), 371-379, 2015.

[8] Ahmad Qasaimeh, Hesham AlSharie, Talal Masoud, “A Review on Constructed Wetlands Components and Heavy Metal Removal from Wastewater”, *Journal of Environmental Protection*, 2015, 6, 710-718, 2015.

[9] Zhengang Liu, Fu-Shen Zhang, “Removal of lead from water using biochars prepared from hydrothermal liquefaction of biomass”, *Journal of Hazardous Materials*, 167 (2009) 933–939, 2009.

[10] K. Jindo, H. Mizumoto, Y. Sawada, M. A. Sanchez-Monedero, and T. Sonoki., “Physical and chemical characterization of biochars derived from different agricultural residues”. *Biogeosciences*, Vol 11, pp 6613–6621, 2014.

[11] B.I. Islam, A.E Musa, E.H. Ibrahim, Salma A.A Sharafa, and Babiker M. Elfaki, “Evaluation and Characterization of Tannery Wastewater”, *JOURNAL OF FOREST PRODUCTS & INDUSTRIES*, 2014, 3(3), 141-150 ISSN:2325–4513.

[12] Adriana Leura-Vicencio , Angel Josabad Alonso-Castro, Candy Carranza-A ´lvarez, Rene ´ Loredo-Portales, Ma Catalina Alfaro-De la Torre, “Removal and Accumulation of As, Cd and Cr by Typha latifolia”, *Bull Environ Contam Toxicol* 90:650–653, 2013.

[13] S. C. Calheiros Cristina, O.S.S. Antonio Rangel and M. L. Paula Castro, “Constructed wetland systems vegetated with different plants applied to the treatment of tannery wastewater”. *Science Direct, Water Research* Vol 41, pp 1790– 17, 2007.

[14] USEPA (2000) “Constructed Wetland Treatment of Municipal Wastewater”, United States (US) Environmental Protection Agency (EPA) Office of Research and Development, Cincinnati, OH, USA.

[15] APHA, A. W. W. A. WPCF. *Standard Methods for Examination of Water and Wastewate*r, 21th. Ed. New York: APHA, AWWA, WPCR, 1, 2005.

SEEC No. 071

CATALYTIC HYDROTHERMAL LIQUEFACTION OF CASTOR RESIDUE: EFFECT ON PRODUCT YIELD AND DISTRIBUTION OF LIQUID PRODUCT

Ravneet Kaur
Department of Chemical Engineering
Dr B R Ambedkar National Institute of Technology Jalandhar
Email: kaur.ravneet23@gmail.com

Poonam Gera
Department of Chemical Engineering
Dr B R Ambedkar National Institute of Technology Jalandhar
Email: chadhap@nitj.ac.in

Mithilesh Kumar Jha
Department of Chemical Engineering
Dr B R Ambedkar National Institute of Technology Jalandhar
Email: jhamkin@yahoo.co.in

Thallada Bhaskar
Thermo-catalytic Processes Area,Bio-Fuels Division
CSIR-Indian Institute of Petroleum, Dehradun
Academy of Scientific and Innovative Research (AcSIR), New Delhi
E mail: tbhaskar@iip.res.in

ABSTRACT

Castor plant is an overgrown perennial shrub, typically found in India, Eastern Africa and tropical regions. Hydrothermal liquefaction of castor plant residue (leaves and stem) was performed at different operating temperatures (260, 280, 300 °C) at residence time of 60 min in the presence of alkali catalyst (KOH, K_2CO_3). The maximum total bio-oil yield ca. 21.2 wt.% was obtained at 300 °C in the presence of 0.5 N K_2CO_3. An increase in bio-oil yield was observed in the presence of catalyst. The obtained products have been analyzed using the Fourier transform infrared spectroscopy, Nuclear magnetic resonance spectroscopy, and Gas Chromatography-Mass Spectrometry, Elemental analysis. The major compounds identified in bio-oil by GC-MS were phenols, acids, esters and alcohols.

Keywords: ***Castor residue, Hydrothermal Liquefaction, Bio-oils, Value added products***

INTRODUCTION

The contribution of fossil fuels such as petroleum, natural gas and coal in world's primary energy consumption are 33, 19 and 24 % respectively. The increase in fuels demands, change in climate and decrease in crude-oil reserves has shifted the global dependence on fossil-based energy resources to renewable energy production technologies. The drawbacks of first-generation biofuels associated with availability and competition with the food industries have led to their replacement by second generation biofuels. Biomass, a second generation biofuel is abundant in nature and carbon-neutral renewable energy resource used for the production of biofuels, bio-chemicals and value- added products.

The conversion routes of biomass to biofuels are thermochemical and biochemical. Thermochemical route involves the heating of biomass in the presence/absence of air or oxygen. The thermochemical process is categorized as: Combustion, Gasification, Pyrolysis and Liquefaction. Hydrothermal liquefaction (HTL) conversion process includes the conversion of biomass in sub-critical water to hydrocarbons [1], and the obtained liquid product is referred as biocrude or bio-oil. HTL gained more attention as compared to other thermal conversion technologies due to its advantages. One of major advantages of hydrothermal liquefaction prevents the need for drying of the feedstocks for producing biocrude.

Castor plant *(Ricinus Communis)* is an evergreen plant from Euphorbiaceae family and genus Ricinus. It is mainly grown in India and Eastern Africa, tropical and subtropical regions. Castor plant is widely found along stream banks, distributed areas, river beds, bottomlands etc. The plant is divided into three parts: seeds, stem and leaves. The maximum production of castor seed is in India and it ranked first with a production of 22,36,000 MT seeds in 2016 [2]. The oil obtained from seeds has many applications. The other parts of the plant include stem and

leaves which contribute to more than 50 % of residue generation per ton of castor plant [3].The kinetic study on castor cake was reported in literature [4], while the first kinetic study on castor residue [5] was reported by Kaur et al., 2017.

To best of our knowledge there is no study reported on catalytic hydrothermal liquefaction of castor residue (leaves and stems) in open literature. The main aim of this work is to study the effect of temperature and catalyst on product yield. The hydrothermal liquefaction of castor residue was carried out at 260, 280, 300 °C at residence time of 60 mins in the presence of KOH and K_2CO_3. Alkali based homogenous catalysts (0.5N KOH, 0.5N K_2CO_3) were used to know the effect on product yield and formation of compounds. The products were analyzed by GC-MS, elemental analysis, FT-IR and NMR.

MATERIAL AND METHODS

Raw Material

The raw material (castor residue) used in this work was collected from Dr B R Ambedkar National Institute of Technology (31.3962° N, 75.5354° E), Jalandhar, Punjab. After crushing and sieve shaking, the obtained fine powder was used for further analysis. The catalyst (0.5N KOH, 0.5N K_2CO_3) was prepared in the laboratory. Proximate analysis, elemental analysis, and component analysis of castor residue was performed. HHV of castor residue and all products were calculated using Dulong's formula:

$$\text{Heating value (MJ/kg)} = 0.338\,C + 1.428\,(H - O/8) + 0.095\,S \quad (1)$$

Apparatus and Experimental Procedure

Hydrothermal liquefaction experiments were conducted in a high-pressure batch autoclave (Parr reactor) at different reaction conditions like temperature and alkaline catalysts (KOH, K_2CO_3). In each catalytic hydrothermal experiment, the reactor was loaded with castor residue and alkaline solutions with ratio of 1:6 (by weight). Then the reactor was sealed and purged with nitrogen for atleast 5 times to remove the inside air. The reactants were agitated vertically with ~ 200 rpm using vertical magnetic stirrer. The reactor was then heated upto desired temperature (260, 280, 300 °C) for residence time of 60 min. The reactor was then left to cool down to the room temperature.

Extraction of Liquid Products and Analysis

After cooling, the gaseous products were vented out, and liquid and solid products were separated out using vacuum filtration. Diethyl ether of equal quality was added to recover the liquid portion and phase separation was carried out to recover organic and aqueous fraction. The obtained organic or ethereal fraction was then dried over anhydrous sodium sulfate to remove the moisture or water content. Diethyl ether was then separated out using rotary vacuum evaporator under reduced pressure. The obtained fraction was then designated as Bio-oil 1 or BO (1). The aqueous phase, designated as WSH are mixture of water-soluble hydrocarbons. The soluble products were extracted out from solid products using acetone in soxhlet apparatus until the solvent in thimble become colorless. The acetone soluble liquid fraction obtained after evaporating the solvent under reduced pressure was weighed and termed as bio-oil 2 or BO (2). The insoluble acetone fraction was then dried at 105°C and designated as Bio-char or (BC).The mass balance equations used in this procedure are:

$$Conversion\ (\%) = \frac{W_{feed} - W_{bio-char}}{W_{feed}} \times 100 \quad (2)$$

$$Bio-oil\ 1\ yield\ (wt.\%) = \frac{W_{ether-soluble}}{W_{feed}} \times 100 \quad (3)$$

$$Bio-oil\ 2\ yield\ (wt.\%) = \frac{W_{acetone-soluble}}{W_{feed}} \times 100 \quad (4)$$

$$Bio-char\ yield\ (wt.\%) = \frac{W_{bio-char}}{W_{feed}} \times 100 \quad (5)$$

$$Gas\ yield\ (wt.\%) = \frac{W(vessel + feed + water)\ before\ HTL - W(vessel + feed + water)\ after\ HTL}{Amount\ of\ feed\ taken\ (g) + amount\ of\ water\ added\ (g)} \times 100 \quad (6)$$

$$Other\ yield\ (wt.\%) = 100 - (bio-oil\ 1 + bio-oil\ 2 + bio-char + gas) \quad (7)$$

W_{feed}: is the weight of feed; $W_{bio-char}$: is the weight of bio-char; $W_{ether-soluble}$: is the weight of ether soluble bio-oil or BO (1); $W_{acetone-soluble}$: is the weight of acetone soluble bio-oil or BO (2). Other yields represent the water - soluble hydrocarbons and some loses.

The optimum ether – soluble fraction Bio-oil 1 or BO (1) were analyzed using FT-IR, GC-MS, NMR and Elemental analysis.

RESULTS AND DISCUSSIONS

Feedstock Analysis

Castor residue has carbon, hydrogen, nitrogen and oxygen content of 43.59 wt.%, 5.56 wt.%, 4.69 wt.%, 46.16 wt.% respectively. The proximate analysis depicts the moisture, ash, fixed carbon and volatile matter content present in castor residue and was 11.14 wt.%, 5.40 wt.%, 9.16 wt.%, and 74.30 wt.% respectively. The high heating value of castor residue calculated using Dulong's formula was 14.43 MJ/kg. Cellulose, hemicellulose and lignin content present in castor residue are 38.42 wt.%, 22.40 wt.% and 20.20 wt.% respectively. The amount of extractives present in castor residue are 16.40 wt.%.

HTL Product Yields

Table 1 depicts the product distribution of castor residue obtained after catalytic hydrothermal liquefaction. The reactions were carried out temperature of 260, 280, 300 °C at residence time of 60 min in the presence of 0.5N KOH and K_2CO_3. Equations (2) to (7) were used to calculate the product yield. It was observed that the maximum total bio-oil yield ca. 21.2 wt.% was observed at 300 °C in the presence of K_2CO_3. The maximum total bio-oil yield ca. 12.2 wt.% was obtained at 300 °C when KOH is used as catalyst. It was observed that the K_2CO_3 enhances the total bio-oil yield as compared to KOH. Similar results were obtained in literature when HTL of wheat husk was done in the presence of both alkali catalysts (KOH and K_2CO_3) at 280 °C for 15 min [6]. The maximum total bio-oil yield of 30 and 31 wt.% was obtained in the presence of KOH and K_2CO_3 respectively. The maximum conversion of 85.0 wt.% was observed at 300 °C in the presence of K_2CO_3. The conversion for KOH varies from 68.6, 77.6, 82.8 wt.% for 260, 280, and 300 °C respectively.

TABLE 1: PRODUCT DISTRIBUTIONS (IN WT.%) OF CATALYTIC HTL UNDER DIFFERENT REACTION CONDITIONS.

Sample Code	Bio-oils		Total Bio-oil	Gases	Bio-char	Other yield	Conversion
	Bio-oil (1)	Bio-oil (2)					
260-60 0.5N KOH	7.2	2.4	9.6	8.3	31.4	50.7	68.6
280-60 0.5N KOH	8.8	1.2	10	5.9	22.4	61.7	77.6
300-60 0.5N KOH	8.6	3.6	12.2	4.9	17.2	65.7	82.8
260-60 0.5N K_2CO_3	15.2	0.2	15.4	7.5	27.4	49.7	72.6
280-60 0.5N K_2CO_3	13.8	0.2	14	10.0	30.8	45.2	69.2
300-60 0.5N K_2CO_3	20.8	0.4	21.2	7.1	15.0	56.7	85.0

HTL Liquid Product Analysis

GC-MS Analysis

Table 2 represents the compounds obtained in BO (1) of castor residue from catalytic hydrothermal liquefaction at 300 °C for 60 mins in the presence of 0.5 N KOH and K_2CO_3. NIST mass spectral database was used for the identification of compounds. The chemical compounds of bio-oil were identified as phenolics, aromatic hydrocarbons, N-contained compounds, aldehydes, ketones. amides, alcohols, and acids. It was observed that the use of catalyst affects the formation of compounds. A maximum area % of 28.2243 of compound 5-Bromo-4-oxo-4,5,6,7-tetrahydrobenzofurazan was observed when KOH is used as catalyst. The area % of the similar compounds was high in case of KOH as compared to K_2CO_3. The formation of compounds 2-Cyclopenten-1-one, Phenol, p-Cresol, Benzene, 3-Methoxybenzyl alcohol, Indole was observed when HTL of castor residue was done in the presence of K_2CO_3.

FT-IR Analysis

Figure 1 shows the FT-IR analysis of BO (1) obtained after catalytic HTL of castor residue at 300 °C. The absorption peak ranges between 3200-3600 cm^{-1} due to N-H and O-H stretching represents the presence of amides/amines and alcohols and phenols. The C-H stretching vibrations at 2800 - 3000 cm^{-1} may indicate the presence of alkanes. The C-H deformation vibrations between 1360-1460 cm^{-1} shows the presence of alkane group. The C=O stretching vibrations between 1680-1800 cm^{-1} indicate the presence of ketones, carboxylic acids, and aldehydes. In addition, the C=C stretching peak between 1400-1600 cm^{-1} suggests the presence of aromatics and the substituted aromatic groups are observed at 675-900 cm^{-1}.The vibrations in the region 1020 - 1300 cm^{-1} were assigned to C-N stretching vibrations which are possibly due to aliphatic amines. Comparing the FT-IR analysis obtained under different catalytic conditions, it was observed that the almost same functional groups are present in both BO samples but at different relative intensity.

TABLE 2: MAJOR COMPOUNDS IDENTIFIED IN BO (1) (AREA, %) USING GC-MS.

RT	Compounds Identified	BO (1) 300 0.5N KOH	BO (1) 300 0.5N K_2CO_3
3.2409	N-Ethylidene t-butylamine		0.8193
3.6387	Cyclopentanone, 2-methyl-		3.4292
4.1647	trans-3,4-Dimethylcyclopentanone		0.667
4.2096	Cyclohexanone, 4-methyl-		0.4799
4.2866	1,3,5,7-Cyclooctatetraene		0.4994
4.3635	1-Butylpyrrolidine		1.3669
4.7741	Cyclopentanone, 2-ethyl-		1.0329
5.6402	Phenol		8.716
6.2753	Pyridine-D5-		0.7471
6.2816	N-.beta.-Hydroxyethylpyrrolidine	1.7107	
6.3267	Pyridine, 5-ethyl-2-methyl-		0.7034
6.4294	2-Cyclopenten-1-one, 2,3-dimethyl-		3.0252
6.795	1-Butanamine, 2-methyl-N-(2-methylbutylidene)-		0.6182
7.1414	p-Cresol		1.8009
7.5199	2-Cyclopenten-1-one, 3,4,4-trimethyl-		7.2258
7.5906	Phenol, 2-methoxy-		2.6185
8.0203	2-Cyclopenten-1-one, 2,3,4,5-tetramethyl-		1.1822
8.8543	1,3-Benzenediamine, 4-methoxy-		0.6514
8.9954	Creosol		0.6023
9.2264	Benzene, 1-methoxy-4-methyl-		1.4603
9.5023	3-Methoxybenzyl alcohol		0.4886
9.7781	Phenol, 3-ethyl-		0.521
9.8873	2-Ethyl-3,5-dimethylpyridine		0.8036
11.4782	Quinoline, 1,2,3,4-tetrahydro-		0.6356
12.3636	Indole		2.3642
14.4934	1H-Indole, 4-methyl-		1.5238
17.7782	Butylated Hydroxytoluene	8.3978	7.0042
24.9248	2-Pentadecanone, 6,10,14-trimethyl-	1.9962	0.8133
26.5416	1,2-Benzenedicarboxylic acid, butyl cyclohexyl ester		0.7387
26.9905	Isophytol	4.3904	1.4842
29.8518	Phytol	4.6194	4.5065
41.7203	Eicosane	3.3327	1.4019
43.0675	γ-Tocopherol	2.2941	1.6776
44.049	Vitamin E	5.1771	2.001
45.1013	Acetamide, N-[4-(trimethylsilyl)phenyl]-		0.5336
45.5759	Stigmasterol	6.0083	2.2365
46.4356	γ-Sitosterol	16.2908	5.4006
46.5576	2-Ethylacridine		1.2037
46.9361	1,4-Bis(trimethylsilyl)benzene		1.5089
47.3786	5-Bromo-4-oxo-4,5,6,7-tetrahydrobenzofurazan	28.2243	
	Total	**82.4418**	**74.4934**

NMR Analysis

Figure 2 shows the NMR analysis of BO (1) obtained at catalytic HTL of castor residue at 300 °C. The NMR spectra provides additional information about functional groups compared to FT-IR spectra for the ability to quantify and compare integration peaks. The spectra 0.5-1.5 ppm represents the protons on aliphatic carbon atoms at least two bonds away from C=C or heteroatom. It was

observed that more aliphatic protons were present for the case of KOH (68.73%) as compared to K_2CO_3. The next region 1.5-3.0 ppm corresponds to protons on aliphatic carbon atoms which may be bonded to a C=C double bond or heteroatom. The protons in this region were less in KOH as compared to K_2CO_3. In the next region, 3.0-4.7 more protons were observed in the case of K_2CO_3, representing the protons on carbon atom next to an aliphatic ether or alcohol or a methylene group that joins two aromatic rings. The region between 4.5-6.0 ppm depicts the presence of aromatic ether protons i.e., lignin derived phenols. The percentage of protons in this region is almost similar for both KOH and K_2CO_3 catalysts. The region of spectrum 6.0-8.5 corresponds to aromatic region, and more aromatic compounds were observed in the case of K_2CO_3.

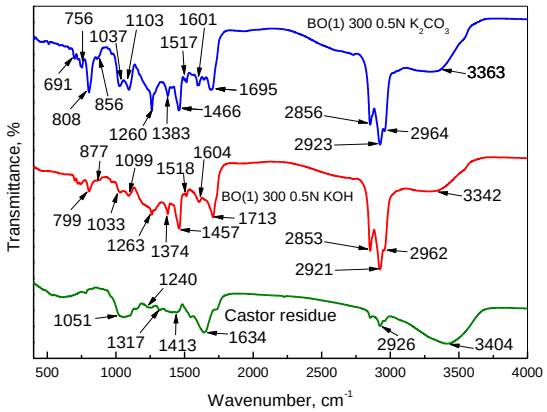

FIGURE 1: FT-IR ANALYSIS OF BO (1)

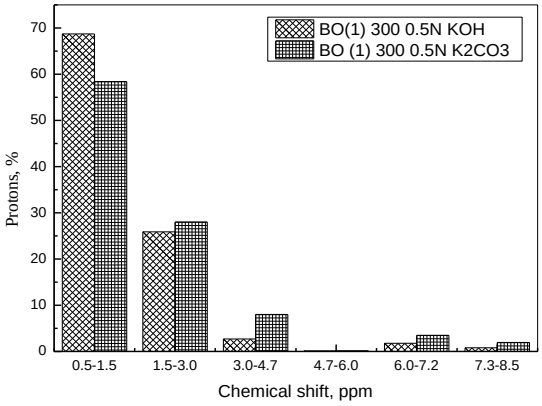

FIGURE 2: NMR ANALYSIS OF BO (1)

Elemental Analysis

Table 3 represents the elemental analysis of BO (1) obtained for both HTL of castor residue using KOH and K_2CO_3 catalyst. BO (1) have carbon content of 62.20 wt.% and 62.80 wt.% for KOH and K_2CO_3 respectively. The oxygen content of BO (1) is less in the case of K_2CO_3 as compared to KOH. The reactions i.e., dehydration (-H_2), decarbonylation (-CO) and decarboxylation (-COO) involved in liquefaction process helps to reduce the oxygen content of BO (1). The heating value of BO (1) for KOH and K_2CO_3 are 32.27 and 33.91 MJ/kg respectively. The reduction in wt.% of nitrogen in bio-oils was observed as compared to castor residue. To make this bio-oils more effective, further denitrogenation and deoxygenation and will be required.

TABLE 3: ELEMENTAL ANALYSIS OF BO (1)

Elements	BO (1) 300 0.5N KOH	BO (1) 300 0.5N K_2CO_3
C (wt.%)	62.27	62.80
H(wt.%)	10.92	11.73
N(wt.%)	2.22	2.62
O(wt.%)	24.59	22.85
HHV (MJ/kg)	32.27	33.91

CONCLUSIONS

Catalytic hydrothermal liquefaction of castor residue was performed in the presence of 0.5 N KOH and K_2CO_3. The total bio-oil yield (wt.%) was highest with K_2CO_3 as compared to KOH. The formation of phenolic compounds were confirmed by GCMS, FTIR and NMR. The use of catalysts promotes the yield and heating value of bio-oil. The HHV of BO (1) for KOH and K_2CO_3 were 32.27 and 33.91 MJ/kg respectively.

REFERENCES

[1] Peterson, A.A., Vogel, F., Lachance, R.P., Fröling, M., Antal Jr, M.J. and Tester, J.W., 2008. Thermochemical biofuel production in hydrothermal media: a review of sub-and supercritical water technologies. Energy & Environmental Science, 1(1), pp.32-65.

[2]Comprehensive Castor Oil Report, 2016. URL http://www.castoroil.in/reference/report/report.html

[3]Bateni, H. and Karimi, K., 2016. Biodiesel production from castor plant integrating ethanol production via a biorefinery approach. Chemical Engineering Research and Design, 107, pp.4-12.

[4]Thiagarajan, J., Srividya, P.K. and Balasubramanian, P., 2016. Thermogravimetric and decomposition analysis of jatropha, castor and pongamia deoiled seed cakes. International Journal of Innovations in Engineering and Technology, 7 (2), pp.417-425.

[5] Kaur, R., Gera, P., Jha, M.K. and Bhaskar, T., 2018. Pyrolysis kinetics and thermodynamic parameters of castor (Ricinus communis) residue using thermogravimetric analysis. Bioresource technology, 250, pp.422-428.

[6]Singh, R., Bhaskar, T., Dora, S. and Balagurumurthy, B., 2013. Catalytic hydrothermal upgradation of wheat husk. Bioresource technology, 149, pp.446-451.

Proceedings of theThird International Conference on Sustainable Energy and Environmental Challenges (3rd SEEC)
18 –21 December, 2018, IIT Roorkee, India

SEEC No. 072

EXPERIMENTAL STUDY OF TWO-PHASE AIR-WATER MIST JET IMPINGEMENT COOLING ON CYLINDER

Chunkyraj Khangembam
Department of Mechanical Engineering
National Institute of Technology Manipur
Email: chunky_kh@yahoo.com

Dr. Dushyant Singh
Department of Mechanical Engineering
National Institute of Technology Manipur
Email: dushyant@nitmanipur.ac.in

ABSTRACT

Experimental investigation on heat transfer mechanism of air-water mist jet impingement cooling on heated cylinder are presented. The cylinder is heated to non-boiling temperature under constant heat flux condition. Multiple experimental tests are conducted to investigate the effect of Reynolds number and mist loading fraction on heat transfer rate. In the experimental parametric study, the Reynolds number Re_d is defined on the outer diameter of the annular air jet,d and varied from 15000 to 30000. The mist loading fraction, f was varied from 0 to 1.0% and the nozzle-to-surface spacing was maintained at h/d=40. The experiment results indicate that increase in mist loading and Reynolds number increases the heat transfer rate. On further investigation, existence of secondary maxima Nusselt number was also noticed.

***Keywords*:** mist jet impingement, heat transfer, mist loading, heated cylinder.

.

NOMENCLATURE

d	nozzle outer diameter, m
D	cylinder diameter, m
f	mist loading fraction
h	nozzle to target surface distance, m
L	length of cylinder, m
Nu	local Nusselt number
Nu_z	Axial Nusselt number
Nu_θ	Circumferential Nusselt number
Nu_{mix}	Stagnation Nusselt number of the air-mist mixture
Nu_{air}	Stagnation Nusselt number of air only condiition
Re_d	Reynolds number based on nozzle outer diameter
$\dot{m}_l$	mass flow rate of water, kg/s
$\dot{m}_a$	mass flow rate of air, kg/s
$\dot{m}_T$	total mass flow rate , kg/s
q´´	heat flux, W/m^2
T	temperature, K

INTRODUCTION

Single phase jet impingement cooling has been widely implemented due to its effecient heat removal capability from heat generation sites. It has shown high heat transfer rate and has been extensively used in applications such as cooling of electronic compomponents, metal cutting processes and food processing unit etc. Sustantial work has been carried out in understanding the heat transfer rate for single-phase jet impingemnt cooling [1-5].

In recent trend, two-phase jet impingement cooling has been implemented, and superior heat transfer characteristic has been observed in such cooling with respect to single-phase jet impingment [6-8]. Mist is the entrainment of very fine liquid droplets in jet of air, and can also be considered as two-phase jet impingement process. Mist are formed due to shear atomization of liquid caused by high pressure annular air jet[9].

Mist jet impingement cooling on cylinder has yet to receive as much focus and significance as mist jet impingement cooling on flat plate. Experimental work has been carried out in boiling and non-boiling region. The area of mist jet impingement in non-boiling region can be further investigated, which gives the motivation of present study of air-water mist jet impingement cooling on cylinder.

Graham et al. [10] carried out experimental study on heat transfer characteristic for air-methanol and air-water mist jet impingement cooling on flat target surface. Experiments were conducted in the non-boiling region for jet *Re* in the range 6,000-10,000;m_l of methanol and water was varied from 3.7-4.1 ml/min and 2.4-6.9 ml/min respectively. Based on experimental study, they proposed an analytical model that predicts the liquid film thickness and rate of heat transfer. Kanamori et al.[11] studied experimentally the effect of air-water mist on heat transfer rate and flow characteristic on a flat target surface in the non-boiling region for *Re* = 12,500-50,000; m_l of water =1 - 3.33 ml/min; f=0.025-0.276, h/d = 2-16. They reported heat transfer rate enhanced with increasing the mass loading of liquid-to-air, increasing Re and decreasing h/d spacing. Lyons et al. [12] carried out experimental study to investigate the relation between heat transfer and fluid flow of air-water mist jet impingement on flat heated plate for h/d = 7.5 and 15.5, $Re_{d(hyd.)}$ = 4800, 7400 and 10300;m_l of water = 0.0046-0.45 ml/min and f = 0.02% -3.8% . They reported that atomization rate and amount of droplet entrainment affects the heat transfer rate, and that droplet diameter decreases with decrease in water flow rate and increase in air pressure. Also increase in heat transfer rate with increase in liquid loading fraction was observed. Quinn et al. [13] investigated the surface wetting and heat transfer phenomena at low, intermediate and high air-water mist loading condition on heated flat surface. Experiments were conducted in the non-boiling region for jet *Re*=4500 with m_l of water = 0.035-0.281 ml/min, f=0.003-0.024, h/d = 5 and 10. Three different regimes of mist loading fraction were reported, where at low mist loading fraction, the liquid droplets impinge on the surface producing small slugs on the surface. These slugs merge with each other in the intermediate loading conditions to form localized films. At high loading conditions these localized films merge to form a complete film of liquid.

Very limited literature is available on mist jet impingement cooling on cylinder. Buckingham et al. [8] investigated the heat transfer mechanism in spray cooling of air-water impingement on cylinder. Experiments were carried out in the boiling region for centre line droplet velocity of 15.3 m/s with m_l of water = 97-603 ml/min. Two distinct heat transfer regime were reported, in radiation dominated region the heat transfer is due to single phase flow. In covection dominated region, evaporation of droplets occurs near the boundary layer increasing the heat transfer rate. Lee et al. [14] also conducted experimental analysis to investigate air-water mist cooling and wetting phenomena on heated cylinder in the boiling region for droplet velocity ranging from 3.55-12.8 m/s with m_l of water = 5-22 l/min. They reported that surface wetting is a result of penetration of droplets into thermal boundary layer and striking the cylindrical surface. They also proposed analytical models which are in good agreement with the experimental data. Issa et al. [15] conducted both experimental and numerical analysis for air-water mist jet cooling of heated cylinder in the nucleate boiling region for air jet Re_d in the range1,000-3,000; m_l of water = 15.7 – 126.18 ml/min; f =1.6 – 15.5, h/d = 100 was maintained. A 2D transient heat transfer model was developed using ANSYS FLUENT for numerical analysis, with droplets modelled in Lagrangian frame and k-ε turbulence model was considered for continuous phase. They reported that the heat transfer coefficient is highest at the stagnation point, and gradually decreases over the cylinder. Based on simulation analysis, it was reported that a liquid film forms on the front portion of the cylinder under low droplet velocities and water flow rates.

To the best of our knowledge, heat transfer study on air-water mist jet impingement cooling on cylinder in non-boiling region is not available. Experimental analysis will be useful in understanding the heat transfer of mist jet impingement on cylinder. Hence, the objective of the present work is to conduct experimental study to investigate the effect of Reynolds number and mist loading fraction on the heat transfer mechanism on heated cylinder subjected to constant heat flux condition in non-boiling region. The variations in heat transfer coefficient along axial and circumferential direction have been reported.

EXPERIMENTAL SET-UP

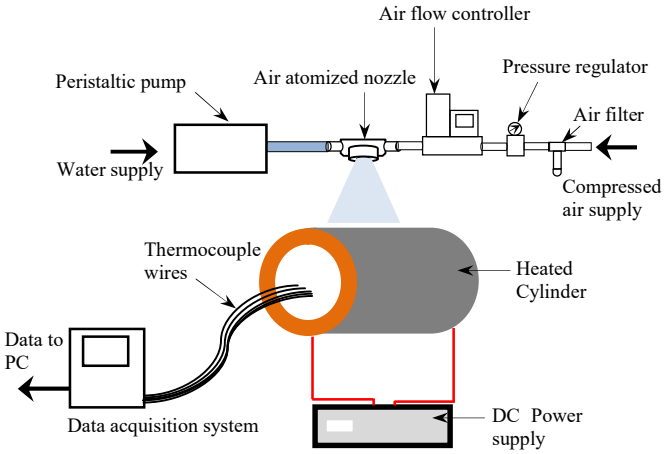

FIGURE 1. Experimental set up.

A schematic diagram of the present experimental set up is shown in Fig.1. Compressed air is supplied to the air atomizing nozzle through an air filter, pressure regulator and a flow control valve. Alicat-MCR-3000SLPM-D-PAR is used to control the air flow, which has an accuracy of ±1% over a range of 0-3000 SLPM. Ravelhiteks RH-P100VS-100 peristaltic pump is used to supply water to the atomizing nozzle. The pump delivers water at 0.1-99.9ml/min with an accuracy of ±1 %. Spraytech DASA 050 nozzle is used to generate the air-water mist.

The diameter and length of the cylinder are 50.5mm and 255mm respectively, and made from a smooth phenolic tube. A thin 25μm SS-304 foil is wound over the tube to obtain a constant heat flux condition.The temperature variation is measured with T-type thermocouples, which are located at specific locations along axial and circumferential direction of the cylinder as shown in Table 1. These thermocouples are then connected to NI Data Acquisition system (DAS) and the temperature readings are recorded in the computer. DC power is supplied to the end terminals of the cylinder, which heat up the SS foil.

TABLE 1: POSITION OF THERMOCOUPLES FROM STAGNATION POINT, T_0

Axial		Circumferential	
T_1	5 mm	T_{11}	30°
T_2	5 mm	T_{12}	45°
T_3	10 mm	T_{13}	60°
T_4	15 mm	T_{14}	90°
T_5	20 mm	T_{15}	120°
T_6	30 mm	T_{16}	135°
T_7	40 mm	T_{17}	180°
T_8	50 mm		
T_9	60 mm		
T_{10}	100 mm		

EXPERIMENTAL ANALYSIS

The mist loading farction (*f*) is defined as the ratio of mass flow of the liquid to that of the total mass flow of the system.

$$f = \frac{\dot{m}_l}{\dot{m}_T} \tag{1}$$

Where $\dot{m}_l$ is the mass flow rate of water and $\dot{m}_T$ is the total mass flow rate of the system, given by:

$$\dot{m}_T = \dot{m}_l + \dot{m}_a \tag{2}$$

The Reynolds number (Re_d) is defined based on the total mass flow and outer diameter of annular air jet opening:

$$\mathrm{Re}_d = \frac{4\dot{m}_T}{\pi d \mu_{eff.}} \tag{3}$$

Where$\mu_{eff.}$ is effective viscosity of mist calculated with the help of Taylor expansion [16].

The local Nusselt number is calculated as:

$$Nu = \frac{q''_{convection}.d}{(T_w - T_{ref.})k_{eff.}} \tag{4}$$

Where *d* is the outer diameter of annular air jet opening, T_w is the local surface wall temperature; $T_{ref.}$ is the temperature near the exit of the nozzle and $k_{eff.}$ is the effective thermal conductivity of the air-mist system.

The convective heat flux is calculated as:

$$q''_{convection} = q''_{all} - q''_{radiation} \tag{5}$$

$$q''_{all} = \frac{VI}{A} \tag{6}$$

Where *V* is the voltage, *I* is the current and *A* is the surface area of the cylinder.

$$q''_{radiation} = \varepsilon\sigma(T_w^4 - T_\infty^4) \tag{7}$$

The parametric study of the present study is shown in Table 2.

TABLE 2: PARAMETERS FOR PRESENT STUDY

h/d	40
f	0, 0.25%, 0.50%, 0.75% & 1.0%
Re_d	15000, 20000, 25000 & 30000

RESULT AND DISCUSSION

The Nusselt numbers along the cylinder were obtained by measuring the local temperature with thermocouples. The variation of heat ransfer rate with respect to mist loading fraction and Reynolds number are presented.

Effect of Reynolds Number

Fig. 2 illustrates the variation of local Nusselt number along the cylinder for $15{,}000 \le Re_d \le 30{,}000$ at h/d=40 and $0 \le f \le 1.0\%$. The heat transfer rate increases with the increase in Reynolds number.

The stagnation nusselt number is high for high Reynolds number. The local Nusselt number decreases along the axial and circulferential direction. A secondary maxima is observed at z/D=0.3 along axial direction and 30° along circumferential direction.

Effect of mist loading

Fig. 3 illustrates the variation of local Nusselt number along the cylinder for $0 \le f \le 1.0\%$ at h/d=40 and $15000 \le Re_d \le 30000$. The heat transfer rate increases with the increase in mist loading fraction.

The local Nusselt number increases from stagnation point to the secondary maxima and decreses monotonically along axial and circumferential direction. The significance of secondary maxima is neglisible for low mist loading, $f = 0$ and 0.25% with respect to higher mist loading.

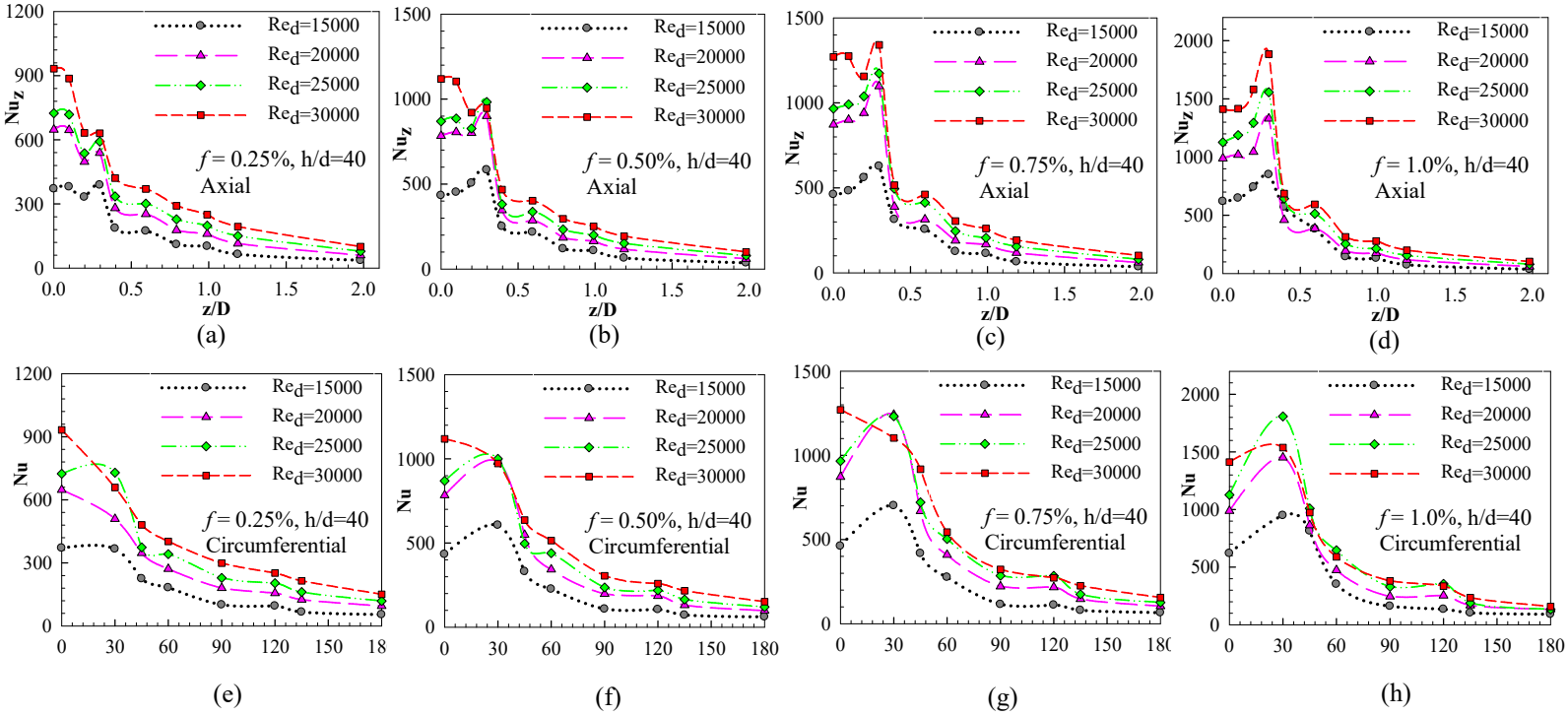

FIGURE 2. Effect of Reynolds number at h/d = 40 and Re_d = 15000, 20000, 25000 and 30000 for (a) f = 0.25%, axial (b) f = 0.50%, axial (c) f = 0.75%, axial (d) f = 1.0%, axial (e) f =0.25%, circumferential (f) f =0.50%, circumferential (g) f =0.75%, circumferential and (h) f =1.0%, circumferential.

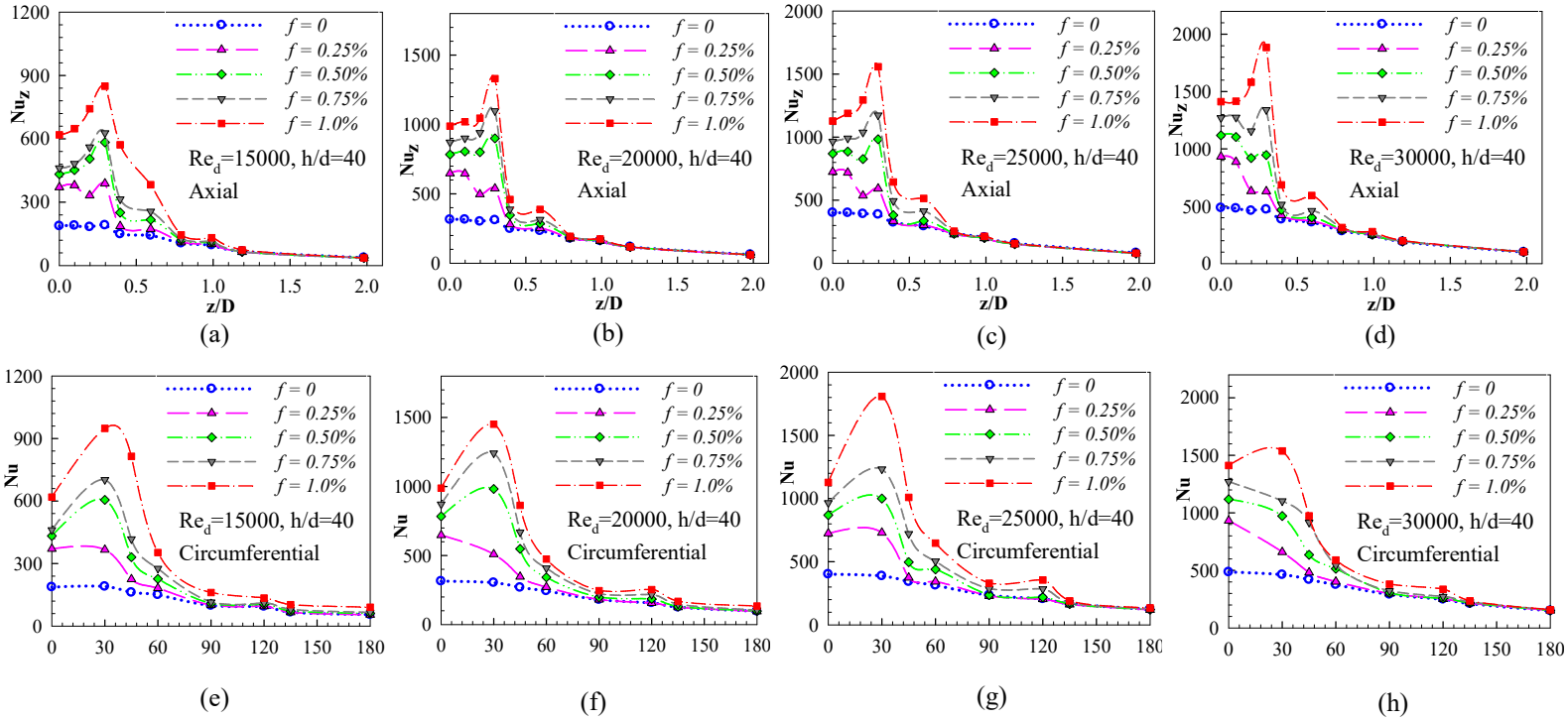

FIGURE 3. Effect of mist loading fraction at h/d = 40 and f = 0, 0.25%, 0.50%, 0.75% and 1.0% for (a) Re_d=15000, axial (b) Re_d=20000, axial (c) Re_d=25000 , axial (d) Re_d=30000, axial (e) Re_d=15000, circumferential (f) Re_d=20000, circumferential (g) Re_d=25000, circumferential and (h) Re_d=30000, circumferential.

The overall increment in the stagnation Nusselt number for the air-mist misture to that of single air condition is shown in Fig. 4. It is clear from the Fig. 4, that heat transfer in air-mist jet impingement is superior to that of single phase airjet impingement cooling.

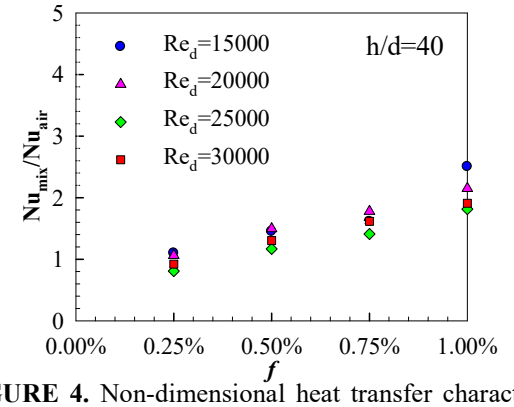

FIGURE 4. Non-dimensional heat transfer characteristic, $\frac{Nu_{mix.}}{Nu_{air}}$ at stagnation point for at f and Re_d.

CONCLUSION

Experimental investigation on the heat transfer rate over heated cylinder has been carried out. And effect of Reynolds number and mist loading fraction has been reported.

The following conclusions can be drawn from the present studies.

1. With the increase in Reynolds number, the heat transfer rate increases in both axial and circumferential direction.
2. Increase in mist loading fraction also leads to increase in heat transfer rate.
3. Secondary maxima in Nusselt number is observed in axial and circumferential direction. However , the significance of the secondary maxima is neglisible for low mist loading fraction.
4. A 1.0% mist loading increases the heat transfer rate by almost 200% with respect to single phase air impingemnt cooling.

ACKNOWLEDGMENTS

Authors are thankful to the Department of Science and Technology (SERB), New Delhi of Project No. ECR/2016/001364, for their financial assistance to set up the facility to carry out this study in Department of Mechanical Engineering at NIT Manipur.

REFERENCES

[1] J. N. B. Livingood, and P. Hrycak, Impingement Heat Transfer from Turbulent air Jets to Flat Plates—A Literature Survey, *NASA Technical Memorandum*, NASA TM X-2778, Lewis Research Center, Cleveland, 1973.

[2] H. Martin, Heat and Mass Transfer between Impinging Gas Jet and Solid Surfaces, *Adv. In Heat Transfer*, vol. 13, pp. 1–60, 1977.

[3] P. Hrycak, Heat Transfer from Impinging Jets: A Literature Review, *AFWAL-TR-81–3054*, New Jersey Institute of Technology, New Jersey, 1981.

[4] R. Viskanta, Heat Transfer to Impinging Isothermal Gas and Flame Jets, *Exp. Thermal and Fluid Sci.*, vol. 6, pp. 111–134, 1993.

[5] Lytle D. and Webb B. W., Air Jet Impingement Heat Transfer at Low Nozzle Plate Spacings, *Int. J. Heat Mass Transfer*, vol.37, pp. 1687-1697, 1994.

[6] J.W. Hodgson, R.T. Saterbak and J.E. Sunderland, An Experimental Investigation of Heat Transfer From a Spray Cooled Isothermal Cylinder, *J. Heat Transfer*, pp. 457–463, 1968.

[7] M.E. Goldstein, Wen-Jei Yang and J.A. Clark, Momentum and Heat Transfer in Laminar Flow of Gas With Liquid-Droplet Suspension Over a Circular Cylinder, *J. Heat Transfer*, pp. 185–193, 1967.

[8] F. P. Buckingham and A. Haji-Sheikh, Cooling of High-Temperature Cylindrical Surface Using a Water-Air Spray, *J. Heat Transfe,* vol. 117, pp. 1018-1027, 1995.

[9] J.C. Lasheras, E. Villermaux and E.J. Hopfinger, Break-up and atomization of a round water jet by a high- speed annular air jet, *J. Fluid Mech.*, vol. 357, pp. 351–379, 1998.

[10] K. M. Graham and S. Ramadhyani, Experimental and Theoretical Studies of Mist Jet Impingement Cooling, *J. Heat Transfer*, vol. 118, pp. 343-349, 1996.

[11] Azusa Kanamori, MunehikoHiwada, JunjiMimatsu, Hiraku Sugimoto and KenyuuOyakawa, Control of Impingement Heat Transfer Using Mist, *J. Thermal Sc. and Tech.*, Vol. 4, pp. 202–213, 2009.

[12] Proceedings, *6th European Thermal Sc. Conference, Eurotherm* , 2012. Oisin F P Lyons, Cian Quinn, T. Persoons and D.B. Murray, Heat transfer and flow in an atomizing mist jet:a combined hot film and shadowgraph imaging approach.

[13] C. Quinn, D.B. Murray and T. Persoons, Heat transfer behaviour of a dilute impinging air-water mist jet at low wall temperatures, *I. J. Heat and Mass Transfer*, vol. 111, pp. 1234–1249, 2017.

[14] Sookwan Lee, Jeeman Park, Piljong Lee and Moohwan Kim, Heat Transfer Characteristics during Mist Cooling on a Heated Cylinder, *Heat Transfer Engineering*, vol. 26, pp. 24–31,2005.

[15] Proceedings, ASME Summer Heat Transfer Conference, 2008. Roy J. Issa, Emily M. Hunt, Freddie J. Davis, Experimental Measurements and Numerical Modelling for the Air-Mist Cooling of a Heated Cylinder.

[16] G. I. Taylor, The Viscosity of a Fluid Containing Small Drops of Another Fluid, Proc. R Soc. A 138, pp.41–48, 1932.

SEEC No.073

CARBON NANO TUBE SUBSTRATE FOR SELECTIVE CATALYTIC REDUCTION (SCR) BASED NO_X REDUCTION

Sandeep Yadav
School of Engineering
IIT Mandi
sandeepyadav8193gmail.com

Akash Kumar
School of Engineering
IIT Mandi
uttambaliyan8dec@gmail.com

Dr. Viswanath Balakrishnan
School of Engineering
IIT Mandi
viswa@iitmandi.ac.in

Dr. Atul Dhar
School of Engineering
IIT Mandi
add@iitmandi.ac.in

ABSTRACT

At present, environmental pollution caused by nitric oxides (NOx) contained in exhaust gases from diesel engines is a serious problem of global significance that urgently needs to be solved. SCR is well known technology for controlling the emissions from lean burning CI engines. In this work, chemical vapor deposition (CVD) technique is used to grow high purity carbon nanotubes (CNTs) as a washcoat material on stainless steel (SS) mesh-based substrate. Scanning electron microscopy (SEM) and transmission electron microscopy (TEM) analysis showed the growth of CNTs on the surface of the SS mesh substrate. Also, experiments with different amount of catalyst loadings (in percentage) and difference in their reduction efficiencies are done. This work investigates the feasibility of CNT based low cost SCR NOX reduction for diesel engines by making it compact, more efficient and affordable.

Keywords: NOx, SCR, Carbon Nanotubes (CNT)

NOMENCLATURE

CNT	Carbon Nanotubes
SCR	Selective Catalytic Reduction
NO_X	Nitric Oxides
DEF	Diesel Exhaust Fluid
CI	Compressed Ignition
CDS	Compact Diagnostics System

INTRODUCTION

Selective Catalytic Reduction (SCR) is the one of the most advanced active emissions control technology system that injects a liquid-reductant agent through a special catalyst into the exhaust stream of a diesel engine for the NO_X removal. The reductant source is usually automotive-grade urea, otherwise known as Diesel Exhaust Fluid (DEF). The DEF sets on a chemical reaction that converts nitrogen oxides into nitrogen, water and tiny amounts of carbon dioxide (CO2), natural components of the air we breathe, which is then expelled through the vehicle tailpipe. It is called selective because it reduces levels of NOx using a reductant within a catalyst system. The chemical reaction is known as reduction where the DEF is the reducing agent that reacts with NOx to convert the pollutants into nitrogen, water and tiny amounts of CO2. When nitrogen is released during fuel combustion it combines with oxygen atoms to create nitric oxide (NO). This further combines with oxygen to create nitrogen dioxide (NO_2). Nitric oxide is not considered to be hazardous to health at typical ambient concentrations, but nitrogen dioxide can be. Nitrogen dioxide and Nitric oxide are referred to together as oxides of nitrogen (NO_x). Nitrogen dioxide is an irritant gas. Environmental and health effects of nitrogen oxides. Elevated levels of nitrogen dioxide can cause damage to the human respiratory tract and increase a person's vulnerability to, and the severity of, respiratory infections and asthma. Long-term exposure to high levels of Nitrogen dioxide can cause chronic lung disease. It may also affect the senses, for example, by reducing a person's ability to smell an odour. High levels of nitrogen dioxide are also harmful to vegetation damaging foliage, decreasing growth or reducing crop yields. Nitrogen dioxide can fade and discolour furnishings and fabrics, reduce visibility, and react with surfaces. Also, to match the new Euro emission standards need of NO_X reduction is there. Table 1. Shows the comparative percentage NO_X reduction data for passenger cars, light motor vehicles (LCVs), light goods vehicles (LGVs) from old to new Euro standard(s).

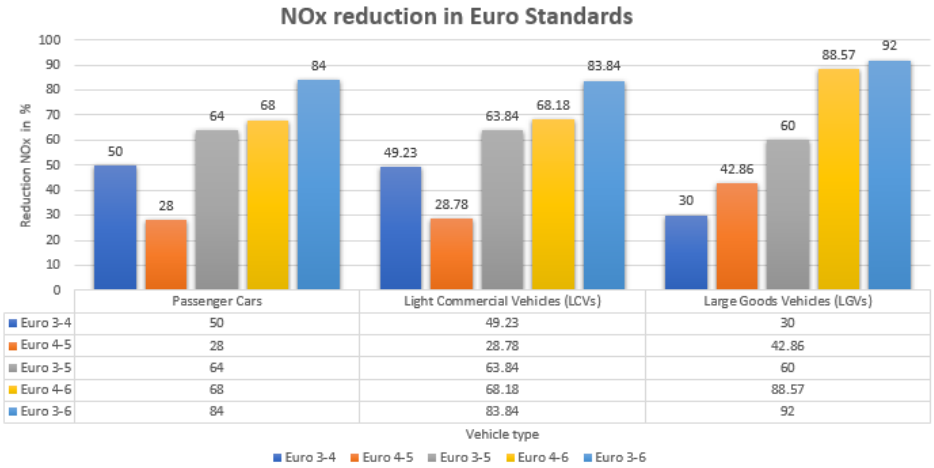

Table. 1. NO_X reduction data for passenger cars, light motor vehicles (LCVs), light goods vehicles (LGVs) from old new Euro standard(s).

Literature review

C.Wang et.al., 2005, it is demonstrated that Metal-exchanged ZSM-5 zeolite catalysts and acetylene as a reducing agent. It was demonstrated that acetylene is a promising reducing agent for SCR of NO in the oxygen-rich conditions. Under reaction conditions of 325°C, 1600 ppm NO, 800 ppm C_2H_2, and 9.95% O_2 in He with GHSV of 17000h-1, a stable NO conversion to N_2 of 76% was achieved over In-H-ZSM-5 catalyst. The acidity of catalyst appears to be critical for the SCR of NO reduction in excess oxygen conditions, by catalysing NO oxidation to NO_2 which is then reduced to N_2 by the reducing agent C_2H_2 over the catalyst. Fig.1. shows the conversion efficiency with respect to temperature.

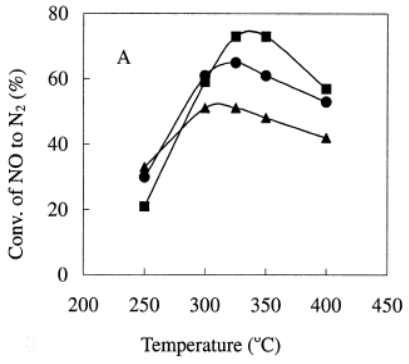

Fig. 1. Conversion of NO as a function of reaction temperature over Ga-H-ZSM-5 (circles), Mn-H-ZSM-5 (squares) and Cr-H-ZSM-5 (triangles). The reactions were run in a feed consisting of 1600 ppm NO, 800 ppm C2H2, 9.95% O2 in He with total flow rate of 50 ml/min over 0.2 g catalysts.

M. Barreau et.al., 2017 used Silver supported catalyst (Ag/Al2O3) and Collaborative effect of ethanol and ammonia (NH_3) i.e.Ethanol (Et-OH), NH_3, Blend (Et-OH+NH_3). The NOx conversion was then ranked between 46 and 95% in the 175–250°C temperature range, while only NO was initially injected. That work demonstrates that co-feeding ammonia and ethanol on a Ag/Al_2O_3 catalyst enables a drastic enhancement of the NOx conversion at low temperature (175–250◦C) using only NO as NO_x (standard SCR condition). The (EtOH + NH_3)-SCR over Ag/Al catalyst has superior NO_X reduction efficiency than both NH_3-SCR and EtOH-SCR in the temperature range 175–500◦C. It is proposed that the hydrogen H* species provided at low temperature by the ethanol dehydrogenation is the main responsible for the deNOx efficiency improvement, in addition to the beneficial concomitant NO_2 formation observed at low temperature with ethanol. Further deNOx improvement was obtained over a dual-coupled catalytic system composed of Ag/Al and a usual NH_3-SCR catalyst (WO_3/Ce-Zr), taking advantage of the remaining NH_3 and NO_2 from Ag/Al catalyst. A promising efficiency of 70% of NOx converted at 200-°C was reached, without dependence to the activity of the upstream oxidation catalyst (DOC). The present results also have practical implications. A unique aqueous solution containing both urea (NH_3 carrier) and ethanol could be used for this purpose, also allowing carrying away a much higher amount of reductant species versus the conventional AdBlue solution.

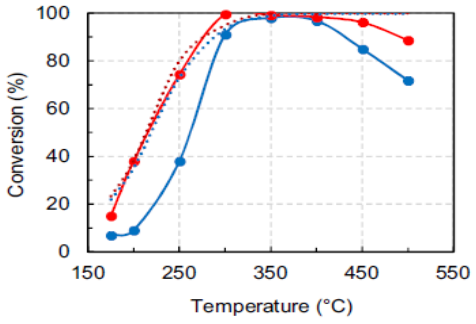

Fig. 2. Comparison of EtOH-SCR (blue) and (EtOH + NH3)-SCR (red) behaviour in NO_x conversion (full line) and EtOH conversion (dotted line) over Ag/Al catalyst.

Y. Zhao et.al., 2017 used Cu-beta zeolite (BEA) catalyst with Cerium and Niobium (Ce and Nb) as additives and HC (hydrocarbon) and NH_3 as a reducing agent. That study showed the effects of Ce and Nb additives on the de-NOx performance of a SCR/CDPF

system based on a Cu-BEA catalyst for a diesel vehicle. The pristine Cu-BEA catalyst with Ce and Nb additives improved the NOx conversion compared to the pristine Cu-BEA catalyst, both under the standard and fast SCR reaction conditions. This result was related to the strength of the intensity ratio as (Cu_2p_3 B peak)/(Cu_2p_3 A peak) for the Ce and Nb added catalysts. At a mild aging temperature of 600ºC, Cu-BEA-Ce and Cu-BEA-CeNb showed better NOx reduction ability, while at an aging temperature higher than 650ºC, the start of agglomeration of the Cu and metal clusters suppressed the de-NOx ability of catalysts. Moreover, the Cu-BEA-Nb catalyst showed better de-NOx performance than the other catalysts after hydrothermal aging at 650ºC; the Nb additive increased the surface acid sites, which are still effective after high temperature aging. After applying C_3H_8 gas to the reaction gas, the NOx conversion and C_3H_8 conversion by the Cu-BEA-CeNb catalyst was significantly affected, whereas the Ce addition to the Cu-BEA catalyst improved the de-NOx ability at high temperature. The Nb addition to the Cu-BEA catalyst improved the oxidation ability and inhibited the HC poison at high temperature. After loading PM, the Cu-BEA-Ce and Cu-BEACeNb catalysts show higher NOx conversion at high temperature, and the de-PM performance did not significantly differ among the four catalysts. The de-PM and de-NOx performances depend on the oxidation and reduction ability of catalysts, respectively. In order to simultaneously remove both PM and NOx in a SCR/CDPF system, the oxidation and reduction reaction sites need to be applied separately. In summary, Cu-BEA-Nb was found to be the most promising catalyst for application in a diesel SCR/CDPF system.Fig.3 shows the NOx conversion of the SCR/CDPF system under standard SCR reaction for channel flow and wall flow conditions. In Fig.3 all the catalysts show a wide temperature window of NO_x conversion of 80% from 225ºC to 550º C under the channel flow condition. Cu-BEA-Nb shows a high NOx conversion of >90% between 350 and 500ºC. Cu-BEA-Ce shows the lowest NO_x conversion among four types of catalysts with a conversion of 80%. The other two catalysts, Cu-BEA and Cu-BEA-CeNb, showed similar NOx conversion of >85%.

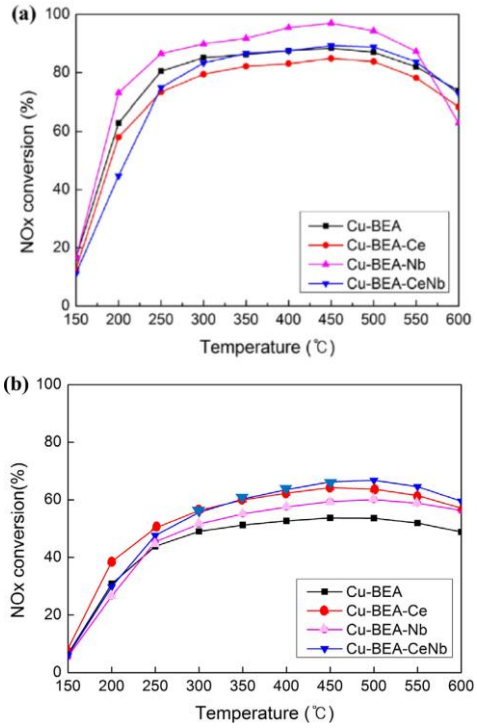

Fig. 3. De-NOx performance of SCR catalysts with various additives under standard SCR reaction (a) channel flow, (b) wall flow.

Experimental Setup

Experimental setup consists of a furnace fitted with quartz tube and electronic temperature control unit, NH_3, N_2 and NO gas cylinders coupled with rotameter for the flow control, removable tedlar gas sampling bag and a CDS system for NO_X characterization. Schematic diagram of the whole system is shown in the fig.4.

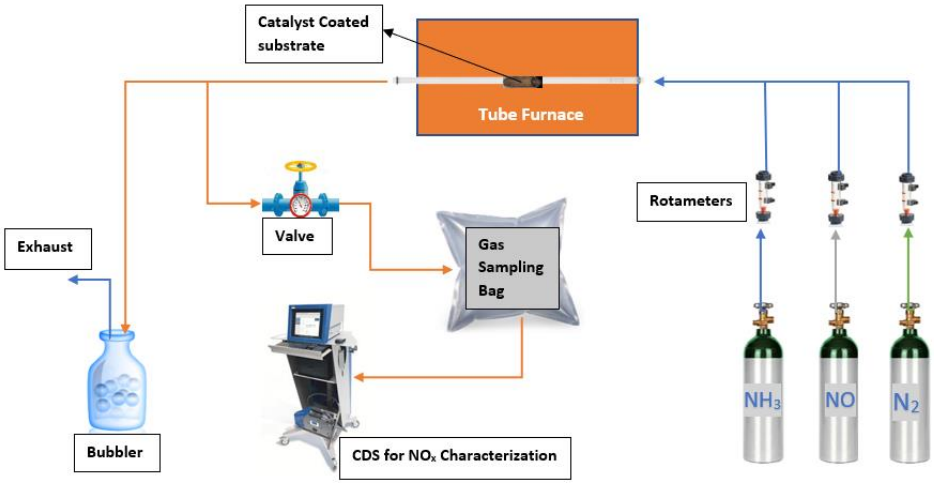

Fig.4. Reactor setup for NOx reduction by SCR, HC-SCR technology, here ammonia or propane used as reducing agent for SCR and HC-SCR respectively.

Results and Discussions

Catalytic reduction with different catalyst loading i.e. 0.01%, 0.04%, 0.1% over different temperatures are done. Also, substrate samples of with CNT growth and without CNT growth tested for percentage NO reduction efficiency. Percentage reduction efficiency may be defined as the ratio of reduced NO ppm to the original NO ppm over 100 scales as defined by equation (1).

$$\text{Percentage NO reduction} = \frac{(\text{NO at input (ppm)} - \text{NO after SCR (ppm)})}{\text{NO at input (ppm)}} \times 100 \quad \ldots\ldots [1]$$

Fig.5 shows the comparative bar chart for both CNT and without CNT based substrate. It shows the role of CNT in NO reduction catalytic reaction if we use it as washcoat materials for different loadings. We can see that at 0.01% catalyst loading we get 10% increment in NO reduction performance by CNT grown SS mesh substrate over bare SS mesh substrate. For at 0.04% catalyst loading we get 7% increment in NO reduction performance by CNT grown SS mesh substrate over bare SS mesh substrate. For 0.1% catalyst loading we get 4% increment in NO reduction performance by CNT grown SS mesh substrate over bare SS mesh substrate.

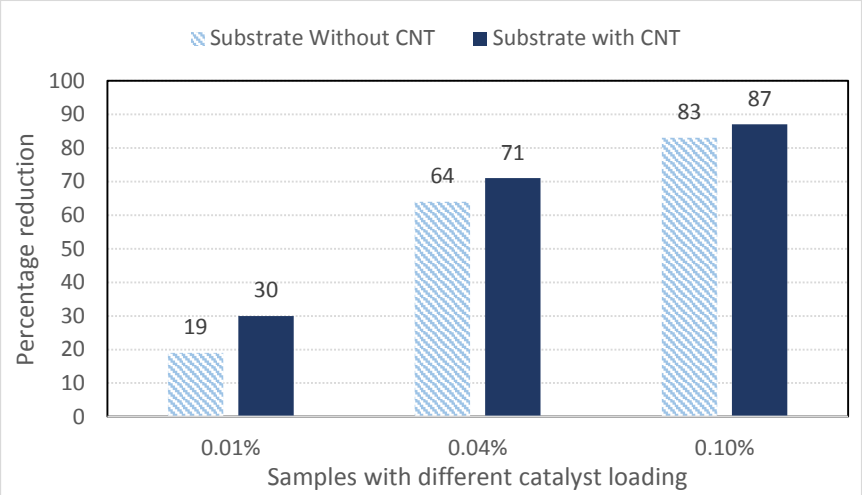

Fig. 5. Bar chart for both without CNT and with CNT based substrate and reduction for different catalyst loading.

REFERENCES

[1] C. Wang, X.wang*, S.Yu and Y. Xu, Acetylene: a new reducing agent used in SCR of NO on zeolite catalysts in an oxygen-rich atmosphere, React. Kinet. Catal. Lett. Vol. 86, No. 1, 59-66, **2005**.

[2] M. Barreau, M.-L. Tarot, D. Duprez, X. Courtois∗, F. Can∗, Remarkable enhancement of the selective catalytic reduction of NO at low temperature by collaborative effect of ethanol and NH3 over silver supported catalyst Applied Catalysis B: Environmental 220, 19–30, **2018.**

[3] Y. Zhaoa, B. Choib, D. Kima , Effects of Ce and Nb additives on the de-NOx performance of SCR/CDPF system based on Cu-beta zeolite for diesel vehicles, Chemical Engineering Science 164, 258–269, **2017**

[4] M.Tech. Thesis, Akash Kumar, CNT grown on stainless steel mesh for developing low cost SCR for diesel engine NO reduction, INDIAN INSTITUTE OF TECHNOLOGY, MANDI, **2018.**

Proceedings of theThird International Conference on Sustainable Energy and Environmental Challenges (3rd SEEC)
18 –21 December, 2018, IIT Roorkee, India

SEEC No.074

INVESTIGATIONS ON INTEGRATING SOFC WITH GAS TURBINE FOR PERFORMANCE ENHANCEMENT AND SUSTAINABLE ENERGY

Pranjal Kumar
Mechanical Engg. Deptt.
PG Scholar,Harcourt Butler Technical University, Kanpur
Email: sachanpranjal3@gmail.com

Onkar Singh
Mechanical Engg. Deptt.
Professor, Harcourt Butler Technical University, Kanpur
Email: onkpar@rediffmail.com

ABSTRACT

Direct energy conversion systems offer advantage over indirect energy systems in terms of their impact on environment but their limited capacity acts as a deterrent. Present work deals with the solid oxide fuel cell based direct energy conversion system integrated with conventional gas turbine based power generation system. It deals with thermodynamic modeling and analysis based on first law of thermodynamics. Here solid oxide fuel cell is integrated with intercooled and reheat type gas turbine for performance augmentation. Based on thermodynamic modeling the performance of considered SOFC-GT integrated system has been analyzed in respect to the fuel utilization factor, cycle pressure ratio and turbine inlet temperature. Results are obtained for arriving at optimal operating condition. The SOFC-GT integrated system under study offers 60.42 % and specific work output of 966.84 kJ/kg at cycle pressure ratio of 10, turbine inlet temperature of 1473 K and fuel utilization factor of 0.85.

Keywords: Intercooling, Reheating, Solid oxide fuel cell, Gas turbine**.**

NOMENCLATURE

A	area (m^2)
HPC	high pressure compressor
LPC	low pressure compressor
HPT	high pressure turbine
LPT	low pressure turbine
h	specific enthalpy (kJ/kg)
m	mass flow rate (kg/s)
N	no.of cell
V	voltage (V)
I	current density (A/m^2)
T	temperature (K)
C_{pair}	specific heat of air (kJ/kg K)
$C_{p\ fuel}$	specific heat of fuel (kJ/kg K)
$C_{p\ gas}$	specific heat of fuel (kJ/kg K)
E	Efficiency
HRVG	heat recovery steam generator
LHV	lower heating value of fuel
SOFC	solid oxide fuel cell
M	mixer
TIT	turbine inlet temperature
Uf	fuel utilization factor
C	combustor
W	work output

Subscripts

cell	SOFC cell
comp	compressor
comb	combustion
fcomp	fuel compressor
poly	polytropic
tur	turbine

INTRODUCTION

Present state of civilization largely depends upon the energy availability and the technological advancements have shown constant increase in the energy demand. Globally, the major share of the

consumed energy is still generated by the fossil fuels.The use of fossil fuel has been causing continuous increase in pollution leading to global warming. That's why researchers are searching promising alternatives to generate pollution free energy with high efficiency. Direct energy conversion systems hold attraction due to their inherent feature of direct generation of electricity. Out of different direct energy conversion systems, the fuel cells have been seen as potential energy conversion system. Fuel cells are electrochemical device which converts chemical energy into electrical energy silently with less or zero pollution. Among various type of fuel cells, the high temperature fuel cell (operating temperature upto 1000^{o}C) such as solid oxide fuel cell (SOFC) is most attractive because of electrolyte being solid in nature and the possibility of its integration with other power cycles due to availability of high temperature exhaust gases.

Literature review of the work carried out in the area of SOFC-GT shows that the performance enhancement of integrated systems needs further studies. The study carried out by Sghaier et al. [1] suggested that the efficiency of the SOFC-GT power plant is higher than the Gas Turbine power plant efficiency. Parametric analysis of SOFC-GT-ORC integrated power system has been done by Zhao et al. [2]. Yahyaoui et al. [3] developed a thermodynamic model for the thermodynamic and electrical study of tabular SOFC and MTG single shaft in PSCAD software. Haseli et al. [4] carried out a thermodynamic simulation for the compressive study of second law of efficiency of a high temperature SOFC combined with a recuperated conventional GT. Eisavi et al. [5] compared different type of SOFC-GT hybrid system and have been conducted environmental, economic analysis of configurations. Calise et al. [6] performed an exergetic analysis of a hybrid solid oxide fuel cell gas turbine system.

The present paper deals with the integration of SOFC with gas turbine (GT) for effective utilization of energy available in the cycle. The considered arrangement has intercooled compression and reheats type expansion in the GT cycle functioning along with the SOFC. The waste heat available from GT is utilized suitably in in the integrated cycle and results in improvement in the efficiency of the combined system.

SYSTEM DESCRIPTION

Figure 1 shows the layout of the SOFC-GT integrated system. Here atmospheric air is compressed in two air compressors namely low pressure compressor (LPC) and high pressure compressor (HPC). Then compressed air at state 4 is preheated through recuperator R1 using the exhaust gas from gas turbine at state 20. Supplementary fuel at state 31 is added as per need into the combustor for achieving desired turbine inlet temperature. The fuel compressor compresses fuel (natural gas) from state 11 to state 12. Again fuel is preheated through recuperator R2 upto state 13. Hot natural gas is mixed in M1 with steam coming from heat recovery steam generator at state 30. Exhaust gases leaving the recuparator R2 are used for providing heat to water coming into steam generator. The mixed fuel stream is further mixed with anode recirculated exhaust coming at state 9 to provide the necessary steam for pre-reforming the methane upto 30% before getting completely reforming in SOFC anode. The air stream at state 5 and the fuel stream at state 15 are sent into the SOFC stack drive for electrochemical reactions in the reaction layers of both electrodes. DC current generated by SOFC through external circuit is converted into AC current by a converter. Highly exothermic electrochemical reaction generates heat for steam reforming reaction and heating anode and cathode streams. In case of incomplete oxidation of fuel in SOFC, the remaining un-oxidized fuel is sent into combustor located down below for burning. Products coming out at the state 16 are utilized to attain the desired turbine inlet temperature (TIT) at state 25 and state 19.

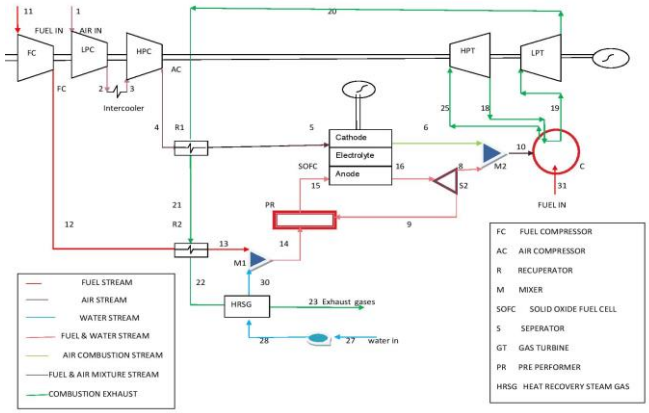

FIGURE 1. Layout of SOFC-GT integrated system

THERMODYNAMIC MODELLING

Thermodynamic modelling of different constituent components is carried out based on first law of thermodynamics as given ahead.

Gas properties model

The specific heat values have been considered as function of temperature and the same is used for estimating the energy interaction. The specific heat model for air and natural gas (100% methane) is considered as detailed in reference [7]. The specific heat of the gases produced after burning fuel in the

presence of excess air is given below as a function of temperature in kJ/kg K.

$$C_{pgas}(T) = 28.9085 - 0.50322 \times 10^{-3} \times T + 9.41292 \times 10^{-6} \times T^2 - 3.82388 \times 10^{-9} \times T^3/28.51 \quad (1)$$

Air compressor model

The outlet temperature of compressor is obtained considering the polytropic efficiency of compressor as;

$$\frac{T_2}{T_1} = \left(\frac{P_2}{P_1}\right)^{\frac{\gamma-1}{\gamma \times E_{poly,comp}}} \quad (2)$$

The compressor is assumed to be carried out with perfect intercooling so,

$$T_1 = T_3 \quad (3)$$

$$T_2 = T_4 \quad (4)$$

Work required for the compressor is determined by applying energy balance equation in kJ/kg as,

$$W_{A,comp} = (h_2 - h_1) + (h_4 - h_3) \quad (5)$$

Fuel compressor model

The outlet temperature of compressor is determined by:

$$\frac{T_{12}}{T_{11}} = \left(\frac{P_{12}}{P_{11}}\right)^{\frac{\gamma-1}{\gamma \times E_{poly,Fcomp}}} \quad (6)$$

Work required for the fuel compressor is determined by applying energy balance equation in kJ/kg as,

$$W_{A,COMP} = (h_{12} - h_{11}) \quad (7)$$

Gas turbine model

The outlet temperature of gas turbine is determined by:

$$\frac{T_{18}}{T_{25}} = \left(\frac{P_{18}}{P_{25}}\right)^{\frac{(\gamma-1)\times E_{poly,tur}}{\gamma}} \quad (8)$$

Reheating in the gas turbine is considered with the assumption detailed below;

$$T_{19} = T_{25} \quad (9)$$

$$T_{20} = T_{18} \quad (10)$$

Work produced by the gas turbine is determined by applying energy balance equation in kJ/kg as,

$$W_{tur} = (h_{18} - h_{25}) + (h_{20} - h_{19}) \quad (11)$$

Solid oxide fuel cell

The direct current (DC) electric power produced by the solid oxide fuel cell is expressed as,

$$W_{sofc} = V_{cell} \times i_{cell} \quad (12)$$

A detailed computer program in C language is written based on thermodynamic modelling of the constituent components of SOFC-GT integrated system.

Result and discussion

The SOFC-GT integrated system has been analysed based on the input parameters detailed in Table 1. The results obtained have been graphically presented in the figures presented ahead.

Table 1 Input parameter of SOFC-GT combined cycle [1,8,9]

Parameter	Value
Compressor polytropic efficiency, %	90
Inlet temp, K	298
Cycle pressure ratio	10
Turbine polytropic efficiency, %	92
Turbine inlet temp, K	1473
Lower calorific value of fuel, kJ/kg	50000
Fuel utilization factor	0.85
Current density, A m^{-2}	4000
Area of cell, m^2	0.04
Cell voltage, V	0.7
Operating temp, K	1073
No. of cell, N	4100
DC-AC inverter efficiency, %	95
Combustor efficiency, %	95
Steam/natural gas ratio	2.5
Pre-reformer operating temperature, K	873
Air composition by mass	O_2: 21%, N_2=79%
Fuel composition by mass	100% CH_4

Figure 2 shows the variation of overall cycle work output of SOFC-GT integrated system with cycle pressure ratio for different fuel utilization factors of 0.65, 9.75 and 0.85. It is seen that overall cycle work output gradually increases as fuel utilization factor in solid oxide fuel cell increases. The increase in cycle work output is also seen with increase in cycle pressure ratio at any fuel utilization factor and constant turbine inlet temperature 1473K.

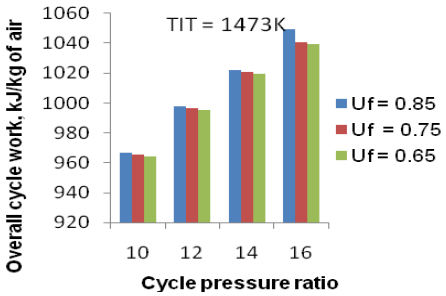

FIGURE 2. Variation of overall cycle work output with cycle pressure ratio for different utilization factors in solid oxide fuel cell.

Figure 3 shows the variation of overall cycle work output of SOFC-GT integrated system with cycle pressure ratio for different turbine inlet temperatures of 1473 K, 1573 K and 1673 K at fixed fuel utilization factor of 0.85. The results depict that the work output increases with increase in turbine inlet temperature for

fixed utilization factor due to increase in gas turbine work output.

Figure 4 shows the efficiency of the SOFC-GT integrated system having higher efficiency as compare to gas turbine cycle due to overall work output increased.

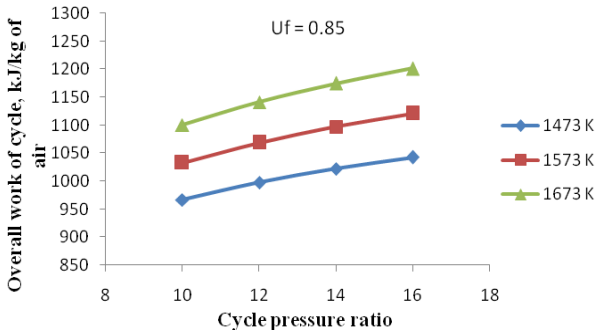

FIGURE 3. Variation of overall cycle work output with cycle pressure ratio for different turbine inlet temperatures at fixed utilization factor of 0.85.

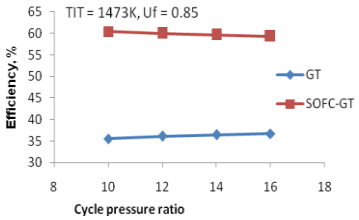

FIGURE 4. Variation of efficiency with cycle pressure ratio for turbine inlet temperature of 1473 K and fuel utilization factor of 0.85

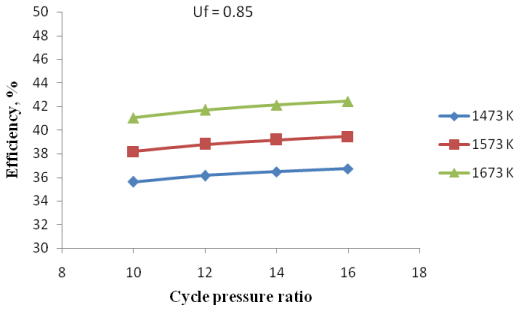

FIGURE 5. Variation of gas turbine efficiency with cycle pressure ratio at constant fuel utilization factor

Figure 5 shows the variation of the gas turbine efficiency with the cycle pressure ratio at constant fuel utilization factor of 0.85. It is seen that the gas turbine efficiency increases with the increase in the turbine inlet temperature.

CONCLUSIONS

Following conclusions are obtained based on the thermodynamic modelling and analysis carried out here.

1. SOFC-GT integrated system is having highest efficiency of 60.42 % as compared to the gas turbine power plant with efficiency of 35.99%.
2. SOFC-GT integrated system has maximum work output of 966.84 kJ/kg at cycle pressure of 10, turbine inlet temperature of 1473 K and fuel utilization factor of 0.85.
3. Integration of SOFC with GT is capable of offering good thermal efficiency due to effective utilization of heat available in the cycle.

REFERENCES

[1] Sghaier Salha Faleh, KhirTahar, Brahim Ammar Ben. Energetic and exergetic parametric study of a SOFC-GT hybrid power plant. International Journal of Hydrogen Energy 2017:1-13.

[2] Zhao Pan, Zhequan Yan, Wang Jiangfeng, Dai Yiping. Thermodynamic analysis of an SOFC-GT-ORC integrated power system with liquefied natural gas as heat sink 2013;38:3352-3363.

[3] Silva de Melo Stefani Vanussi, Yahyaoui Imene, Fardin Jussara Farias, Encarnacao Lucas Frizera, Tadeo Fernando. Power unit SOFC-MTG model in Electromagnetic Transient Software PSCAD 2017:1-12.

[4] Haseli Y, Dincer I, Naterer GF. Thermodynamic modeling of a gas turbine cycle combined with a solid oxide fuel cell 2008;33:5811-5822.

[5] Eisavi Beneta, Chitsaz Ata, Hosseinpour Javad, Ranjbar Faramarz. Thermo-ecvironmental and economic comparison of three different arrangements of solid oxide fuel cell-gas turbine (SOFC-GT) hybrid systems 2018;168:343-356.

[6] Calise F, D'Accadia M Dentice, Palombo A, Vanoli L. Simulation and exergy analysis of a hybrid Solid Oxide Fuel Cell (SOFC)-Gas Turbine System 2006;31:3278-3299.

[7] Bhatt BI, Thakore SB. Stoichiometry. 5th ed. McGraw Hill Publication; 2008.

[8] Singh Ragini, Singh Onkar, Comparative study of combined solid oxide fuel cell-gas turbine-Organic Rankine cycle for different working fluid in bottoming cycle. Energy Conversion and Management 2018;171:659-670.

[9] Siddiqui Osamah, Dincer Ibrahim. Analysis and performance assessment of a new solar based multigeneration system integrated with ammonia fuel cell and solid oxide fuel cell-gas turbine combined cycle. 2017;370:138-154.

Proceedings of International Conference on Sustainable Energy and Environmental Challenges(3rd SEEC), December 18-21, 2018, IIT Roorkee, India

SEEC No.075

Performance evaluation of bioreactor packed with free cell, LDPE and PUF immobilized bacterial consortia for the degradation of polycyclic aromatic hydrocarbon

Ravi Kumar Sonwani, Shivam Kumar, Balendu Shekhar Giri, Ram Sharan Singh, Birendra Nath Rai*

Indian Institute of Technology (BHU), Varanasi-221005, Uttar Pradesh, India

E-mail: raviks.rs.che16@itbhu.ac.in

Abstract

The aim of this work was to investigate a novel approach based on free cell, immobilized low-density polyethylene (LDPE), and immobilized polyurethane foam as packing support in the reactor for fluorene biodegradation. The sludge sample was collected from petroleum refinery to isolate the fluorene degrading bacterial species. The process parameters were optimized for the maximum biodegradation of fluorene by isolated bacterial consortia and found to be: pH 7.0; temperature 35°C and inoculum of 6.25 × 10^7 CFU/mL. The results demonstrate that reactor packed with immobilized PUF show the higher efficiency (90.1% COD removal) compared to the reactor packed with immobilized LDPE (84.1 % COD removal) and free cell (73% COD removal).

Keywords*: Bacterial consortia, fluorene, polyurethane foam, Bioreactor*

Highlights

- *Isolation of fluorene degrading bacterial species from petroleum contaminated sludge.*
- *To study the performance of the free cell, immobilized support bioreactors.*
- *Optimization of process parameters such as pH, temperature, and inoculum.*

Introduction

Polycyclic aromatic hydrocarbons (PAHs) are global environmental pollutant found in soil, air, and sediment (Liang et al., 2017; Bezza et al., 2016; Pugazhendi et al., 2017). The presence of these pollutants in the environment poses the harmful effect to human health and aquatic organism (Demeter et al., 2017). The high stability of these pollutant results in biomagnification and bioaccumulation to the aquatic food chain (Luo et al., 2014; Motorykin et al., 2013). PAHs generally released from the petroleum refinery, oil spills, fossil fuels combustion, and refinery processing (Sonwani et al., 2018). The United States Environmental Protection Agency (Silve et al., 2009) has listed these organic compound as priority pollutants due to their carcinogenic, and mutagenic effects (Sakulthaew et al., 2014). Several Physico-chemical methods have been used remediation of PAHs compound (Lin et al., 2010; Liang et al., 2017).

In the present work, the comparative study of a novel technique based on free cell, immobilized LDPE, and immobilized PUF as supports in a packed reactor was used for the fluorene biodegradation.

Materials and Methods

Isolation and enrichment of bacterial species

The analytical grade fluorene (>98% purity) were purchased from Sigma-Aldrich, India and other chemicals were procured from Merck India. The composition of mineral salt medium MSM (per liter) $K_2HPO_4.2H2O$ 1.5 g, Na_2HPO4 1.2 g, NaCl 0.5, $MgSO_4.7H_2O$ 0.3 g and $(NH_4)_2SO_4$ 0.3 g was used as the nutrient source. The solution also contain trace element such as $CaCl_2$ 2.0 mg, $FeCl_3$ 2.3 mg, $MnSO_4.H_2O$ 5.0 mg, $ZnSO_4$ 5 mg and $(NH_4)_6Mo_7O_{24}$ 1 mg per litre of solution. The pH of the MSM was adjusted to 7.0±0.2 and sterilized by autoclave at 121 ºC for 15 min. The petroleum-contaminated sludge was collected from the site of petroleum refinery for the isolation of bacterial species. PAHs degrading bacteria species were isolated from the petroleum sludge using mineral salts medium (MSM). The bacterial species were isolated using serial dilution method. The details of the isolation procedure have given in the previous study (Sonwani et al., 2018).

Bacterial growth and optimization

The consortia of five bacterial species were pre-culture in nutrient broth to prepare the inoculum for the biodegradation of fluorene. The set of batch experiments were conducted in 250 mL serum bottles. The pre-cultured bacterial inoculum was inoculated in the serum bottle containing 100 mL MSM and fluorene with varying concentration. The batch experiments were performed to optimized process parameters by varying the process variables such as temperature (25.0–40.0 °C), pH (5.0–9.0), and inoculums size (1-6 × 10^7 CFU/mL). The optimized condition obtained during the batch experiment was used for further experiments. All the analysis were performed in triplicate to minimize the error.

Packing support

The recycled waste polymers low-density polyethylene (LDPE) and polyurethane foam (PUF) were used as packing support in the reactor. These are the porous waste material and generally used for the packing of electronic instrument and collected from the campus of IIT BHU. The packing materials were cut into the cubical shape of 1 cm^3. The LDPE and PUF were rinsed with 70% (v/v) ethanol and then washed three times with double distilled water. The packing materials were filled in the separate bioreactor with MSM and glucose to allow the proper growth of biofilm on the surface of supports. After the development of the biofilm, these support were used in the biodegradation study.

Packed bed bioreactor (PBBR)

Three cylindrical borosilicate columns with a height of 65 cm and an internal diameter of 6.0 cm, were filled with packing support. All reactor have the total volume of 1865 mL with 1000 mL of working volume. The solution in reactors were fed by a peristaltic pump (Miclins PP 30 EX). The reactor was aerated by aeration pump (XP-AC-24L Xtra Power) and flow rate was control by rotameter (SRS-MG5, Eureka, Pune). A stone diffuser was placed at bottom of the reactor to maintain the aerobic condition in the reactor.

COD is an effective parameter that is adapted to obtain the level of pollution in a specific wastewater sample (Banerjee and Ghoshal, 2016). The COD of the samples were monitored using COD digester and analyzer (UNIPHOS).

The removal of COD was estimated using Eq. (1)

$$COD\ removal\ (\%) = \frac{COD_{initial} - COD_{final}}{COD_{initial}} \times 10 \quad \text{Eq. 1}$$

The residual fluorene concentration was monitored using a high-performance liquid chromatography (ELICO HL 460, India). The HPLC was equipped with a UV-vis detector (HD 469) and Xtimate C-18 column (4.6 mm × 250 mm × 5.0 µm).

Results and Discussion

Effect of pH

The variation of pH has a significant effect on the enzymatic activity of microorganism. Therefore, an optimum pH is required to obtain the efficient degradation of fluorene. The pH was optimized in the range of 5.0-9.0. It can be observed in Fig. 1, the percentage COD removal was increased as increase the pH up to 7.0 pH and above this pH the COD removal was decline. The optimum COD removal of 76.8 % was obtained at 7.0 pH. As change the pH of the solution to acidic value, the hydroxyl radicals produced which impede the enzyme activity of microorganism (Umar et al., 2017). Similarly, as change the pH of the solution to alkaline value, the removal was decreased due to substrate toxicity (Lin et al. 2010).

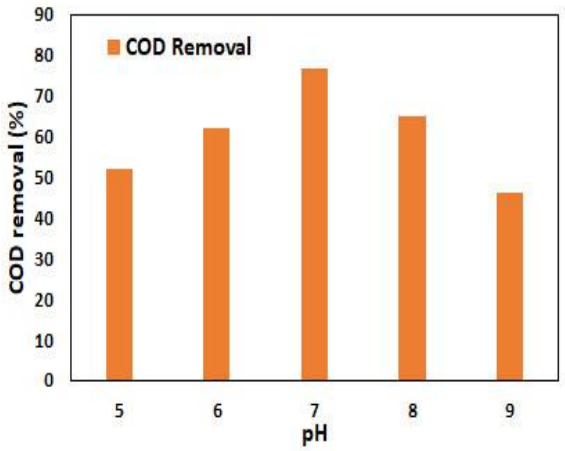

Fig. 1 Effect of pH on percentage removal of COD.

Effect of temperature

Temperature has a profound effect on the degradation of organic substrate. Fig. 2 represent the removal of COD with the variation of temperature (25-40 °C). The optimum COD removal of 81.8% was observed at 35°C. Above this temperature, the COD removal was decline and reached 51.5% at 40°C. The decreased in the COD may be due to inhibition of enzymatic activity at the high temperature. Similarly, the COD removal was decreased as the temperature of

solution decreased. The similar effect of temperature on biodegradation of naphthalene and fluorene has been reported previous researcher (Lin et al., 2010).

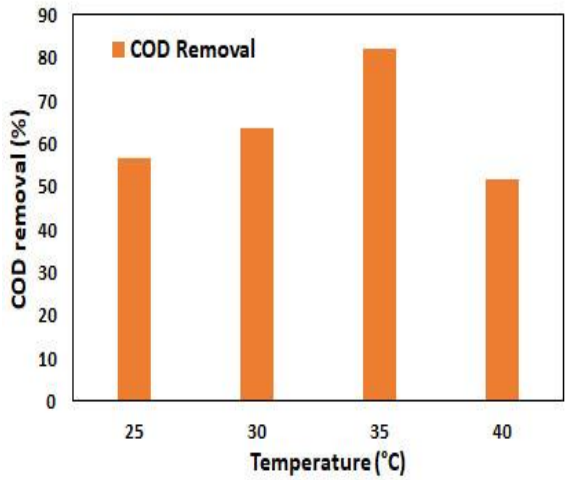

Fig. 2 Effect of Temperature on percentage removal of COD.

Effect of inoculum volume

The inoculum range of 1.0-6.0 mL (1.0 mL =1.25×10^7 CFU/mL) was used to examine its effect on the biodegradation of fluorene. It can be observed in Fig. 3, the percentage COD removal of fluorene increased with increase in the volume of inoculum. The optimum COD removal of 84.2% was obtained at 5 mL of inoculum and further increased in the inoculum no significant removal observed. The similar effect of inoculum was observer by Talha et al. (2018).

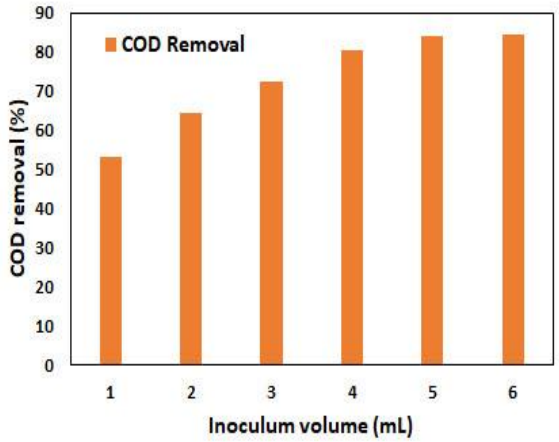

Fig. 3 Effect of inoculum volume on percentage removal of COD.

Performance of packed bed bioreactor for biodegradation of fluorene

Fig. 4 represent the fluorene biodegradation by free cell, immobilized-LDPE, and immobilized PUF. It can be observed from the plot the percentage COD removal was increased with time up-to 7.0 day and further increased in time no significant removal obtained. The maximum percentage COD removal of 73, 84.1, and 90.1 was observed at optimized condition (pH 7.0, temperature 35°C, inoculum 6.25×10^7 CFU/mL) in 10 days. The reactor packed with the immobilized-PUF show the maximum percentage COD removal of 90.1 compared to immobilized-LDPE (84.1%) and free cell (73.0%). More percentage removal of COD in case of reactor packed with PUF as compared to LDPE. This may be due to higher more porosity in the PUF for effective growth of bacterial species (Kureel et al., 2017; Geed et al., 2017).

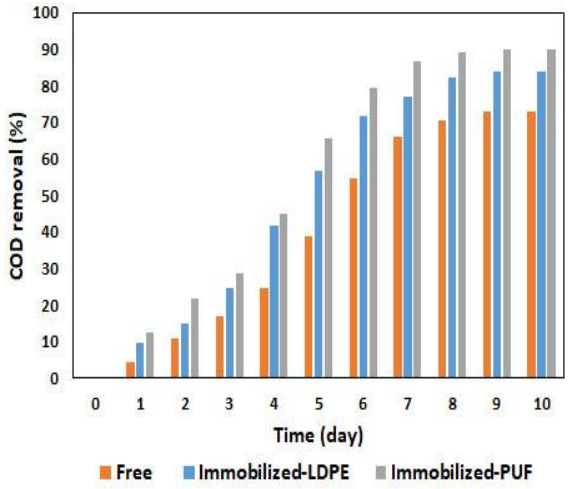

Fig. 4 Biodegradation of fluorene in the free cell, immobilized cells on LDPE, and immobilized cell on PUF.

Conclusions

The microbial consortia isolated from petroleum contaminated sludge was observed to be capable of fluorene degradation in batch bioreactors. The process parameters were optimized for the maximum biodegradation of fluorene by isolated bacterial consortia and found to be: pH 7.0; temperature 35°C and inoculum of 6.25 × 10^7 CFU/mL. The results demonstrate that the reactor packed with immobilized PUF and LDPE show the significant degradation of fluorene than free cell system.

Acknowledgements

The author (Ravi Kumar Sonwani) gratefully acknowledged the Indian Institute of Technology (BHU) Varanasi, UP, India, for providing laboratory facility to complete the work. The authors also acknowledged the Ministry of Human Resource Development (MHRD) for the financial support to conduct the work.

References

Banerjee, A., & Ghoshal, A. K. (2017). Biodegradation of an actual petroleum wastewater in a packed bed reactor by an immobilized biomass of Bacillus cereus. *Journal of environmental chemical engineering*, *5*(2), 1696-1702.

Bezza, F. A., & Chirwa, E. M. N. (2016). Biosurfactant-enhanced bioremediation of aged polycyclic aromatic hydrocarbons (PAHs) in creosote contaminated soil. *Chemosphere*, *144*, 635-644.

Demeter, M. A., Lemire, J. A., Mercer, S. M., & Turner, R. J. (2017). Screening selectively harnessed environmental microbial communities for biodegradation of polycyclic aromatic hydrocarbons in moving bed biofilm reactors. *Bioresource technology*, *228*, 116-124.

Geed, S. R., Kureel, M. K., Giri, B. S., Singh, R. S., and Rai, B. N. (2017) Performance evaluation of Malathion biodegradation in batch and continuous packed bed bioreactor (PBBR). Bioresource Technology, **227**, 56–65.

Kureel, M. K., Geed, S. R., Giri, B. S., Rai, B. N., & Singh, R. S. (2017). Biodegradation and kinetic study of benzene in bioreactor packed with PUF and alginate beads and immobilized with Bacillus sp. M3. *Bioresource technology*, *242*, 92-100.

Liang, X., Guo, C., Liao, C., Liu, S., Wick, L. Y., Peng, D., & Dang, Z. (2017). Drivers and applications of integrated clean-up technologies for surfactant-enhanced remediation of environments contaminated with polycyclic aromatic hydrocarbons (PAHs). *Environmental pollution*, *225*, 129-140.

Lin, C., Gan, L., & Chen, Z. L. (2010). Biodegradation of naphthalene by strain Bacillus fusiformis (BFN). *Journal of hazardous materials*, *182*(1-3), 771-777.

Luo, L., Wang, P., Lin, L., Luan, T., Ke, L., & Tam, N. F. Y. (2014). Removal and transformation of high molecular weight polycyclic aromatic hydrocarbons in water by live and dead microalgae. *Process Biochemistry*, *49*(10), 1723-1732.

Pugazhendi, A., Abbad Wazin, H., Qari, H., Basahi, J. M. A. B., Godon, J. J., & Dhavamani, J. (2017). Biodegradation of low and high molecular weight hydrocarbons in petroleum refinery wastewater by a thermophilic bacterial consortium. *Environmental technology*, *38*(19), 2381-2391.

Sakulthaew, C., Comfort, S., Chokejaroenrat, C., Harris, C., and Li, X. (2014) A combined chemical and biological approach to transforming and mineralizing PAHs in runoff water. Chemosphere, 117(1), 1–9.

Silva, P. T. D. S., Da Silva, V. L., de Barros Neto, B., & Simonnot, M. O. (2009). Phenanthrene and pyrene oxidation in contaminated soils using Fenton's reagent. *Journal of Hazardous Materials*, *161*(2-3), 967-973.

Sonwani, R. K., Giri, B. S., Geed, S. R., and Sharma, A. (2018) Combination of UV-Fenton oxidation process with biological technique for treatment of polycyclic aromatic hydrocarbons using Pseudomonas pseudoalcaligenes NRSS3 isolated from petroleum-contaminated site. , 56(July), 460–469.

Talha, M. A., Goswami, M., Giri, B. S., Sharma, A., Rai, B. N., & Singh, R. S. (2018). Bioremediation of Congo red dye in immobilized batch and continuous packed bed bioreactor by Brevibacillus parabrevis using coconut shell bio-char. Bioresource technology, 252, 37-43.

Umar, Z. D., Aziz, N. A. A., Zulkifli, S. Z., & Mustafa, M. (2017). Rapid biodegradation of polycyclic aromatic hydrocarbons (PAHs) using effective Cronobacter sakazakii MM045 (KT933253). *MethodsX*, 4, 104-117.

Proceedings of the International Conference on Sustainable Energy and Environmental Challenges (SEEC-2018)
18 – 21 December, 2018, IIT Roorkee, India

SEEC No. 076

EFFECT OF ATMOSPHERIC TEMPERATURE AND WIND SPEED ON THE PARABOLIC TROUGH COLLECTOR

Prashant Saini
School of Engineering
IIT Mandi
prashantsaini9997@gmail.com

Satvasheel Powar
School of Engineering
IIT Mandi
satvasheel@iitmandi.ac.in

Pradeep Kumar
School of Engineering
IIT Mandi
pradeepkumar@iitmandi.ac.in

Atul Dhar
School of Engineering
IIT Mandi
add@iitmandi.ac.in

ABSTRACT

From past few years, solar energy has been promoted as a main source of renewable energy. One of the easiest and simplest application of this solar energy is the conversion of solar radiation into heat energy using devices called Solar collectors. In order to enhance the conversion efficiency of these solar collectors, some atmospheric variables that effect the system performance needs to be investigated. For accomplishing these objectives, this paper investigates the effect of atmospheric temperature and wind velocity on the performance of the PTC (Parabolic Trough Collector). The CFD (Computational Fluid Dynamics) analysis of the parabolic trough collector against these parameters shows that wind velocity is inversely proportional to DNI (Direct Normal Irradiance). CFD analysis of Parabolic Trough Collector has been performed on the Beaufort scale with varying Direct Normal Irradiance. On Beaufort Number 0 by varying different solar radiation there is less convectional losses. Convectional losses increase as we move down to Beaufort Number 10. Conversion efficiency of Solar Parabolic Trough Collector is highly co-related with wind velocity and almost negatively co-related with the atmospheric temperature.

Keywords

Parabolic Trough Collector, CFD, Wind Velocity Effect

NOMENCLATURE

CSP	Concentrated Solar Power
PTC	Parabolic Trough Collector
CFD	Computational Fluid Dynamics
HTF	Heat Transfer Fluid
HCE	Heat Collection Element

INTRODUCTION

Parabolic trough collector (PTC) is the most economical concentrator for the indirect generation of steam in solar thermal power plants. Parabolic trough concentrator is simple to manufacture as compared to dish type and compound type concentrators. It requires only single axis solar tacking system [1,2]. The basic schematic diagram of the PTC is given in fig. 1.

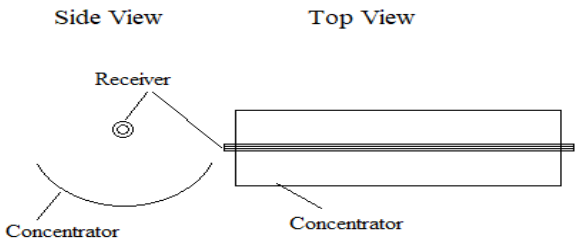

Figure 1. Schematic diagram of PTC.

By using parabolic trough collector, solar irradiance can be focused up to 50 times on absorber tube and hence, heat transfer fluid is heated (300-400°C) [3]. Normally, PTC consists of 3 parts, (i) parabolic reflector, which concentrates solar irradiance on Heat Collection Element (HCE). (ii) HCE, which is usually an absorption pipe made of copper or steel placed at the focus of parabola, (iii) the glass tube, which envelops the absorber tube [4]. The heat transfer fluid passes through the absorber tube and heats up. Parabolic trough collector has capability to achieve high temperature without much drop-in efficiency. PTC is widely used in the process of electricity generation in thermal power plant despite high amount of losses incurred because of poor design of PTC. These losses reduce the efficiency of the PTC to greater extent [5, 6].

Variations in the Zenith angle of the sun results in the variation of solar irradiance. Due to variation in irradiance

the heat flux on the surface of absorber tube also varies. This non-uniformity of heat flux results in non-uniform temperature profile across the absorber tube. There is circumferential variation of heat flux in the receiver. The bottom half of absorber tube receives the maximum solar flux, which leads to higher temperature rise in the bottom half compared to upper half of the absorber tube. In this study, modelling is performed using Fluent software. CFD analysis of parabolic trough collector performed at constant flow rate (i.e. 0.0177 kg/min). Simulation of PTC helps in calculation of heat losses and sizing of the power plant during its earlier design. These simulations also provide an idea how to improve the geometry or a system to minimize various types of heat losses and enhance the efficiency of the PTC [8].

Computational Model

Physical Model

Schematic diagram of PTC and its receiver is shown in figure 2(a) and 2(b). Following assumptions are adopted to model the PTC:

a. Both the ends of receiver are adiabatic.
b. The incident angle modifier is considered as unity, that is true when the incident angle is at zero degree.
c. There should be negligible infrared radiation exchange in between the glass envelop and the absorber surface.
d. The fluid flow is in steady state and incompressible.
e. Infinite long absorber tube is considered to minimized the edge/end loss.
f. Model is theoretically and physically symmetric along the y-z plane. The heat flux profile is symmetrical along the circumference of the absorber tube in y-z plane.
g. The efficiency of the tracking is so good that the optical errors could be neglected.

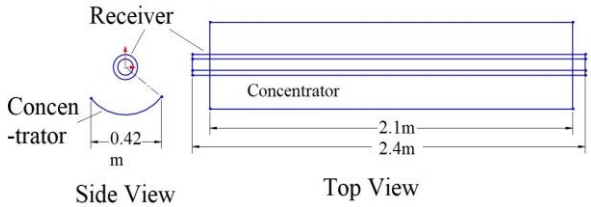

(a)

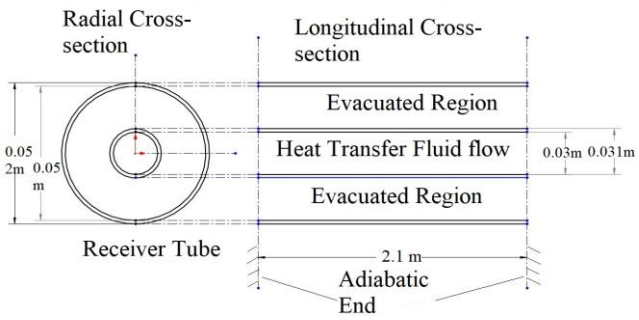

(b)

Figure 2. Schematic diagram of (a) PTC (b) receiver

Numerical approach and methodology:

- Viscosity, density and other thermal properties were kept as constant.
- K-ε turbulent model with enhanced wall treatment is used.
- Incident angle modifier (k) is considered as unity, which is true at an incidence angle of zero.
- There is negligible infrared radiation exchange in between the copper tube and the glass envelop.
- To make the flow incompressible the pressure is considered to be very low.
- Wall boundary condition: all walls are modelled as stationary wall with no slip condition. For the proper handling of viscous effect walls are properly closed and near-wall treatment is applied as a standard wall function.
- Outer surface of the copper tube: non-zero heat flux condition with zero wall thickness and no shell conduction.
- The solar energy flux distribution is calculated by using MCRT Method.
- Mass flow rate or velocity inlet remains constant.
- Coupled scheme is used as the solution method.
- Second order pressure and energy equation are used with pseudo transient condition.
- Second order turbulent kinetic energy and turbulent dissipation rate were used.
- Minimum iteration of 3000 is used for each case.
- Different optical specification of glass is as below:

Table 1. Optical Properties used in CFD

	Type of Spectrum	Incident	Diffused
Reflectance, (r)	Visible	0.08	0.84
	Infrared	0.08	
Absorbtance, (α)	Visible	0.09	0.1
	Infrared	0.09	
Transmitance, (τ)	Visible	0.83	0.75
	Infrared	0.83	

The second order upwind differential scheme is used for the energy and momentum equations. The COUPLED scheme is used for the pressure-velocity interpolation because it is appropriately used to find the density variation with respect to increase in temperature and swirl flows due to gravity.

The convergence of the solution was monitored by keeping the residual target 10^{-5} except the energy equation, for that the target of 10^{-8} is used. Further an extra investigation is performed to ensure the appropriate convergence. The convergence difficulties occur due to the vacuum modeling by using pseudo fluid whose velocity components are kept as zero while the radiational effects are investigated by using the MCRT method [9].

Result and Discussion

Effect of ambient temperature:

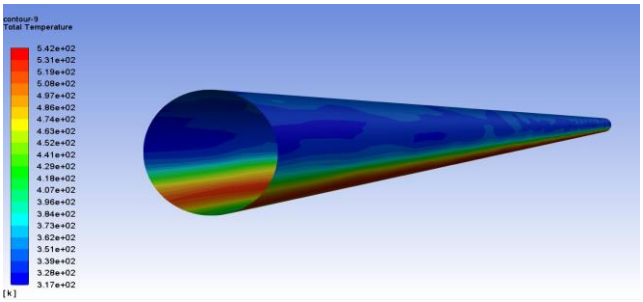

Figure 3. (a) Temperature contour of absorber tube with 500 W/m^2 with zero ambient temperature

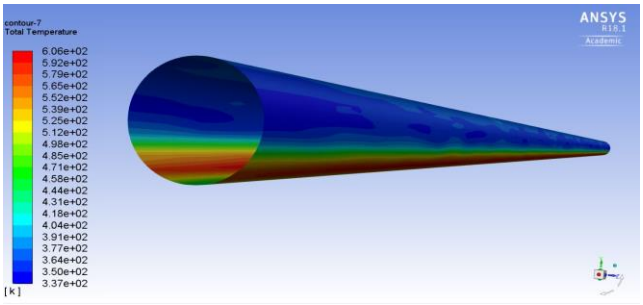

(b) Temperature contour of absorber tube with 800 W/m^2 with zero ambient temperature

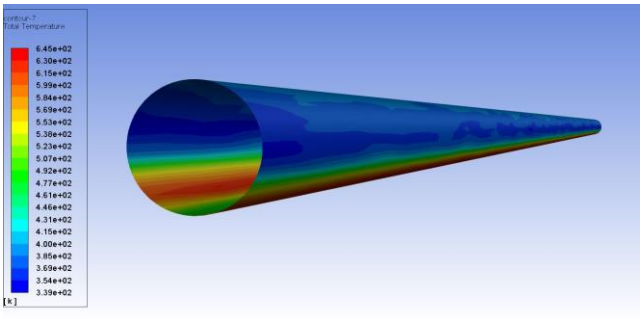

(c) Temperature contour of absorber tube with 1000 W/m^2 with zero ambient temperature

Table 2. Effect of Ambient temperature

S.No.	Ambient Temperature °C	Irradiance W/m^2	Heat Flux W/m^2	Surface Temperature (copper tube) (K)
1.	0	500	19541.78	542.84
2.	0	800	28448	606.82
3.	0	1000	35653	645.2
4.	40	500	20659.8	552.11
5.	40	800	32157.15	619.8
6.	40	1000	41218.42	648.09

Figure 3 (a), (b) and (c) show the temperature contour of absorber tube for different solar radiations (500 W/m^2, 800 W/m^2 and 1000 W/m^2) at 0° ambient temperature. And these contours remain same for the 40-degree Celsius ambient temperature. Temperature is varying with respect to different solar radiation. But by varying the atmospheric temperature from zero to 40 degree Celsius there is very small change in the temperature on the absorber tube as shown in table 2.

Conclusions

From the CFD analysis of PTC (Parabolic Trough Collector) it was observed that wind speed and efficiency have positive correlation while negative correlation with ambient temperature. Furthermore, wind speed is negatively correlated with direct solar radiation. Hence, in conclusion, the ambient temperature and wind speed reduces the thermal performance of the parabolic trough collector.

References

[1] M. Islam, A. Karim, S. Saha, P. K. D. V Yarlagadda, S. Miller, and I. Ullah, "Visualization of thermal characteristics around the absorber tube of a standard parabolic trough thermal collector by 3D simulation," *Iccm*, 2012.

[2] A. A. Hachicha, I. Rodríguez, R. Capdevila, and A. Oliva, "Heat transfer analysis and numerical simulation of a parabolic trough solar collector," *Appl. Energy*, vol. 111, pp. 581–592, 2013.

[3] M. Günther, M. Joemann, and S. Csambor, "Advanced CSP Teaching Materials Chapter 5 Parabolic Trough Technology Authors," *2011*, pp. 1–43, 2011.

[4] M. Romero-alvarez and E. Zarza, "Concentrating Solar Thermal Power," vol. 20072827, no.

September, 2007.
[5] H. Al-Ansary and O. Zeitoun, “Numerical study of conduction and convection heat losses from a half-insulated air-filled annulus of the receiver of a parabolic trough collector,” *Sol. Energy*, vol. 85, no. 11, pp. 3036–3045, 2011.
[6] M. Yaghoubi, F. Ahmadi, and M. Bandehee, “Analysis of Heat Losses of Absorber Tubes of Parabolic through Collector of Shiraz (Iran) Solar Power Plant,” *J. Clean Energy Technol.*, vol. 1, no. 1, pp. 33–37, 2013.
[7] Sargent & Lundy, “Assessment of Parabolic Trough and Power Tower Solar Technology Cost and Performance Forecasts Assessment of Parabolic Trough and Power Tower Solar Technology Cost and Performance Forecasts,” *Rep. No. NREL/SR-550-34440*, no. October, p. 47, 2003.
[8] Z. D. Cheng, Y. L. He, J. Xiao, Y. B. Tao, and R. J. Xu, “Three-dimensional numerical study of heat transfer characteristics in the receiver tube of parabolic trough solar collector,” *Int. Commun. Heat Mass Transf.*, vol. 37, no. 7, pp. 782–787, 2010.
[9] R. Forristall, “Heat Transfer Analysis and Modeling of a Parabolic Trough Solar Receiver Implemented in Engineering Equation Solver,” no. October, p. 164, 2003.

Proceedings of theThird International Conference on Sustainable Energy and Environmental Challenges (3rd SEEC)
18 –21 December, 2018, IIT Roorkee, India

SEEC No. 077

THERMODYNAMICS STUDY OF ENVIRONMENT FRIENDLY AIR / STEAM COMBINED CYCLE

Gaitry Arora
PG Scholar, Mechanical Engg. Deptt
Harcourt Butler Technical University
Kanpur(U.P)-India
Email: gaitry24arora8@gmail.com

Onkar Singh
Professor, Mechanical Engg. Deptt.
Harcourt Butler Technical University
Kanpur(U.P)-India
Email: onkpar@rediffmail.com

ABSTRACT
Gas/Steam combined cycle power plants are extensively used due to their better thermal efficiency but the fossil fuel based gas turbine plants create adversities for the environment. The present work deals with a combined cycle having a gas turbine cycle run on air which is brought up to the state of being expanded using compressor and a heliostat based heating system. The discharge from the gas turbine is sent to heat recovery steam generator for generating steam at the desired pressure and temperature for expansion in the steam turbine. The considered combined cycle configuration has been analyzed using thermodynamic modeling based on first law of thermodynamics. The study involves parametric investigation for arriving at the optimal operating conditions which may give insight into the combined cycle which is free from carbon emission and environment friendly.

Keywords Gas/ Steam combined cycle, heliostat field, intercooling

NOMENCLATURE

Q_s	Solar heat
I_n	Normal irradiation
A_{field}	Heliostat area
Q_{abs}	Heat absorbed by molten salt
Q_{loss}	Heat loss in the central receiver
m_a	Mass of air
$c_p(T)$	Specific heat polynomial for air
T_1	Ambient Temperature
P_1	Ambient Pressure
$\eta_{p,c}$	Polytropic efficiency of compressor
W_{COMP}	Work of compressor
$\eta_{p,t}$	Polytropic efficiency of turbine
LPC	Low pressure compressor
HPC	High pressure compressor
HPT	High pressure turbine
LPT	Low pressure turbine
HPST	High pressure steam turbine
LPST	Low pressure steam turbine

INTRODUCTION
The growing energy demand necessitates new power plants and improvement in the performance of available power plants by incorporating renewable energy resources which helps in carbon free power generation which does not cause environmental degradation.
Literature shows that as the renewable source the solar energy has highest global potential as it is the safe form of inexhaustible free energy so adoption of solar based technologies would lessen the issues related to energy security, climate change and global carbon emission level [2]. It also decreases the consumption of fuel or transportation charges of these non-renewable sources. Different types of solar technologies currently in working are parabolic trough collector (60 ^oC -500 ^oC), solar dish (100 ^oC -700 ^oC) and heliostat field (150 ^oC-1500 ^oC). From this it is cleared that heliostat has the largest and most flexible operating temperature range [3].Amongst all the clean technologies, solar energy serves as an effective renewable energy source to mitigate greenhouse gas emissions and helps to reduce global warming [1]. The amount of solar energy reaching the earth's surface is 6000 times the present global consumption of energy [4]. There is abundant availability of solar radiation of 1700-1900 kwh per kw peak for more than 300 clear sky days in a year. The total installed capacity of CSP in India is 12,288.83 MW till March 31, 2017 which increased four times in two years which was 3743.97 MW in March 2015 [5].
Brief literature review carried out in respect to the present work is detailed herein. Shin et. al[6] showed how combined cycle continues to gain acceptance as a reliable, flexible and efficient base load power generation. Jay et. al

[7] discussed about the problems with conventional power plants, overview and design of various CSP technologies and site selection criteria of CSP in India is outlined. Richa et al. [8] identified the potential sites for installation of CSP and provided solar irradiation data in India. Shaaban [9] worked on Integrated Solar Combined Cycles (ISSC) with steam Rankine cycle and organic Rankine cycle as bottoming cycles. Francesco Calise [10] presented a thermo-economic and environmental comparison between the integrated solar combined cycle and a conventional combined cycle. Anwar O.Binamer[12] developed a mathematical model of a typical integrated solar combined cycle system using engineering equation solver, to evaluate the performance of commercial ISCC power plants. Hogerwaad et.al [13] studied a solar based multigenerational system for power generation, refrigeration and desalination. Chao et. al [14] worked on energy and exergy analysis of solar power tower plants and presented their performances.

Looking upon the potential of solar energy and the ongoing studies, it is evident that the solar powered thermal energy is quite attractive. The present paper deals with the solar powered air run gas turbine cycle combined with the steam run steam turbine cycle. The use of heliostat based heating system for creating working fluid capable of producing positive work in gas turbine offers advantage of no contamination of working fluid. This offers the possibility of recycling the air as working fluid in gas turbine installation while using the energy carried by gas turbine exhaust for generation of steam in heat recovery steam generator (HRSG). The performance investigation of the air/steam run combined cycle is carried out based on thermodynamic modeling of the considered cycle on Ist law of thermodynamics. The results obtained have been analyzed and presented herein.

SYSTEM DESCRIPTION

Fig. 1 shows the schematic of the combined cycle consisting of gas-turbine cycle coupled with a steam Rankine cycle along with heliostat field. The heliostat field reflects solar radiation to a receiver, which carries molten salt. In the current analysis a mixture of work KNO_3 (40 wt. %) & $NaNO_3$ (60 wt. %) is used as a salt. Air enters the compressor at state 1 for being compressed to a state in low pressure compressor then goes to intercooler. here we take perfect intercooling then it compressed from state 3 to higher pressure and temperature at state 4. The compressed air then enters a molten salt to air heat exchanger H1, where it is heated using heat from the molten salt. The high pressure and temperature air is then expanded in the gas turbine to state 5. After expansion in the gas turbine, the low pressure and moderate temperature air passes through the heat recovery steam generator (HRSG), where it exchanges heat with the water delivered by the feed pump of the reheat steam Rankine cycle at state 18. The high temperature superheated steam leaving the HRSG then enters the high pressure steam turbine at state 10. The steam leaving at state 11 is reheated at state 12 and then expanded in low pressure steam turbine with provision of steam bleeding for deaerating the water at state 13. The steam expands in a low pressure steam turbine to state 14 and enters the condenser of the steam Rankine cycle at state 15 where it loses heat to the incoming cold water to provide hot water for process heating and the condensate is extracted using condensate extraction pump at state 16. The deaerated water at state 13 is then delivered to HRSG using feed pumpA few mini-symposia led by eminent experts in selected areas will also be conducted along with the conference. We hope you will be with us at Trivandrum to interact with the international research community.

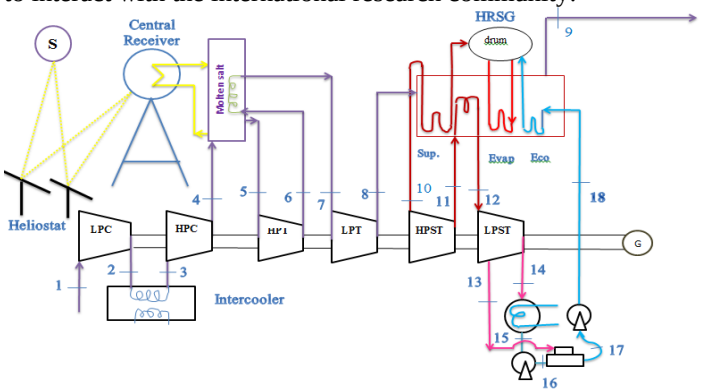

Figure 1 Schematic of air/ steam combined cycle

THERMODYNAMIC MODELLING

The salient features of thermodynamic modelling of the considered configuration are detailed ahead.

Air is considered to be the working fluid for topping cycle with molar composition of 21% oxygen and 79 % nitrogen. The specific heat of air as a function of temperature in kJ/kg-K is given by [12],

$$c_p(T) = 0.999638438 - 0.055205312x10^{-3} \times T + 0.346320281x10^{-6} \times T^2 - 0.140118997x10^{-9} \times T^3$$

Heat gained by air due to temperature variation between any two states 1 and 2-is given in kJ as;

$$Q = \int_{T1}^{T2} m_a \cdot c_p(T)\,dT \quad (1)$$

Considering the polytropic compression process the temperature of air after compression is given by:

$$\frac{T_2}{T_1} = \left(\frac{P_2}{P_1}\right)^{\left[\frac{\gamma-1}{\gamma \cdot \eta_{p,c}}\right]} \quad (2)$$

In the gas turbine run with air as working fluid, considering polytropic efficiency of turbine, the temperature of air after expansion is given by:

$$\frac{T_5}{T_6} = \left(\frac{P_5}{P_6}\right)^{\left[\frac{\gamma-1}{\gamma}\right] \cdot \eta_{p,t}} \quad (3)$$

Heat received from the solar radiation (in Watts) on Heliostat field is given by,

$$Q_S = I_n . A \quad (4)$$

$$Q_{in} = Q_{abs} + Q_{los} \quad (5)$$

Heliostat efficiency can be calculated as

$$\eta_h = \frac{Qin}{In\,Afield} \quad (6)$$

In HRSG, the energy balance yields,

$$m_a . c_p(T) . (T_8 - T_9) = m_w . ((h_{10} - h_{18}) + (h_{11} - h_{12}))$$

An exhaustive computer program in C language has been written based on thermodynamic modeling for studying influence of independent parameters on dependent parameters.

RESULTS AND DISCUSSION

Results are obtained from thermodynamic investigations of the considered air/steam combined cycle based on input parameters given in Table 1. The results have been graphically plotted and analyzed ahead.

Table 1: Input parameter [9,10,13,14]

Parameter, Unit	Symbols	Value
Solar Irradiation, W/m^2	I_n	1000
Total heliostat area, m^2	A_{field}	16666
Heliostat efficiency, %	η_h	75
Receiver efficiency, %	η_R	80
Polytropic efficiency of compressor, %	$\eta_{P,C}$	90
Polytropic efficiency of turbine, %	$\eta_{P,T}$	92
Ambient Temperature, K	T_1	273,283,288,293
Ambient Pressure, bar	P_1	1
Cycle pressure ratio	-	14,16,18,20
Exit pressure of air at Gas turbine, bar	T_8	1.2
HP steam pressure, bar	P_{10}	90
HP steam temperature, K	T_{10}	715
LP steam pressure, bar	P_{12}	5
Condenser Pressure of , bar	P_{14}	0.07
Bleed Pressure, bar	P_{13}	1.2

Figure 2 shows the variation of gas turbine work output with respect to cycle pressure ratio for different ambient temperatures. It depicts that as cycle pressure ratio increases the work output of gas turbine also increases at any ambient temperature. But with increasing ambient temperature at the work output of gas turbine is seen to be decreasing at any cycle pressure ratio.

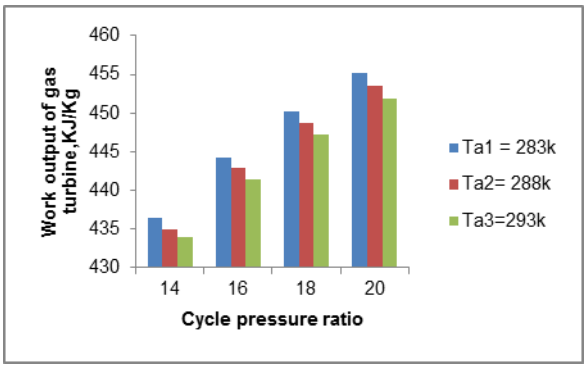

Fig. 2 Variation of work output of gas turbine with respect to cycle pressure ratio at different ambient temperatures

Figure 3 shows the variation of work output of steam cycle with respect to cycle pressure ratio at different ambient temperature it depicts that as the cycle pressure ratio increases exhaust temperature decreases which decreases work output of steam cycle at any ambient temperature.

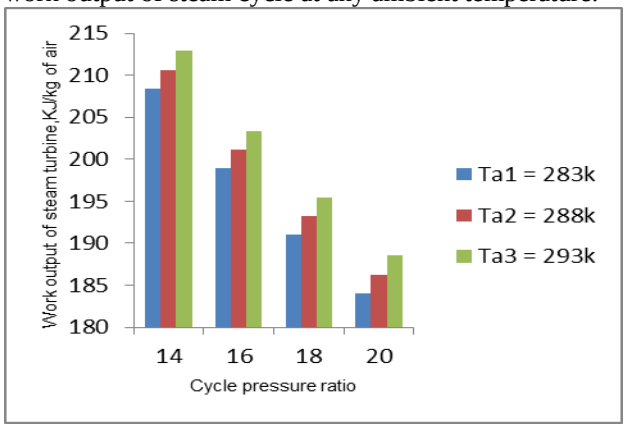

Fig. 3: Variation of work output of steam turbine with respect to Cycle pressure ratio at different ambient temperature

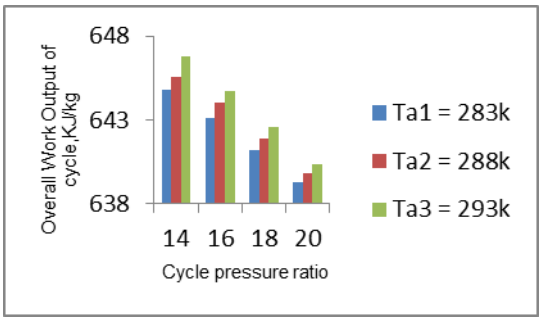

Fig. 4; Variation of overall work output of cycle with respect to cycle pressure ratio at different ambient temperature

Figure 4 shows the variation of overall work output with respect to cycle pressure ratio at different ambient temperature. It depicts that as cycle pressure ratio increases, the overall work output of cycle decreases at any ambient temperature. Figure 5 shows the variation of the gas turbine cycle efficiency with cycle pressure ratio.

The gas turbine cycle efficiency is seen to increase with cycle pressure ratio at any ambient temperature which may be attributed to the increment in positive work being more than increase in negative work. However, the lower ambient temperature offers high efficiency and this may be due to reduction in compressor work.

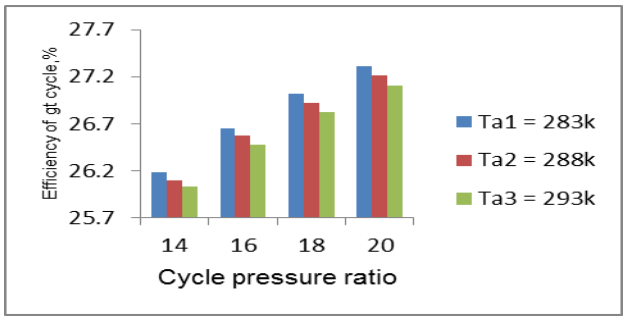

Figure 5 Variation of efficiency of gas turbine cycle with respect to cycle pressure ratio at different ambient temperature

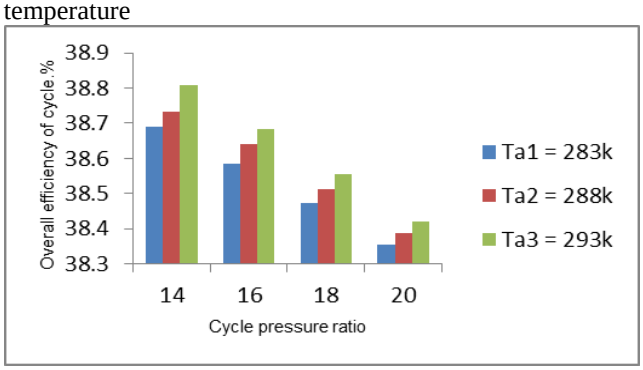

Fig. 6: Variation of overall efficiency of cycle with respect to cycle pressure ratio at different ambient temperature

Figure 6 shows that the overall efficiency of combined cycle decreases as the cycle pressure ratio increases with respect to ambient temperature. It may be attributed to the increase in negative work being more than the increase in positive work. The higher ambient temperature at inlet to compressor yields higher overall efficiency due to better utilization of solar energy.

CONCLUSIONS

Following conclusions have been obtained from this study.

1. The considered solar powered combined gas turbine cycle, steam Rankine cycle does not yield any emissions during its functioning.
2. Efficiency of solar powered air/steam combined cycle is 38.68% at 293K.
3. The increase in ambient temperature leads to increase in overall efficiency of the combined cycle , however the efficiency of gas turbine cycle is lesser at high ambient temperature.

REFERENCES

1. Ramachandra TV, Jain R, Krishnadas G.,2011, “Hotspots of solar potential in India”. Renew Sustain Energy Rev 2011;15(6):3178e86.
2. Ehsanul Kabir, Pawan Kumar, Sandeep Kumar, Adedeji A.Adelodun, Ki-Hyun Kim, “Solar energy: Potential and future prospects”. Renewable and sustainable Energy Reviews 82 (2018) 894-900;
3. Kalogirou,S.A., “Solar thermal collectors and applications,” Prog. Energy Combust.Sci., 30(3),pp.2443-2460.
4. Bosshard P, 2006, “An assessment of solar energy conversion technologies and research opportunities”. GCEP energy analysis, Technical assessment report, Stanford University.
5. Anil Kumar, Om Prakash, Akarshi Dube, 2017, “A review on Progress of concentrated solar power in India”, Renewable and Sustainable Energy Reviews, 79, 304-307.
6. Shin JY, Jeon YJ, Maeng DJ, Kim JS, Ro ST (2002) Analysis of the dynamic characteristics of a combined-cycle power plant. Energy 27: 1085-1098.
7. Jay Prakash Bijarniya, K. Sudhakar, Prashant Baredar, 2016, “concentrated solar power technology in India: A review”, Renewable and Sustainable Energy Reviews, 63, 593–603.
8. Richa Mahtta, P.K. Joshi, Alok Kumar Jindal, 2014, “Solar power potential mapping in India using remote sensing inputs and environmental parameters”, Renewable Energy, 71, 255-262.
9. S. Shaaban, 2016, “Analysis of an integrated solar combined cycle with steam and organic Rankine cycles as bottoming cycles”, Energy Conversion and Management, 126, 1003-1012.
10. M. Rabbani, T. A. H. Ratlamwala, I. Dincer, 2015, “Transient Energy and Exergy Analyses of a Solar Based Integrated System”, Journal of Solar Energy Engineering, ASME, Feb 2015, vol 137/011010-1
11. Stoichiometry, Fifth Edition ,B I Bhatt and S B Thakore, 2010, Mc Graw Hill, 2009.
12. Al-Abdaliya,” integrated solar combined cycle power plant: case study of Kuwait, part 1”, Renewable Energy 131(2019) 923- 937.
13. Janette Hogerward, Ibrahim dincer, Gerg F. Naterer, “Solar energy based integrated system for power generation ,refrigeration and desalination”. Applied thermal engineering 121(2017) 1059-1069.
14. Chao Xu, Zhifeng Wang, Xin Li, Feihu Sun, “ Energy and exergy analysis of solar power tower plants”. Applied thermal engineering 31(2011) 3904-3913.

SEEC No.078

THERMODYNAMIC INVESTIGATIONS ON CARBON CAPTURE IN GAS TURBINE POWER PLANT

Divya Prakash
PG Scholar, Mechanical Engg. Deptt.
Harcourt Butler Technical University
Kanpur (U.P.)
Email: divakardivya2010@gmail.com

Onkar Singh
Professor,Mechanical Engg.Deptt.
Harcourt Butler Technical University
Kanpur (U.P.)
Email: onkpar@rediffmail.com

ABSTRACT
Gas turbine power plants are extensively used for power generation across the world. Generally, the gas turbines are powered using fossil fuels, and the emissions from them have carbon dioxide as one of the major constituents. In view of this, the problem of global warming and air pollution is increasing day by day and there is need to evolve suitable carbon capture and utilization technologies to retrofit them. CO_2 capture system can capture up to 90% of CO_2 from the burnt gases of fossil fuels in power plant and the possible reuse of CO_2 in improving plant performance offers great potential. This paper deals with the study of the emissions from a gas turbine power plant in the combined cycle power at Auraiya U.P. and carbon capture and it's partial utilization in the plant. Results are useful for power sector professionals for making the existing power plants environment-friendly.

Keywords: Gas turbine, Turbine cooling, Carbon capture and storage, PEM Electrolyzer.

.

NOMENCLATURE

C_p	Specific heat (KJ/KgK)
$\dot{m}_a$	Mass of air (Kg/sec)
$\dot{m}_g$	Mass of gas (Kg/sec)
$\dot{m}_c$	Mass of coolant (Kg/sec)
$\dot{m}_f$	Mass of fuel (Kg/sec)
T_b	Permissible blade temperature (K)
T_c	Coolant Temperature (K)
S_{tg}	Stranton No.
CCS	Carbon capture and storage
PEM	Polymer Electrolyte Membrane
TIT	Turbine inlet temperature
CC	Combustion Chamber

1. INTRODUCTION

Increasing the amounts of CO_2 in earth's atmosphere are partly responsible for the rising temperatures, also known as climate change and the problem of global warming. Present scenario of power generation shows that inspite of various power generating technologies available, the cost-effective power still comes from burning fossil fuels such as coal, oil and natural gas. But burning fossil fuels releases CO_2. Keeping the remaining CO_2away from entering the atmosphere is a costly and challenging process and raises the price of electricity by up to 40%.

The literature review shows that there is need to have effective capture of CO_2 and its utilization in the thermal power plants. Jonshagen et al., [1] studied the use of CO_2 capture unit in apower plant, considering the effect of CO_2 capture and investigated how turbomachinery reacts into exhaust gas recirculation. Boubenia et al., [2] studied the CO_2 capture and utilization of captured CO_2 in a gas turbine,This study included the polymer electrolyte membrane electrolyzer to use the water to convert it into hydrogen.Study of CO_2methanation process to convert carbon die oxide to methane, showed that the methane can be used for the power generation using gas turbine, Stangeland et al. [3].Kumar and Singh

[4, 5] presented the investigations on cooling of turbine blades in a combined cycle through the transpiration cooling and film cooling. Magneschi et al. [6], Ou et al. [7] showed in the studies that the carbon capture and storage unit increases the amount of water requirement as compared to without CO_2 capture unit in the power plant.

The objective of the present paper is to capture the CO_2 from the gas turbine unit exhaust of the existing Combined Cycle Power Plantat Auriaya U.P. and then utilizing the collected CO_2 for the production of methane by PEM Electrolyzer and Methanation unit. Further, this methane can be used for the combustion in the same gas turbine and reduces the amount of existing fuel requirement of the plant.

2. System description

Figure 1 shows the schematic of the gas turbine power plant studied here. It shows a gas turbine unit with CCS and PEM electrolyzer and a methanation and oxygen storage unit. Gas turbine plant has a compressor, combustion chamber and turbine.The gas turbine is of cooled type and the same is realized through the air transpiration cooling.

The exhaust from gas turbine plant is sent to carbon capture and storage (CCS) unit for capturing the carbon dioxide. The captured CO_2 is used for the production of methanewhich is used for supplementing the fuel requirement in the combustion process along with the existing fuel. This CCS and methanation process is costly but using this methane as a fuel in combustion chamber reduces the amount of the existing fuel, naphthalene which is used as a primary fuel for the combustion. But the reduction in the requirement of amount of primary fuel reduces the cost of the primary fuel.

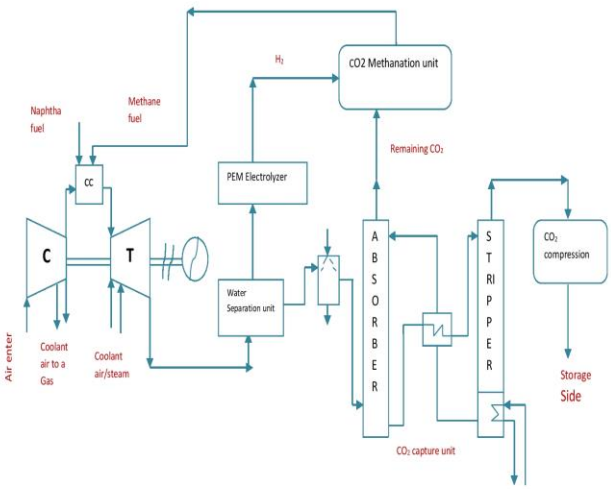

Fig. 1 Gas turbine power plant layout with transpiration cooling, CO2 capture, PEM Electrolyzer, and CO2 methanation unit.

3. Post-combustion CCS plant

The fuel is burned as normal, but before the flue gas travels up the chimney that passes through an absorber column, this is filled with liquid solvents called amines. Now, this CO_2 rich amine mixture is pumped to Stripper column. Here it is heated by the lean amine, where CO_2 is released from the solvents as the chemical link breaks between them. This CCS unit can capture up to 90% of CO_2.

4. Thermodynamic modeling

Thermodynamic parameters of Air and combustion products at different states in the cycle have been estimated considering the specific heat given as a polynomial function.

$$C_p(T) = (a + b * T + c * T^2 + d * T^3 + \cdots) \quad (1)$$

Where a, b, c and d are the polynomial coefficient, values are taken from reference 8.

The enthalpy change in the gas for any temperature range is estimated as follows:

$$\int_{T_i}^{T_e} dh = \int_{T_i}^{T_e} C_p\, dT \quad (2)$$

Compressor work is given as:

$$W_{cmp} = \dot{m}_{a,comp,ex}.h_{a,comp,ex} + \dot{m}_{ci}.h_{ci} + \dot{m}_{a,comp,in}h_{a,comp,ex} \quad (3)$$

Turbine work is given as:

$$W_{turb} = \dot{m}_g h_g + \dot{m}_{ci}h_{ci} - \dot{m}_{exh}h_{exh} \quad (4)$$

Coolant mass requirement in transpiration cooling of gas turbine blades is estimated as follows [4, 5]

$$\frac{\dot{m}_c}{\dot{m}_g} = \lambda * St_g * \ln\left[\frac{Cp_g}{Cp_c} * \frac{(T_g - T_{be}) - \varepsilon_{sw}(T_g - (T_{ci} + \eta_c * (T_{be} - T_{ci})))}{\eta_c * (T_{be} - T_{ci})} + 1\right] \quad (5)$$

Naphthalene is used as a primary fuel burnt in the combustion chamber and the chemical reactions are as follows:

$$C_{10}H_8 + 12(O_2 + 3.76N_2) \longrightarrow 10CO_2 + 4H_2O + 44.4N_2 \quad (6)$$

Methane is used as a secondary fuel in the combustion chamber and the chemical reactions are as follows:

$$CH_4 + 2O_2 \longrightarrow CO_2 + 2H_2O \quad (7)$$

Electrolyzer of water consists two electrodes, a cathode and an anode with the reactions occurring as follows:

(Anode reaction)

$$2H_2O \longrightarrow O_2 + 4H^+(aq) + 4e^- \quad (8)$$

(Cathode reaction)

$$4H^+(aq) + 4e^- \longrightarrow 2H_2(g) \quad (9)$$

Methanation process of Carbon die oxide received from CCS reacts with hydrogen to produce the methane. This methane is utilized for the combustion in same gas turbine unit and, reduces the amount of primary fuel The methanation process, also known as Sabatier process follows the reactions detailed ahead.

(Exothermic reaction)

$CO_2 + 4H_2O \longrightarrow CH_4 + 2H_2O$ (10)

Thermodynamic modeling of different components presented herein is used for writing detailed computer program in C language.

6. Results and Analysis

Based on thermodynamic modeling the results are obtained for the input parameters given in Table 1.

Table 1 Input parameters [4, 5, 9,10]

Input parameters	Values
Compressor polytropic efficiency	90%
Compressor inlet temperature	27°C
Compressor inlet pressure	1.013bar
Combustion chamber efficiency	90%
Turbine polytropic efficiency	92%
Mass of air	405.5 Kg/sec
Mass of naphtha fuel (without CCS)	8.055 Kg/sec
Mass of naphtha fuel (with CCS)	7.055 Kg/sec
Mass of methane (by remaining CO2)	1.00687 Kg/sec
LCV for naphtha fuel	44900 KJ/Kg
LCV for methane gas	50000 KJ/Kg

Figure 2 and Figure 3 depicts the influence of variation of cycle pressure ratio and TIT upon the efficiency of the gas turbine plant and net work output without CCS system.

Figure 4 and Figure 5 depict the variation of cycle pressure ratio and TIT on the efficiency of the gas turbine plant and net work output with the CCS system and methanation unit. Here it is considered that the CO_2 is captured up to 90% by CCS unit and transferred to a storage site and the remaining 10% of CO_2 is utilized for the production of methane. Improved efficiency and work output are found by using CCS system and utilizing the produced methane in the combustion chamber of the gas turbine in comparison to the gas turbine power plant without CCS system and also methane reduce the quantity of primary fluid.

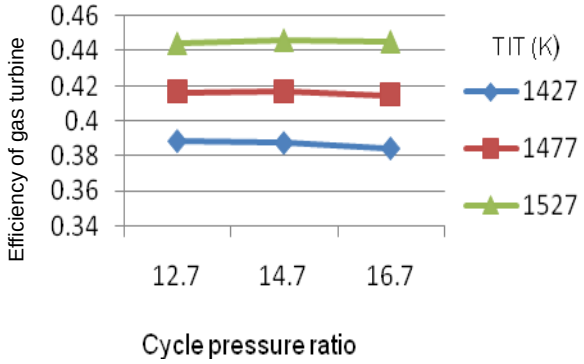

Fig. 2 Cycle pressure ratio and efficiency of gas turbine and TIT (without CCS)

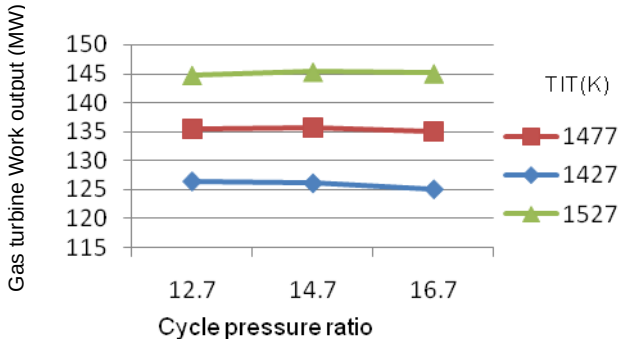

Fig. 3 Cycle pressure ratio and gas turbine work (MW) and TIT (without CCS)

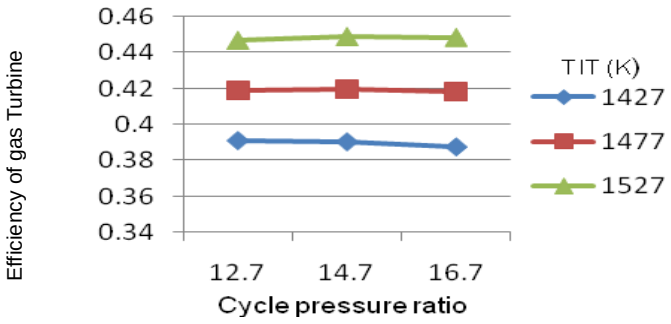

Fig. 4 Cycle pressure ratio and gas turbine efficiency and TIT (with CCS)

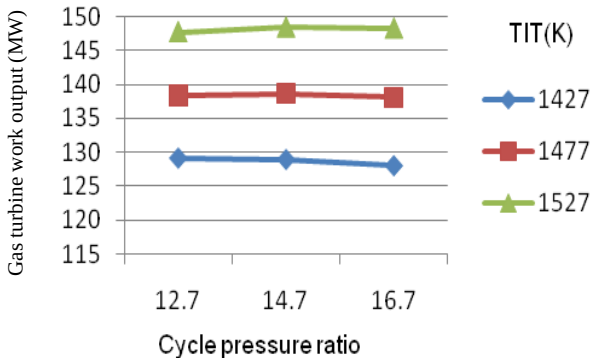

Fig. 5 Cycle pressure ratio and gas turbine work output (MW) and TIT (with CCS)

7. Conclusion

Based on the thermodynamic investigations on carbon capture in gas turbine power plant, the following conclusions have been obtained.

- CO_2 capture system is a futuristic model to capture the CO_2 and to reduce the carbon content from the atmosphere.
- Methanation unit offers potential solution to save the primary fuel requirement with CCS.
- Gas turbine installation is seen to offer increase in efficiency from 44.46 to 44.86% with the introduction of carbon capture, storage and its utilization for methanation.

8. References

[1] KlasJonshagen, NikolettSipocz, Magnus Genrup, A novel approach of retrofitting a combined cycle with post combustion CO_2 capture, Journal of engineering for gas turbine and power, ASME (2011) 011703-7.

[2] A. Boubenia, A. Hafaifa, A. Kouzou, K.Mohammedi, M. Becherif, Carbon dioxide Capture and utilization in gas turbine plants via the integration of power to gas, Petroleum (2017), doi:10.1016/j.petlm.2016.11.013.

[3] KristianStangeland, DoriKalai, Hailong Li, Zhixin Yu, CO2 methanation: the effect of catalysts and reaction conditions, Energy procedia 105(2017)2022-2027.

[4] S Kumar and O Singh, Performance evaluation of a transpiration-cooled gas turbine for the different coolants and permissible blade temperature considering the effect of radiation, Power and energy (2011)

[5] Sanjay, Onkar Singh, B.N. Prasad, Influence of different means of turbine blade cooling on the thermodynamic performance of combined cycle, Applied thermal engineering 28 (2008) 2315-2326.

[6] Guido Magneschi, Tony Zhang, Ron Munson, The impact of CO2 capture on water requirements of power plants, Energy Procedia 114 (2017) 6337 – 6347.

[7] Yang Ou, HaiboZhai, Edward S. Rubin, Life cycle water use of coal and natural gas fired power plants with and without carbon capture and storage, International journal of green house gas control 44(2016) 249-261.

[8] Polynomial coefficients values, htpp://www.colby.edu/chemistry/PChem/Ch7Table.

[9] Ragini Singh, Onkar Singh, Comparative study of combined solid oxide fuel cell-gas turbine-organic Rankine cycle for different working fluid in bottoming cycle, Energy conversion and management 171(2018)659-670.

[10] Fuels-higher and lower calorific values, https://www.engineeringtoolbox.com/fuels-higher-calorific-values-d_169.html

SEEC No. 079

NiO USED FOR THE TREATMENT OF CR(VI) POLLUTED WASTE WATER

Ms. Mamta D. Sardare
School of Chemical Engineering
MIT Acadmy of Engineering Alandi Pune
mdsardare@mitaoe.ac.in

ABSTRACT

As Nickel oxide naoparicle is efficient adsorbent for treatment of Cr(VI) contaminated synthetic wastewater. In this study, a new method combining nanoparticle adsorption and magnetic separation was developed for the removal and recovery of Cr(VI) from wastewater. The nanoparticle was synthesized, characterized and evaluated as adsorbents of Cr(VI), various factors influencing the adsorption of Cr(VI) e.g. pH, initial concentration and existing common ions were studied. Adsorption reached equilibrium within sometime and was independent of initial chromium (Cr) concentration. The adsorption data were analysed and the adsorption mechanism were investigated using X-ray Diffraction (XRD) and by SEM.

Keywords: *Adsorption, Chromium (VI), Nickel oxide naoparicle .*

INTRODUCTION

Water pollution is becoming a most important problem that endangering and effect on all living being and becoming acute every day. The effect of water pollution has effects on gentle balance of nature. Heavy metals like mercury, chromium, nickel, lead, cadmium, copper present in the contaminated water, they present at low concentration in well balance water. However these are present at high concentration as terms of contaminated water. Among these heavy metals chromium hexavalent is considered to be priority. Cr(VI) occur in the effluents produce during the leather tanning, dye fertilizer, electroplating, textile manufacturing, rings water, steel production factories, etc. The chromium hexavalent levels discharged may be ranging from ten to hundreds of mg/l are most important anthropogenic source of chromium (VI) [1,2]

Albadarin et al. (2011) have studied the removal of Cr (VI) from aqueous solution by lignin. The effect of various process parameters such as system pH, ionic strength, initial concentration, adsorbent dosage, presence of other metals (Zn and Cu), and presence of salts were studied. The optimum pH for the removal of Cr (VI) was found to be 2. The adsorption isotherms fitted well with the Freundlich model followed by pseudo second order kinetic reaction model. The maximum metal uptake obtained using Dubinin-Radushkevich and Khan isotherms for Cr (VI) removal are 31.6 and 29.1 mg/g respectively. It was concluded that the 36 adsorption mechanism involves the attraction of both hexavalent chromium (anionic) and trivalent chromium (cationic) onto the surface of lignin [12].

MATERIAL AND METHOD

All the chemicals used in this study were of analytical grade and procured from E-Merck India Ltd and Aldrich. The important chemicals used were Nickel (II) Chloride Hexahydrate ($NiCl_2.6H_2O$), Absolute Alcohol, NaOH (Pellets), Ethanol, and Distilled Water of highest purity was used throughout the study.

1.5 gm of $NiCl_2.6H_2O$ was transferred to 250 ml round bottom flask at room temperature. Then 70 ml absolute alcohol was added in the flask. The Solution was subjected to continuous stirring. 0.5 gm NaOH was dissolved in 100 ml absolute alcohol in another beaker. This Solution was added in $NiCl_2.6H_2O$ solution dropwise .It was stirred for 2 hours. Light green coloured Gel was formed after two hours. Gel was kept for three hours. Filtered and washed with water and Ethanol. Light green coloured precipitate formed. The ppt. was Oven dried at 100^0C for 2 hours. Fine green powder was subjected to Calcination at 290^0C for 30minutes. Black coloured nanopowder of NiOwas prepared.

The effect of initial Cr(VI) concentration on removal efficiency was investigated in the range of 10-100 mg/l for Cr(VI). It is observed that the removal efficiency increased with increasing concentration of Cr(VI) ions in the solution. As the concentration was increased, active sites of NiO were surrounded by more number of metal ions

resulting in increase of uptake of the ions. After reaching the equilibrium the uptake of ions became constant.

RESULT AND CHARACTERISATION

SEM micrographs of Nickel Oxide Nanopowder

The surface morphology of the material is studied by Scanning electron microscopy (SEM) is presented in (Figure 1). The SEM is done for understanding the surface morphology, from Figure that the material is having identifiable pores. It is done at 10.00kv and at 100000 magnification. This mainly shows the pores structures where adsorption of nickel oxide nanopowder can take place.

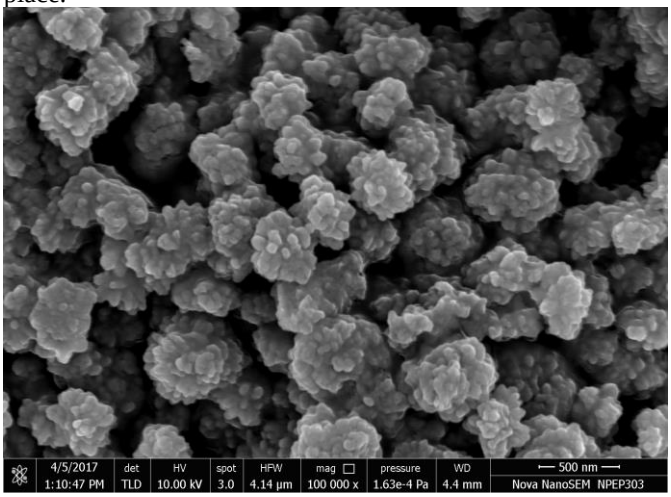

Figure 1: Scanning electron micrographs (SEM) of before adsorption

XRD analysis:

Powdered XRD of the material was obtained by using PHILIPS X'PERT X-Ray Diffractometer with Cu kα radiation (35 kv and 30 mA) at a scan rate of 20/min and was analysed using standard software provided with the instrument. The XRD pattern of the sample is presented in (Figure 2 and 3) few sharp peaks were obtained after loading hexavalent chromium, indicating the sample was partially amorphous in nature. XRD was analysed using standard expert high score.

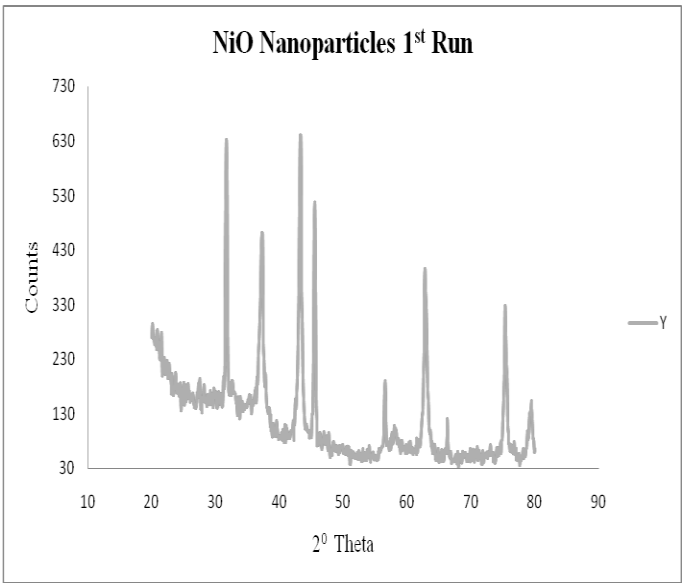

Figure 2: Graph of XRD data for NiO NP (I) run

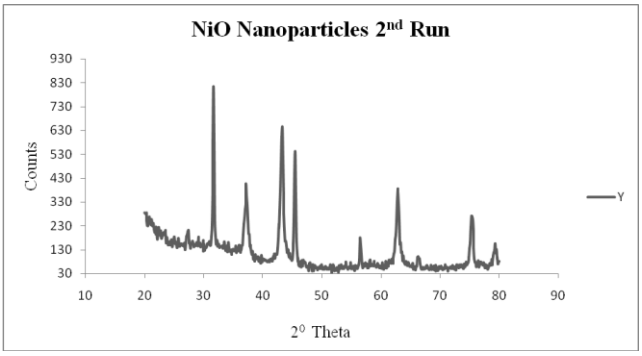

Figure 3: Graph of XRD data for NiO NP (II) run

Effect of adsorbent dose on the removal of Cr(VI) using Nickel Oxidenanopowder

The effect of adsorbent dose on the removal of chromium(VI) is studied in neutral condition (pH 7), at ambient temperature (28±2°C) and contact time of 30 minute for initial chromium (VI) concentration of 100mg/l. The results are shown in (Figure 3). It is evident from the (Figure 3) that the removal of hexavalent chromium raises from 59% to 78.7%, for 0.1 g/100ml of Ceria nanopowder as a hybrid material respectively with initial chromium (VI) concentration of 100mg/l.This results that as adsorbent dose will increases then percentage removal will also increase.

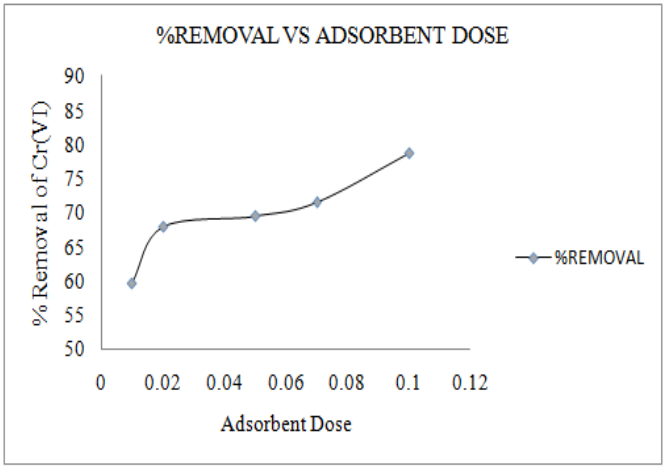

Figure3 : Graph of %removal of Cr(VI) VS adsorbent dose of Nickel Oxide nanopowder at speed 300 rpm and

Effect of contact times on the removal of hexavalent chromium from contaminated waste water

Batch study of chromium (VI) at different contact time is studied for initial chromium (VI) concentration of 100mg/l at pH 7 and adsorbent dose of 0.01mg/l,0.02mg/l,0.05mg/l,0.07mg/l,0.1mg/l keeping all other parameters constant. The result is represented in (Figure 4). It is understand from the (Figure 4) that we get 78% removal at 130 min.This results that as time increase percentage removal also increases.

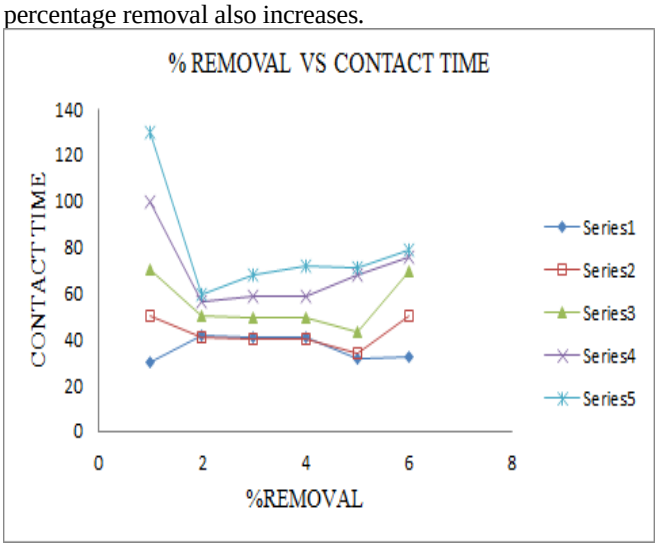

Figure 4: Graph of %removal of Cr(VI) VS contact time of Nickel Oxide nanopowder at 300 rpm speed and pH 7

Effect of adsorbent dose on % removal of Cr(VI) and uptake capcity using Nickel Oxidenanopowder

Chromium uptake capacity and % removal versus adosbent dose for adsorption of chromium is shown in graph in Figure (5) The uptake capacity is decease and % removal is increases as adsorbent dose in increases

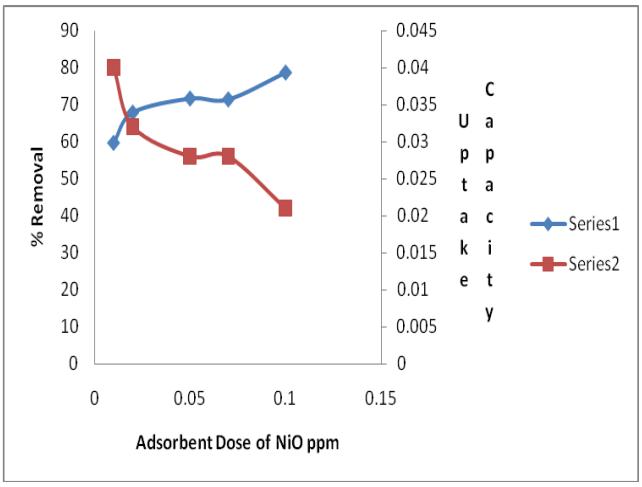

Figure 5: Graph of %removal of Cr(VI) and uptake capcity VS Adsorbent Dose of Nickel Oxide nanopowder at 300 rpm speed and pH 7

CONCLUSION

Nanoparticles of NiO were successfully prepared by SolGel method and prepared sample was characterized by XRD, techniques. Results have shown that prepared sample contains expected chemical composition. Particle size of sample was in Nano Scale range.

Acknowledgments

DST (SERB)-NEW DELHI for sponsored

References

[1]S.Ramasubramaniam, C.Govindarajan, T.Gomathi, and P.N.Sudha, "Removal of chromium (VI) from aqueous solution using chitosan-Starch blend", Scholar Research Library,ISSN 0975-5071.

[2] G. P.Gallios, MiroslavaVaclavikova, "Removal of chromium (VI) from water streams: a thermodynamic study", Environ ChemLett, DOI 10,1007/s10311-007-0128-8, 2008.

[3] A K Bhattacharya, S N Mandal and S K Das, "Removal of Cr(VI) from aqueous solution by adsorption onto low cost non-conventional adsorbents", Indian Journal of Chemical Technology, pp. 576-583, Vol. 13, November 2006.

[4]E.A.Brandes; H.T.Greenaway; Stone, H. E. N. (1956). "Ductility in Chromium". Nature. 178 (587): 587. Bibcode: 1956Natur.178.587B. doi:10.1038/178587a0

[5] National Research Council (U.S.). "Committee on Biologic Effects of Atmospheric Pollutants

(1974)". Chromium. National Academy of Sciences. p. 155. ISBN 978-0-309-02217-0.
[6] National Research Council (U.S.). Committee on Coatings. "High-temperature oxidation-resistant coatings: coatings for protection from oxidation of superalloys, refractory metals, and graphite" (1970). National Academy of Sciences. ISBN 0-309-01769-6
[7] H. K. D. H. Bhadeshia,"Nickel-Based Superalloys". University of Cambridge. Retrieved 2009-02-17.:255-265
[8] C.Baselt, Randall. "Disposition of Toxic Drugs and Chemicals in Man (8th ed.)". Foster City: Biomedical Publications. pp. 305–307. ISBN 978-0-9626523-7-0. (2008)
[9] C.M.Abbott, Isaac Tyson Jr. Pioneer Mining Engineer and Metallurgist, Maryland Historical Magazine, March, pp. 15–25.(1965)
[10] N.Shahruz; M.M.Hossain, World applied Science Journal, 2011, 12 (11), 1981-1986
[11] M.LGulrajan; D.Gupta, Indian Journal of Fibre and Textile Research, 36, pp388-397. (2012)
[12] J.H.Yang; Y.U. Kwon,Bull.KoreanChem.Soc.28,No.7. (2007)

SEEC No.080

EXHAUST HEAT RECOVERY FROM A 4-STROKE DIESEL ENGINE USING A THERMOELECTRIC GENERATOR UNIT

M.Nikhil Mathew
School of Engineering
IIT Mandi
nikhilmathew0308@gmail.com

Sarthak Nag
School of Engineering
IIT Mandi
iamsarthaknag@gmail.com

Atul Dhar
School of Engineering
IIT Mandi
add@iitmandi.ac.in

ABSTRACT

About 30% heat from reciprocating engines is wasted as exhaust heat losses. Recovering some part of this heat is a promising method for improving the efficiency. Exhaust heat recovery (EHR) can be broadly classified in (i) solid state base EHR and (ii) fluid based EHR. Solid state EHR employs thermoelectric generator (TEG) modules to recover exhaust waste heat and convert it to useful electricity. In this work we have used 8 TEGs with the hot side (about Th=523K) being provided by the exhaust gases of a 4-stroke diesel engine and the cold side (Tc=300K) was provided by pumping cold water through a copper channel. Using the above mentioned setup we conducted experiments at different loads and we were able to generate a maximum of 18 Watts of electrical power. This heat recovered from the exhaust has increased the overall efficiency of the system and reduced the temperature of the exhaust gases. This power can be used for running the auxiliary components in the system or reduce the load on the battery thereby reducing its size.

Keywords:Thermoelectric Generators, Exhaust Heat Recovery, Diesel Engine

NOMENCLATURE

V = electrical potential difference

S = seebeck coefficient

ΔT = temperature difference achieved

INTRODUCTION

In early centuries of modern history man was in an attempt to increase the production of energy in order to develop industries, means of transport and quality of life. As the human population is increasing,we are facing an acute shortage of energy sources and there has been a high stress on the earth's environment due to excessive global pollution, majorly due to transportation, power plants and industries [1]. researchers and industrialists have looked mainly to manage energy in a better way, especially by increasing energy system efficiency.This explains the growing interest for thermoelectric generators.

Even though the IC engine is known for producing very high amounts of power and celebrated for being a major prime mover in the transportation industry it still has a maximum efficiency of only about 30-35%. About 30% s lost in cooling and another 35-40% goes out in the form of exhaust gases. Hence if we can combine the above two technologies to recover heat from the exhaust of the engine and convert it to useful electrical energy we could either reduce the size of the battery or eliminate the alternator from the system. The application of TEG to automobiles dates back to early 1900s when Leigh Hale invented a thermoelectric based battery for motor vehicles [12]. Hi- Z Technology developed 1 kW output thermoelectric generator for class eight Diesel truck engines under U. S. Department of Energy and California energy commission funding since 1992 [3]. It employs 72 TEG modules made of bismuth telluride (Bi_2Te_3), The power output increased from 400 W to 1068 W with the attention given to internal design of heat exchanger.

Thermoelectric generators are solid state devices which work on the principle of the seebeck effect. When we place them on the exhaust manifold, due to conduction

we have a higher temperature on one side say the hot side. This heat propels the electrons away from the surface. If we can cool the other side, we can create a good temperature gradient across the module. Hence having fewer electrons on one side and more on the other side will create a voltage difference in the module, this will allow electron movement i.e. electric current. Therefore based on the above discussion we can interpret that greater the temperature difference more the power produced, this relation can be given as

$$V = S\Delta T \qquad (1)$$

A TEG consists of number of thermocouples depending on the size and capacity of the TEG module. A thermocouple is a small unit which is made of *P* type and *N* type semiconductors. These thermocouples are then connected to each other; electrically in series and thermally in parallel and placed between two highly thermally conductive ceramic wafers to form a TEG.

EXPERIMENTAL METHODS AND PROCEDURES

Measurement Of Output Power And Voltage

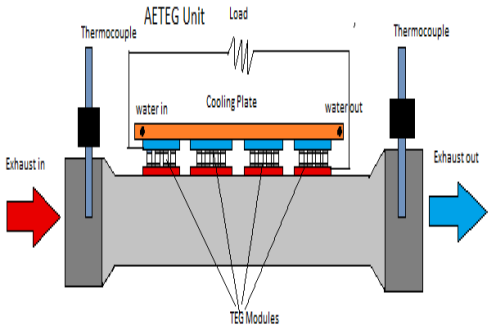

Figure 1: Pictorial representation of the experimental setup

The AETEG unit was fabricated using aluminium sheet of thickness 3 mm which served as a medium of heat exchange between the exhaust and the TEG modules. To measure the exhaust inlet and outlet temperature, two p-type thermocouples were installed at their respective position. For the energy recovery, a total of 8 modules (make: Hi-Z, model: 14V) were used. These TEG modules were chosen as they are bismuth telluride (Bi_2Te_3) based and can operate at high temperatures of 250 ˚C for continuous use and 400 ˚C for intermittent use. 2 parallel arrays containing 4 modules in series in each array were used for experimental studies to maximize both current and voltage in the circuit

Maintaining a constant cold side temperature is very important to increase the potential difference.We used a submersible pump to recirculate water at 8 ˚C over the cold side. For this purpose we used we used a copper plate (as shown in Fig.2) due to its high thermal conductivity with channels milled on to its surface.

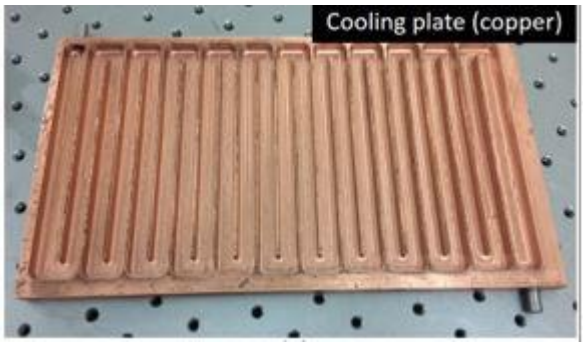

Figure 2 Copper plate used to circulate cold water on the cold surface

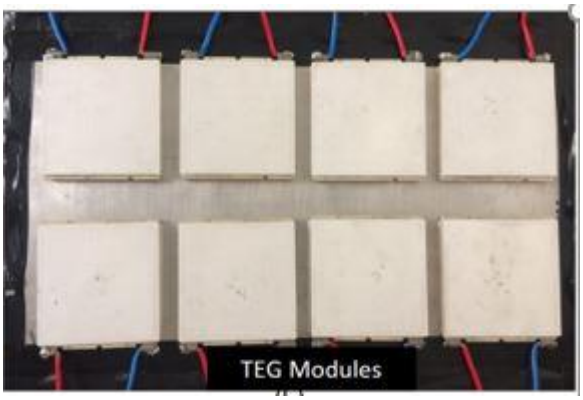

Figure 3 Arrangement of TEG modules

RESULTS AND DISCUSSIONS

The experiment was conducted at 25%, 50 % and 75% loads. The following table and bar graphs show the amount of power and voltage produced in each of he above mentioned case.

Load (%)	Power (watts)	Voltage (V)
25	5.95	4.88
50	12.69	7.12
75	18.83	8.63

Table 1: Results of Experimental Study

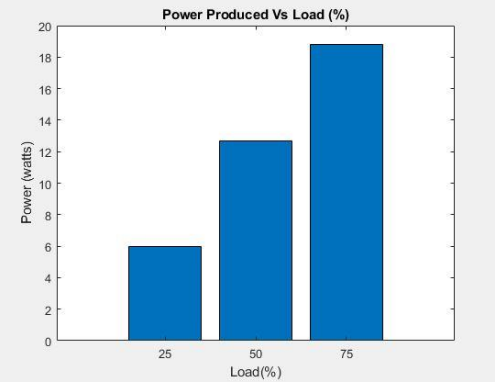

Figure 4 (a) : Power produced Vs Load(%)

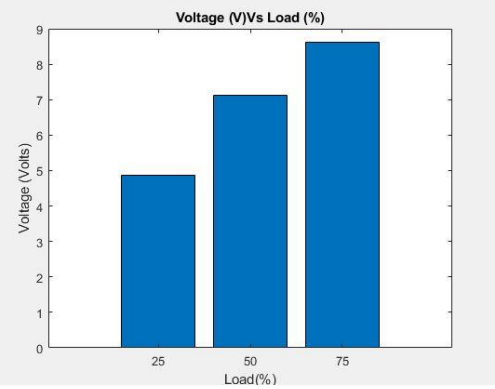

Figure 4 (b) : Voltage Vs Load(%)

Figure 4(a) shows the peak voltage and Fig.4(b) shows maximum power output for the setup. A maximum power output of 18.83 W was obtained at the load of 75%. For the same load, the peak voltage was 8.63 V. As the temperature of the exhaust increases, the net power increases due to the increase in available heat.

REFERENCES

[1] Birol F., 2016, Energy and Air Pollution - World Energy Outlook 2016 Special Report. Paris, France.Author,
[2] Hale LE., 1913. Thermo-electric battery for motor-vehicles. US1134452A,
[3] Bass JC, Elsner NB, Leavitt FA. Performance of the 1 kW thermoelectric generator for diesel engines. AIP Conf. Proc., vol. 316, AIP; 1994, p. 295–8. doi:10.1063/1.46818.

Proceedings of the Third International Conference on Sustainable Energy and Environmental Challenges(3 rd SEEC)
18 –21 December, 2018, IIT Roorkee, India

SEEC No.081

PERFORMANCE ANALYSIS OF TUBULAR AIR PREHEATER USING TAPE INSERTS

Tushar Adgale[a] **Anshul Sharma**[b] **Niraj K Mishra**[c*]
Mechanical Engineering Department[a,b,c]
National Institute of Technology, Uttarakhand, Srinagar Garhwal[a,b,c]
tusharadgale@gmail.com[a] anshul@nituk.ac.in[b] nkm@nituk.ac.in[c]

ABSTRACT

Twisted tape inserts are proven submissive medium for heat transfer intensification. Twisted tape transforms the bulk flow to swirl flow by increasing close wall velocity and reducing the boundary layer enhancing heat transfer. The fluid condition can be transformed from laminar flow to turbulent flow with use of tape insert. Heat exchanger compactness can be achieved by tape inserts, which decrease the exhaust flue gas temperature by increasing their residence time. Ecological health and energy preservation can be achieved through heat transfer augmentation improving heat exchanger performance. Tape inserts are cost effective, have less maintenance, and make heat exchangers compact.

1. INTRODUCTION

With decrease in twist ratio, Nusslet number, friction factor and efficiency enhancement increases [1]. Study mentions that as twist ratio, space ratio increases heat transfer coefficient increases. Increase in space ratio improves friction factor. Nusselt number increases with Reynolds number. Friction factor is higher for tube with tape inserts than for plain tube. Heat transfer rate is higher for smaller space ratio. Pressure loss is decreased by regularly spaced twisted tapes [2]. Twisted tapes with tight twist perform better for short lengths instead of full length. Increase in heat transfer parameters leads to pressure drop. Friction factor reduces for smaller lengths tapes instead of full-length tapes. With increase in Reynolds number, reduction in friction factor and nusselt number increases. Short length tapes reduce Nusslet number marginally as reduction in friction factor takes place by full-length tapes. Twisted tape with uniform pitch performs better than tapes with varying pitch [3]. Full-length tapes provide better heat transfer efficiency compared to short length ones. Increase in Reynolds number leads to increase in Nusslet number [4]. Study describes Serrated twisted tapes with serration width and depth ratio. Nusselt number has direction relation with depth ration and indirect ratio with width ratio. Increase in heat transfer rate is about 72.2% more with serrated twisted tape that to plain tube [5]. Peripheral cut twisted tape perform better in terms of heat transfer and friction factor in comparison to twisted tapes and plain tubes for laminar flow due to turbulence near tube wall. Heat transfer enhancement, Nusslet number, and friction factor increases with increase in depth ratio and decrease in width ratio [6].

With decrease in helical pitch ratio and twist ratio thermal performance decreases while heat transfer rate and friction factor increases [7]. With decrease in twist ratio and clearance ratio Nusselt number and Reynolds number increases [8]. Study refers to effect of taper angle and twist ratio. With decrease in twist ratio and taper angle there was increase in heat transfer enhancement and friction ratio. While thermal performance factor was directly proportional to taper angle and inversely proportional to twist ratio [9]. Study has been made regarding single, double, triple and quadruple number of twisted tapes with co and counter current arrangements. Results show that for greater number of tapes and counter current arrangement Nusselt number and friction factor are better [10]. Nusselt number for corrugated tube that equipped with twisted tapes increases with increasing Reynolds number. Occurrence of high speed takes place due to reduced passage area that leads to swirl flow. Performance of VTT is better than TT [11]. Multiple twisted tapes have better performance in comparison to single twisted tape. Increase in tape number and decrease in twist ratio leads to increase in Nusselt number, friction factor i.e thermal and hydraulic performance [12]. Therefore in the present study the effect of twisted tape inserts in the air preheater (APH) has been investigated numerically.

2. METHODOLOGY

Commercially accessible simulation software Fluent ANSYS 18.0 is used for CFD analysis. Table 1 presents data of APH used for providing combustion air to boiler. The shell-side air flow is

*Corresponding author

489 m^3/hr, flow of tube-side flue gases is 916 m^3/hr, tube span is 1250 mm with 2.3 mm thick. Inlet temperatures of air and flue gas temperature are 26.85^{0}C and 240^{0}C respectively. APH with tube OD 50.8 mm has; 19 number of tubes, 65 mm tube pitch, 14 mm clearance, 312.5 mm baffle spacing, 3 number of baffles and shell diameter of 356 mm.

Table 1. AIR PREHEATER DIMENSIONAL DATA

Air flow rate (m^3/hr)	489
Flue gas flow rate (m^3/hr)	916
Length of tube (l) (mm)	1250
Tube thickness (t) (mm)	2.3
OD of tube (d_0)(mm)	50.8
Number of tubes (N_t)	19
Tube pitch (p_t)(mm)	65
Clearance (c_t) (mm)	14
Baffle spacing (B_s) (mm)	312.5
Number of baffles (N_b)	3
Shell ID (D_s) (mm)	356

The discussed APH 3D model was created using ANSYS Design Modeler. Figures 1 and 2 show three-dimensional model of tube with twisted tape insert APH in ANSYS design modeler. Discretization of the virtual model was done in ANSYS meshing module. Figure 3 shows meshing of 3D model of twisted tape insert tube APH in ANSYS meshing. Table 2 lists discretization data of APH. Proximity and curvature with fine settings were used for meshing. APH with plain tube of OD 50.8 mm is discretized into 362016 numbers of nodes and 1695199 numbers of elements. APH with twisted tape insert tube of OD 50.8 mm is discretized into 361806 numbers of nodes and 1694374 numbers of elements.

Table 2.DISCRETIZATION PARAMETERS

APH (Tubes)	Plain Tube	Twisted Tape Insert Tube
Tube OD (mm)	50.8	50.8
No. of Nodes	362016	361806
No. of Elements	1695199	1694374

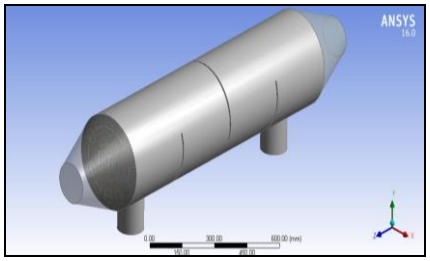

Figure 1. THREE DIMENSIONAL MODEL OF AIR PREHEATER IN ANSYS DESIGN MODELER

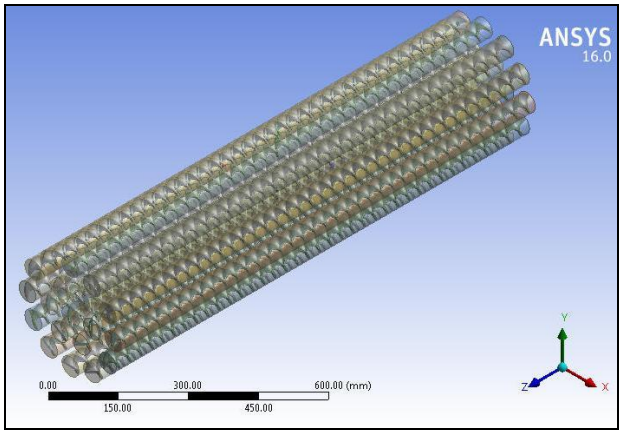

Figure 2. THREE DIMENSIONAL MODEL OF AIR PREHEATER IN ANSYS DESIGN MODELER

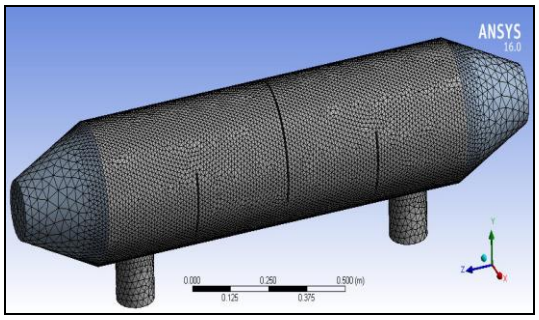

Figure 3. MESHED THREE DIMENSIONAL MODEL OF TUBE WITH TWISTED TAPE INSERT AIR PREHEATER IN ANSYS MESHING

The considered twisted tape insert has rectangular cross section with 45mm width and 3 mm thickness with p/d ratio 1.5 and covering full length of tube.

For simulation analysis Fluent Ansys 18.0 was engaged. Steady state was selected for current study. K-ε, realizable, scalable wall functions turbulence model was used. In cell zone condition, shell was assigned as air fluid zone and tubes as fuel volatiles fluid zone. Mentioned boundary conditions were allotted for air and hot flue gas inlet, hot air and flue gas outlet, tube and shell walls. Mesh interfaces were assigned coupled wall interface. SIMPLEC scheme was deployed for pressure velocity coupling solution method. Second order upwind scheme was assigned for spatial discretization. Hybrid method was used for initialization.

*Corresponding author

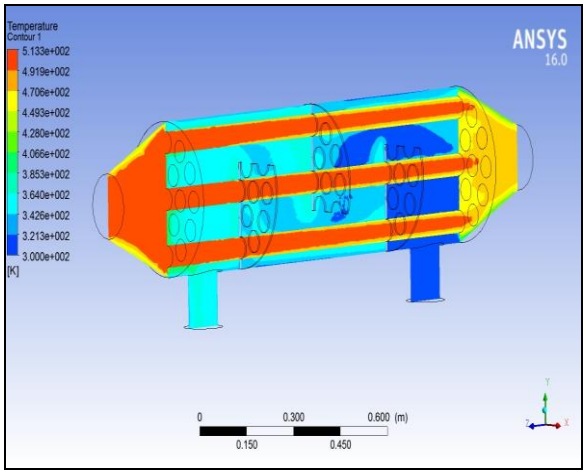

Figure 4. APH AIR OUTLET TEMPERATURE CORRESPONDING TO PLAIN TUBE WITH OD 60.3 MM

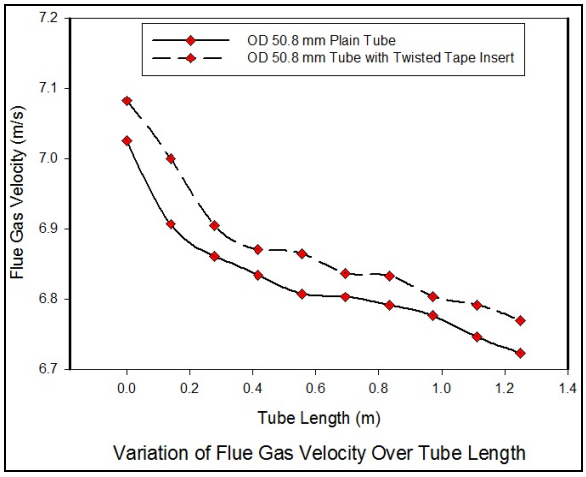

Figure 5. VARIATION OF FLUE GAS VELOCITY OVER TUBE LENGTH

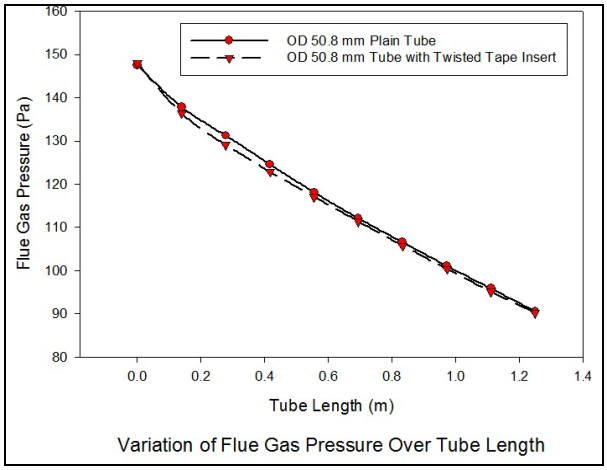

Figure 6. VARIATION OF FLUE GAS PRESSURE OVER TUBE LENGTH

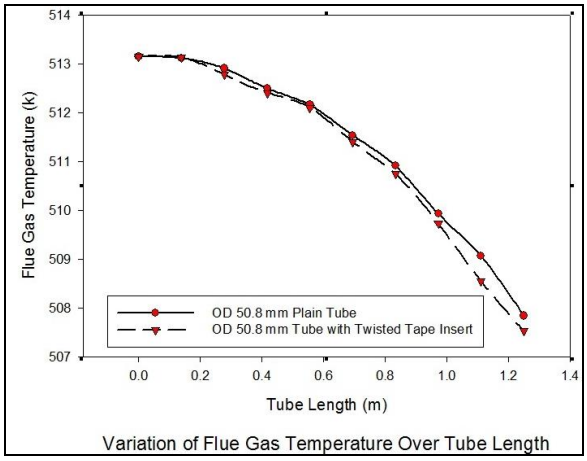

Figure 7. VARIATION OF FLUE GAS TEMPERATURE OVER TUBE LENGTH

3. RESULTS AND DISCUSSION

Figure 5 represents variation of flue gas velocity over tube length. For APH with plain tube of OD 50.8 mm velocity varies around 6.72-7.02 m/s. For APH with twisted tape insert with tube of OD 50.8 mm velocity varies around 6.77-7.08 m/s. While the flue gases enter from inlet duct to the gas compartment the tube plate serves as a barrier in its path and reduces the flow velocity. The flue gases enter the tube forming exit path and hence flow through the tube interior. The velocity of flue gases converges to steady velocity by decreasing from peak velocity and after that remains steady till exit, as the flue gases are sucked by the induced draft fan to extract the gases out of air pre heater. The flue gas velocity is higher in tube with twisted tape insert of OD 50.8 mm than plain tube of OD 50.8 mm.

Figure 6 represents variation of flue gas temperature over tube length. For APH with plain tube of OD 50.8 mm temperature varies from 513.15 to 507.84 K. For APH with twisted tape insert with tube of OD 50.8 mm temperature varies from 513.15 to 507.52 K. In plain tubes the flue gases enter in turbulent pattern and over the length change to laminar flow forming boundary layer, reducing heat transfer. In case of tubes with twisted tape inserts, the flue gases enter the tube and remain in turbulent pattern throughout the length, eliminating formation of boundary layer which increases inertia forces resulting in increased heat transfer. Evidently, the temperature of air will rise and temperature of flue gases will reduce, hence the heat exchange will be better in tubes with twisted tape inserts to that in plain tubes.

Figure 7 represents variation of flue gas pressure over tube length. For APH with plain tube of OD 50.8 mm pressure drop is around 56.94 Pa. For APH with twisted tape insert with tube of OD 50.8 mm pressure drop is around 57.78 Pa.

*Corresponding author

Pressure twisted tape inserts with tube of OD 50.8 mm is higher than in plain tube of OD 50.8 mm, due to decreased flow area, as pressure drop is inversely proportional to open pipe diameter. Similarly, due to presence of twisted tape and increase of friction factor, pressure drop in tube with twisted tape insert is more than in plain tube.

4. CONCLUSIONS

The APH air outlet temperature increases approximately by 5°C (around 1.4%) with the use of tubes of OD 50.8 mm with twisted tape inserts to that in plain tubes. The tube-side pressure drop increases roughly around 1.5 % with the use of tubes of OD 50.8 mm with twisted tape inserts to that in plain tubes. The APH flue gas outlet temperature drops about by around 0.06 % of tubes of OD 50.8 mm with twisted tape inserts to that in plain tubes. The tube side flue gas velocity is approximately higher by 0.1 m/s (around 0.7%) with the use of tubes of OD 50.8 mm with twisted tape inserts to that in plain tubes. In accumulation, use of twisted tape inserts instead of plain tubes boosts heat transfer process. The twisted tape inserts offers subsidiary supplementary heating surface and its geometrical feature creates swirl-turbulence flow that enhances heat transfer process. Further, detail analysis of significant thermal parameters with realistic testing needs to be studied for development of tubular air pre heaters.

REFERENCES

[1] Watcharin Noothong, Smith Eiamsa-ard, Pongjet Promvonge, "Effect of Twisted-tape Inserts on Heat Transfer in a Tube", The 2nd Joint International Conference on Sustainable Energy and Environment (SEE 2006) 21-23 November 2006, Bangkok, Thailand.

[2] Smith Eiamsa-ard , Chinaruk Thianpong , Pongjet Promvonge, "Experimental investigation of heat transfer and flow friction in a circular tube fitted with regularly spaced twisted tape elements", International Communications in Heat and Mass Transfer 33 (2006) 1225–1233.

[3] S. K. Saha, A. Dutta, "Thermohydraulic Study of Laminar Swirl Flow Through a Circular Tube Fitted With Twisted Tapes", Journal of Heat Transfer 123 (2001), 417-427.

[4] Smith Eiamsa-ard, Chinaruk Thianpong, Petpices Eiamsa-ard, Pongjet Promvonge, "Convective heat transfer in a circular tube with short-length twisted tape insert", International Communications in Heat and Mass Transfer 36 (2009) 365–371.

[5] Smith Eiamsa-ard, Pongjet Promvonge," Thermal characteristics in round tube fitted with serrated twisted tape", Applied Thermal Engineering 30 (2010) 1673-1682.

[6] Smith Eiamsa-ard, Panida Seemawute, Khwanchit Wongcharee," Influences of peripherally-cut twisted tape insert on heat transfer and thermal performance characteristics in laminar and turbulent tube flows", Experimental Thermal and Fluid Science 34 (2010) 711–719.

[7] S. Eiamsa-arda, K. Yongsirib, K. Nanana, C. Thianpongb, "Heat transfer augmentation by helically twisted tapes as swirl and turbulence promoters", Chemical Engineering and Processing 60 (2012) 42– 48.

[8] Halit Bas, Veysel Ozceyhan", Heat transfer enhancement in a tube with twisted tape inserts placed separately from the tube wall", Experimental Thermal and Fluid Science 41 (2012) 51–58.

[9] N. Piriyarungrod, S. Eiamsa-ard, C. Thianpong, M. Pimsarn and K. Nanan", Heat transfer enhancement by tapered twisted tape inserts", Chemical Engineering and Processing (2015).

[10] Suriya Chokphoemphun, Monsak Pimsarn, Chinaruk Thianpong, Pongjet Promvonge, "Thermal performance of tubular heat exchanger with multiple twisted-tape inserts" Chinese Journal of Chemical Engineering 23 (2014) 755-762.

[11] H. G. Langeroudi, K. Javaherdeh, "Investigation friction factor and heat transfer characteristics of turbulent flow inside the corrugated tube inserted with typical and V-cut twisted tapes" Heat and Mass Transfer 53 (2018) 1999-2008.

[12] N. Piriyarungrod, Manoj Kumar, C. Thianpong, M. Pimsarn, V. Chuwattabakul, S. Eiamsa-ard, "Intensification of thermo-hydraulic performance in heat exchanger tube inserted with multiple twisted-tapes" Applied Thermal Engineering (2018).

*Corresponding author

SEEC No. 082

FLUORIDE REMOVAL PERFORMANCE OF A NOVAL ADSORBENT

Yogendra Singh Solanki[1] , Madhu Agarwal[1], Sanjeev Gupta[2], Pushkar Shukla[2], A.B Gupta[3]
[1]Department of Chemical Engineering, Malaviya National Institute of Technology, Jaipur, India 302017
[2] Grasim Industries Limited (Aditya Birla Group), Bharuch, Gujrat India
[3]Department of Civil Engineering, Malaviya National Institute of Technology, Jaipur, India 302017

ABSTRACT

Fluoride contamination of water is a major problem in India. World Health Organization(WHO 2004) recommends an upper limit of 1.5 mg/L fluoride in drinking water. Present study reveals performance evaluation studies of Al-Fe-Ac based adsorbent in the fluoride removal from drinking water. The prepared adsorbents were characterized by X-ray diffraction (XRD), scanning electron microscopy (SEM).The material retained amorphous structure and maintained relatively stable fluoride adsorption performance at calcination temperatures lower than 300 ºC. The optimum pH range for fluoride adsorption was 6.0–7.0 and the adsorbent also showed high defluoridation ability around pH 5.5–7.5, which is preferable for actual application. A high fluoride adsorption capacity of 12 mg/g was acquired under an equilibrium fluoride concentration of 50 mg/L, adsorbent dose of 1g/L and pH 7.0. Synthetic sample having Fluoride concentration 2 to 10 mg/L were treated at optimized dosage and residual fluoride was reduced to 0.1 to 1.4 ppm with different adsorbent dose. Residual aluminium in treated water was well within WHO norms for drinking water.

Keywords*:Al-Fe-Ac,de-fluoridation, Adsorbtion, fluoride*

NOMENCLATURE

AL : Alumina

FE :Iron

AC : Activated carbon

INTRODUCTION

Fluoride is classified as of the severely harmful contaminant of water tor human consumption by World Health Organization (WHO) [1].

In India various states namely Assam, Andhra Pradesh, Bihar, Delhi, etc. to have high fluoride concentration in water. The presence of high fluoride content in drinking water makes bones and teeth brittle, harder and dense due to deposition of fluoride as calcium-fluorapatite. It also set the maximum fluoride concentration in drinking water should not exceed 1.0 mg/l.

Fluoride is required in small amount (1.0-3.0 mg/day) on daily basis for prevention of dental problems but taken in large amount can cause dental fluorosis, skeletal fluorosis (Fluorosis is a common symptom of high fluoride ingestion manifested by mottling of teeth in mild cases and embrittlement of bones and neurological damage in severe cases [2], osteoporosis, arthritis, brittle bones, cancer, infertility, brain damage, Alzheimer syndrome, and thyroid disorder, etc. Fluoride can be harmful or beneficial depending upon the amount taken [3]. Human intake of fluoride is mainly from groundwater. Various minerals like fluorite, biotites, and rocks like granite, basalt, etc. are the primary source of fluoride [4]. Industries of glass, ceramic

production produces waste containing high fluoride concentration into discharge into water.

Fluoride concentration (mg/L)	Effects
<1.0	Safe limit
1.0–3.0	Dental fluorosis (discoloration, mottling and pitting of teeth)
3.0–4.0	Stiffened and brittle bones and joints
4.0–6.0 and above	Deformities in knee and hip bones and finally paralysis making the person unable to walk or stand in straight posture, crippling fluorosis.

Table 2.1: Effects of fluoride in water on human health [5]

2. MATERIALS AND METHODS

2.1 PREPARATION OF STOCK SOLUTION

All chemical reagents used in the experiments were purchased from Sigma–Aldrich, mainly including Aluminium chloride ($AlCl_3$), ferric chloride ($FeCl_3$), Activated carbon, Ammonium Hydroxide(NH_4OH), and sodium fluoride (NaF). Those chemical reagents were all of analytical grade and directly used without further purification. Mili-Q water was used throughout the synthesis and treatment processes. Standard stock solution (100 mg/L) of fluoride was prepared by dissolving 0.221 g NaF into 1 L Mili-Q water at room temperature. The solutions for different experiments were prepared by appropriate dilution of the stock solution.

2.2 SYNTHESIS OF ADSORBENT

The composite material in this paper was synthesized by traditional co-precipitation method. In a typical synthesis process, 0.6M $FeCl_3$ and 0.6M $AlCl_3$ were mix to prepare solution A. 100 gm of activated carbon and 3M (NH_4OH) was considered as Solution B and C. Solution C was drop wise added into mixer of solution A and B to maintain pH b/w 6.5-7.0 During process under constant stirring condition at 200 rpm. In order to obtain uniform mixture, the mixed solution was stirred for 30 min after the addition. After filter, the precipitates were washed sequentially with mili Q water and ethanol until chlorine in washed water <0.02% , and dried in oven @ 110°C for overnight. Furthermore, the obtained materials were calcined at different temperatures (from 100 to 500 ºC) for 3 h, respectively. The materials were allowed to cool to room temperature and then used for subsequent adsorption experiments.

2.3 CHARACTERIZATION OF ADSORBENT

The crystalline structure of the adsorbent was characterized using an X-ray diffraction analyzier (XRD) (Pananalytical model-xpert pro) equipped with Cu Ka radiation at a scanning speed of 5º_/min from 5 to 90º. The XRD data were matched with standard JCPDS data. The pH of the systems was adjusted from 4.0 to 10.0 with 0.05 M H_2SO_4 or 0.05 M NaOH. Equilibration of samples was performed by shaking at 25 C for 24 h, and the final pH was measured with a pH meter (Model HI5522,HANNA). The morphologies of adsorbents were determined by Nova Nano 450 scanning electron microscopy (SEM) operating at 15 kV.

2.4 BATCH ADSORPTION STUDIES

The batch adsorption experiments were performed to determine the efficiency of adsorbent and the optimum operating conditions required for effective removal of fluoride from the drinking water. The adsorption experiments were carried out by taking 100 ml of F-solution with varying initial concentration (3 mg/L to 12mg/L). Then varying amount of adsorbent was added in each conical flask and was kept in a water shaker bath (120 rpm) for 1 to 5 hours. Supernatant was separated by filtration using watt men filter paper and analysed for remaining F-content by using thermo orien fluoride ion meter. The amount of fluoride adsorbed by adsorbent at equilibrium q_e (mg/g of adsorbent) was then estimated by Eq. 1

$$q_e = \frac{C_o - C_e}{m} V \qquad (1)$$

Where, C_o and C_e are the initial and final equilibrium concentrations (mg/L) of flouride, respectively, V is the volume of the adsorbate solution (L) and m is the mass of adsorbent added (g). Adsorption experiments were executed at different pH (3 to 11), dosage (1 – 5 g/l), and contact time (1 to 5 hours). Initial pH of the solution was adjusted to desired value with the help of NaOH and H_2SO_4 solution. The percentage removal (% R) of fluoride by adsorbent was calculated by Eq. 2

$$\% R = \frac{C_o - C_e}{C_o} \times 1 \qquad (2)$$

Where C_o and C_e have the same meaning as explained earlier.

3. RESULTS AND DISCUSSION

3.1 X-RAY DIFFRACTION ANALYZIER (XRD)

The crystalline structure of the adsorbent was characterized using an X-ray diffraction analyzier (XRD) (Brucker D-8 Diffractometer, Germany) equipped with CuKa radiation at a scanning speed of 2º per min from 5º to 90º, operated at 40 kV and 40 mA. The XRD data were matched with standard JCPDS data. The XRD pattern of Fe-Al-Ca hydroxides is given in Fig. 1, the amorphous nature of the materials was confirmed by X-ray diffraction patterns.

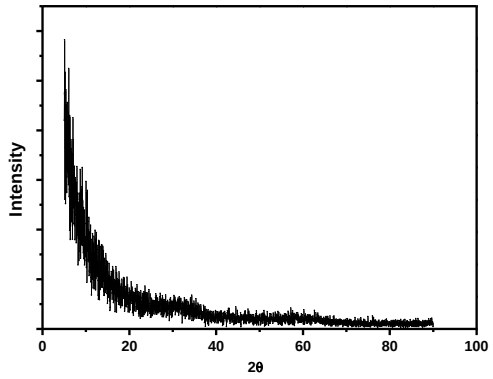

Fig 2 XRD image of the synthesized Fe-Al-Ac Adsorbent

3.2 SCANNING ELECTRON MICROSCOPY (SEM)

The morphologies of adsorbents were determined by Hitachi S-4800 scanning electron microscopy (SEM) operating at 15 kV. The surface morphology of adsorbents are shown in fig.2. The adsorbent shows characteristics of flaky morphology and relatively homogeneous structure

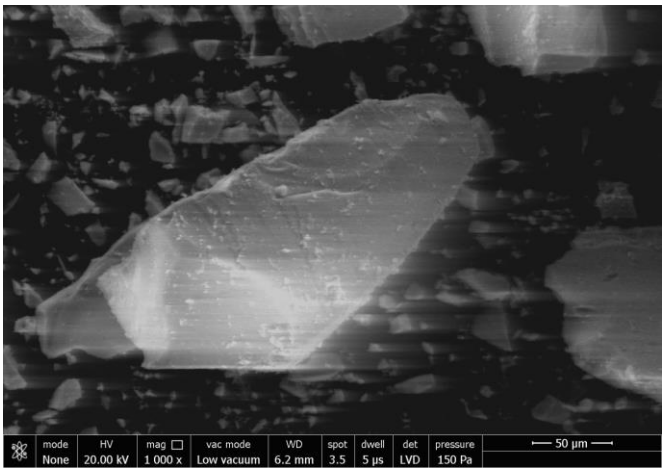

Fig 2 SEM image of the synthesized Fe-Al-Ac Adsorbent

3.3BATCH STUDY

3.3.1 EFFECT OF ADSORBENT DOSE

The effect of adsorbent dose was studied by varying the adsorbent quantity from 1gm to 10 gm maintaining the initial flouride concentration to 7 mg/L, contact time of 2 hour, pH at 7 and temperature 27 ± 2 ºC. The removal of fluoride increases with increasing the adsorbent dose due to increased number of adsorption sites [42]. The trend shown in Figure 4.5 depicts that fluoride removal from 68.4.2% to 97.4% occurs as adsorbent dose increased from 1g/L to 10 g/L. To bring fluoride concentration under permissible limit, 5 g/L of adsorbent dose has been set as optimum dose.

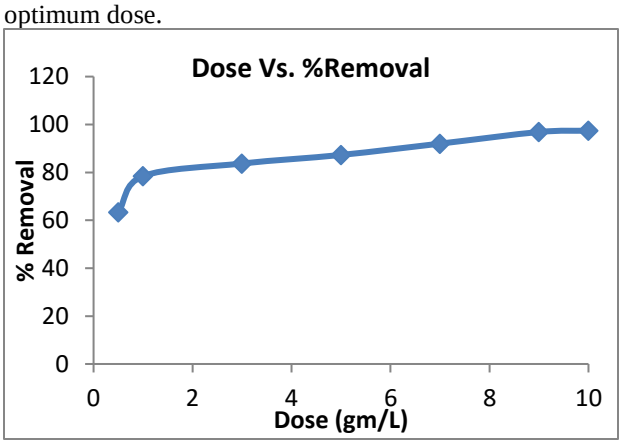

Fig 3 reveal Dose vs.% Removal

3.3.2EFFECT OF INITIAL CONCENTRATION

Batch experiments were performed to study the effect of different initial fluoride concentrations (2, 4, 6, 8 and 10 mg/L) keeping adsorbent dose constant at 5 g/L, pH 7, agitation speed at 180 rpm and contact time to 2 hour. The result as shown in figure 4.6 depicts that the removal of fluoride follows decreasing trend with increasing initial concentration.

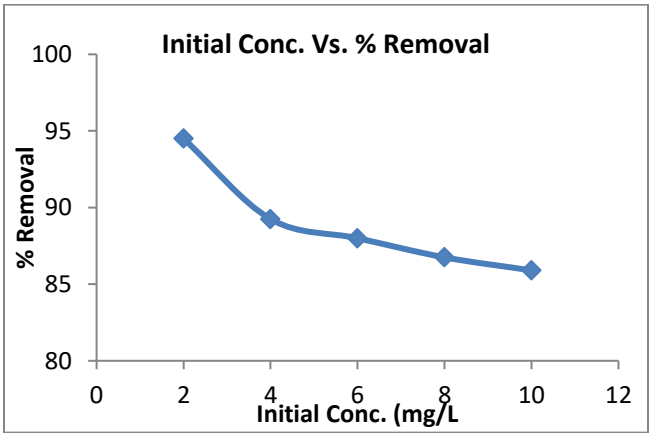

Fig 4 reveal Initial conc. vs.% Removal

3.3.3EFFECT OF CONTACT TIME

All the batch experiments were performed at room temperature with initial fluoride concentration of 7 mg/L using adsorbent dose 5 g/L at pH 7 with agitation speed of 180 rpm in water bath shaker. Figure 4.7 shows the effect of varying contact time from 30 minutes to 180 minutes on fluoride removal. It was observed that in initial 30 minutes percent removal of fluoride increases from (70.2 % to 87.56%) thereafter it becomes constant as all the adsorption sites were occupied and no further adsorption

was possible. Thus 60 minutes was considered as optimum time for maximum arsenic removal at 5 g/L of adsorbent dose.

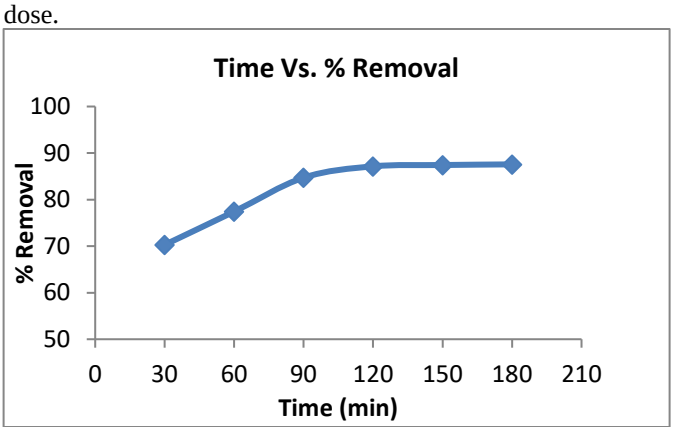

Fig 5 reveal Time vs.% Removal

3.3.4EFFECT OF pH

Figure 6 shows the effect of initial pH on the removal of flouride. The initial pH of reaction mixture plays significant role in adsorption of pollutants as it effect the surface functional group / surface charge of adsorbent as well as solution phase chemistry of pollutant. Removal of fluoride was studied in 3-11 pH range to study the removal behavior in both acidic and basic nature. It was observed that maximum fluoride removal around 92.18% was obtained at neutral pH.

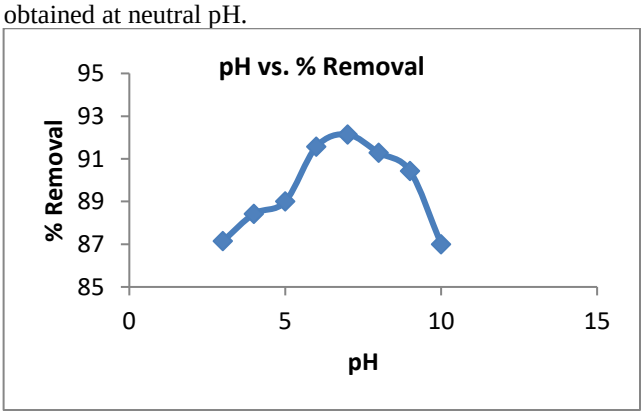

CONCLUSION

In this study, an Fe–Al–Ac amorphous structure was successfully developed for fluoride adsorption. The optimum pH range for fluoride removal was 6.0–7.0 and the adsorbent was also effective at pH 5.5–7.5. A high adsorption capacity of 12 mg /g was acquired at pH 7.0, which was highly competitive compared to other reported adsorbents.In all experiments, residual aluminium was found to be within WHO prescribed limits thus making it a safer de-fluoridating agent.

ACKNOWLEDGMENTS

The authors are thankful to Grasim Industries Limited (Aditya Birla Group), Bharuch, Gujrat and Department of Chemical Engineering, MNIT Jaipur for his kind suport.

REFERENCES

[1] World health organization (WHO), Guidelines for drinking-water quality, guidel drink qual, Third ed., Inc. First Second Addenda, vol. 1, World health organization, Geneva, 1997. (Recomm.) http://www.who.int/water_sanitation_health/dwq/gdwqvol32ed.pdf.

[2] K. Babaeivelni, A.P. Khodadoust, Adsorption of fluoride onto crystalline titanium dioxide: effect of pH, ionic strength, and co-existing ions, J. Coll. Interf. Sci. 394 (2013) 419–427.

[3] A.D. Atasoy, M.O. Sahin, Adsorption of fluoride on the raw and modified cement clay, Clean Soil Air Water 42 (2014) 415–420

[4] WHO, 1985. Guidelines for Drinking Water Quality, vol. 3. World Health Organization, Geneva, pp. 1–2.

[5] Nawlakhe, W.G. and Bulusu, K.R. "Nalgonda technique – a process for removal of fluoride from drinking water." Water Quality Bull. 14 (1989): 218-220.

[6] Nawlakhe, W.G., Kulkarni, D.N., Pathak, B.N., and Bulusu, K.R. "Defluoridation of Water by Nalgonda Technique." Indian Journal of Environmental Health 17, no. 1 (1975): 26.

[7]. S. Chidambaram, A. L. Ramnathan and S. Vasudevan, Fluoride Removal Studies in Water Using Natural Materials, Water SA, 29(3), 339-343 (2003).

[8] Bhattacharjee S, Zhao Y, Hill JM, Percy ME, Lukiw WJ. Aluminum and its potential contribution to Alzheimer's disease (AD). Frontiers in Aging Neuroscience. (6) 62-67 (2014)

SEEC No.083

INDRAYANI WATER TREATMENT BY USING PHOTOCATALYTIC DEGRADATION METHOD

Dipali Sharma, Hitesh Goyal, Neha Singh, Mamta sardare
Chemical Engineering
MITAOE, Alandi Pune, 412105
Email: Dipalisharma1997@gmail.com

ABSTRACT

Water is essence of life, due to industrialization and civilization human devasted the nature. We focused on water sample of river Indrayani. Number of industries are attached with this river and dump their waste water directly in this river. For making water portable we have gone through number of analysis for pH, TDS, Hardness, BOD, COD, heavy metal ions like Zn, total chromium, Iron, Flouride, Coliform and E-Coli.Bismuth oxyiodide is a new upcoming photo catalyst which exhibit excellent photo catalytic performance due to its 3D hierarchical tetragonal structure and less band gap (~1.8 Ev). This catalyst contributes in greatest absorption of visible light due to its less band gap. In this paper, BiOI has been prepared by using ultra sonication method. This paper explores the use of BiOIcatalyst for Indrayani water treatment and includes synthesis and characterization of catalyst as prepared.

Keywords: ***Industrialization, Civilization, Portable, Indrayani, Analysis, ultrasonification, characterization***

.
.

INTRODUCTION

Indrayani a name of Holy River flowing at a place aland in city pune. he **Indrayani** river originates from Kurvande village near Lonavla, a hill station in the Sahyadri mountains of Maharashtra. It flows from east and there to confluence with the Bhima river, through the Hindu pilgrimage centers of Dehu and Alandi. It is revered as a holy river and is associated with such great religious figures such as SantTukaram and Dnyaneshwar. Form the point of origination it covers a distance of 150 km to Alandi. In the way of this river number if industries are dumping their waste water in this river. From this river 152 villages are also connected which takes its water for irrigation purpose. And in rainy season, many organic and inorganic fertilizers, chemicals mixed with water and came in this river, so due to human activities, Lithosphere and hydrosphere both are totally exhausted. Despite of these it becomes lifeline of poor. Villagers take its water directly for drinking purpose, for washing their clothes, automobiles and more. And due to these 70 % people affected by unifactorial hereditary diseases. Maharashtra is fourth one state in which maximum deaths were observed due to water born diseases. Peopled affected by various diseases like gall bladder stone, kidney stones, jaundice, blue baby syndrome, and many more.

Water being essential to life it is much needed to be purified. Due to industrialization and civilization human devasted it. Indrayaniriver is one of those polluted river.

Water samples of Indrayani river was analysed which resulted many of organic and inorganic pollutants. Photocatalytic degradation of water pollutants over semiconductor photocatalyst have attracted much of attention for its potential to decrease environmental pollution. Family of Bismuth oxyhalides is being promising photocatalyst among whichBiOI exhibits best performance under visible light region due to its smallest band gap (~1.8eV) which goes off the limits of other semiconductor catalyst in practical application. BiOI exhibits unique 3D hierarchical tetragonal structure and narrow band gaps which favors better separation of electron hole in the visible light driven photocatalysis.

MATERIALS

CHEMICALS: Bi(NO3)3.5H2O (Bismuth Nitrate)

KI (Potassium Iodide)

NaOH flakes (Sodium Hydroxide)

DYE: Methyl Orange

GLASSWARES AND EQUIPMENTS: Beakers, Funnel, Graduated cylinders, Flask, Crucible, Crucible tong, Watch Glass, Wash bottle, Ring Clamp, Weighing machine, Ultrasonication bath, Oil bath, Oven

LIGHT SOURCE: UV Radiation

METHOD

- Bismuth Oxy-Iodide was prepared using sonication method
- Bismuth Nitrate and Potassium Iodide were kept on ultrasonication for 5 hours.
- When the solution obtains brick red color it is kept for drying.
- Drying was carried out to get crystalline structure in oven for 3 hours to obtain BiOI powder.
- Photocatalysis of Methyl Orange was carried out then using BiOI powder as a catalyst under UV light.

RESULTS

Water analysis report of Indrayaniriver before treatment

Sr. No.	Parameter	Results	Units	
		Chemical Parameter		
1	Sulphate (as SO_4^{-2})	28.0	mg/lit	A
2	Nitrate (as NO_3)	BDL	mg/lit	A
3	BOD(Biochemical Oxygen Demand) (3 day test at 27°C)	10.0	mg/lit	IS
4	COD(Chemical Oxygen Demand)	33.82	mg/lit	IS
5	Hexa Chromium (as Cr^{6+})	250.0	mg/lit	A
		Microbiological Parameter		
1	Total Coliform	1600	MPN/100ml	IS
2	*Escherichia coli*	170	MPN/100ml	IS
		Elemental Parameter		
1	Calcium as Ca	39.11	mg/lit	IS
2	Cadmium as Cd	BDL	mg/lit	IS
3	Iron as Fe	0.02	mg/lit	IS
4	Lead as Pb	0.001	mg/lit	IS
5	Copper as Cu	BDL	mg/lit	IS
6	Manganese as Mn	0.02	mg/lit	IS
7	Magnesium as Mg	9.84	mg/lit	IS
8	Nickel as Ni	0.002	mg/lit	IS
9	Zinc as Zn	0.005	mg/lit	IS
10	Total Chromium as Cr	270.36	mg/lit	IS

BDL: Blow Detectable Limit

Note: For *E.coli* and Coliform <2 can be considered as Absent

The morphology of BiOI has been revealed by SEM images. The as prepared sample have 3D hierarchical structure which is beneficial for the separation of electron hole pair and so its beneficial for photocatalytic activity. The results shown in the below shows the pure sample of

BiOI which appears to be irregular smooth sheet with size 1µm.

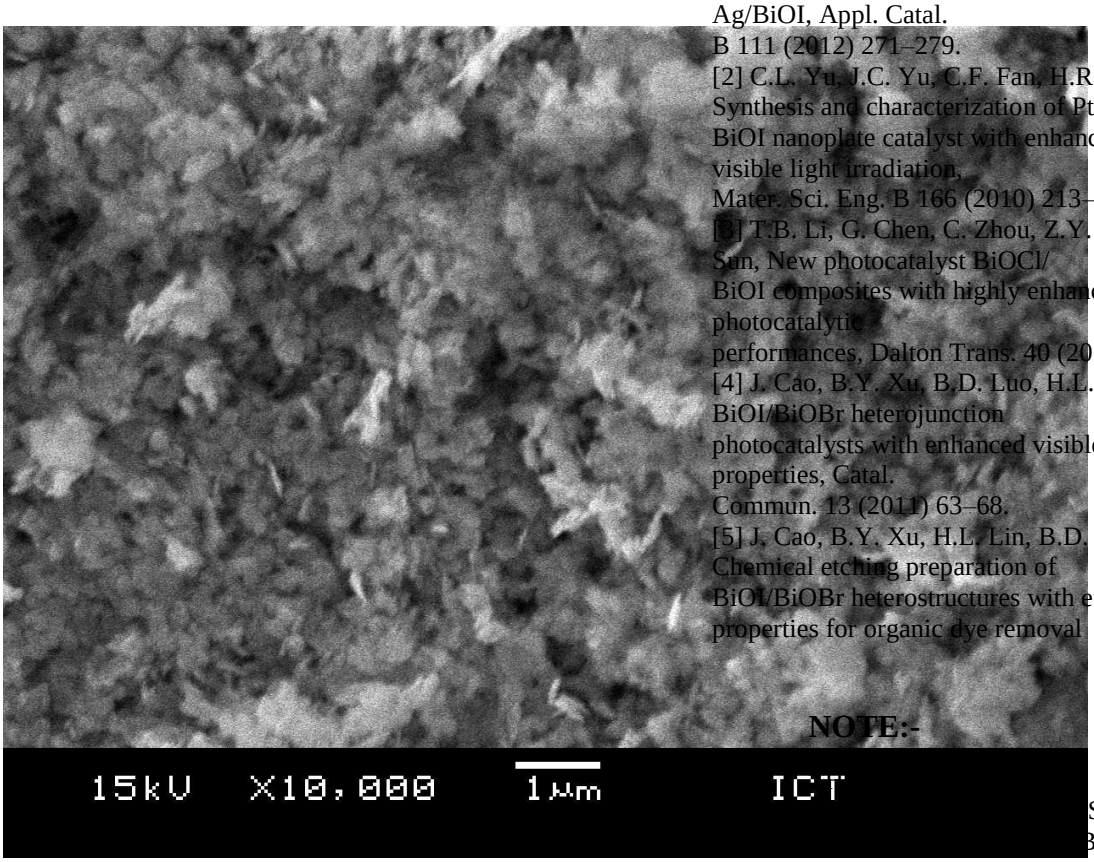

1

CONCLUSION

BiOI absorbs most of the light because of its lowest band gap. In conclusion, BiOI catalyst was synthesized by sonication, precipitation and filtration. As in the SEM image the synthesized BiOIphotocatalyst appears smooth. The as prepared BiOI sample exhibits excellent performance in the performance in degradation of MO under UV radiation. The 3D hierarchical structure has been successfully synthesized. The mechanism of BiOIphotocatalyst has been attributed to effective separation of photogenerated carriers.

REFERENCES

[1]H. Liu, W.R. Cao, Y. Su, Y. Wang, X.H. Wang, Synthesis, characterization and photocatalytic performance of novel visible-light-induced Ag/BiOI, Appl. Catal. B 111 (2012) 271–279.

[2] C.L. Yu, J.C. Yu, C.F. Fan, H.R. Wen, S.J. Hu, Synthesis and characterization of Pt/BiOI nanoplate catalyst with enhanced activity under visible light irradiation, Mater. Sci. Eng. B 166 (2010) 213–219.

[3] T.B. Li, G. Chen, C. Zhou, Z.Y. Shen, R.C. Jin, J.X. Sun, New photocatalyst BiOCl/BiOI composites with highly enhanced visible light photocatalytic performances, Dalton Trans. 40 (2011) 6751–6758.

[4] J. Cao, B.Y. Xu, B.D. Luo, H.L. Lin, S.F. Chen, Novel BiOI/BiOBr heterojunction photocatalysts with enhanced visible light photocatalytic properties, Catal. Commun. 13 (2011) 63–68.

[5] J. Cao, B.Y. Xu, H.L. Lin, B.D. Luo, S.F. Chen, Chemical etching preparation of BiOI/BiOBr heterostructures with enhanced photocatalytic properties for organic dye removal

NOTE:-

PROCEDURE AND SATION LIKE FTIR, BE COMPLETED AND SO THE FINAL RESULTS AFTER PHOTOCATALYSIS WILL BE DISPLAYED IN THE FINAL PAPER

Proceedings of International Conference on Sustainable Energy and Environmental Challenges(3rd SEEC), 18 –21 December, 2018, IIT Roorkee, India

SEEC No.084

COMPARISON OF THE ORIGINAL AND THE MODIFIED v^2f MODEL FOR IMPINGING ROUND JET COOLING FROM A CYLINDER

Ketan A. Ganatra
Department of Mechanical Engineering,
National Institute of Technology, Manipur
ketanganatra0@gmail.com

Dushyant Singh
Department of Mechanical Engineering,
National Institute of Technology, Manipur
dushyant@nitmanipur.ac.in

ABSTRACT

A numerical analysis for the impinging round jet cooling has been carried out. The numerical analysis has been carried out by using two different turbulence models, the original and the modified v^2f. The flow has been assumed as three dimensional, steady and turbulence. The numerical results are obtained for the non-dimensional mean streamwise velocity distribution along the radial direction and the local Nusselt number in the axial direction of the cylinder. For the validation of the fluid flow and the heat transfer characteristics for the impinging round jet, the numerical results are compared with the experimental results of [4-5]. From the comparison of the experimental and the numerical results, the modified v^2f model is found better as compared to the original v^2f model.

Keywords < *Round jet, v^2f turbulence model, cylinder, fluid flow, heat transfer* >

NOMENCLATURE

h	–	Distance between the nozzle exit and the cylinder (m)
Red	–	Reynolds number based on the nozzle diameter,
Nux	–	Axial Nusselt number, |
U	–	Magnitude of the local velocity of the air (m/s)
Y′	–	Radial coordinate ($Y' = \sqrt{X^2 + Y^2} - R$)
$Y'_{0.5}$	–	Radial coordinate for the occurrence of $U = U_{max}/2$
Umax	–	Magnitude of the maximum mean streamwise velocity (m/s)
T_W	–	Cylinder wall temperature (K)
T_{jet}	–	Jet temperature or nozzle exit temperature (K)
k_f	–	Thermal conductivity of the air (W/mK)
y^+	–	Non-dimensional wall distance
X	–	Cartesian co-ordinate in x direction (m)
Y	–	Cartesian co-ordinate in y direction (m)
Z	–	Cartesian co-ordinate in z direction (m)
q″	–	Heat flux (W/m^2)

GREEK

μ	–	Dynamic viscosity of the air (kg/ms)
ρ	–	Density of the air (kg/m^3)
ν	–	Kinematic viscosity of the air (m^2/s)

SUFFIX

j	–	Jet
w	–	Wall

INTRODUCTION

Impinging jets are widely used due to widespread application with much simplicity in the construction. The applications of the impinging jet are cooling of the work pieces in the foundry, cooling of turbine blades and thermal control of electronic equipment. The impinging jet has been a subject of interest due to immediate and selective cooling of the heated surface. The availability of the literature for impinging jet over a curved surface is very less as compared to that over a flat plate [1 – 3]. Kim et al. [4] has carried out an experimental study using the Particle Image Velocimetry (PIV) technique to measure the mean streamwise velocity along the radial direction of the cylinder. They have concluded that with the increase in the value of the Reynolds number, the flow separation is delayed. Tawfek [5] has carried out an experimental study to study the heat transfer characteristics of a round jet impingement from a cylinder. The cylinder is maintained at a constant temperature condition.

The present study focuses mainly on the fluid flow and the heat transfer characteristics for a round jet impinging over a cylinder. The numerical simulation is carried out by the original and the modified v^2f turbulence models. Hence, the present study deals on identifying a better turbulence model from the two models.

PROBLEM STATEMENT

Figure. 1 shows the computational domain used for the present study. The different parameters considered are non-dimensional distance from the cylinder to the jet exit (h/d) and Reynolds number based on the nozzle diameter (Re_d).

The Reynolds number (Re_d) based on the nozzle diameter is defined as,

$$\mathrm{Re}_d = \frac{\rho V d}{\mu}$$

The Nusselt number (Nu) based on the cylinder diameter is defined as,

$$Nu = \frac{q''}{(T_W - T_{Jet})}\frac{D}{k_f}$$

NUMERICAL METHOD

The flow is assumed steady, incompressible and turbulent. The Reynolds time averaged Navier - Stokes equations are used for the numerical simulation. The continuity, momentum and energy equations are as follows,

$$\frac{\partial u_i}{\partial x_i} = 0$$

$$\rho u_j \frac{\partial u_i}{\partial x_j} = -\frac{\partial P}{\partial x_i} + \frac{\partial}{\partial x_j}\left[\mu\left(\frac{\partial u_i}{\partial x_j} + \frac{\partial u_j}{\partial x_i}\right) - \rho\overline{u_i' u_j'}\right]$$

$$\rho u_j \frac{\partial T}{\partial x_j} = \frac{\partial}{\partial x_j}\left[\frac{\mu}{\mathrm{Pr}}\frac{\partial T}{\partial x_j} - \rho\overline{T' u_j'}\right]$$

The numerical simulation is carried out with the open source CFD solver OpenFOAM. SIMPLE algorithm is usedfor the pressure and velocity coupling. The convective and turbulence terms are discretised using Gauss upwind method. The convergence is assumed to be reached when the residuals for all the convective and turbulence terms are less than 10^{-6}.

GRID SENSITIVITY ANALYSIS

A grid sensitivity analysis is carried out with the three different grid sizes having 8 x 10^5, 13 x 10^5 and 20 x 10^5 cells. The sensitivity analysis is carried out by the modified v^2f turbulence model for h/d = 7.5 and Red = 38,800. The grid is generated in such a way that the y^+ value near the walls remains below unity. It is clear from the Fig. 2 that the grid size does not have much effect on the axial distribution of the Nusselt number and hence the grid having the least number of cells are selected for the further analysis.

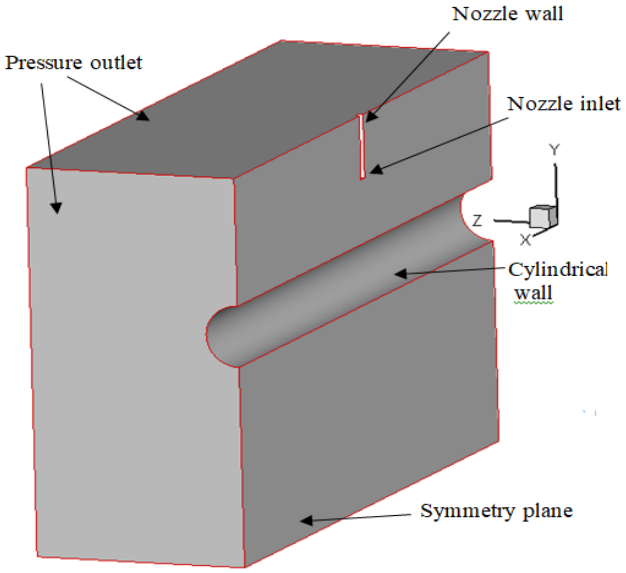

Figure.1 Computational domain used for the present study

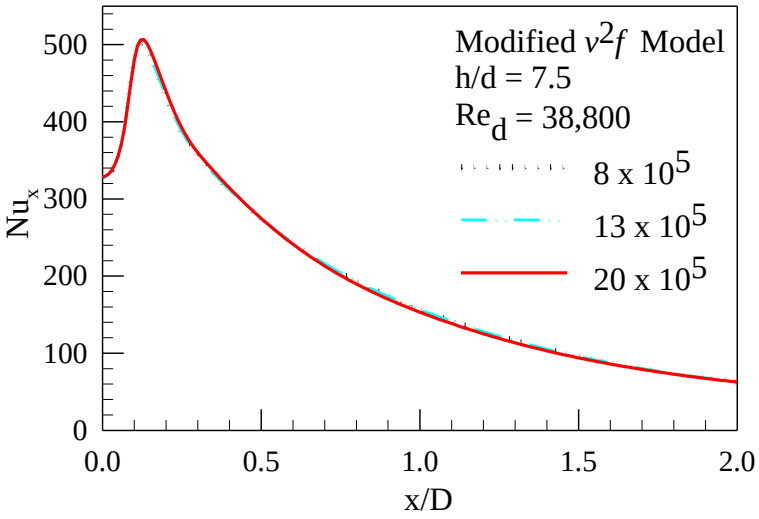

Figure.2 Grid sensitivity analysis with different number of cells

RESULTS AND DISCUSSIONS

Fig. 3 (a) to (c) show the non-dimensional mean streamwise velocity distribution along the radial direction for h/d = 4 and Re_d = 11,800 at various cylindrical angles. As shown in Fig. 2 (a), the experimental non-dimensional mean streamwise velocity is approximately equal to one at the wall. The same value is predicted by the original and the modified v^2f model and also the similar trend of variation of the non-dimensional

mean streamwise velocity is observed by both the v^2f model.

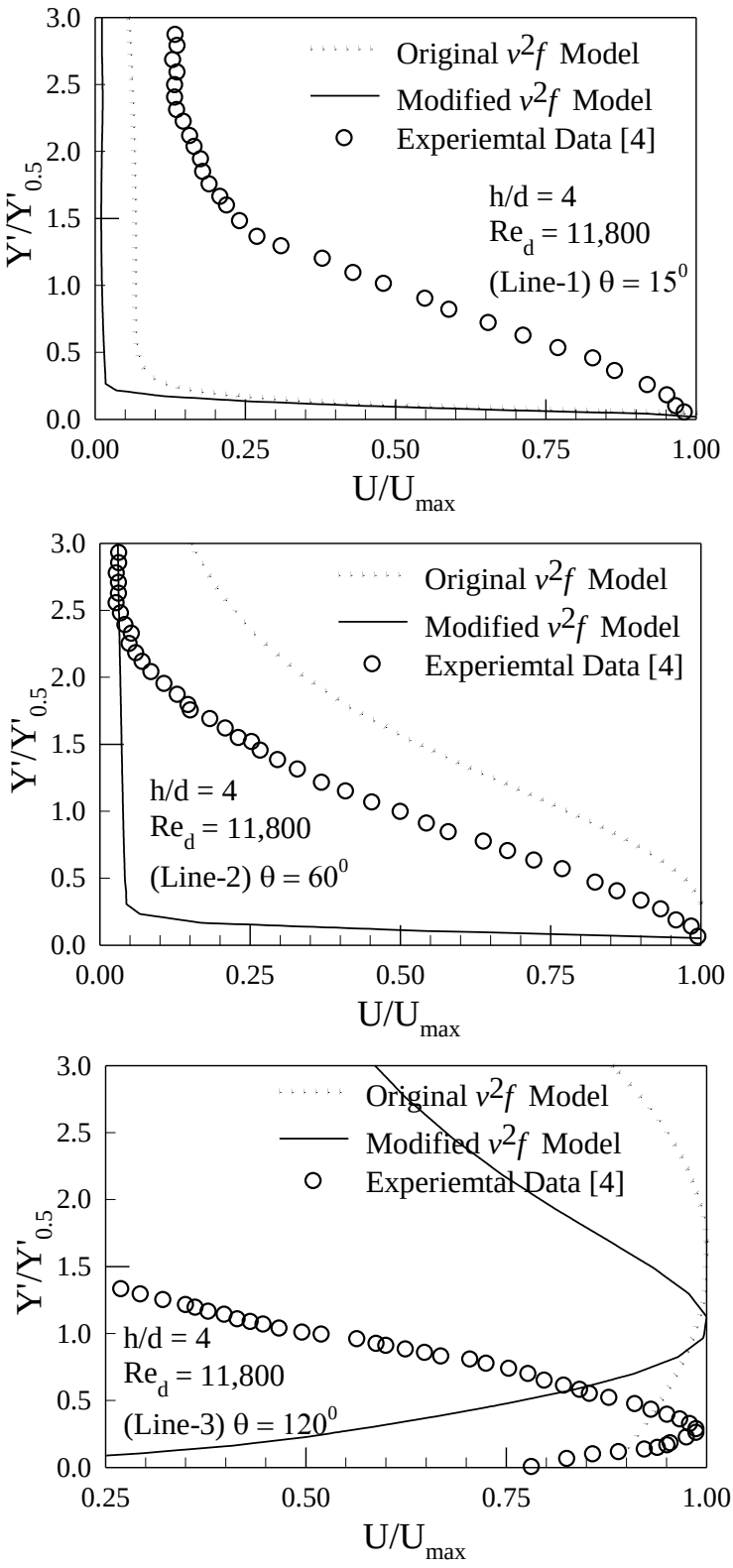

Figure.3 Comparison of the numerical and experimental mean stream wise velocity

Fig. 4 (a) and (b) show the comparison of the experimental and the numerical local Nusselt number in the axial direction of the cylinder for h/d = 7.5 and 15 and Re_d = 38,800. The cylinder is maintained at a constant temperature of 308 K and the temperature of the jet exit to be 300 K. The original v^2f turbulence model over predicts the value of the Nusselt number at the stagnation point while the modified v^2f turbulence model predicts almost the same value as that of experimental value for both the values of h/d = 7.5 and 15. In the wall jet region, the original v^2f turbulence model has two peak at h/d = 7.5 and a single peak at h/d = 15 while the modified v^2f turbulence model has only a single peak for both the values of h/d = 7.5 and 15.

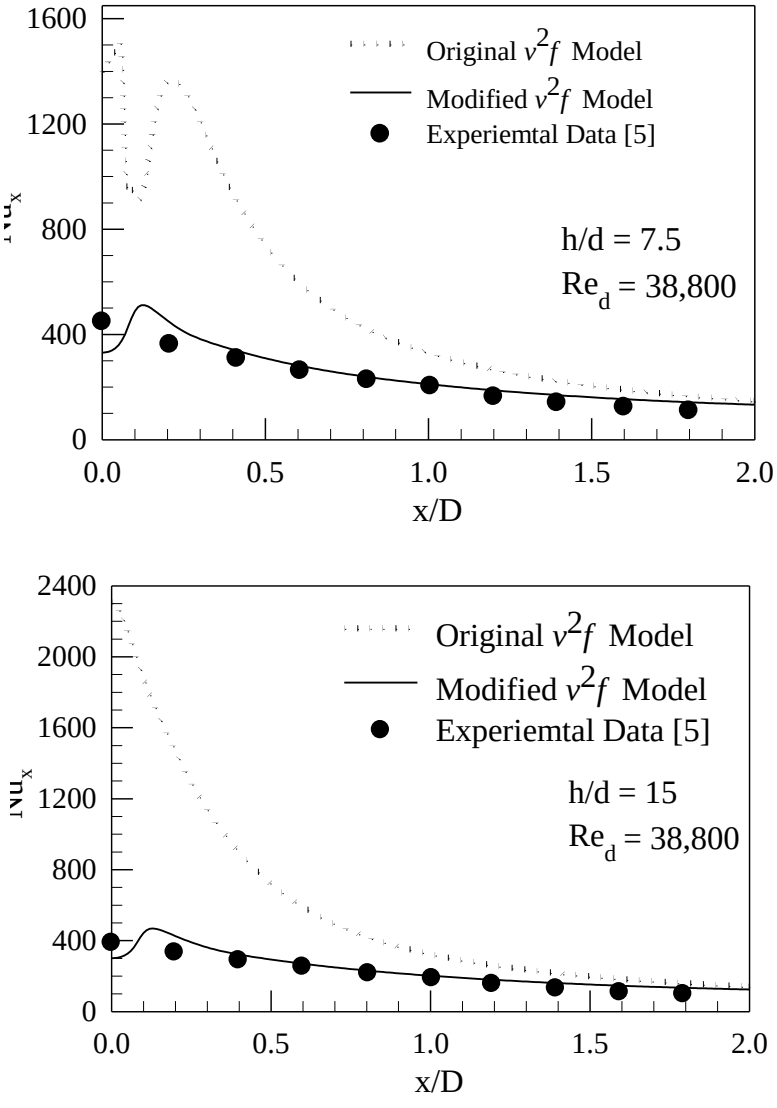

Figure.4 Comparison of the numerical and experimental axial Nusselt number

CONCLUSION

The following conclusions are drawn from the numerical analysis,

1. For predicting the non-dimensional mean streamwise velocity along the radial direction, the modified v^2f model works better as compared to the original v^2f model.
2. The modified v^2f turbulence model predicts the better Nusselt number distribution for both the values of the spacing between the nozzle exit and the cylinder, h/d = 7.5 and 15.

REFERENCES

[1] H. Martain, Heat and mass transfer between impinging gas jet and solid surfaces, Advances in Heat Transfer 13 (1977) 1-60.

[2] R. Viskanta, Heat transfer to impinging isothermal gas and flame jets, Experimental Thermal and Fluid Science, 6 (1993) 111-134.

[3] K. Jambunathan, E. Lai, M.A. Moss, B.L. Button, A review of heat transfer data for single circular jet impingement, International Journal of Heat and Fluid Flow, 13 (1992) 106-115.

[4] M. Kim, H. D. Kim, E. Yeom, and K. C. Kim, Flow characteristics of three-dimensional curved wall jets on a cylinder, Journal of Fluids Engineering, 140(4) (2017), 041201-041207.

[5] A. A. Tawfek, Heat transfer due to a round jet impinging normal to a circular cylinder, International Journal of Heat and Mass Transfer, 35 (1999) 327-333.

[6] D. Singh, B. Premachandran, and S. Kohli, Experimental and numerical investignation of jet impingement cooling of a circular cylinder, International Journal of Heat and Mass Transfer, 60 (2013) 672–688.

[7] D. Singh, B. Premachandran, and S. Kohli, Numerical simulation of the jet impingement cooling of a circular cylinder, Numerical Heat Transfer, Part A, 64 (2013) 1-33.

[8] E. Esirgemez, J. W Newby, C. Nott, S. M. O. V. Otugen, Experimental study of a round jet impinging on a convex cylinder, Measurement in Science and Technology, 18 (2007) 1800-1810.

[9] P. A. Durbin, Separated flow computations with the k- ε – v^2 model, AIAA Journal, 33 (1995) 659-664.

[10] F. S. Lien and G. Kalitzin, Computations of transonic flow the v^2f turbulence model, International Journal of Heat and Fluid Flow, 22 (2001) 53-61.

[11] L. Davidson, P. Nielsen and A. Sveningsson, Modifications of the v2f model for computing the flow in a 3D wall jet, Proceedings of the international symposium on turbulence Heat and Mass Transfer, Antalya, Turkey, (2003) 577-584.

[12] N. N. Mansour, J. Kim, P. Moin, Reynolds-stress and dissipation-rate budgets in a turbulent channel flow, Journal of Fluid Mechanics, 15 (1988) 15 - 44.

[13] OpenFOAM source code user Guide, https://www.openfoam.com/documentation/, 2017.

Proceedings of the Third International Conference on Sustainable Energy and Environmental Challenges (3rd SEEC)
18 –21 December, 2018, IIT Roorkee, India

SEEC No.085

INTERMEDIATE PYROLYSIS:CHEMICAL CHARACERIZATION OF COCONUT SHELL BIO-OIL

Kiran Kumar Dasari
Department of Mechanical Engineering
National Institute of Technology Karnataka
Surathkal
Email: kk2kiran@gmail.com

Veershetty G
Department of Mechanical Engineering
National Institute of Technology Karnataka
Surathkal
Email address: veersg@yahoo.co.in

ABSTRACT

In this work experiments on Intermediate pyrolysis of coconut shells were conducted at temperature 550^oC and 575^oC , three major end products are solid (Bio-char), Liquid (Bio-oil/Tar) and pyro gases. The bio-oil resulted from intermediate pyrolysis at 550^0C and 575^0C was analysed for chemical composition using FT-IR and GC-MS. FT-IR was performed to determine the various functional groups present in the bio-oil. FT-IR spectra showed the presence of alcohols, alkanes and alkenes. The results found consistent when compared with the results of GC-MS. To determine the chemical compounds present in the bio-oil GC-MS was performed. By increasing the temperature, the yield of the liquid increased up to 575^oC at which highest liquid yield of 45.1% is obtained.

***Keywords:* Intermediate pyrolysis, coconutshell, Bio-oil.**

FT-IR (Fourier transform infrared spectroscopy)
GC-MS (Gas chromatography and mass spectroscopy)

INTRODUCTION

With the depletion of the fossil fuels around the world, effective way to solve the energy crisis is finding suitable source of alternative energy. Biomass is a source of all living organic matter with natural grown. Biomass is essential to all human beings. For thousands of years humankind around the world is using biomass a source of energy [1]. In 20th century fossil fuels has made life easy but the nullifying side is the environment is seriously affected. Recent technologies can now convert biomass materials like woody substrates and agricultural residues (sugarcane bagasse, rice husk, straw, cotton stalk, coffee wastes, saw dust, groundnut shells, coconut shells etc.,) into hydrocarbons and value-added chemicals within few hours. Among them thermochemical conversion is one of them [2]. In one year individual kind consumes the equivalent of twelve billion tons of oil. In one year the solar energy received by the earth is equivalent to ninety thousand billion tons of oil and the energy stored in the biomass growth amounts to seventy two billion tons. All the energy needs of public in a year could be made by collecting an hour of sunlight or 1/6th of the biomass production.

Experiments with the coconut shells in a pilot scale fixed bed reactor were conducted at temepratures 550^{o}C and 575^{o}C . In order to determine the functional groups present FT-IR was performed. To determine the chemical compounds present in the bio-oil, GC-MS was done for bio-oil at 550^{o}C and 575^{o}C.

Spectroscopy analysis of coconut shell bio-oil

Fourier Transform infrared spectroscopy:

The FTIR spectrum of coconut shell liquid product obtained at 550^{o}C and 575^{o}C on wet basis is presented in figure 1 and 2 and the corresponding wavelength is summarized in table 1 and 2 Various bonds of C=O, O-H, C=C, and C-O with strong, and medium intensity peaks were annoted

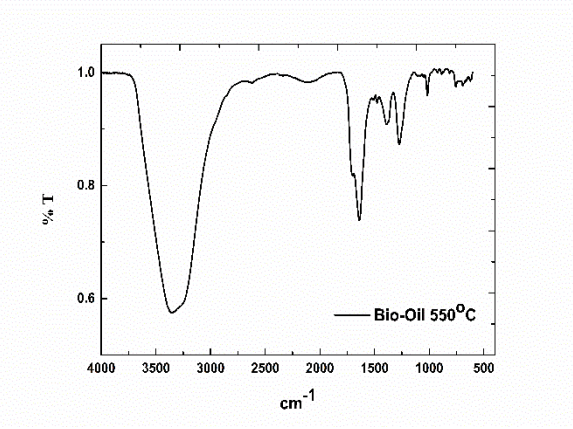

FIGURE 1. FT-IR OF BIO-OIL AT 550^{O}C

Functional group	Wave number (cm^{-1})	Type of vibration
Alcohol/phenol	3353.54	H-bonded O-H stretch (broad strong band)
Ketone or carboxylic acid	1698.59	C=O stretch (strong)
Alkene	1638.53	C=C stretch (medium)
Alkene	1476.4	C=C stretch (medium)
Alkene	1386.87	C=C stretch (medium)
Alcohol/phenol	1274.25	C-O stretch
Ether	1016.22	C-O stretch
Aromatic	756.5	C-H bend
Aromatic	693.12	C-H bend

TABLE 1. FUNCTIONAL GROUPS OF BIO-OIL AT 550^{O}C

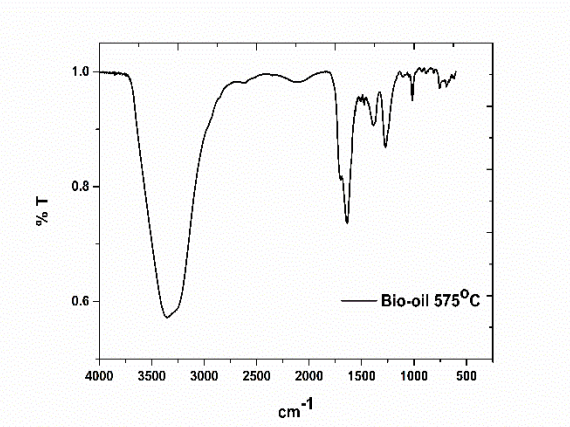

FIGURE 2. FT-IR OF BIO-OIL AT 575^{O}C

Functional group	Wave number (cm-1)	Type of vibration
Alcohol/phenol	3354.07	H-bonded O-H stretch (broad strong band)
Ketone or carboxylic acid	1700.02	C=O stretch (strong)
Alkene	1636.26	C=C stretch (medium)
Alkene	1505.9	C=C stretch (medium)
Alkene	1474.62	C=C stretch (medium)
Aromatic	1387.09	C=C stretch (medium)
Alcohol	1273.08	C-O stretch
Ether	1016.03	C-H bend
Aromatic	756.25, 692.78	C-H bend

TABLE 2. FUNCTIONAL GROUPS OF BIO-OIL AT 575^{O}C

Gas chromatography and mass spectroscopy:

The coconut shell bio-oil at 550^{o}C and 575^{o}C was analysed using GC-MS on wet basis. By matching the corresponding peak from chromatogram the chemical compounds were identified from NIST library. The obtained data prsents 12 and 15 compounds at 550^{o}C and 575^{o}C respectively. The chromatogram is as shown in fig 3 and 4. The compounds are represented in table 3 and 4 with rention time and area%. The coconut shell bio-oil contains ~60% of phenolic compounds, this may be due to the degradation of lignin from coconut shell and moisture impurities present in the bio-oil [3-4].

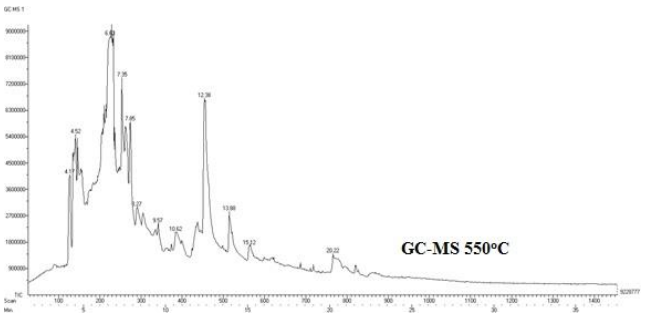

FIGURE 3. GC-MS CHROMOTOGRAM OF BIO-OIL AT 550^{O}C

Peak	Retention time	Area %	Compound Name
1	4.17	6.81	Phenol
2	4.52	10.59	3-Cyclohexen-1-ol, 1-methyl-
3	6.63-6.65	20.13	Phenol, 3-methoxy-
4	7.38	13.14	Methanol, [3-(hydroxymethyl)bicycol[2.2.1]hept-2yl]
5	7.85	10.66	5-Hexen-2-one, 5-Methyl-3-Methylene-
6	8.27	6.88	2,2-Dimethyl-3-vinyl-bicyclo [2.2.1]heptane
7	9.57	5.16	2-Methoxy-6-methylphenol
8	10.62	4.78	8-Decen-2-one, 9-methyl-5-methylene-
9	12.38	10.47	
10	13.88	4.97	2-(2-Methyl-propenyl)-cyclohexanone oxime
11	15.12	3.64	3-Ethoxy-1,4,4a,5,6,7,8,8a-octahydroisoquinoline
12	20.22	2.71	Methyl Z-11-tetradecenoate

TABLE 3. MASS SPECTROSCOPY OF BIO-OIL AT 550^{O}C

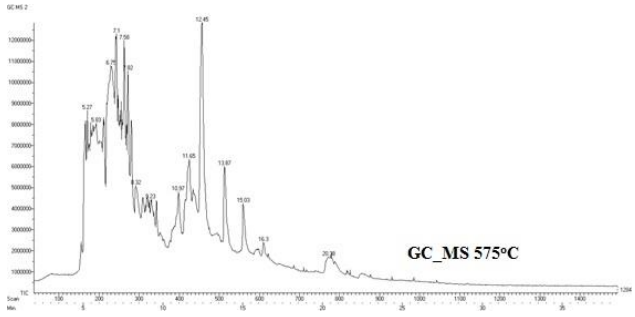

FIGURE 4. GC-MS CHROMOTOGRAM OF BIO-OIL AT 575^{O}C

Peak	Retention time	Area %	Compound Name
1	5.27	8.09	Vinylfuran
2	5.83	8.82	Cis-1,2-Dihydrocatechol
3	6.75	11.64	Phenol, 3-methoxy-
4	7.1	11.31	3-Picoline, 4-amino-, 1-oxide
5	7.58	10.22	5-Hexen-2-one, 5-Methyl-3-Methylene-
6	7.82	9.50	2-Methyl-7-norbornanol
7	8.32	5.50	Phenol, 3-methoxy-
8	9.23	4.77	3-Cyclohexen-1-carboxaldehyde, 3,4-dimethyl-
9	10.97	4.13	2-Isopropylidene-5-methylhex-4-enal
10	11.65	5.99	4-Methoxybenzene-1,2-diol
11	12.45	8.62	2-4-Dimethoxyphenol
12	13.87	4.09	2-(2-Methyl-propenyl)-cyclohexanone oxime
13	15.03	3.12	Morpholine,4-(4-methyl-1-cyclohexen-1-yl)-
14	16.3	2.26	Dimethoxyamphetamine, 2,5
15	20.38	1.87	3,6-Diazzhomoadamantan-9-one Hydrazone

TABLE 4. MASS SPECTROSCOPY OF BIO-OIL AT 575^{O}C

CONCLUSIONS:

Intermediate pyrolysis of coconut shells was carried out at different temperatures. By increasing the temperature, the yield of the liquid increased up to 575^{o}C at which highest liquid yield of 45.1% is obtained. 5. The FTIR analysis showed the presence of alcohols or phenols and other functional groups like aldehydes and ethers. The result is consistent with the findings of GC-MS. Phenol is detected in highest amount and many other phenol derivatives were detected.

ACKNOWLEDGMENTS

We are grateful to M/s Vayu gases, Oils and Carbons, Bangalore, for permitting to carry experiments and providing necessary details of the pilot-plant. We are equally thankful to NITK and IITM for providing necessary research infrastructure.

REFERENCES

[1] McKendry, P., 2002 “Energy production from biomass (part2): Conversion technologies”. Bio Resource Technology, 83(1), May, pp.47-54

[2] Farha, T., Pravakar, M., Snehal,P., 2015 “Intermediate pyrolysis of agro-industrail biomasses in bench-scale pyrolyser: Product yields and its characterization”. Bioresource Technology, 188, pp.258-264

[3] Hasanah, B., 2012 “The chemical composition and physical properties of the light and heavy tar resulted from coconut shell pyrolysis”. J. Pure Appl. Chem. Res. 1 , pp. 26–32.

[4] Sukhbaatar, B., Steele, P., Ingram, L., 2009 “An exploratory study on the removal of acetic and formic acids from bio-oil”. BioResources, 4, pp.1319–1329.

[5] Tanmya, R., Namrata, K., 2016 “Exhaustive study of products obtained from coconut shell pyrolysis”. Journal of Environmental Chemical Engineering. 4(3), pp. 3696-3705

Proceedings of the Third International Conference on Sustainable Energy and Environmental Challenges (3rd SEEC)
18 –21 December, 2018, IIT Roorkee, India

SEEC No. 087

PERFORMANCE ANALYSIS OF CHARGE TRANSPORTING LAYERS IN PEROVSKITE SOLAR CELLS WITH VARYING DEPOSITION TECHNIQUES

Priyanka Kajal
School of Engineering
IIT Mandi
D16008@students.iitmandi.ac.in

Rajeev Ray
School of Basic Sciences
IIT Mandi
D16080@students.iitmandi.ac.in

Satvasheel Powar
School of Engineering
IIT Mandi
satvasheel@iitmandi.ac.in

Suman Kalyan Pal
School of Basic Sciences
IIT Mandi
suman@iitmandi.ac.in

ABSTRACT

Perovskite-based solar cells (PSCs) are the third-generation solar cells with a tremendous increase in power conversion efficiencies within a few years of research. PSCs are organic/inorganic halide based light harvester materials with perovskite crystal structure and a typical chemical composition ABX_3 (where A and B are cations while X are halide anions namely I, Cl and Br e.g. $CH_3NH_3PbI_3$). Though these solar cells have achieved high efficiency but are still striving for long-term stability. The mixed halide perovskites are known to have better stability compared to single halide perovskites. Here, we demonstrate the fabrication of mixed halide-based perovskite solar cells $CH_3NH_3PbI_{3-x}Cl_x$ with and without a charge transporting layer using one and two step solution-based deposition techniques. Various characterization techniques covering optical, structural, compositional were studied. Comparative analyses of different fabricated devices were performed based on efficiency, optical, structural properties. Comparatively better results were obtained from two step and HTL based solar cells because of high crystallinity and fewer defects as compared to a single step.

Keywords
Perovskite, mixed halide, charge transport, crystallinity, stability

NOMENCLATURE

PSC	Perovskite Solar Cell
HTL	Hole Transporting layer
ETL	Electron Transporting layer
HTM	Hole Transporting Material

INTRODUCTION

Perovskite Solar Cells (PSC's) being the 3rd generation thin film-based technology[1]. Perovskite name is given to the material with ABX_3 structure. Perovskites are of great interest in Photovoltaic devices due *Panchromatic light absorption and Ambipolar behavior.*

Perovskite material was discovered in 1839 by a "Gustav Rose" and is named after Russian Mineralogist "Lev Perovski". Application of Perovskites in optical devices and Field effect transistors began in early 1990's while their application in photo energy conversion devices started in 2009 [2], [3].

Miyaska et al. reported about perovskite application as a light absorber on TiO_2 in the structure like DSC. They reported about $MAPbI_3$ and $MAPbBr_3$ based perovskites where they used liquid electrolyte as HTM with the achieved PCE~ 3.8%[4].

Subsequently Park et al. [4] fabricated similar device with PCE~ 6.5% using lower thickness TiO_2 than previous one with liquid electrolyte. It was found that these PSC's exhibits poor operational stability less than hour due to liquid electrolyte usage. Hence there was a great need to replace liquid electrolyte.

Later Kim et al. [4] used $MAPbI_3$ as absorber layer with m-TiO_2 scaffold with spiro-OMeTAD as hole conductor with PCE~ 9.7%. This replacement of liquid electrolyte resulted in better charge extraction by both ETL and HTL with improved stability and efficiency than DSSC's.

With further development in the fabrication methods, material type and architecture development highest achieved efficiency is 22.1% in 2017-18.

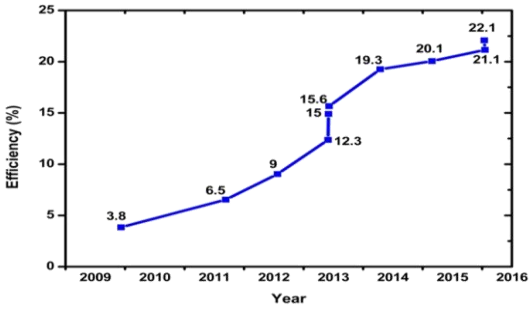

FIGURE 1. Evolution of Perovskite solar cells

EXPERIMENTAL:

Materials:

All chemicals were of analytical grade and used as received. Methyl ammonium iodide (CH_3NH_3I) and 18- NRT TiO_2 paste were purchased from Great cell solar, Australia. Lead (II) chloride ($PbCl_2$), Dimethylformamide (DMF), Ethanol (C_2H_5OH) were obtained from CHD Pvt. Ltd.

Synthesis of $CH_3NH_3PbI_{3-x}Cl_x$:

To prepare the $MAPbI_{3-x}Cl_x$ mixed halide perovskite powder, we reacted a 3:1 molar ratio of purchased MAI (dyesol) $PbCl_2$ powder in 1ml DMF at 60 ºC for 24h by magnetic stirring. Yellow precursor solution of $CH_3NH_3PbI_{3-x}Cl_x$ was obtained.

Characterization:

- **Structural characterization:**

Structural characterization of material was carried out using XRD. During this analysis perovskite material was deposited over the glass containing TiO_2 layer at bottom. The crystallinity of the perovskites incorporated into mesoporous and planar cell architectures was characterized by XRD. The X-ray diffraction analysis is shown in figure 2.

The XRD patterns of perovskite films are shown in Figure 2. The appearances of strong peaks at $2\theta = 14.15°$, 28.5°, 31.87°, 40.54º and 43.23° corresponding to the (1 1 0), (2 2 0), (3 1 0), (2 2 4) and (3 3 0) planes, indicates the formation of the tetragonal perovskite structure, like the previously reported $CH_3NH_3PbI_{3-x}Cl_x$. Along with high intensity peaks some small peaks were obtained at $2\theta = 20.05°$, 24.54°, 35.01°, 50.41°, 52.51° and 58.86° are corresponding to the (1 1 2), (2 0 2), (3 1 2), (4 0 4), PbI_2 and (4 4 0) planes.

The obtained average crystallite size from Debye Scherrer formula is 37.5nm.

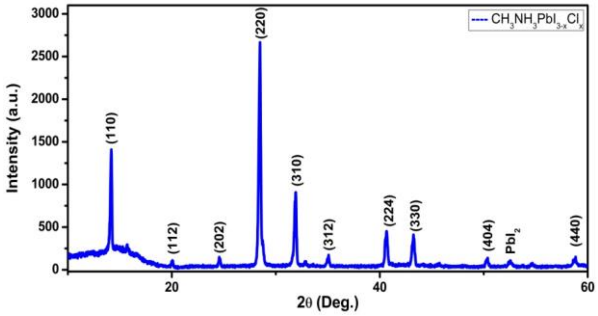

FIGURE 2. XRD pattern of TiO_2/ $MAPbI_{3-x}Cl_x$

Energy-dispersive X-ray Spectroscopy (EDX) coupled with SEM is employed to determine the elemental composition (Figure 3, Table 1). Atomic concentration analysis reveals the content of Cl is very less in obtained perovskite. There are numerous reasons behind that, but fundamental reason is that when we pour MAI and $PbCl_2$ then Pb tries to bond with I rather than Cl and as a result most of the sites are occupied by I and very few sites with Cl. Also, after heating for long Cl get removed from the perovskite structure

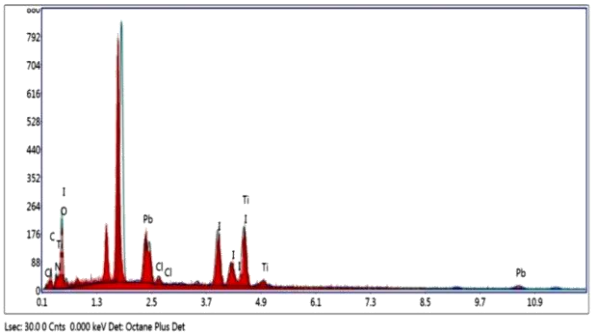

FIGURE 3. EDX pattern of TiO_2/ $MAPbI_{3-x}Cl_x$

TABLE 1: Elemental analysis using EDX

Element	Weight (%)
C	0.59
N	2.36
O	21.79
Pb	18.24
Cl	0.02
I	38.47
Ti	18.53

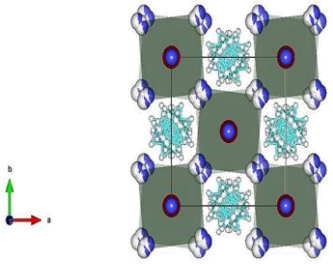

FIGURE 4. Obtained crustal structure of $MAPbI_{3-x}Cl_x$ using VESTA

But the advantage of little Cl doping in $MAPbI_3$ perovskite is improvement in exciton diffusion length and improvement in charge neutrality.

- **Optical Characterization:**

Absorption and photoluminescence spectra of a $CH_3NH_3PbI_{3-x}Cl_x$ perovskite film fabricated at optimum growth condition as shown in figure 5(a, b).

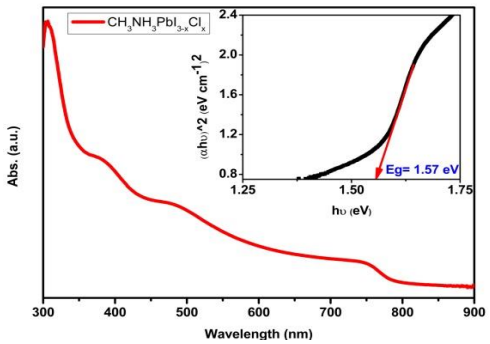

FIGURE 5(a). UV- vis spectroscopy of $CH_3NH_3PbI_{3-x}Cl_x$

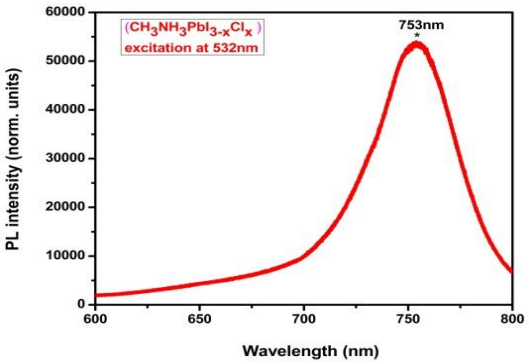

FIGURE 5(b). Photoluminescence spectroscopy of $CH_3NH_3PbI_{3-x}Cl_x$

The perovskite film shows a broad absorption spectrum down to the near-infrared range, whereas its PL band that peaks at ~753 nm reveals an optical gap of ~1.6 eV. The absorption tail at energy below the optical gap is probably due to optical transitions into band tail states (i.e., Urbach edge) caused by traps and defects in the film, of which densities increase in thin perovskite films due to excess grain boundaries. The PL band is caused by electron-hole band-to-band recombination rather than exciton emission because the room-temperature exciton binding energy (~ 12 meV) is smaller than the thermal energy (~ 26 meV). Both spectra clearly show strong absorption and emission in as fabricated thin films. The absorption band edge is positioned at 790 nm (~ 1.569 eV) while the PL peak is positioned at 775 nm (~1.599 eV). The FWHM of PL spectrum is 49.19 nm. There is a 15nm Stokes shift, which corresponds to a 30 meV energy difference between absorbed and emitted photons.

Device Fabrication:

- ***Fabrication:***

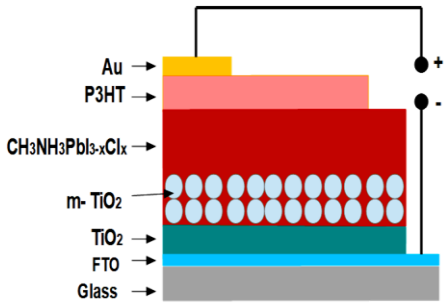

FIGURE 6. Architecture of fabricated PSC

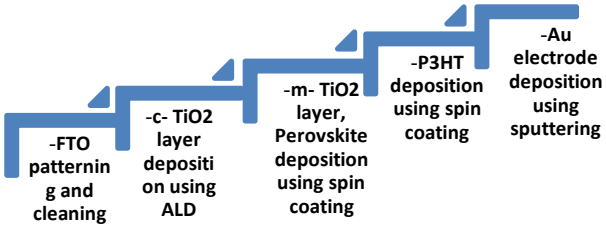

FIGURE 7. Fabrication procedure of PSC

- ***Imaging:***

Cross- sectional imaging of the m-TiO_2/perovskite/ HTM layer was done using SEM. M-TiO_2 and perovskite together results into 710.9nm while P_3HT having thickness of 310.3nm in figure. Also, it is clear from the imaging that obtained films are non- uniform resulting into pin hole formation and increase in resistance which increases losses in PSC and reduces efficiency.

a)

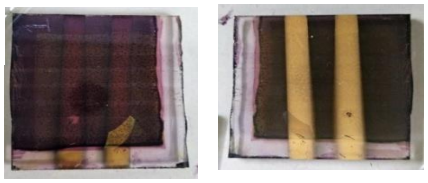

b)

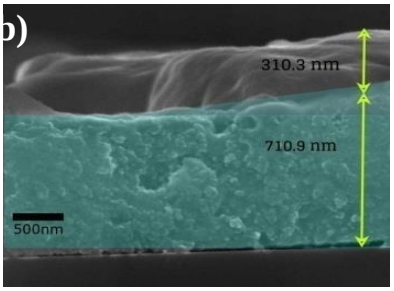

FIGURE 8. a) Front and back Imaging of fabricated PSC; b) Cross-sectional imaging of PSC

Two different types of architectures were fabricated, and a comparative study was carried out between with and without HTL based PSC's. It's been found that in case of without HTL device; there is reduction in V_{oc} which indicates larger recombination losses at the hole-collecting electrode. Incorporating HTLs in perovskite solar cells has been a crucial part towards the achievement of high-performance devices. The main features of an efficient HTL are: a) efficient electron blocking, b) efficient hole extraction. These features can have a major impact to device parameters, e.g. V_{oc} via quasi Fermi level splitting[5].

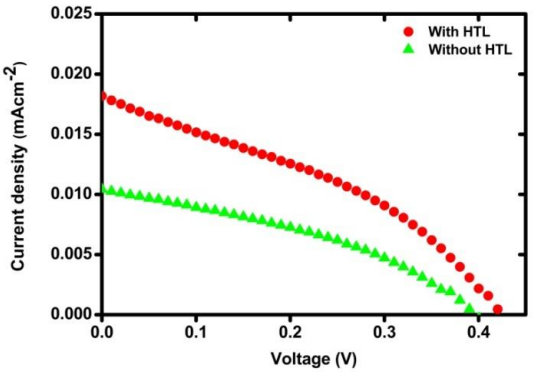

FIGURE 9. JV characteristics of PSC's for HTM and without HTM architectures

TABLE 2: JV characteristics of with and without HTL

	Jsc (mA/ cm^2)	Voc (V)	FF (%)	Efficiency (%)
With HTL	0.018	0.4236	36.5	2.787
Without HTL	0.010	0.39	39.7	1.5

The V_{oc} obtained using non HTL based solar cells is lesser than with HTL based PSC's. It thus results in increase in the recombination in the PSC's leading to reduction in efficiency.

CONCLUSION

Mixed halide perovskite material was synthesized, and crystal structure formation was confirmed by XRD and UV-Vis spectroscopy. Monolithic solar cells with planar PSC architecture were fabricated with and without hole transporting layers. Highest efficiency was achieved with the insertion of hole transporting layer due to better separation of charge carriers and least chances of short circuiting due to increment in the gap between the top and the bottom electrodes.

ACKNOWLEDGEMENTS:

Authors are thankful to IIT Mandi, Advance Material Research Center (AMRC) IIT Mandi, Dr. Viswanath Balakrishnan (Assistant Professor, School of Engineering) IIT Mandi for their valuable support.

REFERENCES:

[1] J. Yan and B. R. Saunders, "Third-generation solar cells: A review and comparison of polymer:fullerene, hybrid polymer and perovskite solar cells," *RSC Adv.*, vol. 4, no. 82, pp. 43286–43314, 2014.

[2] T. Ibn-Mohammed *et al.*, "Perovskite solar cells: An integrated hybrid lifecycle assessment and review in comparison with other photovoltaic technologies," *Renew. Sustain. Energy Rev.*, vol. 80, no. June, pp. 1321–1344, 2017.

[3] D. Zhou, T. Zhou, Y. Tian, X. Zhu, and Y. Tu, "Perovskite-Based Solar Cells: Materials, Methods, and Future Perspectives," *J. Nanomater.*, vol. 2018, 2018.

[4] M. M. Lee, J. Teuscher, T. Miyasaka, T. N. Murakami, and H. J. Snaith, "Efficient {Hybrid} {Solar} {Cells} {Based} on {Meso}-{Superstructured} {Organometal} {Halide} {Perovskites}," *Science (80-.).*, vol. 338, no. 6107, pp. 643–647, 2012.

[5] F. Galatopoulos, A. Savva, I. T. Papadas, and S. A. Choulis, "The effect of hole transporting layer in charge accumulation properties of p-i-n perovskite solar cells," *APL Mater.*, vol. 5, no. 7, p. 076102, 2017.

Proceedings of International Conference on Sustainable Energy and Environmental Challenges (3rd SEEC), December 18-21, 2018, IIT Roorkee, India

SEEC No. 088

Evaluation of Combustion Characteristics of Diethyl Ether–Nitromethane–Diesel Blends in CI Engine

Chandan Kumar[a,b*], K. B. Rana[a], B. Tripathi[a], Ashish Nayyar[b]

[a]Department of Mechanical Engineering, Rajasthan Technical University, Kota–324010, India.

[b]Department of Mechanical Engineering, Swami Keshvanand Institute of Technology, Management & Gramothan, Jaipur–302017, India.

[*]*Corresponding Author Email: chandanpink1988@gmail.com*

Mobile No.:+91–9460481589

Abstract. Continuous consumption of petroleum fuels and atmospheric pollution, have fascinated the development of clean alternative fuels using additives in fuels for better combustion in CI engine. In the current study, diethyl ether and nitromethane were used as oxygenated additives for finding the replacement of diesel with a suitable diesel–diethyl ether–nitromethane blend. For this, experimental investigations were carried out on a VCR diesel engine using diesel–diethyl ether–nitromethane blend in varying concentrations to determine the optimum blending ratio for enhancing performance and reducing exhaust emissions. The considerable performance and exhaust emissions were observed with D–DEE10–NM2.5 (diesel 87.5%, diethyl ether 10%, and nitromethane 2.5%) blend at standard engine parameters. The improvement in engine performance (10.82% increment in BTE) and reduction in emissions (Smoke 29.14%, HC 47.36%) was found using D–DEE10–NM2.5 blend as compared to pure diesel at 100% rated power.

Keywords: *Diesel; Diethyl ether; Nitromethane; Performance; Emission.*

Nomenclature:

BP	Brake power
BTE	Brake thermal efficiency
CAbtdc	Crank angle before top dead centre
CI	Compression ignition
CO	Carbon monoxide
CO_2	Carbon dioxide
CR	Compression ratio
D	Diesel
DEE	Diethyl ether
DME	Dimethyl ether
DI	Direct injection
HC	Hydrocarbons
HSU	Hartridge smoke units
IP	Injection pressure
IT	Injection timing
kg	Kilogram
kJ	Kilojoule
kW	Kilowatt
NE	Nitroethane
NM	Nitromethane
Nm	Newton–meter

NOx	Nitrogen oxides
PM	Particulate matter
ppm	Parts per million
rpm	Revolution per minutes
VCR	Variable compression ratio
v/v	Volume by volume

1. Introduction

Energy plays a significant role in maintaining and improving the economic growth. The diesel engine is continuously dominating in agriculture and transportation sector, due to their beneficial characteristics such as fuel economy, durability, reliability, specific power output[1,2]. However, its use is increasing emissions (i.e., Smoke, CO, CO_2, HC, NOx, PM, etc.) rapidly. For improving the economic growth and controlling pollution, it is essential to improve the combustion characteristics of diesel engine[3–5]. Combustion characteristic may be enhanced by altering the existing engine design parameters such as injection pressure (IP), injection timing (IT), compression ratio (CR), etc. However due to complex design characteristics of the engine, it is quite tricky and expensive[6–8]. Therefore use of blended diesel is a better option to enhance the engine performance and reduce emission simultaneously. Alternative fuel/additives like biodiesel/vegetable oil can be an excellent option to improve the combustion characteristics of the engine, though it may lead to the slight increment in NOx emission[9–11].

A chemical substance which can be added to the diesel in appropriate quantity to improve its combustion properties is known as additive. Many additives (i.e., methanol, ethanol, n–butanol, DEE, DME, NM, NE and n-heptane, etc.) are readily available for blending with diesel and can be used in compression ignition (CI) engines[12–15]. Additives include various advantages[16,17] such as:

- High oxygen content in their molecular structure.
- Can be mixed easily in diesel without any reagent.
- Can be used without any engine modifications.
- Don’t damage the parts of the diesel engine generally.
- No safety and health issue during the preparation of diesel–additives blends.
- May improve the cetane number of the diesel–additives blended fuel.
- Improve the physicochemical properties of the diesel-additives blended fuel, as it is an oxygenated fuel.
- May enhance the BTE of an engine up to 18% without affecting the other parameters.
- May reduce the exhaust emissions by up to 50% or more.

Among the variety of additives, oxygenated additives are mostly used because of their better combustion quality and reduced exhaust emissions[18,19]. Diethyl ether (DEE) and nitromethane (NM) have better combustion characteristics as compared to other additives and diesel[20,21].

As per the reported literature, diethyl ether and nitromethane have superior combustion properties due to high oxygen content, high latent heat, low boiling point, etc. Therefore in the current study, diesel–diethyl ether–nitromethane (D–DEE–NM) ternary blend was used to examine the performance and exhaust emission characteristics of engine experimentally at various concentrations and loads, as the performance of this ternary blend has not been investigated in previous research studies of reported literature.

1.1 Diethyl ether

Diethyl ether is an organic compound which is produced by the condensation of alcohols and commonly used as a starting fuel for some engines. DEE has a low latent heat of vaporization, which provides charge cooling and may responsible for NOx reduction. The performance improvement and emission (CO and HC) reduction can be possible with DEE-diesel blends due to the presence of high oxygen content, higher cetane number and volatility [22,23]. Physico-chemical properties of DEE may play a significant role to know exhaust emission characteristics and decide the appropriate proportion of additives for blending with diesel, which may enhance the performance of the engine. The chemical structure of DEE is as shown in Figure 1.

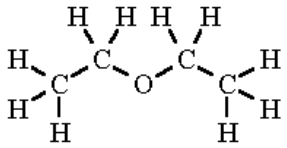

Figure 1. Chemical structure of diethyl ether

Mohanan and Kapilan[24] calculated the performance and emissions characteristic of a single cylinder, four stroke, CI engine with diesel–DEE (5, 10, 15, 20 and 25% by vol.) fuel blend. DEE5 was found to be best option among them to improve the performance and reduce emission simultaneously. Subramanian and Ramesh[25] performed experiments with DEE (5, 10 and 15% by weight) diesel blend on a single cylinder CI engine and reported DEE10 as best blend. Kapilan et al.[26] performed experiments with increasing the percentage of DEE by 1% (up to 10%) and found significant enhancement in BTE and reduction in CO, hydrocarbon and smoke emissions using DEE5.

1.2 Nitromethane

Nitromethane (NM) additives also have the high oxygen content in their molecular structure, which may improve the combustion characteristics of additive–fuel blends and reduce the soot, however it may increase CO and NO_x emissions[27]. The structure of nitromethane is shown in Figure 2.

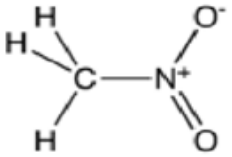

Figure 2. Chemical structure of nitromethane

Performance characteristics of NM–Diesel blends were evaluated in our previous studies[16,20] using vertical, single cylinder, 4-stroke, direct injection (DI), naturally aspirated, variable compression ratio (VCR) CI engine. The results showed the increased BTE with NM–diesel blend at CR 17.5 as compared to pure diesel at CR 17.5 and NM–diesel blend at CR 16.5. The highest BTE (25.15%) was achieved at 100% rated power. NOx emission also reduced using NM–Diesel blend as compared to pure diesel at CR 17.5. NOx emission reduced to a great extent for all loads while reducing the CR (16.5).

2. Experimental facility, materials and methods

2.1. Fuel preparation and physico-chemical properties

Fuel preparation was primary step for the experiments in which 99.0% pure diethyl ether and nitromethane were mixed with diesel fuel. Table 1 shows the various physico-chemical properties of diethyl ether, nitromethane and diesel fuel separately.

Table1. Physico-chemical properties of DEE, NM and diesel fuel [16,20,22,25]

Properties	Diethyl ether	Nitromethane	Diesel
Calorific value (MJ/kg)	36.8	11.3	44.8
Cetane number	125	–	55
Boiling point (˚C)	34	162	195
Density (kg/m^3)	713	1138	829
Latent heat (kJ/kg)	350	561	250
Auto-ignition temperature (˚C)	160	418	315
Viscosity (cSt)	0.23	0.62	2.45
Oxygen content (%)	22	53	00

Concerning above combustion properties, following points should be kept in mind while selecting additives.

- Additives with lower density may help in preparing stable and soluble blend with diesel.
- Lower value of boiling point helps in reducing the ignition delay of combustion stage.
- High latent heat of evaporation results in more cooling intake process, thereby improves volumetric efficiency of the engine.
- Lower viscosity helps in ease the pumping of diesel–additives blend.

Diesel–diethyl ether–nitromethane concentration was taken on v/v percentage for preparation of all D–DEE–NM blends. First, the diesel fuel was taken (as per blending ratio) in the glass container, then diethyl ether (as per blending ratio) was poured drop by drop in diesel as well as homogenized by magnetic stirrer as shown in Figure 3. After that nitromethane (fixed amount 2.5%) was mixed in diesel–DEE blend in the same manner. Above procedural steps were repeated for each fuel blend.

2.2. Test engine

The experiments were conducted on single cylinder, 4-stroke, constant speed, water cooled, direct injection, variable compression ratio, compression ignition engine attached with eddy current dynamometer (air cooled). For varying the CR, lifting and lowering cylinder block arrangement was used without altering the geometry of combustion chamber and stopping of engine. The pictorial view of the experimental facility is as depicted in Figure 3. Table 2 demonstrates all technical specifications of the engine and other measuring equipments.

Figure 3. A pictorial view of the experimental setup

Table 2. Test engine specification

Particulars	**Specification**
Engine –make	Diesel–Kirloskar (TV1)
No. of cylinders	01
Stroke	4 stroke
Cooling	Water cooled
Rated Power	3.75 kW
Max. rpm	1500
Capacity	660 cubic centimeter
Stroke and bore	110 mm and 87.5 mm

Before conducting the experiments, clean and brand new lubricating oil was filled in the oil sump of engine. The experimental result data were monitored and stored in the computer-based LABVIEW software.

2.3. Test procedure

The experimentations on engine were carried out by varying the load from 0 (no load) to 100% of rated power (full load) at constant speed (1500 rpm) using pure diesel and D–DEE–NM blends at normal engine test conditions (CR 17.5, IT 23° CA btdc and IP 210 bar). Each test was carried out for half an hour to achieve steady–state condition before taking the final readings. Once a test is completed with one fuel blend, the remaining fuel blend available in fuel tank and fuel pipeline was eliminated to prevent the alteration of genuine blend ratio.

For all fuel blends, exhaust emissions i.e., HC and smoke density were measured by exhaust gas analyzer (make: AVL–DIGAS) and AVL smoke meter respectively as shown in Figure 3. The non–dispersive infrared radiation principle is used for measurement of HC emissions.

3. Result and Discussion

3.1. Performance characteristic of D–DEE–NM blends:

The performance of engine tested at standard CR (17.5) of engine with different blends of D–DEE–NM is as depicted in Figure 4. Figure 7 shows the values of BTE, smoke and HC for all D–DEE–NM fuel blends and pure diesel at full load condition.

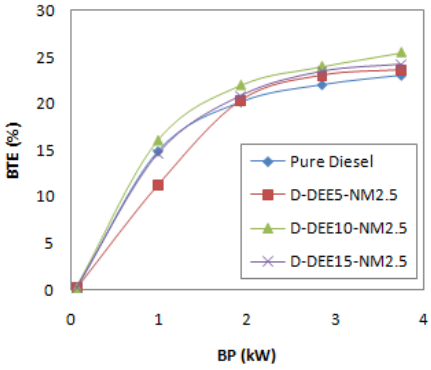

Figure 4. Variation in BTE with BP for D–DEE–NM blends and diesel

It was observed that best BTE values are obtained with D–DEE10–NM2.5 blend among all fuel blends and pure diesel. Diethyl ether has the lower density as compared to the diesel, which helps to make a stable solution of blends. Diethyl ether and nitromethane have higher oxygen content, and DEE has higher cetane number as compared to diesel, and it helps to complete the combustion of fuel due to which increased BTE is obtained. From Fig. 7 it can be concluded that 10.82 % increment in BTE was achieved using D–DEE10–NM2.5 blend as compared to diesel at 100% rated power (full load condition).

3.2.Exhaust emission characteristic of D–DEE–NM blends:

The exhaust emission of engine tested at standard CR (17.5) of engine with different D–DEE–NM blends. Using D–DEE–NM blends, considerable reduction in smoke quantity and HC were obtained as indicated in Figure 5 and Figure 6 respectively.

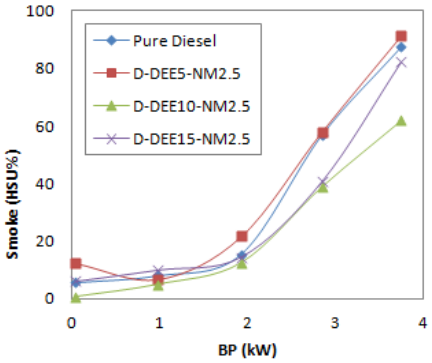

Figure 5. Variation in smoke with BP for D–DEE–NM blends and diesel

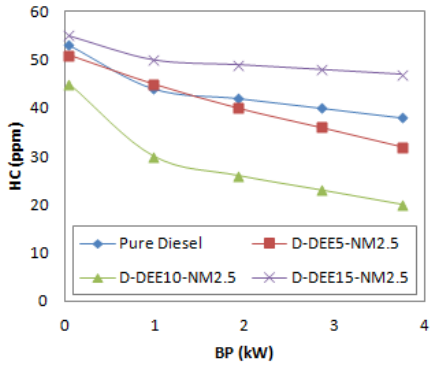

Figure 6. Variation in HC with BP for D–DEE–NM blends and diesel

It is mainly due to the lower density of DEE which makes the blend solution more homogenize; and higher volatility of DEE and nitromethane as compared to diesel, both factors improve the combustion quality. Another aspect for a better result is due to high oxygen content which provides sufficient oxygen to the fuel rich region and oxidizes the smoke. At full load condition, 29.14% reduction in smoke and 47.36% reduction in HC were found with D–DEE10–NM2.5 blend with respect to diesel as summarized in Figure 7. From performance and exhaust emission results as summarized in Figure 7, D–DEE10–NM2.5 was found to be most favorable blend among all fuel blends and diesel for CI engine.

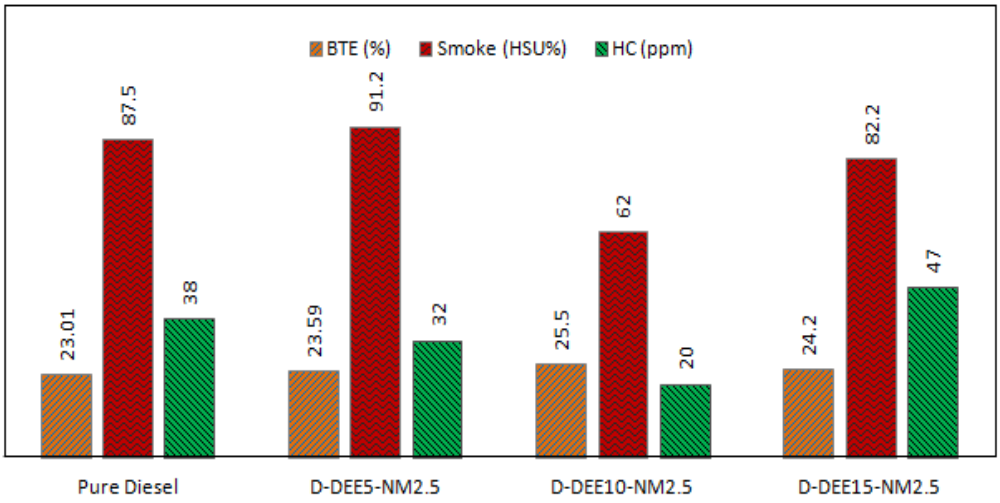

Figure 7. Various outcomes for pure diesel and D–DEE–NM blends at 100% rated power

4. Concluding remarks

The experimental study was carried out to determine the performance and exhaust emissions of VCR stationary CI engine fuelled by diesel–diethyl ether–nitromethane blends. D–DEE–NM blends were tested at normal engine test conditions and compared with diesel to obtain best suitable blending ratio. At normal engine test conditions (CR 17.5, IT 23° CA btdc and IP 210 bar), D–DEE10–NM2.5 blend was found to be the best suitable blend which provides the better combustion characteristics due to rich oxygen content and improved cetane number. D–DEE10–NM2.5 blend improved the engine performance (10.82% increment in BTE) and controlled emissions (Smoke and HC reduced by 29.14%, and 47.36% respectively) simultaneously as compared to pure diesel at 100% rated power.

Acknowledgement

The authors are grateful to Rajasthan Technical University (RTU), Kota and Swami Keshvanand Institute of Technology, Management and Gramothan (SKIT), Jaipur, for providing the facilities for this study. A Special thanks to Dr. S. L. Surana (Director Academics) SKIT, Jaipur for kind support and motivation.

Reference

1. Lin C Y and Huang J C 2003 An oxygenating additive for improving the performance and emission characteristics of marine diesel engines Ocean Eng 30 1699
2. Moghaddam M S, Moghaddam M M, Aghili S, Absalan A and Najafi A 2012 Performance and exhaust emission characteristics of a ci engine fueled with diesel–nitrogenated additives *Int J Chem Eng Appl* 3 363
3. Maricq M M 2007 Chemical characterization of particulate emissions from diesel engines : A review *Journal of Aerosol Sci.* 38 1079
4. Johnson T V 2008 Diesel emission control in review *SAE Int J Fuels Lubr* 1 68
5. Huang H, Zhou C, Liu Q, Wang Q and Wang X 2016 An experimental study on the combustion and emission characteristics of a diesel engine under low temperature combustion of diesel / gasoline / n–butanol blends *Appl Energy* 170 219
6. Roberts M 2003 Benefits and challenges of variable compression ratio (VCR) *SAE Tech. Paper*
7. Sayin C and Uslu K 2008 Influence of advanced injection timing on the performance and emissions of CI engine fueled with ethanol–blended diesel fuel *Int. journal of energy research* 32 1006
8. Zheng M, Asad U, Kumar R, Reader GT, Mulenga MC, Bombardier W et al. 2007 An investigation of EGR treatment on the emission and operating characteristics of modern diesel engines *SAE Tech. Paper*
9. Ameer S and Gopal K R 2012 A review of the effects of catalyst and additive on biodiesel production, performance, combustion and emission characteristics *Renew Sustain Energy Rev* 16 711
10. Behcet R 2011 Performance and emission study of waste anchovy fish biodiesel in a diesel engine *Fuel Process Technol* 92 1187
11. Giakoumis E G, Rakopoulos C D, Dimaratos A M and Rakopoulos D C Exhaust emissions with ethanol or n –butanol diesel fuel blends during transient operation : A review *Renewable and sustainable energy reviews* 17 170
12. Hellier P, Ladommatos N, Allan R and Rogerson J 2013 Combustion and emissions characteristics of toluene/n–heptane and 1–octene/n-octane binary mixtures in a direct injection compression ignition engine *Combust Flame* 160 2141
13. Karabektas M and Hosoz M 2009 Performance and emission characteristics of a diesel engine using isobutanol–diesel fuel blends *Renew Energy* 34 1554
14. Sukjit E, Herreros J M, Dearn K D, Garcia–Contreras R and Tsolakis 2012 A The effect of the addition of individual methyl esters on the combustion and emissions of ethanol and butanol –diesel blends *Energy* 42 364
15. Nabi M N, and Hustad J E 2010 Experimental investigation of engine emissions with marine gas oil–oxygenate blends *Sci Total Environ* 408 3231
16. Kumar C, Bafna M, Nayyar A, Parkash V and Goyal N 2014 Experimental investigation of the performance of VCR diesel engine fuelled by nm–diesel blend *IJETAE* 4 122

17. Goyal N, Nayyar A and Kumar C 2015 Experimental investigation of the performance of VCR diesel engine fuelled by n–butanol diesel blend *International Journal of Research in Engineering and Technology* 4 444
18. Padwa R S, Gupta S, Singh V and Kumar C 2016 Experimental Investigation on the Performance of VCR Diesel Engine Fuelled by E–NM2–Diesel blend *International Journal of Innovative Research in Science, Engineering and Technology* 5 6794
19. Kumar C, Rana K B, Tripathi B and Nayyar A 2018 A comparative study of oxygenated additives for diesel in compression ignition engine *Int. J. Renewable Energy Technology* 9 16
20. Kumar C, Nayyar A, Bafna M, Agarwal A and Parkash V 2015 Analysis of emission characteristic of NM–diesel blend on VCR diesel engine *International Journal of Recent Advances in Mechanical Engineering* 4 115
21. Rakopoulos D C, Rakopoulos C D, Giakoumis E G and Dimaratos A M 2013 Studying combustion and cyclic irregularity of diethyl ether as supplement fuel in diesel engine *Fuel* 109 325
22. Anand R and Mahalakshmi N V 2007 Simultaneous reduction of NOx and smoke from a direct–injection diesel engine with exhaust gas recirculation and diethyl ether *Proc Inst Mech Eng Part D–Journal Automob Eng* 221 109
23. Patil K R and Thipse S S 2014 Experimental investigation of CI engine combustion, performance and emissions in DEE–kerosene–diesel blends of high DEE concentration *Energy Convers Manag* 89 396
24. Mohanan P, Kapilan N and Reddy R P 2003 Effect of diethyl ether on the performance and emission of a 4–S di diesel engine *SAE Tech. Paper*
25. Subramanian K A and Ramesh A 2002 Operation of a compression ignition engine on diesel–diethyl ether blends *ASME Int Combust Eng* 39 353
26. Kapilan N, Mohanan P and Reddy R 2008 Performance and Emission Studies of Diesel Engine Using Diethyl Ether as Oxygenated Fuel Additive *SAE Technical Paper*
27. Kumar C, Rana K B and Tripathi B 2017 Performance and Emission Characteristic of VCR Diesel Engine Using Diesel –Nitromethane blend *International Journal of Engineering Technology Science and Research* 4

Efficiency Enhancement of Flat plate collector using different Nanofluids

Nipun Sharma, Rudraksh Gupta, Sanjeev Anand

ABSTRACT

Flat plate solar collector (FPSC) is a device which collects the solar radiation coming from the sun and is being used in a wide range of thermal applications like water heating, air heating or solar drying purposes. The performance of FPSC depends upon the thermo-physical properties of the working fluid. The Conventional FSPC is less efficient due to the factor that water is used as working fluid. In order to improve the efficiency of collector different nanoparticles are dispersed in combination with water integrated as nano-fluid and are used as working fluid. In this paper, thermal efficiency of FPSC with different nanofluids were theoretically analysed using different technical parameters, meteorological conditions and results were compared when only water was used as working fluid.

Keywords: Solar collector, Nano-fluids, Thermal Efficiency

Proceedings of the Third International Conference on Sustainable Energy and Environmental Challenges (3rd SEEC)
18 –21 December, 2018, IIT Roorkee, India

SEEC No.091

SUSTAINABLE FEEDSTOCK SCENEDESMUS SP. ADIITEC-II AND CHLOROMONAS SP. ADIITEC-III: EFFECT OF INITIAL PH AND NUTRIENT STARVATION ON GROWTH AND LIPID YIELD

Nongmaithem Debeni Devi
Centre for Energy, IIT Guwahati
Email: debeni@iitg.ac.in

Vaibhav V. Goud
Department of Chemical Engineering, IIT Guwahati
Email: vvg@iitg.ac.in

ABSTRACT

Microalgae are the promising feedstock for the sustainable production of biodiesel. The lipid content in the microalgae are transeterified to biodiesel as FA. For the enhancement of lipid accumulation, the novel green algae strainS Scenedesmus sp. ADIITEC-II and Chloromonas sp. ADIITEC-III were cultivated in a two stages process in this study. The first stage showed that both ADIITEC-II and ADIITEC-III grew favorably at pH (7) with the maximum biomass productivity (0.027±0.015gL^{-1}d^{-1} and 0.025±0.017gL^{1}-d^{-1}respectively) and lipid yield (25.85% and 24.5% DCW respectively) at 27◦C. By selecting pH 7 as the optimum growth condition in the second stage, both the strains were grown in nitrogen depletion condition for 24 days. The result brought a significant increase in the total lipid and biomass productivity. Therefore, adjustments to cultivation conditions could serve as an efficient tool for the manipulation of lipid productivity in ADIITEC-II and ADIITEC-III.

.

Keywords: Microalgae, Feedstock, Biomass productivity, Lipid,
.

NOMENCLATURE

FA	Fatty acid
◦C	Degree celcius
DCW	Dry cell weight
sp.	Species
d	day
g	gram
L	Litre
PUFA	Polyunsaturated fatty acids
TAG	triacylglycerides

INTRODUCTION

Microalgae are often regarded as the feedstock of future for sustainable production of biodiesel (Chisti, 2007). The valuable polyunsaturated fatty acids (PUFA) in lipids of microalage are the essential components of biodiesel. However, the low lipid content is one of the major obstacle for the commercialization of the microalgae-derived biodiesel (Cheng-Wu et al., 2002). It is therefore optimization of growth condition is the prime focus for the enhancement of productivity.

Lipid yield and biomass productivity are limited by several factors such as temperature, pH and nutrient availability (Mujtaba et al., 2012). Microalgal species *Chlorella vulgaris* , *Botryococcus* sp. (Banerjee et al., 2002), *Neochloris* sp. (Li et al., 2008) have been reported to have the capacity of accumulating large quantities of lipids under different nutrient starvation and stress condition. (Ren et al., 2013) investigated the strong tolerance of *Scenedesmus* sp to wide range of pH (4-11).

The goal of the study was to optimize the growth contidion of *Scenedesmus* sp. ADIITEC-II and *Chloromonas* sp. ADIITEC-III. Further, the influence of nutrient deficient on lipid accumulation was studied.

EXPERIMENTAL

To investigate the optimum growth conditions and high lipid content, the study was carried out by selecting two novel microalgae strains, *Scenedesmus* sp. ADIITEC-II and *Chloromonas* sp. ADIITEC-III. The study was conducted in a two stage process. In first satge, ADIITEC-II and ADIITEC-III were cultivated in a wide range of pH (4.0-10.0) in BG11 media for 24 days at 27◦C. In second stage, the optimized pH was chosen and nitrogen starvation BG11 medium was provided for the cultivation. The light intensity of 4000 lux with 12/12 hrs dark and light cycle was maintained during the cultivation period of 24 days. All the studies were done in triplicate.

RESULTS AND DISCUSSION

EFECT OF pH

The initial pH of the BG11 media varied from 4.0 to 10.0. The growth analysis was also shown in Tab.1. This study found an interesting phenomenon that the strain ADIITEC-II had strong pH tolerance and grow in wide range of pH (pH 6-10) (Fig 1). The lipid content.also enhanced significantly from 16.44% to 20.44% when pH increased from 4 to 10. The maximum yield of biomass ($0.027\pm0.015 gL^{-1}d^{-1}$) and lipid (25.85%) was obtained at pH 7. (Bartley et al., 2014) found the highest lipid content (24.75%) of *Nannochloropsis salina* at pH 8 This suggested that alkaline pH or pH stress provides flexibility to microalgae cell wall and prevent the release of auto spore thereby increasing the length of cell cycle. Increase in cell cycle accumulated large TAG thereby decreasing membrane lipids (Bartley et al., 2014). Further, ADIITEC-III gave the maximum yield of lipid (24.45%) and biomass productivity ($0.025\pm0.017 gL^{1-}d^{-1}$) at pH 7 (Fig 2). These results indicated that agae lipid content was affected by the pH of the medium. Similar phenomenons were also showed by *Chlorella* (Wan et al., 2012), *Botryococcus* (Ruangsomboon, 2012), *Neochloris* (Li et al., 2008). Thus, the pH was a limiting factor for the biochemical metabolism and affects the enzyme system (Wang et al., 2013) responsible for lipid biosynthesis.

EFFECT OF NITROGEN STARVATION

Lack of nitrogen changes cellular carbon flux to lipid synthesis from protein synthesis and thus increase the yield of lipid (Converti et al., 2009). To investigate the effect of nitrogen starvation in this study, the BG11 medium deprived of nitrogen source was used for the cultivation. The pH of the medium was also maintained at 7. The results were compared with that of normal BG11 medium. The result confirmed the previous reports that nitrogen limitation favoured the significant increase in lipid accumulation. (Li et al., 2008) found the highest lipid productivity of 40% at the lowest nitrate concentration of 3mM. Under nitrogen absence, *Chlorella vulgaris* gave 77.8% of lipid after 2hrs of contimuous light illumination (Mujtaba et al., 2012). It was confirmed that nitrogen source became one of the limiting factor for the enhancement of lipid productivity.

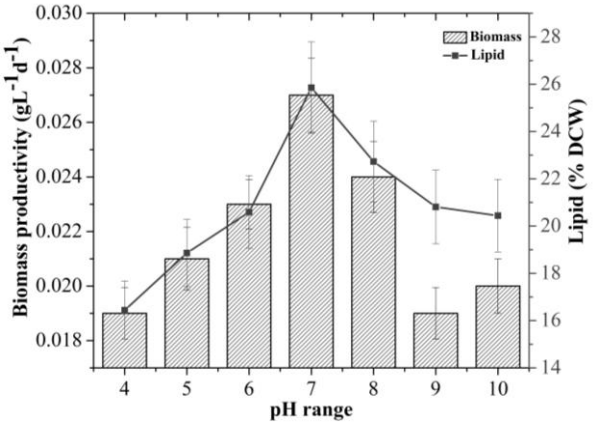

FIGURE 1. Effect of pH on yield of biomass and lipid production of ADIITEC-II.

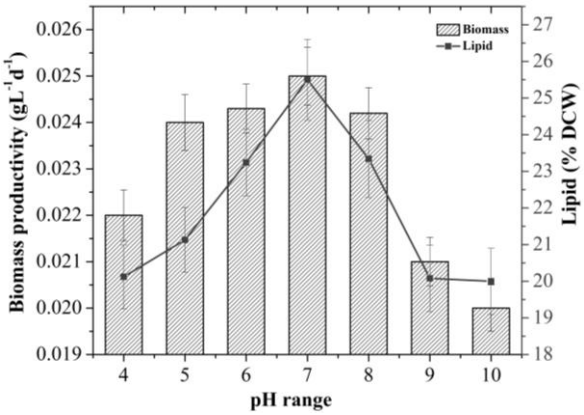

FIGURE 2. Effect of pH on yield of biomass and lipid production of ADIITEC-III

TABLE 1: Growth analysis of microalage obtained at pH 7

Species	Specific growth rate (μ)	Doubling time (hrs)
ADIITEC-II	0.18	3.5
ADIITEC-III	0.21	3.3

CONCLUSION

Adjustments to cultivation conditions of *Snedesmus* sp. ADIITEC-II and *Chloromonas* sp. ADIITEC-III could serve as an efficient tool for the manipulation of lipid productivity. A high amount of lipid production of 25.85%

and 24.5% showed that both the species can be a future source for sustainable biodiesel production.

ACKNOWLEDGMENTS

The authors are grateful to Ministry of Human Resource and Development (MHRD) for providing financial assistantship and Centre for Energy, Central Instrument facilities (CIF), Analytical laboratory of Department of Chemical Engineering and Department of Biosiences and Bioengineering of IIT Guwahati for providing basic research facilities.

REFERENCES

Banerjee, A., Sharma, R., Chisti, Y., Banerjee, U. 2002. Botryococcus braunii: a renewable source of hydrocarbons and other chemicals. *Critical reviews in biotechnology*, **22**(3), 245-279.

Bartley, M.L., Boeing, W.J., Dungan, B.N., Holguin, F.O., Schaub, T. 2014. pH effects on growth and lipid accumulation of the biofuel microalgae Nannochloropsis salina and invading organisms. *Journal of applied phycology*, **26**(3), 1431-1437.

Cheng-Wu, Z., Cohen, Z., Khozin-Goldberg, I., Richmond, A. 2002. Characterization of growth and arachidonic acid production of Parietochloris incisa comb. nov (Trebouxiophyceae, Chlorophyta). *Journal of applied phycology*, **14**(6), 453-460.

Chisti, Y. 2007. Biodiesel from microalgae. *Biotechnology advances*, **25**(3), 294-306.

Converti, A., Casazza, A.A., Ortiz, E.Y., Perego, P., Del Borghi, M. 2009. Effect of temperature and nitrogen concentration on the growth and lipid content of Nannochloropsis oculata and Chlorella vulgaris for biodiesel production. *Chemical Engineering and Processing: Process Intensification*, **48**(6), 1146-1151.

Li, Y., Horsman, M., Wang, B., Wu, N., Lan, C.Q. 2008. Effects of nitrogen sources on cell growth and lipid accumulation of green alga Neochloris oleoabundans. *Applied microbiology and biotechnology*, **81**(4), 629-636.

Mujtaba, G., Choi, W., Lee, C.-G., Lee, K. 2012. Lipid production by Chlorella vulgaris after a shift from nutrient-rich to nitrogen starvation conditions. *Bioresource technology*, **123**, 279-283.

Ren, H.-Y., Liu, B.-F., Ma, C., Zhao, L., Ren, N.-Q. 2013. A new lipid-rich microalga Scenedesmus sp. strain R-16 isolated using Nile red staining: effects of carbon and nitrogen sources and initial pH on the biomass and lipid production. *Biotechnology for biofuels*, **6**(1), 143.

Ruangsomboon, S. 2012. Effect of light, nutrient, cultivation time and salinity on lipid production of newly isolated strain of the green microalga, Botryococcus braunii KMITL 2. *Bioresource Technology*, **109**, 261-265.

Wan, M.X., Wang, R.M., Xia, J.L., Rosenberg, J.N., Nie, Z.Y., Kobayashi, N., Oyler, G.A., Betenbaugh, M.J. 2012. Physiological evaluation of a new Chlorella sorokiniana isolate for its biomass production and lipid accumulation in photoautotrophic and heterotrophic cultures. *Biotechnology and bioengineering*, **109**(8), 1958-1964.

Wang, X., Selvam, A., Chan, M., Wong, J.W. 2013. Nitrogen conservation and acidity control during food wastes composting through struvite formation. *Bioresource technology*, **147**, 17-22.

SEEC No. 093

PERFORMANCE ANALYSIS OF PVT NON METALLIC SOLAR WATER HEATER

Kirti Tewari
Department of Mechanical Engineering, MNNIT Allahabad, Allahabad, U.P, India-211004.
Email:ktkirtitewari@gmail.com,
rme1401@mnnit.ac.in

Rahul Dev
Department of Mechanical Engineering, MNNIT Allahabad, Allahabad, U.P, India-211004.
Email:rahuldsurya@mnnit.ac.in

ABSTRACT

In the present paper, a PVT non-metallic solar water heater (PVNMSWH) made of modified solar collector and Glass-to glass PV module is simulated on MATLAB and validated with the experiments performed in the month of April and December, 2017. The novel solar water heater is made of Fibre-reinforced plastic (FRP) -acrylic and installed at the M.N.N.I.T. Allahabad, Allahabad, U.P India (latitude 25 ^{0}27'N and longitude 81 ^{0}44'). The maximum water temperature in the tank is found to be 65.6°C and 40.0°C in the month of April and December, 2017. Maximum thermal efficiencies have been found to be 43.9% and 38.3% in the month of April and December respectively at 13:00hr and electrical efficiency is found to vary between 11-12.5%. The enviro-economic analysis is carried out and the carbon mitigation cost is obtained as Rs. 1915 per annum.

***Keywords*:** PVT system, Acrylic, transparent storage tank.

.

INTRODUCTION

PVT systems are the solar dvices that produces electricity and heat simultaneously using solar energy. These systems are the integration of solar collector and PV module. Integration of solar devices into one reduces the heat loss. Integration reduces the water temperature and hence results in lower temperature difference between ambient and water temperature, utilizing that amount of heat to produce electricity. Reduced temperature difference between ambient temperature and water temperature inside the collector leads to lower losses [1].

The main comceept of these systems were first introduced by Kern and Russel [2] . Raghuraman [3] studied the thermal performance of PVT flat plate collector using numerical methods. Dubey and Tiwari [4] prested characteristic equation for PV/T system and concluded that energy payback period can be reduced by increasing the overall efficiency of these systems. It can be observed that integration of conventional systems have been focused and analysed in past litertures. Integration of modified systems have been paid little attention. Also a collector made of FRP-acrylic has not been studied in the past. Tiwari and Dev [5] studied the performance of modified solar water heater made of FRP-acrylic collector and storage tank. However they used metal absorber plate. In present paper a modified solar water made on non-metallic materials have been integrated with a glass-to-glass PV module and modelled using MATLAB.

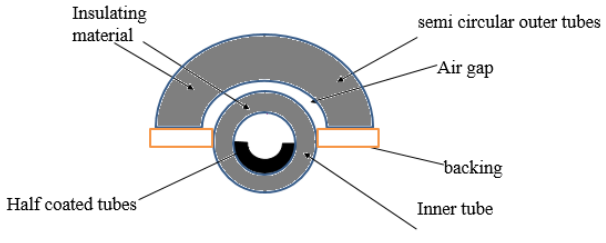

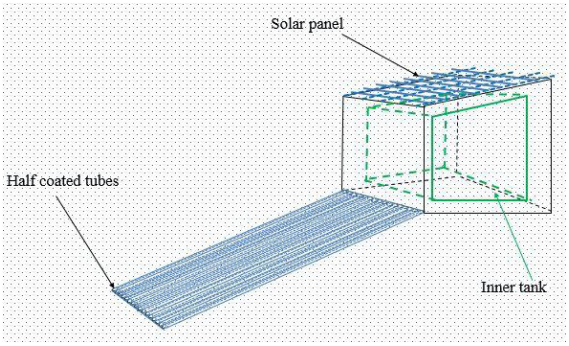

FIGURE 1. Schematic diagram of (a) solar collector (b) PVT non metallic solar water heater

EXPERIMENTAL SETUP AND INSTRUMENTATION

Experimntal Setup

Fig. 1 shows a schematic diagram of components of non metallic solar water heater i.e. solar collector and storage tank. The solar collector is made of 10 thermally insulating material tubes (methyl methacrylate commonly known as acrylic) and these tubes are surrounded by the semi circular tubes of same material on the upper half while the lower half is simply supported by a light support. The inner half of the inner tubes are coated with the SnS-Cu_xS which is an absorptive coating material having absorptance of 0.91. The total collector area is 0.61m^2 and length of each tube is 1m. The collector is connected to the trapezoidal water storage tank of 100L at an angle of 25° (as per laltitude of Alalahabad) and the basin and north wall of the storage tank is made of black painted FRP to absorb the maximum amount of solar radiations. The rest of the walls of the storage tank is made of double layered acylic sheets. Double layered walls reduces the heat loss from the storage tank to the surrounding durig off-sunshine hours. A glass-to-glass PV module of 75 watt is installed at the top surface of the storage tank to produce electricity in addition of hot water and conneted to a load. Thus the system serves as PVT system and this system works on density difference (Thermosiphon system). The water get heated by the combined effect of solar collector and storage tank. The working principle is same as described by Dev and Tiwari [5].

Instrumentation

For the measurement of the temperature of water copper constantan type-T thermocouples were used at the three different heights of North wall in stoare tank and at the ends of the collector tubes. Solar radiation falling at various surfaces of the water heater were measured using the AMPROBE (Model SOLAR-100) solar power meter. Wind velocity and ambient temperatures were recorded using Anemometer (FLUKE Model BTH401).

THERMAL MODELING

The energy balance for each component of the PVNMSWH has been carried out with the following assumptions,

a. The setup is completely water and vapour leakage proof.
b. The heat capacities of coating, FRP, acrylic are negligible.
c. System operates in quasi-steady state regime during the day.
d. The temperature of coating and FRP base are considered to be uniform

The reference for PV cell and nomenclature for water heater are taken from Dubey and Tiwari [4] and Tewari and Dev[6] respectively.

For Solar Cells of PV Module (Glass-Glass):

$$\alpha_c \tau_c \beta_c I_{top}(t) W dx = \left[U_{tc,a}(T_c - T_a) + \eta_c \tau_c \beta_c I_{top}(t)\right] W dx \quad (1)$$

From above equation cell temperature is given by

$$T_c = \frac{(\alpha\tau)_{eff}\, I_{top}(t) + U_{tc,a} T_a}{U_{tc,a}} \quad (2)$$

For Collector

1. For Coating:

$$\alpha_{ct}\left(\tau^2_{acry}\tau_w I_t(t)\right) A_c = h_w A_c (T_{ct} - T_{hw}) + U_1 A_c (T_{ct} - T_a) \quad (3)$$

$$T_{ct} = \frac{\alpha_{ct}\left[\tau^2_{acry}\tau_w I_t(t)\right] + h_w T_{hw} + T_a U_{1d2}}{h_w + U_1} \quad (4)$$

2. For water in tube:

$$\alpha_w\left[\tau^2_{acry}\tau_w I_t(t)\right]\frac{A_{iit}}{2} + h_w A_c (T_{ct} - T_{hw}) = M_{tw} C_w \frac{dT_{hw}}{dt} + \dot{m}_w C_w (T_{hw} - T_{cw}) + U_2 A_{iit}(T_{hw} - T_a) \quad (5)$$

3. For inner surface of inner tube:

$$h_w \frac{A_{iit}}{2} N_t (T_{hw} - T_{ii}) + h_{ct} N_t A_c (T_c - T_{ii}) = N_t A_{iit}(T_{ii} - T_a) U_3 \quad (6)$$

4. For outer surface of inner tube:

$$h_{o1}(T_{ii} - T_{io}) = U_4 (T_{io} - T_a) \quad (7)$$

5. *For inner surface of outer tube:*

$$h_i \frac{A_{iot}}{2}(T_{io} - T_{oi}) = U_5 A_{oit}(T_{oi} - T_a) \quad (8)$$

6. *For outer surface of outer tube:*

$$h_{o2} A_{oot}(T_{oi} - T_{oo}) = h_o A_{oot}(T_{oo} - T_a) \quad (9)$$

For Storage Tank

1. For water in storage tank

$$\alpha_w\left\{I_V(t)A_s + I_H(t)A_{top}\right\}\tau^2_{acry} + \alpha_w\left\{I_E(t)A_E + I_W(t)A_W\right\}\tau^2_{acry} + h_{bw}A_b(T_{bi} - T_{cw}) + h_{nw}A_N(T_{Ni} - T_{cw}) + \dot{m}_w C_w (T_{hw} - T_{cw}) =$$

$$M_{Tw}C_w\frac{dT_{cw}}{dt}+h_{TW}A_s(T_{cw}-T_{sii})+h_{TW}A_{top}(T_{cw}-T_{topi})$$
$$+h_{TW}A_E(T_{cw}-T_{Eii})+h_{TW}A_W(T_{cw}-T_{Wii}) \quad (10)$$

2. For east wall (inner surface of inner layer)

$$\alpha_{acry}\{I_E(t)A_E\}\tau_{acry}+h_{TW}A_E(T_{cw}-T_{Eii})=\frac{K_{acry}A_E(T_{Eii}-T_{Eio})}{t_{acryt}} \quad (11)$$

3. *For east wall (outer surface of inner layer)*

$$h_{kacry}A_E(T_{Eii}-T_{Eio})=h_iA_E(T_{Eio}-T_{Eoi}) \quad (12)$$

4. *For east wall (inner surface of outer layer)*

$$h_iA_E(T_{Eio}-T_{Eoi})=h_{kacry}A_E(T_{Eoi}-T_{Eoo}) \quad (13)$$

5. *For east wall (outer surface of outer layer)*

$$h_{kacry}A_E(T_{Eoi}-T_{Eoo})=h_oA_E(T_{Eoo}-T_a) \quad (14)$$

Similarly heat balance equations for west, north, south and top walls can be writted and following euations can be obtained by solving the equation (1-14). Derivation of Equation (15) and (16) can be referred from Tewari and Dev [6].

Temperature of water in Storage tank:

$$T_{cw}=\frac{1}{\beta^+-\beta^-}\left[\overline{g_1(t)}\left\{\frac{\left(1-e^{-c^+t}\right)}{c^+}-\frac{\left(1-e^{-c^-t}\right)}{c^-}\right\}+\overline{g_2(t)}\left\{\frac{\beta^+\left(1-e^{-c^+t}\right)}{c^+}-\frac{\beta^-\left(1-e^{-c^-t}\right)}{c^-}\right\}\right.$$
$$\left.+T_{hwo}\left(e^{-c^+t}-e^{-c^-t}\right)+T_{cwo}\left(\beta^+e^{-c^+t}-\beta^-e^{-c^-t}\right)\right] \quad (15)$$

Temperature of hot water in tube:

$$T_{hw}=\frac{1}{\beta^+-\beta^-}\left[\overline{g_1(t)}\left\{\frac{\beta^+\left(1-e^{-c^-t}\right)}{c^-}-\frac{\beta^-\left(1-e^{-c^+t}\right)}{c^+}\right\}+\beta^+\beta^-\overline{g_2(t)}\left\{\frac{\left(1-e^{-c^-t}\right)}{c^-}-\frac{\left(1-e^{-c^+t}\right)}{c^+}\right\}\right.$$
$$\left.+T_{hwo}\left(\beta^+e^{-c^-t}-\beta^-e^{-c^+t}\right)+\beta^+\beta^-T_{cwo}\left(e^{-c^-t}-e^{-c^+t}\right)\right] \quad (16)$$

RESULTS AND DISCUSSION

PVNMSWH is simulated on MATLAB using various climatic, operational and design parametrs and the simulated results are validated with the experimental results. Fig. 3 represents the variation of solar radiation (I) (global) and ambient temperature (Ta) in April and December, 2017, with respect to time. Radiations were measured from 7:00hr to 17:00hr. The maximum intensity of measured solar radiation was found to be 1147 W/m^2 and 950W/m^2 at 13:00 and 12:00hr on a particular day of April, 2017 and December, 2017.

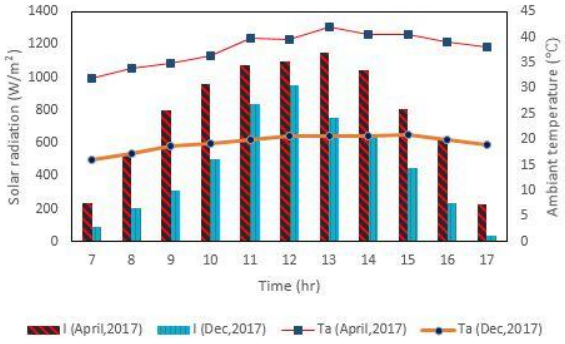

FIGURE 2. Hourly variation of climatic parameters.

Fig. (3a) and (3b) shows the hourly variation of hot water temperature in storage tank and collector tubes respectively for a particular day of April, 2017 and Dec, 2017. The experimental and theoretical results are found to be well agremented. It can be observed that water temperature in tank is increasing till 17:00hr while in the conventional systems like FPC water temperature retards after 14:00hr. This advantage is attributed to the advanced design using transparent storage tank along with the use of thermally insulating materials. The maximum temperature of water in storage tank is obtained as 65.6°C and 40.0°C in the month of April and Dec, 2017 respectively at 17:00hr.

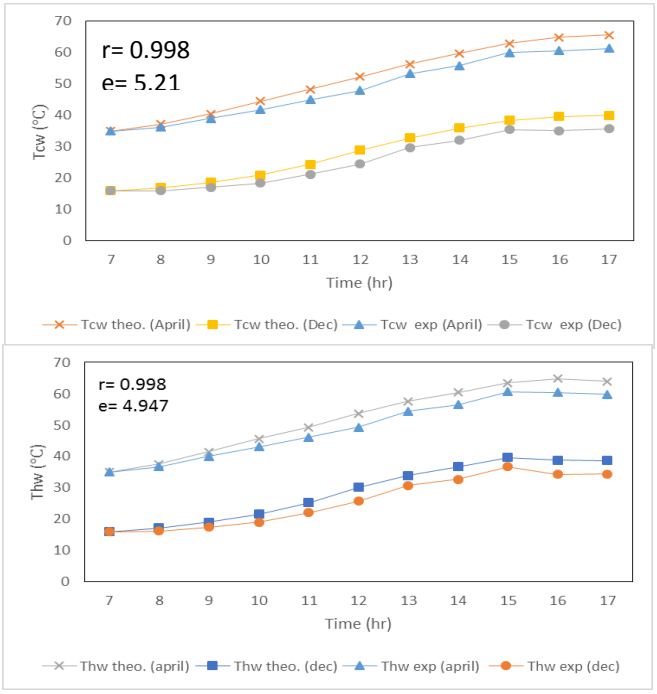

FIGURE 3. Hourly variation of hot water temperaturefor the month of April and December,2017 in (a) storage tank and (b)tubes

Fig. 4 shows the houly variation of cell temperature, coating temperature, thermal efficiency and electrical efficiency of PVNMSWH for the month of April and December, 2017. As the cell temperature decreases, electrical efficiency increases and vice versa. Maximum cell temperature has been found to be 66.6°C and 39.6°C in the month of April and December respectively while cell temperature is found to vary between 11-12%. The coating temperature increases with time and reaches its maximum at 17:00hr with 71.21°C and 50.8°C in April and Decemeber respectively. Coating temperature is very impotant parameter as higher coating temperature leads to higher water temperature flowing in the tube just above the coating. 43.9% and 38.4% has been found to be the maximum thermal efficiency of the PVNMSWH in April and December respectively at

13:00hr. The overall efficiency is the sum of thermal and equivalent electrical efficiency is found to vary between 30 to 69% and overall thermal energy produced by the system is obtained as 857kWh for the year 2017.

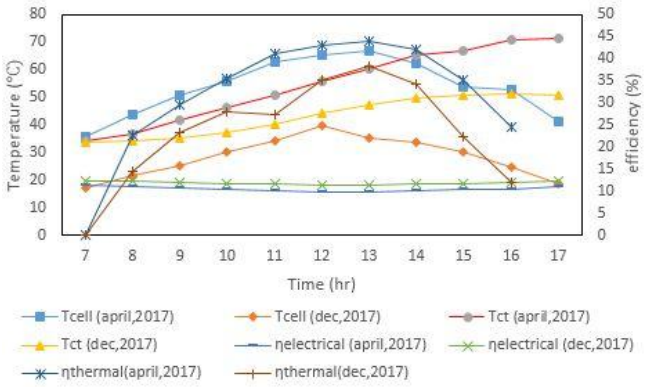

FIGURE 4. Hourly variation of cell temperature, coating temperature, thermal and electrical efficiency

ENVIROECONOMIC AND COST ANALYSIS

Enviroeconomic analysis is very important tool to analyse the carbon mitigartion. 0.982 kg of carbon dioxide is emitted into the environment for the production of 1kWh electricity and annually CO_2 mitigation is calculated as

$$\varphi_{CO2} = \frac{\Psi_{CO2} \times Q_{thermal}}{1000} = \frac{2.04 \times 857}{1000} = 1.748\ tCO_2e \quad (17)$$

Where, ψ_{CO2} is CO_2 equivalent intensity for generation of electricity and earned carbon credit (J_{CO2}) is expressed as

$$J_{co_2} = \varphi_{CO2} \times j_{CO_2} = 1.784 \times 14.5 \times 74.04 \quad (18)$$

j_{co2} is termed as price of one tone of CO_2 which is 14.5 US $ (as per KYOTO PROTOCOL) and the carbon mitigation cost is calculated as Rs.1915 per annum and the total capital cost of PVNMSWH is shown in Tab. [1]

TABLE 1: CAPITAL COST OF PVNMSWH

Components	Quantity × Cost per item (Rs.)	Total cost of item (Rs.)
Inner Acrylic Tubes	10 × 125 per m	1250
Outer Acrylic Tubes	5 × 350 per m	1750
FRP	5.83 sq. ft × 320 per sq. ft	1865.6
Acrylic Sheet	1.68 sq. m × 646 per sq. m	1084.8
Iron Stand	12 kg × 75 per kg	900
Taps	2 × 50 per piece	100
Black Paint	0.5l	150
Fabrication Cost	(506+506*)× 4	4048
Total cost		**Rs.11,148.4 (150.58 US$)**

CONCLUSIONS

The following conclusions has been drawn on the basis of present analysis.

(i) The modified design and thermally insulating material in collector tubes has reduced the need of external insulation, resulting light weight collector and reduced cost and higher heat retention capacity of the system.

(ii)Overall efficiency of the PVT system has been found to vary between 30-69%.

(iii)The maximum variation of tank water temperature with ambient is found to be 27.6°C in April,2017 and 21.1°C in December,2017respectively at 17:00hr.

(iv) The carbon mitigation cost for PVNMSWH is calculated as 1915 per annum and the capital cost of the setup is Rs. 11,148.4 (150.58 US$).

REFERENCES

[1] Dev, R., Tiwari, GN.,2011. "Characteristic equation of the inverted absorber solar still". Desalination, 269, pp. 67–77.

[2] Kern, E.C., Russell, M.C., 1978. Combined photovoltaic and thermal hybrid collector systems". In: Proc. 13th IEEE Photovoltaic Specialists, Washington DC, USA, pp. 1153–1157.

[3] Raghuraman, P., 1981. "Analytical predictions of liquid and air photovoltaic/thermal flat plate collector performance". Journal of Solar Energy Engineering, 103, pp. 291–298.

[4] Dubey, S., Tiwari, G.N., 2008."Thermal modeling of a combined system of photovoltaic thermal (PV/T) solar water heater". Solar Energy, 82, pp. 602–612

[5] Tewari, K., Dev, R., 2018. "Analysis of Modified Solar Water Heating System Made of Transparent Tubes & Insulated Metal Absorber". EVERGREEN Joint Journal of Novel Carbon Resource Sciences & Green Asia Strategy, 5 (1) pp. 62-72.

[6] Tewari, K., Dev, R., 2017. "Theoretical analysis of a proposed solar water heating system made of non-metallic materials". MATTER: International Journal of Science and Technology, 1, pp. 2454.

[7] Tewari, K., Dev, R., 2016. International Journal of Electrical, Computer, Energetic, Electronic and Communication Engineering, Paris. 10, pp. 73.

APPENDIX A: Varius parameters of PVNMSWH

Specifications	Values	Specifications	Values
α_{FRP}	0.9	ρ_w	1000 kg/m^3
α_w	0.6	L	1 m
α_{acry}	0.05	A_{Th}	0.610 m^2
τ_{acry}	0.92	K_{acry}	0.2 W/mK
τ_w	0.35	Rii	0.01m
h_i	2.55W/m^{2}K	Rio	0.0125m
N_t	10	Roi	0.022m
$\dot{m}$	0.02 kg/s*	Roo	0.025m
V_T	100 L	K_{FRP}	0.035 W/mK
t_{Th}	0.06	h_w	200 W/m^{2}K
t_{acryt}	0.003 m	t_{FRPT}	0.005 m
A_N	0.299 m^2	A_E	0.158 m^2
A_S	0.186 m^2	Ab	0.243 m^2
A_{top}	0.268 m^2	Space b/w tubes	0.01 m
Total area of solar cell	0.168 m^2	β	0.72
No. of solar cells	36	A_m	0.233m^2
		h_{bw}, h_{nw}	500

Proceedings of International Conference on Sustainable Energy and Environmental Challenges (3rd SEEC), December 18-21, 2018, IIT Roorkee, India

SEEC No. 094

Numerical Investigations on the Type-II Band Alignment and Quantum Efficiency of Multijunction Solar Cell using Anderson's Rule

Ankul Prajapati[1*], Jatin Kumar Chaudhary[2#], Rajeev Kanth[3], Jukka-Pekka Skön[4], Jukka Heikkonen[5]

1 - UG Student, Department of Mechanical Engineering SVNIT, Surat, Gujarat, 395007, India
2 - UG Student, Department of Electronics Engineering, SVNIT, Surat, Gujarat, 395007, India
3,4 - Savonia University of Applied Sciences, Kuopio 70101 Finland
5 - University of Turku, Turku 20520, Finland
**ankulprajapati7@gmail.com, # jatinkchaudhary@gmail.com*

ABSTRACT

Since the first solar cell was developed, to the present date the low efficiency of the energy conversion has been a matter of concern to the researchers. At, present solar cells are made up of the p-n junction fabrication of the Si or the GaAs which, first, due to high bandgap makes it difficult for the electron emission and decreases the efficiency of the cell, second it cannot utilize the maximum part of the spectrum of the solar energy reaching the earth and hence, most of the energy gets wasted. We have performed numerical studies on semiconducting compounds by using heterojunction methodology for photovoltaic applications to produce solar cells with economic and better performance. Poisson's equation and Anderson's rule has been used to perform the simulations of heterostructure band alignment in Solar Cell Capacitance Simulator (SCAPS 1D®). Band alignment graphs have been plotted for different heterointerface, and quantum efficiency graph has been plotted for the whole model of a solar cell, and the results were analysed.

Keywords

Solar Energy, Photovoltaics, Heterointerface, Anderson's rule, Multijunction.

NOMENCLATURES

G= Generation rate ($cm^{-3}sec^{-1}$)
$N^{\pm}_{D,A}$ = Charged Dopants (cm^{-3})
$U_{n,p}$ - the net recombination rates ($cm^{-3}sec^{-1}$)
D = Electric displacement field ($C\ m^{-2}$)
E = Electric field ($V\ m^{-1}$)
ρ = Charge density ($C\ cm^{-3}$)
ϵ = Permittivity Tensor ($C^2\ N^{-1}\ m^{-2}$)
ψ = Electrostatic Potential (V)
q = Electronic Charge (columb)
n, p = free charges which are electrons and holes respectively. (columb)
ρ_{def} (n, p) – defect distributions

1. INTRODUCTION

The concentration of Greenhouse gases in earth's atmosphere and temperature rise due to human emission of greenhouse gases is increasing day by day. Due to the harsh effects of the energy by the utilization of fossil fuels, the world is shifting its attention from the conventional use of fossil fuels to the use of Photovoltaics and other renewable energy resources [1,2]. But the only problem which persists since the evolution of photovoltaics has been done, is the efficiency of the energy conversion. So, the study in the field of multijunction photovoltaics by using heterointerfaces is primarily motivated by the improvement of energy conversion efficiency. The structure as shown in fig 1 absorbs the most parts of the spectrum of the light and uses it to the maximum because of the presence of multilayer composite materials used. Though heterojunction between different semiconductors have been extensively studied in the literature. Some of the numerical studies have been done on a-Si:H/c-Si and GaAs heterostructure solar cell Using AMPS-1D and CIGS solar cells [3,4,5,6]. In this paper We have explored the different heterointerface layers in a multijunction solar cell where all the layers are intrinsic using Solar Cell Capacitance Simulator (SCAPS-1D). Solar Cell Capacitance Simulator (SCAPS-1D), a one-dimensional simulation programme developed at the Department of Electronics and Information Systems (ELIS) of the University of Gent, Belgium.

The study is concentrated towards the diversion of the Type-II band diagram after the stacking of multiple layers so that the movement of charge carriers can be studied thoroughly. The study of the Quantum Efficiency reflects the potential of the solar cell which it can offer in real life applications. Each layer subjected to the multijunction solar cell has been described by a set of parameters as given in TABLE - 1.

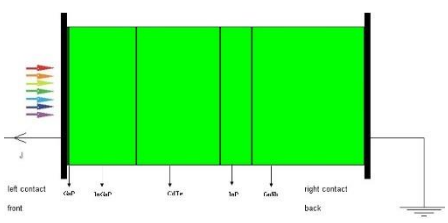

Figure 1 2-D Model of solar cell

2. GOVERNING EQUATIONS & MODELS

SCAPS-1D in order to do all semiconductors simulation uses the Poisson equation and the continuity equations for electrons and holes. The Poisson equation is given as,

$$\frac{\partial}{\partial x}\left(\epsilon(x)\frac{\partial \psi}{\partial x}\right) = -\frac{q}{\epsilon}\left(-n + p + N_A^- - N_D^+ + \frac{1}{q}\rho_{def}(n,p)\right) \quad (1)$$

The continuity equations for electrons and holes is given as,

$$\frac{-\partial j_n}{\partial x} + G - U_n(n,p) = \frac{\partial n}{\partial t} \quad (2)$$

$$\frac{-\partial j_p}{\partial x} + G - U_p(n,p) = \frac{\partial p}{\partial t} \quad (3)$$

For steady state, RHS of equation 2 and equation 3 becomes zero. Where Jn and Jp are electron and hole current densities, and G is the generation rate.

3. SIMULATION SETUP

All simulation has been carried out in standard temperature and pressure. Illumination condition is one sun (=1000W/m^2) with the air mass 1.5, global. SCAPS uses grading parameters. All the layer parameters are graded by uniform composition grading, and settings are considered as position dependent. Numerical calculation of the occupation of the different metastable configurations is done in iteratively way. For different interfaces band to band, tunneling is allowed.

TABLE 1 of Parameters used

Material	GaP	InGaP	CdTe	InP	GaSb
Thickness (µm)	0.030	1.200	1.500	0.560	1.255
Electron Affinity (ev)	3.800	4.160	4.500	4.380	4.060
CB Density of states(cm^{-3})	3.100 E+19	1.300 E+20	7.900 E+17	5.200 E+17	2.100 E+17
VB Density of states (cm^{-3})	1.800 E+19	1.280 E+19	1.300 E+19	1.100 E+19	1.800 E+19
Dielectric Permittivity	11.10	11.62	10	12.5	15.70

4. RESULT & DISCUSSION

The individual band gap of the materials when combined with each other are below:

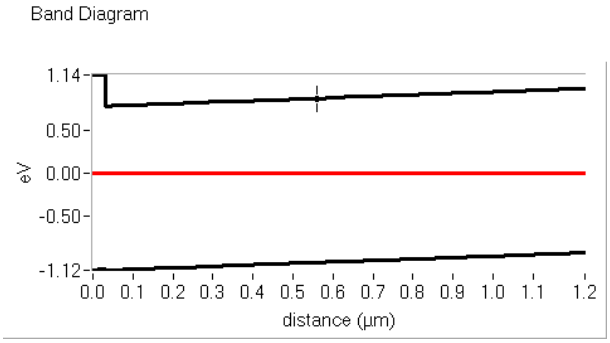

Figure 2 Band Diagram of GaP and InGaP interface

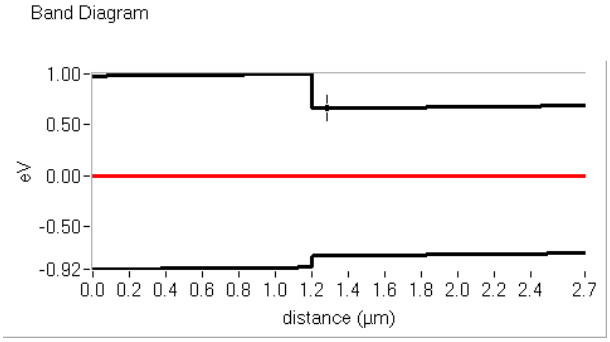

Figure 3 Band Diagram of InGaP and CdTe Interface

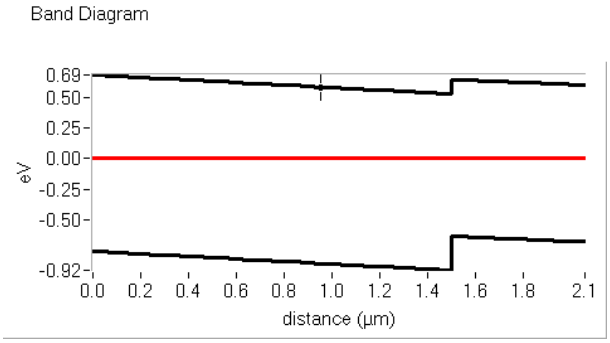

Figure 4 Band Diagram of CdTe and InP Interface

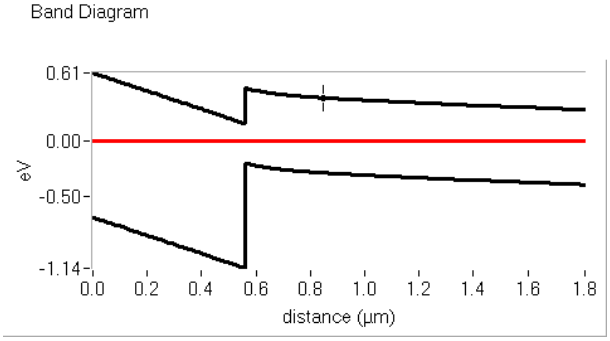

Figure 5 Band Diagram of InP and GaSb interface

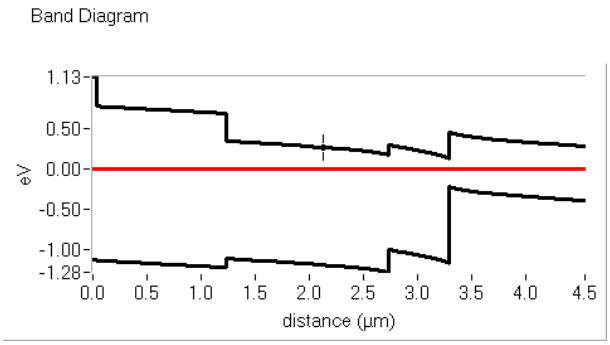

Figure 6 Band diagram of the entire cell

Above mentioned band diagram of the type II band alignment at different heterointerface which assists transport of photogenerated electron and hole pairs to the wide bandgap material. In such a heterostructure, charge carriers of one type (Electrons) can be confined, while the other type (Holes) is not confined. The transportation of the photogenerated charge carriers is very efficient as compared to the single junction heterostructure solar cell.

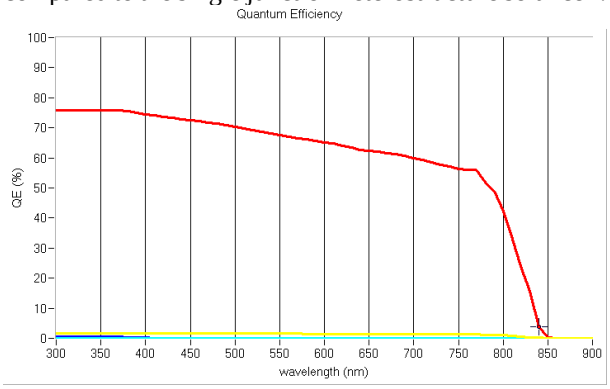

Figure 7 Quantum efficiency of the cell

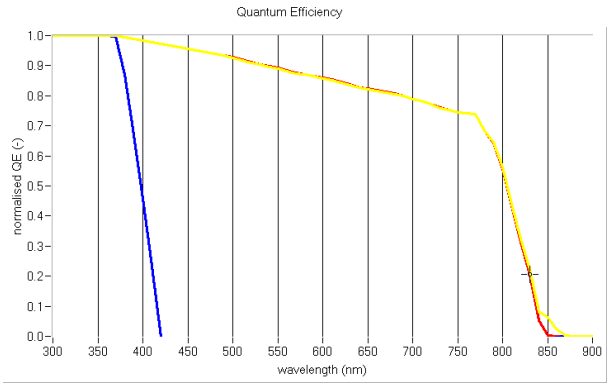

Figure 8 Quantum efficiency of the cell normalized to one.

As from the graph it is seen that the maximum Quantum Efficiency is 78% which reveals the efficient conversion of collected photons to electric current.

5. CONCLUSION

The study of heterojunction multilayered solar cell was done with intrinsic semiconducting compounds using SCAPS 1-D. Analysis of type II band diagram alignment of individual interfaces of the materials and the diagram of the whole cell was done. The five-layered model of the solar cell is efficient in utilizing the maximum spectrum of the solar cell, and hence, the graph of Quantum efficiency is shown. The detailed study of other solar cell efficiency descriptor will be provided in the final paper.

REFERENCES

[1]. Thomas R, Anderson Ed Hawkins and Philip D Jones (2016), "CO2, the greenhouse effect and global warming: from the pioneering work of Arrhenius and Callendar to today's Earth System Models" Endeavour Volume 40, Issue 3, 2016, 178-187.

[2]. Vasilis M. Fthenakis, Hyung Chul Kim, "Greenhouse-gas emissions from solar electric- and nuclear power: A life-cycle study" Energy Policy Volume 35, Issue 4, April 2007, Pages 2549-2557

[3]. Mario Tucci et al., "Contact Formation on a-Si:H/c-Si Heterostructure Solar Cells" Wilfried G.J.H.M. van Sark·Lars Korte Francesco Roca (Eds.) Physics and Technology of Amorphous-Crystalline Heterostructure Silicon Solar Cells, chapter 10.

[4]. Raisul Islam et al., "Si Heterojunction Solar Cells: A Simulation Study of the Design Issues", IEEE transactions on electron devices, vol. 63, no. 12, december 2016.

[5]. Dennai Benmoussa, M. Boukais, H. Benslimane, "Simulation of Hetero-junction (GaInP/GaAs) Solar Cell Using AMPS-1D", journal of nano- and electronic physics Vol. 8 No 1, 01009(3pp) (2016)

[6]. M. Mostefaoui, H. Mazari, S.Khelifi ,A.Bouraiou, R.Dabou. "Simulation of High Efficiency CIGS solar cells with SCAPS-1D software", Energy Procedia 74 (2015) 736 – 744.

Assessment of indoor air quality of construction and renovation site at Rajkot City- A Case Study

Denil Vachhani[1], Nirmit Kapadiya[1], Nisarg Vagadiya[1], Abhishek Gupta[1], Sneha Gautam[1]

[1]Department of Environmental Science & Engineering, Marwadi Education Foundation Group of Institution, Rajkot – 360001, India.

Keywords: INDOOR POLLUTION, AIR QUALITY INDEX, CONSTRUCTION ACTIVITY

ABSTRACT

Due to a rapid increase in the population of India, there is a hyper increase in the demand for residential areas resulting in a large number of constructional activities. Therefore this study mainly focused on exposure to the indoor environment and its health impact on the labour on both construction and renovation site. the result has shown very poor air quality at construction, i.e. prolonged exposure can result in upper respiratory disease, which on later stage can result in cancer and asthma due to deposition of dust, cement in the respiratory tract. Whereas results at renovation site are not so impactful as exposure time is very less as compared to the construction site. The daily average concentration of $PM_{2.5}$ and PM_{10} at construction are 332ug/m^3 and 162 ug/m^3 which is three times to the ambient air quality standards.

INTRODUCTION

Due to a rapid increase in the population of India, there is hyper increase in the demand of residential areas resulting in a large number of constructional activities. With a demand of smart city, need of constructional activity will be at more pace as of today (Esplugues et. al 2010). Constructional activity also leads to an increase in the indoor air pollution for fixed area or for a specific location. Construction activities that contribute to indoor air pollution include land clearing, operation of diesel engines, demolition, burning, and working with toxic materials. All construction sites generate high levels of air pollutions (typically from concrete, cement, wood, stone, silica) and this can carry for very far distances over a long period of time. Due use of this raw materials in construction work there is release of the pollutant such as $PM_{2.5}$, PM_{10}, Humidity, Temperature, CO_2, AQI, TOC which leads to the harmful health effect to the workers and near living society peoples. Among this all pollutants the major amount of the pollutant which is generated is PM_{10}, with the size of less than 10 micron in diameter which is invisible with naked eye. In major cities there is between 20-150 micrograms of particulates (PM_{10} 10 micron) per cubic meter of air. The amount of the PM_{10} over worldwide on the basis of year 2003-2010, as now there will big change in the countries as in the modern era (WHO 2000; WHO 2006).

According to the World Health Organization (WHO) it is today the single biggest environmental health risk with around 3.7 million premature deaths worldwide per year because of the ambient air pollutions (WHO, 2010). Among the most serious indoor air quality health issues is the potential exposure to construction/renovation-generated pollutants in the society areas. The constructions sites or renovation sites provides many potential exposure opportunities to pollutants (Zhao et. al, 2008). As the use of the raw materials for the construction activities such as cement, fine sand, red bricks, soils which lead to the $PM_{2.5}$ and PM_{10}. The application of tile adhesive, roofing materials, paints, and other products used during construction work provide point sources of volatile organic compounds (VOCs). There is also production of CO_2 by the use of the transport vehicles of supply of raw materials and used for the construction works like

digging then filling the concrete trucks, and by the smoking of the workers working at the sites. Similar type of study was carried out by Mandarick et al, 2018 for a photocopying shop at different location within shop.

METHODS

For current study indoor air quality was monitored for construction site and reconstruction activity. Total 2 sites were selected in different areas of the Rajkot. Monitoring of the concentration of pollutant present in indoor environment such as Air quality index, $PM_{2.5,}$ $PM_{10,}$ Humidity, Temperature and CO_2 was carried out. Sampling was done on 12hr basis. Sampling was carried out for a month, twice a week with the help of sensor based instrument of Airveda.

RESULTS & DISCUSSIONS

Sampling was done at two constructional sites, where results shown the variation in AQI, $PM_{2.5}$, PM_{10}, CO_2, Humidity, Temperature along day time. The results at site 1 was average in the morning and it goes high as the work been started, the level of the PM_{10} was high due to the ongoing work of application of the tiles at the site so by the use of adhesive chemicals the range of the PM_{10} reached high, as the range of other parameters where in the average state (Good as per Indian AQI) (Fig 1).

Figure 1: Variation in PM_{10}, $PM_{2.5}$, CO_2 concentration and variation in Humidity, temperature, AQI at renovation site.

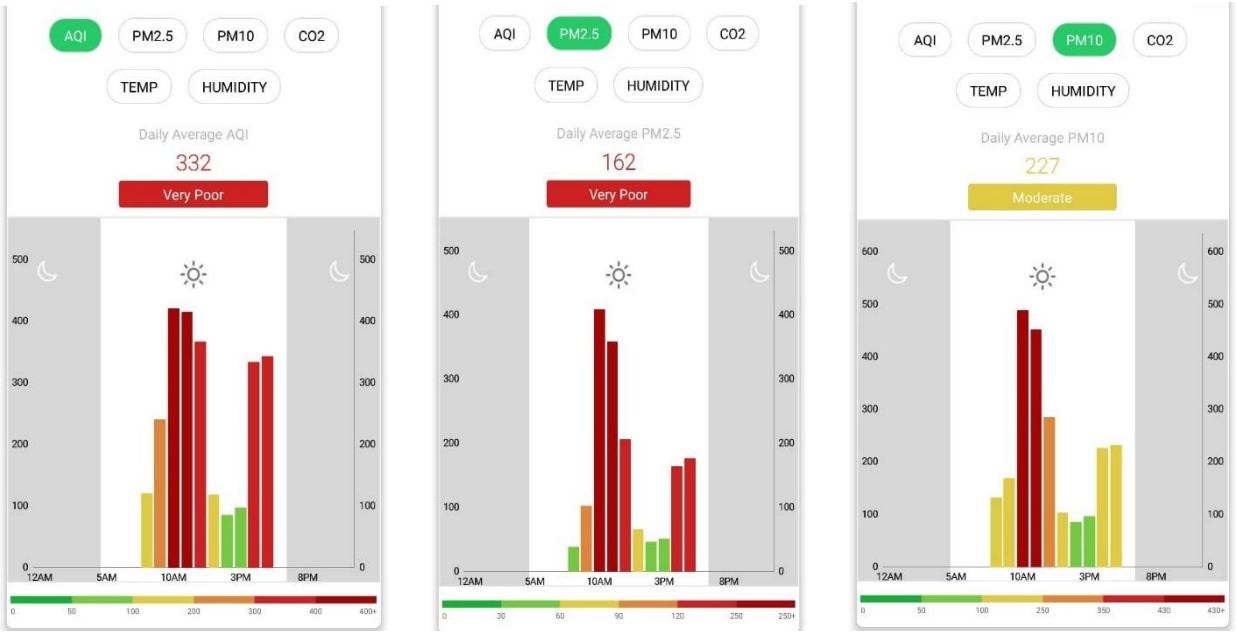

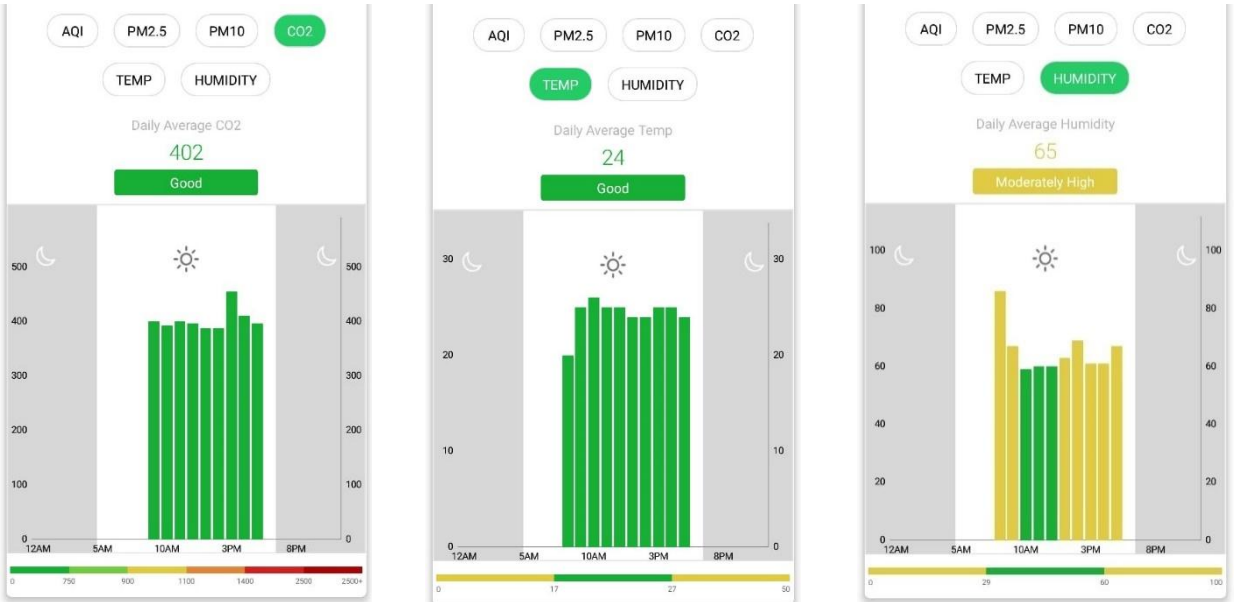

Figure 2: Variation in PM_{10}, $PM_{2.5}$, CO_2 concentration and variation in Humidity, temperature, AQI at construction site.

Result for site 2 i.e. constructional site where cement and concrete based work is going on, was found to be under very poor condition. AQI was very high i.e. 332 (Fig 4) which on higher level. Application of sand, cement, grit & concrete has also resulted in increased concentration of $PM_{2.5}$ and PM_{10}.

A total of 10 sample at each site were collected, variation in PM_{10}, $PM_{2.5}$ were done for day time as shown in Fig 5, Fig 6. In the renovations sites the range of the $PM_{2.5}$ were in very good conditions but due to the flooring work there is peak values in the PM_{10}. It got high due to the use of the adhesive chemicals and other cement materials and grinding work done at the sites

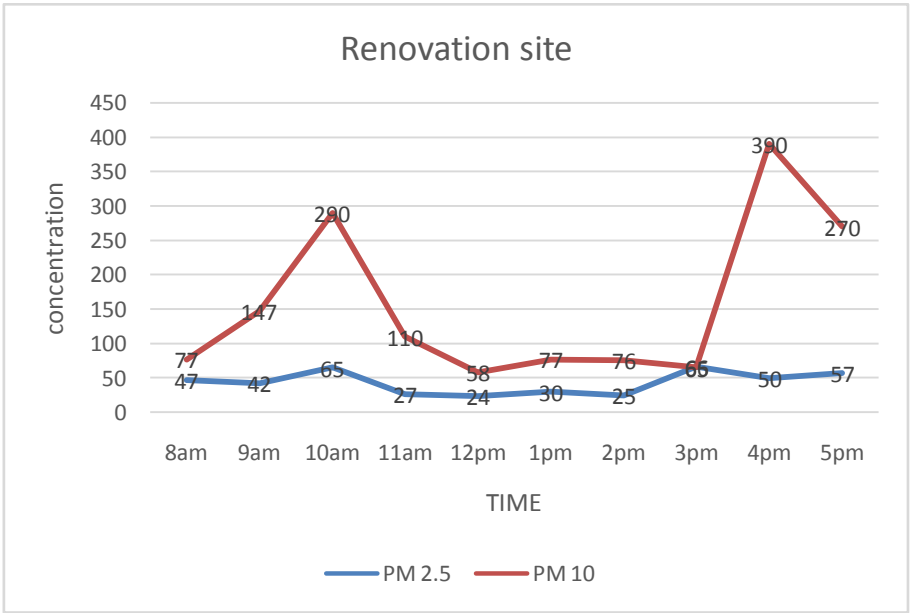

Figure 3: Average concentration of PM_{10}, $PM_{2.5}$ at Site 1

.

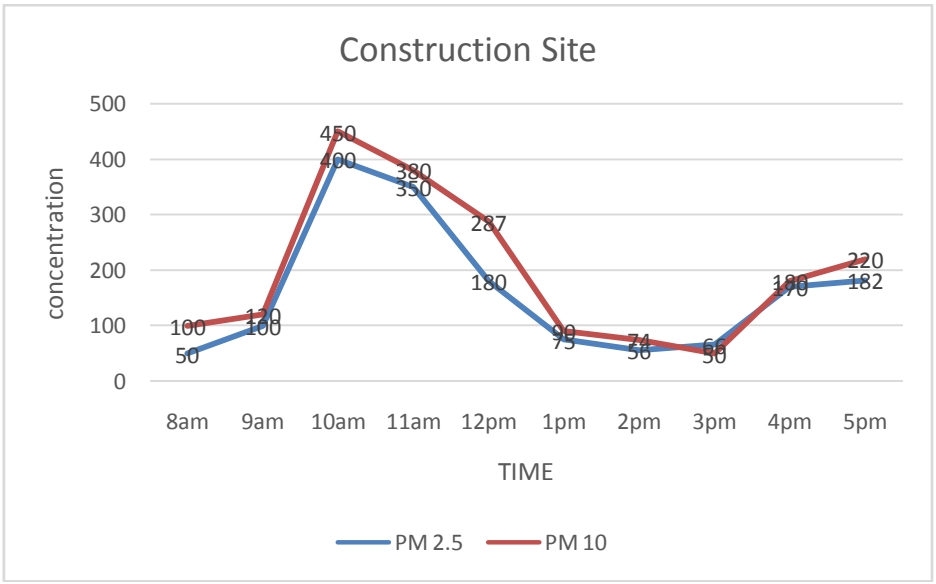

Figure 4: Average concentration of PM_{10}, $PM_{2.5}$ at Site 2

EFFECT OF AIR POLLUTIONS AT CONSTRUCTION SITES: -

The effects due to the generation of pollutant at the constructions sites are very dangerous to the health of the workers and if there is near by society area is there. The effects have two types :- 1) Acute and 2) Chronic; The acute effects are that which can show the result on the spot such as headache, cough, mold spores, itching, eye burning, runny noses which can be caused by the use of the chemicals at the sites for the different purposes. The chronic effects are the effects which are show after the duration of the period or which can be a permanent also. The effects caused are cancer, asthma, skin diseases, stress occurrence, discomfort of working due the unfresh atmosphere, Etc.

REFERENCES

Mandarić S., S. Aksentijević and J. Kiurski (2018). Statistical approach for characterization of photocopying indoor pollution,.*Air Quality, Atmosphere & Health.* 11(7), 867-881.

Esplugues A, F. Ballester, M. Estarlich, S. Llop, V. Fuentes, E. Mantilla and C. Iñiguez (2010) Indoor and outdoor concentrations and determinants of NO_2 in a cohort of 1-year-old children in Valencia, Spain. *Indoor Air*, 20,213–223.

Zhao, Z., Z. Zhang, Z. Wang, M. Ferm,Y. Liang and D. Norbäck (2008). Asthmatic symptoms among pupils in relation to winter indoor and outdoor pollution in schools in Taiyuan, China. *Environ. Health Persp*. 116, 90–97.

WHO (2000). Air Quality Guidelines for Europe. Copenhagen, Denmark. World Health Organization Regional Office for Europe.

WHO (2006). Air Quality Guidelines Global Update 2005. Copenhagen, Denmark, World Health Organization Regional Office for Europe.

WHO (2010). Guidelines for Indoor Air Quality: Selected Pollutants. Copenhagen, Denmark: World Health Organization Regional Office for Europe.

PECTIN / FLYASH BASED BIONANOCOMPOSITE FILM FOR FOOD PACKAGING APPLICATIONS

Keerthana.P, Sri Nidhi.G.R, Vishnuvarthanan.M#

Department of Printing Technology, College of Engineering Guindy, Anna University, Chennai – 600 025. Tamil Nadu. India

#E-mail: vishnuvarthanan.india@gmail.com

In recent times, the demand for the use of packaging materials made of biopolymers has been greatly increased due to the environmental problems occurred by the non biodegradable petroleum based packaging materials (Shankar et al. 2016). In this, the pectin has attracted much attention in food packaging due to the good processing ability, environmental friendly nature and adequate mechanical and barrier properties. The mechanical and barrier properties of biopolymer packaging materials are limited in packaging application. The improvement of such properties can be achieved by reinforcing the nanofillers with the biopolymers and form the composites. It shows high mechanical and thermal properties, low gas and watervapour permeability as compared to neat biopolymer. The coal burning thermal power stations generates large amount of fine powdery by product known as Fly-ash (FA) (Nath et al.2010). It is a mixture of alkali and transition metal oxides mainly of aluminium, iron and silicon with a minimal percentage of potassium, calcium, sodium, magnesium and titanium (Ward et al. 2006). The bionanocomposite films of pectin were reinforced with 1,3,5,7 and 9 wt% of flyash with 1 wt% of glutaraldehyde were prepared by solution casting method.

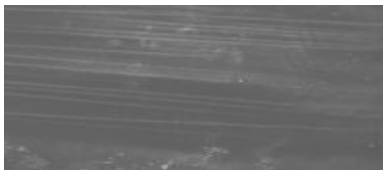

Figure 1: SEM micrograph of pectin / flyash

All the prepared composite films were flexible. The pectin / flyash based nanocomposite films exhibited the rough structures with evenly distributed flyash. The flyash was distributed homogeneously in the surface through the whole film and it was observed in surface view.

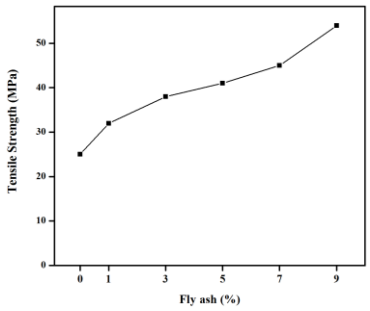

Figure 2: Tensile Strength of Pectin / flyash

The homogeneously distributed nano flyash in pectin attributed to the increase in tensile strength compared to the neat pectin film. This was due to the good interfacial interactions between the pectin and flyash.

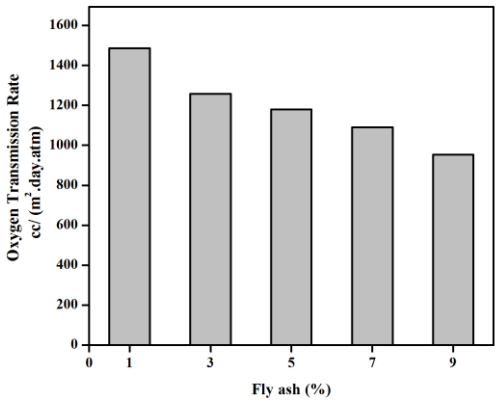

Figure 2: OTR of Pectin / flyash

The addition of nano flyash reduces the oxygen transmission rate (OTR) because of the tortuous path and increases the diffusion path of length.

References:

[1] C.R. Ward, D. French, Fuel 85 (2006) 2268-2277

[2] S.Shankar, N.Tanomrod, S. Rawdkuen, S, J.W. Rhim, 92 (2016) 842-849.

[3] D.C.D. Nath, S. Bandyopadhyay, J. Campbell, A. Yu, D. Blackburn, C.White, 257 (2010) 1216-1221.

SEEC No. 097

CFD ANALYSIS OF LATENT HEAT ENERGY STORAGE SYSTEM WITH DIFFERENT GEOMETRIC CONFIGURATIONS

Naman Bartawal
School of Engineering
Indian Institute of Technology Mandi
Email: naman_bartwal@students.iitmandi.ac.in

Hani Chaudhary
School of Engineering
Indian Institute of Technology Mandi
Email: T17017@students.iitmandi.ac.in

Pushpendra Kumar Shukla
School of Engineering
Indian Institute of Technology Mandi
Email: D16055@students.iitmandi.ac.in

Dr. P. Anil Kishan
School of Engineering
Indian Institute of Technology Mandi
Email: kishan@iitmandi.ac.in

ABSTRACT

Latent heat storage technology is being used worldwide to bridge the gap between supply and demand of energy. The material stores energy during the charging process and releases energy during discharging process. The phase change processes include solidification and melting, boiling and condensation and sublimation and reverse. In spite of having various advantages such as high storage energy density, it suffers from the fact that most Phase Change Materials (PCMs) commonly used have very low thermal conductivity, hence, very slow charging/discharging times. In the current work, a shell and tube type heat exchanger with phase change material on the shell side and heat transfer fluid on the tube side are considered. The effect of flow rate and inlet temperature of heat transfer fluid on melting and solidification times are investigated. The major difficulty encountered in the melting of the PCMs is the accumulation of melted (hot) part at the top while the solid (unmelted) part remains at the bottom, which decreases the efficiency of the system to quite a great extent. An attempt has been made to improve the efficiency of the system by considering various configurations of the heat exchanger.

Keywords: Phase Change Material, Charging/Discharging times, Shell and Tube heat exchanger

SEEC No.098

UTILIZATION OF AGRICULTURAL WASTE FOR THE PRODUCTION OF BIO-OIL AND BIO-CHAR

Sutapa Das
Chemical Engineering /IIT Guwahati
Email: sutapa.das@iitg.ac.in

Dr.Vaibhav V Goud
Chemical Engineering /IIT Guwahati
Email: vvgoud@iitg.ac.in

ABSTRACT

Energy plays a significant role in the everyday activity of human life. The most widely used conventional sources of energy are coal, petroleum, methane, natural gas etc. To reduce the dependency on these natural resources due to many inherent disadvantages, researchers have started to focus on non-conventional renewable resources. Biomass is organic material derived from plants and animals. India being the second largest producer of rice in Asia, it produces huge amount of rice husk as waste. These wastes can efficiently be converted into various valuable products. There are many processes like pyrolysis, gasification, liquefaction etc. to effectively utilise these wastes to produce bio-oil. Pyrolysis is an age old technique, it is basically thermal decomposition of materials at an elevated temperature in an inert atmosphere.. In the current study, based on the TGA analysis, pyrolysis of agricultural residue i.e. Rice husk has been carried out at temperatures ranging from 300 °C to 600 °C along with the varying residence time (20 min – 60 min) . The bio-oil yield of 35wt% which is the maximum is found to be at 500 °C. The composition of bio-oil was determined by GC/MS. Bio-char yield decreased with the increase in pyrolysis temperature.

Keywords: *Renewable Energy,Pyrolysis, biomass, bio-oil yield, bio-char yield, waste utilization*

.

INTRODUCTION

The beginning of this millennium has witnessed the inception of a technological era which will be self-sustaining and moving forward with a limitless potential. With the burgeoning issue of the human population and the ease of accessibility of modern technology, the energy consumption per capita has seen an exponential rise in the last few decades. Conventional sources, like fossils feedstock, are being utilizing to the limit and their potentials are being strained to meet the energy demands. At the current rate of consumption these feedstocks are predicted to last till the turn of the century [2]. To avoid falling into the trap of overdependence on these fuels as the prolonged use of these resources may leave us with scarcity of fuels in future, researchers in have tried to address this issue by finding alternative energy sources. Examples of which include; solar, wind, biomass, hydro, marine, nuclear, geothermal etc. One approach which has the potential to supplement and eventually replace the current fossil fuels, is biofuel. Mixing biofuels into the fossil fuel derivatives being currently used has the added advantage of reducing the carbon footprint along with easing the emission of greenhouse gases to the surroundings.

The major source of this biofuels are the natural, plant based derivatives called biomass. Biomass, is an umbrella term, as it refers to all organic materials that are obtained from plants (including woody material, grass, algae, trees and crops) via natural processes or by intervention of human activities. Another way of looking at it is, it is basically the energy of sun light which is stored in the form of chemical bonds in the plants. In the present scenario, this particular source of energy constitutes nearly 10–14%

of the world energy supply, but has the potential to contribute much more. [1, 2]. According to a report by the European Environment Agency (EEA, 2013), in order to comply with the goal of developing a greener future with a much reduced carbon footprint, 20% of the final energy consumption has to be provided using renewable resources such as biofuels by the end of this decade. Hence, utilizing biomass would only aid our endeavor of reducing our reliance on fossil fuels in a sustainable and eco-friendly. However, one concerning issue has been the traditional usage of biomass, which has many negative effects.

Present-day approaches to the utilization of biomass, with the goal of meeting the energy demands, has been beset with negative environmental consequences [2, 4]. A well-documented example of this is the case-study related to the paddy production in India. India is the second largest paddy producer in the world, and according to the FAO report, in 2016, India produced nearly 165.5 million tonnes of paddy, which is 110.4 million tonnes on milled basis and this corresponded to around 55.1 million tonnes of rice husk generation, which is rather seen as a waste and hence of the overall production 33% of the biomass goes as waste [1_fao]. Rice husk is mainly discarded either by dumping or by open incineration, which results in serious health issues besides contributing to environmental concerns. The resultant ash contains crystalline silica particles which have been deemed hazardous as they fall under the category of dust particulates in the size range of PM 2.5 and PM 10 [2]. Hence, a efforts have are being put in to efficiently utilize these resources for the production of valuable silica-based compounds like nanocomposites, composite fillers, refractory materials and catalysts industries [5]. Studies have been undertaken to enhance the value added products derived from rice husk are already but still this field remains unexplored. The geographic location of the rice husk plays an important role on its composition which mainly consists of 54 – 56% cellulose and hemicellulose, 25% lignin and 20% extractive matter [6]. Along with this, around 15-30% of inorganics, mainly silica is also present [7]. Hence, in addition to the utilization of lignocellulosic composition, the inorganic components such as silica could also be used for the enhancing the overall valuation of this product. One such technique which has embraced for the effective conversion of rice husk is Pyrolysis. Pyrolysis, in addition to being a versatile process is also convenient, economical, established and suitable for a variety of biomass sources leading to the eventual production of bio-oil [8]. Various feedstocks such as wood, sawdust, corn-cob, palm shell, wheat straw, rice straw, rice hulls and peanut shell have been studied as potential sources [9].
Results and Discussion:

Effect of Temperature on Bio-oil and Bio-char yield:

The pyrolysis of rice husk was carried out from 300 to 600°C which is shown in figure 1 . With the increase in temperature, the bio-oil yield initially increased upto 500°C and then decreased at 600°C. Initial temperature of 300°C, is not sufficient for the complete degradation and volatilization of the biomass. With the increase in temperature the bio-oil yield keeps on increasing, however after 500°C, there is a decrease in bio-oil yield to 24wt% from 35wt%. This decrease could be due to the fact that volatile matter products decreases at temperature above 500°C. Also, the decondary cracking starts at this temperature which further decreases the yield. In case of bio-char yield, there is a decrease with increase in pyrolysis temperature. This could be due to the fact that higher temperature promotes the release of volatiles, also due to secondary cracking the gas yield increases with the decrease in bio-char yield. The release of volatiles depends on the degree of breakdown of cellulose, hemicellulose and lignin. Rice husk is also rich in inorganics specially silica, which is also a reason for higher bio-char yield. However the analysis of bio-char showed that with the higher temperature, the carbon content decreased with the increase in pH.

FIGURES

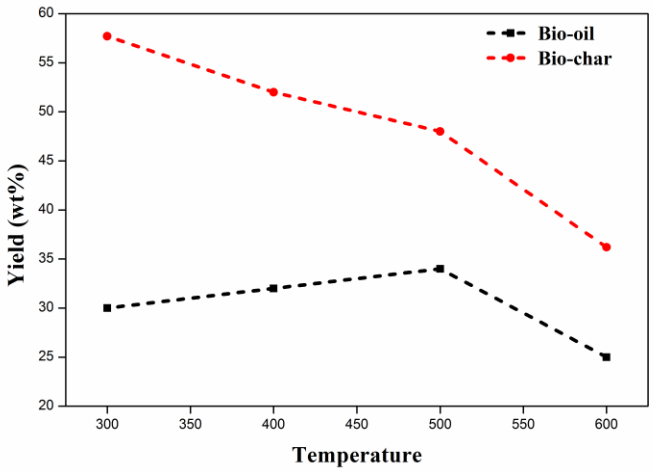

FIGURE 1. Effect of temperature on bio-oil and bio-char yield

REFERENCES

[1] Zhang S, Chen T, Xiong Y. Effect of washing pretreatment with aqueous fraction of bio-oil on pyrolysis characteristic of rice husk and preparation of amorphous silica. Waste and Biomass Valorization, 2018; 9: 861-869.

[2] Patel KS, Gupta S, Ramteke S, Rajhans KP, Nava S, Lucarelli F. Silica Particulate Pollution in Central India. Journal of Environmental Protection, 2016; 7: 170.

[3] Chen D, Liu D, Zhang H, Chen Y, Li Q. Bamboo pyrolysis using TG–FTIR and a lab-scale reactor: Analysis

of pyrolysis behavior, product properties, and carbon and energy yields. Fuel, 2015; 148: 79-86.

[4] Islam MN, Ali MHM, Haziq M. Fixed bed pyrolysis of biomass solid waste for bio-oil. In: ed.^eds., AIP Conference Proceedings. AIP Publishing, 2017; pp. 020015.

[5] Carmona V, Oliveira R, Silva W, Mattoso L, Marconcini J. Nanosilica from rice husk: extraction and characterization. Industrial Crops and Products, 2013; 43: 291-296.

[6] Worasuwannarak N, Sonobe T, Tanthapanichakoon W. Pyrolysis behaviors of rice straw, rice husk, and corncob by TG-MS technique. Journal of Analytical and Applied Pyrolysis, 2007; 78: 265-271.

[7] Mansaray K, Ghaly A. Physical and thermochemical properties of rice husk. Energy Sources, 1997; 19: 989-1004.

[8] Saikia R, Baruah B, Kalita D, Pant KK, Gogoi N, Kataki R. Pyrolysis and kinetic analyses of a perennial grass (Saccharum ravannae L.) from north-east India: Optimization through response surface methodology and product characterization. Bioresource technology, 2018; 253: 304-314.

[9] Mohan D, Pittman CU, Steele PH. Pyrolysis of wood/biomass for bio-oil: a critical review. Energy & fuels, 2006; 20: 848-889.

lysis of rice husk in a fluidised bed reactor. Journal of the Energy Institute, 2011; 84: 73-79.

[29] Abnisa F, Daud W, Jaya Narayan S. Optimization and modeling of bio-oil production from palm shell by pyrolysis using response surface methodology. 2010.

Proceedings of the Third International Conference on Sustainable Energy and Environmental Challenges (3rd SEEC)
18 –21 December 2018, IIT Roorkee, India

SEEC No. 099

EFFECT OF HEATING COIL CONFIGURATION ON ENERGY REQUIREMENTS OF LOCAL HEATING SYSTEM

Pushpendra Kumar Shukla
School of Engineering
Indian Institute of Technology Mandi
Email: D16055@students.iitmandi.ac.in

P. Anil Kishan
School of Engineering
Indian Institute of Technology Mandi
Email: kishan@iitmandi.ac.in

Atul Dhar
School of Engineering
Indian Institute of Technology Mandi
Email: add@iitmandi.ac.in

ABSTRACT

The space heating in residential buildings accounts for a considerable amount of the high-grade electricity consumption. Therefore, understanding the operation and performance of space heating systems becomes crucial in improving occupant's comfort while reducing energy use. The current study will try to demonstrate the energy saving by implementing the local heating when only particular space heating is of interest. In this work, an experimental as well as the numerical study of a dome over a bed, was performed. Various heating coil configurations namely floor coil, roof zig-zag, and roof spiral were constructed to find the best configuration for the localized space heating. Experiments and simulations are carried out with the variable flow rate and varying inlet temperature of the heat transfer fluid. It is found that the floor coil heating gives better results. A temperature difference of 20 ^oC is maintained between the space under consideration with the surroundings.

Keyword: Local heating, energy efficient buildings, energy saving, space heating.

NOMENCLATURE

BTU British thermal units
PCM Phase change material
LHTES Latent heat thermal energy storage
A Heat transfer area (m^2)
C_P Specific heat (kJ/kg)

INTRODUCTION

Buildings account for 20–40% of the total final energy consumption and its amount has been increasing at a rate of 0.5–5% per annum in developed countries [1]. In contrast, energy savings with minimal additional cost can be achieved by smart use of energy. As per US Energy Information Administration 2018 report, the 2400 trillion BTU energy used for space heating. Which is around 27.3% of total energy consumption in the residential sector [2]. In today's time, we all must together think for energy saving possibilities.

The local heating concept is one of the possibilities by which we can save a substantial amount of energy. The idea behind the concept is that when the small area of room/space is needing to be heated, then there is no point to heat full room/space.

In present work, a small attempt is done by which theoretically around 50% amount of energy saving can be achieved. In this work, an insulated dome is constructed over the bed with copper piping for heat transfer. For optimum design, different configurations of the copper piping are considered in the current study. Water is used as heat transfer fluid as it is inexpensive and readily available. So, the concentrated area is heated whenever it is required. In this way not only, energy saving can be done but also environmental benefits can also be achieved.

The solar energy integration can be done with the local heating setup in which PCM based latent heat thermal energy system (LHTES) will be used which will further increase the efficiency of the system.

DESIGN AND SIMULATION MODEL

The experimental setup used for the local heating system (dome over bed), is shown in figure 1a. The geometries used for the numerical simulations with the copper coil at the bottom and on the roof are shown in Figure 1b and 1c.

Figure 1a: Dome over bed local heating experimental setup

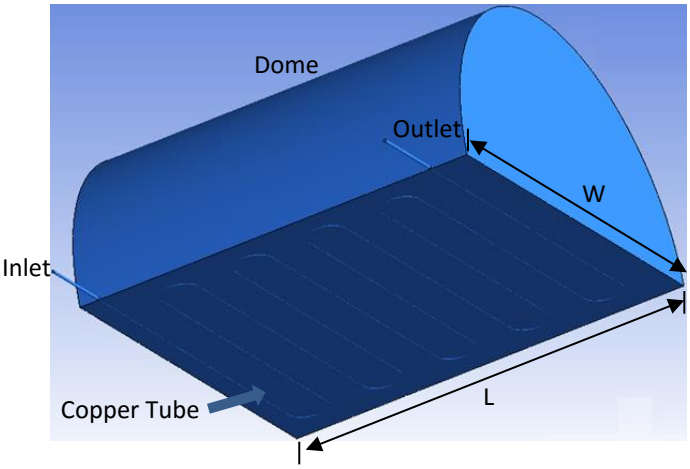

Figure 1b: Dome over the bed with floor coil

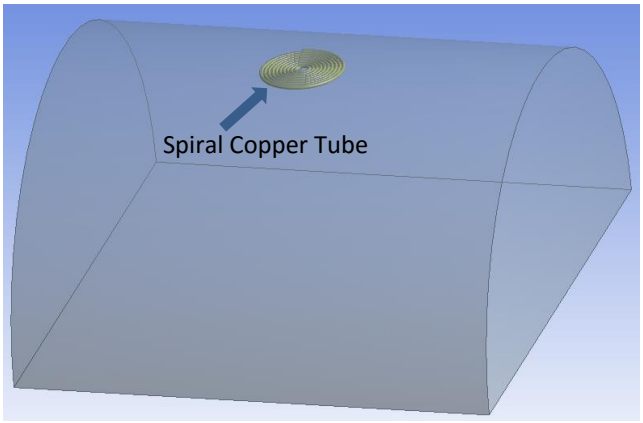

Figure 1c: Dome over bed with spiral coil at top

Hot fluid (water) enters the dome through copper pipe inlet and exits the dome through the outlet. The base of the experimental setup is made with plyboard with a polyester cotton be. The roof of the setup is made with foam. The size of the bed is 6.5 ft x 3 ft.

To start the experiment, water is heated using electric heater up to the required temperature (say, 65 °C). The temperature of the water is maintained with the help of temperature controller. Hot water is circulated through the copper tube using 18 Watts desert cooler pump. Heat is transferred from the heat transfer fluid to the space to keep the space at warm conditions. As the dome is insulated, inside temperature can be maintained around 25°C while the surrounding temperature is around 10°C. The simulation studies of the experiments were performed to find the temperature distribution inside the dome. This distribution will help to have the best heating configuration and for more effective utilization of energy. The dimensions and boundary conditions used for simulations are given in table 1 and 2 respectively.

Table 1: Geometry specifications

PARAMETER	**DIMENSIONS (all in cm)**
Length of bed	60.9 cm (1/3rd of original length)
Width of bed	92 cm
Dia./ Height of dome	46 cm
Dia. of the coil	1.27 cm
Surface area of dome	8798 Sq. cm
Surface area of coil	2231 Sq. cm

Table 2: Initial Boundary Conditions

Description	Boundary Condition	Input Conditions	
		Thermal	Flow
Hot Water Inlet	Mass flow rate	338K	0.5 kg/s
Hot Water Outlet	Pressure Outlet	-	Atm.
Cold Air Inlet	Mass flow rate	283K	0.01 kg/s
Cold Air Outlet	Pressure Outlet	-	Atm.
Walls	wall	Adiabatic	-

Figure 2 shows the results from the experimental study with various copper tube configurations. This graph shows the temperature of the surroundings and the temperatures of the space using floor coil, zig–zag copper coil on the roof, spiral coil on the roof for whole night, from 09:00 PM to 9:00 AM (12 hours) when outside temperature of the room was around 10°C. It is clearly seen that floor coiled

and zig-zag coiled setups give more temperature inside the dome for same input conditions.

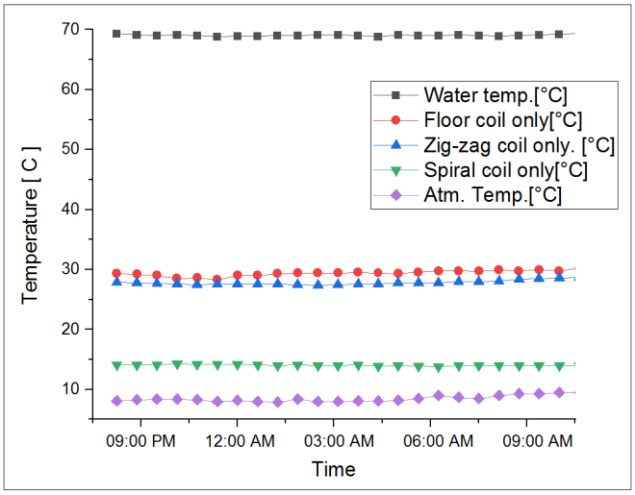

Figure 2: Average temperature at the midpoint of the dome for same inlet conditions for 12 hours

Figure 3 shows the computational domain and boundary conditions used for CFD simulations of the dome over the bed. The Geometry is made in Ansys Design Modular, and Ansys Fluent 18.1 was used for simulations. The whole domain was divided into small control volumes and all the equations are solved for each control volume.

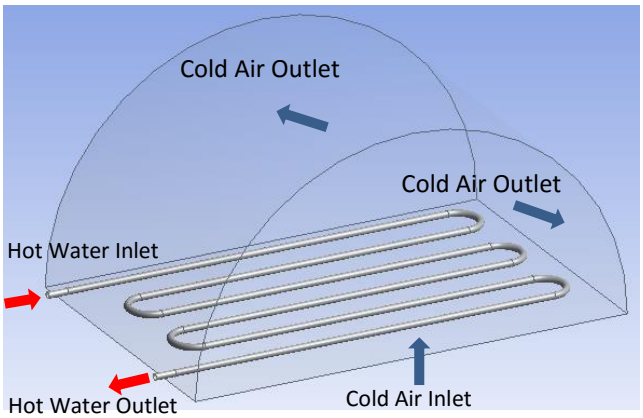

Figure 3: Computational domain for simulations

VALIDATION

The experimental results were used for validation. Four thermocouples were installed in the experimental setup as shown locations in figure 4a. The temperature data were compared at same points and results were found in good agreement with very less error. Figure 4b shows the validation bar graph in the same points. It can clearly seen that the simulation results are very close to the temperatures measured with experimental results. Hence, it is assumed that the equations solved (ref [4]) will provide correct results in the other studies also. Further electrical energy can be replaced by solar energy or any waste heat. In all the cases, the same equations are used without considering the origin of the heat transfer fluid's energy.

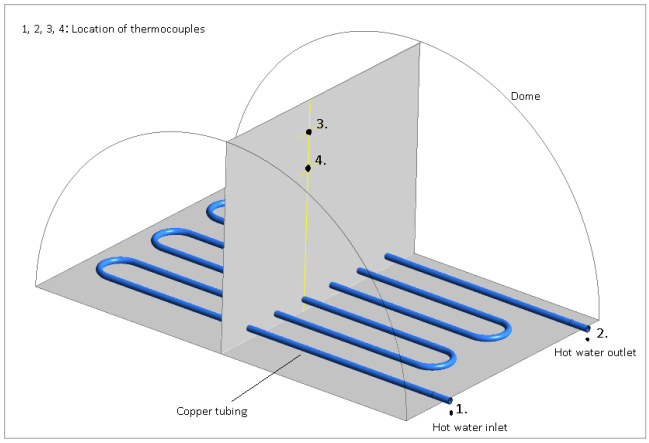

Figure 4a: Location points of thermocouples in the experimental setup

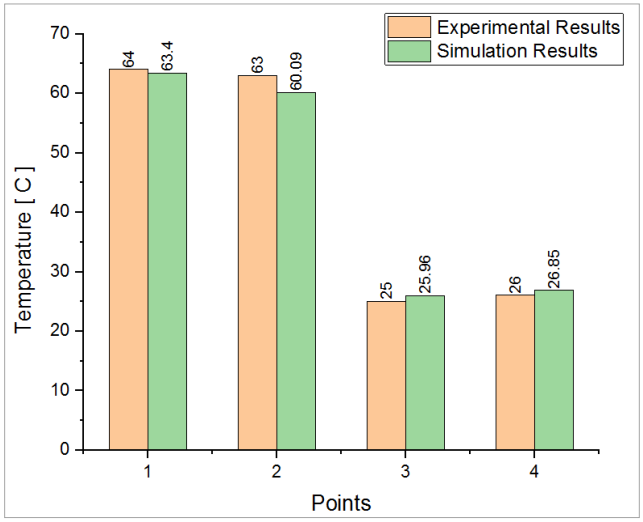

Figure 4b: Validation bar graph in the same data points.

RESULTS AND DISCUSSION

The equations were solved for the given configuration using Ansys Fluent 18.1 for multiple cases with varying mass flow rate (0.25, 0.50 and 0.75 m/s) and hot water inlet temperature (55, 60 and 65°C) for all three configurations. The boundary conditions along with the flow conditions are shown in table 2.

Figures 5a and 5b show the temperature contour for the floor coiled setup, in front and perpendicular plane respectively. In which the average temperature inside the dome is maintained around 25°C.

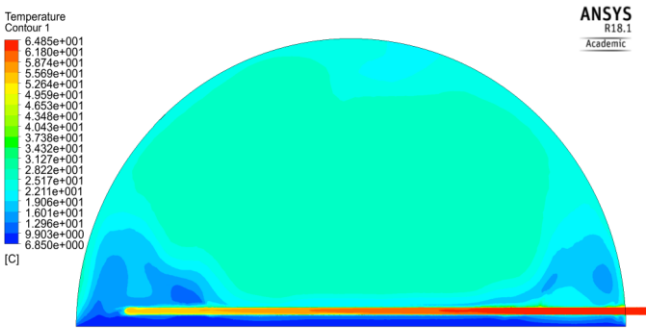

Figure 5a: Temperature contour in front plane

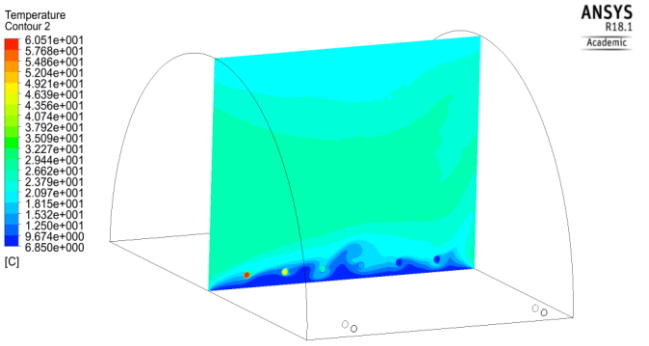

Figure 5b: Temperature contour in perpendicular plane

Figure 6 shows the velocity streamlines inside the dome. It can be seen the air movement throughout the domain and good mixing of various streams. Hence, it can be assumed that the temperature of the space is uniform.

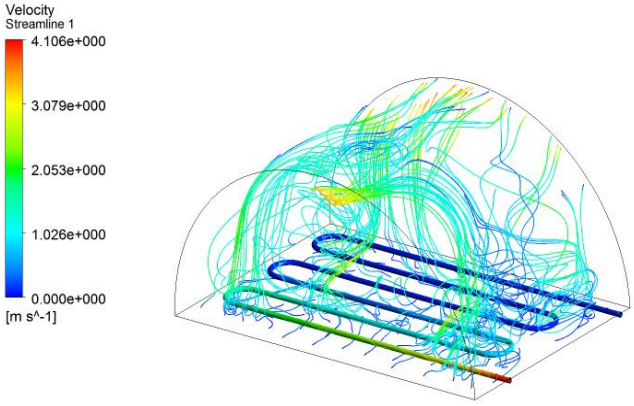

Figure 6: velocity streamlines inside the dome

The temperature variation for floor coiled setup along the height of the dome (yellow line in figure 4a) shown in figure 7a. The ends of the graph are the temperature of the top (dome roof) and bottom (bed ply floor) of the setup. The decrement of temperature at the top is due to heat loss to the surrounding. The figure shows that a temperature difference of 15 ^{o}C can be maintained between the surroundings and space in the dome.

Figures 7b – 7d depict the effect of variation in inlet temperature and mass flow rate of the heat transfer fluid (water). Figure 7b shows the temperature variation along the height of the dome for all three configurations at same inlet conditions. In the case of the spiral coil at the top, heat transfer is mainly by conduction. Hence, the highest temperature is observed near the dome. In the case of floor coil, the heat transfer is by convection. Hence, we see that the temperature of the air is more uniform near the dome. In the case of zig-zag coil, the heat transfer takes place by both fluid conductions as well as convection, because of the orientation of the coil at the roof. Hence, we see a mixed trend in the zig-zag roof coil.

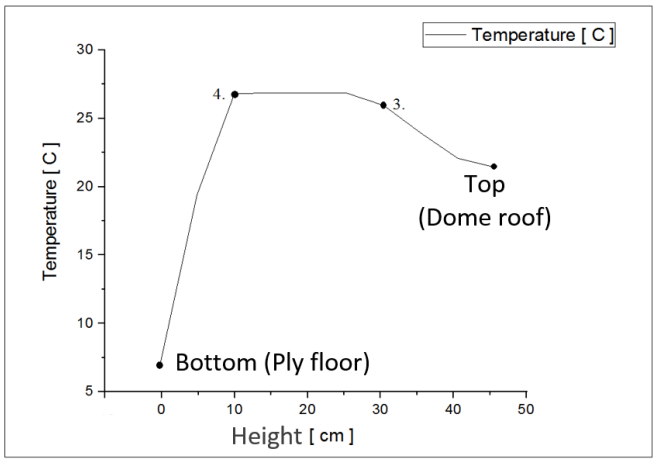

Figure 7a: Temperature variation along the height of the dome (yellow line in figure 4a).

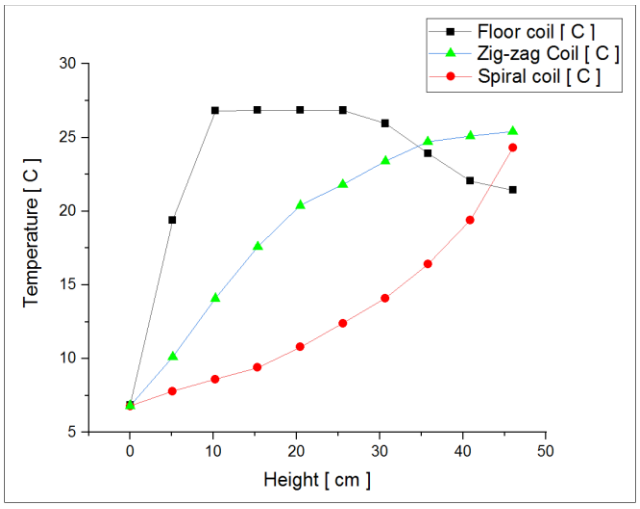

Figure 7b: Temperature variation along the height of the dome

Figure 7c and 7d show the effect of the inlet temperature and mass flow rate of the heat transfer fluid. It has good impact on heat transfer inside the dome, but it is seen that

after a certain limit the effect of mass flow rate and inlet temperature is not that much significant. The heat transfer is improved on the side of the heat transfer fluid due to increase in flow rates and inlet temperatures. But the heat transfer is poor on the air side. Hence, there are optimum values of flow rates and temperatures of the heat transfer fluids in maintaining the space at a prescribed temperature.

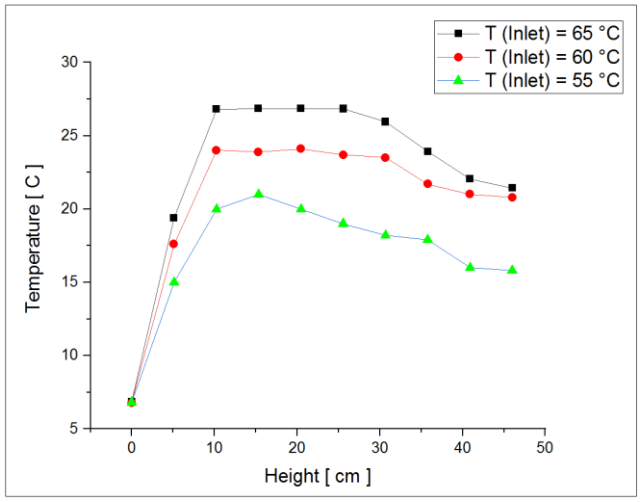

Figure 7c: Effect of hot water inlet temperature variation for floor coiled setup

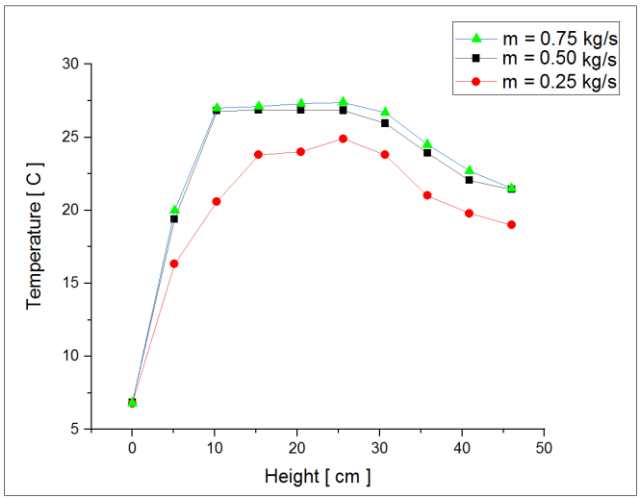

Figure 7d: Effect of mass flow rate variation for floor coiled setup

For the optimum value of flow rates and inlet temperatures of the heat transfer fluids, further simulations are needed to be done.

CONCLUSION

In the current study, an attempt has been made to heat the local space. An experimental setup has been fabricated and experiments were performed with various inlet flow conditions. Numerical simulations were performed with different configurations of the copper coil. Simulations are performed to find the temperature distribution of the space with various flow conditions. It is found that the bottom coil and zig – zag coil will maintain the space above 15 – 20 °C to that of the surroundings. It is also observed that there is a limit in the mass flow rate and inlet temperature of the heat transfer fluid beyond which the improvement in conditions are minimum.

Acknowledgments

Dr. P. Anil Kishan acknowledges the financial support provided by SERB, DST through grant ECR/2015/00526, 'Solar Energy Storage Using Phase Change Materials for Space Heating Applications'.

REFERENCES

[1] Perez-Lombard L, Ortiz J, Pout C. A review on buildings energy consumption information. Energy Building 2008;40(3):394–8.

[2] https://www.eia.gov/outlooks/aeo/pdf/AEO2018.pdf

[3] Lof, G.O.G. (1977) "Systems for Space Heating with Solar Energy" Chapter XII, Applications of Solar Energy for Heating and Cooling of Buildings. ASHRAE GRP 170.

[4] E. Meng, H. Yu, G. Zhan, and Y. He, Experimental and numerical study of the thermal performance of a new type of phase change material room, *Energy Conversion and Management* 74 (2013), 386 – 394.

[5] S. Behzadi and M. M. Farid, Experimental and numerical investigations on the effect of using phase change materials for energy conservation in residential buildings, *HVAC&R Research*, 17:3 (2011), 366 – 376.

[6] Alva, G., Liu, L., Huang, X. & Fang, G. Thermal energy storage materials and systems for solar energy applications. Renewable and Sustainable Energy Reviews 68, 693–706 (2017).

[7] H. Niyas P. Muthukumar, "Performance investigation of a lab-scale latent heat storage prototype - Numerical results", Energy Conversion and Management, 135 (2017) 188–199.

Proceedings of International Conference on Sustainable Energy and Environmental Challenges(3rd SEEC), December 18-21, 2018, IIT Roorkee, India

SEEC No. 101

Remaining Useful Life (RUL) Prediction of Bearing by using Regression Model and Principal Component Analysis (PCA) Technique

Apakrita Tayade
School of Engineering
IIT Mandi
t17007@students.iitmandi.ac.in

Sangram Patil
Department of Mechanical Engineering
V.J.T.I. Mumbai
sangram.patil@gmail.com

Vikas Phalle
Department of Mechanical Engineering
V.J.T.I. Mumbai
vmphalle@me.vjti.ac.in

Faruk S Kazi
Department of Electrical Engineering
V.J.T.I. Mumbai
fskazi@el.vjti.ac.in

Satvasheel Powar
School of Engineering
IIT Mandi
satvasheel@iitmandi.ac.in

ABSTRACT

A wind turbine works under variable load and environmental conditions because of which failure rate has been on the rise. Failure of the gearbox, an integral part of producing wind energy, contributes to 80% of the total downtime for the wind turbine. For ensuring better utilization of the wind turbines, Fault prognosis and condition monitoring of bearings are of utmost importance as it helps to reduce the downtime by early detection of faults which further increases the power output. Included in this paper is the study of vibration signals produced and machine learning approach to determine the Remaining Useful Life (RUL) for a range of faults occurred. The methodology includes statistical feature extraction analysis with regression models.

Further, the feature selection and optimization are done using Principal Component Analysis (PCA) technique which produces training and testing sets which acts as an input parameter for the given model. Weibull Hazard Rate Function is used for calculating the RUL of the bearing. This study shows the potential application of the regression model as a useful tool for degradation performance prediction of bearing.

Proceedings of International Conference on Sustainable Energy and Environmental Challenges (3rd SEEC), December 18-21, 2018, IIT Roorkee, India

SEEC No.102

Improvement in asphalt binder by waste plastic: from waste to wealth

Akanksha Pandey
Department of Polymer and Process Engineering,
Indian Institute of Technology Roorkee, Uttarakhand,
India
Email: apandey@pe.iitr.ac.in

Sumit K. Singh[1]
Department of Polymer and Process Engineering,
Indian Institute of Technology Roorkee, Uttarakhand,
India

Yogesh Kumar[2]
Department of Polymer and Process Engineering,
Indian Institute of Technology Roorkee, Uttarakhand,
India

Sham S. Ravindranath[3]
Assistant Professor
Department of Polymer and Process Engineering,
Indian Institute of Technology Roorkee, Uttarakhand,
India

Abstract:

Increasing awareness for the consumption of enormously generated plastic waste and concern for improving the performance of road stimulated the incorporation of waste into the asphalt binder, which resulted as a reduction in expenditure for road construction with a decrement in piles of waste. The purpose of this short note was to increase the understanding regarding the application of waste material in road construction. For that, some experimental work has been done. Many publications have reported that if the waste material will be used with few percentages of pristine polymers than it is storage stable and shows enhanced properties. Even though it is true if all polymers are recycled like crumb rubber and recycled plastic. So the further studies should be focused on commercialization of binder modification (waste plastic modified binder) via wet process.

Keywords: *Waste plastic, asphalt binder, dry process, wet process.*

Introduction:

Sustainability is a way to maintain the demand of the current system without compromising the availability of resources for future [1]. Resources which are used for road construction are naturally occurring material i.e. asphalt binder, aggregates, lime etc. As the economy and social growth are rising the demand for highways, road is also increasing which causes exhaustive usage of natural resources. To reduce the exhaustion of natural resources and increase the life of pavement alternative ways are budding i.e. binder modification.

In recent year plastic become an inseparable and mandatory component of daily life which causes the increment in demand with the generation of waste. Recently asphalt binder modification has been started by using waste plastics for the consumption of plastic waste and reduction in the landfilling [2,3]. So the purpose of this paper is to accelerate the awareness regarding the waste plastic utilization in the flexible pavement and provide an alternate way for the effective utilization without any difficulties i.e. stripping, raveling, cracking etc.

Norms for waste utilization in the pavement

Application of waste as a pavement material is in practice with varying success ratio, world-widely. Some countries have set the standards and restricted the dosage which helps the respective department at the time of utilizing the existing waste material. Every recycled material which will be used for construction should follow the criteria similar to conventional material. Approximately all countries are focused on the utilization of recycled asphalt; like in USA 15-20 %, recycled asphalt pavement can be used. Similarly, State of Nebraska allow up to 50% RAP, department of transportation, Texas permit 20% usage of RAP and RCA, and Korean state transportation department restricts the use of toxic elements (copper, arsenic, and mercury) present in recycled construction products. The maximum limit of these elements is restricted to 3 mg/l, 1.5 mg/l, and 0.005 mg/l respectively. India is the one country where they have started using waste plastic for the pavement. The maximum dosage decided by CRRI is 8% while as 10 % by Dr. Vasudevan.

Implementation procedure of plastic waste in the pavement

The binder modification has been done from past 30 years, which carries modification by using some specific polymers. In recent years modification becomes a common practice that improves the serviceability of binder, the life of pavement with the increment in construction cost. Hence to reduce the construction cost with desirable properties alternative ways are implemented i.e. waste plastic utilization. For the utilization of plastic waste in the pavement, asphalt binder is modified by using waste plastic. For the binder modification, two different types of processes are in practice. First method cover preparation of plastic and asphalt binder blend by high and low shear mixing and then dumping the aggregates into a prepared blend that is known as a wet process. Many studies have been done on this section. Next method is to coat the aggregates with waste plastic and then add the binder which is known as dry process or Dr. Vasudevan method. The Ministry of Road Transportation and Highways (MoRT&H) has permitted the road laying by using dry process but the application area is limited.

Shortcoming of blending methods

Since the waste plastic and binder blending has two methods one is commercially implemented and another one only limited to the publication. Commercially implemented i.e. dry process has lots of limitations. The process of road laying and material used in this can only be used where average atmosphere temperature goes 25° C or above. At lower temperature cracking will initiate on the road. Another drawback is that it is more prone to stripping because this process smoothens the surface of the aggregate by coating the plastic which reduces the interaction of aggregates with a binder. With this, there is also a possibility of uneven distribution of plastic within the system which will cause mechanical properties deterioration. On the other hand in the wet process, no such problems will occur apart from storage instability. So the target should be focused on the waste plastic modified road by using a wet process with improved storage stability.

Literature Studies

Imran et al, 2016 [4] studied the behavioral change in asphalt binder after modifying it with different waste material i.e. LDPE, HDPE, Crumb rubber. The finding of the study was that the modified binder showed improvement in rheological properties.
M. O. Sulyman et al [5], 2013 studied the effect of crumb rubber and waste LDPE in the performance of asphalt binder. The composition ratio of LDPE and CR was 1:1, 1:1.5, 1:2, and 1:3. The outcome of this study shows that softening point, penetration, and viscosity was increased by 85% against unmodified binder. The 1:3 ratios of LDPE and CR show the best result.

Results

As M. O. Sulyman et al [5] found the impressive result by using CR and waste LDPE, this study shows the effect of SBS and LDPE in asphalt binder. The experiment was started by modifying the Tikitar VG 10 (softening point 48 °C and 85 PEN) with pristine LDPE and SBS. A detailed study on waste LDPE and SBS will be reported subsequently. The overall polymer concentration was 4.5% with the composition ratio of SBS and LDPE was1:3.
The experimental studies i.e. softening point, penetration, rheological analysis by dynamic shear rheometer was performed. The results show that the softening point and penetration value of SBB/LDPE modified binder was 71 and 45 respectively. The performance grading parameter $G^*/\sin\delta$ was $\geq$ 1000 Pa at 63 °C for Tikitar VG10 but modified binder shows $G^*/\sin\delta \geq 1000$ Pa at 80 °C.

Conclusion

The wet and dry both processes are focused toward the utilization of plastic waste in the pavement so that construction and maintenance expenditure can be reduced. The reason of this short note is to increase the awareness regarding the consumption of material in a rightful way. Since the dry process seems a simple way but it has some shortcomings. In case of a wet process having robustness even though all the studies are limited to the publications. The result of this study shows that the incorporation of polymer shows improvement in both conventional as well as rheological properties. So the future work will be focused on the evaluation of on-field performance and a comparison with samples which are made by the dry process.

References

1. Pradeep kumar gautam et al., 2018. “Sustainable use of waste in flexible pavement”. Construction and building materials, 180, 239-253.
2. Rafat Siddique et al., 2008. “Use of recycled plastic in concrete: A review” . Waste management, 28, 1835-1852.
3. Sinan Hınıslıog et al., 2004. “Use of waste high density polyethylene as bitumen modifier in asphalt concrete mix”. Material Letter, 58, 267-271.
4. Imran M. Khan et al. 2016. “Asphalt Design using Recycled Plastic and Crumb-rubber Waste for Sustainable Pavement Construction”. Procedia Engineering, 145, 1557 – 1564.

5. Mohamed O Sulyman et al., 2013. “New Study on Improved Performance of Paving Asphalts by Crumb Rubber and Polyethylene Modification”. Material Science & Engineering 2, 2-4.

.

SEEC No.103

DESIGN ANS ANALYSIS OF SUNFLOWER SOLAR SYSTEM

Rahul Goswami
Mechanical engineering/GLA University
rrg18070@gmail.com

Abhay Singh
Mechanical engineering/GLA University
Abhay.singh_me15@gla.ac.in

ABSTRACT

Solar energy-gathering technology is on the rise which absolutely means good news for our environment. In this paper I will introduce the sun flower solar panel that follows the Sun throughout the day. The detail of design and analyzing parameters has been discussed in this research work. As opposed to the static solar panels this will much like a sunflower, follows the direction of the sun to ensure that it gathers as much sunlight as it can through-out the day. This means it will capable of producing 40% more energy than regular solar panels. Sunflower will capable of generating the electricity which is equivalent of an average household's daily use of electricity. The main advantage of this system is it automatically moves to face the sun throughout the day and at night or during strong winds, it folds itself up back into it's face. It's daily routine consist's of unfolding at the break of down and instantly facing the direction of the Sun.

Keyword: ***Sun flower, Ansys, Solar enegy***

Proceedings of the Third International Conference on Sustainable Energy and Environmental Challenges (3rd SEEC)
18 –21 December, 2018, IIT Roorkee, India

SEEC No. 104

EXPERIMENTATION ON ROTATING DISK BASED WATER PURIFICATION SYSTEM

Sunil Kumar Saini
Department of Mechanical Engineering
Indian Institute of Technology Bombay
Email: 114100007@iitb.ac.in

Milind V Rane
Department of Mechanical Engineering
Indian Institute of Technology Bombay
Email: ranemv@iitb.ac.in

ABSTRACT

A corrugated rotating disk based mass exchanger was used for oxygenation of water. Experimental determination of the mass transfer coefficient and solution oxygenation rates is reported using a batch type aeration equipment. The experiments indicate a strong influence rotational speed and depth of submergence on the mass transfer coefficient. Mass transfer coefficients were determined by linear regression fit between log mean concentration difference and time.

Keywords: ***Rotating Contacting Disk, Aeration, Water Purification, Mass Transfer Coefficient, Sulphite Oxidation***

NOMENCLATURE

a	surface area per unit volume, m^2/m^3
$C_l(t)$	O_2 concentration at time t, mg/l
C_{ln}	logarithmic concentration difference ratio
H	submergence level, mm
He	Henry's constant
k_{la}	volumetric mass transfer coefficient, m/s
$m^*_{O_2}$	O_2 solubilty in water, mg/l
$M_{Na_2SO_3}$	sulphite in solution, g
N_d	number of disks in shaft
R	equivalent radius based on geometrical area, mm
RCD	rotating contacting disk
th	disk thickness, mm
θ	center angle of submergence at disk center

INTRODUCTION

The rivers flowing in Indian subcontinent are the lifeline of more than 1.5 billion people as these rivers provides source of water which is used for different purposes such as drinking, agriculture, and different industrial applications. The banks of these rivers allowed human settelment to flourish and laid down the foundation of ancient civilizations. Indus valley civilisation is one of the notable example which flourished at river Sindhu's bank. These rivers are also contributing to the ground water source in these areas. Due to the immense significance to the human life, these rivers are often called as goddess and mother.

However, these rivers are facing severe pollution problem due to rapid industrialization and population explosion. Ganges and Yamuna which are most important rivers of northern India have become a dumping ground of extremely polluted water coming from industry and untreated sewage system. Water coming from industries contains high concentration of heavy metals such as (Cr, Cd, Pb), phenol derivatives and VOCs (BTX, MTBE, etc.) which affects the aquatic life of these water source [1]. Gharial and Ganges river dolphin are only found in Indian subcontinent and facing threat of extinction [2]. Moreover these pollutants often diffuse into soil and mix with underground water thereby increasing the severity of the problem. Such polluted water is not usable for direct human consumption as it results in severe health problems.

Due to the severity of the problem ***Government of India*** has lunched various schemes such as ***Namami Gange Programme and Yamuna Action Plan [3][4]*** for Cleaning of rivers ***Ganges*** and ***Yamuna*** respectively. These schemes prioritize the treatment of waste water before direct discharge into these rivers. However, in absence of any cost effective and simple technology for water treatment full scale implementation of these schemes is still a challenge.

WATER PURIFICATION TECHNOLOGY: CHALENGES AND SOLUTION

Water aeriation and VOC stripping are important operations which are performed in order to improve the BOD, COD and removal of toxic substances such as BTX from water. In most of the cases these operations are performed at near atmospheric pressure in packed column. Packed column operation suffers from high pressure drop on the air side, flooding and high specific power consumption. Clogging of packing due to algae formation, often results in partial or total shut down of column operation. Treatment of large quantity of water in the municipal corporations limits the use of conventional technology based on packed columns [1].

Bubbling air through water is another technology in which pressurized air is dispersed as fine bubbles in water column with help of sparger. These small bubbles provides large surface area to enable oxygen transfer. Such type of technology is power consuming. Rotating packed bed, mechanical surface aerators are also utilized for above purpose [5]. High power consumption in these mass exchangers make them unsuitable for water treatment technology.

Rotating contacting disk, RCD, or rotating biological contactors, RBC, are often employed for waste water treatment as it can handle large quantity of water with low power consumption [6]. The rotating contacting disk based mass exchanger are usually prepared by assembling the circular disk on a shaft. The contactors are partially submerged in a pool of water and rotated with the help of motor. While rotating the disks pickup liquid film which forms the interphase for gas liquid contact. One of the major drawback of such arrangement is that wetting is only observed in the peripheral section of the disk dipped in water. Use of flat disks limits the mass transfer at the surface. This issues is addressed by texturing the disks and deploying them in series and parallel configurations of the RCD based rotors.

Absorption of gases into any absorber from a mixture of gases is very complex physiochemical process which involves formation of thin liquid film on disk surface, transportation of species from bulk gas phase to liquid film through gas liquid inter phase, mixing of this liquid film into the bulk of liquid, and formation of concentration boundary layer adjacent to the rotating disks. Experimental data is not reported for such textured disk based RCD. Theoretical modelling of these textured disk based RCD will be very complex and time consuming.

This work deals with design, development and deployment of patented multipurpose RCD based mass exchanger [8][8]. Developed mass exchanger was used for water aeration as well as VOC stripping, gas scrubber and horizontal distillation application.

TEST SETUP AND EXPERIMENTATION

The test setup **1** for batch aerator for water is shown in Figure 1. It consists of RCD based mass exchanger which works as a purifier. The rotors **2** were made by mounting the corrugated disk **3** on square shaft **4.** The length of the shaft was taken as 200 mm and total number of disks mounted on shaft were 30. Both ends of the rotor shaft were closed with end plugs **5** in order to hold the end disk. A trough **6** having 305 mm diameter was prepared by bending it in semi-circular manner and inserted in semi-circular groves in a 10 mm acrylic sheet. A 25.4 mm diameter UPVC pipe **7** was glued at the bottom of the trough. This pipe works as probe holder, as the probe is inserted in this pipe for DO measurement. The rotor was rotated using a DC motor **8**. The measurements were performed using a Lutron 5509 O_2 probe **9.** Change in water level in the trough was measured using a 90^o bend tube **10**.

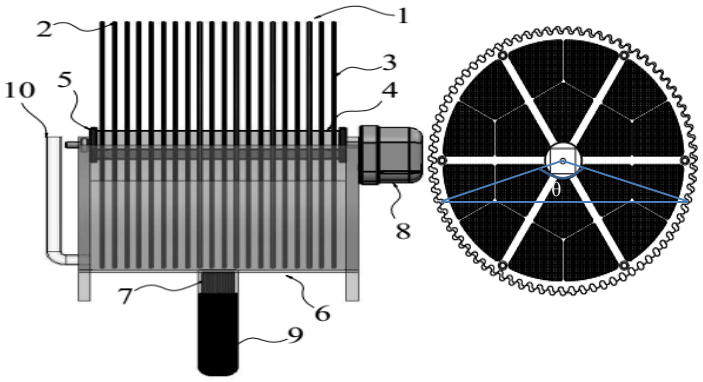

Figure 1: Rotating Contacting Disk Based Mass Exchanger

STOCK SOLUTION PREPRATION

Experiments were performed in batch mode where known volume of solution was filled in the trough. The mass transfer parameters such Oxygen transfer rate, OTR; logarithmic concentration difference ratio ,C_{ln}; and mass transfer coefficients were measured at various liquid submergence level in trough and rotational speed of rotor.

Test solution was prepared in a separate tank and transferred to the trough via 12.7 mm silicon tube. The dissolved oxygen in water was eliminated by adding the sodium sulphite in water.

$$Na_2SO_3 + \frac{O_2}{2} \rightarrow Na_2SO_4 \qquad ...(1)$$

Based on the stoichiometry, 126 g of Na_2SO_3 was added for consuming 16 g of dissolved Oxygen in water. Total amount of Na_2SO_3 (98.5% purity level) required based on the solubility of O_2 in water is 8 mg/l and considering Sodium Sulphite added at 200% excess to the stoichiometric ratio.

$$M_{Na_2SO_3} = \left(1+\frac{exs}{100}\right)\left(\frac{1}{w_{Na_2SO_3.Pur}(\%)}\right)\left(\frac{w_{Na_2SO_3.stoch}}{w_{O_2.stoch}}\right)m^*_{O_2} \quad ...(2)$$

METHODOLGY FOR DATA ANALYSIS

The dynamic method [9] for the determination of volumetric mass transfer coefficient involves the measurement of the O_2 concentration in liquid phase with respect to time.

The mass balance of O_2 in two specific instances t_o and t could be given as

$$\frac{dC_l(t)}{dt} = k_l\, a\left(\frac{C_{O2}}{He} - C_l(t)\right) \quad ...(3)$$

Integrating between two time step t_o and t we get

$$k_l\, a = \frac{\ln\left(\frac{(C_G/He)-C_{O_2}(t)}{(C_G/He)-C_{O_2}(t_o)}\right)}{t-t_o} \quad ...(4)$$

Converting the above equation in terms of solubility

$$k_l\, a = \frac{\ln\left(\frac{m^*_{O2}-m_{O2}(t)}{m^*_{O2}-m_{O2}(t_o)}\right)}{t-t_o} = \frac{C_{\ln}}{\Delta t} \quad ...(5)$$

Here C_{ln} is the logarithmic concentration difference ratio and Δt is the time in which the O_2 content in water reached the C(t). The graph between Δt and C_n are straight lines where slope of the curve represent the mass transfer coefficient.

The specific surface area, a, in this analysis has been considered to be equal to the geometrical surface area. The exposed surface area for partially submerged disk and available for gas liquid contact was calculated using the equation given by Ravetkar and Kale, (1980)[10].

$$a = \frac{A_T}{V} = N_d\left(A_s + A_p\right) + 2R\left(L - N_d t_{th}\right)\sin\left(\frac{\theta}{2}\right) \quad ...(6)$$

Where $A_s = 2\pi R^2\left[\frac{(2\pi-\theta)}{2\pi} + \frac{\sin\theta}{2\pi} - \frac{(1+\cos\theta)}{2}\right]$ and

$A_p = (2\pi-\theta)Rt_{th}$

RESULT AND DISCUSSION

The experiments were performed at various rotational speeds which were achieved by varying the DC voltage from DC power source. The submergence levels 30 mm, 45 mm, 60 mm, 75 mm, were considered for the analysis. For each submergence level experiments corresponding to five rotational speeds 10 rpm, 15 rpm, 20 rpm, 25 rpm, and 35 rpm were considered for the testing.

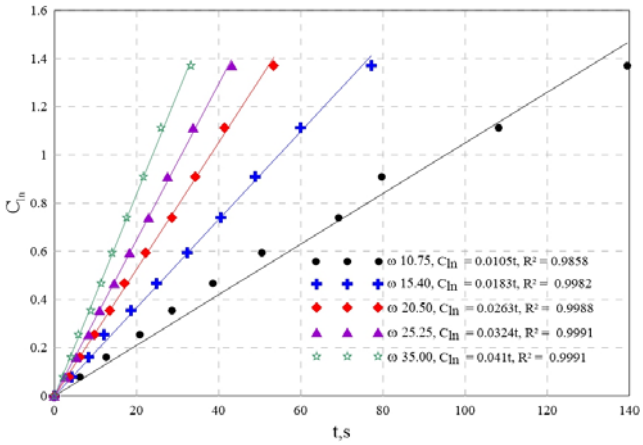

Figure 2: Variation of C_{ln} with time for H 45 mm

The test results for 35% submergence at various speed of rotation is shown in Figure 2. The graph between C_{ln} and t results in various inclined straight lines passing through the origin. The slope obtained by linear fit of these lines provides the value of volumetric mass transfer coefficients. At high rotational speed higher mass transfer coefficient was observed at all submergence level and could be attributed to the high churning effects. The mass transfer coefficient at various submergence level and rotational speed shown in Table 1.

Table 1: Variation of Liquid Phase Mass transfer Coefficient with Rotional Speed

Sr #	ω rpm	K_{la}, 1/s H = 30 mm	H = 45 mm	H = 60 mm	H = 75 mm
1	9.75-10.00	0.0093	0.0105	0.0103	0.0111
2	15.40-16.24	0.0155	0.0183	0.0198	0.0212
3	20.50-21.00	0.0219	0.0263	0.0275	0.0289
4	25.25-26.00	0.0296	0.0324	0.0335	0.0341
5	34.75-35.00	0.041	0.0419	0.0455	0.0486

Similar results were also obtained for the other level of submergence. The values for these tests are shown in Figure 3. To compare the results obtained from the experiments, the volumetric mass coefficients were converted to liquid phase mass transfer coefficient by dividing the volumetric mass transfer coefficient with geometrical surface area. It was assumed that the surface area available for gas liquid mass transfer will be similar to

the geometrical surface area available from the corrugated disks.

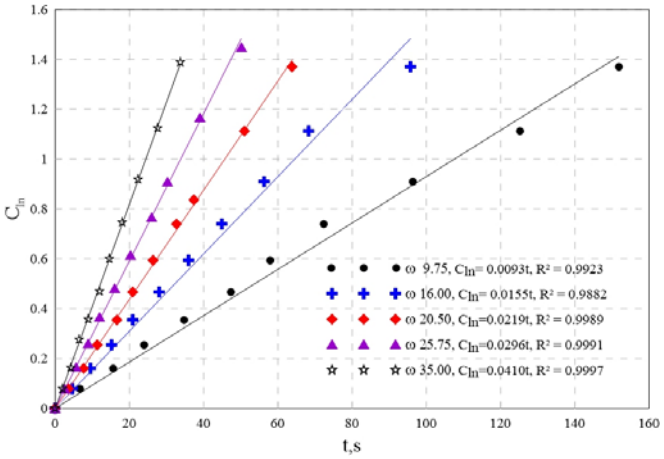

Figure 3: Variation of C_{ln} with time for H 30 mm

The present results are compared with the results from Zeevalkink *et al.*, (1979). (1974) [11]in which they have performed the tests with RCD based contactors under similar experimental conditions. All experiments were performed using flat disks. The comparison of results is shown in Figure 5.

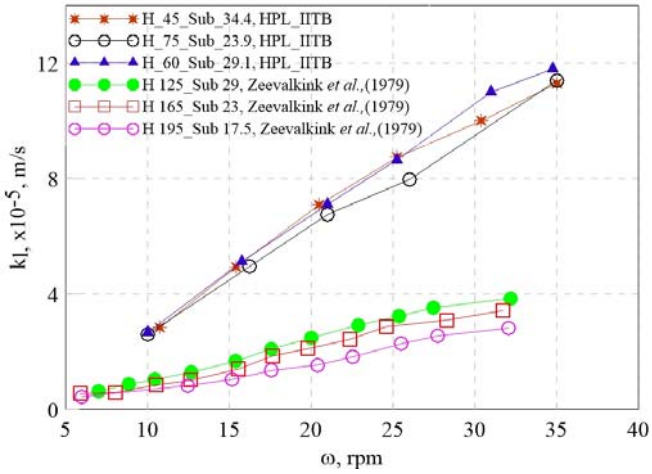

Figure 5: Variation of k_l with rpm at Various Submergence Levels

Corrugated Disk HPL_IITB,) N_{dsk} 30, d_{dsk} 300mm, d_{pitch} 10 mm, t_{dsk} 2.3 mm

Zeevalkink et al., (1979), N_{dsk} 10, d_{dsk} 600mm, d_{pitch} 20 mm, t_{dsk} 20 mm

It is observed that curve of k_l vs ω for noval corrugated disk always lies above the k_l vs ω curve for flat disk based rotors reported by Zeevalkink *et al., (1979).* Comparison between two value at submergenece level ~29% shows that the mass transfer coefficient for HPL_IITB disk found to be 8.6×10^{-5} m/s (25.25 rpm) while for the flat disk reported by Zeevalkink *et al.*, (1979) [11] found to be 3.23×10^{-5} m/s (25.4 rpm). The mass transfer coefficient was for novel HPL_IITB disks was 2.6 times higher as compared to the flat disks. Inspite of the fact that the disk used in the present study are of 300 mm diameter. If the disks size were larger the k_l would have even higher.

CONCLUSION

Mass transfer characteristics of novel corrugated disk were determined using batch process mode. It was found that volumetric mass transfer coefficient found to be dependent on rotational speed and depth of immersion in trough. Mass transfer performance of newly developed HPL_IITB Corrugated disk are found to be 2.66 times higher than the mass transfer performance of flat disk from reported in literature.

ACKNOWLEDGMENTS

Fincial support from Tata Center at IIT Bombay for Funding the Project on TCTD_WEMWBS_125837.

REFERENCES

[1] Hendricks D, 2011, Fundamentals of water treatment unit processes : physical, chemical, and biological, CRC Press,Taylor and Francis Group, 6000 Broken

[2] Rao R J, 2001, "Biological resources of the Ganga River, India" Hydrobiologia, 458: 159–168

[3] http://pib.nic.in/newsite/PrintRelease.aspx?relid=132647 accessed on 10/10/2018

[4] https://nmcg.nic.in/index.aspx accessed on 10/10/2018

[5] Agarwal L, Pavani V, Rao D P, Kaistha N, 2010, "Process Intensification in HiGee Absorption and Distillation: Design Procedure and Applications", Ind. Eng. Chem. Res, 49, pp; 10046–10058

[6] Patwardhan A W,2003,"Rotating Biological Contactors: A Review" Ind. Eng. Chem. Res., Vol 42, pp 2035-2051

[7] Rane M V, Saini S K, 2017, "Modular Rotating Contacting Disk Based Mass and Heat Exchanger", Indian Patent Appl. No 201721029712, DOF 22/9/2017

[8] Rane M V, Kota S V K, 2006, "Contacting Device for Effective Heat And Mass Transfer", Indian Patent, IP203949

[9] Riet K V, 1979, "Review of Measuring Methods and Results in Nonviscous Gas-Liquid Mass Transfer in Stirred Vessels", Ind. Eng. Chem. Process Des. Dev., 1979, 18 (3), pp 357–364

[10] Ravetkar D D and Kale DD, 1981, "Gas Absorption into Non-Newtonian Fluids in Rotating Disc Contactors", Chemical Engineering Science,Vol 36, Issue 2, 1981, pp 399-403

[11] Zeevalkink, J A, Kelderman P, Visser D C, Boelhouwer C 1979, "Physical Mass Transfer in a Rotating Disc Gas-Liquid Contactor", Water Research, Vol.13, Issue 9, pp 913 to 919

SEEC No.105

Comparative analysis of normal concrete by using of granite cutting waste for construction work

Varun Agarwal[1], Garvit Singh[2], Shreyas Dharmeshkumar Desai[3], Kushal Joshi[4]

[1]Department of Environmental Science & Engineering, Marwadi Education Foundation, Rajkot; e-mail: varunkumar.agarwal@marwadieducation.edu.in.
[2,3,4] Department of Environmental Science & Engineering, Marwadi Education Foundation, Rajkot;

ABSTRACT

Ordinary Portland cement, sand and coarseaggregate mixed with normal concrete.it is very high cost cement compare to other. If addition of granite cutting powder with cement in various proportion in normal concrete then cost is low as compare to other normal concrete.day by day its strength will increase.in this particular project we are trying to make green concrete for environment by the help of industrial waste.the shortage of natural materials are decreasing day by day,so we are utilising the industrial material like granite cutting waste is used in concrete by replacing cement.another aim of our project is to reduce cost of concrete.in this project the main focus is given to the cost, the granite cutting is more cheaperthen cement. The made concrete with granite powder has good compressive strength but weak in tensile,to increase the tensile strength we added polyester fiber.by using the fiber in concrete the tensile strength become higher then normal concrete. There are 9 batch we have casted. Batches of compression and split tensile test are OPCAI (50%granite cutting waste) , A2(40%granite cutting waste) , A3(30%granite cutting waste), A4(20%granitecutting waste)A5(60%granite cutting waste), & B1(20%granitr cutting waste+ 125 gm. Fiber) , B2(20% granite cutting waste + 50 gm. Fiber) , B3(20% granite cutting waste + 200 gm. Fiber).

Key words:

Cement, granite cutting waste, coarse & fine aggregates, chemical admixture

Introduction

INDIA is a developing country and infrastructure growth is going high with developing nation and the concrete is a basic need for civil construction. Recycled material is helping hand material in civil construction material. Concrete is an extensively used material across the world. On the other hand recycling of waste without scientific research it will cause environmental problem which is more harmful than normal waste itself.

25Billion tonnes concrete is used by across the world by one year.450 million cubic meter concrete is consumed by INDIA within a one year. After the water it is the mostly consumed material across the world.it is a heterogeneous mixture of cement , aggregates and water.Concrete is used in every single construction sector. We get granite cutting waste from various industries [1]. Each year 112 million tons of granite cutting waste is produce in India.use it in the development enterprises as non-customary material. We are additionally getting advantage as far as quality and decrease in the expense by utilizing this sort of waste material. The most imperative advantage is decreased porousness to water and forceful synthetic compounds. Legitimately restored cement made with rock cutting waste makes a denser item on the grounds that the measure of the pores are lessened. This builds quality and lessens porousness. Quality in cement relies upon numerous variables, the most critical of which is the proportion of water to concrete. Great quality stone cutting waste for the most part enhances functionality or possibly delivers a similar usefulness with less water. The decrease in water prompts enhanced quality. Contains bigger or less responsive particles than Portland bond, critical hydration can proceed for a half year or more, prompting considerably higher extreme quality than cement without rock cutting waste. Today, concrete is utilized in an assortment of creative outlines as a result of its numerous profitable properties,

for example, high compressive quality, firmness, low warm and electrical conductivity and low instability and harmfulness. Be that as it may, concrete is likewise known to be fragile and feeble in pressure and creates splits amid relieving, because of warm development and withdrawal over some stretch of time The ongoing advancement of Secondary fortification in Concrete in different fields has given a solid specialized base to enhancing these lacks.

Filaments are designed Micro Fibers with a one of a kind "Triangular" Cross-segment, utilized in Secondary Reinforcement of Concrete. It supplements Structural Steel in upgrading Concrete's protection from Shrinkage Cracking and enhances mechanical properties, for example, Flexural/Split Tensile and Transverse Strengths of Concrete alongside the coveted change in Abrasion and Impact Strengths [2].

Our primary point of venture is to complete the similar examination between normal concrete by utilizing the rock cutting waste as far as Strength.

2. Materials and methods

Below listed raw material (granite cutting waste) was added to concrete at higher percentage as compare to cement to reduce the cost of concrete and also make the green concrete for environment.

2.1 Raw materials

Granite Cutting Powder: The cutting waste of granite powder was procured from Jalore (Rajasthan), as shown in Fig.1.

Cement: It is as an ingredient in the production andcan be cast in almost any shape desired and once hardened can become a structure element.

Course and fine aggregates: It was used to make up the bulk of a concrete mixture and the important help of course and fine aggregates is to provides significant economic benefits for the final cost of concrete in place , also Controlling shrinkage of the concrete material [2].

Water:A lower water to cement ratio yields a stronger, more durable concrete, while more water gives a free-flowing concrete with a higher slump.

Chemical admixture: Admixtures are materials other than cement, aggregate and water that were added to concrete either before or during its mixing to alter its properties, such as workability, curing temperature range, set time or colour.

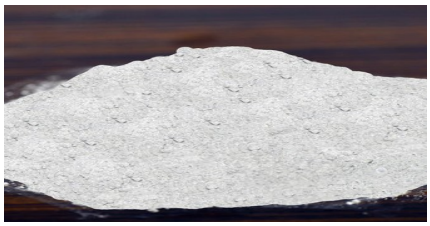

Fig. 1 Granite cutting powder

2.2 Methods

There were various methods to analyse the concrete like Sieving analysis ,initial settling time , final settling time , Compressive strength ,Tensile strength etc [3].

For this project we conduct various methods for testing of concrete.

- **Sieving analysis**
- **Initial selling time**
- **Final settling time**
- **Compressive strength**
- **Tensile strength**

2.3 Testing of material

Table 1 For sieve analysis of aggregates for concrete :

TYPE	SIEVE DESIGNATIONS
Square hole, perforated plate	80-mm, 63-mm, 50-mm, 40-mm, 31.5-mm, 25-mm, 20-mm, 16-mm, 12.5-mm, 10-mm, 6.3-mm, 4.75-mm
Fine mesh, wire cloth	3.35-mm, 2.36-mm, 1.18-mm, 600-micron, 300-micron, 150-micron, 75-micron

2.4 Testing of granite waste using initial and final settling time

It was used to find out the consistency, initial setting time and final setting time of the cement. It has an arrangement to hold the plunger of 10 mm diameter and two other needles which were made to freely fall into a mould filled with the cement paste. Vicat apparatus was used for the determination of settling time which shown in Fig.2.

Fig. 2 Vicat apparatus

Initial settling time: Generally 30minutes require for initial settling time by any cement but it can be increased by adding gypsum up to 60 minutes. Initial setting time is the time from the mixing of the cement and the water to the time when the penetration of the needle is just above 5 mm from the bottom of the base plate or mold.

Final settling time: Generally 10 to 12 hours needs for final settling time by any (OPC).For the final setting time we have to use the third needle which has an larged 5 mm hollow cylindrical base. It is the time for the mixing of the water , when this needle just makes the impression on the surface of the cement but do not penetrate into it.

3. Result & Discussion

3.1 Compressive strength test: The most common performance measured used by the engineer in designing buildings and other structures and it can measured by breaking cube concrete specimens in a compression-testing machine.strength was calculated from the failure load divided by the cross sectional were resisting the

load and reported in units of pound-force per square inch(psi) in US customary units or Megapascals (MPa) in SI units. The results are shown in Table-2.

Table 2 compressive strength results of concrete with use granite cutting waste

No.	Type (cement/granite)	7 days (MPa)	14 days(MPa)	28 days(MPa)
1	40/60	7.43	10.82	24.17
2	50/50	8.01	12.48	25.51
3	60/40	16.80	22.17	28.21
4	70/30	18.12	21.16	30.88
5	80/20	20.52	28.75	30.42

3.2 Tensile strength of concrete: The concrete is not usually expected to resist the direct tension because of its low tensile strength and brittle nature.The test is used to determine the load at which the concrete members may crack. The results are shown in Table-3.

Table 3- Tensile strength with use of granite waste

No	Cylinder (cement : granite)	Tensile strength
1	**50:50**	1.52
2	**80:20**	1.52

3.3 Cost analyses for granite waste cement with Normal cement and Ash cement .

The graph showing (Fig.3) the rate analysis of granite waste cement with other cement, so we conclude that by using of granite cutting waste in cement we make the low cost cement , also we can see that sown in about (Table 3) it is good in tensile strength.

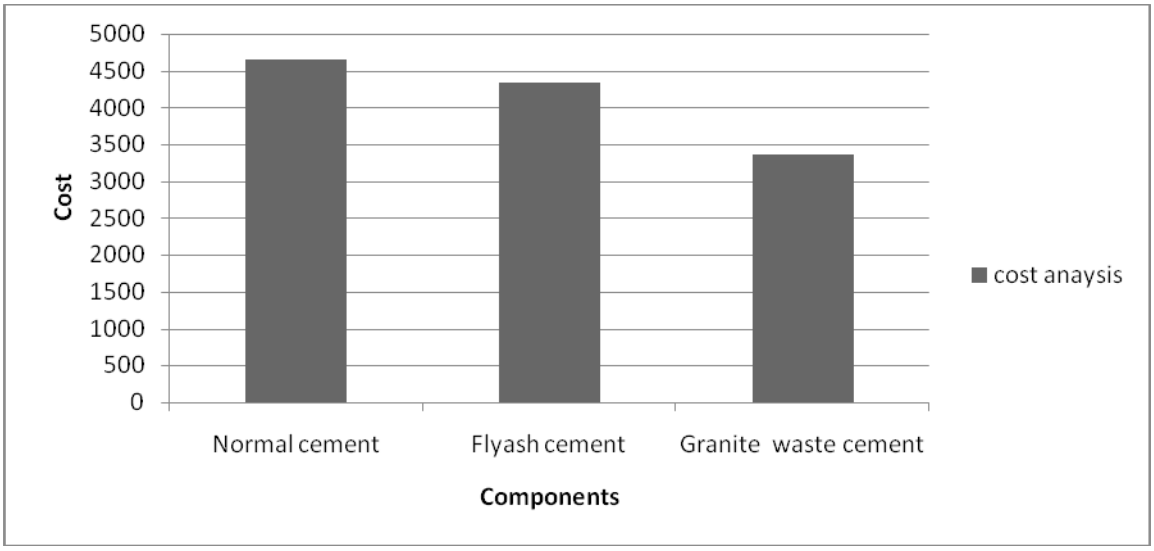

Fig. 3 Cost analysis

Conclusion:

As per initial result (7 days), we conclude that the use of this concrete in PCC, Temporary Road made, Road indicator and non structural member and after 14 days and 28 day we get excellent result, so we can used this mixture in RRC and heavy load bearing structure. Normal Concrete can be made Green Concrete using granite cutting waste in concrete in required amount. Cost criteria is also having positive impact due to use of the granite cutting waste as ingredients in the concrete.

Reference

1) Dhanapandian et al; Utilization Of Granite And Marble Sawing Powder Wastes As Brick Materials, Carpathian Journal of Earth and Environmental Sciences, October 2009, Vol. 4, No. 2, p. 147 - 160

2) Singh S. et al; Sustainable utilization of granite cutting waste in high strength, Journal of Cleaner Production (2016) 1-13.

3) Allam M. E., Re-Use Of Granite Sludge In Producing Green Concrete, Vol. 9, No. 12, December 2014.

SEEC No.106

ENVIRONMENT PROTECTION AND SUSTAINABILITY – An Assessment of Practices in Indian Electric Power Companies

MANIVANNAN R.RAJAN AND L.S.GANESH

Keywords: Sustainability, Environment Protection, India, Electric Power Companies

1. INTRODUCTION

The double whammy of a growing population and massive economic growth has led to massive environmental degradation, threatening the very survival of Planet Earth. For an emerging economy like India, it is an imperative to balance the intertwined objectives of People, Planet and Profits, i.e., the triple bottom line.

Energy is produced by consuming natural resources for meeting the basic needs of economic development and human well-being. However, industries in the energy sector are confirmed polluters of soil, water and air (WBCSD, 2013). Hence, achieving "Energy Sustainability" by correctly balancing energy availability for development; providing affordable and accessible energy for all, and preserving the integrity of the natural environment, is one of the biggest challenges facing humanity, and particularly for India. Electricity is the most widely used form of energy. The variety of challenges faced by Indian Electric Power companies, and the potential opportunities that would be available by their adoption of sustainability principles serve as the prime motivation for the present study.

2. THE RESEARCH PROBLEM: The Challenges of the Triple Bottom Line in Indian Electric Power Companies

All machines, appliances, and gadgets we use at home and at work function on electricity, and a power black-out can be debilitating. The availability of electricity throughout the day, i.e., 24x7, and all around the year, is a basic expectation of people. Besides, electric energy supplies are essential for producing goods in factories, transportation, and commercial activities.

Against this background, India is deeply constrained on the energy front on several aspects:

1. With only 2.45% of the total land area, India holds and supports about 1.3 billion people constituting $1/5^{th}$ of the global population. It is expected to become the most populous nation by 2025 (UNFPA, 2016).
2. Its oil and gas reserves are meagre, and the country is import-dependent (IEA, 2011).
3. It depends on other countries such as Australia for nuclear fuels.
4. Its electricity generation is predominantly based on coal-fired thermal power stations. India's coal reserves, while apparently abundant, are inferior in quality, limiting the usage of indigenous coal and forcing the import of better quality coal. Further, emissions from thermal power plants are considered to have huge adverse environmental impacts and are big contributors of Greenhouse Gases (GHGs) (IEA, 2012).
5. The per capita consumption of energy and electricity are very low compared to the world average, hugely hindering the nation's developmental aspirations (IEA, 2012).

Therefore, the electric power sector is of vital importance to India, in her quest for economic development, poverty alleviation and social inclusive growth. These together unambiguously

show up as the greatest challenge to sustainability of the natural environment and resources, and hence serve as the macro-level justification for this paper.

3. RESEARCH OBJECTIVES AND METHODOLOGY

This paper critically examines the underlying issues pertaining to Environmental protection and Sustainable growth in the context of Indian Electric Power companies (IEPs).

The literature survey covers the following: (a) Academic publications; (b) Company Profiles, Annual Business Responsibility and Sustainability Reports, Investor and other corporate communications, Analysts' reports, of major Indian companies involved in Electric Power Generation, Transmission and Distribution, and (c) Performance of global industry leaders in the Electric Power sector, to identify best practices. The following objectives have been identified following the literature survey.

a) Assess the current status of environmental protection and sustainability initiatives in IEPs, in terms of scope, approaches, programmes, metrics and performance.
b) Identify gaps with reference to literature and best global practices, and identify areas of improvement in terms of approaches, implementation, measurement, impacts and reporting.

To fulfil the above objectives, Content Analysis (CA) is used as the research methodology. It is a technique whereby the presence of certain words or themes in communications is analysed It is a systematic and objective means of describing and quantifying phenomena (Krippendorff, 1980). Hsieh and Shannon (2005) assert that content analysis is "a research method for the subjective interpretation of the content of text data through the systematic classification process of coding and identifying themes or patterns". Krippendorff (2012) defines content analysis as "a research technique for making replicable and valid inferences from texts (or other meaningful matter) to the contexts of their use." The methodology enables systematic identification of major conceptual and contextual themes and their interrelationships within the selected research problem area, and leads to qualitative insights.

4. IMPERATIVES OF SUSTAINABILITY AND ENVIRONMENTAL PROTECTION

The major issues concerning environmental protection are global climate change due to increasing generation of GHGs, global warming, biodiversity loss, changes in land use patterns, fresh water depletion, and mounting solid wastes and related disposal (Rockström et al 2009).

The pivotal role of electric power companies in national economic and social development, and in preserving environmental integrity has been underscored by researchers (WBCSD, 2013) Given the geographic, demographic, socio-economic, and technological status of India, several concerns have been raised regarding the electric power sector, and the implications of its policies and operations to sustainability and environmental protection (IEA, 2012 and WEC and WEF, 2017). The major issues are discussed briefly below:

A comparison of Select Development Indicators on India and the World is given below in Table 1 (WDI 2017, and The Little Data Book, 2017 of World Bank Group).

SELECT WORLD DEVELOPMENT INDICATORS 2017			
	World	**India**	**India's Share**
Population (millions 2015)	7,346.7	1,311.1	17.85%
Surface area (1,000 sq. km in 2015)	1,34,325	3,287	2.45%
Population density (people per sq.km 2015)	57	441	
Urban population (% of total population 2015)	54	33	
Economy			
GDP (% growth 2014-15)	2.7	7.9	
GDP per capita (% growth 2014-15)	1.5	6.6	
GNI, Atlas ($ billions 2015)	77,521.31	2,088.5	3%
GNI per capita, Atlas ($ 2015)	10,552	1,590	
GNI, PPP ($ billions 2015)	1,14,933.5	7,909.9	7%
GNI per capita, PPP ($ 2015)	15,644	6.030	
Environment			
Agricultural land (% land area)	38	60	
Forest area (% land area)	30.8	23.8	
Deforestation (avg. annual %, 2000–15)	0.1	-0.5	
Water and sanitation			
Internal freshwater resources per capita (cu. m)	5,926	1,116	
Total freshwater withdrawal (% of internal resources)	9.3	52.6	
Energy and emissions			
Electricity production (billion kwh 2014)	23,863.9	1,287.4	5%
Energy use per capita (kilograms of oil equivalent)	1,929	637	
Energy from biomass products and waste (% of total)	10.1	23.5	
Electric power consumption per capita (kWh)	3,144	805	
Electricity generated using fossil fuel (% of total)	66.3	81.7	
Electricity generated by hydropower (% of total)	16.2	10.2	
CO2 emissions per capita (metric tons)	5.0	1.6	32%

The above data only reinforces the common perception that India has a long way to go to catch up with most of the developmental indicators, as compared to the world average, let alone with those of the developed nations. While India's per capita GHG emissions are low at about one-third of the world, on an absolute basis, India is in the third place! Though India has no historical responsibility for the accumulated GHGs, international pressure is expected to mount on India to effect big cuts in its emissions, as India is a signatory to the Paris Agreement

A 60% increase in global demand for energy until 2030 has been projected, needing a total investment of US$20 trillion, of which about half would be required in developing countries like India (IEA 2007).

Large corporations, with their power and economic strength, now need to take much more responsibility for development than ever before (Stuart, and Elkington, 1997). Therefore, the role of Electric Power companies in India in managing Sustainability through the 'triple bottom line' approach is crucial and significant. The benefits of this strategy are: Cost and Risk Reduction, enhanced reputation and legitimacy, Innovation and retaining market leadership, adoption of Clean Technologies, and sustained growth (Esty, 2010).

5. FINDINGS OF THE STUDY - THE WAY FORWARD

The task of achieving economic growth and development compatible with climate change efforts demands that India should urgently transition to becoming a 'low carbon economy'. Indian Electric Power companies (IEPs) have a major role to play in achieving this transition.

The study indicates that many of the large IEPs are pursuing sustainability, are at various stages in their journey, but significant gaps still exist in their approach and metrics (IEPs Sustainability Reports, CII, WBCSD, 2018). The smaller organizations are still in a compliance mode, and focusing on certification of their environmental management systems.

All these organizations, irrespective of size and scale, can achieve the twin objectives of growing sustainably and protecting the environment through adopting an integrated sustainability management framework, covering all aspects of environmental protection, with a well-defined set of approaches, a comprehensive set of key indicators and targets, with appropriate action programmes and milestones:

1. Developing a clear map of the value chain processes spanning exploration of fuels-transportation-consumption-generation of electric power-distribution-consumption-disposal of wastes.
2. Identifying all environmental impacts across the value chain: climate change (due to carbon emissions), air pollution (particulate matter, acid rain), ozone depletion, fresh water consumption, water pollution, solid wastes, resource consumption and their intensity, changes in land use patterns, biodiversity,
3. Adopting Clean Energy technologies and processes.
4. Developing an appropriate mix of energy sources and supplies, including Renewable energy.
5. Investing in technologies for alternate materials, carbon capture and energy storage.
6. Focusing on Conservation and Recovery of resources - materials and energy - from the waste streams
7. Achieving Product stewardship: promoting responsible generation and consumption, promoting energy efficiency, developing energy efficient equipment and appliances, labelling of energy products, etc.
8. Engaging actively with a larger set of stakeholders – besides the well-known set of Shareholders, Investors, Suppliers and customers - including Government, academic and research institutions, and civil society.
9. Benchmarking and Innovating to become newer sources of efficiency in value creation and delivery.
10. Driving the concept across the value chain, to derive larger benefits to society, and achieve scale.
11. Embedding the concept of sustainability and environmental protection as core values of the organization

6. APPLICATION OF THE STUDY

The practical and integrated framework of relevant aspects and metrics can be adopted by all Indian Electric Power companies to achieve sustainable growth and environmental protection, while also benefitting from reduction in resource consumption, cost, and environmental footprint; improved operational efficiency; and social inclusion.

SEEC No. 112

Exergy Analysis of DI Diesel engine fuelled with Neem Biodiesel with DEE additive

Veena Chaudhary[1] , R.P.Gakkhar[2]
Mech. & Ind. Engineering Dept. IIT ROORKEE,
Research Scholar[1], Former Professor[2]
Email:veena.mech@gmail.com[1],gakhrfme@gmail.com[2]

ABSTRACT

This study presents the influence of DEE on exergy performance of small DI diesel engine fuelled with neem biodiesel blend NEEM15. Experiments were carried out at speed of 1600 rev/min with five different load levels. DEE is added as an additive with the fuel blend. Exergy parameters namely exergy input, exhaust exergy, exergy destruction, exergetic efficiency, exergy distribution, and sustainability index are determined. It is found that DEE enhances the exergetic performance and reduces the exergy destruction significantly. The exergy efficiency increases by 3-6% by with the use of DEE.

Keywords: Diesel Engine, Neem biodiesel, Exergy analysis, Second law of thermodynamics, exergy destruction, DEE

NOMENCLATURE

A/F	Air fuel ratio
BSFC	Brake specific fuel consumption (g/kW-hr)
BTE	Brake thermal efficiency
BP	Brake power (kW)
$c_{p,ex}$	Specific heat of exhaust gas (kJ/kg-K)
c_{pw}	Specific heat of cooling water (kJ/kg-K)
CV	Lower heating value (kJ/kg)
$\dot{m}_a$	Mass flow rate of air (kg/sec)
$\dot{m}_{eg}$	Exhaust gas flow rate(kg/sec)
$\dot{m}_f$	Mass flow rate of fuel (kg/sec)
$\dot{m}_{cw}$	Cooling water flow rate (kg/sec)
N	Engine speed (Revolution/min or RPM)
P_e	Exhaust gas pressure (bar)
SI	Sustainability Index
$\dot{Q}_{cw}$	Heat carried away by cooling water (kW)
$\dot{Q}_{eg}$	Heat carried away by exhaust gas (kW)
$\dot{Q}_{in}$	Heat input (kW)
T	Torque (Nm)
T_{cw}	Cooling water temperature (K)
T_{eg}	Exhaust gas temperature (K)
T_0	Ambient temperature (K)
T_{wi}	Cooling water inlet temperature (K)
T_{wo}	Cooling water outlet temperature (K)
$\dot{\zeta}_{eg}$	Exhaust exergy rate (kW)
$\dot{\zeta}_{in}$	Exergy fuel input rate (kW)
$\dot{\zeta}_Q$	Exergy rate accompanying with heat transfer (kW)
$\dot{\zeta}_w$	Exergy rate accompanying with work transfer (kW)
η_{II}	Second law efficiency

INTRODUCTION

The fast depletion of fossil fuel reserves and growing concerns of harmful emissions have motivated the investigators to search for the replacement of diesel fuel. Biodiesel is one of the replacement for the diesel since it is biodegradable, nontoxic, sulphur free and can be produced by edible and non-edible oils. It can be used in engine without any modifications. Neem biodiesel is one of the replacement

Exergy analysis is based on the second law of thermodynamics that is gaining interest among the researchers and scientists. Analysis based on exergy is different from the energy. Energy analysis treats all form of energy equally; there is no information about the quality of energy and is inadequate for evaluating the utilization of energy resources

The aim of this investigation is to present influence of DEE on exergy analysis of single cylinder diesel engine using neem biodiesel. In present study the impact of DEE on the variation of exergetic parameters are determined.

Experimental Setup: The experiments were performed on a 4-stroke single cylinder, direct injection diesel engine. The airflow rate was measured by using the air-box method. The engine speed was measured using a magnetic speed pickup**.** All the tests were performed under steady-state conditions. The experiments were conducted at 1600 rev/min. The load and speed were varied using AVL Dycon 201.Type K thermocouples were used to measure the inlet and outlet coolant temperature, intake air temperature and the exhaust gas temperature. The layout of the experimental setup is shown in Figure 1. Table 1 indicates the technical specifications of test engine.

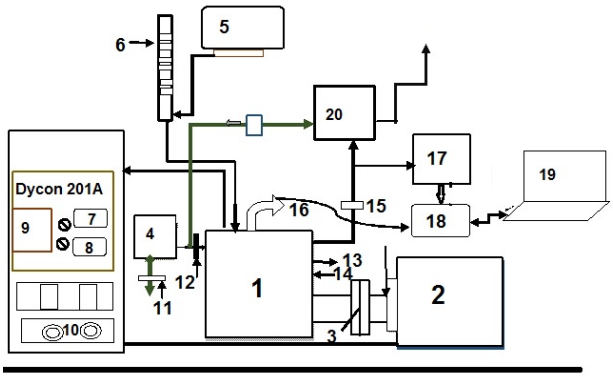

Figure. 1 layout of experimental set up

1 DI Diesel Engine 2. Eddy current dynamometer 3. Universal coupling 4. Air box 5. Fuel tank. 6. Fuel consumption measurement 7. Speed indicator 8. Torque indicator 9 operating mode of dycon panel. 10 throttle control 11. U tube manometer of air box 12. Intake air temperature 13. Water outlet 14. water inlet 15. Exhaust gas temperature 16. Pressure transducer 17. Exhaust gas analyzer 18. DPM 800. 19. Personal computer 20. Exhaust gas surge tank

Table 1. Technical Specifications of Test Engine

Engine	Greaves cotton
Model	GL 600 WII
Number of cylinders	1
Bore (mm)	92
Stroke (mm)	92
Displacement (cc)	611
Maximum power (kW) at rated RPM	8.1
Rated rpm	3000
Compression ratio	18:1

Brake specification fuel consumption (BSFC) is computed by;

$$\text{BSFC}=\left(\frac{\dot{m}_f \times 3600}{BP}\right),\ \frac{kg}{kWhr} \quad (1)$$

The input fuel exergy is calculated as follows

$$\dot{\zeta}_{in}=\dot{m}_f \times LHV \times \varepsilon_f,\ kW \quad (2)$$

$$\varepsilon_f=\left[1.0401+.1728\left(\frac{h}{c}\right)+.0432\left(\frac{o}{h}\right)+.2169\frac{s}{o}\left(1-2.0628\frac{h}{c}\right)\right] \quad (3)$$

where h/c, o/h and s/o are the mass ratios of hydrogen, oxygen, carbon, and sulphur of fuel respectively. Chemical exergy factor are mentioned in appendix 1.

Shaft work exergy or useful work exergy = $\dot{W}$ = Brake Power

The rate of exergy associated with heat going out cooling water is given by:

$$\dot{\zeta}_{cw}=\dot{m}_{cw}\, c_{p,cw}\left[T_{cw,out}-T_{cw,in}-T_o \ln\left(\frac{T_{cw,out}}{T_{cw,in}}\right)\right] \quad (4)$$

Rate of exergy associated with the unaccounted heat loss is computed by;

$$\dot{\zeta}_{unacc.}=\left(1-\frac{T_o}{T_s}\right)\dot{Q}_{unacc.} \quad (5)$$

The exergy destruction is given by equation 6

$$\dot{\zeta}_{dest.}=\dot{\zeta}_{in}-\dot{\zeta}_{eg}-\dot{\zeta}_{cw}-\dot{\zeta}_{W}-\dot{\zeta}_{unacc.} \quad (6)$$

Exergetic Efficiency

It is an indicator of the efficiency of the conversion of fuel input exergy into useful work. Exergetic efficiency is calculated by using the equation 7.

$$\eta_{II}=\frac{\dot{\zeta}_W}{\dot{\zeta}_{in}}=\frac{\dot{W}}{\dot{\zeta}_{in}} \quad (7)$$

Sustainability Index

Sustainability Index (SI) parameter expressed as function of exergetic efficiency indicates the sustainability of the resource for the maximum benefit of the society with minimum negative effects. The sustainability index should not be less than one as mentioned in equation 8.

$$SI=\frac{1}{1-\eta_{II}} \quad (8)$$

Result & Discussion

Figures 2-9 represent the influence of DEE on BSFC, BTE, and exergy parameters of diesel engine fuelled with Neem biodiesel mixed with DEE. Figure 2 shows the influence of DEE on BSFC for Neem15 at speed of 1600 rev/min for different loading conditions. With the addition of DEE, BSFC decreased at all loads. As load increases the BSFC decreases and is minimum at 100% load. As the percentage of DEE increases, the BSFC decreases at all loads. With addition of DEE, the viscosity and density of the biodiesel blend reduce which result in improved atomization and better spray characteristics consequently better combustion of fuel leading to lower BSFC and higher thermal efficiency.

Figures 3 shows the influence of DEE, on brake thermal efficiency for neem biodiesel blend NEEM15 at speed of 1600 rev/min for different loading conditions. It is observed from the figure that the brake thermal efficiency is lower for bio-diesel blend for all loads. The presence of DEE results in increase in the thermal efficiency. As the perentage of DEE increases at any load the brake thermal efficiency increases. 15% DEE-NEEM15 gives the 34.85% thermal efficiency at full load while biodiesel blend NEEM15 without additive gives lower thermal efficiency 31.45%.

Figure 4 presents the variation of fuel input exergy of NEEM15 with DEE at different loads while engine was running at constant speed1600 rev/min. It is observed from

Figure 4 that fuel input exergy decreases with increase in the percentage of additive DEE for all loads. Fuel input exergy increases with the load level. The input exergy is maximum for NEEM 15 at all loads. It depends on the mass flow rate of fuel, at higher load more amount of fuel is injected which increases the fuel input exergy. When additive DEE is added in the fuel blend, the heating value of the blend decreases resulting in the low fuel exergy input at all load conditions as compared to that for NEEM15. With increase in the percentages of DEE, the heating value decreases, which leads to higher fuel consumption as mentioned earlier. 15% DEE gives the lowest exergy input as compared to that for other DEE percentages and NEEM 15 at all load conditions.

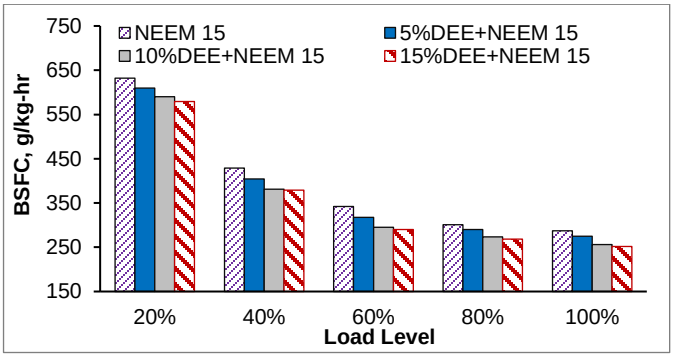

Figure 2 Influence of DEE on BSFC

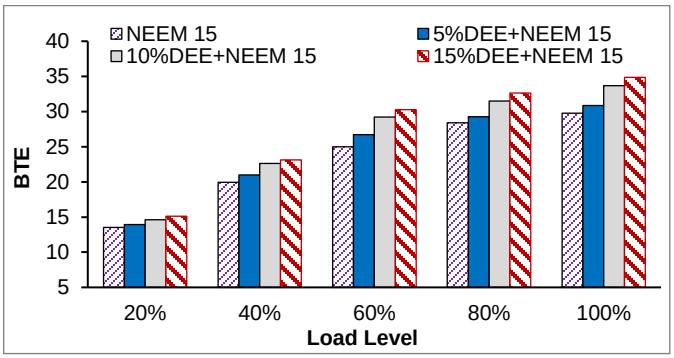

Figure 3 Influence of DEE on BTE

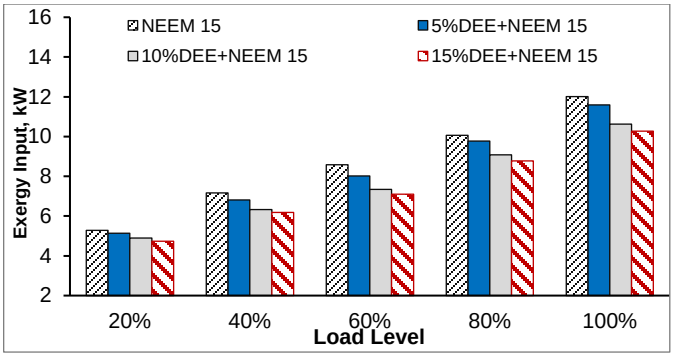

Figure 4 Influence of DEE on Exergy Input

Variation of exergy associated with exhaust energy with load for percentages of DEE at 1600 rev/min is shown in figure 5 It is observed that higher exhaust gas exergy is associated for the 15%DEE+ NEEM15 bio-diesel blend. When DEE is added to the bio-diesel blend the exergy associated with exhaust gases increases. As the percentage of DEE increases the exhaust energy increase. This is due to higher exhaust gas temperature observed for biodiesel and DEE blend for all the load conditions.

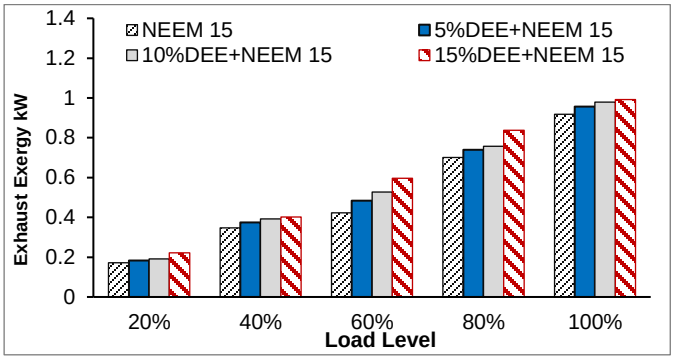

Figure 5 Influence of DEE on Exhaust Exergy

Figure 6 presents the influence of DEE on exergy destruction. As the load increases the exergy destruction also increases. The magnitude of exergy destruction is low at low load conditions. As load increases, the exergy components associated with brake power, exhaust gases, and cooling water increase, leading to high exergy destruction at higher load. Unlike the energy, exergy is not conserved. Exergy destruction is the difference between the total exergy input and exergy associated with exit streams, considering those associated with cooling water, exhaust gas, and brake power.

In the present study, input air exergy has been neglected because air enters the engine at atmospheric temperature and pressure. The exergy destruction is higher for biodiesel blend at all loads. However, when DEE is added to the biodiesel blend the exergy destruction decreases at all loads. For 15% DEE the exergy destruction is lowest.

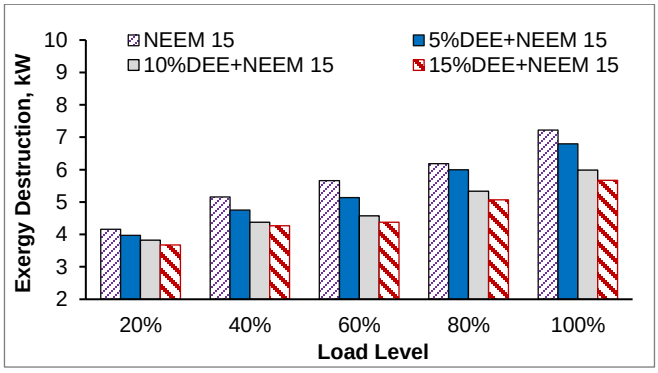

Figure 6 Influence of DEE on Exergy Destruction

Figure 7 represents the influence of DEE on exergetic efficiency at different load conditions for NEEM15 with different proportions of DEE. It is observed that variation trend is similar to brake thermal efficiency while the magnitude is different. The peak value of exergetic efficiency is obtained at higher load condition for all DEE proportions. At low load

condition the exergetic efficiency is lower. Mixing of additive DEE improves the exergetic efficiency significantly, higher efficiency is observed for 15% DEE at any load conditions.
At lower load, the exergetic efficiency is lower. As the percentages of DEE increase in the blend, the improvement in efficiency is observed as indicated in Figure 7.

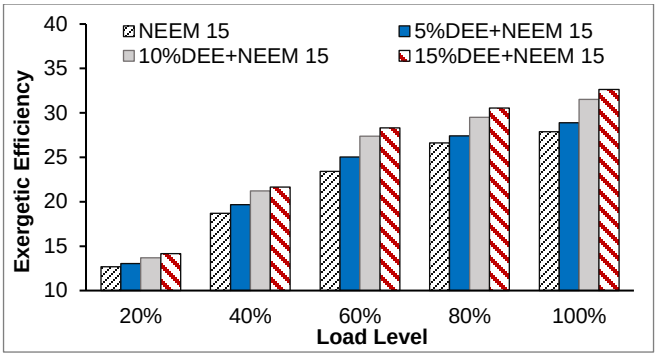

Figure 7 Influence of DEE on Exergetic Efficiency

Figure 8 represents the influence of DEE on sustainability index at varying load condition. The sustainability index is related to the exergetic efficiency and indicates the performance of system effectiveness from sustainability point of view. SI indicates the sustainable nature of the fuel usage in terms of environmental influence and economic feasibility. The 15% DEE with biodiesel blend gives higher SI at any load condition compared to that for 5% and 10% DEE because of higher exergetic efficiency as compared to that for bio-diesel blends.

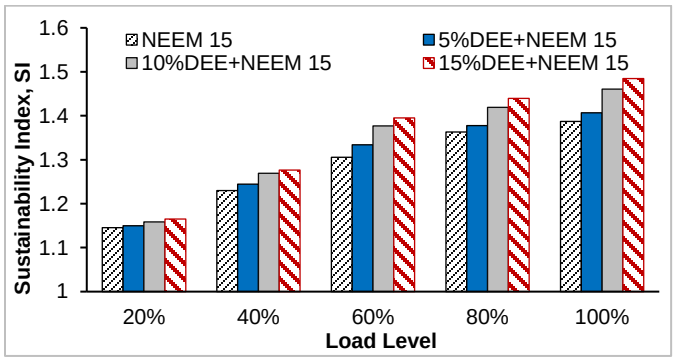

Figure 8 Influence of DEE on Sustainability Index

Figure 9 represents the fuel input exergy distribution percentages to the different components of exergy for 15% DEE+Neem15 fuel blend. It has been observed that with increase in the load, the exergy destruction decreases while the exergy associated with the unaccounted heat losses is very small in magnitude as compared to the other exergy components. The exergy carried by the exhaust gases and cooling water are very small as compared to their distribution in energy analysis. In the exergy distribution, the exergy destruction and useful work are very significant as compared to other components of exergy while in the energy distribution all components play the equivalent role. With the addition of DEE, the exergy destruction reduces at higher load condition with respect to fuel input exergy.
From the comparison of energy and exergy analysis it is clear that energy carried by exhaust gases and cooling water are low grade energy as exergy associated with each of them is quite small. With increase in the load the exergy destruction percentage decreases while the useful work increases. The exergy associated with the uncounted heat losses are very small as compared to that for the uncounted heat losses in energy distribution. Similar observations have been made with the exergy associated with the heat losses with the water.

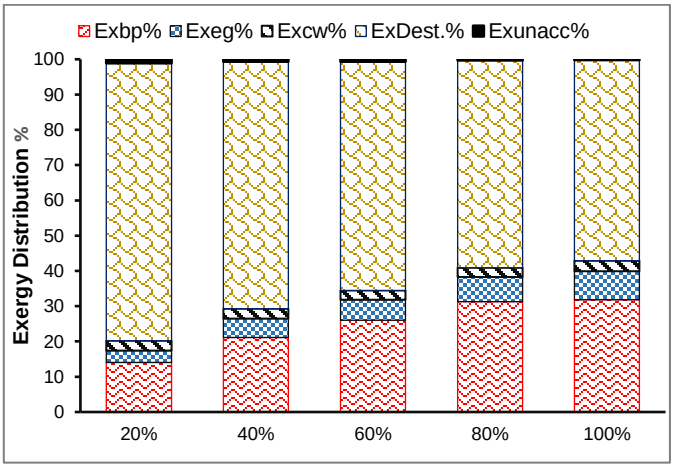

Figure 9 Exergy distribution with 15% DEE+Neem15

Conclusion

Experiments were conducted with the different percentage of additive DEE with the Neem 15 at constant speed of 1600 rev/min and five load conditions. Performance and exergy analysis parameters were compared at different operating conditions.

- It is observed that DEE enhances the performance and exergy parameters significantly.
- Reduction in BSFC is observed by 7.21%, 9.1%, and 10.25% with 5% DEE, 10%DEE, and 15% DEE respectively at speed of 1600 rev/min. Increase in the thermal efficiency is the consequence of lower BSFC with the addition of DEE.
- Brake thermal efficiency is improved by 6.10%, 7.56%, and 8.16% using 5% DEE, 10% DEE, and 15% DEE respectively with Neem 15.
- From the exergy analysis, improvement in exergy parameters is also observed namely; exergy input increased by 7.24%, 10.26% and 12.26% using the 5% DEE, 10% DEE and 15% DEE respectively.
- Significant reduction in exergy destruction by 6.67%, 14.10%, and 16.47% using 5%DEE, 10%DEE, and 15%DEE respectively for Neem15.

Appendix 1 Blend properties

Blend	CV (kJ/kg)	Viscosity	CF
5%DEE+NEEM 15	42440.2	3.27	1.066
10%DEE+ NEEM 15	41748.8	3.11	1.069
15%DEE+ EEM15	41057.4	3.01	1.07

Proceedings of theThird International Conference on Sustainable Energy and Environmental Challenges (3rd SEEC)
18 –21 December, 2018, IIT Roorkee, India

SEEC No.114

AN EXPERIMENTAL STUDY ON PELLETIZATION OF HORTICULTURAL WASTE AND COMBUSTION ANALYSIS

Vaishali Vasudeva
Hans Raj College, University of Delhi
Student
Email: vaishalivasudeva29@gmail.com

Vidushi Pant
Hans Raj College, University of Delhi
Student
Email: vidushipant01@gmail.com

ABSTRACT

Biomass in its densified form i.e., the pellets is more efficient in burning as compared to raw biomass. In the present study, horticultural waste was used to make biofuel pellets. In the first stage, blend of dried grass and leaves, mainly comprising of Cyanodon dactylon and Polyalthia longifolia, was pelletized. In the second stage, saw dust was added to the ground plant waste. Calorific value, ash content, moisture content, ash analysis (Potassium, Phosphate, Silica, Chloride, Cadmium, Mercury, Lead, Arsenic), fixed carbon content, and emission analysis (Particulate matter, Nitrogen oxides, Sulphur dioxide, Carbon monoxide, Methane) was done for both samples. Addition of wood saw dust led to an increase in calorific value of the fuel as well as gaseous emissions.

Keywords*: Biomass, Biofuel, Pellets, Waste, Pelletization*

NOMENCLATURE

N- Nitrogen
P-Phosphorus
K-Potassium
Cl-Chloride
SiO_2-Silica
Cd-Cadmium
Hg-Mercury
Pb-Lead
As-Arsenic
NOx- Nitrous Oxides
SO_2- Sulphur Dioxide
CO- Carbon Monoxide

INTRODUCTION

The average annual decadal growth rate of the energy consumption across the world has increased to 1.7% [1]. This increasing demand is aggravated by the increase of population, primarily in the developing countries. These factors, along with the depleting natural resources, necessitates the shift towards the renewable sources of energy. The Paris Agreement 2015 further urges the signatories to reduce their carbon emissions; this results in a global desire to shift towards green energy alternatives. Biomass is considered as one of the most promising sustainable sources that can be utilized for production of high quality biofuel [2-5].

Plant biomass have low densities, generally in the range of 40 to 150 kg/m^3 (for grasses) [6-7] and 320-700 kg/m^3 (for wood) [8], because of their porous cellular structure. This results in shooting up of the handling and transportation expenses. Densification of plant biomass into pellets results in significant reduction in the costs [9]. Generally, the density of the biomass pellets can be as high as 1000–1400 kg/m^3. Densification process has various advantages: the pelletized fuel has greater structural homogeneity, lower moisture content and hence, higher energy efficiency compared to its raw counterpart [10]. It has the added benefit of convenient handling and easy storage. Pelletized fuel emits lesser particulate matter than the original form and other traditional fuels [11-12]. The major raw materials that are pelletized to be used as a clean biofuel include wood residues (chips, shavings etc.), saw dust, crash crop and agricultural residues (bagasse, rice husk etc.) as well as waste product from the food industry [13-14]. A variety of biomass material has been used in different studies. For example, blends of lignite, xylite and wood chips [15]; wheat straw, barley straw, corn stover and switchgrass [9]; blends of pine, chestnut and eucalyptus sawdust, cellulose residue, coffee husks and grape waste [16], pine, miscanthus, reed canary grass, tall fescue and short rotation coppice willow [17]; bamboo and pine particles [18].

Tapping the potential of grasses as a possible sustainable and renewable source for production of energy efficient pellets has gained momentum in the last few years. The plant cell wall has an amorphous polymer lignin, along with hemicellulose and cellulose (partly crystalline) [19]. These polymers act as natural binders during the densification process of the biomass. Grasses also contain high amounts of extractives, mainly waxes, which are a combination of alkanes, sterols, fatty acids and alcohols [20-21].

The objective of the present study is to investigate the potential of grasses as an energy efficient biofuel by producing densified pellets using in-house horticultural waste that includes the biomass of the grass, viz., *Cynodon dactylon* as well as *Polyalthia longifolia.*

MATERIAL AND METHOD

Material

The raw material, i.e., the horticultural waste was procured from campus of Hans Raj College, University of Delhi. *Cynodon dactylon*, which is the common lawn grass formed the major portion of the waste. The dried and fallen leaf waste comprised largely of the leaves of species *Polyalthia longifolia*. Wood saw dust, which did not form a part of horticultural waste, was procured locally. No additional binder was added to the mixture.

The pellet mill used in the process comprised of a roller and a die (circular metal ring with holes in the periphery), powered by a 3.7 kW motor. The Length/Diameter ratio of the die was 3.5, indicating that the manufactured pellets will be cylindrical in shape having 3.5 cm length and 1 cm diameter of the cross section.

Method

Pellet Production

Two samples were prepared using a blend of grass and leaves (1:1) henceforth referred to as sample A and a mixture of shredded grass, leaves and saw dust in sample B. The overall method followed was same for both samples and can be summarized as follows:

Preprocessing: The freshly cut grass was found to have 40% moisture which needed to be lowered for the shredding purpose. Few days of sun drying and storage reduced the moisture significantly making it suitable for shredding. Leaves were collected in naturally dry state. The length of the plant material was reduced to 2.5 cm using a shredder. The moisture in the shredded grass was found to be 6-7%.

Pelleting: The shredded material (2.5% moisture) was added to pellet mill with some water to aid binding (making final moisture 15%), where rollers grind it to powder and extrude it, forcing it to pass through die holes which effectively compress it into pellets.

Cooling: Pellets leaving the pellet mill at a high temperature and with excess moisture are then cooled and sun dried over a screen to gently cool the hot fragile pellets to room temperature.This results in increased hardness and durability of the pellets.

Screening is required to separate residual fines from the finished pellets before bagging. Fines and fragments collected from screening were returned to the pelletizer.

Bagging: The last step of the pelleting process was to fill the appropriate amount of pellets into bags and seal them.

Fuel, ash and emission analysis

For characterization of fuel- Calorific Value (kJ/kg), Moisture Content (% by mass), Ash Content (%) and amount of fixed carbon (% by mass) were analyzed. The ash obtained after combustion was analyzed for plant nutrients like N, P and K; for potential slag forming elements like SiO_2 and Cl; and presence of heavy metals (Cd, Hg, Pb, As). Analysis of each parameter was carried out following Indian Standards (IS) (Tab 1).

RESULTS

Calorific value of Pellet B (15531.01 kJ/kg) was found to be higher than that of Pellet A (13108.47 kJ/kg) (Tab 1). Other parameters like ash content, moisture content and fixed carbon were found to be lower in saw dust containing pellets (10.2%, 7.17% and 1.38% respectively as against 15.13%, 18.67% and 1.07%). Ash analysis revealed a significant concentration of K present in Pellet A (15.4 mg/kg) and Pellet B (21.2 mg/kg). N, P, SiO_2 and Cl were below detectable limits* in both the samples. Out of the four heavy metals tested, Cd, Hg and As were below detection limit. Pb was found in both the samples having concentration of 5.59 mg/kg and 6.20 mg/kg in sample A and B respectively. Emission analysis showed high particulate matter emissions in case of sample B (338 mg/Nm^3) and in sample A (271 mg/Nm^3). SO_2 and CH_4 were found to be below detection limit but significant amount of NOx and CO were released during combustion. NOx emissions from sample B was higher (66.01 mg/Nm^3) as compared to sample A (51.2 mg/Nm^3). Similarly CO emissions were higher in saw dust containing pellets (40.1 mg/Nm^3) as compared to the sample having grass and leaves (32 mg/Nm^3).

TABLE 1: PARAMETERS ANALYSED FOR BIOFUEL PELLET SAMPLES, VALUES OBTAINED AND THE PROTOCOL USED FOR ANALYSIS.

Parameters	Sample A	Sample B	Protocol
Fuel Analysis			
Calorific value (kJ/kg)	13108.47	15531.01	IS:1448 (P-6)
Ash Content (%)	15.13	10.21	By calculation
Moisture Content (%)	18.67	7.17	By calculation
Fixed Carbon (%)	1.07	1.38	IS:3025 (P-2)
Ash Analysis			
N (mg/kg)	Not detectable	Not detectable	IS:3025 (P-34)

P (mg/kg)	Not detectable	Not detectable	IS:3025 (P-31)
K (mg/kg)	15.4	21.2	IS:3025 (P-2)
SiO_2(mg/kg)	Not detectable	Not detectable	IS:3025 (P-35)
Cl (mg/kg)	Nil	Nil	IS:3025 (P-32)
Cd (mg/kg)	Not detectable	Not detectable	IS:3025 (P-2)
Hg (mg/kg)	Not detectable	Not detectable	IS:3025 (P-2)
Pb (mg/kg)	5.59	6.20	IS:3025 (P-2)
As (mg/kg)	Not detectable	Not detectable	IS:3025 (P-2)
Emission Analysis			
Particulate Matter (mg/Nm^3)	271	338	IS:5182 (P-1)
NOx (mg/Nm^3)	51.2	66.01	IS:5182 (P-7)
SO_2 (mg/Nm^3)	Not detectable	Not detectable	IS:5182 (P-2)
CO (mg/Nm^3)	32	40.1	IS: 5182 (P-10)
Total Hydrocarbons, as CH_4 (mg/Nm^3)	Not detectable	Not detectable	APHA-101

*Detection limits (mg/kg): N=0.1, P=0.05, SiO_2=0.05, Cd=0.002, Hg=0.00002, As= 0.005

DISCUSSION

The present study was conducted with an aim of local utilization of waste in the form of biofuel. Although, the use of herbaceous plant material for pelletization has been a challenge considering its higher moisture content, low fixed carbon and high ash content, we observed significant calorific values associated with both the samples of pellets in our study. The calorific values obtained in our case (13.1-15.5 MJ/kg) is quite comparable to that of mustard crop residue (14.2 MJ/kg) and higher than cow dung cakes (9.79 MJ/kg) [22]. Addition of saw dust improved the calorific value, ash content and moisture content but at the same time increased gaseous emissions, which exceeds the limits set by Central Pollution Control Board. Emission of CO is indicative of incomplete combustion but also depends upon combustion facility and air to fuel ratio. These emissions pose limitation to the use of pellets in a residential setup. Nevertheless, the observation of increased emissions upon mixing saw dust requires further investigation. Out of the four heavy metals tested in the ash, only Pb was detected in significant amount but was found to be in normal concentration as found in soil [23].

In future, the present study has a scope for the investigation of other fuel parameters, for example bulk density, mechanical durability and percentage of fines. In addition to analysis of these parameters, the effect of binders as additives may also be explored. Addition of water and calcium hydroxide suspension, for example reduced the SO_2 emissions [15].

CONCLUSION

Biomass pellets were produced from horticultural waste, comprising of *Cynodon dactylon* and *Polyalthia longifolia*. The pellets were found to have calorific value higher than cow dung cakes and comparable to that of agri-residue. Ash content of the pellets was >10 % and CO and NOx emissions were significant. Lowering of NOx emissions requires further investigations. The pellets generated from horticultural waste has the potential to be used as biofuel in future.

ACKNOWLEDGEMENT

The authors would like to acknowledge Vice Chancellor, University of Delhi and Dr. V. K. Kawatra, Principal Hans Raj College, University of Delhi for providing financial support to the project. We are thankful to the suggestions provided by Mr. P. Raman (TERI) and Dr. Aparna Garg, Dr. Anand Sonkar, Mr. Amar Kumar for this project. We thank Dr. Shantanu Ganguly, TERI library; Librarian, Central Science Library, University of Delhi for allowing us to access the relevant literature on the subject. We are grateful to Mr. A. K. Khater for providing us biomass shredding facility at Kotputli and Delhi Test House and Sima Labs for providing laboratory facility and analytical support. We acknowledge the contribution of Ms. Taanumanshyaa Bhanndari, Ms. Sneha Mittal, Ms. Akansha Gururani, Ms Arushi Mehrotra, Ms Yogeeta Khanna, Ms. Mansi Nagar Mr. Akash Verma and Mr. Naman Tondon.

REFERENCES

[1] British Petroleum UK, 2018. "BP Statistical Review of World Energy". June. 67th Edition. See also https://www.bp.com/content/dam/bp/en/corporate/p

df/energy-economics/statistical-review/bp-stats-review-2018-full-report.pdf
[2] Weldekidan, H., Strezov, V. and Town, G., 2018. "Review of solar energy for biofuel extraction". Renewable and Sustainable Energy Reviews, 88, May, pp.184-192
[3] IEA, International Energy Agency, 2017. "Technology roadmap: delivering sustainable bioenergy". IEA Paris, France.
[4] Rosillo-Calle, F., De Groot, P., Hemstock, S.L. and Woods, J. eds., 2015. The biomass assessment handbook: Energy for a sustainable environment, 2nd Edition. Routledge, New York.
[5] Smeets, E.M., Faaij, A.P., Lewandowski, I.M. and Turkenburg, W.C., 2007. "A bottom-up assessment and review of global bio-energy potentials to 2050". Progress in Energy and combustion science, 33(1), February, pp.56-106.
[6] Adapa, P., Tabil, L., Schoenau, G., Sokhansanj, S. and Bucko, J., 2002. "Compression and compaction behavior of fractionated alfalfa grinds". ASAFICSAE Paper No. MBSK, September, pp.02-206.
[7] Larsson, S.H., Thyrel, M., Geladi, P. and Lestander, T.A., 2008. "High quality biofuel pellet production from pre-compacted low density raw materials". Bioresource technology, 99(15), October, pp.7176-7182.
[8] Simpson W, TenWolde A. "Physical properties and moisture relations of wood". In: Forest Products Laboratory. 2010. Wood handbook—Wood as an engineering material. General Technical Report FPL-GTR-190. Madison, WI: U.S. Department of Agriculture, Forest Service, Forest Products Laboratory. 508 p. Chapter 3.
[9] Mani, S., Sokhansanj, S., Bi, X. and Turhollow, A., 2006. "Economics of producing fuel pellets from biomass". Applied Engineering in agriculture, 22(3), March, pp.421-426.
[10] Xiao, Z., Yuan, X., Jiang, L., Chen, X., Li, H., Zeng, G., Leng, L., Wang, H. and Huang, H., 2015. "Energy recovery and secondary pollutant emission from the combustion of co-pelletized fuel from municipal sewage sludge and wood sawdust". Energy, 91, November, pp.441-450.
[11] Shen, G., Tao, S., Wei, S., Zhang, Y., Wang, R., Wang, B., Li, W., Shen, H., Huang, Y., Chen, Y. and Chen, H., 2012. "Reductions in emissions of carbonaceous particulate matter and polycyclic aromatic hydrocarbons from combustion of biomass pellets in comparison with raw fuel burning". Environmental science & technology, 46(11), May, pp.6409-6416.
[12] Ghafghazi, S., Sowlati, T., Sokhansanj, S., Bi, X. and Melin, S., 2011. "Particulate matter emissions from combustion of wood in district heating applications". Renewable and Sustainable Energy Reviews, 15(6), August, pp.3019-3028.
[13] Verma, V.K., Bram, S., Delattin, F., Laha, P., Vandendael, I., Hubin, A. and De Ruyck, J., 2012. "Agro-pellets for domestic heating boilers: Standard laboratory and real life performance". Applied Energy, 90(1), February, pp.17-23.
[14] Sultana, A., Kumar, A. and Harfield, D., 2010. "Development of agri-pellet production cost and optimum size". Bioresource Technology, 101(14), July, pp.5609-5621.
[15] Heschel, W., Rweyemamu, L., Scheibner, T. and Meyer, B., 1999. "Abatement of emissions in small-scale combustors through utilisation of blended pellet fuels". Fuel Processing Technology, 61(3), November, pp.223-242.
[16] Gil, M.V., Oulego, P., Casal, M.D., Pevida, C., Pis, J.J. and Rubiera, F., 2010. "Mechanical durability and combustion characteristics of pellets from biomass blends". Bioresource Technology, 101(22), November, pp.8859-8867.
[17] Gillespie, G.D., Everard, C.D., Fagan, C.C. and McDonnell, K.P., 2013. Prediction of quality parameters of biomass pellets from proximate and ultimate analysis. Fuel, 111, September, pp.771-777.
[18] Liu, Z., Mi, B., Jiang, Z., Fei, B. and Cai, Z., 2016. "Improved bulk density of bamboo pellets as biomass for energy production". Renewable energy, 86, February, pp.1-7.
[19] Miller, R.B., 1999. Structure of wood. In: Forest Products Laboratory. 2010. Wood handbook—Wood as an engineering material. General Technical Report FPL-GTR-190. Madison, WI: U.S. Department of Agriculture, Forest Service, Forest Products Laboratory. 508 p.
[20] Hamilton, R.J., 1995. "Analysis of waxes". In: Hamilton, R.J., 1995. "Waxes: chemistry, molecular biology and functions". Dundee: Oily press.
[21] Deswarte, F.E., Clark, J.H., Hardy, J.J. and Rose, P.M., 2006. "The fractionation of valuable wax products from wheat straw using CO_2". Green Chemistry, 8(1), pp.39-42.
[22] Harshika, K., Avinash, C. and Kaushik, S.C., 2014. "Comparative study on emissions from traditional and improved biomass cookstoves used in India". International Journal for Research in Applied Science and Engineering Technology, 2(8), pp.249-257.
[23] Zimdahl, R.L. and Skogerboe, R.K., 1977. "Behavior of lead in soil". Environmental Science & Technology, 11(13), December, pp.1202-1207.

Proceedings of the International Conference on Sustainable Energy and Environmental Challenges (3rd SEEC)
18 – 21, December, 2018, IIT Roorkee, India

SEEC No.115

AN ALTERNATIVE LUBRICATION FOR AUTOMOTIVE ENGINES

Vikram Kumar
Dept. of Mechanical Engg.
Indian Institute of Technology Kanpur
Email: vikramk@iitk.ac.in

Sujeet K. Sinha
Dept. of Mechanical Engg.
Indian Institute of Technology Delhi
Email:sks@mech.iitd.ac.in

Avinash K. Agarwal
Dept. of Mechanical Engg.
Indian Institute of Technology Kanpur
Email:akag@iitk.ac.in

ABSTRACT
Lubricating oil is environmentally harmful due to presence of toxic additives such as sulphates, phosphates and heavy metals. These chemicals eventually find their ways to land, water and air and become a hazardous pollutant to the environment. These additives can be reduced in quantity or completely eliminated from the lubricating oil, if friction and wear could be reduced by applying a suitable coating on the mating metallic surfaces to be protected. Polymeric coatings provide great opportunity to modify metallic surfaces with very low friction and wear performance. Further, these coatings have been evaluated for applications in automotive engines.

Keywords: Polymeric coating, Epoxy, Additives, Lubrication.

INTRODUCTION

Because of environmental concerns and government regulations in various countries, there are active efforts made towards diminishing the application of harmful lubricating additives. This important issue could be resolved either by replacing current additives with an environmentally benign formulation or implementing a coating on one of the interacting surfaces, which can reduce friction and prevent wear of the substrate [1].

There are many challenges in developing eco-friendly lubrication. Researchers are paying attention towards finding new additives for industrial lubricants [2]. Throughout the world, researchers are attempting to develop noble lubricant additives with better performance than current additives [2, 3, 4].

Various additives (anti-wear, friction modifier and extreme pressure) are added to enhance the lubricant performance. These additives include zinc dialkyldithiophosphate (ZDDP) and MoDTC etc. The main function of additives is to form a tribofilm after reacting with the contacting surfaces (mainly steels) thus protecting the surfaces from wearing out [5, 6, 7]. It has been recently reported that DLC coatings with ionic liquids as additives provide a possible substitute for ZDDP. Polymers coatings have very low coefficient of friction and wear. The tribological properties such as friction and wear of polymers are dependent on their mechanical properties such as hardness, plastic index, elastic modulus [8], and on their molecular structure.

Polymers are visco-elastic in nature and the energy dissipation during sliding due to viscous hysteresis loss is an important contributor to friction [9]. With polymeric materials, there is an important phenomenon of the formation of transfer film on the counterface [10]. Friction and wear depends upon the nature of transfer layer. Friction is greatly dependent on operational parameters such as load, sliding velocity and temperature.

It is obvious that epoxy (polymer) shows highly improved mechanical and tribological properties, when mixed with appropriate filler material and made in the form of a composite [11,12]. However these studies did not test the efficacy of epoxy and its coatings when used with lubricating oil especially in highly demanding conditions of contact stress and heat. Hence, in the current work, we intend to test graphene- and SN150-filled epoxy as tribological coatings on steel for dry-sliding as well as in the presence of base-oil lubricant without additives. Such

coatings have the potential to be used as boundary layers for the protection of components used in automotive.

Although various coatings, as mention by literature survey as above, it can be concluded that low friction coating can be achieve by replacing conventional lubrication with self lubricating coating.

2. EXPERIMENTAL PROCEDURE

2.1 MATERIALS

Cylindrical shaft (diameter = 40 mm width ~12 mm and roughness ~ 0.40 micron) of D2 steel was coated epoxy/ graphene SN 150 composite. The counterface for all tribological tests is stainless steel (SAE 52100) ball of 4 mm diameter. For lubricated tests, SN 150 (base oil) of Group-I having viscosity index 95 was used.

2.2 SAMPLE PREPARATION

Cylindrical shaft of D2 steel with specifications as mention above was hardened by heat treatment to hardness of 2.75 ± 0.05 GPa. After the heat treatment, cylindrical soft were cleaned. Epoxy composite coating is applied on the cleaned specimen and first cured at room temperature then oven curing at 80 ºC.

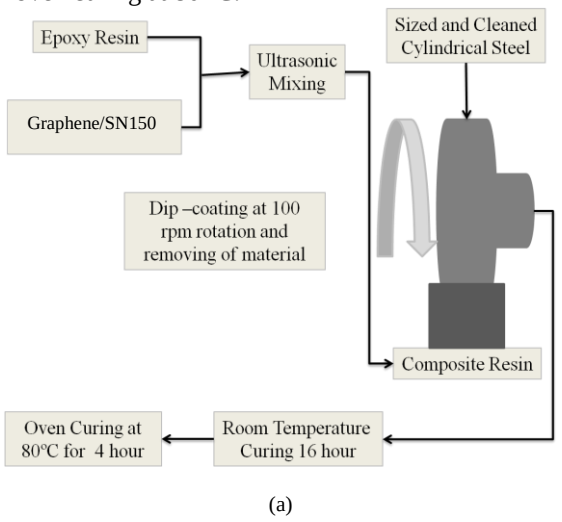

(a)

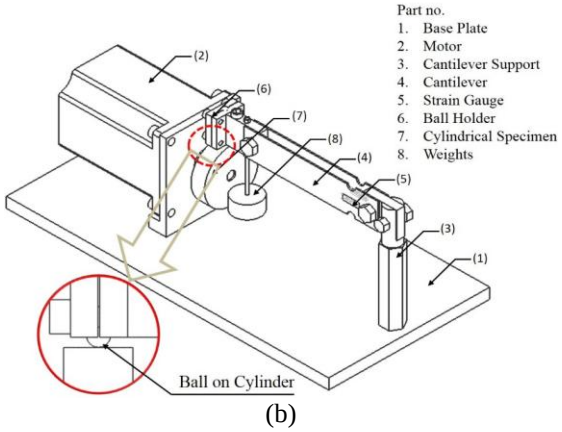

(b)

FIGURE 1. Schematic of (a) sample preparation and (b) Ball-on-Cylinder type tribometer.

3. RESULTS AND DISCUSSION

Tribological investigations of hard coated D2 steel were performed on ball-on-cylinder tribometer under following conditions:

3.1 STRBECK CURVE

Figure 2 presents the steady-state coefficient of friction vs. Sommerfeld number for the epoxy/graphene composites with 10 wt. % SN150. The Sommerfeld number was calculated as ηv/P, where η is the viscosity of the liquid filler, v is the sliding speed in m/s and P is the normal load (10 N). The coefficient of friction was inspected for a fixed number of 5000 cycles at different Sommerfeld numbers. The plot is divided into two zones, based on their frictional behavior w.r.t. the Sommerfeld number, Zone 1 and Zone 2, which represent an abrupt change in the coefficient of friction as the Sommerfeld number increases. In Zone 1, the coefficient of friction increased steeply from 0.04 to 0.06, while in zone 2, it was nearly constant (0.06 – 0.07) for SN150.

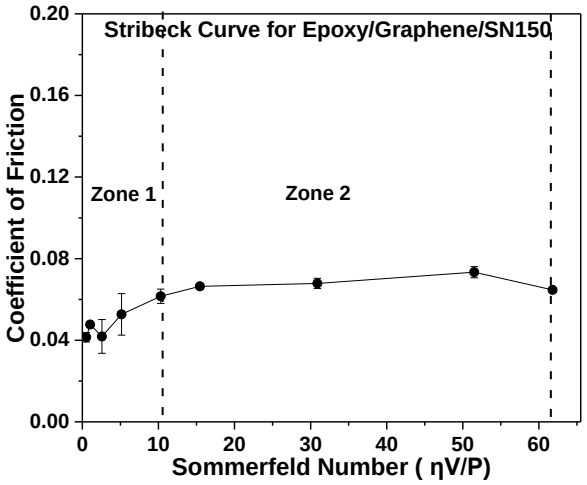

FIGURE 2. Stribeck curve.

3.2 LUBRICATION MECHANISM

A schematic of the coating cross-section with the bonded and mobile lubricant is shown in Figure 3. There is presence of lubricant liquid droplets in the bulk and at the sliding surface, there is mobile lubricant present due to the rupture of those droplets. In the beginning of the sliding process, the bonded and mobile lubricant molecules present on the surface provide sufficient lubrication [12, 13], keeping the coefficient of friction in the range of ~0.042. The trapped droplets of the lubricant are quickly released in the beginning of the sliding process, which maintains low shear stress at the interface. The low

coefficient of friction condition is maintained for 5000 cycles and above because of the in-situ availability of lubricant.

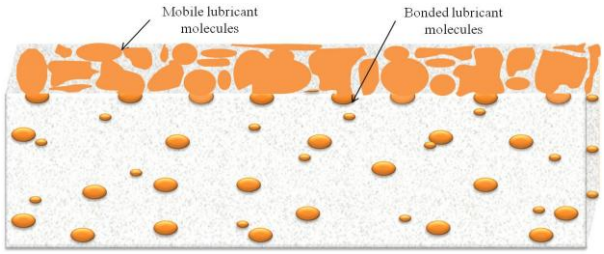

FIGURE 3. Possible sequences of lubrication mechanism at the ball surface interface during tribological test and lubricant distribution in the composite coating.

It is seen that with increasing linear sliding velocity, lubricant displacement increases from the contact point. At low sliding speed, a balance is maintained between the displacements of lubricant from the wear track and re-flows. But at higher speed, the displaced lubricant is not quickly available on the wear track due to insufficient time, leading to lubricant starvation. The repeated movement of lubricant from wear the track causes asperity contact, and the coefficient of friction increases, which leads to wear.

Zone 2 shows a mechanism where lubricant is mixed with the wear debris to form slurry, which provides lubrication. The coefficient of friction is maintained at constant value of ~0.07 – 0.08 for SN150 filled composites.

3.3 SEAR STRENGTH

The shear strength (τ) was calculated using Hertzian contact equations. The equations used for calculation are given below.

$$P = \frac{1}{\pi}\left(\frac{4 * E^{*} * F^{2}}{3 * R}\right)^{\frac{2}{3}} \qquad (1)$$

where F is the applied load during tribological test, R is the effective radius and E* is the effective Young's modulus and is given by the following equation;

$$R = \frac{R_1 * R_2}{R_1 + R_2} \qquad (2)$$

where R1 and R2 are the radius of ball and cylindrical samples. The effective modulus of elasticity is given by;

$$E^{*} = \frac{E_1 * E_2}{E_1(1-\nu_2^2) + E_2(1-\nu_1^2)} \qquad (3)$$

E1, E2 are modulus of elasticity and , are Poisson's ratio of ball and coated samples respectively.

Thus, the relation between contact pressure, coefficient of friction and shear stress is given by the following equation;

Shear stress (τ) = coefficient of friction (μ) x contact pressure (P) i.e.

$$\tau = \mu * P \qquad (4)$$

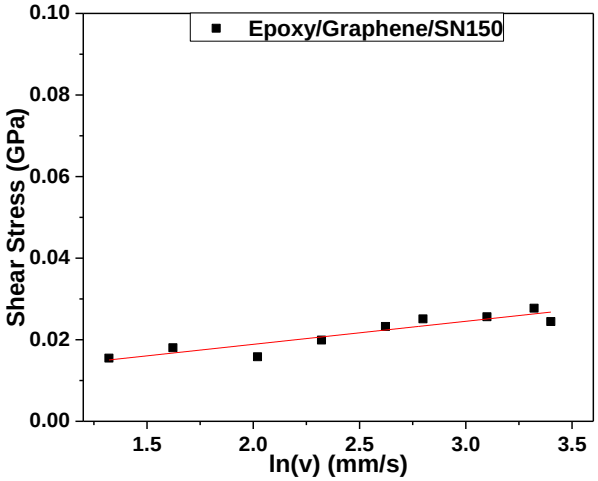

Figure 4. Shear stress (η) versus ln(v) plot for epoxy/graphene/SN150

Figure 4 shows shear stress (τ) as a function of ln (v) plots for epoxy/graphene/SN150 composites tested at the normal load of 10 N and at different sliding speeds for 5000 cycles. The shear stress is calculated by assuming the contact area to be Hertzian contact and the shear stress of interface is coefficient of friction times the pressure applied (Equation 4). The data are fitted to Equation (5), which is given as follows:

$$\tau = \tau_1 + \theta \ln V \qquad (5)$$

The values of τ1 and θ are calculated for epoxy/graphene/SN150 as 0.00758 GPa and 0.00565, respectively. There is an excellent fit of the data to this equation proving that the lubrication mechanism is in the mixed lubrication regime as proposed by Spikes [15]. The data also validate the earlier relation given by Briscoe and Evans [16] for monolayers of carboxylic acids and their soaps. In an earlier work [17], this equation was found to fit the experimental data for a SU-8 (epoxy type molecule) polymer matrix and functionalized PFPE (Z-dol) liquid filler composite. However, the curve fitting parameters are found to be different for different regimes. Hence, such differences were possible for different combinations of matrix and liquid fillers.

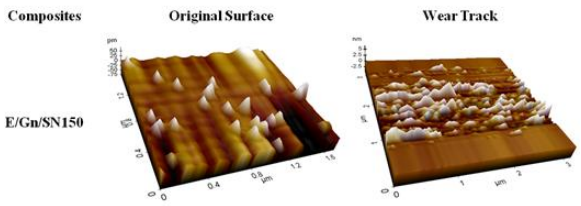

FIGURE 5. AFM images of original and worn surfaces of epoxy/graphene/SN150 (E/Gn/SN150) composites.

Figure 5 provides AFM images of the unworn (original) and worn surfaces for two composites (Epoxy/graphene/SN150). Whereas the original surface was very smooth, the worn surfaces showed many pillars, reduce the contact area, and also contributed to their excellent tribological performance in addition to other effects discussed earlier. These composites showed the lower steady-state coefficients of friction and lowest wear rates.

4. CONCLUSION

Tribological test of epoxy composite coating (epoxy/graphene/SN150) was in the boundary lubrication regime, and gave the lowest coefficient of friction (0.045) at low speed but at higher speed it exhibited little higher coefficient of friction (0.09). The wear rate for epoxy/graphene/SN150 was very low (2.5×10^{-7} mm^3/N-m) at 10 N load and nearly zero at low load of 3 N[18]. This coating can be applied to automotive engine parts where lubrication required.

ACKNOWLEDGEMENT

This research was funded by research grants from the Department of Mechanical Engineering at IIT Kanpur and IIT Delhi, India. We are also thankful to Dr. Ramakumar (Indian Oil Corporation Limited Faridabad, India) for providing base oil SN-150.

REFERENCES

[1] Vizintin J, Kalin M, Dohda K, Jahanmir S. Tribology of mechanical systems: A Guide to present and future technologies. American Society of Mechanical Engineers 2004.

[2] Li J, Ren T, Liu H, Wang D, Liu W. The tribological study of a tetrazole derivative as additive in liquid paraffin. Wear 2000; 246:130–133.

[3] Ren T, Xue Q, Wang H. A study of the tribological properties of S-(lH-benzotriazol-l-yl)-methyl, O, O'-dial~ldithiophosphates as additives in liquid paraffin. Wear 1994; 173:167–170.

[4] Glovnea RP, Olver AV, Spikes H. Lubrication of rough surfaces by a boundary film-forming viscosity modifier additive. Journal of Tribology 2005; 127:223–312.

[5] Varlot K, Kasrai M, Bancroft GM, Yamaguchi ES, Ryason PR, Igarash J. X-ray absorption study of antiwear films generated from ZDDP and borate micelles. Wear 2001; 249:1029–1035.

[6] Barros MI, Martin JM, Le-Mogne T, Vacheret B. Boundary lubrication mechanisms of carbon coatings by MoDTC and ZDDP additives. Tribology International 2005; 38:257–264.

[7] Podgornik B., S. Jacobson, S. Hogmark. Influence of EP and AW additives on the tribological behaviour of hard low friction coatings. Surface and Coatings Technology 2003; 165:168–175.

[8] Nikolai MK, Kovalev AV. Adhesion and Friction of Polymer. Polymer Tribology 2009; 25:2–37.

[9] Bowden FP, Tabor D. Friction, lubrication and wear: a survey of work during the last decade1964.

[10] Bahadur S. The development of transfer layers and their role in polymer tribology. Wear 2000; 245(1):92–99.

[11] Dong B, Yang Z, Huang Y, Li HL. Study on tribological properties of multi-walled carbon nanotubes/epoxy resin nano composites. Tribology Letters 2005; 20:251–254.

[12] Khun N W, Zhang H, Yang J, Liu E. Mechanical and tribological properties of epoxy matrix composites modified with microencapsulated mixture of wax lubricant and multi-walled carbon nanotubes. Friction 2013; 4:341–349.

[13] Bielecki RM, Crobu M, Spencer ND. Polymer-brush lubrication in oil: sliding beyond the Stribeck curve. Tribology Letter 2013; 49:263–272.

[14] Prathima CN, Shivaprakash NR, Rosa M. Espinosa-Marzal, Spencer ND. Exploring lubrication regimes at the Nanoscale: nano tribological characterization of silica and polymer brushes in viscous solvents. Langmuir 2013; 29(32):10149–10158.

[15] Spikes HA. Mixed lubrication—an overview. Lubrication Science1997; 9:221–253.

[16] Briscoe BJ, Evans DCB. The shear properties of Langmuir–Blodgett layers. Proc. R. Soc.Lond. A 1982; 380:389–407.

[17] Saravanan P, Sinha SK, Jayaraman S, Duong HM. A comprehensive study on the self-lubrication mechanism of SU-8 composites. Tribology International 2016; 95:391–405.

[18] Kumar V, Siha SK, Agarwal AK. Tribological studies of epoxy composites with solid and liquid fillers. Tribology international, 2017; 105:27-36.

Proceedings of the Third International Conference on Sustainable Energy and Environmental Challenges (3rd SEEC)
18 –21 December 2018, IIT Roorkee, India

SEEC No.116

EFFECTS OF SPRAY CHARACTERISTICS ON EMISSIONS FROM A METHANOL FUELLED SPARK-IGNITION ENGINE IN INDIAN CONTEXT

Hardikk Valera
Design Program
Indian Institute of Technology Kanpur
Email: hardikk@iitk.ac.in

Avinash Kumar Agarwal
Engine Research Laboratory
Department of Mechanical Engineering
Indian Institute of Technology Kanpur
Email: akag@iitk.ac.in

ABSTRACT

India has a higher percentage of two-wheelers due to its affordability, light weight and ease of maneuver compare to high duty vehicles. But, the two-wheelers are the primary source of air pollution. Un-clean emissions of conventional fuels have motivated Indian researchers to explore alternative fuels. Among of various possible options, Methanol is narrated as a potential alternative fuel because of its high oxygen content, which leads to a reduction in harmful pollutants. However, Emissions from the engines are dependent on fuel atomization and resulting air-fuel mixing. So, it is necessary to investigate the spray characteristics of methanol. This study focuses on the spray characterization of Methanol Blended Gasoline (MBG) using Phase Doppler Interferometry (PDI) for measurement of various Microscopic spray parameters such as Sauter Mean Diameter (SMD), velocity distribution, etc. and emission measurement i.e. CO (Carbon Monoxide), HC (Hydro-Carbon), NO_X (Nitrogen Oxide) at different throttle positions (25%, 50%, 75%, 100%) of 100cc carburettor, using M15 with mineral gasoline as a baseline.

Keywords: ***Methanol, Carburetor, Microscopic spray characteristics, Emission***

INTRODUCTION

Indian market is the largest vehicle class for two-wheeled vehicles, such as mopeds, scooters, and motorcycles, powered by the SI engine. As per the report, two-wheelers industry saw a total sale of 2.01 crore unit sold in the Indian market with 20 percent shot up in the exports.

During Financial Year (FY) 2017-2018, sales of Scooters and Motorcycles increased by 19.90 percent and 13.69 percent respectively, and sales of mopeds are declined by 3.48 percent compared to sales in FY 2016-2017 [1]. These two-wheelers are the significant sources of emissions compared to other vehicles because of its population density. It is necessary to control the emissions because it has a significant effect on air quality, particularly in the urban areas of the country. So, the Indian government is establishing stringent and robust emission norms to control the CO, HC and NO_X by leapfrogging the Bharat Stage (BS) V emission standards to BS VI emission standards. This standard will apply to vehicles manufactured on or after April 1, 2020.

Apart from environmental degradation due to emissions, the demand for energy is also becoming a serious issue as it is expected to increase at a Compounded Annual Growth Rate (CAGR) of 3.5% up to 2040. India imported 37% of its total primary energy demand in 2015-16, whereas the import dependence of natural gas and crude oil has increased to 40% and 81% in 2015-16 concerning 17% and 73% in 2005-06 [2]. However, there has been a dismal growth in the production of domestic oil (CAGR – 1.4%) and natural gas (0.01%) over the last decade. Therefore, it is necessary to explore an alternative fuel which can solve the twin crisis: environmental degradation and depletion of fossil fuels. Exploration of alternative fuels should be by the source of production, its compatibility with existing fuel delivery infrastructure and cost to energy benefits. India is seeing methanol as an alternative fuel and moving towards methanol economy because of its foreseeable benefits as mentioned below.

- India has an enormous quantity of high ash coal which is considered as a prior raw material for methanol.
- Import of methanol is quite cheaper than the conventional fuels if production is not sufficient to meet demand.
- Combustion noise from the methanol is relatively lesser than the gasoline-powered SI engines.
- Methanol-powered SI engine produced lesser harmful pollutants compared to conventional fuels.

Globally many studies have been done to find out the effect of methanol-gasoline blends on emissions vis-à-vis baseline gasoline, are summarised in Table 1. Furthermore, a couple of investigations have been done to study the spray characteristics of methanol vis-à-vis baseline gasoline, are summarised in Table 2.

TABLE 1: IMPORTANT EMISSIONS RESULTS OF METHANOL-GASOLINE BLENDS

G: Gasoline, M: Methanol, GaMb: Gasoline a% (v/v), Methanol b% (v/v)			
Year	Researcher	Fuel used	Concluding Remarks
1985	Emam et al. [3]	G100, M100	CO (↓) NO_X (↓)
1997	Cetinkaya et al. [4]	G100, G97M3, G95M5, G93M7, G90M10,	CO (↓) NO_X (↓) are HC (↑)
2008	Wai et al. [5]	G100, G90M10, G80M20, G15M85	CO (↓) NOx (↓)
2014	Agarwal et al. [6]	G100, G90M10, G80M20	NO (↓), CO (↓), Smoke Opacity (↓), HC (↑)
2015	Li et al. [7]	G100, G85M15	HC (↓), CO (↓), NOx (↑)
2016	Yao et al. [8]	G100, G90M10, G80M20, G70M30, G50M50, G30M70	NOx (↓), HC (↓)
2017	Shetty et al. [9]	G90M10, G85M15, G80M20, G75M25, G70M30	CO (↓), HC (↓), NOx (↓)

The tabulated experimental analysis suggested that Methanol-Gasoline blends can be used as fuel in SI engines. The tail-pipe emission results varied from researcher to researcher and there was no unique trend in results. Reduction in CO and NO_X leads to increase in HC emissions whereas reduction in HC leads to increase in NO_X emissions.

TABLE 2: IMPORTANT SPRAY RESULTS OF METHANOL BLENDS

G: Gasoline, M: Methanol, GaMb: Gasoline a% (v/v), Methanol b% (v/v)				
Year	Researcher	Fuel Used	Concluding Remarks	Device
2001	Choi et al. [10]	G100, G15M85	Spray Angle (↑), Entropy (↑)	Injector
2007	Yanfeng et al. [11]	D100, M100	penetration length (↑), tip velocity (↑)	Injector

As shown in Table-2, a couple of researchers studied the spray characteristic of methanol using an injector. But, in our country, two-wheelers are powered by SI engine with the assistance of carburetor. The carburetor is a robust device comprised of air orifice, pilot jet, main jet, venturi, and butterfly valve. It is used to supply proper air-fuel mixture through mixing, atomizing and vaporizing the volatile fuel with air. Fuel is drawn into the manifold through the main jet because of the pressure difference between the float chamber and the throat of the venturi. Fuel emerging from the carburetor is in the form of column or sheet. Aerodynamic forces are acting on the column or layer of the fuel due to the relative velocity between the air and fuel, which is called the primary atomization of the fuel. Fine droplets occur at the throttle plate due to the high aerodynamic forces, which is called secondary atomization. This entire complex process of carburetion depends on the suction pressure and throttle position, which are correlated with each other.

Moreover, vaporization of fuel mainly depends on the diameter of the droplets which directly depend on the diameter of the jet. However, it has the significant effect on the emissions. So, it is necessary to study the spray characterization of jet-assisted fuel to investigate its impact on the emissions.

The present study aimed to clarify the potential causes of air pressure on the Sauter mean diameter (SMD), and the velocity distribution of the M15 vis-à-vis gasoline. Considering the influence of throttle positions on the suction pressure, a wide range of throttle positions were tested. To this end, emissions were measured from the

same carburetor assisted vehicle at same throttle positions for the M15 vis-à-vis gasoline.

EXPERIMENTAL SETUP

The experiments were conducted in two parts. In the first part, PDI (Phase Doppler Interferometry)-300 is used to measure the droplet size distributions and velocity distributions of test fuel (M15 and gasoline).

PDI primarily uses a Diode-pumped solid-state laser as light sources which are emitted at two wavelengths. Green (532 nm) and blue (473 nm). As shown in Figure-1 the transmitter and receiver have been employed to carry out the spray characterization at various throttle positions (25%, 50%, 75% and 100% throttle). Here, Interference fringes created by the two laser beams, i.e., emitted from the transmitter. When droplet passes from the interfere fringes it reflects the local light intensity on the receiver which directed on to the photomultiplier tubes to produces a typical Doppler burst signal. The frequency of signal gives the information about the velocity distribution as shown in Eq. 1. Moreover, droplet size is found using Eq. 2

$$V = Fs * \Delta 1 \qquad (1)$$

$$D = (Fv * W)/(S * \Delta 2) \quad (2)$$

Where, Fs = Frequency of signal
$\Delta 1$ = Spacing between fringes
Fv =Volume flux,
W = Fringe width,
S= Slope factor, and
$\Delta 2$ =Spatial wavelength

In the second part, Hero HF Deluxe- 100 cc was used to assess the emission characteristics of the test fuels using Horiba; EXSA-1500 as shown in Figure 2. CO, CO_2, HC, and NOx are measured at the same throttle positions and air pressure as used to measure the spray characteristic. Specifications of the test bike are given in Table 3.

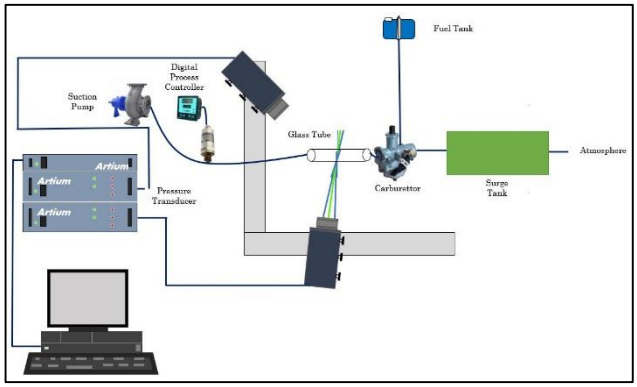

FIGURE 1: SPRAY INVESTIGATION USING PDI

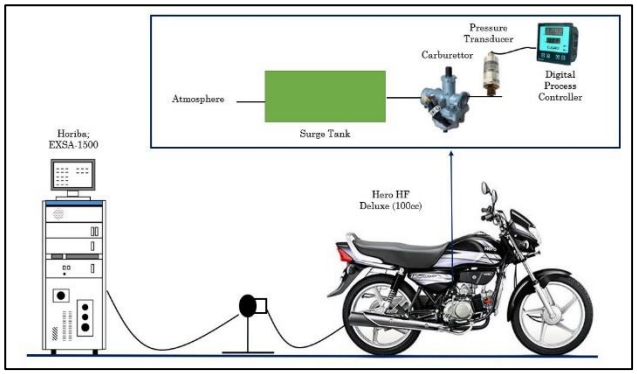

FIGURE 2: EMISSION MEASUREMENT USING TWO-WHEELER

TABLE 3 SPECIFICATION OF THE 100CC HF DELUXE

Type	Air cooled, 4 - stroke single cylinder OHC
Displacement	97.2 cc
Max. Power	6.15 kW (8.36 Ps) @8000 rpm
Max. Torque	0.82 kg-m (8.05 N-m) @5000 rpm
Max. Speed	87 Kmph
Bore x Stroke	50.0 mm x 49.5 mm
Carburettor	Side Draft, Variable Venturi Type with TCIS
Compression Ratio	9.9 :1
Starting	Kick start / Self start
Ignition	DC - Digital CDI
Oil Grade	SAE 10 W 30 SJ Grade, JASO MA Grade
Air Filtration	Dry, Pleated Paper Filter
Fuel System	Carburetor
Fuel Metering	Carburetion

RESULTS AND DISCUSSION

ACKNOWLEDGMENTS

The authors thank the Hero MotoCorp for providing the 100CC HF Deluxe bike and all accessories support.

REFERENCES

[1] Two-wheeler statistics (http://www.siamindia.com/pressrelease-details.aspx?mpgid=48&pgidtrail=50&pid=413)

[2] India's Leapfrog to Methanol Economy - NITI Aayog (niti.gov.in/writereaddata/.../Article%20on%20Methanol%20Economy_Website.pdf)

[3] El-Emam, S.H. and Desoky, A.A., 1985. "A study on the combustion of alternative fuels in spark-ignition engines". International journal of hydrogen energy, 10(7-8), pp.497-504.

[4] Cetinkaya, S. and Celik, B., 1997. "The use of methanol–gasoline blends as fuel in spark ignition engine". In Fifth International Combustion Symposium, Uludag University (pp. 21-23).

[5] Yanju, W., Shenghua, L., Hongsong, L., Rui, Y., Jie, L. and Ying, W., 2008. "Effects of methanol/gasoline blends on a spark ignition engine performance and emissions". Energy & Fuels, 22(2), pp.1254-1259.

[6] Agarwal, A.K., Karare, H. and Dhar, A., 2014. "Combustion, performance, emissions and particulate characterization of a methanol–gasoline blend (gasohol) fuelled medium duty spark ignition transportation engine". Fuel Processing Technology, 121, pp.16-24.

[7] Li, L., Ge, Y., Wang, M., Li, J., Peng, Z., Song, Y. and Zhang, L., 2015. "Effect of gasoline/methanol blends on motorcycle emissions: exhaust and evaporative emissions". Atmospheric Environment, 102, pp.79-85.

[8] Yao, D., Ling, X. and Wu, F., 2016. "Experimental investigation on the emissions of a port fuel injection spark ignition engine fueled with methanol–gasoline blends". Energy & Fuels, 30(9), pp.7428-7434.

[9] AS, D.S. and Antony, A.J., 2017. "Experimental Study on Digital Twin Spark Ignition Gasoline Engine at Different Gasoline-Methanol Blends". International Journal of Applied Engineering Research, 12(13), pp.3817-3821.

[10] Choi, W. and Choi, B.C., 2001. "An investigation of methanol and methanol blended sprays using laser scattering images". KSME international journal, 15(12), pp.1699-1710.

[11] Yanfeng, G., Shenghua, L. and Yu, L., 2007. "Investigation on methanol spray characteristics". Energy & Fuels, 21(5), pp.2991-2997.

Proceedings of the Third International Conference on Sustainable Energy and Environmental Challenges (3rd SEEC)
18 –21 December, 2018, IIT Roorkee, India

SEEC No. 117

EFFECT OF INLET AIR TEMPERATURE ON MACROSCOPIC AND MICROSCOPIC SPRAYCHARACTERISTICS OF METHANOL BLEND FOR TWO WHEELER APPLICATIONS

Ashutosh Jena
Engine Research Laboratory
Department of Mechanical Engineering
Indian Institute of Technology Kanpur
Email: asutosh@iitk.ac.in

Avinash Kumar Agarwal
Engine Research Laboratory
Department of Mechanical Engineering
Indian Institute of Technology Kanpur
Email: akag@iitk.ac.in

ABSTRACT

With the ongoing environmental issues and fuel crisis, the sustainability of the spark ignition (SI) engine in long run would be largely determined by how it adopts with the new alternative fuels. Methanol is seen as the pioneer of alternative fuel movement for SI engines. It has higher octane rating which allows the engine to work under higher compression ratio thus achieving better efficiency. However its high latent heat value makes it more prawn towards wall impingement and poor atomisation. Hence it is of great importance to study its spray plume interaction for optimising the engine performance with methanol. The present study was intended to investigate the effect of inlet air temperature on spray atomisation and penetration of a port fuel injector. Phase Doppler Interferometry (PDI) was used to determine the Arithmetic Mean Diameter (AMD) and Sauter Mean Diameter (SMD). Penetration analysis was done through spray visualisation technique by using a high speed CCD camera. Different air temperature was maintained in a constant volume chamber in which the spray was injected for the experiment.

Keywords: Methanol, spray characteristics, inlet air temperature, Port Fuel Injection.

INTRODUCTION

The past decades have seen significant progress in controlling the tail pipe emissions from automotive engines. Despite this, there is continuous decline in environmental health. This issue is more critical in urban areas. Both SI and CI engines together are major culprits for sick urban air. As far as city traffic is concerned, major portion of it consist of small passenger cars and two wheelers powered by SI engines. These engines are major source of HC and aldehyde emissions. In fact SI engines produce five times more HC then its diesel rivalries [1]. Studies suggest HC can act as a catalyst for developing cancer in humans [2, 3]. Aldehydes may cause irritation and also play a pivotal role in the formation of photochemical smog [4]. Hence to accelerate the progress to cut down emission is need of the hour.

The advancement in SI engine emission regulation is largely connected to better understanding of fuel induction system. Playing with the carburetor design, which has been the warhorse for fuel induction system in SI engine for years, has significantly contributed to bring the CO emissions down [5]. However all modern day cars and two wheelers have switched to the electronic injection technology. At the same time with the burden of fuel price, the world is eagerly looking for the gasoline alternatives.

Among all gasoline alternatives studied, alcohols have gained much attention due to their availability and reliability. Alcohols, mainly methanol can be produced from coal, biomass and natural gas [6]. Despite lower heating value, the fact that it has higher octane rating will allow the engine to run at higher compression ratio thus improving its efficiency. Methanol has higher latent heat of vaporization which would decrease the engine operating temperature. This will bring down the NOx emission. It also increases the oxygen concentration. Abundance of oxygen would help in complete oxidization of carbon and would decrease CO emission.

It is necessary to study the performance of methanol injection system with the conventional design of injection system. These injection systems are in use with gasoline for some time. One of these designs is Port Fuel Injection (PFI) system. In this system, fuel is injected downstream of throttle plate which is back of the valve. This is completely different from carburetor injection system and yet to be understood completely [1]. Hence the manifold design can

be better optimised given the fundamentals like spray formation flow interaction and effect of fuel properties is very well understood.

To study the above mentioned characteristics both macroscopic and microscopic aspects of the spray plume need to be analysed. Microscopic study reveals the atomization quality and fuel dispersion and the macroscopic study helps to analyse the spray penetration which is important to study wall impingement. Studies have found that the wall impingement of fuel has been a common problem for PFI [7]. During transient operation, the fuel film on wall will hinder drivability, increase pollutant emission and hurt fuel economy [8]. Though these issues are more pronounced during cold operation but at the same time liquid drops of fuel have also been spotted in fully warmed up engines with PFI [9]. Microscopic analysis is important to study effect of drag and gravity on micro droplets. Previous studies suggest that the drag is a strong function of Reynolds number (Re) [1]. Hence it seems quite obvious that increasing air temperature will increase atomization as Re itself is a function of air density.

It is quite clear from the previous literature that the spray characteristics plays pivotal role in overall engine performance and determining tail pipe emission. In this paper, our focus is on the effect of inlet air temperature upon spray plume. Both macroscopic and microscopic characteristics of the spray plume are studied for methanol in PFI system.

EXPERIMENTAL SETUP

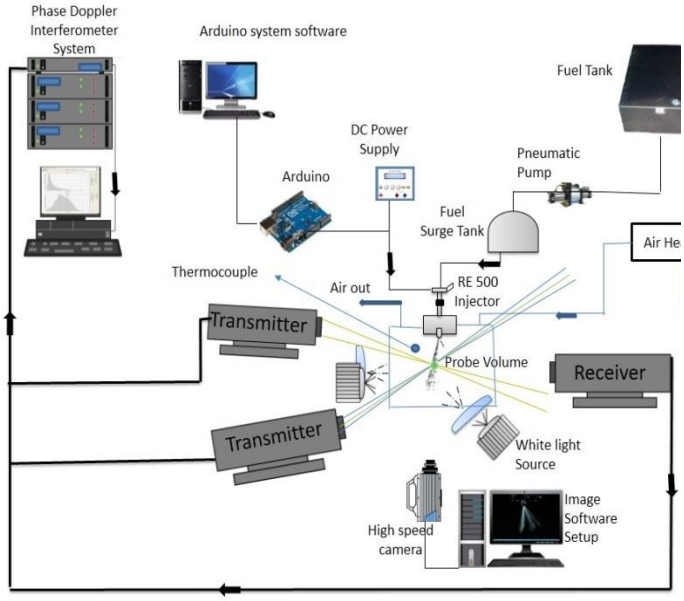

Figure 1: Schematic of macroscopic and microscopic spray characterization setup

A spray chamber was fabricated using glass and ply wood to isolate the spray and maintain the working temperature. The constant volume chamber was fed with hot air from the heater. A steady mass flow rate was maintained to achieve a particular constant temperature inside the chamber. A thermocouple was placed close to the spray plume to note the chamber temperature. The injector was controlled using an Arduino system and software. To study the microscopic spray characteristics Phase PDI technique was employed. AMD and SMD were measured for methanol blend at different chamber temperature (Ambient, 40°C, 60°C). For the macroscopic study, a high speed CCD camera was used along with two flicker free white light source. Spray penetration length, cone angle and spray area were determined using imaging software.

RESULTS AND DISCUSSION

In the present study, tests were carried out using M85 blend for three different temperature conditions (ambient,40°C&60°C).
The analysis was done on the basis of the following parameters.
(i) Arithmetic Mean Diameter(AMD) (ii) Sauter Mean Diameter(SMD) (iii)Spray Penetration length (iv)Spray cone angle (v)Spray plume area.

REFERENCES

[1] Heywood, J.B., 1988, Internal Combustion Engine Fundamentals, McGraw-Hill, New York.
[2] Diaz-Sanchez, D., 1997. The role of diesel exhaust particles and their associated polyaromatic hydrocarbons in the induction of allergic airway disease Allergy 52 (38 suppl): 52–56.
[3] Krzyzanowski, M., Kuna-Dibbert, B. and Schneider, J., Health effects of transport-related air pollution 2005. World Health Organization: Geneva.
[4] Agarwal, A.K., 2007. Biofuels (alcohols and biodiesel) applications as fuels for internal combustion engines. Progress in energy and combustion science, 33(3), pp.233-271.
[5] Liimatta, D. R., et al. "Effects of mixture distribution on exhaust emissions as indicated by engine data and the hydraulic analogy." SAE Transactions (1971): 2213-2238.
[6] Wang, Xibin, et al. "Spray characteristics of high-pressure swirl injector fueled with methanol and ethanol." Energy & Fuels 19.6 (2005): 2394-2401.
[7] Serras-Pereira, J., et al. "Heat flux characteristics of spray wall impingement with ethanol, butanol, iso-octane, gasoline and E10 fuels." International Journal of Heat and Fluid Flow 44 (2013): 662-683.
[8] Servati, Hamid B., and Walter W. Yuen. "Deposition of fuel droplets in horizontal intake manifolds and the behavior of fuel film flow on its walls." SAE transactions (1984): 125-133.
[9] Peters, Bruce D. Laser-Video Imaging and measurement of fuel droplets in a spark ignition engine. General Motors Research Laboratories, 1983.

Proceedings of the International Conference on Sustainable Energy and Environmental Challenges (SEEC-2018)
18 – 21, December, 2018, IIT Roorkee, India

SEEC No.118

OPTIMIZATION OF METHANOL POWERED INTERNAL COMBUSTION ENGINE

Vikram Kumar
Dept. of Mechanical Engg.
Indian Institute of Technology Kanpur
Email: vikramk@iitk.ac.in

Avinash K. Agarwal
Dept. of Mechanical Engg.
Indian Institute of Technology Kanpur
Email: akag@iitk.ac.in

ABSTRACT
Methanol is a substitute for conventional fuel which is used in Internal Combustion (IC) engine. It is renewable, economically and environmentally interesting. In the experiment naturally aspirated single cylinder four stroke diesel engine was modified and used. Methanol is an alternate fuel for IC engines in terms of environment and economical aspect. Port fuel injection method was applied for the substitution of diesel fuel with methanol. The methanol injection is nearly double of diesel as the methanol fuel has lower calorific value than diesel fuel (~53 % of diesel). Diesel was replaced up to 90 % with methanol. Methanol was injected in intake port by two injectors at 3 bar fuel pressure. As the calorific value of methanol is nearly half of the diesel fuel. In this paper, effect of methanol on the IC engine parts and modifications required is studied.

***Keywords**: Methanol, IC engine, Port Fuel Injction.*

INTRODUCTION
Present days our source of energy supply is mostly based on non-renewable source (petroleum). Petroleum based fuels are rapidly depleting. As the energy demand increases there is requirement of more efficient engines. Diesel engine is mainly used in power generation and transportation as they have higher efficiency, but the drawbacks are the pollution (higher generation pollutant such as NOx and soot). These emissions from diesel engines are harmful to human health and environment [1]. To reduce these harmful emissions, there is requirement of new technology and alternative fuel to reduce the undesirable emissions. Future renewable clean alternative fuels are alcohols such as methanol, ethanol, butanol and dimethyl ether (DME). Presently, methanol is used as alternative renewable replacement for fossil fuels [2]. Methanol is produced from natural gas, coal, municipal solid waste, and waste biomass through previously demonstrated technologies [3, 4]. Methanol can be produced from any materials which can decompose in to H2 and CO or CO2 [4].

The effect of premixed methanol on engine performance and emoission characterstics were studied by many researchers. But the effect of diesel injection strattgy on diesel combustion performance was concern of study. Generly diesel fuel was injected at specific injection time based on the engine operation recommendation throughout the test [5, 6]. Fuel injection timing was most important parameter for emission control and efficiency optimization. Performance and emission of diesel engine based on methanol substitution depend on the injection timing of fuel [7]. For the same methanol substitution ratio performance and emission was changed with changing the injection time. Hence methanol substitution effect was not clear in the many studies.

The influence of diesel replacement by methanol on engine combustion and emission performances was rarely studied experimentally, so how is the effect going on needs to reveal. The objective of this study is to discuss the modification in engine and to optimize the percentage of methanol to replace diesel, engine combustion, performance and emission characteristics. Moreover, how to optimize the NOx and soot emissions by adjusting the two parameters was also discussed in this study.

2. EXPERIMENTAL PROCEDURE
2.1. TEST ENGINE
Production-grade single-cylinder, four-stroke, water-cooled, naturally-aspirated, constant speed diesel engine (Kirloskar; DM-10) was used for the experimental test. Technical specifications of the test engine are given in Table 1.

Table 1: Technical specification of Internal Combustion diesel engine.

Engine parameters	Specifications
Make/Model	Kirloskar Oil Engines Limited (KOEL), India/ DM-10
Engine type	Vertical, four-stroke, single-cylinder, constant-speed, direct-injection CI engine
Rated power output	7.4 kW (10 hp)
Rated engine speed	1500 rpm
Bore/ Stroke	102 mm/ 116 mm
Displacement volume	948 cc
Compression ratio	17.5
Nozzle opening pressure	200 bar
Cooling type	Water cooling
Governor type	Mechanical, centrifugal (A2 class)

2.2. ENGINE MODIFICATION FOR DUAL FUEL SYSTEM

In this study dual fuel compression ignition combustion was implemented. Premixed port fuel injection method was adopted for methanol fuel injection at the intake many fold. It consists of methanol injectors, common rail for fuel, pressure regulator, fuel pump, filter and a methanol tank. Methanol injection is controlled by the ECU to control the methanol quantity by changing the injection duration.

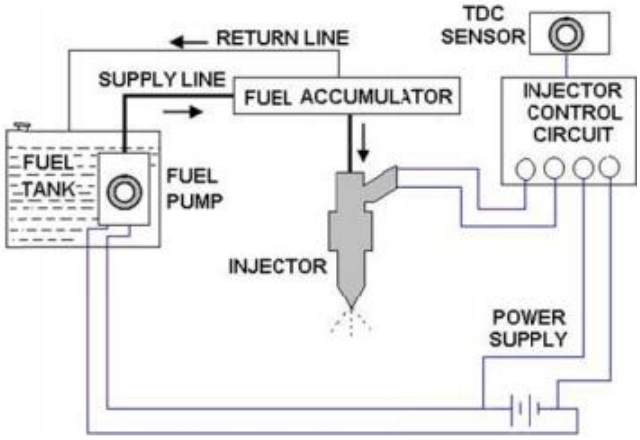

FIGURE 1. Schematic of test enginefuel injection system

2.3 ECU CIRCUIT PREPARATION

ECU circuit is designed and fabricated for methanol fuel injection. It consist of arduino, mosfet, various resister, capacitor and LED. Aurdino program is written according to injection delay and injector opening time required for fuel supply.

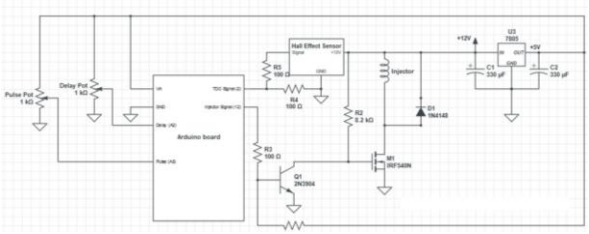

FIGURE 2. Schematic of ECU circuit

ACKNOWLEDGEMENT

This research was funded by research grants from the Engine Research Lab (ERL) Department of Mechanical Engineering at IIT Kanpur.

REFERENCES

[1] Hsieh WD, Chen RH, Wu TL, Lin TH. Engine performance and pollutant emission of an SI engine using ethanol–gasoline blended fuels. Atmos Environ 2002;36(3):403–10.

[2] Balat M. Production of bioethanol from lignocellulosic materials via the biochemical pathway: a review. Energy Convers Manage 2011;52(2): 858–75.

[3] Chmielniak T, Sciazko M. Co-gasification of biomass and coal for methanolsynthesis. Appl Energy 2003, 74(3):393e403.

[4] Olah GA, Goeppert A, Prakash GKS. Beyond oil and gas: the methanol economy. John Wiley & Sons; 2009.

[5] Geng P, Yao CD, Wei LJ, Liu JH, Wang QG, Pan W, et al. Reduction of PM emissions from a heavy-duty diesel engine with diesel/methanol dual fuel. Fuel 2014;123:1-11.

[6] Zhang ZH, Cheung CS, Yao CD. Influence of fumigation methanol on the combustion and particulate emissions of a diesel engine. Fuel 2013;111: 442-8.

[7] Liu JH, Yao AR, Yao CD. Effects of injection timing on performance and emissions of a HD diesel engine with DMCC. Fuel 2014;134:107-13.

Proceedings of the International Conference on Sustainable Energy and Environmental Challenges (3rd SEEC)
18 – 21, December, 2018, IIT Roorkee, India

SEEC No.119

PERFORMANCE AND EMISSION ANALYSIS OF METHANOL FUELED GENSET

Vikram Kumar
Dept. of Mechanical Engg.
Indian Institute of Technology Kanpur
Email: vikramk@iitk.ac.in

Avinash K. Agarwal
Dept. of Mechanical Engg.
Indian Institute of Technology Kanpur
Email:akag@iitk.ac.in

ABSTRACT
The main objective of this investigation is to evaluate performance and emissions of a genset by replacing diesel fuel with methanol. In the experiment single cylinder four stroke diesel engine was used. Methanol fuel was injected in the intake port near to the valve along with heated air. Percentage methanol energy share, injection timing and intake air temperature were optimized. The quantity of methanol and the injection timing were control by tailor made electronic control unit (ECU) on the electronic injector. Brake thermal efficiency (BTE),brake mean effective pressure (BMEP) smoke quantity, nitrogen oxides (NOx) carbon mono oxide (CO) and unburned hydrocarbon (UHC) were evaluated at different load and optimal energy replacement of diesel with methanol.

***Keywords:* *Diesel,* *Methanol, IC Engine*.**

INTRODUCTION

Diesel engines are one of the most efficient sources of power generation. It has high reliability and thermal efficiency with very good fuel economy performance. It can be used many kinds of power generation like stationary power stations, marine power plants and on-road and off-road vehicles [1]. However, the exhaust emissions from diesel engines are main source of air pollution. The diesel fuel combustion process is mixing controlled diffusion combustion. It is difficult to make homogeneous air-fuel premixed mixture before ignition because of its properties such as high viscosity, low volatility and easy ignitability. Thus due to high temperature zones and presence locally rich fuel was main reason to produce high particulate (PM) and NOx emissions [1].

Emissions from diesel engine can be reduced by using alternate fuel in dual fuel operation mode at inlet port and engine performance is also enhanced]. The various alternate fuels are liquefied petroleum gas (LPG), natural gas, bio gas, gasoline, propane, ethanol and methanol [2 – 9]. Methanol was injected for diesel methanol dual fuel in heavy duty diesel engine at constant load and speed. At greater methanol injection (more than 30%) and higher temperature (60 – 70 ºC) had more significant effect on emissions [10]. Operating parameters were optimized by using Taguchi method in a gasoline engine fueled with gasoline, methanol or ethanol. The optimal engine speed was 2400 rpm and compression ratio was 9.0 for all fuels. The optimal ignition timing was 20º CA for alcohol. The performance and emissions were evaluated for optimized engine and compared with conventional engine [11].

Although many researcher has used the methanol as secondary fuel for diesel engine and port fuel techenique has been applied but no one done the maximum energy replacement. In this study, experiments were performed for different energy replacement of diesel by methanol fuel and their effect on performance and emissions were analyzed.

2. EXPERIMENTAL PROCEDURE

2.1 TEST ENGINE

Production-grade single-cylinder, four-stroke, water-cooled, naturally-aspirated, constant speed diesel engine (Kirloskar; DM-10). was used for the experimental test. The tests were performed at 1500 rpm speed and three different loads. Technical specifications of the test engine are given in Table 1.

Table 1: Engine specifications

Engine parameters	Specifications
Make/Model	Kirloskar Oil Engines Limited (KOEL), India/ DM-10
Engine type	Vertical, four-stroke, single-cylinder, constant-speed, direct-injection CI engine
Rated power output	7.4 kW (10 hp)
Rated engine speed	1500 rpm
Bore/ Stroke	102 mm/ 116 mm
Displacement volume	948 cc
Compression ratio	17.5
Nozzle opening pressure	200 bar
Cooling type	Water cooling
Governor type	Mechanical, centrifugal (A2 class)

FIGURE 1. Experimental Setup.

2.2 FUEL AND ITS SUPPLY

Methanol and diesel fuel was used for the experiment diesel engine. Tailor made fuel injection system was developed in intake port by using two injectors. Injectors were connected with fuel pump by using a common rail. Methanol and diesel fuel properties are given in Table 2.

Table 2: Comparison of methanol and diesel fuel properties.

Property	Methanol	Diesel
Formula	CH3OH	C12H26–C14H30
Molecular weight (kg/kmol)	32	170–198
Boiling point, °C	65	180–360
Autoignition temperature, °C	392	315
Cetane number	3-5	40–55
Density, kg/m3	796	820
Octane number	111	--
Kinetic viscosity at 20 °C, mPa s	0.7	3.4
Flash point, °C	11	78
Calorific value (kJ/kg)	23800	44500
Fraction of oxygen, wt%	50	0
Ignition temperature (°C)	470	246

ACKNOWLEDGEMENT

This research was funded by research grants from the Engine Research Lab (ERL) Department of Mechanical Engineering at IIT Kanpur.

REFERENCES

[1] Heywood B. Internal combustion engine fundamentals. New York: McGrawHill; 1988.

[2] Wei LJ, Yao CD, Han GP, Pan W. Effects of methanol to diesel ratio and diesel injection timing on combustion, performance and emissions of a methanol port premixed diesel engine. Energy 2016;95:223-32.

[3] Wang Y, Liu H, Huang ZY, Liu ZS. Study on combustion and emission of a dimethyl ether-diesel dual-fuel premixed charge compression ignition combustion engine with LPG (liquefied petroleum gas) as ignition inhibitor. Energy 2016;96:278-85

[4] Li WF, Liu ZC, Wang ZS. Experimental and theoretical analysis of the combustion process at low loads of a diesel natural gas dual-fuel engine. Energy 2016;94:728-41.

[5] Paykani A, Kakaee AH, Rahnama P, Reitz RD. Effects of diesel injection strategy on natural gas/diesel reactivity controlled compression ignition combustion. Energy 2015;90:814-26.

[6] Barik D, Murugan S. Investigation on combustion performance and emission characteristics of a DI

(direct injection) diesel engine fueled with biogas-diesel in dual fuel mode. Energy 2014;72:760-71.
[7] Yang BB, Yao MF, Cheng WK, Li Y, Zheng ZQ, Li SJ. Experimental and numerical study on different dual-fuel combustion modes fuelled with gasoline and diesel. App Energy 2014;113:416-27.
[8] Lee J, Chu S, Cha J, Choi H, Min K. Effect of the diesel injection strategy on the combustion and emissions of propane/diesel dual fuel premixed charge compression ignition engines. Energy 2015;93:1041-52.
[9] Wu HW, Wang RH, Chen YC, Ou DJ, Chen TY. Influence of port-inducted ethanol or gasoline on combustion and emission of a closed cycle diesel engine. Energy 2014;64:259-67.
[10] Pan W, Yao CD, Han GP, Wei HY, Wang QG. The impact of intake air temperature on performance and exhaust emissions of a diesel methanol dual fuel engine. Fuel 2015;162:101-10.
[11] Balki MK, Sayin C, Sarikaya M. Optimization of the operating parameters based on Taguchi method in an SI engine used pure gasoline, ethanol and methanol. Fuel 2016;180:630e7.
[12] Liu JH, Yao AR, Yao CD. Effects of diesel injection pressure on the performance and emissions of a HD common-rail diesel engine fueled with diesel/methanol dual fuel. Fuel 2015;140:192-200.

SEEC No.120

THERMODYNAMIC EQUILIBRIUM MODELING OF A DOWNDRAFT GASIFIER: STOICHIOMETRIC MODEL

Bhoopendra Pandey
Department of Mechanical Engineering
NIT Uttarakhand, Srinagar (Garhwal),
Uttarakhand, India, 246174
bhoopendrapandey.101622@gmail.com

Yogesh K. Prajapati
Department of Mechanical Engineering
NIT Uttarakhand, Srinagar (Garhwal),
Uttarakhand, India, 246174
yogesh.k@nituk.ac.in

ABSTRACT

This paper presents the mathematical study to predict the syngas composition, calorific value and gasification temperature of biomass based downdraft gasifier. The major products are the composition of CO, H_2 and CO_2. The predicted results of present model are compared with the experimental data. The model results showed good agreement with the experimental data. The effect of moisture content and equivalent ratio are investigated and discussed. The effect of moisture content on production of methane and nitrogen is found very negligible whereas carbon monoxide and hydrogen production have been significantly influenced by moisture content.

Keywords: *Biomass gasification, Downdraft gasifier, Thermodynamic equilibrium modeling.*

NOMENCLATURE

HHV	higher heating value, MJ/kg
m	kmol of oxygen per kmol of feedstock
w	amount of water per kmol of wood
x_i	mole friction of species
k_1 & k_2	equilibrium constant
a, b & d	molar ratio of C/H, C/O and N/C

INTRODUCTION

In the current scenario, biomass has been recognized as a good alternative renewable source of energy. Different types of biomass have been widely used for power production. Their contribution has significant effect on global power production. Direct utilization of biomass for energy or power production is not effective nowadays. Hence, conversion of biomass to desire fuel is one of the most projecting techniques to utilize the biomass for several purposes [1]. Among the different techniques, biomass gasification is one that is based on the thermochemical process to convert the biomass into gaseous fuel (called syngas or producer gas). The syngas or producer gases mainly consist of CO and H_2 with methane, ethylene and other pollutants. This producer gas can be used directly as a fuel to run the internal combustion engine. In Indian perspective, the downdraft gasifier is most utilized gasifier for small-scale power production.

The design of downdraft gasifier plays an important role in the gasification of biomass. However, designing a new gasifier of appropriate size requires a lot of effort and resources. It is also a time consuming and needs considerable experimental facility. Hence, numerical approach is a good technique to get the insight of gasifier and understand the fundamental physics related to gasification of biomass. In addition, it is economical to save the experimentation cost and other resources.

In the literature, several numerical models are available to simulate the gasification process for different types of gasifier with different level of accuracy and model depth [2–4]. Generally, numerical models related to downdraft gasifier are classified into equilibrium and kinetic rate model. Furthermore, equilibrium model have two types stoichiometric and non-stoichiometric model. Zainal et al. [5] used the equilibrium model based on equilibrium constant and predict the final gas composition

for various types of biomass. In their model, oxygen amount was not defined nevertheless it was considered as a variable. However, in most of the literature, amount of oxygen is generally known or fixed. Gambarotta et al. [6] simulated and validated a non-stoichiometric equilibrium model for biomass gasification process.

In the present study, stoichiometric equilibrium model has been developed to predict the gas composition. This model is based on the two equilibrium constant (k_1 and k_2) that are determined for water gas shift reaction and methanation. The model has been validated with Jayah et al. [7] experimental work. The predicted results are found in good agreement with experimental result. The effect of moisture content and equivalent ratio on producer gas are carried out. The effect on producer gas and calorific value of producer gas are discussed in detail.

THERMOCHEMICAL EQUILIBRIUM MODEL

It is assumed in the equilibrium model that all the reactions are in thermodynamic equilibrium. It is expected that all the products of downdraft gasifier achieve thermodynamic equilibrium condition such as pyrolysis product attain thermodynamic equilibrium condition in the reduction zone. Therefore, equilibrium model can be applied on the downdraft gasifier.

The general formula of biomass for single carbon atom is defined as $CH_aO_bN_d$ where a, b and d are the mole ratio of hydrogen-carbon, oxygen-carbon and nitrogen–carbon respectively on dry basis. The global gasification reaction can be represented as follows:

$$CH_aO_bN_d + wH_2O + mO_2 + 3.76mN_2 \leftrightarrow x_1H_2 + x_2CO + x_3CO_2 + x_4H_2O + x_5CH_4 + (3.76m + d/2)N_2 \quad \text{R (1)}$$

Where, w = amount of water per kmol of wood.
m = amount of oxygen per kmol of wood.
x_i = coefficient of constituent of the products.

In the global reaction x_1, x_2, x_3, x_4 and x_5 are generally unknown whereas moisture content helps to determine the value of w. m is generally known for downdraft gasifier. Therefore, five equations are required to determine these values. In which three equations are formulated based on the carbon balance, hydrogen balance and oxygen balance.

Carbon balance $x_2 + x_3 + x_5 - 1 = 0$ (1)

Hydrogen balance $2x_1 + 2x_4 + 4x_5 - 2w - a = 0$ (2)

Oxygen balance $x_2 + 2x_3 + x_4 - w - b - 2m = 0$ (3)

Remaining two-equations are based on the equilibrium constant for methane formation and water gas shift reaction.

$$C + 2H_2 \leftrightarrow CH_4 \quad \text{R (2)}$$

$$CO + H_2O \leftrightarrow CO_2 + H_2 \quad \text{R (3)}$$

$$k_1x_1^2 - x_5 = 0 \quad (4) \qquad \& \qquad k_2x_2x_4 - x_1x_3 = 0 \quad (5)$$

Where the equilibrium constant k_1 and k_2 is calculated from the relation recommended by Zainal et al. [5] and Barman et al.[8] respectively. These five equations have been solved using Newton-Raphson method in MATLAB.

The temperature of the gasifier needs to be known in order to calculate the equilibrium constants k_1 and k_2. The entropy or energy balances equation for global gasification reaction helps to determine the temperature of gasification.

The following energy balance equation has been solved for global biomass gasification reaction.

$$\begin{pmatrix} h^o_{f\,biomass} + w(h^o_{f\,H_2O(l)} \\ +h_{vap}) + mh^o_{f\,O_2} + \\ (3.76m + d/2)h^o_{f\,N_2} \\ +(T_{air} - T_1)\{(3.76m \\ +d/2)c_{pN_2} + mc_{pO_2}\} \end{pmatrix} = \begin{pmatrix} x_1h^o_{f\,H_2} + x_2h^o_{f\,CO} + x_3h^o_{f\,CO_2} \\ +x_4h^o_{f\,H_2O(vap)} + x_5h^o_{f\,CH_4} \\ +(T_2 - T_1)(x_1c_{pH_2} + \\ x_2c_{pCO} + x_3c_{pCO_2} \\ +x_4c_{pH_2O(vap)} + x_5c_{pCH_4} \\ +(3.76m + d/2)c_{pN_2}) \end{pmatrix} \quad (6)$$

Where h_f^o is the enthalpy of energy formation. T_2 is the gasification temperature T_1 is the ambient temperature. $C_{p,i}$ is the specific heat of the species at constant pressure. The specific heat calculated by the empirical formula that has been recommended by Barman et al.[8].

Calculation procedure

To solve the Eqn. (1) to Eqn. (5) for x_1, x_2, x_3, x_4, and x_5 by Newton Raphson method, the values x_i and temperature T are initially assumed. After solving the first iteration, the temperature of gasification is calculated by Eqn. (6) for new values of x_i, same iteration procedure is followed until the gasification temperature value is converged.

RESULT AND DISCUSSION

The above described equilibrium model is used to determine the gasification of biomass. The obtained results from the model are shown in Fig.1 to Fig.5. The present model has been validated with the experimental results of Jayah et al. [7]. Table 1 shows the composition of biomass based on ultimate anslysis.

TABLE 1: Ultimate analyses for various rubber wood [7]

Material	C	H	O	N	S	HHV
Rubber wood	50.6	6.5	42.0	0.20	0.0	19.6

Fig.1 compares the equilibrium model results with experimental results of Jayah et al. [7] at moisture content 16% and at 0.3488 equivalent ratio (ER). It can be observed that the proposed model predicts the results with precise accuracy. The mole fraction of hydrogen, CO, CO_2, CH_4 and N_2 are found to be 22.9%, 20.2%, 9.74%, 0.62% and 43.77% respectively whereas, the experimental values

are 18.3%, 20.2%, 9.7%, 1.1% and 50.7% respectively. The root mean square error 16.54% for CO, hydrogen and CO_2 has been determined.

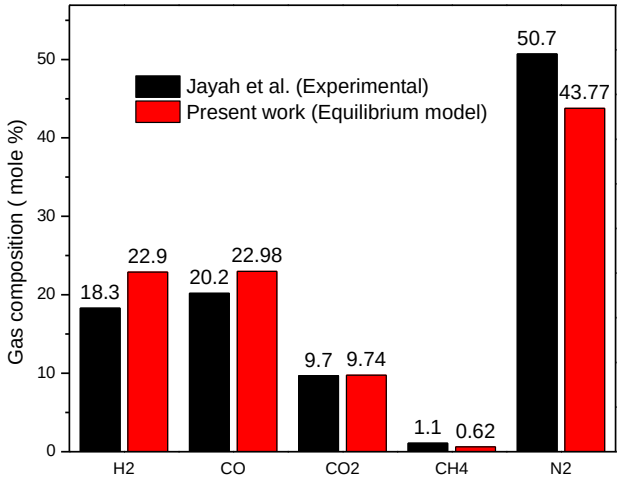

FIGURE 1. Comparison of model results with experimental work of Jayah et al.[7]

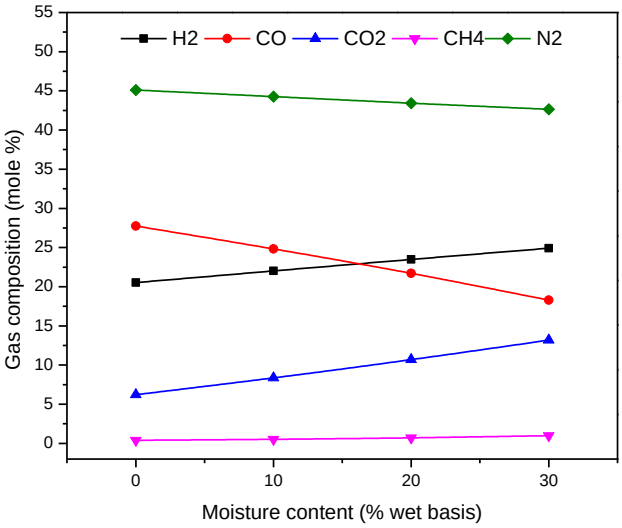

FIGURE 2. Gas composition variation with moisture content for rubber wood biomass

Fig.2 shows the influences on the producer gases with increasing moisture content in the biomass where amount of oxygen supplied is kept fixed at ER 0.3488. It may also be observed that nitrogen is negligibly affected compared to carbon monoxide, hydrogen and carbon dioxide, as expected. The mole frication of H_2 gradually increases from 20.52% to 24.90% when moisture increases in the biomass from dry basic to 40%. Whereas, CO decreases from 27.74% to 18.30% with the increase of moisture content which is the inverse trend of hydrogen formation curve. The methane content is very low in the producer gas, which varies from 0.39 to 0.97%. The hydrogen percentage increases with rise in moisture content. This is because of the effect of water gas and water gas shift reactions. In water gas shift reaction, vapour water reacts with carbon monoxide and form carbon dioxide and produces more hydrogen. Because of water gas shift reaction, the molar percentage of carbon monoxide decreases with increase in moisture content whereas CO_2 curve shows an inverse trend.

Fig.3 shows the effect of moisture content on the gasification temperature and calorific value of product gases. Both the gasification temperature and calorific value of producer gas decreases from 1112K to 1060K and 6.27MJ/m^3 to 5.87MJ/m^3 respectively with an increase in moisture percentage from 0% to 30%.

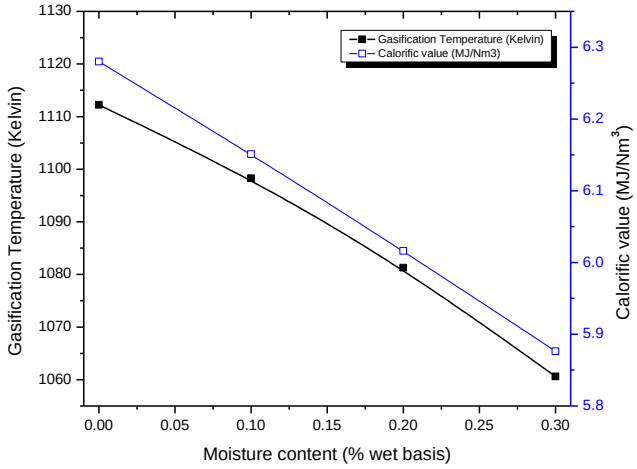

FIGURE 3. Variation of gasification temperature and calorific value with moisture content

Fig.4 illustrates the variation of gas composition during the gasification process with an increase in ER from 0.25 to 0.35 where moisture content is kept fixed at 16%. The mole percentage of N_2 increases from 37.74% to 46.08% with increase in ER from 0.25 to 0.35. The presence of nitrogen in air with oxygen causes the rise in nitrogen mole percentage with increase in ER.

During biomass gasification, ER is the most important and most effective parameter that defines the performance of the gasifier. It also helps to design the biomass gasifier. The heating value is prominently affected by this parameter. However, less value of ER may cause many problems, including low heating value, excessive char formation and incomplete combustion. On the other hand, too much ER will result in an excessive formation of products through complete combustion. In the literature, it has been commonly observed that with increasing ER, CO and H_2 decreases whereas, CO_2 increases. However present model shows reverse trend of CO and CO_2 this may be due to the considered range of ER which may not laying in the optimum range. Methane content also decreases with increase in equivalent ratio.

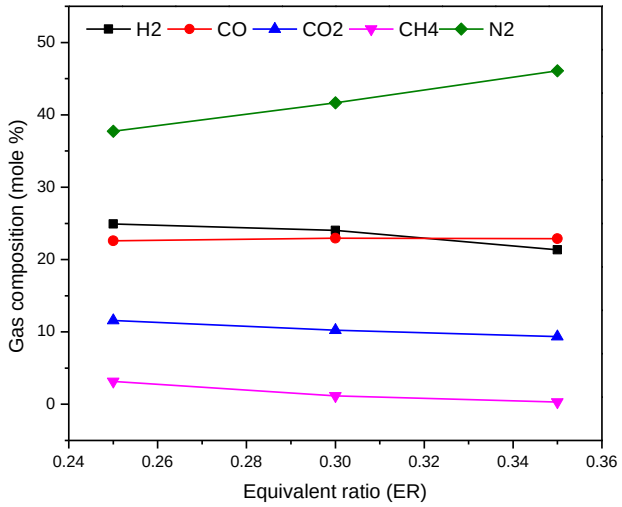

FIGURE 4. Gas composition variation with ER for rubber wood biomass.

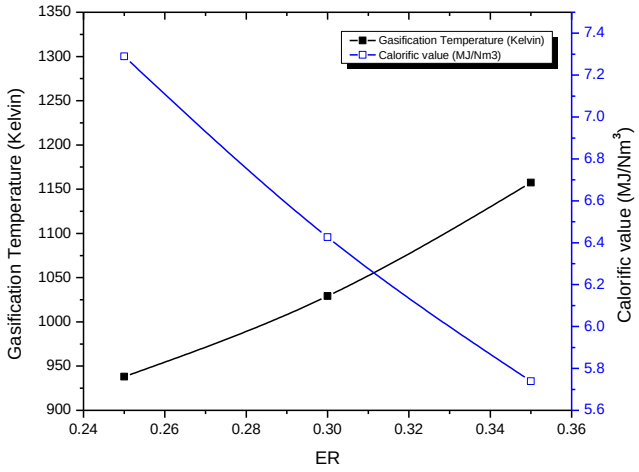

FIGURE 5. Variation of gasification temperature and calorific value with equivalent ratio

Fig.5 shows the variation in the gasification temperature and calorific value with equivalent ratio. As the equivalent ratio increases, the gasification temperature increases due to increase in oxygen supply in the combustion zone triggered by the combustion reaction. The model predicted temperature range are in good agreement with the temperature range suggested in literature.

CONCLUSIONS

The thermal equilibrium model has been developed to predict the composition of producer gas for a downdraft gasifier by using mass balance and energy balance equations. The predicted results reveal that the outcomes of different species are as per literature. The present model is thus showing a promising way to predict the biomass gasification outcomes.

From the analysis, the following conclusions are made:

1. With increase in moisture content, hydrogen percentage increases whereas carbon monoxide shows the inverse trend.
2. Decrease in calorific value and gasification temperature due to increasing the moisture content in biomass.
3. Higher equivalent ratio is responsible for higher content of nitrogen in producer gas.
4. With increase in equivalent ratio, gasification temperature increases due to shifting of gasification reaction toward complete combustion.

REFERENCES

[1] S. K. Sansaniwal, K. Pal, M. A. Rosen, and S. K. Tyagi, "Recent advances in the development of biomass gasification technology: A comprehensive review," Renewable and Sustainable Energy Reviews, vol. 72, no. December 2015, pp. 363–384, 2017.

[2] M. Fani, M. Haddadzadeh Niri, and F. Joda, "A Simplified Dynamic Thermokinetic-Based Model of Wood Gasification Process," Process Integration and Optimization for Sustainability, no. x, 2018.

[3] D. A. Rodriguez-Alejandro, A. Zaleta-Aguilar, V. H. Rangel-Hernández, and A. Olivares-Arriaga, "Numerical simulation of a pilot-scale reactor under different operating modes: Combustion, gasification and pyrolysis," Biomass and Bioenergy, vol. 116, no. May, pp. 80–88, 2018.

[4] A. M. Salem and M. C. Paul, "An integrated kinetic model for downdraft gasifier based on a novel approach that optimises the reduction zone of gasifier," Biomass and Bioenergy, vol. 109, no. December 2017, pp. 172–181, 2018.

[5] Z. A. Zainal, R. Ali, C. H. Lean, and K. N. Seetharamu, "Prediction of performance of a downdraft gasifier er using equilibrium modeling for different biomass materials," vol. 42, 2001.

[6] A. Gambarotta, M. Morini, and A. Zubani, "A non-stoichiometric equilibrium model for the simulation of the biomass gasification process," Applied Energy, vol. 227, no. July, pp. 119–127, 2018.

[7] T. H. Jayah, L. Aye, R. J. Fuller, and D. F. Stewart, "Computer simulation of a downdraft wood gasifier for tea drying," Biomass and Bioenergy, vol. 25, no. 4, pp. 459–469, 2003.

[8] N. S. Barman, S. Ghosh, and S. De, "Gasification of biomass in a fixed bed downdraft gasifier – A realistic model including tar," Bioresource Technology, vol. 107, pp. 505–511, 2012.

Proceedings of the Third International Conference on Sustainable Energy and Environmental Challenges (3rdSEEC)
18 –21 December, 2018, IIT Roorkee, India

SEEC No. 121

Microscopic Spray Characteristics of Methanol Fuelled MPFI Engine Injector

Ankur Kalwar
Engine Research Laboratory
Department of Mechanical Engineering
Indian Institute of Technology Kanpur
Email: ankurkal@iitk.ac.in

Avinash Kumar Agarwal
Engine Research Laboratory
Department of Mechanical Engineering
Indian Institute of Technology Kanpur
Email: akag@iitk.ac.in

ABSTRACT
The study proposes investigations of the microscopic spray characteristics of methanol blended with gasoline fuels in a simulated multi- point fuel injection (MPFI) engine system. Methanol is emerging as a potential alternative fuel due to its higher enthalpy of vaporization, higher octane rating and renewable nature. As atomization of fuel largely affects its combustion, performance and emission quality in an engine environment, it becomes important to study the spray characteristics. The experiment encompasses droplet particle size distribution and velocity distribution determination for different methanol-gasoline blends using Phase Doppler Interferometry (PDI) technique. Three blends namely M15 (15% v/v methanol blended with 85% v/v gasoline), M85 (85% v/v methanol blended with 15% v/v gasoline) and M100 (100% methanol) are compared with baseline gasoline (G100) and Sauter Mean Diameter (SMD), Arithmetic Mean Diameter (AMD), particle size distribution and velocity distribution were experimentally determined in this study.

Keywords: *Methanol gasoline blends, microscopic spray characteristics, MPFI system*
.

INTRODUCTION
Due to global increasing conventional fuels crisis and its deteriorating impact on the environment, the need for switching to alternative fuels has arisen, which need to be evaluated for compatibility along with acceptable engine performance and lower impact on the environment. With that objective in mind, studies on methanol fuel sprays were conducted in this study. Methanol has relatively higher enthalpy of vaporization compared to gasoline, which reduced the charge temperature and hence the combustion temperature is also relatively lower, which reduced the NOx emissions. Its higher octane rating allows increasing the compression ratio of gasoline engine without the danger of knocking. Methanol can be easily produced from environment friendly renewable resources likes high ash Indian coal, municipal solid waste, low value biomass etc. which makes it a comparative green and indigenous fuel [1].

For studying the utilization of a fuel in the automotive engine and assessing its performance and emissions characteristics, which largely depend on how efficient combustion is taking place, atomization and mixing characteristics of the charge were experimentally investigated. Microscopic spray characterization is an important tool for these investigations. In the past, several studies have been done to study macroscopic and microscopic characteristics of different blended test fuels. Han et al. [2] compared spray parameters of fatty acid esters blended with diesel under different fuel injection pressure using common-rail diesel injection (CRDI) system and found that engine variations could be minimized with increasing the fuel injection pressure. From macroscopic spray studies, which involved light intensity characteristics of spray contours, he inferred that diesel and methyl laureate have higher diffusion and

atomization tendency, which resulted in smaller SMD compared to methyl oleate and ethyl oleate. Jing et al. [3] investigated the spray characteristics of diesel blended with gasoline in a CI engine and found that spray penetration, and SMD of the spray decreased as the blending ratio of gasoline in diesel increased, at low fuel injection pressure. Kim et al. [4] performed their study on DME/ iso-butene blends for spray visualization and droplet size distribution and found that DME had higher injection rate peak and showed smaller SMD when compared to DME/ isobutene blends. Yuan Gao et al. [5] investigated spray characteristics of Jatropha oil using experiments and simulations. They reported that spray penetration and spray velocity increased, but spray cone angle is decreased with increasing blending ratio. SMD and spray concentrations were found to be higher for blends as compared to diesel.

Many authors have correlated spray parameters with the engine performance and emissions characteristics. Agarwal et al. [6] carried out studies to analyze the effect of fuel injection pressure and injection timing on spray atomization, engine performance, and emissions from Karanja biodiesel blends using CRDI system. With increasing biodiesel content and higher fuel injection pressure, fuel injection duration decreased slightly. Spray droplet size distribution increased with the blending ratio. 10% Karanja biodiesel blend proved to be useful for improving the thermal efficiency and reducing emissions. Fuel temperature and injector body temperature also affect the spray atomization. Kale et al. [7] compared Butanol isomers with iso-octane using gasoline direct injection (GDI) system at different injector temperature. They reported that spray plumes interact to form a single jet at high fuel temperatures. Spray cone angle and droplet size distribution also reduced, though butanol exhibited larger droplet size distribution compared to iso-octane, at all fuel temperature conditions. From several studies conducted by researchers, it can be concluded that perfect atomization of fuel plays a vital role in almost every aspect of engine operation such as combustion, performance or emissions from the engine. However these are the areas to where viability of methanol blends need to be tested compared to conventional fuels in order to assess their technical viability for engine systems. The analysis of microscopic spray characteristics of gasoline-methanol blends in a MPFI system is therefore one of the important ways to ascertain the same. Three blends namely M15, M85, M100 are compared with gasoline (G100) for spray parameters like sauter mean diameter (D_{32}), arithmetic mean diameter (D_{10}), spray droplet size distribution, and droplet velocity distribution.

EXPERIMENTAL SETUP

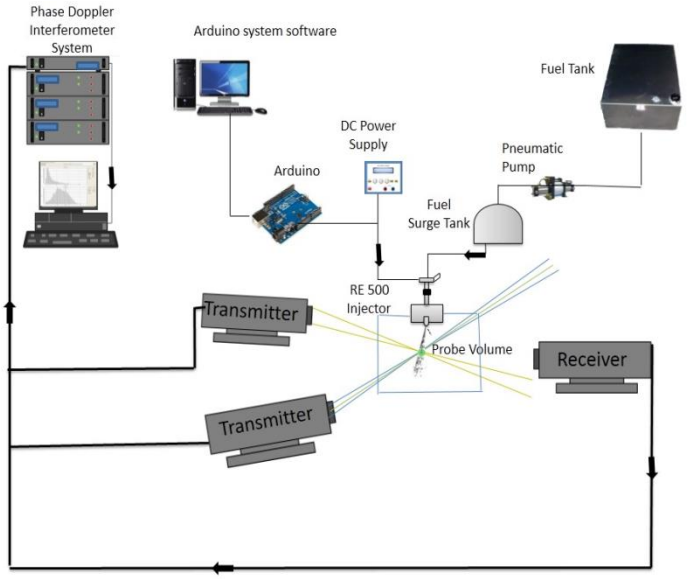

Figure 1: Schematic of microscopic spray characterization setup

Experimental setup for this study consists of a cubic glass chamber (15´´×15´´×15´´) with MPFI injector used in Royal Enfield 500 cc motorcycle, which was mounted on the top to the chamber, as shown in the figure 1. Micro-controller (Arduino) was customized for controlling the injection pulse width of fuel by controlling the pulse to the solenoid MPFI injector. The spray characteristics are determined in ambient temperature and pressure conditions of the chamber and compared with baseline gasoline. The PDI system comprising of 2 transmitter and 1 receiver, which are used for detecting the constructive and destructive interference of fringes of the lasers and then further analyzed to determine the spray droplet size and velocity distributions.

RESULTS AND DISCUSSION

The analysis of results showed variation of various types of diameters (D_{10}, D_{20}, D_{30}, D_{21}, D_{31}, D_{43}, D_{32}), spray droplets size distribution and droplet velocity distribution for methanol-gasoline blends (M15, M85, M100) compared to baseline gasoline (G100).

REFERENCES

[1] Zhen, Xudong. "Methanol As An Internal Combustion on Engine Fuel." *Methanol*. 2017. 313-337.

[2] Han, Dong, et al. "Macroscopic and microscopic spray characteristics of fatty acid esters on a common rail injection system." *Fuel* 203 (2017): 370-379.
[3] Jing, Daliang, et al. "Experimental investigation on the macroscopic and microscopic spray characteristics of dieseline fuel." *Fuel* 199 (2017): 478-487.
[4] Kim, Woong Il, Kihyung Lee, and Chang Sik Lee. "Spray and atomization characteristics of isobutene blended DME fuels." *Journal of Natural Gas Science and Engineering* 22 (2015): 98-106.
[5] Gao, Yuan, et al. "Experimental study of the spray characteristics of biodiesel based on inedible oil." *Biotechnology Advances* 27.5 (2009): 616-624.
[6] Agarwal, Avinash Kumar, et al. "Effect of fuel injection pressure and injection timing of Karanja biodiesel blends on fuel spray, engine performance, emissions and combustion characteristics." *Energy Conversion and Management* 91 (2015): 302-314.
[7] Kale, Rakesh, and R. Banerjee. "Understanding spray and atomization characteristics of butanol isomers and isooctane under engine like hot injector body conditions." *Fuel* 237 (2019): 191-201.

SEEC No.122

Creation of Portable Smart Solid Waste Community bin using Advanced Technologies

In recent times, garbage disposal has become a huge concern in the world. A voluminous amount of waste generated and disposed by means which have an adverse effect on the environment. The common method of disposal of waste is by unplanned and uncontrolled open dumping at the landfill sites. This method is injurious to human health, plant and animal life. Therefore the waste disposal can generate liquid leachate which contaminate surface and ground waters can cause harmful diseases to the human beings and can degrade aesthetic value of the natural environment. When the waste is segregated into biodegradable and non-biodegradable using possible modes, has a higher potential of recovery, consequently, recycled and reused. The biodegradable waste is often converted either biogas or compost. This paper consist of latest surveyed research work in order to contribute to reduce the Environmental pollution caused by the solid waste by proposing a portable smart collection bin with segregation unit having advanced technologies to facilitate the process. The segregation unit will separate the wastes into biodegradable and non-biodegradable components. The separated biodegradable waste is further used to feedstock for biogas plants and non-biodegradable components for recycling.

Keywords: Solid Waste, Community bin, Segregation, Bio-Degradable

SEEC No. 123

COMPARATIVE STUDY OF ELECTRODE MATERIAL FOR TREATMENT OF LEACHATE BY USING ELECTROCOAGULATION

Leachate is wastewater decomposition of organic waste that can contaminate soil and groundwater if it is not handling properly. Contamination by leachate can be prevented by reducing leachate level before the wastewater reaches the ground. One of the methods used to treat the leachate is electrocoagulation. Electrocoagulation is an electrochemical water treatment method where in anode occurred the release of active coagulant as metallic ion, while in cathode occurred the electrolysis reaction in a form of the release of hydrogen gas. In this research, the processing of leachate by electrocoagulation method using copper and iron electrode as cathode and stainless steel as anode. This study is aimed to investigate the effectiveness of electrocoagulation in removing Biochemical Oxygen Demand (BOD), Chemical Oxygen Demand (COD), NH3-N and heavy metals of leachate.

Keywords: Leachate, Electrode, Electrocoagulation, Contamination

Proceedings of the Third International Conference on Sustainable Energy and Environmental Challenges (3rd SEEC)
18– 21December, 2018, IIT Roorkee,India

SEEC No.126

NUMERICAL STUDY OF DIRECT CONTACT MEMBRANE DISTILLATION TECHNIQUE COUPLED WITH NANOFLUID-BASED DIRECT ABSORPTION SOLAR COLLECTOR

Akshay Rathore, Rahul Yadav
Department of Mechanical Engineering
Indian Institute of Technology Ropar, Rupnagar-140001, India
Email: 2015meb1083@iitrpr.ac.in

Dr. Himanshu Tyagi *
Department of Mechanical Engineering
Indian Institute of Technology Ropar, Rupnagar-140001, India
Email: himanshu.tyagi@iitrpr.ac.in

ABSTRACT

In this paper, theoretical study of direct contact membrane distillation (DCMD) unit coupled with the nanofluid-based direct absorption solar collector (DASC) has been carried out. The various influencing parameters affecting the fresh water output have been studied. The mathematical model is prepared for direct contact membrane distillation and direct absorption solar collector and is solved using a MATLAB code. The output is measured in terms of mass of distillate, specific heat consumption. Efficiency of the system is measured against parameters such as inlet temperature of feed water and different salinity ratio. It is observed that mass of distillate water as well as efficiency of the system decrease with increasing water salinity.

Keywords: Direct Absorption Solar Collector, Direct Contact Membrane Distillation, Nanofluids.

NOMENCLATURE

B_m	Mass transfer coefficient [s/m]
c_p	Specific heat [J.kg^{-1}K^{-1}]
D	Diameter of pores [m]
DASC	Direct Absorption Solar Collector
EE	Evaporation efficiency [%]
H_v	Enthalpy of vapors of fresh water [J.kg^{-1}]
h_m	Heat transfer coefficient [Wm^{-2}K^{-1}]
k	Thermal conductivity of fluid [W.m^{-1}.K^{-1}]
Kn	Knudsen number
m_d	Mass flux of distillate water [kg.m^{-2}]
P_d	Partial vapor pressure of permeate side [Pa]
P_s	Partial vapor pressure of Inlet side [Pa]
T_{mf}	Temperature of membrane on hot vapor side [K]
T_{mp}	Temperature of membrane on permeate side side [K]

Greek Symbols

κ	Index of absorption
λ	Wavelength of incident radiation [μm]
ρ	Density [kg.m^{-3}]
θ	Solid angle [str]

Subscripts

diss	Distillate
mf	Evaporator membrane side
mp	Permeate side
spec	Specific

INTRODUCTION

One of the most basic needs of the people throughout the world is access to freshwater, which is depleting at very fast rate [1]. Many dry regions in the world have groundwater with high amount of dissolved salts in them, thus making it unfit for direct human consumption [2]. Due to large scale

industrialization and excessive pollution, the water in rivers and ground water is being polluted and as a result at many places it is not safe for human usage. It has been predicted that there is a possibility of having wars for fresh water in the coming decades, similar to the instability for oil, petroleum and natural gas in this decade [3]. One of the ways this issue of water shortage can be addressed is by the use of desalination. Almost 70% of the surface of earth is covered with sea water (saline), which can be purified. Thus, there is growing focus on the low-cost desalination techniques to meet the increasing demand of fresh water.

Desalination techniques have been known for a very long time. Ships from very old times have been using desalination techniques to harness potable water by evaporation [4]. Thus, this method inspired researchers to develop single stage and multi-stage flash techniques (MSF) and multi effect evaporation (MED) techniques. These processes are basically based upon the concept of heating the fluid to produce water vapor or reducing the ambient pressure so as to reach the flash point at lower temperature and vaporize the water. There are multiple stages/effects through which the seawater passes so as to increase the yield and the efficiency. Many a times these systems are coupled with power plants so as to create a regenerative system and use the waste heat energy from power plant for water desalination. But, there is a disadvantage. Due to the presence of evaporation process, the energy consumption for these processes is very high as the energy required to vaporize the water is 40.8 KJ/mol.

Due to high energy usage of the previous processes, researchers have searched for a more energy efficient method of desalination. Thus, membrane technology (MD) came into picture. Reverse osmosis method, commonly known as RO, was developed which was way more efficient than the previous evaporation techniques [5]. It gives a good amount of yield and is cost effective too. Also, due to advancements in field of membranes, the cost of membranes reduced drastically in the last decade. Thus, over time membrane technologies have became more popular (compared to thermal methods).

Large desalination plants were setup in many countries to produce fresh water with this process. But the major drawback of this process is that it requires high pressure across the membrane, This is usually provided by mechanical pumps which are powered by high powered electrical motors. This requires high amount of electric power which in turn needs to be generated in power plants. This, this process tends to use fossil fuels which are now being exhausted at a very high rate and cause pollution which will eventually lead to climate change and many other problems [6].

An advanced and feasible method: Membrane Distillation Technique - is under research throughout the world. It is a technique that uses low grade thermal energy to drive the desalination process. Water vapor is passed through a hydrophobic membrane separated by hot and cold water stream of water. The nature of membrane is such that it allows water vapor to pass through it and prevents the liquid water and impurities through the pores.

The difference in the temperature on both sides of membrane creates a vapor pressure gradient and causes water vapor to pass through the pores and condense on the other side of the plate. The resultant distillate water is of very high purity compared to the other conventional distillation processes. Due to it being a 'low temperature process', it can be coupled with solar energy which would solve the aforementioned disadvantages of RO technique (i.e. the use of fossil fuels) [7].

Figure 1 shows nanofluid-based direct absorption solar collector with membrane distillation setup. When certain amount of solar intensity irradiation is incident on the glass cover it is absorbed by the solar collector. This absorbed heat is exchange by saline water in heat exchanger and the saline water gets transported in the membrane distillation (MD) unit at the desired temperature. Pure water is collected over the condenser side. A water chiller is also used to cool the water to get transported on condenser side.

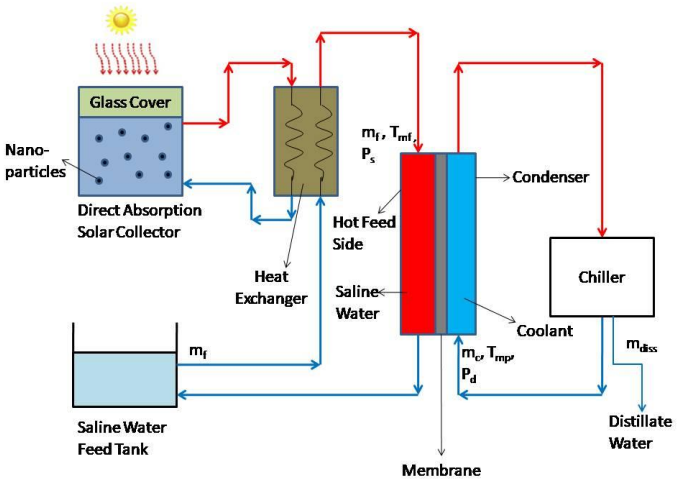

Figure 1: Schematic of direct contact membrane distillation (DCMD) coupled with nanofluid-based direct absorption solar collector (DASC).

NUMERICAL MODELLING

In this section, a mathematical model of a combined system (DASC and DCMD) has been presented. A direct absorption solar collector (DASC) was used in this simulation, in which nanoparticle-laden fluid was used to harness solar energy directly. A detailed description of that system is beyond the scope of this paper, and is given elsewhere [8].

Modeling of Direct Contact Membrane Distillation (DCMD) Unit

Membrane Distillation (MD) was first introduced in the 1960s and was not favorable due to low temperature polarization coefficient [9]. In this process there are three regions where heat transfer takes place. These regions are shown in Fig. 2.

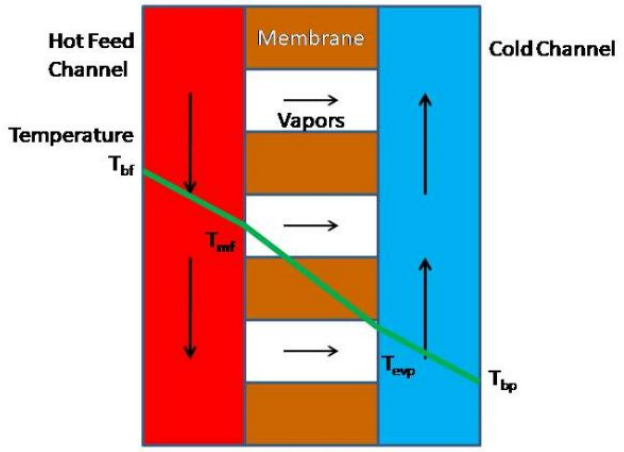

Figure 2: The bulk and membrane interface temperatures where T_{bf} is the bulk feed temperature, T_{mf} is the membrane interface temperature at the feed side, T_{mp} is the membrane interface temperature at the permeate side, and T_{bp} is the bulk permeate temperature. (Adapted from B. Ashoor et al. [10]).

First region: Through feed solution thermal boundary
Second region: Through membrane
Third region: Through permeate solution thermal boundary layer.

Mass transfer inside the DCMD is usually assumed as linear relation between the mass flux (m_d) and the vapor pressure difference through the membrane along with mass distillation coefficient (B_m). Its expression is given as follows [11]:

$$m_d = B_m(P_d - P_s) \tag{1}$$

where P_d and P_s are the partial pressures of water at the feed and permeate sides. In this expression P_d is evaluated by using the Antoine equation at the temperatures T_{mf} and T_{mp}, respectively, such as the following:

$$P = \exp\left(23.328 - \left(\frac{3841}{T-45}\right)\right) \tag{2}$$

where P is the water vapor pressure in Pascal and T is temperature in Kelvin. An empirical correlation describing the saltwater vapor pressure P_s in relation to pure water vapor pressure P_d is given by [12]:

$$P_s = P_d e^{-2.1609\times10^{-4}s - 3.5012\times10^{-7}s^2} \tag{3}$$

The specific thermal energy consumption Q_{spec} required to produce 1 m^3 of distillate is given by:

$$Q_{spec} = \frac{m_d c_p (T_{mf} - T_{co})}{V_{dist.}} \tag{4}$$

where c_p is the specific heat capacity of the feed water and V_{dist} is the amount of distillate water produced in one second.

The expression for EE (evaporation efficiency) is given below in Eq. (5). It is defined as the ratio of the energy transported by the water vapor passing through the pores of the membrane to the total heat transferred across the membrane.

$$EE = \frac{m_d H_v}{m_d H_v + h_m(T_{mf} - T_{mp})} \tag{5}$$

where H_v is the enthalpy of water vapor and h_m is the heat transfer coefficient of polymer membrane. For calculating B_m, various mechanisms have been devised depending upon the Knudsen number (Kn). The Knudsen number (Kn) is defined as the ratio of the mean free path (λ) of the transported molecules to the average pore size of the membrane (d); Kn = λ/d. In this paper, the normal value is taken from reference [13].

RESULTS

In this section, the main output i.e. mass of distillate per unit area (m_d) is plotted against different inlet temperature (T_{mf}) by varying the value of salinity (ranging from 13 to 105 g/kg) and is shown in Fig. 3. It can be seen with increasing inlet temperature from 75 to 95°C, the mass of distillate water increases. On the other hand, with an increase in the water salinity, the amount of distilled water decreases.

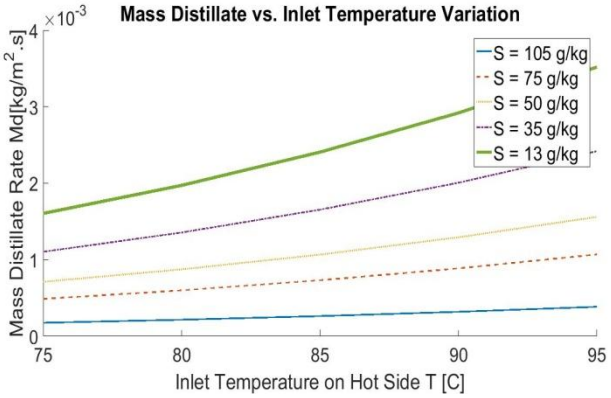

Figure 3: Variation of mass of distillate water vs. inlet temperature.

In Fig. 4 the specific heat consumption (Q_{spec}) is plotted against the inlet temperature variation. The maximum Q_{spec} is achieved for the salinity 105 g/kg. As the salinity value decreases, the amount of heat required decreases as well. But on a specific amount of salinity, with increasing inlet evaporator temperature, the amount of Q_{spec} decreases. Also one point is to be noted here that difference in the amount of heat required for salinity 75 to 105 g/kg is more than that of heat required for 50 to 75 g/kg in spite of comparable same

difference.

In Fig. 5, the evaporation efficiency (*EE*) is plotted as a function of inlet temperature. It can be observed from this figure that with increasing inlet temperature, the evaporator efficiency increases (although temperature is inversely related to *EE*). This is because mass of distillate factor increases more that temperature factor.

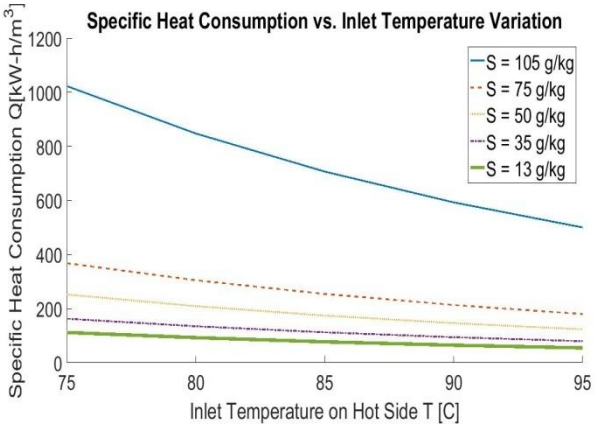

Figure 4: Variation of specific heat consumption vs. inlet temperature.

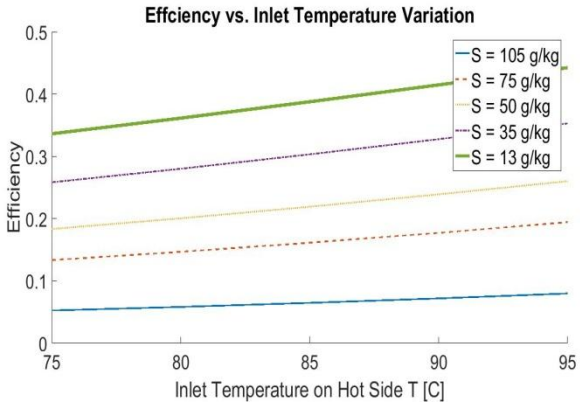

Figure 5: Variation of efficiency vs. inlet temperature.

CONCLUSION

This study presents the results of the numerical study of DCMD system coupled with a nanofluid-based direct absorption solar thermal collector (DASC). The results revealed that maximum mass of distillate water for salinity 13 g/kg at temperature 95^{o}C. The same result was observed with evaporation efficiency (*EE)*. The specific heat consumption (Q_{spec}) was maximum for salinity value of 105 g/kg. For optimum energy consumption, salinity should not be high as it leads to degradation overall output factors such as mass of distillate water and evaporation efficiency (*EE*).

ACKNOWLEDGEMENTS

The support provided by the Department of Mechanical Engineering, IIT Ropar is gratefully acknowledged.

REFERENCES

[1] J. E. Miller, “Review of Water Resources and Desalination Technologies”, Report - Sandia National Laboratories, United States, 2003.

[2] S. E. Moore et al., “Process modeling for economic optimization of a solar driven sweeping gas membrane distillation desalination system”, *Desalination*, Vol. 437, 2018.

[3] S. A. Kalogirou, "Solar Desalination using renewable resources", *Energy and Combustion Science*, 2005.

[4] E. Krell, “A review of the history of laboratory distillation”, *Analytical Chemistry*, Vol. 2 1982.

[5] C. Charcosset, “Desalination using membrane distillation: Experimental studies on full scale spiral wound modules", *Desalination*, Vol. 245, 2009.

[6] M. Elimelech et al, “The Future of Seawater Desalination: Energy, Technology, and the Environment”, *Science*, Vol 333, 2011.

[7] E. Curicio et al., “Membrane Distillation and Related Operations - A Review”, *Separation and Purification Technique*, Vol 34, 2004.

[8] Tyagi, H., Phelan, P. and Prasher, R., 2009. Predicted efficiency of a low-temperature nanofluid-based direct absorption solar collector. *Journal of Solar Energy Engineering*, 131(4), p.041004.

[9] J. Zhang, “Identification of material and physical features of membrane distillation membranes for high performance desalination” *Membrane Science*, Vol. 349, 2010.

[10] B. Ashoor et al., "Principles and applications of direct contact membrane distillation (DCMD): A comprehensive review”, *Desalination*, 2016.

[11] M. Qtaishat et al., “Heat and mass transfer analysis in direct contact membrane distillation”, *Desalination*, Vol. 219, (2008) 272–292.

[12] D. Winter et al., “Desalination using membrane distillation: Experimental studies on full scale spiral wound modules", *Desalination*, Vol. 375, 2011.

[13] J. Lee et al., “Influence of high range of mass transfer coefficient and convection heat transfer on direct contact membrane distillation performance”, *Desalination*, Vol. 426, 2018.

SEEC No.127

PARAMETRIC OPTIMIZATION OF SYSTEM PARAMETERS OF A ROUGHENED SOLAR AIR HEATER WITH V-SHAPED DIMPLED SURFACE

Md. Dilnawaz Azmi
Department of Mechanical Engineering
B. Tech Student
mdilnawaz1234@gmail.com

Dr. Rajesh Maithani
Department of Mechanical Engineering
Assistant professor
rajesh.maithani@dituniversity.edu.in

ABSTRACT

This article deals with the parametric optimization of the geometrical parameters of a solar air heater duct with multiple V-pattern dimpled obstacles. Investigation has been performed to examine the effective efficiency for multiple type V-pattern dimpled obstacles on the heated wall. The flow Reynolds number (Re) is varied from 5000 to 17000, relative dimpled obstacles width (Wc/W_d) in the range of 1 to 6, ratio of dimpled depth to print diameter (e_d/d_d) from 0.5 to 2 and relative dimpled pitch (P_b/e_d) from 8 to 11.The optimum data of effective efficiency for a range of temperature rise parameter ($\Delta T/I$) is obtained that is beneficial to select the geometrical parameter for a particular operating condition.

***Keywords*:** dimpled roughness, solar air heater, exergetic efficiency.

NOMENCLATURE

I	Insolation, W/m^2
W_c	Width of solar air passage, m
W_d	Width of single V-dimpled obstacle, m
P_b	Pitch of dimpled obstacles, m
d_d	Print diameter of dimpled obstacles
e_d	Height of dimpled obstacles, m
Nu	Nusselt number
f	friction factor
ΔT	Air temperature difference
η_{exe}	Exergetic efficiency

INTRODUCTION

The harvesting of heat energy from the solar air heater duct has led to development of novel techniques that enhances the heat transfer coefficient. In the past several investigations brought out an effective augmentation in the heat transfer by diminishing the laminar viscous layer formed between air and heated surface.

The surface of solar air heater is roughened by providing obstacles which are produced by dimples, triangular, ribbed V-pattern obstacles designs which have been investigated on by several researchers [1-3]. Kathkaw et al. [4] investigated the air flows over the heated surface with ellipsoidal dimpled roughness of a solar air heater and found the effect of *Nu* and *f*. The investigation shows that roughened surfaces increases the *Nu* approximately 15.8% folds in comparison to the smooth surface. Lien et al. [5] examined the behaviour of *Nu* and *f* of air flow through a duct which has hemispherical dimple on the heated side of absorber plate and found better heat transfer rate than the passage which was smooth in nature. Hans et al. [6] investigated the effect of multiple V-shaped obstacles on *Nu* and *f* for a roughened solar air heater duct. It was revealed that there was an augmentation in *Nu* and *f* of 6.34 and 5.18 times, respectively in comparison to the smooth surface. Thianpong et al. [7] experimentally studied the *Nu* and *f* of air flow in a duct with surface roughened with triangular obstacle of varying heights. It was concluded that there was significant improvement on *Nu* and *f* in the triangular roughened surface than that of the smooth passage. Maithani and Saini [8] experimentation studied *Nu* and *f* of solar air passage roughened with ribs in the form of V-shaped obstacles having symmetrical gaps and concluded that the highest improvement of *Nu* is about 3.6 folds over the smooth passage. Kumar et al. [9] investigated the thermal and hydraulic performance of a solar air duct with multiple V-shaped dimple on heated surface. After going through the literature review it was decided to analyse and optimise the system parameters with varying operating parameters of Kumar et al. [9].

SYSTEM MODEL

In a solar air heater, the air flows in the lower duct and carry away the heat from the heated surface of the test section from the upper duct. The roughness produced on the absorber plate with number of V-shaped dimpled surface [9] as shown in Fig. 1. This roughness on the absorber plate disturbs the laminar sub layer formed in the vicinity of the heater surface, thus augmenting the heat transfer. The different geometrical parameters of roughness in the form of V-shaped dimpled surface roughness on the absorber plate are Relative dimpled

obstacles width (W_c/W_d), dimpled depth to print diameter (e_d/d_d) and relative dimpled pitch (P_b/e_d). The roughness and flow parameters which are used in this study are depicted in the Table 1.

MODELLING AND CALCULATIONS PROCEDURE

To determine the optimum values of the system parameters, a system model in MATLAB has been formulated that accounts for exergetic components evaluation of a solar air heating system.

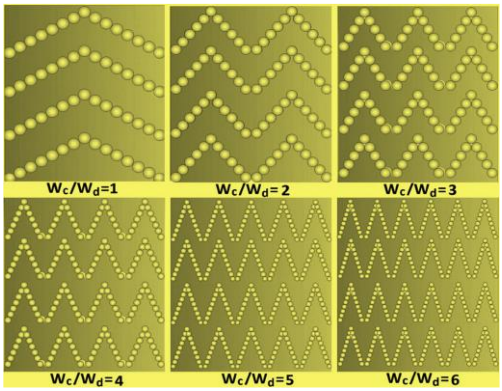

FIGURE 1. Schematic of roughness on absorber plate.

TABLE 1: System and operating parameters

Parameter	Value/range
Relative dimpled obstacles width (W_c/W_d)	1, 2, 3, 4, 5 and 6
Dimpled depth to print diameter (e_d/d_d)	0.5, 1.0, 1.5 and 2.0
Relative dimpled pitch (P_b/e_d)	8, 9, 10 and 11
Temperature rise parameter ($\Delta T/I$)	0.001- 0.04
Insulation (I)	500- 1000

The parametric optimization of V-shaped dimpled surface roughness on the absorber plate of a solar air heater duct based on the criteria of exergetic efficiency analytically (Fig. 2) by using statistical correlations of Nusselt number and friction factor developed by Kumar et al. [26].

$$Nu = 9.35\times10^{-14}\, Re^{1.065}(W_c/W_d)^{2.9832}(e_d/d_d)^{-0.248}(P_b/e_d)^{2.99}(\alpha_a/55)^{-1.09} \times \exp[-0.91\{\ln(W_c/W_d)\}^2] \exp[-0.19\{\ln(e_d/d_d)\}^2] \times \exp[-0.3069\{\ln(P_b/e_d)\}^2] \exp[-2.56\{\ln(\alpha_a/55)\}^2] \quad (1)$$

$$f=2.05\times10^{-5}Re^{-0.6307}(W_c/W_d)^{0.0853}(e_d/d_d)^{-0.162}(P_b/e_d)^{19.13}(\alpha_a/55)^{-0.225}\times \exp[-0.0676\{\ln(W_c/W_d)\}^2] \exp[-0.341\{\ln(e_d/d_d)\}^2] \times \exp[-0.5793 \{\ln(P_b/e_d)\}^2] \exp[-2.30\{\ln(\alpha_a/55)\}^2]$$

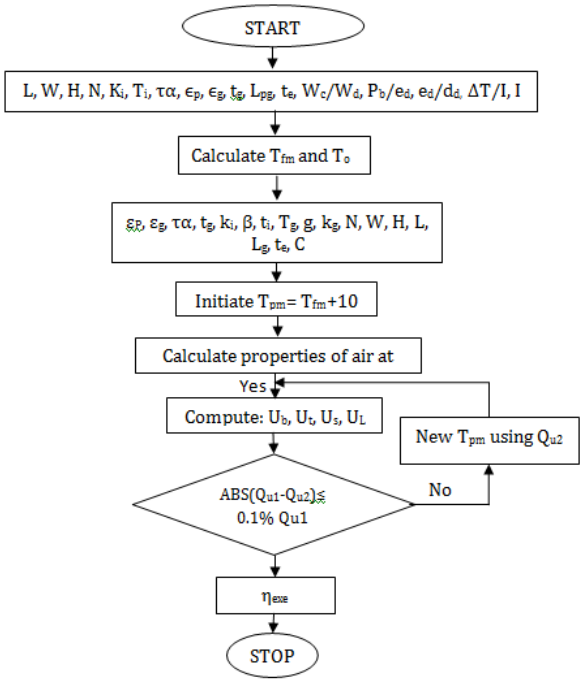

FIGURE 2: Flow chart of calculation procedure.

RESULT AND DISCUSSION

The results of the heat transfer and friction characteristics of V-shaped dimpled surface roughness on the absorber plate of a solar air heater duct has been presented and discussed. The effect of variation of system and operating parameters are discussed.

The enhancement of heat transfer through artificial roughness in the flow passage is always accompanied by increased friction losses. This increases the pumping power required to maintain the flow in the duct and thus the net energy gain reduces. It is, therefore desirable that roughness parameters are selected in such a way that the friction factor should be kept as minimum as possible where as the heat transfer coefficient is to be increased to the maximum possible extent. Such a selection is possible only if the relationships for the heat transfer and fluid flow characteristics of the roughened duct are known.

Effect of Relative Dimpled Pitch (P_B/e_D) on Exergetic Efficiency (η_{exer})

Fig. 3 shows that exergetic efficiency as a function of temperature rise parameter. It can be seen that lower value of temperature rise parameter ($\Delta T/I$) result in negative value of exergetic efficiency because of very high value of mass flow rate that results when temperature rise parameter rise parameter is low after increasing value of temperature rise parameter exergetic efficiency increases. For different values of relative dimpled pitch (P_b/e_d) shown in Fig. 3 the lower exergetic efficiency found at relative dimpled pitch (P_b/e_d) of 11 and high exergetic efficiency at the value 9.

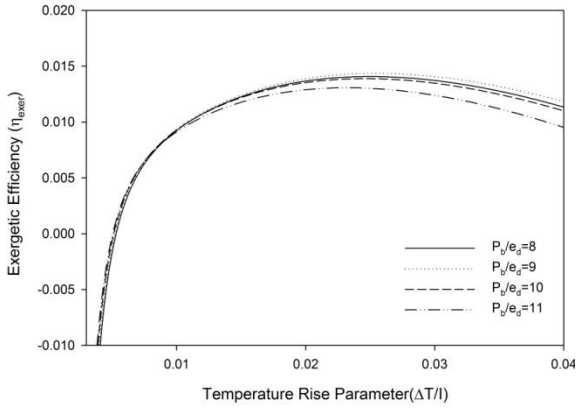

FIGURE 3: Variation of η_{exer} with ΔT/I for different (P_b/e_d)

Effect of Relative Width Ratio on Exergetic Efficiency (η_{exer}):

Fig. 4 shows that exergetic efficiency as a function of temperature rise parameter. It can be seen that lower value of temperature rise parameter (ΔT/I) result in negative value of exergetic efficiency because of very high value of mass flow rate that results when temperature rise parameter rise parameter is low after increasing value of temperature rise parameter exergetic efficiency increases. For different values of Relative width ratio shown in figure the lower exergetic efficiency found for Relative width ratio 1 and high exergetic efficiency found for Relative width ratio 5.

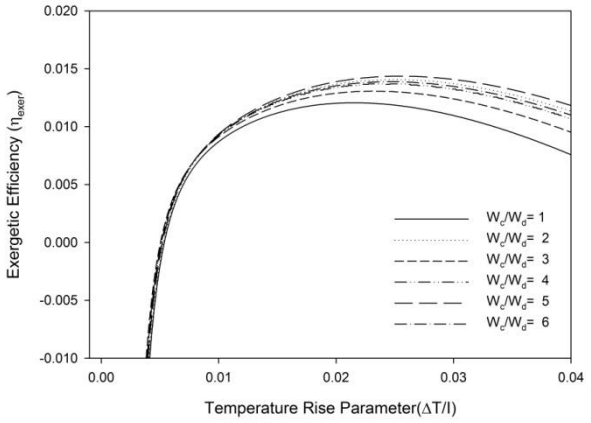

FIGURE 4. Variation of η_{exer} with ΔT/I for different W_c/W_d.

Effect of dimpled depth to print diameter (e_d/d_d) on Exergetic Efficiency (η_{exer}): Fig. 5 shows that exergetic efficiency for different dimpled depth to print diameter (e_d/d_d) as a function of temperature rise parameter. It can be seen that lower value of temperature rise parameter (ΔT/I) result in negative value of exergetic efficiency because of very high value of mass flow rate that results when temperature rise parameter is low after increasing value of temperature rise parameter exergetic efficiency increases. The maximum value of the exergetic efficiency is found to be at dimpled depth to print diameter (e_d/d_d) of 1 and minimum at dimpled depth to print diameter (e_d/d_d) of 2.

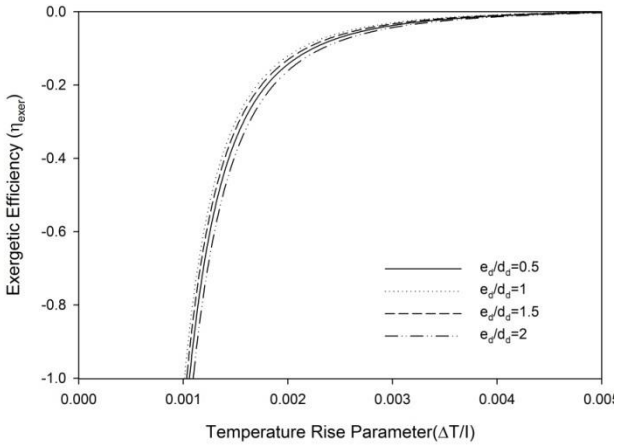

FIGURE 5. Variation of η_{exer} with ΔT/I for different e_d/d_d.

Optimisation of the System Parameters

It is revealed from the Fig. 6 that for the insolation of 1000W/m^2 the optimum value of relative pitch ratio (P_b/e_d) is 12 for the temperature rise parameter (ΔT/I) ranging from 0.001 to 0.003 optimum relative dimpled pitch (P_b/e_d) is 10 for temperature rise parameter (ΔT/I) 0.0032 to 0.004. Beyond this temperature rise parameter (ΔT/I) the optimum relative dimpled pitch (P_b/e_d) value is 8 for all values of temperature rise parameter (ΔT/I). For different insolation optimum values of relative dimpled pitch (P_b/e_d) can be found from Fig. 6.

Design plots [Fig. 6, 7, 8] have been prepared that can be used by the designer to arrived at optimum value of Relative dimpled obstacles width (W_c/W_d), relative dimpled pitch (P_b/e_d) and dimpled depth to print diameter (e_d/d_d) for different values of temperature rise parameter and different insolation.

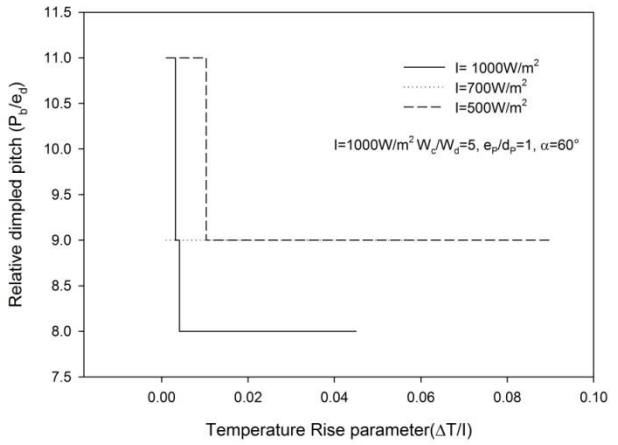

FIGURE 6. Variation of P_b/e_d with ΔT/I.

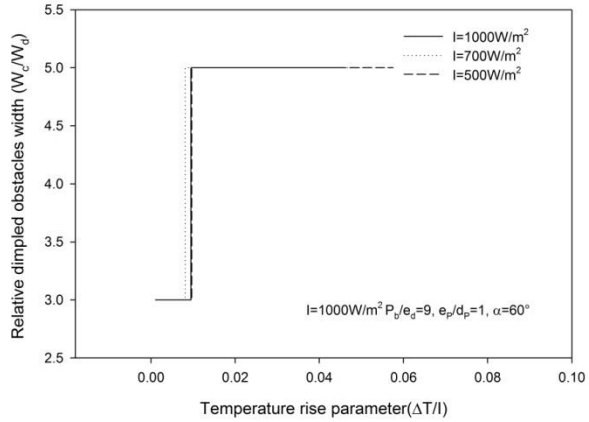

FIGURE 7. Variation of W_c/W_d with ΔT/I.

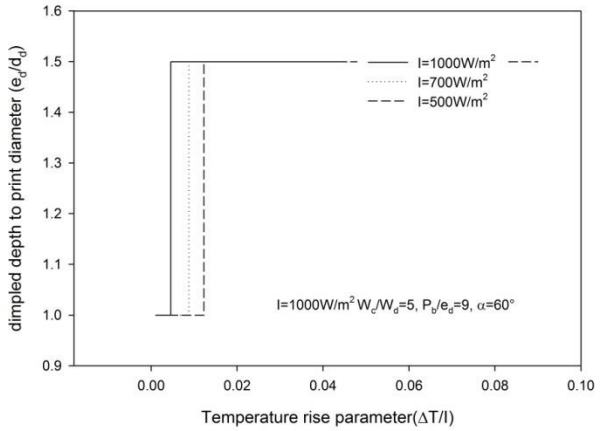

FIGURE 8. Variation of e_d/d_d with ΔT/I.

CONCLUSIONS

This investigation was taken up with the objectives of determining the optimized system parameters on the basis of exergetic efficiency criteria for specified operating condition of solar air heater. The following conclusion can be found on this basis of this work;

1. The maximum exergetic efficiency for the effect of relative dimpled pitch is found at (P_b/e_d =8) with variation of temperature rise parameter (ΔT/I).
2. The maximum exergetic efficiency for the effect of Relative dimpled obstacles width is found at (W_P/W_{AP} = 6) with variation of temperature rise parameter (ΔT/I).
3. The maximum exergetic efficiency for the effect dimpled depth to print diameter is found at (e_P/d_P= 1) with variation of temperature rise parameter (ΔT/I).

REFERENCES

[1] Z. Shen, Y. Xie, D. Zhang, Numerical predictions on fluid flow and heat transfer in U-shaped channel with the combination of ribs, dimples and protrusions under rotational effects, Int. J. Heat Mass Transf. 80 (2015) 494-512.

[2] J. Park, Y.H. Jo, J.S. Kwak,. 2016, "Heat transfer in rectangular duct with perforated blockages and dimpled side walls", International Journal of Heat and Mass Transfer, 97, pp 224-231.

[3] S. Yadav, M. Kaushal, Siddhartha Varun,. 2013, "Nusselt number and friction factor correlations for solar air heater duct having protrusions as roughness elements on absorber plate", Experimental Thermal and Fluid Science, 44, pp 34-41.

[4] N. Katkhaw, N. Voravos, T. Kiatsiriroat, Y. Khunatorn, D. Bunturat, A. Nuntaphan,. 2014, " Heat transfer behaviour of a flat plate having 45° ellipsoidal dimpled surfaces", Case Study in Thermal Engg., 2, pp 67-74.

[5] L.S. Lian, M.X. Rui, W.X. Li,. 2015, " Heat transfer and friction factor correlations for solar air collectors with hemispherical protrusion artificial roughness on absorber plate", Solar Energy, 118, pp 460-468.

[6] V.S. Hans, R.P. Saini, J.S. Saini,. 2010, " Heat transfer and friction factor correlations for a solar air heater duct roughened artificially with multiple v-ribs", Solar Energy, 84, pp 898-911.

[7] C. Thianpong, T. Chompookham, S. Skullong, P. Promvonge,. 2009, "Thermal characterization of turbulent flow in a channel with isosceles triangular ribs", International. Communication in Heat and Mass Transfer, 36, pp 712-717.

[8] R. Maithani, J.S. Saini,. 2016, "Heat transfer and friction factor correlations for a solar air heater duct roughness artificially with V-rib with symmetrical gaps", Experimental Thermal and Fluid Science, 70, pp 220-227.

[9] Anil Kumar, Raj Kumar, Rajesh Maithani, Ranchan Chauhan, Muneesh Sethi, Anita Kumari, Sushil Kumar, Sunil Kumar,. 2017, "Correlation development for Nusselt number and friction factor of a multiple type V-pattern dimpled obstacles solar air passage", Renewable Energy, 109, pp 461-479.

Proceedings of International Conference on Sustainable Energy and Environmental Challenges (3rd SEEC), December 18-21, 2018, IIT Roorkee, India

SEEC No.128

REMOVAL OF TRICLOSAN by *Bacillus licheniformis* FROM DOMESTIC WASTEWATER, MANGALORE REGION

Jayalatha N. A
Research Scholar, Civil Engineering Department, National Institute of Technology Karnataka, Surathkal, Mangalore 575025, Karnataka, INDIA
E-Mail: najayalatha@gmail.com

Chella Purushothaman Devatha
Assistant Professor, Civil Engineering Department, National Institute of Technology Karnataka, Surathkal, Mangalore 575025, Karnataka, INDIA
E-Mail: revacp@gmail.com

ABSTRACT

Triclosan is a disinfection agent present in the personal products and widely distributed in environmental matrices. In recent decade the presence of these emerging pollutants is found in drinking water by adverse effects on humans and aquatic cultures by accumulating on it. Now there is a need of treatment technologies for treatment, therefore bioremediation process is cost-effective with a reduction in secondary pollutants due to the action of organisms on the emerging pollutants. Thus the present study identifies the Triclosan in domestic wastewater and its removal was carried out by Bacillus licheniformis, where 80.89% of Triclosan removal was obtained at 2 hours of the contact period.

Keywords: Triclosan, Solid-Phase Extraction, *Bacillus licheniformis*

INTRODUCTION

In recent decades fresh water receives the Emerging pollutants of pharmaceutical products, disinfectants, antibiotics, analgesics, steroids, antidepressants, antipyretics, stimulants, antimicrobials, fragrances, cosmetics, and many other chemicals [1]. These pollutants are not monitored in the environment thus, effects on humans by its accumulation in the environment. Triclosan is the anti-disinfectant used in many personal care products, after its disposal which leads bioaccumulation in the water body and reaches human health through food chain [2] and also it reached to agricultural land due to use of wastewater for irrigation [3]. The accumulation of Triclosan in plant biomass in algae provides the entry of lipophilic organic contaminants resulting in bioaccumulation factor of Triclosan ranged from 900 – 2100 [4].

The physical and chemical techniques of nanofiltration, ultrafiltration were used in wastewater treatment plants, whereas micellar - enhanced ultrafiltration methods and chemical surfactants of sodium dodecyl sulfate, triton X- 100, tween 20 cetyl trimethyl ammonium bromide were used for the removal of emerging pollutants [5]. These technologies are not cost effective and it forms new kind of pollutants due to the reaction in the process hence use of bioremediation process are utmost importance in present senior. The emerging pollutants of PAH and pesticide removal from polluted marine sediment using *Bacillus licheniformis* were studied [6]. The study focus on the removal of Triclosan from domestic wastewater using *Bacillus licheniformis*.

MATERIALS AND METHODOLOGY

Materials

The dry-freeze form of *Bacillus licheniformis* MTCC 429 was collected from the Microbial Type Culture Collection and Gene Bank, Chandigarh, India. Domestic wastewater was collected from NITK campus treatment plant, surathkal during the rainy season.

Methodology

Inoculum Preparation

The dry form of an organism was grown on nutrient broth at 37°C and130 revolutions per minute (rpm) for 6 hours. The growth of the organism was observed at the optical density at 600 nm [7]

Treatment of Triclosan

The domestic wastewater was filtered through filter paper to remove the suspended particles. The treatment was carried out using 2 ml of domestic wastewater with 1 ml of Incolumn of *Bacillus licheniformis* (2:1 ratio) with direct contact period of 2 hours. The removal efficiency of Triclosan was quantitatively analyzed by HPLC. The sample was extracted by solid-phase extractor using methanol according to [8].

RESULTS

Fig.1. represents the growth of *Bacillus licheniformis* in nutrient broth medium and in Tab.1. tabulated the growth of the organism in garage wastewater and domestic wastewater in terms of optical density and pH. The optical density of more than 2.0 which indicates that the organism reached death phase due to high sediment content in the sample. It observed that the increase in the growth at 6 hours of incubation period with the optical density of 1.412 and change in pH value of 7 to 9 was obtained with its good growth condition for subculturing. Similarly growth of *Bacillus subtilis* having the OD of 0.01 inoculated in media, where exponential growth was started soon after the OD value of 0.1 [9]. Fig.2. shown the growth of Bacillus licheniformis in domestic wastewater (DWW) and garage wastewater (GWW), the optical density was reduced as an increase in the incubation period for both wastewater. Hence it found that inefficiency of nutrients in the sample. The maximum optical density of 1.3, growth of Bacillus licheniformis showed at 6 hours of incubation period using synthetic wastewater [10] and by comparing to garage wastewater, the domestic wastewater showed growth of bacteria up to the certain period.

Tab. 2. represents the presence of Triclosan in domestic wastewater before and after the treatment using *Bacillus licheniformis*. Triclosan removal efficiency of 80.89% was obtained by *Bacillus licheniformis* at 2 hours of the contact period. Thus it represents that *Bacillus licheniformis* was successful can be used for the treatment process. Triclosan concentration of 0.852 and 0.198µg/L was observed for influent and effluents of wastewater treatment plan with conventional treatment [11]. The Triclosan concentration of 2.1, 9 and 8.5 µg/L were observed in August, September and October month respectively for river water sample [11], similarly the present study observed 0.36 mg/L of concentration during the rainy season.

TABLE 1. GROWTH OF *Bacillus licheniformis*

Time (hours)	Optical density	pH
Initial	0.012	7
6	1.412	9

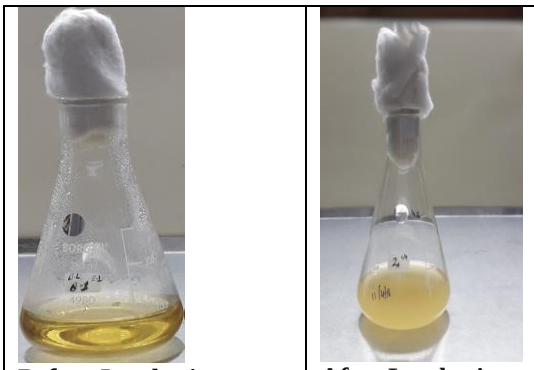

Before Incubation **After Incubation**

FIGURE 1. GROWTH OF *Bacillus Licheniformis* IN NUTRIENT BROTH MEDIUM

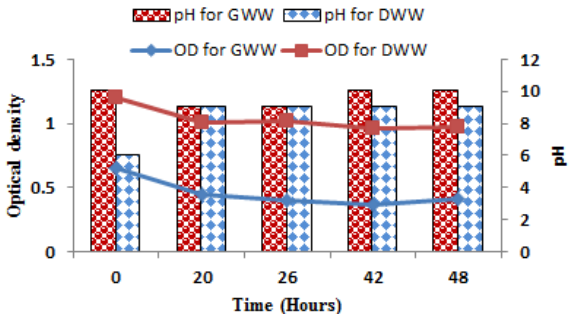

FIGURE 2. GROWTH OF *Bacillus Licheniformis* IN GARAGE WASTEWATER (GWW) AND DOMETIC WASTEWATER (DWW)

TABLE 2. TRICLOSAN CONCENTRATION IN TREATED AND UNTREATED DOMESTIC WASTEWATER

	Triclosan concentration
Before Treatment	0.356 ppm
After treatment	0.068 ppm
Removal	80.89%

CONCLUSIONS

The treatment of Triclosan using *Bacillus licheniformis* obtained the maximum removal efficacy of 80.89% within 2 hours of the contact period. The use of bioremediation process was successful can be used for wastewater treatment with maximum growth was observed in domestic wastewater than the garage wastewater without any external nutrients.

ACKNOWLEDGMENTS

The author acknowledges Dr. Varghese Geordge, H.O.D Civil Engineering Department; National Institute of Technology Karnataka Surathkal, Mangalore for facilitating the work and moral support and also thank Dr. Arun Kumar Thalla, Associate Professor, NITK, Surathkal for helpful suggestions. We acknowledge the H.O.D Chemical Engineering Department for facilitating the HPLC instrument used in this study.

REFERENCES

[1] Sui, Q., Cao, X., Lu, S., Zhao, W., Qiu, Z., Yu, G., 2015. "Occurrence, sources and fate of pharmaceuticals and personal care products in the groundwater: A review". Emerging Contaminants, 1, pp. 14-24.

[2] Olaniyan, L W B., Mkwetshana, N., Okoh, A I., 2016. "Triclosan in water, implications for human and environmental health". SpringerPlus , 5:1639.

[3] Deblonde, T., Cossu-Leguille, C., Philippe Hartemann, P., 2011. "Emerging pollutants in wastewater: A review of the literature". International Journal of Hygiene and Environmental Health, 214, 442– 448.

[4] Ebele, A J., Abou-Elwafa, M A., Harrad, S., 2017. "Pharmaceuticals and Personal Care Products (PCPs) in the freshwater aquatic environment". Emerging Pollutants, 3: 1 – 16.

[5] Acero, J L., Benitez, F J., Real, F J., Teva, F. 2017. "Removal of emerging contaminants from secondary effluents by micellar-enhanced ultrafiltration". Separation and Purification Technology, 181: 123–131.

[6] Ferreira, L., Rosales, E., Danko, A S., Sanroman, M A., Pazos, M M., 2016. "Bacillus thuringiensis a Promising Bacterium for Degrading Emerging Pollutants". Process Safety and Environmental Protection, 101, pp. 19-26.

[7] Lakshmi, B K M., Hemalatha, KPJ., 2016. "Production of Alkaline Protease from *Bacillus licheniformis* through Statistical Optimization of Growth Media by Response Surface Methodology". Fermentation Technology, 5:2, DOI:10.4172/2167-7972.1000130.

[8] Maldaner, L., Jardim I C S F., 2012. "Determination of some organic contaminants in water samples by solid-phase extraction and liquid chromatography-tandem mass spectrometry". Talanta, 100, pp. 38- 44.

[9] Evert-Jan, B., Ridder, A N J A., Lulko, A T., Roerdink, J B T M., Kuipers, O P., 2011. "Time-Resolved Transcriptomics and Bioinformatic Analyses Reveal Intrinsic Stress Responses during Batch Culture of Bacillus subtilis". PLoS ONE, Volume 6, Issue 11.

[10] Hesnawi, R., Dahmani, K., Al-Swayah, A., Mohamed, S., Mohammed, S A., 2014. "Biodegradation of municipal wastewater with local and commercial bacteria". Procedia Engineering, 70, p.p 810-814.

[11] Maria Gavrilescu, M.,, Katerina Demnerova, K., Aamand, J., Spiros Agathos, S., Fava, F., 2015. "Emerging pollutants in the environment: present and future challenges in biomonitoring, ecological risks and bioremediation". New Biotechnology, Volume 32.

[12] Madikizela, L M., Chimuka, L., 2014. "Determination of Triclosan and Ketoprofen in River Water and Wastewater by Solid Phase Extraction and High Performance Liquid Chromatography". S. Afr. J. Chem., 67, 143–150.

Proceedings of International Conference on Sustainable Energy and Environmental Challenges (3rd SEEC), December 18-21, 2018, IIT Roorkee, India

SEEC No.129

OPTIMIZED PRODUCTION PROCESS FOR WCO BASED BIODIESEL BY USING DOE

ANIRUDDHA S. JOSHI
Department of Technology,
Shivaji University, Kolhapur
Email: aditya3909@gmail.com

AJIT B. KOLEKAR
Department of Technology,
Shivaji University, Kolhapur
Email:abk_tech@unishivaji.ac.in

SUDHIR .B. DESAI
YCSRD,
Shivaji University, Kolhapur
Email:desaisudhirb@gmail.com

PRASHIK PATEKAR
Department of Technology,
Shivaji University, Kolhapur
Email-prashikpatekar1996@gmail.com

SAYALI PANDIT
Department of Technology,
Shivaji University, Kolhapur
Email-sayalipandit512@gmail.com

ABSTRACT

Biodiesel, an eco-accommodating fuel is a rising option in contrast to diesel. Crude materials for this bio fuel are generally palatable and non-consumable oils from vegetable sources. Creation cost is one of the real issues to supplant non-renewable energy source with such sustainable choice. Notwithstanding, for biodiesel creation, squander cooking oil (WCO) as a crude material realistic from kitchens, lodgings and sustenance industry might be a less expensive and inexhaustibly accessible alternative. Transfer of such utilized oil causes genuine ecological contamination. Hence changing over it into biodiesel decreases fuel costing as well as weight of treating it to make it ok for condition.

In perspective of this, the work attempted here stresses on actualizing Taguchi Design to upgrade trans-esterification process. The ideal parameters explored are liquor to oil molar proportion 7:1, rate impetus 1%, response time 20 min and temperature 50□ C individually. Biodiesel acquired with the collaboration of these parameters has the most noteworthy yield of 75 %. Besides biodiesel quality is affirmed through testing and investigation.

Keywords: WCO, Transesterification, Taguchi Approach, Biodiesel

I] INTRODUCTION

Transestrification is the most broadly utilized way for biodiesel generation. It is fundamentally a successive response that includes triglycerides decrease to di-glycerides additionally diminished to mono-glycerides which are at long last changed over to unsaturated fat esters. The request of the response may change with the response conditions. The principle factors influencing the whole procedure are molar proportion of liquor to glycerides, impetus compose and focus, response time and temperature. In some cases free unsaturated fats substance and dampness substance of the crude material amay likewise prevent the activity. The explores delight that the regularly acknowledged molar proportion of liquor to glycerides is around 6:1. Base impetuses are more powerful than corrosive impetuses and catalysts. The prescribed measure of base is more often than not somewhere in the range of 0.1 and 1% on weifht premise of the oils. Higher response temperatures accelerate the response and abbreviate the response time. Transestrification of the crude materials to yield biodiesel alongside glycerin as a result which might be isolated from the response blend.

Squander cooking oil, or, in other words costly than unadulterated vegetable oil, is a promising option in contrast to vegetable oil for biodiesel creation. The amount of waste cooking oil created every year by any nation is gigantic. The transfer of waste cooking oil is dangerous, in light of the fact that transfer strategies may debase natural water. Consequently, by utilizing these oils as the crude material, we can lessen the expense in biodiesel generation. The upsides of utilizing waste cooking oils to create biodiesel are the minimal effort and avoidance of condition contamination.

Utilized oil is the crude material feedstock that might be gathered from lodgings, eateries, kitchens, sustenance industry. It is ordinarily known as waste cooking oils (WCOs). It has been advanced as one of the elective sources among other higher review or refines oils being utilized for biodiesel generation. WCO is anything but difficult to gather additionally it is less expensive than other new oils or refined oils. Consequently, by utilizing these oils as the crude material, we can diminish the expense in biodiesel generation. The other intriguing

favorable position of utilizing WCOs to deliver biodiesel is avoidance of condition contamination. These oils if not utilized for biodiesel generation should be treated before their transfer to the earth in order to counteract contamination. Because of the staggering expense of transfer, numerous people arrange WCOs specifically into nature imprudently. In this manner the utilization of WCOs is successful as far as two way advantage. Utilized cooking oil can possibly fuel the pressure start motors. The kinematic thickness of waste cooking oil is around 10 times more prominent and its thickness is around 10% higher than that of mineral diesel. These properties assume crucial job in the burning; accordingly these must be adjusted preceding the utilization of WCO specifically in the motor. Numerous strategies, for example, pyrolysis, emulsification, inclining and transestrification have been produced to lessen the kinematic thickness and particular gravity of vegetable oils. Among these strategies, trans-esterification is the most generally utilized methods. This is a direct result of its relative straightforwardness. It might be completed at typical conditions with the best change productivity and fuel quality also.

II] EXPERIMENTAL

1] Biodiesel Production by Transesterification Method

Trans-esterification process incorporates separation of unsaturated fats from glycerol. Glycerol is an outcome while unsaturated fats are just bio-diesel.Feedstock of Waste Cooking Oil: The formation of waste cooking oil is the limit of cooking temperature and length of use and the material to be used for singed. It is obtained from private, business and current sources from where it is regularly masterminded off into the earth after expansive usage of the equal for fricasseeing sustenances. This waste may be picked as the best choice to secure biodiesel. General advances sought after for securing biodiesel from waste cooking oil are depicted as following:

(i) For methyl ester change, used oil around 100 ml is first preheated to 50ºC. Methanol (by volume) and solid stimulus (by weight) are mixed and blended in an alternate cone formed carafe.

(ii) After that the blended model is incorporated preheated oil test.

(iii) A amass reactor immersed in a water shower, gifted to keep up (± 1ºC) required reaction temperature is used for transesterification. To mix the reactants authentically a steady shaker which changes over the electric power into mechanical shaking is used at impeller speed 300 rpm. This is done at certain predefined reaction times.

(iv) After transesterification the precedent is taken in a confining channel. The mix is made to consent to twenty four hours and subsequently the glycerol is separated.

(v) Excess methanol and dirtying impacts are removed by washing the methyl ester with refined water at 40ºC

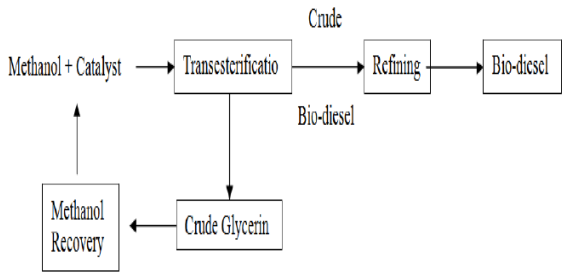

2] Optimization of Production Process

Taguchi's methodology viewed as both vital regions by unmistakably characterizing an arrangement of symmetrical exhibits to structure the analyses and by concocting a standard technique to investigate the outcomes got. Structure of trials by symmetrical exhibits offers incredible trial proficiency.

An improved structure must satisfy two destinations. To start with, the quantity of exploratory trails must be resolved. Second, the conditions for every one of the trails must be indicated. In Taguchi's methodology there are pre-characterized symmetrical clusters which are utilized to choose least conceivable test conditions. For biodiesel creation there are four parametric varieties let us say molar proportion, impetus fixation, raction time and response temperature which impact the generation yield. Each shifting at three levels and according to the enhanced methodology the controlling parameters and their levels are appeared in table 1.

After determination of levels tests are structured based on symmetrical exhibits. From the Orthogonal Arrays (OA), the required number of examinations and their conditions can be concluded. The quantity of parameters and the variety levels of every parameter choose the OA choice. The minimum conceivable number of examinations N is chosen from the quantity of levels L and number of structure and picked control parameters P utilizing the connection N = (L _ 1) P + 1.

The impacts of the four picked parameters at three unique levels have been contemplated by leading just nine investigations according to L9 OA appeared in Table 2. Each analysis has been rehashed thrice with the end goal to limit the blunders.

Table 1: Control Parameters Selection for optimization

Sr.	Process Control Parameters	Level		
		1	2	3
1	Molar ratio (Methanol to Oil)	5:1	7:1	9:1
2	Concentration of catalyst (% weight of KOH)	0.5	1.0	1.5
3	Time of reaction (min)	10	20	30
4	Temperature of reaction (°C)	50	60	70

Taguchi has built up symmetrical exhibits to depict huge number of test circumstances. Symmetrical exhibits are an arrangement of tables of numbers which can be utilized to productively achieve ideal plan. The representative assignment of the exhibit conveys the data on the measure of the analyses. For instance a L8 exhibit demonstrates that 8 preliminaries are required. Each symmetrical exhibit must fulfill adjusting property. As per adjusting property the connections between two levels of elements in trial configuration must be happened approach number of times. For instance if connection between level 1 and level 2 of two unique elements happens thrice then the communications between level 2 and level 1 of these variables must happen thrice.

Choice of an appropriate symmetrical cluster is must to achieve the exact outcomes. To choose reasonable symmetrical cluster first level of opportunity is ascertained by the accompanying condition.

Level of Freedom = P × l−1 (3.1)

Where, P = number of parameters

l = number of levels.

In above case there are four parameters and three quantities of levels so level of opportunity moves toward becoming 8. Presently we should perform least eight analyses to accomplish the require results. This should be possible by choosing a L9 cluster.

Test estimation for Methanol and Oil Volume in one of the runs is given here:

Process Parameters: Molar Ratio for methanol to oil is 5:1 (level 1), Catalyst 0.5 (level 1), Time 10 min (level 1), Temperature 50ºC (level 1): For 100 ml oil, sub-atomic weight of oil = 856 g/mol.

Thus, moles of oil = 100/856=0.1168 moles of oil

Moles of methanol = 0.1168 ×5 = 0.584 moles

Sub-atomic weight of methanol = 32.04

Weight of methanol = 32.02 x 0.584 = 18.7 gm

Liquor Volume = mass/thickness
=18.71/0.79=23.68=24 ml

In this manner for the specific run , 5: 1 molar proportion, 100 ml of oil, Methanol: 24 ml, Catalyst 0.5 gm KOH, time picked is 10 min and the temperature is 50ºC.

The advancement exploratory runs were led in triplicate with the normal of biodiesel yield discovered there.

Table 2: L9 Orthogonal array (3^4)

Sr No.	Control Parameters				% of yield			Average Yield %
	A	B	C	D	Trial1	Trial2	Trial 3	
1	5:1	0.5	10	50	66.66	61.60	70.69	66.31
2	5:1	1.0	20	60	67.74	70.96	64.51	67.73
3	5:1	1.5	30	70	51.61	58.06	66.12	58.59
4	7:1	0.5	20	70	67.74	64.51	80.64	70.96
5	7:1	1.0	30	50	67.16	74.62	67.16	69.64
6	7:1	1.5	10	60	67.74	64.51	67.74	66.67
7	9:1	0.5	30	60	51.61	61.29	48.38	53.76
8	9:1	1.0	10	70	67.74	67.74	50.00	61.82
9	9:1	1.5	20	50	69.44	59.15	59.15	62.58

III] RESULTS AND DISCUSSION

1. Optimization of Process Parameters

The examination of difference for rate yield it very well may be inferred that % yield is fundamentally influenced by the adjustment in molar proportion as it were. This is so on the grounds that 69% most extreme of rate biodiesel yield is gotten at molar proportion of 7:1. Be that as it may, too high molar proportion ought to be

avoidable. This is expected to at most noteworthy molar proportion of 9:1 slightest percent yield 59% was watched. This might be because of having more liquor caused to increment in OH and water content in arrangement. This may require more impetus, temperature and time for response. Alternate parameters like impetus rate, time and temp influenced about comparable altogether on rate yield. Investigations likewise show that percent yield isn't fundamentally changing from preliminary to preliminary. In this manner, it very well may be presumed that the variety in percent yield is predominantly because of progress in molar proportion pursued by impetus rate and time.

The chart of "factorial impact plots" demonstrates these intriguing discoveries. From the chart most noteworthy rate yield is relating to 7:01 molar proportion, 1 % impetus, 20 min time and 50ºC temperatures. Likewise, normal rate yield from this ideal parameters coming about most extreme rate yield is 67.2%.

It was seen that, Expt. NO. 5 indicated best outcome among each of the 9 tests. It was seen that enhanced parameter are Methanol to oil molar proportion ought to be 7:1, KOH impetus ought to be 1%, time ought to be 30 minute at 500C of response temperature. Likewise, this was acquired at most extreme mean yield of waste cooking oil biodiesel as 69.64 %.

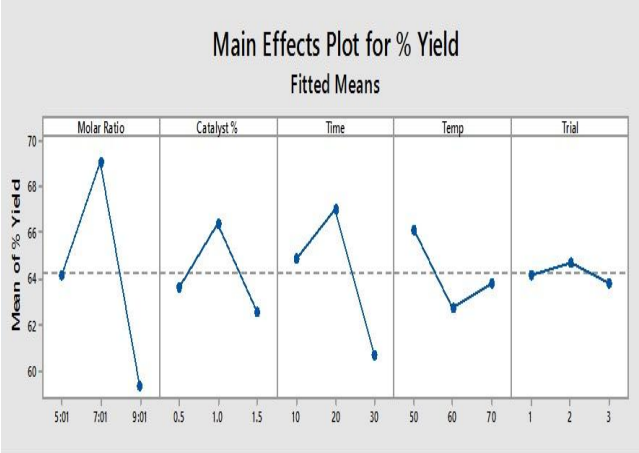

Fig.1. Factorial effects plots

2. Molar Ratios

A standout amongst the most critical factors influencing the yield of ester is the molar proportion of liquor to triglyceride. The stoichiometric proportion for transesterification requires three moles of liquor and one mole of glyceride to yield three moles of unsaturated fat ester and one mole of glycerol. The molar proportion is related with the kind of impetus utilized. A corrosive catalyzed response required a 30:1 Proportion of liquor to oil, while a salt catalyzed response required just a 6:1 proportion to accomplish a similar ester yield for a given response time. In present investigation methanol was taken as liquor. The molar proportion were differed from 5:1, 7:1 and 9:1. The percent yield continues expanding with increment in molar proportion. The 7:1 molar proportion indicated most extreme yield of 69%. In any case, 9:1 and 5:1 indicated second rate consequence of 14% less yield of biodiesel.

3. Catalyst

Impetuses are named salt, corrosive, or chemical. In present work 0.5%, 1% and 1.5% KOH impetus were contemplated. The outcomes demonstrated that 1% impetus gives more yield. The most extreme 67% yield was gotten with 1% impetus. Be that as it may, 6% less yield was watched contrasted with other impetus fixation.

4. Reaction Time

In this present work response times examined were 10, 20 and 30 minutes separately. At 20 minute response time greatest yield of 67% was watched. Notwithstanding, too quick response and too moderate response ought to be maintained a strategic distance from. The too moderate response time of 30 minute came about for 61% yield. This is 9% less yield contrasted with normal response time. This may result because of more buildup of water coming about into more glycerol arrangement and less oil is acquired. Additionally, too quick response was come about into vaporization of oil and water into condenser and subsequently less yield.

5. Reaction Temperature

Transesterification can happen at various temperatures relying upon the oil utilized. The temperature examined were 50, 60 and 70 0C separately. For little volume lesser response temperature is attainable. The response temperature 50 0C demonstrated most extreme yield of 66%. In any case, 70 and 60 0C temperature indicated bring down yield of 63 and 62% individually.

III] CONCLUSION

The accompanying are the imperative conclusions drawn from the present examinations of WCO biodiesel production process.

- The examination of fluctuation (ANOVA) information of % yield it very well may be inferred that % yield is altogether influenced by the adjustment in molar proportion as it were. Different parameters Catalyst %, Time, temperature don't essentially influence % yield.

- Above discoveries are at 5% level of criticalness that is exactness or certainty is 95%. The chart ‘factorial impact plots' additionally bolster above discoveries. From the chart most elevated % yield is comparing to 7:01 molar proportion (33 ml methanol), 1 % impetus (KOH), 20 min time units, and 50ºC temperatures.
- Biodiesel is an eco-accommodating fuel that may construct country economy. It is a rising option in contrast to diesel fuel.

Crude materials for this new fuel are for the most part the oils of eatable and non-consumable seeds from the plants. Be that as it may, current issue for such a development of supplant of the non-renewable energy source by the sustainable alternative is that the quality generation of biodiesel has been costlier. Be that as it may, waste cooking oil (WCO), crude material for biodiesel creation might be a less expensive and copiously accessible alternative which might be from lodging, sustenance industry.

IV] ACKNOWLEDGMENTS

I would like to thank to all whose names, which do not figure here, but have helped me during the tenure of my research work.

V] REFERENCES

[1] Mohammed Abdul Raqeeb and Bhargavi R., “Biodiesel production fromwaste cooking oil”, Journal of Chemical and Pharmaceutical Research, 2015, 7(12):670-681, ISSN : 0975- 7384 CODEN(USA) : JCPRC5.

[2] Jamal Uddin Ahamed, Abdur Razzaq, “Icmere2015-pi-260 production of Biodiesel from waste vegetable oil”, International Conference on Mechanical Engineering and Renewable Energy 2015 (ICMERE2015) 26 – 29 November, 2015, Chittagong, Bangladesh.

[3]N.H. Said, F.N. Anil and M.F.M. Said, “Review Of The Production Of Biodiesel From Waste Cooking Oil Using Solid Catalysts”, Journal of Mechanical Engineering and Sciences (JMES) ISSN (Print): 2289-4659; e-ISSN: 2231-8380; Volume 8, pp. 1302-1311, June 2015.

[4] Nor Hazwani Abdullah, Sulaiman Haji Hasan, and Nurrul Rahmah Mohd Yusoff, “Biodiesel Production Based on Waste Cooking Oil (WCO)”, International Journal of Materials Science and Engineering Vol. 1, No. 2 December 2013.

[5] R. B. Sharma, Dr. Amit Pal, Juhi Sharaf, “Production of Bio-Diesel from Waste Cooking Oil”, Journal of Engineering Research and Applications ISSN : 2248- 9622, Vol. 3, Issue 6, Nov-Dec 2013, pp.1629-1636.

[6] Amit Pala and Surendra Singh Kachhwahab, “Biodiesel Production of Waste Cooking Oil through Ultrasound Cavitation”, International Journal of Engineering Research and Technology. ISSN 0974-3154 Volume 6, Number 3 (2013), pp. 291-306.

[7] Prafulla D. Patil, Veera Gnaneswar Gude, Harvind K. Reddy, Tapaswy Muppaneni, Shuguang Deng, “Biodiesel Production from Waste Cooking Oil Using Sulfuric Acid and Microwave Irradiation Processes”, Journal of Environmental Protection, 2012, 3, 107-113

[8] GokhanÇayl, SelimKusefglu “Increased yields in biodiesel production from used cooking oils by a two-step process: Comparison with one step process by using TGA”, Fuel processing technology 89, (2008), 118 – 122.

[9] MaginLapuerta, Jose M. Herreros, Lisbeth L. Lyons a, Reyes Garcia-Contreras, Yolanda Briceno, “Effect of the alcohol type used in the production of waste cooking oil biodiesel on diesel performance and emissions”, Fuel 87 (2008) 3161–3169.

[10] Marchetti J.M., A.F. Errazu, V.U. Miguel, “Possible methods for biodiesel production”, Renewable and Sustainable Energy Reviews, 11 (2007) 1300–1311.

[11] Van Kasteren J.M.N., A.P. Nisworo, “A process model to estimate the cost of industrial scale biodiesel production from waste cooking oil by supercritical transesterification”, Resources, Conservation and Recycling 50 (2007) 442–458.

[12] Mangesh G. Kulkarni and Ajay K. Dalai, “Waste Cooking OilsAn Economical Source for Biodiesel: A Review”, Ind. Eng. Chem. Res. (2006), 45, 2901-2913.

[13] Zhang Y., Dub M.A., McLean D.D., Kates M., “Biodiesel production from waste cooking oil: Process design and technological assessment”, Bioresource Technology 89 (2003) 1–16.

SEEC No. 131

"EXPERIMENTAL STUDIES ON DEWATERING OF SEWAGE SLUDGE USING SKELETON MATERIAL".

Rashmi. H R*
Research Scholar
Civil Engineering
NITK,Surathkal
Email: rashusmile14@gmail.com

Dr C P Devatha
Assistant Professor
Civil Engineering
NITK,Surathkal
Email: revacp@gmail.com

ABSTRACT

The increase in industrialization and population in the recent days, the sludge production is also increased which has become difficult to handle it. Sludge used to be incinerated, compost and landfilling before disposal, but as it is not economic and environmental friendly most of the researchers are concentrating on the sludge dewatering process which is sustainable technologies so that sludge can be converted to semi solid which will be easy to handle and transport. Some sludge is used to produce to biogas, organic matter and also a source of energy further processing was not done as it contains toxic compounds in it. Hence studies on sludge dewatering can be useful in terms of environmental and economic point of view. To overcome above mentioned issues a skeleton material (Ferro-silicon slag) which is a by-product of the ferro-silicon industry is used, which acts as a rigid lattice structure in the sludge during compression. The present work is on the study of different properties of sludge and dewatering efficiency by using skeleton material. Capillary suction time has been conducted to know the dewatering efficiency using skeleton materials.

Keywords **Sludge**
Dewatering
Slag
Skeleton material.

.

NOMENCLATURE

CST - Capillary suction time
FSS - Ferr-silicon slag
Sec - Seconds

INTRODUCTION

Increasing problem in all waste water treatment plant is the disposal of sludge, during the treatment of waste water different processing will be taken up so that it should meet the discharge limits which routes to the increase in the sludge production. The produced sludge has to be disposed of, due to the increasing amount the sludge, transportation will be difficult, required land for the disposal sometimes issues and also some environmental issues hence it is very much important to reduce the sludge volume and economy **(1).** Sludge is a semi-solid slurry and can be produced as sewage sludge from wastewater treatment processes or as a settled suspension obtained from conventional drinking water treatment and numerous other industrial processes. The sludge quantity varies according to the population and sewerage expansions etc., the sludge content generation is increasing every year which leads to the increase in transportation and handling cost and also impacts on environment **(2).**

During the management of sludge, sludge is used to be treated before by digestion, thickening or conditioned, and also dewatering of the sludge will be taken up before disposing or further treatment to the sludge **(3).** Due to the different physical characteristics of the sludge, which makes much more difficult and complicated in dewatering of sludge therefore it is still a major task to design a treatment system for sludge dewatering **(4).**

Various chemical conditioners are used like cationic polyacrylamide, ferric chloride lime etc,. To increase the efficiency of sludge dewatering(**5**), using chemical conditioners are beneficial because it gives better

efficiency meanwhile it is a disadvantage because as the name itself says chemical usage will be high and sometimes it may affect the environment.so, nowadays to decrease the use of chemical conditioning, physical conditioners are widely used, such as red mud, gypsum, lignite, wheat dregs, coal fly ash and wood chips etc**.(6-11)**

The main aim of this study is to determine the influence of skeleton material on secondary sludge's dewaterability.

MATERIALS AND METHODOLOGY

Sewage sludge was taken from a wastewater treatment plant in NITK, Suratkal, and the sludge was stored at 2°C. The sludge was used within 2 weeks in the dewatering experiments. Before commencing the experiment the stored sludge was kept in a water bath at 20 °C for 30 min.

The skeleton material used here is Ferro-silicon slag which is a by-product during ferrosilicon production.Size:01mm,13mm,100mesh,200mesh,240mesh, 300mesh,325mesh or customized. it is a kind of mixture which contains the main content Silicon (45%~95%) and other components such as C, S, P, Al, Fe.

The sludge characteristics were studied and sludge conditioning will be taken up in jar test apparatus. 200mlof sludge is filled in all 6 beaker and 1st beaker will be the controller later add 1 g skeleton material in rest all 5 beakers vary the pH from 3, 7 and 12 rapid mixing is done at 200 RPM for 10min followed by 30 RPM for 15min slow mixing. Find out the dewatering efficiency by CST. And then change the dose of Skeleton materials like 1, 5, 10, 15 and 20g measure the CST with respect optimum pH. Find out the doseage of skeleton material and pH which influences sludge conditioning.

Capillary suction time (CST) was measured to estimate the sludge filterability and dewaterability. A Whatman #1 marked with two circles of radius 1.5 and 3.0 cm from the centre, with a tube of 1-cm diameter were used for the measurement of CST of the sludge. The sludge samples were poured into the tube and the time taken by the filtrate to wet the circles from 1.5 to 3.0 cm of the Whatman#1 filter paper was noted down (12)

.

RESULT AND DISCUSSIONS

CHARACTERISTICS OF RAW SLUDGE

The initial characterisation of the sewage sludge samples was performed and the values are presented. Table 3.1 shows the characteristics of the sludge sample which are determined according to standard methods

Table 3.1 Characteristics of raw sludge

Sl No	Parameter	Unit	Value
1	pH	-	7.33
2	Electrical Conductivity	Microsimens/cm	323
3	Temperature	Degree	31.2
4	Moisture content	%	91.55
5	Total solids (TS)	mg/L	8450
6	Total dissolved solids	mg/L	500
7	Total suspended solids (TSS)	mg/L	10350
8	Alkalinity	mg/L	2200

The main characteristics of sludge are pH, Moisture content, total solids, Volatile solids, Alkalinity, ect., were determined. The results show the presence of organic matter, and also consists of water and solids that can be divided into mineral and organic (volatile) solids. pH is in the neutral range. There is an increase in alkalinity which has to be reduced in the further process.

3.2 Test to determine the optimum pH

pH is an important parameter for controlling the dewaterability limit, dewatering rate, and energy efficiency.

Table 3.2 Determination of optimum pH

Sl No	pH	CST for FSS(Sec)
1	Controller	78
2	3	70
3	6	63
4	12	32

The results shown in the above table 3.2 project that Skeleton material like FSS is efficient in dewatering in the alkaline range as the CST value was low when compare to acidic and neutral range.

3.3 Estimation of CST dosage

To determine the optimum conditioning dosage, the CST test was conducted. The CST values indicate the filterability or dewaterability of sludge. FSS was conditioned with sludge to examine the effect of dosage on sludge dewaterability measured by CST. The lower the CST, better is sludge dewaterability.

Table 3.3 Determination of optimum dose

Sl No	Dosage(g)	FSS CST(Sec)
1	Controller	71
2	1	32
3	5	53
4	10	58
5	15	63
6	20	69

.

The results show that at FSS dosage at 5 g CST decreased again and started increasing as we increased the FSS dosage up to 20g. The minimum CST achieved was only32 sec for FSS of 1gm dosage. Hence the results (table 3.3) indicates that there is a solid liquid separation happening with these two skeleton material.

CONCLUSIONS

Skeleton material (FSS) were used in sludge to obtain better dewatering capability. Results (CST,) clearly indicate that FSS is performing satisfactorily to use as a skeleton material. Hence it shows that, the skeleton material (FSS) can be used as a physical conditioner which is efficient in solid-liquid separation in dewatering (via CST). Using ferro silicon slag for sludge dewatering gives an sustainable waste management and also constantly contribute in green approach for the waste recycling.

ACKNOWLEDGMENTS

The authors would like to thank the NITK,Surathkal for providing the necessary facilities to carry out this work.

REFERENCES

1. Thapa, K. B.; Qi, Y.; Hoadley, A. F. A., Interaction of polyelectrolyte with digested sewage sludge and lignite in sludge dewatering. Colloids Surf., A: Physicochem. Eng. Aspects 2009, 334, 66-73.
2. Sanin, F. D., Clarkson, W. W. & Vesilind, P.A. (2011), Sludge engineering: The treatment and disposal of wastewater sludges, DEStech Publications, Inc.
3. Vu Hien Phuong To et al., 2016 A review on sludge dewatering indices, Water Science & Technology | 74.1 | 2016.
4. Yan Wu, Panyue Zhang, Guang-ming Zeng, Jie Ye,Haibo Zhang, Wei Fang, and Jianbo Liu, Enhancing sewage sludge dewaterability by a skeleton builder: biochar produced from sludge cake conditioned with rice husk flour and FeCl3, ACS Sustainable Chem. Eng,2016.
5. Chen, C.; Zhang, P.; Zeng, G.; Deng, J.; Zhou, Y.; Lu, H., Sewage sludge conditioning with coal fly ash modified by sulfuric acid. Chem. Eng. J. 2010, 158, 616-622.
6. Lin, Y.-F.; Jing, S.-R.; Lee, D.-Y., Recycling of wood chips and wheat dregs for sludge processing. Bioresour. Technol. 2001, 76, 161-163.
7. .Ning, X.-a.; Luo, H.; Liang, X.; Lin, M.; Liang, X., Effects of tannery sludge incineration slag pretreatment on sludge dewaterability. Chem. Eng. J. 2013, 221, 1-7.
8. Chen, C.; Zhang, P.; Zeng, G.; Deng, J.; Zhou, Y.; Lu, H., Sewage sludge conditioning with coal fly ash modified by sulfuric acid. Chem. Eng. J. 2010, 158, 616-622.
9. Zhang, H.; Yang, J.; Yu, W.; Luo, S.; Peng, L.; Shen, X.; Shi, Y.; Zhang, S.; Song, J.; Ye, N.; Li, Y.; Yang, C.; Liang, S., Mechanism of red mud combined with Fenton's reagent in sewage sludge conditioning. Water Res. 2014, 59C, 239-247.
10. Zhao, Y. Q., Enhancement of alum sludge dewatering capacity by using gypsum as skeleton builder. Colloids Surf. A: Physicochem. Eng. Asp. 2002, 211, 205-212.
11. Zhao, Y.-q.; Allen, S. J.; Sun, G.-z., On the role of gypsum (CaSO4•2H2O) in conditioning and dewatering of a waterworks sludge. J. Guangzhou Univ. (Nat. Sci. Ed.) 2004, 3, 137-142.
12. Lee CH, Liu JC (2000) Enhanced sludge dewatering by dual polyelectrolytes conditioning. Water Res 34:4430 – 4436. doi:10.1016/S0043-1354(00)00209-8 Sludge dewatering by dual polyelectrolyte

SEEC No.132

STUDY AND ANALYSIS OF FLY ASH FOR STOWING IN UNDERGROUND COAL MINE VOIDS

Dr. H. K. Naik*, **Dinesh Reddy Pappu**†

*Associate Professor, National Institute of Technology, Rourkela, Odisha, Pin-769008
† Student, National Institute of Technology, Rourkela, Odisha, Pin-769008
Corresponding author's email: hknaik@nitrkl.ac.in
Corresponding author's Ph. No.: +91-9937115419

Extended Abstract

About 73% of the India's total installed power generation capacity is thermal of which coal-based generation is 90%. Around 85 thermal power stations, besides several captive power plants use bituminous and sub-bituminous coal and produce large quantities of fly ash. High ash content (30% - 40%) coal contributes to these large volumes of fly ash. The country's dependence on coal for power generation has never gone down. The term "fly ash" is used to describe any fine particulate material precipitated from the stack gases of industrial furnaces burning solid fuels. The amount of fly ash collected from furnaces on a single site can vary from less than one ton per day to several tons per month. The characteristics and properties of different fly ashes depend on the nature of the fuel and the size of furnace used. A cause of concern for the future is fly ash management. We have a lot of avenues for use of fly ash, yet we have not yet achieved 100 percent utilization of fly ash generated from coal based thermal power plants resulting in accumulation in ash ponds near the plant and creating environmental hazards to local community. Production of fly ash relies on the coal source, plant activities and numerous more factors. In the present study lime was added with fly ash to gain strength of fly ash to be placed in mine voids for filling purposes. Research facility tests were carried out in our laboratory to assess the strength gain in the fly ash by adding lime to it. Standard proctor hammer test, unconfined compression test, and tri-axial test were carried out to decide about its suitability for placement in mine voids where large amount can be utilized releasing a great stress to the environment. From the results of laboratory study using lime as an additive to the flyash encouraging properties are obtained for filling it in mined out areas. The aim of this study was to find a suitable utilization avenue for a particular fly ash sample depending upon its geotechnical properties and thus reduce the need for vast areas for disposal of fly ash which in turn causes considerable damage to the environment in the form of particulate matter in summer season. By filling these waste materials in underground mine voids this perennial problem of environmental hazard can be addressed suitably.

Key words: *fly ash, coal mine voids, characterization, lime*

1. Introduction

Ground subsidence is a very common phenomenon that is being observed in many coal mining areas. It is caused due to large underground mined out space left out after mining operations have been done. The ground equilibrium will be disturbed as soon as the excavation is done with different forces acting on it. Mine subsidence is the manifestation of gravitational action on strata. Backfilling or sand stowing has been used as a method of filling the voids for decades to counter the effect of subsidence and to improve the pillar recovery. Waste rock, mill tailings, quarried rock, sand and gravel are some of the common types of materials used for backfilling. Later it has been observed that sand or mill tailings tend to remain loose as backfilling material and merely

serve as a temporary working platform and do not offer any lateral stress on the opening walls to improve the stability situation. Due to the high cost of cemented backfills which cost around 10%-20% of the total operating cost of the mines with 75% of that cost taken by cement and also due to the unavailability of river bed sand, the use of fly ash (a by-product of coal based thermal power plants) as the alternative material has been tried to replace the conventional depleting river bed sand. It is an environmentally sound process and is the most feasible option for bulk utilization of fly ash. Using fly ash for filling the voids will save enormous land requirement for ash disposal in ash ponds which is a major issue now all over India. It fills well into the void/cavity as it can easily flow because of its better flowability properties compared to river bed sand.

2. Formulation

The aim and primary objective is to reduce the problem of subsidence so as to protect the surface features by mine void backfilling as well as effective utilizationof fly ash. The specific objectives to meet the goal were the following.

- Characterization of fly ash.
- Determination of physical and chemical properties of fly ash composite material.
- Development of composite materials with fly ash and lime.
- Determination of geotechnical properties such as, Unconfined Compressive Strength (UCS), Brazilian Tensile Strength (BTS) etc.

Following steps were followed in order to complete the project in a sequential way:

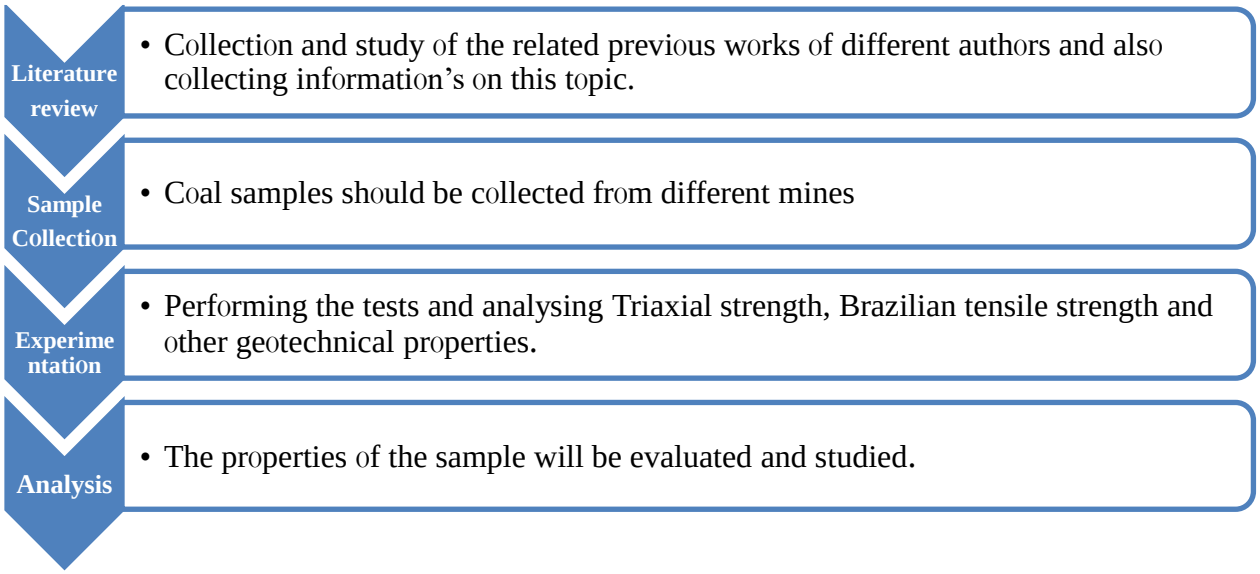

3. Result

The following fly ash Sample is collected from captive power plant **(CPP), National Aluminum Corporation (NALCO),** Talcher, Angul District of Odisha.

Table 1: Moisture content of the collected fly ash

Sl. n0	X in gms	Y in gms	Z in gms	Y – Z in gms	Y – X in gms	M0isture Y –Z/Y –X %
01	34.0557	35.0583	35.0583	0.0021	1.0026	0.209%

Table 2: Density of the collected fly ash

SL. N0.	Am0unt 0f fly ash taken (gm)	Initial reading in (ml)	Final reading in (ml)	Difference in (ml)	True Density in (gm/cc)
1	20	*200*	*210*	10	*2*
2	20	*220*	*230*	10	*2*
3	20	*180*	*190*	10	*2*

Table 3: Permeability of the collected fly ash

Sl.no	Average discharge (Q) ml	Length of specimen in cm (L)	Areaof cross section (A) in cm^2	Time in seconds (t)	Head constant (H)	Coefficient of permeability KT =QL/AtH
01	5.6	10	78	300	6	$3.98*10^{-4}$ cm/sec

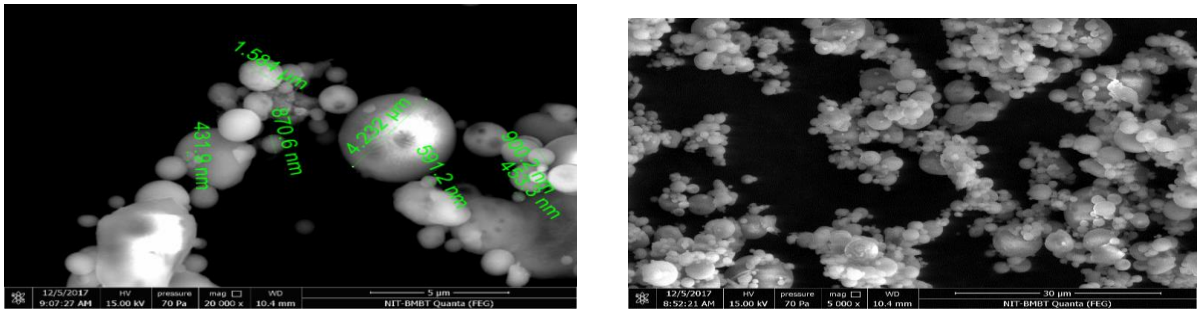

Figure 1: Scanning electron micrographs of the collected fly ash sample

4. Conclusion

The above discussed project has been done to analyze the utilization of fly ash, obtained from the NALCO power plant, for filling underground voids in mines. As per the different tests conducted such as Shear strength, Proctor compaction test, Uniaxial compressive strength test, Permeability test, Moisture Content, True density, Scanning Electron Microscope analysis the following conclusions are drawn: This Fly ash belongs F class, It has very less CaO% (< 10%), The moisture content of the sample were found out to be around 0.209% indicating that all the moisture have been evacuated and they are suitable for the void filling etc. It has an ideal true density; strengthening of composite is due to dispersion strengthening, particle reinforcement and solid solution strengthening. During our personal assessment, we have observed that fly ash composites with 10%, 20% and 30% lime added to it did not show much tensile strength even for a basic setting load. But fly ash composite with 40% lime showed some strength which can be used for filling mine voids.

5. References

(1) Jirina, T., Jan, S., 2010, Reduction of surface subsidence risks by fly ash exploitation as filling material in deep mining areas, Natural Hazards 53, 251-258.
(2) Mishra, D., Das, S.K., 2010. A study of physico-chemical and mineralogical properties of Talcher coal fly ash for stowing in underground coal mines. Materials Characterization 61, 1252-1259.
(3) Bulusu, S., Aydilek, A.H., Petzrick, P., Guynn, R., 2005. Remediation of abandoned mines using coal combustion by-products, J. Geotech. Geoenviron. Eng. 131, 958-969.
(4) Bulusu, S., Aydilek, A.H., Rustagi, N., 2007. CCB-based encapsulation of pyrite for remedial of acid mine drainage, J. Hazard. Materials, doi: 10.1016/j.jhazmat.2007.01.035.

Proceedings of International Conference on Sustainable Energy and Environmental Challenges (3rd SEEC), December 18-21, 2018, IIT Roorkee, India

SEEC No.133

POTENTIAL KERATINOLYTIC ACTIVITY OF *ASPERGILLUS GORAKHPURENSIS* FOR DEGRADATION OF MELANIZED CHICKEN FEATHERS AND SUSTAINABLE DEVELOPMENT

Ranjeeta Bhari*, Rithampreet Kaur

Carbohydrate and Protein Biotechnology Laboratory, Department of Biotechnology, Punjabi University, Patiala 147 002 (Punjab), India; *Email: ranjeetabhari01@gmail.com; Phone: Tel: +91 175 3046262; Fax: +91 175 2283073

Aspergillus gorakhpurensis was investigated for keratinolytic activity on melanized chicken feathers as sole carbon source. The strain showed maximum keratinase production (35.1 U/ml) after 72 h of incubation and completely degraded melanized feathers after 3 days of incubation by releasing melanin embedded in feather matrix. Culture filtrate was analysed for changes in pH, soluble proteins, free amino acids, ammonia concentration, free sulfydryl group and disulfide reductase activity. Highest soluble protein content (1.047 mg/ml) and ammonia (0.989 mg/ml) was observed at 72 h. A substantial increase in free amino acid content (2.701 mg/ml) was observed after 96 h. Free sulfhydryl groups were released and the strain showed high disulfide reductase activity. Scanning electron microscopy showed extensive feather degradation. Fourier transform infrared spectroscopy analysis confirmed the release of melanin after complete degradation of feathers. The strain displayed excellent keratinolytic potential and thus holds promise for sustainable management of keratinous waste.

Keywords: ***Aspergillus gorakhpurensis, Melanized Chicken feathers, Feather Degradation***

Introduction

Chicken feathers are an abundant waste of poultry processing industry, which if dumped untreated may cause environmental pollution and other health related problems [1]. White feathers are composed of hard to degrade keratin, while dark feathers contain both keratin as well as melanin [2]. Melanin is dark colored, insoluble, negatively charged, high molecular weight heterogenous polymer, embedded in the β-keratin matrix [3]. Melanin provides pigmentation and also structural rigidity to feathers by cross-linking proteins and making them more resistant to physical and biological agents [3,4]. Various physical methods such as pyrolysis, adsorption, steam-pressure and incineration have been used for the hydrolysis of melanin [4]. However, this treatment strengthens the structure of keratin by creating cross-linkage between hydrogen bonds [3]. Bleaching agents, ferrous compounds, thioglycollate, copper sulphate, ammonia and sodium sulphite have been reported to hydrolyse melanin [4].

Keratinases are inducible extracellular proteases having the ability to hydrolyse native insoluble keratin. These enzymes are robust, active over wide temperature and pH range [1]. Microbes producing keratinase enzyme are able to degrade keratin and release melanin that can be extracted for commercial use [3]. Melanin possesses physicochemical properties and biological activities that make it suitable biomaterial for wide range of applications in cosmetic, pharmaceutical, electronic and food processing industries [5]. Melanin is used in cosmetics to cure skin disease called vitiligo, caused by a loss of melanin in the skin [6]. Many commercial products contain melanin as active ingredients; including creams that provide protection against UV-light [5]. Sunglasses with high ability to block UV radiations are being fabricated by adding melanin to plastics [4,5]. The synthetic melanin like-molecules are excellent materials for bioelectronics and biomedical purposes, due to their optoelectronic energy-related properties, metal binding capacity, adhesive properties, and their ability to form easy composites with other materials [6]. They possess antimicrobial activity against wide range of food pathogens, indicating its potential applicability in food packaging and processing industries [7]. Melanin can encapsulate the radioactive particles and reduce their spread to groundwater, thus melanins can be used for environmental remediation [5]

Objectives

The present work was carried out to investigate the potential of *Aspergillus gorakhpurensis* to degrade melanised chicken feathers and to evaluate the nutritional quality of the feather hydrolysate.

Materials and methods

Aspergillus gorakhpurensis MTCC547 was grown on minimal salt medium containing melanized chicken feathers as sole carbon source and incubated at 30°C under agitation. The flasks were also visually monitored for complete degradation of feathers. The cell supernatant was used for determination of soluble protein [8], amino acids [9], ammonia [10], sulfhydryl groups [11] and disulphide reductase activity [12] using standard procedures. Degraded feathers at different time intervals were dried and coated with gold alloy using JEOL, JFC sputter coater and then examined under JEOL, JSM-6510 L scanning electron microscope. FTIR was performed to evaluate the melanin released in feather hydrolysate. FTIR spectra were

acquired using a FTIR Tensor 37 spectrometer with ATR Golden Gate in Central Instrumentation Laboratory (CIL), Panjab University Chandigarh. All spectra were recorded from 650-4000 cm^{-1} range.

Results

The strain showed maximum keratinase production (35.1 U/ml) at 72 h of incubation (Fig. 1). The culture showed complete degradation of melanized feathers after 3 days of incubation by releasing melanin embedded in the feather matrix (Fig. 2). There was significant increase in pH from 7.5-8.6 during keratin degradation. The highest soluble protein content (Fig. 3) and ammonia production (Fig. 4). Maximum amino acid content was found to be 2.701 mg/ml at 96 h of incubation (Fig. 5). The maximum concentration of free sulphydryl groups ($16.92x10^{-6}$ M) was observed at 72 h incubation (Fig. 6). Culture supernatant was tested for disulfide reductase activity and high activity was observed at 48 h of incubation (15.75 U). SEM study of hydrolysing feathers by *Aspergillus gorakhpurenis* showed extensive feather degradation at different intervals of time (Fig. 7). Disintegration of barbules apparently started after 24 h of treatment and the surface of feather keratin showed visible crack after 48 h of incubation (Fig. 7b and c). Further, the strain acts on the inner quill keratin making the rachis hollow and transparent after 72 h of incubation and the degradation extends with the breakage of outer quill and prompts the complete degradation of feathers (Fig. 7d). FTIR spectroscopic analysis was performed to study the characteristics of melanin released after degradation of keratin (Fig. 8).

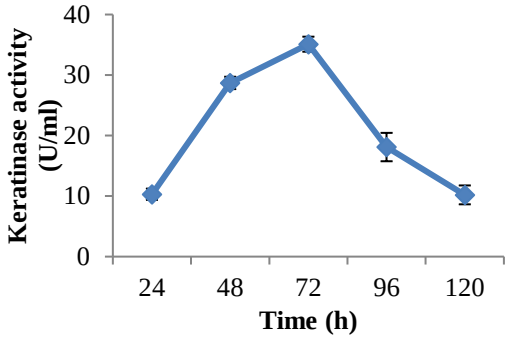

Fig. 1: Keratinase production as a function of time by *Aspergillus gorakhpurensis*.

Control **After 3 days**

Fig. 2: Degradation of melanized chicken feathers by *Aspergillus gorakhpurensis*.

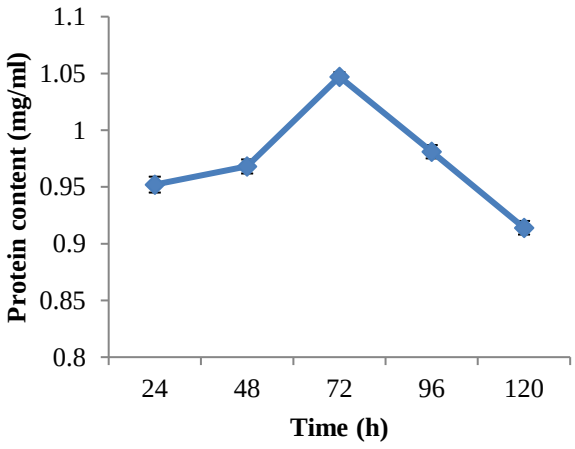

Fig. 3: Estimation of protein content in degraded melanized chicken feathers by *Aspergillus gorakhpurensis*.

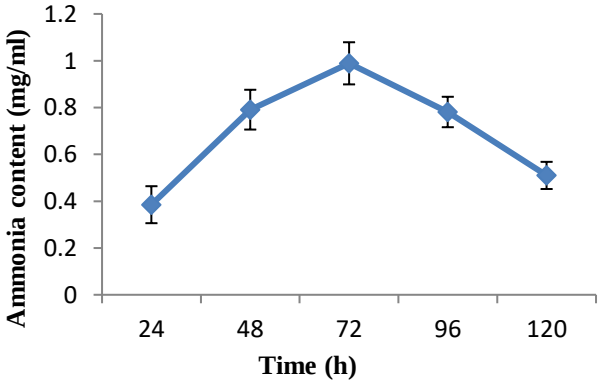

Fig. 4: Estimation of ammonia concentration in degraded melanized chicken feathers by *Aspergillus gorakhpurensis*.

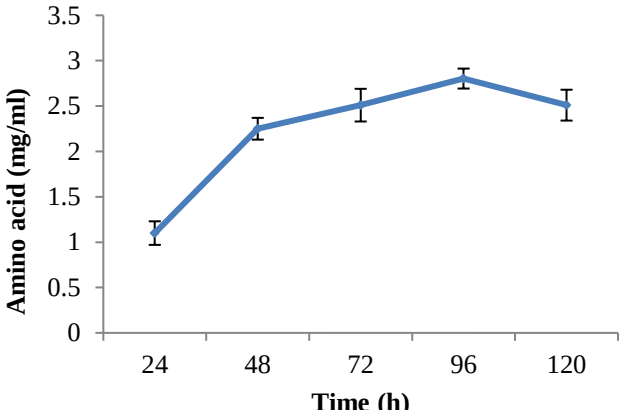

Fig. 5: Estimation of amino acid content in degraded melanized chicken feathers by *Aspergillus gorakhpurensis*.

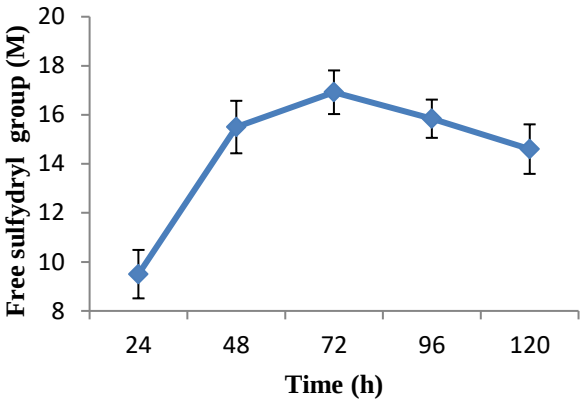

Fig. 6: Estimation of free sulphydryl groups released during degradation of melanized chicken feathers by *Aspergillus gorakhpurensis*.

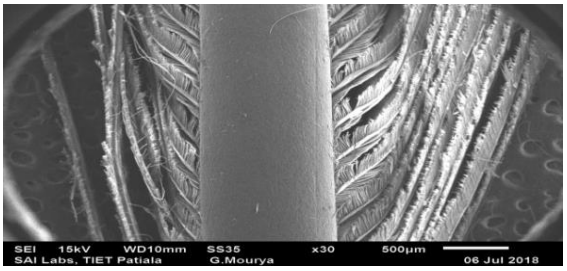

(a)

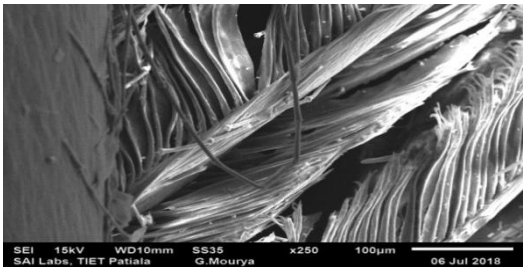

(b)

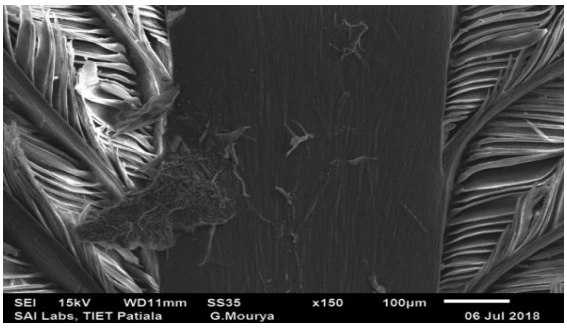

(c)

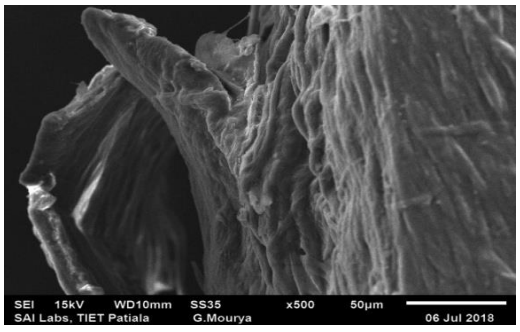

(d)

Fig. 7: Scanning electron micrographs of different stages of feather degradation by *Aspergillus gorakhpurensis* (a) Control (b-c) Colonization of feather barbules by fungi after 24 and 48 h of incubation (d) Complete degradation of the rachis observed after 72 h of incubation.

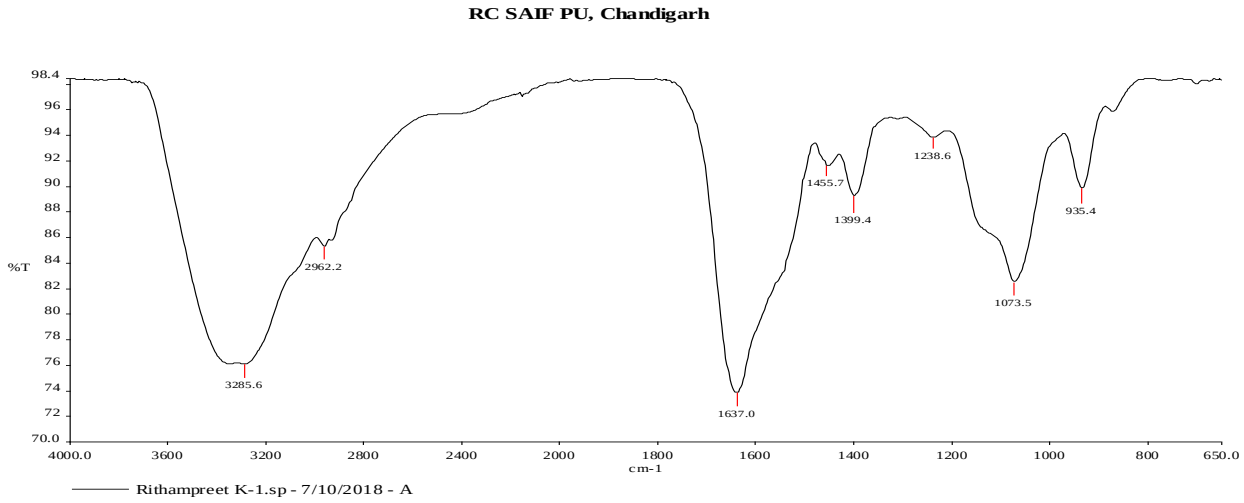

Fig. 8: FTIR spectrum of the melanin pigment obtained after degradation of melanized feathers by *Aspergillus gorakhpurensis.*

References

1. Godheja, J., Shekhar, SK., 2014. "Biodegradation of keratin from chicken feathers by fungal species as a means of sustainable development." International Journal of Bioremediation and Biodegradation, 5: pp. 1-5.
2. McGraw, KJ., Hill, GE., 2006. "Mechanics of carotenoid-based coloration". Bird Coloration, 1: pp. 177-242.
3. Gurav, RG., Tang, J., Jadhav, JP., 2016. "Sulfitolytic and keratinolytic potential of *Chryseobacterium* sp. RBT revealed hydrolysis of melanin containing feathers". 3 Biotech, 6: pp. 145-152.
4. Gunderson, AR., Frame, AM., Swaddle, JP., Forsyth, MH., 2008. "Resistance of melanized feathers to bacterial degradation: is it really so black and white?" Journal of Avian Biology, 39: pp. 539-545.
5. Tarangini, K., Mishra, S., 2013. "Production, characterization and analysis of melanin from isolated marine *Pseudomonas* sp. using vegetable waste". Research Journal of Engineering Sciences 3: pp. 415-419.
6. Sajjan, SS., Anjaneya, O., Guruprasad, BK., Anand, SN., Suresh, BM., Karegoudar, TB., 2013. "Properties and functions of melanin pigment from *Klebsiella* sp. GSK". Korean Journal of Microbiology and Biotechnology, 41: pp. 60-69.
7. Kiran, GS., Dhasayan, A., Lipton, AN., Selvin, J., Arasu, MV., Al-Dhabi, NA., 2014. "Melanin-templated rapid synthesis of silver nanostructures". *Journal of Nanobiotechnology*, 12: pp. 1-18.
8. Lowry, OH., Rosebrough, NJ., Farr, AL., Randall, RJ., 1951. "Protein measurement with the Folin phenol reagent". Journal of Biological Chemistry 193: pp. 265-275.
9. Moore, S., Spackman, DH., Stein, WH., 1958. "Chromatography of amino acids on sulfonated polystyrene resins an improved system". Analytical Chemistry, 30: pp. 1185-1190.
10. Goswami, D., Dhandhukia, P., Patel, P., Thakker, JN., 2014. "Screening of PGPR from saline desert of kutch: growth promotion in Arachis hypogea by *Bacillus licheniformis* A2". Microbiological Research, 169: pp. 66-75.
11. Ellman, GL., 1959. "Tissue sulfhydryl groups". Archives of Biochemistry and Biophysics, 82: pp. 70-77.

.

Proceedings of International Conference on Sustainable Energy and Environmental Challenges (3rd SEEC), December 18-21, 2018, IIT Roorkee, India

SEEC No. 135

RESTORATION OF PHYSICO-CHEMICAL CHARACTERIZATION OF DAIRY SLUDGE BY VERMICOMPOST

Jayalatha N. A[1]
[1]Research Scholar, Civil Engineering Department, National Institute of Technology Karnataka, Surathkal, Mangalore 575025, Karnataka, INDIA
E-Mail: najayalatha@gmail.com

Shreyas A[2]
Kadambari S Teli[3]
Mahendra S Pujari[4]
Vinay Kumar[5]
[2345]Former UG Students, Alva's Institute of Engineering & Technology, Moodabidri, Karnataka, INDIA

ABSTRACT

Vermicomposting is the use of earthworms to form fertile compost using waste organic materials. The composting was carried using dairy waste sludge and compared with soil compost by analyzing the physical-chemical properties. The good fertile compost was obtained for dairy sludge using the earthworms of Eisenia fetida and Eudrilus eugeniae at 5th week. The use of waste organic dairy sludge for composting reduces the landfill with an increase in the fertility in the soil for agriculture with NPK ratio in the compost is good enough for the growth of crops.

Keywords: *Dairy sludge, vermicomposting, physic-chemical property*

INTRODUCTION

India like many other countries has to confront the solid waste management problem due to urbanization, which is a very rapid process and a worldwide phenomenon. Among All industrial activities, the food sectors are highest consumptions of water and generate sludge as waste materials, where the milk industry generates between 3.739 and 11.217 million m^3 of sludge waste per year [1]. The disposal of organic degraded products should be recycled and utilized to sustainable agriculture, therefore the use of dairy sludge for vermicomposting reduce the solid waste management by agricultural usage.

Dewatered and dried sludge is called as biosolid remains problematic due to the high cost of installing sewage sludge stabilization reactors and dehydration systems [2]. The process of subjecting the organic matter to aerobic decomposition, with the help of earthworms is known as vermicomposting. It requires less labor, less time and less expensive method [3]. The dairy sludge and cow dung slurry ratio of 1:2 and 2:2 used with *Eisenia fetida* and *Eudrilus Eugenia* and obtained fertile compost at 55 days [4]. The study was conducted using cow dung and agro wastes in the ratio of 1:1 to 5:1 depending upon availability and it is covered loosely with soil where green waste, paper waste and milk sludge can be successfully decomposed with an increase in the cocoons of the earthworms [3]. Compared to municipal solid waste, dairy sludge have higher N and lipid contents, lower C/N ratios and generally have a more liquid consistency [5].

In this study, the economic and environmentally friendly method of vermicomposting was carried out using waste dairy sludge. The fertility of the compost was compared with soil compost produced by vermiculture.

MATERIALS AND METHODOLOGY

Materials

Dairy waste sludge was collected from Karnataka Milk Factory, Kulashekara, Mangalore and laterite soil, dry leaves, areca nut shells, paddy straws were collected from nearby locality areas. The earthworms of *Eisenia fetida* and *Eudrilus eugeniae* were purchased from Preethi Vermiform Dasanakoppa.

Methodology

Preparation of bin:

The worm bin is the enclosure withholding of food scraps and maintained moisture level in the bed and also bottom outlet was provided to remove the excess water from the bin. The water channel was made attached to the bin to protect the worms from the entry of ants and shelter was made to keep the bed materials with the moistened condition.

Preparation of Worm Bedding:

Bedding materials should be light-weight, biodegradable and retain the moisture to grow earthworms. Worm beds are prepared by filling with first layer as dry areca nut shells up to 10cm, paddy straw up to 10 cm, 10 cm of soil layer and up to 10 to

15 cm thickness dry leave including banana leaves also added.

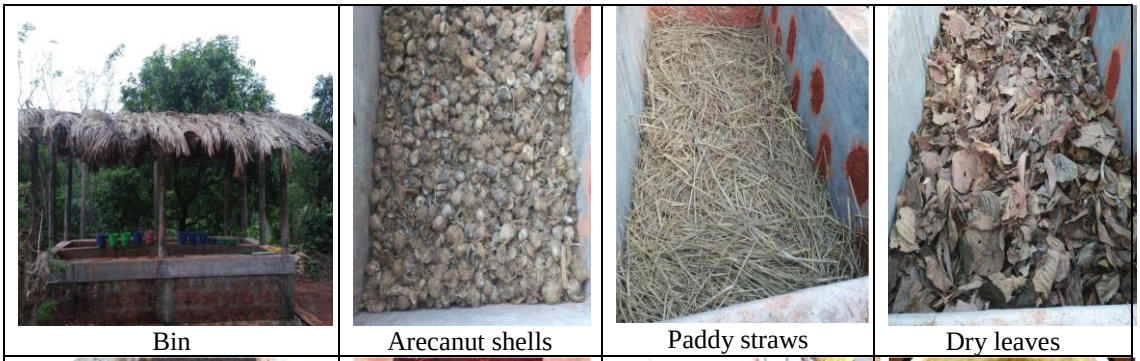

Fig.1.1 Preparation of bedding material for composting and process of vermiculture

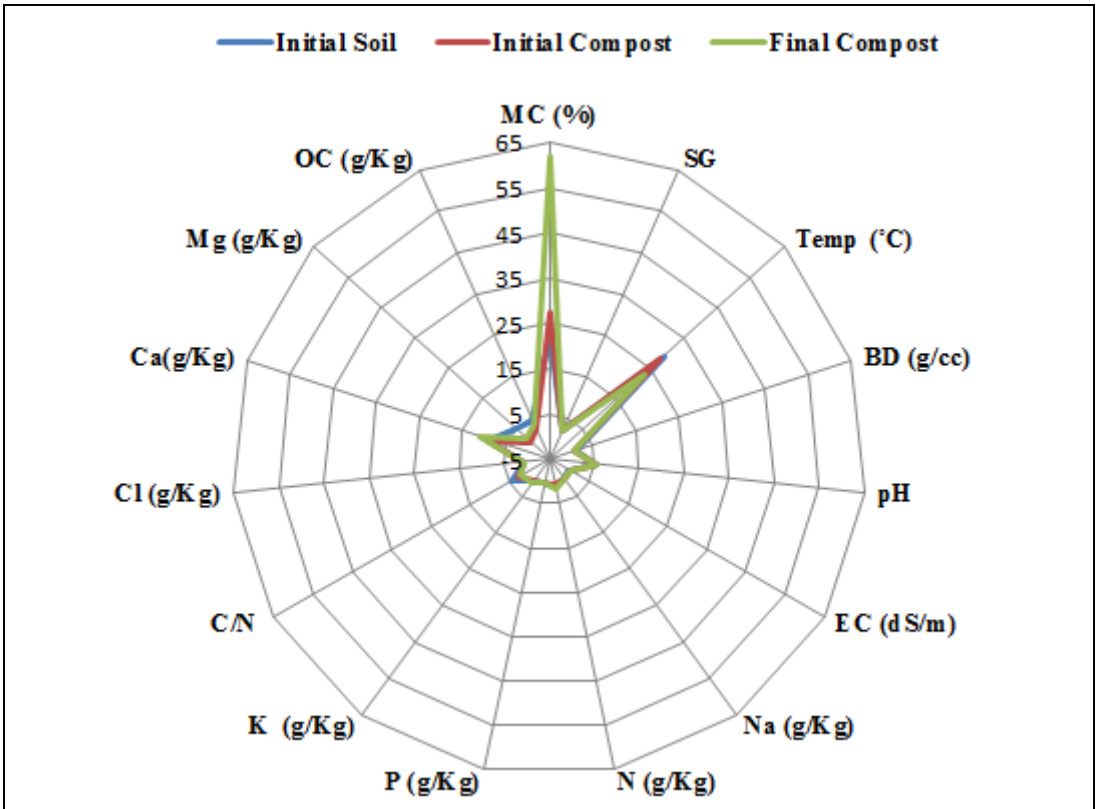

FIG.1. COMPARISON STUDY OF SOIL COMPOST WITH INITIAL CONDITION

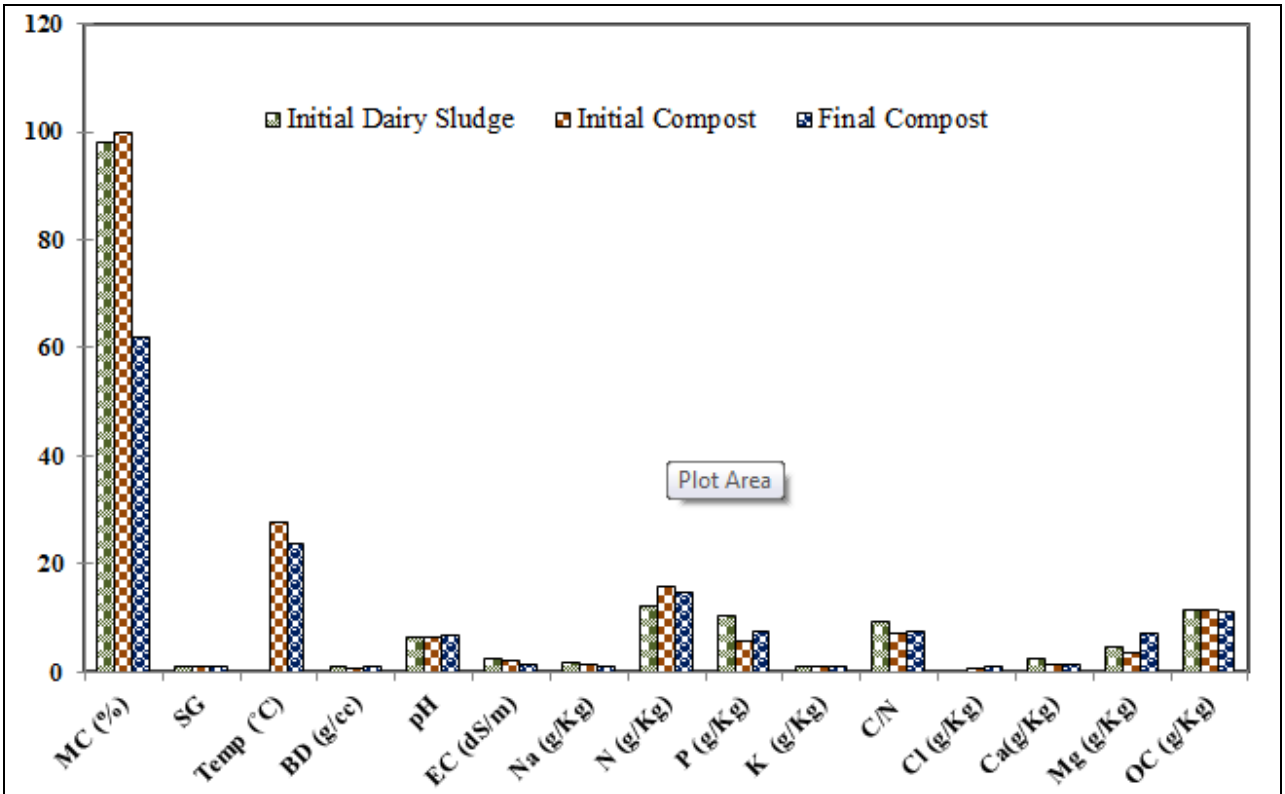

FIG.2. COMPARISON STUDY OF SOIL COMPOST WITH INITIAL CONDITION

Moistening and introducing the worms:

Worms can only live in a moist environment; water was sprinkled to the bin for every 2-3 days to keep it cool and moist in summer. Then 3/4th of the bin was filled with dairy sludge (case 1) and laterite soil (case 2) in two separate bins and mixed once in a day. After 15 days half kilograms of earthworms are introduced into the bins.

Feeding the Worms:

After introducing the worms into the bin food is added to the surface. Banana Stem and Cow dung slurry were used as feeding agents to the earthworms.

Harvesting the vermicompost:

The worms are taken to the new bin after the complete decomposing of the organic materials and final compost was taken from the bin for agriculture purpose.

RESULTS

Management of biosolids remains problematic due to the high cost of installing sewage sludge stabilization reactors and dehydration systems. Generally, dairy sludge contains large quantities of casein, lactose, fat and inorganic salts, besides detergents, sanitizers etc. used for washing.

Fig.1. and 2 represents the comparison study of soil properties with initial and final compost of 100% soil and 100% dairy sludge during initial condition, 1st week of the compost (initial compost) and 5th week (final compost). The moisture content of the soil was 22.69% and increased up to 61.77% during the 5th week of the final compost also the specific gravity has got an increase from 1.707 to 1.76 respectively (Fig.1). Whereas in 100 % dairy sludge the initial moisture content was too high (i.e. 99.97%) and got reduced to 62.13 % in the final compost (Fig.2). Both the cases the pH and electrical conductivity got decreased during final compost. The pH and electrical conductivity of 6.6 and 2500 µS/cm respectively was observed for sewage sludge [6]. In the 100% soil the sodium content was increased at final compost, but in the case of 100% dairy sludge sodium content was decreased from 1.66 g/Kg to 1.07 g/Kg. The nitrogen content in the 100% soil was 0.86 g/Kg at the initial stage and there was increased at final compost (1.4243 g/Kg) and results of vice versa found in dairy sludge.

The Phosphorous content in the 100% soil was decreased and in the case of 100 % dairy sludge, it was increased from 5.95 to 7.69 g/Kg. The phosphorus concentration of initial soil and dairy sludge was 0.19 and 1.05 g/Kg and similar results of

1.07 and 7.48 g/Kg respectively was obtained for rice straw and cow dung [7]. Organic carbon was increased and in 100 % sludge it was decreased at the final stage. The use of *Eisenia fetida* mediated vermi beds showed the reduction in organic carbon as compared to *Eudrilus eugeniae* due to an increase of excretion rate of the species [8] and similarly the organic carbon reduction was observed in 100% dairy sludge.

C/N ratio determines the maturity of the compost and ratio should be less than 15 with preferable value is less 10 [9]. The 4.33 of C/N ratio was observed for 100 % initial soil and at the compost stage it was decreased to 2.221, but in 100 % dairy sludge it was increased (i.e. 7.255 to 7.641). The composting of milk sludge along with paper, garden waste and cow with ratios of 3:1:1 and 7:2:1 respectively obtained the C/N ratio of 21.8, 16.3 [3] at 60days of composting period whereas in the present study both cases showed matured compost fertility with less C/N ratio within 5^{th} week and can be used for the plants. The use of *Eisenia fetida* and *Eudrilus eugeniae* showed high activity in compost formation with reducing the composting period and similar observation was obtained in [10] using Eisenia fetida, Eudrilus eugeniae, and Perionyx excavates of earthworms also showed that use of *Eudrilus eugeniae* for composting reduce detection level of E. coli with the use of organic fraction of Municipal Solid Waste [11].

CONCLUSIONS

Dairy sludge is rich in organic matter and mineral nutrients, particularly nitrogen and phosphorus. Disposal of sludge and waste is a major problem as it leads to serious environmental issues and use of vermicomposting reduced the waste disposal from the dairy industry. The C/N ratio of the final compost was 7.641, and 2.221 respectively for dairy sludge and soil compost. The results of NPK and C/N ratio showed with fertile compost using Eisenia fetida, Eudrilus eugeniae of earthworms.

ACKNOWLEDGEMENT

The author acknowledges Durga Prasad Baliga, H.O.D Civil Engineering Department; Alva's Institute of Engineering and Technology, Moodabidri for facilitating the work and moral support.

REFERENCES

[1] Tikariha, A. Sahu, O., 2014. "Study of Characteristics and Treatments of Dairy Industry Waste Water". Journal of Applied & Environmental Microbiology, Vol. 2, No. 1, pp. 16-22.

[2] Sinha, R K., Bharambe, G., and Bapat, P., 2007. "Removal of BOD and COD Loadings of Primary Liquid Waste Products from Dairy Industry by Vermi-Filtration Technology Using Earthworms". Indian Journal of Environmental Protection, vol-27, No.6.

[3] Desai, N., Tanksalia, A., Soraganvi, V S., 2016. "Vermicomposting – Solution for Milk Sludge". Procedia Environmental Sciences 35, pp. 441 – 449.

[4] Anusha, S., and Pratheeba, P., 2015. "Stabilization of sludge from AAVIN dairy processing plant (Chennai) using Vermicomposting". Journal of Chemical and Pharmaceutical Research, 7(3):846-851.

[5] Quintern, M., Seaton, B., Mercer, E., and Philip Millichamp, P., 2013. "Industrial scale vermicomposting of pulp and paper mill solids with municipal biosolids and DAF sludge from dairy industries". Appita Annual Conference and Exhibition, Melbourne, Vol. 66, No. 4.

[6] Lv, B., Zhang, D., Cui, Y., Yin, F., 2018. Effects of C/N ratio and earthworms on greenhouse gas emissions during vermicomposting of sewage sludge". Bioresource Technology, 268, 408–414.

[7] Sharma, K., Garg, V K., 2018. Comparative analysis of vermicompost quality produced from rice straw and paper waste employing earthworm *Eisenia fetida* (Sav.)". Bioresource Technology, 250, 708–715.

[8] Paul, S., Das, S., Raul, P., Bhattacharya, S S., 2018. "Vermi-sanitization of toxic silk industry waste employing *Eisenia fetida* and *Eudrilus eugeniae*: Substrate compatibility, nutrient enrichment and metal accumulation dynamics". Bioresource Technology 266, 267–274.

[9] Mupondi, L T., Mnkeni, P N S., Muchaonyerwa, P., Mupambwa, H A., 2018. "Vermicomposting manurepaper mixture with igneous rock phosphate enhances biodegradation, phosphorus bioavailability and reduces heavy metal concentrations". Heliyon, 4, e00749.

[10] Hussain, N., Das, S., Goswami, L., Das, P., Sahariah, B., Bhattacharya, S S., 2018. "Intensification of vermitechnology for kitchen vegetable waste and paddy straw employing earthworm consortium: Assessment of maturity time, microbial community structure, and economic benefit". Journal of Cleaner Production 182, 414-426.

[11] Soobhany, N., 2018. "Preliminary evaluation of pathogenic bacteria loading on organic Municipal Solid Waste compost and vermicompost". Journal of Environmental Management, 206, 763-767.

Proceedings of International Conference on Sustainable Energy and Environmental Challenges (3rd SEEC), December 18-21, 2018, IIT Roorkee, India

SEEC No.136

STATISTICAL OPTIMIZATION OF KERATINASE PRODUCTION AND FEATHER DEGRADATION BY *BACILLUS LICHENIFORMIS*

Manpreet Kaur, Ranjeeta Bhari*, Mehak Singh

Carbohydrate and Protein Biotechnology Laboratory, Department of Biotechnology, Punjabi University, Patiala 147 002 (Punjab), India; *Email: ranjeetabhari01@gmail.com; Phone: Tel: +91 175 3046262; Fax: +91 175 2283073

Present study reports keratinolytic potential of Bacillus licheniformis isolated from poultry dump soil. Response surface methodology was employed to improve keratinase production on minimal salt medium containing feathers as sole carbon source. About 2.33-fold increase in keratinase activity was observed at pH 9 and temperature 45°C under shaking (250 rpm) after 48 h of incubation and time for complete degradation of white chicken feathers was reduced to 3 days. Strain was tested for its ability to degrade other keratinous substrates and highest degradation was observed on pigeon feathers followed by human nails, duck feathers, goat horn, sheep wool and human hair. Highest soluble protein and ammonia content was observed on chicken and pigeon feathers after 72 h of incubation. Substantial increase in amino acid content was observed at 72-96 h of incubation in all the substrates tested. Increase in disulphide reductase activity confirms the sulphitolytic potential of the strain.

Keywords: *Bacillus licheniformis,* Response Surface methodology, Keratin Degradation

Introduction

Chicken feathers produced in millions of tons annually are a potent waste generated as a bulk by-product of poultry processing industry, and is one of the major concerns in solid waste management [1]. Feathers are mainly composed of fibrous, insoluble and recalcitrant structural protein called keratin which resists degradation due to extensive network of disulphide bonds, hydrogen bonds and hydrophobic interactions of polypeptides [1, 2]. Various physical or chemical methods for hydrolysis of feathers to feedstuffs and fertilizers are limited due to low yield, poor quality and structural destruction of amino acids such as lysinoalanine and lanthionine [2]. Keratinases are serine or metallo-endoproteases that can degrade both soft and hard keratins by acting on the β-pleated sheets and α-helix structure. A vast variety of bacteria and fungi are known to produce keratinolytic enzymes to degrade keratin [3].

Keratinase have found application in preparation of animal nutrients, protein supplements, leather manufacture, textile processing, detergent formulation, feather meal processing for feed and fertilizer, pharmaceutical and biomedical industries [1-4]. Economic as well as environmental pressure increases interest in using renewable and sustainable raw materials. Composting has been widely known as eco-friendly alternative to managekeratinous wastes into value-added products like feed supplements, amino acids or nitrogen fertilizers [3 ,4]. However, degradation rate of keratinous waste is slow in composting due to highly stable structure of keratin and their resistance to proteolytic enzymes. Addition of keratinase producing microbes to compost provides a new direction for waste management with industrial applications giving rise to green technology for sustainable development.

Objective

The present work was carried out to optimised process parameters (pH, temperature and agitation) to increase keratinase production and feather degradation by *Bacillus licheniformis.* Degradation of different keratin rich substrates and analysis of value added metabolites of feather hydrolysate were also studied.

Materials and Methods

Effect of three independent variables (pH, temperature, agitation) on keratinase production and feather degradation was investigated by central composite rotatable design (CCRD) of response surface methodology (RSM) in 20 experimental runs using Design Expert software version 11.0.2.0. Keratinase activity and feather degradation were determined by coefficient of determination (R^2), analysis of variance (ANOVA) and 3-D plots. The strain was tested for its ability to degrade pigeon feathers, duck feathers, white chicken feathers, human nails, goat horn, human hair andsheep wool. Sterilized MSM supplemented with 1% substrate was inoculated and incubated at 40°C under agitation (150 rpm). Percentage degradation,

changes in pH, keratinase activity, concentration of soluble protein [5], amino acid [6], ammonia [7], free sulfhydryl group [8] and disulphide reductase activity was detected at 24 h intervals upto 5 days.

Results

Maximum keratinase production (42.23U/ml) and feather degradation (92.23%) was observed at pH 9 and temperature 45°C under agitation 250 rpm after 48 h of incubation. Analysis of variance of the quadratic regression model showed the significance of model (Tab. 1). Three dimensional plot surfaces showed the combined effect of three independent variables (Fig. 1 and 2).The plots revealed that the keratinase activity and feather degradation was lower at the lower limits of three independent variables and maximum at pH 9 and temperature 45°C under agitation (250 rpm). *Bacillus licheniformis*was tested for degradation of different keratin substrates (chicken feathers, duck feathers, pigeon feathers, human nails, human hairs, sheep wool and goat horn) at 45ºC under agitation (250 rpm). Degradation was monitored at 24 h intervals for 5days. The strain showed highest degradation to chicken feathers that could be completely degraded in 3 days followed by pigeon feathers (88%), human nails (56%), duck feathers(41%), goat horn (23%), sheep wool (19.2%) and human hairs (17%) showing respective degradation after 5 days. Chicken feathers (42.23 U/ml) and pigeon feathers (38.47 U/ml) showed high keratinase activity after 48 h of incubation while other substrates showed maximum keratinase activity in stationary phase (Fig. 3). The maximum protein content was 1.228 mg/ml in chicken feathers followed by pigeon feathers (0.957mg/ml) after 72 h of incubation (Fig. 4). The maximum amino acid content (0.968 mg/ml) was observed at 72-96 h of incubation in chicken feathers followed by pigeon feathers, human nails, duck feathers, sheep wool, goat horn and human hair (Fig. 5). Maximum production of ammonia (0.986 mg/ml) was estimated in the presence of 1.0% chicken feathers at 72 h incubation followed by pigeon feathers, human nails and duck feathers (Fig. 6). The maximum concentration of free sulphydryl was 2.21×10^{-5}M at 96 h of incubation in chicken feathers followed by pigeon feathers, human nails, duck feathers, sheep wool, goat horn and human hair. Maximum disulphide reductase activity (9.4 U/ml) was observed at 72 h of incubation in chicken feathers followed by pigeon feathers (9.23 U/ml), human nails(7.35 U/ml), duck feathers(7.15 U/ml), sheep wool(4.33 U/ml), goat horn(4.17 U/ml) and human hair(3.57 U/ml). These results demonstrated excellent keratinolytic potential of the strain with the release of value-added products.

Table 1: Variance analysis of response surface quadratic model for keratinase activityand feather degradation by *Bacillus licheniformis.*

Source	Keratinase production (%)				Feather degradation (U/ml)			
	Sum of squares	Df	F-value	p-value	Sum of squares	Df	F-value	p-value
Model	1009.30	9	111.23	< 0.0001	4688.51	9	193.02	< 0.0001
A-pH	626.47	1	621.47	< 0.0001	1914.04	1	709.17	< 0.0001
B-Temperature	4.77	1	4.73	0.0547	808.90	1	299.71	<0.0001
C-Agitation	52.08	1	51.66	< 0.0001	414.13	1	153.44	< 0.0001
AB	7.45	1	7.39	0.0216	12.48	1	4.62	0.0571
AC	2.90	1	2.88	0.1205	31.09	1	11.52	0.0068
BC	1.57	1	1.55	0.2410	11.40	1	4.22	0.0669
A^2	294.32	1	291.93	< 0.0001	1163.96	1	431.26	< 0.0001
B^2	11.73	1	11.64	0.0066	413.42	1	153.18	< 0.0001
C^2	34.99	1	34.71	0.0002	129.52	1	47.99	< 0.0001
Residual	10.08	10			26.99	10		
Lack of fit	7.37	5	2.72	0.1478	22.46	5	4.96	0.0517
Pure error	2.71	5			4.53	5		
Cor total	1019.39	19			4715.50	19		

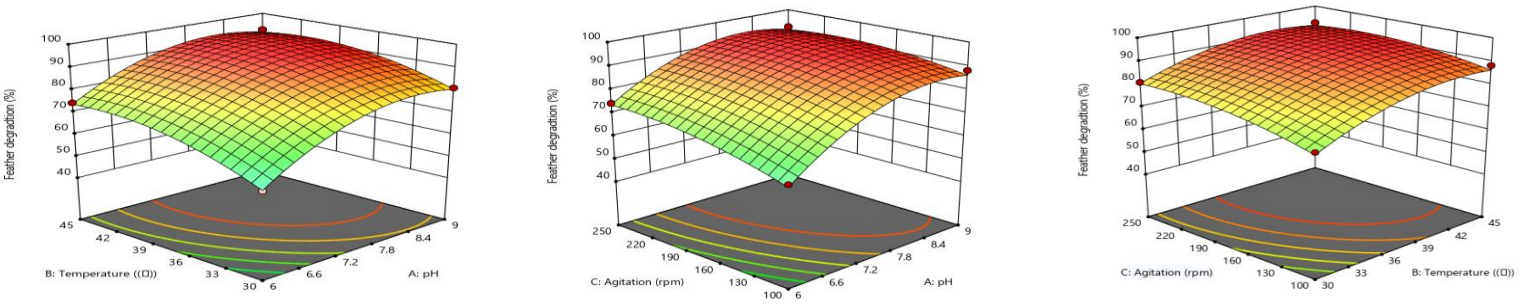

(a) (b) (c)

Fig. 1: Three dimensional plots depicting the interaction of different variables and their effect on feather degradation by *Bacillus licheniformis.*

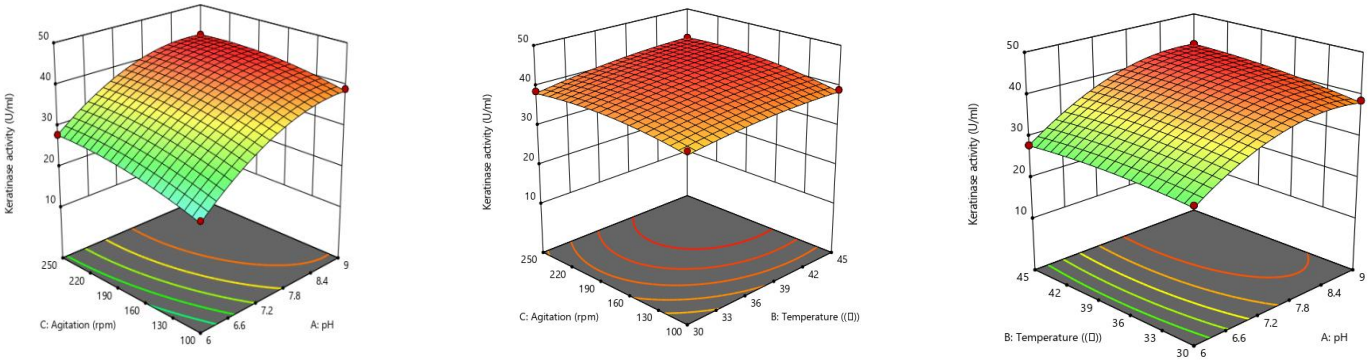

(a) (b) (c)

Fig. 2: Three dimensional plots depicting the interaction of different variables and their effect on keratinase activity by *Bacillus licheniformis.*

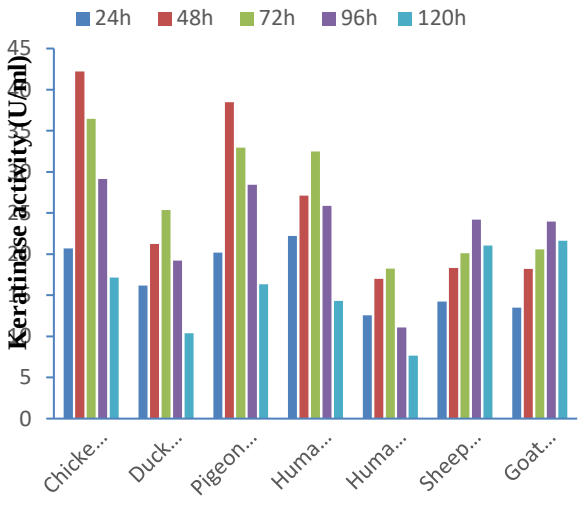

Fig. 3: Keratinase production on various substrates by *Bacillus licheniformis.*

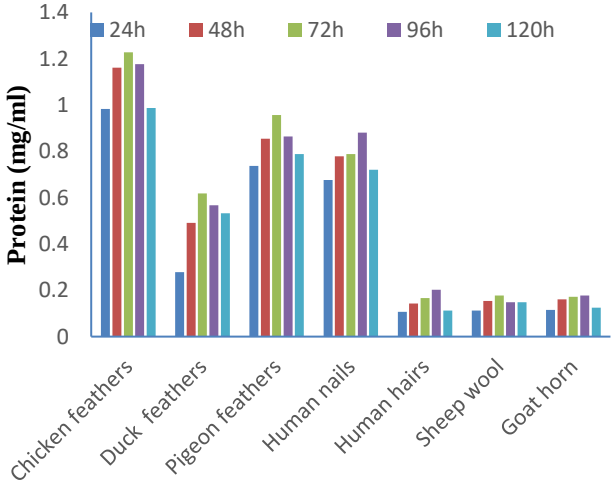

Fig. 4: Protein released on hydrolysis of different keratinous substrates by *Bacillus licheniformis.*

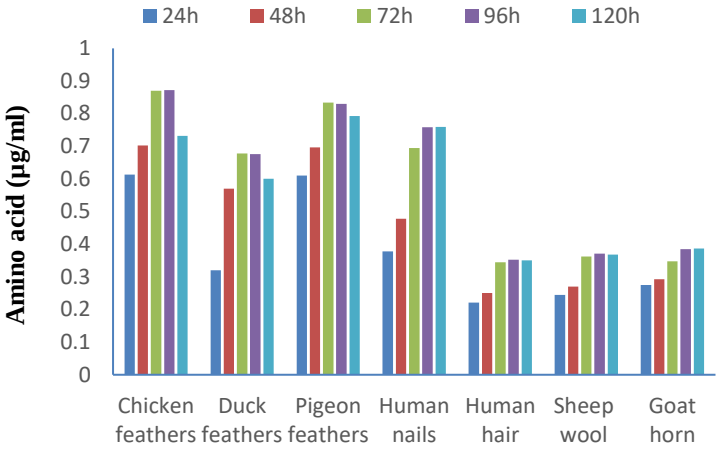

Fig. 5: Amino acid content released on hydrolysis of different keratinous substrates by *Bacillus licheniformis.*

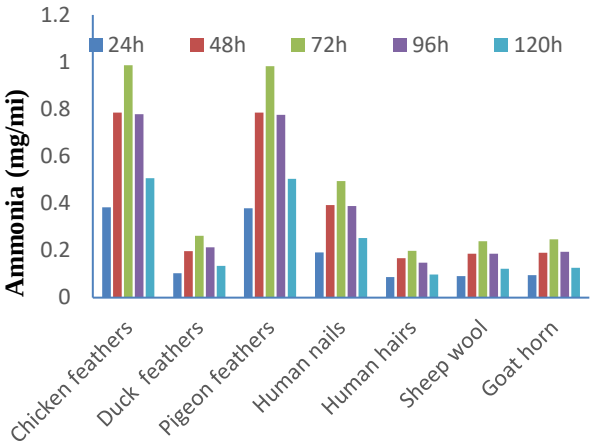

Fig. 6: Ammonia content released on hydrolysis of different keratinous substrates by *Bacillus licheniformis.*

References

1. Brandelli, A., Sala, L., Kalil, SJ., 2015. "Microbial enzymes for bioconversion of poultry waste into added-value products". Food Research International, 73, January, pp. 3-12.
2. Gupta, R., Sharma, R., Beg, QK., 2012. "Revisiting microbial keratinases: next generation proteases for sustainable biotechnology". Critical Reviews in Biotechnology 30, April, pp. 1-13.
3. Tiwary, E., Gupta, R.. 2010. "Medium optimization for a novel 58 kDa dimeric keratinase from *Bacillus licheniformis* ER-15: biochemical characterization and application in feather degradation and dehairing of hides". Bioresource Technology, 101, March, pp. 6013-6110.
4. Verma, A., Singh, H., Anwar, S., Chattopadhyay, A., Tiwary, KK., Kaur, S., Dhillon, GS., 2016. "Microbial keratinase: industrial enzymes with waste management potential". Critical Reviews in Biotechnology, 2, June, pp. 1-16.
5. Lowry, OH., Rosebrough, NJ., Farr, AL., Randall, RJ., 1951. "Protein measurement with the Folin phenol reagent". Journal of Biological Chemistry, 193, pp. 265-275.
6. Moore, S., Spackman, DH., Stein, WH., 1958. "Chromatography of amino acids on sulfonated polystyrene resins an improved system". Analytical Chemistry, 30, pp. 1185-1190.
7. Goswami, D., Dhandhukia, P., Patel, P., Thakker, JN., 2014. "Screening of PGPR from saline desert of kutch: growth promotion in Arachis hypogea by *Bacillus licheniformis* A2". Microbiological Research, 169, pp. 66-75.
8. Ellman, GL., 1959. "Tissue sulfhydryl groups". Archives of Biochemistry and Biophysics, 82, pp. 70-77.

Proceedings of International Conference on Sustainable Energy and Environmental Challenges (3rd SEEC), December 18-21, 2018, IIT Roorkee, India

SEEC No. 137

EFFECTIVENESS OF CATALYTIC CONVERTER IN REDUCING REGULATED EMISSIONS FROM METHANOL FUELLED MEDIUM DUTY SPARK-IGNITION TRANSPORTATION ENGINE

Sagar Srivastava
Department of Mechanical Engineering
Indian Institute of Technology, Kanpur
Email: srivsaga@iitk.ac.in

Avinash Kumar Agarwal
Department of Mechanical Engineering
Indian Institute of Technology, Kanpur
Email: akag@iitk.ac.in

ABSTRACT

Methanol has emerged as one of the most promising alternative fuel for internal combustion engines. Methanol has cleaner emission spectra and leads to lesser emission of pollutants than conventional fuels. These emissions that are harmful, degrading and poisonous to the environment include oxides of carbon (CO, CO_2), nitrogen (NO_x) and sulphur (SO_x). Therefore, methods to decrease the harmful emissions from the methanol-fuelled engines were investigated. For this purpose, catalytic converter is used, and its performance is evaluated in this study. Four typical methanol-gasoline blends, namely- M10, M20, M50 and M85 (M10 represents a blend with 10% v/v methanol and 90% v/v gasoline, and similarly for M20 and others) and G100 (pure gasoline) were used to fuel a medium duty spark ignition (SI) transport engine equipped with a catalytic converter. The effectiveness of the catalytic converter in reducing the regulated emissions of CO, CO_2, NO_x and UHC (Unburnt Hydrocarbons) from the engine was then investigated.

Keywords:

Spark ignition engine, Methanol gasoline blend, Catalytic converter, Alternative fuels, Regulated emissions.

INTRODUCTION

There is an increasing global concern regarding the use of conventional and non-renewable fossil fuels majorly gasoline and diesel. This is attributed to the ever-growing rate of depletion of their limited worldwide reserves, their extensive demand and the use leading ultimately to the environmental degradation and increased fuel prices coupled with an unequal rise in production. Combustion of conventional fossil fuels leads to the emission of various hazardous pollutants such as oxides of nitrogen and sulphur, carbon monoxide, carbon dioxide and often small amounts of lead and phosphorous. These pollutants increase the level of toxicity and global warming in the atmosphere due to their poisonous nature and greenhouse properties respectively [[1],[2]]. There are limited reserves of fossil fuels in the world and these take millions of years to get renewed. The fast depletion of limited reserves of fossil fuels and environmental degradation caused by their use has motivated the scientists to explore alternative fuels.

Feasible and economic renewability and emissions cleaner than their conventional counterparts are the most desirable properties to be sought after in the ideal alternative fuel. The term 'biofuels' is coined for the category of alternative fuels which are produced from renewable biomass resources viz. plants, animals and organic waste and includes biodiesel, vegetable oils (particularly non-edible ones) and primary alcohols [3]. Due to lower torque generation and lower range (much as half) by 100% pure biofuels, they are instead added to gasoline (or diesel) in optimum proportions, and the resulting blends are then used in the engines.

In primary alcohols, methanol is one of the most promising substitutes to be developed as a potential alternative fuel in the SI engines due to its certain properties that are superior to conventional gasoline (Table 1) [[3],[4]]. Because of its higher octane number, the engine can be operated at a greater compression ratio. As compared to gasoline, its higher oxygen content (50%

w/w), lower boiling point and greater flame propagation speed all help in the complete combustion of the fuel and reduce air pollution. Yunju et al. showed that with the increase of the methanol proportion in gasoline, the CO emission decreases by 25% for M85, and the low methanol ratio fuel blends have no significant effect on reducing the NO_x emission while M85 gives an 80% reduction [5].

Table 1. Properties of Methanol and Gasoline

	Methanol	Gasoline
Molecular formula	CH_3OH	C_7H_{16}
Oxygen content (% w/w)	50	0
Molecular weight (g/mole)	32.04	100.2
Density (g/cm^3)	0.792	0.737
Boiling point (normal) (^{o}C)	64	38-204
LHV (MJ/kg)	19.99	43.47
Octane number	111	> 90

Regulated emissions of CO, CO_2, NO_x and UHC are further reduced by use of catalytic converters, which are employed to oxidize CO into CO_2, UHC into CO_2 and water and reduction of NO_x into N_2, which are relatively much less harmful. Krishna et al. [6] examined performance and emission from a single cylinder engine, copper-coated at the inside surface of the cylinder head, fuelled with M20 blend and fitted with a catalytic converter. For CO and UHC, they reported a 20% decrease with the copper-coated engine against the conventional engine. A 40% decrease with copper-coated and installed catalytic converter with no air injection and 60% decrease with copper-coated and installed catalytic converter with air injection was also reported.

In the present study, four different methanol-gasoline blends- M10, M20, M50 and M85 (the number after 'M' indicates the % v/v of methanol in the mixture) and pure gasoline are used to fire a medium duty SI transport engine, equipped with a catalytic converter. The effectiveness of catalytic converter in reducing regulated emission (CO, CO_2, NO_x, UHC) from the engine is studied.

EXPERIMENTAL SETUP

In this study, the experiments were carried out on a four-cylinder, four-stroke, water-cooled, multipoint-port-fuel-injection medium duty SI transport engine (Zen, by Maruti Suzuki). The detailed specifications of the research engine are listed in Table 2. No modifications were made in the original engine for this experiment.

Table 2. Specification of the test engine

Characteristics	Specifications
Model	Maruti Suzuki Zen
Displacement volume	0.993 L
Number of cylinders	Four
Bore/stroke	72/61 mm
Rated torque	66 Nm @ 4500 rpm
Rated power	40 PS @ 6500 rpm
Compression ratio	8.8:1

The engine was coupled with an eddy current dynamometer (ECB50, Dynalec Controls) to regulate its speed and power. The dynamometer controller module in the dynamometer is used to achieve the desired load/speed of the engine. For this experiment, the speed of the engine was fixed at 2000 rpm, and a load of 50 Nm was applied on the engine. Schematics of the experimental setup is shown in Figure 1.

Four different types of methanol-gasoline blends- M10, M20, M50 and M85 and (G100) pure gasoline were used as fuel. These blends are prepared by simple mixing of methanol-gasoline in desired proportions by volume and stirring thoroughly using an electric stirrer.

A catalytic converter was fitted in the exhaust pipe of the engine, which consists of an active catalytic material (namely Palladium (Pd) or Platinum (Pt) and Ruthenium (Ru) or Rhodium (Rh)) in a metal casing which directs the exhaust gas through the catalyst bed. In this process, CO and UHC (Unburnt hydrocarbons) are oxidized by Pd/Pt and NO_x is reduced by Ru/Rh [7].

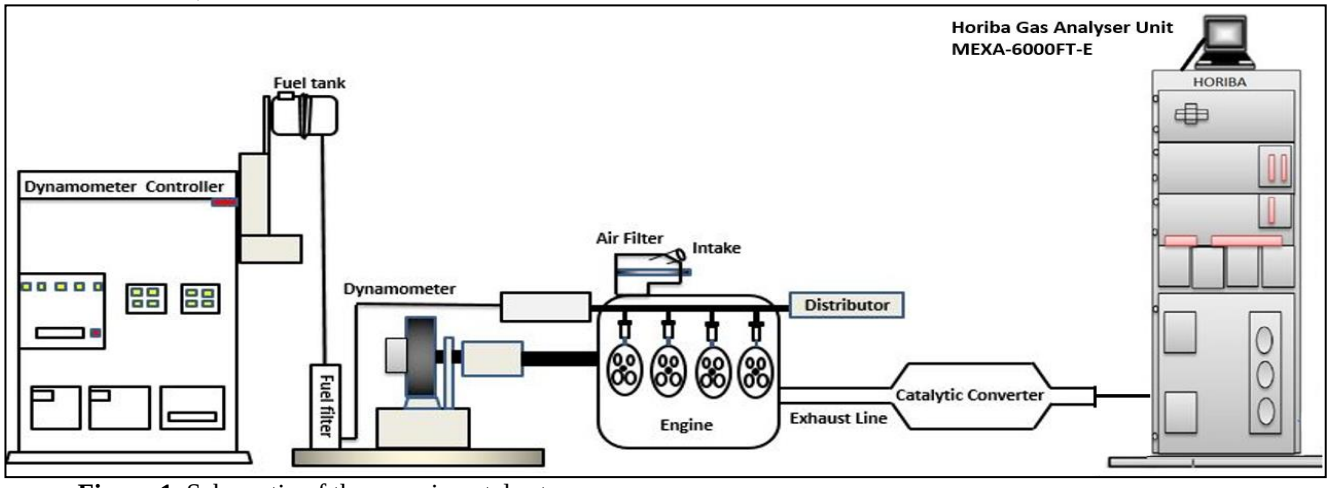

Figure 1. Schematic of the experimental setup

Regulated emissions of CO, CO_2, NO_x and UHC were measured using the Horiba Exhaust Gas Analyser (model MEXA-6000FT-E) for different cases corresponding to different configurations of the converter.

In case-A, the regulated emissions were measured without the treatment of the exhaust gases in the catalytic converter for all the test fuels. This served as a baseline for comparison with case-B, in which the measurements were recorded after the treatment of the exhaust gases in the converter. Thus, this study essentially examines the performance of the catalytic converter in reducing the regulated emissions from a methanol-fuelled SI medium duty transport engine. The effect of introducing methanol into the engine on the regulated emissions is also assessed via its comparison with the baseline gasoline.

RESULTS AND DISCUSSION

The species concentration is plotted against the methanol proportion in the test fuel for each of the species CO, CO_2, NO_x and UHC for cases A and B, namely with and without the catalytic converter respectively.

The effectiveness of the catalytic converter in reducing the regulated emissions is then discussed based on the plots obtained.

REFERENCES

[1] Kampa, M. and Castanas, E., 2008. "Human health effects of air pollution". Environmental pollution, 151(2), pp.362-367.

[2] Mitchell, J.F., 1989. "The "greenhouse" effect and climate change". Reviews of Geophysics, 27(1), pp.115-139.

[3] Agarwal, A.K., 2007. "Biofuels (alcohols and biodiesel) applications as fuels for internal combustion engines". Progress in energy and combustion science, 33(3), pp.233-271.

[4] Elfasakhany, A., 2015. "Investigations on the effects of ethanol–methanol–gasoline blends in a spark-ignition engine: performance and emissions analysis." Engineering Science and Technology, an International Journal, 18(4), pp.713-719.

[5] Yanju, W., Shenghua, L., Hongsong, L., Rui, Y., Jie, L. and Ying, W., 2008. "Effects of methanol/gasoline blends on a spark ignition engine performance and emissions". Energy & Fuels, 22(2), pp.1254-1259.

[6] Krishna, M.V.S. and Kishor, K., 2008. "Performance of copper coated spark ignition engine with methanol-blended gasoline with catalytic converter". Journal of Scientific & Industrial Research, 67, pp.543-548.

[7] Heywood, J.B., 1988. "Internal combustion engine fundamentals". McGraw-Hill Education (India) Private Ltd. Chap.11, pp.649

Proceedings of the International Conference on Sustainable Energy and Environmental Challenges (3rd SEEC)
18 – 21 December, 2018, Roorkee, India

SEEC No. 138

DEVELOPMENT OF A FOUR-CYLINDER DI-METHYL-ETHER FUELLED DIRECT INJECTION HEAVY-DUTY COMPRESSION IGNITION ENGINE

Prashumn
Engine Research Laboratory
Department of Mechanical Engineering
Indian Institute of Technology Kanpur
Kanpur-208016, India
Email: prashumn@iitk.ac.in

Avinash Kumar Agarwal
Engine Research Laboratory
Department of Mechanical Engineering
Indian Institute of Technology Kanpur
Kanpur-208016, India
Email: akag@iitk.ac.in

ABSTRACT
There has been a concern over the emissions from the engines, particularly heavy-duty vehicle engines. With more stringent norms being set up by the different pollution control authorities, there is an urgent need to come up with a solution to reduce the emissions. There has been a significant development in the fuel injection strategies to reduce the emissions in case of compression ignition (CI) engines. Even after the implementation of these strategies, there is still a limit on the amount of reduction that can be achieved. Hence, the use of alternative fuels, particularly the oxygenated fuels is being pushed, so that the Hydrocarbon (HC) and Carbon Monoxide (CO) emissions get significantly reduced. While alcohol-based fuels such as methanol and ethanol have been used in the spark ignition engines, there have been challenges in using these fuels in conventional CI engines due to their poor auto-ignition properties. Ether based fuels, particularly Di-methyl ether, has higher cetane number and hence is a better CI engine fuel. On the other hand, DME has poor lubricative properties and hence in the longer use, it may cause the wear of fuel injection system components. Also, due to its lower viscosity, there are leakage issues that need to be addressed. DME has not been found to be corrosive to the metals, unlike methanol, and hence no major material compatibility issues have to be looked upon. In this paper, the different aspects of DME as a transport fuel will be discussed and solutions to various challenges associated with its implementation in a heavy-duty vehicle engine will be developed. Finally, an experimental setup will be built to test a 4 cylinder, 4-stroke, heavy duty vehicle engine fueled with DME and the performance, combustion and emission analysis of the engine would be done.

Keywords: Compression Ignition, Di-Methyl-Ether, alternative fuel, Soot

INTRODUCTION
It is urgently required to develop the technology to reduce the vehicular emissions in the existing engines without degrading the performance, which does not require major structural changes to the engine. Most of the heavy duty-vehicles are fueled with diesel and the significant depletion in the fossil fuels leads to the questioning of sustainability of these resources. Introduction of cleaner and environment friendly alternative fuels is one of the solutions. DME is a one of best alternative fuel for CI engine.
DME is produced by dehydration of methanol and can be easily produced from coal, biomass, municipal solid waste etc. A brief comparison of the properties of DME and diesel is given in table 1. Due to higher hydrogen to carbon ratio, no connected carbon and presence of oxygen, DME burns cleaner than the conventional diesel fuel. Also, due to lesser soot emissions, strategies like exhaust gas recirculation (EGR) can be used to control the emissions of oxides of nitrogen (NOx).

Due to its higher cetane number (higher than diesel), DME acts as an excellent CI engine fuel. Various studies have

been carried out on common rail direct injection (CRDI) engines fueled with DME. However, in this study we intend to develop a CI engine running on DME where the fuel is injected directly in the cylinder using a conventional mechanical injector and a rotary type mechanical fuel pump. At the room temperature and atmospheric pressure, DME exists as a gas and in order to inject it directly into the cylinder, we need to pressurize the fuel lines. Also, the fuel lines need to be sealed properly in order to prevent leakage. Although metals are resistant to corrosion from DME, but many polymers get deteriorated in presence of DME. Polytetrafluoroethylene (PTFE) does not react with DME and hence can be used to seal the fuel lines.

Property	**Diesel**	**DME**
Oxygen content (mass %)	0	34.8%
Critical temperature (K)	708	400
Liquid density (kg/m^3)	831	667
Cetane number	40-50	>55
Auto-ignition temperature (K)	508	523
Stoichiometric air fuel ratio	14.6	9
Vapor pressure (kPa)	<10	530
Lower heating value (MJ/kg)	42.5	27.6

TABLE 1: Comparison of properties between DME and diesel

Since calorific value of DME is significantly lower than that of diesel, we need to inject higher quantity of fuel. Unlike solenoid based electronic injections systems, where the injection quantity can be controlled by changing the injector open duration through engine control unit (ECU), we need to change the injector nozzle hole diameter and the injector opening pressure. The injector opening pressure can be adjusted by adjusting the spacers above the spring cap.

With the adjustments made in the nozzle hole size and the injector opening pressure, we need to carry out the investigations on the spray behavior at both macroscopic and microscopic scales. Some of the literature available on the spray investigations has suggested that DME atomizes more readily than diesel even at lower injector opening pressures. A typical macroscopic spray image is shown in figure 1.

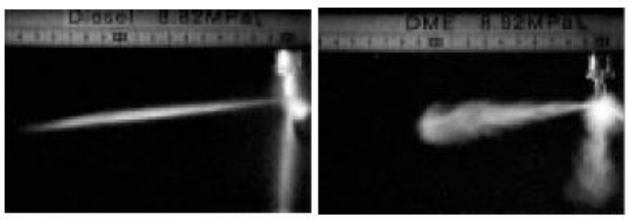

FIGURE 1: Spray images for (a) Diesel and (b) DME with nozzle opening pressure set at 8.82 MPa

EXPERIMENTAL SETUP

To perform the experiments, we will be using a four stroke, four cylinder, naturally aspirated direct diesel injection, water cooled, wet sump lubricated Mahindra LoadKing engine, coupled with an eddy current dynamometer (ECB 200, Dynalec Controls) with load and speed control facility. The detailed specifications of the engine are provided in table 2.

Displaced volume	652cc/cylinder
Stroke/Bore	94/94 mm
Connecting Rod Length	158 mm
Compression Ratio	17.5:1
Number of Valves	2/cylinder
Exhaust Valve Open	56^o BBDC
Exhaust Valve Close	5^{o}ATDC
Inlet Valve Open	10^o BTDC
Inlet Valve Close	18^o ABDC

TABLE 2: Specifications of the engine used

To analyze the real-time in-cylinder combustion data, we will be using Hi-Techniques data acquisition system (meDAQ), with an in cylinder piezo-electric pressure transducer (6013C, KISTLER) coupled to an amplifying unit (5015A00X0, KISTLER) to measure the real time pressures during combustion. A rotary type shaft encoder will be mounted to the crankshaft to record the angular position of the crankshaft. The engine emissions will be analyzed using raw exhaust gas emission analyzer (EXSA-1500, Horiba) which measures the regulated emissions. A detailed schematic for the data acquisition is shown in figure 2.

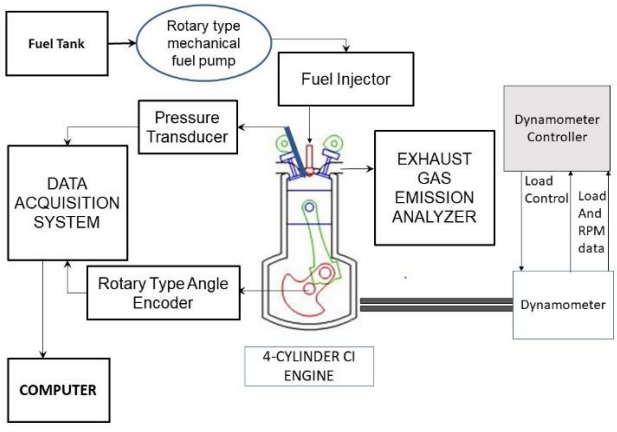

FIGURE 2: Schematic of experimental setup for data acquisition for 4-cylinder CI engine

With the changes done in the fuel injection system, we will need to carry out the macroscopic and microscopic spray investigations at different injector opening pressures for DME. The schematic diagram for the experimental setup for microscopic spray injection studies is shown in figure 3.

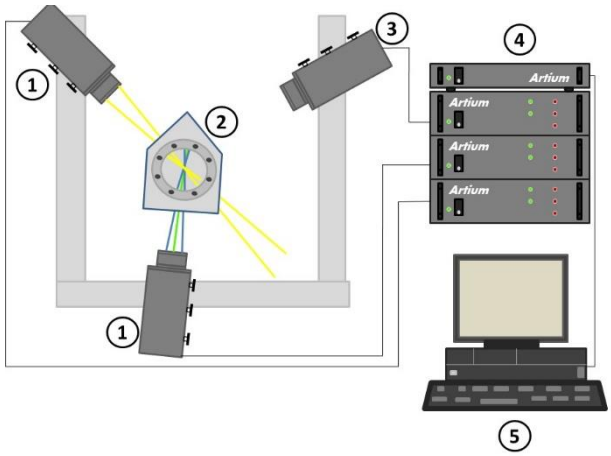

1- Laser beam emitting unit, 2- Constant volume spray chamber, 3- Laser beam receiver, 4- Power box and ASA signal Processor, 5- Computer

FIGURE 3: Schematic of the experimental setup for microscopic spray investigations

As described above, DME exists as a gas at the room temperature and pressure. Hence, we need to pressurize DME fuel supply system in order to ensure that DME reaches the injector in liquid form. Therefore, the fuel tank containing DME will be pressurized up to 10 bar using nitrogen gas cylinder. In order to ensure that the fuel line never develops the issue of vapor locking, an additional pneumatic pump (MSF-22, MAXIMATOR) will be installed after the fuel tank which will pressurize the liquid fuel further to 40 bars. A schematic of the fuel supply system is shown in figure 4.

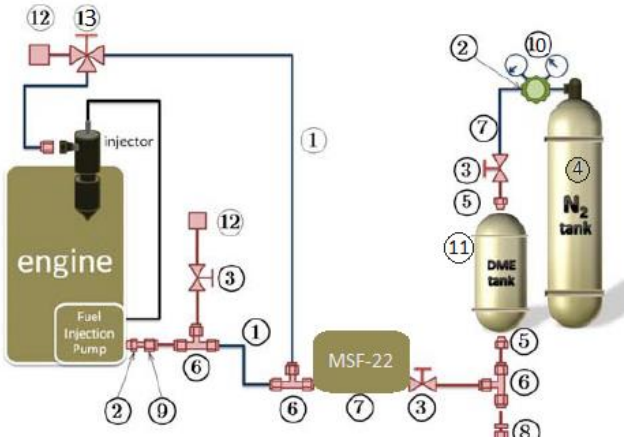

1- High pressure fuel line, 2- Male connector, 3- Ball valve, 4- Nitrogen tank, 5- Tube adapter, 6- Union T- tube, 7- Pneumatic fuel pump, 8- Reducer, 9- Parallel threads male connector, 10- Pressure regulator, 11- DME Tank, 12- Cap tube, 13- 3-way ball valve,

FIGURE 4: Schematic of the experimental setup for fuel supply system

CONCLUSION

The literature available has suggested that there is a significant reduction in the emissions for a conventional CI engine fueled on DME. The experiments will be performed on a 4-cylinder, diesel fueled, heavy duty CI engine which uses a mechanical fuel injection system. The objective of the study is to develop a 4-stroke, four-cylinder, CI engine on 100% DME using direct injection mechanical injection systems. As a part of this study, a retro-fit kit would also be developed to convert the diesel fueled engine to DME fueled engine.

Finally, the study aims to prove the feasibility of DME to replace conventional fossil fuel (gasoline) for existing heavy-duty vehicles, achieving substantially lower emissions (CO, NOx and HC) without any compromise with the power or torque output.

REFERENCES

[1] Wattanavichien K. Implementation of DME in a small direct injection diesel engine. Journal of Renewable Energy and Smart Grid Technology. 2009 Jul;4(2):1-2.

[2] Park SH, Cha J, Lee CS. Reduction of the pollutant emissions from a diesel engine by the application of dimethyl ether (DME) and the control of the intake oxygen flow rate. Energy & Fuels. 2012 Apr 25;26(5):3024-33.

[3] Alam M, Kajitani S. DME as an alternative fuel for direct injection diesel engine. In4th International Conference on Mechanical Engineering, December26-28 2001 Dec 26.

[4] Goto, S., Oguma, M., and Suzuki, S., "Research and Development of a Medium Duty DME Truck," SAE Technical Paper 2005-01-2194, 2005, https://doi.org/10.4271/2005-01-2194.

[5] Hansen, K., Nielsen, L., Hansen, J., Mikkelsen, S. et al., "Demonstration of a DME (Dimethyl Ether) Fuelled City Bus," SAE Technical Paper 2000-01-2005, 2000, https://doi.org/10.4271/2000-01-2005.

[6] Bang, S., Ryu, B., and Lee, C., "An Experimental Investigation on the Spray Characteristics of DME Blended Biodiesel," SAE Technical Paper 2007-01-3631, 2007, https://doi.org/10.4271/2007-01-3631.

[7] Longbao Z, Hewu W, Deming J, Zuohua H. Study of performance and combustion characteristics of a DME-fueled light-duty direct-injection diesel engine. SAE Technical Paper; 1999 Oct 25.

Proceedings of International Conference on Sustainable Energy and Environmental Challenges (3rd SEEC), December 18-21, 2018, IIT Roorkee, India

SEEC No. 139

COMPARITIVE ANALYSIS OF PERFORMANCE, REGULATED AND UNREGULATED EMISSIONS FOR DIFFERENT METHANOL-GASOLINE BLENDS IN A SINGLE CYLINDER TWO-WHEELER MPFI ENGINE

Tushar Agarwal
Engine Research Laboratory
Department of Mechanical Engineering
Indian Institute of Technology Kanpur
Kanpur-208016, India
Email: tushara@iitk.ac.in

Avinash Kumar Agarwal
Engine Research Laboratory
Department of Mechanical Engineering
Indian Institute of Technology Kanpur
Kanpur-208016, India
Email: akhips@iitk.ac.in

ABSTRACT

Vehicular emissions are a major concern in today's world. With the Paris Climate agreement, other Government initiatives and more stringent norms set by Pollution Control Board. It is the need of the hour to find a suitable solution to reduce the vehicular emissions, provide a cleaner environment and a sustainable future for automotive industries. In order to meet such stringent pollution control norms, more and more efforts are required to develop alternatives to conventional fossil fuels. Amongst the alternative fuels, alcohol based fuels (methanol and ethanol) and hydrogen have been the most attractive ones. Methanol is really lucrative to be accepted as an automotive fuel. It has higher research octane number, thus providing higher thermal efficiency and a significant reduction in NOx and CO emissions as compared to simple gasoline fueled engine. On the other hand, very high latent heat of vaporization, corrosive nature and increased formaldehyde emissions are some of the major concerns to be taken care of, before incorporating it as a viable alternative. Many of these shortcomings of methanol can be dealt with blending it with gasoline. Blending about 15% v/v methanol with gasoline has shown to bring down the CO emissions by 65% and unregulated emissions too were reduced. In this study various methanol-gasoline fuel blends like 0% v/v, 15% v/v, 30% v/v, 45% v/v, 60% v/v, 75% v/v and 85%v/v have been investigated for the performance and regulated & unregulated emissions of Royal Enfield 500 CC motorcycle. All the experiments have been performed at engine idling at a constant engine speed of 1100 rpm. The idling fuel maps of ECU have been calibrated to achieve the stoichiometric air-fuel ratio. All other engine physical parameters have been kept same.

This study gave a significant insight into the methanol performance in existing engines and help us to get to know the maximum methanol replacement which is possible in existing engines without deteriorating the performance of engine.

Keywords: Methanol, Gasohols, Fuel maps, ECU, Emissions

INTRODUCTION

Due to environmental concerns, stricter pollution norms and increased global warming, efforts are being made in finding out cleaner and more environment friendly fuels, which can provide better fuel efficiency, while at the same time does not require much structural changes within the engine. Conventional fossil fuel like gasoline is increasingly used for powering light-duty vehicles. The exponentially depleting fossil fuel resources are constantly questioning the sustainability of conventional fossil fuels and their continuation to remain a primary source of energy for automotive industry. Moreover, the pollution control norms related to carbon monoxide (CO), hydrocarbon (HC), oxides of sulphur (SOx) and oxides of nitrogen (NOx) emissions are being revised and made stricter in

quick successions, eventually resulting in higher processing cost for fuels, installation of expensive catalytic convertors or particulate filters in the exhaust system to meet the pollution norms. Introducing cleaner and environment friendly alternative fuel is one of the key solutions. Alcohol based fuels, like methanol & ethanol, hydrogen fuel cells and electric powered vehicles are some of the alternatives that have caught the eye of researchers in recent times.

Methanol can be produced from coal, biomass, biogas etc. It has higher hydrogen-to-carbon ratio and higher research octane number resulting in reduction in HC emissions and better fuel efficiency as compared to gasoline. Nearly all the regulated pollutants like NOx, SOx, CO were substantially reduced for methanol-gasoline blend as compared to conventional automotive fuel.

Multi- port fuel injection requires minimum changes in the engine and no modification of the cylinder head is required. As compared to the direct injection, low pressure fuel pumps and fuel injectors are required in case of MPFI and there is less complexity involved compared to the DI. As the fuel and air are better mixed, the partially rich zones are reduced, hence there is more reduction in NOx formation as compared to DI. However, the higher latent heat of vaporization poses a challenge during the cold start of the engine because the pre-ignition temperatures are reduced due to higher latent heat of vaporization. Also the evaporation of the fuel will be limited due to the high latent heat of vaporization, and hence the cold starting of the engine is a trouble, but blending methanol with gasoline helped to overcome these shortcomings. Initially gasoline was vaporized and start initial ignition and then this in turn aided methanol combustion.

In this study, experimental setup is made for a single cylinder, four stroke, spark ignition engine using various methanol-gasoline fuel blends in port fuel injection. All the experiments have been performed at idling condition at constant engine speed of 1100 rpm. The base fuel maps of various blends were generated and the parameters such as spark timing and injection timing were modified using open engine control unit (ECU) in order to achieve the stoichiometric air-fuel ratio for all blends. The appropriate catalytic converters were then applied in order to reduce the NOx and HC emissions. The regulated and unregulated emissions were measured before and after catalytic convertor.

EXPERIMENTAL SETUP

To perform the experiments, Royal Enfield 500 cc Classic 4-stroke, gasoline fuelled spark ignition engine, coupled to a Dynalec eddy-current dynamometer, with load and speed control flexibility was used. Engine and dynamometer were coupled using direct chain-sprocket coupling. The engine was controlled using Performance Electronics PE3 SP000 open-ECU (engine control unit).

To analyze the real-time in-cylinder combustion data, we used AVL combustion analyzer, with current clamps used to tap low-voltage sensor data. This would help us generate pressure-crank angle curve along with spark timing and fuel injection timing, hence providing us with the data required to build base fuel-maps for gasoline. Subsequently the gasoline fuel maps were tweaked to fine-tune the engine parameters optimized for various methanol-gasoline fuel blends. Bosch wide band lambda sensor along with ETAS conditioning unit has been used to closely monitor air-fuel ratio and calibrate the engine for stoichiometric air-fuel ratio.

For second experimental setup the engine was mounted on motorcycle chassis and coupled with OEM catalytic convertor. EXSA – 1500, MEXA 6000FT-E and EEPS-TSI have been used to measure regulated emissions, unregulated emissions and particulate emissions respectively. The engine exhaust emissions are fed into each of the combustion analyzer using appropriate dilution strategy and then the data of each analyzer is fed into the computer to perform competitive study.

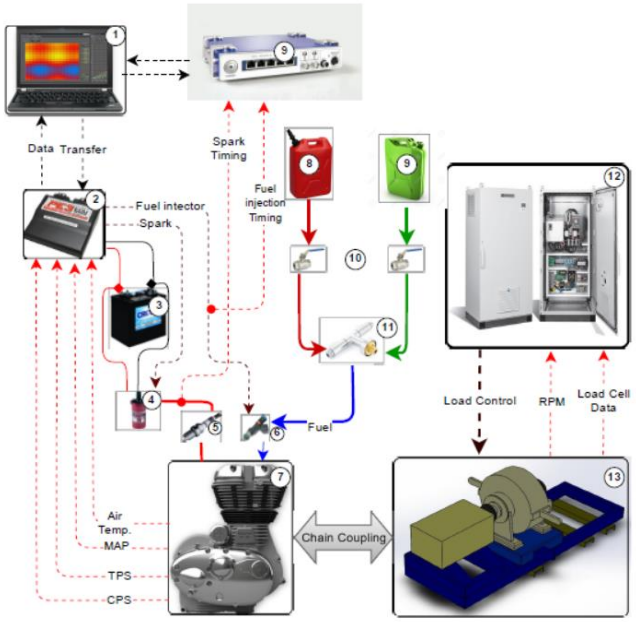

1- Computer interface, 2- Open-ECU, 3- Battery, 4- Ignition Coil, 5- Spark plug, 6- Fuel injector, 7- Test engine, 8- Gasoline fuel tank, 9- Methanol fuel tank, 10- Fuel-line valves, 11- T-joint, 12- Dynamometer controller, 13- Engine-dynamometer setup

FIGURE 1: Schematic of the experimental setup for performance and combustion analysis

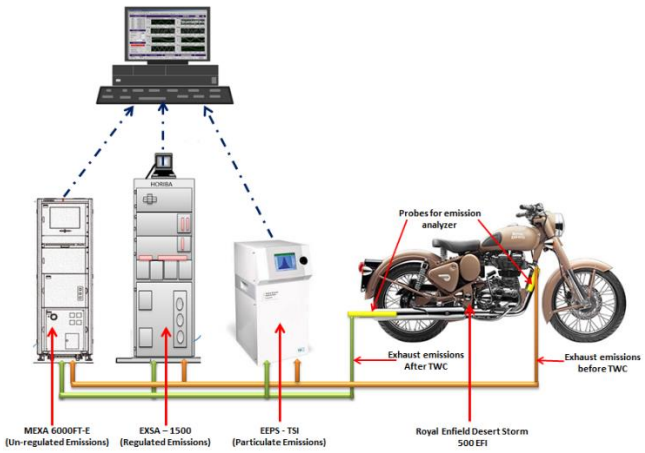

FIGURE 2: Schematic of the experimental setup for regulated and unregulated emission measurement

Results and Discussions

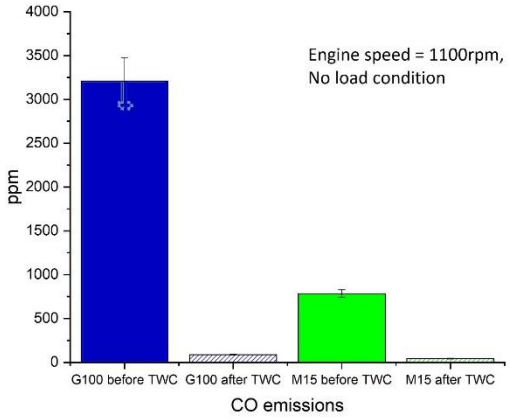

CO emissions were found to be significantly lower in case of M15

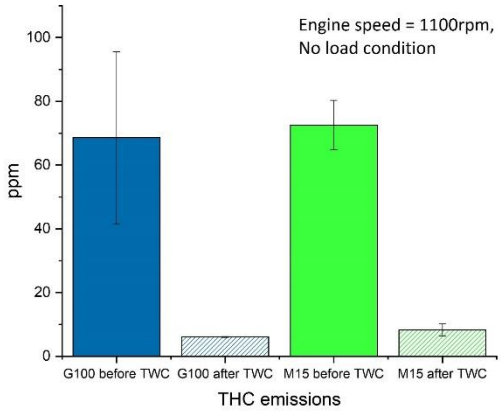

THC emissions in both the fuels were comparable

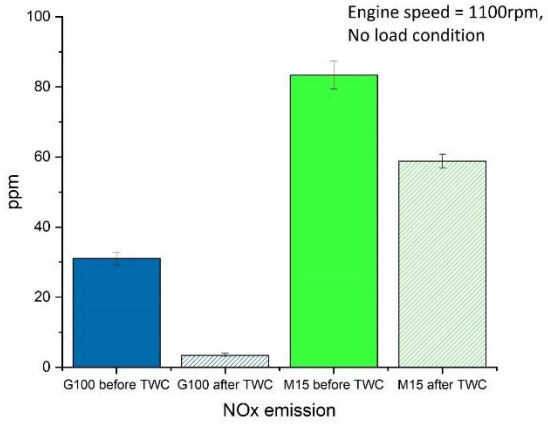

NOx emissions were higher in case of M15, possibly because complete combustion increased the temperatures

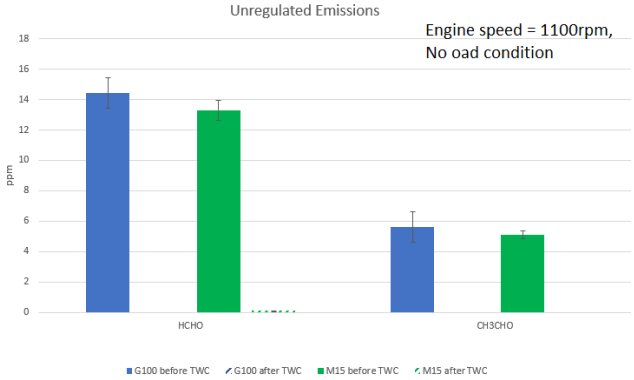

Aldehyde emissions were very low and comparable in both the cases

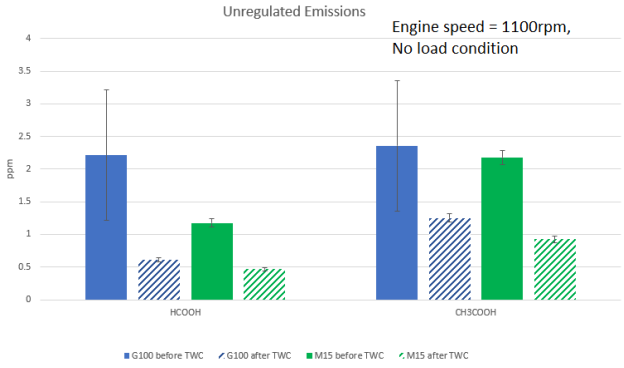

Formic and acetic acid emissions were very low and comparable in both the cases

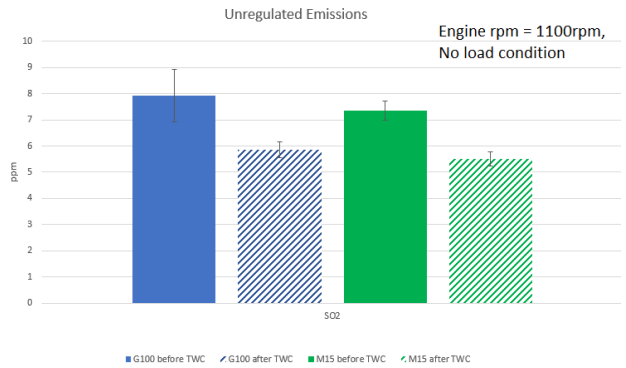

SO_2 emissions were very low and comparable in both the cases

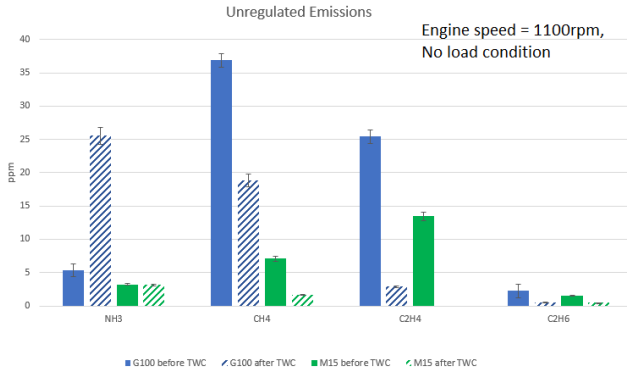

NH_3, CH_4, C_2H_4 and C_2H_6 emissions were very low in both the cases and even lower in case of M15

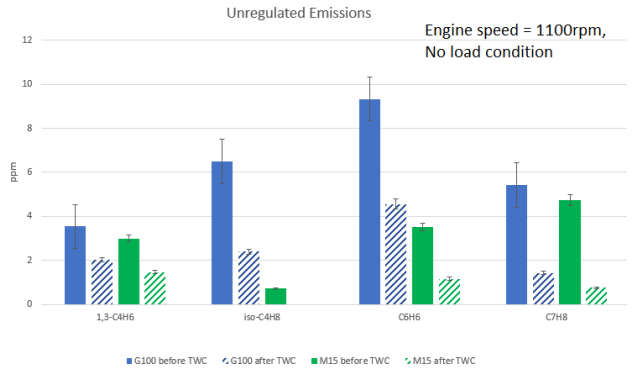

1,3-C_4H_6, iso-C_4H_8, C_6H_6 and C_7H_8 emissions were very low in both the cases and even lower in case of M15

CONCLUSION

- **There was about 65% reduction in CO emissions in case of M15**
- **NOx emissions increased in case of methanol because better combustion resulted in higher in-cylinder temperatures**
- **Formaldehyde emissions from M15 were comparable to those of gasoline**
- **Unregulated emissions in both the cases were generally low and even lower for M15**

REFERENCES

[1] L. Bromberg, D. R. Cohn, 2008. “Effective octane and efficiency advantages of direct injection alcohol engines”, MIT Laboratory for Energy and the Environment Report.

[2] Wyszynski, L., Stone, C., and Kalghatgi, G., 2002, "The Volumetric Efficiency of Direct and Port Injection Gasoline Engines with Different Fuels," SAE Technical Paper 2002-01-0839.

[3] George, S., Schock, H., Gray, C., Hamady, F. et al., 2001, "Design of a High Compression, Direct-Injection, Spark-Ignition, Methanol Fueled Research Engine with an Integral Injector-Ignition Source Insert," SAE Technical Paper 2001-01-3651.

Proceedings of the International Conference on Sustainable Energy and Environmental Challenges (SEEC-2018)
18 – 21, December 2018, IIT Roorkee, India

SEEC No.140

1-D SIMULATION AND MODELLING OF GASOLINE COMPRESSION IGNITION (GCI) ENGINE

Vishnu Singh Solanki
Department of Mechanical Engineering
Indian Institute of Technology Kanpur
Email: vishnus@iitk.ac.in

Avinash Kumar Agarwal
Department of Mechanical Engineering
Indian Institute of Technology Kanpur
Email: akag@iitk.ac.in

ABSTRACT
This research aims to investigate the potential of gasoline compression ignition (GCI) to achieve future engine requirements such as high thermal efficiency with lowering the emissions, such as oxides of nitrogen (NOx) and particulate matter (PM). There is insufficient information available in literature review related to the performance of the GCI engine. Hence, it is difficult to predict the performance of it. Basic route to understanding the behavior of such engine is to create the 1D modeling using GT-POWERv2018. It will help to predict the performance of GCI engine compared to traditional engines. In this study; a 1D model is created to evaluate the performance of the engine at different fuel injection timing. Optimization of injection timing is carried out to achieve the low emission level and high thermal efficiency. Best injection timing is observed at crank angle (CA) 40° before top dead center (BTDC) where, maximum in-cylinder pressure, maximum exhaust gas temperature and better combustion are achieved. But the rate of pressure rise, brake mean effective pressure (BMEP) and brake efficiency are low.

Keywords: 1-D Simulation and Modelling, Low-Temperature Combustion, Gasoline compression ignition, Low NOx and Particulate Emissions, Efficiency improvement.

INTRODUCTION

The highly efficient engine is required to meet the strict emission norms, govern by regulatory bodies. Alternative combustion technology is seen as the plausible route to meet the future engine demand. Advanced combustion technique will serve another important aspect, i.e., preservation of fossil fuel via ensuring lower grade fuel consumption vis-à-vis traditional combustion technology. Furthermore, a combination of advanced engine combustion and after treatment technologies can encounter the present problems related to emissions as well as thermal efficiency.

Considerable research work is going on the engine to improve the performance and emission level of the engine. Compression Ignition (CI) engine is the first choice of any researcher because it has a higher compression ratio and lower pumping losses vis-à-vis Spark Ignition (SI) engine. Hence it has high thermal efficiency. But, CI engine emits higher tail-pipe NOx and PM emission. During the past couple of decades, low-temperature combustion (LTC) is in the center of attraction due to its potential to achieve both, high thermal efficiency and low emissions. GCI is a low-temperature combustion technology, and it can meet BS-VI emission norms with minimal engine modification due to its low fuel injection pressure. Also, this technology reduces the requirement of an exhaust after-treatment system, thus relatively reduces the vehicle cost. This concept is improving the advantage of CI engine via utilizing the traditional fuel of SI engine, i.e., gasoline. But, GCI technology is at the nascent stage of research.

GCI is a low-temperature combustion concept, which uses gasoline, which has a long ignition delay and high volatility. This characteristic can provide more time for mixing so that GCI can achieve low-nitrogen-oxide, low-soot combustion. Furthermore, higher volatility of gasoline is more suitable for premixed combustion as compared to diesel. GCI engine ignites the homogeneous fuel-air mixture at LTC condition without the help of any additional spark energy [5,6]. For the homogeneous fuel-air mixture, fuel is injected early in the compression stroke of the engine cycle. This strategy will provide sufficient time to achieve homogenous fuel-air mixing. However, this strategy also makes it difficult to control the combustion process as the engine load increases.

There is too much of excessive gasoline production in refineries worldwide. In the future, there will be an imbalance in demand for diesel and gasoline. This is because of the shifting of marine transformation on diesel due to environmental consideration. Due to this, the demand for diesel is going up, and the demand for gasoline is going down. Moreover, the octane number of gasoline thus produced is lower since it is originating from mostly the residual heavy crude in the oil wells. This has left much of the low octane number gasoline "Homeless," and the current project of developing GCI technology aims to utilize this surplus refining product efficiently. CI engines have a clear efficiency advantage over the SI engines, and their capabilities can be extended by using a broader range of fuels, which will be advantageous. Optimum fuel specifications require less processing and will have a lower greenhouse-gas footprint. GCI provides a path to mitigate global demand imbalance due to the availability of heavier crude and low demand for lighter fuels and would improve the sustainability of refineries in times to come. The RON of optimum fuel for GCI engines is likely to be around 70, and hence the surplus low-octane gasoline could be used. [7,8]

The main aim of this study is to develop a 1-D model of GCI engine and simulate it to investigate the performance, and combustion characterization at the different start of injection (SOI) with constant engine speed.

2. ENGINE MODELING AND DISCUSSION

2.1. THEORETICAL INFORMATION

Geometric and experimental data is used to build the GCI engine model using GT-POWER (version 2018). It is 1D vehicle simulation software; used by industries and academia to simulate vehicle performance. It is different from the code model (non-predictive model), use to predict engine performance such as power, volumetric efficiency, fuel consumption, etc. It is used to optimize the combustion by varying the different parameter such as injection pressure, injection duration, load, speed, and engine geometry. Other than performance analysis, it can predict tailpipe emissions, acoustic characteristics, in-cylinder temperature, and combustion pressure. GT-POWER engine models are easily converted to real-time fast running models using the software in the loop (SiL) and hardware in the loop (HiL). [9]. It is necessary to have previous knowledge of the start of fuel injection timing, the quantity of fuel, injection duration, fuel properties, and engine geometry data to simulate the 1-D model. A comparison of the simulated results and experimental results is necessary to check the correctness of the model. It is done iteratively by adjusting the parameters to get desire simulation results until some level of agreement is obtained.

2.2. ENGINE DESCRIPTION AND OPERATING CONDITIONS

The 1D GT-POWER GCI engine model used in this study as shown in Fig. 1. It is mono-cylinder GCI engine with a compression ratio of 17.70. In this study, gasoline injector is used with specified specification as listed in the Table1. Specification of the engine is shown in Table 2. Reference intake air pressure has taken as 1.1 bar, which is lower than real engine intake air pressure, i.e., 1.4 bar. Because in a real engine, the pressure loss is encountered due to the friction Otherwise, simulation model would give better performance.

Table 1: Geometric specifications of the mono-cylinder GCI engine model

Parameter	Value
Bore [mm]	83.1
Stroke [mm]	92.0
Connecting Rod Length [mm]	145.8
Total Displacement [L]	0.499
Compression Ratio	17.70
Nozzle Hole Diameter [mm]	0.134
Number of Holes per Nozzle	7
Nozzle Discharge Coefficient	0.86
Inlet Valve Closed (IVC) [CA°]	-164
Exhaust Valve Open (EVO) [CA°]	131
Inlet Valve Open (IVO) [CA°]	346
Exhaust Valve Closed (EVC) [CA°]	384

Table 2: Engine operating conditions for GFCI engine

Parameter	Value
RPM	2000
Injection Start CA° (BTDC)	80°, 60°, 40°, 30°
Rate of fuel injection (g/s)	6
Ref. Pressure [bar]	1.100
Ref. Temperature [K]	300

Direct injection Wiebe Combustion model was used in this simulation work of GCI engine. Wiebe curve is anchored to top dead center (TDC) of the engine cycle. Wiebe exponent and anchor angle is the number of crank angle degrees between TDC and 50% combustion point of the Wiebe curve. The duration of combustion is another important parameter. It relates the 10% to 90% combustion duration.

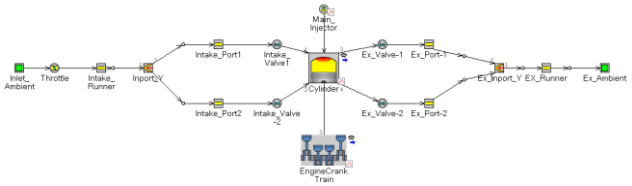

Fig 1: 1D GT-POWER Mono-Cylinder GCI Engine Model

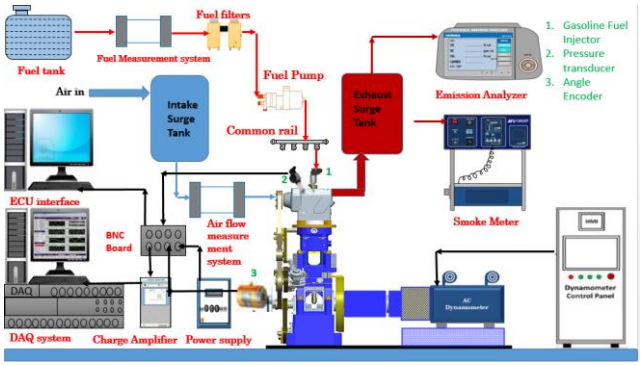

Fig 2: Schematic of the GCI engine experimental setup developed for the next stage of research work

3. RESULTS AND DISCUSSION

3.1 ENGINE COMBUSTION CHARACTERISTICS

In this study, four different injection timing (80°, 60°, 40°, and 30° BTDC) is used. In-cylinder pressure vs. crank angle results is presented in Fig. 3. This result indicates that as we retard the injection timing, the time available for mixing of fuel-air is reduced. The peak pressure value is high in the case of 40° BTDC. But, higher peak pressure in 30° BTDC is noticed for before other injection timing because of high fuel stratification.

Effect of injection timing on the rate of heat transfer is shown in Fig. 4. In SOI 30° BTDC and 40° BTDC, post-combustion takes place. So, the fraction of heat is release after the 25° ATDC.

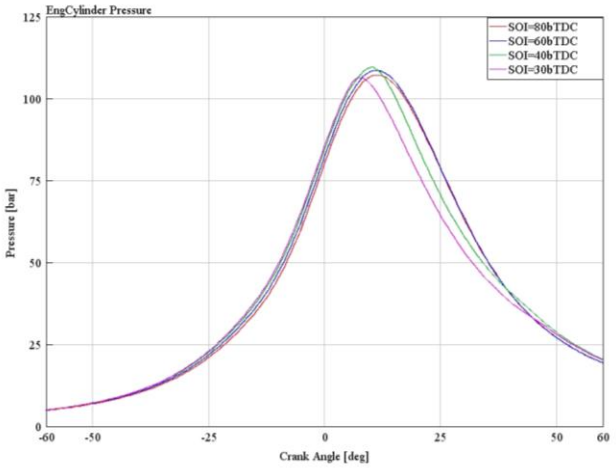

Fig. 3: In-cylinder pressure variation w.r.t. the crank angle at the different injection timing

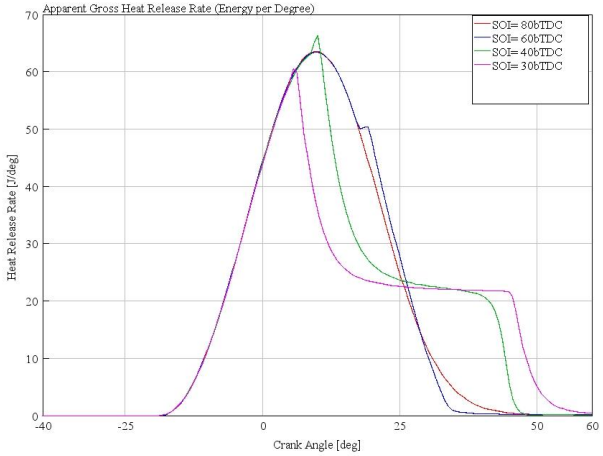

Fig. 4: Heat transfer rate variation w.r.t. the crank angle at the different injection timing

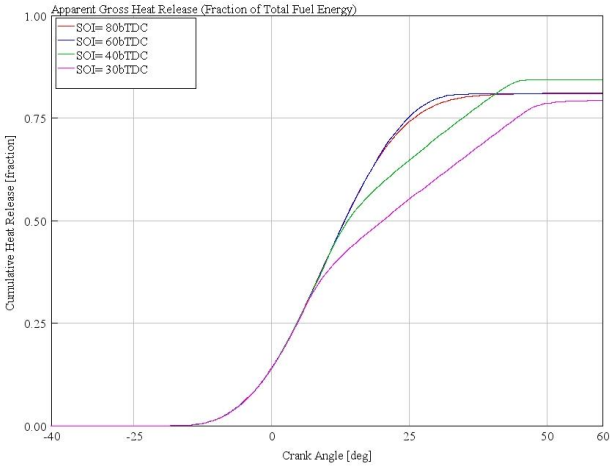

Fig. 5: Variation of the cumulative heat release w.r.t. the crank angle at the different injection timing\

In Fig. 5, a fraction of total energy is presented at different SOI timing. Highest fraction of total energy is obtained in the case of 40° BTDC due to better fuel mixing.

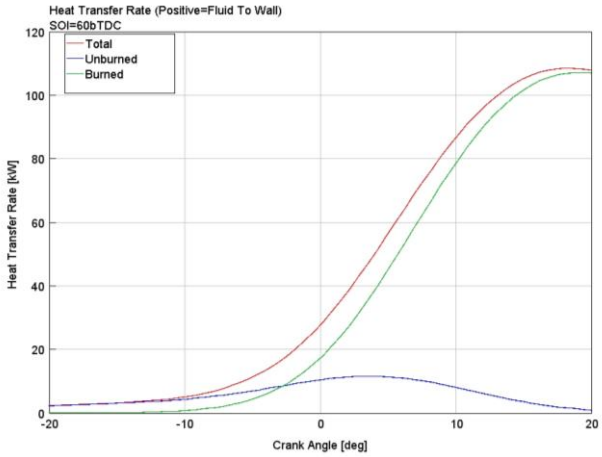

Fig. 6: Fraction of the total, unburned, burned heat transfer rate w.r.t. The crank angle at fixed SOI 60° BTDC.

As shown in figure 6, a large amount of heat is transferred to the burned gases, the only a fraction of heat is supplied to the unburned fuel. Effect of different injection timing on the combustion parameter such as the maximum pressure, the rate of the pressure rise, and exhaust gas temperature is shown in Fig. 7. In the case of 40° BTDC, we are getting maximum pressure and maximum exhaust gas temperature, but the rate of pressure rise is minimum in this case.

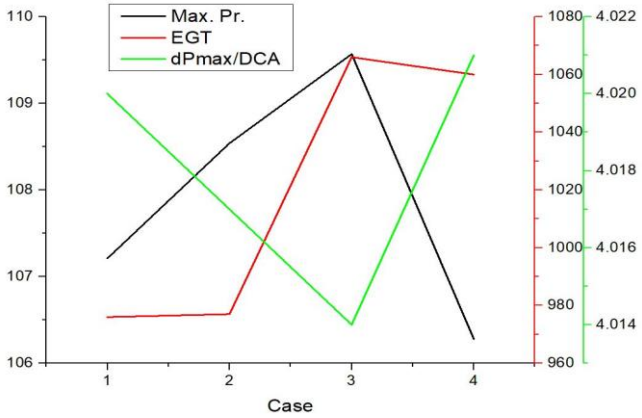

Fig. 7: Effect of injection timing on the maximum pressure, the rate of pressure rise and Exhaust gas temperature.

3.2 ENGINE PERFORMANCE CHARACTERISTICS

As per results as shown in Fig. 8, best efficiency and BMEP are obtained at 80° bTDC but volumetric efficiency at almost same for all the cases.

4. CONCLUSION

It is better to develop GFCI engine technology. It can meet conventional diesel engine efficiency with lower emission. In this study, we found the favorable result regarding the efficiency, BMEP, rate of pressure rise at the 40° BTDC injection timing.

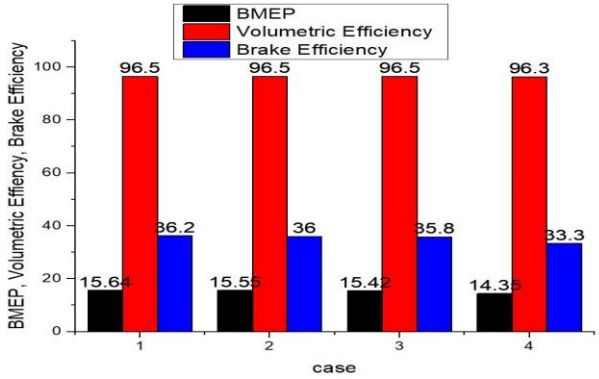

Fig. 8: Variation of BMEP, volumetric efficiency and brake efficiency w.r.t. cases

REFERENCES

[1] Kalghatgi, G., Risberg, P., and Ångström, H., "Advantages of Fuels with High Resistance to Auto-ignition in Late-injection, Low-temperature, Compression Ignition Combustion," SAE Technical Paper 2006-01-3385, 2006,doi:10.4271/2006-01-3385.

[2] Ryan, T (2006): HCCI - Update of progress 2005. 12th Diesel Engine-Efficiency and Emissions Research (DEER) Conference, August 20-24, 2006. Detroit, Michigan, U.S. Department of Energy

[3] Steiger, W. (2006): Future powertrains and fuels for sustainable mobility, Conference on Cost Effective Low Carbon Powertrains for Future Vehicles, 6-7 November 2006. London: IMechE

[4] Farrell, J. and Bunting, B., "Fuel Composition Effects at Constant RON and MON in an HCCI Engine Operated with Negative Valve Overlap," SAE Technical Paper 2006-01-3275, 2006, doi:10.4271/2006-01-3275.

[5] Akihama, K., Takatori, Y., Inagaki, K., Sasaki, S. et al.," Mechanism of the Smokeless Rich Diesel Combustion by Reducing Temperature," SAE Technical Paper 2001-01-0655, 2001, doi:10.4271/2001-01-0655.

[6] Kimura, S., Aoki, O., Ogawa, H., Muranaka, S. et al.," New Combustion Concept for Ultra-Clean and High-Efficiency Small DI Diesel Engines," SAE Technical Paper 1999-01-3681, 1999, doi:10.4271/1999-01-3681.

[7] Kalghatgi G, Gosling C and Wier M-J. The outlook for transport fuels. Part 1. Petrol Technol Q 2016; Q1: 23–31.

[8] Kalghatgi G, Gosling C and Wier M-J. The Outlook for Transport Fuels. Part 2. Petrol Technol Q 2016; Q2: 17–23.

[9] https://www.gtisoft.com/gt-suite-applications/propulsion-systems/gt-power-engine-simulation-software/

Proceedings of the Third International Conference on Sustainable Energy and Environmental Challenges (3rd SEEC)
18 –21 December, 2018, IIT Roorkee, India

SEEC No. 141

EXPERIMENTAL ANALYSIS OF A SMALL-SIZED SOLAR PARABOLIC TROUGH COLLECTOR USING PARABOLIC AND TRIANGULAR SECONDARY REFLCETOR

Alka Bharti
Mechanical Engineering Department
MNNIT Allahabad, Prayagraj-211004, India
Research Scholar
Email: alka31790@gmail.com

Bireswar Paul
Mechanical Engineering Department
MNNIT Allahabad, Prayagraj-211004, India
Assistant Professor
Email: bipaul@mnnit.ac.in

ABSTRACT

In this study, experimental analysis of a small-sized solar parabolic trough collector (PTC) has been done using secondary reflectors. The two types of secondary reflectors, parabolic and triangular were analysed. The experiments were performed with and without secondary reflectors using water as heat transfer fluid at mass flow rate of 0.01 kg/s. The secondary reflectors at the top of the receiver tube can increase the concentration of heat flux at the top surface of the receiver tube and can reduce the circumferential temperature difference at the circumference of the receiver tube. By using the secondary reflectors in parabolic trough collector system, 10.16% and 6.55% improvement in the outlet temperature of heat transfer fluid have been obtained in case of parabolic secondary reflector and triangular secondary reflector respectively in comparison to parabolic trough collector system without secondary reflector.

Keywords*: *Solar parabolic trough collector, Outlet temperature, Thermal efficiency, Secondary reflector.

NOMENCLATURE

m	Mass flow rate (kg/s)
C_p	Specific heat capacity (J/kgK)
T_{in}	Inlet temperature (°C)
T_{out}	Outlet temperature (°C)
η_{th}	Thermal efficiency
Q_a	Energy incident on aperture area of coellctor (W)

INTRODUCTION

A parabolic trough collector is one of the concentrating line focusing solar energy technology. It consists of a parabolic shape trough also known as reflector or collector, a receiver tube (or absorber tube), tracking mechanism, storage tank, circulating pipe and supporting stand. It is a heat exchanging type technology that converts solar energy into thermal energy. The receiver tube is a key component of this technology which is located at the focal line of the parabolic trough. The direct solar radiation that stricks at the aperture area of the collector is reflected towards the bottom surface area of the receiver tube. The receiver tube receives direct solar radiation at the top surface and reflected (concentrated) at the bottom surface area that is subtended by the rim angle of the collector. This heat flux heated the surface of the receiever tube and this heat transfers to the inner surface of the receiever tube by the conduction heat transferring process. A heat transfer fluid circulating through the receiever tube is heated through convection heat transferring process. A hot oil or water, we can observe at the outlet of the receiver tube of an solar parabolic trough collector system. Form a PTC system, steam can be generated directly inside the receiever and indirectly by exchanging heat. In this system, a tracking mechanism is used to track the position of the sun. It can be manual or automatic and in north-south or east-west directions. PTC is usually oriented along the north-south axis and tracking is provided to east-west. East-west orientation requires very little adjustment during the day time. Fig. 1 shows the cross-sectional view of PTC.

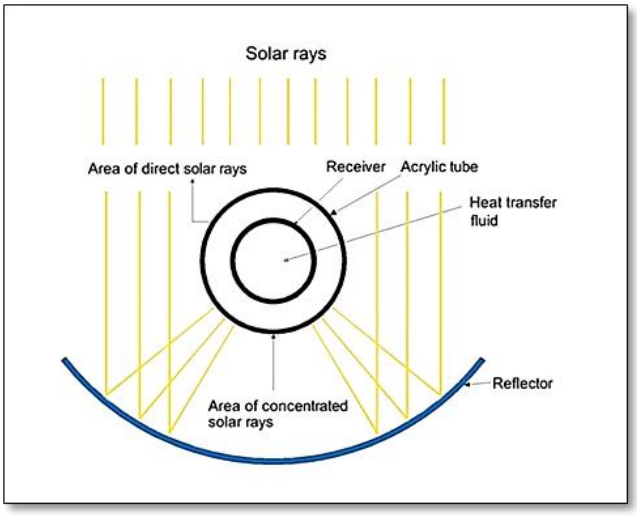

FIGURE 1. CROSS-SECTIONAL VIEW OF SOLAR PARABOLIC TROUGH COLLECTOR

Various studies have been done on solar PTC using water and oil. Valencia et al. [1] conducted experimetnatl study using water as heat transfer fluid. They observed they obtained 47.3°C maximum outlet temperature and 50.57% maximum thermal efficiency. Zou et al. [2] conducted experimental study to evaluate the performance of proposed PTC using water as HTF in cold environment. They have found 67% thermal efficiency of PTC even with solar radiation below 310 W/m^2. Sagade et al. [3] experimentally investigated the performance of prototype parabolic trough which is made of fiberglass-reinforced plastic using water as heat transfer fluid. They concluded that the instantaneous efficiency of the parabolic trough collector increases by 13% and it was 51.67% with receiver tube covered by a glass cover. QiBin et al. [4] conducted experiment and investigate the performance of parabolic trough collector system for solar thermal power generation using synthetic oil as HTF. They found heat loss of 220 W/m for receiver tube with temperature difference of 180°C between atmospheric temperature and collector temperature. Wang et al. [5] numerically analyzed the effects of synthetic oil-based alumina (Al_2O_3) nanofluid on the performance of PTC and compare the performance of PTC using only synthetic oil as HTF. Their results revealed that efficiency of the PTC is higher with nanofluid (Al_2O_3/synthetic oil) than synthetic oil as HTF. Sokhansefat et al. [6] studied about heat transfer enhancement using (Al_2O_3/synthetic oil) nanofluid in PTC. They showed that showed that nanofluid enhances heat transfer better at low operating temperatures. Some researchers have done their study using secondary reflectors in parabolic trough collector. Sundaram and Senthil [7] have done experimetntal study by considering curved and triangular secondary reflectors. They obtained that thermal effieicny improves by 10%. Kun et al. [8] conducted theoretical study of secondary reflectors. They ontained that reduction in circumferential temperature difference on the receiver tube form 25.7 K to 2.3 K. Spirkl et al. [9] numerically optimized different types of secondary reflectors that consist of an involute type inner section with a flat outer section with the tabular tube to boost the concentration level. They observed significant improvement in concentration.

In this study, the effects of secondary reflectors of parabolic and triangular cross-section on the performance of the PTC system have been analysed. The secondary reflectors can minimize the effects of receiver tube misalignment. The receiver tube misalignment is the deviation of the receiver tube center line form the focal line of the collector. The receiver tube misalignment is caused due to various reasons. It can caused due to poor structural design, slope error of reflector, poor installation, tracking error, sagging of the receiver tube due to self weight and weight of the receiver tube and change in the structure due to wind loding and other effects. Due to receiver tube misalignment, the reflected radiations from the collector deviates from its original point that is focal line and goes outside of the receiver tube. These radiations does not take part in the heating of the receiver tube and cause an optical loss. These radiations can be again reflected on the top surface of the receiver tube by using a secondary reflector. In this study, two types of secondary reflectors have been analysed and significant improvements have been obtained.

EXPERIMENTAL SETUP

The experimental set is consists of a collector, a receiver tube, strorage tank, circulating pipe and supporting stand. The supporting frame for collector is made of square cross section stainless steel ribs and the collector (reflector) is made of mirror finished stainless steel sheet, the receiver tube is made of stainless steel and coated with balck paint to increase the absorbtivity. The receiver tube is covered with an acrylic tube to reduce heat losses from the outer surface of the receiver tube. The annulus space between the outer surface of the receiver tube and inner surface of the acrylic tube is filled with air. An storage tank of 300 litres have been used to collect the hot water. The secondary reflector is made of stainless steel and coated with chrome mirror silver vinyl wrap sheet.

EXPERIMENTAL ANALYSIS

The experiments were conducted at Motilal Nehru National Institute of Technology (MNNIT) Allahabad, Prayagraj, Uttar Pradesh, India (25.4358° N, 81.8463° E). The experimetnts were conducted in the month of May, 2018 and using water as heat transfer fluid. The reading were taken from 9 AM to 4 PM. The reading of inlet and outlet temperature of water is measured using a digital thermometer and the solar radiation reading was taken form a weather station isnatlled at the roof top of the

FIGURE 2. EXPERIMENTAL SET-UP WITH SECONDARY REFLECTOR

Mechanical Engineering Department of MNNIT Allahabad. The experimental setup is shown in Fig. 2.

EFFICIENCY CALCULATION

The thermal efficiency of collector is defined as the ratio of the instantaneous useful heat gained by the HTF and the instantaneous direct solar radiation incident (I_d) on the given aperture area (A_a) of the collector (energy incident on aperture area of collector) [10].

$$\eta_{th} = \frac{Q_u}{Q_a} \tag{1}$$

Useful heat gain (Q_u): The amount of heat gained by HTF flowing through the receiver tube.

$$Q_u = m \cdot C_p \cdot (T_{out} - T_{in}) \tag{2}$$

Instantaneous solar beam radiation (I_d) incident on the given aperture area (A_a) of the collector:

$$Q_a = A_a \cdot I_d \tag{3}$$

RESULTS

Fig. 3 shows the variation of global radiation with time for all three conditions that are without secondary reflector (SR), with parabolic SR and with triangular SR. From Fig. 3, it has been observed that the values of global radiation is almost same for without SR and triangular SR condition throughout the day. The value for parabolic SR condition is same to other two conditions from 9 AM to 10:30 AM but after that up to 12 noon the radiation is lower than the other two conditions and from 12 noon to 15:30 PM the radiation for parabolic SR is slightly more than other two conditions. Fig. 4 represents the variation of inlet temperature with time for all three conditions. The small variation in the temperature of water has been observed throughout the day. Fig. 5 shows the variation of outlet temperature with time. It has been observed that the outlet temperature of water for parabolic SR condition is higher than the triangular SR and without SR condition throughout the day due to concentrated radition at the top surface of the receiver tube. The maximum outlet temperature of water is 49.2℃, 47.3℃ and 44.2℃ in case of parabolic SR, triangular SR and without SR cnditions respectively. The outlet temperature increases as the solar radiation increases and observed maximum at 13:30 PM. Though the radiation is maximum at 12:30 PM, the outlet temperature reaches the maximum at 13.30 PM. As the solar radiation will decrease the outlet temperature will not decrease immediately due to high heating capacity of the receiver at that time. Fig. 6 shows the variation of thermal effieicny of collector with time. It can be seen that it is more in case of parabolic SR condition than triangular SR and without SR condition. The triangular SR condition is better than the without SR condition. The Fig. 7 show the variation of circumferntial temeparture of the receiver tube with angle. It can be observed that the circumferential temperature is more uniform in case of parabolic SR condition and triangular SR condition than without SR condition due to concentration of heat flux at the top surface of the receiver tube.

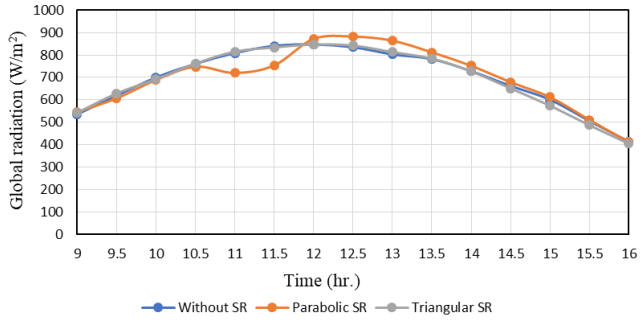

FIGURE 3. VARIATION OF GLOBAL RADIATION WITH TIME

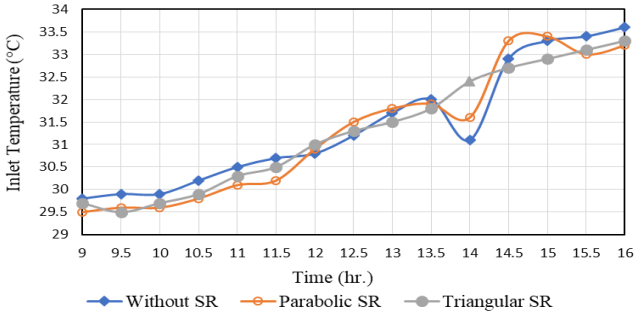

FIGURE 4. VARIATION OF INLET TEMPERATURE WITH TIME

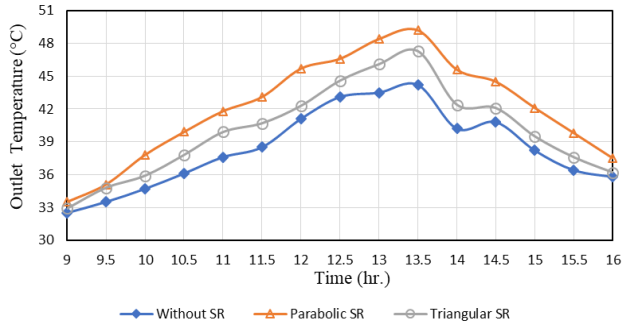

FIGURE 5. VARIATION OF OUTLET TEMPERATURE WITH TIME

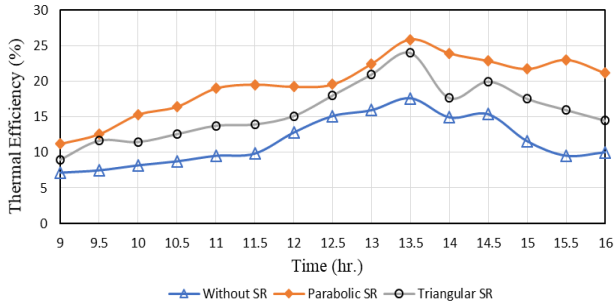

FIGURE 6. VARIATION OF THERMAL EFFICIENCY WITH TIME

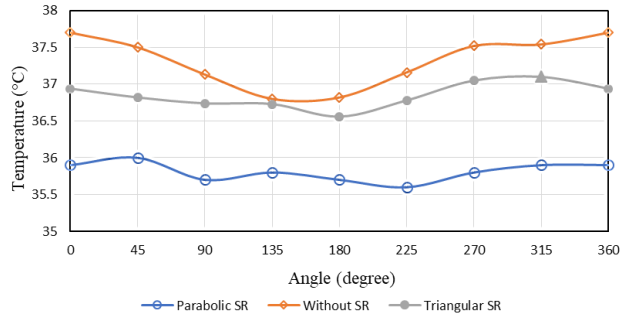

FIGURE 7. VARIATION OF CIRCUMFERENTIAL TEMPERATURE WITH ANGLE

CONCLUSION

The experiments on a small-sized PTC system were performed with and without secondary reflector and a significant imorvement is observed. The performance of PTC system is improved by 10% and 6.55% in terms of outlet temperature of water by using parabolic and triangular secondary reflector incomparison of without SR. The circumferential temperature is obtained more uniform in case of parabolic SR and triangular SR condition in comparison of without SR condition.

ACKNOWLEDGMENTS

This research work was supported by MNNIT Allahabad. We are also thankfull to Dr. Rahul Dev for helping us with the weather station data.

REFERENCES

[1] Macedo-Valencia J, Ramírez-Ávila J, Acosta R, Jaramillo OA, Aguilar JO. 2014. “Design, construction and evaluation of parabolic trough collector as demonstrative prototype”. Energy Procedia, 57 pp. 989–98.

[2] Zou B, Dong J, Yao Y, Jiang Y. 2016. “An experimental investigation on a small-sized parabolic trough solar collector for water heating in cold areas”. Appl Energy, 163 pp. 396–407.

[3] Sagade AA, Aher S, Shinde NN. 2013. “Performance evaluation of low-cost FRP parabolic trough reflector with mild steel receiver”. Int J Energy Environ Eng, 4 pp. 1–8.

[4] Liu, Qibin, Yalong Wang, Zhichao Gao, Jun Sui, Hongguang Jin, and Heping Li. 2010. “Experimental Investigation on a Parabolic Trough Solar Collector for Thermal Power Generation.” *Science China Technological Sciences*, 53(1) pp. 52–56.

[5] Wang Y, Xu J, Liu Q, Chen Y, Liu H. 2016. “Performance analysis of a parabolic trough solar collector using Al_2O_3/synthetic oil nanofluid”. Appl Therm Eng, 107 pp. 469–78.

[6] Sokhansefat T, Kasaeian AB, Kowsary F, Carlo M. 2014. “Heat transfer enhancement in parabolic trough collector tube using Al_2O_3/ synthetic oil nano fl uid” Renew Sustain Energy Rev, 33 pp. 636–44.

[7] Sundaram, P. and Senthil R. 2017. “Thermal Performance Enhancement of Solar Parabolic Trough Collector using Secondary Reflector.” International Journal of Engineering and Technology, 8 (6) pp. 2964-2969.

[8] Wang, Kun, Yaling He, and Zedong Cheng. 2014. “A Design Method and Numerical Study for a New Type Parabolic Trough Solar Collector with Uniform Solar Flux Distribution.” Science China Technological Sciences, 57 (3) pp. 531–40.

[9] Spirkl, Wolfgang, Harald Ries, Julius Muschaweck, and Andreas Timinger. 1997. “Optimized Compact Secondary Reflectors for Parabolic Troughs with Tubular Absorbers.” *Solar Energy*, 61 (3) pp. 153–58.

[10] Marrakchi, S., Leemrani, Z., Asselman, H., Aoukili, A., 2018. “Temperature distribution analysis of parabolic. trough solar collector using CFD, Procedia Manufacturing”. 22 pp. 773-779.

Proceedings of the Third International Conference on Sustainable Energy and Environmental Challenges (3rd SEEC)
18-21 December, 2018, IIT Roorkee, India

SEEC No. 142

NUMERICAL ANALYSIS OF HEAT TRANSFER FOR NON-NEWTONIAN NANOFLUIDS IN AN ELLIPTICAL ANNULUS AT LAMINAR FLOW CONDITION

First Author
Prabhakar Zainith
Department of Mechanical Engineering
NIT Uttarakhand, Srinagar, Uttarakhand
Email: pzainith88@gmail.com

Second Author
Niraj K Mishra
Department of Mechanical Engineering
NIT Uttarakhand, Srinagar, Uttarakhand
Email: nkm.iitg@gmail.com

Third Author
Gyan Sagar Sinha
School of Mechanical Engineering
Kalinga Institute of Industrial Technology Bhubaneswar, Orissa
Email: gyan_it002@yahoo.co.in

ABSTRACT

This paper presents a simulated work on heat transfer analysis of non-Newtonian nanofluid containing CuO nanoparticles with aqueous carboxymethyl cellulose (CMC) as a base fluid in an elliptical annulus. Power law model is used to describe the non-Newtonian nature of nanofluid. The Current research covers a range of nano sized particles 0–4% by volume and Reynolds number in the range of 200–1000. The physical model covers two concentric horizontal pipes used to create an annular space. The outer pipe has diameter of 50.8 mm, 1 mm thickness and 500 mm length. Elliptical pipe has major radius of 9mm with an axis ratio of 1/3. The results concluded that CuO gives 398% higher heat transfer coefficient as compare with pure water. Moreover, significant enhancement in heat transfer has been found with incorporation of elliptical annulus in concentric tube.

Keywords: ***Heat transfer, non-Newtonian nanofluid, elliptical annulus.***

1. INTRODUCTION

The last century was full of struggle for augmenting heat transfer by using the concept of fluid mechanics in different industrial areas. The lower thermal conductivity of ordinary fluids (ethylene glycol, oil, water, etc.) for transporting the heat has been one of the toughest challenges in the field of heat transfer science. The best way to overcome this difficulty is to replace ordinary fluids with some innovative fluids with higher thermal conductivities [1–3].

Nano particles have vast applications in different areas like heat transfer, medical, solar cells etc. Due to their exceptional chemical, physical, structural, and thermal properties from base materials, nowadays nanofluids are extensively used in different industrial areas. The nanofluids were explored by Choi et al. [4] by diffusing different nano-sized particles in the base fluid. Initially the study was limited to the Newtonian behavior of nanofluids, as the time passes the development in the field of heat transfer occurs and researchers showing their interest in non-Newtonian behavior of the nanofluids. Pawar and Sunnapwar [5] experimentally studied for Newtonian and non-Newtonian fluids in helical coils. They concluded that the overall heat transfer coefficient for water is higher than mixer of glycerol-water and sodium carboxymethyl cellulose (SCMC). Bahiraei et al. [6] performed the experiments on non-Newtonian fluid with copper (Cu) nanoparticles in an annulus and investigate the convective heat transfer and flow behaviour in the system. They concluded that on decreasing the annulus diameter, the pressure drop and convective heat transfer coefficient of exterior wall increases while the convective heat transfer coefficient of inner wall decreases

From the above literature review it reveals that the heat transfer enhancement using non-Newtonian nanofluid under laminar flow conditions in an elliptical annulus not investigated in the past. Most of the previous studies were concentrated on different nanofluids under the condition of Newtonian behavior. Therefore the present investigation covers three dimensional heat transfer analysis in an elliptical annulus using CuO based non-Newtonian nanofluid contains aqueous CMC as a base fluid under laminar flow condition.

2. NUMERICAL MODEL

2.1 GEOMETRY

Dawood et al. [7] numerically investigate heat transfer enhancement in an elliptical annulus using ethylene glycol based nanofluid. In the present study the same geometrical conditions were used under power law model for fluids. The present model developed in design module consists of two concentric horizontal tubes. The cross-section shape of inner tube is elliptical having an axis ratio of 1/3, length of tube is 500 mm and the thickness of 1 mm. The

diameter of outer pipe is 50.8mm, 1 mm thickness and 500 mm in length. The material of both the pipes was selected as aluminium.

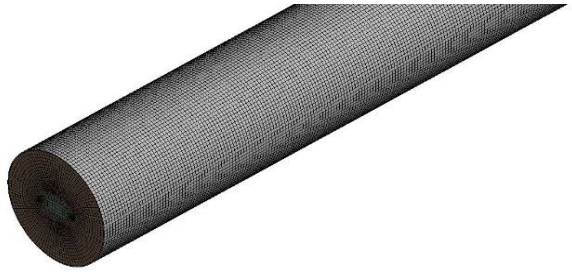

FIGURE 1. Isometric view of physical model

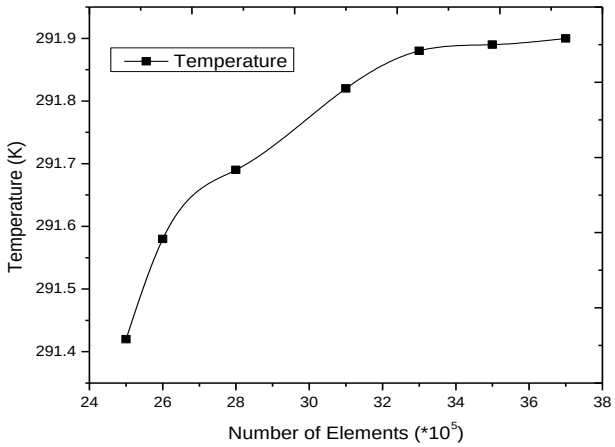

FIGURE 2. Grid independent test

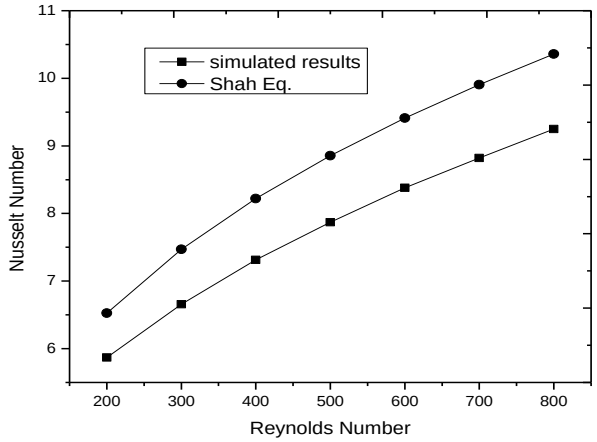

FIGURE3. Validation of simulated result with shah equation

2.2 GRID TESTING AND VALIDATION

To verify the results of mesh, a mesh independence tests were conducted by increasing the number of elements till the nearly constant results were found as shown in Fig. 2. In this grid independent test different values of element size of mesh were numerically investigated for outlet temperature of hot fluid. In the seven different element sizes only three (33×10^5, 36×10^5 and 37×10^5) sizes gives similar results. Thus, the size of 33×10^5 is selected for present simulations. For the confirmation of simulated results the Nusselt number of the elliptical annulus is compared with shah equation [8] with a maximum variation of 10%.

2.3 GOVERNING EQUATIONS

The numerical solution of the heat transfer was carried out using the CFD code FLUENT 18. The basic governing equations, which are used for heat transfer and flow analysis are given below:

$$\nabla.\left(\rho\vec{V}\right) = 0 \tag{1}$$

$$\rho\left(\vec{V}.\nabla\vec{V}\right) = -\nabla p + \nabla.\left[\frac{\mu\left(\nabla\vec{V}+\nabla^{T}\vec{V}\right)}{2}\right] \tag{2}$$

$$\rho C_P\left(\vec{V}.\nabla T\right) = K_f\nabla^2 T \tag{3}$$

Power law model:

$$\tau = K\dot{\gamma}^n \tag{4}$$

Where τ is the shear stress, $\dot{\gamma}$ is the shear rate, K is consistency index and n is the fluid behaviour index. Also the apparent viscosity for the pseudoplastic fluids is given by:

$$\mu = K\dot{\gamma}^{n-1} \tag{5}$$

Where; μ is the apparent viscosity.

These equations are solved with the given boundary conditions to find out the heat transfer coefficient with the increasing Reynolds number.

Nusselt number:

$$Nu = \frac{hD_h}{k} \tag{6}$$

Where, h and k are the heat transfer coefficient and thermal conductivity of fluid, respectively.

The Reynolds number is calculated as:

$$Re = \frac{\rho u_m D_h}{\mu} \tag{7}$$

Where u_m, μ and ρ are mean fluid velocity, dynamic-viscosity of fluid and density, respectively.

The hydraulic diameter (D_h) is calculated as:

$$D_h = \frac{4A}{P} \tag{8}$$

Where, P is wetted perimeter, A is cross-sectional area of the cross-section.

2.4 THERMOPHYSICAL PROPERTIES OF NANOFLUIDS

The thermal properties of nanofluids which are density, specific heat, viscosity and thermal conductivity were calculated by the help of following equations:

The density of nanofluid was find out by using the general formula for the mixture:

$$\rho_{nf} = \phi\rho_{np} + (1-\phi)\rho_{bf} \quad (9)$$

The specific heat of the nanofluid was evaluated from:

$$C_{P_{nf}} = \frac{\phi\rho_{np}C_{P_{np}} + (1-\phi)\rho_{bf}C_{P_{bf}}}{\rho_{nf}} \quad (10)$$

These above equations have been gives significant results for nanofluids on comparing with experimental results by Pak and Cho [9] and Xuan and Roetzel [10].

The Maxwell model [11] was used to find out the thermal conductivity:

$$\frac{k_{nf}}{k_{bf}} = \frac{k_{np} + 2k_{bf} + 2\phi(k_{np} - k_{bf})}{k_{np} + 2k_{bf} - \phi(k_{np} - k_{bf})} \quad (11)$$

Einstein equation is used to determine the effective viscosity of nanofluids having volumetric concentrations less than 5% [12]:

$$\mu_{nf} = \mu_{bf}(1 + 2.5\phi) \quad (12)$$

2.5 Boundary conditions

At the inlet of the annulus, different values of Reynolds number were used depending on the values of inlet velocities, and the inlet temperature was taken as $T_i = 298K$. Also a heat flux of 5000 W/m^2 was given to inner wall of the elliptical pipe. The boundary conditions are:

- Inlet boundary condition:
  $u_r = u_\theta = u_z = 0$, and $T = T_i$ (13)
- At the interface of fluid and wall:

$$u_r = u_\theta = u_z = 0 \text{ and } q_{w,i} = -k\frac{\partial T}{\partial r}\Big| r = r_i \quad (14)$$

- At the outlet (z = L) and over all mass flow rate is balanced.

3. RESULTS AND DISCUSSION

In the present work, laminar heat transfer and fluid flow for CuO based nanofluids having non-Newtonian in nature in a three-dimensional fluid domain through an elliptical annulus is numerically investigated. The dimensions and operating conditions of the present model is described in section 2.0 are used to produce the results presented in this section. The simulations were done for four different values of Reynolds number in the range $200 \leq Re \leq 1000$ and four different nanoparticle concentrations (by volume) ranges from $1\% \leq \varphi \leq 4\%$. For the non-Newtonian nature of nanofluids properties of CMC at 0.4% and 0.8% in an aqueous solution was taken as base fluid. The effect on heat transfer coefficient with the change in CMC concentration and nano particle concentration are discussed in this section.

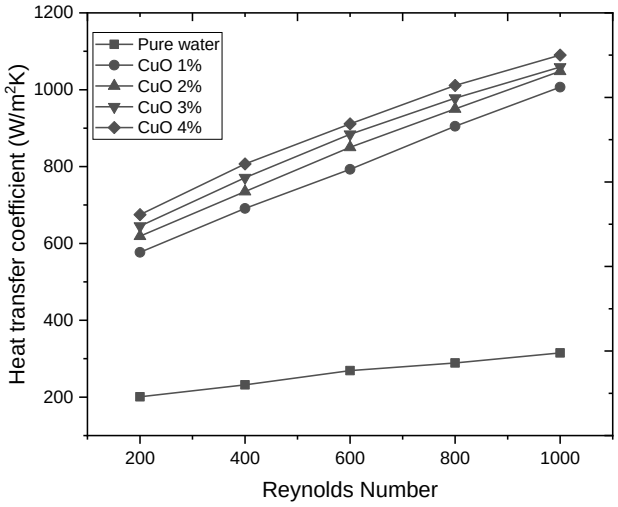

(a)

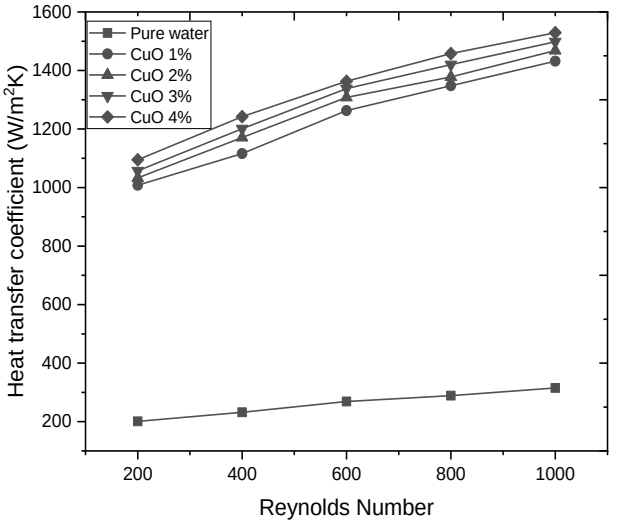

(b)

FIGURE 4. Variation in heat transfer coefficient with Reynolds number of CuO at different particle concentration (a) CMC 0.4% (b) CMC 0.8%

3.1 EFFECTS ON HEAT TRANSFER

The effect of nanoparticle concentration and percentage of CMC on heat transfer in an elliptical annulus are discussed in this section as shown in Figure 4. The numerical analysis was done with a constant heat flux of 5000W/m^2 at the inner section of the elliptical tube. Results reveals that copper oxide

in 0.8% of CMC gives higher heat transfer coefficient as compare to 0.4% of CMC. Moreover heat transfer coefficient at a particular Reynolds number increases with the increase in nano particle concentration. This is due to the increase in the average surface area of metallic particles in the base fluid, which is responsible for better heat transfer rate. Another factor responsible for better heat transfer rate is Brownian motion of particles. Brownian motion is taking place due to random movement of nanoparticles caused by the impact of fluid molecules in the surrounding. Thus, as the concentration of nano sized metallic particles increases more augmentation of heat transfer occurs. The maximum heat transfer coefficient were found 1563 W/m^2 for CuO/water/CMC and nanofluids. These values were obtained at 4% volume concentration in 0.8% CMC aqueous solution. CuO nanofluids gives 398% better results as compare with pure water. The higher heat transfer coefficient is obtained from usage of CuO based nanofluid. The above conclusion reveals that the arbitrary movement of CuO nanoparticles improves the thermal dispersion.

3.2 EFFECTS BY NANOPARTICLE CONCENTRATION

In the present study, effect of nanoparticle concentrations in the range of $1\% \leq \varphi \leq 4\%$ within the laminar flow region have been investigated. Fig. 4 shows that on increasing the volume fraction of nano sized particles the value of Nusselt number increases. The heat transfer coefficient increases from 598 to 1098 for CuO in 0.4% CMC. While the 0.8% CMC gives the higher values of heat transfer coefficient than 0.4% CMC which varies from 1023 to 1563 for CuO. This is because as the nanoparticle concentration increases the metal particles in the fluid increases which is responsible for the thermal conductivity enhancement of the nanofluids. Also uneven and random movement of nano sized particles increases the exchange of heat transfer rate. Other parameters are also affected by increasing the concentration of nanofluids such as specific heat decreases while the density and viscosity increases. In general, the overall effect of all the above properties on increasing the volume concentration results in augmentation of heat transfer rate.

4. CONCLUSIONS

This study covers numerical investigation of convective flow heat transfer in a three dimensional elliptical annulus at a constant heat flux. CuO nanoparticle is used with two different concentrations of CMC as a working fluid. From the above study following conclusion are summarized:

1. The results reveal that the heat transfer rate is remarkably increased by the use of nanofluids. It is concluded that on increasing the fluid velocity and nano sized particles leads to increase in the value of heat transfer coefficient.
2. The CuO nanofluids with 0.8% of CMC gives 398% better heat transfer coefficient, with respect to pure water.
3. The implementation of elliptical annuli over circular annuli accompanied in enhanced heat transfer rate because of aggrandizes mixing of fluids.

4. REFERENCES

[1] Lee, Y. K., 2014. "The use of nanofluids in domestic water heat exchanger". J. Adv. Res. Appl. Mech., 3(1), 9-24.

[2] Sidik, N. C., & Alawi, O. A., 2014. "Computational investigations on heat transfer enhancement using nanorefrigerants". J. Adv. Res. Des., 1(1), 35-41.

[3] Zainal, S., Tan, C., Sian, C., & Siang, T., 2016. "ANSYS simulation for Ag/HEG hybrid nanofluid in turbulent circular pipe". J. Adv. Res. Appl. Mech., 23(1), 20-35.

[4] Choi, S. U. S., Singer, D. A., & Wang, H. P., 1995. "Developments and applications of non-Newtonian flows". ASME FED, 66, 99-105..

[5] Pawar, S. S., & Sunnapwar, V. K., 2013. "Experimental studies on heat transfer to Newtonian and non-Newtonian fluids in helical coils with laminar and turbulent flow". Experimental Thermal and Fluid Science, 44, 792-804.

[6] Bahiraei, M., Khosravi, R., & Heshmatian, S., 2017. "Assessment and optimization of hydrothermal characteristics for a non-Newtonian nanofluid flow within miniaturized concentric-tube heat exchanger considering designer's viewpoint". Applied Thermal Engineering, 123, 266-276.

[7] Dawood, H. K., Mohammed, H. A., Sidik, N. A. C., Munisamy, K. M., & Alawi, O. A., 2017. "Heat transfer augmentation in concentric elliptic annular by ethylene glycol based nanofluids". International Communications in Heat and Mass Transfer, 82, 29-39

[8] Shah, R. K., & London, A. L. 1978. Laminar Flow Forced Convection in Ducts, Academic Press, New York.

[9] Pak, B. C., & Cho, Y. I., 1998. "Hydrodynamic and heat transfer study of dispersed fluids with submicron metallic oxide particles". Experimental Heat Transfer an International Journal, 11(2), 151-170.

[10] Xuan, Y., & Roetzel, W., 2000. "Conceptions for heat transfer correlation of nanofluids". International Journal of heat and Mass transfer, 43(19), 3701-3707.

[11] Chon, C. H., Kihm, K. D., Lee, S. P., & Choi, S. U., 2005. "Empirical correlation finding the role of temperature and particle size for nanofluid (Al_2O_3) thermal conductivity enhancement". Applied Physics Letters, 87(15), 153-107.

[12] Einstein, A., 1906. "Eine neue bestimmung der moleküldimensionen". Annalen der Physik, 324(2), 289-306.

Experimental Study on Electro Chemical Discharge Machining of Sustainable Materials

Pankaj Kumar Gupta[1] and Kishore Debnath[2]

[1]*Department of Mechanical Engineering, National Institute of Technology Uttarakhand, India*

[2]*Department of Mechanical Engineering, National Institute of Technology Meghalaya, India*

Email: pankaj_tnk@rediffmail.com[1], and debnath.iitr@gmail.com[2]

ABSTRACT

The composite materials are important engineering materials and preferred over conventional materials due to their high specific strength and stiffness characteristics. In recent years, a new class of composite materials namely natural fibre reinforced composite materials (NFRC) is emerging at an unprecedented rate because of their eco-friendly sustainable characteristics. These materials have already replaced many conventional materials in a variety of applications. But machining of these materials is a challenging task due to their inhomogeneous nature. The conventional machining of these materials poses several problems such as severe thermal and mechanical damages to the machined surface. Thus there is a wide scope of development of cost-effective machining method for this class of materials. Hence, in the present research endeavour, the nonconventional machining route has been applied to study the machinability of natural fibre reinforced composites. The natural fibre reinforced composites have been developed by hot compression using the film-stacking method. Sisal fibre as reinforcement and polylactic acid as polymer has been used to develop the composites. The fibre weight fraction was kept constant to 20% during the manufacturing of composites. A hybrid machining method namely electro chemical discharge machining method (ECDMM) has been applied for making of holes in the developed composites. ECDMM is the hybridization of two unconventional machining methods: (i) electro chemical machining (ECM) and (ii) electric discharge machining (EDM). The influence of the different input parameters such as duty factor and applied voltage on the material removal rate, hole diameter, heat affected zone, and depth of hole has been investigated. One factor at a time (OFAT) approach has been applied to conduct the experiments as this approach gives a suitable range of process parameters for desired output. The tool diameter 800 µm and electrolyte concentration 20 % were kept constant during experimentation. The result showed that the ECDMM could be a viable alternative to the conventional machining methods for making superior quality holes in natural fibre reinforced composites as shown in Figure 1.

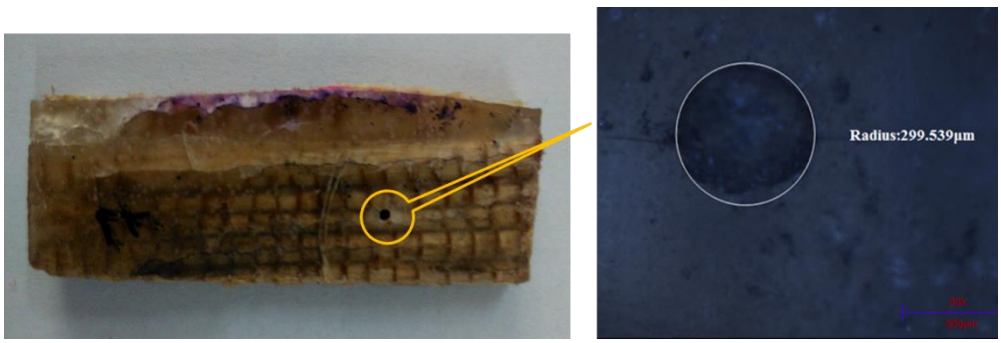

Figure 1 Electro chemical discharge machining of natural fibre reinforced composites

Proceedings of theThird International Conference on Sustainable Energy and Environmental Challenges (3rd SEEC)
18 –21 December, 2018, IIT Roorkee, India

SEEC No.145

ENHANCED LIPID ACCUMULATION IN OLEAGINOUS YEAST UNDER STRESS CONDITION

Km Sartaj
Department of Biotechnology
Research Scholar
Email: kmsartaj@gmail.com

Prof. Vikas Pruthi
Department of Biotechnology
Prof. & Head of Center for
Transportations
vikasfbs@gmail.com

ABSTRACT

The worldwide increase in industrialization has been recognized as serious threat related to environmental deterioration due to the discharge of various waste products and effluents in the surrounding environments. These industrial effluents contain wide varieties of degradable and non-degradable organic toxic chemicals such as phenols, chlorophenol, cresol, butyl phenol and toxic metals such as lead, mercury, chromium, manganese, iron, cobalt, nickel, copper, zinc etc. Consumption of these toxic effluents causes malformation in urban children, neurological disorder, and mutagenic changes etc. The present investigation deals with the utilization of these waste water as a growth media for oleaginous yeast.

Keywords*: *Oleaginous yeast, Degradable.

INTRODUCTION

Economic growth of any country depends on some factors in which energy plays a vital role. Industrialization in all developed countries flourish very well that enhances their economy as well as support job opportunities all over the world and this could be possible because of sufficient energy supply on time. However, current situation is just opposite than before because declined energy supply cannot fulfil the requirement of high energy [1, 2]. Along with this unstable oil prices, energy security, environment protection and concerns, depletion of crude oil supplies are direction of development of alternative sources of energy for reducing unemployment, ensuring energy security and mitigation of toxic gases emission which are harmful for environment and cause pollution. National governments are also making policies, developing strategies, setting targets and investment plans for efficient use of renewable energy resources. However, in India biofuel initiative started in 2003 but choice of raw material for production of biofuel comes under the most important agendas [2]. Although India is the third largest coal producing country (after china and USA) in the world and accounts for about 7.5% of the world's annual coal production [3]. Along with this coal consumption rate is also very high and rapidly increasing day by day. Now India is speedily expanding large economy for which energy demand increasing but to sustain India's 8% average annual economic growth and to support its growing population, India needs to generate two- to three fold more energy than the present [3].

So the world's scientific community is focussing on biofuel that can be an ideal choice to meet these requirements and necessary for future perspectives.

MATERIAL AND METHODS

The present study investigates the effect of stress on growth and lipid accumulation capacity of oleaginous yeast. The selected yeast strain was tested for its ability to intake and grown in minimal media with stress condition.

Lipid accumulation was observed after 6 days of inoculation and was qualitatively estimated by neutral lipid staining. Furthermore lipid was extracted and quantified gravimetrically by modified Bligh and Dyer method. Residual concentration of total carbohydrate and other components in media after six days of inoculation was estimated by phenol sulphuric assay and colorimetric methods. The changes in cell size and morphology were determined by using Image J software and Fe SEM respectively.

RESULT AND DISCUSSION

Enhanced lipid accumulation was observed in cultures having stress conditions. It is reported that nutrient imbalance is one of the factor that is responsible for accumulation of fat in culture medium. When stress cells run out of a key nutrient, usually nitrogen, excess carbon substrate continues to be assimilated by the cells and converted into storage fat.

FIGURES

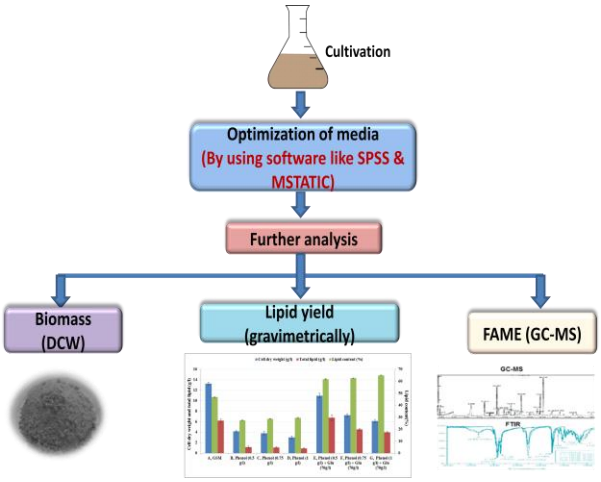

FIGURE 1. METHODOLGY OF COMPLETE PROCESS

ACKNOWLEDGMENTS

Authors are thankful for financial support by JRF fellowship to Km Sartaj from university grants commission, india.

REFERENCES

[1] Shafiee, S. and Topal, E., 2009. When will fossil fuel reserves be diminished?. *Energy policy*, *37*(1), pp.181-189.

[2] Chu, S. and Majumdar, A., 2012. Opportunities and challenges for a sustainable energy future. *nature*, *488*(7411), p.294.

[3] Ratledge, C. and Wynn, J.P., 2002. The biochemistry and molecular biology of lipid accumulation in oleaginous microorganisms. *Advances in applied microbiology*, *51*, pp.1-52.

SEEC No.146

EXPERIMENTAL STUDY ON FLAME CHARACTERISTICS OF SMALL AND MEDIUM SCALE ETHANOL POOL FIRES

Ankit Sharma
Technological Risk Research and Analysis Group (TRAG), Department of Mechanical and Industrial Engineering, Indian Institute of Technology Roorkee, India.
Email: ankit171032@gmail.com

Kirti Bhushan Mishra
Technological Risk Research and Analysis Group (TRAG), Department of Mechanical and Industrial Engineering, Indian Institute of Technology Roorkee, India
Email: kirti.fme@iitr.ac.in

ABSTRACT

From the last few years, ethanol is being increasingly produced and used as a biofuel in India raising their storage and handling volumes. This has also raised concerns for their safe storage and transportation. Hence, to gain practical experiences for their storage tanks, there is a need to study flame characteristics of ethanol pool fire with different diameters. In the present work, three main flame characteristics are experimentally studied namely mass burning rate, flame height and temperature for three diameters - 0.05 m, 0.1 m and 0.2 m. Burning rate comparison of ethanol pool fire with previous experimental results of hydrocarbon (gasoline, diesel) pool fires revealed that they follow a similar trend for the diameters under investigation i.e. first decreasing and then increasing. It was also noticed that the flames are laminar up to 0.1 m after which transition to turbulent zone occurs. Further, it was observed that the flame height and temperature were increasing with the pan diameter.

***Keywords*:** *ethanol, pool fire, burning rate, flame height, flame temperature.*

NOMENCLATURE

d	diameter of the pan (m)
k	extinction coefficient (m^{-1})
m''	mass burning rate per unit area ($kg/m^2.s$)
t	time (s)
T_f	flame temperature (K)
Q	heat release rate (kW)
Z	flame height (m)
ρ	density of Fuel (kg/m^3)
ΔHs	heat of gasification (kJ/kg)
ΔHc	heat of combustion (MJ/kg)

INTRODUCTION

Fossil fuels are getting depleted at a very high rate due to our major dependence on them for energy requirement. Faster depletion and limited available has urged scientists to explore alternative means of energy. Biofuels are one of those alternative solution with the benefit that they are environmental friendly too. They are derived from renewable biomass resources and India is blessed with these resources. So, India is trying hard to tap the maximum potential of biofuels as they will reduce its import dependency, promote a greener environment, create employment generation along with several other benefits [1]. Most commonly used biofuels are mainly biodiesel, and ethanol. From last few years, India is currently focussing on increasing production of ethanol. It has reached to 6th position from the 11th position in the list of world's top ethanol producers within three years and it further plans to thrice its production by 2022 [2]. With the growing usage of ethanol, their storage and handling volume will also increase. Large diameter storage tanks would be required for their storage. Storage tanks are highly prone to accidents as is clearly evident from numerous past experiences and lessons [3]. Some accidents have also happened with ethanol storage tanks. One such

incident took place at Port Kembla in Australia where a large ethanol storage tank of area 800 m^2 got exploded and 4000 m^3 of ethanol burnt away [4]. Other such cases include the ethanol fire in Madison, USA where a large ethanol tank caught fire causing injuries to the workers [5]. The safety issue of these storage tanks hence is a major concern.

In addition, less practical experiences are available for ethanol tank fires. So, there is a need to study their burning behaviour and determine their flame characteristics like burning rate, flame length, temperature, emissive power etc. Prior knowledge of these characteristics will help to understand their fire behaviour and better safety designing of process plants where they are produced and stored. One of the ways to understand their fire dynamics is to experimentally investigate them in pool of various diameters and separately studying their characteristics for each diameter and developing correlations for higher diameters. This is the objective of the current study to investigate pool fire of ethanol in a pool of diameter d = 0.05 m, 0.10 m and 0.20 m and study their characteristics to develop safety measures.

EXPERIMENTAL DETAILS

Set-up

Details of the experimental set up are shown in Fig. 1. Fuel is burned inside the pan placed on a table over a load cell. Three pans made up of stainless steel with inner diameter d = 0.05 m, 0.10 m and 0.2 m were used. Lip height for d = 0.05 m and 0.10 m was 0.10 m while for d = 0.20 m it was 0.05 m. Load cell records the decrease in mass of burning fuel and sends it to the computer via data acquisition system. For recording the flame temperature, K-type thermocouples with a bead diameter of 1 mm were used. These are fixed at a distance of 0 cm, 4 cm, 10 cm, 20 cm and 28 cm for d = 0.05 m and d = 0.10 m from the top of the pan. While for d = 0.20 m, the distance between thermocouples was increased due to higher flame length and were fixed at 0 cm, 10 cm, 20 cm and 40 cm. Data from the thermocouple is recorded in the computer through data logger. Video camera with 30 fps was also installed for recording the experiments for finding out the flame height.

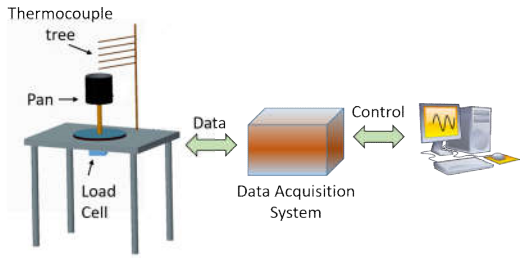

FIGURE 1. SCHEMATIC OF THE EXPERIMENTAL SETUP

Fuel

Fuel used in the experiments was ethanol. The various properties of ethanol are mentioned in Tab. 1.

TABLE 1. PROPERTIES OF ETHANOL [6]

S.No	Property	Value
1.	Density, ρ (kg/m3)	790
2.	Flash point (K)	289.6
3.	Auto-ignition temperature (K)	636
4.	Heat of combustion, ΔHc (MJ/kg)	26.8
5.	Heat of gasification, ΔHs (kJ/kg)	1000
6.	Extinction coefficient, k (m^{-1})	0.4

Procedure

Experiments were performed with three different pool diameters. First d = 0.05 m pan was placed over the load cell and filled up to 95 % height. Small gap was left to avoid spilling of fuel outside due to thermal expansion while burning. An ignitor was used to ignite the fuel initially. Data logger system and video cameras were started to record the mass loss data from load cell and flame temperature data from thermocouples. Readings were taken when the fire was fully developed. All the experiments were performed for three times to ensure repeatability. Similar procedure was carried out for other diameters as well. Ambient conditions taken were 1 bar and 25^0 C with calm wind.

RESULTS AND DISCUSSIONS

Mainly three flame characteristics were studied in the present work - Burning rate, flame height and flame temperature.

Mass Burning Rate

A fixed mass of fuel was burned inside the pan of different diameters for fifteen minutes. Burning rate (m) was determined by calculating the difference in mass of fuel initially (m_i) in the pan and after the experiment (m_f) and dividing it by the total time taken (t).

$$\dot{m} = \frac{m_f - m_i}{t} \quad (1)$$

Figure 2 shows the linear decrease in the mass of ethanol for two diameters. Using equation (1) and dividing by the corresponding pan area, the mass burning rate was calculated for three diameters as shown in Fig. 3. It can be seen from Fig. 3 that burning rate is first decreasing and then increasing for higher diameter. This trend is similar to what is also observed in hydrocarbon fuels like diesel and gasoline [7].

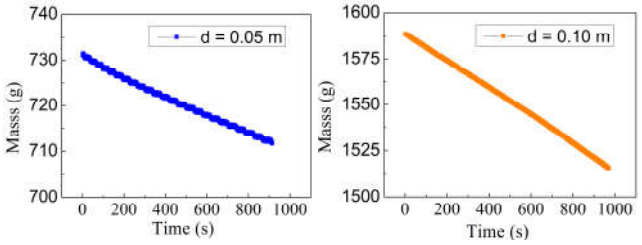

FIGURE 2. DECREASE IN MASS FOR d = 0.05 m AND 0.1 m

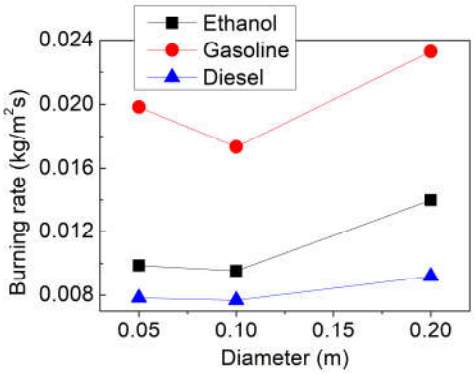

FIGURE 3. COMPARISION OF MASS BURNING RATE (kg/m^{2}s) OF ETHANOL IN PRESENT STUDY WITH GASOLINE AND DIESEL OF PREVIOUS EXPERIMENTS [7]

Flame Height and Appearance

Flame height can be calculated semi-empirically using flame height correlations developed by Heskastad [8].

$$Z = -1.02d + 0.235Q^{\frac{2}{5}} \qquad (2)$$

Where d is the pool diameter (m) and Q is the heat release rate in kW.

In the present study, a video camera was used to visually capture flame appearance and measure flame height. After video processing, flame images at different time steps were captured and are shown in Fig. 4 for d = 0.2 m. It shows the images of flame from the initial stage to steady state. In this case, it took about 2-3 minutes for the flame to reach a fully developed state. Flame height was calculated by visual comparison of images of steady-state flame. Fig. 5 shows the comparison of flame height where it can be seen that with an increase in diameter, flame height is increasing.

One more observation, which is evident from Fig. 5, is that flame is laminar for 0.05 m while for 0.1 m it shows transition stage. For d = 0.2 m, it is nearly turbulent as also seen from Fig. 4.

FIGURE 4. INITIAL IMAGES OF DEVELOPING FLAME FOR d = 0.2 m AT INTERVAL OF 40 s

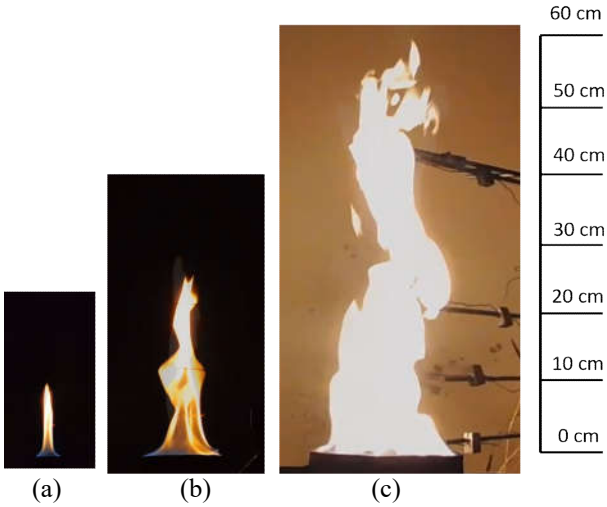

FIGURE 5. FLAME HEIGHT COMPARISON FOR (a) d = 0.05 m, (b) 0.1 m and (c) 0.2 m, AT FULLY DEVELOPED STATE

Flame Temperature

After steady-state flame developed, flame temperature data from K-type thermocouples at various distances from the top of the pan is drawn in Fig. 6. With increasing diameter, flame temperature is also increasing. It was also noticed that for a particular diameter, higher temperature is obtained at the bottom of flame near to the tip of the pan.

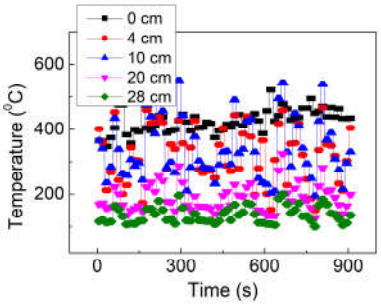

(a) d = 0.05 m

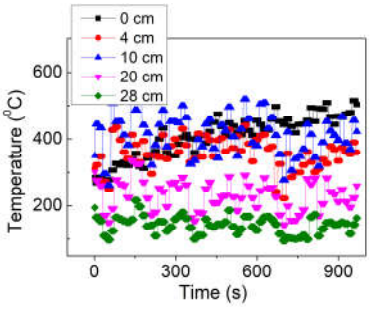

(b) d = 0.10 m

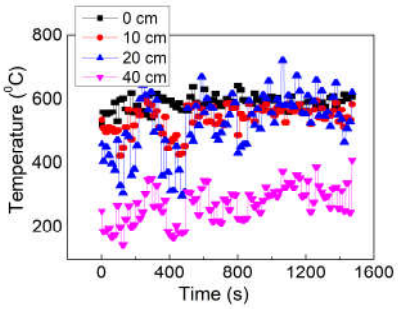

(c) d = 0.20 m

FIGURE 6. FLAME TEMPERATURE OF ETHANOL FOR DIFFERENT POOL DIAMETERS

CONCLUSIONS

In the present work, various experiments were performed to study flame characteristic of small and medium scale ethanol pool fires with three different diameters - 0.05 m, 0.1 m and 0.2 m. A set up was developed to measure the mass burning rate, flame height and flame temperature. Following conclusions can be drawn:

- For the studied diameters, the mass burning rate of ethanol shows a similar trend as obtained in hydrocarbon pool fire. It is first decreasing and then increasing after 0.1 m.
- At d = 0.1 m, the transition is occurring from laminar to turbulent. Hence, d = 0.1 m marks the transition stage which is also similar to hydrocarbon fuels (gasoline and diesel) [7].
- For d = 0.05 m flame is laminar while for d = 0.2 m it is nearly turbulent.
- Flame height and temperature are increasing with pan diameter and higher temperatures are obtained at the bottom of the flame.

Results from this study will aid in understanding the flame characteristics of ethanol pool fire for smaller diameter and developing correlations and appropriate safety distances for their storage tanks. Further studies are being performed for larger diameters [9].

ACKNOWLEDGEMENTS

The authors would like to thank Science and Engineering Research Board (SERB), India for providing the research grant to carry out this project. (Number ECR/2015/0000189)

REFERENCES

[1] H. Gunatilake, D. Roland-Holst, and G. Sugiyarto, "Energy security for India: Biofuels, energy efficiency and food productivity," Energy Policy, vol. 65, pp. 761–767, Feb. 2014.

[2] The Hindu, "'India to triple ethanol production by 2022'- The Hindu," https://www.thehindu.com

[3] K. B. Mishra, K.-D. Wehrstedt, and H. Krebs, "Lessons learned from recent fuel storage fires," Fuel Process. Technol., vol. 107, pp. 166–172, Mar. 2013.

[4] "Fire crews battle fuel tank blaze," BBC News | Asia-Pacific, 2004. http://news.bbc.co.uk

[5] "Three injured in explosion at Madison ethanol plant |," Law and order | stltoday.com, 2011.

[6] V. Babrauskas, "Estimating large pool fire burning rates," Fire Technol., vol. 19, no. 4, pp. 251–261, 1983.

[7] K. S. Mudan, "Thermal radiation hazards from hydrocarbon pool fires," Prog. Energy Combust. Sci., vol. 10, no. 1, pp. 59–80, 1984.

[8] G. Heskestad, "Engineering relations for fire plumes," Fire Saf. J., vol. 7, no. 1, pp. 25–32, Jan. 1984.

[9] Sjöström, Johan, et al. "Thermal exposure from large scale ethanol fuel pool fires." Fire Safety Journal 78 (2015): 229-237.

Proceedings of the Third International Conference on Sustainable Energy and Environmental Challenges (3rd SEEC)
18 –21 December, 2018, IIT Roorkee, India

SEEC No.147

APPLICATION OF CFD TOOL FLACS FOR ADVANCED RISK ASSESMENT IN PROCESS INDUSTRIES

Saumitra Mishra
Technological Risk Research and Analysis Group (TRAG), Department of Mechanical and Industrial Engineering, Indian Institute of Technology Roorkee
Email: smishra@me.iitr.ac.in

Kirti Bhushan Mishra
Technological Risk Research and Analysis Group (TRAG), Department of Mechanical and Industrial Engineering, Indian Institute of Technology Roorkee
Email: kirti.fme@iitr.ac.in

ABSTRACT

The present work addresses the scenario of dispersion and explosion of propane vapor cloud after leakage of the same in an offshore plant. Leakage of flammable and toxic gases in process industries is a problem with increasing concerns. Increment in the uses of H_2S (Hydrogen sulfide) in the industries is drawing more attention to safety from H_2S leakage. As H_2S disperses like a heavy gas and is highly toxic and flammable in nature, the extents of the vapor cloud of more than 10 ppmv concentration are predicted here. LPG (Liquefied Petroleum Gas) is becoming prominent clean source of energy for present and future. Due to the high flammability limits of propane (2.4-10.1 % by volume) leakage is a threat to population and assets in the vicinity. Experiments on such large scale are unrealizable leading to popularization of CFD tools and use of its results in strategic decisions like locations of detectors and pressure panels.

Keywords: *Dense gas dispersion, Vapor Cloud Explosion (VCE), H_2S, Propane.*

NOMENCLATURE

β_j	Area porosity in j[th] direction
β_v	Volume porosity
$\dot{m}$	Mass flow rate (kg/s)
ε	Dissipation of turbulent kinetic energy
μ_{eff}	Effective viscosity (Pa s)
ρ	Density (kg/m^3)
σ_{ij}	Stress tensor (N/m^2)
ζ	Mixture fraction
$C_{2\varepsilon}$	Constant
R_{fuel}	Reaction rate for the fuel (kg/m^{3}s)
Y_{fuel}	Fuel mass fraction
g	Gravitational acceleration (m/s^2)
h	Specific enthalpy (J/kg)
j	Spatial index
κ	Turbulent kinetic energy (m^2/s^2)
P	Gauge pressure (Pa)
p	Absolute pressure (Pa)
t	Time (s)
u	Mean velocity (m/s)
v	Volume (m^3)
x	Length coordinate (m)
$ppmv$	Parts per million volume

INTRODUCTION

The stature of industries in the market is a collective conclusion of various factors, out of which safety has always been on top. The process industries as well as government norms pay a lot of attention to safety nowadays. As the variation in the infrastructure of all industries varies invariably thus it is not possible to perform experiments on every model. An industry can be of size varying in kilometers, and to conduct experiments at this scale is quite cumbersome. CFD (Computational Fluid Dynamics) is an

approach used to tackle with such situations. Dispersion, explosion, fire, blast etc. are some basic accidental scenarios what can occur in the process industry. Many accidents due to vapor cloud explosion have happened over the years across the world [1-4]. There are various CFD tools for modeling these scenarios, some generic CFD codes are FLUENT and CFX; others include some dedicated tools for safety purposes like FLACS (FLame ACceleration Simulator) developed for consequence modeling. Modeling of unobstructed gas flow over flat terrain can also be realized from phenomenological models, but obstructed gas flow in case of heavy gas dispersion depends on gravity-driven spreading and requires complex CFD modeling [5]. Most of the petroleum industries are located offshore or onshore, thus turbulent mixing is a common phenomenon and use of Gaussian tools becomes limited [6]. Vapor cloud dispersion is affected by different factors such as leak rate, leak type, terrain, obstructions, discharge direction and its orientation, weather stability and turbulence conditions, whereas, the vapor cloud explosion after ignition depends on flammability limits, ignition source, and laminar burning velocity etc. This paper highlights the usage of CFD tool FLACS for advanced risk analysis.

METHODOLOGY

In the present study, Favre-averaged transport equations which are shown below for mass, momentum, enthalpy (h), turbulent kinetic energy (κ), the rate of dissipation of turbulent kinetic energy (ε), mass-fraction of fuel (Y_{fuel}) and mixture-fraction (ζ) on a structured cartesian grid are solved using a finite volume method. The standard $\kappa - \varepsilon$ model for turbulence has been used. The accuracy of the CFD solver is second order in space and first/second order in time. CFD solver uses the SIMPLE (Semi-Implicit Method for Pressure Linked Equations) scheme extended with source terms for compressible flows. The CFD solver FLACS has an advantage over the generic CFD tools in terms of simulation time, due to inclusion of porosity concept in the code leading to introduction of β_j and β_v in the equations shown below, analysis in a domain varying in kilometers in reasonable time is possible [7].

Conservation of Mass

$$\frac{\delta}{\delta t}(\beta_v) + \frac{\delta}{\delta x_j}(\beta_j \rho u_j) = \frac{\dot{m}}{V} \tag{1}$$

Momentum equation

$$\frac{\delta}{\delta t}(\beta_v \rho u_i) + \frac{\delta}{\delta x_j}(\beta_j \rho u_i u_j) = -\beta_v \frac{\delta p}{\delta x_i} + \frac{\delta}{\delta x_j}(\beta_j \sigma_{ij}) + F_{o,i} + F_{w,i} + \beta(\rho - \rho_0) g_i \tag{2}$$

Where, $F_{w,i}$ is flow resistance due to walls and $F_{o,i}$ is flow resistance due to sub-grid obstructions given as

$$F_{o,i} = -\rho \left|\frac{\delta \beta}{\delta x_i}\right| u_i |u_i| \tag{3}$$

Transport equation for enthalpy

$$\frac{\delta}{\delta t}(\beta_v \rho h) + \frac{\delta}{\delta x_j}(\beta_j \rho u_j h) = \frac{\delta}{\delta x_j}\left(\beta_j \frac{\mu_{eff}}{\sigma_h} \frac{\delta h}{\delta x_j}\right) + \beta_v \frac{Dp}{Dt} + \frac{\dot{Q}}{V} \tag{4}$$

Transport equation for fuel mass fraction

$$\frac{\delta}{\delta t}(\beta_v \rho Y_{fuel}) + \frac{\delta}{\delta x_j}(\beta_j \rho u_j Y_{fuel}) = \frac{\delta}{\delta x_j}\left(\beta_j \frac{\mu_{eff}}{\sigma_{fuel}} \frac{\delta Y_{fuel}}{\delta x_j}\right) + R_{fuel} \tag{5}$$

Transport equation for mixture fraction

$$\frac{\delta}{\delta t}(\beta_v \rho \zeta) + \frac{\delta}{\delta x_j}(\beta_j \rho u_j \zeta) = \frac{\delta}{\delta x_j}\left(\beta_j \frac{\mu_{eff}}{\sigma_\zeta} \frac{\delta \zeta}{\delta x_j}\right) \tag{6}$$

Turbulent Kinetic Energy

$$\frac{\delta}{\delta t}(\beta_v \rho \kappa) + \frac{\delta}{\delta x_j}(\beta_j \rho u_j \kappa) = \frac{\delta}{\delta x_j}\left(\beta_j \frac{\mu_{eff}}{\sigma_\kappa} \frac{\delta \kappa}{\delta x_j}\right) + \beta_v P_\kappa - \beta_v \rho \varepsilon \tag{7}$$

Dissipation rate of kinetic energy

$$\frac{\delta}{\delta t}(\beta_v \rho \varepsilon) + \frac{\delta}{\delta x_j}(\beta_j \rho u_j \varepsilon) = \frac{\delta}{\delta x_j}\left(\beta_j \frac{\mu_{eff}}{\sigma_\varepsilon} \frac{\delta \varepsilon}{\delta x_j}\right) + \beta_v P_\varepsilon - C_{2\varepsilon} \beta_v \rho \frac{\varepsilon^2}{\kappa} \tag{8}$$

VALIDATION

Validation for the explosion scenario of the present study is done with the help of experimental results obtained from the previous study carried out by Dong Lv et al.[8] Five cases of the previous experimental work are simulated. Boundary conditions are selected such that same conditions that of experimental work can be achieved. Element size of the finite volume is selected based upon grid convergence study. Governing equations are solved using SIMPLE method. Implicit unsteady solver with pre-conditioner is used to solve governing equations. Best practices for estimating loads onto equipment including cylindrical and rectangular shapes as per described by Hansen et al. [9] are also taken

into consideration. As an extensive work has already been carried out for validation of dispersion scenario, therefore that has not been repeated here. Reducing the grid size would naturally lead to a better approximation, but at the same time, the computational expenses are going to increase rapidly. Proper grid independency tests are performed, and grid size was reduced until a refinement of the grid was not producing a result with a change of ±1% from preceding case.

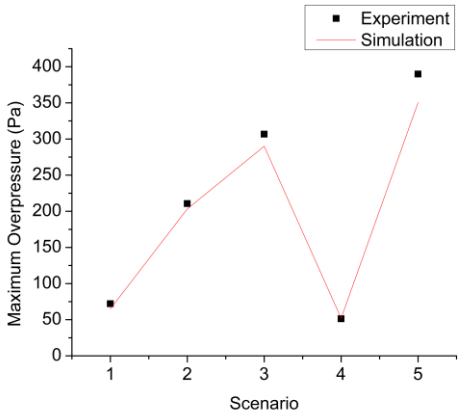

FIGURE 1 RESULTS OF VALIDATION STUDY [8]

From validation study it can be deduced that CFD code is slightly under predicting the overpressure, but is still producing reasonable results.

H_2S DISPERSION

In the original form uses of H_2S (Hydrogen sulfide) are limited. It is being mainly used as a forerunner to produce sulfuric acid, several organosulfur compounds and metal sulfides. Elemental sulfur is also produced using H_2S only. H_2S is colorless hydride gas. It is commonly found as a mixture with natural gas, this mixture of H_2S and natural gas is called as sour gas. H_2S is a toxic gas and in toxicity, it is comparable to carbon monoxide. In petrochemical industries where the chances of the leak of H_2S has high probability, gas detectors are set to alarm at 10-15 ppm. Various short term and long term effects of exposure to H_2S include loss of memory, dizziness, eye irritation, shortness of breath etc. An exposure of short time but high concentration leads to immediate collapse and even a high probability of death.

The density of H_2S is 1.36 kg/m^3 at NTP, which is heavier than air, thus when leakage of H_2S occurs, it disperses as a dense gas. Due to high toxic nature of H_2S and the nature of dispersion being of dense gas, the cloud formation takes place at ground only, leading to an increment in the concentration of gas at the ground with time. The domain contains a storage area and an industry both open to environment as shown in Fig. 2. Leak point is in middle of the storage area. It is seen that when cloud leaves the storage space, the cloud does not advect away with atmosphere but it clinches to the ground and thus a dense cloud formation in the industry starts. The dimensions of the storage space are 25 m × 25 m × 10 m and H_2S leak point is at the center of the domain.

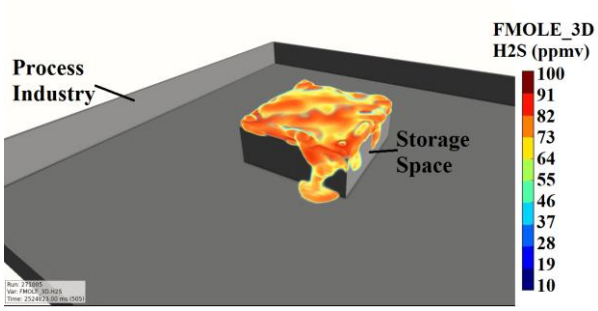

FIGURE 2 DISPERSION OF H_2S IN A PROCESS INDUSTRY

The leak rate is 0.5 kg/s and within an hour the whole industry of 100 m×100 m×10 m gets filled completely where H_2S concentration is varying in between 10-100 ppmv. It can be seen from Fig. 2 that as H_2S cloud flows over the storage space, the cloud does not tend to drift away rather it is settling down in the ground. This is due to the density of the cloud leading to a dense gas dispersion behavior of the cloud. The cloud being of H_2S poses a threat to the people in the vicinity as it is a toxic gas as well as a flammable gas and if an ignition source is present in the extent of the cloud a vapor cloud explosion could take place. With the above prediction the extent of dispersion and explosion can be easily done in the early stages of a project and hence better planning in terms of safety and land use planning can be done.

EXPLOSION AFTER DISPERSION IN OFFSHORE PLATFORM

Figure 3 shows the model of an offshore platform used to extract oil and gases from below the surface of the sea. In these platforms there is always a chance of leakage of petroleum gases. In the present work leakage of propane is taken into consideration and the formation of propane cloud is studied [7].

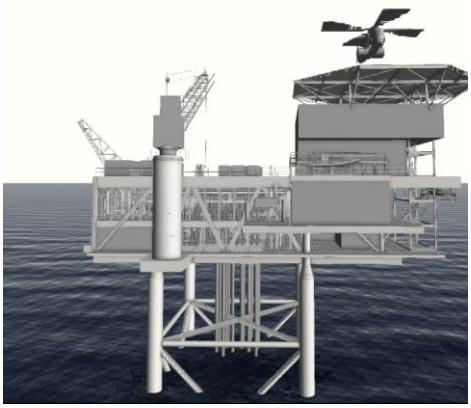

FIGURE 3 MODEL OF AN OFFSHORE PLANT

Figure 4 shows that upon leakage of propane in an offshore platform the flammable vapor cloud will engulf the whole plant within 2 minutes of leakage at the rate of 1 kg/s. These kinds of leakage may occur from the pipe joints or due to rupture of the pipe. The offshore model discussed here is partly confined and a situation of high overpressure is inferred, if an explosion occurs.

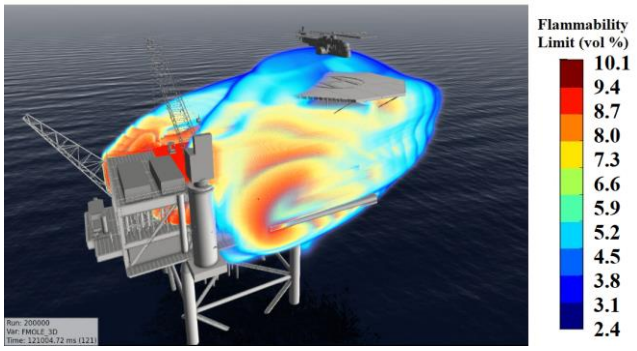

FIGURE 4 DISPERSION IN AN OFFSHORE PLANT

The vapor cloud formed in Fig. 4 is allowed to explode by providing a suitable ignition point, and as the area is partly confined, a maximum explosion overpressure of a magnitude of 20 barg is predicted. Figure 5 shows the area where the overpressure is of highest magnitude. The overpressure of such magnitude is enough for the complete destruction of the platform. Overpressures of this intensity occurs in such a confined space where the volume blockage ratio is high, the event of DDT (Deflagration to Detonation) also can not be ignored from which destruction will be on a larger scale.

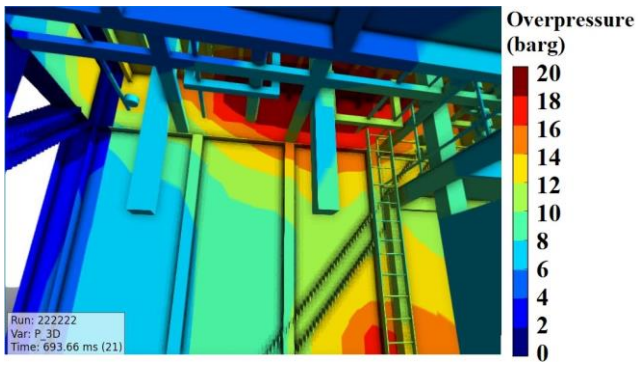

FIGURE 5 EXPLOSION OVERPRESSURE IN A SPECIFIC PORTION OF PLANT

CONCLUSIONS

The application of CFD tools FLACS for multiple dispersion and explosion simulations in 1:1 models of process industries and offshore plants resulted:

- These dispersion simulations can be used to make strategic decisions on heights of boundary walls of storage areas and process industry to contain hydrogen sulfide (H_2S).
- Such dispersion simulations can determine the optimum locations of the gas detectors in a plant.
- The explosion simulation analysis can determine the confined space where the chances are of maximum overpressure generation.
- An installation of pressure panels at those locations will increase safety.
- Inclusion of advanced methods in risk analysis such as discussed in this paper cannot only prevent losses but also will highlight the commitment of industries towards promotion of safety.

REFERENCES

[1] Sadee, C., Samuels, D., and O'Brien, T., 1977. The characteristics of the explosion of cyclohexane at the Nypro (U.K.) Flixborough plant on June 1st, 1974. J. Occup. Accid., pages 203–235.

[2] Knight, H. T., Otway, H. J., and Reider, R., 1971. An unconfined large-volume hydrogen/air explosion.

[3] Burgess, D. S. and Zabetakis, M. G., 1970. Detonation of a flammable cloud following a propane pipeline break: the December 9, 1970.

[4] Makhviladze, G. M. and Yakush, S. E., 2002. Large-scale unconfined fires and explosions. Proc. Combust. Inst., 29(1), 195–210.

[5] Scargiali, F., Di Rienzo, E., Ciofalo, M., Grisafi, F., and Brucato, A., 2005. Heavy gas dispersion modelling over a topographically complex mesoscale a CFD based approach. Process. Saf. and Environ. Prot., 83(3 B), 242–256.

[6] Mazzoldi, A., Hill, T., and Colls, J. J., 2008. CFD and Gaussian atmospheric dispersion models: A comparison for leak from carbon dioxide transportation and storage facilities. Atmos. Environ., 42(34), 8046–8054.

[7] Gexcon, 2016. FLACS v10.5 User's Manual.

[8] Lv, D., Tan, W., Liu, L., Zhu, G., and Peng, L., 2017. Research on maximum explosion overpressure in LNG storage tank areas. J. Loss Prev. Process. Ind., 49, 162–170.

[9] Hansen, O. R., Kjellander, M. T., and Pappas, J. A., 2016. Explosion loading on equipment from CFD simulations. J. Loss Prev. Process. Ind., 44, 601–613.

Proceedings of theThird International Conference on Sustainable Energy and Environmental Challenges (3rd SEEC)
18 –21 December, 2018, IIT Roorkee, India

SEEC No.148

Prediction of multiple fireballs characteristics using FDS

Pushpendra Kumar Vishwakarma[a]
Email: push.vish80@gmail.com

Poomurugan C[a]
Email: poomuruganaero@gmail.com

Kirti Bhushan Mishra[a]
Email: kirti.fme@iitr.ac.in

[a] Technological Risk Research and Analysis Group (TRAG), Department of Mechanical and Industrial Engineering, Indian Institute of Technology Roorkee.

ABSTRACT

Among various type of fires the most vulnerable type of fire scenarios is generation of fireballs from the storage fuels tank explosions. Whenever fireball occurs the thermal radiation from the fireball wreck all the items present in the surrounding environment. Between liquid hydrocarbon fuels and organic peroxides, the organic peroxides are unstable and responsible for the generation of the single and multiple fireballs, give rise to a hazardous thermal explosion. To overcome such problems, analyzing the fireball characteristic by proven numerical code will help us to understand the possible risk involvements and safety measurements needed. In this study the Fire Dynamics Simulator (FDS) is used to predict the fireball characteristics, the code is validated by comparing the experimental data. It's found that FDS predicted the fireball time of generation, shape and flame height with acceptable deviation.

Keywords: ***Organic Peroxide (OP), Fireball, Fire Dynamic Simulator.***

NOMENCLATURE

A_f	Lateral flame surface area (m^2)
D	Diameter of the fireball (m)
F	Geometric view factor
$\dot{m}$	Mass flow rate (kg/sec)
P_w	Partial pressure of water (Pa)
$\dot{Q}_{rad}$	Radiative power (W)
SEP	Surface Emissive Power (W/m^2)
$\overline{T}_f$	Average flame temperature (K)
T_a	Ambient temperature (K)
V	Volume of the fireball (m^3)
$\mathcal{E}$	Emissivity
σ	Stefan- Boltzmann constant(5.67×10^{-8} W/m^2-K^4)

INTRODUCTION

With rapid extension of industry and extensive usage of Organic Peroxides (OP), risk involvement prediction became indispensable. The past noticeable organic peroxide accidents are Fukuoka (Japan, 2000), Edmonton (Canada, 2008), Texas (United States, 2017) [4]. Di-tert-butyl peroxide (DTBP, $C_8H_{18}O_2$) is a kind of common organic peroxide, used as a cross-linking agent and polymerization initiator in rubber and plastic manufacturing. Despite DTBP is considered as one of the most stable organic peroxide, once the runaway reaction happens or in sealed situation when pressure builds up inside tank, and its specific Self Accelerating Decomposition Temperature (SADT) reaching it leads to intense pool fires and multiple fireballs.

Organic peroxides fireballs are distinctly more dreadful compared to hydrocarbon fireballs, Because of its pulsating burning behavior. Unlike hydrocarbon fuels limited studies have been done by various researcher to overcome the risk assessment of organic peroxide fireballs. Blankenhagel *et al*. [1] investigated flame temperature, thermal radiation, sizes of pool fires and fireballs, Roberts *et al*. [2] determined thermal radiation hazards generated from OP and evaluated the safety distances. Mishra [3] analyzed the safety distances based on overpressure and thermal radiation from Russian road carrier accident. Blankenhagel *et al*. [4] developed a new model for OP by modifying the constants present in the known equation. Mishra [5, 6] investigated different diameter DTBP pool fire behavior by experiment and CFD simulation.

There is limited data and literature available for the prediction of the behavior of organic peroxides pool fire and fireball using numerical simulations [7]. Investigating all fireball characteristic by experimental work is both expensive and dangerous. In this regards using the numerical simulation will help us with the much detailed information which can be made available all the times.

Fire Dynamic Simulator (FDS) is most validated and day to day used tool in fire research. It's a Computational Fluid Dynamic model of fire-driven fluid flow, developed by the National Institute of Standards and Technology (NIST) that

solves mass, energy and momentum equations to describe the evolution of fire [8].

To verify FDS capability of predicting fireball characteristics experiment work carried out by Blankenhagel *et al*. [1] has chosen. In his work DTBP is filled inside in steel drum and subjected to outside bonfire. Due to evaporation the pressure increases inside the drum and forms vapor cloud inside drums, when the pressure reaches 2.5 bar, the cap of drum ruptured. When vapor cloud ignites fireballs were generated. The OP mass involved in the fireball vary from 10% to 20% of the original mass available in the drum. This experiment carried out for 20kg and 30kg release of substance.

Numerical Setup

To model DTBP fireball in FDS a 12.8m × 12.8m × 50m height rectangular computational domain was created. The DTBP stored drum having dimension 0.5m×0.5m×0.6m with top surface modelled as fuel supply vent.

Since FDS results are grid dependent the grid independence test was performed with mesh size ranging between 0.3m×0.3m×0.3m, 0.2m×0.2m×0.2m and 0.1m×0.1m×0.1m. It is observed that the deviation between 0.3m and 0.2m being in large percentage and between 0.2m and 0.1m neglible deviation. The cell size of 0.2m adopted for the simulation. The FDS interface supports only the single step, mixing controlled combustion model to account for the evaluation of the fuel gas from its surface of origin through the combustion process. Hence, the combustion process modeled to define the chemical reaction during combustion of DTBP is $C_8H_{18}O_2 + 11.5O_2 \rightarrow 8\ CO_2 + 9\ H_2O$.

Radiation modeling is done through a radiative heat fraction of 0.3, combustion energy to justify the experimentally determined DTBP fire radiative fraction [9]. The induced fireball is driven by density differences, hence buoyancy forces in the vertical direction are considered in the momentum equation to justify the fireball upward motion. Heat release rates are defined with help of ramp-up time for whole burning time for all species. This function allows describing how the heat release varies from ambient to the defined values. Number of thermperature probes and slices placed at different locations to measure the temperature, pressure and heat release rate per unit volume.

A constant specific heat is specified to model the material properties due to FDS limitation. Thermal properties of modelled DTBP in FDS listed in Table 1.

Table 1: Gas phase parameters of DTBP in FDS

Di-tert-butyl peroxide (DTBP)	
Thermodynamic state	Ideal gas
Heat of combustion	36000 kJ/kg
Thermal conductivity	0.02 W/m-K
Refractive index	1.3
Molar mass	0.146 kg/mol
Absorption coefficient	1
Enthalpy of formation	-2.33×10^{-6} J/kg

Figure 1 represents the fluctuations in the mass flow rate of fuel over a certain time period for multiple fireballs of 20 kg (Experiment#1) and 30 kg DTBP (Experiment #2). The multiple fireball developments were observed by the video camera and it was found that three pulses were generated for the multiple fireballs. Each pulse involved approximate 50/25/25 % relative mass compared to the total release.

EVALUATION METHOD

Image Processing

The Surface Emissive Power (SEP) is defined by the Eq.(1) [10]

$$SEP = \sigma.\varepsilon.(\overline{T}_f^4 - T_a^4) \qquad (1)$$

Where σ is the Stefan- Boltzmann constant (5.67×10^{-8} W/m^2-K^4), Ɛ is the emissivity, T_a is ambient temperature and $\overline{T}_f$ is average flame temperature.

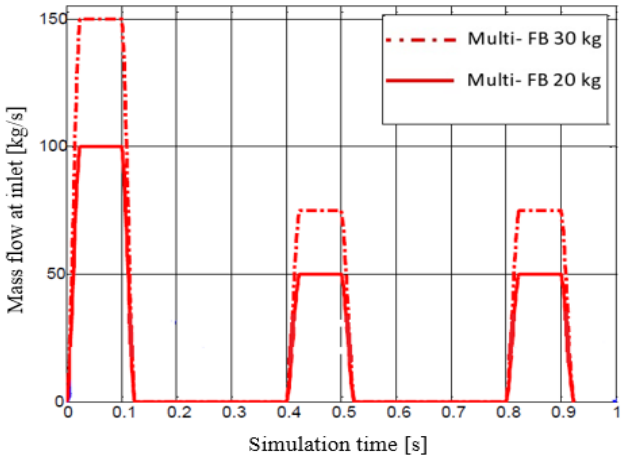

Figure 1 Inlet mass flow rate function for 20 kg and 30kg multiple fireball releases[1]

The screenshots were captured for different time period then processed to obtain the fireball flame height, temperature and SEP. SEP was calculated by defining the isosurface of 800 K. Because, isotherm of the flame boundary temperature T = 800 K is the best fit for the flame appearance [11]. Less valued temperatures doesn't affect the SEP calculation, so the average of below 800 K will be neglected.
The fireball volume V and diameter D calculated by the equation:

$$D = \left(\frac{6V}{\pi} \right)^{1/3} \qquad \textbf{(2)}$$

The obtained images of fireballs captured on different time interval were processed by the help of Adobe Photoshop CS6 software, which was coupled with the Image Processing toolkit. The resulting image files were processed using MATLAB image processing tool to find out the surface area and volume of the fireball, which was generated due to flashing of fuel (DTBP) in a bulk amount due to external heating.

With the knowledge of lateral flame surface area A_f, one can predict radiative power with Eq. (3)

$$\dot{Q}_{rad} = \sigma.\varepsilon.(\overline{T}_f^4 - T_a^4).A_f = \text{SEP} \; . \; A_f \qquad \textbf{(3)}$$

Result and discussion

Flame Shape

The appearance of the fireball is the first indicator of the correct contest between the experiment and numerical data [1].

Figure. 2 shows the instantaneous snapshots of the fireball generated at t = 1.2 sec and t = 1 sec for 20 kg and 30 kg DTBP release respectively.
According to the theory, fireballs are initially momentum driven and buoyancy driven at the end. With the complexity in turbulent FDS simulations well predicted the realtime behavior in terms of flame shape and combustion time of the experimental observed 20 kg and 30 kg fireball.

Flame Height and Temperature

Figure.2 shows the FDS predicted flame height which is virtually equal height of the experimental flame. The FDS predicted maximum heat release rate for 30kg and 20kg release is 195MW and 175MW. The temperature ranges also match with the range of 300K to 1900K.

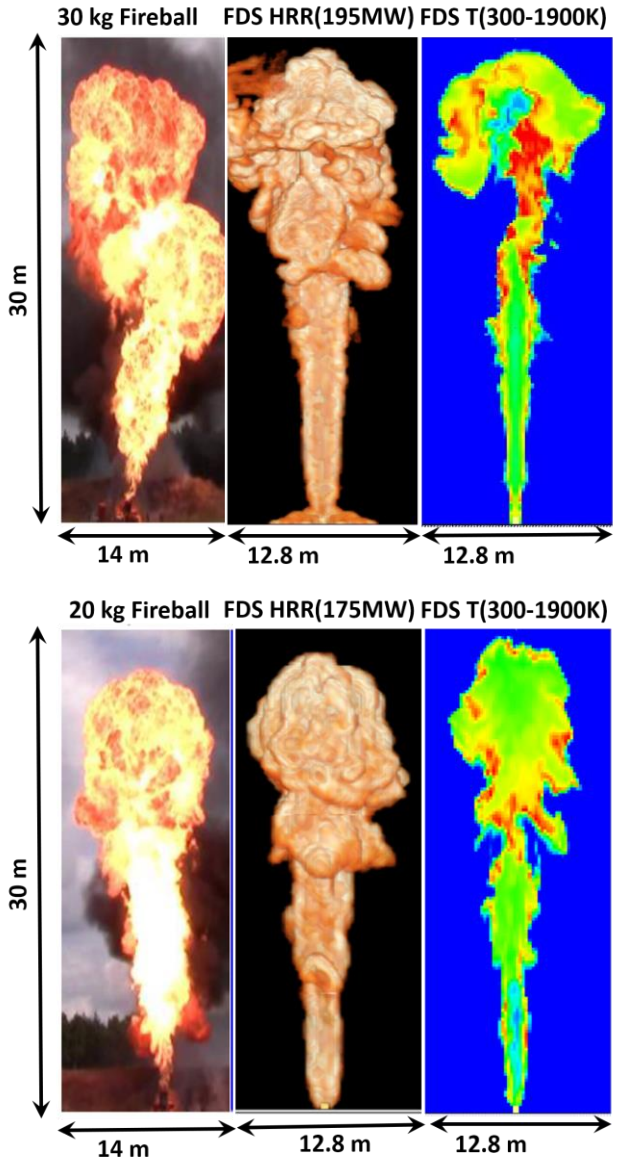

Figure 2 Experimental and FDS predicted flame shape, height, heat release rate and temperature for 30 kg and 20 kg release.

Conclusions

FDS simulations were performed to predict the behavior of DTBP fireballs against the outcomes available from experiments results[1]. FDS simulations were compared and discussed regarding flame temperature, shape, height, SEP and lateral surface area. The following conclusions can be made from the above discussion:

1.The FDS is capable of predicting any organic peroxide fireball characteristics and can be used to calculate the thermal radiation hazrds.
2.This obtained fireball characteristic will helps to predict the safety distances.
3. FDS can also predicts the smoke flow pattern and its toxic cotents much realistically.

References

[1] P. Blankenhagel, K.B. Mishra, K.-D. Wehrstedt, J. Steinbach, Prediction of organic peroxide fireball characteristics using CFD simulation, Digital proceedings of the 8th European Combustion Meeting, 18-21 April 2017, Dubrovnik, Croatia.

[2] T. A. Roberts, R. Merrifield*, and S. Tharmalingam, Thermal radiation hazards from organic peroxides, *J. Loss Prev. Process lnd., Vol3,1990, April*

[3] Mishra K. B., Multiple BLEVE's and fireballs of gas bottles: Case of a Russian road carrier accident, Journal of Loss Prevention in the Process Industries 41 (2016) 60-67

[4] Paul Blankenhagel, Klaus-Dieter Wehrstedt, Sen Xu, Kirti Bhushan Mishra, Jörg Steinbach, A new model for organic peroxide fireballs, Journal of Loss Prevention in the Process Industries 50 (2017) 237–242

[5] K.B. Mishra, Experimental investigation and CFD simulation of organic peroxide pool fires (TBPB and TBPEH), BAM dissertation series 63, Berlin, 2010.

[6] K B Mishra, K D Wehrstedt, H Krebs, Boiling Liquid Expanding Vapour Explosion (BLEVE) of peroxy-fuels: Experiments and Computational Fluid Dynamics (CFD) simulation, The 12th International Conference on Combustion & Energy Utilisation – 12ICCEU, Energy Procedia 66 (2015) 149 – 152

[7] P. Blankenhagel, K.B. Mishra, K.-D. Wehrstedt, J. Steinbach, Thermal radiation impact of DTBP fireballs, Proc. of the 19th Seminar on NTREM (2016) 410-418.

[8] Fire Dynamics Simulator (Version 5) Technical Reference Guide.

[9] S. Siddapureddy, K.-D. Wehrstedt, S.V. Prabhu, Heat transfer to bodies engulfed in di-tert-butyl peroxide pool fires – Numerical simulations, J. Loss Prev. 44 (2016) 204-211.

[10] Casal, J., Arnaldos, J., Montiel, H., Planas, E., Vilchez, J., 2002. Modeling and Understanding BLEVEs. McGraw-Hill, New York book section 22, pp. 22.1–22.27.

[11] Palacios, A., Munoz, M., Darbra, R.M., Casal, J., 2012. Thermal radiation from vertical jet fires. Fire Saf. J. 51, 93–101.

SEEC No.150

Using Machine Learning for Predicting Enthalpy

Accurate thermodynamic data of species is essential for chemical kinetic models to predict the outcomes of complex chemical reactions. Quantum chemistry calculations and experiments can be used to determine all the thermodynamic properties needed; however, these are arduous and time consuming. In this work, we utilize machine-learning algorithms as a tool for quantitative structure property relationship (QSPR) analysis to predict a thermodynamic property (Enthalpy) for a class of reactants and intermediates (Alkanes, alkenes & alkynes) required to build kinetic models. Enthalpy data of alkanes, alkenes and alkynes is taken from Goldsmith et. al [1], Ghahremanpour et .al. [2], NIST [3] and ATcT [4] is used for this study as training, validation and test dataset. Artificial neural networks (ANN's) and Support Vector Regression (SVR) are chosen since they can capture very complex relationships between input and output vectors that are required to map complex properties over dissimilar classes of molecules. Various molecular descriptors [5] consisting of the topological information of species are analyzed for the feature selection to input neural network. In the later part, various parameters of machine learning algorithms are optimized for accuracy. These models can be used to predict enthalpy of molecules with no accurate data in the literature. This work aims at predicting a thermodynamic property for neat stable compounds and thus lays foundation for the further works of predicting other thermodynamic properties and also that of radicals, transport properties leading to solve the challenge of predicting reaction rates.

Ref:

[1] Goldsmith C. F. et al., J. Phys. Chem. A 2012, 116, 9033-9057

[2] Ghahremanpour M. M. et al., J. Chem. Phys. 2016, 145, 114305

[3] https://webbook.nist.gov/chemistry

[4] Active Thermochemical Tables: version 1.122

[5] R. Todeschini and V. Consonni, Handbook of Molecular Descriptors, 11th ed. 2000

Proceedings of the Third International Conference on Sustainable Energy and Environmental Challenges (3rd SEEC)
18 –21 December, 2018, IIT Roorkee, India

SEEC No.151

AHP BASED DRASTIC MODEL FOR GROUNDWATER VULNERABILITY ASSESSMENT IN FATEHGARH SAHIB PUNJAB

Prashant Kumar
Agrionics Department (V1(a))
CSIR-Central Scientific Instruments Organisation
Chandigarh
Email: prashantkumar@csio.res.in
Pras.santu@gmail.com

Sudeshna Bagchi
Agrionics Department (V1(b))
CSIR-Central Scientific Instruments Organisation
Chandigarh
Email: sudeshna_bagchi@csio.res.in

ABSTRACT

DRASTIC is a widely used model to assess the vulnerability of groundwater to contamination across the world. It is used as a rapid regional assessment tool to segregate the regions (vulnerability maps) based on the pollution potential. The weights and ratings of the environmental factors under DRASTIC model are based on DELPHI network technique and there is no scientific explanation for that. There is human subjectivity involved in that. AHP is one of the most optimal techniques for making decisions in situations where there are multiple criteria and multiple alternatives. The present study is an attempt to optimize the weights and ratings of the environmental parameters under DRASTIC Model using AHP. The study also considers the effects of anthropogenic factors towards the groundwater contamination. The resulting groundwater vulnerability map expresses the three classes of severity of groundwater contamination in Fatehgarh Sahib region of Punjab which is facing serious groundwater contamination problem over the years. Such studies are very much useful for the policymakers, town planners and government agencies for groundwater monitoring.

***Keywords*:** Groundwater Contamination, DRASTIC, AHP, Punjab

INTRODUCTION

Groundwater contamination is a burning problem which the entire world is facing. As per United Nation's SDGs, water security is a major challenge to be achieved by 2030 [1]. Groundwater vulnerability assessment is a rapid way of assessing the pollution potential of earth surfaces by index based models. Among the index based models, DRASTIC is the widely used model for its simplicity and usage [2]. DRASTIC model has undergone several modifications over the years but most of the time only ratings have been optimized, keeping weights as per what Aller et al. had suggested [2].

Punjab has been facing serious groundwater contamination problem since decades. The entire Malwa region is facing a serious threat of groundwater contamination. The Malwa region has got maximum patients of cancer. The consumption of polluted groundwater is one of the several causes. Fatehgarh sahib is one of the regions under Malwa zone which is facing serious groundwater quality decline along with reduction in quantity also [3]. The present study optimizes both the weights and the ratings of the fundamental DRASTIC model. Human made causes also contribute significantly towards groundwater contamination. Therefore, anthropogenic factors have also been considered in the empirical equation of DRASTIC model.

METHODOLOGY

The schematic of the methodology is given in Figure 1. The groundwater vulnerability has been assessed using fundamental DRASTIC model and AHP-DRASTICL model and their vulnerability index values and resulting maps have been compared to earmark the potentially vulnerable zones as validated by the water quality parameters.

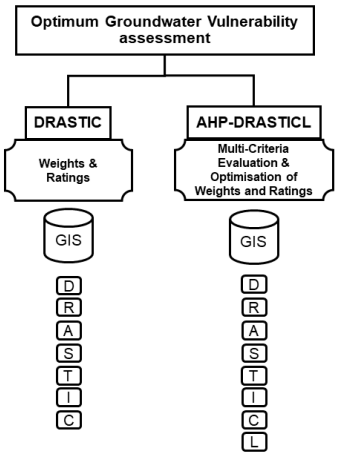

FIGURE 1. SCHEMATIC OF METHODOLOGY

STUDY AREA & HYDROGEOLOGICAL SETTINGS

Fatehgarh Sahib is mainly an agrarian land located in the southern part of Punjab. It is a flat region with no major river. It lies between 30° 25' 00" to 30° 45' 45" N latitude and 76° 04' 30" to 76° 35' 00" E longitude as shown in Figure 2. The total geographical area of the district is 1147 Sq.Km. The study area is divided into five blocks such as Khamanon, Bassi Pathana, Khera, Sirhind and Amloh.

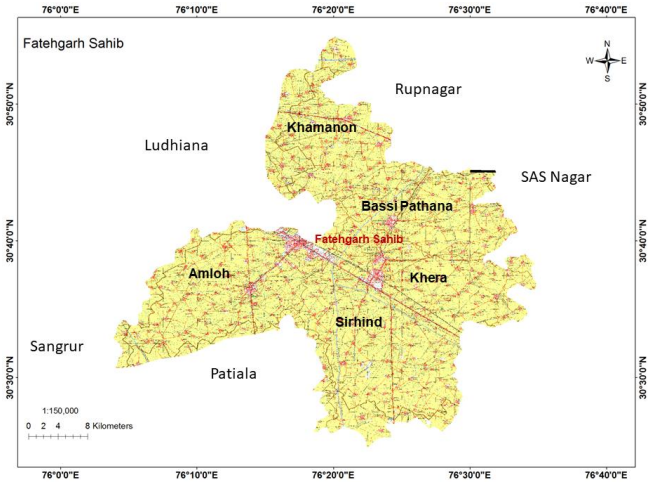

FIGURE 2. GEOGRAPHICAL MAP OF FATEHGARH SAHIB, PUNJAB

DRASTIC MODEL

DRASTIC is an acronym for seven hydro-environmental parameters namely, **D**epth of Water table, Net **R**echarge, **A**quifer Type, **S**oil Media, **T**opography, **I**mpact of Vadose Zone, Hydraulic **C**onductivity. It was developed by Aller et al. in 1987 [2]. It classifies a particular region into different units of potential contamination. The governing equation for the computation of vulnerability index value is given in Equation 1. It uses the relative weights and ratings as decided by experts based on the Delphi network technique.

$$Vulnerability\ Index = \sum_{i=1}^{7} W_i * R_i \quad (1)$$

Groundwater Vulnerability Map

The vulnerability index values range from 103 to 132 when the empirical equation of fundamental DRASTIC model is used and the resulting geospatial vulnerability map is shown in Figure 3. These values have been classified into low (100 - 110), medium (110 - 125) and high (125 - 140) vulnerability classes according to the histogram of the vulnerability index values. As a result, they come under the class of medium vulnerable zone. It is quite noticeable from Figure 3 that most of the part of Fatehgarh Sahib district falls under moderate vulnerability from the perspective of groundwater contamination.

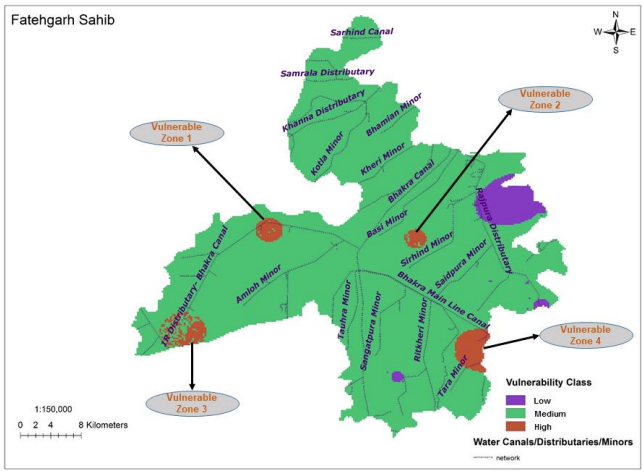

FIGURE 3. VULNERABILITY MAP BASED ON DRASTIC MODEL

Validation: Figure 4 shows the selected sites from where the water sample were chemically analysed and they did possess the toxic elements confirming the highly vulnerable zones. However, there were other regions also as shown in black coloured circles where toxic elements were found in the water samples but these sites were not classified as highly vulnerable zones by fundamental DRASTIC model thereby confirming the lacuna of DRASTIC model in terms of weights and ratings associated with the hydro-environmental parameters of DRASTIC model.

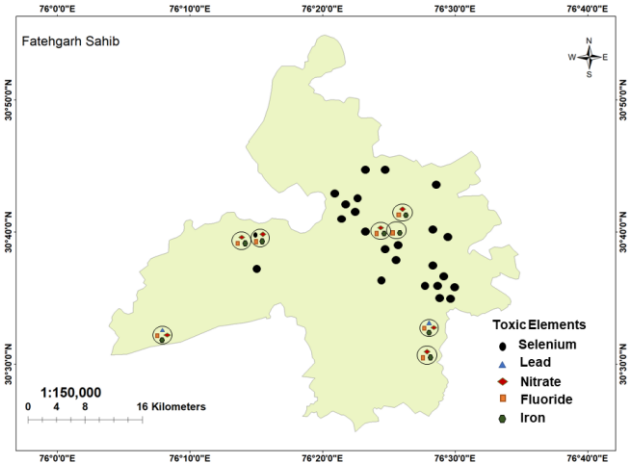

FIGURE 4. WATER SAMPLES FROM SITES FOR VALIDATION

AHP-DRASTICL MODEL

Analytical Hierarchy Process (AHP) is a decision making technique which solves the problem by decomposing a problem into a hierarchy of several smaller problems or sub-problems. It uses Saaty's scale of importance for constructing pairwise comparison of various hydro-environmental parameters [4, 5]. The governing equation of AHP-DRASTICL after considering the anthropogenic factor is given in Equation 2.

$$V\_Index = \sum_{i=1}^{8} W_i \; R_i \tag{2}$$

The hierarchy of the goal (level 0 – Vulnerability index), criteria (level 1 – Weights of DRASTICL parameters) and sub-criteria (level 2 – Ratings of DRASTICL parameters) for the implementation of AHP-DRASTICL is shown in Figure 5.

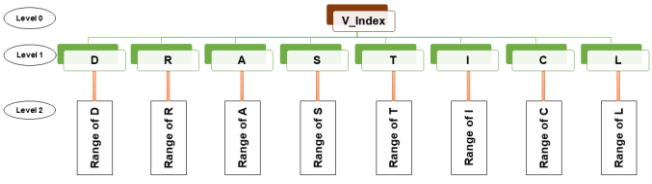

FIGURE 5. HEIRARCHY OF AHP-DRASTIC

Table 1 shows the optimal values of weights and ratings of AHP based DRASTIC model including anthropogenic factor (land use/land cover) parameters.

TABLE 1: AHP-DRASTICL OPTIMIZED WEIGHTS & RATINGS

Parametes	Range/ Types	AHP DRASTICL	
		Weights	Ratings
Depth to water table (m)	0-1.5	0.2113	0.35
	1.5-4.5		0.29
	4.5-9		0.16
	9-15		0.09
	15-23		0.05
	23-30		0.03
	More than 30		0.02
Net Recharge (mm)	0-50	0.1274	0.0327
	50-100		0.0685
	100-175		0.1565
	175-250		0.3109
	More than 250		0.4329
Aquifer Media	Massive shale	0.0773	0.021
	Metamorphic/igneous		0.028
	Weathered		0.047
	bedded sandstone, limestone		
	Shale sequences		0.081
	Massive sandstone		0.081
	Massive limestone		0.155
	Sand and gravel		0.155
	Basalt		0.211
	Karst		0.221
Soil Type	Thin	0.0523	0.211
	Gravel		0.211
	Sand		0.153
	Peat		0.118
	Shrinking clay		0.98
	Sandy loam		0.070
	Loam		0.049
	Silty loam		0.034
	Clay loam		0.025
	Muck		0.018
	Nnon-aggregated clay		0.014
Topography (percent slope)	0-2	0.0318	0.513
	2-6		0.262
	6-12		0.129
	12-18		0.063

	More than 18		0.033
Impact of Vadose Zone	Silt/clay	0.2113	0.0275
	Shale		0.0275
	Limestone		0.0275
	Sandstone		0.0578
	Bedded Limestone		0.0667
	Sand and Gravel		0.0768
	Metamorphic/igneous		0.1072
	Sand		0.1564
	Basalt		0.2211
	Karst		0.2315
Hydraulic Conductivity (m per day)	0.04-4.07	0.0773	0.0274
	4.07-12.2		0.0443
	12.2-28.5		0.0759
	28.5-40.7		0.1437
	40.7-81.48		0.2580
	More than 81.48		0.4506
Land use & Land Cover	Agriculture	0.2113	0.5103
	Settlement		0.2641
	Water		0.1306
	Forest		0.0579
	Barren		0.0372

Groundwater Vulnerability Map

Vulnerability index values range from 105 to 234 with a mean at 208 and standard deviation 13. Based on the histogram of these values, they have been classified into three vulnerable zones low (105 - 195), medium (195 - 221) and high (221 - 234). The vulnerability shown in this map (Figure 6) has seven vulnerable zones as highlighted in red colour. There is a drastic change in this map because of the incorporation of anthropogenic factors as well as optimised ratings and weights as deduced by multi-criteria evaluation technique.

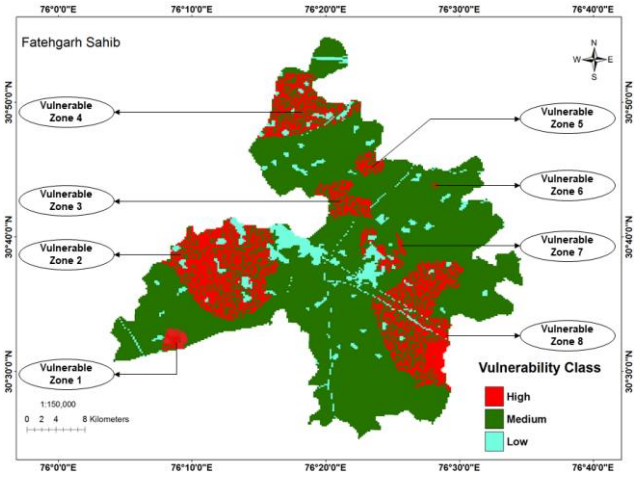

FIGURE 6. VULNERABILITY MAP BASED ON AHP-DRASTICL MODEL

Validation: The vulnerability maps have been validated using water samples from 241 sample locations spread uniformly across the study The ten water quality parameters analyzed are viz. total alkalinity, pH, TDS, Hardness, Magnesium, Sulphate, Calcium, Iron, Fluoride and Nitrate. The cumulative effects of various water quality parameters are considered for validation due to complex and unpredictable dynamics associated with groundwater beneath earth's surface.

CONCLUSION

The inherent lacuna of DRASTIC model is resolved by AHP-DRASTIC model and such studies are very much useful in groundwater monitoring and scientific land use planning.

ACKNOWLEDGEMENTS

The authors are also thankful to all the government departments for providing the hydro-environmental data.

REFERENCES

[1] P. Kumar, P. K. Thakur, B. K. S. Bansod, and S. K. Debnath, "Groundwater: a regional resource and a regional governance," *Environment, Development and Sustainability*, vol. 20, pp. 1133-1151, June 01 2018.

[2] Aller L., Bannet T., Lehar J. H., and Petty R., ""DRASTIC: A Standardized System to Evaluate Ground Water Pollution Potential Using Hydrogeologic Settings."," National Water Well Association Worthington, Ohio1987.

[3] P. Kumar, P. K. Thakur, B. K. Bansod, and S. K. Debnath, "Groundwater vulnerability assessment of Fatehgarh Sahib district, Punjab, India," in *Proceedings of India International Science Festival (IISF) - Young Scientists' Conclave (YSC), Dec 8-11, 2016*, 2016, pp. 115-116.

[4] T. L. Saaty, "What is the Analytic Hierarchy Process?," in *Mathematical Models for Decision Support*, G. Mitra, H. J. Greenberg, F. A. Lootsma, M. J. Rijkaert, and H. J. Zimmermann, Eds., ed Berlin, Heidelberg: Springer Berlin Heidelberg, 1988, pp. 109-121.

[5] P. Kumar, P. K. Thakur, B. K. Bansod, and S. K. Debnath, "Multi-criteria evaluation of hydro-geological and anthropogenic parameters for the groundwater vulnerability assessment," *Environmental monitoring and assessment*, vol. 189, p. 564, October 16 2017.

SEEC No. 152

An Environmentally Friendly approach: Using Coffee as a lubricant for thread cutting application

C.S. Jawalkar
Associate Professor, Punjab Engineering College (Deemed to be University), Chandigarh, INDIA-160012
Email: csjawalkar@gmail.com

Abstract

Advancements in the areas of lubrication have been brought up in this paper. With the stringent Environmental concerns and demand for cheap and eco-friendly lubricants, the user wants to know about such applications and processes which will be of low cost and easy availability. With this in view the various lubricants are reviewed and a brief summary of their properties are discussed.

In machining processes, lubricants play multiple roles, apart from lubricating, the fluid acts as a cutting oil too and its other purposes are for increasing the life of tool, smooth cutting action, better chip removal and improved surface finish. Traditionally mineral oils, cutting oils, mixtures of mineral and cutting oils and chemicals are used in different proportions along with additives. Through this paper an approach with use of coffee (caffeine) as a cheap alternative along its properties are discussed.

The key ingredient in coffee is caffeine (fig-1), which gives it taste and properties. First isolated from coffee in 1820, caffeine has become the most widely used legal drug in the world. It is found occurring naturally in tea leaves, coffee beans, cola nuts, mate leaves and the guarana plant. A white crystalline powder with a melting point of range of 234 to 236.5 °C, caffeine has the chemical name of 1,3,7-trimethylxanthine. It is an alkaloid, meaning that it is an organic molecule containing nitrogen which has pharmacological effects on humans and animals.

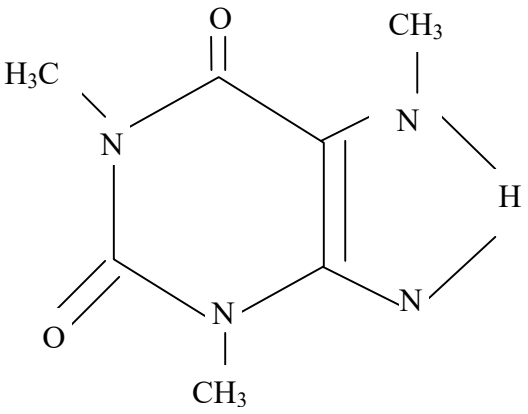

Fig: 1 Chemical Structure of Caffeine

A practical case study on drilling and tapping for an industrial application has been elaborated in the paper. The figure 2 illustrates reduction in average applied forces while using coffee for tapping process in metal cutting. The advantages are enormous such as reduction in cutting force thereby leading to saving in work force, since this process is done manually for larger tap sizes. It presents an environmental friendly approach, as it uses

natural, organic source that can be easily disposed off without causing any harm; additionally, the fragrance it generates motivates and energizes the morale and ambiance of the work area under consideration.

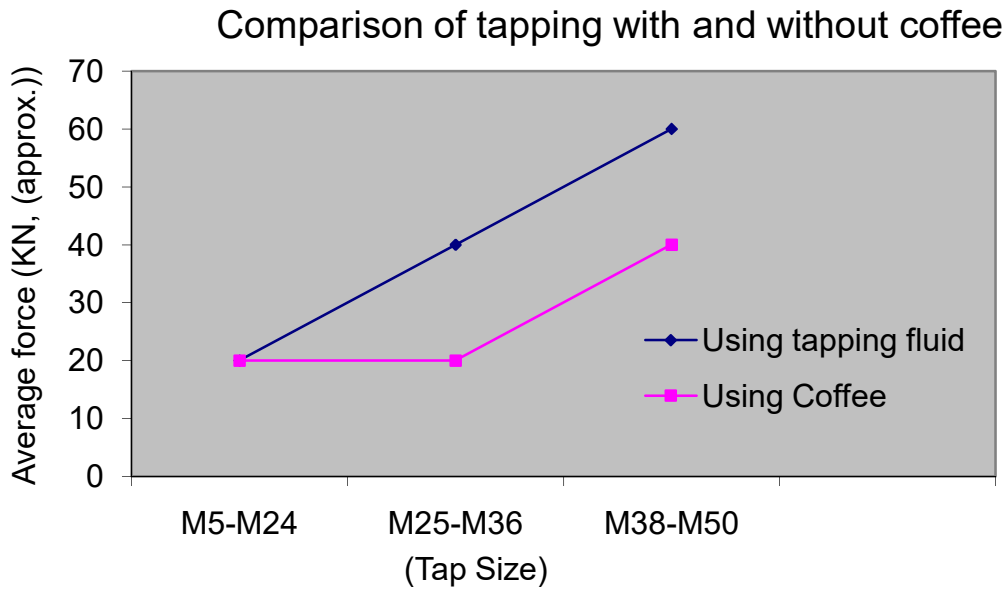

Fig: 2 Graph illustrating average cutting force for different tapping tools

Key Words: Cutting oils, Coffee, Lubricant properties, Tapping

Pre-ignition and knock limits on utilization of Ethanol in Octane – on –Demand concept

Abstract:

Octane-on-Demand (OoD) is a viable contender to reduce global greenhouse emissions from automobiles by utilized a low processed fuel for main driving and efficiency improvements gained thereof. Previous researches have focused on the minimum ethanol content required for achieving a specific load at a given speed. However it is also widely known that ethanol has a high tendency to pre-ignite, owing to its higher laminar flame speed and lower calorific value, leading to higher fuel mass injected into the chamber, thereby increasing the probability of oil dilution. Hence limits on ethanol addition owing to pre-ignition also needs some inspection. In this regard, experiments were performed, using RON 91 gasoline and ethanol, in direct and port injection configurations. Three load points, corresponding to intake pressures of 1.5, 1.75 and 2 bar are used, in conjunction with three speed values, 1500, 2000 and 2500 rpm. In general, it can be said that OoD concept helps suppress pre-ignition innately, by merely splitting the fuel amount going to direct injection. RON 91 gasoline showcased to be the limiting fuel, as it goes from 50 % (v/v) to knock limited gasoline utilization. The large fuel mass at knock limited conditions led to higher fuel-wall impingement and hence, higher tendency to pre-ignite.

Graphical Abstract:

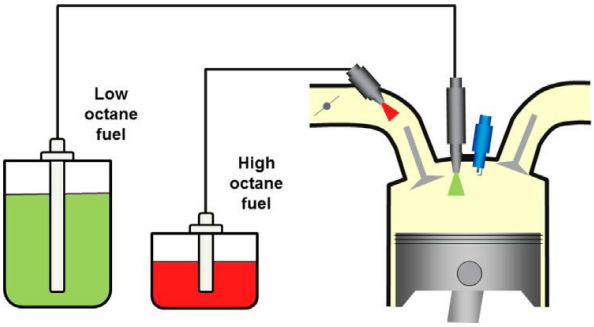

Figure 1. Octane-on-demand methodology

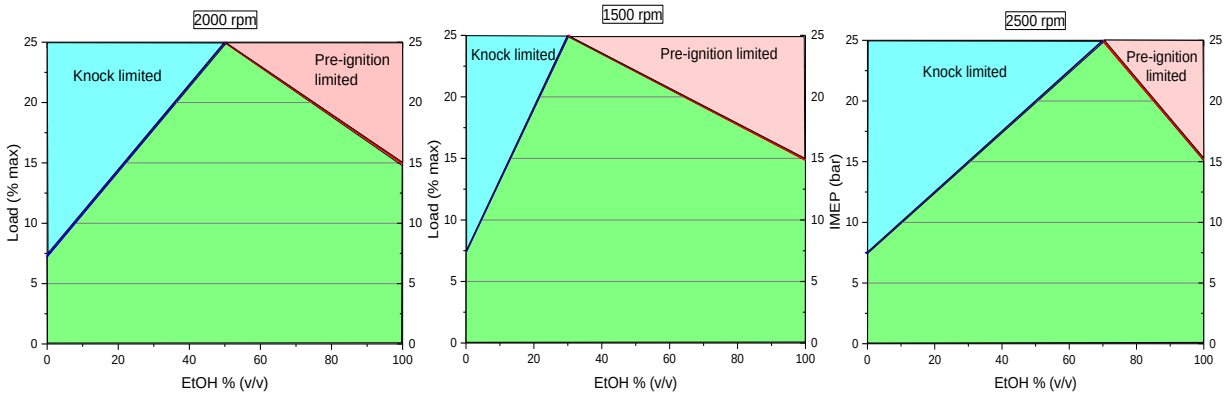

Figure 2. Hypothesis of the Pre-ignition limits on Octane-on-Demand experiments

Keywords: Octane-on-Demand, knocking, pre-ignition, ethanol

Proceedings of International Conference on Sustainable Energy and Environmental Challenges (3rd SEEC), December 18-21, 2018, IIT Roorkee, India

SEEC No.154

INVESTIGATION OF INFLUENTIAL PARAMETER IN THE SUPERCRITICAL FLUID EXTRACTION OF TURMERIC ROOT: A SCREENING DESIGN STUDY

Priyanka
Chemical engineering department
Shiv Nadar University, Dadri
priyanka@snu.edu.in

Shabina Khanam
Chemical engineering department
IIT Roorkee
shabifch@iitr.ac.in

ABSTRACT

Supercritical CO_2 extraction of turmeric root is carried out at different operating conditions to investigate the most influential parameter. Screening design is applied on selected operating parameters such as pressure, temperature, solvent flow rate, particle size and addition of co-solvent considering oil yield as response. These parameters were varied as 200-400 bar, 40-60°C, 5-15 g/min, 0.-0.73 mm and 0-15% of solvent flow rate. % contribution for pressure, temperature, flow rate, particle size and co-solvent are found as 0.1, 63.51, 13.44, 3.07 and 12.29%, which indicates that temperature is the most important parameter and pressure is least important parameter in the extraction of turmeric root. Therefore, it can be concluded that pressure can be fixed at a constant value while varying other parameters for the optimization. Screening design is emerged as a very useful technique to save the time and money also.

***Keywords*:** Turmeric root, Screening design, Supercritical fluid extraction

INTRODUCTION

Turmeric root (Curcuma longa) is a typical rhizome/ perennial herb of Zingiberaceae family, mostly cultivated in the warmer parts of world such as India and China [1]. Turmeric powder is widely used for stomachache as a blood purifier, carminative, appetizer and tonic whereas the essential oil extracted from turmeric root possesses anti-inflammatory, antifungal, antihepatotoxic and antiarthritic activities [1]. To extract oil from turmeric root, supercrticial fluid extraction (SFE), mainly by super-critical carbon dioxide (SC-CO_2) is being used because it results in extract with no organic solvent contamination. There are numerous operating parameters reported in literature affecting the extraction process such as temperature, pressure, solvent flow rate, particle size, addition of co-solvent, extraction time, properties of bed, initial content of oil, type of matrix of raw material and pretreatment of raw materials [2]. These parameters need to optimize for the maximum extraction of solute form solid matrix. For this, widely employed optimization technique i.e. design of experiment is used through various software such as Design expert, Minitab and Quantum XL etc. Design of experiment technique provides a list of experimental runs considering different combination of operating parameters. Number of experimental runs is directly proportional to the number of operating parameters considered. To reduce the number of experimental runs, operating parameters first need to be screened based on their contribution to maximize the extraction yield. Design expert is providing a new feature name screening design to avoid more number of experimental runs which provides least influential parameter of the process. The key objective of Screening design is to find most influential input parameter related to desired output amongst all potential parameters [3].

In present work, SFE technique is used to extract turmeric oil from turmeric root. Screening design is applied on five operating parameters such pressure, temperature, solvent flow rate, particle size and addition of co-solvent considering oil yield of turmeric root as response. Fatty acid analysis of turmeric oil is also performed using GC analysis.

METHODLOGY

SFE Setup and procedure

In present work, SFE (1000F) system, purchased from Thar Technologies Inc., Pittsburgh was used for the extraction of turmeric root oil. The liquid CO_2, supplied from the cylinder, is pressurized by high pressure pump and then mixed with the co-solvent supplied through co-solvent pump. The mixture is heated to a desired temperature through the heat exchanger to attain supercritical conditions. Further, it enters into the extraction vessel where it acquires a desired supercritical temperature and pressure. The turmeric root powder particles were kept into a stainless steel basket placed inside the extractor for easy and fast charging and discharging of the extraction cell. Then extract rich supercritical-CO_2 flows through a cyclone separator where extract is collected at lower pressure through drain value. The extracted turmeric oil was collected from sampling ports located at the bottom of separator in every five minute interval in the separate sample vials. If co-solvent was added, it was removed from the collected extract by

rotary vacuum evaporator and then co-solvent free turmeric oil samples were measured gravimetrically. Total cumulative extraction yield was calculated by summation of all oil samples extracted after 260 minutes. The same procedure was repeated for each experimental run.

Screening design

In present work, screening design was applied on five operating parameters such as pressure (A), temperature (B), flow rate (C), particle size (D) and co-solvent (E) where extraction oil yield (EOY) was considered as response. These parameters were varied as 200-400 bar, 40-60 °C, 5-15 g/min, 0.-0.73 mm, and 0-15% of solvent flow rate. However, extraction time and amount of feed material were fixed at 260 min and 100 g, respectively. EOY was caluculated using Eqn. (1).

$$\text{EOY}(\%) = \frac{\text{Total Oil extracted (g)}}{\text{Solid sample (g)}} \times 100 \qquad (1)$$

Fatty acid analysis

Identification and quantification of fatty acids of turmeric root oil was carried out by using Thermo Trace Ultra Gas chromatograph (Thermo Scientific, USA) by converting fatty acid in to fatty acid methyl estres (FAME). Fatty acid peaks were identified using a standard 37 FAME mixture.

RESULTS

Design Expert 10 (trail version) was used for screening purpose, which suggested 10 numbers of experimental runs using minimum run resolution (iv) varying operating parameters into two levels only as shown in Tab. 1.

Experimental runs provided in Tab. 1 were performed and response was used to evaluate the effect of different terms available in Main effect model as shown in Eqn. (2).

$$\text{EOY} = 0.009408 - 1.667 \times 10^{-6} \times \text{A} + 0.000417 \times \text{B} + 0.000383 \times \text{C} - 0.003459 \times \text{D} + 0.000244 \times \text{E} \qquad (2)$$

To evaluate significance of each parameter on EOY, a student's t-test was performed and plotted as a Pareto chart showing t-value of effect and rank of each parameter which is given in Fig. 1. It shows that pressure is least influential parameter in the SFE of turmeric root whereas temperature is found as most influential parameter. % contribution for each operating parameter are estimated as 0.1, 63.51, 13.44, 3.07 and 12.29% for pressure, temperature, flow rate, particle size and co-solvent respectively as given in Tab. 2. Main effect model, shown as Eqn. (2), is fitted with the experimental data which shows well agreement as R^2 value is close to unity.

TABLE 1: SCREENING DESIGN FOR THE SFE OF TURMERIC ROOT OIL

Run	A	B	C	D	E	EOY
1	200	40	15	0.2	0	0.031
2	400	60	15	0.2	0	0.04
3	400	60	5	0.73	15	0.037
4	400	40	5	0.73	0	0.025
5	200	60	15	0.2	15	0.043
6	200	60	15	0.73	0	0.035
7	400	40	15	0.73	15	0.033
8	200	40	5	0.73	15	0.03
9	400	40	5	0.2	15	0.028
10	200	60	5	0.2	0	0.036

Saturated and unsaturated fatty acid contents of turmeric root oil are found using gas chromatography as shown in Fig. 2. Saturated fatty acids (SFA) identified in the turmeric oil were: Butyric acid, Caproic acid, Caprylic acid, Undecylic acid, Lauric acid, Myristic acid, Pentadecylic acid, Palmitic acid and Arachidic acid whereas unsaturated fatty acids (USFA) were: cis-10-Pentadecylic acid, cis-10-Heptadecenoic acid, trans-9-Oleic acid, cis-9-Oleic acid, Linoleic acid, Linolenic acid,cis-11,14,17-eicosatrienoic acid and cis-5,8,11,14-Eicosatetraenoic acid. Both SFA and USFA are necessary for the human body; however, USFA should be in higher proportion to promote good cholesterol. Oleic acid (cis and trans) is the major monounsaturated fatty acid (MUFA) found in turmeric oil.

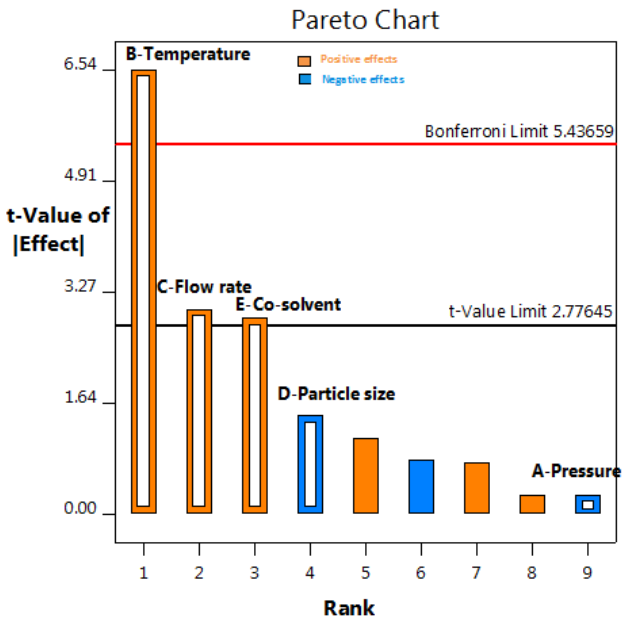

FIGURE 1: RANK OF OPERATING PARAMETERS BASED ON THEIR CONTRIBUTION

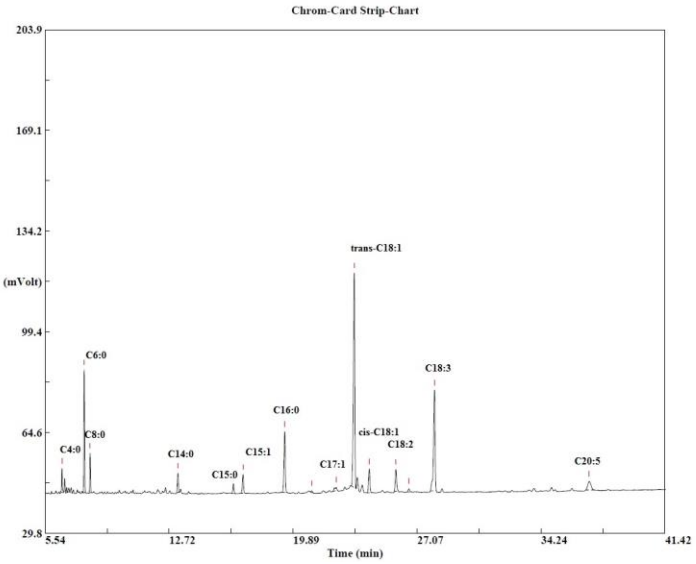

FIGURE 2: GAS CHROMATOGRAPH OF FATTY ACID MIXTURE OF TURMERIC OIL.

TABLE 2: CONTRIBUTION OF TERMS TO MAXIMIZE THE EOY OF TURMERIC ROOT

Term	Sum of squares	Standardized effect	% contribution
A	-0.000333	$2.5*10^{-5}$	0.101616
B	0.00833	0.00015625	63.5098
C	0.003833	$3.3062*10^{-5}$	13.4387
D	-0.001833	$7.5625*10^{-6}$	3.07387
E	0.003667	$3.025*10^{-5}$	12.2955
AB	0.00141421	$3.2667*10^{-6}$	1.32778
AC	0.000333	$6.0167*10^{-6}$	2.44555
AD	0.000942809	$2.0167*10^{-6}$	0.8197
BD	-0.001	$7.35*10^{-6}$	2.9875

CONCLUSION

Screening design study on supercritical fluid extraction of turmeric root oil results that pressure is least influential parameter out of all five parameters such as pressure, temperature, flow rate, particle size and co-solvent. Hence, pressure can be fixed at a constant value while varying other parameters for the optimization. Screening design is emerged as a very useful technique to save the time and money also. Turmeric oil comprises of Oleic acid as monounsaturated fatty acid whereas, Linoleic acid (22.56%) and Linolenic acid (21.3%) are available as major omega-6 unsaturated fatty acid (USFA), which are very beneficial for human health.

REFERENCES

[1] Priyanka. and Khanam, S. 2018. "Influence of operating parameters on supercritical fluid extraction of essential oil from turmeric root". J. Clean. Prod., 188, pp. 816–824.

[2] Rai, A., Mohanty, B. and Bhargava, R., 2016. "Supercritical extraction of sunflower oil: A central composite design for extraction variables". Food chemistry, 192, pp. 647-659.

[3] Sharif, K.M., Rahman, M.M., Azmir, J., Mohamed, A., Jahurul, M.H.A., Sahena, F. and Zaidul, I.S.M., 2014. "Experimental design of supercritical fluid extraction – A review". Journal of Food Engineering 124, pp. 105–116.

ISEES
Membership Form

International Society for Energy, Environment & Sustainability

Membership Form

Photo

I would like to join ISEES and take advantage of all the membership benefits					
First Name		Middle Initial		Last Name	
Membership No. (If you already have):			Designation:		
Age:	Date of birth : Date / Month / Year			Sex: M/F	
Educational Record					
Degree/s:			Specialisation:		
Office Address			**Residence Address**		
City:	State:		City:	State:	
PIN:	Telephone:		PIN:	Telephone:	
Mobile:			Email ID:		
Payment Details (cheque/cash/DD payable at SBI IIT Kanpur in favour of *ISEES*)					
Amount:	Cash/DD /Chq. No:		Date:		
Bank:			Branch:		
Date:			Signature		

	Type of Membership	Annual Membership Fee	Five –Year Membership Fee	Life Membership Fee (10 Years)
India / SAARC Countries	Student Members	1000 INR	---	----
	Members / Fellow	2000 INR	5000 INR	10000 INR
	Corporate	10000 INR	---	50000 INR
USA, Europe and Developed Countries	Student Members	50 US $	---	---
	Members / Fellow	100 US$	250 US$	500 US$
	Corporate	500 US$	---	2500 US$

Mailing Address: Dr. Avinash Kumar Agarwal
Department of Mechanical Engineering, IIT Kanpur
Kanpur 208016, UP, India
08765599882 (Sujeet)
Email: akag@iitk.ac.in

Note: Attach a Demand Draft& a self-attested copy of your ID proof along with the duly filled and signed form.

Schedule of III SEEC

18th - 21st December 2018

Final Schedule of Third SEEC

IIT Roorkee

18-21st December 2018

18th December 2018			
14:00 to 14:30	Inaugural Ceremony		
14:30 to 16:00	Award Ceremony Fellow Induction Ceremony Book Release Function Chief Guest: **Dr. V K Saraswat**, Hon. Member, NITI Aayog		
16:00 to 16:40	High Tea		
16.45 to 17.30	Plenary Talk-1 **Dr. V K Saraswat**, Hon. Member, NITI Aayog		
17.30 to 18.15	Plenary Talk – 2 **Dr. Gurfan Beig**, Safar		
18.15 to 19.45	ISEES Young Scientist and Best Thesis Award Lecture Session (SPL-1)		
20.00 to 23.00	Conference Banquet-1		
19th December 2018			
09.00 to 09.45	Plenary Talk-3 *The Evolution of Laser Ignition Over more than Four Decades* **Prof. Ernst Wintner**, Technical University of Vienna, Austria		
09:50 to 11:20	Session A-1 Advances in IC Engines-1	Session B-1 Solar Energy-1	Session C-1 Environmental Biotechnology-1
11:20 to 11:50	Tea Break		
11:50 to 13:30	Session A-2 Combustion	Session B-2 Environmental Sustainability	Session C-2 Environmental Biotechnology-2
13:30 to 15:00	Poster Session-1 (For all Posters) followed by Lunch		
15:00 to 16:30	Session A-3 Coal and Biomass Combustion/Gasification	Session B-3 Water Pollution	Session C-3 Biomass to Fuels/ Chemicals-1
16:30 to 17:00	Tea Break		
17:00 to 18:30	Session A-4 Advances in IC Engines-2	Session B-4 Solar Energy-2	Session C-4 Biomass to Fuels/ Chemicals-2
18:30 to 19:30	General Body Meeting of ISEES (For ISEES members only)		
19.30 to 20.15	Plenary Talk-4: *Transition to Low Carbon Energy Mix for India* **Dr. Bharat Bhargava**, ONGC Energy Center		
20.30- 23.00	Conference Banquet-2 (Venue: LHC)		
20th December 2018			
09.00 to 11.00	Session A-5 Advances in I.C. Engines-3	Session B-5 Energy and Environmental Sustainability-1	Session C-5 Environmental Biotechnology-3

11:00 to 11:30	Tea Break		
11:30 to 13:00	Session A-6 Atomization and Sprays	Session B-6 Combustion/ Gas Turbines/ Fluid Flow/ Sprays	Session C-6 Sustainable Transportation and Environmental Issues
13:00 to 14:30	Poster Session-2 (For all Posters) followed by Lunch		
14:30 to 16:30	Session A-7 New Concepts in Energy Conservation	Session B-7 Energy and Environmental Sustainability-2	Session C-7 Waste to Wealth
16:30 to 17:00	High Tea Break		
17.00 to 18.00	Plenary Talk 5: **Prof. Ajit Chaturvedi**, IIT Roorkee		
18.00 to 19.00	**Cultural Program** by Students of IIT Roorkee		
19.30 Onwards	**Fellows Dinner** (For Fellows of ISEES and Select Invitees only)		
21st December 2018			
09:00-09:45	Plenary Talk – 6: Dr. Prashant Gargava, Member Secretary, CPCB		
09:50 to 11:30	Session A-8 Rapid Fire Poster Session Engine/Fuels/Emissions	Session B-8 Rapid Fire Poster Session Renewable and Sustainable Energy	Session C-8 Rapid Fire Poster Session Biotechnology
11:30 to 12:00	Tea Break		
12:00 to 12:45	**Panel Discussion** Challenges, Opportunities and Directions for National Energy Security		
12.45 to 01.30	Valedictory Session and Best Paper/ Poster Awards Ceremony		
14:30 to 15.30	Lunch and Closure		

December 18, 2018

Session SPL-1 ISEES Young Scientist and Best Thesis Award Lecture Session		
6.15-6.30 PM	Akhilendra Pratap Singh University of Wisconsin, Madison	Advanced Combustion Techniques for Internal Combustion Engines: Strategies, Achievements and Future Directions
6.30-6.45 PM	Souvick Chatterjee	Innovation Through Integrated and Collaborative Research
6.45-7.00 PM	Nikhil Sharma Chalmers Univ. of Tech., Sweden	Particulate Bound Trace Metals and Soot Morphology of Gasohol Fueled Gasoline Direct Injection Engine
7.00-7.15 PM	Pooja Devi	Materials Engineering for Sustainable Solutions Towards Environment and Energy
7.15-7.30 PM	Vikram Kumar	New Approach for Environment Friendly Lubrication
7.30-7.45 PM	Nithin K.S.	Polymer Nanocomposite Based Spectral Converters: A Considerate Approach Towards Refined Solar Competence and Improved Short Wavelength Harvesting Efficacy of Solar Cells

December 19, 2018

Session A-1 Advances in IC Engines-1		
09:50-10.20	Keynote: V. Ganesan IIT Madras	Trends in Automotive Engines for Emission Reduction
10:20-10:40	Invited: Pravesh Chandra Shukla Indian Institute of Technology Bhilai	Particle Number Emission from Compression Ignition Engines
10:40-10:50	Vikram Kumar and Avinash Agarwal	SEEC-119: Performance And Emissions Of A Methanol Fueled Genset Engine
10:50-11:00	Veena Chaudhary and Rakesh. P. Gakkhar	SEEC-112: Exergy Analysis of DI diesel engine fuelled with Neem Biodiesel with DEE additive
11:00-11:10	Tushar Agarwal and Avinash Agarwal	SEEC-139: Comparative Analysis of Performance, Regulated and Unregulated Emissions for Different Methanol-Gasoline Blends in a Single Cylinder Two-Wheeler MPFI Engine
11:10-11:20	Chandan Kumar, K.B. Rana, Brajesh Tripathi and Ashish Nayyar	SEEC-88: Evaluation of Combustion Characteristics of Diethyl Ether–Nitromethane–Diesel Blends in CI Engine
Session A-2 Combustion		
11:50-12.20	Keynote: Gabrial D. Roy CPNE Consultants	Sustainable Propulsion Fuels: Challenges, Path Ahead
12:20-12:50	Keynote: Debasis Chakraborty Defence Research and Development Laboratory, Kanchanbagh	Numerical Simulation Of High Speed Combustion
12:50-13:00	Denil Vachani, Nirmit Kapadiya, Nisarg Vagadiya, Sneha Gautam and Abhishek Gupta	SEEC-095: Assessment of indoor air quality of construction and renovation site at Rajkot City- A Case Study
13:00-13:10	Gyan Sagar Sinha, Niraj K Mishra and P Muthukumar	SEEC-026: Parametric Analysis of Porous Burner With Pressure Kerosene Cooking Stove
13:10-13:20	Abhimanyu Bandyopadhyay, Sudipta De and Subha Mondal	SEEC-004: Thermodynamic Modelling And Exergy Analysis of a Tri-Generation Process
13.20-13.30	Devashish Chorey and Devendra Deshmukh	SEEC-157: Effect of Multiple Injections on Modified Heavy Duty Single Cylinder Diesel Engine: Spray, Combustion and Emission Analysis
Session A-3 Coal and Biomass Combustion/ Gasification		
15:00-15:30	Keynote: M. Razi Nalim, Purdue University Indianapolis	Cost Reduction & Scale Expansion For Structural Carbon - A Path to Environment Decarbonization
15:30-15:50	Invited: Santanu De IIT Kanpur	Modeling of Turbulent Reacting Sprays
15:50-16:00	Arvind Singh Bisht and N S Thakur	SEEC-12: Pine Needles Biomass Gasification Based Electricity Generation in the Indian Himalayan Region: Drivers & Barriers
16:00-16:10	Anil Kumar Sakhiya, Apoorv Chaturvedi, Vivek Barasara, Krunal Panchal, Darshit Upadhyay and Rajesh Patel	SEEC-27: Elemental and Heat Loss Analysis of Different Feedstock in the Downdraft Gasifier
16:10-16:20	Aravind B, Deepak Kumar Saini and	SEEC-002: A Powerful Miniaturized Thermoelectric based power

	Sudarshan Kumar	generation system using a Stepped Planar Multi-combustor
16:20-16:30	Bhoopendra Pandey and Yogesh Kumar Prajapati	SEEC-120: Thermodynamic Equilibrium Modeling of a Downdraft Gasifier: Stoichiometric Model
Session A-4 Advances in IC Engines-2		
17:00-17:30	Keynote: P.A. Lakshminarayanan Simpson and Co. Ltd, Chennai	Understanding some Aspects of in-Cylinder Behaviour of a Direct Injection Diesel Engine by Experiments
17:30-18:00	Keynote: S. Maji, Delhi Institute of Tool Engineering	Vehicular Emissions and its impact on AQI in Urban Areas
18:00-18:10	Sagar Srivastava and Avinash Agarwal	SEEC-137: Effectiveness Of Catalytic Converter In Reducing Regulated Emissions From Methanol Fuelled Medium Duty Spark-Ignition Transportation Engine
18:10-18:20	Suvam Bhadra, Arnab Das and J Thangaraja	SEEC-23: Comparative Evaluation of Energy and GHG Emissions of Diesel and Biodiesels from Jatropha Oil and Waste Cooking Oil
18:20-18:30	Vishnu Singh Solanki and Avinash Agarwal	SEEC-140: 1-D Simulation and Modelling of Gasoline Compression Ignition (GCI) Engine
Session B-1 Solar Energy-1		
09:50-10.20	Keynote: Himanshu Tyagi IIT Ropar	Sustainable Energy Application: Water Purification
10.20-10.30	Kirti Tewari and Rahul Dev	SEEC-093: Performance Analysis of PVT Non Metallic Solar Water Heater
10.30-10.40	Prashant Saini, Satvasheel Powar, Pradeep Kumar and Atul Dhar	SEEC-76: Effect Of Atmospheric Temperature and Wind Speed on the Parabolic Trough Collector
10:40-10:50	Rahul Dev, Ajaya Bharti, Aman Kumar, Ankit Meena, Amaresh Kumar Singh, Amarendra Kumar and Mohit Dev	SEEC-67: Design, Construction and Thermal Performance of a Solar House
10:50-11:00	Gaurav Kumar, Piyush Pal, Pulkit Agarwal, Rahul Dev and Akhilesh Kumar Chauhan	SEEC-69: Embodied Energy, Pay-Back Period And Cost Analysis of Triple Slope Solar Still Integrated With Glass-Glass PV Module
11:00-11:10	Jatin Kumar Chaudhary, Ankul Prajapati, Rajeev Kanth, Jukka-Pekka Skön and Jukka Heikkonen	SEEC-94: Numerical Investigations on the Type-II Band Alignment and Quantum Efficiency of Multi-junction Solar Cell using Anderson's Rule
11:10-11:20		
Session B-2 Environmental Sustainability		
11:50-12.20	Keynote: Rajiv Sharma, Amity University	Funding Opportunities in India for Clean Energy Research
12:20-12:50	Keynote: Rajeev Kanth Savonia University of Applied Sciences, Finland	Role of Big-Data and Learning Analytics in Innovative Education System
12:50-13:00	Kamal Kumar Agrawal, Rohit Misra, Sandeep Parmar and Ghanshyam Das Agrawal	SEEC-010: Thermal Performance Analysis of Earth-Air-Pipe-Heat Exchanger System with Different Backfilling Materials
13:00-13:10	Kamal Kumar Agrawal, Rohit Misra and Ghanshyam Das Agrawa	SEEC-011: Effect of Soil Moisture Contents on Thermal Properties of Soil for Earth-Air-Pipe Heat Exchanger System
13:10-13:20	Geleta Fekadu and Sudhakar Subudhi	SEEC-019: Novel Experimental Study of Internally Cooled Dehumidifier For Liquid Desiccant System
12:20-13:30	Manivannan R. Rajan and Ganesh L. S.	SEEC-106: Environment Protection And Sustainability – An Assessment of Practices in Indian Electric Power Companies
Session B-3 Water Pollution		
15:00-15:30	Keynote: V S Pruthi IIT Roorkee	Bio-Removal of Cadmium by Microalgae Synchronized With Enhanced Lipid Production
15.30-15.40	Sunil Saini and Milind Rane	SEEC-104: Experimentation on Rotating Disk Based Water Purification System
15.40-15.50	Bharti Saini and Manish Kumar Sinha	SEEC-47: Wastewater Treatment Containing Oil Using Polyvinylidene Fluoride (PVDF) Ultrafiltration Membrane Modified With Functionalized Sio2 Nanoparticles
15:50-16:00	Varun Singh and Mohd Wasi	SEEC-61: Monitoring of Wastewater Quality: A Review
16:00-16:10	Mamta Sardare and Mamta Sardare	SEEC-79: NiO Used for the Treatment of Cr(Vi) Polluted Waste

		Water
16:10-16:20	Rajesh Kumar Venu and Gandhimathi Rajan	SEEC-065:Removal Of Glyphosate From Water By Heterogeneous Fenton Like Process Catalyzed With Nano-Scale Iron Manganese Binary Loaded Zeolite (NIMZ)
Session B-4 Solar Energy-2		
17:00-17:30	Keynote: R.D. Garg IIT Roorkee	Solar Energy with Geomatics for Sustainable Development
17:30-17:40	Sourav Kumar Bagchi, P Srinivasa Rao and Nirupama Mallick	SEEC-003: Feasibility of Utilizing Solar Drying Technique as Energy Efficient Process for the Qualitative Biodiesel Production from a Locally Isolated Microalga Scenedesmus Obliquus
17:40-17:50	Shahinur Rahman and Arif I Sarwat	SEEC-017: Voltage Profile Analysis of a Grid-Tied PV System During Known Intermittent Phenomenon
17:50-18:00	Ankita Sharma, Ravi Shankar Yadav and Dr. Bramha P. Pandey	SEEC-051: Performance Analysis of PbS Colloidal Quantum Dot Solar Cell at Different Absorption Coefficient
18:00-18:10	Kedumese U Mekrisuh, Dushyant Singh and Udayraj	SEEC-066: Numerical Analysis of Effect of Aspect Ratio and Flow Rate on The Performance of PCM Based Thermal Energy Storage System
18:10-18:20	Priyanka Kajal, Rajeev Ray, Satvasheel Powar, Suman Kalyan Pal	SEEC-087: Performance Analysis of Charge Transporting Layers in Perovskite Solar Cells With Varying Deposition Techniques
18:20-18:30	Akshay Rahore, Rahul Yadav and Himanshu Tyagi	SEEC-126: Numerical Study of Direct Contact Membrane Distillation Technique Coupled With Nanofluid-Based Direct Absorption Solar Collector
Session C-1 Environmental Biotechnology-1		
09:50-10.20	Keynote: Michael Sauer BOKU University of Natural Resources and Life Sciences, Austria	Industrial Microbiology for the Valorization of Carbon Containing Side Streams
10:20-10:40	Invited: Thallada Bhaskar, CSIR-IIP, Dehradun	Conversion of Biomass to Low-Sulfur Boiler Fuel and High Value Chemicals
10:40-10:50	Manpreet Kaur, Ranjeeta Bhari and Mehak Singh	SEEC-136: Statistical Optimization of Keratinase Production and Feather Degradation by Bacillus Licheniformis
10:50-11:00	Sartaj Khan and Vikas Pruthi	SEEC-145: Enhanced Lipid Accumulation in Oleaginous Yeast Under Stress Condition
11:00-11:10	Priyanka Priyanka and Shabina Khanam	SEEC-154: Investigation of Influential Parameter in The Supercritical Fluid Extraction of Turmeric Root: A Screening Design Study
11:10-11:20	Lalit M. Pandey and Ravi	SEEC-54: Enhancement of adsorption capacity of designed bentonite/alginate beads for effective removal of methylene blue dye.
11.20-11.30	Ravi Kumar Sonwani, Prarabdh Jain, Balendu Shekhar Giri, Ram Sharan Singh and Birendra Nath Rai	SEE0-058 Biodegradation Of Hexavalent Chromium By Acclimatized Pseudomonas Putida: Optimization And Kinetic Study
Session C-2 Environmental Biotechnology-2		
11:50-12.20	Keynote: Binod Parmeshwaran CSIR-NIIST, Triruvananthpuram	Utilization of Oil Palm Front Biomass for the Production of 2,3-Butanediol
12:20-12:40	Invited: Vivek Kumar Morya Centre for Energy and Environmental Sustainability, Lucknow	Developments in Enzyme-Mediated Single-Pot Fermentable Sugar Production from Lignocellulosic Biomass
12:40-12:50	Priyanka Nath, Arun Dhillon, Kedar Sharma and Arun Goyal	SEEC-006: Protein engineering of carbohydrate hydrolysing enzymes for enhancing activity for improved biomass saccharification
12:50-13:00	Ashish Yewale, Ravi Methekar and Shailesh Agrawal	SEEC-021: Development of Batch Model for Microbial Fuel Cell
13:00-13:10	Kunjan Junghare and Shyam Kodape	SEEC-029: Preparation of Electrochemically Generated Adsorbent using Ultrasonication for Fluoride Removal
13:10-13:20	Puja Mukherjee, Debabrata Bera, Lakshmishri Roy, Samayeeta Ghosh	SEEC-031: Novel approach of the effect of Microencapsulation on antioxidant activity from rice waste distiller's dried grains with soluble
13:20-13:30	Debeni Nongmaithem and Goud Vaibhav V.	SEEC-91: Sustainable Feedstock Scenedesmus Sp. Adiitec-Ii and Chloromonas Sp. Adiitec-Iii: Effect of Initial Ph and Nutrient Starvation on Growth and Lipid Yield
13.30-13.40	Balendu Shekher Giri, Ram Sharan	SEEC-042: Indoor Potted Plant Based Biofilter: Performance

	Singh, Anugunj Pal, Asmita Sarowgi, Yeshaswi Kaushik, V Thivaharan and Abhishek Jaiswal	Evaluation and Kinetics Study
Session C-3 Biomass to Fuels/ Chemicals-1		
15:00-15:30	Keynote: Amit Bhatnagar University of Eastern Finland	Microalgae: A Sustainable Solution for Diverse Environmental Challenges
15:30-15:50	Invited: R Praveen Kumar	Agro Industry Based Biorefineries: Opportunities for Integrated Biorefinery Systems in Cassava Sago Industries
15:50-16:00	Sukanta Roga, Pavan Gomatam and Kanigelpula Abhinash	SEEC-025: Studies of Methanol Production Processes from Various Sources and It's Applications
16:00-16:10	Kaustubh Khaire, Kakali Borah, Arun Goyal and Vijayanand Moholkar	SEEC-007: Pretreatment optimization of sugarcane leaf tops for recovery of holocellulose
16:10-16:20	Philip Bernstein Saynik and Vijayanand S. Moholkar	SEEC-024: A comparative study of the pyrolytic products of pre-treated samples of Arundo donax and Prosopis juliflora
16:20-16:30	Sachin Kumar Tomar and Saswati Chakraborty	SEEC-60: Impact of Thiocyanate (SCN-) on Granular Characteristics after Disintegration of Granules
Session C-4 Biomass to Fuels/ Chemicals-2		
17:00-17:30	Keynote: Daniel CW Tsang The Hong Kong Polytechnic University, China	Urban Food Waste Valorization into Bio-Based Chemicals and Energy
17:30-18.00	Keynote: Sunil K. Khare IIT Delhi	Halophiles As Sources Of Novel Biocatalysts
18:00-18:10	Shalini Sahani and Yogesh Chandra Sharma	SEEC-43: Synthesis of barium cerate as a heterogeneous catalyst for the Biodiesel production; Kinetics and Thermodynamic study
18:10-18:20	Reena Singh and Yogesh Chandra Sharma	SEEC-49: Biodiesel production from microalgal oil using barium-calcium-zinc mixed oxide base catalyst: optimization and kinetic studies
18:20-18:30	Ravneet Kaur, Poonam Gera, Mithilesh Kumar Jha and Thallada Bhaskar	SEEC-71: Catalytic Hydrothermal Liquefaction of Castor Residue: Effect on Product Yield and Distribution of Liquid Product
December 20, 2018		
Session A-5 Advances in I.C. Engines-3		
09:00-09:30	Keynote: R P Gakkhar IIT Roorkee	Exergy Analysis as an Input for Better Engine
09:30-09:50	Invited: Anirudh Gautam	Development of Methanol Fuelled Trainset for Bangalore Suburban Railways
09:50-10:00	Saket Verma, K Kumar, L M Das, S C Kaushik and S K Tyagi	SEEC-035: Experimental Analysis on The Effect of Hydrogen Induction and Manifold Injection in a Diesel Dual Fuel Engine
10:00-10:10	Vikram Kumar and Avinash Agarwal	SEEC-118: Optimization of Methanol Powered Diesel Engine
10:10-10:20	Ankur Kalwar and Avinash Agarwal	SEEC-121: Microscopic Spray Characteristics of Methanol Fuelled MPFI Engine Injector
10:20-10:30	Aniruddha Joshi	SEEC-129: Optimized Production Process For WCO Based Biodiesel By Using DOE
10.30-10:40	Prashumn Prashumn and Avinash Agarwal	SEEC-138: Methyl-Ether Fuelled Direct Injection Heavy-Duty Compression Ignition Engine
10:40-10:50	Dhananjay Kumar and Avinash Agarwal	SEEC-155: 1-D Modelling and Simulation of 4-Cylinder 4-Stroke SI Engine Using GT-Suite
Session A-6 Atomization, Sprays and Combustion		
11:30-12:00	Keynote: Swarnendu Sen Jadavpur University, Kolkata	Instability Control in Natural Circulation Loop
12:00-12:20	Invited: Kirti Bhushan Mishra	What Do We Reliably Know about the Technological Risks of Biofuels?
12:20-12:30	Utkarsha Sonawane and Avinash Agarwal	SEEC-052: To Investigate Macroscopic Spay Characteristics for Methanol Blended Fuels
12:30-12:40	Hardikk Valera and Avinash Agarwal	SEEC-116: Effects of Spray Characteristics on Emissions From a Methanol Fuelled Spark-Ignition Engine in Indian Context
12:40-12:50	Ashutosh Jena and Avinash Agarwal	SEEC-117: Effect of Inlet Air Temperature on Microscopic and Microscopic Spray Characteristics of Methanol Blend for two

		Wheeler Applications
12:50-13:00	Vaishali Vasudeva, Vidushi Pant and Manoj Kushwaha	SEEC-114: An Experimental Study on Pelletization of Horticultural Waste and Combustion Analysis
Session A-7 New Concepts In Energy Conservation		
14:30-15:00	Keynote: V K Shrivastava	**Title Awaited**
15:00-15:20	Invited: Dev Prakash Satsangi B.T. Kumaon Inst. of Tech., Dwarahat	Impact of Miscibility Additives for Methanol-Diesel Blends and Their Impact on Noise, Vibrations and Combustion Characteristics
15:20-15:30	Pushpendra Kumar Shukla, Dr. P. Anil Kishan and Dr. Atul Dhar	SEEC-99: Effect of Heating Coil Configuration on Energy Requirements of Local Heating System
15.30-15.40	Vimal Patel and Mohsinali Batti	SEEC-50: Effect of Intercooler on The Performance Parameters of Axial Flow Compressor
15:40-15:50	Chunkyraj Khangembam and Dushyant Singh	SEEC-72: Experimental Study of Two-Phase Air-Water Mist Jet Impingement Cooling on Cylinder
15:50-16:00	Sandeep Yadav, Akash Kumar, Viswanath Balakrishnan and Atul Dhar	SEEC-073: Carbon Nano Tube Based Substrate for Selective Catalytic Reduction (SCR) based Nox Reduction
16:00-16:10	Chandrashekhar Jawalkar	SEEC-152: An Environmentally Friendly approach Using Coffee as a lubricant for thread cutting application
16:10-16:20	Apakrita Tayade, Sangram Patil, Vikas Phalle, Faruk Kazi and Satvasheel Powar	SEEC-101: Remaining Useful Life (RUL) Prediction of Bearing by using Regression Model and Principal Component Analysis (PCA) Technique
Session B-5 Energy and Environmental Sustainability-1		
09:00-09:30	Keynote: Nitin Labhasetwar NEERI, Nagpur	Nano- and other Low-cost Materials for Cleaner Energy and Environmental Applications
09:30-09:50	Invited: Nirendra Nath Mustafi Rajshahi University, Bangladesh	Energy Sector and Sustainability – Bangladesh's Perspective
09:50-10:00	Rhythm Singh	SEEC-032: Rooftop PV Aspirations of the National Solar Mission and the Renewable Energy Norms of Griha: the Missing Link?
10:00-10:10	Sandeep Anwani and Ravi Methekar	SEEC-046: Economic and Environmental analysis of Recycling Process for Spent Li-Ion Batteries Using Strong Acids
10:10-10:20	Krishna Mani Mishra and Onkar Singh	SEEC-059: Thermodynamic Review Of Trigeneration Systems For Power, Heating And Cooling Requirements
10:20-10:30	Gladstone Philip, Kurien Oomman, Bala Ganesa Moorthy Arumugam, Robin Thomas, Boopathi Arjunan and Kartik G	SEEC-122: Creation of Portable Smart Solid Waste Community bin using Advanced Technologies
10.30-10:40	Preethi Mukkani and Pauline S	SEEC-123: Comparative Study of Electrode Material for Treatment of Leachate by using Electrocoagulation
10:40-10.:50	Mohammad Dilnawaz Azmi and Dr. Rajesh Maithani	SEEC-127: Parametric Optimization of System Parameters of a Roughened Solar Air Heater with V-Shaped Dimpled Surface.
Session B-6 Combustion/ Gas Turbines/ Fluid Flow/ Sprays		
11:00-11:30	Keynote: Amitava Datta Jadavpur University, Kolkata	Sustainability Transition in Indian Power Sector: Role of Distributed Generation
11:30-12.00	Keynote: Rajat Agarwal IIT Roorkee	Competitive Advantages Through Sustainability
12.00-12:10	Pranjal Kumar and Onkar Singh	SEEC-074: Investigations on Integrating SOFC with Gas Turbine for Performance Enhancement and Sustainable Energy
12:10-12:20	Gaitry Arora and Onkar Singh	SEEC-077: Thermodynamics Study of Environment Friendly Air / Steam Combined Cycle
12:20-12:30	Tushar Adgale, Anshul Sharma and Niraj Mishra	SEEC-081: Performance Analysis of Tubular Air Preheater Using Tape Inserts
12:30-12:40	Ketan Ganatra and Dushyant Singh	SEEC-084: Comparison of the Original And the Modified V2f Model for Impinging Round Jet Cooling from a Cylinder
12:40-12:50	Hrushikesh Naik and Dinesh Pappu Reddy	SEEC-132: Study and Analysis of Fly Ash for Stowing in Underground Coal Mine Voids
Session B-7 Energy and Environmental Sustainability-2		
14:30-15:00	Keynote: V. S. Moholkar IIT Guwahati	Xylitol Production From Sugarcane Bagasse
15:00-15:30	Invited: Chandrajit Balomajumder	Delignification and Microbial Hydrolysis for Bioethanol Production

	IIT Roorkee	
15:30-15:40	Abubakar Gado Abubakar, Anbazhagi Muthukumar and Muthukumar Muthuchamy	SEEC-045: Wind-Solar PV Hybrid Electricity Generation and Application to Electric Vehicles, a Sustainable Solution to Carbon Emission Reduction in India
15:40-15:50	Shweta Singh and Saswati Chakraborty	SEEC-048: An Assessment on The Characteristics of Acid Mine Drainage (AMD) in North Eastern Parts of India
15:50-16:00	Jayalatha N A and Chella Purushothaman Devatha	SEEC-128: Removal of Triclosan by Bacillus Licheniformis from Domestic Wastewater, Mangalore Region
16:00-16:10	Rashmi Hr and Devatha C P	SEEC-131: "Experimental Studies on Dewatering of Sewage Sludge Using Skeleton Material
16:10-16:20	Ranjeeta Bhari and Rithampreet Kaur	SEEC-133: Potential Keratinolytic Activity of Aspergillus Gorakhpurensis for Degradation of Melanized Chicken Feathers and Sustainable Development
16:20-16:30	Prashant Kumar and Sudeshna Bagchi	SEEC-151: AHP Based Drastic Model for Grounwater Vulnerability Assessment in Fatehgarh Sahib Punjab
Session C-5 Environmental Biotechnology-3		
09:00-09:30	Keynote: Arvind Kumar Bhatt Himachal Pradesh University, Shimla	Biobutanol: A Combustion Engine Friendly Biofuel Through Biotechnological Intervention
09:30-09:50	Invited: V.K. Garg Central University of Punjab, Bathinda	Solid Waste Management using Vermitechnology
09:50-10:10	Invited: Kashyap Kumar Dubey, Central University of Haryana, Mahendergarh	Strategies for treatment of hospital wastewater using integrated technology
10:10-10:20	Sandeep Anwani and Ravi Methekar	SEEC-020: Reductive Leaching of Spent Li-Ion Batteries to Recover Cobalt Oxalate Using Sulphuric Acid as a Leachant
10:20-10:30	Gisha Singla, Meena Krishania, Pankaj P. Sandhu, Rajender S. Sangwan and Parmjit S Panesar	SEEC-033: Value Addition of Kinnow Juice Processing Industry by-products using Green solvents
10.30-10:40	Y. Nikhileshwar Reddy, Neeraj S. Thakur, Sanjam Chandna and Jayeeta Bhaumik	SEEC-056: Towards the development of pyrrole based photosynthetic nanopigments for the valorization of agricultural biomass via light harvesting
10:40-10.:50	Simarpreet Kaur Chawla and Dinesh Goyal	SEEC-057: Bioconversion of sugars in acid hydrolysates of rice and wheat straw into lactic acid by Bacillus sonorensis DGS15
10:50-11:00	Yogendra Singh Solanki, Madhu Agarwal, Sanjeev Gupta, Pushkar Shukla and A B Gupta	SEEC-082: Fluoride Removal Performance of a Noval Adsorbent
Session C-6 Sustainable Transportation and Environmental Issues		
11:00-11:30	Keynote: S S Jain IIT Roorkee	Effect of Pavement Conditions on Road Safety
11:30-12:00	Keynote: M Parida IIT Roorkee	Sustainable Urban Mobility Strategies for Indian Cities
12:00-12:20	Invited: R. P. Singh, IIT Roorkee	Microalgal Biofuel: Molecular Strategies and Implications
12:20-12:40	Invited: Inderdeep Singh, IIT Roorkee	Sustainable Composite Materials: Expectations and Reality
12:40-13:00	Invited: Bhola R. Gurjar IIT Roorkee	Current Status of $PM_{2.5}$ Pollution and Its Mitigation in India
Session C-7 Waste to Wealth		
14:30-15.00	Keynote: S N Naik IIT Delhi	A Biorefinery Approach For The Utilization Of Waste Generated From Natural Indigo Dye Production Process
15.00-15:20	Invited: Deepak Pant Central University of Harayana, Mahendergarh	Economy in Waste Plastic Recycling
15.20-15.40	Invited: Vinod Kumar Center of Innovative and Applied Bioprocessing, Mohali	Production and purification of a robust L-asparaginase having low-glutaminase activity from Bacillus Sp.: In vitro evaluation of anti-cancerous properties
15:40-15:50	Nagendra Prasad Yadav and Abhishek Kumar	SEEC-022: Prediction of Potential of Energy Generation from Municipal Solid Waste Through Incineration Technology
15:50-16:00	Ankita Mukherjee, Dr. Biswajit Ruj, Dr. Parthapratim Gupta and Dr. A.K.	SEEC-040: Pyrolysis of waste Polyethylene Terephthalate (PET): A Strategy for Plastic Waste to Product Recovery

	Sadhukhan	
16:00-16:10	Rengarajan Manivannan and Gopinath S	SEEC-062: A Practical Framework for Pursuing "Wealth from Waste" In Indian Industries
16:10-16:20	Sherin Parwin P.M, Sathiya Prabhakaran S.P, Swaminathan G	SEEC-068: Feasibility of The Textile Effluent Sludge as An Alternate Raw Material for Cement Production
16:20-16:30	Varun Agarwal, Garvit Singh, Kushal Joshi and Shreyas Desai	SEEC-105: Comparative analysis of normal concrete by using of granite cutting waste for construction work

December 21, 2018

Session A-8 Engine/Fuels/Emissions Rapid Fire Poster Session - I (4 Minutes Each Including Q&A) (4 Best Poster Awards)		
SEEC-008	Ajit Kolekar and Aniruddha Joshi	Performance Analysis of C.I. Engine by Using DME Fuel
SEEC-013	Harishchandra Dhumal, Amardeep Dongare, Nikhil Raut and Ajit Kolekar	Computational Simulation of Domestic Burner With Different Fuels and Varying Geometry of Bores
SEEC-015	Debjit Kundu, Sourav Sarkar, Achintya Mukhopadhyay and Swarnendu Sen	Numerical Study of a Laminar Flat Plate Boundary-Layer Diffusion Flame With Fuel Injection
SEEC-030	Sukanta Roga, Gundumogula Pavankumar and Shiva Seri	Study of Specific Outputs and Emission Characteristics of Engines by Using Suitable HCNG Fuel Blending
SEEC-036	Kamlesh Sasane	Design and Development of A Six Stroke Engine to Reduce Pollution Levels And Improve Efficiency
SEEC-041	R S Krishna	Bulk Utilisation of Fly Ash in Mining
SEEC-078	Divya Prakash and Onkar Singh	Thermodynamic Investigations on Carbon Capture In Gas Turbine Power Plant
SEEC-080	M. Nikhil Mathew, Sarthak Nag and Atul Dhar	Exhaust Heat Recovery From a 4-Stroke Diesel Engine Using a Thermoelectric Generator Unit
SEEC-085	Kiran Kumar Dasari and Veershetty Gumtapure	Intermediate Pyrolysis: Chemical Characterization Of Coconut Shell Bio-Oil
SEEC-092	Mritunjay Kumar Shukla, Rahul Reddy Chada and Om Prakash Sharma	Lubricity Of 2, 5-Dimethylfuran–Gasoline Blends And Prospects as an Si Engine Fuel
SEEC-097	Pushpendra Kumar Shukla, Dr. P. Anil Kishan and Hani Chaudhary	CFD Analysis of Latent Heat Energy Storage System With Different Flow Conditions
SEEC-115	Vikram Kumar, Sujeet K Singh and Avinash Agarwal	An Alternative Lubrication for Automotive Engines
SEEC-146	Ankit Sharma and Kirti Bhushan Mishra	Experimental Study on Flame Characteristics of Small and Medium Scale Ethanol Pool Fires
SEEC-148	Pushpendra Kumar Vishwakarma, Poomurugan C and Kirti Bhushan Mishra	Prediction of multiple fireballs characteristics using FDS
SEEC-153	Eshan Singh, Kai Morganti and Robert Dibble	Pre-ignition and knock limits on utilization of Ethanol in Octane – on –Demand Concept
SEEC-158	Vishal Jagadale and Devendra Deshmukh	Combustion, Emission and Performance analysis using EGR in Diesel engine fuelled with Methanol and Diesel Blend
Session B-8 Renewable and Sustainable Energy Rapid Fire Poster Session - II (4 Minutes Each Including Q&A) (4 Best Poster Awards)		
SEEC-018	Saloni Chaudhary and Dr. Raghavendra G. Rao	To Make a Frame Work of Input-Out for Sustainable Development of Clean Energy- A Review of New Holland Fram Industry
SEEC-090	Nipun Sharma, Rudraksh Gupta and Sanjeev Anand	Efficency enhancement of Flat plate collector using different nanofluids
SEEC-096	Keerthana P, Sree Nidhi G.R and Vishnuvarthanan M	Pectin / Flyash Based Bionanocomposite Film for Food Packaging Applications
SEEC-098	Sutapa Das and Dr. Vaibhav V Goud	Utilization of Agricultural Waste for The Production of Bio-Oil and Bio-Char
SEEC-100	Gaurav Chhaparwal, Ram Dayal and Ankur Srivastava	Thermal Hydraulic Performance Enhancement of a Solar Air Heater Exploiting Von-Karman Effect by Suspended Wires.
SEEC-102	Akanksha Pandey, Sumit Singh, Yogesh Kumar and Sham S. Ravindranath	Improvement in Asphalt Binder by Waste Plastic: From Waste to Wealth
SEEC-103	Rahul Goswami, Abhay Singh, Piyush	Design and Analysis of Sunflower Solar System

	Singhal and Abhinav Dwivedi	
SEEC-107	Ashwini Chaudhary, Ankur Srivastava and Gaurav Chhaparwal	Heat Transfer Enhancement and Thermal Performance of Solar Air Heater With Different Artificial Roughness: A Review
SEEC-108	Sainath Navale and Sanjaykumar Dalvi	Design And Development of a Parabolic Solar Cooker for Cooking
SEEC-109	Mukesh Ruhela and Neetu Panwar	Low Cost Waste-Water Remediation Technologies: A Review
SEEC-110	Neetu Panwar and Mukesh Ruhela	Consequences of Environmental Resources Degradation in Context to the Sustainable Development Goals
SEEC-141	Alka Bharti and Bireswar Paul	Experimental Analysis of a Small-Sized Solar Parabolic Trough Collector Using Parabolic and Triangular Secondary Reflcetor
SEEC-142	Prabhakar Zainith, Niraj K Mishra and Gyan Sagar Sinha	Numerical Analysis of Heat Transfer for Non-Newtonian Nanofluids In An Elliptical Annulus at Laminar Flow Condition
SEEC-144	Pankaj Kumar Gupta and Kishore Debnath	Experimental Study on Electro Chemical Discharge Machining of Sustainable Materials
SEEC-147	Saumitra Mishra and Kirti Bhushan Mishra	Application of CFD Tool Flacs for Advanced Risk Assessment In Process Industries
SEEC-150	Kiran Kumar Yalamanchi, Monge-Palacios Manuel, Francesco Tutino, Xin Gao and Mani Sarathy Subram	Using Machine Learning for Predicting Enthalpy
SEEC-159	Tanvi Verma and Soumitra Satapathi	Water Remediation Based on Electrospun Ceramic Hollow Nanofiber Membranes
SEEC-160	Jitendra Bahadur and Kaushik Pal	Fabrication of ambient stable low temperature planer perovskite solar cell
Session C-8 Biotechnology Rapid Fire Poster Session - III (4 Minutes Each Including Q&A) (4 Best Poster Awards)		
SEEC-005	Subha Mondal and Sudipta De	Performance Assessment of An Organic Flash Cycle (OFC) Using R1234ze(Z) as The Alternative Working Fluid Of R245FA
SEEC-014	Sonam Tantuvoy and P. Hari Prasad Reddy	Removal of Arsenic by adsorption using Neem Leaves (Azadirachta Indica)
SEEC-018	Saloni Chaudhary and Dr. Raghavendra G. Rao	To Make a Frame Work of Input-Out For Sustainable Development of Clean Energy- A Review of New Holland Fram Industry
SEEC-028	Bedotroyee Chowdhury, Lakshmishri Roy and Debabrata Bera	Application of Condensed Distillers Syrup Ethanol Industry Waste for Heavy Metal Removal from Wastewater
SEEC-037	Riti Thapar Kapoor	Biotreatment of Acid Magenta Dye by Rice Husk : A Sustainable Tool for Agro-Waste Management
SEEC-055	Saima Saif and Mohammad Saghir Khan	Biosorbing Potentials of Pseudomonas Aeruginosa SFP1 to Combat Cr(VI) Stress In Cicer Arietinum Seedlings
SEEC-063	Dr. K P Suhasini and Dr. P Mangaveni	Green Synthetic Approach of 1,7-Bis(Substituted Phenyl)1,6-Heptadene-3,5-Diones
SEEC-064	Sweta Singh, Atul Grover and Madhu Bala	Nitrate Supplemented Medium for Enhanced Biomass of Chlorella Sp. DBRF-1
SEEC-070	Sudarsan J S, Payal Maharathi, Pranjal Singh B and Sri Hari V	Tannery Wastewater Treatment with Constructed Wetland Using Biochar Mixed Substrate as an Adsorbent.
SEEC-075	Ravi Kumar Sonwani, Shivam Kumar, Balendu Shekher Giri, Ram Sharan Singh and Birendra Nath Ra	Performance Evaluation of Bioreactor packed with LDPE, PUF immobilized bacterial consortia for the degradation of Polycyclic Aromatic Hydrocarbon
SEEC-083	Dipali Sharma, Hitesh Goyal, Neha Singh and Mamta Sardare	Indrayani Water Treatment by Using Photocatalytic Degradation Method
SEEC-089	Koushik Singha Roy, Alkesha Naik, Ashwini Trivedi and Abhishek Gupta	Bioprospecting of Exopolysaccharides for Amelioration of Soil Quality
SEEC-124	Aquib Jawed, Ravi and Lalit M. Pandey	Synthesis of Nano-Structured Al-Doped Zno for Effective Removal of Heavy Metals
SEEC-135	Jayalatha N A, Shreyas A, Kadambari S Teli, Mahendra S Pujari and Vinay Kuma	Restoration of Physico-Chemical Characterization of Dairy Sludge by Vermicompost
SEEC-149	Hardik Gamdha and Umeshkumar Khare	Advanced Oxidation Processes for the Removal of Refractory COD and Ammoniacal Nitrogen from Pharmaceutical Wastewater: A Review
SEEC-156	Uplabdhi Tyagi, Neeru Anand and Dinesh Kumar	Amalgamation of Ionic liquid and Solid acid catalyst for the conversion of cellulose into Sugars and 5-Hydroxymethyl furfural

Sponsors

Diamond Sponsors

TEQIP-3
Technical Education Quality Improvement Programme

Gold Sponsors

सत्यमेव जयते
Department of Science and Technology (DST)
DST

Bronze Sponsors

UTTAR PRADESH BIOENERGY DEVELOPMENT BOARD

Publishing Partners

Springer